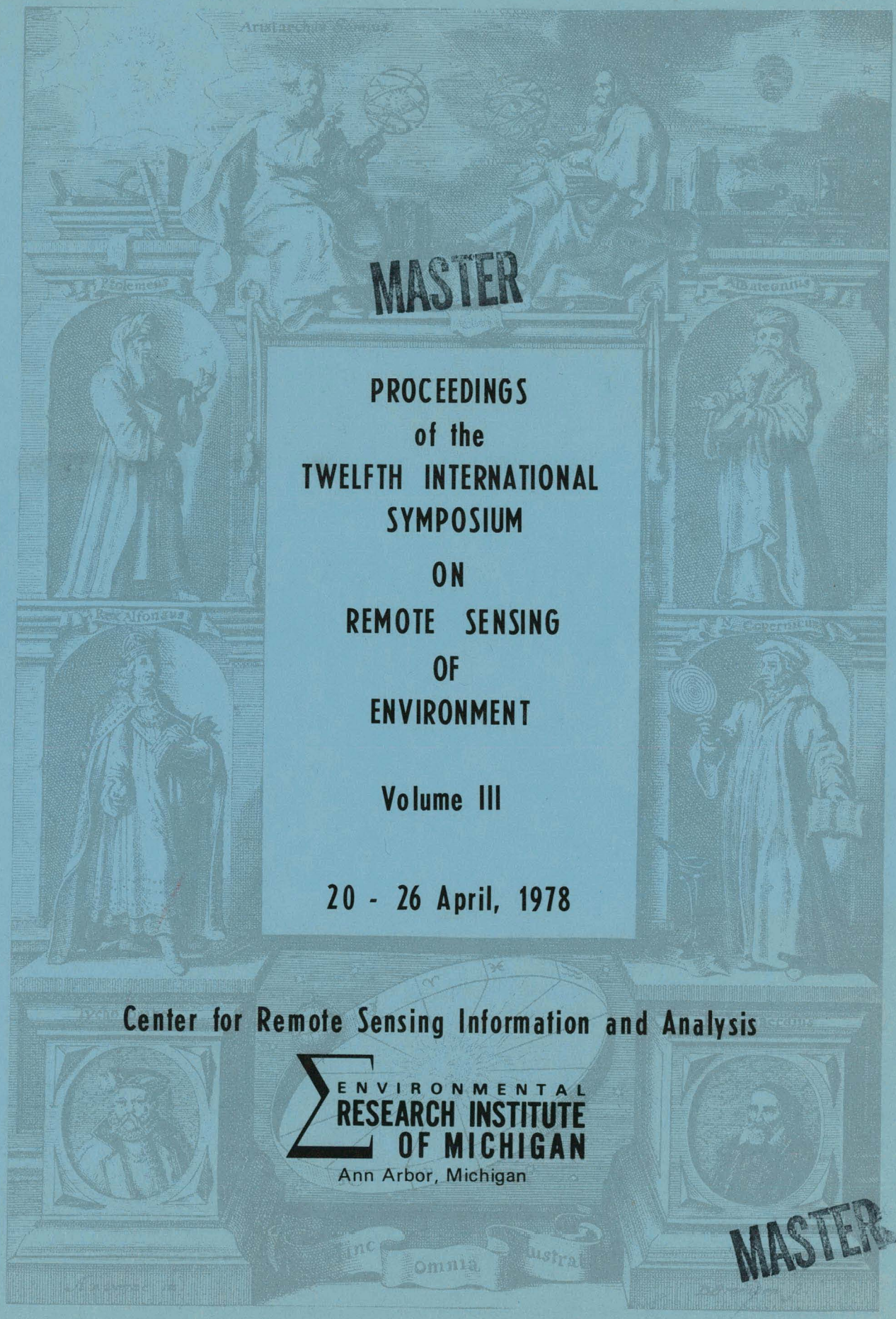

MASTER

PROCEEDINGS of the TWELFTH INTERNATIONAL SYMPOSIUM ON REMOTE SENSING OF ENVIRONMENT

Volume III

20 - 26 April, 1978

Center for Remote Sensing Information and Analysis

ENVIRONMENTAL RESEARCH INSTITUTE OF MICHIGAN
Ann Arbor, Michigan

MASTER

DISTRIBUTION OF THIS DOCUMENT IS UNLIMITED

DISCLAIMER

This report was prepared as an account of work sponsored by an agency of the United States Government. Neither the United States Government nor any agency Thereof, nor any of their employees, makes any warranty, express or implied, or assumes any legal liability or responsibility for the accuracy, completeness, or usefulness of any information, apparatus, product, or process disclosed, or represents that its use would not infringe privately owned rights. Reference herein to any specific commercial product, process, or service by trade name, trademark, manufacturer, or otherwise does not necessarily constitute or imply its endorsement, recommendation, or favoring by the United States Government or any agency thereof. The views and opinions of authors expressed herein do not necessarily state or reflect those of the United States Government or any agency thereof.

DISCLAIMER

Portions of this document may be illegible in electronic image products. Images are produced from the best available original document.

NOTICES

Reproduction Notice. Reproduction in whole or in part is permitted for any purpose of the United States Government. This document has been approved for public release and sale; its distribution is unlimited.

Final Disposition. After this document has served its purpose, it may be destroyed. Please do not return it to the Environmental Research Institute of Michigan.

CONF-7804163--(Vol. 3)

CONTENTS

	Page
Executive Committee	ii
Program Committee	iii
Abstract	iv
Editorial Note	v
Program	vii
Registrants	xxxiv
Messages	lxiii
Session 1	
Opening Remarks Honorable Jose J. Leido	1
Keynote Address His Excellency Ferdinand E. Marcos	5
Luncheon Address, The Role of Science and Technology in Development Sander M. Levin	11
Session 2	
Remote Sensing Program of the Philippines C. R. Roque	17
The Application of Remote Sensing in Support of the National Program for the Inventory and Evaluation of the Country's Natural Resources (Indonesia) Pranoto Asmoro	27
A Review of Remote Sensing Activities in Singapore Chong Yean Joo	35
Thailand National Remote Sensing Program: Past, Present & Future Sanga Sabhasri, et al.	37
Remote Sensing Activities in India: A Country Report K. R. Rao	43
Session 3	
The Application of Remote Sensing for Development in Australia J. F. Ryan	55
Bangladesh Landsat Programme, A Review of the Programme and a Report on the Activities Anwar Hossain, et al.	63
Satellite Remote Sensing Activities in Iran B. Jazayeri and F. Naderi	69
Remote Sensing Activities in Japan Kaoru Mamiya	81
Applications of Remote Sensing to the Study of the Agricultural and Natural Resources (Iran) M. A. Sharifi	95

DISCLAIMER

This book was prepared as an account of work sponsored by an agency of the United States Government. Neither the United States Government nor any agency thereof, nor any of their employees, makes any warranty, express or implied, or assumes any legal liability or responsibility for the accuracy, completeness, or usefulness of any information, apparatus, product, or process disclosed, or represents that its use would not infringe privately owned rights. Reference herein to any specific commercial product, process, or service by trade name, trademark, manufacturer, or otherwise, does not necessarily constitute or imply its endorsement, recommendation, or favoring by the United States Government or any agency thereof. The views and opinions of authors expressed herein do not necessarily state or reflect those of the United States Government or any agency thereof.

DISTRIBUTION OF THIS DOCUMENT IS UNLIMITED

Page

Remote Sensing Activities in the German Democratic Republic
H. Kautzleben, et al. 113

Pakistan National Programme of Remote Sensing Applications
M. Shafi Ahmad 123

Session 4

Argentina Remote Sensing Program
Miguel Sanchez Pena 125

Bolivian National Earth Resources Technology Satellite Program
Carlos E. Brockmann 131

Remote Sensing Activities in Malaysia
Ealich Mohd. Nor 133

Resources Assessment and Remote Sensing in Costa Rica
Rodolfo E. Quiros Guardia, et al. 139

Italian Activities in the Domain of Remote Sensing
R. Cassinis 145

Earth Resources Satellite Remote Sensing in New Zealand
P. J. Ellis 159

Session 5

The Role of Science and Technology in Development
Henry A. Arnold 175

The United Nations Role in Satellite Remote Sensing
H.G.S. Murthy 179

Remote Sensing Technology and New Development Trends in Latin America
Pierre-Marie Adrien 187

Remote Sensing Technology Transfer The Canadian-Peruvian Approach
F. P. DuBois and W. D. Bruce 203

Transfer of Remote Sensing Technology for the Benefit of Developing Countries-A Case Study in Bangladesh
Anwar Hossain 213

Session 6

Monitoring Environmental Pollution by Remote Sensing
P. A. Vass and J. L. van Genderen 219

Control of Oil Pollution by Remote Sensing Along the Shores of France
Jean-Claude Mourlon 235

Remote Sensing for Oil Pollution Control Along the Coastal Waters of the U.S.
J. R. White and L. R. Breslau 239

Remote Sensing for Air Pollution Control
A. R. Barringer and J. H. Davies 257

Remote Sensing and Land Use Impact Assessment
Thomas H. Pierce, et al. 271

Page

Session 7

Ground Truth Collection Techniques
T. W. Wagner and D. S. Lowe 277

Remote Sensing Data Collection; A Review of Aircraft and Satellite Systems
J. T. Smith 283

SPOT: The French Trial Earth Observation System
A. M. Gaubert 289

Microwave Sensors and Sensor Systems
R. W. Larson and E. Schanda 297

Session 8

Information Extraction With Human Interpreters
C. E. Olson, Jr. 323

Digital Image Analysis of Landsat Data
W. L. Alford 329

A Review of Current Remote Sensing Satellite Reception and Preprocessing Technology
A. B. Park and W. M. Strome 355

Landsat-D, A Systems Overview
V. V. Salomonson 371

Session 9

A World Wide Approach to Remote Sensing and Mineral Exploration
W. D. Carter and L. C. Rowan 387

Energy and Remote Sensing Applications
R. A. Summers, et al. 395

Digital Processing Applied to Geology
Carlos Brockmann 415

Session 10

Forest Mapping and Inventory Techniques Through Visual Analysis of Landsat Imagery: Examples from Thailand
S. A. Morain and B. Klankamsorn 417

Potential Applications of Space Radar for Agricultural Monitoring in the Wet Tropics
D. S. Simonett 427

A Land Use Information System Based on Statistical Inference
W. H. Wigton and H. F. Huddleston 429

Methods for Using Landsat Data in Large-Area Resource Inventories
D. G. Moore 443

Session 11

Satellite Surveillance of Physical Water-Quality Characteristics
G. K. Moore 445

Remote Sensing Floods and Flood Plains, Victoria, Australia
D. T. Currey 463

Page

The Definition of Hydrologic Model Parameters Using Remote Sensing Techniques
R. M. Ragan and V. V. Salomonson 481

Remote Sensing Use in Hydraulic Planification in Mexico
J. A. Diez Perez 497

Water Resources Investigations in West-Central Iran, Using Multistage, Multispectral and Repetitive Sampling
M. S. Akhavi 503

Session 12

An Overview on the Utilization of the Japanese Geostationary Meteorological Satellite
N. Murayama and N. Kodaria 505

A Decade of Collection of In-Situ Environmental Data Utilizing Earth Orbiting Satellites
H. S. Moore and J. H. Puerner 507

Global Climate Analysis Utilizing Remotely Sensed Data
W. A. Sprigg 513

Remote Sensing of Areal Rainfall Rates by a Ground Based Microwave Radiometer
Leu Dar-ren, et al. 523

Acoustic Radar and Remote Sensing in the Boundary Layer of Atmosphere
Lu Nai-ping, et al. 535

Session 13

Use of Change Detection in Assessing Development Plans: A Philippine Example
J. C. Coiner and R. C. Bruce 547

Remote Sensing, Geographic Information Systems, and National Land Planning: Some Central American and Caribbean Experiences
R. L. Shelton and S. E. Tilmann 567

Procedures for Land-Use Analysis in Developing Countries: Examples from Southeast Asia
S. Wacharakitti and S. A. Morain 587

Remote Sensing in National Planning for Developing Countries: Relations Between Physical and Economic Planning
D. S. Simonett 597

Session 14

Remote Sensing of the Oceans - A Review
G. A. Morgan 599

Surface Radar Observation of Sea Ice
Tadashi Tabata 619

Marine Applications of the NIMBUS-G Coastal Zone Color Scanner
T. M. Vanselous, et al. 621

An Overview of Remote Sensing Oceanography in the United States
J. W. Sherman, III 639

Page

An Experiment on a Popular Multispectral Image Optical Process
Huang Hsuan 653

Lidar Remote Sensing of Lower Atmosphere
Institute of Atmospheric Physics, Peking 661

Theoretical Analysis on Remote Sensing of Atmospheric Parameters by Scintillations of Light
Chou Hsiu-chi, et al. 671

Poster Session A

Oceanic Wave Imagery and Wave Spectra Distortions by Synthetic Aperture Radar
R. K. Raney and R. T. Lowry 683

Earth Orbital Photography by the Large Format Camera
Farouk El-Baz and R. J. Ondrejka 703

NS001MS - Landsat-D Thematic Mapper Band Aircraft Scanner
R. R. Richard, et al. 719

Improving Land Cover Classification by Image Stratification of Landsat Data
Wayne G. Rohde 729

Modeling to Estimate and Optimize Multispectral System Performance
S. L. Green and H. L. Schlesinger 743

Landsat Images of Part of the U.S. Trust Territory of the Pacific Islands and Other Pacific Outlying Areas
W. D. Carter and J. M. DeNoyer 755

Principal Component Greenness Transformation in Multitemporal Agricultural Landsat Data
R. A. Abotteen 765

Spacial Correlation and its Effect Upon Classification Results in Landsat
J. D. Tubbs and W. A. Coberly 775

Elimination of Atmospheric Effects from Remote Sensor Data
R. E. Turner 783

Application of Remote Sensing to Reconnaissance Geologic Mapping and Mineral Exploration
R. W. Birnie and J. D. Dykstra 795

An Example of the Merging of Landsat, Topographic, and Aeromagnetic Data in a Geologic and Hydrologic Study of a Karst Region: Claunch, New Mexico
W. A. Fischer, et al. 805

Correlation Studies Between Linear Features Observed in Landsat Imagery and Earthquake Epicenters for a Region South of Peking, People's Republic of China
R. K. Vincent, at al. 825

Simultaneous Use of Geological, Geophysical, and Landsat Digital Data in Uranium Exploration
A. E. Prelat, et al. 835

Page

Quantitative Evaluation of Habitat Conditions for Effective Waterfowl Management by Computer Manipulation of Landsat Classified Data
J. E. Colwell, et al. 845

Application of Landsat Imagery in the Geological and Soil Investigations in the Central Western Desert, Egypt
E. M. El Shazly, et al. 857

Remote Detection of Reinforced-Concrete Delamination in Bridges by Infrared Thermography
G. G. Clemena and W. T. McKeel, Jr. 867

Remote Sensing of Snowpack With Microwave Radiometers for Hydrologic Applications
J. C. Shiue, et al. 877

A Quantitative Assessment of Changes in Land Formations Along the Coastline of Bangladesh
M. A. H. Pramanik, et al. 887

A Small Grant Program for Remote Sensing Technology Transfer
T. W. Wagner and D. S. Lowe 899

Large-Scale Demonstration of Aquatic Plant Mapping by Remote Sensing
L. E. Link and K. S. Long 907

Applications of Modeling to Analysis and Processing of Landsat Data
W. A. Malila, et al. 917

Improving Forest Cover Classification Accuracy from Landsat by Incorporating Topographic Information
A. H. Strahler, et al. 927

Procedural Guide for Vegetation Analysis
J. A. Messmore and T. C. Vogel 943

Use of Landsat in the Study of Forest Classification in the Tropical Jungle
W. A. Danjoy and F. G. Sadowski 947

Poster Session B

Electromagnetic Scattering Properties of Soils and Snow
D. A. Ellerbruch, et al. 957

SURTRACE™, An Airborne Geochemical System
A. R. Barringer, et al. 975

Cloud Effects on Ultraviolet Photoclimatology
A. E. S. Green and J. D. Spinhirne 991

Data Screening and Preprocessing for Landsat MSS Data
P. F. Lambeck, et al. 999

The Application of Conventional Aerial Photography and Interactive Computer Graphics in Mapping Natural Phenomenon
W. H. Kuyper 1009

A Guide to Area Frame Sampling Utilizing Landsat Imagery
W. H. Wigton, et al. 1013

An Analysis of the Spatial and Temporal Distribution of Surficial Waters in the Minnedosa Wetland District of Manitoba, Canada
R. Steffensen and A. M. Smith 1015

Page

Image Enhancement of Side-Scan Sonar Mapping
B. P. Luyendyk, et al. 1025

Use of Remote Sensing to Quantify Construction Material and to Define Geologic Lineaments Dickey-Lincoln School Lakes Project, Maine
H. L. McKim, et al. 1027

Targeting Exploration for Nickel Laterites in Indonesia With Landsat Data
J. V. Taranik, et al. 1037

Groundwater Exploration in Northwestern Tamil Nadu, India With Landsat Data
R. K. Vincent, et al. 1053

Low Cost Hydrographic Mapping
D. K. Warne 1063

Problems and Concepts in Remote Sensing of Land Use
L. E. Link and H. Struve 1073

Identification and Delineation of Urbanized Areas Using Landsat Data
D. L. Dietrich, et al. 1083

Airborne Multispectral Survey of Intertidal Vegetation in Alaska
F. C. Polcyn, et al. 1091

Optical Remote Sensing of Chlorophyll in Ocean Waters
W. H. Wilson, et al. 1103

Radar Monitoring of Surface and Internal Glacial Flow and Iceberg Movement
Ben Drake, et al. 1115

The Use of SAR Systems for Iceberg Detection and Characterization
R. W. Larson, et al. 1127

Wheat Production Forecasts Using Landsat Data
R. F. Nalepka, et al. 1149

Delineation of Soil-Landscapes in the Sudd Region of Sudan on Landsat Imagery
B. K. Worcester and D. G. Moore 1155

Analysis of the Dynamics of Shifting Cultivation in the Tropical Forests of Northern Thailand Using Landscape Modeling and Classification of Landsat Imagery
L. D. Miller, et al. 1167

New Developments in Tropical Forest Inventories
L. Sayn-Wittgenstein 1187

Transferring Remote Sensing Technology: Activities of TAC
S. A. Morain 1199

Poster Session C

Image Registration for Thermal Inertia Mapping, and its Potential Use for Mapping of Soil Moisture and Geology in Australia
D. A. Pratt and C. D. Ellyett 1207

A Five Channel MSS for Aircraft Platform
G. Joseph and D. S. Kamat 1219

Analog/Digital Image Processing System "TIAS"
H. Shimoda and T. Sakata 1229

Page

Atmospheric Effects and Their Correction in Airborne Sensor and Landsat MSS Data
Y. Kawata, et al. 1241

Estimating the Proportions of Classes in a Boundary Pixel
R. Krishnan and S. Natarajan 1259

Analysis of a Transformation Model of Satellite Radiances into Reflectances
G. Rochon, et al. 1267

Airborne Lidar Aerosol Measurements Over the US and Europe
Ch. Werner, et al. 1279

A Structural and Lithologic Interpretation of Northwestern Cebu Island, Republic of the Philippines, Using Multi-Level Remote Sensor Data and Computer-Assisted Image Processing Techniques
R. S. Punongbayan, et al. 1287

Geologic and Hydrogeologic Study in the Tamilnadu State of South India Using Landsat Data
S. Thillaigovindarajan and A. S. Andrawis 1289

Use of Satellite Imagery to Assess Forest Deterioration in Eastern Thailand
Boonchna Klankamsorn 1299

Simulated Retrievals of the Tropical Atmosphere From a Projected Advanced Satellite Sounding System
L. D. Kaplan, et al. 1307

Quantitative Description and Analysis of Remotely Sensed Water Quality Distribution
Y. Yasuoka, et al. 1309

Comparative Results of Conventional and Digital Land Cover Collection Methodologies for Input to Hydrologic Modeling
R. R. Sasso, et al. 1319

Application of Landsat Data to Monitor Desert Spreading in the Sahara Region
A. M. Brera and F. Shahrokhi 1329

Remote Sensing of Squatter Areas in Hong Kong
C. P. Lo 1339

Thematic Map of Lombok Island From Landsat Computer Compatible Tapes
Z. D. Kalensky, et al. 1349

Sediment/Siltation Monitoring Within a Tidal Basin Using Repetitive Landsat CCT Data
I. L. Thomas 1367

Detection of Eutrophication Processes From Air and Space
U. Horstmann, et al. 1379

A Landsat Inventory of the Agricultural and Forest Resources in Bangladesh
M. U. Chaudhury, et al. 1391

Landsat Assisted Forest Inventory of the Philippine Islands
H. M. Lachowski, et al. 1401

Page

The Use of Color Infrared Aerial Photography to Detect Plants Attacked by Tropical Fruit Flies
W. G. Hart, et al. 1409

New Brunswick Potato Area Estimation From Landsat
P. N. Mosher, et al. 1415

Poster Session D

Some Recent Developments in Remote Sensing Instruments and Measurement Systems
E. H. Velten, et al. 1421

The First European Ocean Color Scanner Experiment in the Southern Bight of the North Sea-EURASEP Project
B. Møller Sørensen, et al. 1431

Integration of Landsat Data and National Land Data System
Shunji Murai, et al. 1441

An Airborne Remote Sensing Project in Japan-JAFSA Project
Hiromichi Toyota, et al. 1451

Between Scene Registration Accuracy in Landsat Time Sequencing
G. D. Lodwick 1461

Computer Classification and Delineation of Types Using Landsat Data in Two Areas of Tropical Forests in India
N. V. Madhavan Unni 1471

Analytical Positioning of Thermal IR Imagery for Monitoring Volcanic Activity
Mitsuru Nasu 1481

Processing and Analysis of Landsat Data Covering the Baguio Mineral District, Northwest Luzon, Philippines
R. S. Punongbayan, et al. 1489

An Evaluation of Landsat Technology for Operational Use by Nepal Resource Agencies
A. S. Andrawis, et al. 1503

Geological Interpretation of Landsat-1 Imagery of Mindoro Island, Philippines
Juanito C. Fernandez, et al. 1513

Operational and Experimental Use of SMS/GOES Digital Satellite Data
Marshall P. Waters, III 1529

Application of Satellite Imagery to Flood Plain Mapping in Thailand
George Whitehouse, et al. 1545

Systematic Interdisciplinary Analysis With Stereo and Transfer Scope Application
Clyde E. Renz 1555

Jonglei Canal Project, Sudan-A Landsat Imagery Approach
E. M. El Shazly, et al. 1563

Ring-Ditch Fortifications in the Rewa Delta, Fiji: Archaeology From the Air Using Panchromatic, Infrared, and Color Photography
J. T. Parry 1573

Page

Advance in the Research and Use of Remote Sensors in Natural Resources Development Studies - Chile
Arnoldo Ortiz 1583

The Modulation of the Radar Backscattering Cross Section by Long Ocean Waves
Werner Alpers and W. L. Jones 1597

Applications of Landsat and Skylab Imagery in Mexico: Detection of Erosion and Forest Damage
D. Rodriguez-Bejarano 1609

Remote Sensing Inputs into a Wetland Rice Regional Production Model (Java)
Jean-Paul Malingreau 1617

Applied Research on Remote Sensing in the Field of Agriculture
S. Haketa, et al. 1649

Remote Measurements of Vegetative Cover in Surface Mines
J. E. Carrel, et al. 1653

Problems Associated With Organising Remote Sensing Applications in a Developing Country
Chris Nanayakkara 1665

Experiments in the Use of Remote Sensing From Satellite and Aerial Photography for Forest Inventory
Piran Wiroatmodjo 1671

Poster Session E

Infrared Remote Sensing on Geothermal Areas by Helicopter
M. Sekioka and K. Yuhara 1679

Digital Image Rectification and Enhancement on a Minicomputer: Analysis of Results
M. J. McDonnell 1687

Landsat User Needs and Administrative Responses: Density Scales, Data Catalogues, Image Annotation
Allan Falconer, et al. 1697

Extraction of Soil Information From Vegetated Area
Michikazu Fukuhara, et al. 1707

Land Cover Studies Using Landsat MSS Digital Data: Cartographically Corrected Lineprinter Output
J. R. Hardy 1717

Evaluation of Wavelength Groups for Discrimination of Agricultural Cover Types
R. Kumar 1729

The Use of Landsat Imagery for Marine Pollution Studies
Chong Yean Joo 1741

Remote Sensing for Nuclear Power Plant Siting, Bataan Peninsula, Republic of the Philippines
Barry S. Siegal, et al. 1743

Landsat Digital Enhancement Techniques for Mineral Exploration in Australia
A. A. Green, et al. 1755

Page

Remote Sensing and Inventory of Mineral Resources in Part of Chandrapur District, Maharashtra, India
K. S. Misra 1763

Analysis on Multi-Date Landsat Data
S. Chandrasekhar and M. Maruthachalam 1769

Soil Moisture Determination and Snow Classification With Microwave Radiometry
E. Schanda, et al. 1779

Detection and Monitoring of Water Hyacinth (Eichhornia crassipes) Infestation in Laguna De Bay Through Multispectral Digital Analysis of Landsat Imageries
Ricardo T. Bina, et al. 1791

Landsat Interpretation for Development Studies
J. W. Trevett 1799

The Ten-Ecosystem Study: Landsat ADP Mapping of Forest and Rangeland in the United States
E. P. Kan and F. P. Weber 1809

Application Study of Remote Sensing to Saury Fisheries in Japan
Sei-ichi Saitoh, et al. 1827

Water Management and Control Via the Global Meteorological Satellite System
Warren L. Sharp 1837

Determination of Wheat Acreages From Landsat Imagery in the Narrabri District of New South Wales, Australia
A. J. Parsons and E. A. Fitzpatrick 1849

A Study on Computer Analysis of Land Use Classification of Metro Manila
Alejandro Pascual and Wellman Silonga 1859

Mapping Tropical Vegetation Zones in the State of Veracruz, Mexico
M. Soto, et al. 1871

An Interpretation of Northern Thailand Swiddening and Multiple Cropping Systems Using Multidate Landsat Images and Computer Compatible Tapes
Michel Bruneau and Thuy Le Toan 1883

Use of Large Scale Aerial Photographs for Ecological Studies in a Grazed Arid Ecosystem
R. B. Hacker 1895

Some Notes on the Experiences of LAPAN (The Indonesian National Institute of Aeronautics and Space) in the Development of Remote Sensing in Indonesia
Mahsun Irsyam 1909

Poster Session F

Sonar Imagery of Sea-Floor Objects
Lloyd Breslau 1917

Vegetation Mapping of Nigeria From Radar
J. W. Trevett 1919

Spectral Characteristics in UV-V-IR of Materials in Requena and La Esperanza Dams and Their Detection by Remote Sensing
P. Ruiz Azuara and L. Lemus Hidalgo 1937

Page

Japan's Receiving and Processing Facilities for Landsat Data
Y. Haruyama and Y. Yamamoto 1947

Application of Texture Analysis and Image Enhancement Techniques for Remote Sensing
Joji Iisaka, et al. 1957

An Economic Way of Data Handling and Reproduction of Landsat Data
Suvit Vibulsresth, et al. 1973

Landsat-Digital Data as a Tool in Quaternary Geological Mapping in the Coastal Plain of the Malaysian Peninsula
A. E. Prelat, et al. 1985

Zone of Mineralization in the Northern Part of South Sulawsei and its Structural Control, as Observed From Landsat Imagery
Suwijanto 1993

A Study of Airborne Gamma-Ray Spectrometry for Geological Mapping
V. R. Slaney 1995

Resources Engineering Investigations - An Approach and Output Applicable to 'Chandrapur Project'
A. Parthasarathy 2011

Photographic Remote Sensing at Chiba University (a) Studies of Kumano River Water and (b) Analysis of Concrete Moisture by Simulation
Hidesaburo Genda, et al. 2019

Multi-Level Inventory and Monitoring of Wetlands on the Swan Coastal Plain, Western Australia
F. R. Honey, et al. 2027

Thailand's Littoral Mudflats as Interpreted From Landsat Imagery
Nissai Sriplung 2045

Coral Reef Mapping Using Landsat Data: Follow-Up Studies
Ricardo T. Bina, et al. 2051

The Application of Remote Sensing in Marine Research in Indonesia
D. P. Praseno, et al. 2071

The Application of Remote Sensing Techniques to Forest Vegetation Surveys in Tropical Areas and Urban Fringe Land Use Problems in Costa Rica
Timothy K. Cannon, et al. 2081

Automatic Classification of Reforested Pinus Spp. and Eucalyptus Spp. in Mogi-Guacu, S.P., Brazil Using Landsat Data
Y. E. Shimabukuro, et al. 2091

Therman Infrared Remote Sensing of Soil Moisture: What Can be Expected From HCMM Data?
Ferdinand J. Bonn 2101

Grassland and Forestry Applications From New Zealand Landsat Data
G. Ross Cochrane 2109

Page

Poster Session G

Volcanic Gas Eruption Velocity Sensor Using a Spatial Filter
Suteo Tsutsumi, et al. 2121

Automatic Collection of Environmental Ground Truth Data in Chile by Employing Earth Orbiting Satellites
Mauricio Araya F. 2131

Design of Decision-Tree Classifier for Remote Sensing Applications
Z. Chen and L. Y. Tseng 2141

Land Use Map Compilation System From Aerial MSS Data
Sotaro Tanaka 2151

The Production of 1:250,000 Maps of Precision Rectified and Registered Landsat Imagery Using the MDA Image Analysis System: Initial Results
R. Orth, et al. 2163

Landsat and Photographic Remote Sensing for Arid Land Application in Australia
P. T. Tueller, et al. 2177

A System for the Coherent Processing of Remote Sensing Imagery
J. C. Lummaux and S. Braconne 2193

The Varied Applications of Satellite Remote Sensing Practiced by the Federal Institute of Geosciences and Natural Resources of the Federal Republic of Germany
R. Muhlfeld 2199

Increased Visibility From the Invisible A Comparison of Radar and Landsat in Tropical Environments
R. H. Gelnett, et al. 2205

Remote Sensing Applications for Geological Mapping of Pahangan Sheet, Central Kalimantan, Indonesia
Turus Soejitno 2217

Geomorphology and Natural Resources of the Coipasa Area Using Landsat Imagery
Milton Suarez M. 2227

Ionospheric and Satellite Observations for Studying the Dynamic Behavior of Typhoons and the Detection of Severe Storms and Tsunamis
R. J. Hung and R. E. Smith 2245

The Use of Landsat Data to Minimize Flooding Risks Caused by Ice Jams in Alaskan Rivers
J. M. Miller and T. E. Osterkamp 2255

"TELL-US" A Combined Surface Temperature, Soil Moisture and Evaporation Mapping Approach
A. Rosema, et al. 2267

Sedimentation Pattern and Land Formation Studies in the Feni and Little Feni River Estuaries Using Landsat Imageries
M. A. H. Pramanik, et al. 2277

Using Intermediate Remote Sensing Technology Projects for National Development in the Yemen Arab Republic and the Republic of Sri Lanka
Harold Haefner, et al. 2285

Page

Land Use Inventory of North Thailand Using Landsat Imagery
Manu Omakupt 2297

U. S. Coast Guard Utilization of Remote Sensing Techniques for Ocean Surveillance
J. R. White, et al. 2307

An Ecological Approach to Resources Inventory; The Photomorphic Analysis of a Landsat Image of Central Java
Jean-Paul Malingreau and Priyadi Santoso 2313

Remote Sensing Applications to Wildlife Management in the U.S. Fish and Wildlife Service
A. D. Marmelstein 2315

Experiment to Evolve Methods for Separation and Identification of Agricultural Crops From Multispectral Information
R. S. Ayyangar 2323

Determination of Spectral Signatures of Vegetated Surfaces by Radiometric Ground Measurements
Werner Fischer 2333

Mangrove Inventory of the Philippines Using the Landsat Multi-Spectral Data and the Image 100 System
Ricardo T. Bina, et al. 2343

Session 15

Future Operational Earth Resources Programs
(Including statements by: E. Risley, D. Keller, C. Spohn, M. Strome, I. Pikus, J. Hielkema, D. Simonett, W. Fischer, R. Vincent, J. Cook, J. van Genderen, S. Pena, F. Rudin and C. Roque. Also included is a presentation of L. W. Morley, Barriers to Realizing Remote Sensing Benefits) 2353

Report on Commercial Exhibits 2379

Author Index

TWELFTH INTERNATIONAL SYMPOSIUM ON
REMOTE SENSING OF THE ENVIRONMENT
20-26 April 1978
MANILA , PHILLIPINES

JONGLEI CANAL PROJECT, SUDAN
A LANDSAT IMAGERY APPROACH

E. M. El Shazly, M. A. Abdel Hady, M. M. El Shazly,
M. A. El Ghawaby, A. B. Salman, I. A. El Kassas,
S. M. Khawasik, M. M. El Rakaiby and H. El Amin

Remote Sensing Center
Cairo, Egypt

ABSTRACT

One of the most accepted means of overcoming the water losses at Bahr El Jebel in Southern Sudan, estimated at 12,250 million m^3 annually, is its canalization through a canal some 280 km long connecting Jonglei on Bahr El Jebel with Malakal on the White Nile. This scheme is called the Jonglei Canal Project.

The regional mapping and study of the huge Jonglei Canal Project area represent an ideal case for the application of LANDSAT imagery interpretation especially in view of the inaccessibility of most of its coverage, notably in the long rainy season. The implementation of this work has been carried out through LANDSAT imagery interpretation in both the dry season and the wet season, together with low reconnaissance flying, ground field work along passable roads and tracks, and extensive laboratory analyses. Maps have been accordingly constructed for the geological and environmental units, structural lineations, lineation density, surface drainage, surface water bodies and groundwater potential, soils, land use, vegetation cover, and infrastructure. Thematic extraction maps and computer printouts are prepared on the basis of the previously mentioned maps. In this communication the soils, land use and vegetation cover of the project area are not given. LANDSAT imagery interpretation has thus provided, within less than eighteen months, including the preparatory period, a regional picture for such a unique area of investigation covering 165,000 km^2 on a scale of 1:500,000.

INTRODUCTION

The River Nile originates in Central Africa where it starts to flow under the name of Victoria Nile. It assumes the names Albert Nile and Bahr El Jebel at the eastern end of Lake Albert and at Nimule on the southern border of Sudan respectively. At El Sudd Region in Southern Sudan Bahr El Jebel enters an almost flat alluvial plain where the river course becomes highly ramified and infested by swamps largely covered with vegetation, there the main channel of Bahr El Jebel is sufficient to carry its water discharge when the water is low, however, Bahr El Jebel overflows its banks as the water rises leading to great losses of water by seepage, evaporation and evapotranspiration (Hurst, et al., 1932-present). During the months of May, June, July, August, September, October, November and December the average monthly discharge of Bahr El Jebel at Mongalla normally exceeds two thousand m^3, while in the months of January, February, March and April the average monthly discharge is less than two thousand m^3.

Alternative ideas have been presented to overcome the huge water losses at Bahr El Jebel which exceed twelve thousandmillion m^3 annually, however, the currently most accepted project in this respect is the Jonglei Canal Project. The latter implies the canalization of Bahr El Jebel through a canal some 280km long connecting Jonglei on Bahr El Jebel with Malakal on the White Nile. There is also a new suggestion that the proposed canal may connect, Bor, instead of Jonglei with Malakal. The amounts of water expected to be saved through the execution of the project are needed for land reclamation in Egypt and the Sudan. Rainfall, inflow of water and bad drainage at El Sudd Region in Southern Sudan, through which passes Bahr El Jebel, lead to the predominance of a high water level and a swampy environment in the region under discussion. There, human well being, infrastructure, animal life, vegetation and the whole environment are adversely affected by the huge swamps dominating El Sudd Region which isolate the human communities and animal gatherings for most of the year or for long periods of time. The canalization of Bahr El Jebel is expected to ensure water control in the concerned region and its best utilization for the progress of its population.

An area of 165,000 km^2 (Fig. 1) has been mapped by the utilization of LANDSAT-1 imagery interpretation on a scale of 1:500,000 which is conceived as the only way to map this area with sufficient accuracy in a short period of time. This is especially true as various parts of the area of study are hardly accessible notably during the rainy season which lasts from March to November in the south and from April to October in the north with an annual average of about 1000 mm and 800 mm respectively. LANDSAT images covering the area have been examined in both the dry season and the wet season. Imagery interpretation has been greatly supported by low reconnaissance flying, ground field work in the dry season, and laboratory analyses of the samples collected during the field season.

Several maps have been constructed for Jonglei Canal area by the application of the previously mentioned techniques, however, in this paper only a central part and a northern part of each of the maps of the drainage in the dry season (Fig. 2, 3), structural lineations (Fig. 4, 5) and geological and environmental units (Fig. 6, 7) are shown on a scale of approximately 1:1,000,000.

In this paper the geomorphology, drainage and water conditions, the structural lineations and the geological and environmental units, with special reference to the central and northern part of Jonglei Canal area, are very briefly reviewed.

GEOMORPHOLOGY, DRAINAGE AND WATER CONDITIONS

The geomorphology, drainage and water conditions in the studied Jonglei Canal area are closely related to the geology and structure of the area on one hand, and to the prevailing climate to which the area is exposed on the other hand.

Geomorphologically the area under discussion,, may be subdivided into four major units ranging from lands of the relatively highest altitude to lands of the relatively lowest altitude. These major units are as follows: basement upland unit, lateritic-covered unit, seasonal flood plain unit and perennial flood plain unit.

The basement upland unit covers mainly the southern part of the studied area where the oldest rocks belonging to the Precambrian basement are outcropping. The drainage pattern dominating in this unit ranges from the dense dentritic to the trellis types. The drainage lines themselves are characterized by being narrow and deep, and they are obviously controlled by structure, geology and relief. The direction of water flow in the drainage channels is directed to east and west in the vicinity of Bahr El Jebel and to north in other locations,

The lateritic-covered unit is mainly of lower altitude in comparison to the previously mentioned unit. The lateritic-covered unit exhibits characteristic morphology, and it is divided into two subunits according to relief. The

first southerly sub unit is represented by a relatively high undulating land with dense drainage lines, while the second is illustrated by a lower plain which is partly covered by clay. Most of the drainage channels in the lateritic-covered unit, especially on the western side, drain into elongated lakes before draining finally into Bahr El Jebel (Fig. 2).

The seasonal flood plain unit extends to the north and to the east of the main river courses. It is formed of slightly undulating clayey land with sand ridges about 1 m high. The plain is flooded in particular during the rainy season with water brought from the surrouding high lands. The drainage lines in the seasonal flood plain unit are characterized by the presence of long tributaries and the dendritic pattern.

The perennial flood plain or El Sudd plain unit possesses the lowest altitude in the area of study, and it covers the neighbourhood of Bahr El Jebel and Bahr Ez Zaraf. The plain in question is characterized by a complicated drainage pattern, and highly meandering network of channels or separate ones connected with Bahr El Jebel and Bahr Ez Zaraf (Fig. 2, 3). The channels are essentially shallow and wide, and they form in certain parts perennial swamps and lakes.

One of the main advantages of the application of LANDSAT imagery is the delineation of the drainage lines intersecting and influencing the course of the canal project, to be constructed from Jonglei to Malakal, both in the wet and in the dry season.

It can be seen from the foregoing the close links, illustrated by the regional mapping conducted, between the surface water distribution and the geomorphology and drainage which are in turn directly related to geology, structure and relief. It may be also demonstrated that the sediments deposited during the previous geological history of the area of study especially Um Rawaba and Yirol Formations control the watertable level and the salinity of the groundwater.

GEOLOGY AND STRUCTURE

The delineation of the geological and environmental units through the application of the technology of LANDSAT imagery interpretation has allowed the mapping of 25 units in the mapped area of which 13 are of Quaternary age possessing direct impact on the environment of the considered area. The remaining 12 represent the igneous-metamorphic basement and the Phanerozoic small igneous bodies, as well as, the Cretaceous sedimentary Yirol Formation.

Using the same technology, a structural lineation map has been constructed for the same area which shows 878 lineaments representing in particular fractures including faults and folds. Statistical analysis and computation of these lineaments have been used as basis for the construction of rose diagrams and a lineation density map for the whole area. The produced maps may be compared with the south sheet of the geological map of the Sudan (Vail, 1974), illustrating in a clear manner the superiority of the space-borne technology applied in mapping the Jonglei Canal Project area.

The present studies have shown that the dominating environment is greatly dependent on its geological and tectonic history which has led to the creation of the semiclosed sedimentary basin limited to the north, south, east and west by the igneous-metamorphic basement rocks. The fractures and fault sets delineated caused the downthrowing of the basin and the upthrowing of the older basement. The sets attain NNW-SSE and NW-SE, ENE-WSW and NE-SW, and NNE-SSW and WNW-ENE trends while the fold traces belong to N-S, NW-SE, NE-SW and ENE-WSW trends. It is also evident that the courses of Bahr El Jebel, Bahr Ez Zaraf and the White Nile, apart from the less important drainage lines are superimposed on the lineaments (Fig. 4, 5). This structural picture is much more elaborate than that given by Whiteman (1971) who stated that most of the structural trends in Southern Sudan vary from 160° to 180°, i.e., NNW-SSE to N-S .

The sediment distribution in the sedimentary basin extending from Juba in the south to Nuba mountains in the north, and apparently starting with Yirol Formation and the intervening basement ridges (Fig. 6, 7) are controlled by structural lineaments. These sediments act as aquifers and aquicludes to groundwater seeping into the ground from riverine and rainfall sources. Basement ridges and basement configuration under the sedimentary cover control the aquifers both regionally and locally. It is thus demonstrated that the distribution of surface water which influences greatly the environment and the groundwater aquifers in the studied area is largely controlled by its geological and tectonic history as revealed emphatically from satellite imagery interpretation.

At the same time the execution of Jonglei Canal would consider the encountered structural lineaments and geological units in its path. The structure is generally quiet in this part of the area, however, additional detailed studies are required in the vicinity of the projected canal.

REFERENCES

HURST, C. M. G., et al. (1932 - present) The Nile Basin Series. Government Press, Caire, Egypt.

VAIL, J. R., Compiler (1974) Geological Map 1:2,000,000, South Sheet, The Democratic Republic of the Sudan and Adjacent Areas. Directorate of Overseas Surveys, London, U.K.

WHITEMAN, A. J. (1971) The Geology of the Sudan Republic. Clarendon Press, Oxford, U.K.

FIGURES: 1, 2, 3, 4, 5, 6, 7.

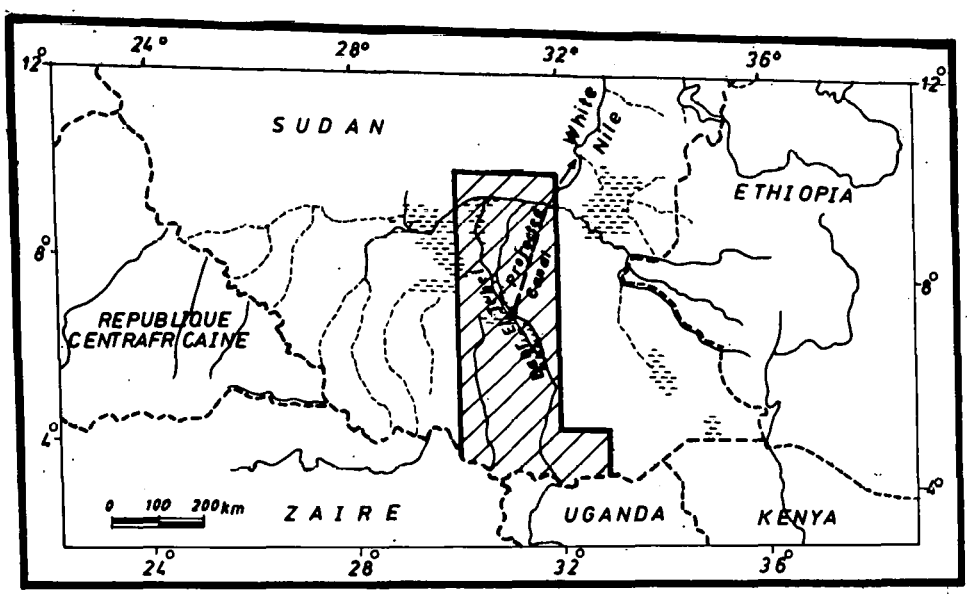

FIGURE 1. INDEX MAP SHOWING LOCATION OF JONGLEI CANAL AREA, SOUTHERN SUDAN, INVESTIGATED BY LANDSAT-1 IMAGERY INTERPRETATION.

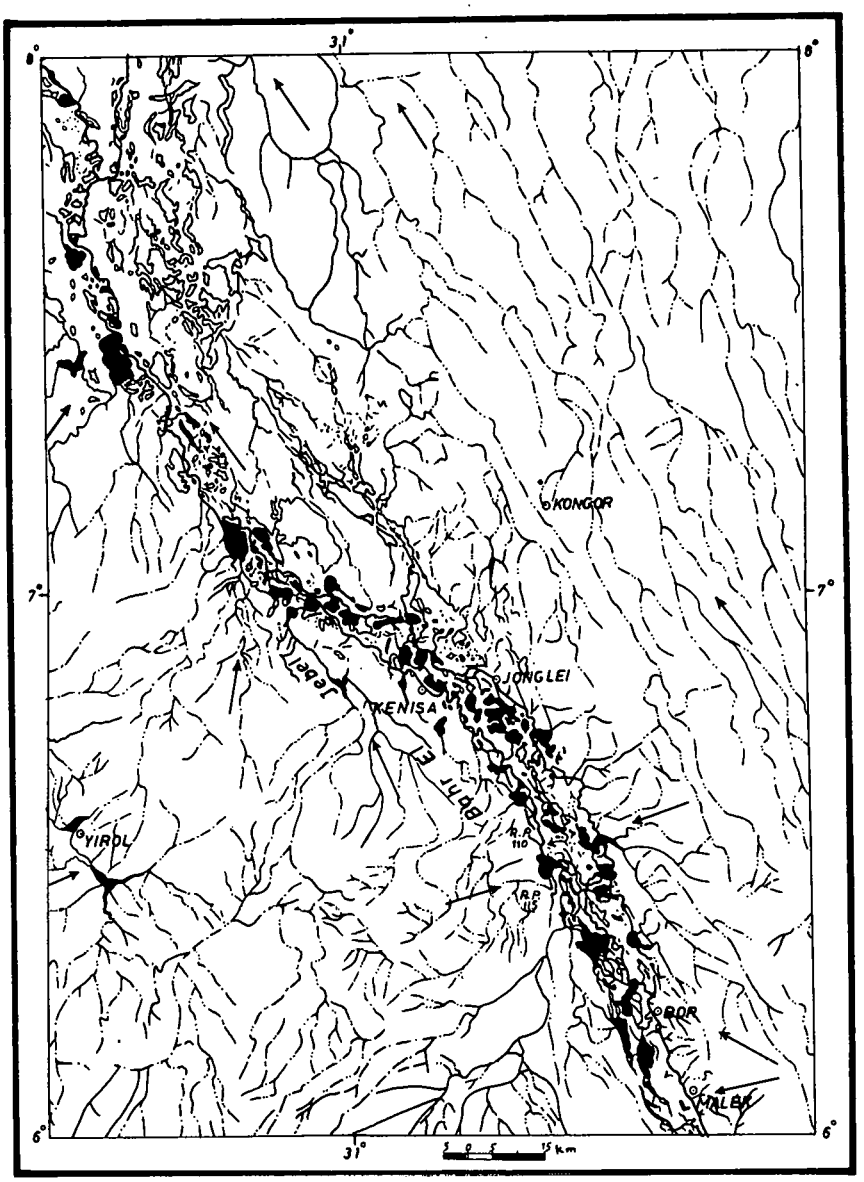

FIGURE 2. DRAINAGE MAP OF THE CENTRAL PART OF JONGLEI CANAL AREA BASED ON LANDSAT-1 IMAGERY INTER-PRETATION IN THE DRY SEASON.

- Lakes and Water Ponds
- Shallow Water Bodies
- Main River Course
- Main Drainage Lines
- Minor Drainage Lines
- Direction of Water Flow
- Cities and Towns
- Settlements and Small Towns
- Missionaries
- R.P 115 Reference Point

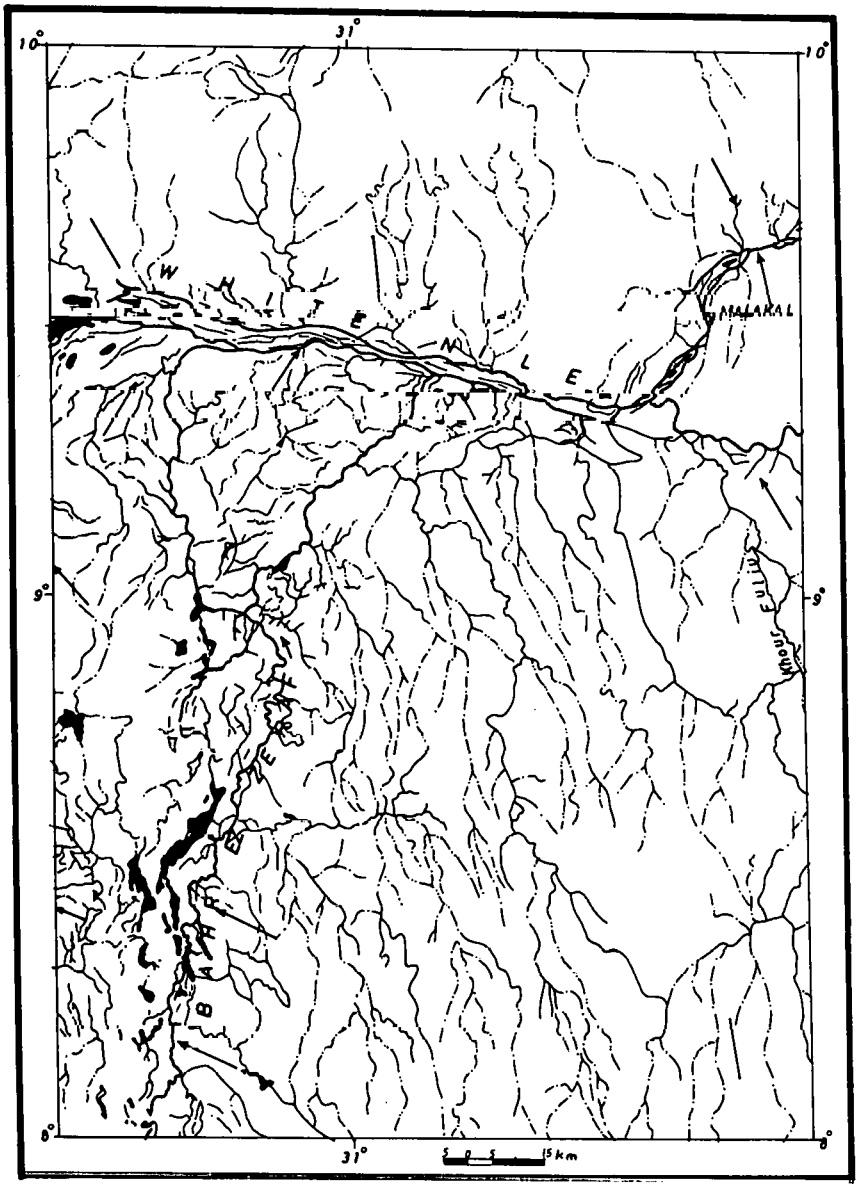

FIGURE 3. DRAINAGE MAP OF THE NORTHERN PART OF JONGLEI CANAL AREA BASED ON LANDSAT-1 IMAGERY INTER-PRETATION IN THE DRY SEASON.

- Lakes and Water Ponds
- Shallow Water Bodies
- Main River Course
- Main Drainage Lines
- Minor Drainage Lines
- Direction of Water Flow
- Cities and Towns
- Settlements and Small Towns
- Missionaries
- R.P 115 Reference Point

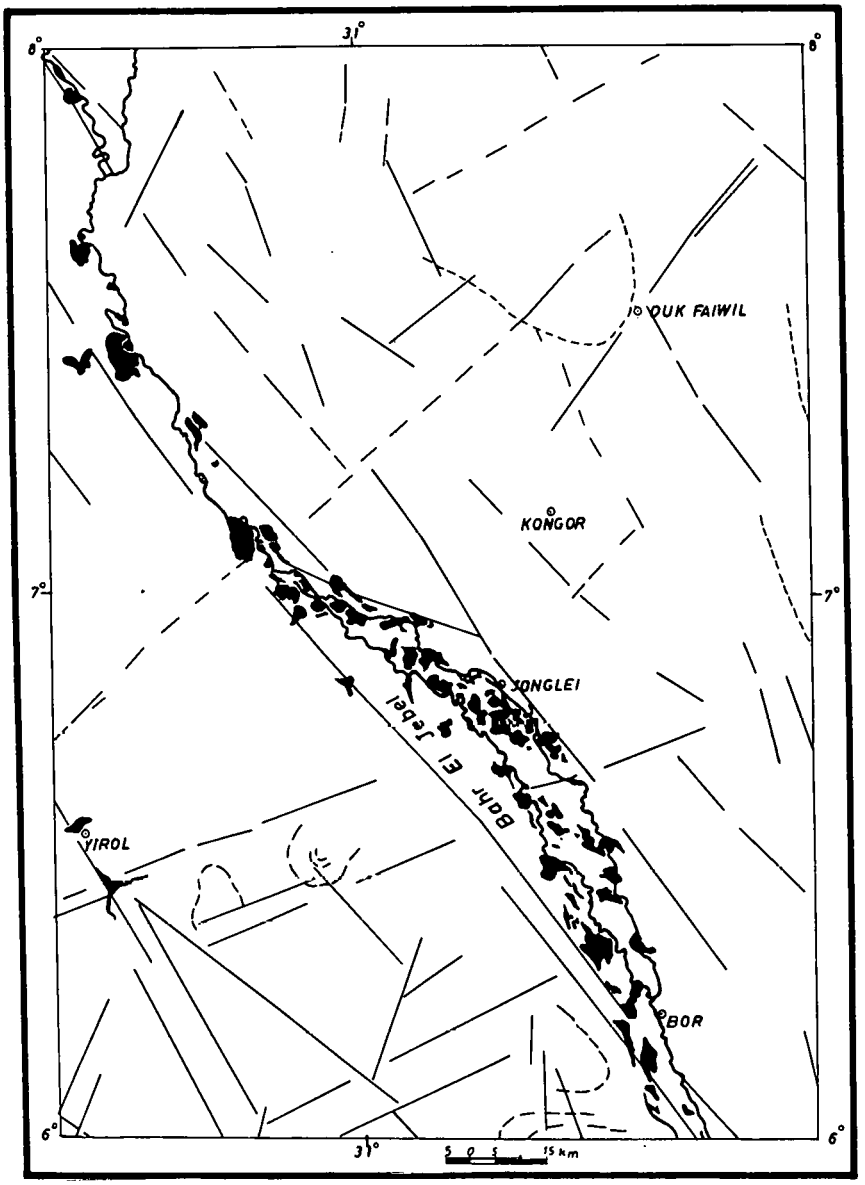

FIGURE 4. STRUCTURAL LINEATION MAP OF THE CENTRAL PART OF JONGLEI CANAL AREA BASED ON LANDSAT-1 IMAGERY INTERPRETATION.

- Lakes and Water Ponds.
- Fractures Including Faults
- Fold Traces
- Settlements and Small Towns

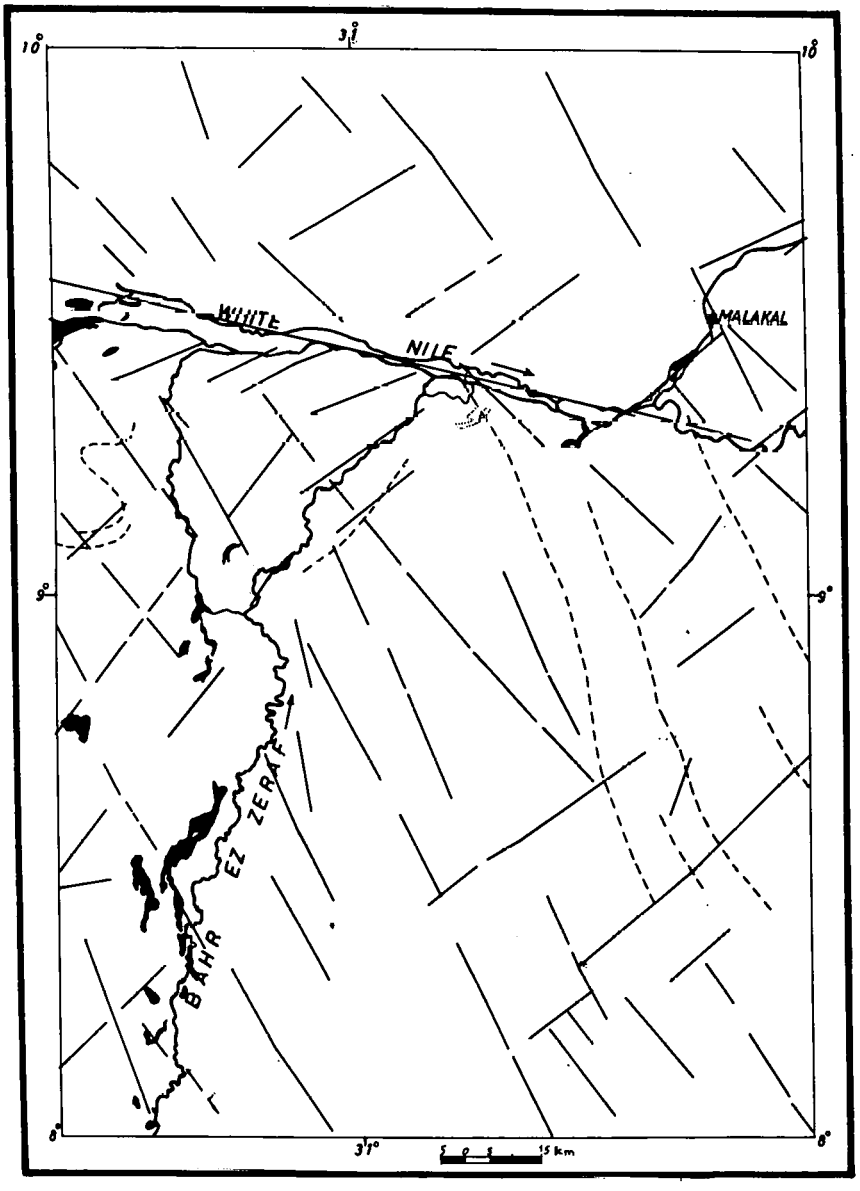

FIGURE 5. STRUCTURAL LINEATION MAP OF THE NORTHERN PART OF JONGLEI CANAL AREA BASED ON LANDSAT - 1 IMAGERY INTERPRETATION.

- Lakes and Water Ponds
- Fractures Including Faults
- Fold Traces
- Foliation and/or Bedding Traces In Granitoids
- Cities and Towns

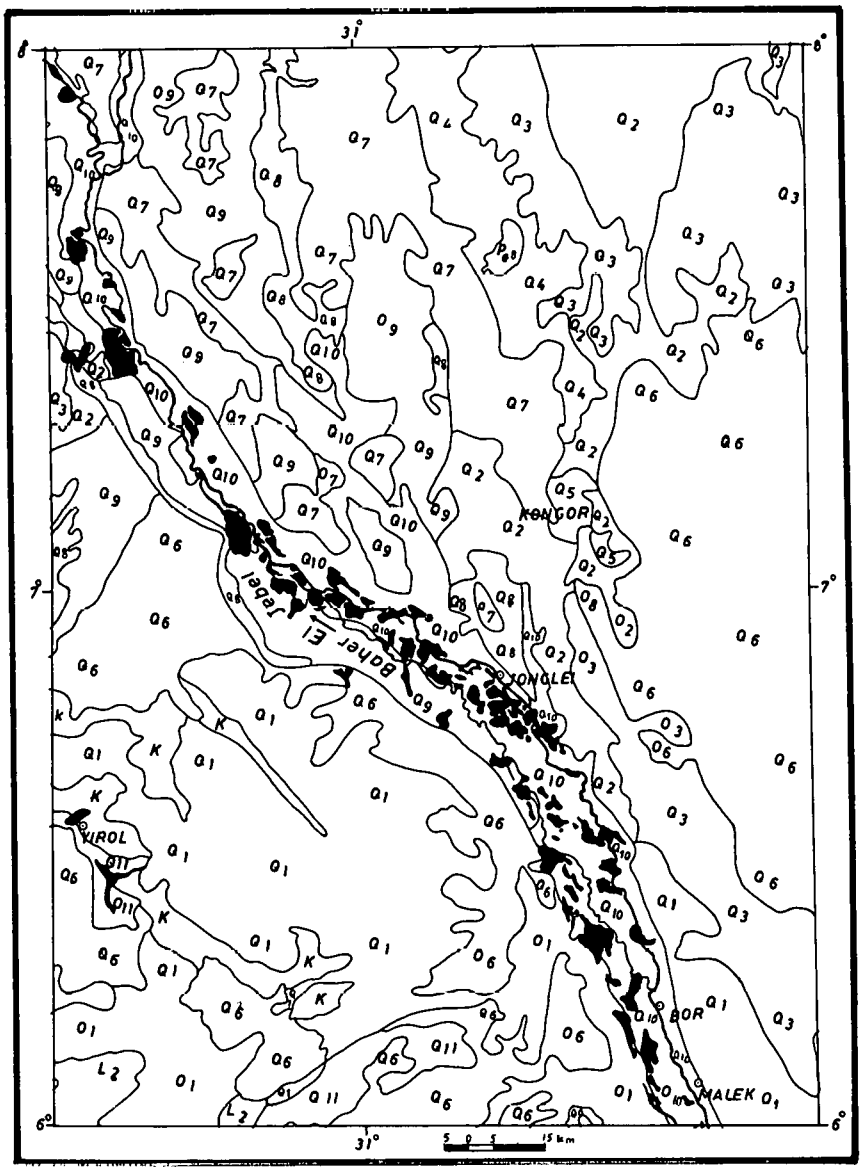

FIGURE 6. MAP OF GEOLOGICAL AND ENVIRONMENTAL UNITS IN THE CENTRAL PART OF JONGLEI CANAL AREA BASED ON LANDSAT-1 IMAGERY INTERPRETATION AND FIELD INVESTIGATIONS.

- Q11 Wadis. Filled With Relatively Coarse Alluvium, Draining Mainly Basement
- Q10 Soil, Perennially Flooded Under Deeper Water
- Q9 Soil, Perennially Flooded Under Relatively Shallow Water
- Q8 Soil, Flooded In Wet Season, Under Deeper Water
- Q7 Soil, Flooded In Wet Season, Under Relatively Shallow Water
- Q6 Fine Clay
- Q5 Clay and Silty Clay
- Q4 Silt
- Q3 Sandy Clay
- Q2 Sand
- Q1 Coarse Sand and Gravel
- L Lateritic Exposures; Apparently Locally Transported
- K Yirol Formation
- Pe8 Granitoids

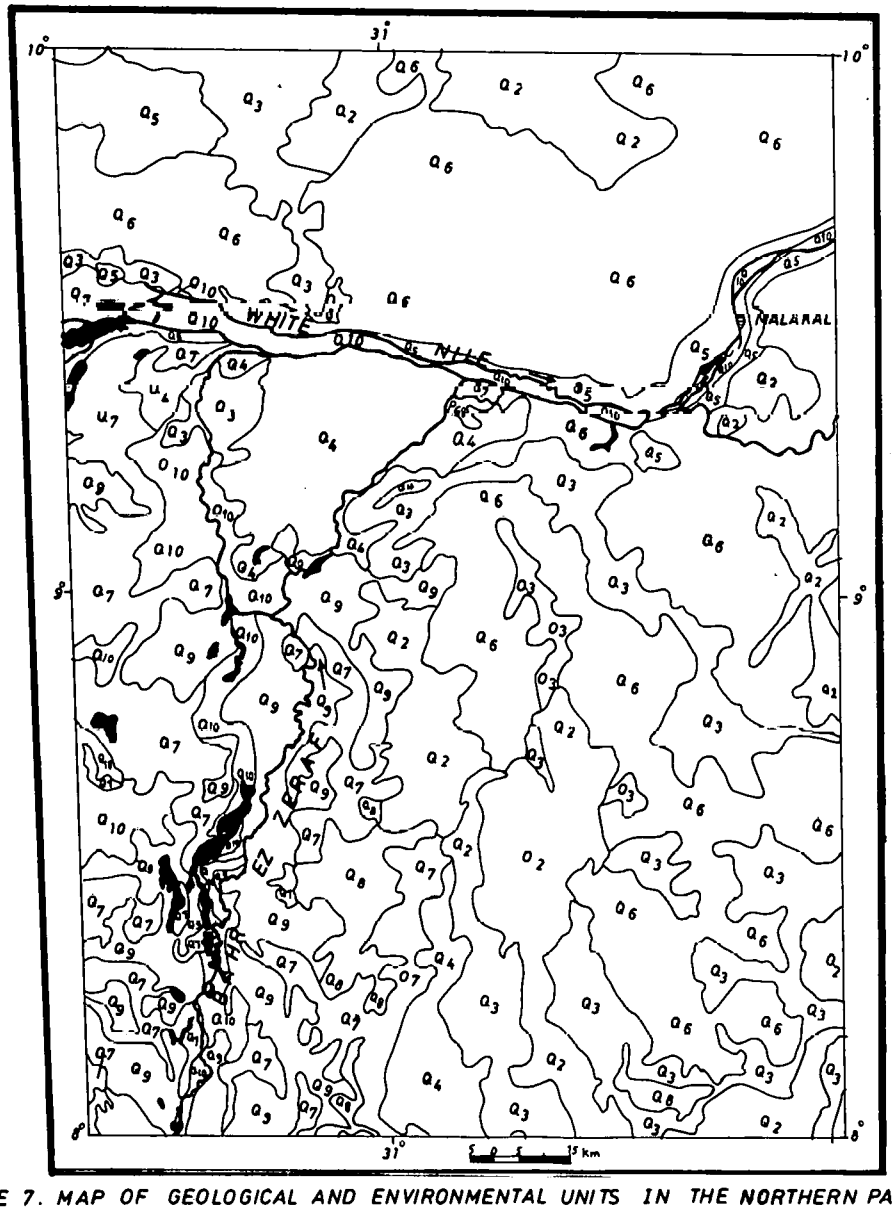

FIGURE 7. MAP OF GEOLOGICAL AND ENVIRONMENTAL UNITS IN THE NORTHERN PART OF JONGLEI CANAL AREA BASED ON LANDSAT-1 IMAGERY INTERPRETATION AND FIELD INVESTIGATIONS.

- Q10 Soil, Perennially Flooded Under Deeper Water
- Q9 Soil, Perennially Flooded Under Relatively Shallow Water
- Q8 Soil, Flooded In Wet Season, Under Deeper Water
- Q7 Soil, Flooded In Wet Season, Under Relatively Shallow Water
- Q6 Fine Clay
- Q5 Clay and Silty Clay
- Q4 Silt
- Q3 Sandy Clay
- Q2 Sand
- Q1 Coarse Sand and Gravel
- PEB Granitoids

RING-DITCH FORTIFICATIONS IN THE REWA DELTA, FIJI: ARCHAEOLOGY FROM THE AIR USING PANCHROMATIC, INFRARED, AND COLOR PHOTOGRAPHY

Dr. J. T. Parry

Department of Geography, McGill University
Montreal, Quebec, Canada

Fijian fortifications have received some attention in the archaeological and historical literature, but there are few detailed, regional studies. The first scholarly treatment was provided by Elsdon Best, a New Zealand ethnologist, who treated Fijian fortifications in the concluding chapter of his monograph on Maori villages (Best, 1927). During the next forty years little archaeological work was undertaken in Fiji, and there is only one relevant publication - a monograph dealing with the megalithic culture of Melanesia (Riesenfeld, 1950), in which there is a discussion of the origins and characteristics of Fijian fortifications. The New Zealand Archaeological Association organised a conference on fortifications in the south Pacific in 1967, and this seems to have stimulated considerable interest in the problems of cultural diffusion, particularly in relation to methods of fortification and warfare (Green, 1967). However, it was not until two years later that the first field study of Fijian fortifications was published (Palmer, 1969). This was particularly valuable because it provided a classification of fortification types. In addition, it demonstrated the value of air photo interpretation as a research method in this type of investigation, and pointed up the need for detailed regional investigations. So far only two studies of this type have been attempted, a monograph dealing with fortified sites on Taveuni (Frost, 1974), and a monograph dealing with ring-ditch fortifications in the Rewa delta (Parry, 1978). The weapons and tactics of Fijian warfare have been examined in an excellent recent study by Clunie (1977), which contributes greatly to the understanding of the role and function of defensive fortifications.

Although archaeological research in Fiji has been somewhat limited, the evidence suggests that fortified sites occur throughout the group, with the greatest concentration in the deltas and alluvial flats on the eastern or windward side of the islands. During the nineteenth century, the Rewa delta was one of the most densely populated areas in Fiji, indeed in the whole south Pacific region. It was noted for the extent of its cultivated land and for its fertility, renewed at frequent intervals, by the spread of silt-laden waters from the Rewa and its distributary channels. The area was also noted for almost continuous local warfare in which "crop lands were laid waste, villages were left in smouldering ruins, and the common people were butchered wholesale" (Derrick, 1950). Settlements of this period display the characteristic ring-ditch type of fortification, which served as a crude but effective defence against surprise attack. In its simplest form, this consisted of an outer bank and a roughly circular ditch or moat enclosing a fenced habitation area, which was reached by causeways.

Ring-ditch settlements are now largely abandoned as a result of the peaceful conditions following cession of the islands to Britain, and the dramatic decline in population due to the epidemic diseases of the late nineteenth century. The traces of former occupance are very difficult to identify in the field because of the rapid regeneration of swamp forest, and in certain areas, the superposition of plantation agriculture. Fortunately for the archeologist, all disturbances of the ground leave their mark in one form or another, sometimes in subtle configurations of the micro-relief, more often in textural variations of the vegetation canopy, or anomalies in the soil composition and moisture regime which are transmuted in the pattern of crop growth. Such indicators are difficult to detect on the ground, but from the air they are often revealed with startling clarity, the regular geometric outlines of man-made features showing through the irregular textures of the natural cover. With careful interpretation, it is possible to rediscover the past and to discern the salient features of settlement and cultivation patterns that have been superimposed by later features and remain only as vestiges in the landscape palimpsest.

THE REWA DELTA IN THE 18TH AND 19TH CENTURIES

The Rewa delta occupies an area of approximately 250 square kilometres in south-eastern Viti Levu, and geologically it is very recent. Alluvial deposits provide a relatively thin veneer overlying sandy marine sediments, which form the floor of the delta. The inner margin of the delta is marked by an abrupt break of slope representing a former coastline cut in relatively weak volcanic marls and tuffs.

In the delta, a fairly typical set of landforms has developed comprising levees, delta-bar fingers, backswamps, beach ridges, and mangrove swamps. The first task in the investigation was the preparation of a landform map of the delta using medium scale panchromatic photography. Major changes in the delta environment during the last two centuries became apparent as the mapping progressed. Sudden shifts in the pattern of distributary channels due to flood breaching of the levees was demonstrated, and the channel pattern at three specific dates in the 18th and 19th centuries was established by combining the historical evidence from contemporary journals with the evidence derived from air photo interpretation using soil and vegetation indicators.

Delta environments are essentially low-lying. The highest parts of the Rewa delta are no more than 6.5 metres above mean sea level, and the water table is close to the surface throughout the area. During dry periods it stands at depths of 2 to 4 metres in the levee zones, between 0.5 and 1.5 metres in the levee backslopes and higher backswamp areas, and in the low backswamp and coastal marsh it is within 0.3 metres of the surface. As indicated in Fig. 1 there is a close relationship between landforms, soils, and drainage conditions. Settlement sites are obviously severely limited by these conditions, the only habitable zones being the levees, abandoned levees, and delta-bar fingers.

Although subject to flooding, the Rewa delta was formerly a very productive area for various types of aquatic and sub-aquatic taro - the edible aroids belonging to the family araceae. The most favoured crop in the 19th century was the giant swamp taro (Cyrtosperma chamissonis, Fijian via kana), which had the great advantage of being able to withstand injury resulting from natural hazards such as flood and storm that would seriously damage other crops. Many parts of the delta are not suited to the production of via kana, and by a process of trial and error the better soils came to be known by the early cultivators. The soil series, their textural characteristics, and their limitations for via cultivation are indicated in Fig. 2.

The pattern of suitability for via cultivation that emerges from an examination of the soil characteristics is very similar to the pattern of site control on settlement. The better drained alluvial soils of the levees and backslopes offered the best settlement sites and because of the higher content of soluble base elements and nutrients these soils were also more suitable for via gardens than the gley and coastal saline soils. However, the alluvial soils are relatively restricted and so many communities were forced to make use of unfavourable soils.

RING-DITCH FORTIFICATIONS AND THEIR INTERPRETATION ON AIR PHOTOS

One of the prime concerns of Fijian communities until the mid-nineteenth century was protection from surprise attack. The majority of village sites appear to have been selected with an eye to defence, and in the Rewa delta, very considerable effort was expended in constructing defensive moats or ring-ditches with earth banks around the perimeter. Calculations indicate that between 7,000 and 10,000 cubic metres of material was moved in excavating a typical ring-ditch.

In its basic form, the ring-ditch fortification consisted of a roughly circular earth bank and a water-filled ditch, enclosing a fenced habitation area. Access was by means of causeways, generally four in number, and more or less equally spaced in a quadriform pattern, leading to gateways in the fence. Fortunately there are several contemporary descriptions of ring-ditch fortifications in the 19th century literature, and when considered together they provide a fairly comprehensive account. Even more valuable is a painting based on the field sketch of J. Glen Wilson, an artist attached to the scientific staff of H.M.S. Herald engaged in hydrographic work in the south Pacific in 1855-6. An enlargement of part of the painting is shown in Fig. 3.

The fences and gates of ring-ditch sites have long since disintegrated, but the ditches, banks and causeways are relatively substantial features and their presence can be detected even when overgrown by swamp forest. The sites are revealed in different ways on air photos, and it is part of the interpreters task to recognise the various indicators, such as surface microrelief, shadows and tonal anomalies resulting from differences in illumination, vegetation and crop marks resulting from differential growth or species clustering, and anomalous patterns of soil moisture or standing water. The air photo image types encountered in this study are illustrated in Fig. 4; some are well known in the literature of aerial archaeology, others are encountered less frequently.

The air photo analysis commenced with examination of medium scale photography which was available for the greater part of the area. Large scale panchromatic and modified infrared photography was available for only limited areas; however, this was especially useful for a detailed examination of several major sites. Color obliques were obtained for most of the major sites, and these proved to be particularly valuable in detecting small details.

Provisional scanning of each set of photos with a hand magnifier was followed by stereoscopic examination with an ODSS II. As each ring-ditch site was detected, it was plotted directly onto a 1:50,000 topographic map. Four aspects of the morphology of each site were examined - shape, size of habitation area, number of ditches, number of causeways and their orientation. Size measurements were made with a circle templet, and causeway orientation was recorded using a magnifying comparator. The soil type and site conditions were assessed from the photo tone and texture characteristics. The data for each site was codified using an alphanumeric / symbol classification system as illustrated in Fig. 5.

As the analysis progressed, it became apparent that some of the air photo contrast marks by their very nature must represent older sites, whereas, other forms indicated relatively recent abandonment. An attempt was made to establish the relative age relationships as indicated in Fig. 6. It was established from historical sources that several sites which now exhibit positive:negative relief marks or negative vegetation marks were occupied in the mid-19th century, but deserted by the time of the earliest surveys of native lands at the close of the century. Thus, the probable date of abandonment was in the 1870's or 80's. The next stratum of air photo contrast marks represents abandonment at an earlier stage because the relief is subdued and the vegetation more completely regenerated. The probable date of abandonment of these sites was the late 18th century. The most indistinct air photo traces (shadow and tonal contrast differences and crop marks) represent sites occupied during the 17th century, and probably abandoned during the early 18th century.

THE SETTLEMENT PATTERN IN THE 19TH CENTURY

The air photo is a very effective tool in analysing distribution patterns and making an inventory of discrete features such as ring-ditch sites. In addition, the aerial perspective allows the researcher to integrate all of the site factors in seeking an explanation of the raison d'être for a particular settlement.

A total of 605 ring-ditch sites was identified, and a close correspondence between site conditions and settlement density was established. The preferred sites included the higher beach ridges of the strand zone, the seaward margin of the marine terrace bordering the inner margin of the delta, 'swamp island' sites on outliers of volcanic tuffs standing above the delta surface, the delta-bar fingers, and the present and former levees. The relative frequency of occurrence of ring-ditch settlements according to site type is illustrated in histogram form in Fig. 7. In the central part of the delta 32% of the sites occur on present or former levees, 33% on delta bars, 23% on levee backslopes, and only 11% in backswamp and mangrove environments.

THE MORPHOLOGY OF RING-DITCH SETTLEMENTS

The basic shape of the ring-ditch fortifications in the Rewa delta is annular; however, two other fortification types were encountered - the ring-square and the polygonal form. The annular ring-ditch is the most common: 94% of the sites identified were enclosed by circular ditches and only 4% by ring-square forms. Polygonal fortifications, with a series of rectilinear banks and ditches intersecting at obtuse angles, accounted for only 2% of the total. However, these settlements are large with multiple ditches and offset maze type causeways. It is possible that the polygonal fortification type is a variant of the ring-square representing an adaptation of the basic form to suit site conditions.

The mean size of the fortified sites was found to be 0.3 hectares, which reflects the socio-economic structure of Fijian society in the 18th and 19th centuries with relatively small kin groups - tokatoka and mataqali - organised in loose federations with obligations of service and tribute (Fig. 11). The very large fortified sites with habitation areas of between 1.5 and 4.5 hectares were either local centres or the settlements of the bati mataqali, whose function was to provide warriors in time of war.

The smaller and medium sized settlements (91% of the total) were protected by a single ditch, and the causeways exhibit a simple quadriform pattern. The larger settlements often had elaborate fortifications with double ditches, and 22 settlements (3% of the total) were found with between three and five ditches. In these sites, the causeways do not lead directly to the habitation area, but are offset either to left or right after crossing each ditch (Fig. 8). This type, which has been termed the offset maze, would cause considerable confusion to an attacking force by dispersing the disorienting the warriors.

THE AGRICULTURAL ECOSYSTEM AND THE POPULATION DENSITY

The swamps of the Rewa delta presented one of the most difficult agricultural environments of the south Pacific, yet a highly specialized agricultural ecosystem based on the giant swamp tara (Fijian, via kana) was developed. Via gardens were prepared by creating a semi-permanent arrangement of small plots, separated and partly surrounded by ditches (Fig. 9). The gardens are now abandoned and overgrown, but the traces are discernible from the air. Two types of garden systems were recognised in the air photo analysis - the reticulated and the grid-iron (Fig. 10). The distribution of former gardens was mapped, and the total area is estimated at 5,200 hectares, with 92% classified as reticulated and 8% as grid iron.

In the nomenclature of Denevan and Turner (1974), the via garden is considered as a type of raised or ridged field. Improved drainage results from the banking and ditching process, and the material dug from the ditches and spread on the garden plots helps to maintain their fertility by supplying minerals and organic matter. In addition, the soil structure is improved, allowing easier root penetration and better aeration. The via garden is a highly specialised ecosystem: a sophisticated way of utilising an environment subject to flooding, and one requiring a high degree of social organisation and work force coordination. Considerable effort was required in the creation of the gardens and also in their maintenance. However, this was rewarded with high returns, because the system allowed semi-continuous use of the gardens with long cultivation periods separated by short fallows.

One of the most difficult problems facing the archaeologist is that of estimating the population of a prehistoric culture. Even more fundamental is the problem of the interrelationship between population and food production. This is particularly significant in the Rewa delta, because it is clear that intensive agriculture supported a dense population, thus raising the question as to whether the agricultural system was responsible for the demographic situation or conversely, whether the large population had necessitated intensive agricultural practices.

Air photo analysis adds a new dimension because it provides a reasonably accurate indication of the number and size of settlements in the area. It is apparent that if a specific population figure could be assigned to a particular settlement in each of the size classes in the histogram (Fig. 11) then the data could be used to derive the total population for the area as a whole. Careful search of the ethnohistorical literature provided population estimates for several ring-ditch sites which could be positively identified in the field. These sites allowed the construction of a kind of population rating curve as shown in the lower section of the histogram. Using the curve, it can be estimated that a ring-ditch settlement in size class 10, for example, would have a population of approximately 300. Making due allowance

for the fact that the sites were not all synchronous it is possible to extrapolate population figures for the Rewa delta as a whole. In the early to mid 19th century it is estimated that the total population was between 35,000 and 40,000. The population density for the delta as a whole would have been approximately 150 per square km. and if one considers only the cultivated garden areas, the effective population density was approximately 730 per square km. Such a density would have put a very heavy demand on agriculture, necessitating intensification: the adoption of successively more sophisticated practices with a resulting increase in productivity to meet the needs of an increasing population. The establishment and extension of via gardens into progressively more difficult backswamp areas provides the evidence for population pressure and agricultural intensification in the Rewa delta.

Perhaps the most important contribution of this study is the addition of another case history to the increasing body of evidence supporting the view that in many parts of the humid tropics, forest and swamp were able to sustain a very dense population. It also demonstrates the potential for air photo interpretation methods in treating some of the problems in tropical archaeology.

REFERENCES

Best, E. 1927. The Pa Maori, Bulletin no. 6, New Zealand Dominion Museum.

Clunie, F. 1977. Fijian weapons and warfare, Bulletin no. 2, Fiji Museum.

Denevan, W.M. and B.L. Turner, 1974. "Forms, functions and associations of raised fields in the old world tropics", Jour. of Tropical Geog. Vol. 39, pp. 24-33.

Derrick, R.A. 1950. A history of Fiji, Govt. Press, Fiji.

Frost, E.L. 1974. Archaeological excavations of fortified sites on Taveuni, Asian and Pacific Archaeology Series, no. 6, Univ. of Hawaii.

Green, R. 1967. "Fortifications in other parts of tropical Polynesia," Newsletter, New Zealand Archaeol. Assoc., Vol. 10, no. 3, pp. 96-113.

Palmer, J.B. 1969. "Ring-ditch fortifications on windward Viti Levu," Archaeology and Phys. Anthropology in Oceania, Vol. 4, no. 3, pp. 181-197.

Parry, J.T. 1978. Ring-ditch fortifications in the Rewa delta, Fiji: air photo interpretation and analysis, Bulletin no. 3, Fiji Museum.

Riesenfeld, A. 1950. The Megalithic culture of Melanesia, E.J. Brill, Leiden.

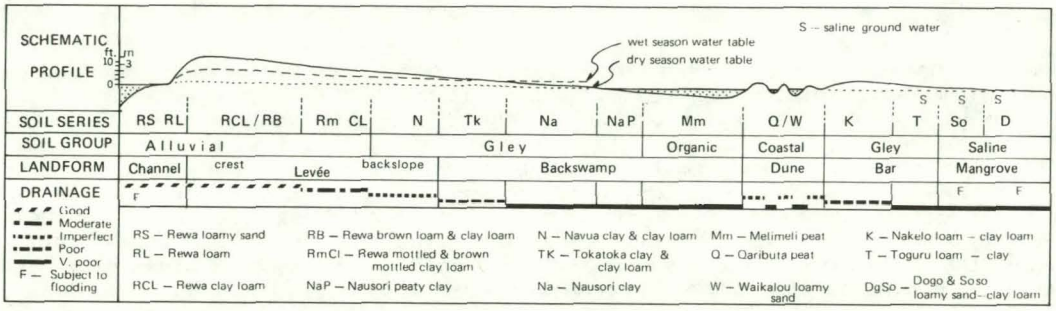

Fig. 1. Schematic profile illustrating the relationship between landform, soil type, water table and drainage in the Rewa delta.

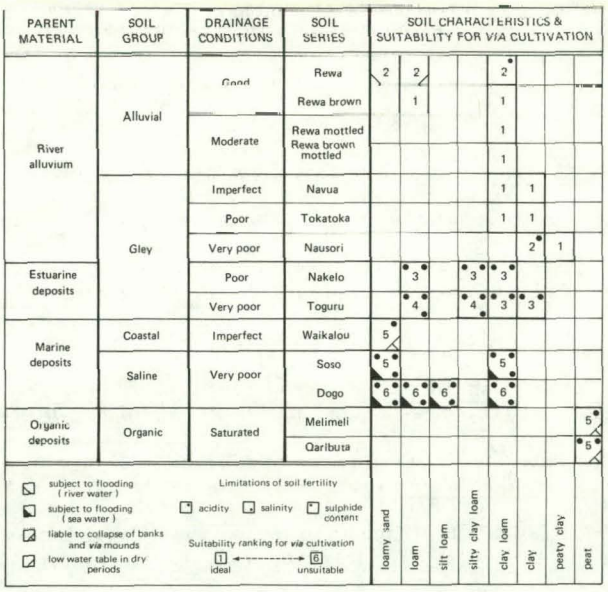

Fig. 2. Soils of the Rewa delta and their suitability for via cultivation.

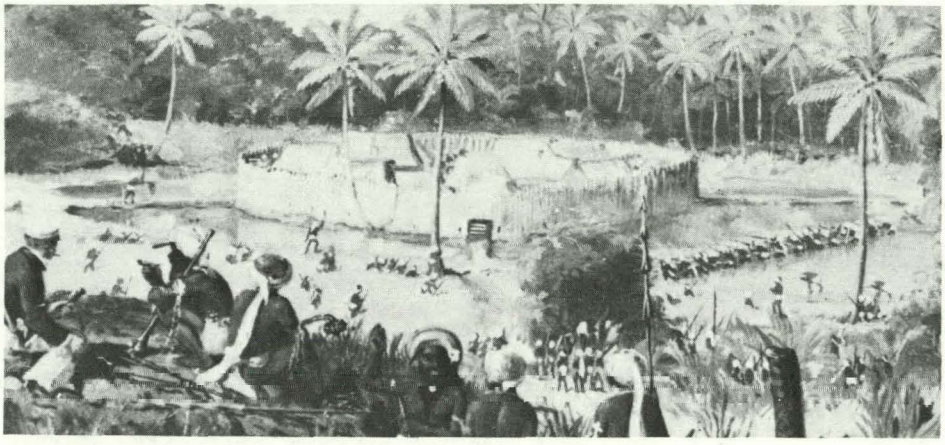

Fig. 3. The ring-ditch fortification at Vewara, Nadi Bay, Vanua Levu, from the painting by J. Glen Wilson, 1856.

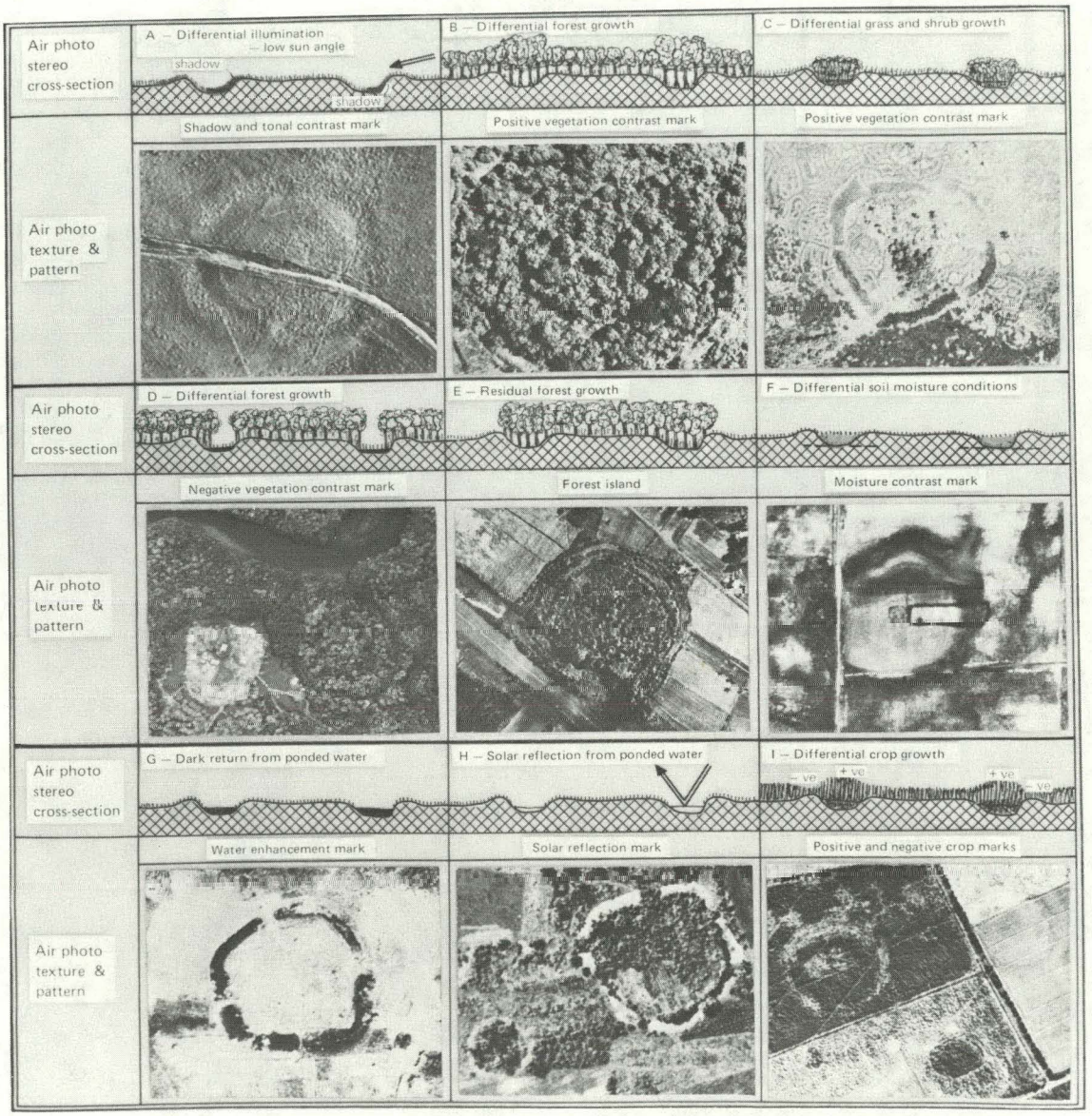

Fig. 4. Illustrative key to air photo image types of ring-ditch fortifications.

Air Photo Ref. No. & Quadrat	Air Photo Image Type	Size	No. of Ditches	Causeways No.	Causeways Orientation	Site Type & Soil Characteristics		Contemporary Place-name	Additional Notes
71/1 29 SE	A4(c)	16	1	4	0, 120, 210, 275	Ó	4 scl	Vunuku	S. Limit of via gardens, edge of mangrove

Fig. 5. Sample extract illustrating the layout of the air photo interpretation data sheet.

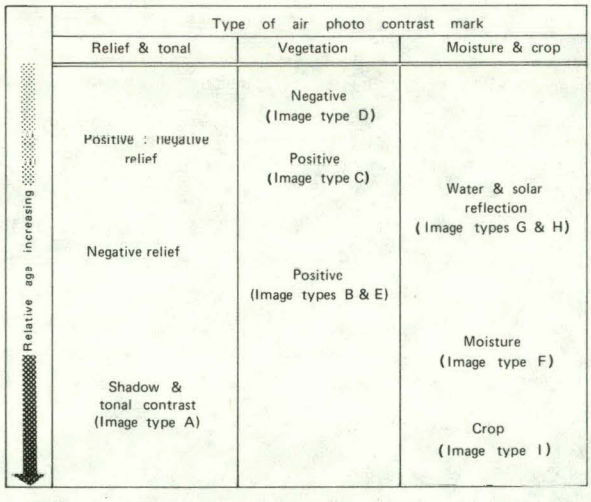

Fig. 6. Probable age relationships of the various types of air photo contrast marks.

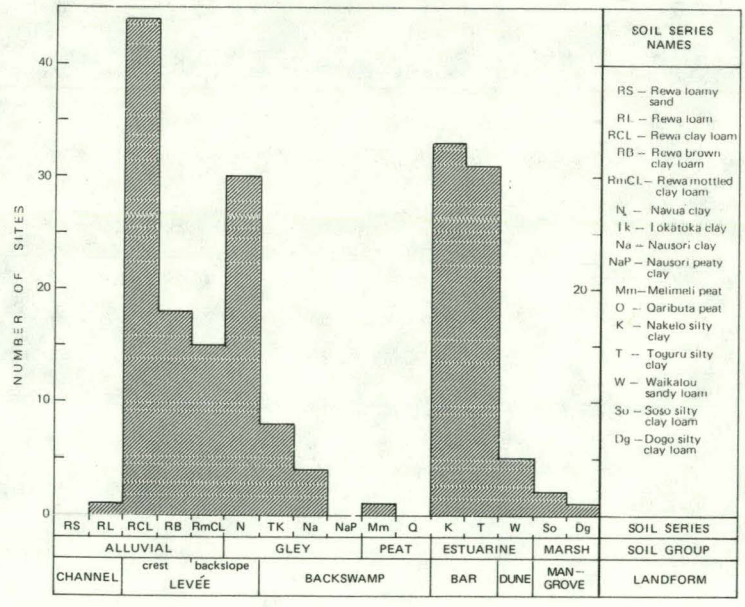

Fig. 7. Frequency of occurrence of ring-ditch sites according to landform and soil type in the central section of the Rewa delta.

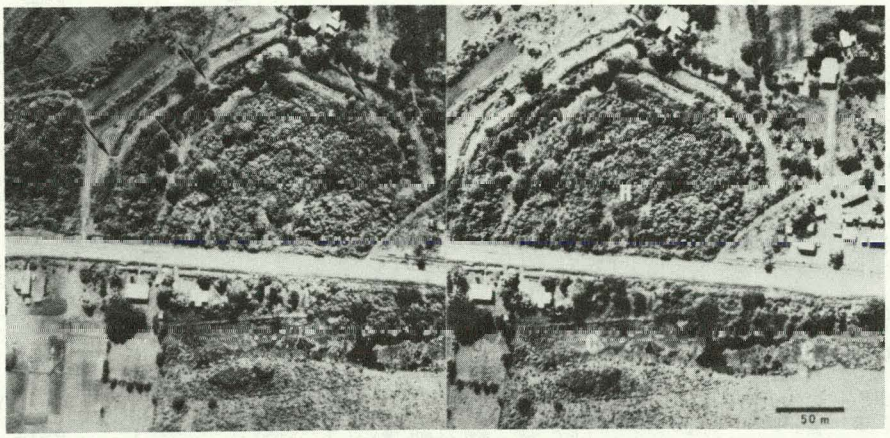

Fig. 8. Stereogram of the offset maze type causeways and multi ditch polygonal fortifications at Nadali.

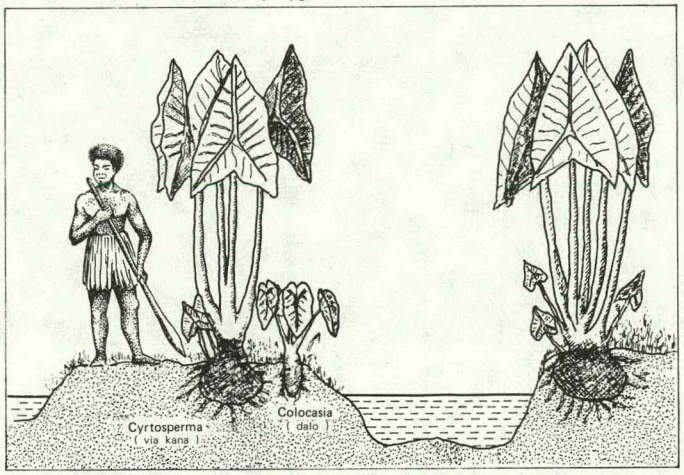

Fig. 9. Schematic cross section of part of a via garden.

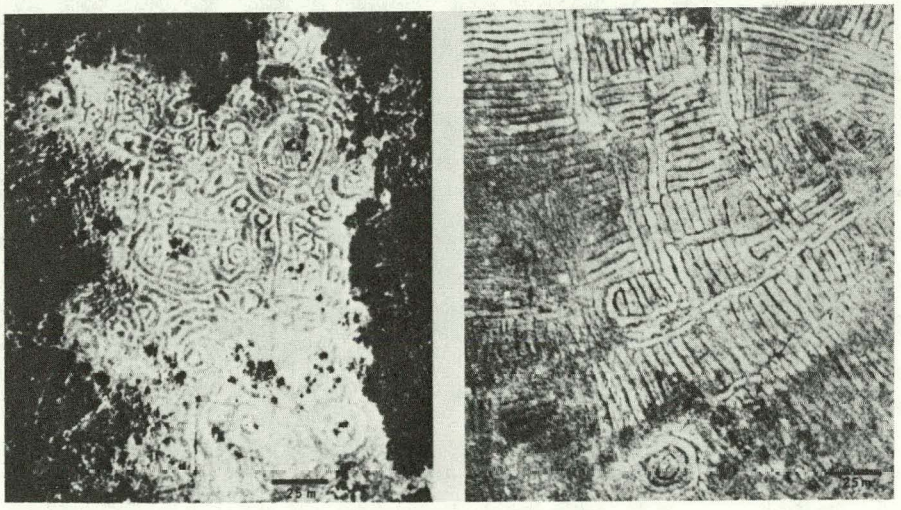

A. Reticulated via gardens belonging to Nabouciwa village on Sawai island.

B. Grid-iron via gardens in the Mokani backswamp.

Fig. 10.

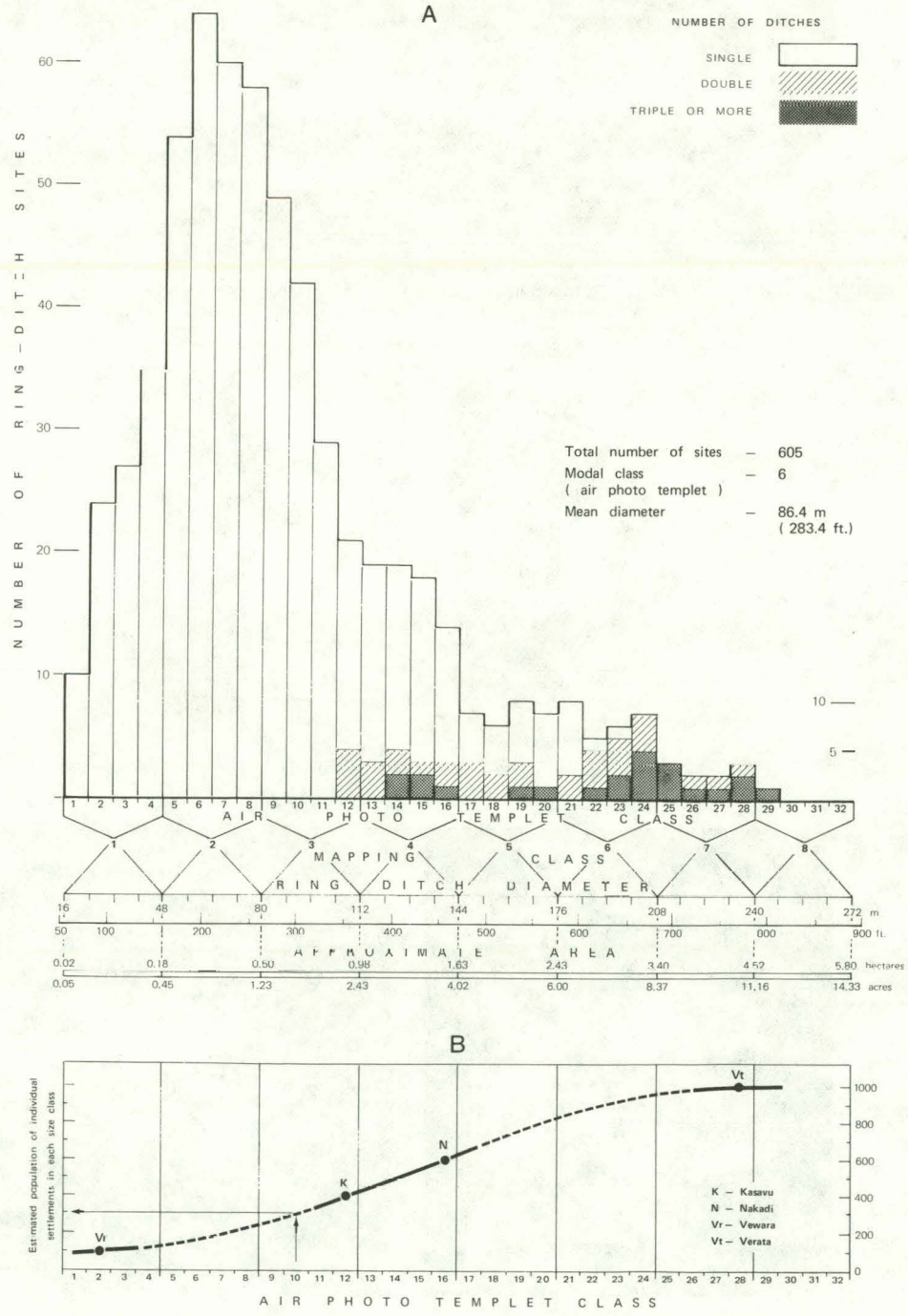

Fig. 11. Frequency distribution histogram showing sizes and numbers of ditches for ring-ditch settlements in the study area and an estimated population rating curve.

ADVANCE IN THE RESEARCH AND USE OF REMOTE SENSORS IN NATURAL RESOURCES DEVELOPMENT STUDIES - CHILE

ARNOLDO ORTIZ - GEOLOGIST

NATURAL RESOURCES RESEARCH INSTITUTE - IREN/CORFO
SANTIAGO, CHILE

SUMMARY

The Natural Resources Research Institute (IREN) an official organism was created in 1964 as an specialized institute whose aim are tho natural resources integrated studies. IREN has based its research on the utilization of remote sensors.

In 1973 the use of aerial multiband images was initiated as an analitical way of use to detect some aspects of soils, water and plants in an utmost agricultural region, with highly satisfactory results, so its use was adopted for special agricultural studies.

In 1975 IREN established a program of evaluation of the use of LANDSAT images in natural resources integrated studies related to geology, geomorphology, hidrology, soils and vegetation. It was considered an area in the southern part of Chile where IREN had enough regional information to do this evaluation. The results were optimum and the LANDSAT images were considered as a useful research instrument.

Through experience obtained in 1975 a new program was established for the use of LANDSAT images in the survey of natural resources in the northern part of Chile. The purposes of the program were : provide cartographic data at a regional level in, geology-mining, geomorphology, soils, climate and hidrology previously to a human resource evaluation, so to define development feasibility programs at a regional level; and, establish satellite images as a normal research tool.

The photographic material was :
22 black-white images; bands 4, 5, 6 and 7 scale 1:500.000
22 false color composite images scale 1:1.000.000 and 1:250.000
22 transparent positive images; bands 4, 5, 6 and 7 scale 1:3.360.000 used in the multiespectral viewer.

The following methology was applied :
- LANDSAT images analysis, in different wavelength bands and scales.
- LANDSAT false colour images interpretation, through the multiespectral viewer.
- Descriptive legends generated by data obtained from the images.
- Location of field areas as recognition patterns for the different studies.
- Field-checking to evaluate sample sites, descriptive legends and image interpretation.
- Final cabinet for definitive cartography.

The conclusions obtained with this new experience are developed in the following pages.

1. INTRODUCTION

The Natural Resources Research Institute (IREN) is an organism of the Chilean Government, whose aim are the natural resources integrated studies at national and regional levels with a view to promoting effective and sustained socio-economic development plans.

IREN was created in 1964 and, since then, the utilization of remote sensors has increased steadily introducing new techniques and tools of interpretation to know and evaluate CHILE's natural resources potential. In 1973, new experiences were initiated with aerial multiband images as an analytical means to detect some aspects of the soils, waters and plants in an agricultural sector of utmost importance due to its export fruit production.

The result of the experience led to highly satisfactory conclusions, and its use was adopted for special agricultural surveys.

In 1975, as a consequence of a program proposed by the Instituto Panamericano de Geografía e Historia (History and Geography Pan American Institute), an OAS's organ, IREN established a program for the evaluation of the use of LANDSAT satellite images in natural resources integrated studies, especially as regards geology, geomorphology, hydrology, soils and vegetation.

For this evaluation, an area was considered in the South of Chile whose ecological conditions are those of a cold humid area, in which IREN had enough regional information.

The results, from a regional point of view, and at a recognition scale, were optimum, thereof, it was considered as a useful research instrument to make surveys of the natural resources in the South of the country, where basic knowledge of the resources has not been detailed so far.

2. INVENTORY OF NATURAL RESOURCES THROUGH LANDSAT IMAGES IN THE NORTH DESERTIC AREAS OF CHILE.

With the experience obtained in 1975, an official program was established the following year for the use of LANDSAT images to make a survey of natural resources in the desertic region in the North of Chile between parallels 17° 45' and 25° 30' S meridians 68° 30' and 70° 30' W approximately.

The region under study covers an area of 211,812 Km^2, comprising what is considered America's most desertic zone.

- Main Objectives

To provide cartographic information of the natural resources in an integrated form, as a step prior to the evaluation of their interrelation or interdependence, both between themselves and in respect to other socio-economic aspects, to define development feasibility programs at a regional level.

To establish satellite images as a normal research tool as a means to develop new study techniques which will permit an advance in an ever increasing knowledge of the phisical resources, to allow the optimization of their use without degradation of the ecosystem.

3. ORGANIZATION

The program was carried out entirely by IREN's technicians, partially advised in the technical aspect by Michigan"s ERIM.

The studies carried out were the following : Geology-Mining; Geomorphology; soils and vegetation, apart from the surveys of services and infrastructures, population, hydrographical and weather characteristics, which

were carried out through statistical data.

The photographic material was :
22 black and white images in the bands 4, 5, 6 and 7; scales 1:500.000
22 false color composition images, bands, scales 1:1.000.000 and 1:250.000
22 transparent positive images, bands 4, 5, 6 and 7; scale 1:3.360.000 used in the multiespectral viewer.

4. METHODOLOGY

Evaluation of the existing descriptive information.

Analysis of LANDSAT images, selecting the bands which, in the specialist opinion were more useful in their research.

Analysis and interpretation of false color composition images by means of the multiespectral viewer according to each speciality.

Elaboration of descriptive legends from the data offered by the images.

Establishment of cartographic resources patterns for each resources.

Field checking to verify the samples and descriptive legends sites.

Drawing of subject charts with the corresponding final legends.

5. RESULTS

These will be analyzed according to each resources researched.

Geology-Mining

The proposed objective was to find evidence that structural controls of the earth's crust are at least partly related to the existence of mineral deposits.

To study this theory every surface feature was detected and charted through LANDSAT images resulting in an overlay of fractures which covers the whole region under study and also nearby areas.

The LANDSAT images turned out to be very useful due to their ortophoto characteristics. The sun's relatively low angle allowed to detect a great number of megalineaments which had not been previcusly spotted.

The fracture overlay was later used to determine the preferential directions and intersection or convergency degree of the detected lineaments.

The direction of the layers was determined in IO degree segments and at the same time their density was classified stablishing nodal values according to the number of layers that intercross or converge in five categories.

Finally nodal measurements of the same type were added to these measurements forming curves of nodal isodensity.

A second overlay was independently prepared with the already known ores and an overlay with regional geological information was later prepared.

These three overlays were finally superposed to detect the connection between mining and fractures and regional geology.

High category isodensity areas proved to have a greater concentration of mineral sectors besides having an ore selection to the effect that minerals such as copper, iron and manganese are controlled by NS fractures, while gold, lead, zinc and silver layers as main elements are controlled by E-W fractures which continue deeply to the east.

Extrapolating relations we have : geology-mining structure; I8 new areas in copper, manganese, iron, silver, lead, and zinc deposits were detected which have been recomended as most important for exploratory research studies.

In this task, LANDSAT images turned out to be of utmost importance due to the integrated regional vision, an easiness of interpretation, plus saving time and money.

We have learned through this experience that satellite images have opened a way to a vast field of geological studies and their derivations, which with the traditional methods would have required at least years.

Working with LANDSAT images, only six months were necessary reducing the detailed exploration to no more than 50.000 Km^2 which represents over 40% of the total area.

- Geomorphology

The geomorphological chart has two objectives.

- Final chart as information to make decisions in the stablishment of human settlements as well as an infrastructure and risk prevention.
- Support base chart for later service of soils, water and derivates.

For the region under study it was of utmost importance to count with a geomorphological chart showing the dynamics of the earth's forms as all them correspond to past shaping processes or paleoforms which at present are unbalanced due to the exogene prevailing conditions with the constant danger to the existing infrastructure and human elements.

The geomorphological interpretation was carried out based on two elements: the regional geology and the use of LANDSAT images.

In this study the satellite images abundantly provided the necessary data to stablish the correlations between the various individualized forms because of their integrating view of the regional scape and the detection of the agradation process affecting the regional dynamics.

Using basically black and white images at a scale of 1:500.000 it was possible to detect and chart over 30 earth forms within the big geographic mark which define the studied area.

Through color composition in the multiespectral viewer an analisis was made of the relations between the forms and the hydric, vegetation and the ecological processes, which permited a final definition of a homogeneous scapes key for the later definition of equipotential development areas on which it would be possible to establish integrated development projects.

- Vegetal Layer

Although the region is very poor in vegetal elements it is nevertheless necessary to count with chartographic information and nature as a direct means to stablish ecological zones which were later used for the descriptive report of the native shape of the region.

With some very fragmentary descriptive information the interpretation of LANDSAT images was carried out based fundamentally on multiespectral viewer color composition.

For this research, use was made of positives corresponding to two different dates : November and April. It was possible to establish the behaviour of vegetation before and after the dry season, in the East area, which has an indirect influence as far as the central part of the territory.

Through interpretative methods I2 vegetal forms were detected which were later field checked and subdivided in associations for a final chart at a

scale of 1:500.000.

Soils

Due to the harsh conditions of the area, the use of the soil is limited to small valleys, oases and the Eastern high plateau. Nevertheless studying soil resources at the regional level was deemed necessary, not only in case of a possible farm use, but also as basic information for a possible use of material classifield as non-metallic minerals.

The objective is to know the distribution, characteristics and general aptitude of the soils at a survey level, and this was based on existing fragmentary descriptive information, on geomorphological charts and analyses of LANDSAT images.

For the analyses, use was made of images in bands 4 and 5 of the electromagnetic spectrum; in these bands, units were differentiated through tonal variations of greys based on geomorphological information.

This method permitted the identification and charting of about 60 associations with areas of a minimun of 6.000 up to 300.000 hectares. Using 5 and 7 band images definition was obtained of hydric charactetistics and limiting elements of soil use such as stoniness, saltiness active eolian deposits which completed the information to characterize each mapped unit.

As a result from a complex visual analysis of images, soil checking and other direct or indirect data a synoptical chart of the region was made, showing all the mapped associations with their parental material characteristics, weather, vegetation topography, average height, limiting potential aptitude area of each association percentage in relation to the region's total area.

Through this method it has been possible to identify I5 soil associations which will possibly have farm use and which would, therefore be advisable to be thoroughly studied.

6. CONCLUSIONS OF THE USE OF LANDSAT IMAGES

- Extremely good results have been obtained as a research tool of natural resources at a survey level.

- The possibility to scan vast areas with an image allows the integrated research of physical resources and their interrelation and interdependance; this work the traditional methods of interpretation of low altitude air surveys result difficult and costly.

- Counting with images in band 4 of the electromagnetic spectrum notably widens the interpreting possibilities, permitting the comparison of phenomena observed in the Earth's crust in a bigger wavelength, making possible a more detailed interpretative method.

- Obtaining multiespectral viewer color composition images, or by Diazo process, is a highly useful means to define, based on the hihg refractancy degree, the vegetal and lithological types and the soils of the area under study.

- Because of the scale and resolution of the images, their use is limited to a survey level information, but, at the same time, allows the reduction of the more detailed studies to really important sectors, obviating the need to re-cover large zones.

- IREN will continue to encourage the use of remote sensors in natural resources studies. This concept is already evident, as, at present, a research program of the present use of soils through digital processing of LANDSAT images is being implemented. This program is being developed jointly with NASA and the Direcciòn General de Aguas (Water General Bureau) of the Chilean Government.

Fig. 1 LANDSAT 1, band 5 image, showing the biggest EW canyons through the desert, North of Chile.

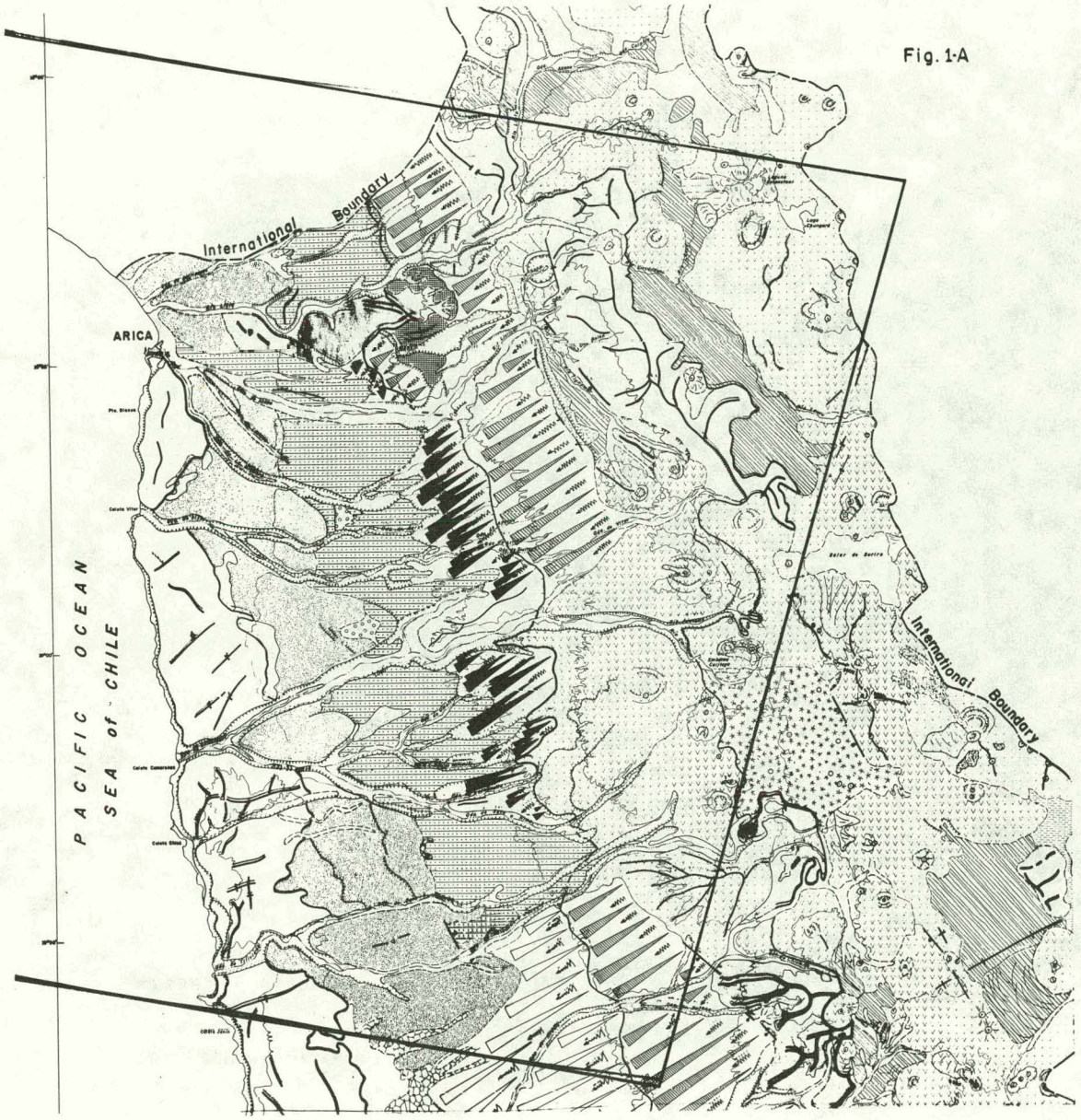

Fig. 1-A Map of Geomorphology from LANDSAT 1, interpretation of Fig. 1.

Fig. 2 LANDSAT 1, band 7 image, used for soil interpretation.

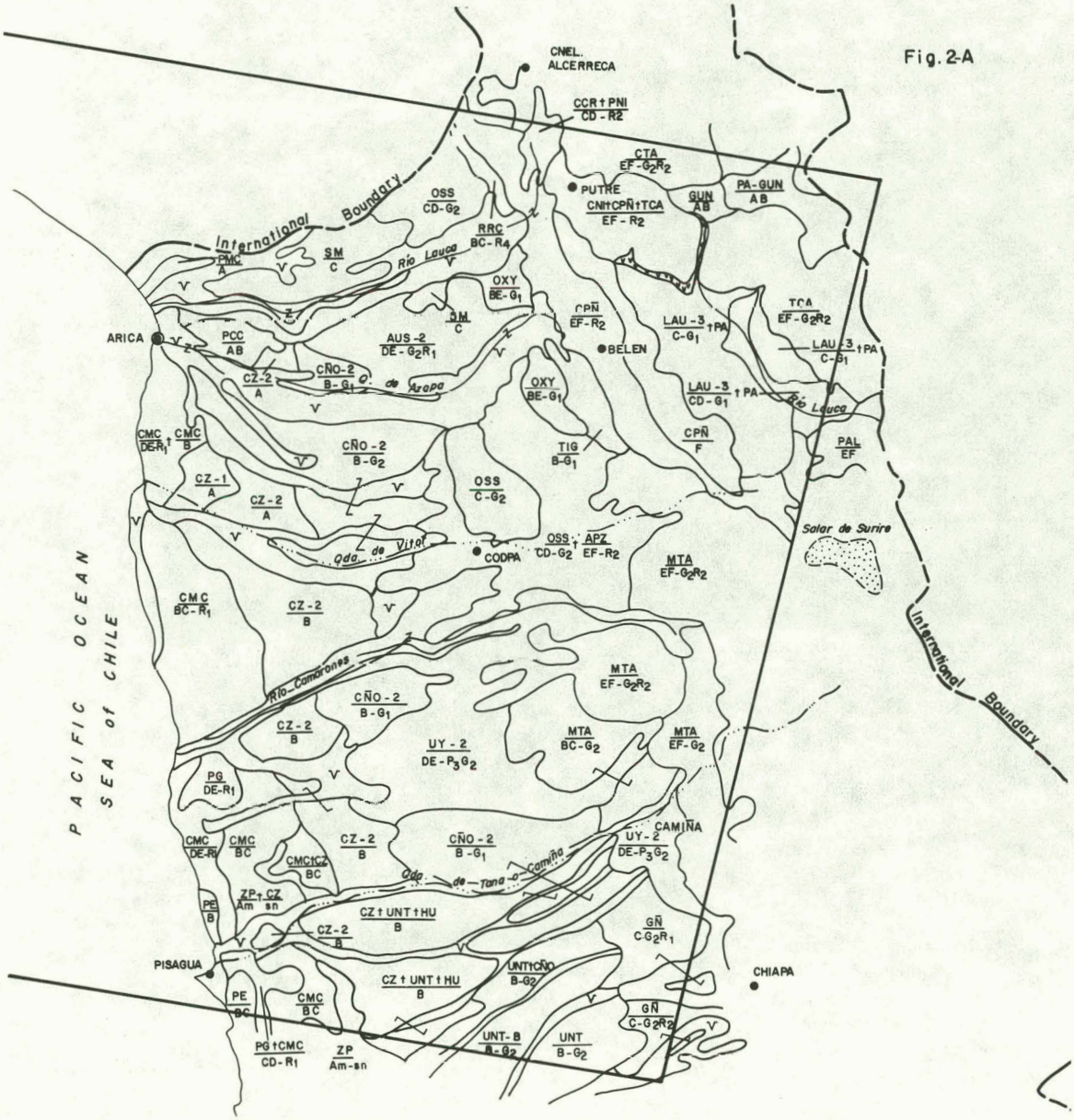

Fig. 2-A Classification of soil associations from LANDSAT 1 band 7 image. Includes type and restriction factors.

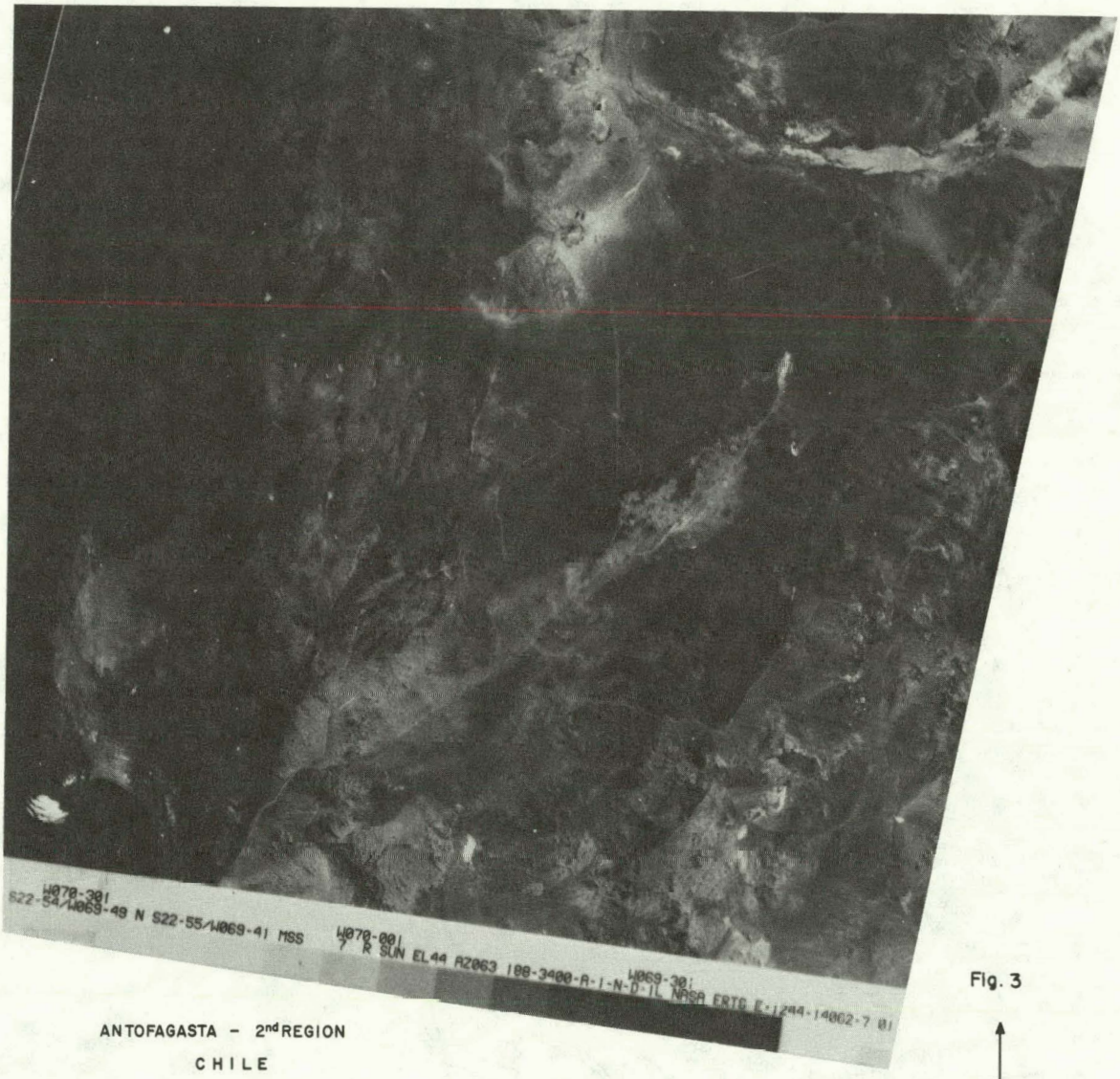

Fig. 3 LANDSAT 1 band 7 image of central Antofagasta region in the North of Chile.

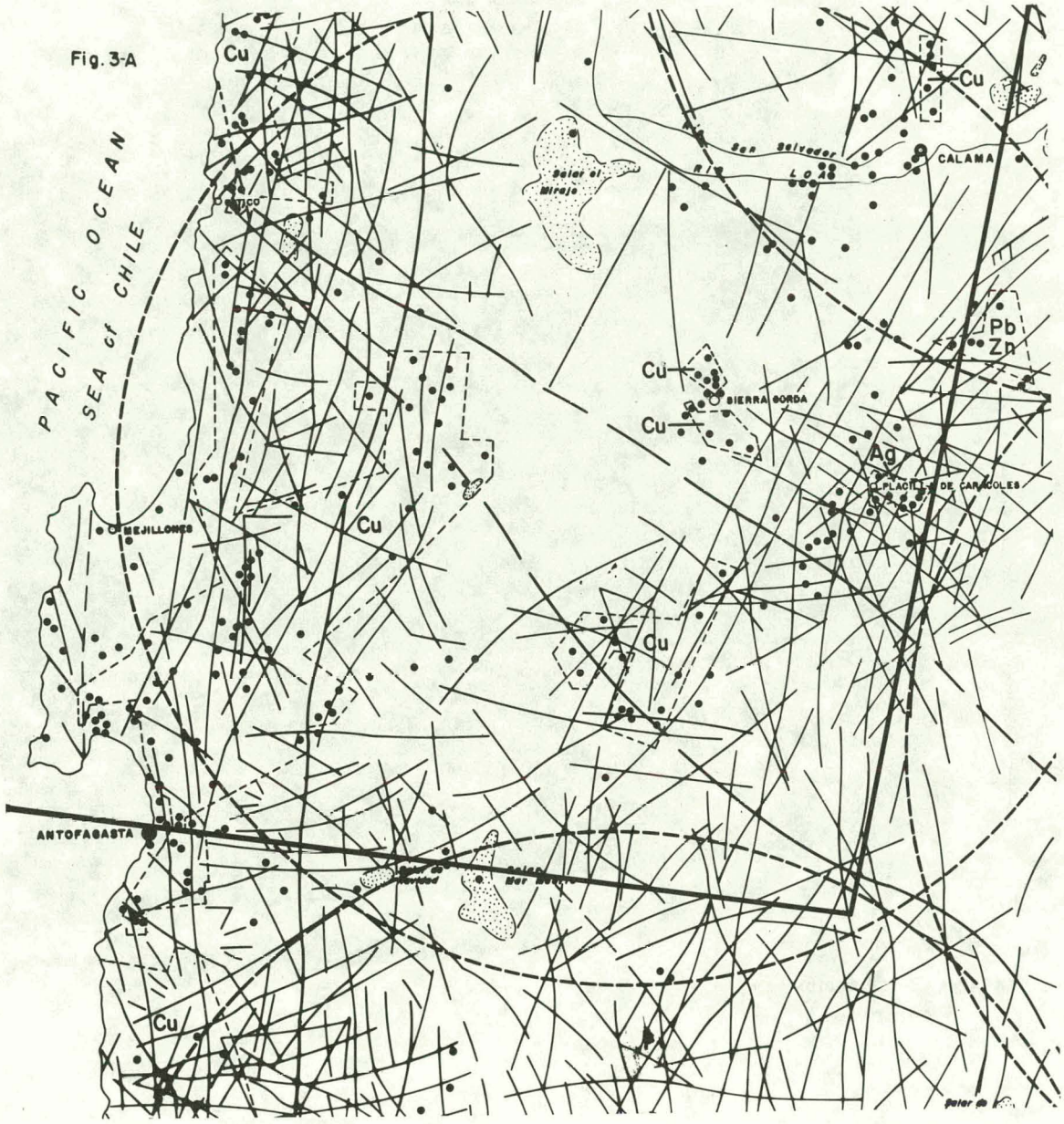

Fig. 3-A Relation of copper, silver, lead and zinc ore deposits to linear NS fractures from LANDSAT 1, interpretation of Fig. 3.

Fig. 4 LANDSAT 1 band 6 image showing the eastern part of The Andes Range and central part of Tarapaca desert.

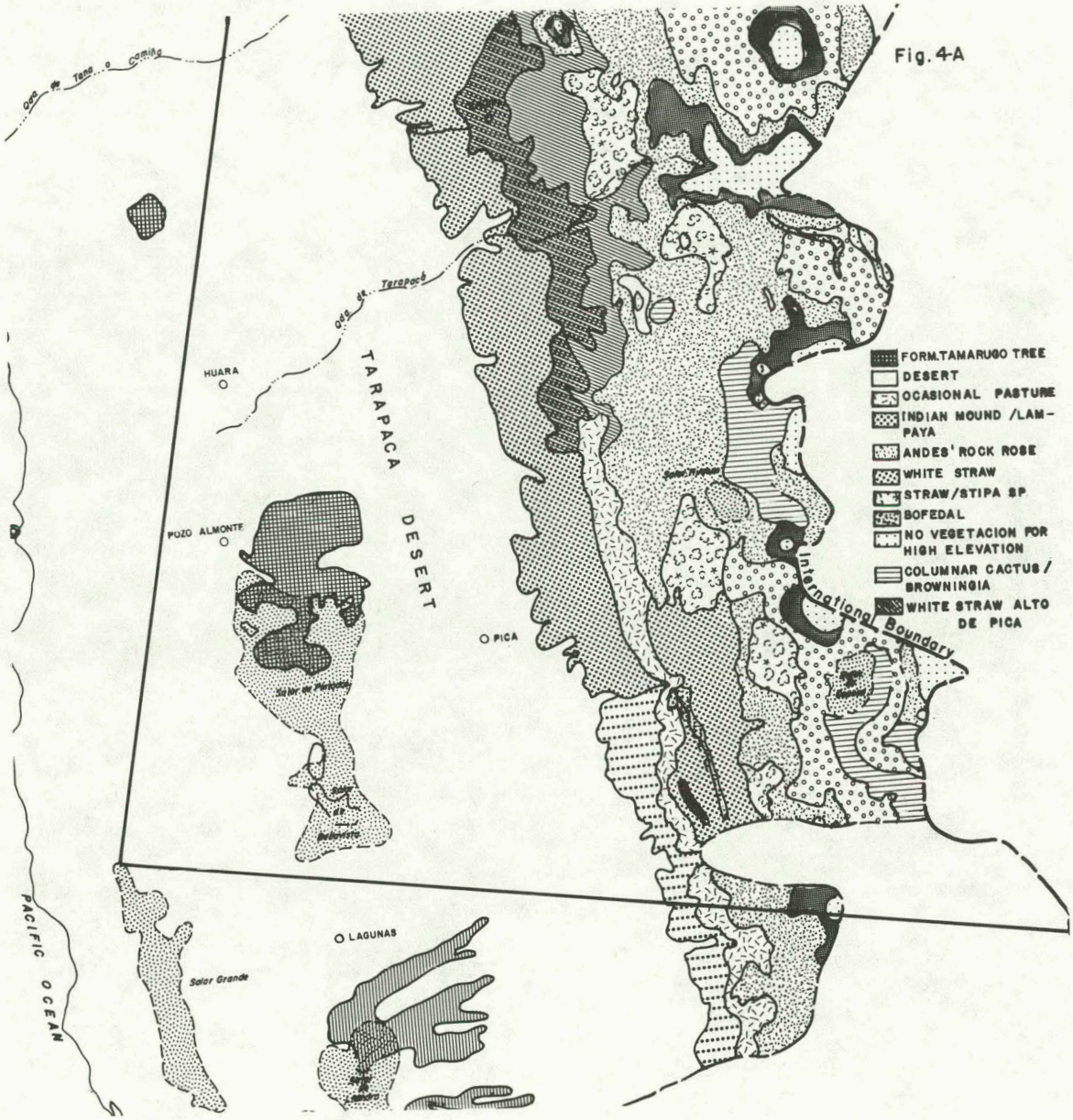

Fig. 4-A Natural plant association through interpretation of LANDSAT 1 band 6 image.

THIS PAGE

WAS INTENTIONALLY

LEFT BLANK

THE MODULATION OF THE RADAR BACKSCATTERING CROSS SECTION BY LONG OCEAN WAVES

Werner Alpers

Institut für Geophysik, Universität Hamburg, and
Max-Planck-Institut für Meteorologie,
Hamburg, FRG

and

W. Linwood Jones

NASA Langley Research Center
Hampton, Virginia 23665, USA

ABSTRACT

The modulation transfer function which relates the backscattered microwave power to the long ocean wave field was measured in the North Sea during JONSWAP 75. Results from this tower experiment with an X-band scatterometer are presented and compared with the two-scale wave model (relaxation-time model).

1. INTRODUCTION

Weather and wave forecasting could be improved considerably if information about sea state were available on a global scale and quasi synoptically. Therefore much effort is being devoted to developing an all-weather system for measuring ocean surface waves from satellites. The requirement that the system must be operational day and night and independent of weather conditions is met by microwave sensors. Active microwave sensors which have the potential to provide information about two-dimensional ocean wave spectra from satellites include the synthetic aperture radar (SAR) and the two-frequency-scatterometer (2 FS) (ALPERS and HASSELMANN, 1978). An L-band SAR will be flown on SEASAT which is due to launch in May, 1978. The two-frequency technique will be tested on a SPACELAB flight late 1980.

Backscattering of microwaves at ocean surfaces at oblique incidence angles is primarily caused by Bragg scattering on short ripple waves, which have wavelengths comparable to the wavelength of the microwaves. Therefore to first order the backscattered microwave signals contain only information about the small scale structure of the ocean surface. However, these small scale structures are modified by the long ocean waves, and thus cause a modulation of the backscattered microwave power.

This modulation permits spectra of long ocean waves to become detectable by microwave techniques. If microwave measurements (obtained e.g. by imaging radars or 2 FS) are to be converted into ocean surface spectra the modulation transfer function must be known.

A tower experiment with an X-band scatterometer was carried out during JONSWAP 75 (Joint North Sea Wave Project) in September 1975 in the North Sea with the prime objective to measure the modulation transfer function which relates the backscattered microwave power to the long wave field. Measurements

of this kind had been performed previously only in a wave tank (KELLER and Wright, 1975).

2. THEORY

2.1 Definition of the modulation transfer function

The transfer function $R_{\underline{K}}(\hat{\underline{k}})$ describing the modulation of the backscattered microwave power P by the long ocean waves is defined in wave number space by

$$P_{\underline{K}} = P_0 \left[1 + \int \left(R_{\underline{K}}(\hat{\underline{k}})\, z(\hat{\underline{k}})\, e^{i(\hat{\underline{k}}\underline{x} - 2\pi \hat{f} t)} + c.c. \right) d\hat{\underline{k}} \right] .$$

$z(\underline{\hat{k}})$ is the Fourier transform of the long wave field amplitude,

$$\hat{\zeta} = \int \left(z(\hat{\underline{k}})\, e^{i(\hat{\underline{k}}\underline{x} - 2\pi \hat{f} t)} + c.c. \right) d\hat{\underline{k}} ,$$

P_0 the backscattered power in the absence of long surface waves and $\underline{K}$ the 3-dimensional wave vector of the incident microwave. c.c. stands for complex conjugate. We assume that the modulation of P depends only linearly on the long wave field, which implies that $R(\underline{\hat{k}})$ does not depend on $z(\underline{\hat{k}})$. We expect that this assumption is correct for low and moderate sea states.

P as well as $R(\underline{\hat{k}})$ are functions of wave number, incidence and azimuth angle ϑ of the incident microwave radiation and of polarization.

According to the theory of single-input linear systems the transfer or response function $R(\underline{\hat{k}})$ is given by

$$R(\hat{\underline{k}}) = |R(\hat{\underline{k}})|\, e^{-i\theta} = \frac{1}{P_0} \frac{1}{P_{\hat{\zeta}}(\hat{\underline{k}})} P_{\hat{\zeta},P}(\hat{\underline{k}}),$$

where $P_{\hat{\zeta}} = F(\underline{\hat{k}})$ is the 2-dimensional wavenumber spectrum of the long waves and $P_{\hat{\zeta},P}$ the cross spectrum of $\hat{\zeta}$ and P. In terms of the coherence function

$$\gamma_{\hat{\zeta},P} = |\gamma_{\hat{\zeta},P}| e^{-i\phi} \quad (0 \le |\gamma_{\hat{\zeta},P}| \le 1),$$

the spectrum P_p of the backscattered power P, and $P_{\hat{\zeta}}$ we obtain

$$|R(\hat{k})| = |\gamma_{\hat{\zeta},P}| \left(\frac{P_P}{P_{\hat{\zeta}}} \right)^{1/2} \cdot P_0^{-1} \qquad \text{and} \qquad \theta = \phi$$

2.2 Two-scale wave model

Within the two-scale or composite-wave model introduced by WRIGHT (1968), the modulation transfer function can be expressed as the sum of two terms,

$$R = R^{tilt} + R^{hydr.}.$$

R^{tilt} describes the modulation of the backscattered power due to the change in local depression angle induced by the long waves and $R^{hydr.}$ the modulation due to the hydrodynamic interaction between short and long waves, which results in an asymmetric distribution of short Bragg scattering waves with respect to the long wave field.

The tilt modulation transfer function can be calculated by using Bragg scattering theory. Fig.1 shows a plot of $R^{tilt}(i\hat{\underline{k}})^{-1}$ as function of incidence angle for the case that the long ocean wave with wavenumber $\underline{\hat{k}}$ propagates in look direction of the antenna and that the polarization is horizontal both for transmit and receive (an isotropic PHILLIPS spctrum for the short BRAGG scattering waves is assumed). Note that R^{tilt} is a purely imaginary function.

The tilt modulation depends on the angle φ between look direction of the antenna and the direction of propagation of the long wave: it is maximal for $\varphi = 0^{o}$ and 180^{o}.

The hydrodynamic modulation transfer function has been calculated by KELLER and WRIGHT (1975) and ALPERS and HASSELMANN (1978) by using a WKB-type interaction theory. This interaction model is called relaxation time model in KELLER and WRIGHT (1975).

If the ratio of the group velocity of the short waves to the group velocity of the long waves is taken as expansion parameter and if again a PHILLIPS spectrum for the short waves is assumed, then in this theory

$$R^{hydr.}(|\underline{\hat{k}}|)^{-1} = 4.5\,\frac{2\pi\hat{f}}{\mu}\left(1+\left(\frac{2\pi\hat{f}}{\mu}\right)^{2}\right)^{-1}\left(\frac{2\pi\hat{f}}{\mu}-i\right)\cos^{2}(\hat{\underline{k}},\underline{k}),$$

where $\underline{k}$ is the wave vector of the short wave spectral component and $i = \sqrt{-1}$ (see ALPERS and HASSELMANN, 1978). Note that $R^{hydr.}$ is a complex function and depends on angle. When applied to Bragg scattering, $\underline{k}$ must be replaced by $\pm 2\,\underline{K}$, where $\underline{K}$ is the projection of the wave vector of the incoming microwave onto the horizontal plane. μ is a parameter which has to be determined by experiment.

μ^{-1} is sometimes called "relaxation time constant". In Fig.2 modulus and phase of $R^{hydr.}|\underline{k}|^{-1}$ are plotted as function of $2\pi\hat{f}/\mu^{-1}$.

3. THE EXPERIMENT

The modulation experiment was carried out during phase 2 of JONSWAP 75 from the sea-based platform "PISA" situated in the North Sea area 27 km off the island of Sylt, Germany.

The antenna of the scatterometer was mounted to an outrigger of "PISA" approximately 1o m above mean sea level (see Fig. 3). The scatterometer is a coherent CW system operating at a frequency of 9.5 GHz (X-band). Amplitude and phase of backscattered power P as well as Doppler shift f_d is recorded in a logarithic scale. The half-power beamwidth of the antenna is 5 degrees, such that the footprint is normally between 1 m and 1.5 m.

The non-directional long wave spectrum is measured by two resistive wavestaffs (W-1 and W-2), supplied by the German Hydrographic Institute.

4. DATA ANALYSIS

The transfer functions in the frequency-domain are obtained by calculating first the spectra and cross spectra of the time series. The analysis presented here is carried out with a frequency resolution of o.o3 Hz and 4o degrees of freedom. Thus the total record length is about 11 minutes.

Since the time series of the backscattered power P(t) is given in a logarithmic (dB) and the surface elevation $\hat{\zeta}(t)$ associated with the long waves in a linear scale, one obtains

$$R(\hat{f}) = \frac{1}{P_{\hat{\zeta}}}\,P_{\hat{\zeta},\frac{\Delta P}{P}} = \frac{1}{10\log e}\,\gamma_{\hat{\zeta},10\log P}\left(\frac{P_{10\log P}}{P_{\hat{\zeta}}}\right)^{1/2}$$

5. EXPERIMENTAL RESULTS

Measurements of the modulation transfer function were carried out under a variety of sea and wind conditions. As an illustrative example we present here the time series number 14-1, which was obtained on Sept. 8, 1975 around 14:3o h local time.

The incidence angle of the antenna beam is 5o° and the azimuth angle 319° N. The local wind speed measured at 14:oo h is 6.4 m s^{-1} and 6.9 m s^{-1} at 15:oo h, the wind direction is 2o5° N. Fig. 4 shows the geometry for this particular measurement. The non-directional long wave spectrum P measured by the oblique wavestaff is plotted in Fig. 5 together with the spectrum of the modulated backscattered power (in dB). Fig. 6 shows the spectrum of the Doppler shift (in dB) of the backscattered microwave signals. For comparison we have inserted in this plot again the long wave spectrum.

We notice that the long wave spectrum has two swell peaks, one at o.o9 Hz and the other at o.21 Hz, and a wind wave peak at o.33 Hz.

Fig. 7 shows the coherence of the time series $\zeta(t)$ and $P(t)$, and the calculated modulation transfer function $R_{\hat{k}}|\hat{k}|^{-1}$ in frequency space. $R_{\hat{k}}|\hat{k}|^{-1}$ is 1o.5, 8.6 and 1o.2 at those frequencies where the coherence is $\geq$ o.5.

6. DISCUSSION OF RESULTS

The analysis of this and other time series shows that, in general, $R_{\hat{k}}|\hat{k}|^{-1}$ does not increase with frequency. According to two-scale wave theory $R_{\hat{k}}|\hat{k}|^{-1}$ should increase or remain approximately constant (see Fig. 2). (The dimensionless tilt modulation transfer function should be almost independent of frequency f). The latter case only can occur when the relaxion parameter μ is sufficiently small, i.e. when $2\pi\hat{f}\mu^{-1} \gg 1$.

A small relaxation constant (e.g. $\mu \leq$ o.2 s^{-1}) implies a small phase of the hydrodynamic transfer function, i.e. a small phase shift between the crests of the long waves and the maximum of the short wave spectral energy. (A positive phase indicates that the maximum of the spectral energy is shifted in the direction of wave propagation).

Note that the modulus of the hydrodynamic transfer function attains its maximum value in the limit $\mu \to 0$.

If we assume that all assumptions are correct which enter in the derivation of R^{tilt} and R^{hydr}, then the maximum of the modulus of $R_{\hat{k}}|\hat{k}|^{-1}$ is given by

$$\left(|R_{\hat{k}}||\hat{k}|^{-1}\right)_{max} = \left(|R_{tilt}|^2|\hat{k}|^{-2} + 4.5\right)^{1/2}.$$

In the example considered here (ϑ = 5o°, HH polarisations) this maximum value should be approximately 9.5.

We have calculated the dimensionless modulation transfer function $R|\hat{k}|^{-1}$ also from a number of other time series. If only those values are kept for which the coherence is greater than o.5, then we find that $|R||\hat{k}|^{-1}$ varies between 3.6 and 13.5 depending on incidence and azimuth angle and wind conditions.

By summarizing the results from all time series analysed so far, we conclude that the modulus of the measured modulation transfer function is almost always close to its maximal possible value, or larger than predicted by the two-scale wave model.

Finally we want to point out that a very small phase shift between the long wave crests and the maximum of the short wave spectral energy yields

also a very small upwind-downwind asymmetry of the radar cross section which is in contradiction to experimental results. The highest value for the upwind-downwind asymmetry is calculated in the two-scale wave model when μ is chosen to be of the order of 1, which leads to a phase shift around 45 degrees. (For $\mu \to \infty$ we also obtain a vanishing upwind-downwind asymmetry.) But even with this value of μ only upwind-downwind asymmetries smaller than 1.5 dB can be obtained in this model. Since often upwind-downwind asymmetries even larger than 3 dB have been measured with X-band radars, we conclude that the two-scale theory is unable to explain these asymmetries. Strong non-linear effects -- like Rayleigh scattering at air bubbles on the leeward side of the long waves -- could be the explanation.

ACKNOWLEDGEMENT

We want the thank Prof.K.Hasselmann for many helpful discussions. Dr. K. Richter from the German Hydrographic Institute built the wavestaffs and we are greatly indebted to him for making the wave data available.

REFERENCES

Alpers, W. and K.Hasselmann, "The two-frequency microwave technique for measuring ocean wave spectra from an airplane or satellite". Boundary-Layer Meteorology, Special issue on Radio Oceanography, 1978 (in press)

Keller, W.C. and Wright, J.W., "Microwave scattering and straining of wind-generated waves." Radio Science, 10, 139-147, 1975

Wright, J.W., "A new model for sea clutter", IEEE Transactions on Antennas and Propagation (USA), AP-16, 217-223, 1968

FIGURE CAPTIONS

Fig. 1: Dimensionless tilt modulation transfer function as a function of incidence angle calculated from Bragg scattering theory.

Fig. 2: Calculated dimensionless hydrodynamic modulation function (relaxation-time model). In the upper part the modulus is plotted and in the lower part the phase.

Fig. 3: Geometry of the tower-scatterometer experiment.

Fig. 4: Geometry of measurement number 14-1.

Fig. 5: Non-directional ocean wave spectrum $P_{\hat{\zeta}}$ measured by wavestaff W-1 and spectrum $P_{10 \log P}$ of backscattered microwave power (in dB).

Fig. 6: Spectrum of Doppler shift $P_{10 \log fd}$ (in dB) together with the non-directional ocean wave spectrum $P_{\hat{\zeta}}$.

Fig. 7: Measured dimensionless modulation transfer function in frequency-domain together with the coherence of the time series $\hat{\zeta}(t)$ and 1o log P (t).

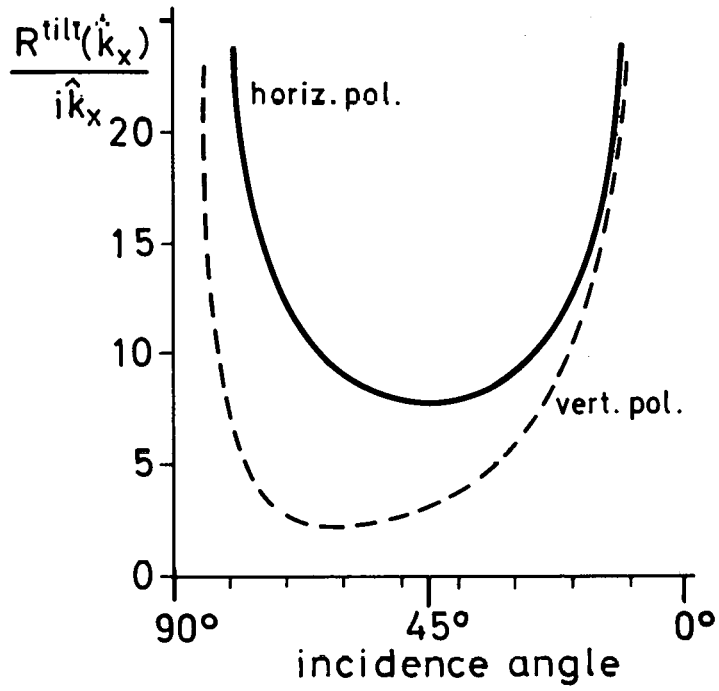

Fig. 1: Dimensionless tilt modulation transfer function as a function of incidence angle calculated from Bragg scattering theory.

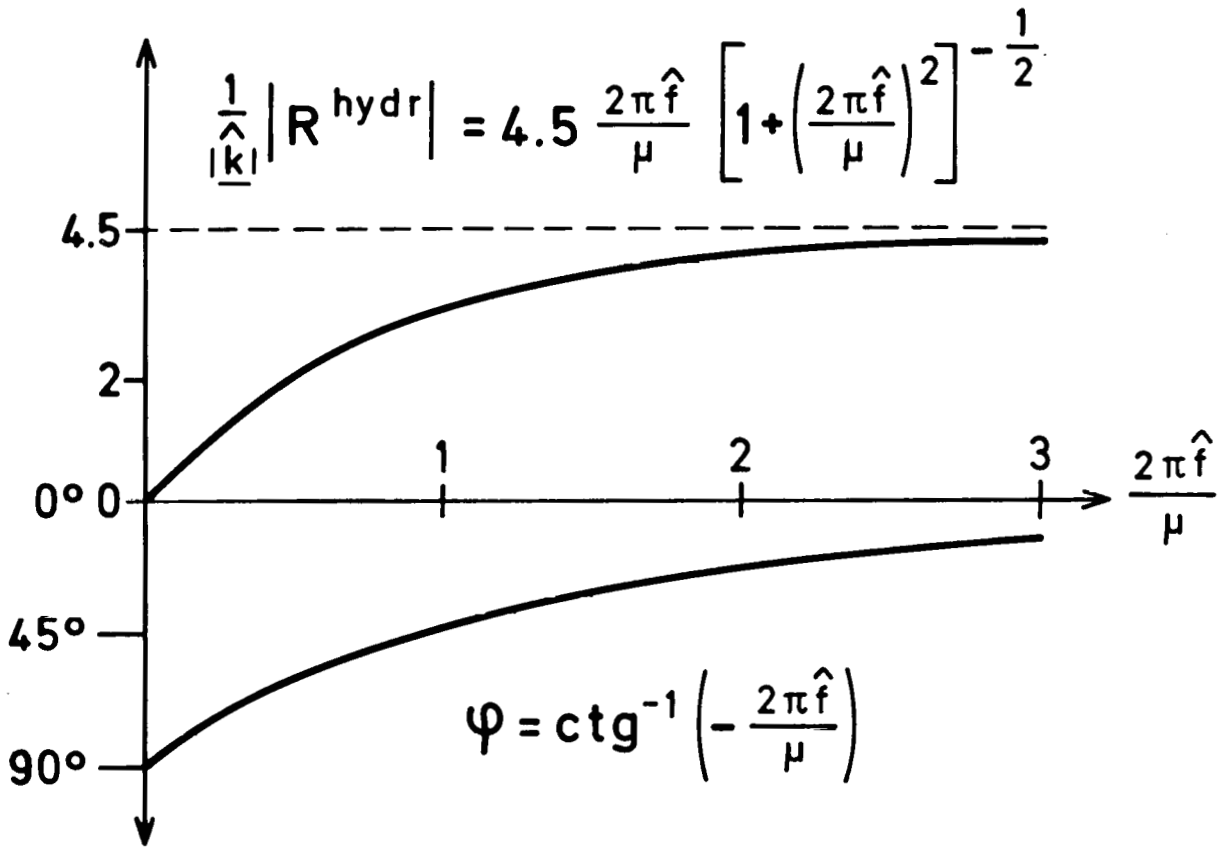

Fig. 2: Calculated dimensionless hydrodynamic modulation function (relaxation-time model). In the upper part the modulus is plotted and in the lower part the phase.

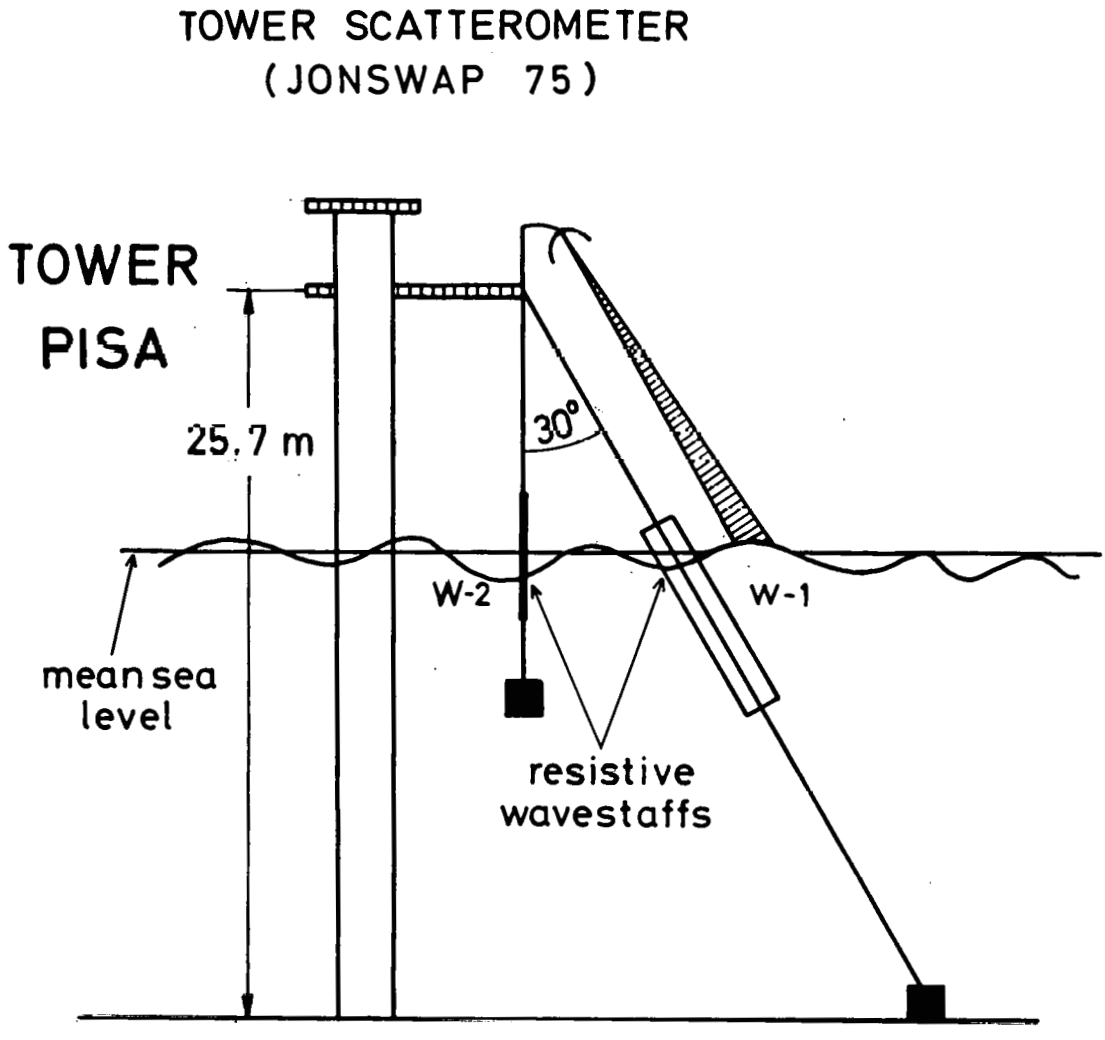

Fig. 3: Geometry of the tower-scatterometer experiment.

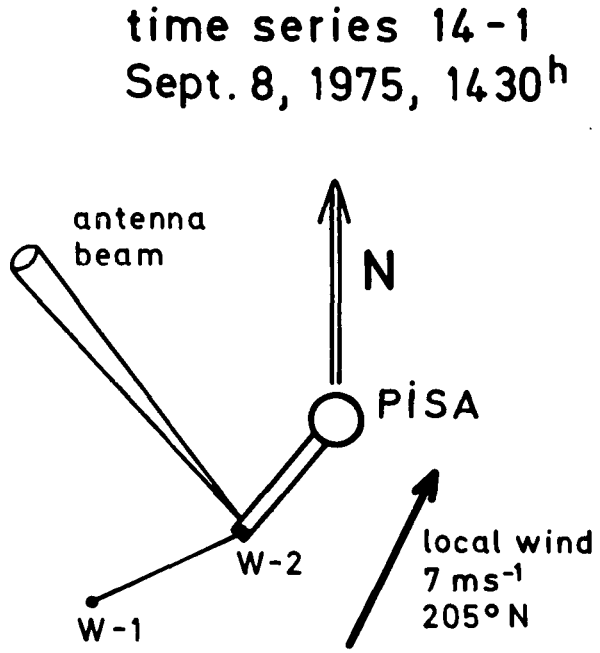

Fig. 4: Geometry of measurement number 14-1.

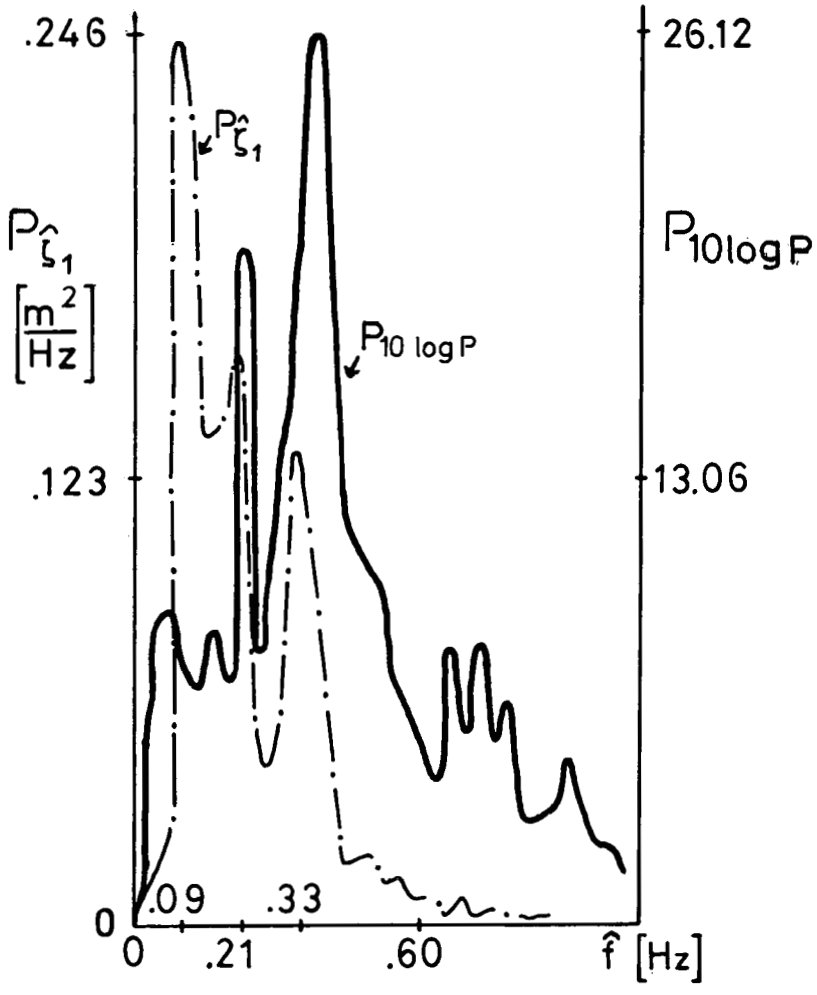

Fig. 5: Non-directional ocean wave spectrum $P_{\hat{\zeta}_1}$ measured by wavestaff W-1 and spectrum $P_{10\log P}$ of backscattered microwave power (in dB).

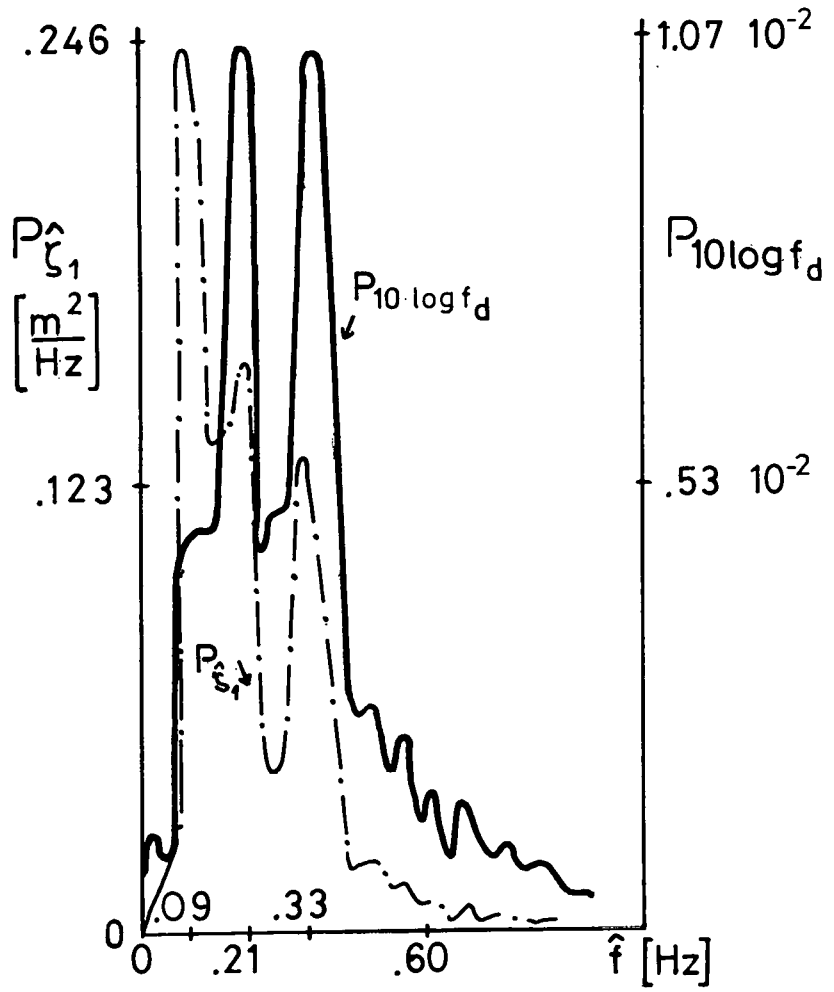

Fig. 6: Spectrum of Doppler shift $P_{10\log f_d}$ (in dB) together with the non-directional ocean wave spectrum $P_{\hat{\zeta}_1}$

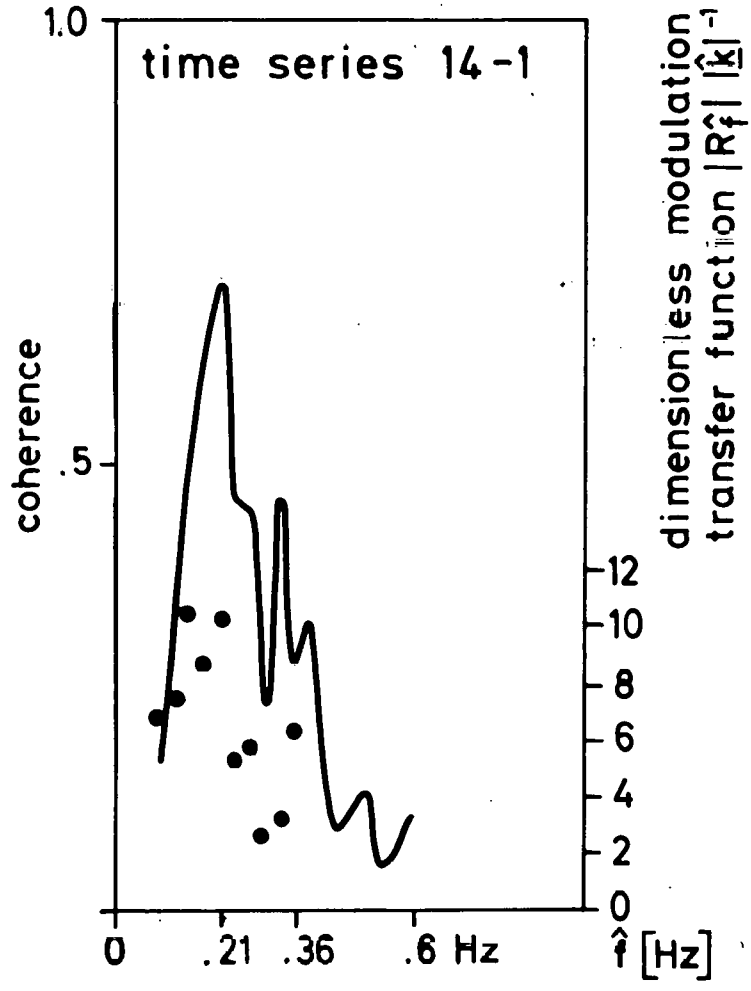

Fig. 7: Measured dimensionless modulation transfer function in frequency-domain together with the coherence of the time series $\hat{\varphi}_1$ (t) and 10 log P(t).

APPLICATIONS OF LANDSAT AND SKYLAB IMAGERY IN MEXICO: DETECTION OF EROSION AND FOREST DAMAGE

D. Rodriguez-Bejarano
School of Natural Resources
The University of Michigan
Ann Arbor, Michigan 48109

ABSTRACT

Detection of erosion and forest insect damage was tried out in two regions of Mexico: the central part of the State of Puebla and the northeast region of the State of Guerrero. LANDSAT and SKYLAB imagery were used, together with convontional aerial photography and ground checking. Results showed the possibilities of applying this type of data to extensively affected areas. The examples derived could very well serve to teach natural resources students the limitations and possibilities of visual interpretation of LANDSAT and SKYLAB data in Mexico.

INTRODUCTION

Remote sensing technology is fast becoming one of the most important tools in formulating management policies in developing countries. But their potential has not been completely utilized by developing countries, among other reasons because (1) the applications in these countries have been sporadic and contingent upon some international organization program (UN, AID, World Bank, etc.), and (2) the lack of trained personnel in remote sensing that is permanently stationed (i.e. nationals) in the needed areas.

The application of remote sensing techniques in developing countries has seen an upsurge in recent years in the form of aid, grants, development programs, etc. The second problem, the lack of permanently stationed trained personnel, needs more attention. Although in most remote sensing programs there is some type of technology transfer scheme from the sponsoring organization to the recipient country, its impact is minimized due to the fact that the technician in the developing country will himself require trained helpers which are not normally available. These trained helpers should come from universities, colleges, or specialized training schools in the recipient country. Thus, aside from training local counterparts it is necessary that the recipient country provide its own manpower, trained in its own centers (universities). For this it is necessary to strengthen the remote sensing curricula offered in developing nations. Two basic steps need to be taken in order to accomplish this: (1) train university teachers in remote sensing, and (2) have these people develop their own curricula in their own countries given their particular problems and technical infrastructure (trained personnel and instrumentation available).

To demonstrate the latter, a study was implemented at the Department of Forestry of the National School of Agriculture in Chapingo, Mexico, using LANDSAT and SKYLAB data and visual techniques to detect erosion and forest damage.

BACKGROUND

Since 1966 Mexico has been using the data provided by NASA's programs to gather information on the earth's natural resources. There have been several applications of LANDSAT and SKYLAB data in Mexico in soils classification,

land use, water resources, erosion, mineral resources, and geological surveys. However, neither methodologies nor information of results have had enough effect in shaping natural resources policies. This has been due mainly to: poor communication between agencies in charge of natural resources study, and a lack of a clear-cut national plan to use natural resources (Rodriguez-Bejarano, Calderon, 1977).

The erosion problem in Mexico is at best hazy. Although censal data sets at 30.0 million Ha the area totally eroded, a recent study detected only 6.3 million Ha (Garduño, et al., 1975). The problem is further compounded by the fact that at least two governmental institutions (National Forest Inventory and Commission on Studies of Mexico's National Territories) are presently involved in mapping erosion and both are using different definitions of erosion (Rodriguez-Bejarano, Calderon, 1977). But whichever the figure we use, the eroded area of Mexico could go between 3% to 15% of its total land area.

The forested land area of Mexico (temperate and tropical forests) covers 44.4 million Ha or about 22% of its territory (INF, 1977). This area is plagued by a host of problems: mismanagement, fires, insect and disease attacks and population pressures especially in areas around Mexico City.

Insect attacks by bark beetles (Dendroctonus spp.) are localized in the temperate regions in the States of Mexico, Puebla, Michoacan, Durango, and Guerrero. Several attempts by the National Forest Research Institute of Mexico have been made to identify the attacks and set up protection and combat plans. Unfortunately, the extension of the attack is not fully known and plans have been drawn on field data without much use of remote sensing techniques. Although some uses of conventional aerial photography and color infrared aerial photography have been made (Moncayo-Ruiz et al., 1970), the state of the art leaves much to be done.

Applications of LANDSAT imagery to land erosion detection and monitoring are found in the literature (Bowden, Pruitt eds., 1975; Williams, Carter eds., 1976) and the techniques have been applied in Mexico (Rodriguez-Bejarano, Calderon, 1977). The same can be said about forest insect attacks (Bowden, Pruitt, eds., 1975; Heller, 1975) although there is not general agreement as to the accuracy of LANDSAT detection especially in small areas. But the author knows no attempt being made in Mexico to use LANDSAT or SKYLAB data to detect forest insect attacks.

EROSION AND FOREST STRESS DETECTION

The two areas selected for this study are shown in Figure 1. They were chosen on the basis of three criteria: (1) there existed sufficient data for the areas (i.e. aerial photography, LANDSAT and SKYLAB coverage, and some ground data); (2) both had serious problems of resource using which make them desirable as show cases, and (3) they were reasonably near to the center of operation and thus easily accessible by remote sensing course groups.

Erosion Detection. The area surveyed for the erosion study is located east of Puebla, capital of the State of Puebla. Agriculture in the two traditional forms, rain-fed and irrigated, is the principal activity of this area. Apparently most of the area was deforested early in the Spanish colonization period and now suffers from very serious erosion problems.

Similar conditions and erosion intensity exist in the area near Chapingo, State of Mexico (Figure 2). This area was used as a reference pattern (training set) for the study. A mosaic of the area was produced using conventional aerial black and white panchromatic photography taken by CETENAL (Commission on Studies of Mexico's National Territories) at a 1/50,000 scale. The mosaic showed erosion as well as rain-fed and irrigated agriculture areas. The area covered by the mosaic was located in a false color composite (FCC) LANDSAT image* at a 1/500,000 scale, thus producing the reference pattern for erosion and agriculture. The FCC image, covering an area from 18°00' N to 19°30' N and 99°00' W to 97°30' W, was taken on May 1973, which corresponds

* Image ID number: 81307162855G200-C

to the dry season in the area.

The erosion reference pattern in the FCC image appeared whitish and somewhat yellowish. The eroded areas are often surrounded by a bluish rim which in the FCC image can be directly related to dying or sickly vegetation. Immediately after this bluish surroundings comes a red or pink color area that represents healthy tree or green bush vegetation. This corresponded to mixed conifer forests and rain-fed agricultural areas. Thus, erosion was flanked by this type of agriculture and forests. Ground data from the area showed spreading erosion due to devegetation and deforestation for agriculture purposes, done by the peasantry of the area.

This reference pattern was used to detect eroded areas in the study region of Puebla. Erosion is here characterized by white areas surrounded by light blue and pinkish rims. The whiter and bigger the area the more pronounced the erosion. So, areas with very intensive erosion showed very white and large; while areas with little erosion showed as whitish-yellowish and an in-between erosion showed as the transition between the extreme of the two types. To the east of the severely eroded area there was a large irrigated agricultural area.

At the same time the eroded area was located in SKYLAB photography: color, color infra-red, B&W Panchromatic and B&W infra-red.* This served the purpose of illustrating eroded areas in different types of emulsions. For this purpose the same scale as the FCC, 1/500,000, was utilized: the SKYLAB photography taken in September, 1973, which is already rainy season in Mexico, did not show substantial differences from the FCC as far as extension of eroded area. This meant that weather conditions did not alter the vegetated area and that eroded land was not being reduced due to more available water (rainy season). It could also be that in September, the beginning of the rainy season, not enough vegetation had appeared in marginal areas to make a difference, making it necessary to use data from December (later on in the rainy season).

Also for illustrative purposes the study area was enlarged to 1/100,000 scale from B&W negatives of the four LANDSAT bands.

Forest Stress Detection. This study was conducted in a pine-covered area in the north eastern part of the State of Guerrero (Figure 3). This part of Mexico is rugged terrain where the principal activities are forestry exploitation and low production agriculture. The particular forest of this region has been selectively exploited, poorly managed, and constantly affected by forest fires. All these activities have contributed to a decreased forest vigor and could have been the cause of insect attacks.

Forest vegetation which has been affected by insect attacks is easily detected in color infra-red photography. Healthy vegetation appears red while stressed vegetation appears pinkish, yellowish and bluish depending on the stage of attack. In high altitude, small scale color infra-red photography, such as SKYLAB's, relatively large areas of stressed vegetation can be detected. Color and color infra-red SKYLAB photography taken in August 1973, and at a 1/500,000 scale was obtained for the general area.** A particular area was detected in the color photograph and then in the color infra-red. The reason to select this area was a color change that appeared to be caused by vegetation stress that could be attributed to: (1) burned area which was regenerating (it was thought to be burned since a common practice in the area is to clear-cut and burn for agricultural land), and (2) insect or disease attack. If the area had been burned, chances were that it was covered by vegetation sometime before and no color change would be observed in the multidate imagery. But if the cause for the color change was due to insect or disease stress in the forest vegetation then this change will most likely persist.

Thus, when a similar color change was detected in a FCC LANDSAT image***

*Photograph ID numbers: G30A046082000, G30A045082000, G30A047082000, G30A044082000.

**Photograph ID numbers: G30A045081000 and G30A046081000

***Image ID number: 81577162455A2

taken in November 1972 the second possibility was thought to be the cause of the color change. To prove this point a general area known to be affected by the bark beetle Dendroctonus frontalis ZIMM was located in the image and the color change detected. Then a field visit was scheduled.

The particular area is located north of Acapulco, near a small village called La Providencia which is accessible by a dirt road, difficult to travel in the rainy season. The principal pine species present in the area are Pinus pringlei, P. leiophyla, P.pseudostrobus, P. ayacahuite, P. herrerai and P. strobus-chiapensis (Gonzalez-Espinoza et al., 1977). The attack, initially reported in 1968, concentrates almost exclusively on two species: Prinus pringlei and P. herrerai, the former being the most severely attacked (Gonzalez-Espinoza et al., 1977). The field visit, performed in mid November 1977 confirmed the finding in the FCC image. During this visit slides in color and color infra-red of the area were taken to show the conditions of forest damage to remote sensing students.

RESULTS

This study showed the possibility of using LANDSAT and SKYLAB data to detect erosion and forest damage of relatively large areas. The maps, mosaics, annotated photographs and images, overlays and slides could be used in classroom activities to show capabilities of remote sensed data in monitoring resources. All the work was developed under what we may assume to be similar conditions existing in educational institutions common to developing countries.

Erosion can be visually detected and mapped initially into three different categories: areas intensively, moderately, and slightly eroded. A map of these types of erosions is shown in Figure 4. Forest insect damage was detected, mapped and measured, again using manual techniques. The affected area was delineated on the FCC image, a map produced at 1/500,000 scale (Figure 5) and the area measured using a dot grid. Area estimation of the insect damaged area using a dot grid showed 12,682 Ha, which differed from a 1976 ground and helicopter estimation set at 10,000 Ha (Gonzalez-Espinoza et al., 1977). This suggests an underestimation since the image used in the study was taken in 1972 and the area affected has probably extended rather than shrunk in the 1972-76 period.

CONCLUSIONS AND RECOMMENDATIONS

The remote sensed data could be used for actual information gathering for classroom examples and within the means of a normal remote sensing course. Using the methodology described several examples could be developed to cover particular resource management aspects and show prospective users (students) what the possibilities are for LANDSAT and SKYLAB.

Erosion of agricultural areas and hill-lands is a serious problem in emerging nations, so that visual and quick ways should be developed to detect and monitor its advance using available infrastructures (personnel and instrumentation). The same can be said for forest damages, especially in high value forests such as the case presented here.

It is suggested that this particular experiment be continued with more recent data so a monitoring system of the erosion and damage processes could be set up.

REFERENCES

Bowden, L.W. ed. and Pruitt, E.L., asst. ed. Manual of Remote Sensing. Vol. II. Falls Church: American Society of Photogrammetry, 1975.

Garduño, H., Garcia-Lagos, R., and Garcia-Simo, F. Present and Potential Land Use Mapping in Mexico. Proceedings of the NASA Earth Resources Survey Symposium, Vol. I-C, pp. 1823-1839. Houston, 1975.

Gonzalez-Espinoza, M., Reyes-Rodriguez, B. and Zerecero-Leal, G. "Estudio Fitosanitario de los Montes Comunales de Tixtlancingo y Ejidales de Sta. Rosa, Pueblo Viejo y Las Compuertas, Municipio Coyuca de Benitez, Edo. de Guerrero." Report SARH, SFF, Mexico, 1977. (Mimeographed).

Heller, R.D., tech. coord. Evaluation of ERTS-1 Data For Forest and Rangeland Surveys. USDA Forest Serv. Res. Paper PSW-112. Berkeley, 1975.

Inventario Nacional Forestal (INF). Estadisticas del Recurso Forestal de la Republica Mexicana. SARH, SFF Publication No. 42. Mexico, 1977.

Moncayo-Ruiz, F., Estrada-Escobar, F. and Perez-Romero, C. Manual para el Uso de Fotografias Aereas en Dasonomia. Mexico: SAG, SFF, INF, 1970.

Rodriguez-Bejarano, D. and Calderon, A. A Review of the Uses of LANDSAT Imagery in Mexico. Proceedings 1977 ASP-ACSM Fall Technical Meeting pp. Little Rock, 1977.

Williams, Jr., R.S. and Carter, W.D., editors. ERTS-1: A New Window on Our Planet. Geological Survey Professional Paper 929. Washington: U.S. Gov. Printing Office, 1976.

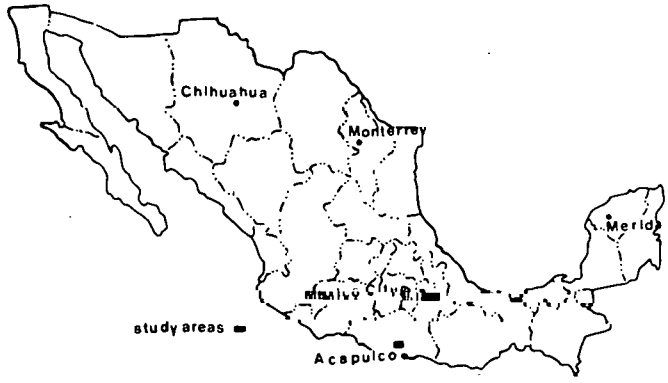

Figure 1 : General location of study areas in Mexico.

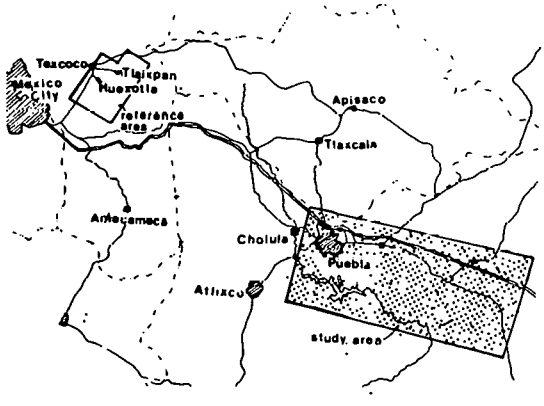

Figure 2 : Location of erosion study area.

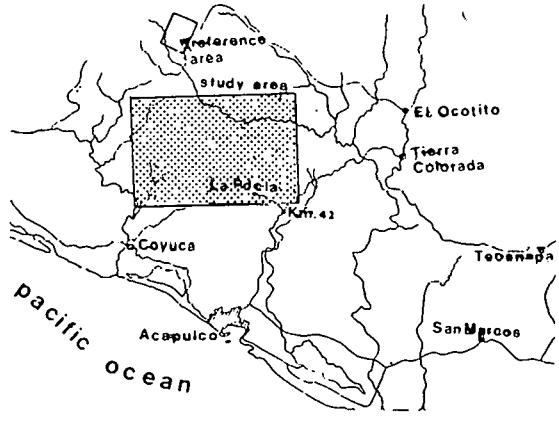

Figure 3 : Location of forest damage study area.

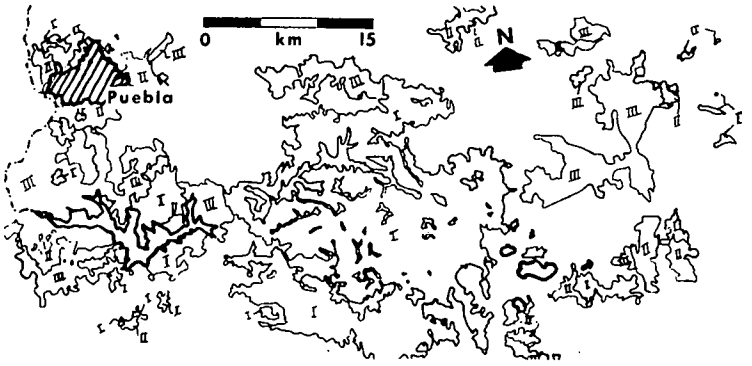

Figure 4 : Map showing different types of erosion : intensive (I), moderate (II), slight (III).

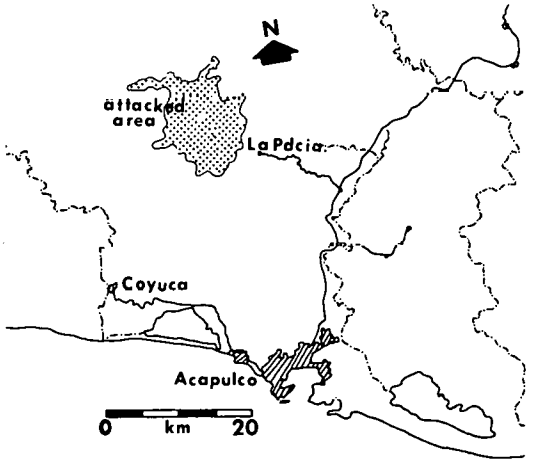

Figure 5 : Map showing extent of bark beetle attack.

THIS PAGE

WAS INTENTIONALLY

LEFT BLANK

REMOTE SENSING INPUTS INTO A WETLAND RICE REGIONAL PRODUCTION MODEL (JAVA)

Jean-Paul Malingreau

Universitas Gadjah Mada
Yogyakarta - INDONESIA

ABSTRACT

A conceptual model of wetland rice regional production is presented with particular application to the Javanese *sawah*. Two sub-models are analyzed : a Crop Area sub-Model (CAM) and a Crop Yield sub-Model (CYM). Field observations have shown that a very large spatial and temporal variability in production factors can be found over sometimes small areas. The stratification of the landscape into Homogeneous Production Areas (HPA) is therefore basic to the modeling strategy proposed here. The main crop and environmental parameters (planted variety, water availability and occurence of pests) are evaluated over a biological time scale. Remote sensing technology can provide significant inputs at the stratification level as well as at the actual monitoring level but applications are still limited.

1. INTRODUCTION

Although the worldwide food situation has somewhat improved since the shortage threat of the beginning of the decade, the issue remains very critical in many countries experiencing a rapid population growth together with an increasing per capita food consumption.

Indonesia for example, with its 132 millions people and a rate of population growth of approximatively 2.3% per year is far to be self sufficient in the production of rice, its staple food. It is reported that the country will have imported about 2.6 millions tons of rice by the end of the 1977/78 fiscal year; this represents over 30% of the world market supply. In such situation, statistics on rice production are quite understandably critical data for development planning. They have acquired indeed an overriding influence on the economic situation and the socio-political stability of the country. And it has been said that rice production parameters such as harvested acreage, yields, inputs and prices, are regarded at the local as well as at the national level as a "general barometer of success or failure of economic policy" (Grenville, 1977).

The very importance of the theme of self-sufficiency in rice production at the national level calls for the development of a series of "tools" appropriately designed for keeping a permanent (or near permanent) record of the production. Although no economic theory seems to be able to precisely quantify the benefits which will accrue from an improved crop information system, it is fairly evident that production estimates at or near harvest are vital data on which a wide range of decisions on rice policy can be based (i.e., purchases on international markets, stock building, price support, food relief operations, design of improved strategies for agriculture production development etc...).

The Indonesian Goverment, through its Central Bureau of Statistics in collaboration with the Ministry of Agriculture has already taken several steps toward improving its crop statistical reporting services; such steps include for example the monthly reporting of crop situation by agricultural extensions agents at the sub-district level (*kecamatan*) and the establishment of a very large number of yield measurement plots across the country. However, the complexity of the situation typical of a traditional agriculture "on the move" coupled with the very wide variety

of situations in which paddy is grown in Indonesia (in a spatial and temporal dimension) makes speedy and accurate rice production inventories a task of major proportions.

As in many other countries of the world, there is room in Indonesia for improvements in the assessment of crop production. Remote sensing supported global information systems have been presented as having the potential of servicing agriculture with local or global frequently updated relevant information (Colwell, 1976, Estes, 1974. Moore, 1977. National Academy of Science,1975). In the humid tropics however, technological support for the implementation of such a system at an operational level is still in an early research and development phase. Research and applications in this field have indeed mainly concentrated on temperate and subtropical regions of the world. Thus, a very limited amount of information only is available to-day on the use of remote sensing for agricultural inventories in the traditional intensively cultivated paddy lands of the tropics in general and of the Far-East region in particular[+]. Drewes (Drewes, 1975) in India, Heydt and McNair (Heydt, 1973) in the Philippines and a group of european scientists (DeCarolis, 1974. LeToan, 1977) in southern France and Italy, have reported on some preliminary work dealing with the use of air-photography and satellite imagery for irrigated rice inventories.

The present paper deals with the conceptualization of a wetland rice production model as adapted to conditions encountered on the Island of Java and with an evaluation of the potential of remote sensing technology for providing inputs to the model. It is based on some preliminary observations made during an on-going investigation carried out in the Cimanuk River Basin (West Java) using conventional and multispectral air-photography and satellite imagery. The research is divided in the three following parts which will be reviewed hereafter.

First, as for any crop, but maybe the more so for wetland rice in the tropics, the design of an acceptable model of production presupposes a fairly intimate knowledge of the range of field situations in which the crop is grown. This familiarization is effected during field investigations carried out on a monthly basis (over a wet and a dry season) and covering a wide range of environmental settings.

Second, a conceptual model of production is being elaborated on the base of specific observations made during field investigations and on the sum of the relevant knowledge which has already been accumulated on the agronomy of rice in Indonesia and other parts of the world.

Third, the present and potential capabilities of remote sensing technology for providing appropriate inputs into the model is assessed.

These three distinct aspects of the problem are quite obviously overlapping : each one of them somewhat conditions the approach taken in the analysis of the others.

The final objective of a crop production model is to be operative in a predictive mode. It has nevertheless been found premature to venture in the difficult terrain of crop production forecasting before accurately ascertaining the feasibility of actually monitoring field activities and environmental parameters.

2. THE PHYSIOGNOMY OF THE JAVANESE SAWAH[++]

Anyone somewhat familiar with traditional wetland rice cultivation in the humid tropics is well aware of the complexity of situations associated with this intensive farming system.The sawah in Java is the focal point of a very dense web of delicately interconnected physical, biological, socio-economic and cultural influences. Its present methods of cultivation are guided by tradition as well as by modern farming technology and by socio-cultural forces as well as by economic incentives. It is obvious that accounting for all these variables is hardly feasible especially when one wants to work at a regional or broader scale. Two main criteria have been guiding the selection of the most appropriate variable to be monitored during field data collection : at first the retained variables have to be amenable to parametrization in model formulation

---

[+] This is somewhat surprising considering that among the major food crops rice is second only to wheat and that the asian paddies occupy approximatively 124 millions hectares and produce 91% of the world total (FAO, 1974).

[++] *Sawah* is the Indonesian word for a terraced area destined to wetland rice cultivation (irrigated or rainfed).

and second , they have to be, whenever possible, amenable to remote sensing measurement. These two criteria are not limitative but have been used as overall guidelines.

In this perspective, visible quantifiable parameters related to crop production have naturrally received preferential treatment. Thus the grouping of these parameters in a set of "physiognomic" characteristics of *sawah* (Malingreau, 1976).

A short review of those characteristics augmented by additional relevant field observations is given hereafter. The following points are not pretended to give a complete picture of actual rice crop growing situations but to highlight the main *sawah* features which are thought to be important in the present approach.

2.1. Wetland rice is cultivated on level fields surrounded by low grassy bunds. The terraces are formed on slopes ranging from close to 0% in nearly flat alluvial plains to up to 50 - 60% in highly dissected mountainous areas. The shape and average size of the fields depends upon the landownership pattern and the topography (terrace requirement); square to rectangular fields of up to a few ha or irregular plots of a few square meters are found(TABLE I). But because of their irrigated nature, wetland rice fields are often found in groups (*golongan*) depending upon water delivery from a unique canal. Problems of spatial cohesiveness present particular importance as shown in paragraph 2.9.

2.2. There are basically two types of wetland rice cultivation systems on Java : the irrigated and the rainfed *sawah* (respectively 74 and 26% of the total *sawah* of Java - Soemartono,1974).

2.2.1. In the irrigated type, the bunded fields are artificially supplied with water (by gravity flow system for 95% of the area - Agricultural Census 1963). If enough water is available they may support a continuous crop of rice (2 per year or 5 in two years)[+]. Other types of cropping patterns are :
- 1 crop of rice in the rainy season and no crop in the dry season.
- 1 crop of rice in the rainy season and a secondary crop[++] in the dry season (see point 3.4).

2.2.2. The rainfed *sawah* depends entirely on rainfall for its water supply. The bunded terraces support only one crop of rice planted at the onset of the rainy season.When the rainfall pattern is appropriate, a secondary crop is sometimes grown before or after the rice.

2.3. Water is the main determinant of cropping pattern and crop performance.

2.3.1. In the absence of storage facilities,there is no straightforward correlation between water availability to the crop and the classification of an area as being "irrigated". The term should be understood as "irrigatable", or irrigated if and when water is available. As irrigation water is directly dependent upon river runoff, it is mainly available at the time of the highest rainfall. In many rice growing area irrigation water can in fact be considered as only supplementing the local rainy season precipitation, or at the most, extending the cropping season of a few months after the end of the rains (storage reservoirs are still rare, river base flows are low). Where storage facilities do exist, cropping calendars can be obtained from the agency in-charge.

2.3.2. On Java, the rainfall is generally sufficient during the rainy season to sustain at least one crop of rice (Oldeman, 1975). It is therefore a fair generalization to say that during the rainy season, all the land which is physically prepared for wetland rice (bunded fields) supports at least one crop. Irrigation can then be considered as supplementing the rainfall.Because of the large influence of orographic lifting on rainfall, the high lands generally exhibit a less concentrated rainfall pattern (with the notable exception of rainfall shadows). Runoff water which is more readily available on mountain slopes and better rainfall usually insure the production

---

[+] three crops in a year are reported but rare

[++] a secondary crop in *sawah* (*palawidja*) can be constituted among others by cassava, corn, sweet potatoes, vegetables, groundnuts, beans, tobacco, ...

of two crops of rice per year.

2.3.3. The physiographic setting of a production area has been found to give extremely valuable indications on the crop water environment (Malingreau, *op.cit*). Elevation, topography, hypsometric characteristics, relative setting in the landscape, ratio catchment area/area of utilization, are important parameters which can be derived from such an analysis. Additionally, the present cropping pattern reflecting the present utilization by the farmers of the local set of seasonally variable resources can also be taken as an indicator of water availability in a given area. As indicated in part 4, these observations are of pivotal importance in a remote sensing approach to crop monitoring.

2.3.4. The air temperature is very uniform during the year and, except at high elevations, has no prominent effect on rice growth. Improved varieties show very little or no photoperiodic sensitivity; seasonal varieties show a relative flexibility in their planting time because it is the panicle primordia initiation and thus the time of harvest which is controlled by day-length (Tanaka, 1976). There is therefore no "obligated" uniform date for planting rice in a given area; field water availability determines the time of nursery and field preparation. And although the basic division between the dry and the wet season broadly sets the cropping pattern - especially in low lands with pronounced dry seasons - it is not uncommon to find, over a small area, fields at almost any stage of growth. Overall crop calendars are therefore to be 'modulated' by weather and hydrological data. Table II illustrates this important characteristic of the physiognomy of a rice growing area, it gives the monthly harvested area expressed as a % of the yearly harvested area for three districts (*Kabupaten*) in West Java. It can be easily observed that the monthly distribution of harvested area is more even as the altitude increases; correlation with rainfall patterns can be established.

2.3.5. Floods in the rainy season and drought in the dry season are the two water related limitant factors to be considered. Plant resistance to stress is related to the intrinsic tolerance characteristics of the planted variety, the intensity of the event (as measured for example by the number of days of its occurence) and its timing. Critical stages can be recognized. It is usually possible by field survey to establish the flood/drought situation of a given area for years of average weather conditions. In a monitoring scheme, it will however be necessary to determine on a regular basis (i.e. monthly[+])
- the area affected by the event at each level of intensity
- the stage of the crop
- the yield loss
- the non-harvested area.

2.3.6. There is a land classification used locally for determining the real estate value of *sawah*. It is primarily based on a detailed up-to-date assessment of water availability conditions at the field level.

2.3.7. Water discharges data in irrigation systems are seldom available. The present cropping pattern especially in the dry season has been found to be a good indicator of general irrigation conditions (Malingreau, *op. cit.*).

2.4. The number of rice varieties which are planted is very large. An increasing share of the planted acreage is however occupied by improved varieties (30 - 35% at the national level - McIntosh, 1975). Determining the extent of the adoption of high yielding varieties (HYV's) is an important element of the evaluation because of its overriding influence on the production (differential responses to inputs). It is however not easy to assess on a distributed geographical base. Participation to the intensification programme (BIMAS-INMAS) is one indicator of the use of HYV's (improved seeds are part of the package); the technological level of the farmers or the state of the irrigation systems are others. But the adoption of

[+]daily water balances which are often recommended for crop production studies cannot realistically be contemplated in regional studies of this sort.

improved varieties is also much influenced by socio-economic considerations, local customs and taste preference and by the previous year performance of the crop (resistance to pests). The crop duration (transplanting-harvest) and the relative duration of each stage vary considerably from one variety to another (Table III); the average local temperature(correlated with elevation) will also determine the length of the growing period.

2.5. Given the very large variability of *sawah* conditions which can be found at any time of the year, it is important, when remote sensing data collection is contemplated, to define a series of possible types of land cover observed in actual field situations (these will later be translated into photophenological stages assembled in a"photo-crop calendar"- Hay, 1974). Seven main types of land cover associated with wetland rice cultivation can be observed :

1. dry soil : in dry season mainly; the color depends upon the soil type and the presence of organic material.
2. flooded field : during field preparation stage; the water depth varies from 1 to 10 cm. The water can be clear or muddy.
3. growing crop : the cover is partitioned between water and green matter until the canopy is closed. The correlation between % cover (or LAI) and the phenological stage depends largely upon the variety (tillering, leaf geometry) (IRRI, 1970).
4. maturing crop : progressive yellowing of the plants.
5. stubble : after harvest the stubble and straws are left on the fields until plowed in for the next crop.
6. secondary crops or grass : with particular land cover characteristics; field are usually not flooded.
7. burns are frequent in some areas(clearing before plowing).

2.6. Experimental results in the Philippines have shown that because of a higher level of solar radiation, the dry season yield may be 25% higher than the wet season one (IRRI, 1972).The same observation has been made by numerous other authors (Moomaw, 1964. Roumasset, 1976)+. Evidence of differences between the two seasons yields is however difficult to detect in aggregated data; this is thought to be mainly due to the fact that water is, during the dry season, an important constraint offsetting the beneficial effects of higher radiation.

2.7. The level of fertilizer application can much vary from one farm to the other; however aggregate values seems to be related to the farmer awareness of the technology (participation to intensification programs), the adopted cropping pattern and the irrigation status of the area. Urea and triple super-phosphate are the most commonly employed fertilizers (mixed in 3 or 4 to 1 proportions). The 1973 figures indicate that the level of fertilizer application in the four Javanese provinces is still below half of the amount which would maximize grain yield (Table IV). It is likely though that if the present trend remains (12% annual growth in fertilizer use between 1964 and 1975), fertilization will not be a major limiting factor to maximum production. Some production functions such as the one given in figure 1 are available from experimentations on Java and are very useful for studying the response of various rice varieties at different levels of nitrogen applications.

2.8. Large pest outbreaks are frequent and are considered as very serious constraints to production. Among the most frequently reported pests are the leaf- and grasshoppers (*wereng*), the army worms and the stem borer. The *wereng* is almost ubiquitous and may cause extremely heavy damages in some areas (100 % losses are sometimes reported). Epidemiological studies which could serve as the basis for accurate monitoring and prediction development are not available. Rats also take a heavy toll on field crops. Reports seem to indicate that their population is on the increase in paddy fields (losses of up to 20 % are reported).

2.9. The observations made in all the above points related to the large variety of crop environmental influences, cultural practices and types of land covers, raise the problem of defining units of production having a certain homogeneity in terms of resources endowment, field operations (temporal dimension) and visual (image) characteristics. A tentative hierarchical classification of the levels of aggregation which can be recognized in *sawah* is given in Table IV.

+) see also vanIttersum (1972) who has calculated potential rice yields at various latitudes on the base of radiation levels.

3. CROP PRODUCTION MODEL

3.1. CROP PRODUCTION MODELING

Crop production modeling is basically concerned with predicting the condition of the crop at the time of harvest through a constant or time punctual evaluation or measurement of its performance during the growing period (Park, 1976). Crop models can be based on the measurement of a single set of crop cultural or environmental factors. Examples of this type of models are the agro-meteorological models such as the one developed by Robertson (Robertson, 1973) or the "true" remote sensing models such as the one based on crop multispectral reflectance characteristics (Colwell, 1975) or on the crop stress degree day (Idso, 1977).

More often though, various crop models are of the hybrid type in the sense that they make use of sets of variables related to crop parameters. The LACIE project for example makes use of remote sensing, statistical and climatological yield models, in combination, for monitoring and forecasting wheat production in the Great Plains of the United States (McDonald, 1977).

The wetland rice crop production model (CPM) which is presented hereafter in its conceptualized form is basically a hybrid-type monitoring model. Inputs are indeed derived from agronomic, climatological and hydrological observations supplemented by a remote sensing approach to data collection. As already indicated in the introduction it has been felt that prior to allowing the use of a prediction function itself, any mechanism of crop production evaluation must demonstrate adequate monitoring capabilities. In a situation such as the one found in Java where crop growing conditions and farming activities are highly diversified both in time and space, an intermediate monitoring system could already provide extremely valuable information on "what is actually going on". This type of information is indeed very slow and difficult to collect by conventional means. Consideration of a predictive nature have therefore been excluded at this stage.

The difficulty of devising a viable wetland rice production model in such a complex agroecosystem is by no means underestimated; the development of such a model is therefore seen as a process of an iterative nature which can be summarized as follows.

The first step focuses on the statement of the problem as perceived during preliminary contacts with field situations. This also allows the setting of time and space limitations of the analysis. The second step consists in the formulation of the model itself. It is performed in two distinct phases : all the variable directly and indirectly influencing crop production at a regional level are first exhaustively reviewed, and then hypotheses are expressed regarding the relationships linking the various model components.Relationships considered as the most relevant for the understanding of the system under study are analysed in priority. At this stage the model is considered as being "conceptual".

The initial model is then progressively modified in the light of inferences drawn from the collected data or, in other words, the conceptual model is progressively adjusted to the "real world" as this latter becomes better understood. The last two steps include calibration and testing. The calibration involves the adjustment of model parameters within the stratification framework until an acceptable fit between observed and calculated data is achieved. An independent testing is usually added before the model is put in a fully operational mode.

At the present time our research is seeking to identify the major model components and to establish how they interact in a geographical reference system (landscape stratification).

3.2. THE NATURE OF CROP PRODUCTION

The proposed CPM has been divided in two dependent sub-models :

- a Crop Area sub-Model (CAM)
- a Crop Yield sub-Model (CYM)

The following discussion on the nature of agricultural production will help to clarify the subdivision which has been proposed.

The agricultural production is the result of the crop performance (Yield) over a certain area (Acreage) or

$$P = Y \times A$$

$$\text{tons} = \text{tons/ha} \times \text{ha}$$

The acreage can be taken as planted acreage (A_p) or harvested acreage (A_h). The difference between the two being the abandonned area (A_a) (*fuso*). A_a can also be considered as the A_p over which Y = 0.

In Indonesia, separate estimates of planted area, harvested area and yield are made on a monthly basis per sub-district. The final production estimate being the sum of the individual production estimates progressively aggregated from the local to the national level. Planted and harvested acreages are reported by the farmers to their village chiefs who in turn report to the agriculture agents; yields are estimated from test plots distributed over the sub-districts.Crop reporting units therefore coincide with the regular administrative units subdividing the whole territory of the country. These units can, and often do, encompass a large and heterogenous territory.

A more natural approach is to stratify a given region in homogeneous production areas (HPA). An homogeneous production area is a portion of the landscape considered as having a certain degree of internal homogeneity in its endowment in production resources. It can be characterized by a given cropping pattern (i.e. 1 or 2 crops a year or more) and by a given yield level.

The production in the i^{th} HPA is

$$P_i = A_{h.i} \times Y_i$$

The total regional production is given by

$$P = \sum_{i=1}^{n} (A_{h.i} \times Y_i)$$

The delineation of the HPA requires the definition of a set of stratification criterias. Dealing with wetland rice and its extreme dependency upon an appropriate water supply (irrigation and rainfall), water availabillty comes naturally to mind as a first criteria of stratification. This parameter (already widely used as a qualitative sense in agroeconomic surveys) has a direct influence on the size of the planted area in the HPA, the A_h / A_p ratio and the yield level which can be attained. Water related parameters can be devided in two groups : climatic and hydrologic. In the present study, a large basin (400,000 ha) has been divided according to a corresponding two levels stratification scheme. In a first step the area is divided in agroclimatic zones following a rainfall pattern classification defined by IRRI for wetland rice (IRRI, 1974).

The second step makes use of the correlation which has already been noted above between the surface water availability conditions of an area and its physiography (Malingreau, *op. cit.*). The relevant physiographic units are delineated on air-photos and topographic maps.

A third level of stratification has been added to take into account the actual cropping pattern and the agrotechnical level of management which may vary within the strata defined above. The Table III summarizes the criterias of stratification at the three levels.

The subdivision of the landscape into homogeneous production area presents noteworthy advantages :

- it allows the evaluation of crop performance on a more sound ecological base.
- it allows the "unpacking" of highly aggregated census data in a more agronomically suited space and time dimensions.
- it is well suited to remote sensing techniques of data collection which allow the measurement of physical processes in a distributed rather than lumped model.
- it increases the efficiency of on-site sampling.

3.3. THE WETLAND RICE CROP PRODUCTION MODEL

The generalized crop production model can be expressed as follows

$$(CPM) = (CAM) \times (CYM)$$

or the crop production is the result of the interaction between a crop area model and a crop yield model (they have been called sub-models in the present study). The CAM and CYM are dependent sub-models for in a context of limited production resources (i.e. water, labor) the yield will be somewhat acreage dependent.

A series of requirements/assumptions which are to be taken into account in the model formulation are listed hereafter :

- the production model is operated at the HPA level which is considered homogeneous in its endowment of production factors.
- the biophysical environmental parameters are considered as acting on the crop within an agrotechnical framework defined at the third level of the stratification; a series of assumptions related to crop responses to these parameters are to be accepted during the first stage of model formulation. These assumptions mainly pertain to the representativity of experimentally derived crop production functions.
- model parameters have to be as possible amenable to easy field collection and remote sensing measurement.

3.3.1. sub-MODEL I : THE CROP AREA MODEL (CAM)

The land use situation on Java is such that very little additional land can be put under *sawah* cultivation[+]. Each HPA can therefore be characterized by a maximum area (A max-fixed variable) which within its confines is terraced for wetland rice production.

The seasonally planted area can be evaluated by the application of a land utilization function (LUF) to the maximum area

$$A_p = (A_{max} \times LUF)_{\text{per season}}$$

$$\text{with} \quad 0 < LUF < 1$$

The time framework in which this formula is applied is the season (example in Table VII). Yearly values of planted area do indeed not allow the application of season specific environmental parameters of crop performance. As the time of planting during the season is also of relevance in the present model, A_p values are monitored on a monthly basis and then aggregated per season.

The LUF is determined by

- the water availability at the beginning of the season[++]. It can safely be assumed that in normal years the rainy season planted area is close to the maximum area, (otherwise the presence of *sawah* would be unjustified); the dry season LUF value will vary between 0 (i.e. for rainfed *sawah*) to 1 (fully irrigated *sawah*).
- the adoption of certain cropping pattern which is sometimes conditioned by factors other than water availability (i.e. economic incentives, prophyllaxy).
- the risk factor : in unreliable water availability conditions, the farmer will speculate on the probability of receiving an adequate amount of irrigation water at critical periods. The rainfall pattern at the end of the rainy season seems to be influential in the farmer decision to plant a dry season crop in poorly irrigated area (Malingreau and Trojer, 1977).
- the labor availability : although it is assumed that labor distribution can have some influence on the staggering of planting operations at the onset of the season it is not considered as a limitant factor in a seasonal perspective.

Instead of using the harvested area value for calculating production we have elected to keep the planted area value up to the end of the crop season and to apply to it a zero yield if the crop has not been harvested. In this event the production per HPA can be represented by the

---

[+]Between 1963 and 1973 the acreage extention of *sawah* was only of 4% on Java (1963 and 1973 Agricultural Census).

[++]Rainfall and acreage have been found to be highly correlated on Java (I.S. Park, 1975).

following formula :

$$P_{HPA} = [\{A_{p.1} \times Y_1\} + \{A_{p.2} \times 0\}] \text{ for the season}$$

with $A_{p.2}$ being the non-harvested area.

This approach seems to be more compatible with a spatially distributed monitoring procedure in which the actual location of the failing crop is sought after. It also makes allowance for clarifications concerning the "no yield" situation. Additionally, remote sensing monitoring models will usually make the "season start" difference between planted and non planted areas,but will not be able to account for non-harvested areas.

3.3.2. sub-MODEL II : THE CROP YIELD MODEL

Several type of crop yield models are presently under testing or, in some instances, already applied to operational situations. Four main kinds can be recognized; the regression type models such as the factorial yield weather model proposed by Robertson (*op.cit.*), the growth models (deWit, 1965. Milthorpe, 1974) where biomass is calculated by simulating assimilation processes during the plant development, the recently developed deterministic models relating crop phenology (as measured by multispectral sensors for example) and yield estimates (Colwell, *op.cit.*), and the relative yield models (also called yield reduction and loss function models) increasingly applied in socio-economic studies such as the ones related to constraints identification(IRRI, 1975. Herdt, 1975)+.

The loss function model has been adopted in the present study because it is considered the most appropriate in situations where data are scant and for use in a remote sensing oriented approach. The model can be expressed as follows (Fig. 2) : if we assume that at the time of planting, the crop, submitted to a local set of bio-physical environmental influences has the potential to reach a certain yield called 'potential yield' (Y_{pot}), we can consider the actual yield (Y_{act}) obtained as a result of agricultural management, as a fraction of the potential yield or,

$$Y_{act} = Y_{pot} \times \text{loss function}$$

In applying this model for assessing rice yield constraints, Herdt (Herdt et al, 1975) makes the distinction between "maximum possible yield" and the "maximum potential yield obtained in the farmers environment". The first value is the yield which can be obtained in a given site when all the crop production factors are optimal (best combination of environmental and management factors in ideal experimental situation).The "potential yield" is considered as the yield which the farmers can reach by making the best use of the production resources existing in his particular site and within the present socio-economic circumstances.
Although on purely agronomic grounds,arguments strongly lean in favor of using the "maximum possible yield" concept, we have elected to retain the farmers "potential yield" one. This decision is mainly pragmatic. Indeed, masimum possible yields can only be obtained in careful experimental settings which are still rare in Indonesia. Additionally, preliminary field observations lead us to believe that the potential yields are fairly well represented by those obtained in the demonstration plots (DEMPLOTS) now being established in many villages. These are fields cultivated by renowned "good farmers" using production resources within their reach and under the best management scheme available to them (use of HYV's fertilizers and pesticides package, support from extension services).

In each homogeneous area defined above we will therefore use an average productivity value of Y_{pot} derived from the DEMPLOTS located within its confines

$$Y_{pot.\ HPA_i.\ var_n} = \bar{Y}_{DEMPLOT.\ HPA_i.\ var_n}$$

on a seasonal basis

These potential yields can only be calculated for the improved varieties (they are indeed the only ones planted in the demonstration plots); the results can obviously not be translated into

+see also Hall, 1970. Wang, 1963. Nix. 1969. Feyerherm, 1977.

yields of local varieties. A detailed assessment of varietal yielding ability derived from still scanty field experiments and farm observations appear difficult to achieve at this stage and very general yield values are to be retained for local varieties.

The application of a loss function necessitates an evaluation/measurement of the effect of constraints during time increments coinciding with crop life development stages. In a practical monitoring perspective, these time increments are chosen to coincide with crop growth stages and field practices but also with "visual" crop canopy characteristics (photo-phenological stages). The division of the crop life into phenological and tentative photo-phenological stages is given in Table VIII together with a summary of the *sawah* visual characteristics at each stage.

Three production factors only have been included as variables in the present model, namely: water availability (precipitation and irrigation), occurence of pests and diseases and radiation level during the last 45 days of the crop. Other production factors such as the use of improved varieties and fertilizer application are considered as fixed seasonal parameters characterizing each homogeneous production area (TABLE IX).

Evaluating the impact of stress on a potential yield remain a difficult operation, especially when carried out over large areas. This impact is a function of the stress and the time of its application during the biological time scale defined above. Production functions established in experimental conditions can provide some background support to the evaluation but are obviously limited because not including interaction effects as they may apply in a specific spot. In the absence of detailed field water measurements, we also have to report to the simpler "stress-day" concept as defined by Godwin (1971) : it is the "number of days, accumulated over the whole crop duration or portions of it (i.e. critical period) during which the stress intensity is greater than a prescribed value". For all practical purposes, a wetland rice field may be considered under stress as soon as the soil moisture level is below saturation, or as soon as there is no water pondage. This criteria has been used by Whickham(1973) for large area water balance modeling. Locally derived information on varietal recovering abilities after drought or flood are also precious when trying to decide on treshold values beyond which the conditions become limitant.

The impact of pests and diseases seems to be even more difficult to evaluate and there is a great deal of guess work involved in this operation. The first information sought after is evidently the "where" and "when" of the pest attack. The intensity of the attack is then to be assessed. No present information gathering system is able to collect those data on a short time basis. Varietal resistance and application of pesticides are also to be taken into account. Estimates are made in percent of crop losses derived from field observations and interviews.

The following list includes the data necessary for operating the proposed model per land stratification unit (HPA). In order to link these "data requirements" with an analysis of remote sensing potential for collecting them, the subdivision per photo-phenological stages has been retained (see TABLE VIII).

General HPA parameters : A_{max}
Type of *sawah*; agroclimatic zone
Agrotechnical level
Level of fertilization
Use of varieties (HY's and Local in %) Area.

t_o : field preparation, nursery stages

time increment : n_o days
decision variables: area under preparation
state variable : rainfall, runoff

t_1 : transplanting

time increment : n_1 days
decision variables : A_p planted area
planted varieties % of A_p
state variables : rainfall
number of days with/without standing water

, number of days of excess flooding

t_2 : tillering -maximum tillering

time increment : n_2 days
decision variables : -
state variable: rainfall
number of days with/without water
pest outbreaks (% A_p)
crop parameter: LAI; % ground cover
multispectral characteristics

t_3 : reproductive stage

time increment : n_3 days (constant for varieties)
decision variables: -
state variable : rainfall
number of days with/without standing water
pests outbreaks (% A_p)

t_4 : ripening and harvest

time increment : n_4
decision variable : A_h
state variables : pests, rats (% A_p)
number of days with/without water
radiation level during ($t_{harvest}$ - 45) days

End of season HPA Y_{pot} from DEMPLOTS and field observations.

4. REMOTE SENSING INPUTS

As already indicated in the introduction, little research has been done so-far on the applicability of remote sensing technology to the study of agricultural production in the tropics. It seems therefore justified to carry this short review of possible inputs in a crop production model at a potential as well as actual perspective. Both approaches are however very much user oriented and the conclusions presented hereafter are the result of a "matching" between model data requirements as reviewed in the previous parts of this paper and sensor capabilities.

Inventory and monitoring are the two modes under which operational remote sensing is to be examined in the present context. Inventorying production resources pertains to the assessment of the nature, location and extent of the permanent elements of the environment supporting the crop and monitoring crop production consists in collecting time related data (repetitive observations) on both crop environmental variables (water, pests, nutrients) and crop intrinsic parameters(such as areal extent and growth stage). These two modes will respectively preside to the recognition/ stratification of rice growing areas and the evaluation of the seasonal conditions influencing the crop performance (Fig. 3).

4.1. INVENTORY

The inventory aspect of the use of remote sensing imagery assumes a particular importance in the process of stratifying the landscape into homogeneous production areas. Stratification necessitates at first the identification and delineation of the *sawah* area (viz. the area permanently terraced for wetland rice production). This can be easily done on small scale air-photos(1/50,000). On satellite imagery the accuracy of delineation of *sawah* will very much depend upon the time of photography and the type of land cover/land use complexes of which rice fields are part.A general observation is that the imagery acquired at the end of the dry season (when most of the fields are fallow) allows a better identification by contrast between the dry level *sawah* soil and the surrounding land usually occupied by evergreen plants (mixed gardens, homestead gardens,swamps...) or irregular soil surface (plowed dry fields) (Malingreau, 1975). Since the signatures of large rice growing areas are a composite of many individual land cover signatures, the determination, for each strata, of the period of the year during which spatial variability is minimum will help to refine this selective time punctual inventory procedure. However, as indicated earlier in the

description of *sawah* this ideal uniform "physiognomy" might never be observed in many areas; it is therefore important that any proposed remote sensing system exhibits an "all stages" *sawah* identification capability (see section 4.2.). The second step in the stratification is to analyze the "setting" of an area of production in the landscape[+]. This physiographic approach to *sawah* classification (Malingreau,1976) is easily amenable to remote sensing data collection techniques and it has been performed with success over large areas using small scale air-photographs. These results in fact lead us to assume that the complete 1/100,000 scale air-phptographic coverage of the whole of Indonesia will represent a major tool in an approach of this sort. The LANDSAT images do not yield consistent results in this respect because of the lack of stereoscopic coverage and the quasi absence of shadows due to an already high sun angle at the time of overpass. Further work is being conducted using the multistage approach.

The third level of stratification retained in the present model necessitates the collection of field data on cropping patterns and agrotechnical levels of management. This field exercise can be largely facilitated by a prior analysis of air-photos and satellite images for directing the sampling procedure. Additionally, as shown in the following section, the monitoring of an area will provide most of the necessary information for establishing the local cropping patterns.

4.2. MONITORING

4.2.1. The identification of the rice crop stage

Crop growth is a dynamic process submitted to time related environmental influences which, in order to evaluated, must be under constant or repeated selected time punctual observations. Since most of the crop factors act differently upon the crop depending upon its stage of growth/development, the first required characteristic from a remote sensing system of data collection is an ability to usefully discriminate between the most critical of those stages. This capability would in addition insure an all time *sawah* identification.

In the course of this analysis it has been found that a certain compromise had to be made in the choice of photo-phenological stages; visual analysis alone of multispectral imagery does indeed not allow the identification of every desirable phenological stage of rice growth and a grouping has to be made; this aggregation unfortunately prevents the precise identification of important stages such as the transplanting and the panicle initiation/heading. Transplanted rice can only be detected after 15 to 20 days by infrared photography even at very large scale(1/5,000) and it is expected that the first day of plant visibility is not less than that value for LANDSAT images. The spectral reflectance changes occuring in the plant canopy during the phasal development of rice varieties has not yet been studied in detail and it is difficult with the presently available multispectral imagery to segregate the reproductive phase from the vegetative one. Once the canopy has reached full cover the only observations performed so far is the lightening in color at the start of the ripening period. Obviously the complex spectral signature behaviour of the crop will much depend upon the time interval or overlap between LAI development, maximum tillering, panicle initiation, heading and flowering. Varietal characteristics and environmental conditions are important parameters in this respect (Tanaka, *op.cit.*).

The total field preparation/plant cycle/harvest period has been divided into five photo-phenological stages which are described hereafter. The accompanying reflectance curves have been derived from a rough evaluation of total values of each stage in the four LANDSAT bands (green, red, infrared I, infrared II), supplemented by large scale multispectral imagery analysis.

Photophenological stage 1. Field preparation and early transplanting period. (Fig. 3a)
The area appears dark to light blue on the infrared color composite. The fields exhibit higher reflectance characteristics in the green and red bands if the water contains sediments. Geometric patterns can often be identified because the fields are usually irrigated by groups (*golongan*) under the command of a unique secondary and tertiary canal. Contrast is good with surrounding dry or planted area. Confusion may arise with burned areas.

[+]The setting in the landscape has been found to be a major factor determining the endowment of an area in production resources (mainly water).

Photophenological stage 2. Growing stage to full cover period (Fig. 3b).
From 20 to 25 days after transplant, changes in field reflectance due to growing vegetation will begin to appear. The color composite image goes from a blue to pinkish blue, bluish red and finally bright red. Because of the progressive covering of the water layer by vegetation, the green and infrared reflectance will increase as the red one will stay more or less stationary or decrease progressively if during the stage 1 the field was covered with muddy water. The detection of differential growth modes and rates between varieties would necessitate a closer sequence of images than what is available at the present time[+].

Photophenological/stage 3. End of growing stage, reproductive stage and beginning of ripening (Fig. 3c).
The field being almost fully covered by green vegetation shows a typical vegetation reflectance curve. As indicated above, crude image analysis does not reveal changes during this stage. The determination of the exact timing of panicle initiation and heading presents however some importance for evaluating the impact of water stress on production[++].

Photophenological stage 4. Ripening. Progressive yellowing of the crop up to harvest (Fig. 4d).
The color composite image shows a change from red to light red and then yellow color. This stage is associated with a slight increase in reflectance in the green and IR bands and a sharp reduction in red wavelength absorptance.

Photophenological stage 5. Post harvest period.
The ground is usually covered by broken stalks (in the traditional harvesting method, only the panicle is removed with a small hand-knife). Water may already be brought onto the field for the next crop. This shows up as overall lowering of reflectance values in all bands. The color composite image appears brownish.

When used in conjunction with appropriate field controls, a time discriminant analysis such as the one described above can clearly provide a sound base for "driving" a crop production model. The major bottleneck in applying this monitoring method in the tropics is the lack of acceptable sequence of images because of high cloud coverage (see Section 4.3.). Additionally, field observations and real time analysis of large scale multispectral images of *sawah* have shown that varietal (crop intrinsic) characteristics and environmental influences play a determinant role in the dynamic behavior of the reflectance properties of the canopy. This introduces undue complications in any tentative to generate a set of multispectral curves corresponding to crop system. Clearly, one has to resort here to spectral values frequency analysis whose complexity requires digital processing.

4.2.2. The identification of rice varieties.

The acreage of planted varieties classified in a first approximation as 'High Yielding Varieties' and 'Local Varieties' is an important parameter to be seasonally assessed in a regional model. Two main sets of identification clues have been used in this respect. They both necessitate the compilation of fairly detailed ground truth data. Spectral varietal differentiation is the first method which comes to mind has being the closest to visual identification of plant varieties. It is of common observation indeed that HYV's have a darker green color than the local varieties. The geometry of the plant is also quite different (HYV's have erected leaves). Fields planted with HYV's can be easily be detected and identified on color infrared and red large scale multispectral images taken during the vegetative phase of the crop. They exhibit a deeper red coloration on the former (higher reflectance) and a darker tone on the latter (higher absorptance). The second approach to differentiate between varieties is to make use of local cropping patterns. Because of the different length of their growing periods, the two groups of varieties will not follow the same calendar. Imagery taken at the time of harvestof one variety for example will show field planted with the other by contrast; areal proportions have been measured with succes on large scale multispectral imagery using this procedure. It requires however the collection of often highly localized cropping patterns data. Stratification is difficult because each farmer tend to be very independent in his choice of variety. The LANDSAT images have not been analyzed for varietal differentiation because of the lack of real time ground truth data.

[+]Research needs in this respect are reviewed in "The use of remote sensing technology for the study of agriculture production in Indonesia". Malingreau, 1978, in preparation. Center for image Interpretation and Integrated Survey, UGM. Yogyakarta.

[++]Cfr. Idso 1977 and his analysis of albedo increase at heading stage for irrigated wheat.

4.2.3. Monitoring the crop growing conditions.

The monitoring of crop growing conditions provides the basic data on which to evaluate the loss function applied to the potential yield. Two limiting factors are reviewed hereafter, namely water stress and pest attack. When reflecting on the usefulness of a remote sensing system having the capability of monitor drought or pest induced crop stress, an important aspect of its applications comes immediately to mind. This aspect pertains to the function of a "warning system" in a crop protection/ development framework. What is required indeed from advanced technology is not only to merely confirm ground observations (which are in fact quickly and accurately made if only slowly aggregated); instead,remote sensing observations should either precede ground observations (pre-visual stress detection) either allow the expansion of point field observations in the two dimensional plane (spatial aspects). In order to make maximum use of either approach, a review of the relevant affects of stress on the rice crop is essential. Such a review is only partly available to-day and its operational value is still questionable. Thus the likelihood of obtaining early detection of stress over large areas using the presently available technology still appears very low.

It is generally accepted that a maximum rice yield requires the field to be maintained under flooded or saturated conditions. The objective of monitoring will therefore be to assess pondage/ non pondage situation during the growth of the crop paying particular attention to specific critical stages such as rooting, panicle formation and heading. This seemingly simple observation is however difficult to make over large areas by conventional field reporting methods. Remote sensing technology presents the potential to provide some of these important water related data; a literature review suggests however that early claims of detecting crop stress from orbiting satellite have so far exceeded accomplishments and that operational crop water status remote sensing monitoring still presents many difficulties. For lack of solution within our present reach we will therefore apply ourselves to a clear statement of the problem. The capability which will be required from a monitoring system is simply to descriminate between field "saturation/no saturation" conditions on a repetitive base (once every other week) for the duration of the crop over an homogeneous production area. Direct water observation can be made up to the time of closing of the crop canopy (depending upon the varietal LAI development characteristics). After the 100% canopy closure has been reached,indirect clues such as changes in crop reflectance or differential crop-air temperature (Idso, *op.cit.*) have to be used. The approach is summarized in figure 5.

Pest attack as well as drought usually results in changes in the flux of energy reflected or emitted from the altered vegetation as compared to healthy one. Visual observations of pest manifestations (yellowing of leaves, wilting, reddish spots, sclerotic aspect ....) are commonly used as diagnostic criteria in ground surveys. The increase in reflectance associated with the attack and its detection by photographic multispectral methods have been documented by DeCarolis (*op.cit.*) who also mentions the possibility of segregating "healthy rice" from "sick rice" using thermal infrared scanning. Large scale IR and red air-photos of rice growing areas in Java have also shown color/tone variations related to crop stress status. Quantification of the effect of the stress on production is however difficult for lack of transform functions between deviation of reflectance properties from the normal and yield loss+.

4.3. LANDSAT AND WETLAND RICE MONITORING IN INDONESIA.

The NASA Earth Resources Satellites are frequently mentioned as having been successfull in supporting crop production data collection exercises. This assertion has however not been clearly validated in the case of rice in the tropics. In Indonesia, for example, there is indeed a whole range of technical, manpower and institutional roadblocks preventing the broadscale application of the orbiting platform imagery to agricultural inventories.

The major technical problem affecting the availability of imagery originates from the fact that the much praised sequential coverage ability of the satellites has not yielded the expected results during the last five years of the two LANDSAT's operation.Only 2.6% (frames with 0 - 30% clouds) or 4% (frames with 0 - 50% clouds) of the total number of imaging positions taken by

+Hass (1975) and Carneggie (1975) have addressed this problem in the context of range conditions evaluation. The applicability of some of their approaches to wetland rice is under study.

LANDSAT I and II over Indonesia have produced acceptable images. Cloudiness is obviously an important deterrent to short wavelength multispectral remote sensing in the tropics but the lack of ground receiving station in this region of the world coupled with shortcomings of the on-board image recording devices, and a surprising inactivation of LANDSAT II cameras over the country also contribute to this meager output (Malingreau 1978). The paucity of images available over the main agricultural production areas (Java, Bali) is even further aggravated by the fact that most of the good quality frames are concentrated over one season only as shown by the figure 7. No coverage is therefore available during the rainy season or during the crucial transition between the rainy and the dry season. The bulk of the imagery of Java, Madura and Bali was taken mainly during the few months immediately preceding the rainy season, period during which many fields are fallow.

The ground resolution characteristics of the Landsat imaging system has often been presented as a limitation to accurate agricultural inventories in areas where the size of the fields are less than the resolution value. It is usefull, in this respect however to take account the already mentioned spatial cohesiveness of the paddies which, because of their dependence upon irrigation water, are always present in groups presenting a certain spatial and temporal continuity. It is on the base of those spatial units that the images have been evaluated and although it has been found that the exact location of small sawah areas interspersed with other land use types is often difficult to determine with precision[+], the detection of areas of a few hectares has been successfully performed using a multistage approach in the uplands of Sulawesi (Malingreau, 1975). The optimal time for such an analysis being the dry season when fields in small depressions between hillocks are covered by dry soil and stubble while the surrounding land is occupied by green bush/tree vegetation or dry field with bare roughly plowed soil. The problem of inventorying planted varieties can however not be solved using the LANDSAT images because changes are occuring from one field to another and most of the fields have a surface smaller than the ground resolution. A multistage sampling scheme has to be considered in this case.

The frequency of coverage is also of particular importance when considering the use of remote sensing for monitoring the crop. The improved rice varieties which have a total life cycle of 120 days are visible on small scale imagery for only 90 days of that period (plants are not visible at nursery and transplanting stages). Crop growth is fast and the maximum acceptable interval between two images is estimated at three weeks (4 images over the season). Two weeks seems the optimal (6 images over the crop season). The probability of having this sequence of images with present orbiting system appears dim and serious consideration should be given to all-weather imaging devices planned for the next satellite generation.

5. CONCLUSION

Given the spatial and temporal diversity of wetland rice production systems in Java, it can be readily recognized that a remote sensing system presenting synoptic and sequential capabilities offers definite advantages for the collection of relevant data. Present results of investigations on the applications of this new technology are still limited. The work reported in this paper indicates however that there is a potential for devising crop production data collection systems supported by a whole range of remote sensing products. At this stage the lack of appropriate LANDSAT coverage makes mandatory the adoption of a multistage approach making large use of conventional or multispectral air-photography as well as of satellite imagery. The operational value of such an approach is however questionable on economic grounds alone.

The stratified sampling procedure associated with the present model is based on an assessment of hydro-climatic conditions, cropping patterns and technical level of management, leading to the delineation of homogeneous production areas. This preliminary landscape stratification using combined ground and remote sensing parameter measurements assumes a particular importance when one considers the lack of spatially distributed production data presently available and the large variability of growing conditions which may be found in aggregated standard reporting units. The operation of defining and mapping the HPA's is basic to the proposed approach because it narrows down the range of values taken by environmental parameters which are to be evaluated over specific geographical areas.

Listing the data required for monitoring the rice crop is a necessary step in trying to validate the available remote sensing technology. The present analysis seems to indicate however

[+] in the Philippines, Heydt (1973) had to resort to triangulation to locate field sites.

that a complete reappraisal of this technology in a more regionally (conditions specific) oriented context is necessary. Technology cannot be used alone. If indeed improvements in rice production evaluation present a significant economic importance at a national or regional level (southeast Asia), the problem should be reviewed from the start in a comprehensive fashion taking into account all the technical, institutional as well as economic aspects of this complex agricultural production evaluation system. And then only should the data collection technology be designed and tailored to the expressed needs. Furthermore, the introduction of remote sensing technology in this specific area should be made in conjonction with progressive adjustments of current data collection systems to which data derived from the imagery should be considered as complementary inputs.

ACKNOWLEDGEMENT

The assistance of LAPAN (Jakarta) for acquiring the large scale imagery of the Citarum River Basin is gratefully acknowledged.

BIBLIOGRAPHY

Agroeconomic Survey, 1976. Agricultural census in 33 villages located in major rice producing area of Indonesia. Research Note No. 6. Bogor. Indonesia.

Carneggie, D.M., 1975. Usefulness of Landsat data for monitoring plant development and range conditions in California annual grassland. Proc. NASA Earth Resources Survey Symposium. Houston (Texas).

Colwell, J.E. and G.H. Suits. 1975. Yield prediction by analysis of multispectral scanner data. Final report. NASA CR-ERIM 109600-17-F. ERIM. Ann Arbor(Michigan).

Colwell, R.N. 1976. Some considerations relative to the making of globally uniform resources inventories by remote sensing. Paper presented at NATO-sponsored Advanced Research Institute. Hamilton. Bermuda.

DeCarolis, C. and G.M. Lechi. Relievi da terra e dall'aereo nell'infrarosso fotografico e termico su campi di riso affetti da "giallume". Revista Il Riso. Anno XXII. March 1974.

DeWit, C.T. 1965. Photosynthesis of leaf canopies. Agric. Res. Rept. No. 663. Centre for Agric. Publ. and Doc. Wageningen. 57pp.

Estes, J.E. and L.W. Senger. Ed. 1974. Remote sensing techniques for environmental analysis. Hamilton Publishing company.

FAO. 1974. Yearbook of Crop Production Statistics. Rome.

Feyerherm, A.M., E.T. Kanemasu, and G.M. Paulsen. 1977. Response of winter and spring wheat grain yields to meteorological variations. Final Report Contract NAS9-14282.

Godwin, R.J., W.D. Lembke, and B.A. Jones. 1971. Design of irrigation pumping rates in a humid region. Trans. Amer. Soc. Agr. Engin. 14: 875-878.

Grenville, S.A. Survey of recent developments. BIES. Vol. XII, No 3. March 1977.

Haas, R.H. *et al*. 1975. Monitoring vegetation condition from Landsat for use in range management. Proc. NASA Earth Resources Survey Symposium. Houston (Texas).

Hall, W.A. 1970. Some problems in the application of systems analyses in water resources systems. Proc. IId. Int. Seminar for Hydrology Professors. IHD.

Hay, C.M. 1974. Agricultural inventory techniques with orbital and high altitude imagery. Photogrammetric Engineering 60(11).

Herdt, R.W. and R.H. Bernsten. 1975. Methodology for assessing rice yield constraints. International Rice Agro-Economic Network. Working Paper 2. Intern. Rice Res. Inst. Los Banos. Philippines.

Heydt, H.L. and A.J. McNair. 1973. Engineering analysis of ERTS data for Rice in the Philippines. Proc. Symp. A.S.P. Management and Utilization of Remote Sensing Data. Sioux Falls (SD).

Idso, S.B., R.D. Jackson and R.J. Reginato. Remote sensing of crop yields. Science. Vol. 196 : 19-25. April 1977.

International Rice Research Institute. 1970. Rice Production Manual. Los Banos. Philippines.

International Rice Research Institute. 1970. Annual Report. Los Banos. Philippines.

International Rice Research Institute. 1974. An agroclimatic classification for evaluating cropping systems potential in Southeast Asia rice growing regions. Los Banos. Philippines.

International Rice Research Institute. 1975. Annual Report. Los Banos. Philippines.

Ismunadji, M., I. Zulkarnaini, A. Prawirosamudro and F. Yazawa. 1973. Productivity of some major Java soils with special reference to yield and nitrogen nutrition of lowland rice. Contr. Central Res. Inst. of Agr. No 7. Bogor. Indonesia.

LeToan T., P. Cassirame, J. Quach. 1977. Inventory of rice fields in France using Landsat and aircraft data. Proc. XIth Int. Symp. on Remote Sensing of Environment. Ann Arbor. Michigan.

Malingreau, J.P. and A. Suroto. 1975. The usefulness of remote sensing technology for land evaluation in Indonesia. Paper presented at the Joint UN/FAO Regional Seminar on Remote Sensing Applications. Jakarta.

Malingreau, J.P. 1976. Cropping patterns and water management in sawah. A case study of image interpretation. FAO INS 72/011. Working Paper No 12. Bogor. Indonesia.

Malingreau, J.P. 1978. It's 9 O'clock! an Earth Resources Satellite must be going over Indonesia. Indonesian Journal of Geography. (forthcoming). Jogjakarta. Indonesia.

Malingreau, J.P., and H. Trojer. 1976. Observations on the agroclimatology and cropping patterns in the Cimanuk River Basin. unpublished. FAO 72/011. Bogor. Indonesia.

MacDonald, R.B. and F.G. Hall. 1977. LACIE, a look to the future. Proc. XIth Int. Symp. on Remote Sensing of Environment. Ann Arbor. Michigan.

McIntosh, J.L. and E.S. Suryatna. 1977. Cropping systems research and implementation. Central Research Institute for Agriculture. Bogor. Indonesia. Annual Report 1975-1976.

Milthorpe, F.L. and J. Moorby. 1974. An Introduction to Crop Physiology. Cambridge Un. Press.

Ministry of Agriculture. Agricultural Census. 1963. Jakarta. Indonesia.

Moore, D.C. and V.I. Myers. 1977. Progress and needs in agricultural research, development and applications programs. Proc. XIth Int. Symp. on Remote Sensing of Environment. Ann Arbor.Michigan.

National Academy of Science. 1975. Practical Applications of Space Systems. Supporting Paper No. 4. Agriculture, Forest and Range. Washington, D.C.

Nix. H.A. and E.A. Fitzpatrick. 1969. An index of crop water stress related to wheat and grain sorghum yields. Agr. Met. 6. pp. 321-333.

Oldeman, L.R. 1975. An agroclimatic map of Java. Contr. Centr. Res. Inst. Agric. Bogor. No 17.

Park, A. 1976. A crop production alarm system. ERTSAT. Washington D.C.

Park, J.S. 1975. Development of forecasting methods for paddy hectarage harvested in Indonesia. Central Bureau of Statistics. Jakarta.

Robertson, G.W. 1973. A factorial yield weather model for wheat. Proc. WMO Symposium.Agrometeorology of the wheat crop. World Meteorological Organization Publ. 396.

Roumasset, J.A. 1976. Rice and Risk. Decision Making Among Low Income Farmers. Nth. Holland Publ.

Soemartono, 1974. Bercocok Tanam Padi. Yasaguna. Jakarta.

Tanaka, A. 1976. Comparasion of rice growth in different environments. in: International Rice Research Institute. Climate and Rice. Los Banos. Philippines.

vanIttersum, A. A calculation of potential rice yields. Neth.J.Agric. Sc. 1971 (10-21).

Wang, J.Y. 1963. Agricultural Meteorology.

Whickam, T. Predicting yield benefits in lowland rice through a water balance model. in: International Rice Research Institute. Annual Report 1973. Los Banos. Philippines.

range of sizes ha	average size ha	% size distribution			
		0-.49 ha	.5-.99 ha	1.0-1.99 ha	2 and more
0.01 - 3.77	0.64	72	14.6	8.9	4.5

TABLE I. AVERAGE AND PERCENTAGE SIZE DISTRIBUTION OF IRRIGATED RICE FIELDS IN THE WEST JAVA PROVINCE (500 HOUSEHOLDS SAMPLE). WET SEASON 1970/71
Source : Agroeconomic Survey. 1976.

Kabupaten	elevation m	Jan	Feb	Mar	Apr	May	Jun	Jul	Aug	Sep	Oct	Nov	Dec	Total ha
Indramayu	0	0	0	1	17	34	16	6	11	14	1	-	-	141,517
Sumedang	300+	2	7	11	21	18	5	3	13	12	6	3	1	53,028
Garut	600+	6	8	6	8	14	12	9	7	6	6	7	11	73,616

Peak values have been underlined

TABLE II. MONTHLY HARVESTED AREA OF PADDY EXPRESSED AS A PERCENTAGE OF THE TOTAL YEARLY HARVESTED AREA FOR THREE REGENCIES (KABUPATEN) IN WEST JAVA.
Source : Lembaga Penelitian Pertanian. Bogor. Laporan Kemajuan No.3. 1976.

Variety	Growing period+
IR - 28	105
IR - 30	110
IR - 34	135
Local varieties	up to 165 days

+including nursery time

TABLE III. GROWING PERIOD OF A FEW PADDY VARIETIES ON JAVA

Province	Kg/ha urea + T.S.
West Java	125.56
Central Java	127,17
East Java	132.33
Jogjakarta	179.83
Java average	141.2
Java average for intensification programme only	172.11

TABLE IV. FERTILIZER USE IN WETLAND RICE OF JAVA
Source : Ministry of Agriculture 1973 Census.

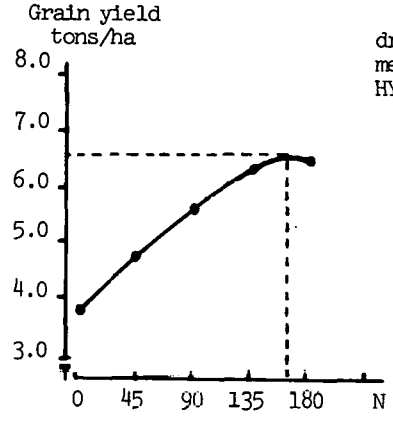

FIGURE 1. GRAIN YIELD RESPONSE CURVE TO INCREASING RATES OF N APPLICATION ON RICE (JAVA). from Ismunadji, 1973.

level of aggregation	corresponding administrative unit (s)	variability of plant and environmental factors within level of aggregation
plant	-	-
field	farm (managerial unit)	. natural biological variability . uneven field conditions
golongan: group of fields . continuity in space . uniformity in time	hamlet, village	. plant variety . inputs: fertilizers pesticides
group of *golongan:sawah* in various physiographic settings . continuity in space . non uniformity in time	village, district	. plant variety . climate: precipitation radiation temperature . water availability . inputs: fertilizers pesticides
region/watershed . non continuity in space . non uniformity in time	group of districts	all of the above
island	group of provinces	idem
country	group of provinces	idem

TABLE V. LEVELS OF AGGREGATION OF WETLAND RICE PRODUCTION UNITS

Level I	: AGROCLIMATIC STRATIFICATION (based on number of months with P>200 mm. IRRI, 1975)
Level II	: PHYSIOGRAPHIC STRATIFICATION and correlation with surface water availability conditions
Level III	: CROPPING PATTERN and AGROTECHNICAL LEVEL (if necessary after level II)

TABLE VI. WETLAND RICE PRODUCTION MODEL. Stratification of the landscape into homogeneous production area (HPA).

	A_{total} sawah (ha)	rainy season 1975 - 76			dry season 1976		
		$A_{planted}$	LUF	A_{harv}	$A_{planted}$	LUF	$A_{harvested}$
Lohbener	5540	5540	1	4543	4489	0.81	1546
Losarang	6789	5889[+]	0.87	2723	1193[++]	0.18	680

[+] flood

[++] water shortage

TABLE VII. LAND UTILIZATION FUNCTION (LUF) PER SEASON FOR TWO SUB-DISTRICTS OF THE INDRAMAYU DISTRICT.
Source : Agriculture Service. Indramayu. Annual Report 1976.

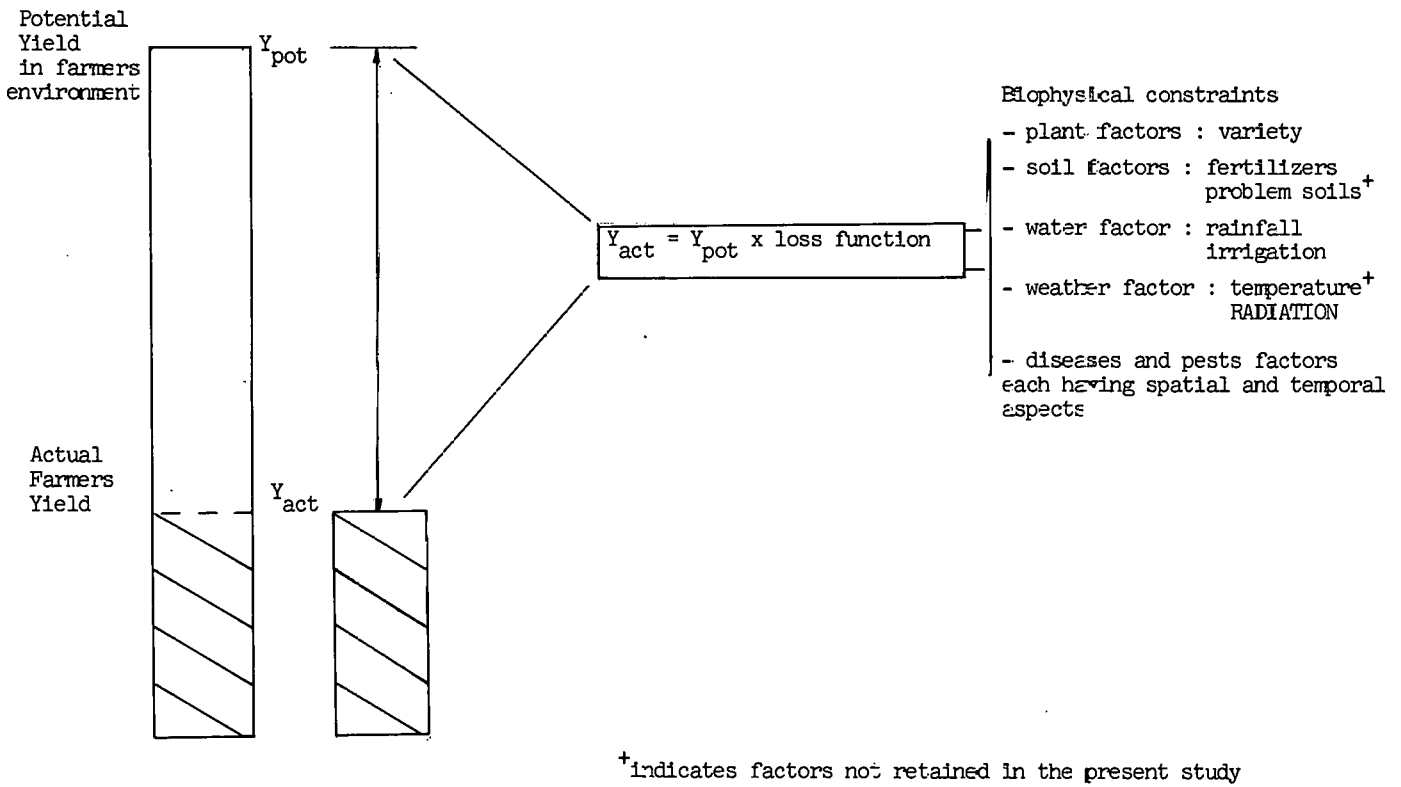

FIGURE 2. SCHEMATIC REPRESENTATION OF THE LOSS FUNCTION OR RELATIVE YIELD MODEL (based on IRRI, 1975).

phenological		photo-phenological stages	land cover	albedo
phases	stages			
FALLOW	-	f	dry soil, stubble	high
VEGETATIVE	t_0 : field, nursery preparation	t_0	water	low
	t_1 : transplant	t_1	water, green seedlings	low
	t_2 : tillering to maximum tillering		progressive closing of water by green cover[1]	increasing
REPRODUCTIVE	t_3 : panicle initiation	t_2	green cover	plateau
	t_4 : heading		green cover	?[2]
	t_5 : flowering		green cover	?
RIPENING	t_6 : ripening	t_3	yellowing/browning of plants	slight increase[3]
	t_7 : harvest		dry plants	?

[1] the time to reach maximum LAI (just before heading) depends upon varieties and environmental conditions; various growth curve types can be identified (Tanaka, 1976); full cover is reached at LAI=3 (Allen, 1968).

[2] Idso (1977) indicates that albedo data appear to exhibit characteristic variations allowing the identification of a critical wheat growth period. No similar results have been reported for rice.

[3] an increase in reflectance of *sawah* close to harvest has been detected on a BW set of infrared air-photographs (Malingreau, 1976)

TABLE VIII. PHENOLOGICAL, PHOTO-PHENOLOGICAL STAGES OF WETLAND RICE GROWTH AND ASSOCIATED LAND COVER

Temporal unit of yield evaluation: the season Spatial Unit of yield evaluation: Homogeneous Production Area (HPA)			
		variables	stratum parameter (ct)
	$Y_{potential}$	-	measured in DEMPLOTS for HYV. From farmers, for local varieties.
	Y_{actual}	· water availability · occurence of pests · radiation level · interactions	level of fertilization agrotechnical level

TABLE IX. COMPONENTS OF A REGIONAL YIELD MODEL

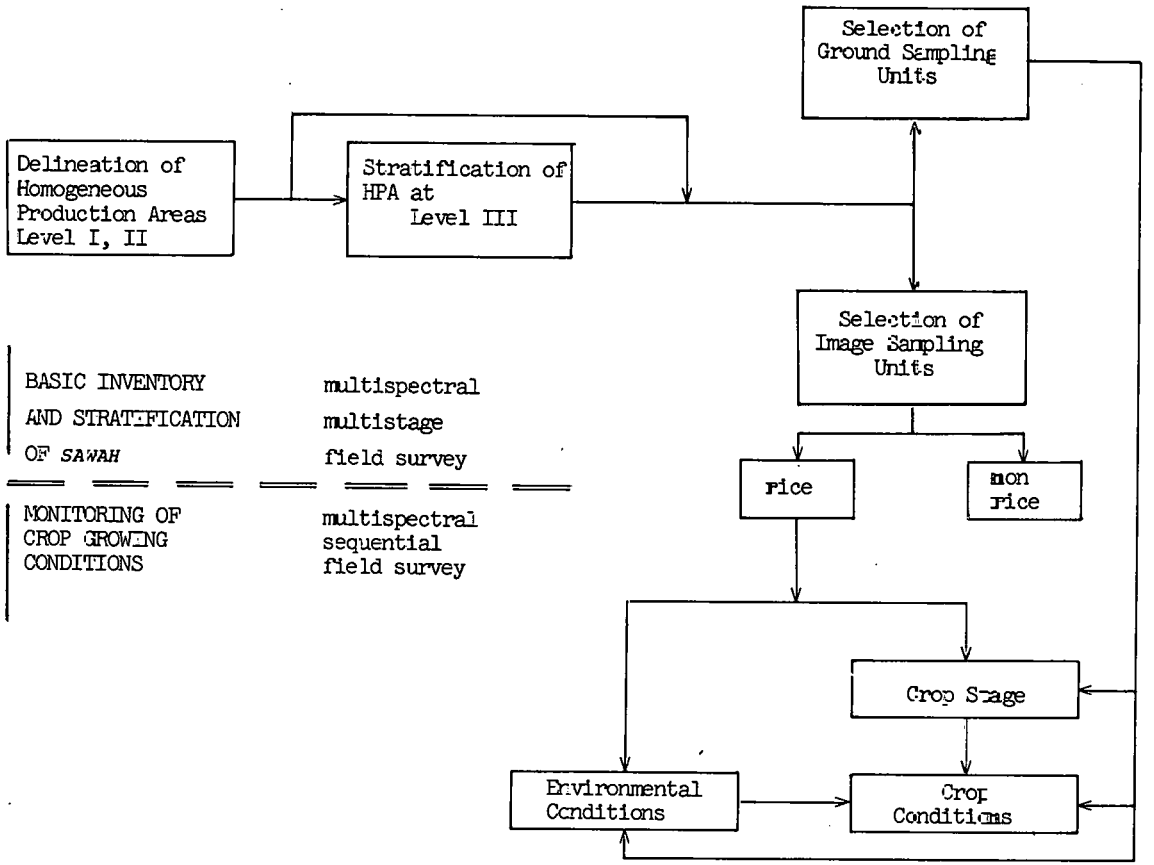

FIGURE 3. GENERAL PROCEDURE FOR INVENTORYING AND MONITORING WETLAND RICE PRODUCTION USING REMOTE SENSING TECHNIQUES.

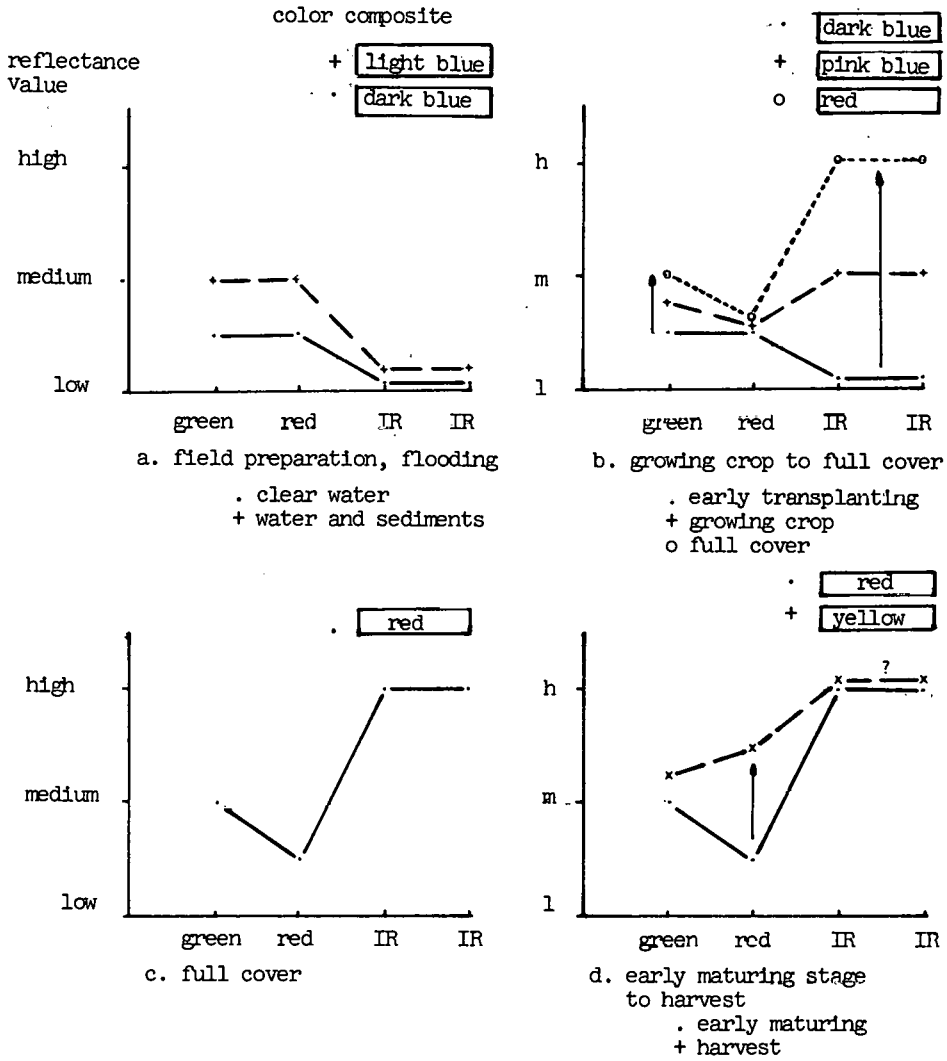

FIGURE 4. Evaluation of the reflectance values of a rice crop at various photo-phenological stages in the four LANDSAT bands.

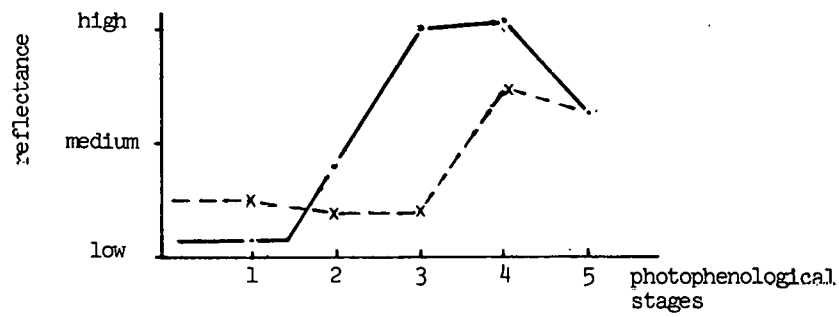

FIGURE 5. Evaluation of changes in the red (x) and infrared (.) reflectance values of a rice crop during successive stages.

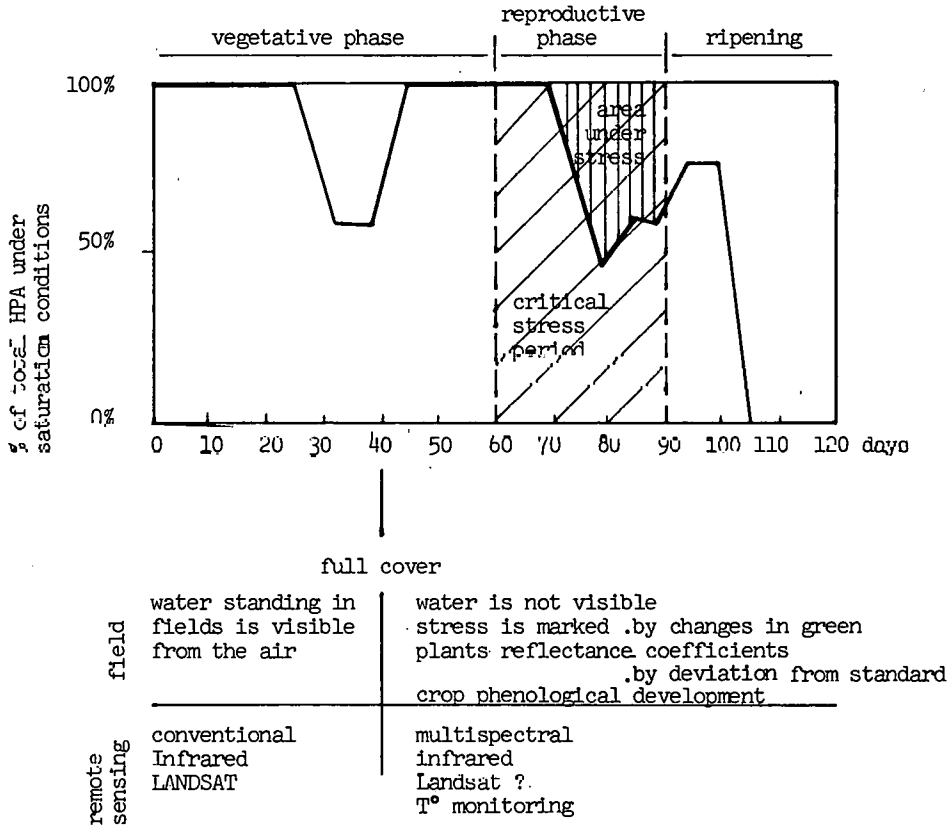

FIGURE 6. REGIONAL EVALUATION OF WATER STRESS IN SAWAH; data requirements in time and space framework.

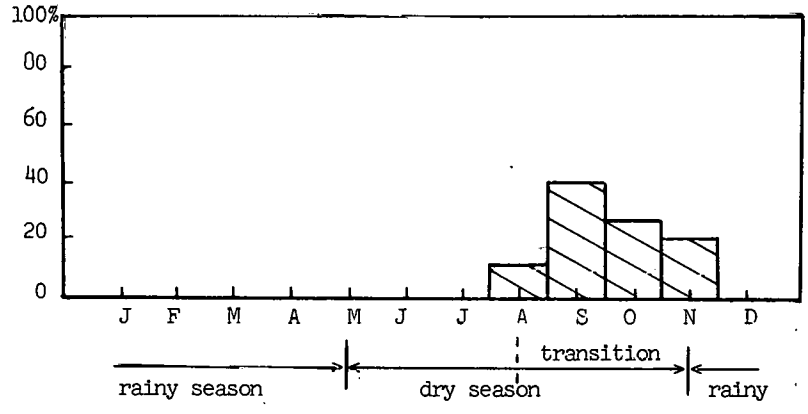

FIGURE 7. LANDSAT I IMAGES AVAILABILITY 1972-75 JAVA MADURA, BALI. 0-30% cloud cover. Total 37.

APPLIED RESEARCH ON REMOTE SENSING IN THE FIELD OF AGRICULTURE

S. Haketa G. Miyakawa

Statistics and Information Department,
Ministry of Agriculture and Forestry, Japan

T. Michino T. Yamamoto

NAC Incorporated, Japan

ABSTRACT

A fundamental research project about Remote Sensing application in the field of agriculture has been performed since 1974.

Purpose of the project is to make fundamental investigation and research about Remote Sensing technique. In the case of such a relatively small country as Japan, which has usually small-size crop fields and consequently has many kind of crops in relatively small area, there exists special problem to make accurate crop acreage summation through Remote Sensing method.

An airborne multi-band camera, developed recently, has been selected as sensor, and ground image processing equipments, also developed recently, have been utilized for information extraction. These equipments consist of analog systems such as additive color viewer and multi-color data system, and digital systems such as image digitizing system, data analysis system with inter-active color image display co-operated with small size computer.

At the 1975 experiments multiband camera images were analyzed through densitometer and mini computer, classification was examined with simple quadrangular decision rule, and rice, mulberry, navelorange, etc were classified with reasonable accuracy.

At the 1976 experiments multiband camera images were digitized by specially designed digitizing system, and then ten kind of crops were classified through multi-dimentional cell method. Acreage of individual crop was calculated with inter-active manner. Accuracy of over 90 percent was obtained at optimum condition in both classification and acreage summation.

The research project is still continuing in 1977 fiscal year, utilizing airborne digital multi-spectral scanner and improved digital image processing techniques.

1. INTRODUCTION

1.1. General approach for local condition

Concerning with relatively small country as Japan, sizes of crop fields are usually so small that, low altitude (airborne) remote sensors and co-operating data processing systems are considered to be indispensable. Furthermore, in order to utilize Remote Sensing method onto practical governmental affairs, it is necessary to research that how much extent the latest Remote Sensing technique may apply into the field of agriculture, to survey where is physical and technical problem actually.

These are the reason that Ministry of Agriculture and Forestry, Japan, had intended to initiate the experimental project about Remote Sensing at 1974, and development of an airborne multiband camera in Japan at the same year which provides more improved performance had encouraged to promote the research project against local condition of Japan.

1.2. Outline of progress of the 1974 - 1975 experiments

(1) Outline of the 1974 experiments

Preliminary trial was performed through combination of airborne multiband camera and analog image processing system, and found that reflections from each of these crops have considerable variance in both of grey level and spectral pattern. Test result suggested that natural condition of both of crop field and sun illumination will affect reflective signals mainly.

(2) Outline of the 1975 experiments

a) Purpose of the experiment

Purpose of the experiment of this year was to examine first simple statistical approach through mini computer for data processing.

b) Test field and data acquisition

A couple of test field (Maebashi & Kumamoto) was selected in Japan, and objective crops of rice plant, mulberry, navel orange were selected.

Flights for data acquisition was carried out at 5th, 12th August 1975, with altitudes of about 1,500m each. Airborne Multiband Camera was utilized and provided 122 scenes of four-band images on KODAK 2424 film.

c) Data processing and analysis

Multiband film images were analyzed through new analog processing system (Multi Color Data System 4200C) at first in order to search spectral characteristics of objective crops. The system has three channel parallel-piped classification function by manipulation (without software), which is very useful for analyzing multiband film images quickly. The system also provides simple acreage summation function concerning with classified subject which helps preliminary study of multiband camera data considerably.

A conventional spot densitometer was used for converting multiband film density information of individual unit field into numerical data, which were fed into mini-computer for further statistical analysis such as histogram analysis and four channel quadrangular classification.

d) Test results of the 1975 experiments

Histogram analysis:

Histograms of each crops provided by mini-computer showed considerable variance as in Fig. 1-1., and reason of variance was considered mainly to be variation of ground coverage by individual crop. That is, histograms of mulberry indicate that coverages of green leaves of mulberry over ground are various usually.

Classification results analysis:

Because of considerable overlap of spectral characteristics between crops as shown in Fig. 1-1., determination of decision-rule for classification was put into trade-off between "detectability" and "pureness", as shown in appendix. That is, when severe decision-rule was determined, inverse-pureness (error that extracting wrong crop) will decrease, while inverse-detectability (error that missing objective crop) will increase.

By-band ratio data were provided for rejecting atmospheric effect, and decision-rules were determined as an restriction of value of ratio data.

Representative decision-rules and classified results are shown in Table 1-1. The Table shows that "correctness" of rice or mulberry will take 90% in optimum case.

2. DESCRIPTION OF THE 1976 EXPERIMENTS

2.1. Purpose of the 1976 experiments

The experiments of 1976 had considered to be the final year of our research project which utilize airborne multiband camera for data acquisition, and also to be final stage for finding that how much extent an airborne multiband camera can be applied for agricultural surveillance purpose.

In order to verify quality of multiband camera image objectively, conversion of film image to digital data was performed through specially designed digitizer, and then digital data were fed into computer system to perform further analysis.

2.2. Outline of performance of the 1976 experiments

Multiband film images obtained by airborne multiband camera were fed into additive color viewer for human interpretation. Results of interpretation were utilized for both of image digitizing and inter-active classification by computer. Classified results were summed up to find crop acreages and refered to "true" acreage data of each crop which were prepared from land-use map or from multiband image through graph-pen system. Finally, classified results of test area on digital image data were converted into color images through laser beam image recorder.

Performance chart of the 1976 experiment are shown in Fig. 2-1.

2.3. Test field and subjects (crops)

Test field of 1976 experiments was selected at Obihiro, Hokkaido, Japan, where located an experimental station of the Ministry of Agriculture and Forestry of Japanese Government.

Three flight course was decided upon three test areas as Nooshi, shooei, and shuchiku. Unit fields of total number of 706, in which had single species of crop, and almost of which had acreage size of 1,000 - 50,000m^2 , were selected in the test field. 288 of unit fild among them only had "ground truth" data about both of crop species and acreage values.

Ten species of subjects (crops) were selected in the test field. These were rice-plant, potato, corn, wheat, oats, pasture, beet, redbean, soybean, kidneybean and others. Total number of individual crop field are shown in Table 2-1.

2.4. Data Acquisition of the 1976 experiments

Data acquisition by an aircraft was carried out on Jul 23 - 24, 1976, at altitude of 3,000m, then about 1,800m square of ground area was exposured in single scene of multiband film.

Airborne Multiband Camera MB-490, developed in Japan, was used as image sensor. The camera provides brighter, uniformly exposured, less distorted images, which will bring improved products for Remote Sensing purpose.

2.5. Data processing and analysis of the 1976 experiments

(1) Image interpretation by additive color viewer

Multiband image films obtained by MB-490 camera were copied (inversed to posi film) and then interpreted through Additive Color Viewer AC-90 in order to make preliminary analysis, that is, to find exposure condition, to prepare spatial (geographical) and intensity (density) information for digitizing, and to predict classification availability between crops for computer processing.

These preliminary interpretations by additive color viewer assisted further processing and analysis of multiband data to considerable extent about time & cost reduction.

(2) Conversion of film image to digital data

Film images acquired by multiband camera were digitized and put into CCT (Computer Compatible Tape) through Image Digitizing System IDS-800, which provides exclusive multiband film stage for preparing pre-digitizing registration (positional matching between band). Performance of digitizing was that, maximum image size of 800 x 500 pixels per frame, grey level of 8 bits (256 steps) per pixel. Pre-digitizing registration by film stage results registration error of within few pixels. Field size corresponding to one pixel was about 2m square in this experiments.

Post-digitizing re-registration was achieved by computer (as described later) and registration error were reduced within one pixel. Also grey level non-linearity of the digitizer was compensated by computer as described later.

(3) Inter-active classification by NTIPS

Multiband image data on CCT were fed into a computer system named NTIPS (NAC Total Image Processing System)[1].

At first, mis-registration errors between band were re-adjusted within one pixel by inter-active manner through color display system of NTIPS, and then calibration of grey level errors during digitizing also were performed by NTIPS which resulted error of within 2 steps.

Supervised (training method) classifications were performed through color display system of NTIPS. Classification method used in the 1976 experiments was to utilize decision rule of "multi-dimensional cell" type, and performed by "unequal priority" manner which has been reported[2] as preferable for crop discrimination. Simple manual classification function with three bands on color display system of NTIPS was useful for setting decision rules of four-bands cell and finding priority between crops considerably.

In this year's experiments, different training sets (that is, different decision-rules) of same crop were provided in accordance with individual test areas (that is, with individual flight lines). Because of both difference of circumstantial condition during data acquisition and fluctuation of performance of the image digitizing system, classification results are considered to be affected theoretically and practically.

Classified results were displayed in color, and supervised, and then decision rule were re-adjusted for improved classification.

Representative results of classification are shown in Table 2-1.

(4) Post-classification acreage summation and image recording

Spatial information (positional data of ridge way around unit field) were instructed into computer by inter-active manner in order to improve calculation accuracy of crop acreage, and then acreage summation by pixel counting had carried out about each crop classified. Ground truth data about acreage values of each unit field were prepared from both land-use maps and multiband camera images through Graph Pen System GP-3 as shown in Fig. 2-1.

Acreage summation results are shown in Table 2-2.

Finally, digital data of improved classification results were fed into Laser Beam Image Recorder ST-600 to produce color film images for recording.

2.6. Consideration on test results of the 1976 experiments

(1) Consideration about classification results

Generally speaking, classification results shown in Table 2-1 are considered to be reasonable compared to that of previous year's and that reported before[2] . According to our experience of this year, classification accuracy would be improved to some extent if it was allowable to repeat same procedure furthermore by changing cell width independently and slightly.

One of the factors, that will affect considerably onto spectral reflection from crop field, is coverage factor of crop leaves over ground. For example, wheat which covers over ground to large extent will shows relatively same reflectance pattern between different area, on the other hand, red bean which has relatively small coverage over ground will shows relatively different reflectance patterns between different area, as shown in Fig. 2-2. Difference of spectral pattern about such a crop as red bean will be brought by differences of both of coverage factor and ground reflection, and this kind of difference will be utilized for discrimination key between crops in some case.

(2) Consideration about results of acreage summation

When comparing the results of acreage summation (Table 2-2) to the results of classification (Table 2-1), it could be denoted that, in actual crop acreage surveillance from Remote Sensing data, classification accuracy will be dominant in general. About automatic acreage summation of individual unit field classified well, accuracy of resulted acreage data will reach over 90% in the case of relatively large field, and accuracy will be reduced because of "ridge way effect" in the case of relatively small field. About inter-active instruction method which used in the 1976 experiments, accuracy of acreage value on individual unit field will be nearly 100%, but the method will be accompanied with considerable time consumption in general. Trials for developing automatic techniques which reduce "ridge way effect" by detecting ridge way information automatically are considered to be recommendable.

3. CONCLUSION

In accordance with three year's experiments which utilize airborne multiband camera as data acquisition sensor, we have found that, the multiband camera can provide not only fine images for human interpretation but also high quality of images for digital processing.

Also we have found that further improvement of Remote Sensing techniques are desirable in order to apply Remote Sensing method onto practical agricultural field more smoothly.

Furthermore, such kind of researchs are considered to be expectable as that, finding inter-relation between yield of individual crop and integrated spectral reflectance pattern of whole crops. Because, for this kind of research, so called classification error will affect less onto the result of surveillance when utilizing severe decision-rules for classification.

Our experimental project is continuing at 1977 fiscal year, utilizing airborne digital multispectral scanner for data acquisition, and also developing more improved data processing techniques.

Classification availability about rice－plant (Maebashi)

Decision rule	$0.7 < \frac{R}{B} \leqq 1.0$	$0.5 < \frac{IR}{B} \leqq 1.1$	$0.7 < \frac{R}{B} \leqq 0.9$	$0.8 < \frac{IR}{R} \leqq 1.4$
Items / Crops	Extracted rice field / Total rice field	Percent of unit field classified as rice	Extracted rice field / Total rice field	Percent of unit field classified as rice
Rice	90.6 %	74.7 %	72.5 %	90.8 %
Mulberry	—	13.5	—	4.6
Others	—	11.8 (percent correct)	—	4.6 (percent correct)

Total number of unit field: rice 242, mulberry 145, Others 63.

Classification availability about mulberry (Maebashi)

Decision rule	$0.3 < \frac{R}{B} \leqq 1.1$	$1.1 < \frac{IR}{B} \leqq 1.3$	$0.9 < \frac{R}{B} \leqq 1.1$	$0.4 < \frac{IR}{R} \leqq 1.4$
Items / Crops	Extracted mulberry field / Total mulberry field	Percent of unit field classified as mulberry	Extracted mulberry field / Total mulberry field	Percent of unit field classified as mulberry
Rice		20.2	—	28.9
Mulberry	54.7 %	72.1 %	86.1 %	52.4 %
Others	—	7.7 (percent correct)	—	18.7 (percent correct)

Table 1－1 Classification results at the 1975 experiments.

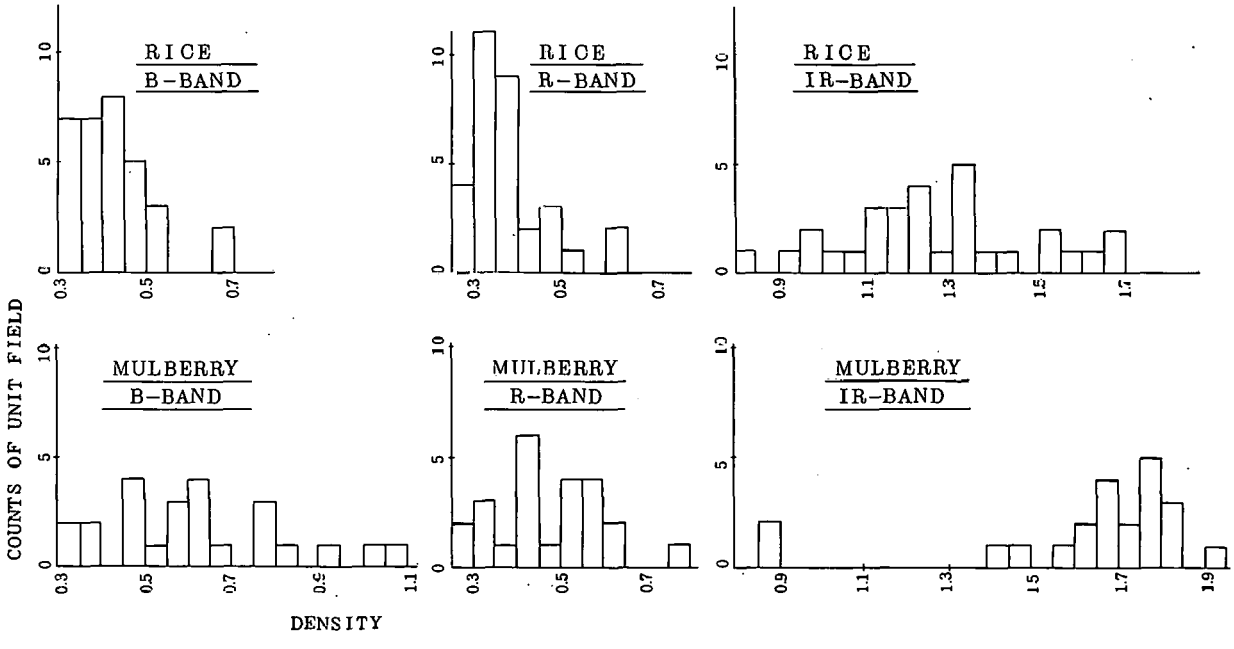

Fig 1－1 Histogram patterns at the 1975 experiments.

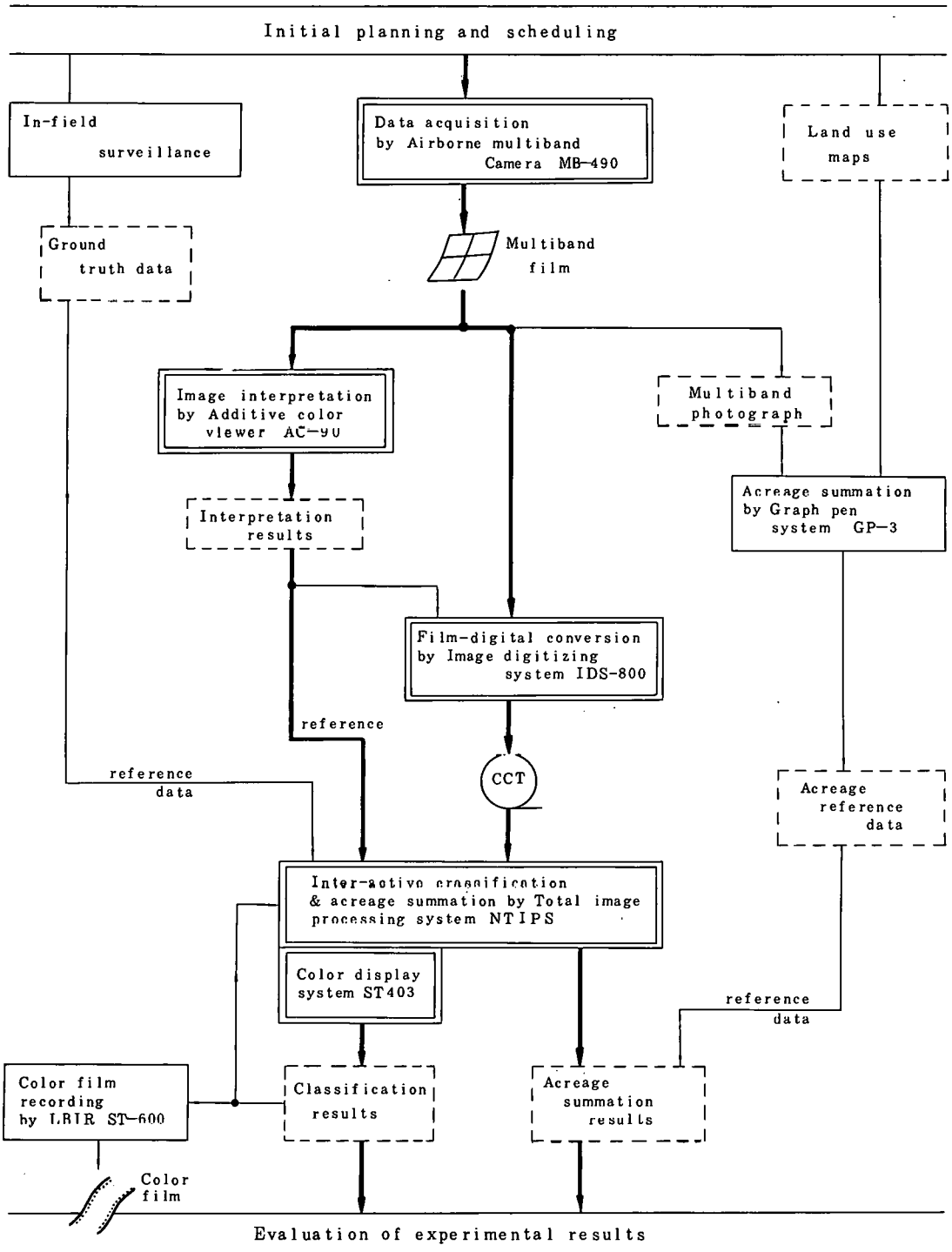

Fig 2 – 1 Performance chart of the 1976 experiments.

Items / Crops		Total number of field	Classified results										
			% correct	a	b	c	d	e	f	g	h	i	j
Potato	a	24	79%	19					3				2
Corn	b	16	94		15			1					
Wheat	c	12	92			11							1
Oats	d	2	50				1						1
Pasture	e	5	80		1			4					
Beet	f	11	73	1					8				2
Red bean	g	8	38							3			5
Soy bean	h	0	—								—		
Kidney bean	i	0	—									—	
Others	j	42											

— Nooshi area, FLT JUL 24. 1976 —

Potato	a	26	81%	21									5
Corn	b	23	57		13						1	2	7
Wheat	c	18	100			18							
Oats	d	11	0		1		0					2	8
Pasture	e	16	31			1		5		1			7
Beet	f	13	76						9				4
Red bean	g	15	67		2					10		3	
Soy bean	h	10	20		1			1		2	2	4	
Kidney bean	i	16	25		3						1	4	8
Others	j	52											

— Shoei area FLT. JUL 24. 1976 —

Determination priority a(most) → j(least)

Table 2—1. Classification results at the 1976 experiments.

Items / Crops	Potato	Corn	Wheat	Oats	Pasture	Beet	Red Bean	Soy Bean	Kidney Bean	Others	
Ground truth acreage	6,522	4,533	5,865	404	2,382	5,282	2,894	868	1,818	1,172	(are)
Remotely sensed acreage	5,872	4,741	5,434	235	1,668	4,984	2,485	520	1,299		(are)
Percent Correct	90.0	104.6	92.7	58.2	70.0	94.4	85.9	59.9	71.4		(%)

Table 2—2. Acreage summation results at the 1976 experiments.

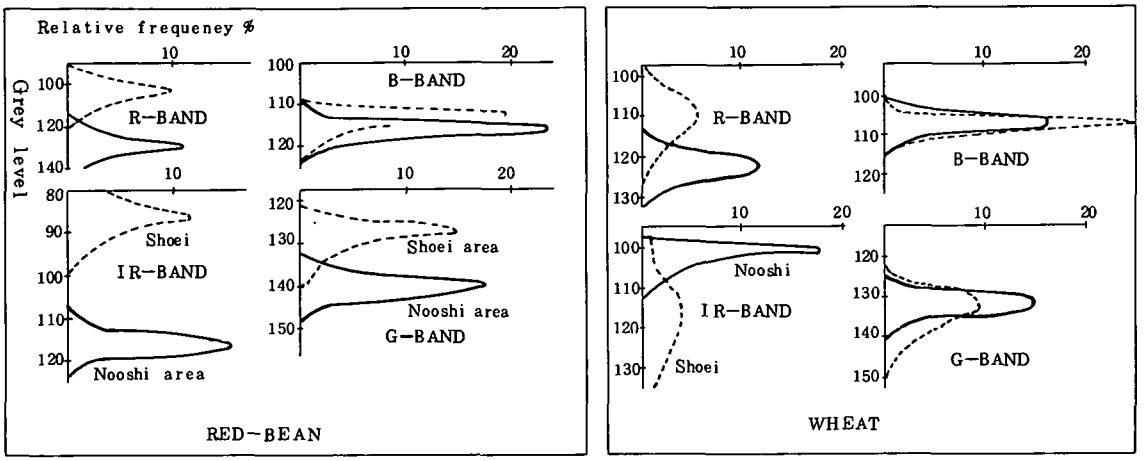

Fig 2-2 Histogram patterns at 1976 experiments.

(Reference)
[1] T. Michino "A total system for Remote Sensing"
US-Japan Seminar on Image Processing in Remote Sensing, Nov. 1976.
[2] D.H. Von Steen, W.H. Wigton "Crop identification and acreage measurement utilizing Landsat imagery"
USDA-NASA Report March 1976.

(Acknowledgement)
The research project has been supported mainly by people of The Hokkaido National Agricultural Experiment Station, and by Mr. T. Takahashi & Mr. S. Yamazaki, NAC Incorporated.

APPENDIX

Simplified signal detection theory from noisy input

Probability of error P(E) when detecting signal from noisy input will consist of "error that missing signal" and "error that accepting noise", and will be denoted as:

$$\left.\begin{aligned} P(E) &= P_S \cdot P_M + P_N \cdot P_F \\ P_S &+ P_N = 1 \end{aligned}\right\} \quad \text{---------- (1)}$$

where P_S: Probability that signal will exist in input data.
P_N: Probability that noise will exist in input data.
P_M: Probability that missing signal which should be extracted.
P_F: Probability that extracting noise which should be rejected.

"Decision-rule" means determining value of P_M and P_F. Inter-relation between P_M and P_F will vary in accordance with individual test condition, but usually P_M is in inverse-proportional to P_F. So, "severe" decision-rule means selecting large value of P_M and consequently small value of P_F.

Speaking roughly, when P_S takes large value, P(E) will nearly proportional to P_M, and when P_S comes near 0.5, P(E) will be affected less by P_M.

THIS PAGE

WAS INTENTIONALLY

LEFT BLANK

REMOTE MEASUREMENTS OF VEGETATIVE COVER IN SURFACE MINES

J. E. Carrel, C. J. Johannsen, T. W. Barney, and W. McFarland [1]

University of Missouri - Columbia
Columbia, Missouri 65201, USA

ABSTRACT

Vegetative ground cover, an important indicator of surface mine reclamation, can be remotely determined by two low cost, semi-automatic techniques. The first utilizes a leaf area meter to measure the extent of vegetation as represented by darkened spots on clear plastic overlays made from aerial photographs of minelands. The second utilizes an image analyzing computer to scan, digitize, and classify ground cover detected in the same aerial photographs. Both methods are rapid and highly (85-95%) accurate, although the computer system is more versatile. Digital image analysis can be coupled with many types of remotely sensed data to monitor surface mining and mineland reclamation anywhere in the world.

1. INTRODUCTION

Although surface mining for coal and other deposits is ancient, it was done on a small scale until the twentieth century. With the advent of power machinery capable of rapidly moving great masses of earth, strip mining of coal became one of the most productive methods to obtain fuel (Saperstein and Secor, 1973). After World War II, in the United States the production ratio of surface to underground mined coal changed markedly, increasing from 11 percent in 1940 to 44 percent in 1970 (Siehl, 1972). Projections for the next several decades indicate that the intensity of strip mining should increase across the country as coal is used to augument domestic energy supplies (Walsh, 1974; Singer, 1977).

Much attention has been focused on artificial and natural reclamation of mined lands by plants. Revegetation of surface mines is the outcome of many interactions among biotic and abiotic components. Biotic elements can be separated into three taxonomic categories: plants, animals, and microbes. These organisms not only constitute a vital, complex ecological community, but they also depend upon the soil and air for their existence. Because the success of plant colonists is so clearly tied to properties of materials on or near the surface, it is necessary to study the relationships between living and nonliving entities, to use the "ecosystem approach." Particular emphasis has been placed on the effects of soil acidity, soil texture, nutrient availability, extreme surface temperatures and slope on revegetation of spoils. Such interrelationships have been stressed in the proceedings of recent symposia on the ecology and reclamation of devastated lands (Hutnik and Davis, 1973; Lenihan and Fletcher, 1976; Anonymous, 1977).

---

[1] Associate Professor of Biological Sciences, Professor of Agronomy, Research Specialist in Agronomy, and Assistant Professor of Bioengineering Programs.

Few studies of plant succession on strip mines in the Midwest have been conducted. The early work of Croxton (1928) dealing with revegetation of Illinois coal strip mines was by and large elaborated upon or extended by subsequent authors (for example, Ashby, 1964; Brewer and Triner, 1956; Haynes and Klimsta, 1975). However, a major difference exists between their findings and those of other workers. Whereas Croxton (1928) described the process of revegetation in terms of waves or stages across an entire area, Byrnes and Miller (1973) later found that cover is established through formation of a patchwork of many vegetation islands that slowly encroach on the intervening bare patches. Similar results were reported for natural revegetation of coal spoil banks in central Pennsylvania (Bramble and Ashley, 1955), West Germany (Bauer, 1973), and Great Britain (Brierley, 1956). Hence, mined lands naturally undergo a rapid but highly patchy colonization by grasses, herbs, shrubs, and a few pioneer trees, some of which have economic value. On the other hand, all the aforementioned studies suggest that the time for natural succession to a climax vegetational community may be on the order of 70 to 100 years or even much longer.

The great variability among the observed rates and patterns of revegetation is partly due to the means by which the areas of vegetation were estimated. Bramble and Ashley (1955) employed the Braun-Blanquet (1932) technique for estimating the areas of cover. This involves visually estimating the cover and assigning it to one or five cover classes (0-5, 5-25, 25-50, 50-75, 75-100%). The Braun-Blanquet estimation is only one of a number of releve methods in which some type of estimation analysis is required. The releve method is a classification scheme in which species presence or absence is considered more important than minor variations in quantity. The method is therefore primarily qualitative and applicable to small, homogeneous habitats. To obtain more quantitative data, it is necessary to use some type of ordination method. Ordination, evolved primarily from timber survey, is used in large communities that are heterogenous in undergrowth and habitat. Various ordination methods and their applications are described in depth by Mueller-Dombois and Ellenberg (1974). We use several of these techniques in conjunction with photographic analyses.

Remote sensing has been utilized by mining companies for site planning and production monitoring for many years. More recently, remote sensing has been shown to be a feasible tool for mineland reclamation. Jackson et al. (1975) encouraged the use of remote sensing for monitoring mining operations. The use of aerial photography, especially black and white views, during field inspections of mined areas was recommended by Reinheimer et al. (1973). Johnson and Heinrich (1976) utilized color infrared aerial photography in the identification and subsequent measuring of morphologic units contained in strip coal mining operations typical of western North Dakota. Chase (1973) demonstrated that LANDSAT images can be used to detect and monitor new and unclaimed stripping activities. He further noted that tonal gradations in the different bands could probably be enhanced by computer processing techniques to separate degrees of vegetative reclamation. Gilbertson (1973) showed that differences in vegetative cover can be detected in large areas. Rogers et al. (1974) employed computer processing of LANDSAT data to identify reclaimed areas, partially reclaimed areas, water and water with sedimentation in minelands for a five county area in eastern Ohio. Alexander et al. (1975) reported on the feasibility of using machine processed LANDSAT multispectral data to accurately monitor the extent and location of current strip mining activity and assess the effectiveness of reclamation and pollution adatement procedures. Utilizing a band-ratio classification scheme, Anderson et al. (1975) used LANDSAT data to accurately measure strip mined acreage in western Maryland. Whitebay and Barr (1977) were successful in locating surfaced mined areas and delineating revegetated zones within the affected area utilizing low-cost Diazo processing and manual interpretation techniques.

The objectives of our research are (1) to develop characterizations of specific revegetation patterns resulting from various reclamation methods within representative sites of selected old and new coal strip mines; (2) to extend the developed surface characterization to large mined areas using remote sensing methods; and (3) to provide detailed vegetative information in a format suitable for use by reclamation planners and monitors. Our work is conducted in Missouri, USA. Because coal mining methods drastically changed after Missouri's Surface Mining Law was enacted in 1972, we are studying both pre-law and post-law sites at the same strip mines.

2. SURFACE OBSERVATIONS AND AREA METERING OF VEGETATION

The purpose of this section is to prepare verified land cover maps of surface mines for use as reference standards in the computer image analysis of mineland reclamation. Both ground level and low altitude aerial methods are employed. Low altitude aerial photographs are obtained from existing photographic coverage (Barney and Johannsen, 1976) or from our own flights.

2.1 COVER CLASSIFICATION

Large scale (1:3,000) vertical aerial photographs of a surface mine are printed either in black and white or in color. The scale is verified in two ways. In the laboratory, large (10^3m) distances between features indicated on U.S.G.S. topographic maps (1:24,000) are compared with those visible in the photographs. In the field, small (10^2m) distances measured with a tape are compared with those visible in the photographs.

Cover classification in a surface mine proceeds in a step-wise fashion. First, the perimeter of a mineland is marked on the photographic print. A silhouette of the entire mine is made by inking a clear plastic overlay. In a similar fashion transparent overlays of the total vegetation, woody vegetation and water are prepared. Darkened areas (mm^2) are measured individually using a leaf area meter (Carrel et al., 1977) and their real areas are calculated by multiplication by the verified scale factor. The areas occupied by bare soil or herbaceous vegetation are calculated by subtraction. Finally, relative abundance of the different cover classes is determined.

The results for a hilly pre-law and a graded post-law site at the same surface mine are presented in Table 1. Both mines were reseeded aerially in 1975 with the same pasture mixture. The pre-law site contains 20.8% vegetative cover vis-a-vis 48.4% for the post-law site. If one ignores water area, the post-law site contains enough vegetative cover to satisfy requirements of Missouri's surface mine reclamation law.

Vegetative cover in surface mines is verified in randomly located 30X30 m quadrats. The procedure, described in detail by Carrel et al. (1977), involves comparison of cover measurements made by walking thirty 30 m transects spaced 1 m apart in a quadrat with cover measurements made by metering the area darkened in on an overlay of the aerial photograph of the same quadrat. Whereas resolution at ground level is $0.1m^2$, resolution in the aerial prints is $0.5m^2$.

Results of vegetative cover verification are shown in Figure 1. There is a significant correlation ($r=0.95$, $p < .01$) between the direct and low altitude remote measurements of vegetative cover. Hence, error in low altitude aerial determination of cover classes is insignificant.

2.2 VEGETATION IDENTIFICATION

Vegetation growing in surface mines is separated into two categories: woody and herbaceous. Trees and shrubs have a different texture and color in aerial photographs than do grasses and legumes, so the two classes are readily differentiated by a trained observer. In minelands artifically seeded with forage species, woody plants are rare and individually identifiable. For example, 0.4% of the area of the pre-law site and 0.1% of the post-law site cited in Table I are covered by woody species.

Plant species composition and abundance in surface mines are measured by quadrat sampling along transects. Quadrats ($0.5m^2$) are established at 30m intervals along parallel transects spaced 200m apart across a mine. The above-ground plant biomass is clipped and segregated by species for dry weight determinations.

The results for a pre-law site that was aerially seeded with a mixture of Kentucky 31 fescue and alfalfa are provided in Table II. While the two pasture species dominate, as is indicated by their large importance values, several other small species are common and some small or large species are rare. Most weedy plants occur in places with little other vegetation.

3. COMPUTER ANALYSIS

The purpose of this section is to perform digital image analysis of aerial photography obtained over reclaimed minelands, identifying areas of vegetation, bare soil and water. The analysis utilizes large scale 70 mm false color infrared (CIR) positive transparencies and 9 in. x 9 in. CIR paper prints.

3.1 COVER CLASSIFICATION

Photographs are digitized with a Spatial Data Model 108 Computer Eye at a resolution of 256 x 240 points with 256 gray levels. The digitized image is displayed on a Ramtex GX200 Color Display at a resolution of 256 x 240 points with 16 levels in each of 3 colors, which theoretically gives 4096 different shades of color. A Model GP-3 Graf Pen is used for interactive data manipulation and processing with the display. Digitized images and programs are stored and retrieved using a 9 track, 800 bpi tape drive and several disk drives. Programs written in Fortran IV with some special purpose assembly language subroutines are operated on a DOS PDP-11 computer system.

Two approaches are used to classify the digital data. One approach is a cluster analysis technique based on each point's gray level. A histogram showing general trends in gray level distribution is generated for each scan (Figure 2). From the histogram, thresholds are estimated for each of the 3 cover classes and the image is subdivided into 3 separate, binary images (Figure 3). The 3 subimages are assigned a color and then they are recombined to produce a tricolor image on the display screen.

A second approach to classify the digital data uses selected training fields to arrive at average gray values that are representative of each of the 3 cover types. Because most mine sites generally are small, only 4 or 5 pure training fields are used for each category. Training fields are entered into the computer by interacting with the display system using the Graf-Pen.

The classification routine allows the Graf-Pen to be used to delineate the mine site as seen on the displayed image. Only the outlined area from the scan is classified using a minimum distance decision scheme. The resulting point by point classification is then printed and totaled on a line printer (Figure 4). A scaling factor is applied to the total points and the area is determined for each class.

3.2 COVER VERIFICATION

Two techniques are used to evaluate the accuracy of computerized classifications. One technique involves dividing the computer printout into equally sized grid cells and comparing the results to those from the equivalent grid in a large scale (1:6,000), CIR aerial photographs which is manually interpreted. The grids are registered and numbered so that each cell on the computer printout and aerial photo cover the same geographical area. The results of this comparison are shown in Table III.

Most misclassifications listed in Table III are due to the large variation in the intensity of reflection by bare soil. In a total of 231 cells classified as bare soil, 26 cells were misidentified. In a total of 240 cells classified as vegetation, 61 cells were misidentified. In both cases, dark shale material on the mine surface was confused with the surrounding vegetation and water. Vegetation and water usually appear darker than most bare soil on photographic positives.

The grid cell comparison technique itself introduces error into the results. Imperfect grid registration, unequal grid cell size, distortions in the aerial photograph and the scanned imagery cell affect the accuracy of verification. Computer printout resolution is degraded by imposing a 7 x 7 point grid to match the 50ft x 50ft grid used on the ground truth photo. Each point on the printout covers an area of 7.1 ft x 7.6 ft. The comparison technique calls for the cells to be classified by their predominant cover. A smaller grid size would allow a more accurate assessment of printout results. Unfortunately the 50 ft x 50 ft grid cell was the smallest size that could accurately be constructed for 1:6,000 scaled mineland photo.

Accuracy of computer classification is also evaluated by comparing area figures generated by the computer with those made by direct surface observations. As indicated in Table IV, computer interpretations can produce large absolute errors but still yield small (< 10%) relative errors.

Cover characteristics of minelands determined by computer classification differ from surface observations in part because perimeters used in both analysis are not uniform. It simply is impossible to duplicate a mine's boundaries exactly with a Graf Pen when it is drawn by hand on the computer screen. Another factor is the difference in spatial resolution between the two methods. The effective spatial resolution of the computer image exceeds 5 m^2. In general one cannot measure objects less than 2 times the effective spatial resolution and the preferred ratio between working resolution and effective spatial resolution is 5:1. In contrast, surface observations and area metering of mineland cover have a resolution less than 0.5 m^2, 10 times better than in the computer technique. On the other hand, a single scan computerized interpretation requires approximately 45 min., whereas surface observation of the same strip mine may take 20 hr. Thus, a trade-off between spatial accuracy and temporal efficiency is achieved with computer image analysis.

4. CONCLUSIONS

We have demonstrated that both area metering and digital image analysis of low altitude, vertical aerial photographs are fast, low cost approaches to determine accurately the extent of revegetation in surface mines. These methods cannot replace ground surveys for cover verification nor can they compete on a large scale with more sophistocated monitoring schemes that utilize machine processed LANDSAT data, aircraft scanner data, or conventional aerial photo interpretation methodologies. However, our approaches offer a substantial saving in time and money to persons who must make policy decisions based on the degree of revegetation in single surface mines. Thus, the subjectivity now inherent in many decision processes regarding a mineland reclamation could be greatly reduced or eliminated.

5. ACKNOWLEDGEMENTS

We thank L. Bouchard, S. Weems, T. Hotrabhavananda, A. Leavitt, E. Kogler, and R. Crane for technical assistance. This research is supported by US ERDA (DoE) contract E(11-1) 2758 and by US DA/CSRS contract 648-15-20.

6. REFERENCES

Alexander, S.C., Baumgardt, D., and Dein, J. 1975. Mapping and Classification of Strip Mines and Acid Drainage Through Digital Analysis of Landsat-I Multispectral Scanner Data. Proccedings, NASA Earth Resources Survey Symposium, Houston, Texas.

Anderson, A.T., Schultz, D., and Buchman, N.E. 1975. Landsat Inventory of Surface-Mined Areas Using Extendible Digital Techniques. NASA/Goddard Space Flight Center.

Anonymous. 1977. Fifth Symposium on Surface Mining and Reclamation. Natl. Coal Assoc./Bitum. Coal Res., Wash., D.C., 319 pp.

Ashby, W.C. 1964. Vegetation development of a strip-mined area in southern Illinois. Trans. Ill. St. Acad. Sci. 57: 78.

Barney, T.W. and C.J. Johannsen. 1976. Index to Aerial and Space Photographic Coverage of Missouri. Extension Division Publication M-102. University of Missouri, Columbia, Mo.

Bauer, H.J. 1973. Ten years' studies of biocenological succession in the excavated mines of the Cologne lignite district. Paper III-2. In Ecology and Reclamation of Devastated Land, R.J. Hutnik and G. Davis eds. Gordon and Breach, N.Y., 1: 271.

Bramble, W.C. and Ashley, R.H. 1955. Natural revegetation of spoil banks in central Pennsylvania. Ecology 36: 417.

Braun-Blanquet, J. 1932. Plant sociology. (Trans. by G.O. Tuller and H.S. Conrad), McGraw-Hill Book Company, N.Y.

Brewer, R. and Triner, E.D. 1956. Vegetational features of some stripmined land in Perry County, Illinois. Ill. Acad. Sci. Trans. 48: 73.

Brierley, J.K. 1956. Some preliminary observations on the ecology of pit heaps. J. Ecol. 44: 383.

Byrnes, W.R. and Miller, J.H. 1973. Natural revegetation and cast overburden properties of surface-mined coal lands in southern Indiana. Paper III-3. In Ecology and Reclamation of Devastated Land, R.J. Hutnik and G. Davis eds. Gordon and Breach, N.Y. 1: 285.

Carrel, J.E., DeMott, J.E., and Zwight, D.M. 1977. Surface mine revegetation: area metering of ground cover. Fifth Symposium on Surface Mining and Reclamation: 8-11.

Chase, P. 1973. Ecological Effects of Strip Mining in Ohio, NASA. Report E73 - 1003.

Croxton, W.C. 1928. Revegetation of Illinois coal stripped lands. Ecology 9: 155.

Gilbertson, B.P. 1973. Growth and Decline of Vegetation of Mine Dumps. NASA, ERTS Report E73-10326.

Haynes, R.J. and Klimstra, W.D. 1975. Illinois Lands Surface Mined for Coal. Coop. Wild. Res. Lab., S. Ill. Univ. 201 p.

Hutnik, R.J. and Davis, G. eds. 1973. Ecology and Reclamation of Devastated Land. Gordon and Breach, New York, 1 and 2.

Jackson, R., Vincent, R., Wilcock, L., Schuchman, R., and Davis, C., March 1975, "Remote Sensing of Strip Mines", Final Report, USDI, Bureau of Mines.

Johnson, G. and Heinrich, M. 1976. Monitoring Strip Coal Mining and Reclamation Activities With Color Infrared Imagery. Innovations in Land Use Management. University of North Dakota, Grand Forks, N.D.

Lenihan, J. and Fletcher, W.W. 1976. Environment and Man. 4. Reclamation. Academic Press, N.Y.

Mueller-Dombois, D. and Ellenberg, H. 1974. Aims and Methods of Vegetation Ecology. John Wiley and Sons, N.Y.

Reinheimer, C.J., Wallace, A.G., Kassler, E.O., November 1973, "Remote Sensing Techniques for Field Inspections", MDC A2596, Prepared by McDonnel Aircraft Company, St. Louis for USGS, Reston, VA. 22092.
Rogers, Robert, Reed, L. and Pettyjohn, W. 1974. Automated Strip Mine and Reclamation Mapping from ERTS. NASA Report E74-10490.
Saperstein, L.W. and Secore, E.S. 1973. Improved reclamation potential with the block method of contour stripping. Research and Applied Technology Symposium on Mined-Land Reclamation, Bituminous Coal Research, Monroeville, PA.: 25.
Siehl, G.H. 1972. Mined land reclamation requirements: issues, actions and arguments. Lib. Congr. Res. Serv.
Singer, S.F. 1977. Soil and coal: a cost-benefit inquiry. Science 197: 213.
Walsh, J. 1974. Problems of expanding coal production. Science 184: 336.
Whitby, L. and Barr, D. 1977. Evaluation of LANDSAT Imagery For Mined Land Studies. Annual Meeting of the Missouri of Science, St. Louis, Mo.

TABLE I. COVER CHARACTERISTICS OF TWO ADJACENT SITES IN A MISSOURI STRIP MINE

	Area (m^2)	Cover (%) Total	Cover (%) Land
Prelaw Site			
Vegetation			
Herbaceous	25,679	20.4	21.8
Woody	547	0.4	0.5
Subtotal	26,226	20.8	22.3
Bare Soil	91,517	72.7	77.7
Land	117,743	93.5	100.0
Water	8,173	6.5	----
Total	125,916	100.0	----
Postlaw Site			
Vegetation			
Herbaceous	117,830	48.3	52.6
Woody	212	0.1	0.1
Subtotal	118,042	48.4	52.7
Bare Soil	105,807	43.4	47.3
Land	223,849	91.8	100.0
Water	20,005	8.2	----
Total	243,854	100.0	----

TABLE II. VEGETATIVE SPECIES COMPOSITION OF A PRE-LAW SITE SEEDED TO PASTURE IN A MISSOURI STRIP MINE

Species	Frequency		Biomass		Importance Value*
	Absolute	%	g/m^2	%	
Medicago sativa	.813	34.2	81.6	41.1	75.3
Festuca elatior	.653	27.4	81.3	41.0	68.3
Melilotus officinalis	.120	5.0	7.4	3.7	8.7
Ambrosia bidentata	.186	7.8	1.6	.8	8.6
Typha latifolia	.080	3.4	9.6	4.8	8.2
Polygonum pennsylvanicum	.133	5.6	4.2	2.1	7.7
Lactuca canadensis	.146	6.1	.06	.4	6.5
Echinocloa muricata	.040	1.7	2.7	1.4	3.1
Apocynum cannabinum	.013	.5	4.2	2.1	2.7
Rumex crispus	.053	3.3	.69	.4	3.6
Agrostis hiemalis	.013	.5	1.9	1.0	1.5
Salix interior	.026	1.1	.78	.4	1.5
Trifolium hybridum	.013	.6	.51	.3	.9
Setaria glauca	.013	.6	.26	.1	.7
Gleditsia tricanthos	.013	.6	.26	.1	.7
Poa pratensis	.013	.6	.36	.1	.7
Eupatorium serotinum	.013	.6	.24	.1	.7
Unidentified shrub	.013	.6	.12	.1	.6
Asclepias incarnata	.013	.6	.05	<.1	.6
Lepidium sp.	.013	.6	.005	<.01	.6
Total	2.380	100.4	198.5	100.0	200.4

*Importance Value = % Frequency + % Biomass for a given species.

TABLE III. ACCURACY OF COMPUTER CLASSIFICATIONS FOR A SURFACE MINE EVALUATED BY GRID CELL TECHNIQUE

Surface Level Categories	Computer Classification			Total # of Grid Cells	% Correct
	Bare Soil	Vegetation	Water		
Bare Soil	205	22	4	231	89
Vegetation	57	179	4	240	75
Water	8	1	52	61	86

TABLE IV. ACCURACY OF COMPUTER INTERPRETATIONS VERIFIED BY SURFACE OBSERVATIONS FOR TWO SITES IN A MISSOURI STRIP MINE

	Surface Observations		Computer Interpretations		Computer Error	
	Area (Hectares)	Cover (%)	Area (Hectares)	Cover (%)	Area (Hectares)	Cover (%)
Pre-Law Site						
Vegetation	2.6	21	4.8	32	+ 2.2	+ 11
Bare soil	9.2	73	8.5	57	- 0.7	- 16
Land	11.8	94	13.3	89	+ 1.5	- 5
Water	.8	6	1.6	11	+ .8	+ 5
Total	12.6	100	14.9	100	+ 2.3	
Post-Law Site						
Vegetation	11.8	48	12.7	56	+ 0.9	+ 8
Bare soil	10.6	43	7.5	33	- 3.1	- 10
Land	22.4	91	20.2	89	- 2.2	- 2
Water	2.0	9	2.4	11	+ .4	+ 2
Total	24.4	100	22.6	100	- 1.8	

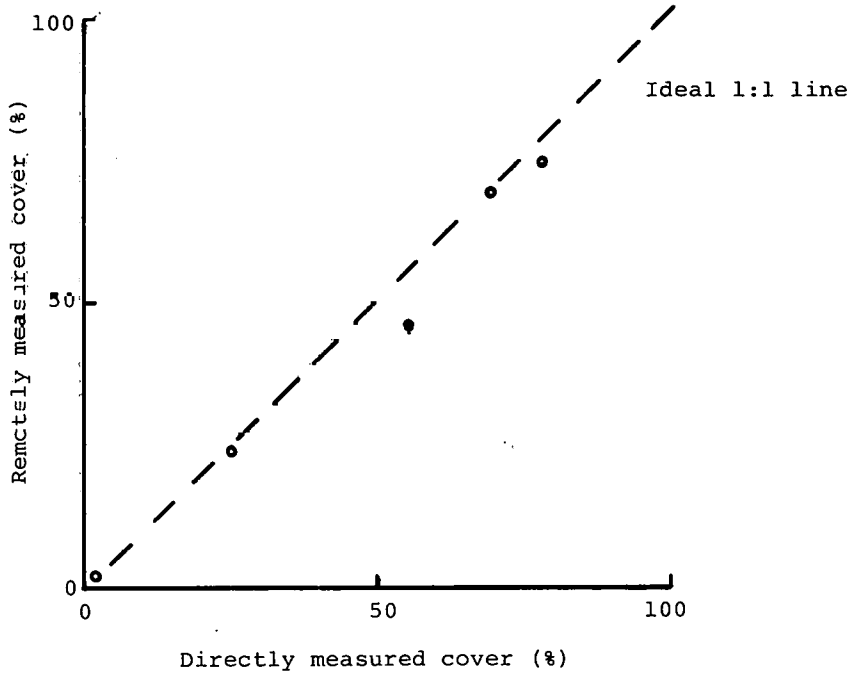

Figure 1. Verification of vegetative cover measured with the area metering method. Data for five 30 x 30 m quadrats are shown.

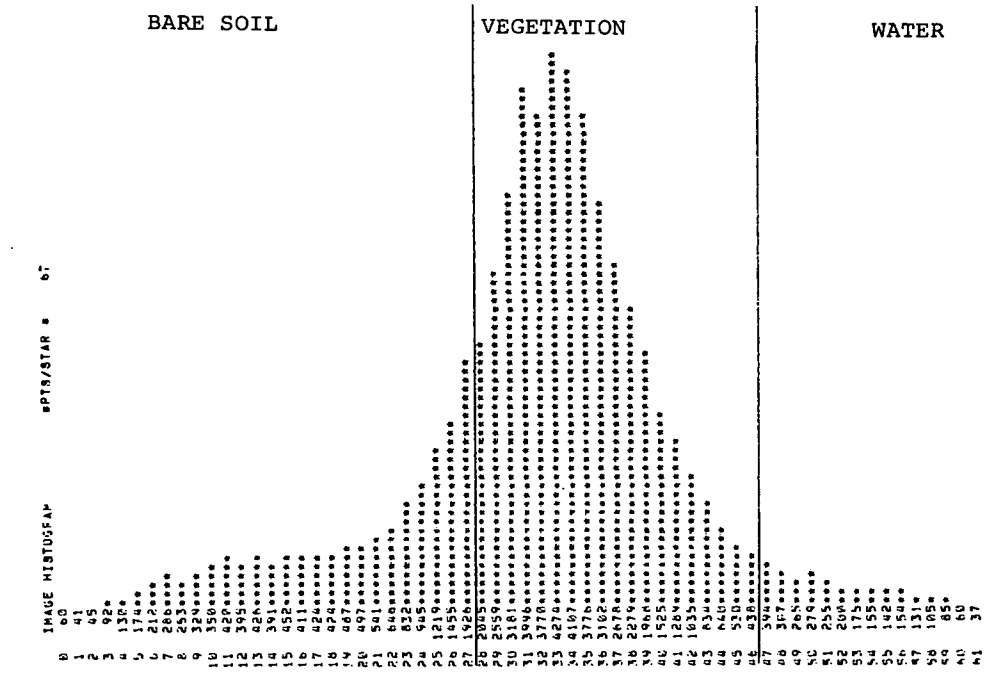

Figure 2. Gray level histogram for a digitized image of a strip mine.

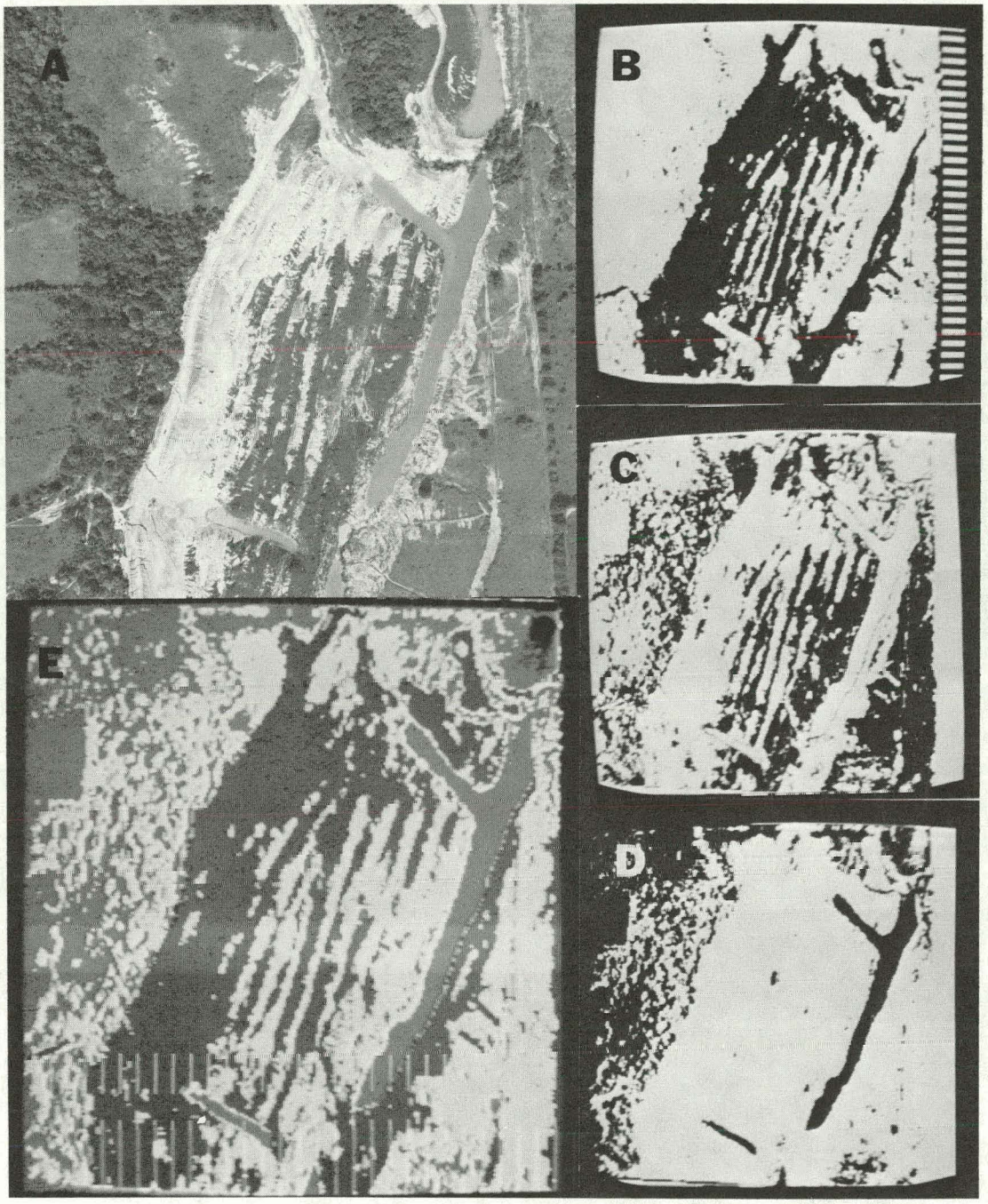

Figure 3. Digital mapping of cover in strip mines. A: Vertical aerial photograph (1:7,500) of a pre-law site in Missouri. B,C,D: Bare soil, vegetation, and water as digitally mapped by computer responses to the aerial photograph. E: Compostie map reconstructed from the images in B,C, and D.

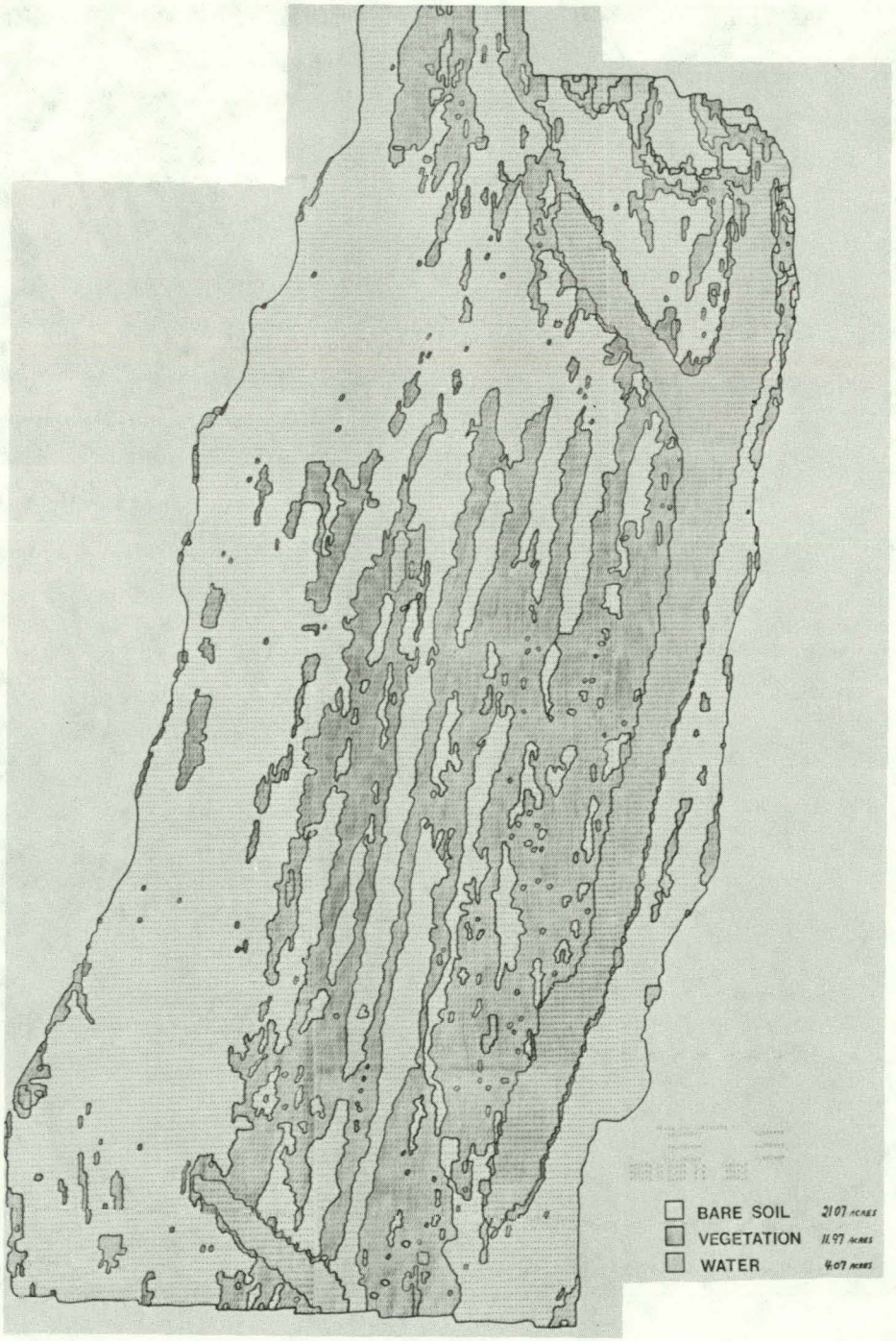

Figure 4. Computer printout of digital image in Figure 3E. This map is used for verification of cover classifications in a strip mine.

PROBLEMS ASSOCIATED WITH ORGANAISING REMOTE SENSING APPLICATIONS IN A DEVELOPING COUNTRY

Chris Nanayakkara

Center for Remote Sensing
Survey Dept. of Sri Lanka, Colombo.

ABSTRACT

The problems that one has to face in organising an operational Remote Sensing Unit in a developing country is discussed, giving many possible approaches to these problems and suggestions on the different levels of sophistication in technique. The case in Sri Lanka and its approach to the problems is described. Possible solutions are taken up for discussion with suggestions for improvements in technology transfer and training aspects.

Many developing countries have commenced Remote Sensing Applications at some level or other.

Why did these countries start on this activity ? Why do others propose to start ? Why do some of them consider expansion of this activity or propose going to higher levels of sophistication and investment ? What are the possible applications ? What are the benefits ? How does one start ? At what level ? What are the other problems ? How does one get information ? How to choose the level of sophistication and investment ? Who does one consult ? How does one build up the technical know-how within the country ?

These and many other questions crop up at some time or the other when an organisation in a developing country wishes to exploit this recently developed technology.

The detailed answering of the first three questions starting with "why" is outside the scope of this paper. In brief, they include the wide publicity given to Remote Sensing and the spate of publications that claimed a very wide spectrum of applications and solutions to almost all the problems of obtaining accurate up-to-date resources information and agricultural, land-use data etc., required for developing and improving the economy of a developing country. It also became advantageous to the Agencies responsible for introducing and improving this technology to claim vast advantages of this methodology in helping the developing countries. Manufacturers of equipment completed the natural trend of diversification of types and approaches to data acquisition and processing. However, Remote Sensing has now come to stay and is undergoing improvements and changes. A developing country with limited resources and a cautious attitude hardly finds it possible to keep pace with these changes and new developments.

The answers to the subsequent questions could be obtained by a proper and pragmatic assessment of the needs of each country for the type of data and information provided by remote sensing. At this stage one may consider the present capabilities of the remote sensing techniques as well as the likely improvements in reliability, resolution, data processing etc., in the near future.

Many organisations in developing countries are still either reluctant or slow to make firm commitments to develop operational systems for Remote Sensing. This is due to many reasons and it can be seen that many of them are valid ones. They are listed below : -

(a) The uncertainity of obtaining the required data, in the case of the Landsat System. Due to restrictions in tape-recorder capacity on board the satellite, the countries that are not within the range of a Landsat receiving station are finding it more and more difficult to obtain coverage during the required seasons or obtaining any regular coverage.

(b) The high cost of establishing a Landsat receiving station, as well as the lack of proper regional co-operation to economise on the cost is another set-back. Even if one is prepared to chance the heavy cost, further uncertainty results as regards the continuity of compatible satellite systems.

(c) Likely changes in the Data Acquisition Systems and the consequent likelihood of specialised and expensive equipment going out-of-date.

(d) Uncertainty of continued coverage by Landsat or similar systems for long term applications.

(e) Wide variety and constant updating of data processing systems. Such changes and improvements occur during the development phase of any new technology. The recent changes in these systems have forced the smaller or cautious organisations into a "wait-and-see" attitude. The fear of specialised and extremely expensive processing equipment becoming out-of-date is a major justification for caution.

(f) Lack of reliable information regarding processing techniques and equipment. This may be due to the fact that technology is in the development phase or due to competitiveness and the secretive attitude of the manufacturers.

(g) Lack of good text books or references.

(h) Lack of well-organised training facilities at different levels. There are many workshops, seminars and symposia organised for international participants. While these serve a very useful purpose, they do not adequately cater to the needs for training at different levels. What is required is a scheme of training Scientists and Users. This scheme should be a systematic development of the fundamentals, techniques and applications. The courses should be so designed that the different types of trainees (such as Managers, Users, Data Processing and Analysis groups or Applications groups in specialised fields such as Geology, Agriculture, Hydrology etc.,) may be channelled into their respective specialisations, after a general introduction into the broad field of Remote Sensing. By this process an organisation could develop a multidisciplinary working group with the capability to carry out data processing and analysis for specific applications. At the commencement, such a group could operate at a basic or lower level using simple techniques and later undertake more sophisticated levels as they develop confidence in the techniques and as the usefulness of the applications is established and diversified.

(i) The limited resolution of Satellite Remote Sensing Data.
The presently available Landsat 2 type of data has a limited spatial resolution, especially when one considers land-use or crop inventory type of information. This limitation is even more apparent when we consider areas which have complicated land-use practices and where the crop types are spectrally confusing, changing from season to season or is grown in small parcels of land with complicated spatial characteristics. This is mostly so in areas coming under traditional village-type of landuse. Such situations are very common in the developing countries.

In fact, the publicity given to the wide variety of applications for Landsat data has generated a situation where the decision makers and planners have been made to believe that this technique is an instant solution to their problems of landuse and crop inventory information. This has caused a considerable amount of embarrassment to the remote sensing people and in many instances it may have had a negative effect as far as introducing and propagating this technique is concerned.

(j) On the other hand, the extremely large cost of Airborne multispectral remote sensing data acquisition, processing and presentation presents the other extreme. Airborne systems are very costly and require sophisticated technology for acquisition and processing either in analogue or digital modes. They generate a vast volume of data which is difficult to process and present, if one tries to make use of all the units of data or at least the majority of the data units. Statistics can be obtained accurately. However, for actual applications one requires the location and the spatial characteristics at some stage or the other. At this stage one wonders if the expense is justifiable and if other or simpler systems of data acquisition such as B/W aerial photography would not be equally good.

(k) The lack of reliable techniques in between these extreme choices is a matter that needs careful study.

(l) Over-selling. Remote Sensing has been a victim to the "over-sell" technique for many years. One can pick a large number of publications giving series after series of papers describing "significant results" and successful applications. Many of them do not carry careful descriptions of the techniques used but present very good results and positive conclusions. Widest possible spectrum of applications is claimed. Many of them have apparently been carried out under ideal situations and perhaps in areas that had extensive and homogeneous crop cover with a definite and uniform crop calender which is not common in the tropics.

The same remarks apply to the manner in which equipment and other products were introduced.

Inspite of these problems, Remote Sensing Techniques have come to stay and are likely to be adapted by developing countries at some level or other. In fact, it is realised that the applications of remote sensing are more useful and pertinent for the development endeavours of these countries than to the industrialised or developed countries.

Choice in techniques and level of technology.

If one considers just the Landsat type of data and their possible applications, one is confronted with a fairly wide choice in deciding on an operational system. This is on the assumption (discussed later) that this system will yield the desired information.

First of all, one has to decide on how to obtain the data; either directly from the Satellite transmissions or through a Data Centre. Lacking a receiving facility one decides the latter. Here too, the choice of data products and their relative merits have to be considered. After obtaining the information as to the availability of coverage, one has to decide between : -

(a) 1:3.3 million scale bulk B/W +ve or -ve transparancies,
or
(b) 1:1 Million scale bulk B/W +ve or -ve transparancies,
or
(c) 3 band color-composites,
or
(d) precision-processed products
(scale of product, +ve or -ve transparancy or color prints etc.,)
or
(e) on M.SS. Computer Compatible Tapes.

This choice will, of course, be influenced on the level of processing and analysis to be utilised to transfer this data to the type of information that one desires.

At the lowest level, using B/W bulk transparancies and simple photolab equipment one could enlarge individual bands and prepare interpretations using overlays and combine this multiband information for a better analysis. A similar procedure may be adopted with the 1:1 Million B/W transparancies, resulting in a better working scale of 1:250,000 or slightly larger. The 3-Band color composites combined with rather simple optical devices such as a Zoom Transferscope offers a very useful device for interpretation and inserting the data onto a base map.

On the other hand, one may decide to prepare one's own color composites using a simple process such as Diazo Film which requires only an ordinary ozalid type of machine for the exposure and the ammonia developing process required. Or, one may go on to color printing of the composites, through a slightly more sophisticated process. The precision-processed products may be used in a similar manner with somewhat better results in accuracy of representation.

In deciding between these choices one must consider the delay in obtaining specially processed photographic products as compared to the fast delivery time of bulk or standard products, and, of course, the additional cost.

The processing of Computor Compatible Tapes to yield the required information, requires a computor terminal and operational software, either developed in-house for simple processing and analysis or transferred from an already developed system. Here too, one can think of many levels at which the digital processing, analysis, interpretation and presentation can be performed. Here the level of sophistication can be very high with a consequent escalation in the cost of equipment and processing time. Even at the higher levels, there is a wide variety of hardware and software systems to choose from.

As one considers other airborne remote sensing systems the choices increase and the variety of other decisions involving cost, risk of equipment going out-of-date, time factor, maintenance, dependance on outside agencies etc., come into the picture.

The Case of Sri Lanka.

In Sri Lanka, the development of Remote Sensing applications has undergone the following stages : -

(a) being attracted to the advantages of the wide variety of applications ;
(b) the desire to keep pace with this developing technology ;
(c) the evaluation of the need for up-to-date landuse and crop data for national planning and development ;
(d) caution in expending valuable foreign exchange ;
(e) evaluation of the state-of-the-art with forseeable improvements, and finally
(f) a step-by-step approach to developing an operational center for Remote Sensing.

The need for such data was studied. Investigations were designed through the assistance of ERIM to study the feasibility of using Landsat Data for crop inventory.

Commencing from the simplest level of using enlargements of B/W bulk data the level of processing, interpretation and analysis was systematically raised to the use of optical devices, aerial photography for ground-truthing, preparation of Diazo Color Composites, use of the Zoom Transferscope and color composite printing. This development and the feasibility studies have revealed the possible applications and the limitations of the system.

A further development was towards the digital approach. A simple computer program adapting the LIGMALS program of Harvey Wagner (ERIM) to the small capacity (48K) general-purpose computer system was made operational. This has enabled comparison studies between the visual and the digital modes of processing and analysis. The long delay in obtaining the CCTS as compared to the comparatively fast delivery time of photographic products is noted.

Further developments planned include, the use of analogue type color display and analysis systems and interactive computor terminals for better digital processing of the CCTS.

Throughout this process of development, the size of the country, the type of data required, timeliness of the information, the benefits and cost were the major factors that influenced the decisions arrived at. Emphasis was also placed on obtaining reference material, training of Sri Lanka personnel and the building up of a self-reliant, in-house working group for photographic and digital processing. A multidisciplinary working group, for applications in the specialised fields, is organised. Considering the small size and the economic level of the country, steps are also taken to centralize the facilities under the Center for Remote Sensing as a User Facility to be shared by all interested groups or individuals.

An outline. The decision making process to solve the problems associated with organising remote sensing applications can now be outlined as follows : -

(a) Define your objectives
(b) List your data or information requirements such as -

Crop Inventory,
Land Use,
Resources (Forestry) etc.,

(c) Define how and for what purpose you will use this data ;
(d) Assess the benefits of using this information and discuss with the actual users as to exactly how it is to be presented and its potential uses in the decision-making, planning or development processes.
(e) Assuming that the data is to be presented in the form of a map (in the first instance), define the desired scale, minimum resolution or unit that needs representation and the desired accuracy required.
(f) Compare the sources presently available (within your Organisation or in another allied agency) to provide such or similar data.
(g) Are these sources inadequate ? If so, how or why ? Can they be improved or, supplemented to satisfy the needs ? If so, assess the costs and the requirements in technical, personnel, equipment etc.,
(h) Can the presently available system be used as the base for inserting the desired data ?
(i) Now select a suitable remote sensing technique to fit your needs.
(j) Assess the costs, requirements in technology, personnel etc.
(k) Compare with the results of costs etc., arrived at for (g).
(l) Select the level of sophistication in remote sensing required. Consider one step higher than your first assessment and compare costs etc.
(m) Assess the timeliness of the data acquisition, processing and presenting systems. Does this meet your requirements ? Consider delays in the remote sensing data procurement and analysis.
(n) Consider reliability, continued availability, the need for co-operation with other organisations in other countries, the need to keep pace with a developing technology etc.

CONCLUSIONS:

It is felt that the need for better texts, reference material, training programs and consultancy services is important and opportune. The forming of an international professional group to advice on these aspects is desirable. The auspices of International and National Professional Bodies and Research Organisations as well as those of the United Nations, FAO etc., to co-ordinate or even organise this activity is most desirable.

The aspects of regional co-operation of satellite receiving stations, sharing of other facilities (including Airborne Remote Sensing Systems) as well as unbiased information on the capabilities and limitations of the various systems may be some of the important matters that need the attention of such a co-ordinating body as proposed.

EXPERIMENTS IN THE USE OF REMOTE SENSING FROM SATELLITE AND AERIAL PHOTOGRAPHY FOR FOREST INVENTORY

by

Piran Wiroatmodjo

Directorate of Forestry Planning

Bogor, Indonesia

ABSTRACT

The objectives of these experiments were :

1st : To find out the usefulness of satellite imagery for forest inventory. For this purpose some experiments were made on different types of primary forests as well as on plantation forests.

2nd : To find out a basic method for quantitative analyses of forest stand from vertical photographs. The experiments were carried out in the low-land Dipterocarps forest of Kendilo watershed, East Kalimantan.

The results of the experiments may be described as follows :

1. Satellite imagery is useful for
   a. identification of forested areas.
   b. identification of the types of primary forests
   c. rough stratification of forests in flat terrains up to those with gentle hills based on forest stand density
   d. rough stratification of teak plantation forest in flat up to those with gentle hills based on age class.
2. There is a significant linear correlation between parameters of forest stands of trees with diameters of 20 cm and up (in this context the average number of trees and stand volume per hectare of forested area) and the crown density percentage measured directly from 1 : 24,000 scale vertical aerial photographs, so that a quantitative analysis of forest stand can be established from aerial photographs.

PREFACE

The forest cover of Indonesia is approximately 1,200,000 sq.km or about 60% of the total land surface. During this decade the volume of forest production, especially wood, has increased rapidly and has made forestry the second most important export commodity producing natural resource. The increasing role of forestry in the national economic development requires more appropriate management in order to produce the maximum benefit and to sustain forest production. Management can be carried out only on the basis of right planning founded on reliable data obtained in a quick and inexpensive method, especially data on extent, distribution, volume and composition of stands. These considerations have motivated the author to investigate possibilities of utilizing remote sensing for forest inventory.

The research used as basis of this poster paper is the first part of the research into remote sensing utilization in forestry, comprising identification of forest areas, forest types and other vegetations from satellite imagery and estimation of stand volumes and composition from aerial photos. The research was carried out in the area of Cepu, Java, Kalimantan, Sulawesi and Sumbawa island.

The results of the research prove the usefulness of remote sensing techniques for national as well as provincial forest inventory. This research is an essential step in developing remote sensing for forest inventory purposes in Indonesia.

CHAPTER I. IDENTIFICATION OF FORESTED AREAS AND FOREST TYPES

1. MATERIAL AND AREA OBSERVATION

To probe the possibilities of identifying forested areas and forest types, an analysis has been carried out from ERTS-1 imageries, vertical aerial photos and some field observations. The materials and the terrain observed can be described as follows :

ERTS - 1 imagery

Java : Colour composite from bands 4, 5 and 7 scale 1 : 1,000,000, and black and white, scale 1 : 500,000, paper print, taken in September - October 1972 and September 1973 with sun elevation ranging from 49^{o} to 58^{o}. All of these ERTS - 1 imageries were taken in dry season.

Kalimantan : Colour composite from bands 4, 5 and 7 scale 1 : 1,000,000 and black and white scale 1 : 1,000,000 from band 5, paper print, taken in September 1972 and in July 1973 with sun elevation ranging from 48 to 56 degrees.

Sulawesi : Colour composite from band 4, 5 and 7 scale 1 : 1,000,000, paper print, taken in September - October 1972 with sun elevation ranging from 48 to 58 degrees.

Sumbawa : Colour composite from bands 4, 5 and 7, scale 1 : 1,000,000, paper print, taken in September 1972, with sun elevation 51 degrees.

Aerial photographs

Java : Cepu teak plantation forest, vertical, scale 1 : 30,000 with normal angle camera black and white panchromatic film, taken on June 15, 1975.

Kalimantan : West Kalimantan vertical aerial photographs, scale 1 : 50,000, taken with wide angle camera, black and white panchromatic film, in 1969 - 1970.

Sulawesi : South East Sulawesi vertical, scale 1 : 60,000, taken with wide angle camera, black and white panchromatic film, in 1969.

Ground truth

Forest map : Java, scale 1 : 250,000, of 1972 - 1975 and Cepu forest complex 1972. Sumbawa, scale 1 : 1,000,000, of 1975.

Ground survey : Kalimantan in 1970 - 1977.

Conditions of the areas observed.

The areas observed have different forest types and vegetation types and have various types of topography, climate, soil and land-use.

2. ANALYSIS AND RESULTS

Reflection of electromagnetic waves from stand depends on :

a. the quantity and the quality of the electromagnetic waves received.
b. the physical conditions of the stand.
c. the physiological conditions of the component trees of the stand.

The quantity and the quality of the electromagnetic waves the vegetation receives depend, among other things, on : the elevation of the sun, atmospheric conditions especially cloud and mist, and the field topography. The radiation of electromagnetic waves from the sun is at its height when the sun is at right angle with the horizontal plane. While the field topography, particularly the field inclination, has its bearings on the quantity of the electromagnetic waves from the sun. Every element of component trees of the vegetation absorbs and reflects parts of the electromagnetic waves received. So the density of every area unit and its structure may influence the quality and the quantity of the reflectance. The physiological conditions of the component trees of the vegetation, especially the chlorophyll and water content and anatomic structure, affect the strength of the reflection.

In the visible region of electromagnetic waves, from 400 to 750 nm, the absorption of light by pigment, particularly chlorophyll, is dominant, while near infra-red region, from

750 - 1350 nm is the region of high reflectance where the degree of reflectance depends mainly on the anatomical structure of leaves. Both of these regions are considered effective for edentifying and analyzing stands.

ERTS - 1 imageries now available are of the bands 4, 5, 6 and 7, in the wave-lengths of 500 - 600, 500 - 700, 700 - 800, 800 - 1100 nm respectively, all of which are in visible and near-infra red regions. Based on the above-said physics, the imageries are expected to produce data on the distribution of forests even the types and composition of stands. Analysis is aimed at identifying distribution, extent and stands of :

a. natural forest
   1. mangrove forest
   2. littoral forest
   3. swamp forest
   4. peat forest
   5. lowland rainforest
   6. highland rainforest
   7. lowland monsoon forest
   8. highland monsoon forest

b. plantation forest
   9. teak forest
   10. conifer forest
   11. forest of other species.

In which forests are defined as tree-covered areas with interlacing crowns. It should be noted that with this identification, similarities of tones are possible between forest and :

12. horticultural estate
13. brushland
14. resettlement areas with horticultural plants
15. secundary forest with pioneer trees and low stand volume
16. alang-alang or grass-land and shrubs
17. nipa or thatch palm — 16 open land
18. wet and dry ricefield.

Phenomena on ERTS - 1 imageries used for identification and analysis are : colour, grey density, pattern and topography of the area. ERTS - 1 imageries are examined on a light-table and lens and aerial photos are examined under mirror-stereoscope. In colour composite imageries, trees emanate a red colour, whereas in black and white they emanate a darker tone.

From the examination it can be concluded that :

1. Mangrove forests can be identified clearly and can be distinguished from nipa and brushland.
2. The existence of littoral forests can be ascertained, though they are hardly distinguish-able from adjoining dry-land forests.
3. Swamp forests, can be identified, and can be distinguished from brushland, mangrove and dryland. The discrepancy between forest boundaries on ERTS - 1 imagery and those on aerial photos is mainly caused by the difference in scale and technique used in mapping.
4. Peat forests can be distingushed from swamp forests. On the whole, peat forests have a greater density than swamp forests.
5. Dryland forests are identifiable. Analitical results of ERTS - 1 imagery of Sumbawa island, hardly show any difference between rain forests and monsoon forests. In areas where the tone is strongly effected by topography, differences in stand density are difficult to notice.
6. In lowland areas in Central Java, teak plantation forests can be distinguished from Pinus merkusii and mixed species plantation forests. But the difference become vage when those three forest types are situated in areas where there is no pronounced dry season, such as in Wilis area, East Java. Tone differences in Cepu teak plantation forests are compatible with age class differences (map 1).
7. Rubber plantations can be distinguished from any type of primary natural forest.

Identification of other vegetation types, such as brushes, decayed secundary forests, grassland, rice-fields and open-land, does not give much difficulty.

3. C O N C L U S I O N

a. From colour-composite ERTS - 1 imagery we can map out vegetation types and forest types.

b. Distribution and extent of plantation forests can be identified as long as the coverage is large enough.
c. ERTS - 1 imagery can be used as the basis of a more intensive forest inventory.

CHAPTER II. STANDING STOCK ESTIMATION

1. SITE AND MATERIAL

The Kendilo river watershed, East Kalimantan, has been selected for this research. Its' position is between 115°53' - 115°56' East and between 1°43' - 1°53' South. The area amounting 5502 hectares, has a slightly undulated topography and its altitude is 100 - 400 m above sea level. The average rainfall is 2572 mm per year with no pronounced dry season. The soil belongs to latosol, red-yellow podsolic and litosol soil types.

The forests are dry-lowland tropical rainforests. The upper crown layer is dominated by Dipterocarps, Koompassia, Cratoxylon and Durio. The second layer is dominated by Lauras and Anacardias. Field observations have recorded the existence of 103 species in this area.

Aerial photographs used in this research have the following description : taken in July 1973, with normal angle camera, focal length 152.55 mm, black and white panchromatic film on the scale of 1 : 24,000.

2. DATA COLLECTING METHOD

Data collecting from aerial photos as well as from the field is done by sampling. The steps taken can be outlined as follows :

a. Stratification of the forest on photos according to crown over density.
b. Fixation of plots on aerial photos for every stratum, measuring 2 hm x 3 hm actual size.
c. Measurement of crown density using crown cover scale with 5 % class interval.
d. Mapping.

Data collecting in the field was done with double sampling. Each sample on photos is presented by 6 circle plot of 0.1 ha each (actual field size), allocated systematically. Scheme of sample plot location shown on map 3. On every sample plot the breast-high diameter and the height of the free bole of every sound tree are measured. The volume of the free-bole is calculated using the form factor 0.7. From the results of the field measurements the average number of trees and the average of stand volume per hectare of forested area of each stratum can be calculated producing dependent variable (Y), while crown closure in the photo is independent variable (X). Hereunder follows a list of dependent variables :

Group 1, all tree species

Y 1,	average number of trees per ha (N), diameter	>= 20 cm
Y 2,	average volume per ha (V) of trees, diameter	>= 20 cm
Y 3,	N	>= 35 cm
Y 4,	V	>= 35 cm
Y 5,	N	>= 50 cm
Y 6,	V	>= 60 cm

Group 2, all commercial tree species

Y 7,	N	>= 20 cm
Y 8,	V	>= 20 cm
Y 9,	N	>= 35 cm
Y10,	V	>= 35 cm
Y11,	N	>= 50 cm
Y12,	V	>= 50 cm

Group 3, commercial export species

Y13,	N	>= 20 cm
Y14,	V	>= 20 cm
Y15,	N	>= 35 cm
Y16,	V	>= 35 cm
Y17,	N	>= 50 cm
Y18,	V	>= 50 cm

Group 4, Dipterocarps

Y19,	N	>= 20 cm
Y20,	V	>= 20 cm
Y21,	N	>= 35 cm
Y22,	V	>= 35 cm
Y23,	N	>= 50 cm
Y24,	V	>= 50 cm

3. ANALYSIS AND RESULTS

A graphical examination has been made to select the suitable regression equation for each Y on X correlation. It appears that conventional linear regression equation is may fit. The regression equation between variables may, theoritically speaking, form parabola or hyperbola assymptotic to a line parallel with X axis. It may also be a linear regression that goes through the origin. These reasonings lead to the following regression :

1). $Y = A + B.X$
2). $Y = B.X$
3). $Y = A + B.\ln(X)$
4). $\ln(Y) = A + B.\ln(X)$
5). $Y = \frac{1}{A + B.X}$

All constanta are calculated using the least squared technique, with the help of computer Q1 in the PL 1 language. A regression is considered effective, if the correlation coefficient (= r) is higher than 0.7 and has a lower squared residuals total and standard deviation.

The computations have resulted in regression considered the best for each pairs of variables as follows :

1.	$\hat{Y}\ 1 = 108.878 + 0.754.\ X$	r = 0.478	*
2.	$\hat{Y}\ 2 = 24.982 + 2.843.\ X$	0.880	
3.	$\hat{Y}\ 3 = 24.148 + 0.633.\ X$	0.679	*
4.	$\hat{Y}\ 4 = 5.744 + 2.759.\ X$	0.876	
5.	$\hat{Y}\ 5 = 0.905 + 0.504.\ X$	0.831	
6.	$\hat{Y}\ 6 = 28.139 + 2.454.\ X$	0.852	
7.	$\hat{Y}\ 7 = 11.669 + 0.704.\ X$	0.633	*
8.	$\hat{Y}\ 8 = -34.769 + 2.413.\ X$	0.800	
9.	$\hat{Y}\ 9 = -0.980 + 0.511.\ X$	0.749	
10.	$\ln(\hat{Y}10) = -3.869 + 2.017.\ X$	0.839	
11.	$\hat{Y}\ 11 = -2.991 + 0.340.\ X$	0.701	
12.	$\hat{Y}\ 12 = -39.754 + 2.031.\ X$	0.773	
13.	$\hat{Y}\ 13 = -9.779 + 0.758.\ X$	0.746	
14.	$\hat{Y}\ 14 = -47.267 + 2.302.\ X$	0.757	
15.	$\hat{Y}\ 15 = -7.485 + 0.486.\ X$	0.741	
16.	$\hat{Y}\ 16 = -46.292 + 2.162.\ X$	0.756	
17.	$\hat{Y}\ 17 = -7.147 + 0.368.\ X$	0.776	
18.	$\hat{Y}\ 18 = -39.620 + 1.812.\ X$	0.683	
19.	$\hat{Y}\ 19 = -14.370 + 0.664.X$	0.724	
20.	$\hat{Y}\ 20 = -55.674 + 2.241.\ X$	0.738	
21.	$\hat{Y}\ 21 = -10.782 + 0.479.\ X$	0.725	
22.	$\hat{Y}\ 22 = -54.240 + 2.144.\ X$	0.738	
23.	$\hat{Y}\ 23 = -8.835 + 0.365.\ X$	0.745	
24.	$\hat{Y}\ 24 = -51.101 + 1.965.\ X$	0.722	

Note : * less effective regression equation.

The linear regression equation for Y 10 is :

$Y\ 10 = -\ 38.408 + 2.278.\ X \qquad r = 0.806$

Student's t tests have shown that each of all A's, B's and r's is significant different from zero, except the values of A for Y4, Y5, Y7, Y9 and Y11. Anyhow, linear regressions through the origin always resulted a bigger total of recidual squared, so that conventional linear regression equations remain to be considered the best.

4. D I S C U S S I O N

Analitical results have proved that there is a significant linear correlation between standing stock, calculated for all species as well as for groups of species, and crown clasure percentage measured from 1 : 24,000 scale aerial photos, so that standing stock estimation can, in principle, be done with the help of vertical aerial photos.

The above - meant regressions are valid only for the forests where the research has been made, or for other forests with stand compositions, of which the diameters and tree species do not differ very much from those in the area of research.

Standing stock calculation for the whole area can be done by substitution of crown closure percentages in the regression equations resulting from the above analysis and by multiplying the outcome by the area of the forest concerned, while the crown closure percentage can be measured by means of sampling.

This method can be applied to the inventory of extensive forest area. Data collecting in the field serves to be used in calculations to obtain regression equations suitable for the areas concerned. Further studies should be made into the possibilities of establishing regression equations that is applicable to each forest type.

5. C O N C L U S I O N

1. There is a significant correlation between standing stock (expressed in the average number of trees and volume per hectare of forested area) and the crown closure percentage measured from vertical aerial photographs.
2. The double sampling technique of standing stock estimation using aerial-photos may be recommended, at least for low-land tropical rain forest.

L I T E R A T U R E

American Society of Photogrammetry 1975 : A Manual of Remote Sensing, Volume I, II, American Society of Photogrammetry, Falls. Church, Virginia.

Kalensky. Z and J.M. Wightman, 1976 :
Automatic forest mapping using remotely sensed data, Invited paper XVI IUFRO World Congress, Oslo, Norway.

Loetsch, F. and K.E. Haller, 1964 :
Forest Inventory I ; Bl. V. Verslagsgesellschaft, Munchen Basel Wein.

Steenis. C. G.G.J. van, 1957 :
Tropical lowland vegetation, the characteristics of its types and their relation to climate.

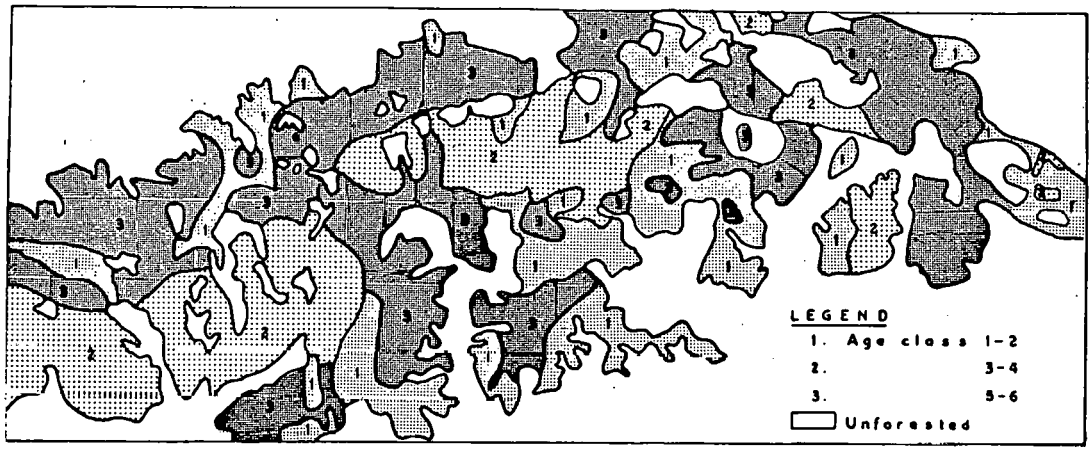

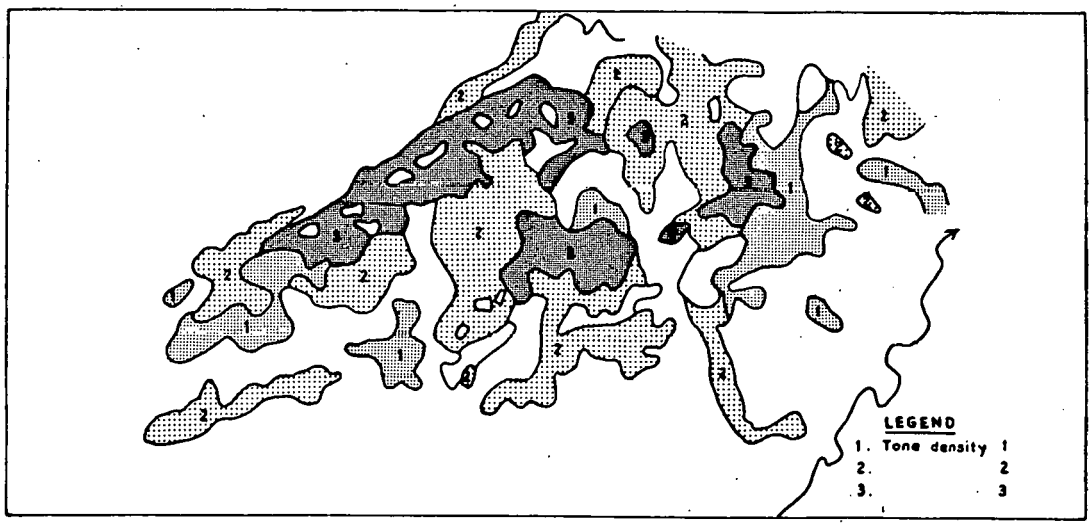

M A P 1 . Teak plantation forest in Cepu, Central Java, scale 1 : 250,000
Above : Compiled from aerial photo.
Bottom : From color composite ERTS - 1 imagery.

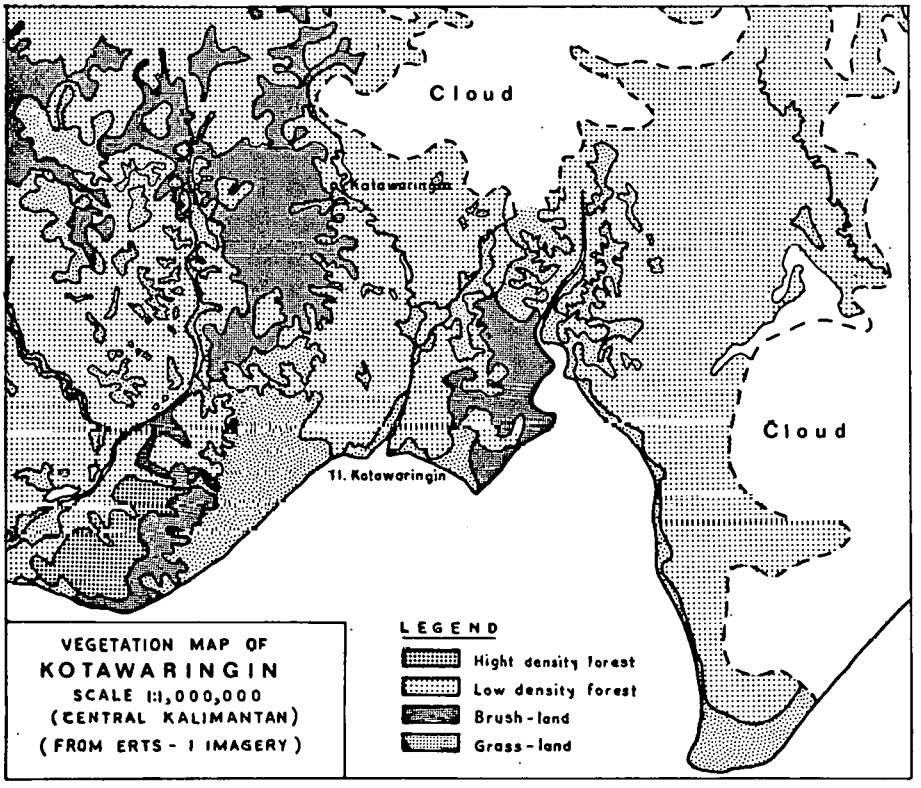

M A P 2

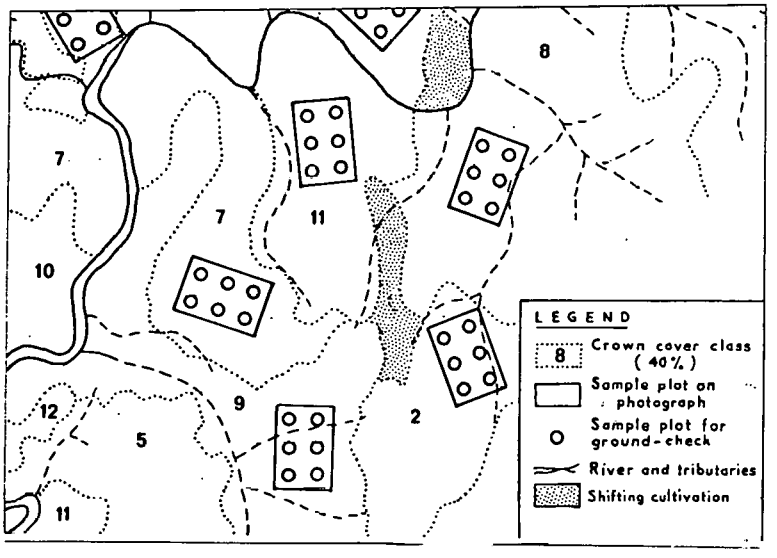

M A P 3. Scheme of the sample plots location

INFRARED REMOTE SENSING ON GEOTHERMAL AREAS BY HELICOPTER

M.SEKIOKA

INSTITUTE OF METEOROLOGY, THE DEFENSE ACADEMY, YOKOSUKA, JAPAN

AND

K.YUHARA

FACULTY OF ENGINEERING, KYUSHU UNIVERSITY, FUKUOKA, JAPAN

ABSTRACT

A technique is developed to determine surface temperature distributions by using a helicopter-borne infrared thermographic instrument, the Canon CT-5B Thermocamera, giving thermal images of television type. Making a helicopter with an open hatch on its floor, through which a thermal images are photographed, to hover over the target area, the temperature distributions with high resolution can be obtained in projection on a horizontal plane. The two experimental surveys were performed for several subregions of an active volcanic island, Satsuma-iwojima island, Kagoshima, Japan. In the first survey, an attempt to print out digitally the ratio of areas between each adjacent isotherm on the isothermal image is sufficiently carried out with an isothermal area processor. A method converting the isothermal pattern of geothermal fields to a distribution of heat discharge will be applied to such a ratio of areas of isothermal patterns thus obtained in the near future. In the second one, effects of atmospheric absorption and emission between the sensor of the Thermocamera and the target area are evaluated using a newly developed helicopter-borne radiosonde system to correct the surface temperatures measured by the Thermocamera.

1. INTRODUCTION

Many aerial measurements of the surface temperature distribution by using infrared thermometers and infrared line-scanning radiometers operated on board of an aircraft have been carried out in geothermal and volcanic areas. These surveys have an advantage in rapid measurement of the temperature patterns in a vast area, but it is not suitable to the detailed analysis of patterns.

On the other hand, surveys with helicopter-borne instrumentation have been also interested in such a measurement. Colacino et al. (1976) carried out in the period of 1971-1972 several experimental surveys, by a Barnes PRT-5 radiometer installed on board of a helicopter of the Italian Navy, of the surface temperatures on the Garda lake, Italy. Owing to the low altitude and low-speed flight of a helicopter, such a survey can bring about high-resolution temperature data over a relatively small domain. But, since the data thus obtained by using an infrared radiometer are only along the flight path of a helicopter, interpolation and extrapolation are required to determine the temperature patterns.

A survey with the helicopter-borne thermographic instrument which gives

a thermal image of television type may enhance an advantage of utilization of helicopters. Making a helicopter to hover over a target area, the temperature distribution of the area, dimension of which depends on the hovering height, can be instantaneously obtained as a thermal image projected on a horizontal plane without any interpolation and extrapolation.

In the present paper, the two surveys are reported which were operated in February and December of 1976 over an active volcanic island, Satsuma-iwojima island, and its peripheries by using helicopter-borne Canon Infrared Thermocamera CT-5B. In the first survey, an isothermal area processor printed out digitally the ratio of areas between each adjacent isotherm on the isothermal pattern (Yuhara et al., 1978). A digital ratio thus acquired can facilitate an application of a formula (Sekioka and Yuhara, 1974) converting the isothermal pattern of geothermal fields to the distribution of heat discharge.

In the second survey, a newly-developed helicopter-borne radiosonde system (Sekioka, 1978) was employed to correct the Thermocamera-obtained data for effects of atmospheric absorption and emission between the sensor of the Thermocamera and the target areas.

2. SATSUMA-IWOJIMA ISLAND

As seen in Fig.1, Satsuma-iwojima island, Kagoshima, Japan, which is located near 30°47'N and 130°16'E about 40 km southwest of the main land of Kyushu, has an active volcano, Iwodake (704 m), at the eastern part of the island, and many fumaroles are found in its summit crater and around its mountainside. Many hot springs with various chemical compositions also flow out below the sea surface and react with sea water to make reddish and yellow-whitish sediments which develop the several small discolored sea areas surrounding the island.

3. DESCRIPTION OF THE THERMOCAMERA CT-5B

The Canon Infrared Thermocamera CT-5B, made by Canon Inc. in Japan, consists of two parts, the thermocamera head and the display unit. The specifications of the Thermocamera are as follows: the objective temperature range is -20 to 1850°C; the spectral band pass is 8 to 14 μm; the detectable temperature differences are 0.12°C at 30°C and 2.0°C at 500°C; fields of view are 18 deg and 30 deg in the horizontal and vertical directions, respectively; the number of picture elements is 120,000 and the image-scanning time is 5 sec. The thermal image taken by Canon CT-5B can be selected among monochromatic continuous temperature pattern, 5-stage discontinuous isothermal pattern and 10-stage discontinuous isothermal pattern.

As the thermocamera head is cooled with liquid nitrogen, direct sensing through the open hatch by tilting it downward is impossible, and, therefore, an indirect sensing is carried out through a mirror attached in front of the thermocamera head as shown in Fig.2. Reflectivity of a mirror which is made by coating an aluminium-vaporized float glass with silicon dioxide is 94 to 95 % within the present band pass. Mirror images can be normalized electronically in the display unit of the Thermocamera.

4. EXPERIMENTAL SURVEY I

Using a helicopter, Fuji-Bell 204B of Nakanihon Air Service Co., observations were performed on 21 February 1976 over Nagahama bay, Shin-iwojima island and Monogusa solfataric field (see Fig.1). Following is a summary of the paper by Yuhara et al. (1978) for this survey. Since fields of view are 18 deg and 30 deg in the horizontal and vertical directions, respectively, approximate areas of the target are from 95×160 m to 160×270 m corresponding to the hovering heights of 300 to 500 m. The helicopter hovered about 5 minutes over each target area.

An isothermal area processor, which prints out digitally the areal ratio of isothermal zones on the isothermal pattern, one of thermal images obtained by the Thermocamera, is combined with an on-line, real-time-measuring system. A data recorder Sony DFR-3415 is also used on board. Input of a thermal data

from the thermocamera head into the data recorder can be processed to get the various temperature pattern mentioned above by using the display unit in a laboratory after landing of the helicopter. This makes hovering time shorten. In the present case, *in situ* direct input of 5-stage discontinuous isothermal pattrn into the isothermal area processor, by which the ratio of five isothermal areas is printed out, is also done during a hovering time. The measuring system is shown in Fig.3.

On the other hand, during hovering of a helicopter, color photographs of the target areas were also taken to collate with their thermal images.

(a) Nagahama bay:

Fig.4 is a photograph of Nagahama bay. The area surrounded by a jetty and a landing pier which are seen at the upper right and the central parts, respectively, is a fishing port. Hot spring water wells up from the bottom of this port near its beach and dyes sea water red. Fig.5 shows the 5-stage discontinuous isothermal pattern of Nagahama bay ranging from 14.0 to 20.0°C inside a frame indicated on Fig.4. The maximum sea surface temperature in the port is seen as some white spots indicating temperature above 18.8°C along the beach. Outside of the range of 17.6 to 18.8°C surrounding the maximum temperature spots, a zone of 16.4 to 17.6°C is found. A low temperature strip with range of 15.2 to 16.4°C along the beach is due to breakers mixing cold air with warm sea water.

Such a temperature distribution that the maximum temperature spots stand in a line parallel to the beach is more minute than that measured by a remote controlled, unmanned boat on 15 August 1976 (see Fig.6) excepting the absolute value.

(b) Shin-iwojima island:

Fig.7 is an aerial view of Shin-iwojima island located at about 2 km east of Satsuma-iwojima island. It is a new volcanic island formed by a submarine eruption in December of 1934. Surface temperature distribution over the central part of Shin-iwojima island inside a frame indicated on Fig.7 is shown in Fig.8 with the 5-stage isothermal expression same as in Fig.5. It is seen that sea surface temperatures have the maximum value above 18.8°C at the innermost of the southern cove and decrease gradually outward to the range of 16.4 to 17.6°C. While in the northern cove, the maximum sea surface temperature is in the range from 17.6 to 18.8°C less than the southern one. These distributions give more information than the previous results (Yuhara et al., 1977). Ground surface temperatures of the island are generally in the range from 15.2 to 16.4 °C, but a somewhat higher temperature region in its middle part with range of 16.6 to 17.6°C may be owing to an old-and-now-inactive crater.

(c) Monogusa solfataric field:

At the western foot of Iwodake, there is an active solfataric field called Monogusa. Fig.9 shows a part of this area where several fumaroles are located around a block of lava rock. Fig.10 is the 5-stage isothermal expression inside a frame indicated on Fig.9. High temperature regions above 19.8°C include those fumaroles.

5. EXPERIMENTAL SURVEY II

5.1.HELICOPTER-BORNE RADIOSONDE SYSTEM

A success of Experimental Survey I was followed by Experimental Survey II. It is attempted in the survey to correct the surface temperatures obtained by the helicopter-borne Thermocamera for effects of atmospheric absorption and emission below a hovering level of helicopter, by using a recently developed helicopter-borne radiosonde system (Sekioka, 1978).

The principal units of the helicopter-borne radiosonde system are a radiosonde, a receiving and recording equipment and a winch.

A cylindrical radiosonde measures 10 cm in diameter and 36 cm in height and weights 1700 gr. It is designed for use with a nyron string let out from the winch set up on the floor of a helicopter. The dry- and wet-bulb tempera-

ture elements employ thermistor thermometers and the pressure unit has an aneroid capsules. Specifications of the radiosonde are as follows; detection range of -10 to 40°C for dry-bulb temperature, 0 to 40°C for wet-bulb temperature, 5 to 35°C for water temperature and 930 to 1030 mb for pressure, and sensitivities of ±0.3°C for all temperatures.

Radio transmitter sends out 2-second-continuous signals of water temperature, wet-bulb temperature, dry-bulb temperature and reference temperature every 8 seconds, on the carrier frequency of 398.5 MHz.

The winch gives a descending rate of 3 m/sec to the radiosonde. Length of a nyron string counted by a counter every 10 m is about 500 m. After a downward measurement the radiosonde is pulled up to a helicopter with ascending rate of 3 m/sec by the winch.

The receiving and recording equipment is loaded on a helicopter and a four elements Yagi antenna is fixed downward at a corner of the open hatch.

5.2.EQUIVALENT BLACKBODY TEMPERATURE

Referring to NASA's definition, the equivalent blackbody temperature is obtained as follows (details of a practical procedures are found in Fujita et al. (1968)): The effective radiant emittance is computed from

$$W = \int_0^\infty B(\lambda,T)\phi_\lambda d\lambda \qquad (1)$$

which denotes that portion of blackbody radiant emittance which would be detected by a sensor with a spectral response ϕ_λ. The spectral response of the Thermocamera ranges from 8 to 14 μm.

The radiation transfer equation can be written as

$$W = \int\int \phi_\lambda B(\lambda,T)d\tau d\lambda + \int e_s \tau_{s\lambda}\phi_\lambda B(\lambda,T_s)d\lambda \qquad (2)$$

where τ denotes the transmissivity of the atmosphere from the sensor to any level and τ_s the transmissivity to the background radiation with temperature T_s and emissivity e_s of the emitting surface. Emissivity of the surface of sea water and geothermal fields can be assumed to be unity by citing the previous investigations (e.g., Sekioka and Yuhara, 1974). By equating equations (1) and (2), the equivalent blackbody temperature can be obtained.

The transmissivity in equation (2) for a specific wavelength in the atmospheric window region is a function of the effective optical path u_e only. The transmissivity between a helicopter and a specific layer is computed by dividing the atmosphere into for layers of 10 mb. The effective optical path u_e is given by

$$u_e = \frac{1}{g}\int_{P_a}^{P} q\,\frac{P}{P_0}\,dP \qquad (3)$$

where P_a is the pressure at the hovering level, P_0 1013.25 mb, g the acceleration of gravity and q the mixing ratio. A relation between the emissivity and the effective optical path in the window region is shown by Wark et al.(1964).

5.3.MEASUREMENT

Experimental Survey II was operated on 14 and 15 December 1976 over some target areas in Satsuma-iwojima island (see Fig.1) by using a two-engine helicopter V-107 of the Japan Ground Self Defense Force, which has also an open hatch of 80×80 cm on its floor. The Thermocamera and the radiosonde system are installed on board of V-107.

A case of Heikenojo cape (see Fig.1) observed at 0935 JST on 15 December 1976 is, as an example, reported here. Yellow-whitish sediment spreading along the coast of Heikenojo cape extends zonally toward the offing. Fig.11 is a 5-stage discontinuous isothermal pattern at the yellow-whitish zone and its perifery in the offing of Heikenojo cape. It ranges from 15.0 to 21.0°C. While, the vertical profile of mixing ratio q computed from the dry- and wet-bulb temperatures and pressure observed above the yellow-whitish zone during the in-

frared remote sensing by the helicopter-borne radiosode system is shown in Fig. 12, with the vertical temperature distribution and the water temperature. With these data the equivalent blackbody temperature is 19.1°C corresponding to the sea surface temperature of 21°C. This rather large damping of the sea surface temperature is due to cold air temperature between the hovering height of 290 m and the sea surface in spite of rather low mixing ratio. Absorption by CO_2 can be ignored (Fujita et al., 1968).

In order to correct the temperature distribution taken by the Thermocamera for atmospheric absorption and emission, the sea surface temperature is changed from 17 to 23°C at 2°C intervals while keeping the overlaying atmosphere unchanged, as was done by Fujita et al. (1968). Corresponding equivalent blackbody temperatures have damping effects of 1.7 to 2.0°C.

6. CONCLUSION

An infrared remote sensing scheme by a helicopter was established through the two experimental surveys mentioned here. The Thermocamera, the data recorder and the isothermal area processor operated on board of a helicopter bring about high-resolution isothermal pattern projected on a horizontal plane.

The helicopter-borne radiosonde system corrects, during the thermal measurement, those data mentioned above for effects of absorption and emission of water vapor in the atmospheric layer below the hovering level of a helicopter. The corrected high-resolution temperature patterns of the surface is accomplished finally.

Such patterns will be converted to the heat discharge patterns by using a formula developed by Sekioka and Yuhara (1974) when the vertical wind shear near the earth's surface can be observed. The radiosonde system is, therefore, modifying to equip a wind sensor.

ACKNOWLEDGMENTS

The Experimental Survey II was supported by the 1st Helicopter Brigade, J GSDF. The helicopter-borne radiosonde system was manufactured by Meisei Electric Co., Ltd. in Japan.

REFERENCES

Colacino,M.,Giorgi,M.,Guerrini,A. and Vivona,F.,1976, Thermal Surveys on the Lake Garda by Infrared Equipments: Arch.Met.Geoph.Biokl., ser.A, vol.25, pp.159-170.

Fujita,T.,Baralt,G. and Tsuchiya,K.,1968, Aerial Measurement of Radiation Temperatures over Mt.Fuji and Tokyo Areas and Their Application to the Determination of Ground- and Water-Surface Temperatures: Journ.Appl.Meteor., vol.7, pp.801-816.

Sekioka,M.,1978, Helicopter-borne Radiosonde System and Its Experimental Use: (to be published)

Sekioka,M. and Yuhara,K.,1974, Heat Flux Estimation in Geothermal Area Based on the Heat Balance of the Ground Surface: Journ.Geophys.Research, vol.79, pp.2053-2058.

Wark,D.Q.,Alishouse,J. and Yamamoto,G.,1964, Variation of the Infrared Spectral Radiance near the Limb of the Earth: Appl.Optics, vol.3, pp.221-227.

Yuhara,K.,Sekioka,M and Ehara,S.,1978, Infrared Measurement on Satsuma-iwojima Island, Kagoshima, Japan, by Helicopter-borne Thermocamera: Arch.Met. Geoph.Biokl., (to be published).

Yuhara,K.,Sekioka,M. and Yoshida,T.,1977, Measurement of Sea Surface Temperatures by Remote Controlled, Unmanned Boat: Water Temperature Research, vol.20, pp.4039-4048 (in Japanese).

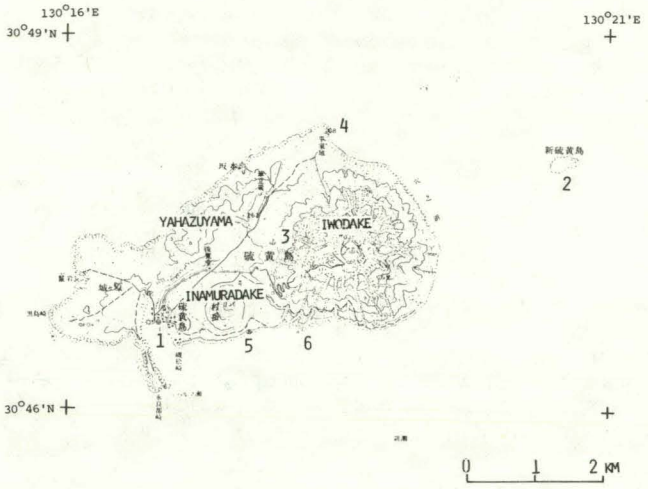

Figure 1. MAP OF SATSUMA-IWOJIMA ISLAND AND ITS PERIPHERIES
1: Nagahama bay, 2: Shin-iwojima island, 3: Monogusa solfataric field, 4: Heike-nojo cape, 5: Akayu spa and 6: Higashi spa.

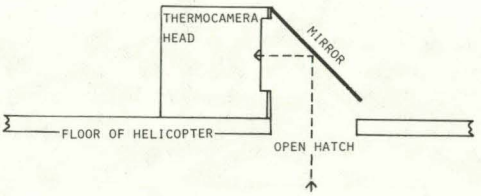

Figure 2. THERMOCAMERA HEAD WITH A MIRROR

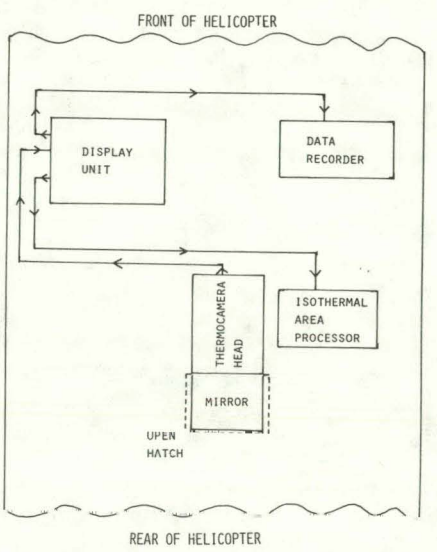

Figure 3. ARRANGEMENT OF MEASURING SYSTEM

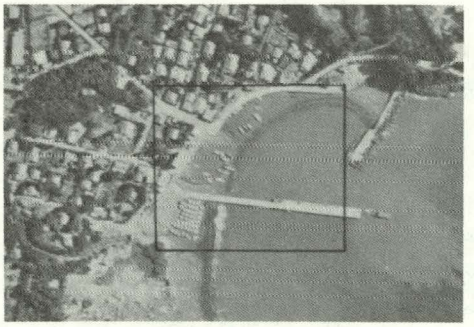

Figure 4. AERIAL VIEW OF NAGAHAMA BAY
Frame indicates limits of thermal image shown in Figure 5.

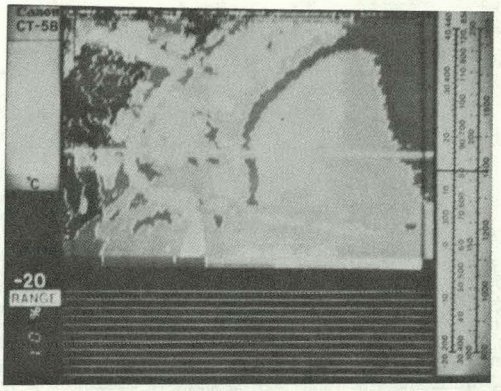

04.9 35.7 34.6 16.8 06.5

Figure 5. 5-STAGE DISCONTINUOUS ISO-THERMAL PATTERN OF NAGAHAMA BAY
Temperature range are, from black to white, 14.0 to 15.2°C (6.5%), 15.2 to 16.4°C (16.8%), 16.4 to 17.6°C (34.6%), 17.6 to 18.8°C (35.7%) and above 18.8°C (4.9%), respectively. Numerals in parentheses are the ratio of covering areas of each isothermal zone.

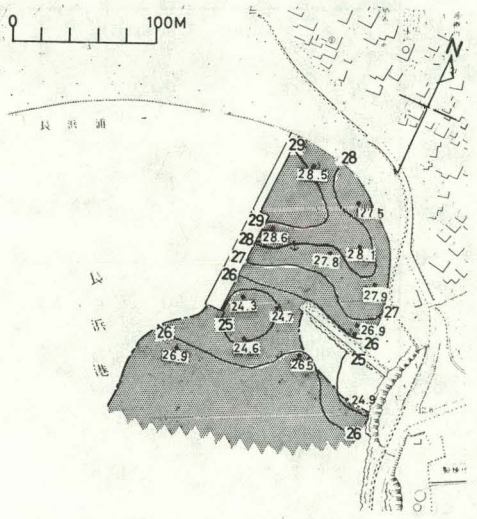

Figure 6. TEMPERATURE DISTRIBUTION OBTAINED BY THE REMOTE CONTROLLED, UNMANNED BOAT IN AUGUST OF 1976.

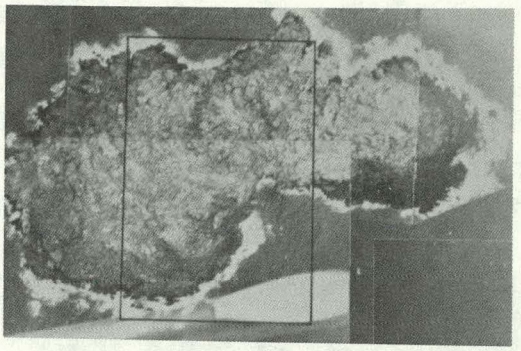

Figure 7. AERIAL VIEW OF SHIN-IWOJIMA ISLAND
Frame indicates limits of thermal image shown in Figure 8.

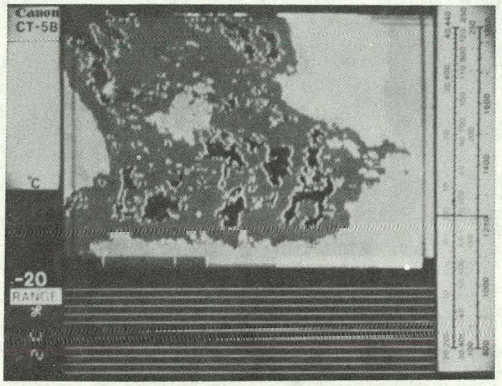

06.6 08.9 24.6 52.1 08.1

Figure 8. 5-STAGE DISCONTINUOUS ISO-THERMAL PATTERN AT THE CENTRAL PART OF SHIN-IWOJIMA ISLAND
Temperature ranges are, from black to white, 14.0 to 15.2°C (8.1%), 15.2 to 16.4°C (52.1%), 16.4 to 17.6°C (24.6%), 17.6 to 18.8°C (8.9%) and above 18.8°C (6.6%), respectively.

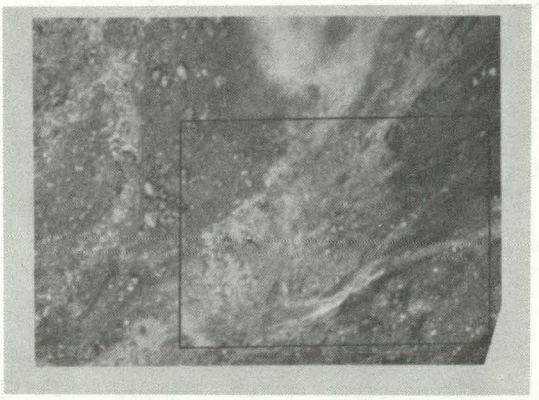

Figure 9. AERIAL VIEW OF MONOGUSA SOLFATARIC FIELD
Frame indicates limits of thermal image shown in Figure 10.

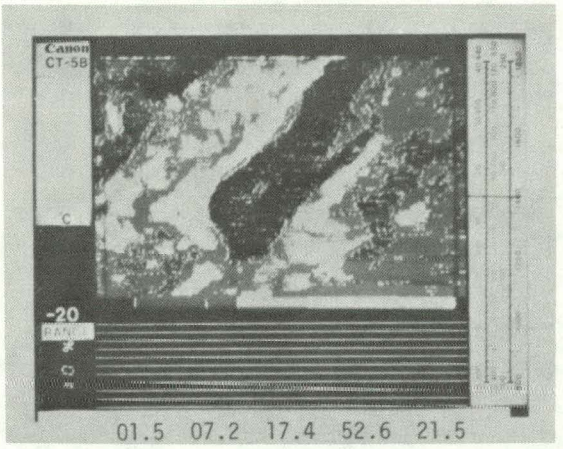

Figure 10. 5-STAGE DISCONTINUOUS ISOTHERMAL PATTERN OF MONOGUSA SOLFATARIC FIELD
Temperature ranges are, from black to white, 15.0 to 16.2°C (21.5%), 16.2 to 17.4°C (52.6%), 17.4 to 18.6°C (17.4%), 18.6 to 19.8°C (7.2%) and above 19.8°C, respectively.

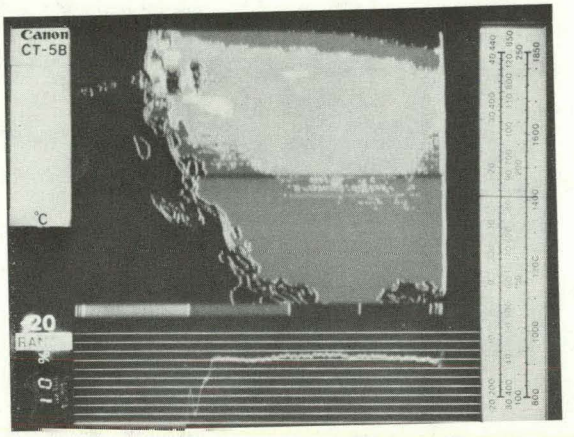

Figure 11. 5-STAGE DISCONTINUOUS ISOTHERMAL PATTERN OF HEIKENOJO CAPE
Temperature ranges are, from black to white, 15.0 to 16.2°C, 16.2 to 17.4°C, 17.4 to 18.6°C, 18.6 to 19.8°C and above 19.8°C, respectively.

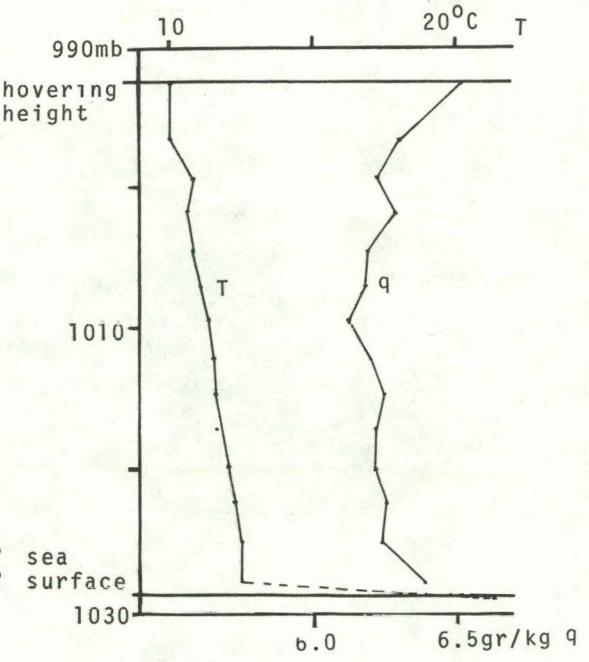

Figure 12. VERTICAL PROFILES OF TEMPERATURE AND MIXING RATIO AT THE OFFING OF HEIKENOJO CAPE
Temperatures are in °C and mixing ratios are in gr/kg.

DIGITAL IMAGE RECTIFICATION AND ENHANCEMENT ON A MINICOMPUTER: ANALYSIS OF RESULTS

M J McDonnell

Remote Sensing Section
Physics and Engineering Laboratory
Department of Scientific and Industrial Research
Lower Hutt, New Zealand

ABSTRACT

New Zealand involvement in the LANDSAT II investigation program has led to the rapid development of a digital image processing facility within the Remote Sensing Section of the Physics and Engineering Laboratory of the Department of Scientific and Industrial Research. Our recently acquired Optronics C-4300 Colorwrite machine is being used to write our processed imagery directly out as a colour transparency. This paper describes the digital image rectification and enhancement techniques which we have developed for use on a minicomputer.

1. INTRODUCTION

Because of New Zealand's involvement in the LANDSAT II investigation program, the Remote Sensing Section of the Physics and Engineering Laboratory (PEL), DSIR, has, since 1975, been regularly receiving LANDSAT imagery of New Zealand. This imagery is available both as computer compatible tapes (CCTs) containing the original digital data, and as photographic transparencies. In addition, transparencies from a number of aircraft multispectral photographic photographic surveys are also available at PEL. These can be digitised on the Remote Sensing Section's flying spot scanner.

Qualitative research work can often satisfactorily be accomplished using the transparencies directly. However, because of the versatility offered by computer processing techniques, serious quantitative work requires the use of digital data. The usefulness of the digital data increases rapidly as the resolution is improved. LANDSAT imagery of the best possible resolution can be obtained if the imagery is corrected for the many geometric distortions present in it and written out on a photographic transparency using a machine such as the Optronics C-4300 Colorwrite (which we have recently acquired and interfaced to a Varian 620f computer). In addition, it is usually desirable to have the corrected imagery displayed at a convenient scale in a suitable map projection. This correction process is called image rectification.

In order to utilise the available dynamic range of the film transparency to best advantage, it is desirable to preprocess the image data before writing it to the display device. This preprocessing, which is called image enhancement, can compensate for the distribution of radiance levels within the original scene, and the characteristics of the display device, the film transparency, the film processing, and the human eye.

2. IMAGE RECTIFICATION

We have developed a package of Fortran computer programs which will perform a full geometric rectification of a LANDSAT subimage on the HP2100 minicomputer at PEL. With this system, it is possible to produce a rectified image at any scale in any desired map projection. An uncorrected LANDSAT image typically contains geometric distortions equivalent to about 300 m

on the ground, whereas our rectified imagery typically has an r.m.s. error of 50 m which is less than the size of a LANDSAT picture element or pixel. Our system can also be used to rectify aircraft imagery so that it is in register with a map.

The image rectification system developed for use on our HP2100 computer is based on the system developed by Van Wie et al (1975, 1976) at the Goddard Space Flight Center but differs from it in certain key respects. These differences will be made clear as the rectification system is discussed in detail in the following sections.

The reason for developing our own rectification system is mainly financial. The Goddard system would involve us in too much expenditure for computer time on a large computer. However, we have available an HP2100 minicomputer for which we are not charged. The Goddard system will rectify whole LANDSAT scenes in the UTM projection. Our system will rectify a LANDSAT subimage on the HP2100 in any desired mapping projection. The size of the input subimage depends on the extent of the rotation required. This is due to the limited core storage available. For example a small input image (e.g. 128 x 128 pixels) can be fully rotated, whereas a large input image can only be rotated by a small amount.

2.1 DISTORTION SOURCES

There are many sources for the geometric distortions present in LANDSAT imagery. These distortions depend on the detailed technical specifications of LANDSAT and have been discussed in detail by Van Wie et al (1975, 1976) and Bernstein et al (1975). They will now be summarised here before our rectification system is described.

An aspect ratio of 1.4:1 in the LANDSAT imagery is due to the sampling distance being 57 m along but 79 m across scan lines. This is not a serious problem. The angular velocity of the MSS scanning mirror is not constant. This leads to an along scan line distortion in the form of a sine error function which is zero at the end of each scan line and goes through one cycle along each line. The amplitude of the sine error function is about 450 m but varies slowly with time and is different for LANDSAT 1 and 2. This has the effect of decreasing the along scan sampling distance in the middle of each scan line.

Individual MSS bands are misregistered by up to six pixels along scan ines. This is corrected by NASA when preparing the CCT by the insertion of appropriate registration fill characters at the start and end of each scan line.

Additional pixel misregistrations within each band are caused by the delays between sampling each of the 24 individual MSS sensors. An additional offset every six lines is caused by the effect of the earth's rotation during each mirror scan. These errors can be simply compensated for by adding a correction term to each column when a LANDSAT image coordinate (row, column) is calculated.

Variations in the mirror period lead to slight variations in the number of samples in a line. This is compensated for by NASA by regularly inserting synthetic pixels as required so that the resultant line length is constant. These synthetic pixels cause an average error of 28.5 m and can be removed when the CCTs are reformatted. We have not considered it necessary to remove this error.

Further distortion is caused by the satellite's attitude, velocity, and changes of roll, pitch and yaw. In addition the altitude and velocity of the

satellite can vary during the 28 seconds or so required to record a whole LANDSAT image.

Panoramic distortion occurs because samples are taken at nominally constant angular intervals of the mirror's movement rather than at equal distances on the ground. A similar effect along scan lines is caused by the earth's curvature.

Because of the central perspective of LANDSAT an object on the ground will appear to be displaced by a distance depending on its height and its distance from the centre of the scan line it is on. This displacement can be as much as 300 m for the top of a mountain of height 3000 m at the edge of a LANDSAT image. This produces a discrepancy when the image is compared to a map produced with an orthogonal perspective. When LANDSAT imagery is viewed, it should be taken into account that it has been correctly produced for a central perspective. The discrepancy between a map and a LANDSAT image produced in this way is only serious for mountains near the edge of a LANDSAT image.

Further geometric distortions can be introduced in the rectification process by the nature of the map projection in which the LANDSAT image is to be produced. These distortions are negligible for orthogonal map projections such as the Universal Transverse Mercator (UTM) Projection. However, they can be more serious if for example the axes of the map are in latitude and longitude. This can lead to nonlinear effects that are difficult to compensate for using our rectification procedure.

2.2 RECTIFICATION PROCESS

The Goddard approach to the rectification problem is firstly to explicitly correct the input LANDSAT image for the effects of sensor delay, the earth's rotation and the mirror velocity profile to give a corrected input image. The next step is to deduce a suitable mapping function from the UTM map projection to the corrected input image. Let the co-ordinates for the input image, the corrected input image and the map be (R,C), (U,V) and (X,Y) respectively. The Goddard system has available an affine transformation or a polynomial mapping function. For the polynomial mapping function, which is the more accurate, coefficients C_i and D_i are required for the general mapping described by

$$U = C_o + C_1 X + C_2 Y + C_3 X^2 + C_4 XY + C_5 Y^2 + C_6 X^3 + C_7 X^2Y + C_8 XY^2 + C_9 Y^3 + \ldots\ldots\ldots\ldots$$

$$V = D_o + D_1 X + D_2 Y + D_3 X^2 + D_4 XY + D_5 Y^2 + D_6 X^3 + D_7 X^2Y + D_8 XY^2 + D_9 Y^3 + \ldots\ldots\ldots\ldots$$

The desired order of polynomial is chosen according to the mapping accuracy required. Next the C_i and D_i are computed by means of a least squares fit to a number of known ground control points (GCPs). The coordinates of each GCP are normally measured in both the input LANDSAT image and the map. The input image co-ordinates are then converted to corrected input image coordinates and the least squares fit is done between the GCPs in the corrected input image and the map. The above polynomial mapping function is intended to compensate for all errors which have not been explicitly corrected in the corrected input image. This technique can compensate for all the errors discussed in the previous section except for those caused by the central perspective of LANDSAT. This error is not correctable by a polynomial mapping function, although it is possible to correct the image for a single

chosen height (e.g. sea level). This correction can be achieved by adjusting each GCP by an amount which depends on its altitude and distance from the satellite track through the centre of the image. This correction appears to have been neglected by Van Wie et al. If a GCP is taken on top of a mountain it could cause an error of several pixels.

Our approach is somewhat different. We have noted that the effect of the earth's curvature and the panoramic distortion (for a given height) along rows both have the form of a sine error function to a good approximation. Thus, these errors can be included in the correction for the mirror velocity profile by adjusting the sine amplitude to an optimum value. This optimum value can be simply found by plotting the mean absolute GCP error against the sine amplitude, and choosing the amplitude which gives the minimum error. For the example image discussed in section 2.3, this optimum amplitude is 0.55 pixels. The optimum amplitude will vary with the map projection used and it will also vary slowly with time. Correcting for the earth's curvature and perspective distortion at the same time as the mirror velocity profile gives a new corrected input image and reduces the need to use a high order polynomial mapping function. We accept the minor constraint that our map image should be a rectangle with sides parallel to the map coordinate axes. In this case the function for mapping a rectangle on the map into a quadrilateral in the corrected input image has the form

$$U = C_o + C_1X + C_2Y + C_3XY$$

$$V = D_o + D_1X + D_2Y + D_3XY$$

A function for mapping from the corrected input image to the map is not required in the rectification process.

This particular mapping function has some special properties. Firstly, straight lines on the map parallel to the co-ordinate axes, map into straight lines on the corrected input image. However, other straight lines on the map, map into curved lines (see for example the diagonals in Fig. 1). This is caused by the XY term in the polynomial. Secondly, and most importantly, the sampling grid in the corrected input image, corresponding to the rectangular desired output image on the map, is formed by the intersection of a grid of straight lines. For each output image row, the endpoint coordinates of the corresponding corrected input image sample line are obtained by adding a constant amount to the previously used sample line endpoint coordinates. Similarly the sample coordinates along each corrected input image line (corresponding to an output image row) are simply obtained by incrementing the previously used sample coordinate by a constant amount.

This leads to a considerable saving in computation time. Each sample coordinate needed in the corrected input image (corresponding to an output image sample) does not have to be calculated separately by means of the polynomial function above. Van Wie et al overcome the problem of the time required to calculate the polynomial mapping function for each output image sample by superimposing a coarse grid system upon the output image, mapping this grid onto the corrected input image and then performing bilinear interpolation between grid lines. Our system is considerably simpler, but cannot obtain the accuracy possible with the highest order (e.g. 4) polynomial mapping functions used by Van Wie et al. Our model of a sine error function along scan lines, which is implemented efficiently by a table lookup method, compensates satisfactorily for nonlinear distortions along scan lines. However, we have made no attempt to correct for nonlinear distortions which occur across scan lines and are caused mainly by variations in the velocity and pitch of the satellite while scanning an image. We have found these distortions to be minor and a small price to pay for the computational efficiency and simplicity of our rectification procedure.

A further advantage of our quadrilateral mapping function is that, being of a low order, it is stable at the edges of the image. Also, although the GCPs should be well spread out, our mapping function is not over sensitive to their location.

For each required geometrically corrected output image sample, its corresponding coordinate is calculated first in the corrected input image and then (straightforwardly) in the input image itself. The final radiance value is then obtained by nearest neighbour, bilinear or cubic interpolation as is done by Van Wie et al. Results for an example LANDSAT image are discussed in section 2.3.

Nearest neighbour is the fastest and cubic the slowest, but most accurate interpolation technique. In our experience bilinear interpolation is a satisfactory compromise between the requirements of speed and accuracy.

Our rectification system has been implemented on our HP2100 minicomputer system. This system has 32 K (16 bit words) or core storage, a single 800 BPI magnetic tape unit and uses a 2.5 M byte disk unit to store the image to be rectified. One output image row is calculated at a time, using data stored in core, after which it is written out to magnetic tape. Data stored in core is updated from disk when required. The size of image which can be rectified is limited either by core storage or disk storage depending on how much the image to be rectified has to be rotated. The amount of this rotation determines how many input image rows are needed in core to calculate each output image row. A 128 x 128 pixel input image can be rotated as much as is desired. A LANDSAT image of an area 13.7 km square can be produced in the Transverse Mercator projection used in the New Zealand inch to the mile map series. This is assuming that the output image has its edges parallel to the map grid lines. In these cases the limit on image size is core storage because of the extent of rotation required. It is possible to define map projections which require very little rotation. From a computational point of view the most suitable projection of this type is the Space Oblique Mercator projection (Colvocoresses 1974). However, for our purposes it is desirable to be able to register rectified imagery with maps in common use in New Zealand. For this reason we are producing rectified images whose edges are parallel to grid lines on a map formed by rotating the standard New Zealand Transverse Mercator grid by -12.5^{o} about its artificial origin. The size of image which can be rectified in this way is limited by our disk storage. A quarter of a full LANDSAT scene can at present be fully rectified. A whole LANDSAT scene can be rectified if only even rows and columns are used in the input image. The resolution obtainable in this way is sufficient for the preparation of a mosaic of New Zealand.

Later this year it will be possible to use our rectification system on our Varian minicomputer using two 800/1600 BPI magnetic tape units to fully rectify a whole LANDSAT scene. It should be noted that the limitations in image size (in pixels) discussed above apply only to the input image. The size of the output image is generally constrained by the amount of data which can be stored on a magnetic tape. Each rectified image is produced on tape in a form suitable for direct outputting on our Colorwrite machine.

2.3 RECTIFICATION RESULTS

Our rectification system has so far been used on six LANDSAT scenes and one set of multispectral aircraft negatives which had been scanned on an Optronics photoscan device at Massey University. Results obtained for LANDSAT 2 scene 2334-21123 are discussed in this section.

Nineteen points suitable for use as GCPs were chosen by inspection of the LANDSAT scene. Some of these points were the centres of small lakes and

forest road intersections, but most were acute water-land interfaces. A number of shaded computer lineprinter outputs and New Zealand standard inch to the mile (1:63360) Transverse Mercator (TM) maps were then obtained which included all the GCPs. The coordinates of each GCP in the LANDSAT image and the map were then determined by examining, for each GCP, the appropriate shaded printout and map together. To obtain reasonable accuracy (i.e. $\pm$0.5 pixel in the image row and column coordinates and $\pm$20 yards in the map coordinates) it is most important that the printout and map should be examined together. Our experience is that the best type of GCP is a land-water interface with the land forming an acute angled peninsula. Such GCPs are readily available throughout New Zealand. An advantage of using land-water interfaces is that only MSS band 7 needs to be printed out to locate the GCP.

In Table I the input image coordinates and the corresponding map coordinates are given for the nineteen GCPs. The GCPs were then compensated for the effects of their heights and transformed to the corrected input image. A least squares mapping function was then derived for various amplitudes of the sine error function. The resultant average error in metres is plotted in Fig 2 against the amplitude of the sine error function. From this plot it was deduced that the optimum amplitude was 6.55 pixels in the along scan direction. The resulting mapping error in meters for each GCP using this amplitude in the sine error function is shown in Table I. This error is the distance between the result of mapping the GCP in map coordinates to the image, and the GCP measured in image coordinates.

It should be noted that the errors for each GCP in Table I include contributions from the errors in measuring the GCPs in the map and the image. These contributions may well be the main part of the errors shown in Table I. More images need to be processed, and the processed images need to be compared to maps before the mapping accuracy of this method can be fully evaluated. However, initial tests indicate the accuracy is sufficient for our purposes.

3. IMAGE ENHANCEMENT

We have found that the visual quality of imagery produced on our Colorwrite machine is strongly dependent upon the enhancement techniques used to preprocess the image data before writing it to the Colorwrite. The first stage in setting up the Colorwrite machine involves choosing colour film transparency material, film processing conditions, and lamp voltages (for each colour) that ensure a satisfactory film dynamic range can be obtained for each primary colour. We have initially obtained satisfactory results using Kodak daylight Ektachrome 64 film push processed to 1½ stops.

The number n written form the computer to the Colorwrite for each pixel ranges from 0 to 255. The next step is to obtain, for each primary colour C, $D_C(n)$ where D_C is the resultant diffuse spectral density on the transparency material. $D_C(n)$ is found by writing a grey wedge out on the Colorwrite, and sampling the density along it with a colour densitometer. These samples are then typed into a computer where $D_C(n)$ is obtained by linear interpolation. It is then straightforward to calculate a lookup table L(n) such that $D_C(L(n))$ is a linear function of n. A linear ramp preprocessed in this way and then written to the Colorwrite for each primary colour, will thus produce a grey wedge which is linear in diffuse spectral density (for each primary colour).

However, the eye is not, as is often assumed, uniformly sensitive to changes in diffuse spectral density. (i.e. the sensitivity of the eye to changes in diffuse spectral density varies with diffuse spectral density). To a good approximation, its sensitivity actually decreases linearly with increases in diffuse spectral density (CIE Technical Committee Report, 1972).

Knowledge of this relationship allows us to define a quantity V_c, which we call visual density, by

$$V_c = D_c - 0.139\ D_c^2$$

The eye is uniformly sensitive to changes in visual density on a transparency. This is true over a fairly wide range of background illuminations which includes commonly used light tables.

Two other forms of preprocessing are commonly included in our enhancement procedure. The above techniques are concerned with calibrating the display device. These techniques are related to the distribution of radiance levels within the actual image to be displayed. For each of them, a count is taken, for each colour band, of the number of times each radiance level occurs. For each band, the image data within a chosen range (e.g. 20-50) may be linearly stretched to fill the available range (0-255). Usually, the chosen range will include most of the level occurrences found in the count. Alternatively, the image may be enhanced by histogram equalisation (Andrews, 1974). Ideally, this makes each visual density level on the final transparency equally likely. In practice, however, histogram equalisation is implemented by means of a nonlinear mapping which distributes the visual density levels as evenly as possible. For each band, stretching and histogram equalisation are both implemented by means of a lookup table. To save computation time, we combine the required lookup tables into a single table.

Histogram equalisation improves the contrast of levels that occur often at the expense of those that occur rarely. This results in an image which on general viewing conveys more information to the eye than the corresponding stretched image, so long as the number of radiance levels used in the original image is not too low (e.g., 10 or less). For a particular application, detail of interest can be further enhanced at the expense of detail which is of less interest.

For general viewing of LANDSAT imagery we have found that histogram equalisation produces images that are substantial improvements upon those produced by the corresponding linear stretch. Furthermore, the eye correction we have discussed produces a significant improvement in visual quality over images which are linear in diffuse spectral density. If it is desired to make prints of the best possible quality (rather than transparencies), then the calibrations discussed above should be applied to the print. Imagery supporting the above conclusions is to be displayed at the poster session of this conference, but is not reproduced here because of the cost of colour printing.

4. CONCLUSIONS

We have shown that it is practicable to rectify large LANDSAT subimages on a minicomputer system. The geometric accuracy of our rectified imagery is sufficient for a wide range of applications. We have also summarised the practical experience we have gained in enhancing and displaying LANDSAT imagery on an Optronics C-4300 Colorwrite machine.

REFERENCES

Van Wie, P, Stein, M (1976) "A LANDSAT digital image rectification system." Report X-931-76-101, Goddard Space Flight Centre, Greenbelt, Maryland.

Van Wie, P, Stein, M, Puccinelli, E, Fields, B (1975) "LANDSAT digital image rectification system preliminary documentation", Information Extraction Division, Goddard Space Flight Centre.

Bernstein, R, Ferneyhough, D G, (1975) "Digital image processing", Photogrammetric Engineering and Remote Sensing 41, 12, 1465-1476.

Colvocoresses, A P, (1974) "Space Oblique Mercator" Photogrammetric Engineering and Remote Sensing 40, 8, 921-926.

Andrews, H C, (1974) "Monochrome digital image enhancement", Applied Optics 15(2): 495-503.

Technical Committee Report of the CIE, No 19 (TC.3.1) 1972.

GCP Number	Image (pixels)		Map (yards)		Error (meters)
	Row	Column	Northing	Easting	
1	2001.2	180.2	377180	311220	29
2	1917.0	2155.5	357610	435460	67
3	1412.5	208.0	426220	326610	87
4	1003.0	2188.5	433830	458860	77
5	1166.3	1266.2	432600	397700	86
6	385.0	546.0	508040	371460	95
7	313.8	1402.5	502370	426290	72
8	240.5	2945.5	487700	523490	34
9	1359.3	3205.5	390300	513020	13
10	2024.2	169.6	375350	310050	22
11	1441.2	286.3	422800	330810	24
12	1009.7	2169.1	433550	457590	4
13	413.0	584.0	505050	373250	82
14	253.4	693.4	517110	383770	63
15	255.5	741.5	516220	386610	37
16	300.0	799.2	511750	389170	16
17	347.7	812.0	507580	388840	24
18	385.0	781.8	504890	386060	50
19	393.0	790.8	504100	386450	55
Mean absolute error					49

TABLE I. RECTIFICATION RESULTS

(Image and map co-ordinates, and mapping errors for 19 GCPs for LANDSAT scene 2334-21123.)

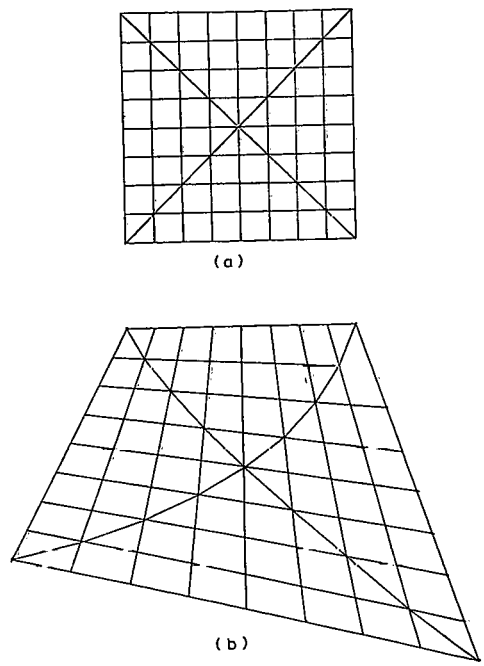

Figure 1. EXAMPLE MAPPING

(Example mapping of a rectangle on a map (a) into a quadrilateral in the corrected input image (b).)

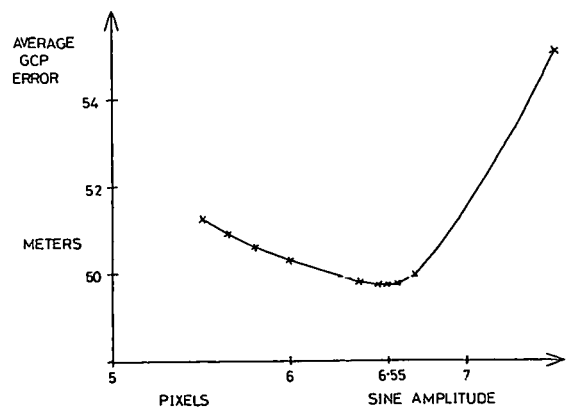

Figure 2. EFFECT OF VARYING SINE AMPLITUDE

(Average GCP error in meters versus amplitude of the sine error function in pixels in the along scan direction.)

THIS PAGE

WAS INTENTIONALLY

LEFT BLANK

LANDSAT USER NEEDS AND ADMINISTRATIVE RESPONSES:

DENSITY SCALES, DATA CATALOGUES, IMAGE ANNOTATION

Allan Falconer

Department of Geography, University of Queensland,
Brisbane, Australia

Donald Gray

Department of Science,
Canberra, Australia

Andrew A. Green,

Commonwealth Scientific & Industrial Research Organization,
Sydney, Australia

ABSTRACT

The present procedure of system interrogation and the consequent response to users which is necessary in order to identify a Landsat image, order and receive it can, apparently be simplified by the use of an illustrated image catalog. The illustrated catalog can be rapidly compiled using existing system procedures based on the Canadian ISISFICHE model and using off-set litho printing. The consequent ease of consultation of the catalog and the flexibility in forming weekly, monthly or annual catalogues alongside the daily catalogue system appear as major advantages. The illustrated catalog provides the user with a ready reference to the position of cloud cover within the scene and the major locational detail is visible also. An improved method of annotating the grey scale on individual bands and thus making colour composites easier to analyse is also described. In total a system of receiving stations providing quicklook imagery and a catalogue service backed by a central processing facility creating images as required by user demand, appears to offer an efficient use of regional resources. It may be a useful model for future planning of facilities amongst nations receiving Landsat data.

1. INTRODUCTION

The user of Landsat data requires, in a timely manner, copies of data tapes or images in forms which are easy to use and free of obvious problems. For many users the end product is a photograph or photo-image-map which may or may not require the expense of substantial computer processing in its creation. Common to all users is the desire for high quality cloud free scenes of appropriate date and location. Many users are also concerned that the images should not prove to be an expensive source of embarrassment by providing views of clouds when detail of the land area is required. Images which provide views of areas adjacent to those desired are a similar source of embarrassment. Feature identification is often best achieved in a particular season, and user interest in the passage of fires, rainstorms, snowstorms, or the 'green wave' can often only be sustained by the appropriate temporal selection of images.

The current system of image selection offered to the potential user is efficiently operated but is not in itself ideal for its purpose. The typical system of requests and responses is given in figure 1. An initial enquiry receives the response of an introduction to the system; a request for an geographical computer search can then be completed. The completion and return of the form results in a listing of scenes for the requested area. This listing provides a vast amount of coded information which requires an additional sheet of explanation to facilitate its interpretation. On receipt of such a print-out the potential user seeks for a scene which has zero cloud cover, excellent quality in all four bands, is available in colour composite, and was compiled from data gathered at a desired season in an appropriate year.

Searching such output is a difficult task especially when the number of pages of computer output is large. There is the further complication that several images may meet the user's criteria and a full evaluation requires either travel to a browse file, or the purchase of the cassettes of images for use on microfilm readers. The further possibilities, namely purchase of all the suitable images or the purchase of a randomly selected image lead to expense, frustration or delay unless the random selection by chance provides an ideally suited image.

It is only on receipt of the images ordered from the system that most first-time users become fully aware of the image quality and scene content. This awareness occurs only after the ordering decisions and payment have been completed and is particularly important in cases where there is some cloud cover in the images. In such cases the location of the cloud may be of critical importance in determining the further use of the image.

Figure 1 illustrates the linkages between events in the obtaining of suitable data for a given project. The most desirable link would be the direct satisfaction of user needs in reply to the initial enquiry. This however, can rarely be achieved when the user is enquiring with the purpose of obtaining data. Thus, in figure 1, link A and link B are desirable but not realistically obtainable, as the definition of scene, season, year, band, cloud cover, and image quality are important in determining the product to be supplied. Link C reduces the time between the expressed need for imagery and the delivery of it but requires a tedious search of catalogues to define the image required and a particularly perplexing search if a series of images are required for mosaicing.

Links 1 and 2 represent the interaction of a user with the system in a manner which is almost inevitable unless an illustrated catalogue is used. Data ordered either from existing catalogues or from a requested computer print-out cannot be evaluated until received. The elapsed time in dealing with the system plus the necessary pre-payment for images which may be of little value mean that several circuits around links 1 and 2 may be required before the desired goal is achieved. Within the user's subsystem there is often a need for ready reference catalogues to identify data at short notice so that an existing project may be extended either in area or through time. Searching through existing computer-printed "stock inventories" for these purposes is often a severe problem.

Many of these initial problems can be solved by integrating the catalogue system with the production of "quick-look" imagery and the system of path and row identifiers for Landsat scenes. Path, row and date uniquely identify each Landsat scene at a given nominal centre. Thus images for a certain scene centre can be requested and the existing system of geographical search yields a listing of scenes for that centre. However, scenes for adjacent centres are difficult to identify and it becomes a painstaking task to search for images at a given season to use in the construction of a mosaic. The problem of determining the location of cloud within the image remains.

2. INTEGRATION OF SYSTEMS FOR CATALOGUE PRODUCTION

Existing systems of image production provide the raw materials for an illustrated image catalogue and, by amending the system-flow, a low-cost highly efficient catalogue system can be developed. The Canadian system

which produces "quick-look" data processes the data tapes within a short-time of the satellite pass, makes the images available either in individual prints at 1:1,000,000 scale or in 70mm format. In addition all the imagery collected on a given day is formatted into a microfiche and mailed to subscribers. This product of Integrated Satellite Information System (ISIS) Ltd., is known as ISISFICHE.

The 70mm format band 5 images which are the raw material for the daily microfiche are a resource which can be used for a further catalogue system. Because the data from one day of orbits over a nation consist of images along widely separated paths, the coverage is contiguous only along the paths. Searching these fiche by date is more convenient than searching the computer print out ordinarily supplied to the user. The fiche have the added advantage that the location and type of cloud cover can be readily observed.

If the band 5 images used in the creation of the microfiche of the image received each day are then reassembled in a series of standard frames a larger area of contiguous coverage can be achieved. Thus a microfiche of images for seven adjacent paths and five rows gives a set of 35 images or one weeks production of imagery over a standard area of some 1,197,875kms of the earth's surface (not allowing for overlap). This system then permits the use of a standard frame using the international path and row identifiers and the dates of image collection. Figure 2 illustrates such a standard frame for images around Brisbane, Australia (095-079). Such a frame can be easily created and used for each seven day cycle.

If each frame is then filled with the correct 70mm quicklook image of band 5 over the seven days the frames can be photographed using a 125mm x 100mm format which gives a conventional microfiche product. Higher resolution can be achieved by using appropriate microfilm equipment. By rephotographing the same original in a standard off-set litho platemaker a conventional A4 size offset litho printing-plate can be produced. This can be used to create a page of a visual catalogue of Landsat data. Figure 3 is a specimen page in which a selection of scenes has been used to evaluate the technique. In figure 3 the images in each path (column) and row location are not correct except for Brisbane (095-079). Column 100 contains test images which were originally in colour except for row 080 which is entirely a selection from the many dollars worth of cloud covered imagery purchased by one of the authors. All of figure 3 excluding row 080 and column 100 consists of six columns and four rows. Row 076 contains band 4 images, Row 077 contains band 5 images row 078 band 6 images and row 079 band 7 images.

Row 077 offers particularly useful detail because it shows band 5 images which would be the standard item for inclusion in such a system. Figure 4 illustrates a standard page from the non U.S. data catalogue and Figure 5 an extract from the typical computer print out in response to a geographic computer search request. The value of the illustrated catalogue system is its flexibility and its direct communication with the user. From the miniature scenes ready identification of cloud location is possible. Major location features are also readily identifiable in band 5 images (row 077).

The value of this identification of cloud extent and location and major feature identification can be appreciated by comparing figure 3 with figure 4 and 5. The initial catalogue page printed by the offset litho process shows only computer digits (figure 4) and contains information about 35 scenes. The information requires explanatory detail provided on another (offset litho) printed sheet. Figure 3 provides information for 35 scores and requires little or no further coding information. Figure 5 is a specimen response to a request for a geographical data search. The quantity of output for a 35 scene area is large, and requires explanation to permit the data to be decoded. Although the user possess an invaluable fund of information about sun angle and azimuth, image centre and corners, and other detail the critical factors remain cloud cover date and location. Thus a catalogue of the type shown in figure 3 provides more information of immediate value to the potential user.

Costs have not been fully evaluated but the cost of preparing an offset litho printing plate does not differ greatly in the case of the two types of information illustrated in figures 3 and 4. As each catalogue page becomes available it is a resource which can easily be reprinted, or distributed, and provides a permanent, easy reference. For the duration of the Landsat program so far, any 35 scene area within the United States will have had a total of approximately 200 overpasses by Landsat sensors by the end of 1978. Because of cloud cover not all these scenes will be of value to users. In consequence the 200 page illustrated catalogue for a chosen 35 scene area would represent the maximum catalogue and cycles for which no usable data were gathered would provide for a reduction in the total page count.

For a catalogue operation by subscription, persons interested in a specific area could receive, by mail, a catalogue page of each 7 day cycle over the requested area. The advantage of mailing one sheet for low cost off-set litho material which can be easily read by the recipient contrasts with the present packaging of computer print out or the expense of microfiche production and the need for the recipient to have access to a microfiche viewer.

Catalogue pages can be accumulated into annual catalogues (20 pages p.a. for each Landsat satellite over each 35 scene area) and distributed to subscribers and users in each area. The interest of individual states or nations and of researchers in specific areas should be satisfied through the detail readily available in an illustrated catalogue. Further embellishment is possible as the NASA scene identification code can be written under each scene but the simplicity of the path, row and date as a unique definition of the scene appears to offer many advantages.

A consequence of such a system is the flexibility of organisation which it permits. It becomes possible to establish one major image production centre to serve the needs of several receiving stations. Each receiving station, equipped with its "quicklook" facility and the consequent catalogue operation serves as a user oriented prime contact in the system. Scenes which are partially obscured by cloud do not have to be processed beyond the "quicklook" or catalogue stage until a user requests them and so a larger component of enquiries to the main image production centre is reduced. The existing computerized system of cataloguing becomes primarily an internal "stock control system". It is no longer in such great demand for user search requests and the illustrated catalogues of Landsat data are readily available for consultation on an area basis. Thus the catalogues would become fully oriented to user needs rather than organised by a computerized stock-control system as at the present time.

3. GREY SCALES AND ANNOTATION

Once the user receives the image in photographic form further problems are innate in the system. Although the image carries a standard grey-scale the units of reflectance recorded on the Landsat tape are not directly and clearly associated with the image. To offset this problem it is proposed that a sequence of automatic annotation of the grey-scale be added so that the units of energy recorded by each step are indicated numerically at each step of the grey-scale. Some of the present difficulties with the interpretation of colour composite images in photographic form can be solved by the relocation of the grey-scales for each of the images so that band 4 has the grey-scale located to the left of the image band 5 in the conventional position, band 6 to the right of the image and band 7 above it. The locations of grey-scales for all bands other than that of the image itself should be masked. This then results in a colour positive which shows at a glance the bands used and permits the intensity of the bands to be measured by densitometer measurement of the "grey"-scale associated with each separate colour used in the print. The annotation of the grey-scale also permits the quantitative contribution of each band to the colour composite to be assessed.

4. CONCLUSION

The integration of an existing image production system at present used

in creating "quicklook" imagery and a cataloguing procedure using offset lithography and miniature images can result in a flexible and comparatively low cost catalogue system. The system proposed permits the use of microfiche, or offset litho prints of data for a specific area on a regular basis. A subscription service mailing the product of each 7 day cycle of imagery over an area is also possible. Thus a subsriber requiring immediate knowledge of the content of Landsat imagery can use the existing technology of the facsimile transmission of quicklook data. The existing service of the ISISFICHE type where a daily mailing of the days imagery conveys the quicklook information to a user (at the discretion of the postal service) remains available.

The new possibility is for a standard area of 35 scenes to be documented on a seven day cycle and mailed to subscribers. Each cycle then is recorded for the subscriber who receives either a microfiche or offset print of the images. The delivery time is subject to the mail service but dispatch should be about a day after the receipt of the last image in the sequence and eight days after the reception of the first. It becomes in effect an 18 day subscriber service.

Accumulation of these sheets into annual groups permits the issuing of an illustrated annual catalogue of images at low cost for subscribers. The receiving stations operating a quicklook system and catalogue service can therefore be independent of the central processing centre. A central processing centre can create imagery on demand annotating the grey-scale as outlined above. One central processing centre may be able to handle the data for several receiving stations particularly if the administrative demands on the system are reduced by the catalogue system outlined here.

The concept can easily be given a further dimension; for example certain areas of interest can be catalogued by miniature prints which illustrate all available imagery over a small area or a single standard scene. The use of images arranged on a page in temporal sequence may be a further useful elaboration of the proposal. In total the flexibility, low cost, and speed of the proposed system seem to offer great advantages. The fact that it can be operated using conventional equipment, low cost materials and the standard product of a "quicklook" system seems to enhance the potential value to users.

ACKNOWLEDGEMENTS

The assistance of the University of Queensland Printery, and of Mr E.E. Savage and Miss D. Flemming of the Department of Geography has been invaluable in the preparation of this manuscript. Their assistance is gratefully acknowledged.

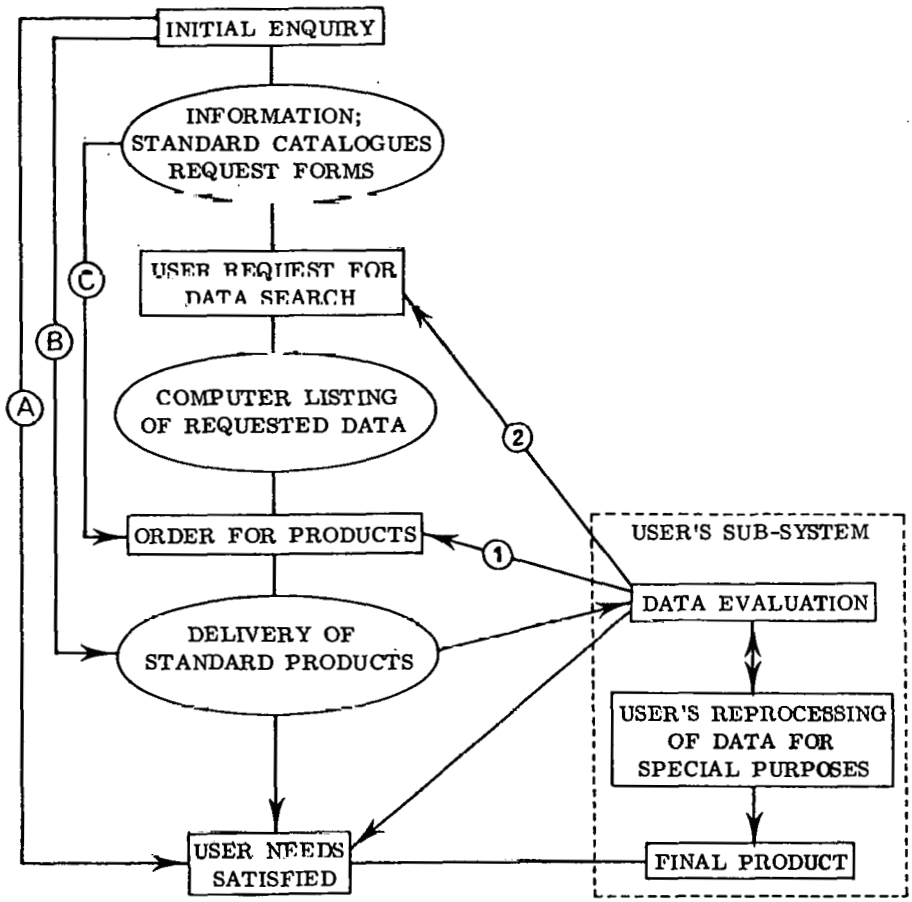

Figure 1 Flow chart of user/data center interaction

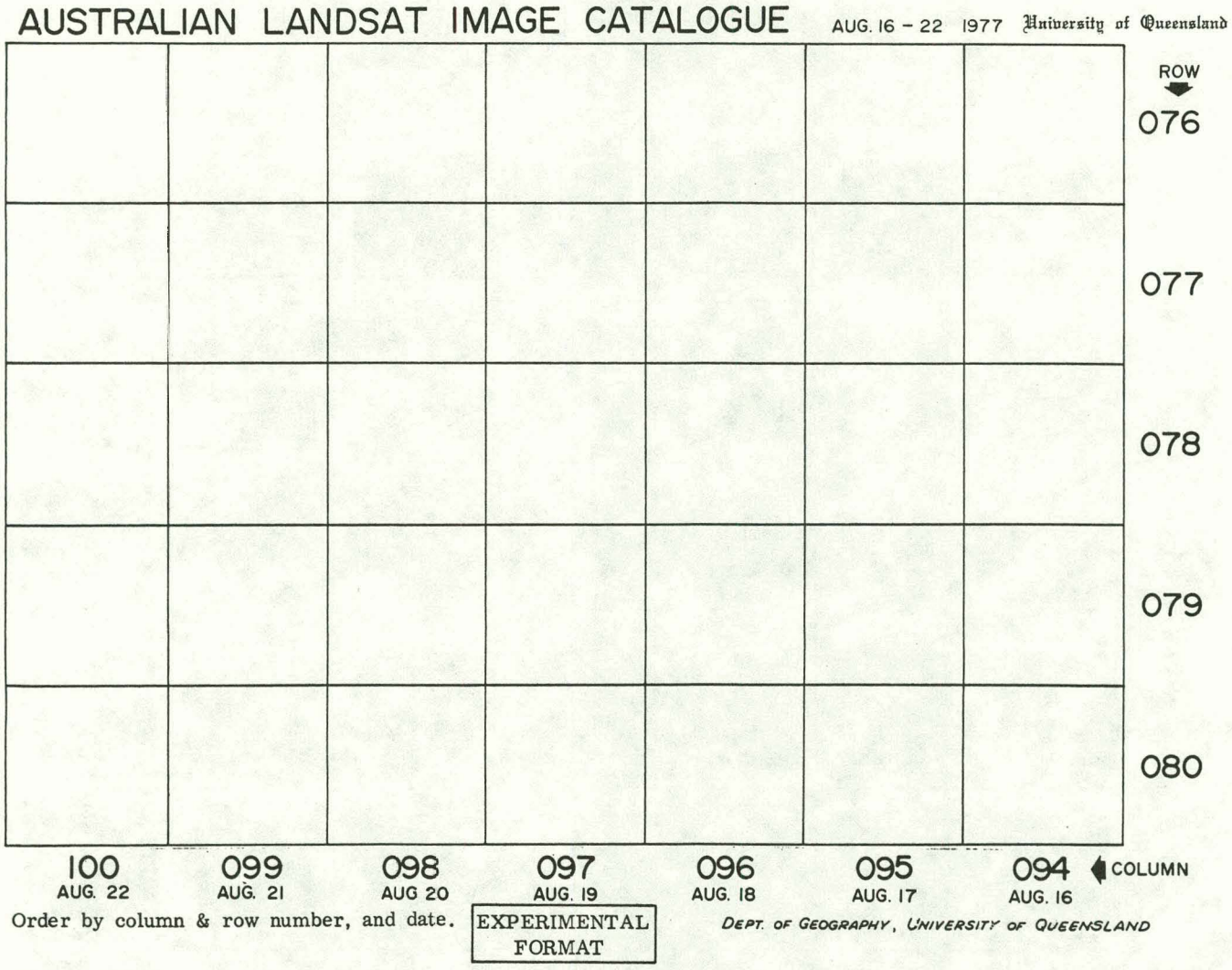

Figure 2 An outline catalogue page using Path (column) and Row identification

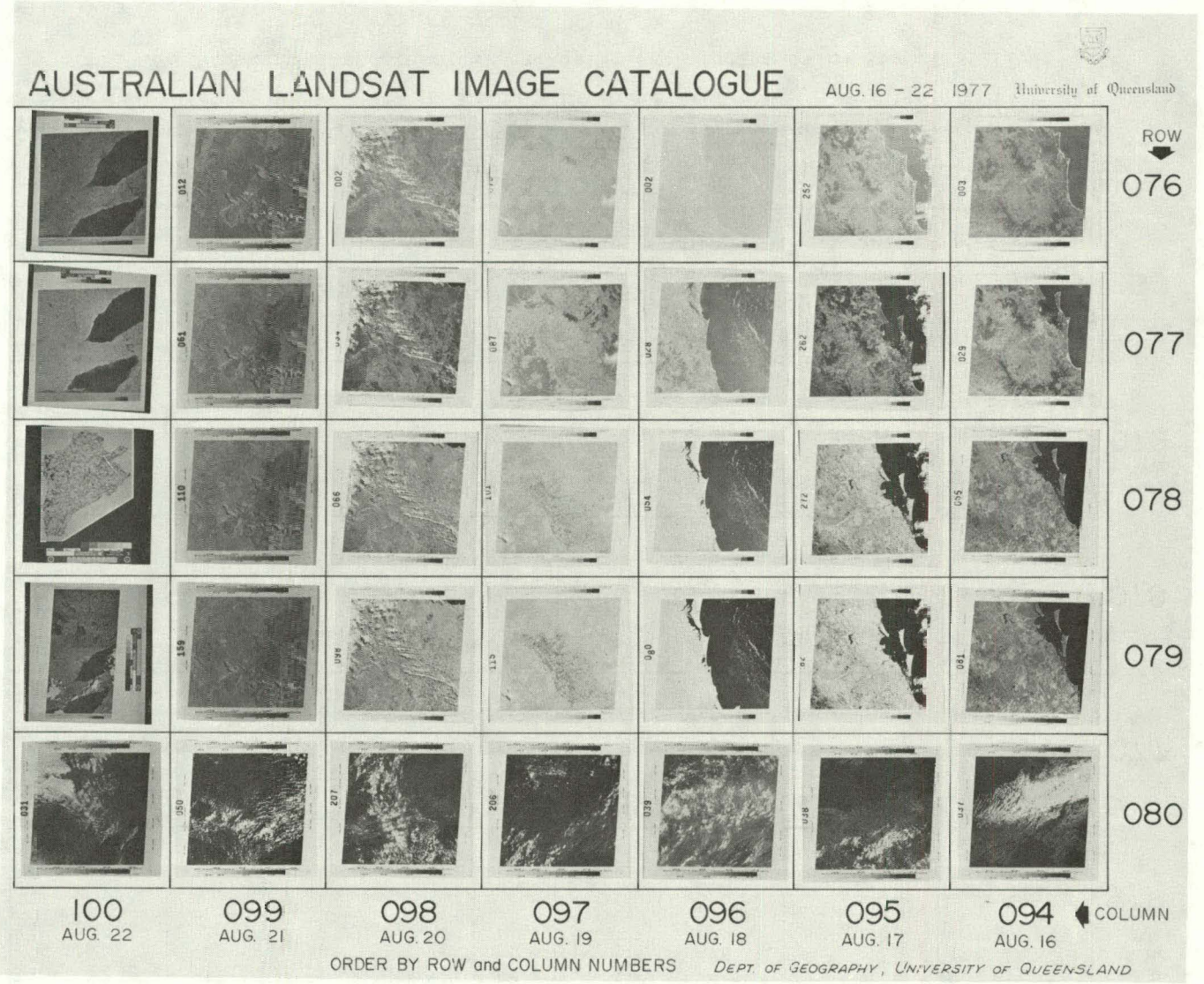

Figure 3 Sample page with an assortment of images (not correctly located by path and row)

PRINCIPAL POINT OF IMAGE LONG	LAT	OBSERVATION ID	MICROFILM POSITION RBV	ROLL NO./ IN ROLL MSS	DATE ACQUIRED	CLOUD COVER %	ORBIT NUMBER	SUN ELEV.	SUN AZIM.	IMAGE RBV 123	QUALITY MSS 45678	PRODUCTS B P P B P C C D D
04647E	2141S	1109-06205	00000/0000	20007/0173	11/09/72	40	1513	57.8	87.4		GGGG	
04646E	3013N	1172-06571	00000/0000	20012/0672	01/11/73	40	2392	30.1	146.6		GGGG	
04645E	5835N	1360-07343	00000/0000	20025/0978	07/18/73	70	5014	49.6	149.1		GGGG	
04645E	2142S	1127-06210	00000/0000	20008/1179	11/27/72	30	1764	57.7	95.6		GGGG	
04644E	3017N	1010-06563	20001/1027	00000/0000	08/02/72	90	133	59.5	107.2	GGG		
04644E	0843N	1330-06903	00000/0000	20024/0713	06/18/73	10	4595	55.0	61.2		GGGG	
04644E	2131S	1361-06202	00000/0000	20026/0586	07/19/73	60	5027	32.6	45.0		GGPP	
04644E	7725S	1185-03341	00000/0000	20013/1370	01/24/73	100	2571	20.4	87.3		GGGG	
04643E	2559N	1351-06523	00000/0000	20025/0727	07/09/73	0	4888	61.3	90.4		GGGG	
04643E	0126N	1167-06365	00000/0000	20012/0078	01/06/73	80	2322	48.0	126.8		GGGG	
04642E	1548S	1290-06251	00000/0000	20021/0185	08/09/73	0	4037	41.4	48.4		PGPG	
04641E	1432N	1313-06445	00000/0000	20022/1392	06/01/73	10	4358	59.3	71.1		GGGG	
04641E	1428N	1349-06443	00000/0000	20025/0825	07/07/73	0	4860	57.5	70.5		GGGG	
04639E	7528N	1233-09073	00000/0000	20017/0203	03/13/73	60	3244	11.6	181.2		GGGG	
04639E	3013N	1208-06574	00000/0000	20015/0898	02/16/73	20	2894	37.2	138.9		GGGG	
04639E	3009N	1118-06573	00000/0000	20008/0481	11/18/72	100	1639	35.0	150.6		GGGG	
04639E	2015N	1350-06483	00000/0000	20025/0679	07/08/73	50	4874	59.9	79.8		GGGG	M
04639E	0127N	1149-06371	00000/0000	20011/0082	12/19/72	50	2071	49.2	129.6		GGPP	
04637E	2437N	1009-06523	20004/0044	20004/0045	04/01/72	0	119	59.7	96.4	GGG	GGGG	M
04637E	2423N	1063-06524	00000/0000	20004/1350	09/24/72	0	872	53.0	128.3		GGGG	
04637E	2428N	1171-06530	00000/0000	20012/0566	01/10/73	0	2378	34.2	143.6		GGGG	M
04636E	3431N	1173-07014	00000/0000	20013/0321	01/12/73	20	2406	27.0	148.6		PGPG	
04636E	0709N	1042-06403	00000/0000	20002/1494	09/03/72	10	579	57.2	87.2		GGGG	
04636E	0131N	1203-06372	00000/0000	20015/0655	02/11/73	20	2824	49.7	113.9		GGGG	
04636E	0104N	1041-06363	00000/0000	20002/1426	09/02/72	10	551	55.4	77.6		GFFF	
04636E	1714S	1074-06244	00000/0000	20005/0535	10/05/72	10	1025	54.3	73.6		GGG	
04635E	3859N	1156-07062	00000/0000	20011/0843	12/26/72	0	2169	22.8	153.2		GGGG	
04635E	3437N	1011-07010	20001/1215	00000/0000	08/03/72	10	147	58.5	115.4	GGG		
04634E	5559N	1323-07300	00000/0000	20024/0327	06/11/73	20	4498	53.8	146.7		GGGG	
04634E	3439N	1191-07015	00000/0000	20014/0288	01/30/73	10	2657	29.9	145.3		GGGG	
04634E	1259N	1169-06450	00000/0000	20012/0321	01/08/73	20	2350	41.7	136.5		GGGG	
04633E	3021N	1226-06575	00000/0000	20016/1277	03/06/73	20	3145	42.9	134.4		GGGG	
04633E	2434N	1153-06532	00000/0000	20011/0563	12/23/72	60	2127	34.0	146.6		GGGG	
04633E	1843N	1170-06490	00000/0000	20012/0435	01/09/73	20	2364	38.1	140.3		GGPG	M
04633E	1303N	1151-06451	00000/0000	20011/0341	12/21/72	30	2099	42.2	139.5		GGGP	
04633E	0132N	1221-06373	00000/0000	20016/0826	03/01/73	40	3075	51.9	104.4		GGGG	
04633E	2300S	1073-06203	00000/0000	20005/0395	10/04/72	20	1011	51.1	66.8		GGGG	
04632E	1848N	1152-06492	00000/0000	20011/0444	12/22/72	10	2113	38.2	143.3		GPPG	

KEYS: CLOUD COVER % ..... 0 TO 100 = % CLOUD COVER. ** = NO CLOUD DATA AVAILABLE.
IMAGE QUALITY ..... BLANKS=BAND NOT PRESENT/REQUESTED. R=RECYCLED. G=GOOD. F=FAIR BUT USABLE. P=POOR.
PRODUCTS ALREADY MADE ..... R=MADE FROM RBV. M=MADE FROM MSS. B=MADE FROM RBV AND MSS.

Figure 4 Typical page from data catalog

EROS DATA CENTER
SIOUX FALLS, SOUTH DAKOTA 57198
PHONE 605-594-6511 FEDERAL TELECOMMUNICATIONS SYSTEM PHONES USE 754-7151

REPORT NO. D1026-1
DATE 09/28/77
TIME 12:08
PAGE 1

CONTACT NUMBER C00717900S TERMINAL 0096
KMW

15 ACCESSIONS

POINT REFERENCE RETRIEVAL

PATH	ROW	PATH	ROW	PATH	ROW	PATH	ROW
105	066	105	067	105	068	106	066
106	067	106	068				

QUALITY 5 CLOUD COVER 30%

DATA TYPE MULTISPECTRAL

IMAGERY TYPE	SCENE ID	PATH,ROW	FILM	SOURCE	QUALITY	CLOUD	EXPO	DATE	SCENE CENTER POINT	SCENE SCALE	MICROFILM	CCT	CCP
LANDSAT-1 (MSS)	8102600032SN0	105,066	B&W	2.2"	8,8,8,8	30%		08/18/72	SC8D43M13S E143D19M40S	1:3,369,000	12000020155	P	Y
CORNER POINT COORDINATES=#1:S08D05M24S E144D20M32S ,#2:S07D50M16S E142D44M14S ,#3:S09D36M06S E143D55M17S ,#4:S09D20M53S E142D18M36S													
LANDSAT-1 (MSS)	8102600032SN2	105,066	FCC	7.3"	5	30%		08/18/72	SC8D43M13S E143D19M40S	1:1,000,000	12000020155	P	
CORNER POINT COORDINATES=#1:S08D05M24S E144D20M32S ,#2:S07D50M16S E142D44M14S ,#3:S09D36M06S E143D55M17S ,#4:S09D20M53S E142D18M36S													
LANDSAT-1 (MSS)	8142200030SN0	105,067	B&W	2.2"	8,8,8,8	30%		09/18/73	S10D11M22S E142D5[illegible]M31S	1:3,369,000	12000290899	P	P
CORNER POINT COORDINATES=#1:S09D32M44S E143D51M44S ,#2:S09D18M56S E142D14M51S ,#3:S11D03M44S E143D27M45S ,#4:S10D49M51S E141D50M25S													
LANDSAT-1 (MSS)	8138600034SN0	105,067	B&W	2.2"	8,8,8,8	30%		08/13/73	S10D03M46S E142D5[illegible]M36S	1:3,369,000	12000290148	P	P
CORNER POINT COORDINATES=#1:S09D25M02S E143D51M50S ,#2:S09D10M38S E142D14M07S ,#3:S10D56M49S E143D27M13S ,#4:S10D42M19S E141D49M03S													
LANDSAT-1 (MSS)	8102600035SN0	105,067	B&W	2.2"	8,8,8,8	10%		08/18/72	S10D10M24S E142D5[illegible]M26S	1:3,369,000	12000020156	N	P
CORNER POINT COORDINATES=#1:S09D32M37S E144D30M33S ,#2:S09D17M22S E142D23M51S ,#3:S11D02M22S E143D35M15S ,#4:S10D48M01S E141D58M07S													
LANDSAT-2 (MSS)	8212923510500	105,068	B&W	2.2"	5,5,8,5	30%		05/31/75	S11D34M52S E142D1[illegible]M59S	1:3,369,000	22300071812	P	P
CORNER POINT COORDINATES=#1:S10D56M41S E143D41M13S ,#2:S10D41M12S E142D02M46S ,#3:S12D02M42S E143D15M27S ,#4:S12D15M05S E141D36M30S													
LANDSAT-1 (MSS)	8138600C415N0	105,068	B&W	2.2"	8,8,8,8	30%		08/13/73	S11D36M35S E142D3[illegible]M12S	1:3,369,000	12000290149	P	P
CORNER POINT COORDINATES=#1:S10D51M54S E143D31M46S ,#2:S10D37M24S E141D53M37S ,#3:S12D23M42S E143D07M02S ,#4:S12D09M04S E141D28M22S													
LANDSAT-1 (MSS)	8117000C445N0	105,068	B&W	2.2"	5,5,8,6	20%		01/09/73	S11D45M01S E142D3[illegible]M17S	1:3,369,000	12001200375	P	P
CORNER POINT COORDINATES=#1:S11D06M22S E143D36M14S ,#2:S10D52M26S E141D58M44S ,#3:S12D37M31S E143D12M55S ,#4:S12D23M27S E141D34M04S													
LANDSAT-1 (MSS)	8102600041SN0	105,068	B&W	2.2"	8,8,8,8	0%		08/18/72	S11D37M02S E142D3[illegible]M56S	1:3,369,000	12000020157	N	P
CORNER POINT COORDINATES=#1:S10D59M17S E143D40M23S ,#2:S10D43M57S E142D03M14S ,#3:S12D13M03S E143D14M52S ,#4:S12D14M35S E141D37M13S													
LANDSAT-1 (MSS)	8102700090SA0	106,066	B&W	2.2"	8,8,8,8	30%		09/19/72	S08D31M52S E141D2[illegible]M25S	1:3,369,000	12000020255	P	P
CORNER POINT COORDINATES=#1:S07D53M31S E142D52M53S ,#2:S07D39M16S E141D16M51S ,#3:S09D24M24S E142D28M30S ,#4:S09D10M04S E140D51M45S													
LANDSAT-2 (MSS)	8223823574500	106,068	B&W	2.2"	5,5,8,5	20%		09/17/75	S11D30M00S E141D15M59S	1:3,369,000	22001400401	P	P
CORNER POINT COORDINATES=#1:S10D51M11S E142D18M13S ,#2:S10D36M12S E140D39M17S ,#3:S12D23M42S E141D52M58S ,#4:S12D09M36S E140D13M30S													
LANDSAT-1 (MSS)	8140500093SN0	106,068	B&W	2.2"	8,8,8,2	20%		09/01/73	S11D31M21S E141D05M46S	1:3,369,000	12300290491	P	P
CORNER POINT COORDINATES=#1:S10D52M53S E142D06M55S ,#2:S10D38M32S E140D29M25S ,#3:S12D24M05S E141D42M21S ,#4:S12D09M37S E140D04M20S													
LANDSAT-1 (MSS)	8120700110SA0	106,068	B&W	2.2"	8,8,8,8	10%		02/15/73	S11D27M08S E141D05M39S	1:3,369,000	12001500295	P	P
CORNER POINT COORDINATES=#1:S10D48M05S E142D07M16S ,#2:S10D33M55S E140D28M45S ,#3:S12D2[illegible]M16S E141D42M49S ,#4:S12D09M59S E140D03M46S													
LANDSAT-1 (MSS)	8117100C035N0	106,068	B&W	2.2"	8,8,0,5	30%		01/10/73	S11D48M06S E141D29M32S	1:3,369,000	12001200300	P	P
CORNER POINT COORDINATES=#1:S11D09M34S E142D10M35S ,#2:S10D55M26S E140D33M04S ,#3:S12D34[illegible]M41S E141D46M14S ,#4:S12D26M27S E140D08M12S													
LANDSAT-1 (MSS)	8106300100SN0	106,068	B&W	2.2"	8,8,8,5	10%		09/24/72	S11D37M35S E141D32M07S	1:3,369,000	12000041322	P	P
CORNER POINT COORDINATES=#1:S10D58M48S E142D13M32S ,#2:S10D44M34S E140D35M26S ,#3:S12D3[illegible]M32S E141D49M04S ,#4:S12D16M11S E140D10M26S													

1706

Figure 5 EROS Response to user request for Geographic Computer Search

EXTRACTION OF SOIL INFORMATION FROM VEGETATED AREA

Michikazu FUKUHARA, Shigechika HAYASHI
Hokkaido National Agricultural
Experimental Station, Hokkaido

and

Yoshizumi YASUDA, Ichio ASANUMA, Yasufumi EMORI
Institute of Color Technology,
Chiba University, Chiba

and

Joji IISAKA
Scientific Center, IBM Japan, Tokyo

ABSTRACT

Mix or interaction of vegetation signal on soil information decrease the performance of soil identification and mapping.

This paper discusses a simple technique to eliminate the vegetation signals from the remotely sensed data and to extract soil imformation from vegetated area. This paper, also, demonstrates the usefulness of the technique.

1 INTRODUCTION

On the application of remote sensing technique for identification and mapping of soil condition, there is a limitation that, in an area to be surveyed, often only a portion of the soil exposed to aerial view. To maximize bare siol areas, it is necessary to collect the remote sensing data from vegetated areas preferably in the spring, prior to substantial crop growth. Even then, there will be areas of perennial vegetaion, winter crops,or cultural development for which no direct soil imformation will be obtainable from the remotely sensed data.

In order to extract soil imformation from the vegetated area and to analyze soil condition, mix or interaction of vegetation reflectance on the soil reflectance should be eliminated. In this paper, a simple technique to eliminate the vegetation reflectance mixed on the soil reflectance is discussed and the effectiveness of the technique on soil mapping is demonstrated.

2 THEORY

Variations of spectral characteristics due to vegetation growth change, vegetation cover change, and soil condition change can be two-dimentionally expressed by a relationship between red and infrared spectral bands.
A nIR/R reflectance ratio is sensitive to vegetation growth, biomass, and vegetation cover (Kanemasu, 1974). The nIR/R ratio, also, tend to normalize the effects of varying soil reflectance due to varying soil type, contents of soil organic matter, and soil moisture (Colwell et al, 1975).

A more important feature is that, according to increasing of vegetation cover, the co-ordinates of each soil reaches a co-ordinates of 100 percent vegetation cover; point P (PR, PIR), as shown in Fig. 1 (Fukuhara et al, 1975). Mixed reflectances of soil and crop for red and infrared bands, (R, IR), are given as follow;

$$R = c\ PR + (1 - c)\ SR \qquad \text{---------- (1)}$$

$$IR = c\ PIR + (1 - c)\ SIR \qquad \text{---------- (2)}$$

where, PR and PIR are red and near infrared reflectances of the vegetation, respectively, SR and SIR is red and near infrared reflectances of the soil respectively, and c is vegetation cover. By elimination of c from the equations (1) and (2), following equations are derived;

$$\frac{R - SR}{PR - SIR} = \frac{IR - SIR}{PIR - SIR} \qquad \text{---------- (3)}$$

Let point P (PR, PIR) be the origin and transform the co-ordinates. Then, the equation (3) is rearranged as follow;

$$k = (PIR - IR) / (R - PR) = (PIR - SIR) / (SR - PR) \qquad \text{---------- (4)}$$

As (PIR - SIR) / (SR - PR) is constant for each soil type, k is considered to be a indicator of each soil type.

3 PROCEDURES

3.1 STUDY AREA

Test area is located in north-west part of Obihiro city in Hokkaido. It has 67 trainning fields as shown in Fig. 2 . Soil types in the test area are as follows; (1) Black ando soil with very rich humus (WV-1), (2) Black ando soil with rich humus (WV-2), (3) Brown ando soil with humus (DV), (4) Alluvial soil with rich humus (AL-2), and (5) Alluvial soil with humus. Crop types in the test area are (1) Winter wheat (high vegetation cover) (W), (2) Beet (B), (3) Potato (P), (4) Corn (C), and Bare soil (S). The other classes in the test area are (1) Sand, (2) River or water (R), (3) Grass field (G), and (4) Forest (F).

Trainning fields were selected on the basis of a conventional soil survey map. Table 1 shows a relationship between soil type, crop type, and their trainning field numbers.

3.2 MSS DATA and CCT for ANALYSIS

MSS data were collected over the study area by DAEDALUS DS-1250, from an altitude of 12,500 ft at 13.00 hours on June 5th,1976. The MSS data had 11 spectral bands and an instantaneous field of view of approximately 10 meters. Six of the 11 bnads were chosen, digitized, and used in the computer analysis; three in the visible portion of the spectrum (0.42-0.45, 0.55-0.60, and 0.65-0.69), two in the near infrared (0.7-0.8 and 0.8-0.9), and one thermal infrared (8-14μm). As the MSS data had sun angle and look angle effects and channel misregistration, pre-processing algorithms for mean angle response correction and channel registration were applied to the data before analysis.

3.3 SPECTRAL FEATURES OF TRAINNING FIELDS AND RATIO DATA

To obtain the coefficients (PR and PIR) in the equation (4) or the co-ordinates of P in Fig.1 , the statistics of counts of the trainning classes in red and near infrared band were computed. Fig. 3 shows two dimentional plots of CCT counts of red and infrared bands. A broken line in the figure shows the bare soil group.

Solid lines show the loci of the same soil types according to the vegetation cover change. The lines are gathered to point P. The point P means co-ordinates of 100 percent vegetation cover. The ratio transformation, (PIR - IR)/ (R - PR), are found to be useful for the purpose of extracting soil information, where PIR and PR are coefficients being approximately 160 and 0 respectively for this study.

New ratio transformation, (160 - IR2)/R, were computed (channel 16 in Table 2). Additionally, 16 of ratio channels were computed, as shown Table 2. The best subset of two, three, or four channels from 23 channels were determined based upon statistical distance (Swain 1972) and were used for the soil mapping by using computer-implemented pattern recognition technique. Computed soil maps produced by these various procedures were evaluated with respect to their correlation with conventional soil survey map.

4 RESULTS

4.1 DETERMINATION OF THE BEST CHANNEL COMBINATION FOR ANALYSIS

As the ratio transformation of equation (4) decrease classification performances of water and forest areas, the ratio cannot solely be used and must combine to use with another channels. The best subset of two, three or four channels was determined from the 23 channels based upon the statistical distance among classes and weighting the average distance. This allows the assignment of priorities according to the need to correctly distinguish soil type.

4.1.1 BEST SUBSET OF TWO CHANNELS

A subset of ch 11, (R/IR2), and ch 16, (16-IR2)/R, gave the best separability for soil classification.
Average separation of this subset was 1.860, but the minimum pairwise separation was not enough as 1,280. This means that any subset of two channels is not enough for soil mapping.

The subsets which gave high average separation were combination of ch 16, (160-IR2)/R with other channels such as ch 5(IR), ch 12(R/IR2), ch 15((IR2-R)/ (IR2+R)), and ch 18((B+G+R)/(IR1+IR2)).
This means that the ratio transformation as equation (4) is very useful for the purpose of extracting soil information. Channel 18,(B+G+R)/(IR1+IR2),correspond to the selected ratio, (V/IR), for mapping siol features(Kristof et al,1974).

4.1.2 BEST SUBSET OF THREE CHANNELS

Two subsets of 3 channels were selected based on the value of the minimum pairwise separation;

(a) ch3(R), ch5(IR2), and ch16((160-IR2)/R)
(b) ch5(IR), ch15((IR2-R)/(IR2+R)) and ch16((160-IR2)/R)

Those all channels consists of red and near infrared spectral bands and their combination. In the best subset (a), value of minimum pairwise separation was 1.590 and avarage separation was 1984. Pairs which gave lower separability than 1800 were (1) AL-1 with W and AL-2 with W, and (2) AL-2 bare soil and DV with B and P. By using a ratio related to vegetation cover or biomass such as ch11, ch15 and ch18, the lower separability between AL-1 with W and AL-2 with W was improved. This improvement was done by the difference of wheat growth due to the difference of soil type.

4.1.3 BEST SUBSET OF FOUR CHANNELS

By using 4 channel, the minimum pairwise separation increased to 1700 and more. The best subset of four channel combinations for soil classification was

as follows;
(a) ch3(R), ch5(IR2), ch16((160-IR2)/R) and ch18((B+G+R)/(IR1+IR2))
In this case, spectral bands which were used were Blue, Green, Red, IR1 and IR2. Subsets of four channels which include thermal bnad were as follows;
(b) ch3(R), ch5(IR2), ch14(IR2/TIR) and ch16((160-IR2)/R)
(c) ch2(G), ch14(IR2/TIR), ch16((160-IR2)/R) and ch18((B+G+R)/(IR1+IR2))

To reduce the number of those spectral bands, next 2 subsets of four channels were selected.
(d) ch3(R), ch5(IR2), ch11(R/IR2) and ch16((160-IR2)/R)
(e) ch3(R), ch5(IR2), ch15((IR2-R)/(IR2+R)) and ch16((160-IR2)/R)
This shows an ability of soil mapping with data of red and infrared bands and their transformations.

4.2 SOIL MAPPING

Soil maps were computed by using multispectral pattern recognition technique (Lindenlaub, 1973). For the convenience of the comparison, a small area in the test area are shown in Figure 4 - Figure 7. Figure 4 shows a conventional soil survey map with surface vegetation. Figure 5 shows a classification with the simple ratio transformation; 16 ((160-IR2)/R). Soils AL-1, DV, AL-2, WV-2 and WV-1 were assigned the symbols A, B, C, D, E, respectively. Grass and forest which had high vegetation cover as 80 percent or more were assigned the symbol. Sand and water area were assinged the symbol S and W, respectively. To decrease misclassifcation, the soil area were thresholded as 3 percents and the thresholded areas were left blank on the printouts.

There is some agreement between the soil survey map and the computer printmap. The wheat fields were classified into correct soil classes, although fields had 50 - 70 percent vegetation cover with wheat. Problems were that some soils were classified into water area(W), and water area was misclassified into one of the soil classes, as pointed out by the previous statistical distance study.

Figure 6 shows a classification with single channel of 18 ((B+G+R)/(IR1+IR2)). In this case, the bare soil field were classified with some dependability. But the field with vegetation;corn and beet on surface,were not successfully identified.

Figure 7 shows a classification with the best subset of three channels. There is resonable good agreement between the soil survey map and the computer printmap. Separation of river, forest and grass were also successful. 74.7 percents of average performance by soil classes were obtained although they contained vegetated area.

The classification in a circumference area of high look angle or high scanning angle were successful if ratio transformation channels as ch7 - ch23 in Table 2 were used. Although pre-processing for mean angle response correction were applied to original CCT data, the classification in a circumference area were relatively poor with untransformed channels 1 - 6.

5 CONCLUSIONS

In order to extract soil information from vegetated area and to analyze soil condition, mix or interaction of vegetation reflectance on the soil reflectance should be eliminated. For this purpose, a simple ratio transformation, k=(PIR-IR)/(R-PR), were theoretically derived. In the transformation, PR and PIR are coefficients which derived from the co-ordinates of 100 percent vegetation cover. PR and PIR were approximately 0 and 160, respectively, for this study. The coordinates of high vegetation cover such as forest and grass will be used instead of the coordinates of point P (PR, PIR).

The usefulness of the transformation were investigated and shown by the channel selection based upon the statistical distance between classes and by multispectral pattern recognition. The simple ratio transformation is considered to especially sensitive to the degrees of the soil organic matter content.

The work described in this paper was supported by JAFSA project in Japan.

REFERENCES

1) E.T. Kanemasu, "Seasonal canopy reflectance patterns of wheat, sorghum,and soybean" Remote Sensing of Environment, 3 (1); (1974)
2) J.E.Colwell and G. H. Suits, "Yield prediction by analysis of multispectral scanner data" NASA-CR-141865, ERIM 109600-17-F, p57 (1975)
3) M.Fukuhara and S.Hayashi, "Remote Sensing of agricultural area by using multiband photography" Proceedings of 1st Remote Sensing Symposium p.13, Tokyo,Japan, November 25-26, 1975 (in Japanese)
4) P.H.Swain et al, "Comparison of the divergence and β-distance in feature selection." LARS Information Note 020871 (1972)
5) S.J.Kristof and A.L.Zachary, "Mapping siol features from multispectral Scanner Data" Photogrammetric Engineering. 40 p1427 (1974)
6) J.C,Lindenlaub, "Guido to multispectral data analysis using LARSYS." LARS Information Note 062873 (1973).

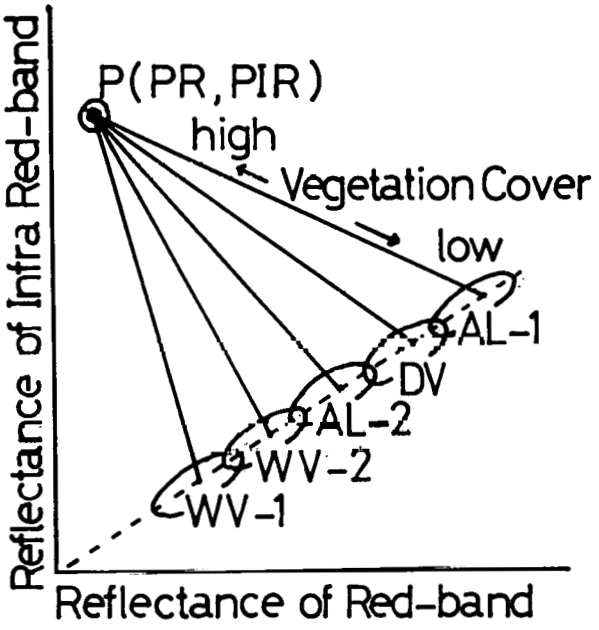

Fig. 1 Illustration of Relationship between Soil Types and Vegetation Covers in a Space of Red and IR spectral Bands.

Table 1 Relationship between Soil organic matter content, Vegetation Cover and Trainning Field.
Numerals in the Table are Numbers of Each Trainning Class.

Soil Type \ Vegetation Type		low ← Vegetation Cover → high				
		S 0 %	B 10-20 %	W 50-70 %	G	F 80 % <
rich	WV-1	3	5	3		1
↑	WV-2	4	4	4	1	2
Soil Organic Mutter	AL-2	4	3	2	1	
	DV	5	4	2	1	5
↓	AL-1	4	2	2	2	
	Sand	1				
poor	Water	2				

S:Bare Soil or Corn, B:Beet or Potato, W:Wheat, G:Grass, F:Forest

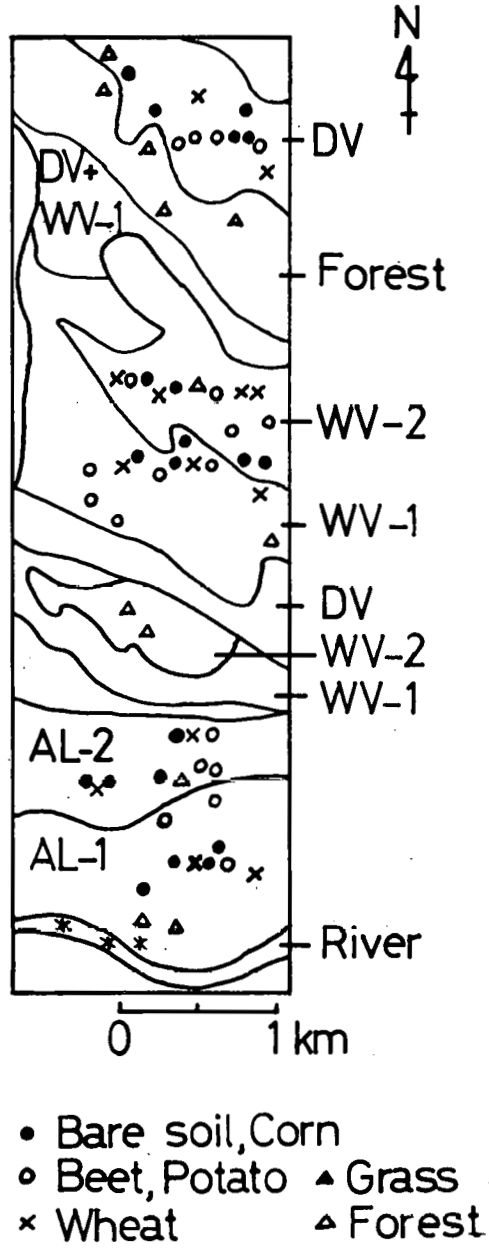

Fig. 2 Conventional Soil Survey Map of Test Area.

WV-1 --- Black ando soil with very rich humus
WV-2 --- Black ando soil with rich humus
DV --- Brown ando soil with humus
AL-2 --- Alluvial soil with rich humus
AL-1 --- Alluvial soil with humus

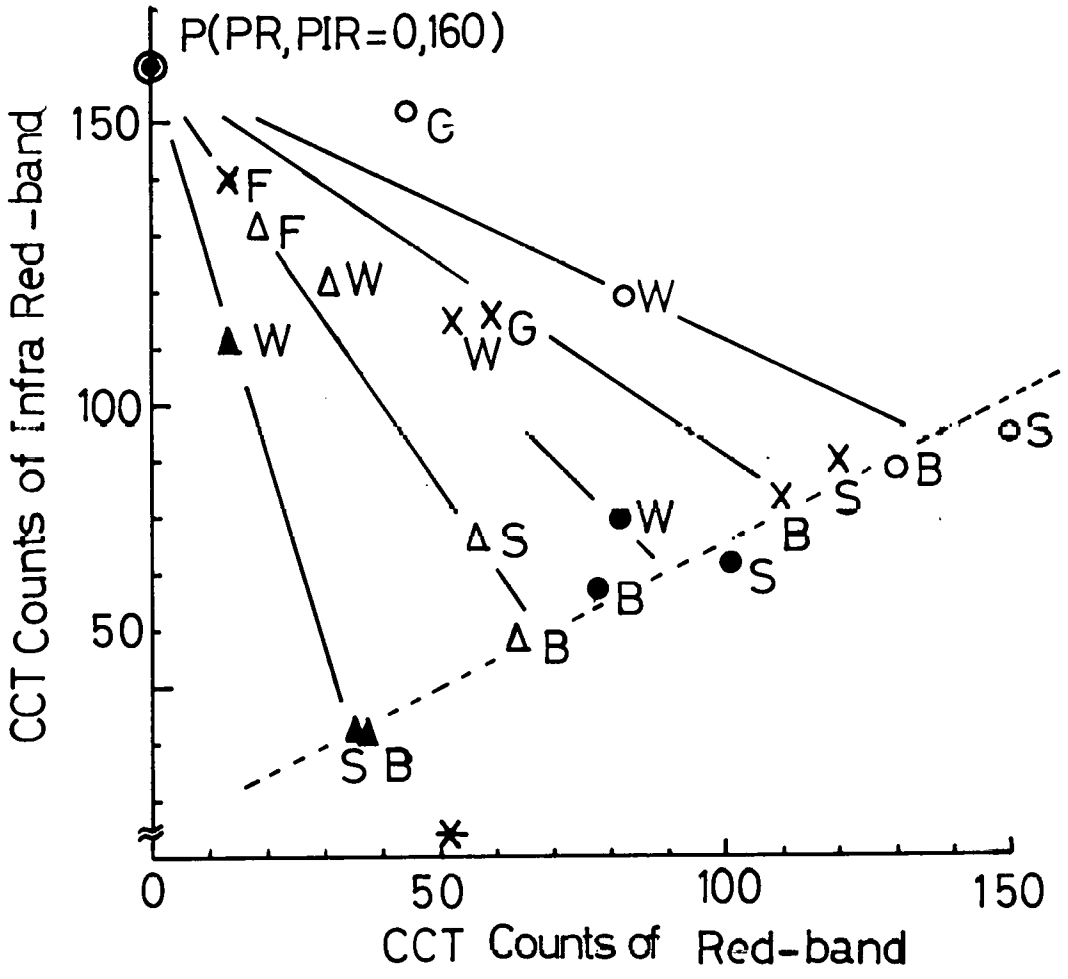

Fig.3, Two Dimentional Plots of CCT Counts of Red and Infrared Bands for Each Trainning Class.

Table 2 , CCT channels for Analysis.

CCT ch. NO.	Spectral band & ratio	CCT ch. NO.	Spectral band & ratio	CCT ch. NO.	Spectral band & ratio
1	B(0.42-0.45 m)	8	G/R	17	(255-TIR)/R
2	G(0.55-0.60 m)	9	G/IR2	18	(B+G+R)/(IR1+IR2)
3	R(0.65-0.69 m)	10	G/TIR	19	B/(B+G+R+IR1+IR2)
4	IR1(0.70-0.79 m)	11	R/IR1	20	G/(B+G+R+IR1+IR2)
5	IR2(0.80-0.89 m)	12	R/IR2	21	R/(B+G+R+IR1+IR2)
6	TIR(8.5-12 m)	13	R/TIR	22	IR1/(B+G+R+IR1+IR2)
7	B/R	14	IR2/TIR	23	IR2/(B+G+R+IR1+IR2)
		15	(IR2-R)/(IR2+R)		
		16	(160-IR2)/R		

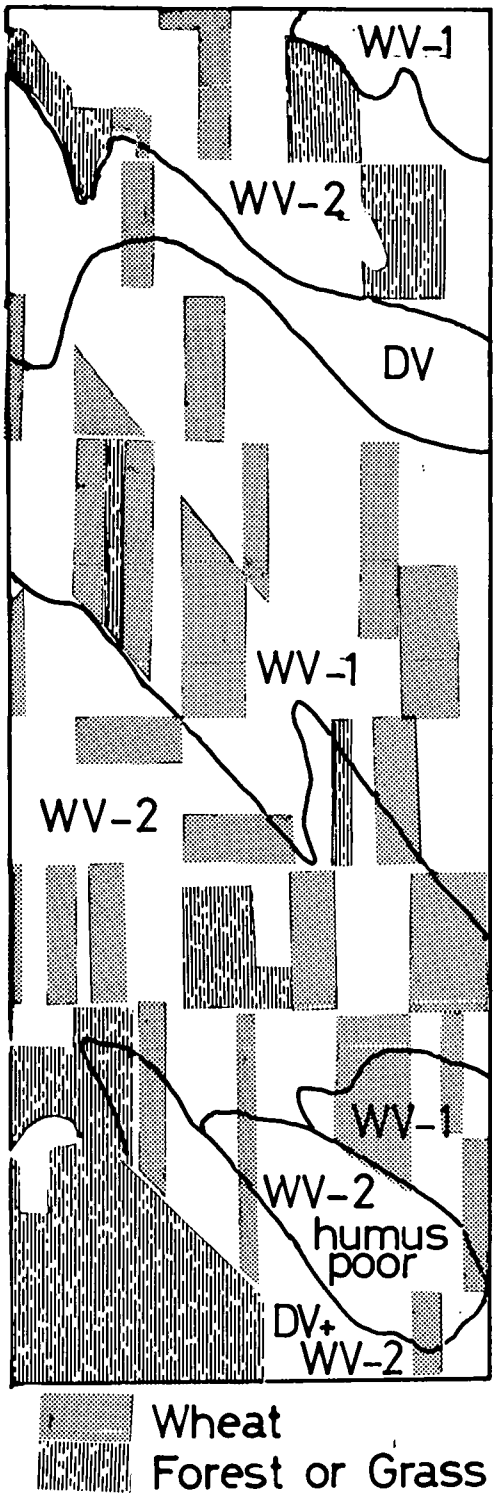

Fig. 4 Soil Survey Map of a part in the test area, with Surface Vegetation.

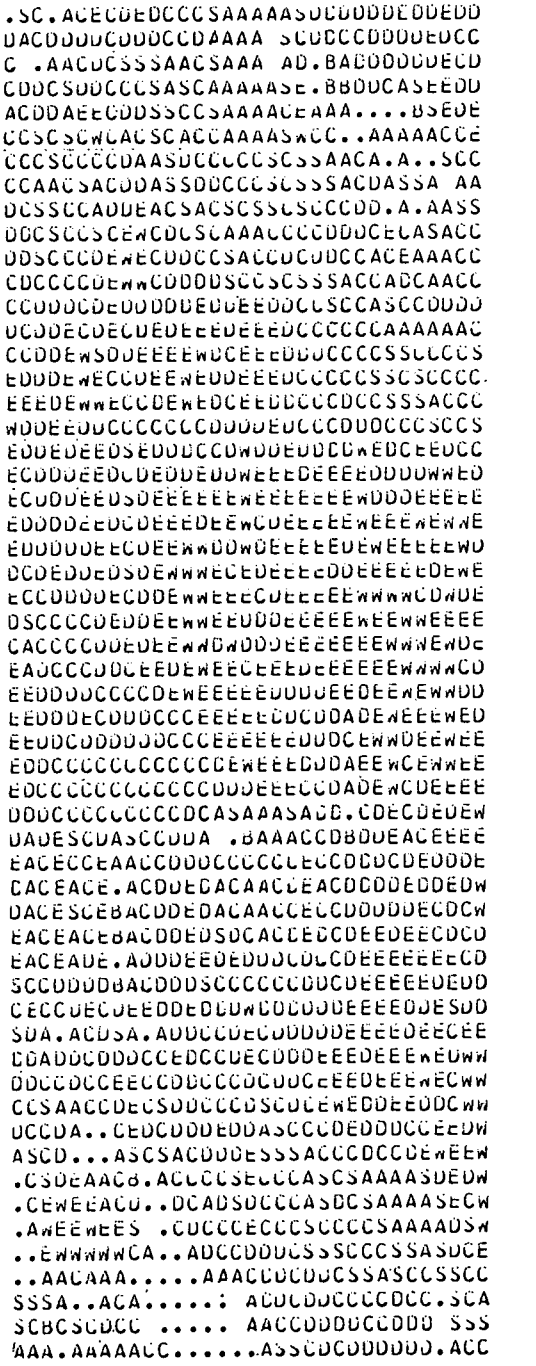

Fig. 5, Computer Classification using Channel 16. Legend; A:AL-1, B:DV, C:AL-2, D:WV-2, E:WV-1, S:Sand, W:Water, (.):Forest and Grass, ( ):Others

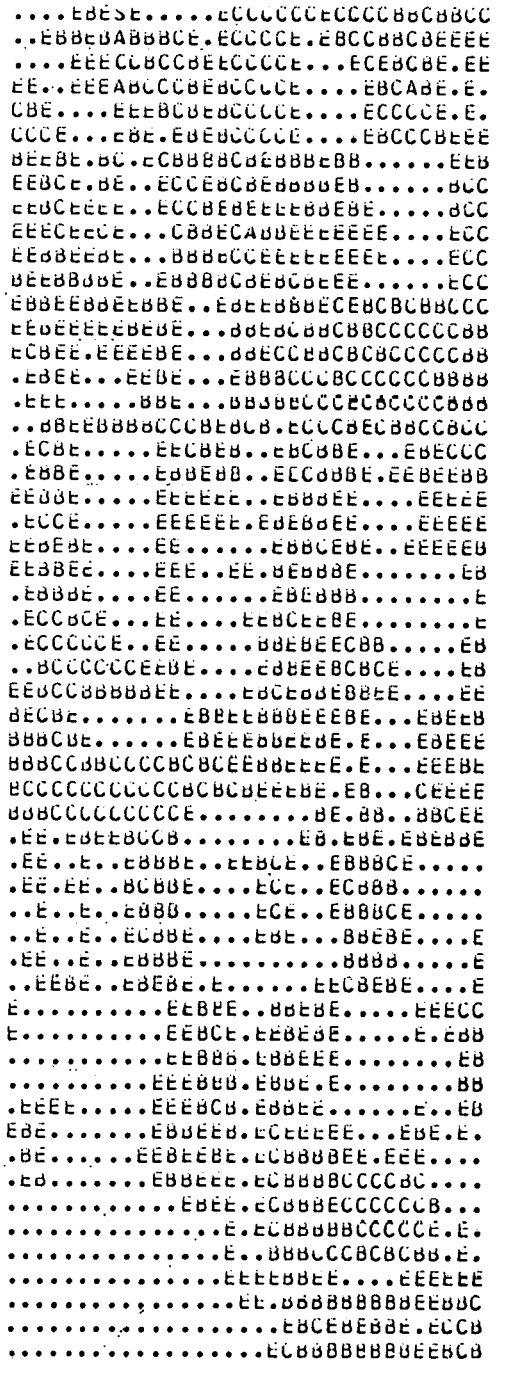

Fig. 6, Computer Classification using channel 18. Training Class Symbols are the same as im Fig. 5

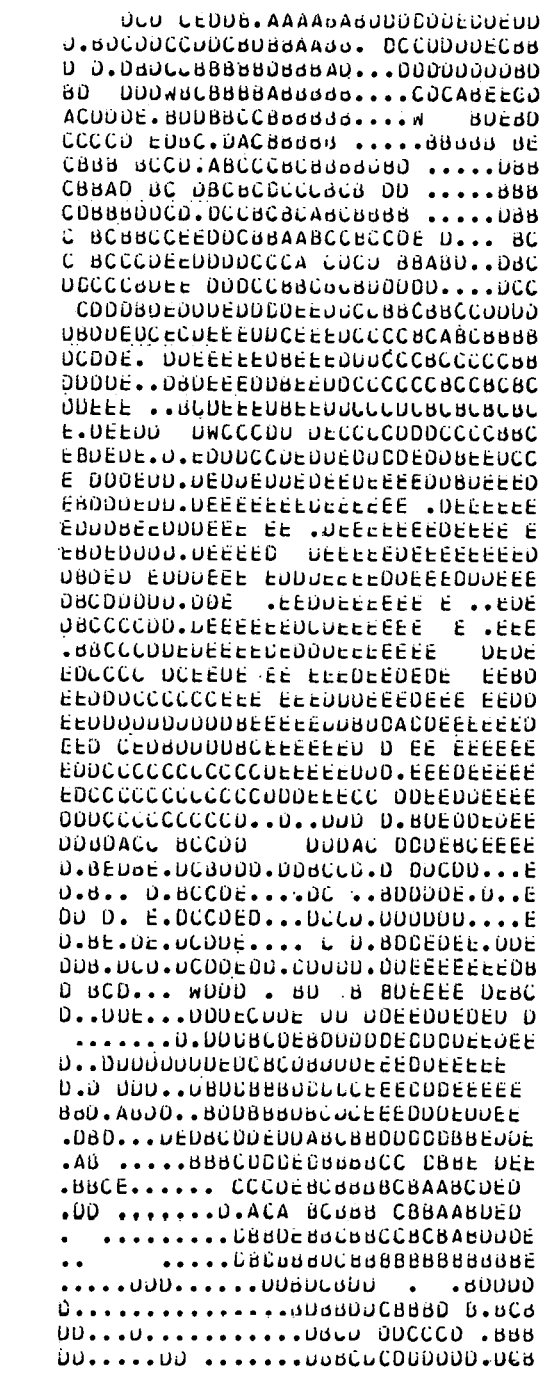

Fig. 7, Computer Classification using the best three channels.

LAND COVER STUDIES USING LANDSAT MSS DIGITAL DATA:

CARTOGRAPHICALLY CORRECTED LINEPRINTER OUTPUT

J.R. Hardy

University of Reading,
Reading, England.

ABSTRACT

A suite of programs is described, and methods are suggested for the processing of Landsat MSS digital data using a general purpose computer, standard FORTRAN and a standard lineprinter for output. Methods and algorithms for producing cartographically corrected lineprinter output are discussed, enabling the output to be overlaid accurately on a 1/25,000 map to facilitate interpretation and classification. Methods of performing areal computations are given.

1. INTRODUCTION

Landsat MSS data are obtainable in two forms - images on film or paper, or digital data on computer compatible tapes (CCT's). Much more frequent use is made of images for interpretation than of the digital material. Among reasons for this may be because difficulties are imagined in processing the digital data, and because many such studies reported make use of expensive dedicated hardware, not commonly available. This paper aims to show that neither of these difficulties need stand in the way of processing and interpretation of Landsat MSS digital data, by reporting a method using

1) A general purpose computer

2) Standard lineprinter output

3) Programs written in standard FORTRAN

Examples of the output of the programs are given in the illustrations at the end of the paper.

A suite of such programs has been written by the author, with advice and assistance from Mr. Richard Dann and staff of the Computer Centre, University of Reading, and from Mr. C.D. Agar, who acted as research assistant on the project during the summer of 1977. The programs have been implemented on the University's ICL 1904S computer, and now serve as a base for the research programs of several workers. The programs, or corresponding ones, could presumably be implemented on any similar general purpose computer installation.

The main purpose of this paper is to describe the cartographic correction algorithms which have been developed and implemented, rather than the actual classification procedure, although the methods used are exemplified by a particular classification example.

Particular advantageous features of the system are:

1) Actual digital values or classifications for every pixel on the CCT can be displayed, at 1/25,000 scale.

2) The output can be modified and cartographically corrected to overlay a 1/25,000 map, with errors of a few millimetres at most, corresponding to 100 metres or less on the ground. Thus individual pixels can be located on a map with reasonable accuracy, and classification limits estimated or modified. If the lineprinter output is reproduced at contact scale on transparent film, it can be suitable for field use with the corresponding map.

3) Accurate areal computations can be automatically carried out for classifications. These areal computations can if necessary be made for areas defined by map grid lines.

4) The basic method used for the map fitting of the output, that of linear least squares transformations, can be applied to enable matching of data from CCT's for different dates. A simple nearest neighbour classification is used for this purpose.

Problems which may be encountered in using the system for other purposes may include:

1) Due to the fixed size of a lineprinter symbol, display at scales smaller than 1/25,000 require either photographic reduction of the original, or omission of say alternate pixels to give a display at 1/50,000. To retain pixel symbols that are individually legible without magnification lineprinter output cannot be reduced by much more than twice. The reduced illustrations (Figures 3 and 4) are at a scale of approximately 1/100,000. Classification maps can of course be reduced by more than twice if individual characters do not have to be read. Alternative output devices, such as a graph plotter, could be used for increased accuracy and variable scale.

2) Due to the large scale of the output, the area that can be handled in one batch by the Reading University computer has a maximum size of about 1000 km^2, but this restriction is shared with a number of dedicated hardware systems.

2. GENERAL DESCRIPTION OF THE PROGRAMS

A single 9 track 1600 b.p.i. CCT can hold the data for a single Landsat scene in all four channels. The data are pixel interleaved (Thomas, 1975). Only a small section of this tape can be handled at one time in the Reading University and most other general purpose computers, and this is most conveniently handled by choosing a suitable small area of interest, the maximum size of which must not be more than about 1000 km^2 on the ground. The position of the area on the tape is most conveniently estimated by reference to an image of the scene if available.

The first programs used separate the CCT data for the four MSS channels for the selected area, and write each channel data on a separate 'tapefile' stored on disc, with each record length on the tapefile corresponding to a scene line for the selected area. Three such programs were required, one each for Landsat 1/Eros Data Center, Landsat 2/Eros Data Center and Landsat1/Landsat 2/Fucino/Telepazio CCT's. The Fucino/Telespazio tapes are in the Canadian format. These programs were written by Mr. Richard Dann of the Computer Centre, University of Reading. The remaining programs described were written by the author, with the exception of program LLST, which was originally written by Mr. C.D. Agar and modified by the author.

The disc tapefiles are then available for further processing. The first task is to obtain some form of visual output, to answer as far as possible the questions 'what do the radiance values represent on the ground?', and 'where

is the selected area actually located?'.

The basic data for all further work are provided by output from the program QUARRY, of which a specimen part is shown in Figure 1. A set of A-format symbols is devised and output, using overprinting, such that 64 or 128 distinctive symbols are produced, one for each numerical value on the tapefile. These QUARRY outputs, one for each of the four channels, enable the actual CCT digital radiance value for each pixel to be determined by inspection, for reference in classification determination.

Histograms, one for each channel, are also produced, showing the number of pixels having each radiance value.

Outputs from program QUARRY may enable location of the area to be estimated, but it is probable that a SLICE output may be more suitable (Fig. 2). This, as its name implies, groups the complete range of pixels in a single channel into a specified number of groups or slices, allots a symbol to each slice, and outputs the result. The most generally useful initial output can be made by reference to the histogram to divide the area into a chosen number of slices, each with an approximately equal number of pixels.

These outputs must be used to identify homologous points on the lineprinter output and on the corresponding map, and coordinates must be determined for each point in the Landsat pixel and line coordinates system and in a map grid easting and northing coordinate system. Approximately ten such points will suffice. (Hardy, 1978).

Using these points, a linear least squares transformation is carried out, using program LLST. The 'observed' and 'calculated' values of each point are given in the output, together with the differences, with their means and standard deviations. Any unusually large discrepancies between a single pair of observed and calculated values must be investigated and resolved if possible. A transformation with good quality data for a single tapefile area will have standard deviations of around 50 metres or less in eastings and northings (Hardy, 1978).

The constants calculated in these transformations provide the bases for cartographic correction of the lineprinter output, accurate areal calculations, and the registration of scenes of different date. The algorithms for these purposes are described in the next section.

Map corrected QUARRY outputs can now be produced, and overlaid on a standard map to allow classification limits to be estimated and corrected in successive approximations. Figure 3 illustrates such an output, corrected from Figure 1. Figure 4 shows a map corrected cuboid classification of the same area into woodland (w) and non-woodland (·), based on the QUARRY information. Figure 5A shows classification confined to an area specified by grid coordinates. Figure 5B is a map of the same classification prepared manually from a combination of topographical maps, air photographs and field checking, while Figure 5C is a copy of the topographical map. Figures 4-5 show various versions of a classification of a test area near Reading, England, into woodland and non-woodland. (Hardy and Agar, 1978). Figure 6 shows a two date classification (March and June), enabling classes of trees to be separated within the woodland areas.

Other programs available are ratio and edge enhancement programs, and programs to test and correct for six line banding.

3. THE CARTOGRAPHIC CORRECTION ALGORITHMS FOR A SINGLE SCENE

Homologous points are selected for each of which coordinates are determined

in the CCT pixel and line system (P and L) and in a map grid system of eastings and northings (E and N).

Sums and cross products are obtained to formulate four sets of normal equations, one set of which is given as an example below:

$$na + \Sigma Pb + \Sigma Lc = \Sigma E \qquad (1)$$

$$\Sigma Pa + \Sigma P^2 b + \Sigma LPc = \Sigma PE \qquad (2)$$

$$\Sigma La + \Sigma LPb + \Sigma L^2 c = \Sigma LE \qquad (3)$$

where $\Sigma P = \sum_{i=1}^{i=n} Pi$, $\Sigma P^2 = \sum_{i=1}^{i=n} P^2 i$, $\Sigma LP = \sum_{i=1}^{i=n} LiPi$ etc.

and n = the number of points

The solution of equations (1) to (3) above permits the determination of a calculated value of E from known values of P and L: Ecalc = a + bP + cL.

Three further corresponding sets of normal equations must be formed and solved, to determine the transformation constants a to m. These enable calculated values of E, N, P and L for any point to be obtained as follows:

$$Ecalc = a + bP + cL \qquad (4)$$

$$Ncalc = d + eP + fL \qquad (5)$$

$$Pcalc = g + hE + iN \qquad (6)$$

$$Lcalc = j + kE + mN \qquad (7)$$

The constants a to m are obtained using program LLST (Linear Least Squares Transformations) using the n values of Pi, Li, Ei and Ni. The constants may then be applied to yield cartographic corrections, areal calculations and registration of scenes of different date.

Pixel dimensions are obtained as follows. The eastings increment between two adjacent pixel centers on the same line is given by constant h, in the same units as the original eastings, while northings increment between the same two points is given by constant e. Thus the along scan line dimension of a pixel is given by $PX = \sqrt{b^2 + e^2}$, and by similar reasoning the along track dimension of a pixel is given by $PY = \sqrt{c^2 + f^2}$. The area of a single pixel is thus PX. PY. K, where K is a constant for conversion of units to yield areas in hectares, acres or other units as appropriate. By simple counting procedures as classification proceeds, areal computations can be carried out using these figures.

From the pixel dimensions, scale corrections may be calculated. A single pixel symbol occupies 1/10 x 1/8 inches on the lineprinter if printed at 8 lines per inch (an option available on most lineprinters compared with the normal 6 lines per inch). This is 2.54 x 3.175 mm, and at a scale of 1/25,000 corresponds to 63.5 x 79.375 metres on the ground. The resemblance of these figures to the average pixel separation of 57 x 79 metres is too close not to be exploited in countries where topographic maps at 1/25,000 are available.

The largest adjustment is required in the along scan line scale. The most accurate method of adjustment involves resampling of the pixels across the line. Simple nearest neighbour resampling has been used in the program described.

Let the total number of pixels across a line being processed in a batch be PPuncorr. The number of pixels to be displayed has to be reduced to

$$PPcorr = PPuncorr. PX / 0.0035,$$

the constant 0.0635 being used if the grid units and pixel dimensions are in kilometres, with adjustment for other units if necessary.

The actual pixel number, NPcorr, of the pixel to be displayed at each lineprinter position from 1 to PPcorr is given by

$$NPcorr = NINT\ (0.0635\ NPuncorr/PX),$$

where NINT is the FORTRAN function for the nearest integer to a given real number.

Similar reasoning may be applied to yield along track corrections of scale, but in practice it has been generally found that the correspondence of the lineprinter line scale separation of 79.375 metres at 1/25,000 to the along track pixel dimension is so close that a correction is required only once in several hundred lines of output, so that it is generally neglected for economy of computation.

In programming these pixel omissions to give a correct scale output, care must be taken if areal computations are also being carried out to ensure that the latter are performed on all pixels before any omissions are made.

The requirements for accurate map correspondence mean that one further major correction has to be made. This is the inclusion of the shear effect which results from the rotation of the earth beneath the satellite's orbital path. This results in the displacement of successive scan lines westward as the descending orbit progresses, with the angle between the scan line axis and the suborbital path differing by about 3^{0} from a right angle.

A good correction of the lineprinter output for this effect may be achieved as follows: The angle described above, of approximately 3^{0}, can be determined from the transformation constants. The angle PE between the eastings and scan line axes is given by

$$\angle PE = \tan^{-1}(e/b)$$

while the angle LN between the northings and along track axes is given by

$$\angle LN = -\tan^{-1}(c/f) \qquad \text{(Figure 7)}$$

These angles are typically of the order of $\angle PE = 13^{0}$ and $\angle LN = 104^{0}$ or -16^{0}. The angle of shear correction, $\angle SC$, is given by $\angle SC = \angle LN - \angle PE$, and is of the order of -3^{0}. This angle is used in the programs, but henceforth the minus sign is ignored.

The implementation of this correction is carried out by displacing the line printer output to the right on the paper at the head of the output, leaving a blank margin on the left. The size of this margin is calculated in the program by determining the integer next greater than the product of the total number of lines to be processed and the tangent of the skew correction angle SC.

As each line is processed, the tangent of the angle SC is multiplied by the total number of lines processed, and each time this value passes an integer, the whole display is stepped one character to the left.

Application of these algorithms will produce a display which is a close map fit (Figure 4), but whose horizontal and vertical axes are, as stated above, along the scan line axis of the satellite data and orthogonal to it, rather than north-south and east-west. To produce a lineprinter output with the latter axes would be impracticable in terms of computer time and programming. A grid overlay for such an output may be calculated and drawn on by manual methods, and up to now this has been considered the most accurate and convenient method of application of a grid. (Figures 3 and 4).

4. PROCESSING OF GIVEN MAP GRID AREAS

There are obvious disadvantages in areal computations performed for areas which are bounded by arbitrary line and pixel limits on the satellite data. It would be more convenient to determine classified areas limited by either map grid lines or administrative boundaries. The former is the simpler of the two tasks and has been accomplished.

A practicable upper limit for a single batch to be processed on a single width of lineprinter paper at a scale of 1/25,000 is 5km x 5km, 25km^2.

The grid area is displayed as before with the scan line axis of the satellite data corresponding with the lines of the lineprinter outputs, rather than east-west, and thus a grid area is displayed obliquely on the printout (Fig. 5A).

The grid limits of the area to be processed are defined in the data deck by the eastings and northings of the four corners, and are described as Ene, Nne, Enw, Nnw, Esw, Nsw, Ese, Nse, with E and N denoting eastings and northings and the suffixes ne etc., describing the corner to which they refer. The worker must of course ensure that the whole of the specified grid area lies within the total tapefile area.

The line and pixel limits of the grid area to be processed must first be determined (Figure 8). The upper and lower limits of the lines to be processed, L1 and L2 respectively, are defined by

$$L1 = \text{NINT}\ (j + k.\ Ene + m.Nne)$$

$$L2 = \text{NINT}\ (j + k.\ Esw. + m.Nsw)$$

The first and last pixels in a line to be processed, P1 and P2 respectively, are defined by

$$P1 = \text{NINT}\ (g + h.\ Enw + i.Nnw)$$

$$P2 = \text{NINT}\ (g + h.\ Ese + j.Nse)$$

For each line between L1 and L2 to be processed, the first and last pixels in that line, marking the limits of the grid area, must be determined. For this purpose, the grid area must first be divided into zones, as indicated in Figure 8, by the determination of L3 and L4.

$$L3 = \text{NINT}\ (j + k.\ Enw + m.Nnw)$$

$$L4 = \text{NINT}\ (j + k.\ Ese + m.Nse)$$

For each line in Zone A, between L1 and L3, the first pixel in that line to be processed, P3, is given by a rearrangement of (5)

$$N = d + eP + fL$$

in which N is defined as the northernmost grid limit, Nne, and the number of the line being processed, LX, is known, to yield P3

$$P3 = \text{NINT}\ \{(Nne - d - f.LX)/e\}$$

In Zone B, between lines L3 and L4, P3 and P4 are defined by

$$P3 = \text{NINT}\ \{(Enw - a - c.LX)/b\}$$

$$P4 = \text{NINT}\ \{(Ene - a - c.LX)/b\}$$

In Zone C, between lines L4 and L2, P3 and P4 are defined by

$$P3 = NINT\ \{(Enw - a - c.LX)/b\}$$

$$P4 = NINT\ \{(Nse - d - f.LX)/e\}$$

The combination of these pixel and line limits with the scale and shear corrections and areal computation methods outlined in the previous section can be used to produce outputs such as those in Figure 5A, in which map corrected output is limited to the specified grid area. The somewhat wavy appearance of the east and west margins is caused by the combination of integer displacement of pixel symbols to the right to conform with the north-south boundary lines, and to the left to implement the shear correction. The accuracy of the areal computations is indicated by the figure for the total area processed, which has always so far been within 0.25% of the correct value for the grid area.

5. MULTITEMPORAL COMBINATIONS OF SCENES

The system described permits, by a further extension, the registration of data for the same area from two or more scenes of different date. Tapefiles are required of areas from the different scenes which correspond closely, although not necessarily exactly, in their limits. Linear least squares transformations must be performed on each scene to be processed. The area to be processed must be represented completely on all scene tapefiles to be used, and for this purpose it is frequently necessary to process an area smaller than any one of the individual tapefiles.

One scene must be chosen as the 'master' for classification purposes. Pixels are processed on this master scene and data from other scenes are registered to it. For economy of computation, this registration is accomplished using scene-to-scene transformations. To obtain these it may be necessary to carry out scene-to-map transformations for each scene, as it is often impossible to find reliable homologous points on one scene and another acquired at a different season. A scene-to-scene transformation may then be computed from any two scene-to-map transformations.

Pixel (P_2,L_2) on scene 2 may be found by determination and application of the transformations

$$P_2 = NINT\ (p + q.\ P_1 + r.\ L_2)$$

$$L_2 = NINT\ (s + t.\ P_1 + u.\ L_1)$$

The major programming change required for multitemporal registration is that, while it is simplest to work on a single scene one line at a time, holding only that line in store, with a multitemporal combination it may be necessary to hold three lines or more of the 'second' scenes in store as well as the appropriate single line of the 'master' scene, because of slight differences in orientation of the lines on the two scenes.

A practical example of the use of such a multitemporal combination is given by a project carried out by the author and C.D. Agar for the British Forestry Commission in which the requirements were to separate woodland from non-woodland for a test area in Britain, and further, for the woodland areas, to differentiate as far as possible different types and species of trees. It proved possible to separate woodland from non-woodland using digital data for March 1973. However, no reliable separation of woodland types was found possible using the March data. Inspection of June 1973 data suggested that tree type separation would be possible, but tests showed that the initial separation of woodland from non-woodland was very poor on the June data. So a solution was adopted of separating woodland from non-woodland on the March data,

and for pixels thus classified as woodland, the homologous pixel for June was found and classified into one of four woodland types. An output is illustrated in Figure 6. The results of the study are reported elsewhere (Hardy and Agar, 1978).

6. CONCLUSION

The suite of programs described enables Landsat MSS digital output to be displayed at a scale of 1/25,000 to sufficient accuracy to enable individual pixels to be attributed to the corresponding ground areas. This allows estimates of initial classification limits to be made with reference to areas for which detailed ground information is available. Later classification estimates can be revised, with errors of omission and commission clearly shown on the map overlay. Similar overlays can also be used in the field with suitable preparation on clear film.

Accurate areal computations are possible for all map corrected classifications, within map grid limits if required. The precision of classification permitted by the use of digital data is available, with accurate registration of channels and scenes from different dates. The system is operated on a general purpose computer, using standard FORTRAN as the programming language and a standard lineprinter as output device, making processing of digital Landsat MSS data more widely available.

ACKNOWLEDGEMENTS

The author wishes to acknowledge the assistance of Mr. C.D. Agar who was his research assistant during the summer of 1977 on much of the work reported in this paper, and the assistance and advice of Mr. Richard Dann and other members of the staff of the Computer Centre, University of Reading. Mr. Agar was salaried by the British Forestry Commission, who also paid for computer time involved.

REFERENCES

J.R. Hardy, Methods and accuracy of location of Landsat MSS points on maps, paper accepted for publication in *Journal of the British Interplanetary Society*, 1978.

J.R. Hardy and C.D. Agar, A study of the potential of Landsat MSS digital data for woodland census in Britain, paper accepted for publication in *Journal of the British Interplanetary Society*, 1978.

V.L. Thomas, *Generation and Physical characteristics of the Landsat 1 and 2 MSS Computer Compatible Tapes*, NASA, Goddard Space Flight Center, 1975 (Document X-563-75-223).

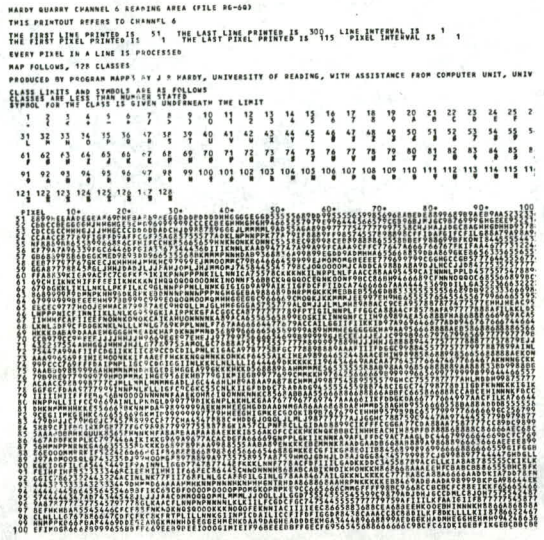

Figure 1. Sample output of program QUARRY

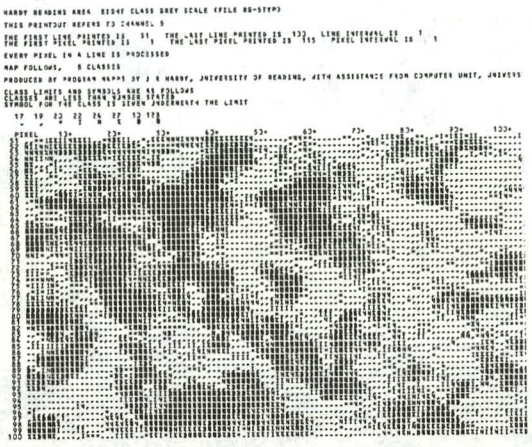

Figure 2. Sample of program SLICE (same area as Figure 1)

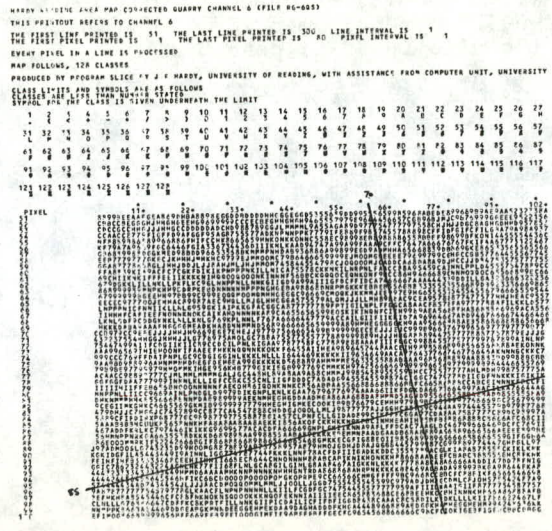

Figure 3. Map corrected QUARRY output with manually prepared grid overlay (same area as Figure 1)

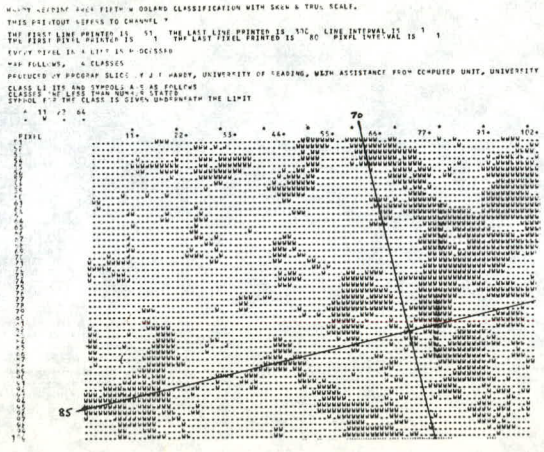

Figure 4. Map corrected cuboid classification for woodland/non-woodland (same area as Figure 1)

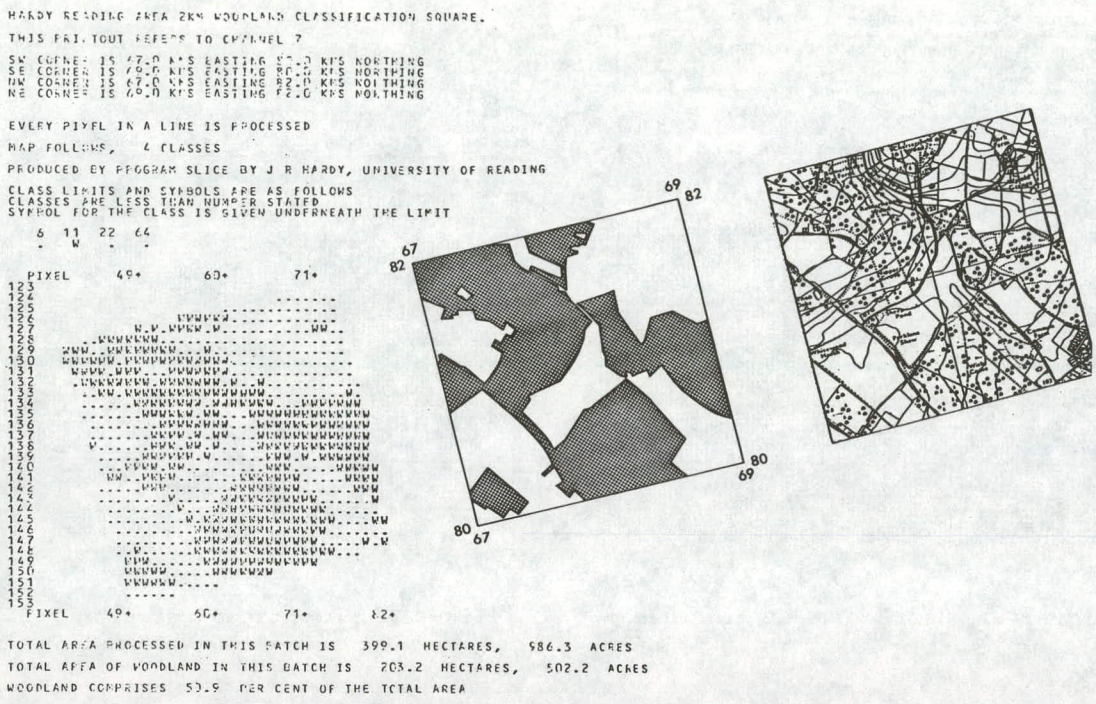

Figure 5. Cuboid classification for woodland/non-woodland for a 2km x 2km grid area (A), with manually prepared 'truth' map (B), and Ordnance Survey topographic map (C). Originals were at 1/25,000 scale. (Details in text, page 3).

Figure 6. Part of 5km x 5km classification into four types of woodland, and non-woodland, combining scene data from March and June 1973.

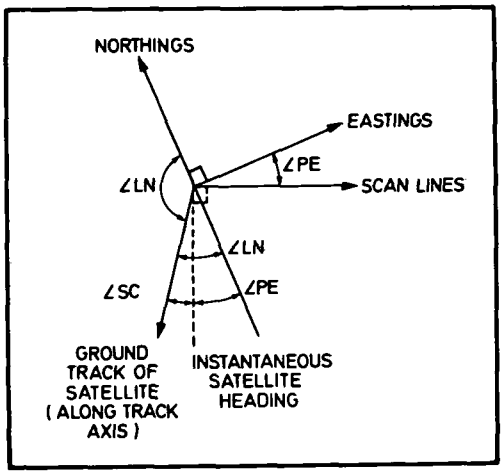

Figure 7. The relation and angles between the scan lines and along track axes, and the northings and eastings axes. (see text, page 5).

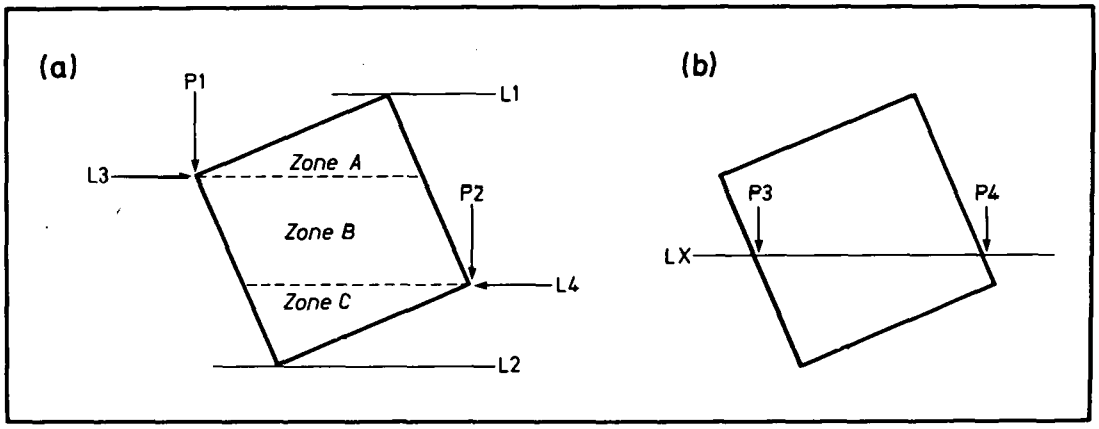

Figure 8. Limits and zones of a map grid square area defined on the pixel and line system of a Landsat tapefile (see text, pages 6-7).

THIS PAGE

WAS INTENTIONALLY

LEFT BLANK

EVALUATION OF WAVELENGTH GROUPS FOR DISCRIMINATION OF AGRICULTURAL COVER TYPES

R. Kumar

Instituto de Pesquisas Espaciais - INPE
Conselho Nacional de Desenvolvimento Científico e Tecnológico - CNPq
12.200 - São José dos Campos, SP, Brazil

ABSTRACT

Multispectral scanner data in twelve spectral channels, in the wavelength range 0.46 to 11.7 μm, acquired in July 1971 for three flightlines, were analysed by applying automatic pattern recognition techniques. These twelve spectral channels were divided into four wavelength groups (W1, W2, W3 and W4), each consisting of three wavelength groups -- with respect to their estimated probability of correct classification (P_c) -- in discriminating agricultural cover types. The same analysis was also done for the data acquired in August, to investigate the effect of time on these results. The effect of deletion of each of the wavelength groups on P_c, in the subsets of one to nine channels, is given. Values of P_c for all possible combinations of wavelength groups, in the subsets of one to eleven channels are also given.

1. INTRODUCTION

Multispectral scanner (MSS) data were analysed in subsets of one to twelve spectral channels, in the wavelength range 0.46 to 11.7 μm, for selected flightlines of the 1971 Corn Blight Watch Experiment[1]. These twelve spectral channels were divided into four wavelength groups (W1, W2, W3 and W4), each consisting of three spectral channels (Table I). The purpose of this study was to determine the statistical separability of multispectral measurements from agricultural cover types for evaluation of these wavelength groups. The agricultural cover types selected were: corn, soybeans, green forage (hay & pasture), and forest. In particular, the objectives of the study were: (1) To study the effect of deletion of all possible combinations of the four wavelength groups -- W1, W2, W3 and W4, on the statistical separability and corresponding estimated probability of correct classification (P_c) of the agricultural cover types. (2) To develop a criterion for evaluation of a combination of wavelength groups, based on the estimation of the probability of correct classification obtained by using this combination of wavelength groups in discrimination of agricultural cover types. (3) To investigate the effect of time on these results.

The literature review of the statistical separability of agricultural cover types was done by Kumar and Silva (1977)[2]. In addition, they analysed the multispectral scanner data in wavelength range 0.46 to 11.7 μm for three flightlines. They found that in the subsets of one to six spectral channels, the combination of wavelength regions (where V, N, M and T denote the visible, near infrared, middle infrared and thermal infrared wavelength regions, respectively): V, VM, VNM, VNMT, VVNMT, VVNMMT, respectively, were found to be the best choices for getting good overall statistical separability of the agricultural cover types for the data acquired on July 16 as well as August 12.

An effort was made to explain these results on the basis of spectral properties of agricultural cover types. The overall statistical separability of the agricultural cover types was found to be greater for the data of August 12 than the data of July 16. Kumar[3] (1977) did a further analysis of similar nature, to evaluate explicitly each spectral channel, each wavelength region and all possible combinations of wavelength regions for statistical separability, in terms of estimated probability of correct classification for agricultural cover types. Deletion of the channel 7 (0.61 to 0.70 μm) reduced P_c by about two percent. The deletion of each of the other channels caused no reduction, or less reduction, in the values of P_c, as compared to this channel. The deletion of the spectral channels constituting the visible wavelength region caused more reduction in P_c, as compared to the spectral channels constituting any of the other wavelength regions. The deletion of the spectral channels of near infrared wavelength region caused relatively small changes in the values of P_c. In the subsets of one to six spectral channels, the combination of wavelength regions V, VM, VMT, VNMT, VVNMT, VVNMMT; and T, NT, VNT or VMT, VNMT, VVNMT or VNMMT, VVNMMT were found to be the best choices for the data of middle of July and middle of August respectively.

Since the spectral channels were divided into four wavelength regions, the results obtained could be interpreted on a physical basis; on the other hand, each wavelength region (V, N, M, T) is not represented equally, in the sense that each wavelength region does not have the same number of spectral channels. The author does not have data of a multispectral scanner where each wavelength region has equal number of channels. However, the author felt a definate need for doing an analysis of similar nature by dividing the available twelve spectral channels (Table I) into four wavelength groups -- W1, W2, W3 and W4, each wavelength group consisting of three channels, so that each wavelength group is equally represented in the sense that it has an equal number of channels. In addition, this analysis is more complete in the following aspects: (1) The effect of deletion of all possible combinations of the four wavelength groups on the estimated value of P_c is given. (2) In addition to the average values of P_c, maximum as well as minimum values of P_c for all possible combinations of wavelength groups in the subsets of one to twelve spectral channels are given.

2. METHOD OF ANALYSIS

Multispectral scanner data in twelve spectral channels in the wavelength range 0.46 to 11.7 μm, collected with an optical-mechanical scanner at altitudes of 914 to 2133 meters (3000 to 7000 feet) over Western Indiana were analysed by applying automatic pattern recognition techniques. The wavelength bands of these twelve spectral channels are given in Table I. The data of three selected flightlines, acquired in July of 1971, were analysed. Each of these three flightlines had fair or good amount of each of the four agricultural cover types: corn, soybeans, green forage and forest. These three flightlines were selected carefully so that these combined could be considered to be representative of the four agricultural cover types in the Western Indiana.

Black and white photography and gray scale printouts of the spectral channels of the flightlines were used to aid in locating the boundaries of the fields on the Digital Display. Sufficient number of fields of each agricultural cover type were selected carefully so that they could be assumed to be representative of the flightline.

Using the same three flightlines and twelve spectral channels, an identical analysis was performed on the data acquired in August of 1971, to study the effect of time on the statistical separability of agricultural cover types. The multispectral scanner data was acquired on both dates (July and August) between 10.30 a.m. and noon time (local solar time). In addition, these data were of good quality and free from problems like lack of sufficient ground observations, excessive cloud cover, etc. The analysis was done for the data acquired in July and August, because corn and soybeans have reached their maximum vegetative growth by these times, and one month of time is sufficient for significant changes to occur in the spectral properties of agricultural cover types. The author wanted to avoid the analysis of data from late

September afterwards, because soybeans are harvested in September-October. The author tried to keep all the variables other than time uniform in the two (July and August) sets of data as far as possible. For example, an effort was made to select about the same field boundaries for the two sets of data. A total of more than 550 fields taken from three flightlines were analysed.

Each field was treated as an independent unit and the fields of the same agricultural cover type were put in the same class. The statistics algorithm was used to compute the mean vector and covariance matrix (mean and standard deviation) of the classes. Histograms of the agricultural classes defined above were used to check unimodality of the statistical distributions in individual channels. The classes were redefined to eliminate distinct multiple modes. Divergence is defined for any two density functions. In the case of normal variables with unequal covariance matrices, divergence in n spectral channels $C_1, C_2, \ldots, C_n$ is given in terms of mean vectors and covariance matrices of the classes[4,5].

A modified form of the divergence D_T, referred to as "transformed divergence", has a behavior[4,6] more like the probability of correct classification than the divergence, D.

$$D_T = 2\{1 - \exp(-D/8)\} \tag{1}$$

Transformed divergence has been used throughout this study.

Although divergence only provides a measure of the distance between two class densities, its use has been extended to the multiclass case by taking the average over all pairs[7]. Let D_{Tij} denote the divergence between classes i and j of a certain flightline, then the average divergence over all class pairs of four classes (each agricultural cover was treated as a separate class) is given by

$$D_{TAVG} = \frac{1}{6}\left[D_{T12} + D_{T13} + D_{T14} + D_{T23} + D_{T24} + D_{T34}\right] \tag{2}$$

$$\text{Let } D_{TMIN} = \text{minimum of } \left\{ D_{T12}, D_{T13}, D_{T14}, D_{T23}, D_{T24}, D_{T34} \right\} \tag{3}$$

Let superscripts 1 and 2 with the symbol "D_T" denote the values of transformed divergence for the data acquired in middle of July and middle of August respectively. Let D^1_{TMIN1}, D^1_{TMIN2}, and D^1_{TMIN3} be the values of D_{TMIN} (see eq. (3)) in first, second and third flightline, respectively, for the data acquired in middle of July.

$$\text{Let } \bar{D}^i_{TAVG} = \frac{1}{3}\left[D^i_{TAVG1} + D^i_{TAVG2} + D^i_{TAVG3}\right] \quad , i = 1, 2 \tag{4}$$

$$\text{Let } \bar{D}^i_{TMIN} = \text{minimum of } \left[D^i_{TMIN1}, D^i_{TMIN2}, D^i_{TMIN3} \right] \quad , i = 1, 2 \tag{5}$$

Assuming each agricultural class has a multivariate gaussian distribution, the feature selection processor was used to find $\bar{D}^1_{TAVG}$ and $\bar{D}^1_{TMIN}$ in <u>all possible</u> combinations of one to twelve spectral channels out of the available twelve spectral channels.

$$\text{Let } \bar{D}^i_{TMAX}\left\{ \text{subset of r spectral channels} \right\} = \max\left\{ \bar{D}^i_{TAVG} \right\}, \; i = 1, 2 \tag{6}$$

maximized over all possible subsets of r spectral channels out of the available twelve spectral channels. From the values of the average transformed divergence, classification accuracy can be reasonably predicted from the results of Swain et al. (1973)[6].

Table I gives the wavelength interval and the corresponding wavelength group of each of the twelve spectral channels. Tables II and III give the effect of deletion of each of the four wavelength groups and all possible combinations of the four wavelength groups respectively on $\bar{D}^1_{TMAX}$ and $\bar{D}^2_{TMAX}$, in terms of the corresponding estimated probability of correct classification (P_c).

To fulfill one of the main objectives of the study -- evaluation of all possible combinations of wavelength groups -- the following criterion is proposed.

Each of 12 available channels of the multispectral scanner can be placed in one of the four wavelength groups W1, W2, W3 and W4 (Table I). Thus, any combination of spectral channels can be called as the corresponding combination of the wavelength groups. For example, channel combination 1 4 7 10 is called "combination of wavelength groups W1 W2 W3 W4". For a given combination of wavelength groups, for example, W1 W2 W3 W4, D_{TAVG} and the corresponding value of P_c were calculated using the curve of Swain and King[6], for all possible combinations of four spectral channels that constitute the combination W1 W2 W3 W4. The minimum, maximum and the mean of these values of P_c were calculated for all possible combinations of wavelength groups, in the subsets of one to twelve spectral channels, and is shown in Table IV, for the data of middle of July as well as middle of August.

3. RESULTS AND DISCUSSION

Table II shows that deletion of each of the wavelength groups causes the following maximum reductions in P_c for the data of July: W1 (0.5, subset of five channels), W2 (0.4, subset of four channels), W3 (1.0, subset of one channel), W4 (2.3, subset of two channels). The corresponding values for reductions of P_c for the data acquired in August are: W1 (0.2, subset of nine channels), W2 (0.3, subset of nine channels), W3 (0.5, subset of three channels), W4 (1.5, subset of one channel).

Each wavelength region (visible, near infrared, middle infrared and thermal infrared) contains independent valuable information. Deletion of W4 causes more reduction in P_c than deletion of any of the other wavelength groups because it is the only group that contains all the spectral channels of two wavelength regions -- middle infrared and thermal infrared. Deletion of W3 causes more reduction in P_c than W1 or W2 because it has one spectral channel in the visible and two in the near infrared wavelength region, whereas W1 or W2 has the spectral channels only in the visible wavelength region.

Similarly Table III shows that, among the combinations of two wavelength groups, the deletion of W3 and W4 causes most reduction in P_c, because it has all the spectral channels of the near infrared, middle infrared and thermal infrared wavelength regions and one spectral channel of the visible wavelength region. Similarly, among the combinations of three wavelength groups, deletion of W2, W3 and W4 causes the most reduction.

Table IV is quite useful, since it evaluates all possible combinations of wavelength groups in the subsets of one to eleven spectral channels, in terms of P_c. It shows that in the subset of one channel, W1 has the highest value of P_c. This is mainly because channel 7 (red) is an excellent channel for discriminating agricultural cover types. Besides other reasons pointed out by Kumar and Silva[2] (1977), the separability of agricultural cover types in this channel was relatively high due to their low variance in this channel. In the subset of two to four spectral channels, the combination of wavelength groups W2 W4, W2 W3 W4 and W1 W3 (2W4), respectively, for the data of July; and W3 W4, W2 W3 W4 and W2 W3 (2W4), respectively, for the data of August, are found to be the best choices. This work has much application to

feature selection (i.e. selecting best subset of m spectral channels, out of N available channels, of the existing multispectral scanners), and deciding wavelength bands of future satellites.

The author gratefully acknowledges: the Laboratory for Applications of Remote Sensing, Purdue University, for their permission to use the multispectral scanner data, obtained under the NASA Grant No. 15-005-112; Dr. Nelson de Jesus Parada, the Director of the Instituto de Pesquisas Espaciais (INPE), for his permission to publish this work; Dr. Celso de Renna e Souza and Dr. Derli Chaves Machado da Silva, for their continuous encouragement and assistance; Mr. Nandamudi L. Vijay Kumar, for his help in preparation of the tables.

REFERENCES

1. Bauer, M.E., in M.E. Bauer (ed.), "1971 Corn Blight Watch Experiment Final Report", National Aeronautics and Space Administration, Lyndon B. Johnson Space Center, Houston, Texas, 1974.

2. Kumar, R. and L. Silva, "Separability of Agricultural Cover Types by Remote Sensing in the Visible and Infrared Wavelength Regions", IEEE Transactions on Geoscience Electronics, Jan. 1977.

3. Kumar, R., "Evaluation of Spectral Channels and Wavelength Regions for Separability of Agricultural Cover Types", Proceedings of the Eleventh International Symposium on Remote Sensing of Environment, Environmental Research Institute of Michigan, Ann Arbor, Michigan, 1977.

4. Swain, P.H., "Pattern Recognition: A Basis for Remote Sensing Data Analysis", LARS Information Note 111572, Laboratory for Applications of Remote Sensing, Purdue University, W. Lafayette, Indiana, 40 p., 1972.

5. Marill, T. and D.M. Green, "On the Effectiveness of Receptors in Recognition Systems", IEEE Trans. on Information Theory, Vol. IT-9, pp. 11-17, 1963.

6. Swain, P.H. and R.C. King, "Two Effective Feature Selection Criteria for Multispectral Remote Sensing", in International Joint Conference on Pattern Recognition (LARS Information Note 042673, Purdue University), Washington, D.C., 1973.

7. Fu, K.S. and P.J. Min, "On Feature Selection in Multiclass Pattern Recognition", Technical Report TR-EE 68-17, School of Electrical Engineering, Purdue University, W. Lafayette, Indiana, 1968.

TABLE I. WAVELENGTH BANDS OF THE SPECTRAL CHANNELS

Channel No.	Wavelength Band (Micrometers)	Wavelength Region	Wavelength Group
1	0.46 - 0.49	visible	1
2	0.48 - 0.51	visible	1
3	0.50 - 0.54	visible	1
4	0.52 - 0.57	visible	2
5	0.54 - 0.60	visible	2
6	0.58 - 0.65	visible	2
7	0.61 - 0.70	visible	3
8	0.72 - 0.92	near infrared	3
9	1.00 - 1.40	near infrared	3
10	1.50 - 1.80	middle infrared	4
11	2.00 - 2.60	middle infrared	4
12	9.30 - 11.70	thermal infrared	4

TABLE II. EFFECT OF DELETION OF EACH WAVELENGTH GROUP ON THE PERCENTAGE OF CORRECT CLASSIFICATION

Number of channels in the subset	Values of Probability of Correct Classification Estimated from D_{TMAX}									
	A_0	A_1	A_2	A_3	A_4	B_0	B_1	B_2	B_3	B_4
1	84.3	84.3	84.3	83.3	84.3	85.4	85.4	85.4	83.9	85.4
2	89.2	89.2	89.2	88.3	86.9	91.1	91.1	91.1	90.6	90.4
3	90.9	90.9	90.9	90.2	90.0	94.3	94.2	94.3	93.8	93.5
4	92.6	92.6	92.3	92.2	90.6	96.2	96.2	96.1	95.0	95.0
5	93.9	93.7	93.7	93.8	91.8	96.8	96.8	96.7	96.7	95.9
6	94.6	94.2	94.2	94.4	92.4	97.3	97.3	97.1	97.1	96.2
7	95.0	94.6	94.7	94.7	93.0	97.5	97.5	97.3	97.2	96.4
8	95.4	95.0	95.1	94.9	93.5	97.7	97.6	97.5	97.3	96.5
9	95.7	95.2	95.4	95.0	93.7	97.8	97.6	97.5	97.3	96.5
10	95.9	np	np	np	np	97.8	np	np	np	np
11	96.0	np	np	np	np	97.8	np	np	np	np
12	96.1	np	np	np	np	97.9	np	np	np	np

Note: This table gives the values of percentage probability of correct classification (P_c) estimated from the values of D_{TMAX} (see eq. (6)), Swain and King (1973)[6]. A_0, A_1, A_2, A_3 and A_4 denote the values of P_c when using all available channels, deleting spectral channels in the wavelength groups 1, 2, 3 and 4 respectively for the data acquired in the middle of July. B_0, B_1, B_2, B_3 and B_4 denote corresponding quantities as A_0, A_1, A_2, A_3 and A_4 respectively for the data acquired in the middle of August. "np" denotes that this channel combination was not possible.

TABLE III. EFFECT OF DELETION OF COMBINATION OF WAVELENGTH GROUPS ON THE PERCENTAGE OF CORRECT CLASSIFICATION

DATA OF JULY.

(A) Values of Probability of Correct Classification (P_c) Estimated from $\overline{D}_{TMAX}$ (see eq. (6)) After Deletion of Combination of Wavelength Regions

N	P_c^*	W1W2	W1W3	W1W4	W2W3	W2W4	W3W4	W1W2W3	W1W2W4	W1W3W4	W2W3W4
1	84.3	84.3	83.30	84.3	82.68	84.3	83.30	82.68	84.3	83.30	81.59
2	89.2	89.2	88.33	86.38	86.85	85.79	84.74	86.12	86.88	86.06	83.70
3	90.9	90.9	90.18	86.96	90.84	89.62	88.40	88.56	89.51	86.45	83.94
4	92.6	96.26	92.25	90.50	91.21	90.87	88.86	np	np	np	np
5	93.9	92.89	92.90	91.35	91.93	91.64	91.64	np	np	np	np
6	94.6	93.89	93.62	92.29	92.91	92.68	92.67	np	np	np	np

DATA OF AUGUST

(B) Values of Probability of Correct Classification (P_c) Estimated from $\overline{D}_{TMAX}$ (see eq. (6)) After Deletion of Combination of Wavelength Regions

N	P_c^*	W1W2	W1W3	W1W4	W2W3	W2W4	W3W4	W1W2W3	W1W2W4	W1W3W4	W2W3W4
1	85.4	85.4	83.88	85.4	83.88	84.05	83.51	83.62	83.88	83.51	83.51
2	91.1	91.1	90.95	90.57	90.01	90.26	88.14	90.88	90.71	88.93	84.20
3	94.3	91.64	93.95	93.55	93.62	92.33	90.53	92.17	92.10	89.36	85.47
4	96.2	95.77	95.96	95.01	95.16	94.50	90.71	np	np	np	np
5	96.8	96.44	96.69	96.26	96.05	95.88	92.05	np	np	np	np
6	97.3	96.77	96.77	96.38	96.18	96.01	93.89	np	np	np	np

Note: "np" denotes that deletion of combination of wavelength regions was not possible. W1, W2, W3 and W4 denote wavelength groups 1, 2, 3 and 4 respectively (see Table I).
N = Number of channels in the subset
$P_c^* = P_c$ Without Deletion

TABLE IV. EVALUATION OF COMBINATION OF WAVELENGTH GROUPS

WGC	(A) P_c Avg	(A) P_c Min	(A) P_c Max	(B) P_c Avg	(B) P_c Min	(B) P_c Max
N = 1						
W1	80.7	79.67	81.59	82.7	81.91	83.51
W2	80.4	78.15	83.33	82.6	81.93	83.51
W3	75.8	66.01	84.30	84.7	83.30	85.39
W4	81.2	80.37	82.65	82.0	80.13	83.88
N = 2						
2W1	83.1	82.37	83.70	84.3	83.52	85.03
W1W2	83.8	82.50	84.74	85.1	83.51	88.14
W1W3	85.2	84.20	85.79	89.4	85.52	90.36
W1W4	86.3	85.39	86.85	89.4	88.32	90.01
2W2	84.3	82.62	86.06	86.4	85.24	88.93
W2W3	85.2	83.74	86.38	89.7	86.18	90.57
W2W4	86.4	85.14	88.83	89.7	89.24	90.36
2W3	84.3	77.44	86.88	89.1	85.13	90.71
W3W4	85.5	83.59	89.21	90.5	89.21	90.84
2W4	85.3	84.56	86.12	89.8	86.32	90.88
N = 3						
3W1	83.9	83.9	83.9	85.46	85.46	85.46
(2W1)W2	84.9	83.96	86.22	86.4	84.90	88.71
(2W1)W3	86.3	85.36	87.97	90.6	86.45	91.88
(2W1)W4	88.3	86.82	88.55	90.7	89.44	91.00
W1(2W2)	86.0	84.93	88.40	89.3	88.17	90.88
W1W2W3	86.8	85.60	88.75	90.7	88.40	93.53
W1W2W4	89.0	86.17	89.83	90.9	90.19	92.70
W1(2W3)	88.5	86.90	89.62	91.7	90.39	92.50
W1(2W4)	89.9	89.13	90.44	92.2	90.36	93.62
W1W3W4	89.2	88.51	90.51	92.3	91.10	94.29
3W2	86.4	86.40	86.40	89.4	89.4	89.4
(2W2)W3	86.8	85.74	89.54	90.6	89.15	92.42
(2W2)W4	89.0	86.12	90.61	91.6	90.49	92.81
W2(2W3)	88.9	86.61	89.96	92.3	91.51	93.55
W2W3W4	90.0	88.15	90.89	92.7	90.89	94.15
W2(2W4)	89.8	88.59	90.18	92.5	90.73	93.95
3W3	89.5	89.50	89.50	92.1	92.10	92.10
(2W3)W4	89.5	85.55	90.33	92.5	91.14	93.60
W3(2W4)	89.1	86.26	90.86	92.5	91.33	93.00
(3W4)	88.6	88.60	88.60	92.2	92.2	92.2

WGC	(A) P_c Avg	(A) P_c Min	(A) P_c Max	(B) P_c Avg	(B) P_c Min	(B) P_c Max
N = 4						
(3W1)W2	85.8	85.23	86.83	88.4	86.67	89.18
(3W1)W3	88.3	86.89	88.53	90.8	89.55	92.28
(3W1)W4	89.4	89.27	89.53	91.0	90.14	91.50
(2W1)(2W2)	86.8	85.91	88.86	90.2	89.59	90.71
(2W1)W2W3	88.8	88.01	90.07	92.7	89.24	94.06
(2W1)(2W3)	89.8	88.89	90.66	92.7	91.62	93.93
(2W1)W2W4	89.9	89.01	90.22	92.8	90.74	93.72
(2W1)W3W4	90.7	90.09	90.96	93.8	90.28	95.10
(2W1)(2W4)	90.2	89.83	91.06	93.6	91.21	94.80
W1(3W2)	88.6	88.30	88.84	90.9	90.57	91.41
W1(2W2)W3	89.4	88.43	90.93	92.2	90.24	94.46
W1(2W2)W4	90.6	89.71	91.14	93.5	91.78	94.93
W1W2(2W3)	90.3	89.06	90.62	94.0	92.39	94.95
W1W2(2W4)	90.6	89.89	91.77	94.5	92.02	96.02
W1W2W3W4	90.3	89.67	91.38	94.6	91.45	96.07
W1(3W3)	90.7	90.50	90.87	93.8	92.87	94.50
W1(2W3)	90.7	90.53	91.70	94.6	93.76	95.45
(2W3)(2W4)	90.7	89.75	92.26	95.0	94.82	95.77
W1(3W4)	90.9	90.81	91.21	95.0	94.82	95.16
(3W2)W3	89.5	88.85	89.90	91.6	90.54	92.78
(3W2)W4	90.8	90.48	91.17	92.8	92.36	93.62
(2W2)(2W3)	90.2	89.08	90.85	93.7	92.66	94.46
(2W2)W3W4	90.2	90.10	91.42	94.3	91.85	95.66
(2W2)(2W4)	90.6	89.85	92.25	95.0	92.84	95.96
W2(3W3)	90.9	90.53	91.30	94.5	93.87	95.01
W2(2W3)W4	90.7	90.09	91.94	95.1	94.15	95.88
W2W3(2W4)	91.0	90.45	92.55	95.5	94.08	96.17
W2(3W4)	90.6	90.34	91.24	95.3	95.16	95.45
(3W3)W4	90.9	90.62	91.29	94.7	94.36	94.82
W3(3W4)	90.8	89.81	91.74	95.2	95.10	95.30
W1W3(2W4)	91.1	90.75	92.09	95.1	92.89	96.11
N = 5						
(3W1)(2W2)	90.8	90.7	90.9	93.5	93.41	93.62
(3W1)W2W3	89.5	89.4	89.57	94.3	94.21	94.46
(3W1)W2W4	90.6	90.48	90.68	90.7	90.6	90.8
(3W1)(2W3)	91.8	91.71	91.93	93.5	93.4	93.63
(3W1)W3W4	91.26	91.21	91.35	95.3	95.07	95.47
(3W1)(2W4)	91.6	91.50	91.69	95.2	95.14	95.32

TABLE IV. CONTINUATION

WGC	(A) P_c Avg	(A) P_c Min	(A) P_c Max	(B) P_c Avg	(B) P_c Min	(B) P_c Max
(2W1)(3W2)	88.6	88.38	88.90	95.04	95.01	95.08
(2W1)(2W2)W3	92.2	92.0	92.4	95.2	95.03	95 35
(2W1)(2W2)W4	91.4	91.26	91.56	95.2	94.99	95.39
(2W1)W2(2W3)	91.2	91.16	91.26	95.6	94.95	96 43
(2W1)W2W3W4	91.5	91.19	92.09	96.0	95.64	96 42
(2W1)W2(2W4)	91.8	91.22	92.56	95.1	95.05	95 15
(2W1)(3W3)	91.7	91.13	92.41	95.5	94.95	96 00
(2W1)(2W3)W4	91.8	91.21	92.50	95.9	94.97	96.57
(2W1)W3(2W4)	92.2	91.50	92.94	95.7	95.28	96.05
(2W1)(3W4)	91.8	91.46	92.01	95.0	94.95	95.12
W1(3W2)W3	91.3	91.25	91.5	95.1	95.03	95.22
W1(3W2)W4	91.4	91.29	91.56	95.2	94.93	95.64
W1(2W2)2W3)	91.3	91.24	91.45	95.8	94.97	96.59
W1(2W2)W3W4	91.7	91.18	92.62	96.0	94.97	96.76
W1(2W2)(2W4)	92.9	91.83	93.77	95.6	94.97	95.90
W1(2W2)(2W3)	91.5	91.19	91.83	96.0	95.10	96.70
W1W2(2W3)W4	91.9	91.26	92.89	96.4	95.01	96.81
W1W2(2W4)W3	92.3	91.16	93.95	95.4	95.71	96.65
W1W2(3W4)	92.2	91.38	92.62	95.7	95.16	96.26
W1(3W3)W4	92.0	91.56	92.34	95.2	95.24	96.63
W1(2W3)(2W4)	92.9	91.90	93.94	95.3	95.85	96.71
W1W3(3W4)	92.4	91.94	92.74	95.4	95.0	95.70
(3W2)(2W3)	91.4	91.20	91.55	95.5	95.05	95.81
(3W2)W3W4	91.5	91.22	91.67	95.6	95.26	95.94
(3W2)(2W4)	92.5	92.42	92.54	95.8	95.16	96.09
(2W2)(3W3)	92.7	92.6	92.75	95.4	95.29	95.48
(2W2)(2W3)W4	92.0	91.50	92.42	95.8	95.18	96.45
(2W2)W3(2W4)	92.3	91.22	92.97	96.3	95.12	96.69
(2W2)(3W4)	92.1	90.40	92.90	96.4	96.26	96.69
W2(3W3)W4	92.1	91.56	92.58	96.2	95.43	96.44
W2(2W3)(2W4)	92.4	91.32	93.70	96.3	95.71	96.81
W2W3(3W4)	92.3	91.64	93.64	96.6	96.34	96.80
(3W3)(2W4)	92.4	91.95	92.89	96.1	95.77	96.42
(2W3)(3W4)	92.6	92.55	92.72	96.4	96.21	96.54
N = 6						
(3W1)(3W2)	94.0	94.0	94.0	96.4	96.4	96.4
(3W1)(2W2)W3	92.3	92.12	92.53	94.9	94.75	95.18
(3W1)(2W2)W4	92.0	91.82	92.23	96.3	96.12	96.45
(3W1)W2(2W3)	92.57	92.51	92.65	96.3	96.15	96.42
(3W1)W2W3W4	93.25	92.97	93.55	96.3	96.15	96.35

WGC	(A) P_c Avg	(A) P_c Min	(A) P_c Max	(B) P_c Avg	(B) P_c Min	(B) P_c Max
(3W1)W2(2W4)	93.5	93.31	93.68	97.2	97.05	97.37
(3W1)(3W3)	93.0	93.0	93.0	96.2	96.2	96.2
(3W1)(2W3)W4	93.0	92.58	93.81	96.3	96.13	96.50
(2W1)W3(2W4)	93.0	92.62	93.78	96.4	96.34	96.52
(3W1)(3W4)	92.5	92.5	92.5	96.3	96.3	96.3
(2W1)(3W2)W3	92.61	92.47	92.70	97.0	96.91	97.14
(2W1)(3W2)W4	92.65	92.55	92.78	97.3	97.12	97.44
(2W1)(2W2)(2W3)	92.74	92.55	92.97	96.4	96.38	96.69
(2W1)(2W2)W3W4	92.7	92.62	94.15	96.4	96.32	96.69
(2W1)(2W2)(2W4)	93.5	93.22	93.81	97.1	96.85	97.31
(2W1)W2(3W3)	92.81	92.54	93.87	96.4	96.38	96.71
(2W1)W2(2W3)W4	92.8	92.53	94.33	96.6	96.38	96.98
(2W1)W2W3(2W4)	93.6	92.60	93.76	96.6	96.44	96.87
(2W1)W2(3W3)	92.9	92.63	93.51	96.4	96.35	96.48
(2W1)(3W3)W4	92.8	92.55	94.21	96.6	96.40	96.86
(2W1)(2W3)(2W4)	93.7	92.63	94.02	96.7	96.44	96.92
(2W1)W3(3W4)	93.0	92.91	93.12	96.67	96.44	96.82
W1(3W2)(2W3)	92.70	92.55	92.87	96.45	96.40	96.56
W1(3W2)W3W4	93.7	92.92	94.08	96.5	96.36	96.60
W1(3W2)(2W4)	93.8	93.62	94.81	97.2	97.08	97.35
W1(2W2)(3W3)	93.2	92.52	93.95	96.52	96.40	96.74
W1(2W2)(2W3)W4	92.9	92.54	94.34	96.7	96.47	97.11
W1(2W2)W3(2W4)	93.8	92.52	94.42	96.8	96.60	97.08
W1(2W2)(3W4)	93.6	92.63	94.02	96.6	96.32	96.86
W1W2(3W3)W4	93.0	92.55	94.59	96.8	96.40	97.19
W1W2(2W3)(2W4)	93.8	92.55	94.55	97.0	96.6	97.26
W1W2W3(3W4)	93.8	92.63	94.25	96.6	96.49	96.96
W1(3W3)(2W4)	94.02	92.84	94.25	97.0	96.63	97.13
W1(2W3)(3W4)	94.65	94.41	94.82	97.2	96.92	97.35
(3W2)(3W3)	92.75	92.75	92.75	96.41	96.41	96.41
(3W2)(2W3)W4	93.32	92.81	93.74	96.5	96.42	96.80
(3W2)W3(2W4)	93.6	93.51	93.72	96.57	96.50	96.91
(3W2)(3W4)	93.6	93.6	93.6	96.77	96.77	96.77
(2W2)(2W3)(2W4)	93.7	92.55	94.14	96.7	96.47	97.05
(2W2)W3(3W4)	93.7	92.60	94.08	97.0	96.68	97.22
W2(3W3)(2W4)	93.8	92.55	94.25	96.8	96.51	97.16
W2(2W3)(3W4)	93.7	92.68	94.23	97.0	96.80	97.26
(3W3)(3W4)	94.50	94.50	94.50	96.8	96.8	96.8
(2W2)(3W3)W4	92.8	92.71	93.00	96.4	96.43	96.60

TABLE IV. CONTINUATION

WGC	(A) P_c Avg	(A) P_c Min	(A) P_c Max	(B) P_c Avg	(B) P_c Min	(B) P_c Max
N = 7						
(3W1)(3W2)W3	93.8	93.69	94.02	96.5	96.41	96.65
(3W1)(3W2)W4	93.92	93.72	94.13	96.65	96.52	96.78
(3W1)(2W3)(2W3)	93.9	93.65	94.17	97.0	96.73	97.29
(3W1)(2W2)W3W4	94.0	93.78	94.35	96.6	96.35	96.91
(3W1)(2W2)(2W4)	94.12	93.91	94.42	96.72	96.41	97.17
(3W1)W2(3W3)	93.93	93.68	94.21	96.73	96.6	97.08
(3W1)W2(2W3)W4	94.0	93.81	94.48	96.81	96.69	96.96
(3W1)W2W3(2W4)	94.32	94.25	94.45	96.8	96.57	97.11
(3W1)W2(3W4)	94.3	93.98	94.65	96.82	96.60	96.95
(3W1)(3W3)W4	94.0	93.68	94.59	96.91	96.83	97.02
(3W1)(2W3)(2W4)	94.3	93.87	94.42	96.92	96.81	97.15
(3W1)W3(3W4)	94.41	94.25	94.61	97.01	96.92	97.23
(2W1)(3W2)(2W3)	94.15	93.85	94.37	96.65	96.60	96.78
(2W1)(3W2)W3W4	94.21	93.95	94.45	96.72	96.68	96.80
(2W1)(3W2)(2W4)	94.2	93.98	94.36	96.70	96.51	96.85
(2W1)(2W2)(3W3)	94.03	93.68	94.31	96.74	96.60	96.93
(2W1)(2W2)(2W3)W4	93.9	93.68	94.80	96.95	96.87	97.22
(2W1)(2W2)W3(2W4)	94.3	93.83	94.74	97.0	96.60	97.24
(2W1)(2W2)(3W4)	94.2	93.68	94.36	96.8	96.69	97.31
(2W1)W2(3W3)W4	94.0	93.70	94.93	97.0	96.71	97.38
(2W1)W2(2W3)(2W4)	94.4	93.81	94.88	97.1	96.60	97.33
(2W1)W2W3(3W4)	94.3	93.77	94.69	96.9	96.74	97.28
(2W1)(3W3)(2W4)	94.4	93.79	94.67	97.1	96.95	97.33
(2W1)(2W3)(3W4)	94.4	93.85	94.72	97.2	96.83	97.45
W1(3W2)(3W3)	93.9	93.65	94.23	96.8	96.61	97.13
W1(3W2)(2W3)W4	93.9	93.68	94.29	96.7	96.60	96.93
W1(3W2)W3(2W4)	94.4	93.81	94.71	96.9	96.60	97.22
W1(3W2)(3W4)	94.5	94.17	94.69	97.1	97.04	97.16
W1(2W2)(3W3)W4	94.1	93.68	94.38	96.8	96.60	97.07
W1(2W2)(2W3)(2W4)	94.4	93.71	95.01	97.0	96.66	97.28
W1(2W2)W3(3W4)	94.5	93.68	94.93	97.2	96.93	97.49
W1W2(3W3)(2W4)	94.5	93.76	95.05	97.1	96.71	97.43
W1W2(2W3)(3W4)	94.85	94.05	95.32	97.3	97.02	97.52
W1(3W3)(3W4)	94.71	94.67	94.92	97.2	97.04	97.32
(3W2)(3W3)W4	93.92	93.85	94.01	96.66	96.66	96.66
(3W2)(2W3)(2W4)	94.2	93.68	94.44	96.9	96.84	97.14
(3W2)W3(3W4)	94.2	94.14	94.36	97.2	96.96	97.29
(2W2)(3W3)(2W4)	94.3	93.77	94.65	97.0	96.84	97.28
(2W2)(2W3)(3W4)	94.4	93.98	94.63	97.3	97.16	97.46
W2(3W3)(3W4)	94.5	94.31	94.69	97.4	97.21	97.50

WGC	(A) P_c Avg	(A) P_c Min	(A) P_c Max	(B) P_c Avg	(B) P_c Min	(B) P_c Max
N = 8						
(3W1)(3W2)(2W3)	92.3	92.07	92.39	96.2	96.02	96.42
(3W1)(3W2)W3W4	92.9	92.50	93.83	96.4	95.14	96.90
(3W1)(3W2)(2W4)	94.1	92.86	94.48	96.7	96.45	96.87
(3W1)(2W2)(3W3)	92.8	92.76	92.86	96.38	96.34	96.47
(3W1)(2W2)(2W3)W4	93.9	92.71	94.42	96.8	96.42	97.05
(3W1)(2W2)W3(2W4)	94.2	92.63	94.90	97.0	96.38	97.32
(3W1)(2W2)(3W4)	94.4	94.12	94.84	97.2	97.08	97.28
(3W1)W2(3W3)W4	94.2	94.02	94.50	96.9	96.56	97.14
(3W1)W2(2W3)(2W4)	94.5	92.90	95.01	97.1	96.68	97.37
(3W1)W2W3(3W4)	94.7	94.34	94.97	97.3	97.17	97.46
(3W1)(3W3)(2W4)	94.7	94.23	95.03	97.1	97.01	97.23
(3W1)(2W3)(3W4)	94.8	94.46	94.99	97.3	97.25	97.35
(2W1)(3W2)(3W3)	92.9	92.81	93.62	96.4	96.33	96.44
(2W1)(2W2)(2W3)W4	94.1	93.72	94.53	96.8	96.51	97.10
(2W1)(3W2)W3(2W4)	94.5	93.51	94.97	97.0	96.53	97.34
(2W1)(3W2)(3W4)	94.8	94.69	94.93	97.25	97.23	97.28
(2W1)(2W2)(3W3)W4	94.4	94.10	94.76	97.0	96.72	97.22
(2W1)(2W2)(2W3)(2W4)	94.6	93.51	95.28	97.2	96.87	97.44
(2W1)(2W2)W3(3W4)	94.8	94.28	95.22	97.4	97.14	97.56
(2W1)W2(3W3)(2W4)	94.8	94.23	95.31	97.3	96.89	97.52
(2W1)W2(2W3)(3W4)	94.9	94.44	95.31	97.4	97.17	97.61
(2W1)(3W3)(3W4)	95.0	94.91	95.09	97.4	97.19	97.46
W1(3W2)(3W3)W4	94.4	94.08	94.78	97.0	96.83	97.11
W1(3W2)(2W3)(2W4)	94.7	93.91	95.24	97.2	96.93	97.65
W1(3W2)W3(3W4)	94.9	94.66	95.16	97.51	97.49	97.55
W1(2W2)(3W3)(2W4)	94.9	94.25	95.57	97.3	97.13	97.53
W1(2W2)(2W3)(3W4)	95.0	94.31	95.37	97.5	97.34	97.64
W1W2(3W3)(3W4)	95.1	94.86	95.37	97.5	97.31	97.68
(3W2)(3W3)(2W4)	94.6	94.19	94.88	97.2	97.14	97.34
(3W2)(3W3)(3W4)	94.8	94.63	94.88	97.4	97.35	97.53
(2W2)(3W3)(3W4)	94.9	94.84	95.01	97.5	97.44	97.59
N = 9						
(3W1)(3W2)(3W3)	93.7	93.70	93.70	96.55	96.55	96.55
(3W1)(3W2)(2W3)W4	94.3	94.12	94.67	97.0	96.83	97.20
(3W1)(3W2)W3(2W4)	94.7	93.89	95.09	97.2	96.72	97.40
(3W1)(3W2)(3W4)	95.03	95.03	95.03	97.34	97.34	97.34
(3W1)(2W2)(3W3)W4	94.6	94.44	94.84	97.1	96.92	97.31
(3W1)(2W2)(2W3)(2W4)	94.5	93.96	95.33	97.3	97.05	97.52
(3W1)(2W2)W3(3W4)	95.1	94.71	95.29	97.5	97.29	97.62

TABLE IV. CONTINUATION

WGC	(A) P_c Avg	(A) P_c Min	(A) P_c Max	(B) P_c Avg	(B) P_c Min	(B) P_c Max
(3W1)W2(3W3)(2W4)	95.1	94.65	95.39	97.4	97.16	97.58
(3W1)W2(2W3)(3W4)	95.2	94.84	95.39	97.5	97.37	97.65
(3W1)(3W3)(3W4)	95.37	95.37	95.37	97.52	97.52	97.52
(2W1)(3W2)(3W3)W4	94.7	94.51	94.97	97.1	97.05	97.28
(2W1)(3W2)(2W3)(2W4)	95.0	94.40	95.43	97.4	97.14	97.53
(2W1)(3W2)(3W4)	95.2	95.09	95.37	97.5	97.35	97.64
(2W1)(2W3)(3W3)(2W4)	95.2	94.67	95.62	97.5	97.29	97.61
(2W1)(2W2)(2W3)(3W4)	95.3	94.78	95.62	97.6	97.46	97.70
(2W1)W2(3W3)(3W4)	95.4	95.37	95.60	97.6	97.43	97.74
W1(3W2)(3W3)(2W4)	95.2	94.67	95.60	97.5	97.38	97.56
W1(3W2)(2W3)(3W4)	95.4	95.07	95.58	97.6	97.50	97.71
W1(2W2)(3W3)(3W4)	95.5	95.28	95.67	97.7	97.59	97.76
(3W2)(3W3)(3W4)	95.22	95.22	95.22	97.64	97.64	97.64
N = 10						
(3W1)(3W2)(3W3)W4	95.0	94.84	95.10	97.3	97.19	97.35
(3W1)(3W2)(2W3)(2W4)	95.2	94.72	95.52	97.5	97.28	97.59
(3W1)(3W2)W3(3W4)	95.45	95.41	95.47	97.6	97.46	97.68
(3W1)(2W2)(3W3)(2W4)	95.4	94.95	95.71	97.5	97.43	97.67
(3W1)(2W2)(2W3)(3W4)	95.5	95.14	95.69	97.7	97.56	97.76
(3W1)W2(3W3)(3W4)	95.66	95.64	95.67	97.7	97.59	97.79
(2W1)(3W2)(3W3)(2W4)	95.5	95.05	95.82	97.6	97.52	97.65
(2W1)(3W2)(2W3)(3W4)	95.6	95.45	95.82	97.7	97.62	97.76
(2W1)(2W2)(3W3)(3W4)	95.7	95.60	95.88	97.8	97.68	97.82
W1(3W2)(3W3)(3W4)	95.7	95.58	95.85	97.8	97.74	97.82
N = 11						
(3W1)(3W2)(3W3)(2W4)	95.6	95.33	95.87	97.6	97.59	97.70
(3W1)(3W2)(2W3)(3W4)	95.8	95.73	95.85	97.7	97.68	97.80
(3W1)(2W2)(3W3)(3W4)	95.9	95.83	95.98	97.82	97.76	97.85
(2W1)(3W2)(3W3)(3W4)	96.0	95.88	96.02	97.80	97.80	97.83
N = 12						
(3W1)(3W2)(3W3)(3W4)	96.15	96.15	96.15	97.88	97.88	97.88

Note: (A) and (B) denote the data of July and August respectively. P_c Avg, P_c Min, and P_c Max denote the average, minimum and maximum values of the probability of correct classification respectively. W1 W2 W3 W4 denotes all channel combinations constituting this combination of wavelength groups in the subset of four channels. For example: 1 4 7 10, 2 5 8 11, 3 6 9 12 etc.
WGC = denotes wavelength group combination in N channels.

THIS PAGE

WAS INTENTIONALLY

LEFT BLANK

THE USE OF LANDSAT IMAGERY FOR MARINE POLLUTION STUDIES

Dr. Chong Yean Joo

University of Singapore
Republic of Singapore

SUMMARY

A Landsat scene of the southermost tip of the Asian mainland covers not only a very busy international waterway, the Straits of Singapore/Malacca, connecting the Pacific Ocean with the Indian Ocean, but also land areas of three countries where intense developments are being carried out.

These developments include the reclamation of land from the sea, the clearing away of primary forests, the creation of new population centers, the building of industrial complexes, the damming of rivers to provide new water reservoirs, the construction of land, sea, and air transportation facilities and the establishment of recreational areas both on land and in the sea.

The benefits to be derived from such developments are immense. The related impact on the environment of man's activities on such a huge scale is also being closely watched in order to ensure that these benefits are not obtained at the high cost of undesirable environmental pollution.

Remote sensing can play a useful role in supplementing the numerous ground level environmental studies. This presentation concerns the use of Landsat data to:

(a) obtain a precision image data base upon which overlays may be made to study the changes taking place;

(b) provide a synoptic view of the region indicating how developments in one area can possibly influence marine pollution in the coastal zones of another area.

To construct an image data base, accurate matching of pixel coordinates in Landsat data with point coordinates on a map, are made with the aid of suitable control points. These control points would have to be easily identifiable in Landsat data. Various types of control points are shown as they appear against their surrounding background in computer line prints in the various bands, side-by-side with low altitude photographs. The suitability of using these control points in the thermal infrared band is also indicated.

A regional view of large scale current and circulation patterns is shown in Skylab and Landsat imagery. The high incidence of cloud cover in this humid tropical region, limits present studies to only those involving long term changes, such as for example the siltation of the sea bottom in the Straits of Singapore/Malacca.

Siltation is accelerated by the clearing of forested areas leading to increased erosion of soil. During the heavy rains of the monsoon seasons, large quantities of soil are washed into the rivers from where they are carried into the sea. The siltation of the sea bottom could lead to changes in the existing stable hydrological regimes. When used in conjunction with data from a recently completed four-nation joint hydrographic survey, Landsat imagery provides base-line data for detecting changes, that could affect shipping routes in this important busy Straits.

Using the suspended particles as a natural tracer, Landsat imagery provides a synoptic view of the dispersal of pollutants discharged by the rivers into the sea. This is useful in studying what effect a particular land development has on specific recreational areas along the coast and on islands in the sea.

In the clear shallow waters, where depths are known, attenuation coefficients and bottom reflection characteristics are compiled for bands 4 and 5 using both the single channel and the ratio methods. The bottom reflection characteristics are compiled for sand, flourishing corals and dead corals, with a view to distinguishing life and dead corals in Landsat data.

In water discharged by rivers into the sea Landsat data is used to obtain relative density contours of suspended matter. Statistics of radiance levels in the various bands are also compiled for identifying the nature of the pollutants in the water particularly those discharged from palm oil and rubber processing factories.

REMOTE SENSING FOR NUCLEAR POWER PLANT SITING, BATAAN PENINSULA, REPUBLIC OF THE PHILIPPINES

Barry S. Siegal, Frederic G. Snider, and N.R. Tilford

Ebasco Services, Incorporated
2211 West Meadowview Road
Greensboro, North Carolina 27407

ABSTRACT

The siting of the first nuclear power plant in the Republic of the Philippines entailed an extensive remote sensing study to help evaluate tectonics, volcanism, and the structural setting of potential site regions. Over 10,000 square km of Side-Looking Airborne Radar was obtained, covering Mt. Pinatubo south to the Taal-Banahao volcanic area and from the west coast of Luzon east to Laguna de Bay; these data were analyzed concurrently with Landsat imagery, thermal IR imagery, and black and white and color aerial photography. Analysis included photographic processing, color additive viewing, Ronchi rulings and stereoscopic viewing, where applicable. Results of the remote sensing study, in conjunction with seismological and field and laboratory analyses, provided an effective method of identifying and evaluating potential sites. Initial phases of the remote sensing study revealed that several of the proposed site regions were unsuitable because of fracturing, gravity movements, or volcanic hazards. SLAR imagery proved invaluable throughout the study in guiding field activities, unraveling structural settings and volcanic stratigraphy. As a result of the siting investigation, Napot Point was selected for the site of the first nuclear power plant in the Republic of the Philippines.

1. INTRODUCTION

The siting of a nuclear power plant requires proper attention to many technical, licensing, and socio-economic factors. Questions concerning public safety, environmental impact, costs, site development requirements, and proximity to load demand must be considered to determine site suitability. Geological and seismological considerations must include those factors necessary to provide reasonable assurance that the nuclear power plant can be constructed and operated at the site without undue risk. Information on earthquakes, quantitative vibratory ground motion, faulting, volcanism, ground water conditions, foundation characteristics, and other engineering related items must be determined as early as possible in the site evaluation study.

Siting investigations for nuclear power plants therefore require a multidisciplinary, phased program to evaluate in a focusing manner regions favorable for site development, with the ultimate selection of several candidate areas for site confirmation studies. Site selection studies are more difficult whenever information is scarce or nonexistent and the geologic setting is complex. In such instances, remote sensing techniques employing electromagnetic radiation in the visible, infrared, and microwave wavelength regions can provide a cost-effective

and time-efficient means of identifying regional geological features such as fault systems, which may rule out particular locations for futher study. In more detailed regional assessments and site confirmation studies, remote sensing techniques may also provide basic information on structure, stratigraphy, geomorphology, and ground water and may help guide field operations, providing data on access routes, topography, outcrop location, and ground cover. Siting of the first nuclear power plant in the Republic of the Philippines provided a unique opportunity to use remote sensing techniques in a geologically complex region which had been little studied.

2. REMOTE SENSING PROGRAM AND OBJECTIVES

Remote sensing studies in the Republic of the Philippines began in 1974 as part of an overall site evaluation study of the Bataan Peninsula.(Philippine PNAR, 1977). The site evaluation study was the culmination of various investigations undertaken since the 1960's by the National Power Corporation, the International Atomic Energy Agency, and the Philippine Atomic Energy Commission. During the remote sensing studies (1974-1978), extensive field and laboratory investigations augmented interpretation of imagery and permitted re-evaluation of earlier interpretations. The remote sensing investigations took account of the unique nature of the terrain (seismologically and volcanologically active), heavy vegetation cover, inaccessibility, and minimum existing geologic information to provide a regional assessment and to help identify potential sites for further study. The study was integrated with and provided baseline data for field investigations, seismology and geochemical studies, environmental assessments, and offshore geophysical programs. As conceived, the specific objectives of the remote sensing study included the following:

1) Identifying linear features which could be the surface expressions, of faults or fractures.

2) Locating volcanic centers.

3) Determining stratigraphy and relative geochronology between the volcanic and tectonic events within Zambales-Bataan volcanic highlands.

4) Locating coastal and near-shore hot springs and delineating zones of offshore suspended sediment concentration and movement.

Information from the remote sensing study, together with that from other ongoing studies, was to be used to select potential sites, and to prepare the required Safety Analysis Reports for licensing.

The first task of the remote sensing study included the planning and execution of a flight mission to obtain Side-Looking Airborne Radar (SLAR), color aerial photography, and thermal infrared photography for selected portions of the Bataan Peninsula. The imagery was used to supplement existing aerial photography and Landsat MSS images.

SLAR imagery using the Motorola APS/AN-94D (X-band) real-aperture system was obtained for 10,000 square km extending from Mt. Pinatubo south to the Taal-Banahao volcanic area and from the west coast of Luzon east to Laguna de Bay (Figures 1 and 2). Flight lines were north-south with a two-look direction. Contact prints were prepared from the 1:250,000 acquisition scale, enlarged to 1:100,000 scale for more detailed study. The nominal scale of the imagery was small enough to denote regional features, yet large enough to highlight terrain relief features in relation to site-specific details. Ground resolution was approximately 20 m. Linear features such as fish pond dikes as little as one meter wide can be identified.

Color and black and white aerial photography was flown at a scale of 1:8000 for the Bataan Peninsula coastline from Eman Point south to Caybobo Point. Black and white aerial photography at scales of 1:8000 and 1:15000 was also obtained within a 10-km radius of Bagac; it was used to supplement existing 1:15000 scale black and white aerial photographs of the entire Bataan Peninsula and 1:20000 photography for the Mapalan Point region.

A predawn mission was also flown to acquire thermal infrared imagery for the entire coastline of the Bataan Peninsula. A Daedalus 60 thermal infrared line-scanner, 0.5 milliradian spot size, 0.1°C temperature sensitivity, was used. The volcanic highland area was not flown because of the dense vegetation cover and extreme topographic relief. Natural variations in geologic properties or topography can easily overwhelm geothermal fluxes of several hundred heat flow units in all but the flattest, most homogeneous terrains (Watson, 1975).

Relatively cloud-free Landsat imagery was available for the study region and was analyzed with the other imagery by various image enhancement and interpretative techniques. Analysis of the imagery was performed primarily by unaided visual examination, stereoscopic techniques, or light table projection. In the examination, images were viewed from several directions to help insure recognition of significant, but subtle, linear features and to minimize interpretive errors from spurious alignments. Measures were also undertaken to minimize operator bias (Siegal, 1977).

3. RESULTS

3.1 REGIONAL EVALUATIONS

The first phase of the remote sensing study was directed at evaluating three potential site regions, Zambales, Bagac, and Southern Bataan (Figure 3), as to their suitability for nuclear power plant development. The studies were undertaken concurrently with seismological and field mapping investigations and were directed at identifying faults, landslide scars, areas of recent volcanism, and physiographic features which could channel volcanic material toward potential sites in the event of future volcanism.

Analysis of SLAR (Figure 4) and Landsat images (Figure 5) revealed distinct, pervasive fracturing in the Zambales region. These fractures occur in a suite of mafic-ultramafic rocks that are considered obducted sea floor. Available information suggested that major faults are common, the closest forming the boundaries of the east-west trending San Antonio Graben. The Graben is seismically active and its southern margin is 18 km north-northwest of the site area. An active offshore feature related to subduction along the Manila Trench, the West Luzon Trough, also occurs only 15 km from the Southern Zambales Peninsula. These factors eliminated the Zambales region from further consideration.

The Southern Bataan region was found to be situated on a broad, gently sloping fan of volcanic material originating near the summit of Mt. Mariveles. The location of a site on this broad plain would make it especially susceptible to potential damage from even small volcanic events. No structural features in this region could be found on the imagery or in the field; however, microseismic activity was noted nearby. Magnetic maps of the area showed a possible structural feature directly offshore San Jose Point, which was considered the source of the microearthquake activity. These factors eliminated the Southern Bataan region as a potential site area.

The Bagac region was found to be underlain by a thick sequence of pyroclastic rocks related to the Mt. Natib and Mt. Mariveles volcanic cones. Coarse volcanic breccia is the dominant lithology, although tuffaceous rocks and volcaniclastic sedimentary units are preserved in some areas. Extensive outcrops along the South China Sea coast were examined. No evidence of faulting was discovered on the images or in the field. No historical earthquake epicenters are located in the

region, and the imagery suggested that several parts of the region provide excellent protection from volcanic hazards. The advantages of the Bagac region over the Zambales and Southern Bataan regions suggested it should be considered the candidate site area. Six specific sites within this region were therefore selected for detailed analysis: Napot Point, Mapalan Point, Bagac I and II, Saysain Point, and Caybobo Point, as shown in Figure 1. Caybobo Point was eliminated early in the investigation due to the lack of natural protection from volcanic activity and its nearness to a possible parasitic vent noticed on SLAR images. The Mapalan Point site was eliminated because it displayed morphological characteristics suggesting it was part of a large slide block that rotated and slid 1-2 km down slope of Mt. Natib. Although the natural topography of the area provides excellent protection from volcanic hazards, existence of a possible glide plane beneath the point ended consideration of Mapalan Point as the primary site. Saysain Point was eliminated because of a lack of natural protection from volcanic events and a deep weathering profile. Both Bagac sites were eliminated because of susceptibility to river and tsunami flooding, liquefaction, and anticipated construction dewatering problems. The Napot Point site, however, afforded a high degree of natural protection against volcanic events, no threat of flooding or tsunami damage, and excellent foundation stability; it was therefore chosen as the preliminary site.

3.2 SITE CONFIRMATION STUDIES

Choice of a primary site ended the first phase of the siting studies. Further investigations were designed to evaluate thoroughly seismic and volcanic risks to the proposed plant and fulfill all nuclear licensing requirements. Remote sensing data were used extensively during this phase of the project, in both seismic and volcanic risk investigations. Techniques used and the results of some of these investigations are briefly described below.

Confirmation of Regional Structures

The first task of the site confirmation study was to denote regional structures on the images and determine their possible extent where unknown. Most of the known faults can be distinguished on the images. The Philippine Fault and the Marikina Graben (see Figures 6 and 7) and their related structures, for example, are distinct on Landsat images by topographic and tonal expression. The Philippine Fault is defined by abruptness of the southern boundary of the Caraballo and Cordillera Mountains although the northernmost extension of the fault can only be inferred due to a lack of surface expression. Faulting in the Central Valley is also apparent on Landsat images. The 90-km long, northwest-trending fault at the boundary of the Zambales Mountains and the Central Valley is relatively distinct by tonal expression near Lingayen Gulf and by topography at the base of the Zambales Mountains, but it cannot be traced south of Mt. Pinatubo. The fault appears to be covered by Pliocene-Quaternary pyroclastic deposits from Mt. Pinatubo.

The San Antonio Graben is clear on both SLAR and Landsat images (Figures 4 and 5). On Landsat images, the distinction results primarily from a tonal change due to difference in spectral reflectance between the ultramafic rocks of the Zambales Mountains and the surficial covering of Holocene sediments within the graben. The northern boundary of the graben is very apparent topographically and is outlined in part by the path of the Santo Tomas River. The southern boundary of the graben is distinct on the imagery by tone and topography.

Topographic change across the graben is especially distinct on SLAR images. Variations in tonal expression of the graben and the adjacent region are due to an apparent difference in the surface roughness of the ultramafics of the Zambales Mountains and the Holocene sediments of the graben.

The San Antonio Graben, an active fracture zone and a potential Safe Shutdown Earthquake (SSE) feature is recorded on geologic maps extending west-northwest a distance of 20 km. Westward, geophysical and seismic data suggest the fault extends through the Luzon Trough. Eastward, seismic data suggests the fault extends toward the Central Valley. This interpretation is strengthened from analysis of SLAR images; several linear features appear to correspond with the southernmost fault and extend toward the Central Valley. Although the San Antonio Graben is mapped as two bounding faults, its appearance on imagery and field investigations suggests a series of step faults.

Faulting in the area of Laguna de Bay is also distinct. On Landsat images (Figure 7) faulting associated with Marikina Graben is clear as far south as San Pedro. The trace of the fault is not distinct further south because of excessive cloud cover on the available imagery. On SLAR images (Figure 2), the fault can be traced toward Lake Taal.

Estimating Regional Structural Trends

Regional structural trends were delineated on SLAR and Landsat images by preparing frequency distribution plots to characterize the tectonic trends within the major physiographic provinces[1]. The dominant fracture patterns of the study area occur primarily in three concentrations, northwest, northeast, north-south. Sets of northwest-trending fractures show up well in Batangas on Landsat and SLAR images where they interconnect a linear chain of volcanoes. In the Bataan volcanic chain the fractures are not as distinct, because the volcanoes are larger and have extensive sheets of less eroded pyroclastic deposits.

The northwest system appears to have played a major role in the process of magma emplacement. Northeast fractures trend at right angles to the volcanic belt and appear to concentrate in areas with volcanic cones. It seems highly probable, therefore, that the volcanoes developed at the intersection of major northwest and northeast fracture swarms. The third set of north-south fractures appears unrelated to the volcanic belt. They also occur in distinct swarms, causing major longitudinal depressions. The westernmost swarm delineates the eastern border of the southern Zambales Range and may be partially responsible for the formation of Subic Bay. A second swarm occurs in Batangas; a third follows the shore east of Manila and crosses Taal. In each of these three areas the principal faults dip east and form the western borders of grabens. Their origin is probably related to that of the Central Valley.

Cross-cutting fractures are evident in a number of places. The tectonic chronology, however, cannot always be determined, because fracturing appears to have been more or less synchronous. East of Taal, however, the north-south faults appear to be younger than some northeast and northwest sets. Horizontal offsets are mostly apparent and appear due to vertical motion. It is possible, therefore, that fractures originating by strike slip were rejuvenated by vertical movements during the major phase of regional uplift accompanying volcanism.

As seen on the images, the west flank of Balakibok is thoroughly fractured by northeast and northwest-trending faults. The northwest set is also quite conspicuous in the Zambales Mountains; here these faults cut and offset north-northwest and north-northeast trending sets. The structure of the ultramafics, therefore, appears to be characterized by an older north-northwest, north-northeast conjugate fracture system and the tectonic framework of the Bataan volcanic belt to be dominated by the younger northwest-northeast system. Tectonic relationships can be found for other regions in the study area. In general, field observations support the above remarks and suggest a correlation between age of material and fracture orientation.

1 In the analysis, consideration was given to the preferrential enhancement of linear elements by each of the data acquisition systems, and measures were taken to minimize misidentification of linear features due to spurious trends of diverse ground features, artifacts resulting from illumination conditions, instrument response, and operator subjectivity.

Volcanic Stratigraphy

The probability of volcanic eruption and its possible effects on the site area was one of the major factors addressed in the site confirmation studies. Remote sensing studies assisted field and laboratory investigations in determining the relative ages of volcanic deposits, in the search for the youngest volcanic units, and as a guide to subsequent field mapping and sampling. These data were supplemented by an extensive program of sampling for geochemical, radiometric, and paleomagnetic analysis. The major volcanoes nearest the site were primary concerns. These peaks are, north to south: Mt. Pinatubo, Mt. Balakibok, the Mt. Natib volcanic complex, and Mt. Mariveles, peaks consisting primarily of coarse pyroclastic deposits. Lava flows are typically thick but not areally extensive, and are limited to the summit areas of the volcanoes. A few intrusive bodies, visible on the imagery as isolated rounded hills, are exposed on the flanks of several peaks. Lahars are exposed in many of the major radial stream valleys, and appear on the imagery as smooth, gently sloping units. Some of the clearly visible characteristics of the nearby volcanoes are described briefly below.

Mt. Pinatubo

Interpretation of the imagery suggests that the western side and small parts of the northern and eastern sides of Mt. Pinatubo comprises several distinct ignimbrite deposits. Surface roughness and degree of incision suggested these deposits are relatively young; later radiometric dating of carbonized wood within them yielded ages as young as 600 years. The ignimbrite material appears to have originated from one or more point sources near the peak of Mt. Pinatubo. The northern, eastern and southern flanks of Mt. Pinatubo consist mainly of volcanic deposits, highly dissected by stream incision and apparently the oldest exposed materials on Mt. Pinatubo. The eastern area is probably the oldest. The upslope pointing "V" shape of the topography is typical of the oldest deposits in the region.

Mt. Balakibok

The east flank of Mt. Balakibok differs from the west flank on both SLAR and Landsat imagery. The east flank has "minimum" topograpic relief and less surface roughness. It is composed of younger pyroclastic material with grass cover. There is some indication on SLAR imagery of fossil landslides with eastward movement. Numerous circular topograpic peaks are evident, suggesting many small volcanic centers.

Mt. Natib

The physiographic boundary between Mt. Balakibok and Mt. Natib is accentuated on imagery by east-west trending stream channels, controlled primarily by topography. Distinct northeast and northwest fracture systems transgress Mt. Natib, which nevertheless, has a well developed radial drainage pattern. Measurements of joints in exposed pyroclastic rocks indicate that this fracture set is dominant in the older volcanic units. No offsets were observed or discovered on the imagery or in the field. The fracture system does not appear in the younger volcanic sequences on Mt. Natib.

The surface material comprising the eastern flank of Mt. Natib has "smooth" surface roughness and is relatively homogeneous in character, as suggested by its light and uniform tone on SLAR imagery. A small crater, approximately 3 km in diameter immediately adjacent to and east of the major caldera of Mt. Natib, delineates the westernmost extent of the material. This crater is considered the source of the lobate deposit of pyroclastic material. Lateral extent of the pyroclastic blanket could not initially be determined because of similar reflectance of the other surficial materials (soils and sedimentary deposits) on the lower flanks. Later field examination showed this lobate deposit to be sequence of thin, (1-5 m) pumice-bearing, weakly consolidated, pyroclastic flows. The

imagery suggest that there are actually two overlapping sequences in the same area, representing two episodes of volcanic activity. Slight differences in surface texture suggested an age relationship later verified in the field. Paleomagnetic dating of pumice clasts suggest an age of less than 100,000 years for the younger sequence.

Mt. Mariveles

Mt. Mariveles is a morphologically young volcano with a well developed radial drainage pattern. Mt. Limay, a smaller peak on the eastern flank of Mt. Mariveles, appears to be morphologically younger than Mt. Mariveles. Mt. Samat, a small parasitic cone on the northeastern flank, also appears younger than the main cone. A southeast-extending fan-shaped feature occurs on the southern flank of Mt. Mariveles. Expression of this area on the imagery suggests the feature is the youngest volcanic material on Mt. Mariveles. Mariveles Harbor, at the extreme southern tip of the Bataan Peninsula, is a partially drowned and buried volcanic center; the harbor itself is the drowned central crater area. The northern part of this volcanic cone is buried by younger deposits from Mt. Mariveles.

Assessment of Volcanic Risk

The assessment of volcanic risk to a site on the Bataan Peninsula was approached in several ways. The temporal distribution of volcanic activity near the site was determined by two different stochastic time-series analyses developed by Stepp (1972) and Wickman (1966). A total of 52 samples of lava flows and intrusive bodies were dated radiometrically; ages ranged from 4.1 to 0.19 million years. The time series analyses suggested that during the period between 2.2 and 0.5 million years ago, the maximum rate of volcanic activity was about 120 significant events per million years. During the last 500,000 years the rate has slowed remarkably; only two samples of lava flows are in this age range.

The distribution and extent of young pyroclastic deposits observed on the imagery provided invaluable data as to the type of volcanic eruption characterizing the peaks in the area. In addition, the ages of the youngest pyroclastic deposits (600 years for Mt. Pinatubo, perhaps 100,000 for Mt. Natib) are significantly younger than the youngest sampled lava flows (0.19 my). Without guidance from the imagery, the sampling of the youngest volcanic deposits could not have been assured.

4. CULMINATION OF INVESTIGATION

Remote sensing studies and field and laboratory investigations culminated in selection of a site for the first nuclear power plant in the Republic of the Philippines, which fulfilled all applicable nuclear licensing requirements, with recommendation of specific design criteria for the plant.

Determination of the magnitude and possible generators of the Safe Shutdown Earthquake was based on historical seismic data and the length of major structural features as determined on the imagery. A conservative estimate of the maximum possible acceleration at the site was made using the results of the seismic studies and the attenuation characteristics of the site.

Evaluation of the data obtained from intensive study of the volcanoes near the site indicated that volcanic ash fall is the only credible volcanic hazard. The site location and the topographic characteristics of the area would protect it from other likely hazards. Investigations in Luzon and compilations of worldwide data led to determination of a design basis ash-fall and its probability of occurrence. The mathematical techniques used for evaluation of volcanic risk paralleled closely the techniques used in seismic analysis.

5. REFERENCES CITED

Preliminary Safety Analysis Report, Philippine Nuclear Power Plant Unit 1, 1977, Submitted by Ebasco Services, Inc. to National Power Corporation, Manila.

Siegal, B.S., 1977, Significance of operator variation and the angle of illumination in lineament analysis on synoptic images, Modern Geology, v. 6, p. 75-85.

Stepp, J.C., 1972, Analysis of completeness of the earthquake sample in the Puget Sound area and its effect on statistical estimates of earthquake hazard: Proceedings of the International Conference on Microzonation 2, 897-910. NTIS P.B. 219-383.

Watson, K., 1975, Geologic applications of thermal infrared images, Proc. IEEE, 63, 128-137.

Wickman, F.E., 1966, Repose-period patterns of volcanoes. Parts I-V, in Arkiv for Mineralogi och Geologi, v. 4, p. 291-367.

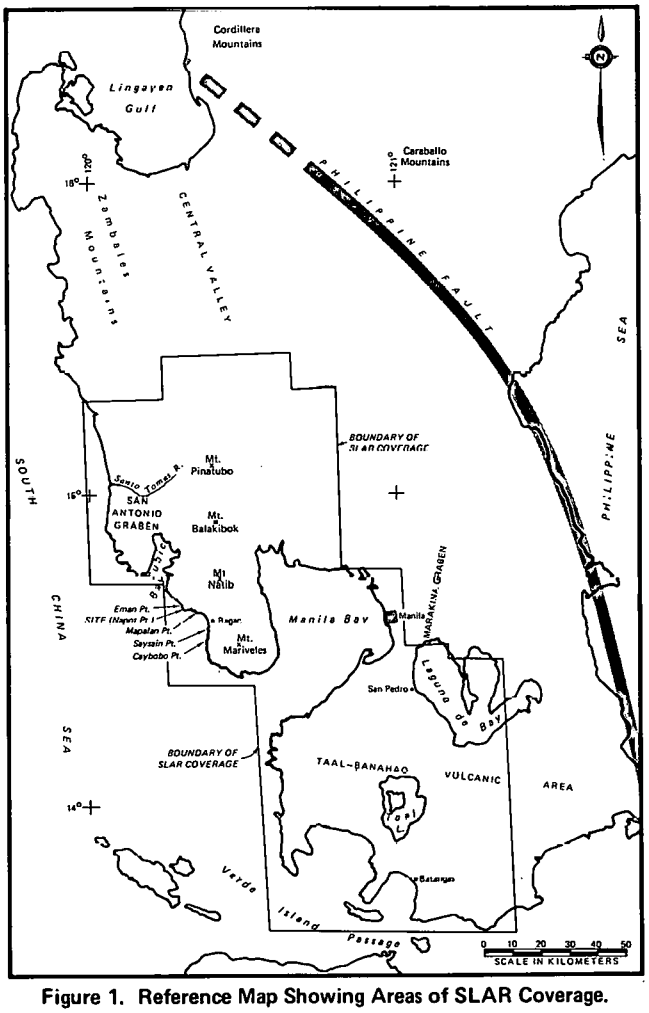

Figure 1. Reference Map Showing Areas of SLAR Coverage.

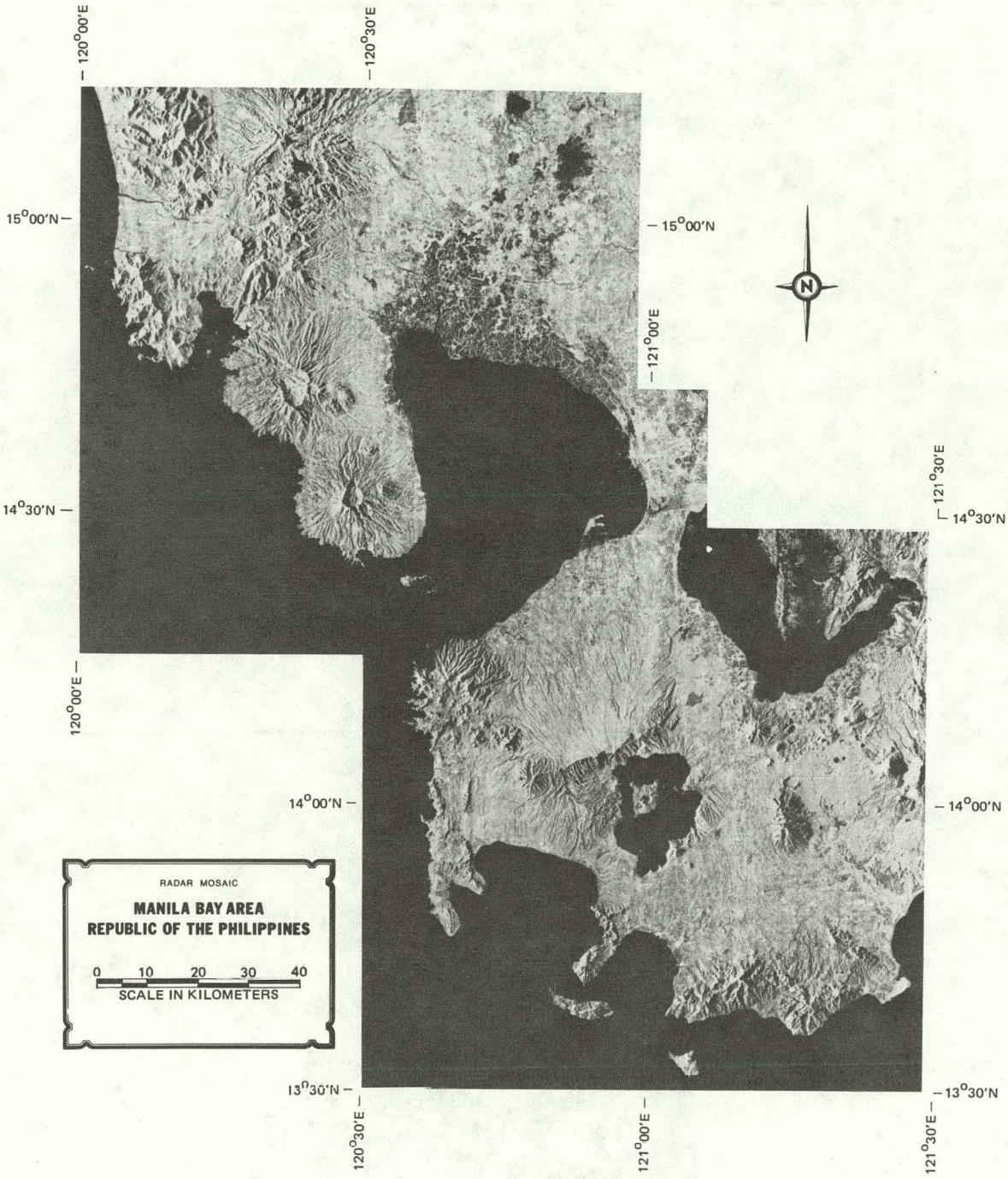

Figure 2. East-look SLAR Mosaic.

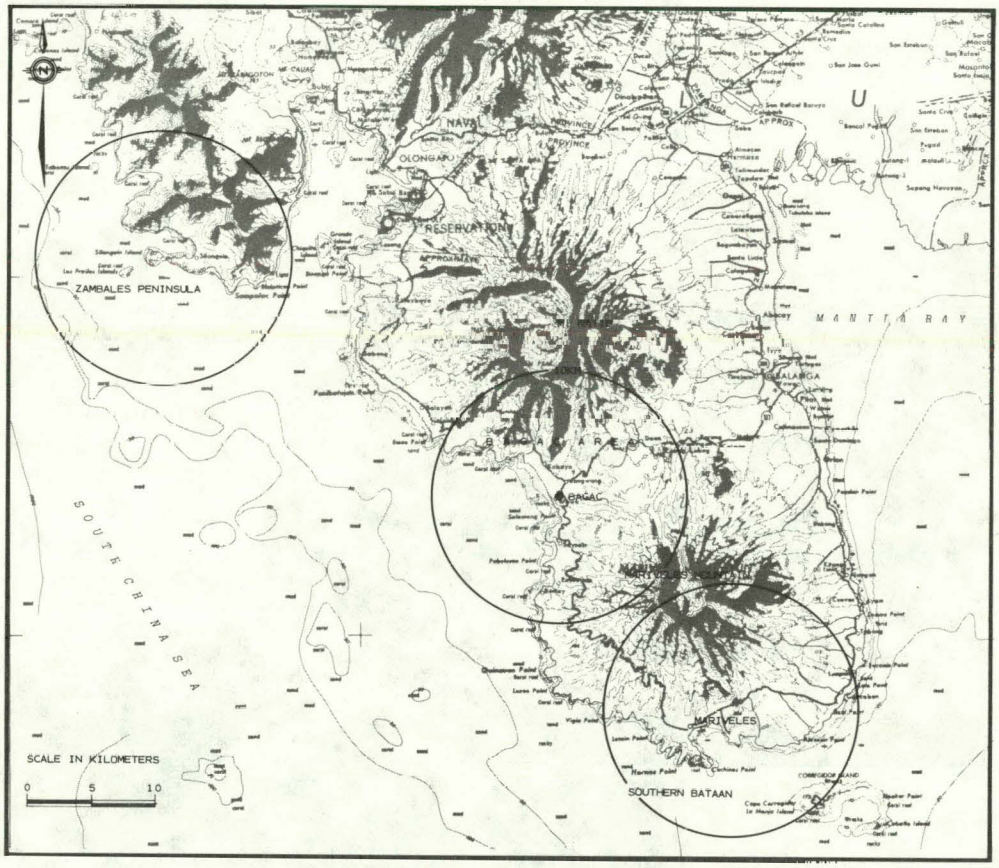

Figure 3. Potential Site Regions.

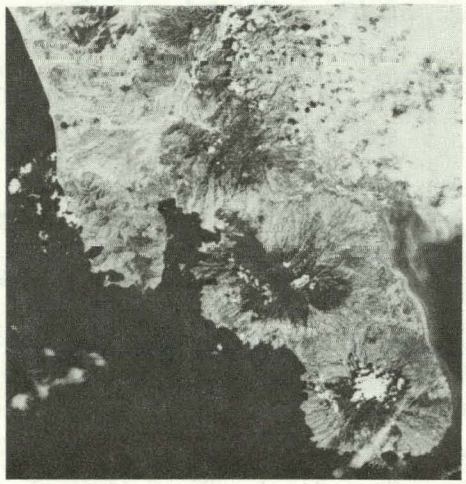

Figure 5. Landsat Image of Bataan Peninsula and Surrounding Area.

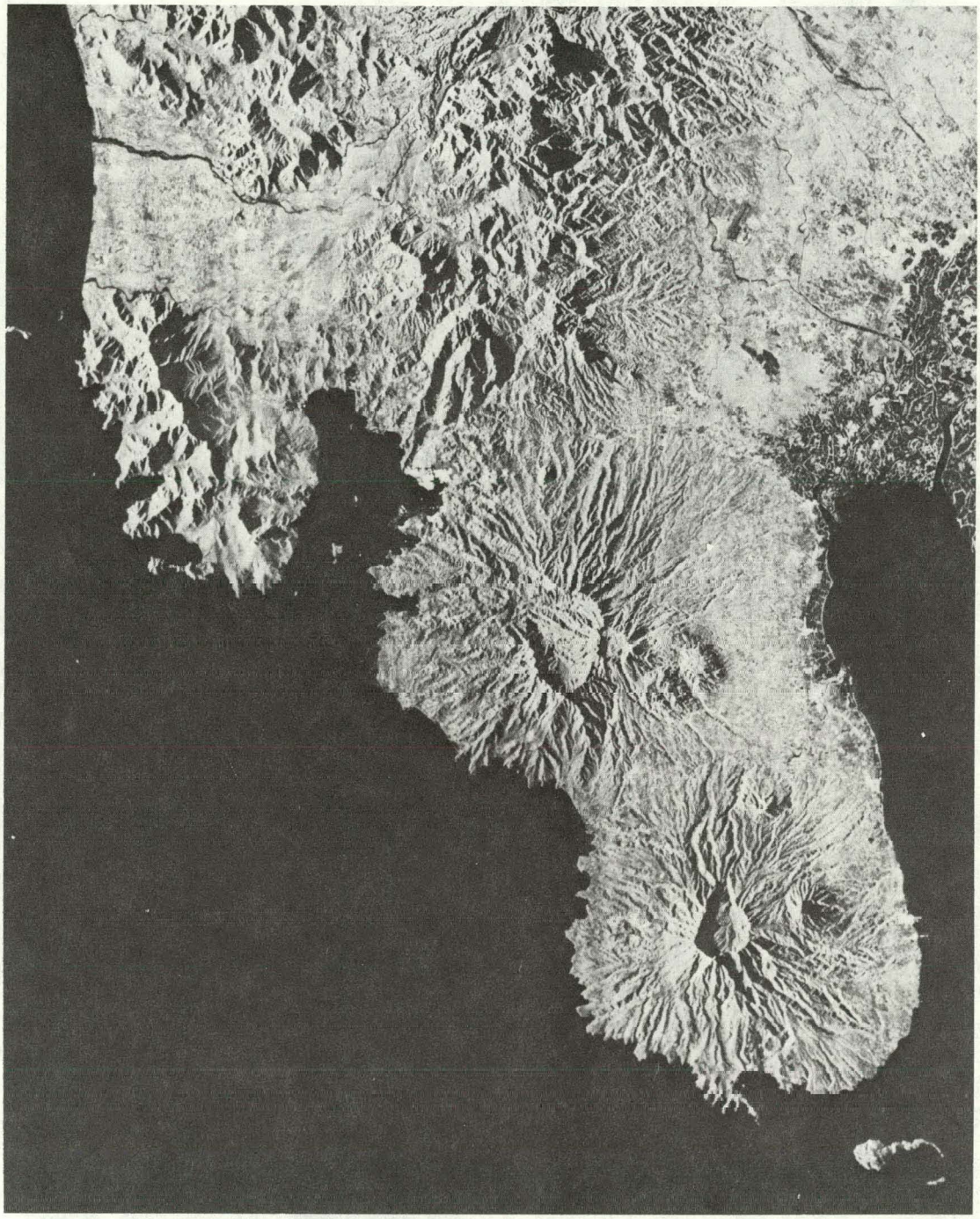

Figure 4. Enlargement of SLAR Image for Bataan Peninsula.

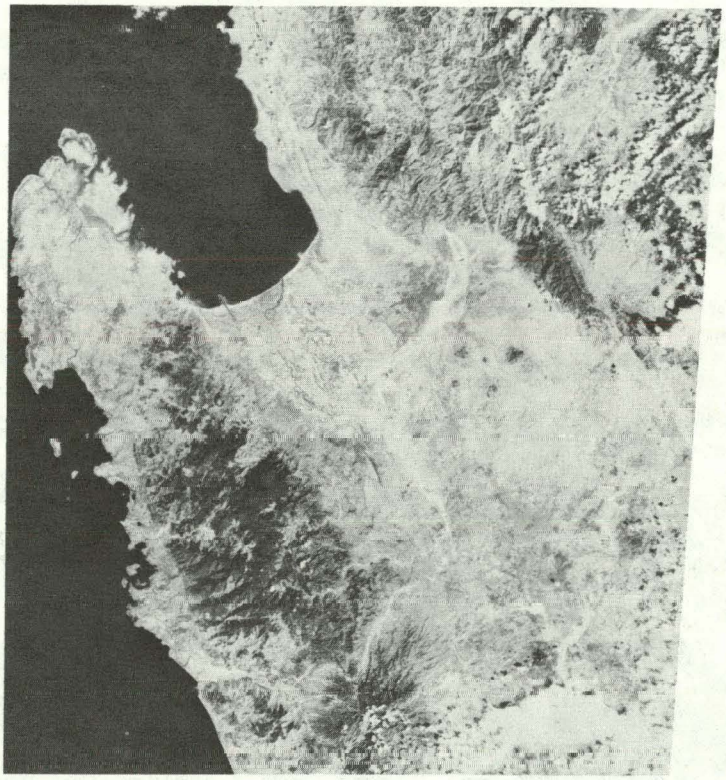

Figure 6. Landsat Image of the Northern Portion of the Central Valley.

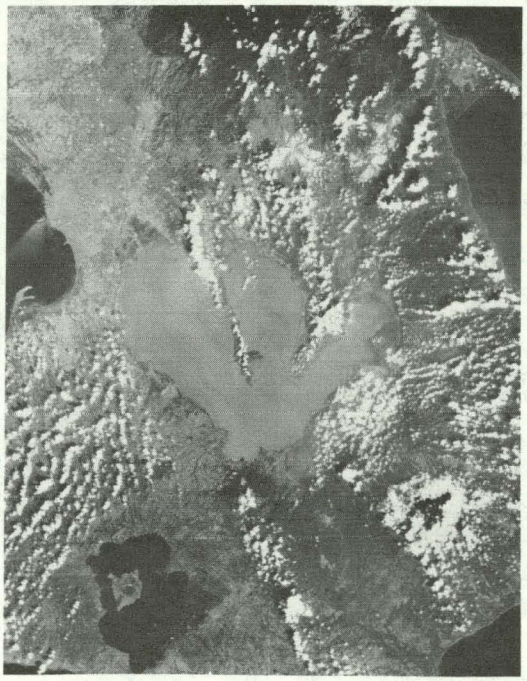

Figure 7. Landsat Image of the Laguna de Bay Region.

LANDSAT DIGITAL ENHANCEMENT TECHNIQUES FOR MINERAL EXPLORATION IN AUSTRALIA

A.A. Green, J.F. Huntington and G.P. Roberts

CSIRO Division of Mineral Physics
North Ryde, NSW, Australia

ABSTRACT

A Landsat image processing system is discussed. The system is based around a mini-computer with image display on an interactive TV system and a film recorder. Software has been developed to provide enhancement techniques including contrast modification, ratioing, spatial filtering, stereo pair production and multi-spectral classification.

The system has been used to produce computer enhanced images of approximately one third of Australia in a continuing effort to develop optimum enhancement techniques for each of Australia's major mining areas.

1. INTRODUCTION

When Landsat imagery first became available in Australia the initial response among the user community was unenthusiastic. To some extent this attitude was due to a natural conservative approach to this new form of data. However, it was also due in part to the very poor quality imagery which was available, typically from 5th and 6th generation masters. For this reason the CSIRO Division of Mineral Physics embarked on a program to produce optimum quality photographic products for photo-interpretation. This program has resulted in the development of a Landsat digital image processing facility for the production of enhanced imagery for many diverse research groups in Australia.

The aims of the project are twofold. The first is to optimize Landsat image restoration techniques within the constraints of acceptable execution times on a mini-computer and the needs of potential users. This involves improving the radiometric quality of the image as much as possible and implementing basic geometric corrections.

The second aim is to manipulate this "cleaned up" data by enhancement techniques selected for the problem at hand. The selection of enhancement over classification is deliberate. We feel the interpretation of classification results is made difficult by the absolute nature of the decision made by the computer. Geological photo-interpretation involves an inference about subsurface features from their surface expression. This inference is often made on the basis of very subtle criteria and usually needs as much textural and contextural information input as possible. The absolute nature of decisions made by most classification procedures can tend to obscure this other information.

With this thought in mind special emphasis has been given to the design of optimum enhancement procedures for each of the important metallogenic provinces of Australia.

2. HARDWARE

The hardware is based around a Hewlett-Packard 21MX mini-computer with 32K of memory running under the RTE-II operating system. There are 17.5Mbytes of

disc storage, two 1600 BPI magnetic tape drives and three interactive terminals.

Image display is via an Optronics Photowrite and an interactive colour TV system. The Photowrite takes 8" x 10" sheet film suitable for the production of approximately 1 : 1 000 000 scale images.

The TV system, which was designed and built in the division, has a 512 x 512 pixel display and can operate in a colour mode with 32 grey levels for each primary colour, or in monochrome with 256 grey levels. The TV monitor is refreshed from 16K bit CCD recirculating memories which can be written from the CPU. The computer can update individual pixels or whole scan lines in the display and has a graphics overlay channel which can be modified by a cursor and read back to the computer.

The image can be updated in either a scrolling or overwriting mode. Various sizes of software-generated ASCII characters for the graphics overlay channel are available with output at the current cursor position.

3. SOFTWARE

Particular care has been given to the development of software so as to minimize execution times while still retaining a modular system which can be easily modified. This has been done by using machine level coding for all operations on individual pixels, while control operations executing only once per scan line have been written in FORTRAN. Where memory constraints permit, look-up procedures are used instead of repeating calculations for each pixel.

The programs can be separated into a number of distinct classes according to their function. Execution times for the main classes are shown in Table I.

3.1 REFORMATTING

In order to produce whole scene products conveniently on the Photowrite (without access to large disc storage) it is necessary to reformat the normal NASA Landsat tapes so that the data blocks for each scan line are adjacent on the reformatted tape. In this process we label each block, record scene histograms in each band, compute the means and variances of each of the 24 detectors on the MSS and search for and replace bad data lines resulting from sensor drop out. The reformatted tape then becomes the working data source and the NASA original goes into an archive.

3.2 INPUT AND RADIOMETRIC CORRECTION

A standard input routine provides random access to any or all bands of any part of any scan line in the image. Each line is then radiometrically corrected for six-line striping and decompression noise.

The destriping correction is made by forcing each of the six detectors in each band to have the same mean and variance for the whole scene - in effect normalizing them to the same gain and offset.

The correction for decompression noise is made by recompressing the data in bands 4,5 and 6 using the standard NASA decompression tables (1) and the calibration data provided at the end of each data block. The data are then decompressed once more using a 6th order polynominal fitted through the NASA decompression tables.

These two corrections are implemented in conjunction with a linear contrast stretch to produce a range from 0 to 255. It is this stretch which enables the effective removal of the unwanted noise which had been introduced by the necessity of rounding to a six or seven bit number in the first place. Figure 1 shows the improvement in image quality obtained by removal of the decompression noise.

3.3 IMAGE DISPLAY

Output routines are available for the Photowrite and the TV system which

accept a scan line of data, format it for the appropriate device and output the line. Geometric corrections for aspect ratio and earth rotation are also provided in these routines by a nearest neighbour interpolation procedure.

The need for further in-line geometric corrections such as sensor offset, mirror velocity profile, or removal of synthetic pixels has been investigated. However, it was decided that the extra accuracy obtained in the resampling process is not worth the increased computer time involved. Geological applications depend mainly upon the location of areas of interest relative to other local features which can be identified in the scene. The availability of exact geographical coordinates is not of major concern for most current geological problems.

3.4 CONTRAST MODIFICATION

This routine allows the enhancement of single bands by linear contrast stretching, logarithmic and exponential stretching, histogram equalization and general procedures for histogram modification.

The linear contrast stretch is normally provided in the restoration phase outlined above. Logarithmic stretching uses the folmula

$$y=\mathrm{sgn}(x-x')A\log|(x-x')|$$

This produces a sigmoidal curve where the point of inflection is at x' and the severity of the stretch increases with the value of A (a normal logarithmic stretch is obtained when x'=0). This function is useful when we seek increased contrast in a small range of levels (centred at x') without completely destroying the information in other levels.

Exponential stretching is provided by the inverse of the above procedure.

The normal histogram equalization routines produce a flat output histogram, but the routine can produce any required shape for the output histogram.

The single most effective enhancement of images has been gained through the combination of the six-line striping correction and a standard linear contrast stretch. The logarithmic and exponential stretches were developed to deal with certain specific, but not uncommon, geological environments in Australia, partly those involving very wide tonal ranges in a single area of interest.

3.5 RATIOS

The current software allows ratio images of any two bands to be made. The resulting ratios can then be subject to the same contrast modification procedures outlined above. This additional step is performed on each line of ratio data as it is computed.

We have found that it is always necessary to perform a contrast stretch on ratio images and that histogram equalization is usually the most effective procedure.

3.6 SPATIAL FILTERING

Several forms of subtractive box filtering have been implemented. The basic form outlined in (2) is defined by

$$y=(1-f)(x-\bar{x})+fx+c$$

where f is the fraction of the original image retained, $\bar{x}$ is the local average brightness around the central point with value x and c is an additive constant to ensure a non-negative value for y.

We have also implemented functions defined by

$$y=(1-f)\mathrm{Log}(x-\bar{x})+fx+c$$

and

$$z=\exp(y)=\exp\{(1-f)(w-\bar{w})+fw+c\}$$

where w=log(x) and Log is the sigmoid shaped function above with a point of inflection at zero.

These operations can be carried out with box sizes up to 51 by 51 pixels using an efficient algorithm which retains a local running average line and does not recompute averages for each pixel.

Figure 2 shows an example of an image which has been processed with the second of the above three schemes.

3.7 STEREO PAIR PRODUCTION

A program is available for the production of synthetic stereo pairs of Landsat images when some form of z axis (height) information is provided. The general aim with this technique is to subdivide image information and represent it to an interpreter in the most interpretable form. Images have been written using the image brightness as the z component (Figure 3). These provide an interesting enhancement of textural patterns in the scene and aid the interpreter in relating discontinuously expressed features of varying brightness. Work is under way to produce stereo pairs with geophysical data, such as gravity or magnetics, as the z component.

3.8 CLASSIFICATION

The usefulness of classification procedures for geological problems is a difficult question. We have implemented an eight class parallelepiped classifier with output to three film positives which when combined as a colour composite produce a classification map.

In general, however, we have preferred to direct our major effort into enhancements which optimally display the information content of the raw data. We would prefer to have a photo-interpreter rather than a computer making decisions about the nature of the geology. Optimally, such decisions must use other characteristics (e.g. texture, shape, context, experience) as well as spectral response to differentiate or identify geological features. Also, normal classification procedures do not easily cope with mixed signatures of different proportions or spatially varying signatures. These are extremely common in geological interpretation, either due to changing ground cover or condition, or to "facies" changes in the rocks themselves.

However, classification procedures do have an ability to assess accurately the spectral similarity of terrain features. In seeking to display the results of this sort of processing to a photo-interpreter we have developed a procedure for writing images of the Mahalanobis distance D of any given pixel from the mean of some selected training area. Here D is defined by

$$D=(X-M)'S^{-1}(X-M)$$

Where X is the four dimensional vector defined by the four Landsat bands, M is the mean vector for the training area and S is the covariance matrix for the training set.

This image does not display yes/no decisions as to what some feature is, but provides a measure of how similar an unknown area is to some known area. The technique also tends to retain textural and contextural information better than a normal classified image. Figure 4 shows an example of this technique.

4. SYSTEM USAGE

The basic system as outlined above has been in operation for the past two years, during which time a considerable amount of routine enhancement has been performed. Some twenty mining companies and various state and federal survey organizations have cooperated in projects to analyse these data.

Approximately one third of Australia or some 150 scenes have been processed to enhanced imagery. It is planned to extend the coverage to the whole of Australia in the next two years. The results of this work are available to the public through three licenced commercial distributors with a small price increase over the normal copies available from NASA generated images.

The interactive TV system has not been in operation long enough to assess its full potential. However, it is already of very considerable benefit in determining optimum enhancement techniques. The long turnaround time enforced by the slow speed of the Photowrite, the nature of the photographic process and the need to use a colour additive viewer is reduced enormously.

Further, the scale of the display (1:80 000) matches that of the RC-9 aerial photography which is available for most of Australia. By using the TV display, the RC-9 photography, and high quality colour composites at a scale of 1:100 000, we hope to develop an interpretation facility which could usefully contribute in the early stages of a 1:100 000 scale mapping program.

While software development is continuing, the above techniques are being utilized in a research project to optimize digital processing techniques for each of the major Australian mining provinces. The terrain of interest varies from the arid Precambrian shield of Western Australia through tropical and sub-tropical areas in the Northern Territory to the temperate and semi-arid areas of the Lachlan Geosyncline. The differing climates, geological expression and cultural patterns in these areas all create different image processing problems, if we are to extract all the geological information that is in the Landsat data.

5. REFERENCES

(1) Soha, J.M., Gillespie, A.R., Abrams, M.J. and Madura, D.P. Paper presented at *CALTECH/JPL Conference on Image Processing Data Sources for Commercial and Scientific Applications*, Pasadena, 1976, pp. 4-1 - 4-9.

(2) Thomas, V.M. *Generation and Characteristics of the Landsat 1 and 2 MSS Computer Compatible Tapes.* Document Number X-563-75-2 Goddard Space Flight Center, November 1975, Appendix E.

TABLE I. TYPICAL EXECUTION TIMES FOR OUTPUT OF WHOLE LANDSAT SCENES TO THE PHOTOWRITE

Contrast modification	40 min
Ratio images	80 min
Spatial filtering	80 min
Stereo pair production	120 min

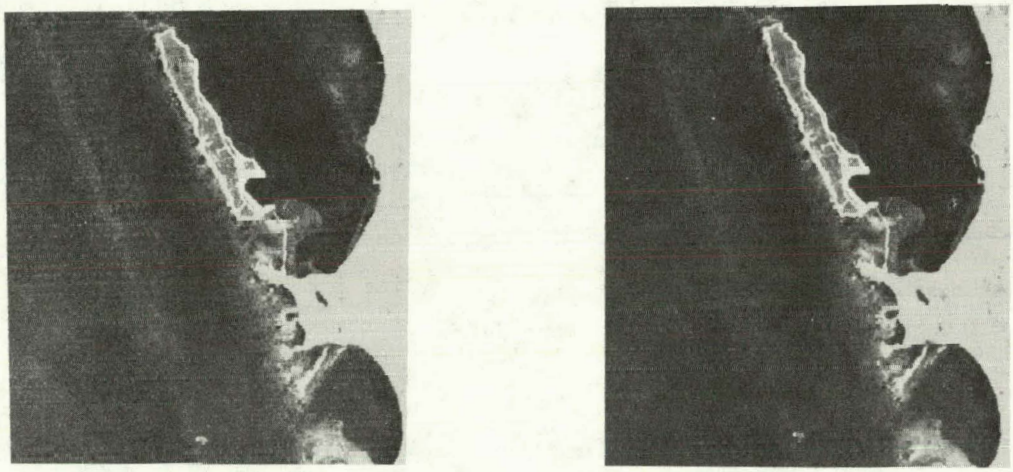

(a) (b)

FIGURE 1. CONTRAST STRETCHED IMAGES OF THE AREA OFFSHORE FROM PERTH, WESTERN AUSTRALIA. Both images have been corrected for sixth line striping effects. However the image with no decompression correction (a) has considerable in line noise, much of which is removed in the recompression/decompression processing (b).

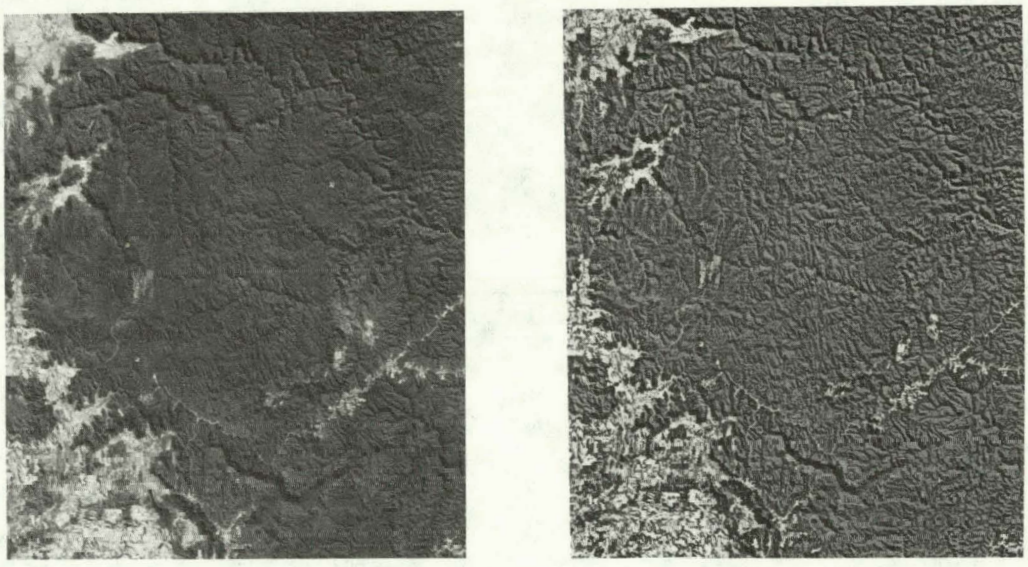

(a) (b)

FIGURE 2. AN AREA OF THE BLUE MOUNTAINS TO THE WEST OF SYDNEY, NSW WHERE DIFFICULTIES HAVE BEEN EXPERIENCED WITH ROOF FAILURE IN UNDERGROUND COAL MINES. This image in (b) has been processed with a subtractive box filter (box size 21 x 21) in order to enhance fracture patterns expressed in the topography. The normal image (a) is shown for comparison.

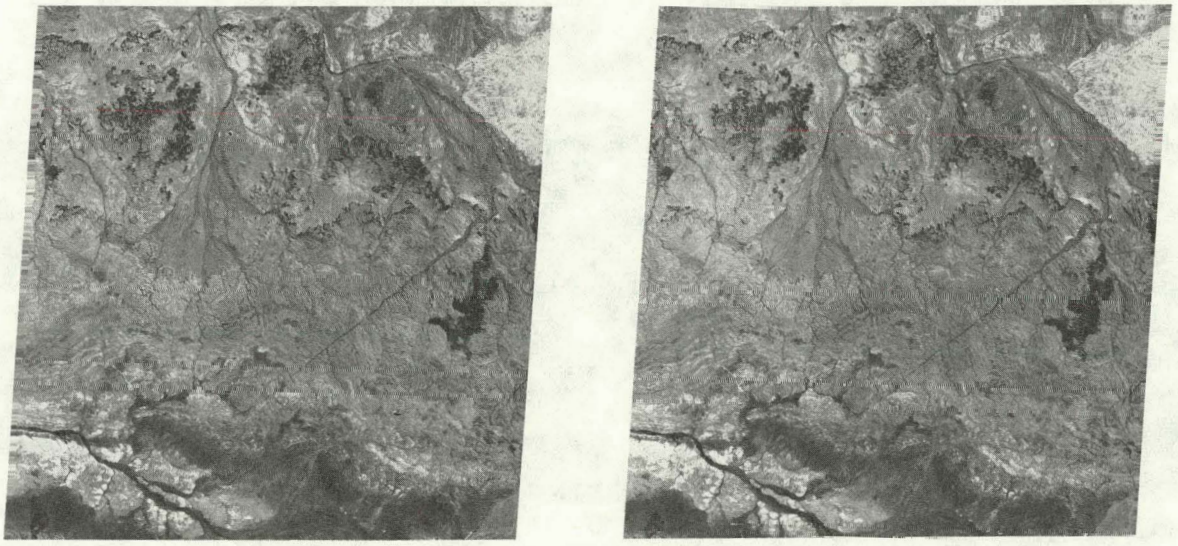

FIGURE 3. STEREO PAIR OF THE FORTESCUE AREA IN WESTERN AUSTRALIA. The brightness of each Landsat pixel has been used to compute a lateral shift for the pixel giving an apparent height proportional to the brightness.

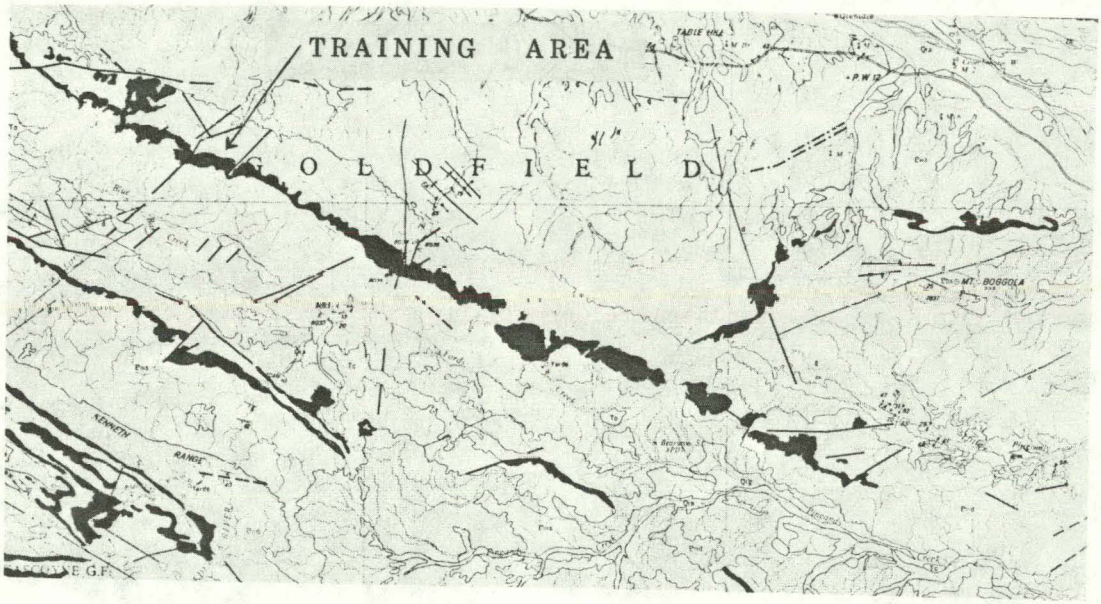

FIGURE 4. DISTANCE IMAGE OF THE ASHBURTON GOLDFIELD IN WESTERN AUSTRALIA. The training area (arrow) is a part of a series of outcropping dolerite sills. The darker the tone the more likely that area is to be similar to the training area. The dark areas on the corresponding map show the existing mapping of the dolerites in the region.

REMOTE SENSING AND INVENTORY OF MINERAL RESOURCES IN PART OF CHANDRAPUR DISTRICT, MAHARASHTRA, INDIA.

K. S. Misra
Centre of Studies in Resources Engineering,
Indian Institute of Technology, Bombay, India.

ABSTRACT

Remote sensing techniques have been found to be of immense help in highlighting certain interesting geological features, which have a direct bearing on the inventory of mineral resources in southern part of Chandrapur district of Maharashtra. The area comprises mainly four geological units, viz. Archaean unclassified crystallines, Precambrian metasedimentaries of Pakhal Group and younger sedimentaries belonging to Gondwana Super Group and Deccan Trap basaltic flows. The Archaean crystallines comprise schists, migmatites, granites, pyroxene granulites, quartzites, banded hematite quartzite, basic sills and pegmatite veins. The Pakhal metasedimentaries include quartzitic sandstones, interbedded slates and quartzitic sandstones, siliceous limestone and slates. Gondwanas are represented mainly by shales, sandstones, conglomerates and limestone.

From structural point of view, the area includes the upper part of main Godavari graben running in NW-SE direction and presents a very complicated and long tectonic history. In all six episodes of deformation due to compressive forces, interspersed with three episodes when tensional forces were active, are discernible in the study area.

The faults and lineaments developed during the tectonic deformations, have been easily picked up on aerial photographs and Landsat imageries, and are found to be the sites of hydrothermal mineralization in various parts of the area. The Thanevasana base metal mineralization as well as barite mineralization near Kopela village are situated on the fault planes running in NW-SE direction. A number of associated sister faults are the subject of intensive study for the inventory of mineral deposits.

INTRODUCTION:

For elucidating the regional geological setting a mosaic of Landsat imageries, covering an area of about 80,000 sq.kms. in Central India including parts of the states of Maharashtra, Andhra Pradesh and Madhya Pradesh, has been interpreted and a geological map has been prepared. For detailed study an area of about 5,000 sq.kms. covering southern part of Chandrapur district of Maharashtra has been taken up for the details of geology for the inventory of mineral resources, using the techniques of photointerpretation and selected field checks.

Four major geological units are demarkated and an interesting tectonic history is deciphered in the study area. Apart from it various major and minor faults and lineaments which are picked up very easily by the remote sensing techniques have been found to have important bearing on the inventory of hydrothermal mineral deposits.

Stratigraphy and Lithology:

The area comprises mainly four stratigraphic units, viz. Archaean crystallines, Pakhal metasedimentaries, Gondwana sedimentaries and Deccan

Trap basaltic differentiates. The general geological succession is as follows:

Stratigraphic units.		Lithology	Age	Equivalents
Deccan Traps		Basalt and basaltic differentiates.	Upper Cretaceous to Eocene.	Deccan Traps of Western India.
x x x x x x x x x x x x		Unconformity x x x x x x x x x x x x x x x x x x		
Gondwana Super Group.	Chikiala Series.	Conglomerates, ferrugineous sandstones. buff coloured shales and clays.	Permocarboniferous to Cretaceous	Gondwanas of Central India.
	Kota Series.	Limestone, sandstone and shales.		
		Fault		
Pakhal Group.		Quartzitic sandstones, interbedded slates and quartzitic sandstones stromatolitic and non-stromatolitic limestones and slates.	Precambrian	Cuddapah
x x x x x x x x x x x x x x		Unconformity x x x x x x x x x x x x x x x x x x		
Archaeans		Granites and migmatites, schists, banded Hematite quartzite, ferrugineous quartzites, metabasic sills, pyroxene granulites, diorites, quartzites, vein quartz and pegmatites.	Archaean	Dharwars of South India

Archaeans: Pascoe (1950) believed that the well marked bands of banded hematite quartzite which have been termed as Dharwar rocks belong almost certainly to the Iron Ore Series. The crystallines in which banded hematite quartzite bands occur includes schists, migmatites, granite, diorite, quartzite, basic sills, pyroxene granulites and minor intrusions of vein quartz and pegmatites. The magnetite is associated with quartz magnetite rocks. The crystallines are strongly foliated having strike direction of NW-SE. This NW-SE strike is the most common direction not only in the present area but also in the Dharwars of adjacent areas of Central India.

Pakhals: The sedimentary formations consisting of quartzitic sandstone, conglomerate, limestone, slates overlying the Archaeans in the Pranhita-Godavari valley were classified by King (1881) as Pakhal Series and an younger Sullavai Series. The two having being correlated by him with the Precambrian, Cuddapahs and Vindhyans respectively. Raman (1975) however due to similarity in lithology of the members of the two groups, their close proximity and presence of some members in both the groups suggested that the so called Sullavai Group of sediments are equivalent to Pakhals. The present author agrees with Raman (1975) as neither any marked distinction in lithology nor an unconformity is noticed in the area to separate them into two groups.

Gondwanas: The Gondwanas are divisible into two series, viz. Kota Series and Chikiala Series. The Kota Series consists principally of coarse, loosely compacted sandstones with some subsidiary bands of shale and a prominent band of limestone. While Chikiala Series consists of light brown, red, yellow and buff coloured ferrugineous sandstones and thick bands of conglomerates with white quartz pebbles. The junction between the Kota Series and Chikiala Series is obscure. Pascoe (1950) considered the Kota Chikiala succession to be more or less equivalent to the Jabalpur Group of Lower Cretaceous age.

Regional Geological Setting:

The present area includes the upper part of main Godavari graben running in NW-SE direction which is mantled on NE and SW sides of crystalline rocks of Archaean age. The Gondwana sedimentaries occupy the central part of the graben and are bounded by Pakhal metasedimentaries on either side. Thus the youngest and least deformed rocks lie in the core portion of the graben and the intensity of deformation and metamorphism increases both towards NE and SW direction. The river Godavari flows in the central part of the graben from Sironcha to the Bay of Bengal, and river Pranhita a tributary of the Godavari occupies the main graben in the area N and NW of Sironcha.

The Gondwanas are separated from Pakhals by a set of boundary faults on either sides which are running in almost NW-SE direction. While the contact between Pakhals and Archaean crystallines is unconformable wherever it is away from the central part of the graben and it is of tectonic significance near the central part of graben. The outcrops of Pakhals forming NW plunging synclinal structure in the central part of the area close to the river Pranhita appear to be uplifted enblock along a set of NE-SW and NW-SE running faults.

Structure and Tectonics:

The area presents a complicated structural pattern and a long tectonic history. The foliation in Archaean crystallines, bedding and foliation in Pakhal metasedimentaries and bedding planes in Gondwana sedimentaries mainly trend in NW-SE direction. Three episodes of folding are discernible in crystallines, followed by two episodes of folding in Pakhal metasedimentaries and one after the deposition of Gondwana sedimentaries. Interspersed with these deformations due to compressive forces, three episodes of deformation due to tensional forces have further complicated the overall structural disposition. The sequence of deformational episodes is as shown in the enclosed table.

The important fact thus emerges out is that, the area has been repeatedly subjected to compressional and tensional forces over a long period of time from Archaean period upto the end of Cretaceous. Various geological evidences thus suggest that the development of Godavari graben started in early Precambrian times due to tensional forces in the crust of the earth. The existing NW-SE foliation in Archaean crystallines facilitated block faulting due to which the graben has come into existence. Deposition of Pakhals took place in this graben during the later part of the Precambrian. This was followed by the advent of compressional forces resulting in the folding of Pakhals on NW-SE axis during Ist deformation and on NE-SW axis during second deformation. Later during the early Permocarboniferous times the graben has again got enlarged due to tensional forces to accommodate the deposition of Gondwana sedimentaries. After the Gondwana sedimentation compressional forces appeared again from NE and SW direction folding the Gondwanas also on NW-SE fold axis. After this deformational episode the central part of Godavari graben has been

faulted again due to tensional forces in such a way that Gondwanas are separated from Pakhals by a boundary fault running in NW-SE direction.

Inventory of Mineral Resources:

The detailed geological map prepared by remote sensing techniques has been found to be of great help in planning investigations for the inventory of mineral resources in the southern part of Chandrapur district. The regional extent of outcrops of limestones and banded hematite quartzite of economic importance have been easily delineated by these methods. Apart from it the major and minor faults and lineaments which have been picked up on the aerial photographs and Landsat imageries have a direct bearing on the hydrothermal mineral deposits. The NW-SE running boundary fault separating Gondwanas with the Pakhals along with its sister faults has been found to have isolated mineral occurrence all along its length. In the NW part of the area base metals like copper, lead and zinc are found in Thanevasana area and in the SE part near Kopela barite mineralization is noticed along this fault.

Conclusions:

Remote sensing techniques are found to be of great importance in elucidating the geological features and inventory of mineral resources in the southern part of Chandrapur district of Maharashtra. The area comprises four major geological units viz. Archaean unclassified crystallines, Pakhal metasedimentaries, sedimentaries belonging to Gondwana Super Group and Deccan Trap basaltic flows. From structural and tectonic point of view the area is very interesting as six episodes of deformation due to compressive forces, interspersed with three episodes of deformation due to tensional forces are recognized in the area. Faults and lineaments developed during these deformations have been found to be the sites of hydrothermal mineralization of base metals and barite.

REFERENCES

King, W.,	1881	The Geology of the Pranhita - Godavari Valley. Mem. Geol. Surv. Ind. Vol. 18.
Poscoe, E.H.,	1950	A Manual of the Geology of India and Burma, Misc. Pub., Geol. Surve, Ind. Vol.I and Vol.II.
Raman, R.	1975	The Relationship between the Pakhal and Sullavai Groups in part of the Pranhita-Godavari Valley in Chandrapur district, Maharashtra, Misc. Pub. Geol. Surv. Ind. No.23, Part 1.

TABLE SHOWING SEQUENCE OF DEFORMATIONAL EPISODES

Geological Time	Deformational Episode	Type of Forces	Direction of Forces	Results
Permocarboniferous to Cretaceous	III rd	Tensional	NE-SW	Boundary faulting separating Gondwanas from Pakhals
	II nd	Compressional	NE-SW	Folding of Gondwanas on NW-SE axis.
	I st	Tensional	NE-SW	Enlargement of Godavari Graben to accommodate Gondwana sedimentaries.
Precambrian	III rd	Compressional	NW-SE	Folding of Pakhals on NE-SW axis formation of structural domes and basins.
	II nd	Compressional	NE-SW	Folding of Pakhals on NW-SE axis, low grade metamorphism and development of axial plane schistosity.
	I st	Tensional	NE-SW	Development of Godavari graben
Archaean	III rd	Compressional	E-W	Open folding of Archaean Crystallines on N-S axis.
	II nd	Compressional	NW-SE	Tight folding in Archaean crystallines on NE-SW axis, development of structural domes and basins and L_2 lineation.
	I st	Compressional	NE-SW	Folding of Archaean crystallines on NW-SE axis, development of main axial plane foliation parallel to fold axis, high grade metamorphism, migmatization, intrusion of basic sills and development of L_1 lineation.

PHOTOGEOLOGICAL MAP OF SOUTHERN PART OF CHANDRAPUR DISTRICT, MAHARASHTRA, INDIA

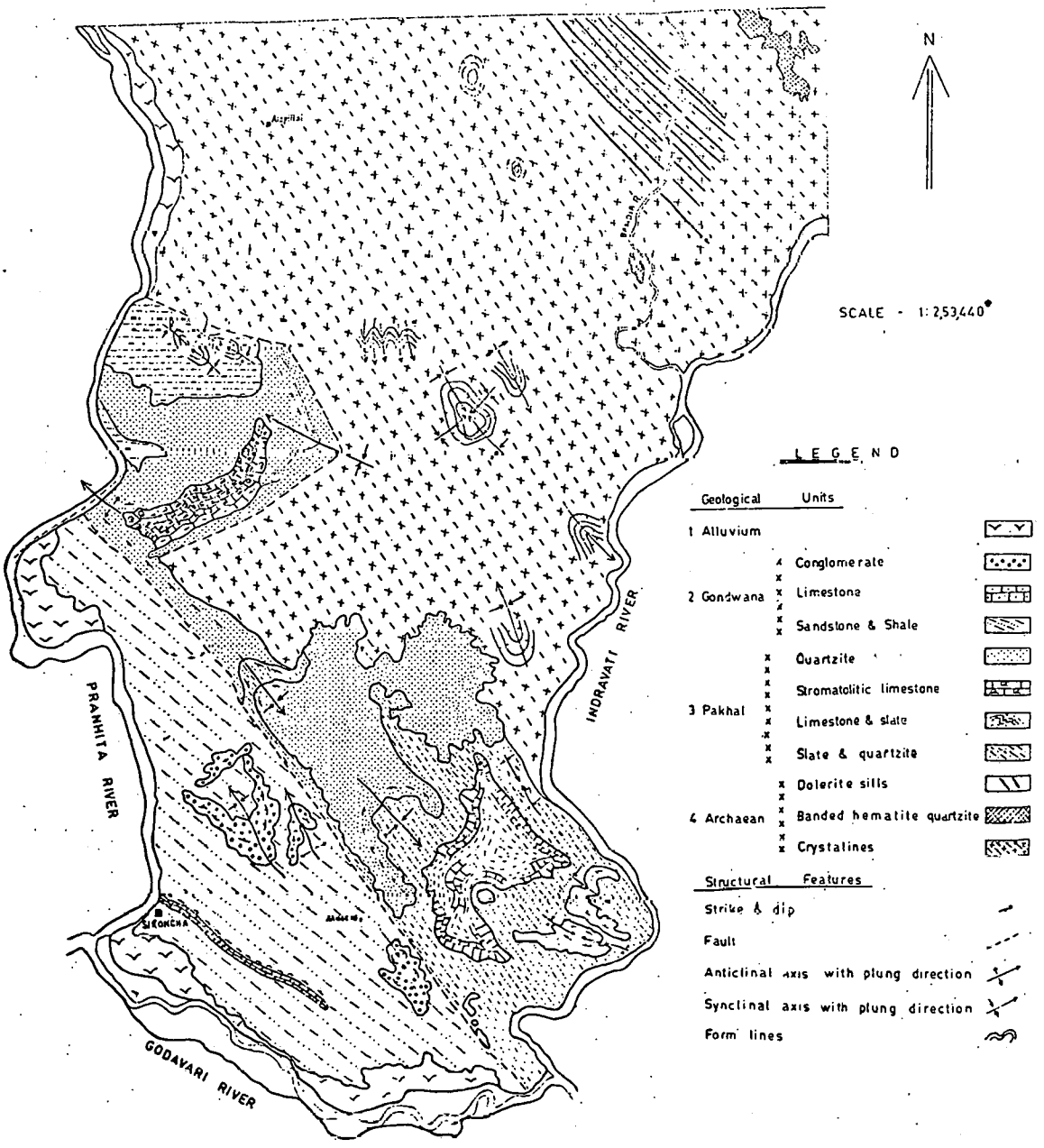

ANALYSIS ON MULTI DATE LANDSAT DATA

S.CHANDRASEKHAR AND M.MARUTHACHALAM
NATIONAL REMOTE SENSING AGENCY, SECUNDERABAD (INDIA)

1. INTRODUCTION

Detection of surface change phenomenon is one of the important applications of remote sensing. Remote sensed data can be acquired in many ways i.e. using Aircraft, Balloons and Satellites. Each method has its own advantages and limitations. One specific and important advantage of opting for remote sensed data using satellites is the global coverage over long period of time and also repetitive coverage at regular intervals. For our study Landsat data in the form of Computer Compatible Tapes (CCTs) provide the basic input and it is supplemented by imageries. Each scene covers a ground area of approximately 185 km x 185 kms and contains 3240 picture elements and 2340 scan lines. Each picture element contains the energy reflected from ground surface of 57 m x 79 m and this energy will be recorded in four spectral bands. For temporal study, multi date data pertaining to the area under study is to be selected.

For our analysis two areas (one in Punjab and another in Andhra Pradesh in India) were considered. For these areas, multidate data tapes were available and also imageries. One important aspect to be considered in multidate analysis is the registration of the image pertaining to different dates. There are different registration techniques and depending upon the size of the area each technique will be best suited. Two techniques are used for registration and these are explained in future paragraphs. For classification of data, supervised technique using maximum likelihood decision rule assuming Gaussian distribution of data is adopted. For multidate data the dimension of the measurement vector becomes large the technique of principal component transformation is used to reduce the dimension of measurement space but still retaining the maximum information content. The detailed technique of analysis and also discussion of results are as follows.

2. ANALYSIS PROCEDURE

2.1. REGISTRATION

Two techniques were used for registration of images. In the first method, check points (control points) are identified in both the images and their coordinates are noted. The average shift in coordinates will be determined and this shift will be used for the transformation of one image point to another.

If X_1, Y_1 are the coordinates of a point in image (1) and X_2, Y_2 are the coordinates of the point in image (2), then the transformation used will be

$$X_2 = X_1 + \Delta X$$
$$Y_2 = Y_1 + \Delta Y \qquad (1)$$

where ΔX, ΔY is the shift computed by recording the difference in coordinates at control points.

The other method uses the technique of affine transformation. The transformation can be expressed as

$$X_1 = a_1X_2 + b_1Y_2 + c_1$$
$$Y_1 = a_2X_2 + b_2Y_2 + c_2 \qquad (2)$$

where (X_1, Y_1) and (X_2, Y_2) are the coordinates of a point in images designated as (1) and (2) and a_1, b_1, a_2, b_2, c_1 and c_2 are constants that define the transformation and which can be determined.

The determination of these constants are as follows:

Record the coordinates of certain points which can be identified in both the images. Let us designate them as (X,Y) pairs. Then a two dimensional least square fit is performed to estimate these constants.

Equation (2) can be expressed as

$$Y\,a = b \qquad (3)$$

where a = d-component weight vector $(a_1, a_2, \ldots a_d)$

b = n-component column vector $(b_1, b_2, \ldots b_n)$

Y = n x d matrix; n = Number of control points

The least square solution will be

$$a = (Y^tY)^{-1}\,Y^tb \qquad (4)$$

When once the weight vector is determined the transformation of points from image (1) to image (2) will be reduced to a matrix multiplication defined by equation (2).

Using the transformation matrix the predicted values at the control points in image (2) can be computed using the coordinates of image (1). The actual value is also known. Hence the RMS error can be calculated and this gives an idea of the goodness of the fit achieved.

2.2. CLASSIFICATION

The classification technique adopted for single date as well as multidate analysis is the supervised technique using maximum likelihood decision rule. Basically what a classifier does is to map a multi-dimensional measurement vector also designated as feature vector into an integer number called class number. If we designate this vector as X then the classifier can mathematically be defined as mapping using a function F such that

$$F(X) = K \Rightarrow 1 \quad K \leq n \qquad (5)$$

where

K is an integer between 1 and n

n Number of classes

$\Rightarrow$ Mapping operation.

There are many ways to define the mapping function F. One method is to define F using certain parameters that characterise each class. These

parameters can be determined by supplying known data for these classes which are called Training Set Data.

For a given vector X and total number of classes n, we get n values of the function. These functions are called Discrimant functions. The assignment is made to that class for which the discrimant function attains maximum value.

If we represent the discrimant function by g decide class K for which X belongs such that

$$g_k(X) > g_i(X) \text{ for } i = 1,2,....n;\ i \neq K \qquad (6)$$

we let

$$g(X) = P(X/i)$$

where

P(X/i) is the probability that feature X belongs to class i and assign X to class K for which g is maximum. Such a classifier is also called the Maximum Decision likelihood rule classifier.

If an assumption is made saying that the distribution of X is Gaussian P(X/i) can be expressed in terms of mean vector and covariance matrix.

$$P(X/i) = \frac{1}{(2\pi)^{n/2} |\Sigma_i|^{1/2}} \exp\left[-\frac{1}{2}(X-\mu_i)^T \Sigma_i^{-1} (X-\mu_i)\right] \qquad (7)$$

where

P(X/i) is the likelihood of Vector X to Class i

n = Dimension of measurement Vector X

Σ_i = Covariance matrix for i^{th} class

μ_i = Mean Vector for Class i

$|\Sigma_i|$ = Determinant of

From the training set data μ and Σ can be computed for each class.

2.3. DIMENSIONALITY REDUCTION

The reduction in dimensionality of the measurement vector is achieved in the following manner.

A Linear transformation such as

$$Y = TX \text{ with } m < n \qquad (8)$$

where

Y = Transformed vector (m x 1)

T = mxn matrix

X = Original vector (n x 1)

can be used to reduce the dimension from n to m (m<n). This transforms an original n dimensional vector to a new m dimensional vector Y whose dimension is less than that of X. In addition if it minimises the error $\|Y - X\|^2$ it is equivalent to saying that most of the information contained in X in a space of higher dimension will be retained in a space of lower dimensionality. One such method to choose T is to have Eigen vectors of the covariance matrix

arranged as coloumns of T and retaining only that many rows corresponding to m. It can also be proved that if an assumption is made that vector X is Gaussian distributed the transformed vector Y will also be Gaussian distributed.

The maximum likelihood decision rule can be used to classify Vector Y, which is having lower dimension.

The parameters of the distribution in new space can be derived from computed parameters of original vector space. These can be expressed as:

$$\mu_{new} = T \quad \mu_{Old} \tag{9}$$

$$\Sigma_{new} = T^T \Sigma_{old} T \tag{10}$$

where new, old are the mean vectors in new and original space. new, old are the covariance matrices and T transformation matrix that is used to transform X. The results of application of the above techniques to the selected data set is explained.

3. RESULTS AND DISCUSSIONS

3.1. PUNJAB AREA

For the analysis of Punjab area, two data tapes pertaining to the same area were selected (September 72, March 75). To check the quality of the data, the tapes were displayed on the image processing facility available. Sutlej river which is prominent feature in the area under analysis was identified in both the tapes and the approximate region is fixed by noting the scan line/ pixel from the display panel.

Further, the required area was extracted and a gray scale map for bands 5 and 7 was printed. Using this and also supplementing this information with imagery and topomaps training areas were identified. Three different water classes were identified and labelled as Deep water (about 15' indepth), Medium water (about 8' indepth), Shallow water (about 4' indepth) and others were wet settlement and dry settlement. Using the maximum likelihood decision rule the training sets were classified. The average accuracy of classification was 97.9% for September data and 86.1% for March data. The number of pixels falling under each class using the statistics computed from the training area is shown in Table I (under heading T_1/T_1).

Next for T_2 data T_1 area training sets are used. The results of classification are shown in Table I (under Column T_2/T_1).

The two tapes were merged by giving the shift. This shift for the selected area is 217 scan lines and 66 pixels. A synthetic 8 band data tape is created and classified using T_1 training set data. The results are shown in Table I under column $T_1 + T_2/T_1$.

From the results we can conclude that there is decrease in shallow and medium water pixels from September to March data. This is expected as September is a monsoon season whereas March is comparatively dry period. Also area under dry settlement which is quite significant in March has been reduced in September data. This is for the reason that dry settlement area has changed to shallow water areas in September. These results correlated well with the actual field data available (Rainfall data for the above periods shown in Table Ia).

3.2. ANDHRA PRADESH AREA ANALYSIS

Another area selected for analysis is portion of the scene located in Godavari district of Andhra Pradesh. For this area we had multidate tapes and also the selected portion of the scene contains distinguishable features such as water, river sand, forest, cropland etc.

The details of the scene are given below:

Tape ID 1163 - 0426100 Exposure dt 2.1.1973

Tape ID 1181 - 0426000 Exposure dt 20.1.1973

To have a preliminary idea about the data these tapes were displayed on the Image Analysis System. The beginning of the Godavari River which appears in both the scenes was observed. The approximate analysis area was read from display panel.

For accurate registration and also for selection of training set, the gray map of both the images (Bands 5 and 7) were taken.

The coordinates (scanline/pixel) of six control points which can be identified without ambiguity in both the images were recorded. As the area of interest in small (240 scanlines x 320 pixels) the registration was done computing the average shift at these control points. The shift is 82 scan lines and 65 pixels.

With the help of gray map and also imagery, six different classes were identified and training fields were selected. The classes were designated as Riversand, Forest, Fallow, Cropland, Hill shadow and Riverwater. The training set selected lies in the common area of both images. With the help of this training set data, necessary statistical parameters were computed and the training fields were first classified using the maximum likelihood decision rule. The results of classification are shown in table II.

The two tapes were merged by giving the shift vector and a synthetic 8-band tape was generated. This 8-band vector was classified using training set data for time T_1 and also for time T_2. The details of the results are given in table II.

From the temporal analysis we can infer that features such as riverwater, riversand, forest and hill shadow have practically not changed where as there is a significant change in fallow and cropland categories. Since January is harvest season due to cutting of the crops, the cropland area has reduced and as a consequence fallow land area has increased.

The results obtained are more or less the same when T_2 data is classified using training sets for the period T_1 and vice-versa and also using stored statistics for one period and using it for classification of data for another period. Table III gives some of the details.

TABLE I

RESULTS OF CLASSIFICATION OF PUNJAB AREA

Area of interest:
(240 scanlines x 210 pixels)

DATA SET 1 (Designated as T_1) Sep 72, Lines 1 - 250, Pixels 600-809

DATA SET 2 (Designated as T_2) Mar 75, Lines 218-467, Pixels 666-875

CLASSIFICATION TABLE

Class Name	Pixel Count		
	T_1/T_1	T_2/T_1	$T_1 + T_2/T_1$
Deep water (15')	354	290	300
Medium water (8')	15125	10612	12082
Shallow water (4')	28735	6784	5456
Wet settlement	2989	1055	2609
Dry settlement	5297	33759	32053
Total	52500 each		

T_1/T_1 indicates T_1 data T_1 Training set
T_2/T_1 indicates T_2 data T_1 Training set
T_1+T_2/T_1 indicates Merged T_1, T_2 data with T_1 Training set.

TABLE IA

RAINFALL (IN CMS) DATA OF PUNJAB AREA (From Government Records)

(Average of month given in bracket and its preceding month)

Place	1972 (September)	1975 (March)
Ropar	10.30	2.60
Ludhiana	7.50	2.82
Sangrur	6.20	0.55
Patiala	10.10	3.00

TABLE II

RESULTS OF CLASSIFICATION OF ANDHRA PRADESH AREA

Area of Interest:
(240 scanlines x 320 pixels)

DATA SET 1 (T_1) Exposure Date 2.1.73, Tape ID 1163-0426100
Lines 919 - 1158; Pixels 7 - 326

DATA SET 2 (T_2) Exposure Date 20.1.73, Tape ID 1181-0426000
Lines 1001 - 1240; Pixels 72 - 391

CLASSIFICATION TABLE

Class Name	% OF PIXELS IN EACH CLASS			
	T_1/T_1	T_2/T_2	T_1+T_2/T_1	T_1+T_2/T_2
River Sand	3.70	3.98	2.85	3.71
Forest	25.80	23.60	27.79	26.37
Hill Shadow	24.57	22.46	23.83	23.13
River water	4.30	4.85	5.57	5.42
Fallow	27.15	35.06	28.64	30.50
Cropland	14.48	10.05	11.32	10.87

T_1/T_2 represents T_1 data T_1 Training set.

T_2/T_2 represents T_2 data T_2 Training set.

T_1+T_2/T_1 represents Merged T_1, T_2 data and T_1 training set.

T_1+T_2/T_2 represents Merged T_1, T_2 data and T_2 training set.

TABLE III

RESULTS OF CLASSIFICATION OF ANDHRA PRADESH AREA

Class Name	% OF PIXELS IN EACH CLASS			
	T_{2D}/T_{1S}	T_{1D}/T_{2S}	T_{1D}/T_{2A}	T_{2D}/T_{1A}
River sand	4.02	3.66	3.74	4.12
Forest	23.76	24.50	26.12	28.12
Hill shadow	23.36	22.92	23.26	21.62
River water	5.98	5.42	5.21	4.10
Fallow	31.19	29.84	25.32	30.9
Cropland	11.69	13.66	12.35	11.14

T_{2D}/T_{1S} indicates T_2 data classified using T_1 training set statistics.

T_{1D}/T_{2S} indicates TT_1 data classified using T_2 training set statistics.

T_{1D}/T_{2A} indicates T_1 data classified using T_2 area training sets.

T_{2D}/T_{1A} indicates T_2 data classified using T_1 area for training set.

THIS PAGE

WAS INTENTIONALLY

LEFT BLANK

SOIL MOISTURE DETERMINATION AND SNOW CLASSIFICATION WITH MICROWAVE RADIOMETRY

E.Schanda, R.Hofer, D.Wyssen

Institute of Applied Physics
University of Berne, Switzerland

A.Musy, D.Meylan, C.Morzier

Institute of Agricultural Engineering
Federal Institute of Technology, Lausanne, Switzerland

W.Good

Federal Institute of Snow and Avalanche Research
Weissfluhjoch/Davos, Switzerland

ABSTRACT

Results of our investigations on the microwave emission of snow and soil under controlled conditions are reported. Three radiometers at 4.9, 10.5, and 21 GHz have been used for the studies on soil moisture at three test sites, different in type of soil and covering a wide range of moisture contents, during the second half of 1977. Five radiometers at 4.9, 10.5, 21, 36, and 94 GHz are in use for the studies on the snow cover at a well-equipped high-altitude site, where all grades of snow are available during the seasons since early 1977. A classification of conventional snow parameters by the microwave emission due to a statistical algorithm yields very promising results.

1. INTRODUCTION

Long term observational programs on the microwave emission behavior of soil and snow have been started early 1977 in combined efforts of the three participating institutes. The Institute of Applied Physics Berne (IAP) group, basing on previous experience in controlled investigations of microwave emissivity, e.g. [1], and in interpretation of microwave radiometer data from satellites, e.g. [2], is aiming for comprehensive and statistically significant information on the microwave emission of natural media. This has to serve for reliable interpretation of data from future satellite-borne microwave sensor systems in earth-surface or atmospheric applications [3]. The group of the Institut de Génie Rural Lausanne (IGR), primarily engaged in hydrological studies of the soil, initiated the common soil moisture project within the framework of a larger remote sensing project of this institute, and makes various test areas with infrastructure available, and performs the determina-

tion of the hydrological and meteorological parameters. The Swiss Institute of Snow and Avalanche Research (SFISAR) makes its high altitude test site Weissfluhjoch, 2540 meters above sea level, with infrastructure and the regular snow parameter determination available. Additionally, an algorithm for snow classification, developed at SFISAR, is the basis for collaboration on statistical classifications of snow parameters due to the measured microwave properties.

At previous occasions preliminary results of the first snow measuring season [4], qualitative interpretations and additional observational results [5], and a comprehensive utilization of the snow data of the first season in a clasification procedure [6] have been described.

Concerning the soil moisture measurements, first results and preliminary estimations on their usefulness have been given [7].

2. TEST SITES AND INSTRUMENTATION

The microwave sensor package used until now consists of five simultaneously operated radiometers, with specifications given in Table I.

TABLE I

Microwave Multichannel Radiometer

Center Frequency [GHz]	4.9	10.5	21	36	94
Bandwidth [GHz]	0.2	0.8	0.8	0.8	2.0
Sensitivity [K] (at 1 sec Integration Time)	$\leq$ 0.1				0.2
Viewing Angle [°]	all between nadir and zenith				
Polarization [°]	any				
Beamwidth [°] (3db)	$\sim$10				

These radiometers are mounted in a common instrument cabin, occasionally together with auxiliary instruments as a thermal i.r. radiometer and a Hasselblad camera. This cabin is mounted on a 16 m high tower of light framework at the snow test field, or it is hoisted up by a crane to 12 meters altitude at the various soil test fields. During the past soil measurements only the three lowest frequency channels of the microwave radiometer have been employed. At the snow measurements the 94 GHz channel is sometimes not used or its results are not taken into consideration because of the influence of clouds and precipitation on this channel.

The following conventional snow parameters are determined regularly (full program every two weeks, reduced program daily): depth, layering, ram-hardness, temperature profile, moisture (free water), total water equivalent, meteorological history, cristallographic properties, grain size parameters. Air and snow temperature (at the surface and at 10 cm depth) and moisture determination on a coarse empirical scale (handtest) are continuously observed.

The snow test site is common with the high altitude test area of the SFISAR at 2540 meters which is regularly observed by this institute and made available to our microwave investigations, including logistic support. During the winter season (December-May) all types of alpine snow quality can be observed.

The supporting measurements on soil are: Classification of soil type and roughness, nearly all microwave measuring cycles (all frequencies, all incidence angles, vertical and horizontal polarization) are accompanied by taking almost simultaneously soil samples of the upper layer of approximately 2 cm depth for laboratory determination of the moisture content; temperature profile, surface temperature by thermal infrared radiometer, moisture profile by neutron absorption method, meteorological history are determined on a less regular basis.

During the summer and fall period of 1977 three test areas in the south-west part of Switzerland with distances of about 60 to 80 kms between each other have been used:

- Vouvry with essentially loamy-sandy soil,
- Changins with loamy and clay soil,
- St.Aubin with very heavy, mixed soil (about half clay).

At each test site one or two test fields have been investigated during periods of two to three weeks. The surface roughness was ranging from smoothed (r.m.s. height variation about 2 to 3 cm), harrowed (about 5 cm) to ploughed (about 10 to 15 cm).

3. MICROWAVE EMISSION DUE TO SOIL MOISTURE

In the following only a few examples are presented out of the large amount of recorded measurements. It is not yet possible to derive distinct conclusions because:

- only a part of the material has been evaluated so far,
- there is not yet sufficient statistics to discriminate clearly the effects of moisture, type of soil and roughness,
- of the low degree of accuracy, in particular in the moisture determination (accuracy of measurement, number and choice of samples, lacking profile within the upper 10 to 20 cm),
- of the lack of any useful and reliable theoretical approach for the interpretation of the radiation behavior of this type of heterogeneous media with rough surfaces.

Therefore, the presented examples can only be used to estimate the trend in a more qualitative way. Figure 1 compares the brightness temperatures of two test fields at 4.9 and 21 GHz as a function of viewing angle. There are at least three qualities differing:

- the type of soil: very heavy mixed, half clay, in St.Aubin, loamy-sandy in Vouvry;
- roughness: r.m.s. about 10 to 15 cm (ploughed) with measuring along the furrow in St.Aubin, smoothed (r.m.s. about 2 to 3 cm) in Vouvry;
- moisture per weight of the dry soil: ~51% in St.Aubin, ~35% in Vouvry.

At a first glance the effect of surface roughness determines the differences: Fresnel-like behavior with clear splitting for vertical and horizontal polarization at 6 cm wavelength, much less pronounced at 1.5 cm; on the smoothed field almost independent on viewing angle at the rough surface. The effect of increasing moisture is to reduce the brightness temperature: less moisture in the field of Vouvry increases the brightness temperature of the wavelength which is shorter than the roughness scale. On the very rough

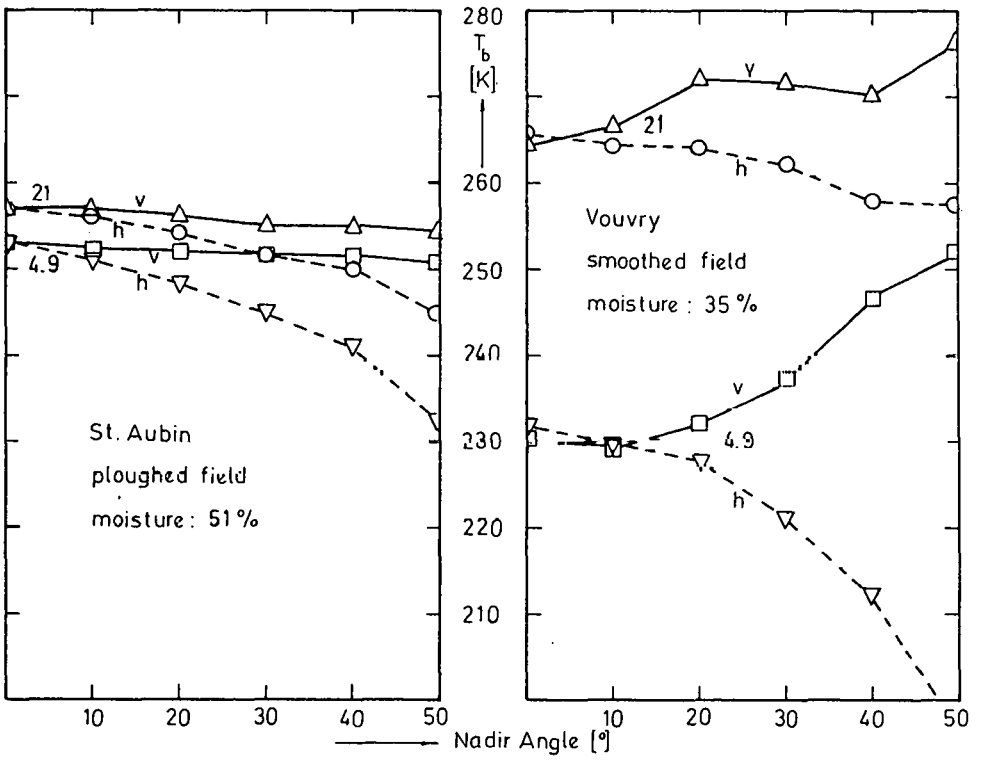

Figure 1:

Microwave brightness temperature at 4.9 GHz and 21 GHz for vertical and horizontal polarizations as a function of the viewing angle measured off nadir ploughed field: r.m.s. height variation approximately 10 to 15 cm, smoothed field: r.m.s. about 3 cm.

surface however due to multiple scattering the brightness temperature cannot attain the low value which would be expected according to its high degree of moisture content.

Figure 2 shows the temporal development of the moisture content and the proper emissivities (ratio of brightness temperature and physical temperature) measured in the three channel radiometer in nadir looking position during one week. The times of taking soil samples for the laboratory moisture determination are roughly coinciding with the time of microwave measurements. Decreasing moisture corresponds with increasing emissivity for the whole period as well as to some extent within even single days.

Figure 3 summarizes the results of four fields presenting three different types of soils, a wide range of moisture content and strongly differing surface roughness. The results of only two frequencies are given. The large spread of the measuring points indicates the rather high degree of inaccuracy created mainly by the moisture determination. One has to be cautious in deriving conclusions on the sensivity of the method and on quantitative relationships between moisture and emissivity. But for an estimation of the trend the measured points have been used for a linear regression, expressing the emissivity by $e = mw+k$ as a linear function of the moisture content w per weight of dry soil, with m = regression coefficient and k = constant. The lines in Figure 3 are according to this procedure. The quantities m and k are given in Table II.

Table II

Coefficients of the regression lines of Fig.3

	4.9 GHz		21 GHz	
Testfield	m	k	m	k
Vouvry	-0.31	0.89	-0.21	0.96
Changins	-0.84	1.03	-0.46	1.03
St.Aubin (smooth)	-0.34	1.05	-0.21	1.02
St.Aubin (rough)	-0.10	0.94	-0.03	0.93

The coefficient m represents the sensitivity to detect changes of the moisture contents. One has to be cautious in applying the values of m and k: in view of the large spread of the points measured so far, the coefficients in Table II are simulating a much too high accuracy; the estimated error of these values is in the order of 0.1.

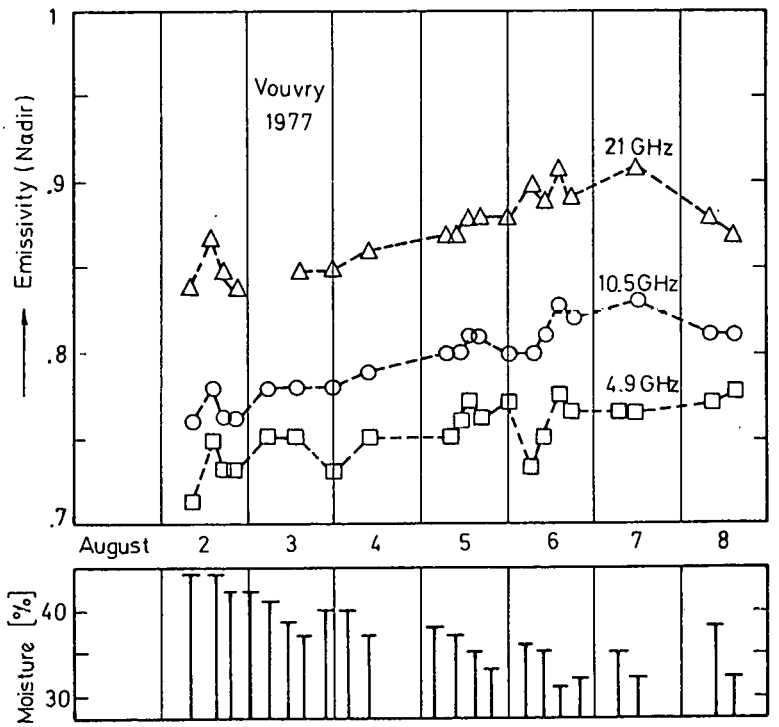

Figure 2: Temporal development of the moisture content per weight of dry soil and of the associated emissivities 4.9, 10.5 and 21 GHz during one week.

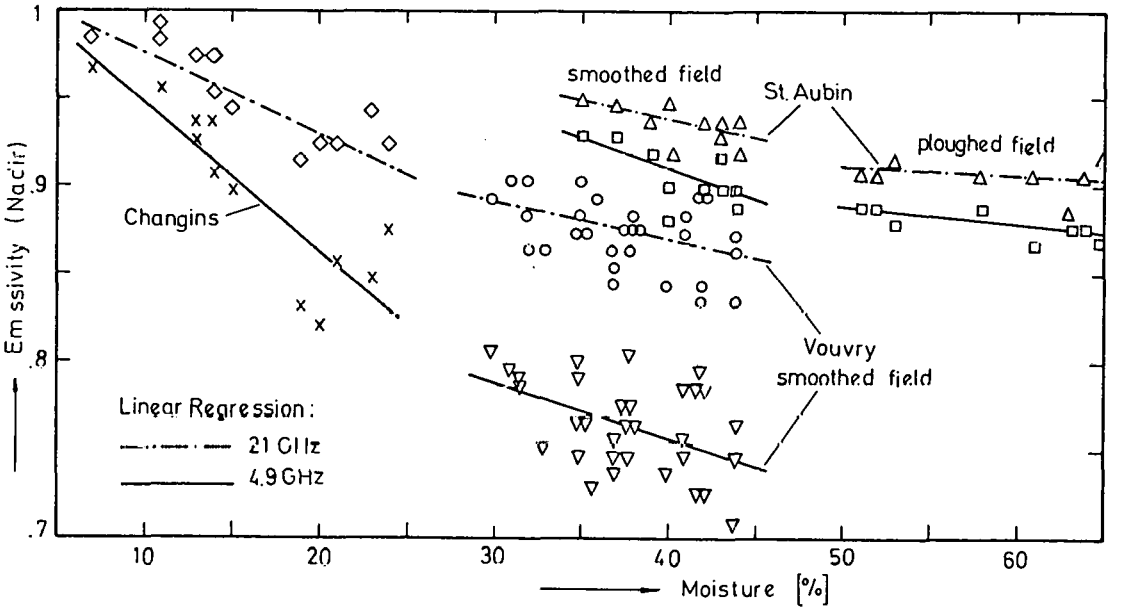

Figure 3:

Microwave emissivities of 4 different test fields at 3 locations in wide ranges of moisture content. Regression lines due to coefficients of Table II. The field in Changins is also ploughed (r.m.s. = 15 cm).

4. MICROWAVE EMISSION OF SNOW

Additionally to earlier published results [4, 5, 6], we present here typical emission properties of very dry snow of the early winter season. At the altitude of the snow test field (2540 m) the snow cover of the winter 1977/78 has been built up by dry snow accumulated to a depth of 1 to 1.5 meter at temperatures never above minus 5 degrees centigrade, and therefore without any melting metamorphosis until about mid-March. During the measuring campaign 1976/77, which was started in March 77, we never have met the same situation; even large accumulations of new dry snow were always occurring on top of old snow. This time the whole layer of snow was highly permeable to the microwaves down to the underlying soil. The microwave attenuation was found to be less than 0.5 db/m at 10 GHz, the mean density of the total snow layer was approximately 295 kg/m^3.

The following figures represent therefore the resulting emission of a layer of dry snow and the underlying soil. Figure 4 shows the brightness temperature as a function of the viewing angle for horizontal and vertical polarization. The character of the angular dependence is simpler than in most of the spring conditions with layers of very different properties. The stronger decrease for the 10.5 GHz as compared to the other channels cannot yet be explained.

Figure 5 shows the spectral behavior of the brightness temperature derived from the same measurement cycle as presented in Figure 4. These results are typical for all measurements during the early winter season. The curves for different days (at any time of a day) of this period are significantly

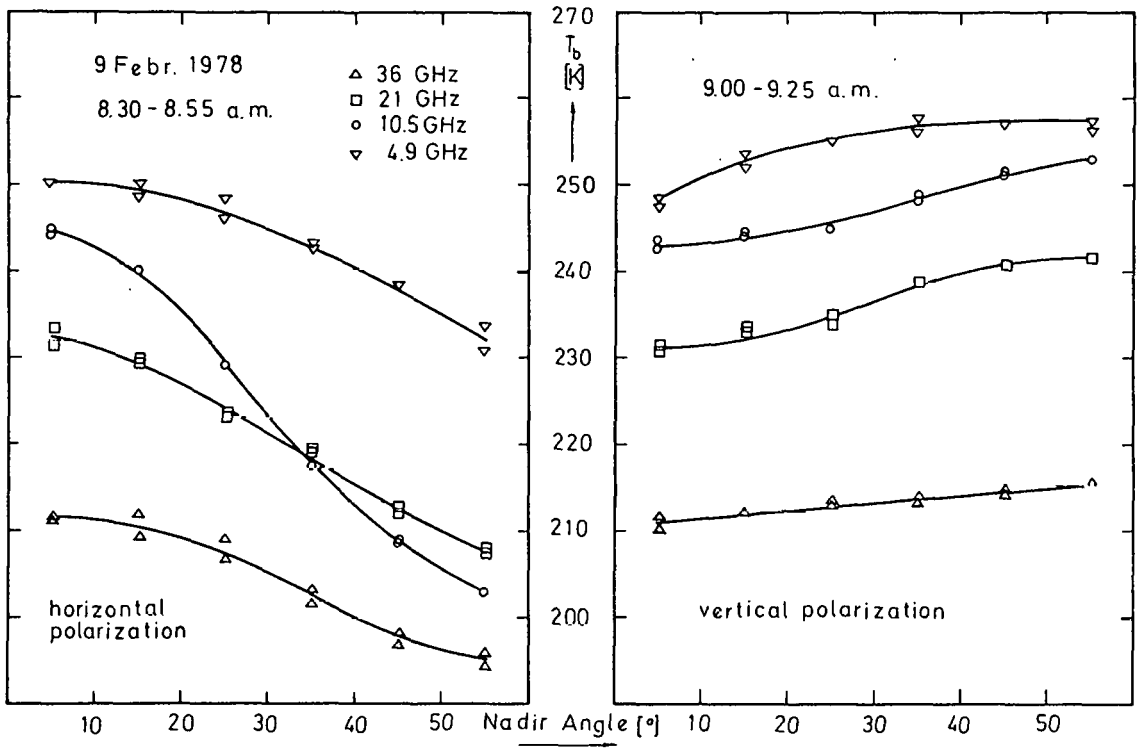

Figure 4:

Microwave brightness temperature of a 1 to 1.5 meter thick layer dry snow as a function of the viewing angle. Snow surface temperature: -19.5° C.

similar and to a large extent indistinguishable.

5. CLASSIFICATION OF SNOW QUALITIES DUE TO MICROWAVE EMISSION

A statistical method used previously by one of us [8] for snow classification is now applied to the microwave measurements of snow, and an analysis of the measurements of the first season has been completed recently [6]. The measured brightness temperatures of the early winter season 77/78 are noticeably affected by the underlying soil due to the highly permeable dry snow, therefore the classification procedure has not yet been started for this complex situation until results of the joining period of the first melting metamorphosis are available.

For the purpose of this symposium the main results of [6] are summarized here. All the measured data are analyzed by correlation, factorial and cluster analyses. Various selections out of the available measured data can be made to concentrate the analysis on the most significant data (e.g., the 94 GHz data present deteriorated information due to the atmospheric effects on the measurement, therefore they can better be eliminated). The brightness temperatures measured in one cycle (e.g., at four frequencies 4.9, 10.5, 21, and 36 GHz, at 5 nadir angles 10°, 20°, 30°, 40°, 50°, at one polarization) are constituting a vector of n (e.g., 20) components. If this measuring cycle was occurring p times during the whole observation period, on the resulting p x n matrix a correlation analysis can be applied yielding a n x n correlation

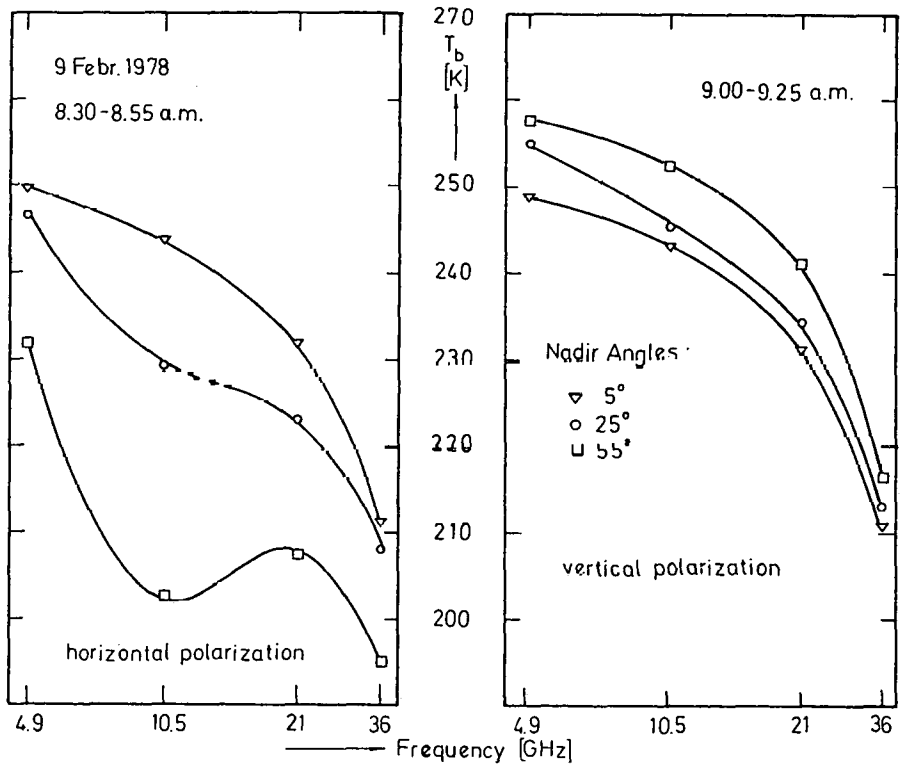

Figure 5:

Microwave spectrum of the brightness temperature of a 1 to 1.5 meter thick layer of dry snow at various viewing angles.

matrix which displays the degree of common information (≤1) between the components row- or column-wise. Along a factor analysis the linear dependences between the individual measurements at a specific snow quality are determined, yielding an orthonormal reference frame. This defines a number of axes (linear combinations of the mean values of brightness temperatures measured under given experimental conditions, i.e. with given conventional snow parameters) along which a fraction of the total variance is displayed. The cluster analysis (unsupervised classification) compares the distances between individual vectors and centers of masses of groups (clusters) and vectors are regrouped to obtain a minimum value for the sum of the squared distances. Taking the dataset containing all vectors with four frequencies and five position angles as indicated above, but now including those vectors with the second polarization, we arrive at 131 vectors of the whole observation period in spring 77. Figure 6 shows the distribution of these vectors as projected on the first two axes (F1, F2) of a six dimensional space constructed by the factorical analysis. Centers of masses of seven non-hierarchical clusters (numbers in circles) and the number of vectors belonging to the different clusters are indicated. According to the construction of the space by factorial analysis the amount of information decreases with increasing axis-number. Hence Fig.6 contains about 88% of the information of the measured data.

In order to associate these clusters to conventional snow parameters a coarse snow classification of the uppermost 10 cm layer, as it is used for quick look by experts, has been applied during our measurement periods and can be utilized for our purpose in Table III.

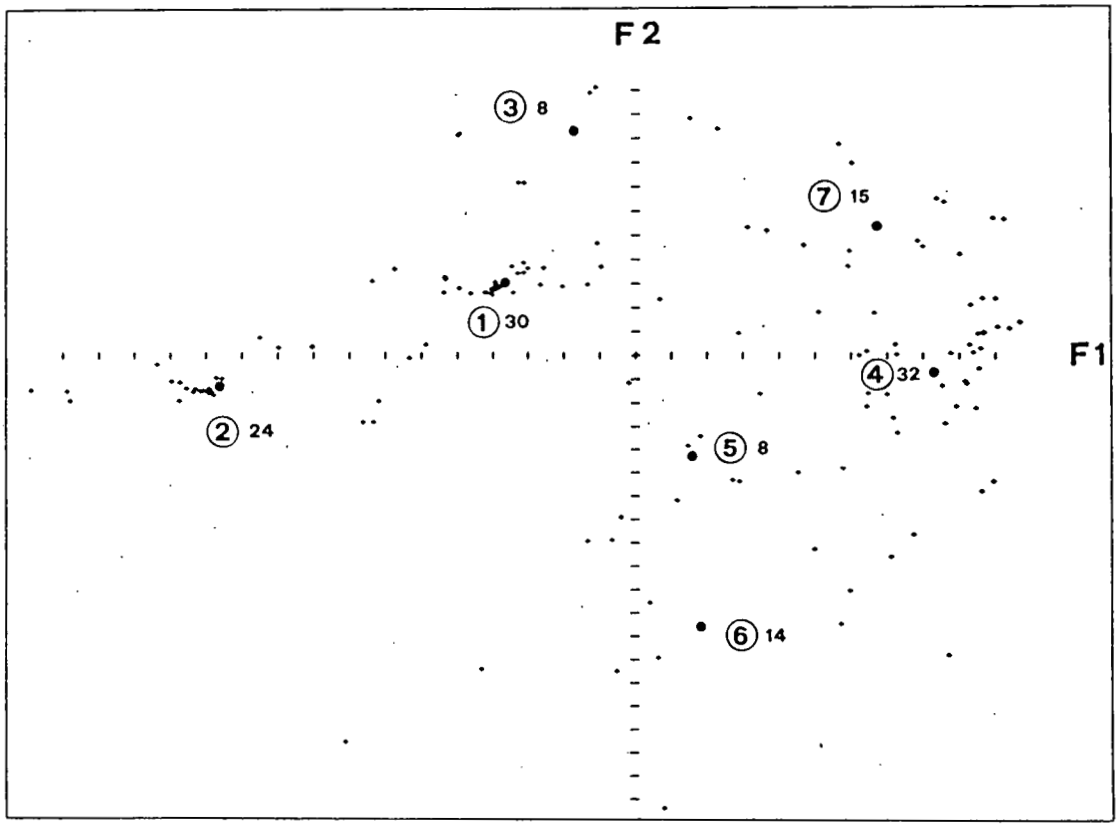

Figure 6:

Projection of the 131 vectors of all measuring cycles, containing the channels 4.9, 10.5, 21, 36 GHz, the nadir angles 10, 20, 30, 40, 50 degrees and both polarization, onto the first two axes of a 6-dimensional space. Seven clusters can be isolated.

It can be recognized that of all measured situations dry snow can be distinguished from humid or from wet snow. Even dry ice can be discriminated from new or old dry snow. However, no clear distinction between humid and wet snow is possible by the data sets investigated so far.

This statistical method will be used also for the more recent snow emission data. It may however be regarded in a more general sense as a useful tool also for other experiments on natural phenomena (soil moisture, vegetation) where the statistical independence of the various information channels is a priori unknown.

We acknowledge herewith the support of the soil moisture project by the Swiss National Science Foundation.

Table III

Percentage of measurement cycles (vectors) belonging to a given snow quality which can be associated to one of the 8 clusters. In parantheses numbers of measurement cycles belonging to a given snow condition. Total number 194 is the sum of the vectors used in Figure 6 plus those at viewing angles 15, 25, 35, 45, 55 degrees. For definition of the snow qualities and for associations of other data sets see [6].

Cluster	Dry (90)			Humid (62)				Wet (42)		
	new (72)	old (6)	ice (12)	new (38)	old (12)	ice (6)	spring (6)	old (18)	ice (6)	spring (18)
1	53	50								
2	46	50								
3			100							
4				92	50	100	50	56		6
5					25		50	17		
6					17			22	67	17
7								6	33	33
8				5						33
not classified	1			3	8					11

6. REFERENCES

[1] Schanda, E., Hofer, R., "Scattering, Emission and Penetration of Three-Millimeter Waves in Soil", Proc.URSI, Specialist Meeting Microwave Scattering and Emission from the Earth, 141-149, (1974), University of Berne, Switzerland.

[2] Künzi, K.F., Fisher, A.D., Staelin, D.H., Waters, J.W., "Snow and Ice Surfaces Measured by the Nimbus-5 Microwave Spectrometer", J.Geophys. Res., 81, 4965-4980, (1976).

[3] Schanda, E., Künzi, K.F., Hofer, R., "Microwave Experiments for Spacelab and Nimbus G", Proc.Colloque de GDTA sur l'utilisation des satellites en télédétection, 21 - 23 Sept. 1977, St.Mandé, France.

[4] Schanda, E., Hofer, R., "Microwave Multispectral Investigations of Snow", Proc. 11th Internat.Symposium Remote Sensing of Environment, 601-607, (1977), Ann Arbor, Mich., USA.

[5] Hofer, R., Schanda, E., "Signatures of Snow in the 5 to 94 GHz Range", in press: Radio Science (1978).

[6] Hofer, R., Good, W., "Snow Parameter Determination by Multichannel Microwave Radiometry", submitted to: Remote Sensing of Environment, (1978).

[7] Meylan, P., Musy, A., Morzier, C., Wyssen, D., Hofer, R., "Etude de la Variation Spatio-Temporelle de l'humidité du Sol par Télédétection", Proc. Colloque Internat. L'Observation Spatiale de la Terre et la Gestion des Ressources Planétaires, 6 - 11 March 1978, Toulouse, France.

[8] Good, W., Langham, E.J., "Erkennung und Parametrisierung geometrischer Strukturen von Landsat-Bildern", Informatik Fachberichte, 8, (1977), Springer-Verlag Berlin.

THIS PAGE

WAS INTENTIONALLY

LEFT BLANK

DETECTION AND MONITORING OF WATER HYACINTH (Eichhornia crassipes) INFESTATION IN LAGUNA DE BAY THROUGH MULTISPECTRAL DIGITAL ANALYSIS OF LANDSAT IMAGERIES

Ricardo T. Biña, Robert Jara, Ernesto Lorenzo, and Benjamin de Jesus, Jr.

Natural Resource Management Center
Visayas Avenue, Diliman, Quezon City
Republic of the Philippines

ABSTRACT

In an effort to determine the potential of LANDSAT data in the detection and monitoring of water hyacinth (Eichhornia crassipes) infestation in Laguna de Bay, the Natural Resources Management Center conducted initial studies to find out what information are obtainable from LANDSAT data, in preparation for LANDSAT C Program. Preliminary results indicate that a number of information vital in the management of water hyacinth infestation such as patterns of distribution, density estimates, area coverage, etc. can be obtained from LANDSAT data through visual and digital analysis using the Image 100 System.

INTRODUCTION

Infestation of water hyacinth (Eichhornia crassipes) is a major environmental problem in several areas of the lake, Laguna de Bay. They are not only navigational hazards but in several cases cause fouling of water resulting in the death of aquatic life including several tons of milkfish which are commercially cultured in fishpens along the lake shores. Effective control and management of this pest require several data input which include: (1) standing stock (2) productivity rate (3) areal and temporal distribution (4) dispersion pattern (5) areas of rapid growth (6) extent of damage. To obtain these information necessitates extensive survey of the entire lake as well as periodic monitoring. Due to the extensive size of the lake (c.a. 91,136 has) such undertaking would entail a considerable manhour input and huge financial costs if done through conventional ground survey methods and aerial photography. The use of LANDSAT multispectral data as a cost-effective and economical substitute method for obtaining certain levels of information is well known and proven. With the recent acquisition by NRMC of facilities for the digital processing of LANDSAT data, (Image 100 System) plans are now being prepared to make use of the forthcoming LANDSAT C Program for the monitoring of water hyacinth infestation and other relevant environmental problems in Laguna de Bay. Prior to this, a study was conducted to evaluate and assess the effectiveness and potentials of LANDSAT imageries and interactive digital analysis techniques in obtaining the various information enumerated above. This paper reports on the results of the said investigation.

METHODOLOGY

Only two LANDSAT computer compatible tapes representing overpasses in December 1972 (LANDSAT 1) and April 1976 (LANDSAT 2) were available for this study. Video observation of the two LANDSAT scene overviews revealed anomalous features over the lakewater area which are particularly prominent in the near-infrared bands (MSS 6 and MSS 7). In the 1972 3-band composite imagery (Fig. 1) the said anomalous features appear as high-reflectance line with lateral striations extending for approximately 25 km. along the eastern shore of West Bay and as high-reflectance circular and undulating line with striations in the East Bay. In the 1976 imagery (Fig. 2) such anomalous features appear as high-reflectance solid mass right on the eastern shorelines of the West Bay and as high-reflectance circular and polygonal solid mass in the East Bay. Collation of secondary information and available aerial photographs of Laguna de Bay confirmed the suspicion that these anomalous features are water hyacinth massed along the boundaries and within the fishpen areas. To study these features in detail, four subscenes, each measuring 480 X 480 pixels, were extracted from each CCT to cover the entire lake. Each subscene area was read directly from the CCT into the Image 100 refresh memory where the digital data are transformed into video display of a 3-band false color composite imagery. Video image enhancements were performed by digital contrast stretch of near-infrared bands and by ratioing processes. Using the enhanced imageries as guides, the spectral signatures of water hyacinth masses were obtained by cursor-training of infested and non-infested areas in the video display and reading their four MSS band gray level values via the single cell and N-cell signature acquisition algorithms. By comparing the spectral histograms of the infested and non-infested areas, spectral parallelepiped cells associated with water hyacinth masses were identified. Another digital program enabled each pixel with water hyacinth-associated parallelepiped cell to be displayed in the video, color-coded. The result is a video display of color-coded infested areas. Level slice of MSS 6 and MSS 7 produced five color-coded categories within the infested areas. Video-halftone and alphanumeric theme prints were produced from the video display and evaluated against available ground information.

RESULTS AND DISCUSSIONS

Video and hardprint analyses of processed imageries reveal a potential number of useful information on water hyacinth infestation not readily available via conventional methods. Inspection of the enhanced imagery (Fig. 3) shows patterns of distribution of water hyacinth, indicating areas of high and low infestations as well as extent of areal damage to fishpens. Given a repetitive coverage over a time period, the point of origin, movement pattern and areas of high productivity can easily be determined. Likewise, such occurence of infestation can be correlated with gross water quality changes which can be digitally mapped out. Using spectral signature acquisition algorithms, the characteristic low gray level values of non-infested water on near infrared bands (Table 1) can be exploited to pinpoint any emerging infestation even if such is not visually detectable in the imageries. Since the pixel-band gray level values are radiometric averages from one-half hectare of land per water surface, the fluctuations in the four-band spectral signatures of water hyacinth masses are interpreted as a function of plant density (plant cover per unit area) and variations in water quality. This is indicated by the inverse relationships between the visible bands and near-infrared bands (Fig. 4) where areas of high infestation manifest low gray level values for MSS 4 and MSS 5, and high gray level values for MSS 6 and MSS 7 and vice-versa. Using various digital programs available in the Image 100 System, pixels containing the same gray level values for MSS 6 and MSS 7 can actually be mapped out, color-coded, and the total area occupied automatically computed. With real-time ground sampling, it is possible to correlate MSS 6 and MSS 7 gray level values with plant cover and biomass so that the total standing stock and subsequently the productivity rate could be estimated.

CONCLUSION

An investigative program featuring the above analytical schemes is presently being planned to be executed in real time in conjunction with LANDSAT C coverage in 1978. To be included in this investigation is the determination of the relationship between MSS 6 and MSS 7 gray level values of water hyacinth which at present is being hypothesized as manifestation of growth and morphological variations among these plants.

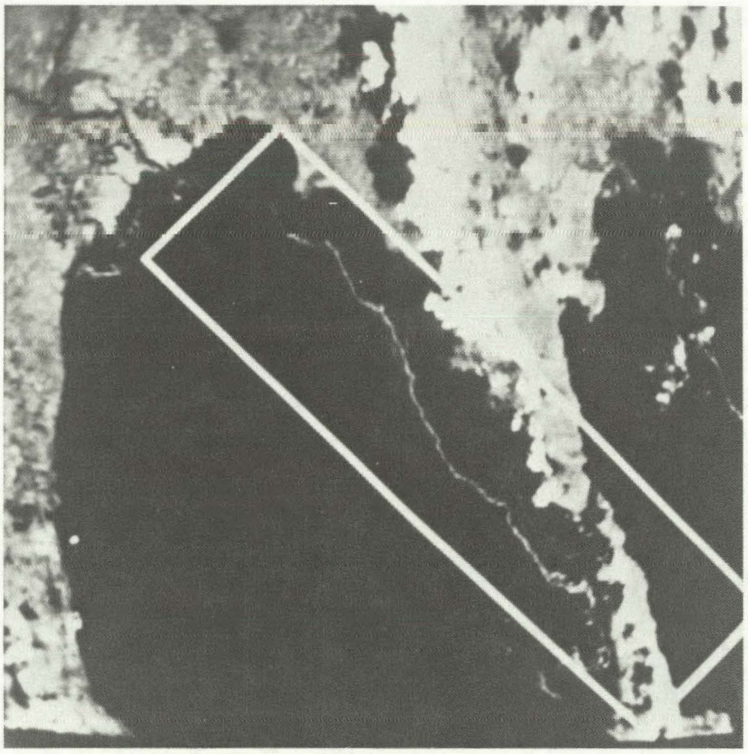

Fig. 1. Three-band composite imagery showing water hyacinth infested areas in Laguna de Bay (LANDSAT Scene No. 1153-01463).

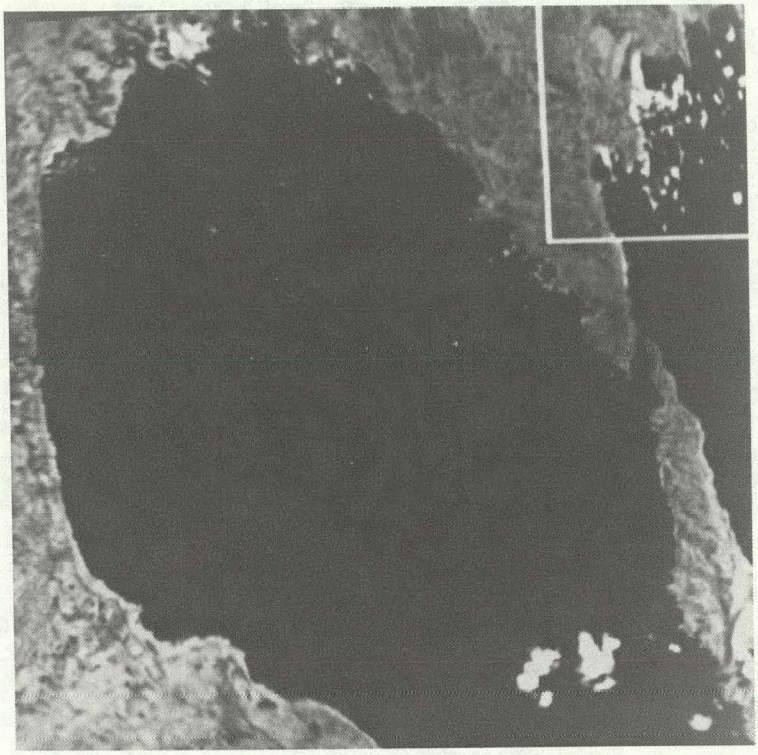

Fig. 2. Three-band composite imagery showing water hyacinth infested areas in Laguna de Bay (LANDSAT Scene No. 2455-01294).

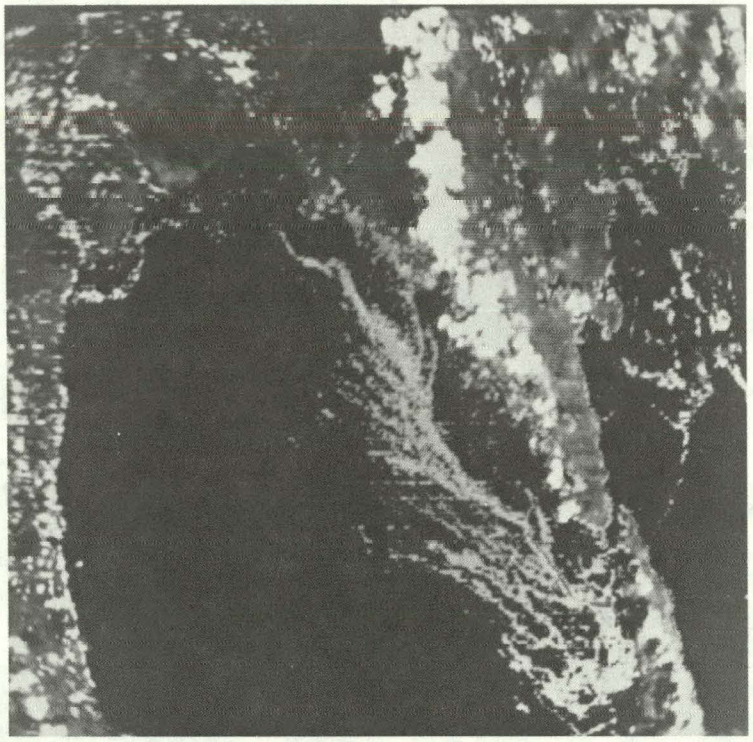

Fig. 3. Spatial patterns of distribution of water hyacinths on an enhanced three-band composite imagery.

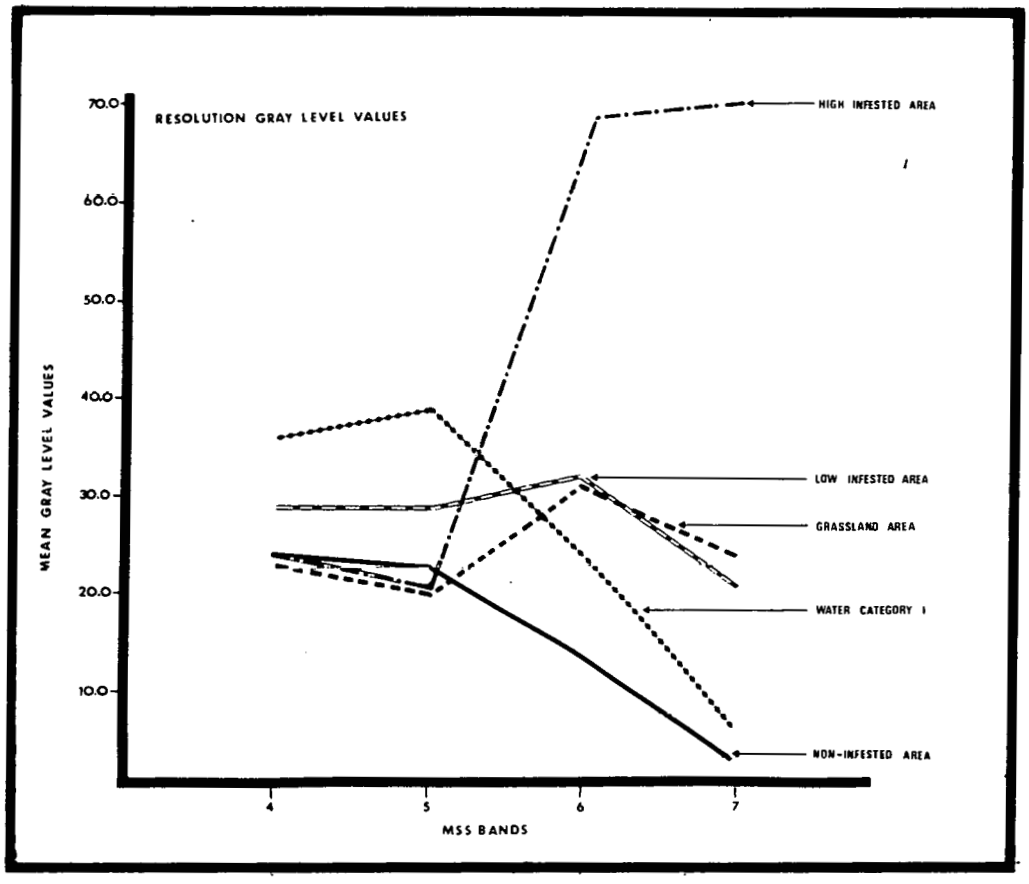

Fig. 4. Relationship of the mean gray level values of high-infested area, low-infested area, water category 1, non-infested area, and grassland area.

Table 1. Mean spectral signatures of water hyacinth infestation in Laguna de Bay.

CATEGORY	CLASSIFICATION	BANDS	1972 DATA SPECTRAL LIMITS	1972 DATA MEAN VALUES	1976 DATA SPECTRAL LIMITS	1976 DATA MEAN VALUES
1	Highly Infested Areas	4	34 - 43	37.0	21 - 28	23.5
		5	22 - 31	27.1	17 . 25	21.4
		6	25 - 36	29.9	58 - 99	69.5
		7	13 - 24	19.6	50 -100	69.7
2	Low Infested Areas	4	34 - 43	37.5	28 - 33	29.5
		5	22 - 31	27.1	27 - 32	29.3
		6	20 - 36	26.0	21 - 38	32.2
		7	10 - 34	18.8	16 - 28	21.1
3	Water Quality 1	4	40 - 43	41.2	32 - 35	39.0
		5	28 - 32	29.6	30 - 37	33.3
		6	17 - 20	19.0	17 - 24	20.2
		7	8 - 10	8.9	4 - 6	5.0
4	Water Quality 2	4	42 - 50	44.3	34 - 39	36.1
		5	33 - 39	33.8	38 - 43	39.5
		6	19 - 28	21.8	21 - 28	24.9
		7	8 - 14	10.7	4 - 10	6.0
5	Water Quality 3	4	37 - 40	38.6	28 - 32	29.0
		5	26 - 29	27.2	26 - 30	28.5
		6	15 - 19	16.8	11 - 18	15.9
		7	6 - 10	7.1	0 - 4	3.2
6	Coastal Waters	4	32 - 36	34.8	21 - 26	23.9
		5	22 - 28	25.2	20 - 27	22.9
		6	17 - 28	20.0	11 - 24	14.0
		7	4 - 10	10.7	2 - 6	3.3
7	Non-Infested Area	4	33 - 38	36.2	25 - 31	28.9
		5	22 - 28	25.9	28 - 35	30.4
		6	11 - 15	13.8	18 - 25	20.1
		7	0 - 6	4.6	2 - 8	5.1
8	Grassland	4	28 - 32	29.9	22 - 26	23.0
		5	18 - 22	20.5	18 - 22	20.6
		6	15 - 30	24.3	15 - 45	30.9
		7	8 - 30	20.3	8 - 42	23.7

LANDSAT INTERPRETATION FOR DEVELOPMEMT STUDIES

J. W. Trevett

Hunting Technical Services Limited
Borehamwood, Herts., England

INTRODUCTION

This paper outlines the experience of Hunting Surveys Limited, Hunting Geology & Geophysics Limited and Hunting Technical Services Limited who together form the main division of Hunting Surveys and Consultants Limited. These companies are engaged upon conventional mapping, geological and geophysical prospecting and land and water resources consultancy.

The majority of projects that are undertaken are for development studies or in developing countries, frequently existing maps are out of date, poor or non-existant, while air photography is equally unavailable or too expensive to acquire for the specific project.

Since its introduction LANDSAT has found a firm place in the data sources used by the companies, hardly a project is now undertaken that does not use the imagery in some way and some of the projects are wholly based upon the use of various forms of remote sensing.

It is not suggested that any of the methods used are new advanced techniques, rather they are a practical application of LANDSAT for conventional use and show how, without recourse to computer based technology, the imagery can still provide invaluable information.

As a conclusion some comments are made about more advanced technology and its application to development studies.

PLANIMETRIC MAPPING

The term planimetric is used specifically here since without stereoscopic cover LANDSAT can never be used to provide contour information.

LANDSAT provides a synoptic view over a very large area, because of the height of the satellite, distortion due to terrain is minimised and the scale distortions on the projection used mean LANDSAT provides an aothographic first base map.

Its use for map production largely depends upon the ultimate use of the map itself. If precise planimetric mapping is required, conventional mapping from air photographs still provides the most detailed data source for larger scales (above 250,000). For use by thematatic mappers however it is an ideal mapping medium for planimetric detail.

This does not mean that LANDSAT cannot play a role in more detailed map, it can and does. Conventional air photography has to be related to a second survey data base if it is to be used for anything other than reconnaissance mapping. In many areas access is difficult and the cost of providing additional survey data is high, if the existing survey data could be supplemented by other accurate locational control this would reduce the time and expense involved in field survey for photogrammetry.

Such an application occurred in a project in the Sultanate of Oman where

the shape of the land area, the disposition of available field-surveyed control points and the pattern of photographic flying made traditional photogrammetric methods of block adjustment unsatisfactory for certain areas. The decision was made to use LANDSAT imagery to provide the additional control required and accordingly the LANDSAT images were enlarged and scaled to fit identifiable field-surveyed points and a mosaic made fitted to this control.

The completed map was constructed from air photographs picking up the known control points and scaling to fit additional identifiable detail on the LANDSAT mosaic. The result is a detailed map produced at 1:100,000 scale completed with a saving in time and expense but showing more detail than would have been possible from the LANDSAT alone.

A less obvious but equally invaluable use of LANDSAT has been in the planning and execution of flying airborne surveys whether photographic or for geophysical sensing. In remote, poorly mapped areas, accurate navigation, is all too often a problem. It has been known for the aircrews to fly the wrong area because of poor control data and lack of ground detail.

LANDSAT images, are used to mark accurately the area to be surveyed and in desert regions the general tonal changes provide the navigator with recognisable features that can be used to chart the flight lines. By checking the rush prints produced in the field with imagery a rapid check of cover can be accomplished.

Similar techniques are applied to geophysical surveys and the flight lines can be plotted reliably onto the LANDSAT image, the synoptic view also assists the geophysicist with the final data interpretation.

A contract carried out in Southern Sudan illustrates how LANDSAT can be used to provide a high grade revision of an existing map series.

The 1:250,000 maps of Sudan are the only large scale data source available for much of the country. They are excellent maps considering the date they were surveyed and the conditions under which they were produced. Most of the data was supplied at the turn of the century being compiled from camel traverses by a number of explorers and British Army personnel. As a piece of mapping history they are unique; as a basis for planning and implementing extensive development schemes they leave much to be desired.

To re-map the vast areas concerned would be a major undertaking requiring a number of years to complete and the urgent need is to provide additional use of resources for immediate benefit to the people concerned.

Using LANDSAT imagery a major survey was carried out covering an area of 200,000 square miles dominated by the river Nile and the vast plains which have little outcropping geology.

The project was remarkable for the vast area surveyed in a short period and also for the use of an integrated system of satellite imagery, aerial photography, Doppler and Toran which was used to overcome extraordinary navigation problems.

An example of the comparison of the existing 1:250,000 map and that mapped from the LANDSAT show how an area where only a minor drainage pattern was previously shown with some vague references to swamps, in fact contains a complex drainage pattern (Figure 1). This information alone could have a significant influence on the selection of an area for possible agricultural development.

It is interesting to note that the Bahr el Ghazal shown on all maps as a tributary to the Nile and a supplementary contributing source to that river, is in fact a loop from the Nile and all the drainage in that area is using water derived from the Nile and eventually returned to that river.

FIGURE 1

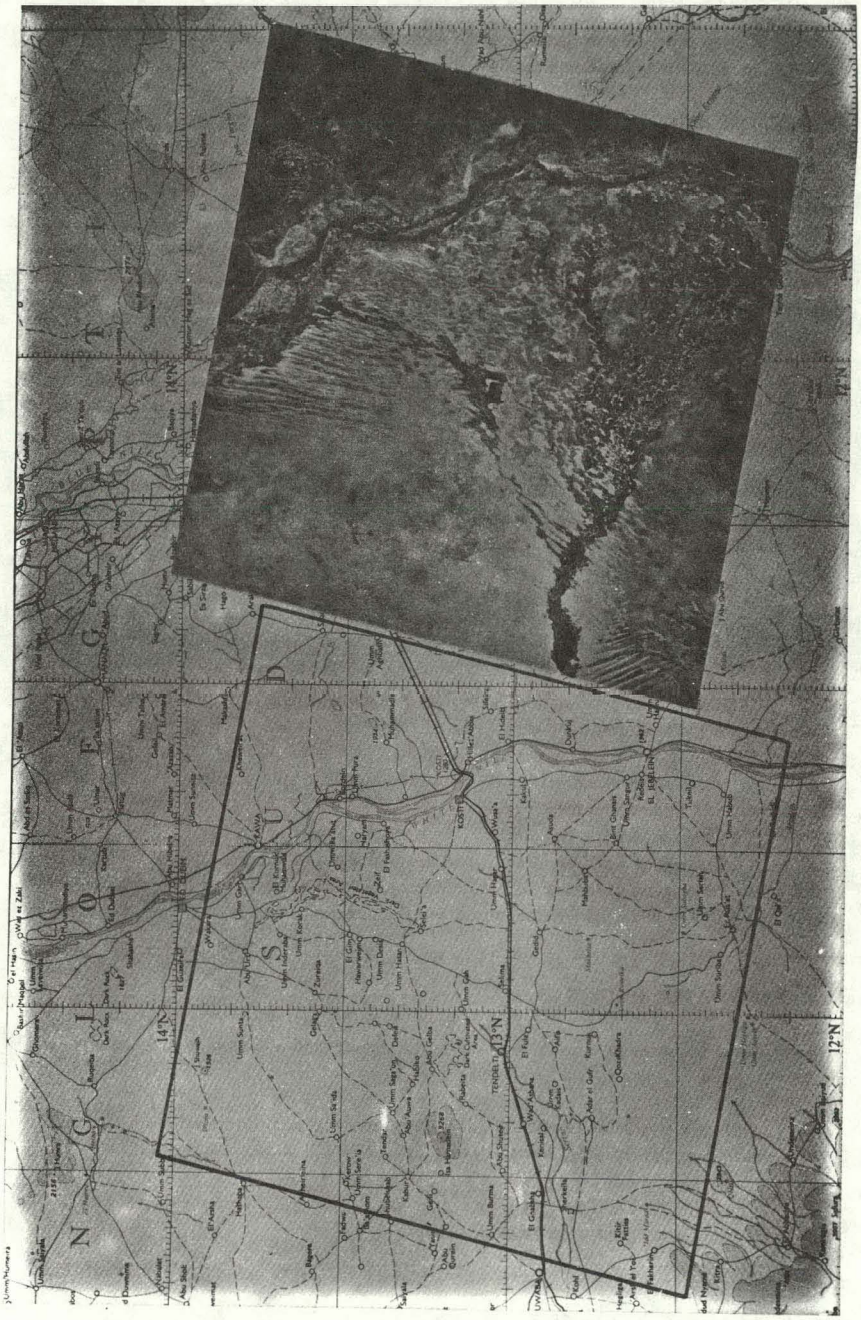

A comparison of the Landsat image with an existing 1:250,000 map, Sudan.

As a result of work in Sudan, LANDSAT imagery is always used by Hunting companies to check existing map reliability before commencing a survey.

GEOLOGICAL AND GEOPHYSICAL MAPPING

The previous section has already indicated how LANDSAT imagery is used to assist geophysical surveys.

The imagery has also been used for a number of important geological studies. Perhaps one of the most striking examples of how data from LANDSAT interpretation can add vital information to conventional surveys occurred in Ethiopia.

Before LANDSAT imagery became available a geological mapping project had been undertaken in Northern Ethiopia, the mapping was based upon interpretation of air photography and compiled onto mosaics constructed from these photographs. When LANDSAT became available an exercise was carried out to compare the interpretation of the imagery with the previous interpretation.

The synoptic view of LANDSAT revealed significant structural trends which had been masked on the air photos due partly to the limited view of each print but also attributable to the small directional errors and distortions introduced by the effect of severe terrain on mosaicing.

As with all earth science surveys a strong reliance upon field work to identify formations and confirm possible mineralisation, the situation is not expected to change where detailed surveys are concerned.

LANDSAT does provide an overview of a region enabling structural trends to be identified and significant geological features to be identified.

From the initial interpretation the most effective field study programme can be identified, routes are planned and sampling sites identified.

A great deal of work has been carried out in making an interpretation of the potential of a region based upon the analysis of linears. As has been described, LANDSAT with its broad overview, can reveal linear trends that would otherwise be missed and the directional trends of all linears plotted with greater reliability.

LAND AND WATER RESOURCES

Land resources in this context is taken to include land use, vegetation, geomorphology, forestry and soils.

Such is the value of LANDSAT for these studies that no project in these disciplines is undertaken without examining the imagery, where it exists, as an essential part of the survey.

The value of LANDSAT as a base map has already been highlighted, nowhere is this of more significance than in land and water resource studies.

In the first instance as a total record of a countries surface features it is used to identify areas with a high potential for development and to eliminate those areas which for reasons of terrain, accessibility or other factors should not be considered for development study.

In early resources studies, projects for development were viewed in isolation, that is as a pocket or area of land which could be developed without considering its impact on the total region.

Recent development studies tend to be on a regional basis. Agricultural or other development is seen as part of a total plan for developing or controlling

FIGURE 2

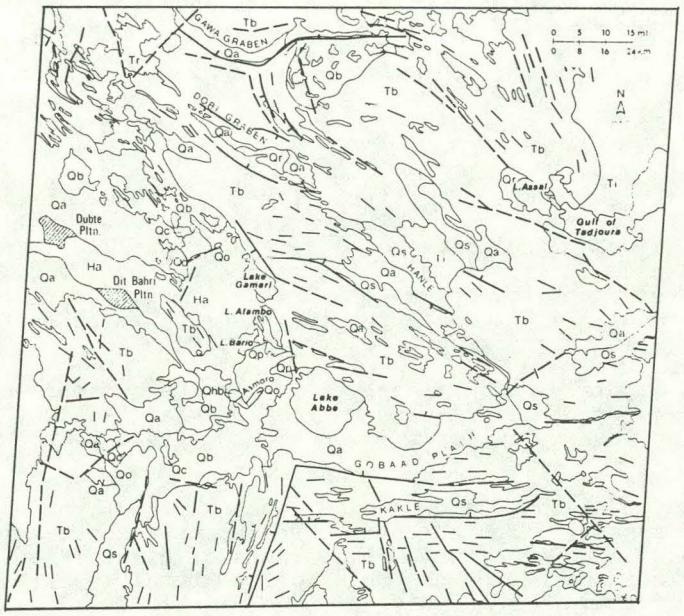

—+— Rift-type faulting, with downthrown side indicated where known

— — Linears indicating regional faulting — Short linears indicating joints and local faults

PLEISTOCENE AND HOLOCENE

Ha—Holocene sands, silts and clays.
Qa—Holocene and Pleistocene sands, silts, clays, conglomerates, reef limestones.
Qc—Recent basalt lava.
Qr—Evaporites, mainly salt pans.
Qs—Fans, screes and outwash plains.
Qb—Basaltic lava flows and related spatter cones.
Qo—Siliceous domes and pyroclastic flows; rhyolites, pantellerites, obsidians.
Qp—Picritic basaltic flows and related spatter cones.
Qhb—Hyaloclastite ash rings.

MIOCENE

Tb—Stratoid basaltic lavas affected by tectonics.
Tr—Lava flows and domes; predominantly rhyolitic. } Afar Group
Ti—Complex unit of ignimbrites and pumice.

Sources: Photogeological Map of the Southern and Central Afar compiled by Ceri James. 1972. U.N. Ethiopia Geothermal Survey.
Geological Map of Ethiopia compiled by V. Kazmin, 1973

Photogeological map of Central Afar, Ethiopia compiled from ERTS imagery.

From D.E. Parry's paper (Photogrammetric Record 8(43): 65-80 (April 1974)

a larger area. The need to conserve areas of natural vegetation, to preserve river catchments and landscapes or wildlife, and to view the impact of development on the general ecology of a region are all taken into consideration.

To see development in this wider context requires a broader total view of a region. In many countries LANDSAT provides this broad overview of the total resource base so that development can be seen in the context of total impact on the surrounding region.

A National Cropping Plan survey was carried out in 1975/76 for Iran where two major problems were revealed.

In the first instance the statistical returns showed the total amount of land under agriculture, but nowhere was it recorded where all this developed land occurred. The major agricultural zones were of course well known, the area along the Caspian coastline, a large irrigation project near Tehran and the Desful basin development for instance. This still left a significant acreage unaccounted for and if a National Cropping Plan was to be devised it was essential to know where other agriculture existed.

To order a complete national survey by air photography would have been time consuming and prohibitively expensive, fortunately cloud free LANDSAT cover of all Iran was available and even without enhancement, vegetated areas showed up clearly.

Interpretation of the 250,000 colour composites of the whole country revealed that the remaining agricultural development existed as valley bottom strips in the hills and numerous small pockets of cultivation scattered across a wider area. Thus apart from the major agricultural areas, all other agriculture consisted of small, isolated schemes unsuitable for development or extension and LANDSAT supplied the first reliable location of these areas.

The geomorphology of Iran is such that it forms a natural drainage basin to the centre of this country with no proper drainage outlet. One of the most significant geological formations in the region is the FARS formation which form extensive salt bands in the surrounding hills. The total result is an evaporation basin for water already charged with salt to form large saline lakes and salt affected soils.

These salt pans are continually being replenished and extended, any planned development must take into account the salinity problem and areas that are saline or could become saline in the future, have to be avoided. The geological maps showed the location of the FARS beds, hydrological information provide data on the salinity content of rivers and the existing soils map showed the extent of saline soils at the time of survey. What was required was an assessment of the spread in salinity since the soil survey was made and how it related to the geology and geomorphology.

The saline soils showed up clearly on the LANDSAT imagery so the extent of these areas was mapped as accurately as possible and the interpretation compared with the soil survey data. Where no changes had taken place the correlation of the two boundaries was very close, where salinity had increased the new areas could easily be identified. These new or extended areas tied in with the spread that could be expected from the geology and hydrology.

No attempt was made to grade salinity since any form of salinity ruled out an area for development.

As part of the final map series, a map was produced showing the saline areas fromthe soil map, the FARS beds and the comparative salinity of streams together with the new saline areas identified from LANDSAT.

The LANDSAT work carried out in the Sudan has already been referred to for other purposes. Hunting Technical Services have a number of major projects for land and water resources studies in the Sudan and all have made extensive use of the LANDSAT imagery in the field, in one area a study was being made which included recommendations for cattle centres, fattening lots, water points, marketing etc. All the cattle farming in the region is nomadic herds and it was required to map current watering points, migration routes and to assess the vegetation available for increasing the cattle population.

The LANDSAT imagery was used to map the total drainage pattern over the project area, to identify existing watering points and main migration routes and the principal vegetation units. The interpretation was used for a preliminary assessment of development potential and to plan the subsequent detailed field studies.

HTS through its partnership with an engineering consultancy are one of the two partners forming Groundwater Development Consultants who are currently employed on a project covering a large part of Saudi Arabia to study the groundwater potential of the region and the possibility of areas suitable for agricultural development that could be supplied by any groundwater.

In such a barren area the maps cannot show much detail and dune patterns or tonal changes may be the only features by which to locate field positions.

Colour composites of LANDSAT imagery are again providing a vital information base and being used to identify areas of potential which would benefit from a more detailed soil survey, to plan field work, for navigation, and a base for the land survey teams, for flight control on air surveys, to assist the hydrogeological interpretation and its application in the location of offshore fresh water springs is being investigated.

The projects so far described are all in arid regions and it may appear that LANDSAT is only of use in such areas. This is only in so much as cloud free cover more readily exists for these areas, in other regions where there is almost continuous cloud cover, LANDSAT has less application although some cover is now available of most areas.

LANDSAT imagery was used in Southern Thailand to help locate areas of smallholder rubber and oil palm cultivation, it also provided essential data on the extent of logging in the forest areas. Interpretation is more difficult in heavy vegetation cover but a good interpreter with local field knowledge can still derive a great deal of useful data.

In Nigeria HTS have an expert working with the Federal Department of Forestry to interpret imagery of Nigeria and to train local staff in remote sensing. Results so far achieved show that by conventional interpretation it is possible to map the main vegetation zones, to identify forest reserves and more important to be able to identify reserves that are being illegally logged or are under pressure from agriculture.

FUTURE APPLICATIONS

All the projects so far described have used LANDSAT imagery in its straight forward photographic form, not the computer enhanced product nor digital analysis. In general the only equipment used has been a large hand lens although more recent work, in the last 12 months, has used the I^2S mini-adcol colour additive viewer.

As a general policy all the earth scientists employed on projects are expected to familiarise themselves with the use and interpretation of LANDSAT.

By using imagery in this mode both in the office and in the field on projects, they have become familiar with and respect its potential. The projects

demonstrate how a great deal of very useful information can be extracted from this photographic LANDSAT product, information that can greatly assist resources surveys and development planning.

The companies have kept a close watch on the developments being made in digital analysis and are now employing these techniques more and more on projects that would benefit from its use.

To have introduced the techniques earlier could well have meant bringing in a specialist team, such a team would have ignored the vast potential of knowledge and experience already with the field staff and probably not have gained the confidence of these staff in the product.

All the staff have now become interested in the potential of LANDSAT and are ready to move to the next phase of development. When full digital analysing techniques are installed the same policy will be followed with all staff operating the equipment for their own projects.

The future usage of LANDSAT will no doubt rely heavily upon digital analysis if only for the basic reason that there will be no other way to handle the amount and variety of data available. Many of the experimental and standard techniques developed for regions with distinctive signatures such as the LACIE project for the major wheat areas, will find applications in the more complex land use regions of the world. The companies are using digital analysis and computer based systems and are looking to such techniques to extend their services for development studies.

Perhaps the most important future use of satellite imagery in development studies will be for monitoring. Irrigation projects rely for their success, on the controlled use of water; too much water applied in some areas could raise the water table and eventually turn the fertile land into a swamp or a saline pan, too little and cultivation will drop in yield or fail completely. Agricultural returns are notoriously inaccurage especially in developing regions where farmers are suspicious of the use of the returns and fear taxation reprisals. Regular satellite imagery over an area with continual comparison of seasonal results could monitor the use of water, possible seepage from canals, the advent of salinity and provide support information on crop returns and maybe yields.

For regional development the use of monitoring increases, illegal logging of forest reserves, erosion hazards, crop diseases, extent of disaster damage from floods, fires, hurricanes etc. When the success of a development project is often finely calculated and dependent for its success upon careful use and management of resources, a regular imaging system for monitoring, independent of human influence has obvious advantages.

The present LANDSAT has the disadvantages of non-penetration of cloud cover, for many development areas the future will look to the development of a satellite borne land imaging radar system. It is hoped that experiments based upon Seasat will provide some indication on how efficient such a system would be.

The basic use of LANDSAT imagery for development studies is seen as an additional data source for earth scientists and our policy has been one of use by the earth scientists involved in the project and not an interpretation by head office specialists. In this way the experience of the staff is utilised but more important the same staff engaged upon the interpretation carry out the subsequent field checking. Ground truth or field checking has always been an important part of any interpretation study and the value of LANDSAT interpretation is increased many times by this operation. LANDSAT or any other imaging cannot be a substitute for field studies, it may be possible, for example, to identify vegetation changes but only field work will identify the species involved.

In short satellite imagery is not a panacea for all mapping problems for development studies but it is a highly useful tool in the armoury of the practical earth scientist. Furthermore, although digital analysis is essential to release the full potential of the data obtained, development studies can still be carried out and derive great benefit from the use of the standard photographic product.

THIS PAGE

WAS INTENTIONALLY

LEFT BLANK

THE TEN-ECOSYSTEM STUDY: LANDSAT ADP MAPPING OF FOREST AND RANGELAND IN THE UNITED STATES*

Edwin P. Kan

Lockheed Electronics Company, Inc.
Systems and Services Division
Houston, Texas

F. P. Weber

U.S. Department of Agriculture
Forest Service
Houston, Texas

ABSTRACT

The Ten-Ecosystem Study was designed to assess the maximum information content of Landsat data and its utility for large area classification using a uniform technical approach on the 10 generalized forest and rangeland ecosystems of the United States. Conclusions on the feasibility of using Landsat remote sensing automatic data processing methods, selecting the best seasons, analyzing costs and the effects of site complexity, miscellaneous analysis, problems, and recommendations were derived from 2 years of study, the project being three-fourths completed.

1. INTRODUCTION

The Ten-Ecosystem Study (TES) was designed to uniformly assess the utility of Landsat remote sensing technology when tested on forest and rangeland classifications over 10 broadly defined ecosystems in the 49 continental United States [1]. Using a unified automatic data processing (ADP) approach, one site from each ecosystem was studied. This repetitive endeavor permitted a systematic, uniform comparison between site analyses and a summation of the overall feasibility conclusions.

Much diversified research [2 through 9] on Landsat remote sensing applications has been conducted in the past, resulting in general and specific conclusions. However, these conclusions are difficult to compare because investigators used different ADP schemes and different evaluation techniques and operated under various time and resource constraints. Conclusions were obtained on forest and rangeland type mapping accuracies, areal measurement accuracies, mapping by administrative boundaries, single-date and temporal analyses, registration accuracies, utility of preprocessing and postprocessing, and other techniques. TES was designed to generate similar conclusions in a uniform mode such that they could be assessed across the different ecosystems of the United States.

In TES, multiple study sites were investigated in two analysis modes using the same ADP system; the analysis results were evaluated using the same statistical sampling scheme; and the analyses were performed under the same time and resource constraints. The design of the two analysis modes, the type separability study and the simulated inventory study,† reflected the time and resource constraints that were placed on any operational environment. The former study investigated the maximum information content in Landsat multispectral scanner (MSS) data;

*This work was performed under the National Aeronautics and Space Administration Contract NAS 9-15200 at the Lyndon B. Johnson Space Center, Houston, Texas, in cooperation with the U.S. Department of Agriculture, Forest Service.

†The phrase "simulated inventory" was used to connote the operational environment where resources such as time, manpower, and ground truth were limited. In this analysis mode, MSS data classification was performed; no actual ground inventory was made.

the latter study investigated how well ADP techniques could extend limited ground truth over large area mapping efforts.

For the study, the 49 continental United States were divided into 10 generalized forest and rangeland ecosystems: (1) Coastal Range and Rocky Mountain Conifers, (2) Northern Hardwoods, (3) Northern Conifers, (4) Chaparral-Pinyon-Juniper, (5a) Oak-Pines, (5b) Southeastern Pines, (6) Boreal, (7) Rangeland, (8) Pacific Coast, and (9) Central Hardwoods (fig. 1). This classification is a generalization of the Shantz and Zon classification [10] and is more general than the 43-ecosystem classification given in the Resources Planning Act Assessment [11]. The decision on such a classification and the choice of the study sites within the ecosystems were made by the study sponsors, the U.S. Department of Agriculture (USDA), Forest Service and the National Aeronautics and Space Administration (NASA).

The TES is a research project of the current Nationwide Forestry Applications Program, a cooperative USDA, Forest Service and NASA program performing and sponsoring research and development on advanced remote sensing technology, and has been performed at the Earth Observations Division at NASA/Lyndon B. Johnson Space Center (JSC). Completion of TES is expected by September 1978.

2. TES PROJECT DESIGN

2.1 OBJECTIVES, SCOPE, AND STUDY SITES

TES was designed to uniformly assess the information content of Landsat MSS data and to uniformly assess the success of Landsat classification over large areas, to arrive at an integrated set of feasibility conclusions on Landsat MSS ADP remote sensing as applied to the forest and rangeland ecosystems of the 49 United States. Secondary objectives include establishing the best seasons for ADP analyses, identifying ADP analysis problems and solutions for site-specific problems, and transferring the technology to users, such as the USDA, Forest Service.

One site from each of the 10 ecosystems (fig. 1) was studied. Each site covered either one complete county or a 60- by 60-kilometer (37- by 37-mile or 900 000-acre) area, whichever area is smaller.[1] Classification accuracies at two analysis levels (section 2.2), classification maps, and statistical tabulations were summarized by administrative units.

In TES, Landsat MSS data were used as the mapping data base. Aerial photography (primarily NASA high-altitude flight 1:120 000-scale color-infrared photographs), a site familiarization field trip plus published literature, and personal knowledge from Forest Service foresters resident at or near the sites were used as supplementary information for data analysis.

The study sites chosen to represent the 10 ecosystems (fig. 1) are (1) Grand County, Colorado; (2) Warren County, Pennsylvania; (3) St. Louis County, Minnesota; (4) Sandoval County, New Mexico; (5) Kershaw County, South Carolina; (6) Fort Yukon, Alaska; (7) Weld County, Colorado; (8) Grays Harbor County, Washington; and (9) Washington County, Missouri. The fifth site, Kershaw County, represented two ecosystems, Oak-Pines and Southeastern Pines; hence, only nine sites in 10 ecosystems. In some cases, the choice of these sites was influenced by current or recent remote sensing and inventory work performed at or near the sites. For example, the USDA, Forest Service had a 1977 spring survey in Kershaw County. The Bureau of Land Management was performing a remote sensing project in Alaska close to Fort Yukon, and the Forest Service was interested in the proposed Porcupine National Forest site at Fort Yukon. The Pacific Northwest Commission, Department of Natural Resources of the State of Washington and NASA were performing a remote sensing inventory project in Washington, including the Grays Harbor County area.

---

[1] A 60- by 60-kilometer area could be covered by four screens of Landsat data on the ADP system used by TES, the Interactive Multispectral Image Analysis System, model 100 (Image-100). Site sizes were thus limited after considerations were made on data throughput rates, machine time availability, and project time and manpower resources.

2.2 ANALYSIS MODES AND LEVELS

As a feasibility study, TES was designed to play two roles: (1) to perform a type separability study to determine the extent of forest and rangeland details obtainable from Landsat MSS ADP analysis and (2) to conduct a simulated inventory study to determine how successfully ADP technology can extend limited ground truth for large area classification.

The type separability study investigated the maximum information content in Landsat MSS data by deriving classification accuracies of training fields in the site. The identities of these fields were checked by previous field visitation, by reliable image interpretation, or by other information sources.

The simulated inventory study provided a better understanding of test accuracies by investigating the success of extending limited ground truth in large area classification. The analysis was constrained to the use of photointerpreted vegetation classes over a representative contiguous 10-percent area of the site; this portion was deliberately not field checked. Spectral signatures were then developed from this 10-percent area and were used to classify the entire 60- by 60-kilometer site.

The TES investigated two hierarchial levels (table I), which were modified from the classification system presented by Anderson [12]. Since the Level I forest, nonforest, and water features were aggregates of Level II features, they were not studied separately. In Level II, forest was categorized into softwood and hardwood, and nonforest was categorized into grassland and other. Level III analysis consisted of the discrimination between specific timber and grassland types and the distinction between census and noncensus water (larger or smaller than 16 hectares, respectively). The minimum width and size requirement was 1 picture element (pixel), approximately 60 meters, for all features. Analysis of mapping all land features, with a minimum 4-hectare size, was also attempted.

The softwood, hardwood, and grassland categories actually connoted more specific vegetation communities and associations because of the potential vegetation that specifically exists in each ecosystem. For example, in the Northern Hardwoods Ecosystem, hardwoods refer to beech, birch, and maple; in the Pacific Coast Ecosystem, softwoods refer to Douglas firs, western red cedars, and western hemlock (table II).

2.3 TECHNICAL APPROACH

This section discusses the analysis flow for each site, the manning configuration, the data, and the instruments used in TES [13]. Figure 2 illustrates the sequence of the six major tasks performed for each site analysis. Each task was scheduled for 6 weeks; hence, each completed site analysis took approximately 9 months.

2.3.1 PRELIMINARY ANALYSIS

The objectives of the preliminary analysis task were (1) to screen the available Landsat data to select the best two data sets for ADP analysis and (2) to gather specific information on the site and on the vegetation characteristics.

The first objective was met by a photointerpretation analysis of the Landsat imagery and available aircraft photographs, followed by a simple grid-dot evaluation and comparison between both interpretations. The mathematical measure used to select the best data sets was the probability of correct classification (PCC), which is based on the similarity of the dot classifications.

The second objective was met by collecting and studying literature on the site, by visiting the site, and by coordinating with forest experts resident at or near the site. Ancillary information included Forest Service maps, soil and geology maps, topographic maps, statistical summaries, and technical reports and papers.

2.3.2 PREPROCESSING

The preprocessing task consisted of (1) temporal registration of two Landsat images, (2) registration of Landsat data to a geographic map base, (3) registration and overlaying administrative boundaries (e.g., county boundaries) on Landsat data, and (4) analysis of Landsat imagery and aerial photographs for locating training areas.

The image-to-image and image-to-map registration processes included selecting control points, determining a least-squares-fit bilinear mapping polynomial, transforming one image to a base by nearest-neighbor mapping, rotating and rescaling the image, and composing the image and the base. The administrative boundaries were located via a coordinate digitizer and transformed and overlaid onto the Landsat data. Training field locations were either similarly digitized or cursored into the ADP processor during interactive online sessions.

2.3.3 PROCESSING — TYPE SEPARABILITY STUDY

This task was designed to determine the maximum Landsat MSS information content regarding the power to discriminate between vegetation classes at Level II and Level III.

All available training data were examined for their classification accuracies at Level II and Level III. A nonparametric statistical classifier was used in conjunction with a nonparametric maximum likelihood decision rule that resolved overlaps. The supervised classification method was used.

2.3.4 PROCESSING — SIMULATED INVENTORY STUDY

This task was designed to determine how successfully ADP technology could extend limited ground truth for large area classification. The amount of ground-truth data was limited in that the training signatures were developed from a representative 10-percent area of the site, with the aid of aerial photographs but without the benefit of ground checking.

By interactively developing the spectral signatures that best classified the 10-percent area, these signatures were used to classify the entire 60- by 60-kilometer site. The results were classification maps and area (proportion) summaries. These maps and statistics were then evaluated for their accuracies and precisions. Only Level II classifications were performed.

2.3.5 POSTPROCESSING

The output from this task consisted of classification map products in photographic and lithographic forms, in color separation or line-boundary formats, and at different scales and different resolutions.

A postprocessing computer algorithm [14,15] was developed to remap the classification maps to different resolutions. The present word "resolution" pertained to the minimum mapping size of each mapped unit. Prior to this postprocessing, each object in the classification map was at least 1 pixel in size. A 4-hectare minimum "smoothed" object size was used for all land classes; a 0.4-hectare size was used for noncensus water bodies and a 16-hectare size was used for census water bodies.

2.3.6 EVALUATION

The classification results from the simulated inventory study were evaluated for (1) classification map accuracy PCC, (2) area (proportion) accuracies for the Level II features, and (3) their utility as auxiliary information for improving area estimation from random sampling of photographic (or ground) plots.

To achieve these, random sampling units were drawn from the site classification map and compared with aerial photographs, which served as the source of ground truth. Two stages of random sampling were employed. The primary sampling units (PSU's), the first stage, were 50 by 50 pixels in size, a size which produced sufficiently good registration between the Landsat imagery and the aerial photographs. The secondary sampling units (SSU's), the second stage, were 2 by 2 pixels in size, which permitted proportion estimates on the photographs to be compared against the Landsat classification. The SSU locations were allowed to fluctuate plus or minus 1 pixel in all four directions to minimize the effects of misregistration residual errors and edge pixel effects [13].

Each SSU was evaluated for a correct and incorrect classification by a sum-of-squares criterion; the average of these decisions over all SSU's gave the overall classification map accuracy PCC.

Simultaneously, the proportions of each Level II feature were summed for each PSU and were tested for differences between the Landsat classification and the ground truth. To obtain the

accuracy of the ADP area summation over the entire site (the so-called naive estimate), the naive estimate was tested against the regression estimate. The regression estimate served as the ground truth over the entire site.

Regression analysis and regression estimates were performed to investigate the utility of a Landsat classification to improve areal estimation in a two-phase sampling scheme [16]. Areas could be estimated by random sampling aerial photographic (or ground) plots and expanding these estimates to the entire site. However, it was expected that Landsat data would reduce the variance of these estimates when used in a regression estimate, two-phase sampling model. The regression equation was obtained by analyzing the Landsat PSU classification against the PSU classification proportions on the photograph. Statistical tests of significance and calculation of the reduction of variance were performed.

2.3.7 REPORTING

A series of four reports was produced for each site. The first three were informal reports covering the first task, second and third tasks, and fourth and fifth tasks, respectively. The fourth and final report[2] was more formal and received NASA and Forest Service distribution.

An interim TES report has been published [17] and the final TES report is planned. An interim workshop was conducted in September 1977, and a final workshop is planned in September 1978 to present the results to NASA and the Forest Service.

2.3.8 MANNING CONFIGURATION

The execution of the six tasks for each site was scheduled in a staggered fashion so that the project's resources could be best utilized. For example, in the first 6-week period of the Site I, task 1 took place; in the second 6-week period, task 2 was performed for Site I and task 1 was performed for Site II.

A three-man team was the concept used in TES. The overall supervision of the six-task site analysis was assigned to an interdisciplinary site scientist. Overseeing the execution of a specific task was assigned to a specialized analyst. A general analyst, who relieved most of the routine work and who was rotated among the different sites and tasks, was assigned to each team.

2.3.9 DATA AND INSTRUMENTS

Landsat MSS imagery, aerial photographs, field information, and ancillary data were used. Landsat-1 and Landsat-2 MSS color composites and digital data on computer-compatible tapes were used. NASA high-altitude flight color-infrared photographs at scales of 1:60 000 and 1:120 000 were used as the main source of ground truth. Photographs acquired by other Government agencies were also used, when available, for auxiliary information. Field information was acquired via a field trip and the cooperation of the foresters resident at or near the site. Ancillary data consisted of maps, literature, statistical summaries, etc.

The ADP computer systems included the Image-100, Earth Resources Interactive Processing System (ERIPS), the Data Analysis Station, Univac 1108 and 1110 computers, and a NOVA minicomputer at NASA/JSC. The bulk of the ADP analysis was performed on the Image-100 System. Filming of classification maps was partially done with the electronic film recorder in the Data Analysis Station. Coordinate digitizing was done on a Dell Foster, model RSS-400, digitizer. Photointerpretation equipment consisted of a Richards light table, Bausch and Lomb Zoom Transfer Scope, an Old Delft scanning stereoscope, and other standard equipment. A hand-held, programmable electronic calculator, the Texas Instruments SR-52, was used extensively during the evaluation phase.

---

[2]These reports are titled "The Ten-Ecosystem Study (TES), Site (number), (county), (state), Final Report," published by Lockheed Electronics Company, Inc., in 1977 and 1978. The major authors and site scientists of these site reports were: R. D. Dillman (Site I), C. A. Reeves (Site II), J. E. Weaver (Site III), W. E. Parkhurst (Site IV), R. D. Dillman (Site V), J. F. Ward (Site VI), J. E. Weaver (Site VII), J. C. Prill (Site VIII), and W. F. Echert (Site IX).

3. SITE ANALYSIS AND EVALUATION SUMMARY

Tables III through VI summarize the important analysis results for the nine sites. (Blanks indicate that the data were not available at the time of publication.) Detailed tabulations and discussions can be found in the respective site reports.[3]

Table III lists the results of the type separability study, in which training fields were examined for the maximum Landsat information content; for the Landsat data which were chosen for ADP analysis; for the maximum Level II classification accuracies (the data sets are given in parentheses); and for the Level III accuracies between species and classes.

Table IV provides the evaluation results from the simulated inventory study. Level II classification was performed here. The overall classification map accuracy PCC, obtained from random sampling evaluation, is tabulated in the second column. The four columns under "mensuration" investigate the bias of the ADP area mensuration by checking random samples and the summation over the entire site. The last five columns discuss the two-phase sampling and regression analysis results, which infer the utility of Landsat analysis for use as auxiliary information to improve areal estimates obtained by simple random sampling of aerial photographic plots.

Table V is a simplistic cost analysis of the project. Only direct manpower, ADP equipment hours, and field analysis cost (the major contributors to the overall cost) were considered here.

Table VI presents some geometric parameter comparisons. It includes Landsat pixel size, as related to site latitude and elevation, and the precision of the image-to-image and image-to-map registrations.

4. DISCUSSION ON ANALYSIS RESULTS

This section analyzes the implications of the results from the TES for using Landsat data in large area forest and rangeland mapping; discusses the results pertaining to selecting the best seasons, costs and site complexity related to ADP analysis, and miscellaneous analyses; and discusses problems and recommendations. Note that these observations will not be conclusive until the project is completed in September 1978.

4.1 LANDSAT DATA INFORMATION CONTENT

The information in table III suggests that, with sufficient training information, Landsat could produce excellent Level II classifications but not consistently good Level III classifications in all ecosystems. For the major Level II classes, training accuracies were in the high 90 percentile.[4] For Level III discrimination between species or types, accuracies ranged from 9 to 98 percent.[4] The separation of water into census and noncensus water (greater than, equal to, or less than 16 hectares) was always achievable using the geometric discrimination method in ADP postprocessing.

No definite advantages of temporal classifications versus single-date classifications were apparent in Level II analysis. In fact, using the Image-100 nonparametric classifier on the training areas, all accuracies were very high and close to one another in the 90 percentile. Any increase or decrease in accuracies might be due to chance.

4.2 LANDSAT ADP LARGE AREA CLASSIFICATION

Four conclusions could be drawn on the simulated inventory study (table IV), which was constrained such that the spectral signatures were developed from a contiguous 10-percent area of the site without the benefit of field checks and were used in subsequent classifications of

---

[3] See footnote 2.

[4] The training accuracies seemed too high, especially in some Level III classifications. This could be attributed to the insufficient size of training data and to the idiosyncrasy of the nonparametric classifier on the Image-100 System.

the entire 60- by 60-kilometer site. This environment simulated operational inventory projects where resources and ground truth were limited. Only Level II classifications were performed. Classification statistics were always summarized by administrative units.

4.2.1 OVERALL CLASSIFICATION MAP ACCURACY PCC

The PCC provided a measure for test accuracies as compared to the training accuracies obtained in the type separability study. The PCC was obtained by a random sampling of the classification map.

For sites where the vegetation was homogeneous and occurred in large contiguous patterns, PCC's were in the high 80 percentile and above. Otherwise, PCC's as low as 70 percent were obtained.

As is inherent in any sampling results, the PCC's were provided with a confidence interval; a 0.9-confidence level was used. A maximum ±5-percent error was attempted with the upper limit of 25 PSU's (corresponding to an overall 0.1-percent sampling). This ±5 percent was not always achieved under the stated constraints; hence, a maximum ±6.1 percent was accepted.

4.2.2 MENSURATION

Another criterion of classification accuracy was the accuracy of area measurement. It is expected that if the classification is good the area measurement is normally accurate (but not vice versa).

Table IV shows that for well-classified sites (i.e., sites having a PCC in excess of 80 percent), the area measurements of major classes were obtained by ADP with insignificant biases. On the other hand, when the PCC fell below 80 percent, the major classes tended to be underestimated.

The TES statistical sampling evaluation method was considered appropriate because complete mensuration of the ground truth was not feasible and was too expensive. Random cluster sampling was used in TES with a maximum of 0.1 percent sampling, corresponding to 250 generic sampling units. Features that occurred in small proportions were not adequately sampled and were not evaluated.

The two tests performed under mensuration produced compatible results. The first test checked the bias of area proportions exhibited in random cluster samples. The second test compared the ADP naive estimate to the regression estimate, the regression estimate being considered as the truth plus or minus a precision. The ADP naive estimate was that number produced from ADP classification for a given class over the entire site. The regression estimate was a precise, two-phase sampling attribute that was derived from expanding and improving ground-truth sampled areas.

4.2.3 TWO-PHASE SAMPLING AND REGRESSION ANALYSIS

A two-phase sampling and a regression analysis were conducted to check the utility of a Landsat ADP classification for use as auxiliary information to improve areal estimates by random sampling of aerial photographic (or ground) plots. The data used here were those from the same cluster samples used in evaluating the classification map accuracy and mensuration. For example, the regression equation between softwood ADP proportion and the ground-truth proportion was developed and tested for significance. Then, by substituting the ADP naive estimate for softwood in the regression equation, an adjusted and improved regression estimate was derived. The standard error and the reduction in variance over the random ground-truth sample estimate were calculated.

Table IV shows that all the regression analyses were significant, with the reduction of the proportion varying from 55 percent to 97 percent, depending on the complexity of the site/ecosystem data (as reflected in the PCC). Standard errors of these regression estimates were between 0.01 and 0.031. These standard errors were generally within 10 percent, relative to their area measurement, and even within 3 percent in the case of hardwood estimation in Site II.

These results implied that Landsat ADP classification results could be used effectively as auxiliary variables to improve area estimates obtained primarily by random sampling of aerial photographic plots.

4.2.4 EFFECTS OF LOCATION OF TRAINING SIGNATURES

To test the possible effects of constraining the development of training signatures to a 10-percent contiguous portion of the site, an additional analysis was made on Sites I and II. Denote the previously stated method of developing signatures as Method 1 and the analysis method of developing training signatures from throughout the site as Method 2. These signatures were used to classify the entire site.

The Level II classification results, map PCC, and areal estimates from Methods 1 and 2 were compared by their classification of the major Level II classes, with the following conclusions. The PCC's from Method 1 were insignificantly different, at a 0.95-confidence level, than the PCC's from Method 2. The naive area estimates of the major classes were more accurate in Method 2; that is, the estimates were closer to the regression estimate plus or minus a precision. However, the regression estimates from both methods compared favorably; and, as expected, Method 2 gave a more precise regression estimate. Table VII shows the sample analysis results from Site II.

These results implied that, for a 60- by 60-kilometer study site such as in TES, the resource constraint of limited contiguous ground truth did not have a significant effect on classification and area mensuration accuracies. However, the more expensive spreadout ground-truth method could provide more precise results.

4.3 BEST SEASON, COST, AND SITE COMPLEXITY

The best seasons which were chosen for the site analysis included late spring and/or summer. The choice of the best single date or the temporal composite for ADP analysis was not consistent among the sites, which might result from the closeness of the training accuracies for the single-date data and the temporal data. In fact, high residual misregistration errors in the temporal data could cancel any possible advantage derived from temporal analysis. Errors in excess of 1 to 2 pixels could exist in the registration of natural vegetation landscapes unless extreme caution is exercised. However, these errors might be unavoidable except in cases where definite, permanent landmarks are available for registration.

The selection of best dates reflected the season or seasons when the growth of vegetation was rigorous, when shadow effects were not adverse to ADP analysis, and when snow cover was minimal. In some sites, poor weather also prohibited the selection of more than four dates from 4 years of Landsat coverage for preliminary image analysis.

The current simplistic cost analysis in table V shows a cost of between 11.7 to 18 cents per hectare. Considerable fluctuation occurred between sites because of the differences in experience of the team scientists during the site analyses and because of the variation in the complexity of the site.

Site complexity can be described by many parameters, including topography, vegetation community diversity, edaphic vegetation diversity (i.e., diversity caused by changes resulting from overgrazing, soil erosion, fire, etc.), transition rate between vegetation types, and average size of homogeneous vegetation.

Topography, and hence shadows, made ADP site analysis complex because more diverse spectral signatures necessitated extra training areas. It was found in the Grand County, Colorado, Site I area that aspect could be used as a differentiating factor for Level III classification. That is, softwoods facing northwest, west, and southwest could be differentiated from softwoods facing east and northeast with an overall accuracy of 79 percent (table III). This accuracy was much higher than the classification accuracy between lodgepole pine and spruce-fir (49 percent).

Vegetation diversity and the slow transition between vegetation types necessitated establishing multiple training signatures, which could be difficult to accomplish. By correlating the overall classification map accuracy PCC of different sites to the average width of homogeneous vegetation in the sites, a strong relationship was obtained. The correlation analysis had a coefficient of determination (r^2) of 0.83.

Site complexity only affected the ADP image analysis proceedings; caution was used in selecting small features and diverse signatures. The site complexity was manifested in classification and area determination accuracies.

4.4 MISCELLANEOUS ANALYSIS

Table VI shows the Landsat pixel sizes, site latitude, elevation range, and registration precision for eight of the sites. Landsat pixel sizes fluctuated from 0.44 to 0.46 hectare and were calculated using the Jacobi method on the registration mathematics [13]. Any trend that could relate the pixel size to the site latitude and elevation was too weak to be discerned.

Using an average of 15 control points, image-to-image registration produced between 1.0 and 2.0 pixels root-mean-squared (RMS) error, and image-to-map registration had more than 100 meters in errors in most cases. Note the trend in Site II (Warren Co., Penn.) and Site III (St. Louis Co., Minn.) of good image-to-map registration and poor image-to-image registration; this was attributed to the fact that obvious landmarks existed on at least one image, rendering good image-to-map registration, and to the changes of these vegetation landmarks, rendering poor image-to-image registration. In case of the Site IV semidesert environment, image-to-image registration was good, but image-to-map registration was poor. The former was the result of good contrasts in the desertlike scenes, and the latter can be attributed to using an outdated topographic map.

In Site VI (Fort Yukon, Alaska), an attempt was made to study the effects of variations in the density of spruce stands and in the vegetation cover over tundra on Landsat signatures. It was suggested that a winter scene would provide contrasts between different density classes. The separation results between grass tundra and brush tundra showed an average of 86-percent accuracy for the March data set that had snow cover. However, the temporal August-September data set was found to be better than the winter data set in providing separation between dense spruce and sparse spruce (table III).

The change detection capability of Landsat was investigated using Site VI (Fort Yukon, Alaska) and Site VIII (Grays Harbor Co., Wash.); the results of this analysis are pending. Site VI had a large, burned area (6000 hectares) which was visible on the latest of the three selected dates. Site VIII had intensive lumber logging activities. A demonstration was planned to investigate and locate these two changes.

4.5 PROBLEMS AND RECOMMENDATIONS

Although the TES results have aided in the uniform intersite assessment of Landsat MSS data utility in forest and rangeland mapping, problems in several technical areas remained unresolved. The technical areas are system design; classification, registration, and evaluation; and user modeling.

4.5.1 SYSTEM DESIGN

Fundamental to all remote sensing image classification efforts are area size, signature development, and automation. In TES, the size of study sites was designed to be 60 by 60 kilometers covering four (512 by 512 pixels) analysis screens. Ground truth existed in a limited 10-percent contiguous portion of the site. Signature development was performed in an interactive and an iterative mode on the responsive Image-100 System; hence, simulating a clustering approach in developing signatures. The classes under study were general and could be evaluated readily in the 10-percent area during an interactive ADP session. Extreme automation was not required in TES because of the limited data to be studied as compared to the manpower available.

For future countywide, National forest, regional, or statewide studies, a similar approach to large area classification, such as TES, could be applied. The mode of signature development might differ depending on the feasibility of obtaining ground truth. A grid sampling approach [18] or a cluster sampling approach [19] could be used. It was suggested that the grid sampling approach would provide more streamlined data analysis and automation [18].

For nationwide or even global remote sensing applications, it is not feasible to use the wall-to-wall classification technique used in TES. In order to reduce the quantity of data to a tractable size, statistical sample cluster segments must be selected according to certain statistically valid criteria. An analysis procedure, similar to one used in reference 18, would be necessary.

To substantiate and to realize the true potential of the assessment conclusions from TES, further large area demonstrations are necessary; and depending on the assumptions of the project, the TES approach could be adopted or modified.

4.5.2 CLASSIFICATION, REGISTRATION, AND EVALUATION

Some questions concerning classification on the Image-100 nonparametric classifier need clarification. The use of the nonparametric classifier instead of the maximum likelihood classifier seems to provide excessively high accuracies on training areas, which might provide inaccurate Landsat feasibility conclusions on maximum accuracy and best date selection. The optimal radiometric resolution for classification needs further analysis; resolution in each data channel means the effective number of data values considered in the classification and could be changed by expanding or condensing the data range. Signature development by training fields, clustering, or interactive analysis is discussed in section 4.5.1.

Registration precision is necessary for valid temporal analysis. Again, depending on the size of the area to be registered, a rubber-sheet mapping method using control points might or might not be adequate. Large area registration may require additional corrections for Landsat flightpath and sensor geometry deviations from the normal. The relative importance of the overall system performance in registration precision is yet to be explored.

Evaluation techniques seem to fall short of complete enumeration, and some sampling design is necessary. As such, the precise location (i.e., registration of the same samples on the data to be evaluated and on the ground-truth base) is vital. Consistency in ground rules in evaluation is also important. Random sampling with equal probability tends to suppress the contribution caused by minority features; some stratification needs to be employed, especially if the minority features are to be evaluated more carefully.

4.5.3 USER MODELING

TES objectives were primarily focused on the classification and mensuration aspects of Landsat remote sensing. The questions of yield, productivity, growth, mortality, resource management, data information storage and retrieval, and the many facets of user requirements should be investigated.

To this end, mathematical models need to be developed, tested, and evaluated. Experiments on and integration of multisource, multiplatform, and multisensor data should be attempted. Data systems and data manipulation technology, geared to users' needs and interests, should be developed. Above all, further demonstrations and remote sensing application projects should be continued in order to realize the benefits of this computerized space technology.

5. SUMMARY AND CONCLUSIONS

With the completion of three-fourths of the TES project, the trends of the conclusions have surfaced on the uniform assessment of the information content of Landsat MSS data and its utility for large area classification. The TES project plan required the analysis of one site from each of the 10 generalized forest and rangeland ecosystems in the 49 continental United States. To date, the analyses of six of these ecosystems have been completed, and the analyses of the remaining sites have been initiated. The uniform assessment was made possible by performing the analyses in a standardized environment and under a uniform set of assumptions and constraints. Conclusions derived from TES might have been derived in prior individual studies, the comparison of which could be difficult across the United States because of their nonuniform operating constraints.

In TES, Level II and Level III classifications were attempted. Level II refers to the separation of softwoods, hardwoods, grassland, water, and others. Level III refers to discrimination between types (species) and the discrimination of census and noncensus water

(larger or smaller than 16 hectares). The softwood, hardwood, and grassland categories actually connote more specific vegetation communities and associations because of the potential vegetation that exists in each ecosystem.

By examining the maximum information content in Landsat MSS data, it was found that Level II classifications were excellent but Level III classifications were not consistent. For major Level II classes, accuracies were in the high 90 percentile. For Level III discrimination between species or types, accuracies ranged from 9 to 98 percent. The separation of water into census and noncensus water (greater than, equal to, or less than 16 hectares) was always achievable using the geometric discrimination method in ADP postprocessing. These conclusions were drawn by examining the training data. Insufficient data might have given rise to high accuracies which, nonetheless, reflected upper bounds on Landsat information content.

The conclusions made on the utility of Landsat MSS data in Level II large area classification were inferred from four analyses. The system design in these analyses constrained the development of spectral signatures to a 10-percent contiguous portion of the site without ground truth. In the first analysis of overall classification accuracy, the PCC's were above 85 percent for homogeneous sites where vegetation occurred in large contiguous patterns; otherwise, PCC's were as low as 70 percent. The second analysis of mensuration accuracy of major classes showed that area measurements obtained by ADP analysis had insignificant biases for sites having PCC's above 80 percent; otherwise, the areas tended to be underestimated. The third analysis, the two-phase sampling and regression analysis, showed that Landsat could always improve areal estimates that were obtained via simple random sampling aerial photographic (or ground) plots; the improvement ranged from 55- to 97-percent reduction in estimate variance. The fourth analysis of system design showed that, for the 60- by 60-kilometer sites, area estimations compared favorably regardless of whether signatures were developed from a 10-percent contiguous sampling or from a spreadout sampling over the site; however, the latter could provide more precise estimates.

Routine analysis by administrative units was demonstrated to be feasible in TES. Minimum area mapping (other than 1 pixel) was demonstrated operationally using an ADP postprocessing method. Additional conclusions on miscellaneous analysis, geometric parameter comparison, cost analysis, and problem and solution identification were made from the current analysis of TES.

These feasibility analysis results implied that Landsat could effectively be employed to map and produce area measurements for Level II land cover features. Mapping accuracies of these features were consistently high. ADP classification in a 60- by 60-kilometer site could be performed almost as accurately when ground truth was confined to a 10-percent contiguous area as compared to when ground truth was spread over the entire site. Direct area tabulations from ADP classification provided sufficiently accurate figures. Also, Landsat ADP classification could be used as auxiliary information to improve areal estimates obtained by random sampling of aerial photographic plots. ADP classification was also developed to a stage where routine operation was feasible. Overall, the TES uniform assessment of Landsat utility in remote sensing applications encourages larger, user-oriented, and more operational demonstrations in order that the full potential of Landsat be realized.

6. ACKNOWLEDGMENT

The many facets of the TES were made possible only through the devotion and support of many people. Special thanks are offered to R. D. Dillman and A. V. Mazade of Lockheed Electronics Company, Inc., and R. E. Joosten of NASA.

7. REFERENCES

1. Kan, E. P.: The Ten-Ecosystem Study Investigation Plan. Lockheed Electronics Co., Inc., Technical Report LEC-8667 (also NASA Technical Memorandum JSC-11533), Sept. 1976.

2. Reeves, R. G., ed.: Manual of Remote Sensing. American Society of Photogrammetry (Falls Church, Va.), 1975.

3. Erb, R. B.: The ERTS-1 Investigation (ER-600): A Compendium of Analysis Results of the Utility of ERTS-1 Data for Land Resources Management. NASA TM X-58156 (JSC-08455), NASA/JSC (Houston), Nov. 1974.

4. Colwell, R. N.: An Integrated Study of Earth Resources in the State of California Based on ERTS-1 and Supporting Aircraft Data. NASA CR 5-21827, July 1973.

5. Heller, R. C.; Aldrich, R. S.; Driscoll, R. S.; Francis, R. E.; and Weber, F. P.: Evaluation of ERTS-1 Data for Inventory of Forest and Rangeland and Detection of Forest Stress. USDA, Forest Service Research Paper PSW 112, 1975.

6. Mead, R.; and Meyer, M.: Landsat Digital Data Application to Forest Vegetation and Land-Use Classification in Minnesota, Final Report. NASA Contract NAS 5-20985, June 1977.

7. Kan, E. P.; Ball, D. L.; Basu, J. P.; et al.: Data Resolution Versus Forestry Classification and Modeling. Proc. Second Symp. Machine Processing of Remotely Sensed Data, Purdue Univ. (W. Lafayette, Ind.), June 3-5, 1975.

8. Hoffer, R. M.; and Staff: Natural Resource Mapping in Mountainous Terrain by Computer Analysis of ERTS-1 Satellite Data. LARS Research Bulletin 919, 1975.

9. Haralick, R. M.: Texture Analysis of Forestry Multispectral Scanner Data. NAS CR 9-14453, Jan. 1976.

10. Shantz, H. L.; and Zon, R.: Natural Vegetation. Atlas of American Agriculture. Government Printing Office (Washington, D.C.), 1924.

11. Resources Planning Act, Summary, Assessment and Program. USDA, Forest Service, Aug. 1975.

12. Anderson, J. R.; et al.: A Land-Use Classification System for Use With Remote Sensor Data. U.S. Geological Survey Circular 964 (Washington, D.C.), 1976.

13. Kan, E. P., ed.: Technical Analysis Procedures for the Ten-Ecosystem Study. Lockheed Electronics Co., Inc., Technical Report LEC-9379, Dec. 1976.

14. Kan, E. P.: A New Computer Approach to Map Mixed Forest Features and Postprocess Multispectral Data. Proc. of ACSM/ASP Convention (Seattle, Wash.), Sept. 28 — Oct. 1, 1976.

15. Kan, E. P.: A Remote Sensing Application: Preprocessing and Postprocessing Aspects of Forestry Data Analysis. Digital Signal Processing. Western Periodicals (San Francisco, Calif.), 1978. (Also in Lockheed Electronics Co., Inc., Technical Report LEC-8669, Oct. 1976.)

16. Hansen, M. H.; Hurwitz, W. N.; and Madow, W. G.: Sample Survey Methods and Theory, Volume I. John Wiley and Sons, Inc. (New York), 1953.

17. Kan, E. P.: The Ten-Ecosystem Study Interim Report. Lockheed Electronics Co., Inc., Technical Report LEC-10539 (also NASA Technical Memorandum JSC-12924), Aug. 1977.

18. MacDonald, R. B.; and Hall, F. G.: LACIE, A Proof of Concept Experiment in Global Crop Monitoring. Proc. Midcon 77. IEEE Electronics Show and Convention (Chicago, Ill.), Nov. 8-10, 1977.

19. Krebs, P. B., et al.: Multiple Resource Evaluation of Region 2 USDA, Forest Service Lands Utilizing Landsat MSS Data, Final Report. NASA Contract NAS 5-20984, July 1976.

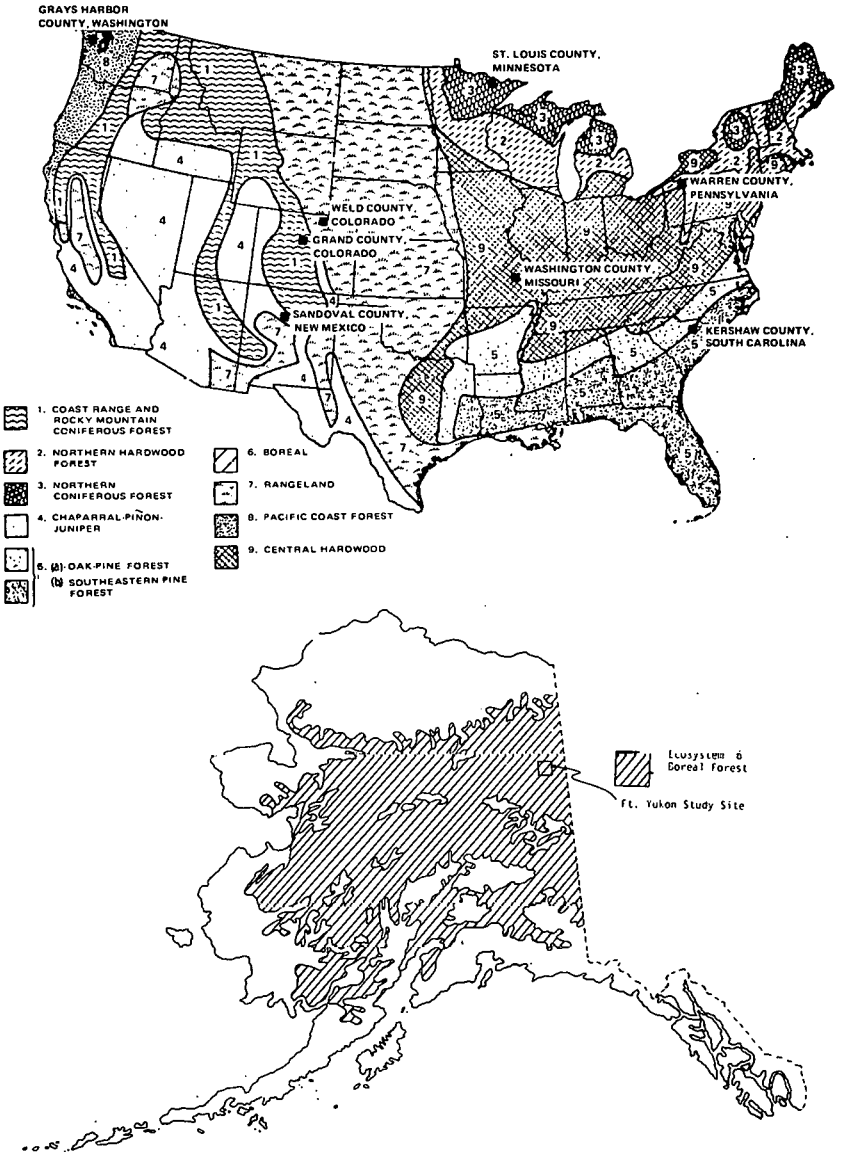

FIGURE 1. FOREST AND GRASSLAND ECOSYSTEMS IN THE UNITED STATES.

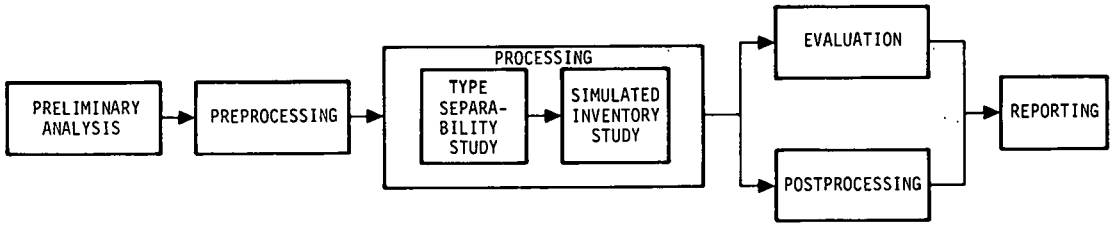

FIGURE 2. TECHNICAL FLOW FOR EACH SITE ANALYSIS IN TES.

TABLE I. TES ANALYSIS LEVELS

Level I	Level II	Level III
Forest	Softwood	E.g., loblolly vs. shortleaf pine; softwood vs. mixed softwood and hardwood
	Hardwood	E.g., maple vs. oak
Nonforest	Grassland	E.g., annual grassland vs. mountain meadow; sagebrush vs. grassland
	Other	Includes cropland, urban, bare soil, rock, etc. No distinction made in TES.
Water	Water	Census and noncensus water [greater than, equal to, or less than 16 hectares (40 acres)].

TABLE II. VEGETATION COMMUNITIES AND ASSOCIATIONS SPECIFIC OF ECOSYSTEMS

Site/forest ecosystem	Specific vegetation communities and associations		
	Softwood	Hardwood	Grassland
1. Coastal Range and Rocky Mountain Conifers	Piñon-juniper, ponderosa pine, Douglas fir,[b] lodgepole pine,[b] and spruce-fir[b]	Oak woodland and aspen[b]	Bluegrass, muhly, fescue, and sedges
2. Northern Hardwoods	Yellow pine,[b] eastern white pine, pine-hardwood, and spruce-fir[b]	Oak-hickory, cove and bottomland, beech,[b] birch, and maple[b]	Bluestem and panicum
3. Northern Conifers	Jack pine,[b] red pine,[b] eastern white pine, swamp conifer,[b] black spruce, and spruce-fir-hardwood[b]	Aspen[b]	Sedges and rushes
4. Chaparral-Pinyon-Juniper	Piñon-juniper,[b] ponderosa pine, Douglas fir, lodgepole pine, and spruce-fir	Scrub oak woodland[b] and aspen	Blue grama and galleta
5a. Oak-Pine[a]	Yellow pine,[b] pine-hardwood,[b] and eastern white pine	Oak-hickory and cove and bottomland[b]	Cultivated rye and bluegrass
5b. Southeastern Pine[a]	Longleaf pine,[b] slash pine, loblolly pine,[b] shortleaf pine, ponderosa pine, spruce-pine, and Atlantic white cedar		
6. Boreal	Spruce[b]	Intolerant hardwood[b]	Sedges, bluegrass, and fescue
7. Rangeland		Cottonwood	Blue grama, buffalo grass, and salt grass
8. Pacific Coast	Spruce-hemlock,[b] Hemlock-cedar,[b] and Douglas fir[b]	Alder[b] and maple	Three-awn, fescue, and sedges
9. Central Hardwoods	Pine-hardwood[b] and eastern red cedar[b]	Oak-hickory,[b] mixed hardwood, and elm-ash-maple	Bluestem and panicum

[a]The fifth site, Kershaw County, South Carolina, represents two ecosystems.

[b]These species are specific in the selected sites.

TABLE III. MAXIMUM TRAINING CLASSIFICATION ACCURACIES FROM THE TES TYPE SEPARABILITY STUDY[a]

Site	Landsat data	Level II class accuracy, %				Level III analysis	
		Softwood	Hardwood	Grassland	Water	Class	Accuracy, %
I	08/15/73 10/03/74 Temporal	99.8 (Oct.)	86.1 (Aug.)	99.1 (Oct.)	100 (Oct.)	Pasture/sagebrush Lodgepole pine/spruce-fir Softwood aspect: NW, W, SW, NE, and E	84/98 (Aug.) 9/99 (Aug.) 70/89 (Aug.)
II	09/05/72 05/06/75	80.0 (Sept.)	100 (May)	98.2 (May)	100 (May)	Maple/oak	94/50 (May)
III	07/03/73 09/26/74	99.7 (July)	98.9 (Sept.)	100 (July)	100 (July)	White spruce/fir	42/55 (July)
IV	05/07/75 08/05/75 Temporal	99.7 (May, temporal)	100 (May, temporal)	99.8 (Aug., temporal)	100 (Aug., temporal)	Oak/cottonwood Juniper/pine	Not separable Not separable
V	05/24/75 02/19/76 Temporal	99.2 (Feb., temporal)	100 (Temporal)	100 (Feb., temporal)	100 (Feb., temporal)	Pine/mixed/hardwood Slash pine/loblolly pine	91/89/97 (Temporal) 89/89 (Temporal)
VI	09/03/73 03/02/74 08/27/76 Temporal	99.9 (Temporal)	99.0 (Temporal)	99.0 (Temporal)	99.9 (Temporal)	Sparse spruce/dense spruce Grass tundra/brush tundra	92/66 (Sept., Aug., temporal) 82/88 (Mar.)

[a]The Landsat data information content was investigated.

TABLE IV. TES SIMULATED INVENTORY STUDY EVALUATION RESULTS[a]

[Level II classification]

Site	(1) Overall classification accuracy (random sampling) PCC, 0.9-confidence level, %	Class considered in mensuration and regression	(2) Mensuration					(3) Two-phase sampling and regression analysis				
			Bias[b] of ADP area over random sampling, 0.9-confidence level	Entire site				Regression equation between Landsat (p) and ground truth ($\hat{p}$)	Coefficient of determination, r^2	Significance of regression, 0.9-confidence level	Regression estimate standard error, %	Variance reduction, %
				ADP naive estimate, P_N	Regression estimate, P_R	0.9-confidence level	Bias[c] of ADP area, 0.9-confidence level					
I	75 ± 5.4	Softwood	Negative bias	0.28	0.37	(0.32, 0.42)	Negative	$p = 0.98\hat{p} + 0.10$	0.77	Yes	3.1	74
II	87 ± 6.1	Hardwood	Insignificant	0.72	0.74	(0.72, 0.76)	Insignificant	$p = 0.94\hat{p} + 0.07$	0.84	Yes	2.1	80
III	76 ± 5.1	Softwood	Insignificant	0.24	0.26	(0.23, 0.28)	Insignificant	$p = 1.01\hat{p} + 0.02$	0.92	Yes	1.5	92
		Hardwood	Negative	0.34	0.42	(0.39, 0.45)	Negative	$p = 1.05\hat{p} + 0.06$	0.93	Yes	1.5	93
		Water	Insignificant	0.09	0.11	(0.08, 0.14)	Insignificant	$p = 0.98\hat{p} + 0.03$	0.97	Yes	1.5	95
IV	94 ± 3.9	Softwood	Insignificant	0.06	0.07	(0.04, 0.10)	Insignificant	$p = 1.11\hat{p} + 0.00$	0.92	Yes	2.0	91
		Grassland	Insignificant	0.04	0.05	(0.04, 0.06)	Insignificant	$p = 0.98\hat{p} + 0.01$	0.97	Yes	1.0	97
V	70 ± 5.7	Softwood	Negative	0.25	0.32	(0.28, 0.36)	Negative	$p = 0.87\hat{p} + 0.10$	0.71	Yes	2.2	68
		Hardwood	Negative	0.16	0.24	(0.20, 0.28)	Negative	$p = 0.90\hat{p} + 0.10$	0.62	Yes	2.3	55

[a]The evaluation parameters are (1) classification map accuracy, 2) mensuration precision, and (3) two-phase sampling and regression analysis.

[b]Bias refers to comparison between the ADP area estimates and the photointerpreted ground truth. Negative bias means an underestimate from ADP.

[c]Bias refers to comparison between the ADP naive estimate and the regression estimate, which acts as ground truth.

TABLE V. A SIMPLISTIC COST ANALYSIS[a]

Site	Man-hour	Computer console hour	Filming hour	Digitizing hour	Travel, $	Site size, hectare	Cost, cent/hectare
I	1893	112	23	31	1145	310 000	18
II	1195	73	30	24	1402	304 900	12
III	1714	168	18	141	1487	316 100	23
IV	1943	122	20	19	1210	309 600	21
V	1483	94	21	21	1406	303 000	15
VI					3354	314 300	
VII					1063		
VIII					1886		
IX					887		

[a]Total cost = (Man-hours × $12) + (computer hours × $300) + (filming hours × $100) + (digitizing hours × $15) + (field trip travel, 1 wk.)
Hourly rates are approximate rates obtained informally from Government sources; the computer used was mainly the Image 100 System.

TABLE VI. MISCELLANEOUS ANALYSES

Site	Landsat MSS pixel size, hectare	Site latitude, degrees North	Site elevation range, meter	Registration RMS error	
				Image-to-image (pixel)	Image-to-map, meter
I	0.46	40:00	2250 - 3940	1.4	101
II	0.44	41:45	365 - 490	2.0	139
III	0.46	47:30	365 - 550	2.0	112
IV	0.46	35:30	1980 - 3430	0.9	170
V	0.45	34:15	38 - 188	2.0	128
VI	0.46	66:44	200 - 782	1.0	55
VII		40:26	1390 - 1840		
VIII		47:15	0 - 2000		
IX		37:57	210 - 520		

TABLE VII. RESULTS OF EVALUATING TWO METHODS OF DEVELOPING SPECTRAL SIGNATURES FOR LARGE AREA CLASSIFICATION

[Site II hardwoods area estimation]

Method / Results	Classification by signatures developed from 10% contiguous area	Classification by signatures developed from throughout site
Naive areal estimate	0.723	0.744
Regression equation	$p = 0.937\hat{p} + 0.066$	$p = 0.99\hat{p} + 0.004$
Regression, r^2	0.836	0.916
Improved regression estimate	P = 0.937 (0.723) + 0.066 = 0.743	P = 0.99 (0.744) + 0.004 = 0.740
Standard error	0.021	0.015
Confidence interval	(0.722, 0.764)	(0.725, 0.755)
Overall Level II classification PCC	87% ± 6.1%	88% ± 4.9%

THIS PAGE

WAS INTENTIONALLY

LEFT BLANK

APPLICATION STUDY OF REMOTE SENSING TO SAURY FISHERIES IN JAPAN

Sei-ichi SAITOH and Sei-kichi MISHIMA

Research Institute of North Pacific Fisheries
Faculty of Fisheries
Hokkaido University
Hakodate, Japan

Joji IISAKA

Tokyo Scientific Center
IBM Japn ,Ltd.
Tokyo, Japan

Osamu ASAOKA

Meteorological Research Institute
Meteorological Agency
Tokyo, Japan

ABSTRACT

As a practical approach, an attempt were made to combine remote sensing data and data base management system for marine living resources assessment. Study area were chosen from the water off the SANRIKU coast and saury Cololabis saira (BREVOORT) were chosen as a study resources. Commercial fishing data were prepared from data base and compared with LANDSAT MSS data by non-parametric clustering analysis. High C.P.U.E. cluster were well correspond with water class SEA-4 classified by LARSYS program.

1. INTRODUCTION

In recent years the management of marine living resources has become a pressing problem in every part of the World's oceans. On one hand, the development of remote sensing from satellites has opened the first possibility of surveying the entire globe in reasonably short period of time. But remote sensing technique is still unfamiliar with fisheries science community although there is the need for real-time information about the environmental conditions of marine living resources.

Remote measurement of chlorophyll concentration of the world's oceans from satellite observation could potentially be extremely useful for assessments of productivity in large areas (Atwell,1976). Through the food-chain in the oceans, as a large-scale ecological system, it is possible to estimate fish productions approximetry, but it is necessary to establish data base for management of the large volume of data from vast seas.

As a practical approach, we attempt to combine remote sensing data and data base management system for marine living resources assessment. The objective of this study is to demonstrate the feasibility to catch the fish migration patterns

by using remote sensing data and data base management system.

Study area is chosen from the water off the SANRIKU coast (a part of the Northeastern district of the mainland of Japan). This area is one of the most important fishing ground of epipelagic fishes and has the dynamic features in ocean structure that oceanic fronts formed in boundary zone between the Oyashio system and the Kuroshio system. Moreover, we focussed saury, Cololabis saira (BREVOORT) which is commercially important speacies, and also migratory and epipelagic species. Selected study season is September and October, south-going period of saury fish school from offshore of eastern Hokkaido to offshore of the SANRIKU coast.

This paper discusses the relationship between the results of non-parametric clustering analysis for commercial fishing data and LANDSAT MSS data and classification results of sea water by LARSYS program.

2. DATA COLLECTION

LANDSAT MSS data covering study area was gathered in October 2, 1972. On the other side, commercial fishing data and biological measurement data were gathered from September 20 to October 10, 1972 by several fisheries experimental laboratories and Tohoku Regional Fisheries Research Laboratory. The commercial fishing data contains fishing date, fishing position, fishing methods, fishing yield, number of haul, C.P.U.E.(catch per unit of fishing effort), and sea surface temperature. The biological measurement data includes body length, body weight, sex, gonad weight, thickness index. The commercial data overlaped spatially LANDSAT data from October 5 to October 8. There is time lag about 3 days to 6 days between both data.

3. DATA BASE MANAGEMENT SYSTEM

For the future study, we are going to plan the Marine Living Resources Assessment (MLRA) Data/Base for fisheries management and at the same time sea-truth data banks. This data base is composed of four main tables, TIME, LOCATION, ENVIRONMENT, MLR (Fig. 1). MARSDEN SQUARE CHART (MS) is employed for one of the Location table because of world ocean mesh data. In this data base, it is possible to make mesh data from both MSCMESH and JFB, also to prepare coast line data as a map in parallel.

As a first step, we developed the saury data base as one of "Fish Type" in MLR table, and utilize "SEQUEL XRM" data base management, which is a prototype Database System built to experiment with relational processing techniques, for listing up commercial fishing data of saury. "SEQUEL" means Structured English QUEry Language and is one of the data base management system. This technology offers a solution to managing the information contained in the numerical models (Chamberlin, 1974). The following simple example indicates how to use "SEQUEL".

If the data base contains the following tables COMFISH and BIOFISH

COMFISH(YYMMDD,CATCH,HNC,CPUE,LAT,LONG,FBLOCK,STEMP)
BIOFISH(YYMMDD,LAT,LONG,BL,BW,GW,STEMP,SAMPNO)

The COMFISH table gives each fishing date, fishing yield, number of haul, C.P.U.E., Latitude of fishing point, Longnitude of fishing point, Japanese fisheries block no., sea surface temperature. The BIOFISH table gives each fishing date, Latitude, Longnitute, body length, body weight, gonad weight, sea surface temperature, sample no..

(1) Question: "List the C.P.U.E., Latitude, Longnitude, sea surface temperature, and fishing date of all COMFISH data located in the area from 141°31' to 143°00' in Latitude and from 38°00' to 40°00' in Longnitude" is expressed as follows:

```
SELECT   CPUE,LAT,LONG,STEMP,YYMMDD
FROM     COMBISH
WHERE    LAT BETWEEN 14130 AND 14300
         AND
         LONG BETWEEN  3800 AND  4000;
```

(2) Question: " List the mean body length and mean body weight of fish catched in october 2, 1972 where sea surface temperature was greater than 18.0°C " is expressed as follows:

```
SELECT   AVE(BL),AVE(BW)
FROM     BIOFISH
WHERE    YYMMDD=721002
         AND
         STEMP>180;
```

4. DATA ANALYSIS

LARSYS image processing program developed at Pardue University is used for digital image processing and "linear" contrast stretching method is employed to enhance the oceanic informations.

An attempt is made to classify the sea water masses by using LARSYS programs. Moreover, as apost-processing, image smoothing by 5X5 filter is carried out to erase the effects of "stripping" and isolating pixels in classification map.

On one hand, list of commercial fishing data in LANDSAT covering area is easily producted by using "SEQUEL". For non-parametric clustering analysis, statistical values (mean and standard deviation) of LANDSAT MSS data in the area, about 1km by 1 km, surround commercial fishing point are calculated respectively. The parameters for non-parametric clustering analysis are chosen as follows : C.P.U.E., the subtraction mean of MSS 5 CCT counts from mean of MSS 4 CCT counts, mean of MSS 4 CCT counts, and sea surface temperature. In this analysis, we make the assumption that the subtraction mean of MMS 5 CCT counts from mean of MSS 4 CCT counts expresses approximately the gradient of spectral reflectance curve of sea water for several different concentrations of chlorophyll as calculated with Hulburt's (1943) equations (Fig. 2).

The results of non-parametric clustering analysis are compared with the classification map of sea water masses to investigate the relationship between LANDSAT MSS data and commercial fishing data.

5. RESULTS AND DISCUSSION

Contrast stretched imageries (MSS 4 and MSS 5) are shown in Fig. 3 and post-processed classification map with pattern tracing map are shown in Fig. 4. In classification of sea water masses, it is possible to separate into 8 classes : class names are SEA-1, SEA-2, ---,----SEA-7, and COASTAL. The location with symbolof class of commercial fishing points are shown in Fig. 5.

By non-parametric clustering analysis, two clusters are obtained and distance between clusters is calculated at 2.19727. 2-dimensional cluster map of C.P.U.E. and the subtraction MSS 5 from MSS 4 is shown in Fig. 6. In comparision with Fig. 5 and Fig. 6, high C.P.U.E. cluster is well correspond with class SEA-4.

The isothermal line of sea surface temperature at 20°C from late September to early October is shown in Fig. 7. There is so rapidly moving of water mass in LANDSAT covering area when MSS data are obtained in earky October. On the

other side, sea surface temperature of commercial fishing points are between 18.0°c and 19.9°c in LANDSAT covering area, and in this year fishing ground were formed in relatively high sea surface temperature water at about 20°C against usually 17°c (Matsumiya, 1976). Therefore, it is considered that sea surface temperature were not so influence to fish distribution that the distribution were determined by other environmental factors. Thus, it is interesting with water caractaristics of water class SEA-4. SEA-4 has high gradient in spectral curve between MSS4 and MSS5, so that it may be relatively high chlorophyll concentration water and we must consider that there is good feeding environment for zooplankton as a food of saury. But, futher investigation for these factor except sea surface temperature with sea truth is necessary.

In the future study, it is necessary to develop the multistage sampling system with thermal and wind informations of TIROS-N, and thermal and ocean color data of LANDSAT-C satellites.

6. ACKNOWLEDGMENT

The authors are grateful to Dr. Shinichi FUKUSHIMA, Tohoku Regional Fisheries Research Laboratory, for providing the commercial fishing data and biological measurement data of saury.

7. REFERENCES

(1) Atwell, B.H. (1976) : Remote sensing of chlorophyll concentration: State-of-the- ART 1975., NASA-TM-X-74635., 35p.

(2) Chamberlin, D.D. and Boyce, R.F. (1974): SEQUEL: A structred english query language., Proc. of ACM SIGFIDET Workshop.

(3) Fromm, F.R. and Northouse, R.A. (1976): CLASS: A nonparametric clustering algorithm., Pattern Recognition, Vol. 8, pp. 107 -114.

(4) Fukushima, S. (1976): Synoptical analysis of migration mechanism of Northwestern Pacific saury., Ph. D. Thesis, Hokkaido University. (in Japanese).

(5) Kerr, S.R. and Neal, M.W. (1976): Analysis of large-scale ecological system., J. Fish. Res. Board. Can., Vol. 33, pp.2083 -2089.

(6) Matsumiya, Y. and Tanaka, S. (1976): Numerical implication between the distribution of surface temperature and the saury fishing ground in the Pacific Ocean off North Japan., Jour. Jap. Soc. Fish. Oceanogr., Vol.29, pp.30 - 40.

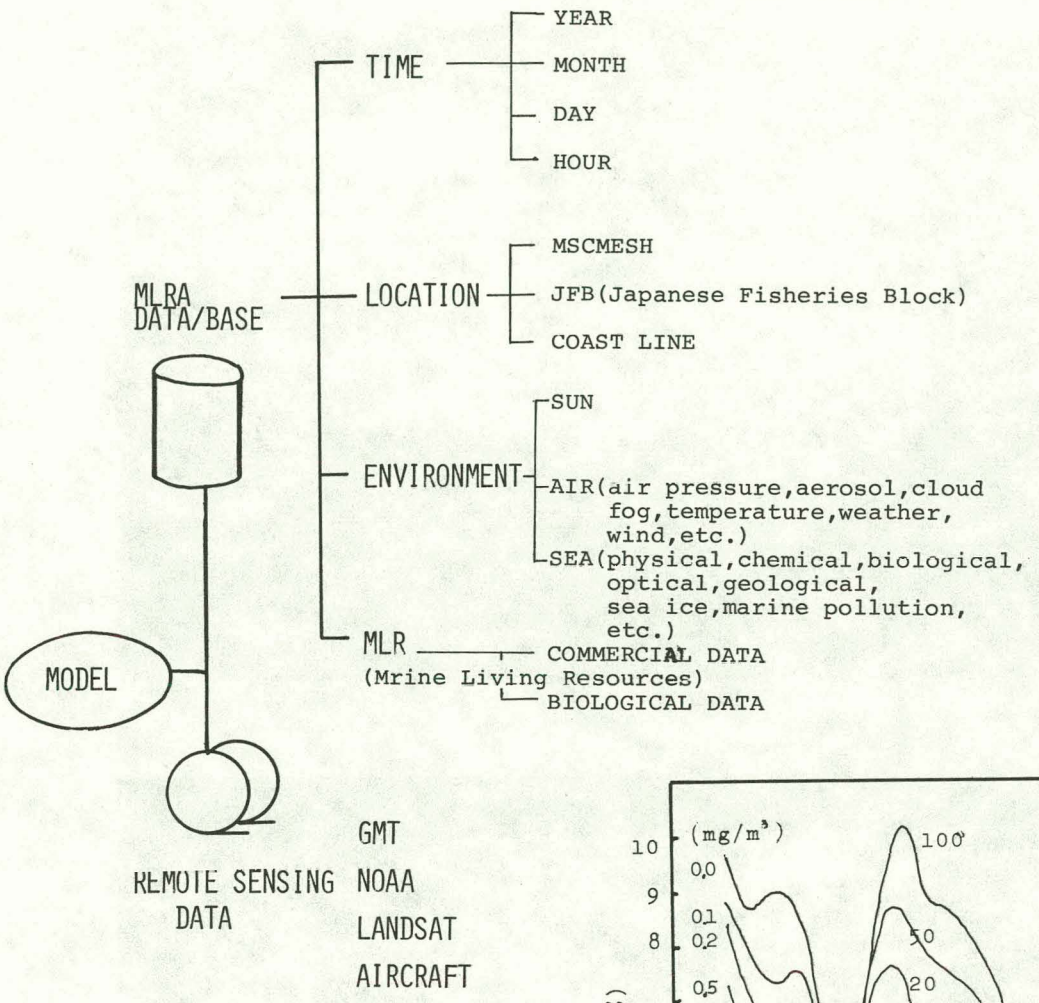

Fig. 1 Scheme of MLRA DATA/BASE

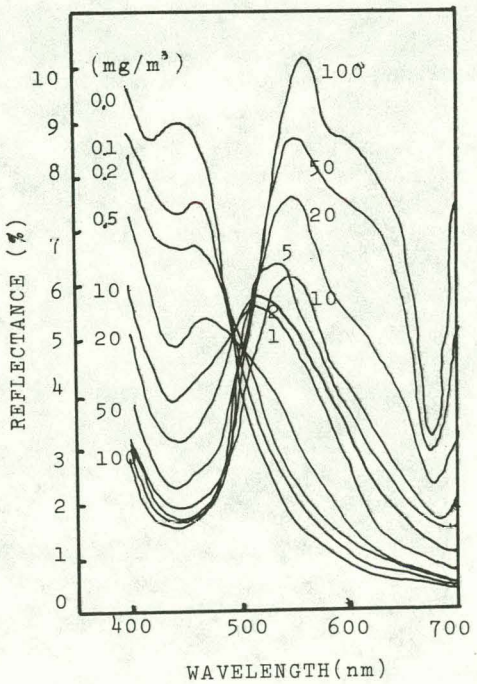

Fig. 2 Spectral reflectance of sea water for several different concentrations of chlorophyll (mg/m), as calculated with Hulburt's (1943) equations. (After Atwell,1976)

MSS 4

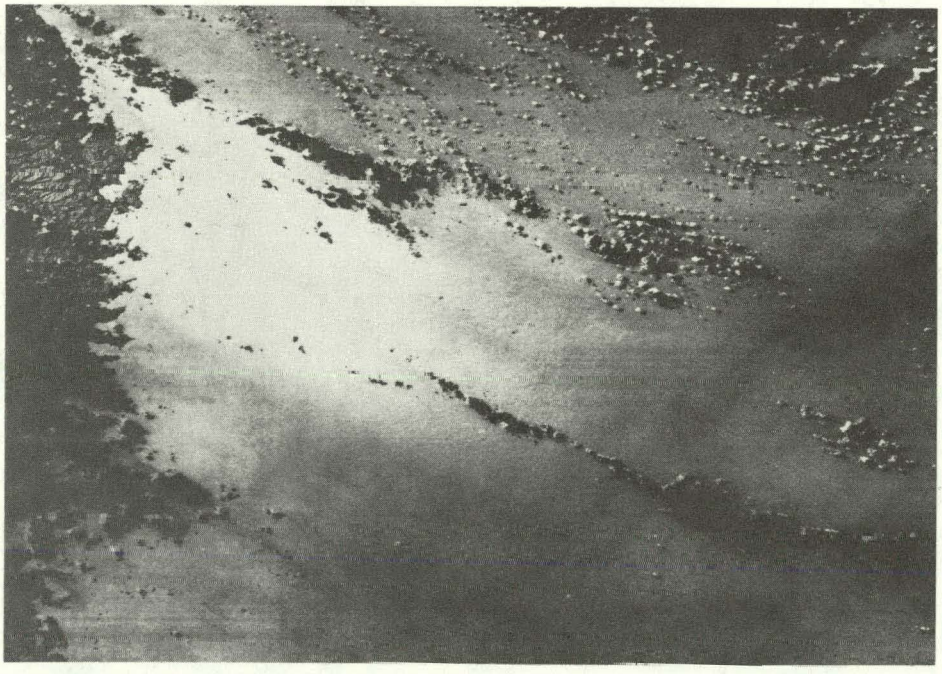

MSS 5

Fig. 3 Contrast stretching imageries of LANDSAT-1, October 2, 1972.(range, MSS4:18<DN<24; MSS5: 8<DN<15).

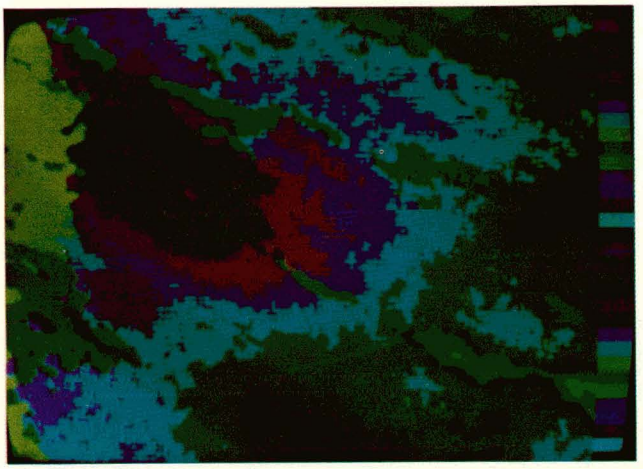

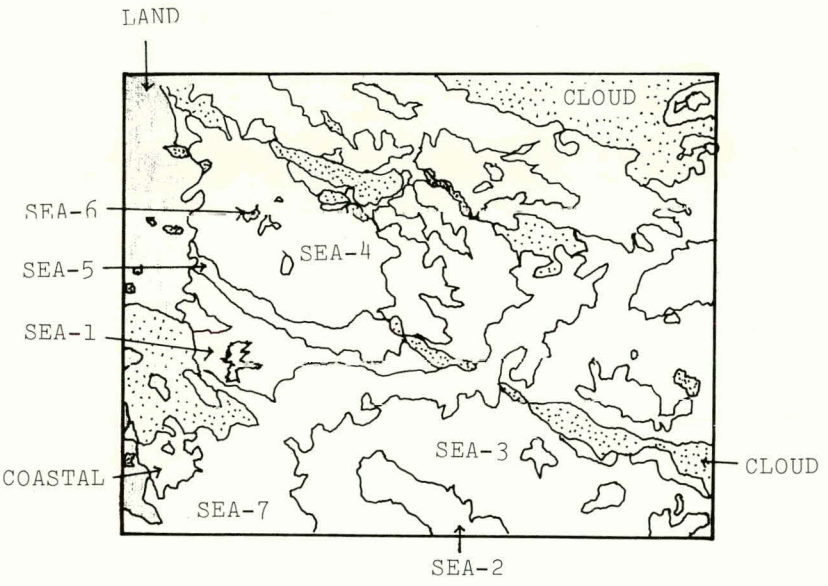

Fig. 4 Post-processed classification map and pattern tracing map.

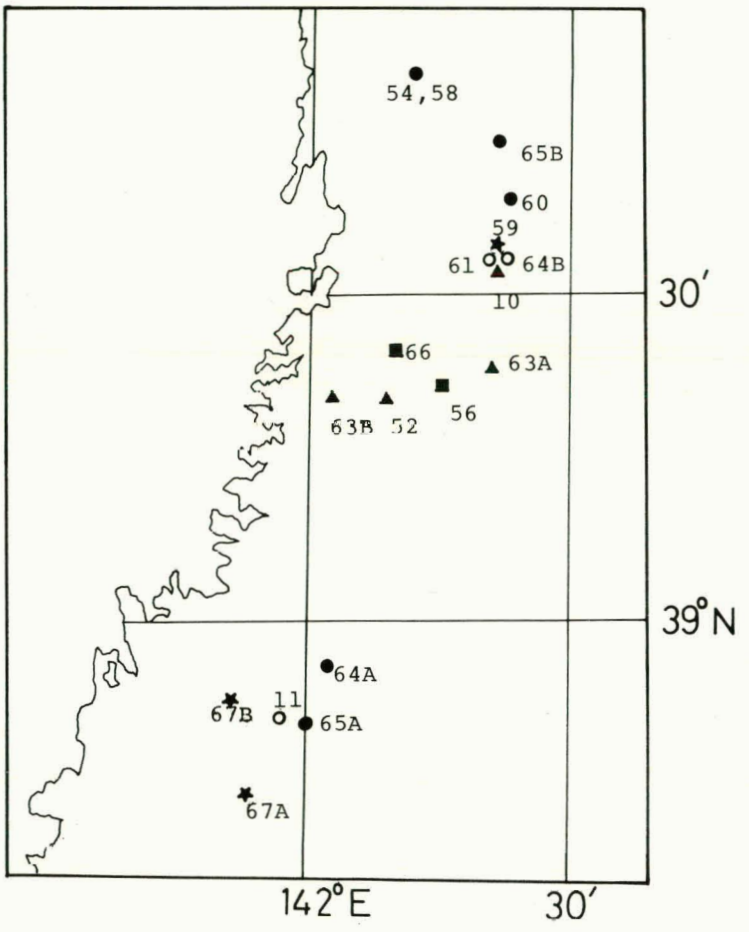

Fig. 5 Location map of commercial fishing points.
(●:SEA-1, ▲:SEA-4, o:SEA-5, ■:SEA-6, ★:cloud covering point)

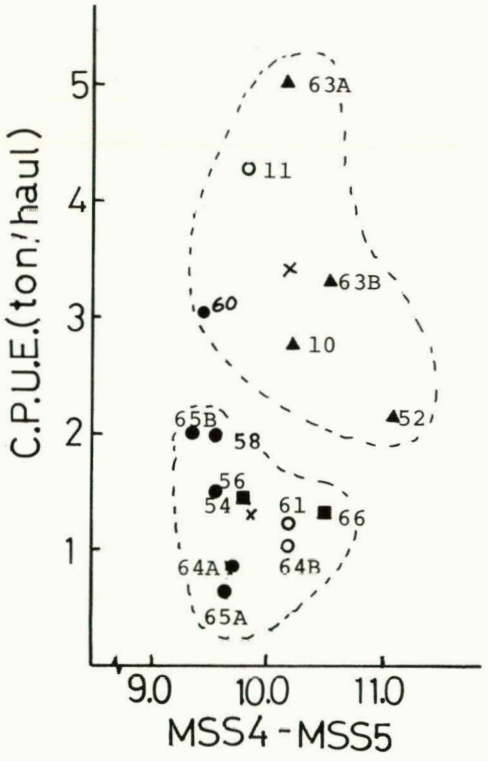

Fig. 6 2-dimensional cluster map.
(×:cluster center)

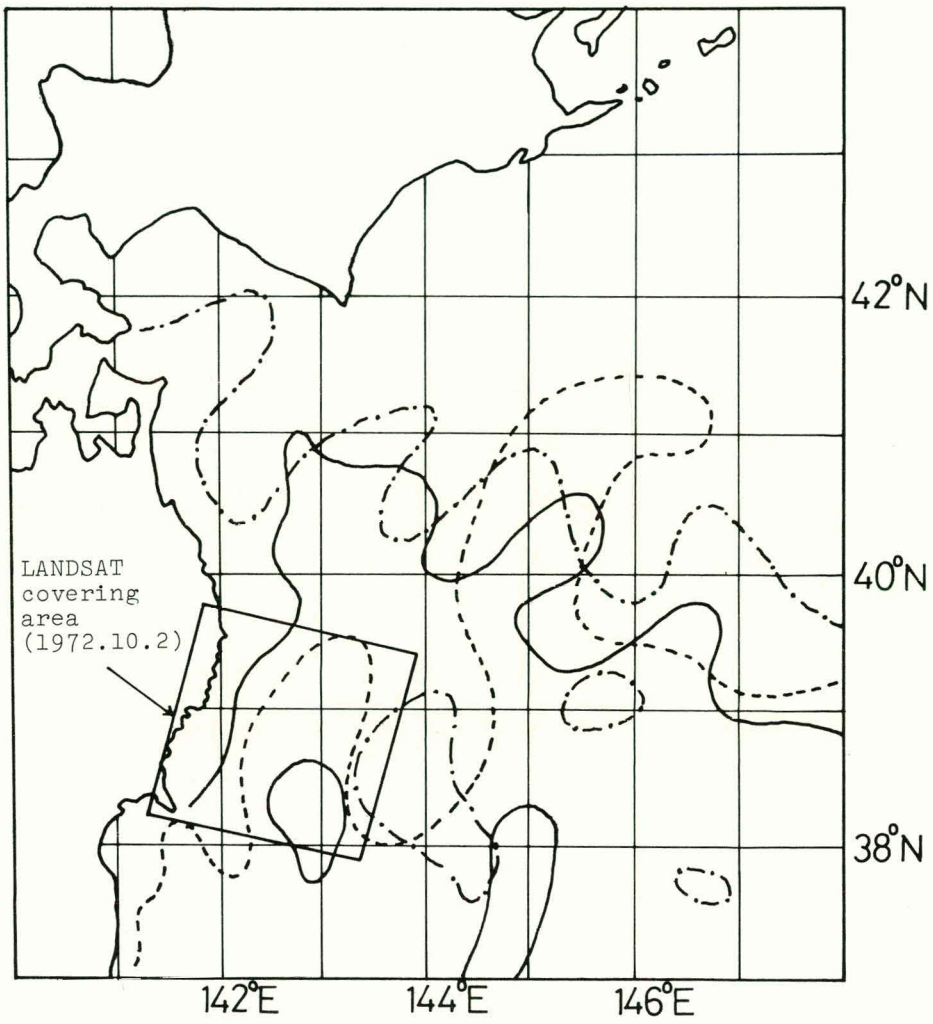

Fig. 7 LANDSAT covering area and isothermal line of sea surface temperature at 20°C in the water off SANRIKU coast.

(—·—·—·—: September 26 - 30, 1972
————: October 1 - 5, 1972
- - - - - - - - -: October 6 - 10, 1972)

THIS PAGE

WAS INTENTIONALLY

LEFT BLANK

WATER MANAGEMENT AND CONTROL VIA THE GLOBAL METEOROLOGICAL SATELLITE SYSTEM

Warren L. Sharp*

Lower Mississippi Valley Division/Mississippi River Commission
Vicksburg, Mississippi 39180

1. A SYSTEM IN THE LOWER MISSISSIPPI RIVER BASIN

A fully automated water resource data collection system is in the early stage of operation in the lower Mississippi River Basin by the Corps of Engineers (Corps). The Central Receive Site is located in the River & Reservoir Control Center of the Corps in Vicksburg, Mississippi. The initial phase of the system, which is designed to aid water control managers over a vast area, includes 57 reporting stations throughout the lower valley. Sixteen of the stations are on the main stem Mississippi River, 15 are at Corps reservoirs, 24 on principal tributaries, and 2 are on the Atchafalaya River outlet to the Gulf of Mexico. Seven of the stations are in the Cooperative Stream Gaging Program of the Corps and U. S. Geological Survey. Several other offices of the Corps and National Weather Service located outside the lower valley are also using the Central Receive Site.

All of the water data stations report to the Center via earth satellite every 4 hours, at which time data recorded at the sites within the 4-hour interval are also reported. All of the existing stations report water level. Precipitation is reported from most of the stations and water quality will ultimately be reported from several select stations.

The principal physical components of the system consist of: automatic measuring equipment for the parameters just mentioned; environmental (water) data transmitters containing memory; earth satellites; a Central Receive Site; and a data communications processor (minicomputer) linked with small remote user terminals. These components are discussed in this paper in terms of their role in the system, including mention of special features which I think will be of interest to you. In addition, comparison with other more conventional data collection systems, the potential for technology transfer to other areas of the world, and some uses of the data are discussed very briefly.

2. MEASURING EQUIPMENT

Conventional automatic recorder-type rainfall and water level measurement equipment is being used in the system. Strip charts and punched paper tape may remain in use. A special study was recently conducted to evaluate on-the-shelf water quality sensors for use in the system, including cost comparison and hands-on testing of a few sensors for compatibility with the environmental (water) data transmitters and parameter measurement sensitivity. The report on this study, which found none of the sensors suitable for in-situ monitoring, is available to any who may want it. Water quality parameters in need of monitoring are temperature, pH, DO, conductivity, turbidity, and certain ions.

*Chief, River & Reservoir Control Center, Lower Mississippi Valley Division, Corps of Engineers, 1400 Walnut Street, P. O. Box 80, Vicksburg, Mississippi 39180

3. ENVIRONMENTAL (WATER) DATA TRANSMITTERS

Environmental (water) data microprocessor/transmitters (EDT) are installed at the recorder stations to relay data to either the Geostationary Operational Environmental Satellite (GOES) Data Collection System (DCS), or to the Land Satellite (LANDSAT). See figure 1. It will be shown later why LANDSAT, formerly the Earth Resources Technology Satellite (ERTS), is much less suitable for water management and control activities than the GOES system. A special transmitter was designed for the data collection system to include several important features that enhance utility. Some of these features are: capability to monitor four digital recorders plus 8 analog (see figure 3); transmission in either the GOES or LANDSAT modes; 832-bit memory; 16-bit digital and analog conversion to 8-bit digital word sizes; American Standard Code for Information Interchange (ASCII); AC or DC; and essentially unaffected by weather conditions. The transmitter is contained in a relatively small drum, 11-1/2 inches in diameter by 14-1/2 inches high, which will accommodate easy installation in the recorder shelters. The drum will protect against moisture and, to some degree, against vandalism. Separate antennas for the GOES and LANDSAT systems are furnished with each transmitter. Full memory data (832 bits) and station identification can be transmitted in 25.6 seconds every 4 hours via the GOES system. Transmission of data in sets consisting of 64 bits/set in the LANDSAT mode can be programmed to occur on either 90- or 180-second intervals; however, the data can only be retrieved at 12-hour (approximate) intervals. Also, full memory cannot be transmitted during the LANDSAT orbit.

Each EDT contains a time clock accurate to 30 seconds per year, which is used to activate transmission. All of the variable setup data, such as the GOES/LANDSAT mode, transmit interval, data collection between transmissions, memory usage, message formatting, and instrument configuration are programmed into the EDT through switches on a "test set" that is provided by the manufacturer. Each transmitter should be checked once or twice each year for drift and other performance. Conversion from GOES to LANDSAT mode, or vice versa, is accomplished by connecting the appropriate antenna cable, rotating a switch on the EDT, and reprogramming the microprocessor and time clock in the transmitter container using the test set.

The cost of the EDT, approximately $3,000, is expected to reduce substantially in the future since design and production have been established and because "more intelligent" EDTs are in an advanced state of development. These second generation EDTs will convert raw data to engineering units at the field stations, which, in turn, will permit a substantial reduction in the cost for a Central Receive Site.

4. EARTH SATELLITES

The GOES and LANDSAT systems are used to relay data from the recorder stations to the Central Receive Site at Vicksburg, Mississippi. The GOES system is provided by the National Oceanic and Atmospheric Administration (NOAA) and the LANDSAT system by the National Aeronautics and Space Administration (NASA). Three GOES are stationary above the equator at an approximate altitude of 22,500 miles at positions 75, 105, and 135 degrees west longitude. These three satellites contain identical channel frequencies and the center one serves as a spare. When a station is reporting in the GOES mode, the data are relayed by each GOES in operation; therefore, the same bit stream of data can be received from either satellite by redirecting the transmitting and receiving antennas. Omnidirectional antennas will be tested with the EDTs later.

There are 150 channels on each GOES. Several of the channels will relay data from self-timed transmitters and some are for interrogable-type transmitters. The assignment of channel frequencies is controlled by the National Environmental Satellite Service (NESS), NOAA. Four self-timed channels, 7, 35, 55, and 67, have been assigned to the Corps for exclusive use. Complete dedication of the channels is vital for water management and control

activities, especially during flood emergencies. It will be explained later how these channels and others, if assigned when needed, can be used by any and all Corps Districts in the United States.

All EDTs at Corps stations are self-timed and cannot be interrogated. Interrogation capability, which is needed for water management, is not used because of the added cost for transceivers and because interrogation can only be made by NOAA, NESS at Wallops Island, Virginia. As stated earlier, transmission in both the GOES and LANDSAT modes is controlled by a self-contained clock.

The polar orbiting LANDSAT passes within good communication range of the same point on earth at our latitude about every 12 hours at an altitude of approximately 500 miles. Acquisition of water data via LANDSAT is a major improvement in terms of cost and utility over conventional telemetry systems; e.g., landline and microwave systems. However, the infrequent and limited data-relay capability of this satellite for a given hydrometeorological or water quality station, and the relatively high cost for a tracking receive station impose a significant limitation on using LANDSAT for real-time water control management activities. In view of these constraints, water data will only be monitored via GOES and capability on the LANDSAT system will be discontinued.

5. RECEIVING EQUIPMENT

The Central Receive Site for the automated data collection system located at Vicksburg, Mississippi (figure 2), is owned by the Corps and operated by the staff of the River & Reservoir Control Center, Lower Mississippi Valley Division (LMVD) and Mississippi River Commission. Receive sites are commonly termed ground stations. Prior to installing the facilities in Vicksburg, the Corps contributed funds for installation of an experimental interagency GOES/LANDSAT ground station for DCS at Bay St. Louis, Mississippi, which is operated by the National Space Technology Laboratories (NSTL), NASA.

The satellite data acquisition and processing system at NSTL is considered experimental in nature, and there is no mandate to maintain its current posture or to provide a permanent operational service. However, the need is rapidly growing for applications of both the LANDSAT and GOES systems. Even though LMVD has become independent of NSTL on the GOES system, a continued interface is maintained between LMVD and NSTL for developmental purposes.

The GOES receive site at Vicksburg consists of a 30-foot-diameter, fixed-type receiving antenna, which will normally be directed toward the east satellite at 75 degrees west longitude directly above the equator. Although termed a fixed antenna, it can easily be oriented toward the west satellite at 135 degrees west longitude, or to the spare in the event a power failure occurs in the east satellite. Also, the capability to home in on the satellite whenever it drifts is provided with indoor remote control. The 1,500-pound receiving antenna is mounted on the roof of the LMVD office. A phaselock receiver and multichannel (four) demodulation unit, which operate simultaneously on all channel frequencies, provide the capability to collect data from 240 stations per hour, giving a total system capacity of 960 stations since all stations report at 4-hour intervals. The receiver and other parts of the system will accommodate several additional demodulation units, which will eventually be necessary to enlarge the network of stations. The reporting scheme is explained in detail later in the paper.

6. DATA COMMUNICATIONS PROCESSOR

Data processing equipment for the regional ground station in the River & Reservoir Control Center consists of a minicomputer with disc storage and dial-up communications capability. Principal components of the automatic data processing (ADP) system consist of: a Data General NOVA 840 minicomputer, CRT/keyboard terminal, arithmetic hardware unit, disc cartridge storage, a real-time clock, synchronous and asynchronous data communication channels, and a printer. In addition, a 19-inch Tektronix graphics terminal is interfaced with the NOVA 840 and a national ADP time-share system.

The configuration has the advantage of a real-time disc-operating system, which allows around-the-clock unattended operation. Any authorized user having a compatible terminal with dial-up phone capability may access the data base. Also, communication equipment is being installed to send data to users automatically at prescribed times. The communications capability will permit data programming and control information interchange with other ground stations, if desired. A list of ADP equipment is shown in Table II.

7. TIME ORDERED REPORTING NETWORKS

The preferred maximum time required to gather data from a network of water data stations in many watersheds is 10 to 15 minutes, with 30 minutes considered a moderate time lapse and 1 hour an absolute maximum. The time of concentration of storm runoff in watersheds and the need to enter data in water control computer models constitute the need to cluster reports and to report frequently. Thirty minutes has been adopted for trial initially. Constraints to consider in achieving this include: 25.6-second time required to transmit full memory and station identification in the GOES mode from a data collection station; 30-second possible annual drift in transmission time at a station; anticipated increase in the number of stations in the network; and the requirement by NOAA, NESS to make maximum utilization of satellite channels. Since data collected during a short period of time from relatively large regions are a requirement by water control managers, and because additional data from the region are seldom needed until a few hours have lapsed, the following plan was established which complies with the above constraints.

The stations on a given channel are scheduled to transmit at 1-minute intervals, allowing 60 stations to report in 1 hour on each channel. The four Corps channels can be monitored simultaneously, as well as others when added. A 4-hour reporting interval was selected to avail the channels for use by the Corps nationwide; i.e., the interval equals the number of time zones in the United States (U.S.). Each channel is available to District offices in different time zones at their same local times. For example, offices in the eastern time zone can use the channels from 6 to 7 a.m., local standard time (7 to 8 DST), followed by use of the channels in the central time zone, again 6 to 7 a.m., local standard time . . .etc., for the Rocky Mountain and Pacific time zones. Automated data collection just prior to normal working hours provides information on prevailing conditions for immediate use by water control managers. On this basis, subsequent reporting periods on standard time via GOES in each of the four time zones will be 10 to 11 a.m., 2 to 3 p.m., 6 to 7 p.m., 10 to 11 p.m., and 2 to 3 a.m. As mentioned earlier, data can be measured and stored in the EDT microprocessor at the data collection stations during the 4-hour intervals for transmission at the times mentioned above.

Data are displayed in the Center in near real-time on a CRT and on a map of the lower valley using light emitting diodes at key stations.

Data sets with automatic dialers will be installed on the synchronous and asynchronous ports to enable unattended data transmission to users. Also, the data can be accessed at any time by the District offices and other authorized agencies using dial-up I/O terminals. Standard-grade telephone lines are used for all communication by the processor, at least initially. Some requirements of the data management software for the communications processor are listed in Table III.

8. USE OF THE DATA

The staff of the River & Reservoir Control Center is responsible for water management and control of the water resources projects of the lower Mississippi River Basin downstream of St. Louis, Missouri. Data from stations in the U. S. outside the lower valley are also received at the Center via GOES, converted to engineering units, and disseminated in near real-time over landline to other Corps offices in the nation that have water management responsibilities. Increased development of water resources projects in the basin and severe weather events during the years 1973, 1974, and 1975

demonstrated a need to improve water control activities in the lower Mississippi River Valley and possibly the entire basin. Initial efforts have already been made by the River & Reservoir Control Center to broaden the roles of water control management and data communications. The first phase of the automated hydrometeorological data collection network via satellite was completed in fiscal year 1977. Additional stations are being installed and others are planned for the future. Activities are underway for evaluation and adaptation of water control models to better perform data handling, hydrologic forecasting, and water control decision-making tasks.

A sophisticated model for routing the Mississippi River that accounts for dynamic changes in river regimen and provides for operation of Mississippi River and Tributaries (MR&T) flood control features is in the final stages of adjustment and application. This model and others require input data in a real-time mode which is provided by the existing network, additional reporting stations, and the satellite data collection system. The most efficient manner for applying the models is through automatic collection and massaging the large quantities of data involved. The communications processor permits water control managers to make more efficient use of other computer facilities. It is also planned to establish a permanent data bank in a non-real-time mode at a large central processing unit (CPU) vendor facility to accommodate investigative-type water control activities. Conversion of the form of data, verification, and frequent or continuous interaction (real-time) with the data bank are not practicable on a large diversified processing computer. This is especially true for a multiuser facility, because it would require a high-priority interrupt for immediate access and turn-around which would conflict with other processing.

In addition to real-time water control activities, studies will be conducted in the near future to better define water control capabilities of the project under present conditions. A preliminary investigation will be made to improve the capability for water control, including consideration of physical (structural) changes in the MR&T portion of the overall Mississippi River water resource system. The communications processing system will accommodate data handling aspects of this task.

Developments under the direction of water control managers in LMVD are being closely coordinated with other organizational elements to ensure suitability for application elsewhere by the Corps. Appreciable savings can be realized in data collection hardware and software, satellite channel usage, and in application of water control models as a result of these developments. The satellite data collection system in LMVD will increase the dependability of data acquisition and, in turn, improve the efficiency of water control activities by providing necessary information directly to water control managers. In summary, the system will:

* Permit real-time interaction between a minicomputer dedicated to water management and control activities, data collection networks, and water control managers.

* Ensure continued real-time collection, processing, and dissemination of data via GOES/DCS.

* Convert data to usable engineering units and adapt to special formats.

* Provide a data bank for real-time use.

* Permit graphics interaction in the processing of data.

* Provide a terminal to Corps or commercial computers to process large-volume water control data.

9. TECHNOLOGY TRANSFER

The Global Meteorological Satellite System (GMSS) is making it possible to utilize completely automated environmental data collection systems throughout most of the world at a fraction of the cost of any other means of

data collection. With the new technology, a network of water data stations and a GMSS ground station, or Receive Site Facility (RSF), is highly competitive to the most modern landline or radiotelemetry data collection systems in terms of cost, timeliness, and accuracy. One Central Receive Site can collect, convert, and disseminate data to many users in real-time. Data can be processed several times each day from several hundred water data stations deployed in a drainage area of several hundred thousand square miles by using low-power EDTs.

A receive site facility can also include equipment to receive imagery of the earth's surface and cloud cover within and surrounding the water management area. Storm- and flood-warning systems can be enhanced for river basins and for the land-sea interface. Ground truth data can be obtained for ready comparison, correlation, and verification of other satellite imagery, such as that from LANDSAT. Data can be reported and used from remote locations where collection by conventional means is prohibitive for various reasons. In general, the new technology can make it much easier to provide to water control managers, hydrometeorological data and information that are vital for decision-making processes.

The hydrologic data collection network, meteorological imagery, and water management system for the lower Mississippi River Basin that has been operational on the GOES system since February 1977, clearly demonstrates the potential for worthwhile application in other areas. Design of a relatively low-cost GMSS receive site facility for both DCS and imagery can be installed essentially anywhere in the world where the technology is needed, to varying degrees of sophistication. The author, by special request from authorized officials, is presently providing assistance in designing such a system to be considered for installation in Southeast Asia.

10. BIBLIOGRAPHY

World Meteorological Organization, World Weather Watch, Global Observing System - Satellite Sub-System, Information on Meteorological Satellite Programmes Operated by Members and Organizations, WMO - No. 411, Secretariat of the World Meteorological Organization, Geneva, Switzerland, 1975.

Program Plan for Prototype Geostationary Operational Environmental Satellite Data Acquisition System for Corps of Engineers, Lower Mississippi Valley Division, by the National Aeronautics and Space Administration, National Space Technology Laboratories, Bay St. Louis, Mississippi 39520, July 1975.

Program Plan for Design and Fabrication of Displays for Corps of Engineers, River & Reservoir Control Center, Lower Mississippi Valley Division, by the National Aeronautics and Space Administration, National Space Technology Laboratories, Bay St. Louis, Mississippi 39520, November 5, 1975.

Preliminary Instruction Manual for the Convertible Data Collection Platform (Water Data Transmitter and Microprocessor) and Related Equipment by LaBarge, Inc., Electronics Division, P. O. Box 36, Tulsa, Oklahoma 74011, November 1975.

NOAA Technical Memorandum NESS 67, Data Collection System Geostationary Operational Environmental Satellite: Preliminary Report, National Oceanic and Atmospheric Administration, National Environmental Satellite Service, Washington, D. C., March 1975.

Annual Report, River & Reservoir Control Center, Lower Mississippi Valley Division and Mississippi River Commission, Corps of Engineers, 1400 Walnut Street, Vicksburg, Mississippi 39180, fiscal year 1977.

TABLE I. ACRONYM DEFINITIONS

ADP	-	Automatic data processing
ADR	-	Automatic data recorder
ASCII	-	American Standard Code for Information Interchange
CPU	-	Central processing unit
CRT	-	Cathode ray tube computer console or terminal
DCS	-	Data Collection System on GOES
DST	-	Daylight saving time
EDT	-	Environmental (water) data microprocessor/transmitter
ERTS	-	Earth Resources Technology Satellite, NASA
GMSS	-	Global Meteorological Satellite System
GOES	-	Geostationary Operational Environmental Satellite, NOAA
I/O	-	Input/Output
LANDSAT	-	Land satellite. Obtains land imagery data
LMVD	-	Lower Mississippi Valley Division, Corps of Engineers
MR&T	-	Mississippi River and Tributaries. A vast water resources project in the lower Mississippi River Valley consisting of channel improvement, levees, dikes, storage reservoirs, and other features.
NASA	-	National Aeronautics and Space Administration
NESS	-	National Environmental Satellite Service, NOAA
NOAA	-	National Oceanic and Atmospheric Administration
NSTL	-	National Space Technology Laboratories, NASA

TABLE II. COMMUNICATION PROCESSING EQUIPMENT

NOVA 840 with 64K memory	1 each
Automatic program load	1 each
Real-time clock	1 each
Console CRT	1 each
Disc System	
Disc Control	1 each
Disc adapter and power supply	1 each
Disc drive unit, 1.25 M words	2 each
Disc drive unit, 10 M words	2 each
Printer	
Printer I/O interface	1 each
Printer control	1 each
Printer serial matrix 165 cps 132 columns	1 each
Asynchronous Communication	
I/O interface board	4 each
Time-share I/O interface	4 each
Data set I/O parts - 1 @ 110; 1 @ 300; and 2 @ 1,200 baud	4 each
Precision crystal for 110 baud	1 each
Precision crystal for 300 baud	1 each
Synchronous Communication	2 each
Synchronous line adapter (parts) 1 @ 2,000 baud; 1 @ 4,800 baud	
Paper Tape System	
I/O interface board	1 each
Paper tape reader control	1 each
High-speed paper tape reader	1 each
Paper tape punch control	1 each
Paper tape punch	1 each
GOES/DCS Interface	
General purpose I/O board	2 each
Wire wrap pin and socket option	2 each
Graphics Terminal	
Precision Crystal Oscillator	1 each
Timeshare I/O interface	1 each
CRT Graphics Terminal. 19 inch	1 each
Hard copy unit	1 each
Date General I/O interface	1 each
Data Communications option	1 each

TABLE III. DATA MANAGEMENT SOFTWARE TASKS

* Monitor initial network of stations every 4 hours. Allow for network expansion, additional satellite channels, and more users, with no restriction on duration the system is on line. Real-time clock with manual override capability should control duration system is on line.

* Monitoring times (standard time) via GOES: 2-3 a.m., 6-7 a.m., 10-11 a.m., 2-3 p.m., 6-7 p.m., 10-11 p.m.

* Convert data to engineering units while monitoring network (water level, precitipation, water quality, other).

* Include option to send data to other users during monitoring cycle on a per-user basis; i.e., by toggle or entry on console, control automatic distribution of data to each user by the auto-dialer immediately after it is monitored. May choose to furnish the data at night, or user may not have auto-receive capability at outset and may add later.

* Provide option to print data at receive site during monitoring cycle, or after monitoring is completed.

* Include name of station, station number, and parameters names in output format, and, of course, the parameter values and time monitored. One line per station, if possible. Permit future modification to format.

* Store data on disc in minicomputer regardless of whether sent by auto-dialer to other users. Store in both raw data form and in engineering units. Retain data on file in mini for 15 to 18 months, if possible, which would extend through both the calendar and water year to accommodate ready use of the data and report preparation.

* Update arrays with real-time data for the electrical display while network is being monitored, such that the updating of a parameter being monitored will track the network monitoring scheme when the display is turned on.

* Provide arrays in systems software for the digital display that can be filled by applications software when network is not being monitored.

* Develop applications software program to address and fill any of the systems software arrays for the digital display (when network is not being monitored), either from disc to the array, or from keyboard console to the array; e.g., average daily stage, delta precipitation versus time, convert stage to discharge.

* Compute midnight to midnight daily averages for certain parameters following the 2-3 a.m. GOES and 11-12 p.m. ERTS monitoring cycles. Data measurement interval may be hourly. Include option to send to users by same provisions as above. Store in disc for ready access.

* Enable LMVD and other users to access mini files any time of day or night.

* Permit jobs to be run on NOVA in Fortran in background mode, with as much memory available for use as possible.

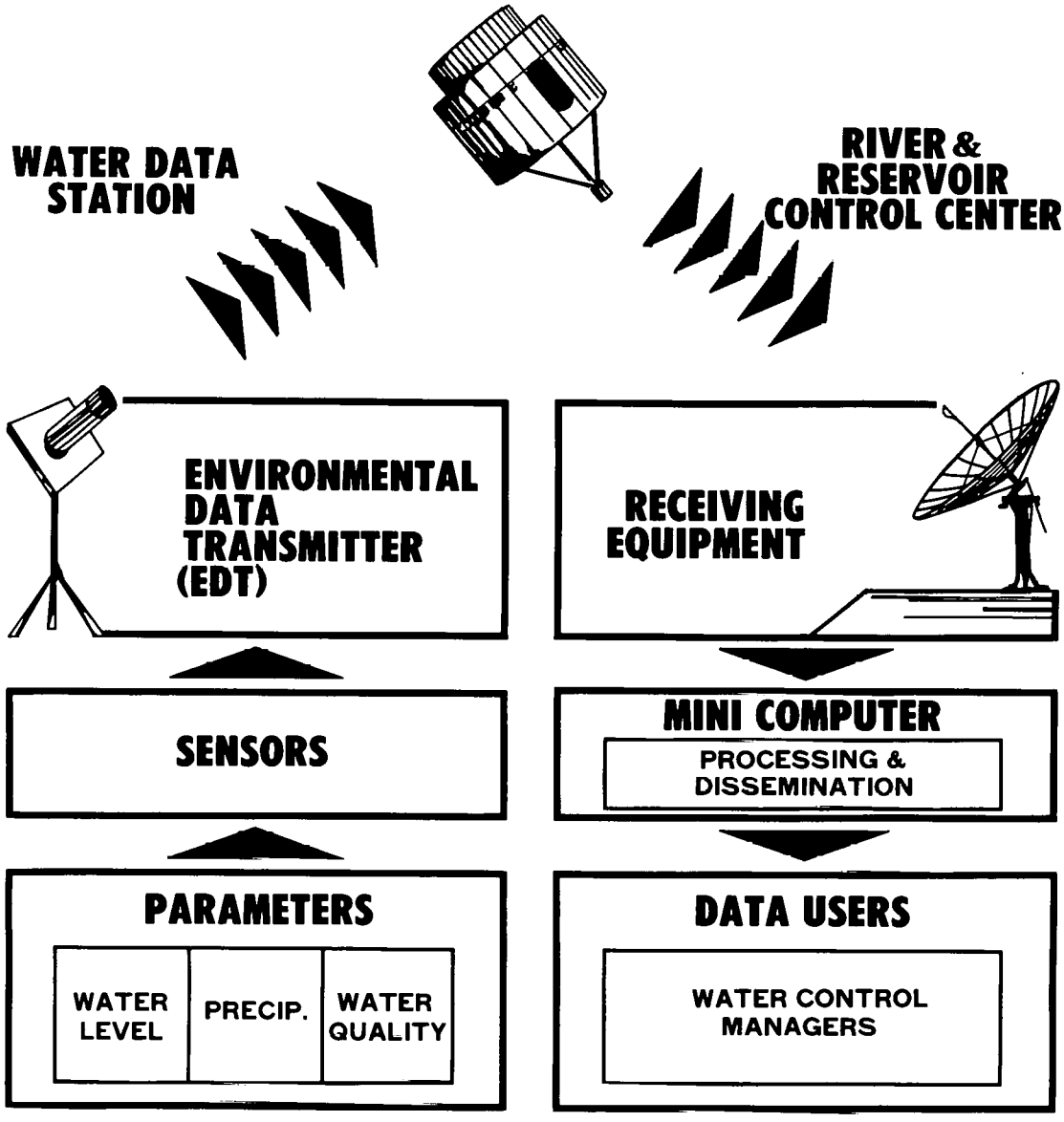

Fig. 1 Environmental Data Collection via GOES/DCS for Water Management and Control of the Lower Mississippi Basin

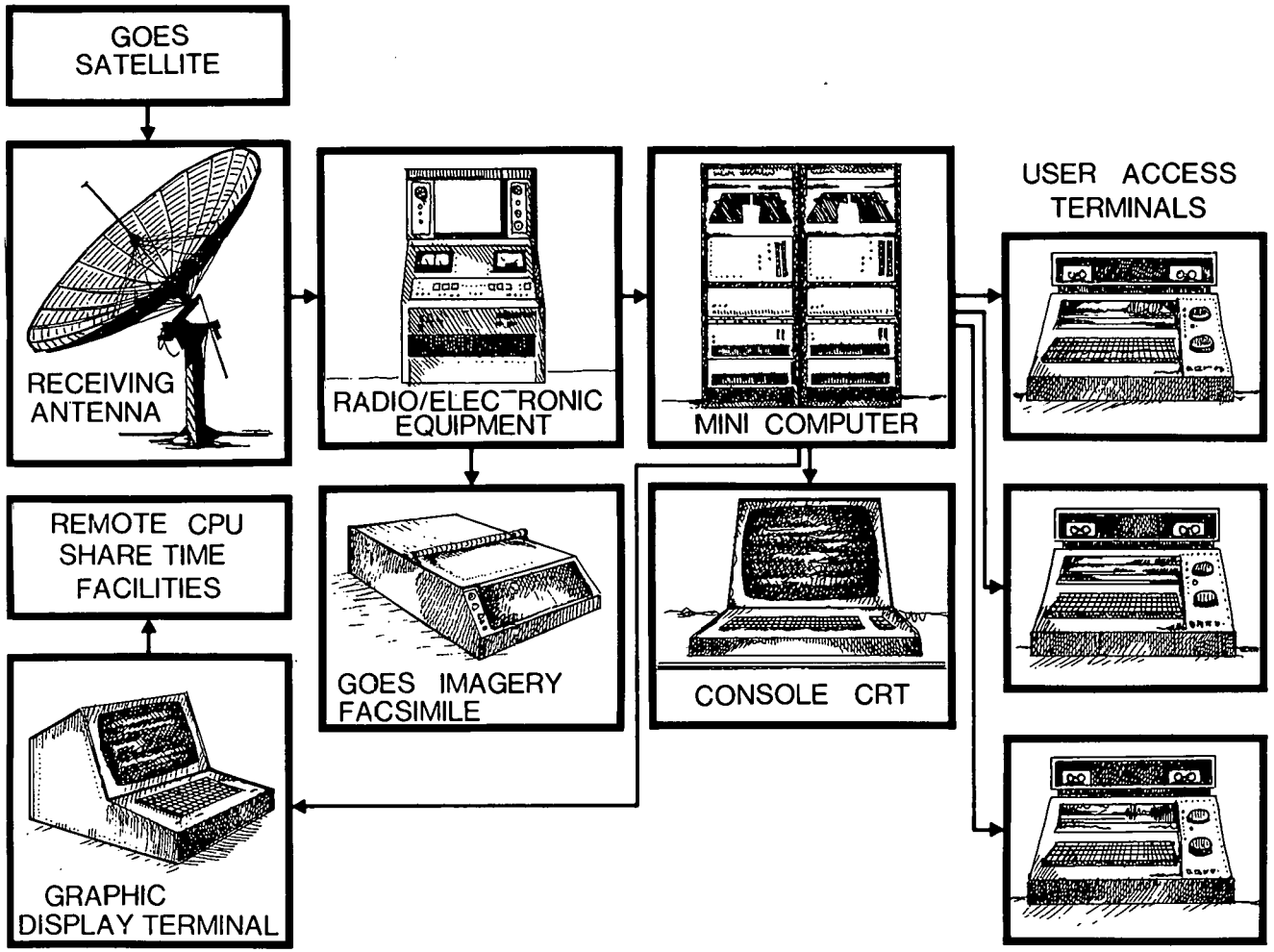

Fig. 2 GOES/DCS Receive Site in the River & Reservoir Control Center, Vicksburg, Mississippi

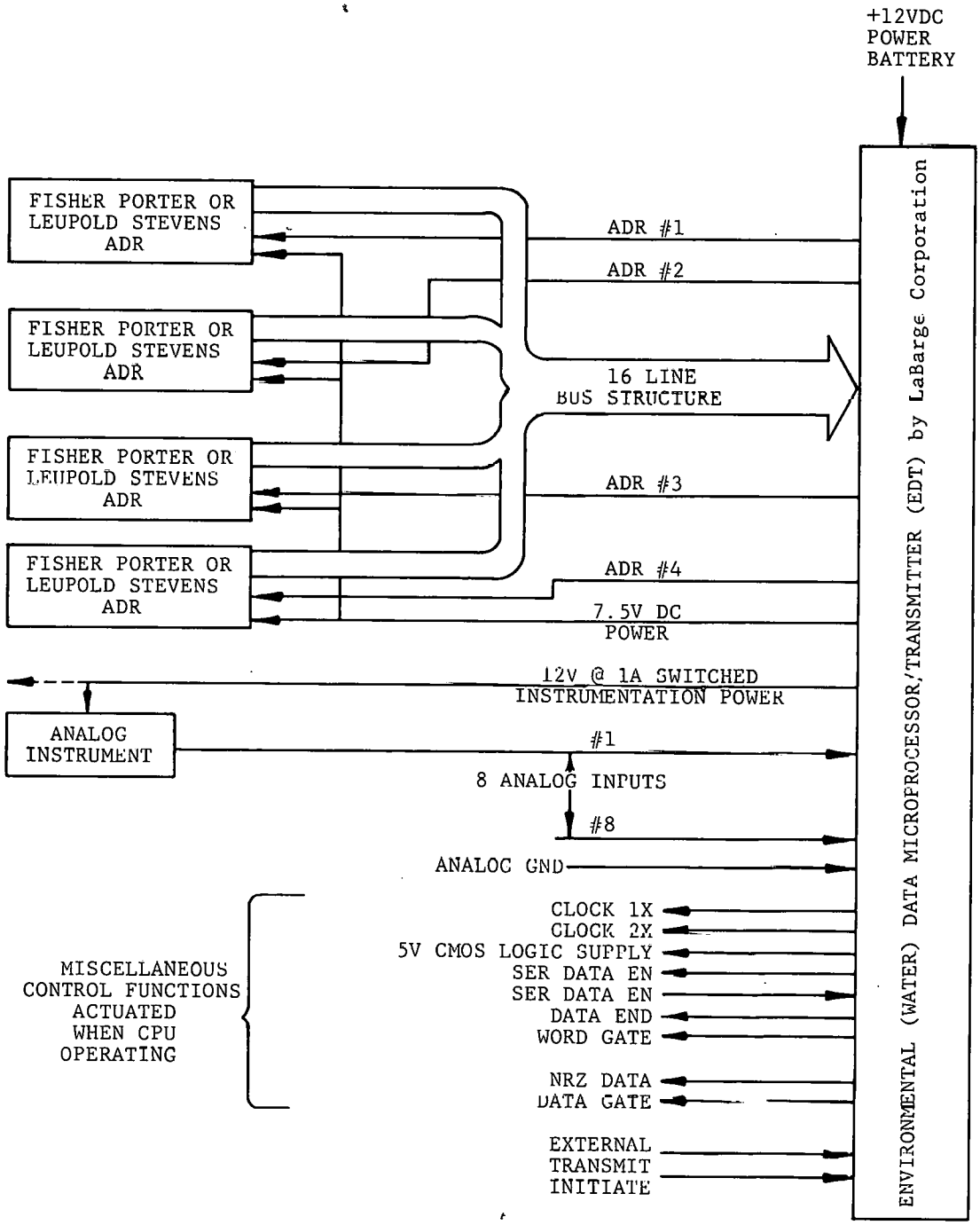

Figure 3. Electrical Interface

DETERMINATION OF WHEAT ACREAGES FROM LANDSAT IMAGERY IN THE NARRABRI DISTRICT OF NEW SOUTH WALES, AUSTRALIA

A.J. Parsons & E.A. Fitzpatrick

School of Geography
University of New South Wales
Sydney, Australia

ABSTRACT

For the 1975 wheat-growing season all LANDSAT-2 imagery obtained between May (the time of sowing) and November (the time of harvesting) was analysed for three study areas in the Narrabri district of New South Wales, Australia with the object of determining optimum times for identifying areas planted to wheat, the spatial variability in the identifiability of areas planted to wheat, and the value of using sequential imagery for correcting errors of misclassification.

It is found that best results are obtained in early June, corresponding to the period immediately after sowing when all areas planted to wheat appear as bare ground, and in late September, when the crop is in head but not begun to ripen. Considerable spatial variability in the accuracy of determination of areas planted to wheat is obtained. By using in conjunction the imagery for two dates upon which acceptable results are obtained, errors of misclassification can be reduced.

Results of this study indicate that for operational use of LANDSAT data for wheat-area mapping in the New South Wales wheat belt the total survey area must first be stratified into smaller areas in which crop phenology, terrain type and soil type are uniform. The study also shows that repeated analysis of imagery obtained at optimum times during the growing season may help to eliminate most Type II errors of misclassification.

1. INTRODUCTION

Early estimates of wheat production at the district, state and national levels are of considerable benefit in organizing the storage, transport, and sale of the crop. A basic requirement for such estimates is a knowledge of the area planted to wheat and of the progressive effects on the crop of weather conditions that ultimately influence grain yield. It is in this context that work on the Large Area Crop Inventory Experiment (LACIE) has been undertaken in the U.S.; this programme is worldwide in scope and is based upon the timely utilisation of LANDSAT multispectral data to appraise the area of crop harvested, and upon an interpretation of surface climatic data to estimate grain

yield on a unit area basis (MacDonald, 1976). Encouraging results have been obtained by Morain and Williams (1975) using such methods in an area of winter wheat production in southwest Kansas, U.S.A. Recent work by Idso et al. (1977) suggests that multispectral data from repetitive satellite monitoring may be useful in yield estimation as well as for crop area determination.

As an initial step toward assessing the feasibility of making crop area estimates for districts within the New South Wales wheat belt, we examined the identifiability on LANDSAT-2 imagery of paddocks planted to wheat in the Narrabri district, one of the major producing areas in the northern part of the wheat belt (see fig. 1). Should acceptable estimates of area planted to wheat be possible early in each season, then regularly updated district production forecasts should be possible by combining such estimates with yield predictions based on routinely collected climatic data (e.g. Nix and Fitzpatrick, 1969; Greacen and Hignett, 1976).

The amount of data potentially obtainable from LANDSAT during any one wheat growing season is considerable. At an eighteen-day overpass interval, there are on average ten to twelve viewing dates yielding between forty and forty-eight separate images. Planned increase in the frequency of LANDSAT overpasses may double the amount of data forthcoming. Even allowing that cloud on the dates of some overpasses will appreciably reduce the volume of useful data, any attempted analysis of all data over the whole of the growing season would be a formidable and costly task. For practical reasons, therefore, there is a need for investigating the extent to which the most useful information for crop identification may be concentrated in a few images. In this preliminary study, we analysed by visual means all available good quality imagery for the 1975 growing season in an attempt to identify:

(i) those images that would be most usefully analysed in any operational system to estimate district wheat acreage, and

(ii) whether there is any spatial variation in the identifiability of areas planted to wheat within a single district.

Visual interpretation of the LANDSAT-2 imagery was used as an exploratory method on the assumption that comparable rates of successful crop recognition could be achieved by computer-based techniques working directly from coded LANDSAT data held on magnetic tapes. Clearly any operational system applicable for an entire district, or for the whole of the wheat producing area of the state or nation, would require some form of automated classification.

2. DESCRIPTION OF THE STUDY AREA

The study area lies within the Namoi catchment in the North West Slopes and Plains region of New South Wales (see figs. 1 & 2). Within this general area, three smaller areas for study were chosen: one to the north of Narrabri (area A on fig. 2), one to the north-west (area B on fig. 2), and the third to the west of Narrabri (area C and fig. 2). The topography of these areas is mostly flat; in areas B and C slopes are less than 1^{o} and only in part of area A do slopes attain 3^{o}. With the exception of parts of area A where Tertiary basalts outcrop, all areas are underlain by alluvium. Because of local differences in the alluvium and the effect of outcrops of basalt, soils differ between the three areas (Hird, 1975). In area C soils are hard alkaline red-brown earths derived from the coarser alluvial deposits of the Namoi River. Soils of area B are grey and black, self-mulching, and mainly developed on the finer alluvial sediments. Area A is characterised by a variety of soils reflecting the more diverse parent materials found in that area. Soils here are generally similar to those of area B and are found together with brown clays and black earths derived from the sedimentary rocks and basalts of the Nandewar ranges to the east.

Differences in the physical character of the three areas are reflected in paddock sizes. Area B has the largest mean paddock size (81ha), area C the smallest (46ha) and in area B paddock size is more variable with a mean of 56ha

Small grains (mainly wheat) are the dominant winter crop in all three areas (see fig. 2). In the 1975 season approximately 67 percent of area A, 56 percent of area B, and 46 percent of area C was planted to wheat.

Figure 3, which is based upon crop developmental phases identified by Fawcett and Carter (1975), shows a crop calendar for wheat grown in the Narrabri district. Usual agronomic practice is for land previously used for wheat production to be plowed soon after harvesting and left as bare follow through late summer and autumn. All land preparation operations preliminary to planting are usually completed not later than early June. The actual date of sowing wheat in this area is highly opportunistic, depending on the time of occurence of rains which producers judge as adequate for effective germination and seedling establishment. The 1975 season conformed generally well with the temporal pattern of phasic development shown in fig. 3. Reported plantings within the area sampled for this study were with few exceptions between mid-June and mid-July, and harvesting was carried out mostly from about mid-November to mid- December.

3. LANDSAT IMAGERY

For the 1975 growing season good quality imagery for only eight overpasses is available up to the time of harvesting. Positive transparencies (9 by 9 inches) of the four multispectral scanner (MSS) bands for each of the eight dates were obtained, providing 32 images for analysis. The dates of these overpasses are shown by the solid arrows on fig. 3. On June 28 cloud covered most of areas A and B, and also it appears that high level cloud reduced the quality of the image over area C on that date. This overpass is therefore of limited value. On September 8 and November 1 cloud obscured all of part of areas B and A, respectively, and so an interpretation was possible only for the other two areas on these dates.

4. GROUND TRUTH DATA COLLECTION

In May 1976 visits were made to all properties within the selected study areas. Information was collected on land use during the 1975 growing season from each farmer. Prior to these visits an outline map was prepared for each property at a scale of 1:31,360 showing the boundaries of the property and locations of buildings, tracks and bores as shown on available topographic maps. Each farmer was then requested to fill in on the map the individual paddock boundaries and to indicate the area of each paddock, its land use for the 1975 growing season, and the dates of planting and harvesting the wheat crop.

The accuracy of these sketches was subsequently checked by comparing the paddock areas drawn on the map with the acreages given and summing all the areas to give a comparison with the known acreage of the property. In all cases the sum of paddock acreages was acceptably close to that for the whole property. Where individual estimated acreages per paddock did not agree with the size drawn, the map was adjusted accordingly. In no case was the error so great that the plan of the property could not be corrected with confidence. This information was then compiled on one land use map for the three study areas at a working scale of 1:100,000. The land use information collected by these methods is incorporated into fig. 2.

5. ANALYSIS OF LANDSAT IMAGERY

Because of the multispectral and sequential nature of LANDSAT data, the variability of terrain, spatial differences in crop phenology and in agricultural practice, the task of identifying areas planted to wheat is a complex one. The problem can be expressed as one in which answers to the following questions are sought:

(i) Are areas planted to wheat more easily identified on some MSS bands than others?

(ii) Can areas planted to wheat be more reliably identified at particular stages in the crop calender (fig. 3)?

(iii) Can subsequent imagery be used to validate, or improve upon, estimates made early in the season?

(iv) What is the effect on identifiability of a different phenology based upon a different agricultural practice?

(v) Is it possible to allow for the fact that all areas planted to wheat will not look the same at any one LANDSAT overpass because of differing planting dates or varieties leading to non-synchronous phasic development?

(vi) Can other small grain crops with closely similar life-form and phenology be distinguished from wheat?

(vii) Do different conditions of land form and/or soil type affect the identifiability from LANDSAT data of areas planted to wheat?

From the analysis of LANDSAT imagery from the Narrabri area during the 1975 season we attempt to provide answers to these questions.

Interpretation of the imagery was carried out using a Bausch and Lomb Zoom Transferscope to enlarge the imagery to a scale of 1:100,000 for mapping onto base maps. The three study areas were treated separately, and for each the task was to interpret and map all areas that appeared the same as, or similar to, one given area (one large paddock known to be wheat). Results of this analysis are given in table I. For each overpass the percentage of the known wheat area that is correctly identified is given in the first line, and the degree to which wheat areas are confused with other ground cover types is shown by the percentage values given in the second line. Results for that part of area B in which wheat is produced using irrigation are shown separately, though interpretations are made on the basis of similarity of appearance to a wheat paddock not irrigated.

Some minimum standard for acceptable identification is needed. We arbitrarily decide (a) that for an interpretation to be acceptable then at least 95 percent of the true wheat acreage must be identified, and (b) that the total identified area must be within 10 percent of the true value. The form of this standard is comparable to that adopted for LACIE, (see MacDonald, 1976) but the actual criteria are slightly more stringent.

Acceptable results are obtained for June 10 for area B (excluding the irrigated area) using MSS bands 5, 6 and 7 and for area A using bands 6 and 7. After that date acceptance results are not obtained again until September 26 when, using MSS band 7, acceptable results are obtained for areas A and B. For area C acceptable results according to the adopted criteria are never obtained, though it should be noted that the two dates on which acceptable results for the other two areas are obtained also give some of the best results for area C. For the irrigated part of area B, acceptable results are obtained only on October 14 using MSS band 5.

These results may be interpreted in terms of the known crop phenology. Early in the season areas of bare ground can be readily identified on both bands 6 and 7. Incorrect identification is minimal at this time. This applies also to the equivalent images of May 5 and, as far as can be assessed, to those of June 21. We can infer that in May not all areas have been plowed so that some areas are not represented. We can also expect that by the time sowing has been completed all bare areas will have been identified to an acceptable standard of accuracy. For the 1975 season the imagery of June 10 gave the optimum information. No areas of wheat were identified on May 5 or June 28 that were not also identified on June 10. If we can assume that all these areas were to be planted to wheat, then, for areas A and B, our preliminary estimate of wheat acreage is likely to be sufficiently accurate to be useful. When the crop is in head, it again has a distinctive reflectance value on MSS 7. With the exception of area C, an acceptable standard of identifiability is obtained at this time.

Errors of classification are twofold. Type I errors are those where areas of wheat are not identified, and type II errors are those where areas are wrongly identified as wheat. By minimising the chances of type II errors, we can produce an estimate of wheat acreage that will almost always be an underestimate. An area that is misclassified in June is unlikely to be misclassified again in September unless it is planted to a crop having a very similar life-form and reflectance in the measured bands, and also a similar phenology. Accordingly, therefore, we compared the results obtained from the September classification with those for the June classification. With the exception of a few small areas planted to barley in areas A and C, type II errors had not been made. Of the 95 percent of the true wheat acreage identified in June in areas A and B, all was subsequently reclassified as wheat in September. For area C discrimination later in the growing season is so poor that there was little chance that any of the 85 percent of true wheat area identified in June would fail to be similarly identified in September. Nevertheless, because of the absence of type I errors in September, the June estimate was validated.

8. DISCUSSION

The results of this analysis give affirmative answers to the first three questions posed earlier. The answers to the other four questions are not satisfactory and need further discussion.

Because the identification of wheat is based only upon reflectance values, any crop with a very similar phenology and life-form will be almost indistinguishable from wheat. Our ground truth investigations indicated that in 1975 there was no difference between sowing and harvesting times for wheat and barley and so discrimination between them was not possible. Barley is rarely grown in area B whereas in areas A and C barley may be sown over an area equal to about one-tenth of the area planted to wheat.

Wheat grown under irrigation has a different phenology from dryland wheat. It is planted later and harvested earlier. It is unlikely, therefore, that the two will appear similar on LANDSAT imagery at a time when they are easily distinguishable.

Whereas area B and, for the most part, area A are characterised by large paddocks and very little uncultivated land, area C has smaller paddocks and considerably more rough scrub interspersed with cultivated land. These factors, together with the effects of lower fertility soils on the growth of wheat in area C, probably account for the lower level of accuracy in wheat identification in area C.

7. CONCLUSION

These results indicate that for the Narrabri area only limited success is obtained in identifying areas planted to wheat from LANDSAT imagery by visual interpretive methods. For some areas accurate estimates can be obtained using imagery from June and September only. However, where agricultural practices are diverse, where paddock sizes are small, and where land is poorer, accurate estimates cannot be made. It seems unlikely that a more accurate estimate can be obtained for area C, but it may be hoped that for the irrigated part of area B an accurate estimate could be obtained by taking as the reference a known area of irrigated wheat rather than wheat grown solely on natural rainfall. Because the area under irrigation is relatively small in this study, it has not been possible to test this.

As a result of this work certain guidelines for any operational system that uses LANDSAT data to determine wheat acreage at the district level are suggested:

(i) The district must first be subdivided into areas in which land form, soil type and agricultural practice are relatively uniform.

(ii) For each such area, estimates of wheat acreage must be made separately using those LANDSAT data that are most likely to provide accurate results. With exception of the irrigated part,

imagery from May/June and late September are most useful in the Narrabri area.

(iii) For each area the likely percentage of land devoted to crops with a similar phenology and life form must be determined by ground truth observations and the estimate for the area adjusted accordingly.

(iv) For each area likely accuracy of the estimate should have been determined by an experiment similar to the one reported here, and the total district acreage given confidence limits accordingly.

With a sufficient input of ground truth information of this type, it seems reasonable to expect that reliable estimates of district wheat acreages can be obtained from LANDSAT data

REFERENCES

Fawcett, R.G. and Carter, O.G., 1973. Effects of plant density, time-of-sowing and fallow water on available soil water under spring wheat. Aust. J. Exp. Agr. and Animal Husb. 13, 714-7.

Greacen, E.L. and Hignett, C.T., 1976. A water balance model and supply index for wheat in South Australia. Tech. Paper No. 27, CSIRO Division of Soils.

Hird, C., 1975. Ch. 5. Soils in Narrabri Technical Manual, Soil Conservation Service of New South Wales.

Idso, S.B., Reginato, R.J., Jackson, R.D., 1977. Albedo measurement for remote sensing of crop yields. Nature, 266, 625-628.

MacDonald, R.B., 1976. The Large Area Crop Inventory Experiment. Paper presented to the 2nd Annual William T. Pecora Memorial Symposium, Souix Falls, South Dakota.

Morain, S.A. and Williams, D.L., 1975. Wheat production estimates using satellite images. Agron. J., 67, 361-364.

Nix, H.A. and Fitzpatrick, E.A., 1969. An index of crop water stress related to wheat and grain sorghum yields. Agric. Meteor., 6, 321-337.

TABLE I. ACCURACY OF WHEAT ACREAGE ESTIMATES OBTAINED FROM LANDSAT IMAGERY

DATE OF OVERPASS		MSS 4			MSS 5			MSS 6			MSS 7		
		STUDY AREA			STUDY AREA			STUDY AREA			STUDY AREA		
		A	B+	C	A	B+	C	A	B+	C	A	B+	C
5/5/75	1.	60	80(100)	80	65	70(40)	70	70	90(20)	65	80	90(20)	75
	2.	25	60(60)	40	20	60(45)	20	5	5(45)	15	5	5(40)	5
10/6/75	1.	75	95(95)	75	80	95(20)	75	95	95(20)	85	95	95(20)	80
	2.	10	35(50)	20	10	10(40)	20	5	5(40)	15	5	5(45)	10
28/6/75	1.	*	*	80	*	*	75	*	*	85	*	*	80
	2.			20			20			10			5
21/8/75	1.	90	90(80)	50	90	85(80)	60	65	90(80)	70	70	90(85)	70
	2.	10	35(60)	20	15	30(45)	20	15	5(0)	10	15	10(0)	5
8/9/75	1.	55	*	80	55	*	55	65	*	65	65	*	95
	2.	40		20	15		10	15		50	15		50
26/9/75	1.	90	85(20)	60	75	90(20)	60	85	80(25)	95	95	95(40)	90
	2.	15	5(0)	15	10	5(0)	5	10	10(0)	60	5	5(0)	50
14/10/75	1.	95	85(70)	70	85	85(95)	50	90	80(10)	90	80	75(20)	90
	2.	15	5(5)	15	10	5(5)	15	15	60(0)	40	10	10(0)	60
1/11/75	1.	*	75(20)	90	*	90(20)	90	*	65(0)	80	*	75(15)	85
	2.		25(0)	50		5(50)	50		60(0)	60		50(0)	80

1.= % OF WHEAT ACREAGE CORRECTLY IDENTIFIED TO THE NEAREST 5%.

2.= % OF AREA IDENTIFIED AS WHEAT THAT IS NOT WHEAT TO THE NEAREST 5%.

+ = EXCLUDING IRRIGATED AREA FIGURES FOR WHICH ARE GIVEN SEPARATELY IN PARENTHESES

* = AREA OBSCURED BY CLOUD.

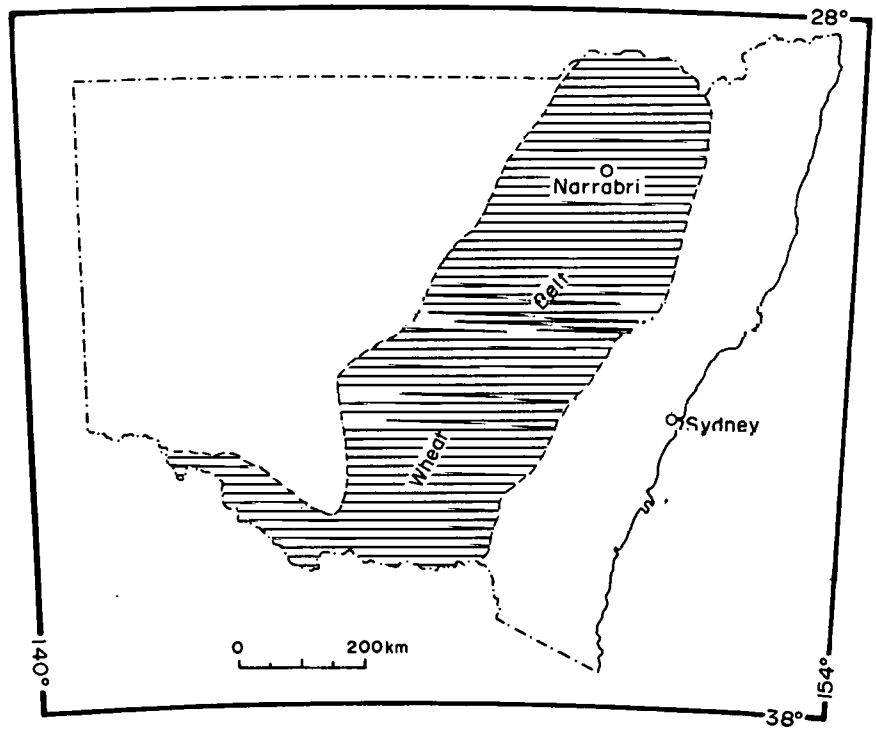

Figure 1. LOCATION OF STUDY AREA

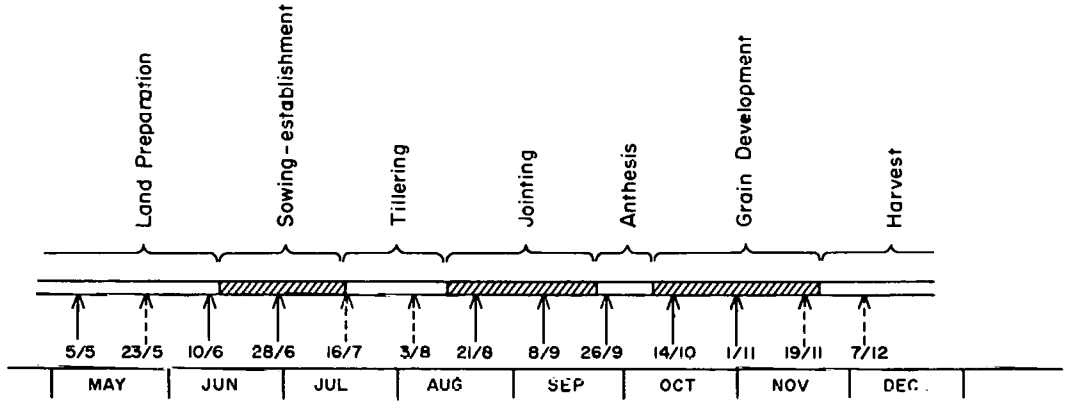

Figure 3. TIME OF LANDSAT-2 OVERPASSES IN RELATION TO TYPICAL CALENDAR OF FARMING OPERATIONS AND CROP DEVELOPMENT

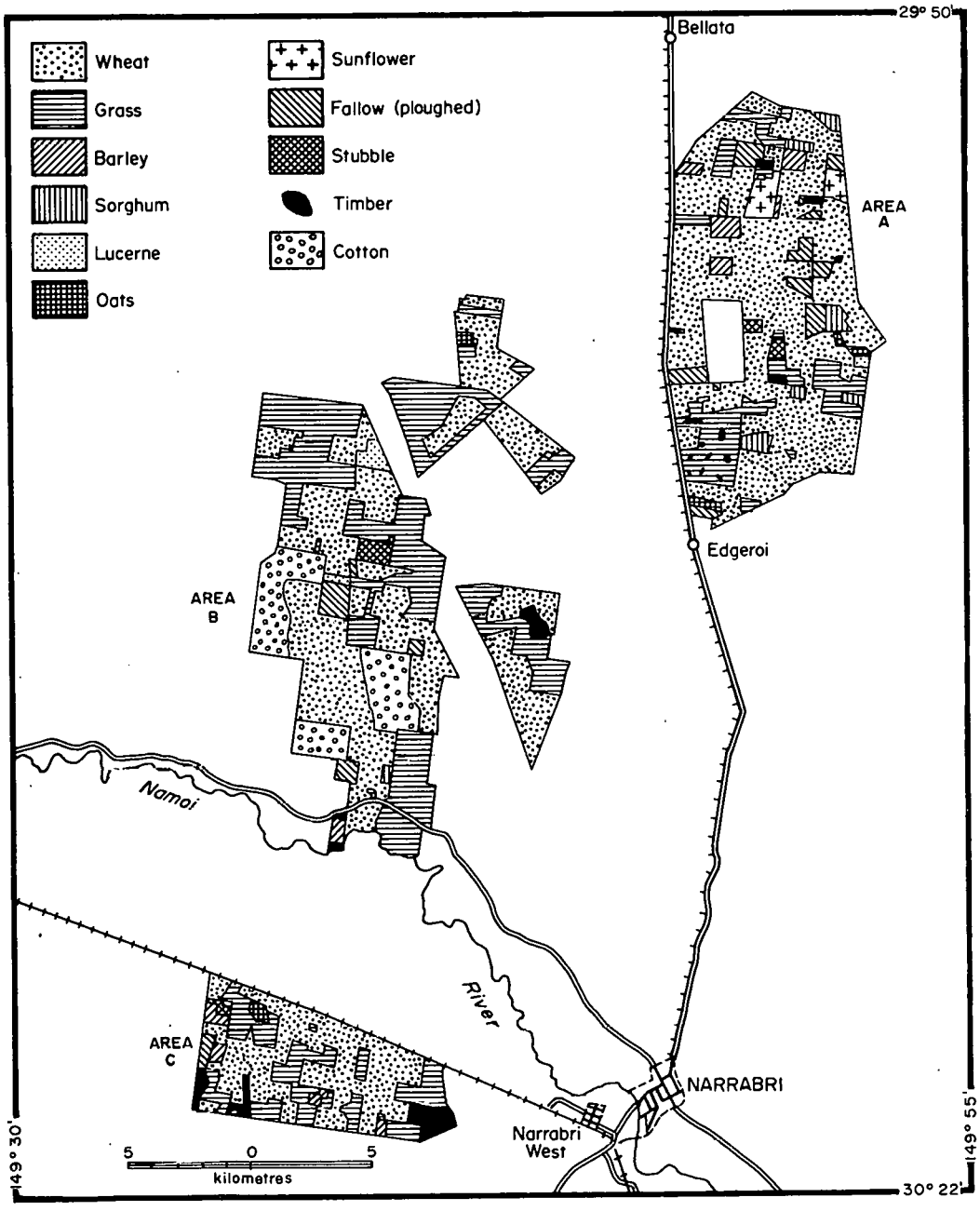

Figure 2. LOCATION OF AND LAND USE WITHIN STUDY AREAS

THIS PAGE

WAS INTENTIONALLY

LEFT BLANK

A STUDY ON COMPUTER ANALYSIS OF LAND USE CLASSIFICATION OF METRO MANILA

Alejandro Pascual and Wellman Silonga

Natural Resources Management Center
Department of Natural Resources
Diliman, Quezon City
Philippines

ABSTRACT

Digital analyses utilizing the Interactive Multispectral Image Analyzer System were undertaken to classify the existing land use patterns within Metro Manila. Using CCT data three subscenes at scale 1:100,000 projected on the CRT (TV screen) were extracted from Landsat I Scene No.1153-0146300 and LANDSAT II Scene No. 2455-012945, dated December 23, 1972 and April 21, 1976, respectively. These subscenes were processed utilizing digital techniques and various computer programs incorporated in the Interactive Multispectral Image Analyzer System in order to come up with a more refined land use classification.

Comparisons were made between the 1972 and 1976 subscenes and changes were noted down. To show the accuracy and reliability of the data obtained from the LANDSAT imagery, the 1976 LANDSAT statistical data gathered from the Analyzer were correlated with existing data gathered by the Metro Manila Commission in 1976. which utilized conventional ground survey methods.

Preliminary comparative evaluation of the data obtained with the existing source data maps indicated the extensive changes and growth that transpired in the area during the period 1972-1976.

The results of the evaluation of broad land use categories derived from satellite data could be useful to conceptual studies in land form changes and environmental development planning.

INTRODUCTION

Resource management and comprehensive land use planning require factual information on the nature, location and extent of present use of the land and total land resources. As such, all environmental components should be considered to be able to evaluate the impact of the proposed changes in planning of development policies.

In line with the objective of government agencies involved in resource management and development, this study was initiated to provide an initial evaluation of LANDSAT imagery for land use inventory and mapping; develop techniques of operational computer analyses of satellite multispectral data

into meaningful land form classification and other associated land use categories; and to determine the reliability and accuracy of such data obtained. Through the use of LANDSAT data, detection of the changes in the various land use categories between CCTS taken at different times could be easily monitored.

Metro Manila, the study area, is composed of four cities and 13 municipalities inhabited by some 6,925,000 million people. It was selected because of its rapidly growing population and industries and diversified pattern of urbanization. The whole area is divided into three zones, namely: (1) Inner Core - the multi-nucleated area which constitute the highest density of population growth; (2) Intermediate Core - the less dense but rapidly urbanizing area characterized by selected urban concentration and suburban residences along linear development corridors formed by major transport routes; (3) Outer Area - the lowest density area compared to other zones and characterized by large tracts of agricultural land and hilly terrain.

METHODOLOGY

Data analyses and processing were perfomed with the aid of the Interactive Multispectral Image Analyzer, otherwise called Image-100. The primary function of this system is to extract thematic information from multi-spectral imagery. This is done through statistical measurements of radiometric properties of the objects within the spectral limits of the imageries, complemented by the analyst's visual and statistical interpretation of the data presented.

SOURCE DATA. The available LANDSAT imageries covering the area of interest at the time of the study are LANDSAT I Scene No. 1153-0146300 taken in December 23, 1972 and LANDSAT II Scene No. 2455-012945 taken in April 21, 1976. For data interpretation, references used are topographic maps sheet No. 3263-II and 3163-II at 1:50,000 scale compiled by the U.S. Army Map Service utilizing photogrammetric methods and the land use photo-mosaic map at 1:25,000 scale prepared for the Human Settlement Commission. Ground truth investigations were performed on the areas which were not familiar to the interpreters to resolve doubts.

DATA PROCESSING. A working scene with an area of approximately 663 square kilometers covering the area of interest was extracted from the LANDSAT overview frames of 1972 and 1976, respectively, then loaded into the computer refresh memory and subsequently displayed on the TV-monitored screen.

Parametric modification was made to assign the best radiometric resolution or discrete gray levels that will be most suitable in the image analysis, which in this case was 128 gray level resolution for each nad used. To eliminate the effects of clouds, which was prevalent in the 1976 CCT, truncation offsets were established at (0,0) for band 4; (20,65) for band 5; (0,0) for band 6; and (11,48) for band 7! Only bands 5 and 7 have truncation offset values since these bands were used for extracting the data.

Prior to signature acquisition, enhancement of the image quality of the sub-scenes generated were accomplished utilizing pre-processing program. Cosmetic line patch was employed on a band by band basis to remove the bad scan lines and video noises present on each band.

Digital mapping was executed using the following spectral pattern recognition programs: (1) single cell signature acquisition; (2) multi-cell signature acquisition; and (3) semi-unsupervised clustering.

Training areas of known physical features in conjunction with the source data maps were selected on the image through the use of an adjustable electronic cursor. This is called the single cell acquisition training wherein a signature consisting of the feature space volume is enclosed by a single cell. Spectral values of the picture elements or "pixels" within the training area were measured. The limits of these spectral values define a four-dimensional parallelepiped in the spectral space. All the pixels on the entire imagery projected on the CRT were then compared with the parallelepiped limits and all

those falling within the bounds defined in the training area were alarmed and displayed on the TV-monitored screen.

Multi-cell signature acquisition obtained the multi-dimensional histogram of the training sites, thereby defining the multi-cell signature. Prior to this, the number of cells to be searched was displayed. During acquisition, the spectral values of the pixels in the training site were tested against the cell bounded by the single cell signature. The acquisition process utilized a binary search technique, whereby large empty regions of spectral space were quickly eliminated. The pixels corresponding to each of the elemental cells were accumulated, thus, defining a multi-dimensional histogram.

The semi-unsupervised clustering permitted the partitioning of the feature space of a multi-cell signature into the most spectrally separable classes. The clustering process was an automatic mode but the number of clusters depended on the interpreter's option. Analysis was repeated until a satisfactory result was obtained.

The various band combinations such as bands 4,5,6 and 7 bands 5,6 and 7; bands 6 and 7; bands 5 and 7; and band 7 were tried utilizing semi-unsupervised clustering for more refined classifications. The same training sites were utilized for both the 1972 and 1976 sub-scenes.

Bands 5 and 7 were found to be the best band combinations for land use and were used subsequently with seven (7) broad land use categories identified. (See Table I). These categories were stored on thematic channels displayed on the original image data base (CRT) and subsequently saved on magnetic tapes for future retrieval.

RESULTS

Output generated was in the form of a thematic printout map of the study area at scale 1:100,000. These categories were tabulated (Table I) to show the changes that occured from 1972 to 1976. Seven major land use categories were identified.

From TABLE I, it could be noticed that commercial and industrial areas had been combined, as well as riceland and grassland. This was done because segregation of these categories was difficult as the ranges of their spectral signatures were almost quite similar. The only way to separate these categories is to have a large training area, which the study did not offer. Metro Manila had a jumbled and mixed-up land use categories, causing the occurrence of overlapping signatures and misclassification. It was noted that some clusters did not conform to the uniformity of the actual urban patterns. It was possible, therefore, that any picture element at the image scale could comprise a complex conglomeration of categories.

A combination of bands 5 and 7 were utilized in order to come up with a more refined land use classification. Band 5 showed the cultural features which were dominant in Metro Manila, while band 7 showed the land formation features. Built-up areas were distinctly delineated using the semi-unsupervised technique in band 7. The classifications identified in this band were as follows:

(1) commercial/industrial areas; (2) high density residential areas; (3) low density residential areas; and (4) street patterns.

Thematic classification of commercial district and street patterns were combined to form the commercial/industrial areas. Similarly, high and low density residential areas were combined

Comparison of the results of analyses using bands 5 and 7 with the photomosaic land use map of Metro Manila indicatesa fairly good correspondence of the two sources of data.

The feature composition of the categories used as basis in the delineation of the categories are described hereunder:

1. Residential - Single, duplex,or condominium type of buildings with high reflective galvanized roof with few trees along the streets.

2. Commercial/industrial - Large buildings and complexes with high reflective concrete roofs along the major streets.

3. Parks/open spaces - Open field with few trees and bare lands, mostly newly-reclaimed areas and denuded areas.

4. Brushland - Predominantly tall grasses and second growth trees of medium height.

5. Riceland/Grassland - Rice paddies with scattered small trees along the dikes and contiguous spaces.

6. Wooded Areas - Predominantly tall trees in clusters.

7. Fishponds - Shallow mud-diked salt and fresh water fish paddies.

Table II shows the spectral bounds statistics of the various land categories. Resolution value of 128 has been used to meet the discrete gray level value information.

Table III shows the hectarage comparison between the data gathered by Metro Manila Commission (MMC) in 1976 and 1976 LANDSAT imagery of the different land use categories.

DISCUSSION OF THE RESULTS

Results gathered from 1972-1976 satellite imagery of the area shows an increase residential by 54.38%, which is typical of a growing metropolis (See TABLE I). The increase could be attributed to the economic growth that created a concentration of population attracted by better opportunities and employment in the area, and also, due to the government's program to provide low cost mass housing facilities, especially to the low-income sector of the population. Consequently, former ricelands, grasslands, brushlands and other idle lands, particularly those along the fringes of the commercial/industrial areas, gave way to residential subdivisions. This explains the decrease in hectarage of the previous categories. Open spaces increased due to the denuded areas caused by the cutting of trees and mainly due to the reclamation projects of Dagat-Dagatan offshore and areas along the Manila Bay. This accounts for the decrease of fishponds and wooded hectarage.

The sub-scene extracted from the CCT did not cover exactly the whole of Metro Manila as portions of Quezon City, Navotas, Malabon, and Caloocan City to the North, and Las Piñas to the south were ommitted. Likewise, the whole towns of Valenzuela and Muntinlupa were not covered. The other two classified sub-scenes for each CCT's generated which were covered in the central sub-scene would entirely ruin the quantification of the said classification, since it covered some areas which are not part of Metro Manila area. Furthermore, we had difficulty in delineating the exact boundaries of the desired area due to the minuteness of the LANDSAT overview scale.

Spectral bounds define the characteristics of a given object or material as a function of its reflectance of electromagnetic radiation at a number of discrete wavelengths (visible and/or non-visible). The spectral bound consists of feature space cells having some user-defined relationship.

From Table II, it could be noticed that vegetation canopies have lower spectral bound values in band 5 and tend to increase parabolically in band 7 and likewise in the upper bounds. The dominant features of reflectance curve for vegetative canopies are due to both the absorbing pigments, moisture content

and the internal structure of the leaves.

The relectance values of soils decrease from lower bound in band 5 to the lower bound in band 7 and likewise, in the upper bounds. Organic matter content, mineral content, grain size and distribution contribute to the spectral reflectance curve for a specific soil identification. Finer grain sizes mean increased spectral reflectance value as shown in the increase of spectral bounds in open spaces. Water exhibits also the same characteristics as those of soil.

The percentage of accuracy as shown in Table III shows a relatively good correspondence between the data gathered by conventional ground survey methods and that of the 1976 LANDSAT overview which was even cloud-covered. The great concentration of clouds are within the inner core of Metro Manila where the commercial/industrial areas are located. Hence, the increase of the commercial/industrial hectarage for 1976 was only 0.71%.

For the areas partially covered in the central sub-scene, the ratio between the squares of the total area of each land use category in the municipality or city partially covered to the total area of each land use category in Metro Manila was applied to the ground data gathered by the Metro Manila Commission. This ratio was subtracted from the total area of each land use category in Metro Manila Commission data.

The Metro Manila Commission showed a much detailed classification as it did the study by the conventional ground method. Commercial, industrial, institutional and utilities in the MMC classification were matched with the commercial/industrial categories in the LANDSAT imagery since these are almost of the same spectral signature characteristics.

It could be noticed in Table III that brushlands are added to parks and open spaces since, here, brushes are present at relatively big quantities and are often included in parks and open spaces.

CONCLUSION

Data from computer-analysis of satellite imagery aided by intelligent human evaluation and decision can produce good land use maps which are beneficial and useful to resource development planners and decision makers.

Broad land use categories on Level I and Level II classes are reasonably defined on LANDSAT imagery and tangible analysis results can be extracted through improved computer analysis techniques.

Plausible potentials of data of LANDSAT imageries in land use could be geared toward large mapping, urban change detection and land use inventory.

Detection of the changing land use pattern could easily be monitored using LANDSAT imagery through the timely processing of satellite data.

Reflectance values of vegetative canopies tend to increase parabolically from band 5 and 7 while spectral reflectance values of water and soil tends to decrease from band 5 to band 7. For soils, the finer the grains are, the higher the range of spectral bounds (both lower and upper limits.)

Evaluation of certain classes have results of minimum reliability so that continuing researches are being undertaken for better computer-analysis techniques to improve the accuracy of the outputs and to increase the information extraction from satellite imagery.

TABLE I

HECTARAGE COMPARISON OF THE DIFFERENT LAND USE CATEGORIES

	CATEGORIES	AREA IN HAS. (1972)	AREA IN HAS. (1976)	INCREASE	DECREASE
1.	Residential Areas	9,638	14,879	54.38%	
2.	Commercial/Industrial	8,394	8,453	0.71%	
3.	Riceland/Grassland	8,693	5,625		35.29%
4.	Parks)Open Spaces	2,594	2,893	11.53%	
5.	Brushlands	9,597	7,749		19.26%
6.	Fishponds	1,490	954		35.97%
7.	Wooded Area	970	154		04.12%
	TOTAL	41 376	40,707		

TABLE II

STATISTICAL COMPARISON OF THE SPECTRAL BOUNDS OF EACH OF THE LAND USE CATEGORIES

	CATEGORIES	BAND	SPECTRAL BOUNDS (1972) Lower	Upper	(1976) Lower	Upper
1.	Residential Areas	5	17	37	37	47
		7	12	34	30	46
2.	Commercial/Industrial	5	18	40	18	47
		7	10	26	12	34
3.	Riceland/Grassland	5	15	41	17	60
		7	32	70	24	90
4.	Parks/Open Spaces	5	29	61	40	93
		7	32	70	24	90
5.	Brushlands	5	16	26	27	47
		7	32	54	42	54
6.	Fishponds	5	13	18	11	22
		5	2	14	2	10
7.	Wooded Area	5	14	19	11	23
		7	30	50	32	44

* Resolution used = 128

TABLE III

Comparison of the Area of the Land use Categories Gathered by the Metro Manila Commission and the Computer Analysis of LANDSAT Imagery.

Categories	Area in Has. (LANDSAT Imagery) 1976	Area in Has. (MMC) 1976	Accuracy
1. Residential Areas	14,879	17,829	83.45%
2. Commercial/Industrial	8,453	8,950	94.45%
3. Riceland/Grassland	5,625	6,066	92.73%
4. Fishponds	954	1,298	73.50%
5. Parks/Open Spaces/Brushland	10,642	8,269	77.70%

NOTE: There was no available data of the quantification of the different land use categories of Metro Manila for the year 1972.

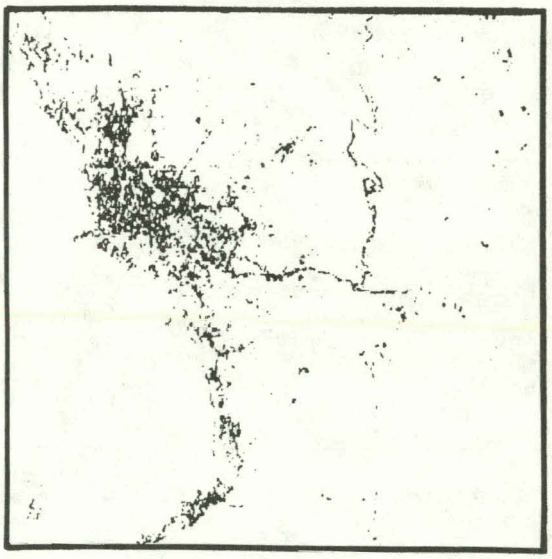

Fig. I - A computer generated binary printout showing the extent of commercial and industrial areas within Metro Manila in 1972.

Fig. II - A computer generated binary printout showing the extent of residential areas within Metro Manila in 1972.

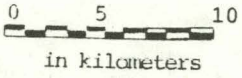

Fig. III - A computer generated binary printout showing the extent of commercial and industrial areas within Metro Manila in 1976

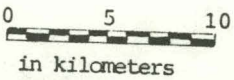

Fig. IV - A computer generated binary printout showing the extent of residential areas within Metro Manila in 1976.

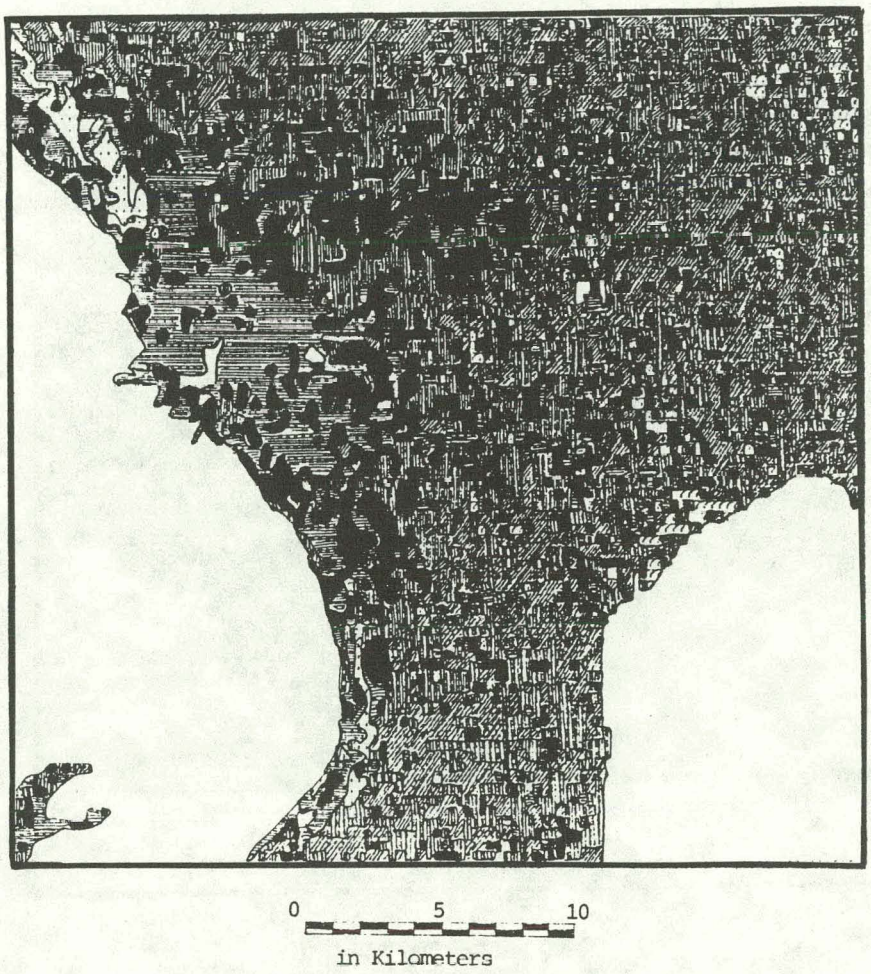

Fig. V - A computer generated alphanumeric printout showing the different land use categories within Metro Manila in 1972.

Open Spaces

Grassland/Riceland

Commercial/Industrial

Residential Areas

Brushland

Wooded Areas

Fishponds

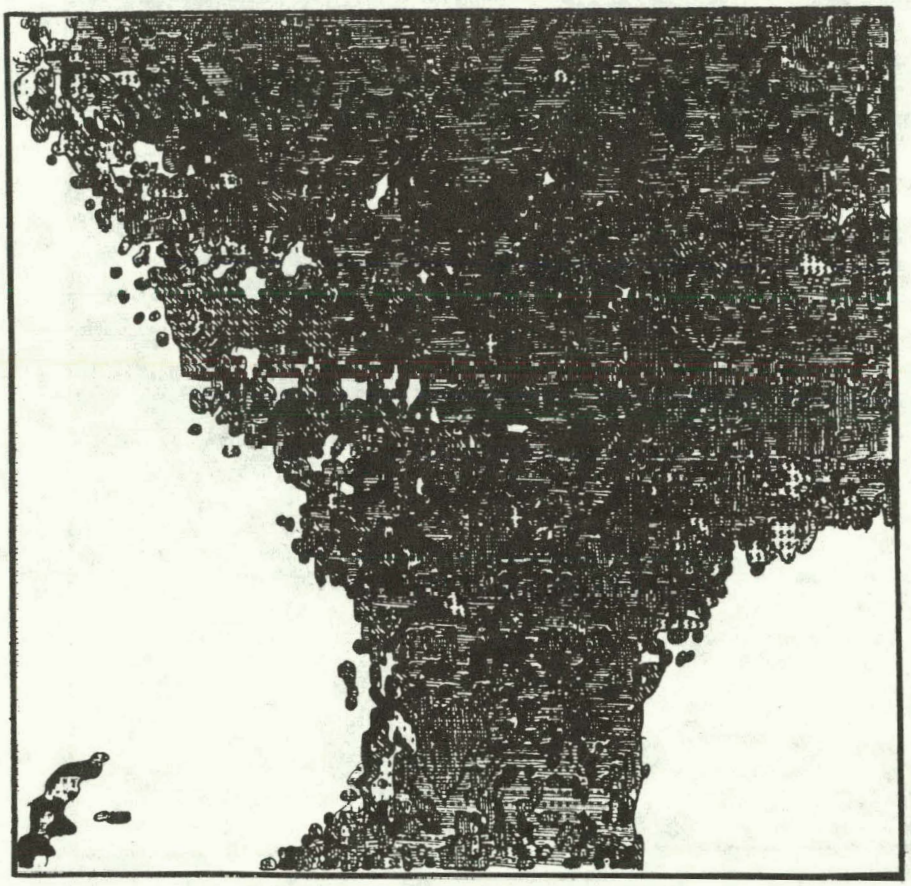

Fig. VI - A computer generated alphanumeric printout showing the different land use categories within Metro Manila in 1976.

Brushland

Commercial/Industrial

Grassland/Riceland

Residential Areas

Fishponds

Open Spaces

Clouds

REFERENCES:

Baldridge, P.E., Goesling, P.H., Leone, F., Minshall, C., and Rodgers, R.H, "Ohio's Statewide Land Use Inventory; An Operational Approach for Applying LANDSAT Data to State, Regional and Local Planning Program". Proceedings of the NASA Earth Resources Survey Symposium. Houston, Texas, June, 1975.

Anderson, J.R., and Witmer, R.E., "The National Land Use Data Program of the U.S. Geological Survey." Proceedings of the NASA Earthe Resources Survey Symposium. Houston, Texas, June, 1975.

Reining, P., and Egbert, D., "Interactive Multispectral Analysis of More Than One Sonrai Village in Niger, West Africa." Proceedings of the NASA Earth Resources Survey Symposium, Houston, Texas, June, 1975

Lundelius, M.A., Chesnutwood, C.M., Garcia, J.E. and Erb, P.B., "A Comparison of Land Use Determinations Using Data From ERTS-1 and High Altitude Aircraft." Proceedings from Symposium on Significant Result Obtained From the Earth Resources Technology Satellite 1. New Carrolton, Maryland, March 5-9, 1973

Hannah, J.H., Thomas, G.L. and Esparza, F., "Satellite Information on Orlando, Florida." Proceedings of the NASA Earth Resources Survey Symposium, Houston, Texas, June, 1975

Simpson R.B., and Lindgren, D.T., "Land Use of Northern Megapolis." Proceedings from Symposium on Significant Result Obtained From the Earth Resources Technology Satellite 1, New Carrolton, Maryland, Mar. 5-9, 1973

Branch, M.C., et al., "Urban Environments: Inventory and Analysis." Manual on Remote Sensing, Washington, American Society of Photogrammetry

Image-100 User's Manual, Ground System Department, Space Division, General Electric Company, Daytona, Florida

Image-100 System's Description, Ground System Department, Space Division, General Electric, Daytona, Florida

THIS PAGE

WAS INTENTIONALLY

LEFT BLANK

MAPPING TROPICAL VEGETATION ZONES IN THE STATE OF VERACRUZ, MEXICO

by

M. Soto, F. Lozano, C. Mejía, J. A. Diez, and M. Medina

Instituto de Biología, UNAM,
Instituto de Investigaciones sobre Recursos Bióticos,
and
Comisión del Plan Nacional Hidraúlico
Mexico

ABSTRACT

This article presents a detailed study of tropical vegetation zones using numerical analysis of Landsat data. The study area is totally within the state of Veracruz, Mexico, and reaches from the Cofre de Perote mountain to the town of Actopán. It is a complex ecological mosaic controlled by diverse factors such as altitude (from 250 to 4200 m), varied relief, position with respect to winds, etc. These factors, combined with intensive human activity, produce a great variety of vegetation communities, including high pastures, pine forests, low deciduous forests, coffee plantations, sugar cane plantations, orchards, and others. Analyses were based on a single image from 1973, and were made with SIADIS, the System for Automatic interpretation of Satellite Images of the Remote Sensing Department of the Commission of the National Hydraulic Plan of Mexico. Results consist of a detailed vegetation map of the study area, and demonstrate the usefulness of Landsat for vegetation mapping of tropical areas.

1. INTRODUCTION

One of the most urgent needs of the developing countries is self knowledge. Their plans for economic development depend strongly on an accurate knowledge of their abundant vegetation resources. However, traditional methods of inventory of vegetation zones are slow and costly. In many cases, the very resources being inventoried are disappearing before they can even be well understood.

The study presented here demonstrates that Landsat is quite useful in tropical regions, and hence of value to developing countries. It shows, in particular, that tropical regions can be studied with great success using numerical analysis of Landsat images.

Many specialists have the responsibility of inventorying vegetation

resources. However, even though they recognize their responsibilities, they are limited by the lack of economic resources and sometimes human resources. But in addition, they have been impeded by the very nature of the methodologies available to them.

Although the advent of earth resources satellites seemed promising to researchers in developing countries, most studies of remote sensing have been made in temperate countries. There the vegetation is homogeneous since forests tend to have a single dominant species or only a few, and land use is relatively constant over large areas. The tropical areas, by contrast, are heterogeneous. They are formed of many codominant species, and land use is very diverse, with fields divided into relatively small areas.

This study was undertaken with two motives. The first was to continue the development of techniques for the use of Landsat in tropical areas of Mexico. The other, more practical motive, was to map in great detail the vegetation of the study area.

2. BACKGROUND

Tropical vegetation is important for Mexico. It provides a significant economic asset, especially for the production of coffee, sugar cane, and fruit. Knowledge of these tropical natural resources is high in priority, especially since these zones are rapidly being altered and often destroyed by man.

It is important to note that despite the richness of tropical forests, they are fragile. They are quite vulnerable, and they can easily be damaged irreparably. Unfortunately we have many examples of their destruction in Mexico, including some cases in which nothing remains but drastic evidence of soil erosion. At this time the pace of alteration is so accelerated that many zones are being destroyed before they can be known and quantified as resources.

Because of this problem, an integrated program of studies of the tropical state of Veracruz was established in 1967. The new program was called "Flora of Veracruz" and was designed to develop a comprehensive inventory of the vegetation resources of the state (Gómez-Pompa and Nevling, 1970). Veracruz forms a large area along the Gulf of Mexico with very interesting ecological characteristics. It is on the edge of the northeastern arid zone, where the wealth in endemic species is great. Its elevation varies from sea level on the gulf to 5000 m at Mount Orizaba (Citlatepetl), the highest point in Mexico. Its relief varies from the very flat gulf coastal plain to mountain ranges of very high relief, part of the Sierra Madre Oriental and the Eje Neovolcánico ranges of Mexico. These and other characteristics make Veracruz an ecological mosaic that is very complex, interesting, and rich in natural resources.

One of the principal tasks of the Flora of Veracruz project is to elaborate a detailed map of vegetation which reflects potential and actual vegetation. This is especially high in priority since human activities are very intense in the Veracruz area.

With this in mind, a first stage of the work involved tests of remote sensing, including the numerical analysis of Landsat images, in studies of tropical vegetation (Soto et al., 1975 and 1976). This was done in the Johnson Space Center of NASA in Houston, Texas, in facilities of the Health Applications Office and the Lockheed Electronics Company.

These first steps demonstrated that remote sensing with Landsat could be very useful in studies of Veracruz. As a result, more detailed studies were made of a part of Veracruz, the Alchichica-Perote region (Soto et al.,

1977). This second step was made in collaboration with the Remote Sensing Department of what was then called the Secretariat of Hydraulic Resources of Mexico.

With this experience, a new experiment was made in the region from the Cofre de Perote mountain peak to the gulf coast, a very complex region. In a distance of 75 km we encounter elevations which vary from sea level to 4200 m, with consequent gradients of temperature. In addition, the region has distinct humidity gradients because of the humid winds from the northeast and the mountain ranges to the west and south.

The study of this region continues with the same Remote Sensing Laboratory, now a part of the Commission of the National Hydraulic Plan of Mexico.

2.1 LOCATION AND PHYSIOGRAPHY

The study area, which we have called the Cofre de Perote-Coast area, is defined by the following coordinates:

upper western edge	lat. 19°42'12" N.	long. 97°10'18" W.
upper eastern edge	lat. 19°35'12" N.	long. 96°26'48" W.
lower western edge	lat. 19°23'30" N.	long. 97°15;12" W.
lower eastern edge	lat. 19°16'30" N.	long. 96°31'42" W.

It is located in the southern end of the Sierra Madre Oriental, which starts in the Big Bend region of Texas and ends at the Cofre de Perote, where it touches the Eje Neovolcánico. The latter reaches to the coast near the 20° parallel, with only 75 km between the Cofre de Perote and the coast (Tamayo, 1962).

The altitude gradient is very marked. Cofre de Perote is at 4200 m, and the town of Rinconada, near the coast, is at 250 m. The latter is the eastern limit of these studies; our Landsat tape of the coastal areas was found to be unusable. (Fig. 1)

2.2 CLIMATOLOGY

Because of the high relief and the variation of altitude, we find a wide range of climatic types in the study area, from cold to hot, and from humid to subhumid. Following the climatic classification of Köppen as modified by García (1964), the following climates appear: (Fig. 2)

Cold

ETH	Cold tundra

Temperate (average annual temperature between 5° and 18°C)

C(fm)	Humid with abundant rain all year (the dryest month has more than 40 mm of precipitation)
C(m)	Humid with rains in the summer
$C(w_1)$	Subhumid with rains in summer, P/T (the moisture index of Lang) between 43.2 and 55.0
$C(w_2)$	Subhumid with summer rains, P/T greater than 55.0

Warm (average annual temperature between 5° and 18°C)

(A)C(fm) Humid with rain all year (the dryest month has more than 40 mm of precipitation)

(A)C(m) Humid with summer rains

Hot (average annual temperature between 22° and 24°C)

Aw_2 Subhumid with summer rains, P/T greater than 55.3

Aw_1 Subhumid with summer rains, P/T between 43.2 and 55.3

Aw_0 Subhumid with summer rains, P/T less than 43.2

3. METHODOLOGY

Machine classifications were made with the SIADIS system (System for the Automatic Interpretation of Satellite Images), which was developed in the Remote Sensing Department of the former Secretariat of Hydraulic Resources, which now forms part of the Commission of the National Hydraulic Plan of Mexico.

The Landsat image used in this study, 1306-16231, was taken May 25, 1973. This date corresponds to the end of the dry season.

After selecting the study area, grey maps (symbol-density maps) were made in each of the four channels. Based on these, and with existing knowledge of the area, about fifteen relatively homogeneous training fields were chosen. These were used for machine classification, resulting in tentative vegetation maps with thirteen classes, printed by the computer with alphanumeric symbols. Each character on this listing represented a pixel, and each class was represented by a distinct symbol. This map was colored by hand, and its details verified in the field.

Since some vegetation zones were mixed, a second classification was made, this time with 22 classes, skipping every other line and sample (each character represented four pixels). This map was also colored by hand and verified in the field.

Once the zones were verified, definitive training fields were chosen and the final, definitive machine classification was made.

3.1 GROUND TRUTH

Many field trips were made to identify and locate the classes that appear in the trial classifications. To help in the identification of training fields, two flights were made in a light aircraft provided by the government of the state of Veracruz.

Extensive use was made of the data bank of the Flora de Veracruz. Printouts were used to provide information on species and types of vegetation of several sites in the study area.

Training sites chosen for the final classification are listed in the following table:

TRAINING SITES

Cofre de Perote
High pasture of the Cofre de Perote
High pine forests on the Cofre de Perote
Basaltic outpouring near Las Vigas
Near Naolinco
Basaltic outpouring to the north of Jalapa
Area of the sugar cane mill, La Concha
Mount Macuiltepec in Jalapa
Area of San Andresito
Area of Coatepec
Area near Ursulo Galván
Area around Teocelo
Area of Xico
Area around Consuelo
Area of the Laguna de Miradores
Area around Rinconada
Area near Actopán

4. RESULTS

The zone is a complex mosaic of vegetation communities, due to environmental conditions and the variety of human activity. Figure 3 shows the results of the final machine classification of the entire study area.

This plate constitutes a map of soil use. We have identified both primary (natural) and secondary communities, the latter being the result of disturbances, in the majority, by man. With the latter there are many diverse levels of perturbations, the most serious being the loss of the soil by erosion. We also find communities which we might call "created", which are sustained by man, such as the various crops.

To describe and define the natural communities we choose as base the classification proposed by Miranda and Hernández (1963) and Gómez-Pompa (1978). For some of the secondary communities we adopt the criterion of Gómez-Pompa (1965 and 1978), and for those we call "created," we use their characteristics or simply the name of the crop.

It is interesting to note that some areas known to be different were classified as the same in the machine classification. This occurred because these areas have similar radiances. Nevertheless, even these areas are delimited (since they are in non-contiguous areas), and this is the important result for mapping.

The communities found in the study area are discussed below.

PINE FOREST.- This forest occupies the cold and temperate part of the study area between 3500 and 4000 m (the tree line). It is composed of Pinus hartwegii (Miranda, 1963, and Gómez-Pompa, 1978). Below 3000 m, down to 2000 m, we find that the forest is composed of Abies religiosa and by Pinus spp. (Fig. 4). In the final map (Fig. 3) these forests correspond to the purple color and occupy 4820 Ha.

PINE FOREST OF "MALPAIS" (BADLANDS).- This pine forest develops on basalt outpourings in the study area. These forests are composed of Pinus teocote, but rather sparcely due to the scarcity of soil. These communities have been studied in detail by Ortega (1978). On the final map they correspond to a light blue color and cover 1,760 Ha.

PINE-OAK FOREST.- This association is very frequent in Mexico. In the study area this community is localized in the regions between 2000 and 3000 m (Fig. 4), in the outpourings of basalt to the northeast of the Cofre de Perote, and near the villages of Coacoatzintla and El Esquilón (Ortega, 1978).

Towards lower elevations this community is frequently found in damp places where they are protected by small canyons. On the map they correspond to a pink color and cover 12,180 Ha.

The pine-oak forests are also found over the areas of high relief, where they give the appearance of ribs, or crests. In these cases we think that the information from the satellite is responding to the terrain rather than the vegetation. However, it is valid to say that these zones contain pine-oak forests, since they were so recognized in the field. On the map these correspond to a light green color. They cover 6,310 Ha.

DECIDUOUS FOREST.- This is composed of trees that lose their leaves in response to the cold season (Miranda, 1963). This is also called a cloud forest since fogs are present with great frequency. It has been studied in detail by Miranda and Sharp (1950). In the study zone its dominant species is Liquidambar macrophylla and diverse species of Quercus. It occupies regions between 900 and 1600 m, where the climate is transitional (warm humid, (A)C(m)).

Note that this community in the classification appears equal to the coffee zones. Even in low flights in light aircraft it is difficult to differentiate the deciduous forest from the coffee zone when the former has not lost its leaves.

On the map, light green corresponds to a deciduous forest in the dairy basin as described below. However, towards the east, the same color corresponds to coffee plantations.

HIGH ALTITUDE GRASSLANDS AND HIGH PLAINS.- Here the dominant species are grasses, principally Stipa Muhlenbergia and Festuca (Miranda, 1963). In the study area they are found above 4,000 m, where the climate is cold (ETH). Some authors, such as Miranda (1963), feel that these are at least in part secondary vegetation caused by the destruction of the pine forests. On the final classification they appear in gold, with an area of 4,790 Ha.

MIDDLE-ALTITUDE OAK FOREST.- This forest occupies the low, hot parts of the zone. It is characterized by small trunks. The principal species in the zone is Quercus oleoides. This type of oak has been considered by several authors (Miranda, 1959; Gómez-Pompa, 1966 and 1978; and Toledo, 1969) to be relicts of a mesic vegetation which existed in the past, these being the oak forests which adapted to hotter, dryer conditions. On the plate they correspond to purple and cover 19,920 Ha.

SAVANNA.- This term has been used to describe very distinct types of vegetation. We use it in the sense of Gómez-Pompa (1978) to describe the tropical pastures of low altitude with or without scattered trees, whose soils have problems of drainage; they usually have a well-defined layer of clay.

We need to note that we have not made an exhaustive study to define whether this type of vegetation in the lower part of the study area is really a natural savanna or whether it is savanna-like secondary vegetation. Nevertheless, we have listed it as savanna to correspond with its physonomic characteristics. Our doubt comes from the fact that at higher elevations we find similar groupings (yellow on the map) to which we have also attributed to pastures, but derived from cut-over or abandoned areas. On the map savannas are represented by yellow and cover 42,920 Ha.

LOW DECIDUOUS FOREST.- This zone is characterized by the moderate height of the trees, less than 15 m, and the fact that they lose their leaves in the dry season. In the study area they are found below 400m. Even though the structure of the communities of vegetation varies, depending on the region, the most frequent components cited by Gómez-Pompa (1978) are Cordia dodecandse, Crescentia alata, Enterolobium Ciclopcarpum, Piscidia pisupula, Tabebuia chrysantha, and Tabebuia rosea. On the map they correspond to a strong blue color, and they cover an area of 35,120 Ha.

SECONDARY VEGETATION.- This term refers to communities of vegetation that grow after the natural, or primary, vegetation has been cut. These stands are different from primary communities but can easily be confused with them.

The study area has been disturbed since early times, and therefore the presence of secondary vegetation is no surprise. The ones we find are derived from pine or pine-oak forests. The most frequently found genera are Alnus, Mirica, and Carpinus. These trees are small, less than 10 m tall. On the map these zones correspond to a turquoise color in the upper part (2000 to 3000 m).

Nevertheless, in the basaltic outpourings to the north of Jalapa, the vegetation is not secondary. Rather, it is a low deciduous forest (Ortega, 1978), whose characteristics, at least in tree size, is similar to secondary vegetation. We feel it will be necessary to use an image from the dry season to see if it is possible to separate these two groups in the machine classification.

DAIRY PASTURES.- This type of vegetation is one we have included as created and sustained by man. It corresponds to the dairy region which is called the dairy farm basin. On the map it corresponds to an orange color. It covers 22,660 Ha.

COFFEE ZONES.- As indicated, coffee zones in the machine classification appear to be the same as the deciduous forest since the sensor sees only the overstory trees. We detected coffee zones around Teocelo, Coatepec, and the region to the east.

SUGAR CANE.- This crop appears on the classification map as dark green. We visited the cane areas of El Castillo, east of Coatepec, Naolinco, and the Actopán basin. They cover an area of 8,700 Ha.

ORCHARDS.- These zones correspond to light orange on the plate. They may contain citrus, a variety of mango (petacón), or papaya. The trees are mixed in size but less than 5 m. In many cases the orchards are mixed, making their classification more difficult. These zones cover 6,150 Ha.

POTATO FIELDS?.- It is very possible that the magenta zones of the map correspond to fields of potatoes because they lie in high parts of the pine-oak forests. Nevertheless, we were not able to locate an exact training field. It will be necessary to make more field trips to locate them.

ERODED ZONES.- Eroded zones are associated with red, tan, and pale green (an ivory green) in the plate. Our deductions are based on the fact that these colors predominate in the city of Jalapa. On the other hand, the red color in the southern parts of the study area correspond to the most eroded regions that we visited.

Taken together, the eroded zones measure 19,345 Ha, which is quite large considering the size of the test area.

The tan color in the surroundings of El Castillo have the special name of "tepetate" soils, which characterizes them as very argillaceous and impermeable. They cover 7,550 Ha.

We were not able to locate an exact training field corresponding to the pale green areas, and we were therefore unable to determine the degree of erosion in these areas.

UNIDENTIFIED ZONES.- There were two zones we did not identify, the ones colored light yellow and pink. The yellow ones are associated with pastures of the dair basin, and they appear to involve some state of growth of that

pasture land vegetation. We would need several training fields to verify this interpretation. The pink zones are associated with the city of Jalapa.

5. CONCLUSIONS

It is evident that remote sensing offers great possibilities for the study of tropical vegetation. The fact that we have been able to define the vegetation of such a complex area confirms this. It must be said, nevertheless, that the need for ground truth is great. We would not have been able to obtain these results if we had not had all the advanced information which we used, in effect the product of ten years of floristic studies.

The map that we obtained is more than a vegetation map. It is a map of land use. We do not consider it definitive, but it is certainly more than 80% correct. This is especially good since we used an image from May of 1973, the latest available, but we collected ground truth in 1976 and 1977.

We believe that we are still quite far from the automatic identification of vegetation resources of tropical areas. Still, this is not discouraging. With our experience to date, we know that we are working with a technology that is adequate to our needs. It will be necessary in the future to experiment in other regions, and in other dates. In addition, the analysis of images of a given area from several dates, that is to say, multitemporal analysis, will resolve problems of zones which appear identical on a single date.

6. ACKNOWLEDGEMENTS

The authors express appreciation for the help of Dr. L. E. Giddings in various phases of this work, including its translation to English; to Dr. Arturo Gómez-Pompa for reviewing it and offering helpful suggestions; to the biologists Wilfredo Márquez and Roberto Ortiz, and to Sr. Ismael Calzada for their collaboration in our field trips; to Sr. Felipe Villegas for the fine drawings; to Srta. María Bernardina Bello for her help in the laboratory; and to Sr. Lino Monrroy for his help in coloring the various maps. In particular, we wish to express our sincere appreciation for the collaboration of the Office of Security of the state of Veracruz.

7. REFERENCES

CETENAL. 1970. Carta de Climas CETENAL, Secretaría de la Presidencia, México, hoja: Veracruz. Mapa a color, escala 1:500000 (Impreso al reverso "Sistema de Clasificación de Koeppen modificado por García para adaptarlo a las condiciones de la República Mexicana" y gráficas de precipitación y temperatura). Elaborado por el Instituto de Geografía, UNAM.

García, E. 1964. Modificaciones al sistema de clasificación climática de Koeppen (para adaptarlo a las condiciones de la República Mexicana). Offset Larios, México, D.F. 71 p.

Gómez-Pompa, A. 1965. La vegetación de México. Bol. Soc. Bot. Méx. 29:76-120

Gómez-Pompa, A. 1978. Ecología de la vegetación de Veracruz. Compañía Editorial Continental, S.A. México. 91 p.

Gómez-Pompa, A. y L. I. Nevling. 1970. La Flora de Veracruz. An. Inst. Biol. Univ. Nal. Autón. México 41, Ser. Botánica (1):1-2.

Miranda, F. and A. J. Sharp. 1950. Characteristics of the vegetation in certain temperate regions of eastern Mexico. Ecology 31:313-333.

Miranda, F. and X. Hernández. 1963. Los tipos de vegetación de México y clasificación. Bol. Soc- Bot. Méx. 28:29-179.

Ortega, O. R. 1978. Estudio de la vegetación y la flora de una corriente de lava (Malpais) al NE del Cofre de Perote. Tesis en preparación. Esc. de Biología, Universidad de Veracruz. Jalapa, Ver. México.

SARH--Dirección de Agrología. 1977. Perspectivas del desarrollo agroeconómico del estado de Veracruz. Secretaría de Agricultura y Recursos Hydráulicos. México. 116 p.

Soto, M., A. Gómez-Pompa, F. Menéndez, y G. Arp. 1975. Uso de los sensores remotos en el Programa Flora de Veracruz. In: Memorias de la Primera Reunión sobre el aprovechamiento de los datos derivados de los satélites tecnológicos para el estudio de los recursos naturales. Comisión Nacional del Espacio Exterior. Secretaría de Comunicaciones y Transportes. México.

Soto, M., A. Gómez-Pompa, F. Menéndez, and G. Arp. 1976. Uso de los satélites para el estudio de la vegetación tropical. Ciencia y Desarrollo, México 2(7):3-6.

Soto, M., F. Lozano, A. Diez, C. Mejía, y S. Villa. 1977. Estudio piloto de la vegetación en la región Alchichica-Perote por medio de percepción remota. Publ. Inst. Invest. Rec. Bióticos 2(3):19-36 México.

Tamayo, L. J. 1962. Geografía General de México. Instituto Mexicano de Investigaciones Económicas. México. Vol. 1. 561 p.

Toledo, V. M. 1969. Diversidad de especies en las selvas altas de la planicie costera del Golfo de México. Tesis Fac. de Ciencias, UNAM. México, D.F. 55 p.

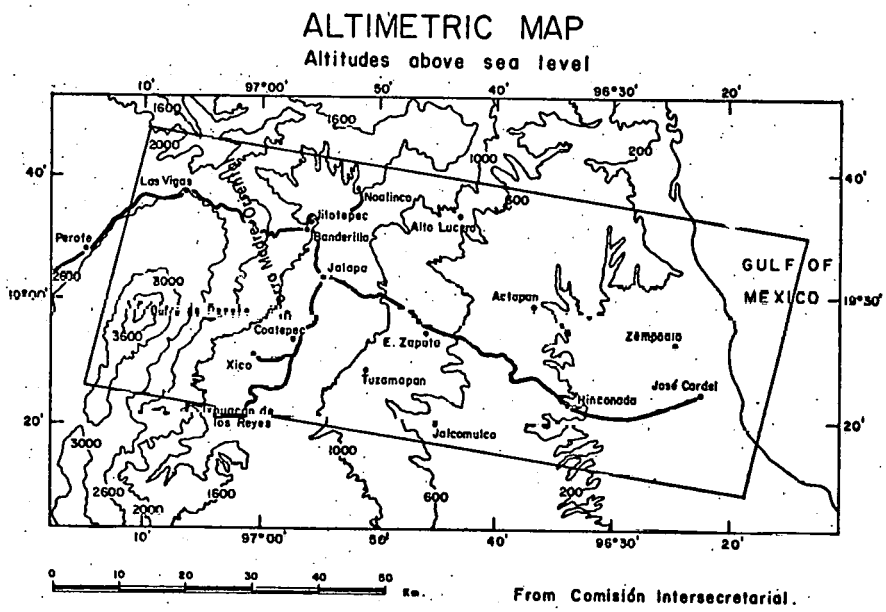

Figure 1. ALTIMETRIC MAP

(In addition to contours, this map shows some of the towns used to identify training fields)

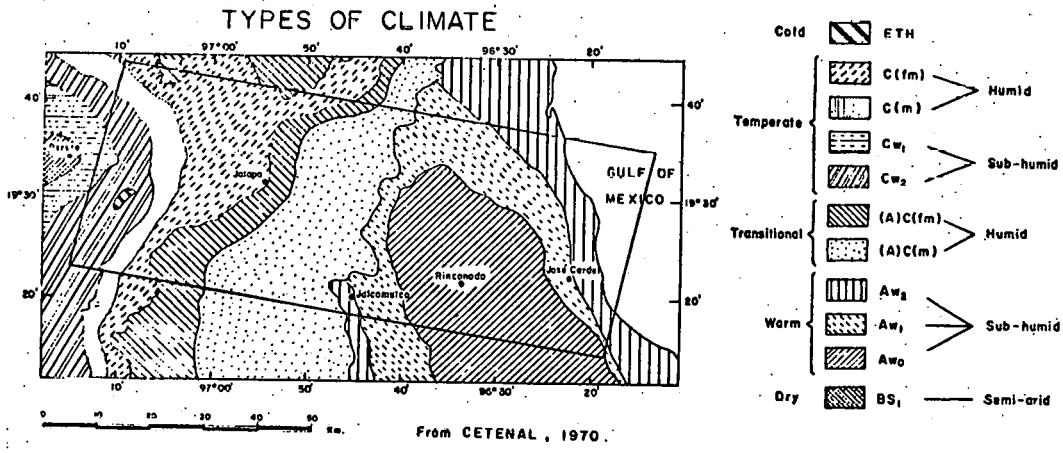

Figure 2. CLIMATES OF THE TEST AREA

(After the climatic classification of Köppen, as modified by García (1964)

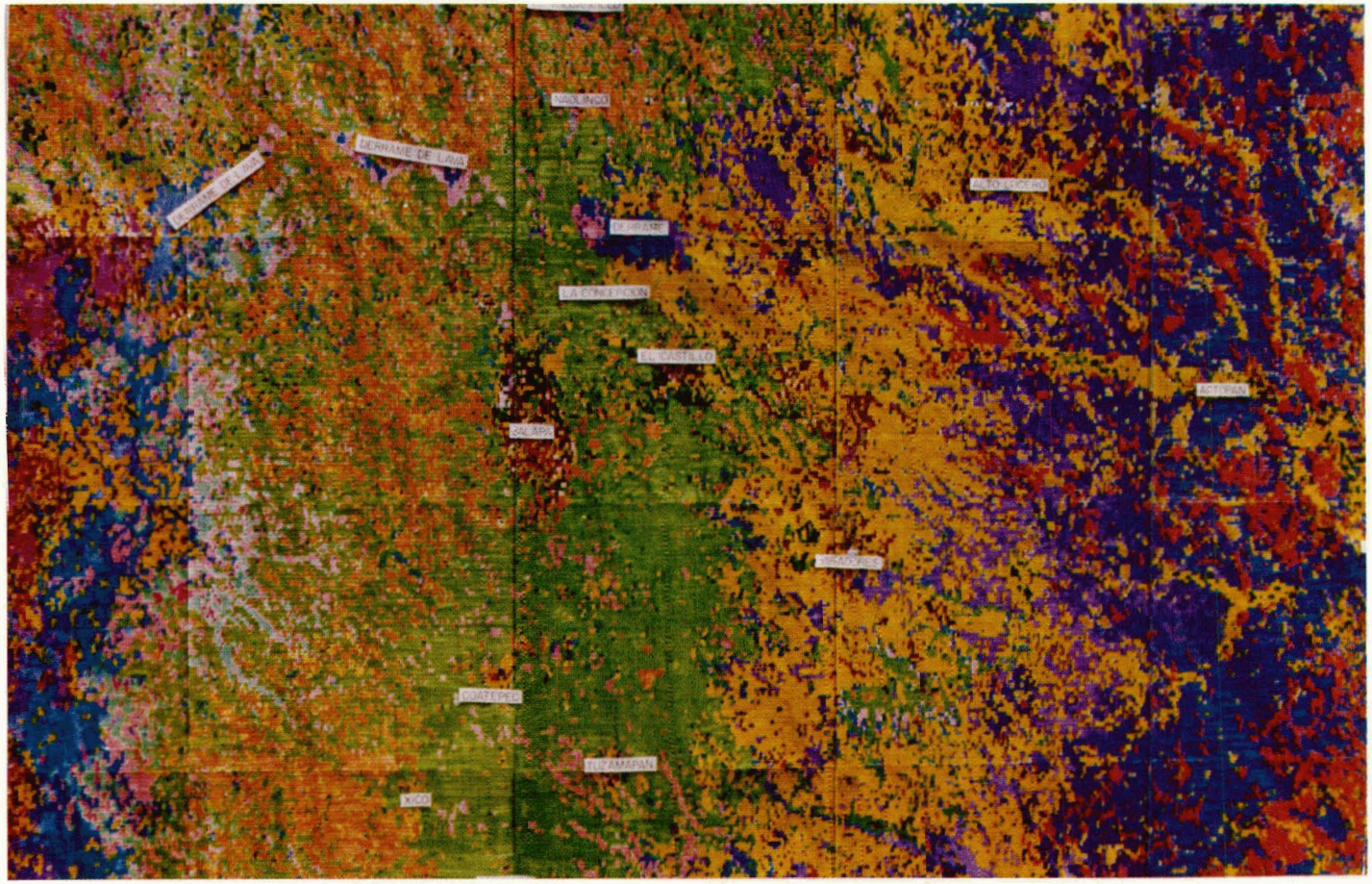

Figure 3. HAND-COLORED CLASSIFICATION MAP

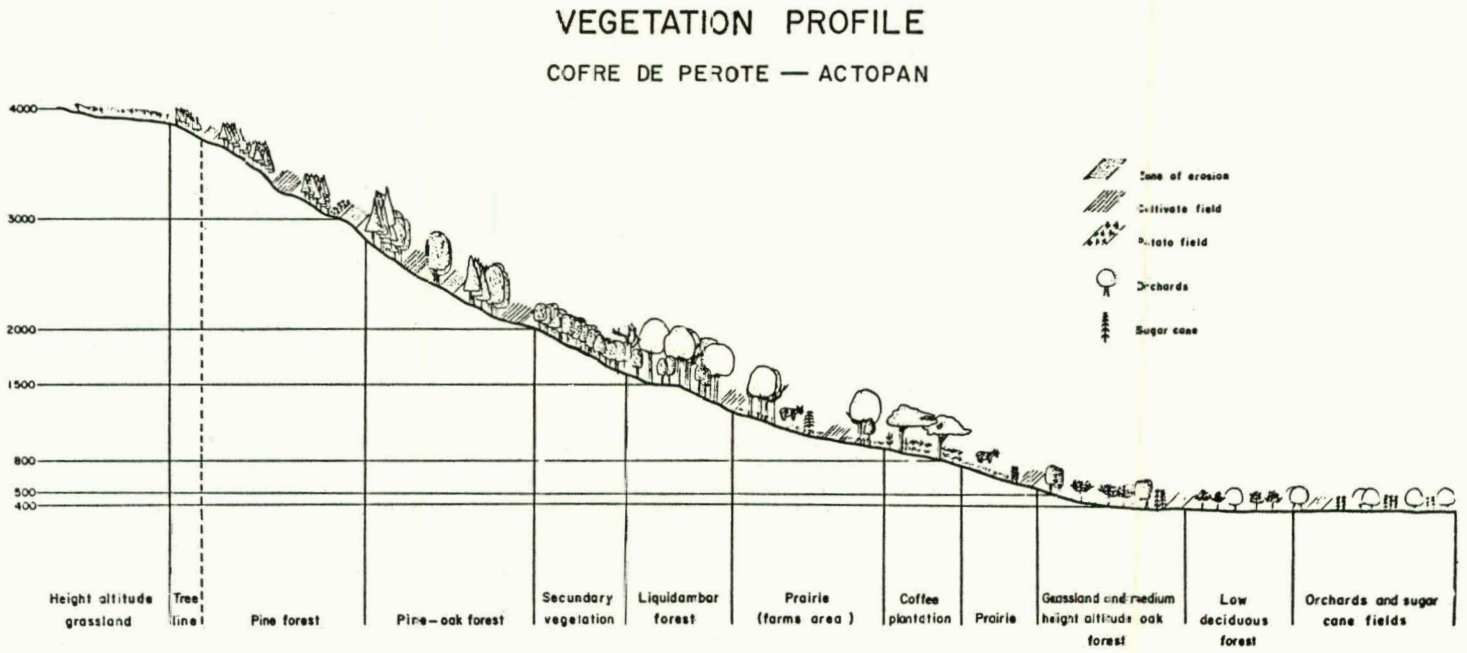

Figure 4. PROFILE OF VEGETATION FROM THE COFRE DE PEROTE TC THE TOWN OF ACTOPÁN

(The straight line distance is about 50 km)

AN INTERPRETATION OF NORTHERN THAILAND SWIDDENING AND MULTIPLE CROPPING SYSTEMS USING MULTIDATE LANDSAT IMAGES AND COMPUTER COMPATIBLE TAPES

Michel BRUNEAU
Centre d'Etudes de Geographie Tropicale - Bordeaux

Thuy LE TOAN
Centre d'Etudes Spatiales des Rayonnements - Toulouse

ABSTRACT

A photo-interpretation analysis of uplands west of Chiang Mai, Northern Thailand, at three different dates (band 7) during the dry season shows the progression of fires (burnt areas). The overall features of the area (uplands and lowlands) is given by interpreting the 27th january 1973 and 8th april 1975 color composite images. Classification of CCT tapes of a part of uplands and lowlands, using supervised methods, gives forest types, swidden area, savanna, paddy fields in the highlands east of Doï Inthanon, and changes of irrigated agriculture between january and march in the alluvial plain.

INTRODUCTION

AREA, GOALS OF THE STUDY AND DATA DESCRIPTION

This paper is mainly concerned with the study of land use types in lowlands and uplands of peninsular Southeast Asia using multidate black and white band 5 and 7 Landsat 1 and 2 images, color composites and computer compatible tapes. The particular area choosen is the Chiang Mai Valley and the hills and mountains ranging on its western side (18 - 19° N lat, 98 - 99° E long). It comprises a sequence of all characteristic vegetation types and land use forms of Northern Thailand.

Chiang Mai alluvial plain is covered with irrigated paddy fields on which two or three crops a year are grown, owing to a high Thai population pressure. After a first paddy crop during wet season, a second one or one or two successive dry commercial crops such as soybean, peanut, tobacco, vegetables are planted for dry season. On the upper old alluvium non irrigated terrace scrubs, deteriorated woodland, fruit trees orchards and fields are found.

On the uplands three forest types range from the bottom to the top : dry deciduous Dipterocarps forest (clear forest or woodland), mixed deciduous or semi-deciduous forest, dense evergreen lower mountain forest. Slash and burn shifting cultivation is the main land use which is differentiated in two types. Between 500 and 1 500 meters Karen and Lua hill tribes grow dry rice on swiddens for one year followed by a fallow period of 7 to 10 years with secondary forest regrowth. Above 1 000 meters Meo and Tibeto Burmese tribesmen clear forest to grow maize and poppy on the same hoed field for 5 to 10 years in succession after what a savanna or tree savanna follows instead of a forest regrowth.

Our knowledge of this area derives largely from data collected during field research in 1969-70, 1973-74 and 1977. Complete aerial coverage of the area in 1969 at 1/50 000 approximate scale and in 1972 at 1/20 000 are available. From these air photos interpreted we have drawn two colour maps (not yet published) that we used as main ground truth : one at 1/250 000 from the 1969 coverage on the overall area, the other at 1/25 000 of the Doï Inthanon area (1) from the 1/20 000 aerial coverage.

There are two approaches taken in this study from Landsat data. The first one is a photo-interpretation analysis of two early dry season images (27 january and 14 february 1973) and two late dry season images (21 march and 8 april 1975). Black and white band 5 and 7, color composites of these dates were used in 1/500 000 and 1/1 000 000 enlargements. The second part is a machine analysis of digital datas of the same area taken from two Landsat CCT tapes (27 january 1973 and 3 march 1975). Supervised classification methods are used for multidate and multispectral analysis of the same landscapes as in photo-interpretation. Comparison of both results is worth of interest.

1. PHOTO-INTERPRETATION ANALYSIS

1.1 BURNT AREAS AND SWIDDENS (BAND 7)

During dry season burning of large areas (savannahs, woodland or clearings in the forest) is a major phenomena which is expanding with the advancement of the drought. A multidate approach is necessary in such a matter (27 january, 14 february 1973, 21 march, 8 april 1975). One color composite image (27 june 1973) and three black and white band 7 1/500 000 enlargements are available on the transect (Fig. 1).

a. 27 january - 14 february 1973

This is the first part of the dry season and the cool season. Fires are still uncommon. Only one area is concerned, the Mae Chaem Valley where slopes with rocky soils, very dry, are covered by clear forest and savannahs. This is the first and only place to be burnt at this date on the maped area.

b. 21 march 1975

Fires have stretched and intensified in the same area (Mae Chaem Valley) towards the North and on the western margin of Chiang Mai basin. The image is more black. Most of the lowlands with woodland and savannas are at least partly burnt. Highland savannas (upper 1000 meters) have been already touched (Doï Inthanon area). Burned marks are still scarce.

c. 8 april 1975

Eighteen days later fire marks have been considerably extended on the whole area, mainly in the lowlands. Compared with 21th march, marks have been blurred (dark grey instead of black on band 7) in the lowlands. In the dense deciduous or evergreen forests, in the highlands, new black spots appear scattered. Some are large spot and represent blocks of newly burnt swiddens, these are small spots corresponding to smaller blocks. This landscape is related to Karen shifting cultivation system that has conservationary methods for environment. Especially Karen use to control escape fires or accidentally ignited out breaks in the vicinity of fallow swiddens.

In the highland savannas due to poppy growers burning is more generalized in space than eighteen days before.

(1) Doï Inthanon is the highest peak in Thailand culminating at 2 590 meters of altitude.

The map (Fig. 1) shows the extension of burning areas during second part of dry season from a stage where fires are strictly limited to particular edaphic conditions (in february) to an overall extension on the landscape.

1.2 COLOR COMPOSITE IMAGES

a. 27th january 1973

Two broad units can be easily delineated : the highlands where red and pink colours are prominent and lowlands (basin and valleys) with clearer (white) or darker (blue) colours and red spots of various shapes (Fig. 2).

Dark red areas, not very extensive, are located on highest altitudes (more than 1 500 meters). That is dense evergreen lower mountane forest which is quite well represented on the highest peak (Doï Inthanon).

Around these red dark spots white pink areas are still in highlands (upper than 1 000 meters). Small blue scattered spots are obvious in these areas especially around Doï Inthanon. This is trees savannas following poppy cultivation by some tribal populations (Meo, Yao or Tibeto Burmese). The blue spots are marks of the first fires which burn every dry season the savanna but are still very few in january, it is a cool season in mountain areas. South West of Doï Inthanon in the Mae Chaem Valley savanna partly due to edaphic conditions, partly to human action (wood cutting) is clearer (white color) and has burnt already in some parts (blue spots) as previously mentionned (Fig. 1).

On most of the highlands (mountain and hill areas) colour varies from purple to light red. This is mixed semi deciduous forest and, lower, clear forest (400 to 1 200 meters elevation). It is not possible on this image to differentiate mixed forest from clear forest.

In the lowlands stubbly paddy fields are displaid in white. They are at this date already harvested. Blue colors bring out ploughed paddy fields and irrigated for a second paddy crop or for a commercial crop (peanut, soybean, tobacco...). Along rivers and streams red lines and spots are dense fruit trees orchards where human settlements are located. Irrigated crops loom out almost solely in the Chiang Mai Valley.

On the basin fringes, especially south and north of Chiang Mai Valley, a mosaïc of red, blue and white colours, being red purple on the whole, not well distinguished from the mauve and red colour of the highlands, correspond to old alluvium terraces covered by deteriorated woodland, orchards and various field crops.

b. 8th april 1975

Highland landscapes are quite different from the previous image. Heat and a more advanced dry season help extension of fires and patches of burnt which are much more numerous and large than on the january scene. Fire is the main factor modifying forest landscapes (Fig. 3).

Highlands marked by numerous dark spots (black or dark blue) on a red background are the shifting cultivation area with highest population density. It is between 500 and 2 590 meters a part of the mixed deciduous forest, dense evergreen forest and high altitude savannah due to human action. To distinguish burnt swiddens from scrub or savannah fires it is necessary to refer to the previous image where savannahs are delineated. That is impossible to do on this image, even for evergreen mountain forest which appears quite obviously on the january scene.

Another hilly area with a red background and few dark spots is the same environment but with a lower human pressure, burnt swiddens and fires being smaller and more scattered. The semi deciduous or evergreen forests are better preserved.

Mauve, blue, white and purple colours prominently dark represent lower hills and valleys with woodland or semi deciduous forest in which the under wood has been burnt at the end of the dry season.

At lower altitudes blue and mauve are predominating more obviously, red tending to disapear. These hills and terraces are covered by woodland, scrub more or less deteriorated with orchards and field crops scattered. Burnt areas have extended but are blended in the whole.

In the alluvial plain's paddy fields white or light blue colour show predominance of stubbly paddy fields and mosaic of blue, white and red irrigated paddy fields used for a second rice crop or for a commercial field crop (peanut, soybean, vegetables, tobacco...). On the western and northeastern edge of the Chiang Mai basin two more red areas (mosaic of blue and red but with predominance of the later) correspond to areas where these field crops have a better vegetation cover (mostly peanut and soybean).

Comparison of two Landsat images from two different periods of the vegetation and crop cycle is worth teaching for the overall knowledge of the eco and agro systems. It helps to delineate the main spatial units at small scale. Some of them can be accurately identified at one date only : evergreen mountain forest and savanna due to human action in january, clear forest and scrub in april. Some land use types (burnt swiddens or field crops with thick vegetation cover) can be seen also at only one date (april). On the other hand the delineation of irrigated cropping areas and stubbly paddy fields is possible at these two different dates.

2. MULTIDATE DIGITAL DATA ANALYSIS

Classification technics are applied on multispectral data of 3rd march 1975 Landsat 2 (E-2040-03111) for the Doi Inthanon site and on data of the 2 dates 27th january 1973 Landsat 1 (E-1188-03224) and 3rd march 1975 Landsat 2 for the Chiang Mai basin site.

2.1 PROCESSING METHODOLOGY

Prior to classification training sets (samples) are selected on Landsat images according to knowledges of the area and to aerial photo-interpretation. The analysis of sample responses aims to study the clustering of multidimensional data (multispectral and multitemporal), e. g. to point out clusters of pixels in the sense of their spectral values. Adequate class number can also be determined by this way.

The concept of supervised classification is applied. Unsupervised methods are considered only when no knowledges of the area are available, or when a preliminary study showed that sample clusters are well separated.

The method used is the non parametric method with weighted euclidian distance between any vector to be classified and the mean vectors of the classes of interest. Since the usual euclidian distance assigned the same importance to every class the classification performance is improved by using a weighting factor which is the inverse of the variance of the classes. Then the distance between a pixel x and any class y_k is the following :

$$d^2 : (x, y_k) \rightarrow (x - Gy_k)^t \cdot \sum_k^{-1} \cdot (x - Gy_k)$$

where Gy_k is the barycentre of y_k and $\sum_k = \left| \sigma_k^2 \right| \times I$ is the total covariance matrix of the class y_k.

The effectiveness of the classification methods is checked by mean of the performance matrices between ground truth and classification result.

2.2 DOI INTHANON MOUNTAIN AREA CLASSIFICATION RESULT

The date of march is choosen for identification of the upland forest types because the deciduous formations have lost their leaves in this late dry season period and they can be separated from the evergreen formations.

The supervised four bands classification of the 3rd march 1975 gives five classes (Fig. 4) :

- dense or semi-dense forest in the shade
- dense or semi-dense forest
- savanna, swiddens and fallows
- woodland
- paddy fields and bare soils (road in construction).

1,47 % of pixels only are not classified, most of them being very dark shadows.

Paddy fields and bare soils on one hand, savanna, swiddens and fallows on the other hand are well differentiated from forests and between them. Wocdland or clear forest is not much represented in this area (2,68 % of the pixels). The two other forest types, dense evergreen mountain forest and semi-dense mixed deciduous forest, are not accurately distinguished because the topography casts shadows. The forest types classification is biased by this phenomenon (cast shadow) (Fig. 5).

Two different landscapes, savanna due to Meo poppy cultivation and swiddening area (swiddens and forest regrowth on fallows) of Karen people are not separable in the classification. They cover 40,37 % of the area, dense and semi-dense forests covering 50,7 %. Savanna is in most cases tree savanna, and neighbouring clearings (swiddens and fallows on different stages of regrowth) are small patches (less than one hectare). These two landscape units can be well differentiated on aerial photographs but not from Landsat data whose ground resolution is not high enough.

2.3 IRRIGATED MULTIPLE CROPPING IN CHIANG MAI ALLUVIAL PLAIN CLASSIFICATION RESULT

Two digital data tapes, 27th january 1973 and 3rd march 1975, were superposed and a supervised classification of land use types, that changed and that did not change between these two dates, was done on band 5 and 7 of both (Fig. 6).

Six classes are quite well distinguished as one can see on the performance matrix (Fig. 7). Four of them dont change between the two dates :

- dry stubbly paddy fields and bare soils

- inundated paddy fields and swamps

- woodland and thicket more or less deteriorated

- orchards and settlements.

The two other classes are changing between january and march, between middle and end of dry season :

- ploughed and irrigated paddy fields after harvest time (27th january) becoming covered by canopied crops (3rd march) which are soybeans, peanuts, tobacco, beans...

- stubbly paddy fields (27th january) becoming inundated paddy fields (3rd march).

There is some muddle or overlapping between woodland and orchards. Their appearance being sometimes the same, it is quite normal. Another confusion can occur between ploughed and irrigated paddy fields on one hand and inundated paddy fields on the other hand. That is no wonder because of the imbrication of these two types and the small size of the fields. Mae Ping river is classified sometimes with inundated and swampy areas, sometimes non classified.

Multidate digital data analysis is a good tool for second or third crops mapping during dry season in such an irrigated plain. Second rice crop and orchards are accurately delineated. Field crops are quite well sorted out too.

CONCLUSION

Landsat 1 and 2 data of different dates in dry season are the best available remote sensing data for an up to date mapping of swiddening and multiple cropping areas of the valleys and mountains of continental Southeast Asia. The area mapped in this paper has been selected because it represents the main vegetation and cropping systems of such a region. Multidate photo-interpretation analysis of band 7 gives good information about the progressive extension of fires in the uplands during dry season. Interpretation of color composite images of beginning or middle and end of dry season gives the main landscape units : forest types and land use types. They are interesting especially for the mountain shifting cultivation area, because digital data analysis does not give good results in this respect. Topographic cast shadow alter the classification of forest types and savanna cannot be accurately separated from swiddens and fallows. On the other hand multidate supervised classification is a good mean for inventory of multiple cropping areas in irrigated alluvial plain or valley. The results are more accurate than by photo-interpretation technics of Landsat images.

REFERENCES

Le Toan, T., Cassirame, P., Kuach, J. "Inventory of rice-fields in France using Landsat and aircraft data", Eleventh International Symposium on Remote Sensing of Environment, 25-29 april 1977, Ann Arbor, Michigan, 13 p. (forthcoming).

Bruneau, M., Le Toan, T. "Les clichés ERTS 1 et la cartographie des paysages en milieu tropical : le cas de la Thaïlande septentrionale, Bulletin de la Société Française de Photogrammetrie, 61, 1976, pp. 123-149.

Le Toan, T., Bruneau, M. "Utilisation des données Landsat pour la cartographie en milieu tropical (Nord de la Thaïlande), Colloque du GDTA, Paris, 1977, 10p. (forthcoming).

Bruneau, M. "Ray et utilisation des terres hautes dans la Thaïlande septentrio-

nale", in "Etudes de Geographie Tropicale offertes à Pierre Gourou", Mouton, Paris, 1972, pp. 101-118.

Bruneau, M., Cabaussel, G. "Dynamique de paysages de montagne (Doï Inthanon, Thaïland)", colour map 1/25.000, 4 insets, CEGET, Bordeaux, Institut français de Pondichery, Pondichery, 1977.

Bruneau, M., Cabaussel, G. "La dynamique des paysages en zone tropicale : essai de cartographie dans la region de Si Satchanalai (Thaïlande septentrionale), Travaux et Documents de Geographie Tropicale, CEGET, Bordeaux, 9, 1973, 73 p., 1 colour map.

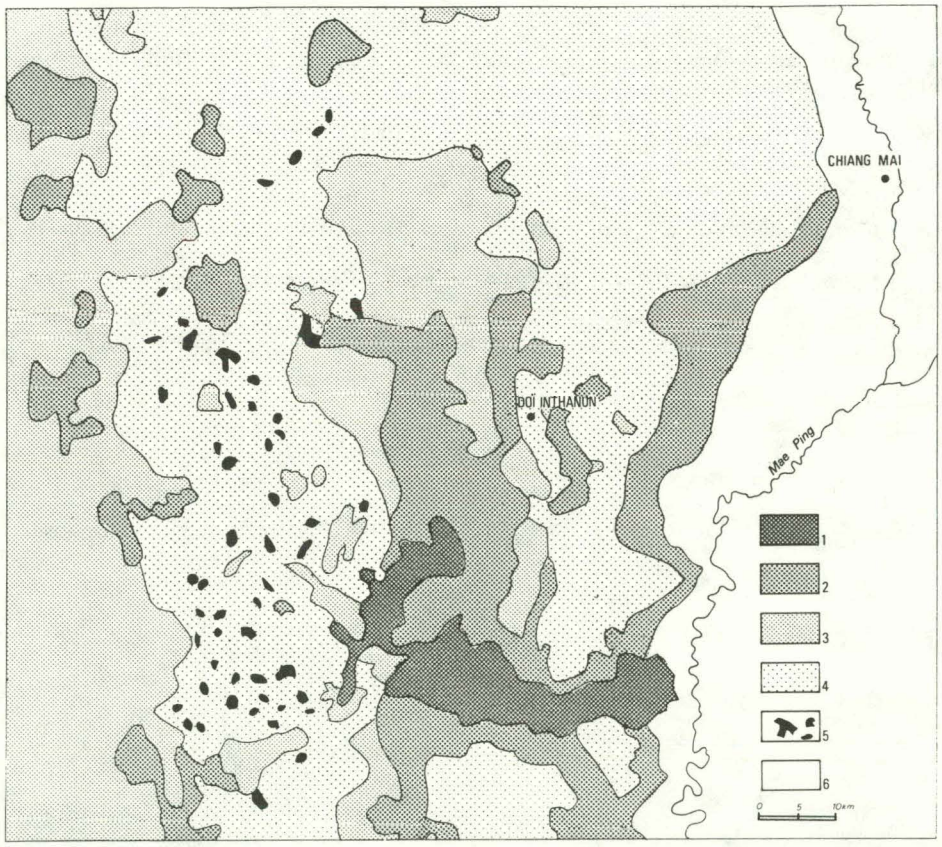

Figure 1. FIRES FROM MIDDLE TO END OF DRY SEASON WEST OF CHIANG MAI
(Landsat 1 and 2 images)

1 Burnt areas 14th february 1973
2 " 21th march 1975
3 " 8th april 1975
4 Scattered burnt clearings in the forest (8th april 1975)
5 Blocks of burnt swiddens (8th april 1975)
6 Cultivated alluvial plain

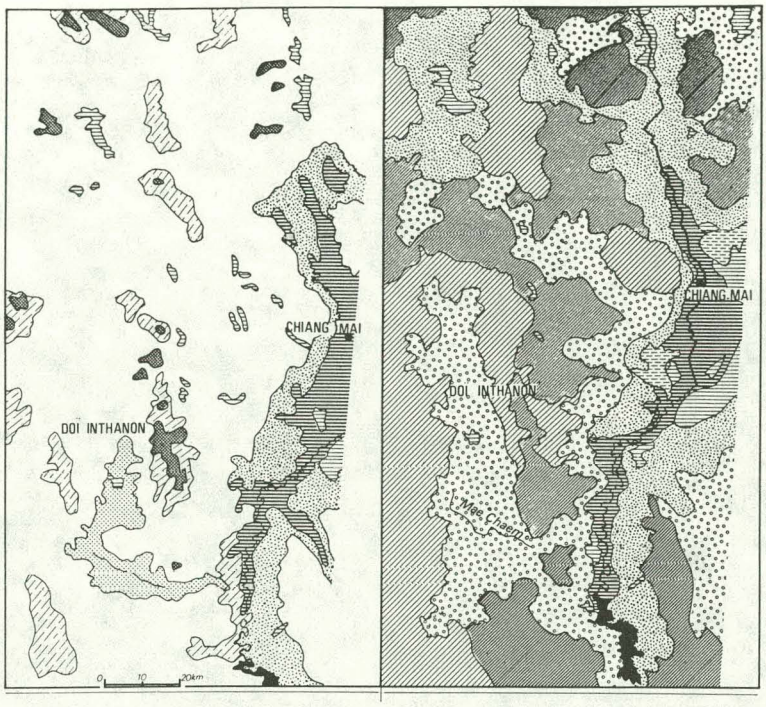

Figure 2. 27th JANUARY 1973 (Landsat 1) Figure 3. 8th APRIL 1975 (Landsat 2)

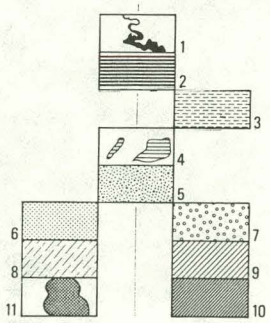

1 Reservoir, stream
2 Irrigated paddy-fields
3 Dry second-cropping on paddy-fields canopied (soybean, peanut...)
4 Stubbly paddy-fields
5 27th january deteriorated woodland and field-crops on terraces and hills
8th april deteriorated woodland, field-crops and burnt areas on terraces and hills
6 Lower mountain soil and human savannas
7 Lower mountain mixed and open forests deteriorated and partly burnt
8 Highland anthropogenic tree savanna
9 Lower mountain mixed deciduous and evergreen forests with anthropogenic savannas and patches of burnt
10 Lower mountain mixed deciduous and evergreen forests not much cleared and burnt
11 Lower mountain evergreen dense forest

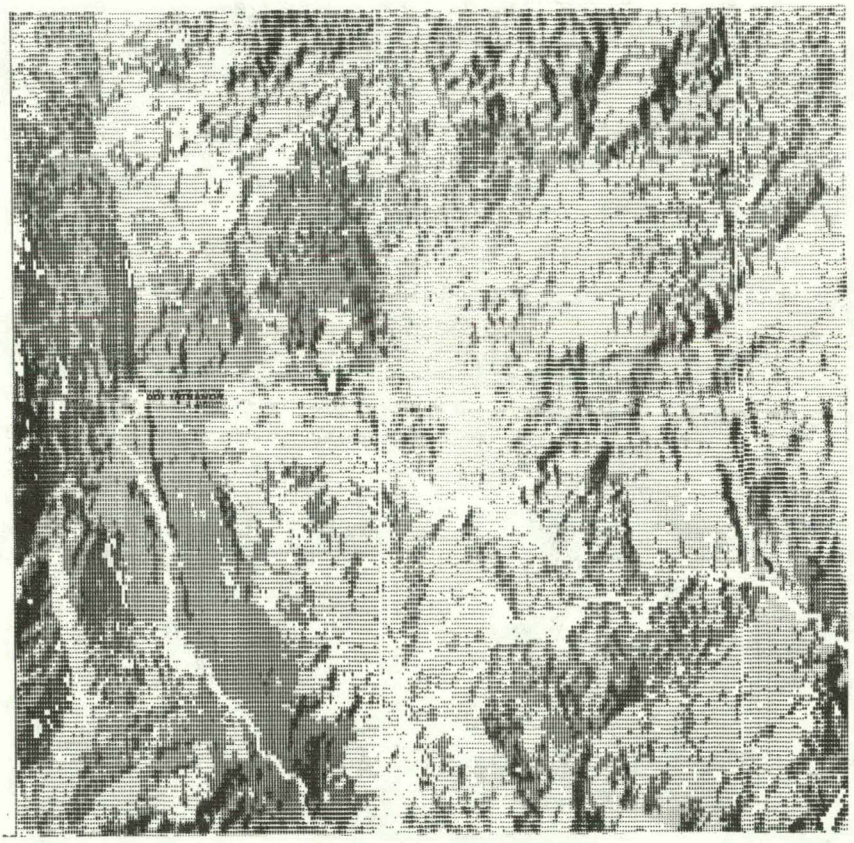

Figure 4. Doï Inthanon mountain area multispectral classification (3rd march 1975)

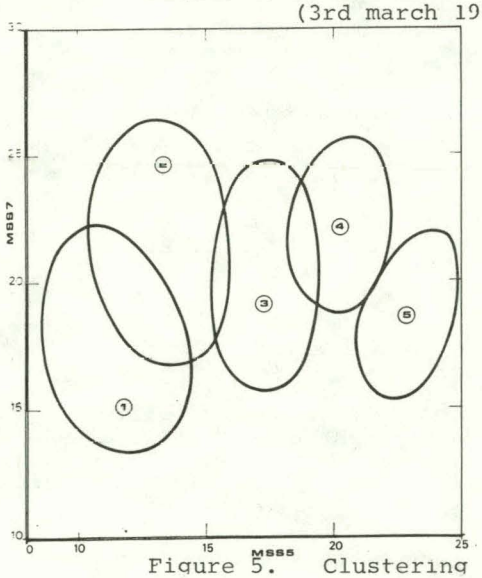

LEGEND

1 Dense or semi-dense forest in the shade

2 Dense or semi-dense forest

3 Savanna, swiddens and fallows

4 Woodland

5 Paddy fields and bare soils

SAMPLES

1 Evergreen dense forest

2 Mixed deciduous semi-dense forest with swiddens and fallows

3 Woodland

4 Savanna

5 Paddy fields and bare soils

Figure 5. Clustering of sample responses in the MSS5 MSS7 plane

The clustering of sample pixels is showed in the figure 5 where evergreen dense forest and mixed deciduous forest are partly mixed as well as woodland and savanna. Dry fields only can be identified without ambiguity.

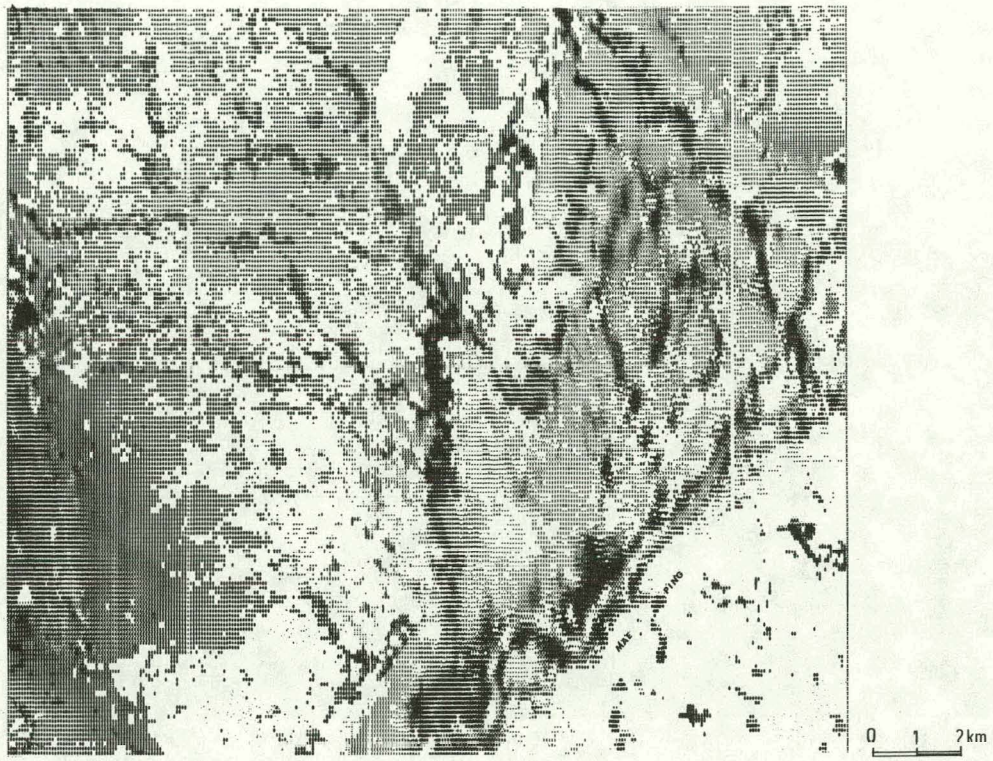

Figure 6. Multiple cropping in Chiang Mai irrigated alluvial plain, multidate and multispectral classification (27th january 1973, 3rd march 1975)

Classes	1	2	3	4	5	6
1	71	0	25	2	0	2
2	0	73	0	0	20	7
3	0	2	93	5	0	0
4	0	0	2	90	7	0
5	0	22	0	6	70	0
6	0	0	0	0	0	100

LEGEND

1 Dry stubbly paddy fields and bare soils

2 Inundated paddy fields and swamps

3 Woodland and thicket more or less deteriorated

4 Orchards and settlements

5 Ploughed paddy fields (january) becoming covered by canopied crops (march)

6 Stubbly paddy fields (january) becoming inundated paddy fields

Figure 7. Performance matrix (Chiang Mai)

THIS PAGE

WAS INTENTIONALLY

LEFT BLANK

USE OF LARGE SCALE AERIAL PHOTOGRAPHS FOR ECOLOGICAL STUDIES IN A GRAZED ARID ECOSYSTEM

R. B. Hacker

Department of Agriculture
South Perth, Western Australia

ABSTRACT

Colour aerial photographs at a scale of approximately 1:250 were used to obtain plant inventories for six study sites in a multi-layered arid zone community. Species were divided into size classes based on canopy area. Coordinates for each individual, read from the photographs, were transformed to ground coordinates and used to produce plant counts in contiguous quadrats. Multiple pattern analysis of these data revealed the major features of community variation and their corresponding scales of pattern. Within-site variation in grazing pressure was the major factor influencing community pattern in three sites. Responses of the major species to grazing were clearly defined. Aggregation of shrubs around the relics of older populations of trees or large shrubs, or under the canopies of living individuals, primarily determined (or at least influenced) vegetation pattern on the remaining sites. The presence of these relics is thought to impose a weak fundamental pattern on this community.

1. INTRODUCTION

Applications of large scale aerial photographs for rangeland research have become more widespread in recent years. Reported research has mainly involved such aspects as species identification, cover determination, evaluation of soil surface condition, community type discrimination and film type/scale comparisons (e.g. Carneggie and Reppert 1969, Driscoll 1969, Driscoll *et al.* 1970, Carneggie *et al.* 1971, Driscoll *et al.*, 1974).

Large scale aerial photographs also provide the means of recording plant inventory data, and the spatial arrangement of plant populations, without excessive field work (West and Goodall, 1971). Such information has been used in the present study for ecological investigations of a grazed arid zone ecosystem.

2. AREA DESCRIPTION AND STUDY SITE DESIGN

Field data were collected in a multi-layered vegetation community in the arid winter rainfall zone of Western Australia. Average annual rainfall is approximately 200 mm. Winter rainfall (May-June) is most reliable but heaviest falls result from occasional cyclonic disturbances in summer.

The vegetation consists of a sparse over-storey of mulga (*Acacia aneura*) with a mid-storey of shrubs among which *Eremophila leucophylla* is dominant on ungrazed or lightly grazed areas. Other species of *Eremophila* and species of *Maireana* are also present. Under heavy grazing *E. leucophylla* is progressively eliminated. The ground storey is dominated by the perennial grass *Eragrostis xerophila* while a variety of annual herbs and grasses are present under suitable seasonal conditions. In the study area, this community is found on flat or slightly rounded interfluves between drainage lines which carry run-off towards a lake (usually dry) several miles distant. The associated soil type is a deep (generally > 1 m), non-saline loamy sand of neutral - slightly acid reaction.

Data for six study sites, each 256 m x 35 m (approximately 0.9ha) are reported. These sites exhibited differences in range condition as evidenced primarily by differences in the density of *Eremophila leucophylla*. Long term grazing by sheep is the primary factor responsible for range degradation in this ecosystem although cattle have grazed the area intermittently.

Site boundaries were permanently marked with white painted tyres placed at 30.48 m (100 ft) intervals along the length of the transects. These markers served as visual navigational aids during photographic flights and provided ground references for scale determination.

3. AERIAL PHOTOGRAPHY

Colour stereo photography of all sites was obtained in October 1975 from an altitude of 500 ft (152 m). A Vinten 70 mm camera fitted with a 152 mm (6 in.) lens was vertically mounted externally on a Cessna 182 aircraft for this purpose. Four sites were photographed with Kodak Aerocolor negative film (type 2445) and the remaining two with Kodak Aerochrome MS (type 2448). All films were developed to the negative and used to produce enlarged prints (X4), at a scale of approximately 1:250, for field work.

4. DATA COLLECTION

Shrub and tree species were inventoried for each site by annotation of photo-overlays in the field. Seedlings were distinguished on the basis of predetermined definitions involving height and degree of morphological development. Individuals unresolved on the photographs were located accurately by reference to resolved features of the vegetation or soil mosaic and the approximate outline of plants obscured by tree canopies was marked on the overlays. A total of 10 400 individuals, representing 12 species, was recorded on the six study sites.

Non-seedling populations of 8 of these species were broken into size classes on the basis of canopy area, determined by super-imposing overlays (on which canopies were outlined in accordance with strict conventions) on a 1 mm grid. Actual areas were calculated from photo areas and size class boundaries for each species determined by natural breaks in the canopy area frequency histograms based on samples of 46-113 individuals. Non-seedling populations of selected species were thus broken into two-four size classes. For the remaining four species, subdivision proved difficult and only seedling and non-seedling size classes were differentiated. Subdivision produced a total of 38 size classes for the 12 species (including seedlings). Population data are presented in Table 1.

Cartesian coordinates for all individuals in each study site were extracted by referring the overlays to a 1 mm grid with coordinates estimated to the nearest 0.25 mm. Individuals were simultaneously classified into the appropriate size class so that the record for each plant, written directly onto computer coding sheets, consisted of species code, size class code, and X and Y coordinates in the photo system. These coordinates were subsequently transformed to ground coordinates by plane transformation using the least squares method. The appropriate equations are of the form

$$X_2 = aX_1 + bY_1 + c$$

$$Y_2 = -bX_1 + aY_1 + d$$

where (X_1Y_1) are the coordinates of a plant in the photo system and (X_2Y_2) are its coordinates in the ground system. Known ground coordinates for the corners of each annotated transect segment, and their corresponding photo coordinates, are used to determine the constants a, b, c, and d.

These transformations account for scale differences, origin shifts and angular rotation between photo and ground coordinate systems but not for displacement of points in the photo system due to tilt or relief. These sources of error are considered negligible since the ground surface is essentially horizontal and photography is approximately vertical. After transformation coordinate data could be manipulated in a variety of ways to provide input for later analyses.

Photographs were used directly to provide a quantitative measure of the density of stock tracks, taken as an index of long term grazing pressure. The length of interpretable track was measured by means of a map meter in each of the eight 32 m x 35 m subsections of each site. Quadrats scaled directly on the photo overlays permitted the extraction of some data which could not be obtained by manipulation of the transformed coordinates. Details appear in succeeding sections.

5. THE ANALYTICAL APPROACH

Primary data analysis aimed at determining a representative area for this community, if one existed, as a guide to future sampling. Plant counts in 64 contiguous (4 m x 35 m)

quadrats were determined for each site and subjected to the multiple pattern analysis (M.P.A.) procedure of Noy-Meir and Anderson (1970). Mathematical descriptions of the technique are presented by Noy-Meir and Anderson and Walker *et al.* (1972).

Briefly, species-in-site scores (x_{ij}; i=1,2...n, j=1,2...m) for m species in n (=64 in this case) primary sites are combined in pair-wise fashion to produce total scores and means for blocks of 2, 4, 8 etc. units. Each block size or scale, s, is an integer multiple (usually 2) of the preceding block size and the number of blocks of size s is $n_s = n/s$. The deviation of any species-in-site score (x_{ij}) from the species mean ($\bar{x}_j$) may thus be expressed as the sum of the deviations of the mean score for species j at each block size from the mean score for the next largest block in which the smaller block is located, mean score for the largest block size produced by the pairing being expressed as a deviation from the mean of the whole transect. In matrix notation,

$$D = \sum_s D_s$$

where D is the (n x m) matrix of deviations for primary site scores and D_s is the (expanded) matrix of deviations of mean scores at block size s from the means of the next largest block size.

At each block size, a between-species variance-covariance matrix is calculated

$$V_s = \frac{1}{d_s} D_s' D_s$$

where d_s is the degrees of freedom for block size s, and these are added to produce a combined variance-covariance matrix

$$V = \sum_s V_s.$$

Principal components analysis applied to the matrix V yields eigenvectors ν and latent roots λ which are related by

$$V\nu = \lambda\nu. \qquad (1)$$

Eigenvectors provide a species ordination and are standardised such that

$$\nu'\nu = \lambda \qquad (2)$$

The proportion of the total variance accounted for by each component is defined by the ratio of λ to the trace of V. From (1) and (2), it follows that

$$\nu'V\nu = \lambda^2$$

and

$$\lambda = \frac{\nu'V\nu}{\lambda}$$

Since V may be decomposed into its component matrices, V_s, a similar partitioning of λ may also be achieved so that the contribution of each block size to a component of community variation (λ_s where $\lambda = \sum_s \lambda_s$) may be calculated and plotted against block size by analogy to the conventional (univariate) pattern analysis (Greig-Smith, 1952).

Vectors of species loadings, ν, may be used to produce vectors of scores for primary sites, μ, by the equation

$$\mu = \frac{D\nu}{\sqrt{\lambda}}$$

This method of calculating site scores is used by Noy-Meir and Anderson (1971) and Walker *et al.* (1972). In the present study, site scores are calculated as

$$\mu = D\nu$$

and the vectors are then post-standardised by $(\frac{\lambda}{\mu'\mu})^{\frac{1}{2}}$ so that for the rescaled vectors, μ_r,

$$\mu_r'\mu_r = \lambda$$

A series of super-imposable ordinations for sites at each block size may be obtained by averaging primary site scores within each block.

Several modifications of this basic algorithm are feasible which differ in the weightings given to species, sites or scales. These have been discussed by Noy-Meir and Anderson (1971) and Walker *et al.* (1972). In the present study the above algorithm has been used throughout for unstandardised analyses. For standardised analyses, primary species-in-site scores have been divided by maximum species score in order to equalise (approximately) the influence of rare and abundant species.

All computations were performed on the CSIRO Cyber 7600 computer using the programme package described by Nicholls (1977).

Two data sets were analysed for each site. Five per cent analyses are based on species, or groups of adjacent size classes within a species, which account for 5 per cent or more of the total population. Both standardised and unstandardised analyses were conducted on these data sets. One per cent analyses refer to data sets including rarer species or size classes which contributed at least one per cent of the total population. These data were always standardised before analysis.

6. RESULTS

The efficiency of the first three components for all analyses is detailed in Table 2. These components account for at least 85 per cent of the total variance for the 5 per cent analyses but their efficiency is reduced when rarer species (or size classes) are introduced in the 1 per cent analyses.

The patterns displayed by the variance (λ_s) - block size graphs are summarised in Table 3. As in univariate pattern analysis, peaks in these graphs are generally interpreted as indicating contagion or clumping at the corresponding scale. Variances, however, are now generalised "phytosociological" variances and are components of the total community variance. This interpretation has only been accepted, in the present study, in those instances in which λ_s values were not shown to be a simple function of the distance between block centers. The linear regression of log λ_s on log spacing was tested initially for all analyses following the approach adopted by Goodall (1961) to interpretation of the (univariate) Greig-Smith analysis. When this regression is significant, the variance pattern is more consistent with a general trend in community composition or total density along the transect rather than with a repetitive mosaic pattern.

Table 3 reveals no consistent scale of pattern for either the first or second components of the 5 per cent analyses or for the first component of the 1 per cent analyses. Pattern at block size 16 is evident on four sites for the second component of the 1 per cent analyses but for the remaining sites, the linear regression is significant so that no repetitive pattern can be inferred. The major factors of community variation thus provide no evidence for the existence of a representative area in this community which could serve as a guide for future sampling. If such a representative area did once exist, grazing differentials between sites have apparently eliminated any trace of it from the first two components of community variation. It is notable, however, that for four of the six sites the third component for the standardised analyses does reveal a consistent scale of pattern, at block sizes 8 and 16 for the 5 per cent and 1 per cent data respectively, and that for the remaining two sites, pattern is evident at the adjacent block size. Such shifts in the position of the major peak could possibly be accounted for by starting point effects (cf. Usher 1969). Some weak fundamental pattern may this be postulated in this community but its influence in determining total community pattern is largely obscured either by local environmental effects or by differences in the degree of grazing disturbance between sites.

Examination of the vectors of species loadings for both 5 per cent and 1 per cent analyses revealed that for 4 of the 6 sites, the major contrast on the first axis involved some size class of *Eremophila leucophylla* and size classes of either *Maireana planifolia* or *Eremophila* sp. Such contrasts were evident on other axes as well but in only one instance (1 per cent analysis, site 1, first component) were the latter species contrasted with each other. Since *Eremophila leucophylla* decreases under grazing in this community, these contrasts suggested the possible existence of within-site variation in grazing pressure which

had been hitherto unsuspected. Track density profiles were therefore determined for each site, at a scale corresponding to blocks of 8 units in the multiple pattern analyses, and examined in relation to the block ordinations at this scale.

For sites 3, 4 and 6, the first component of community variation was clearly associated with internal grazing heterogeneity as defined by the track density profiles (Fig. 1). Species responses to grazing may thus be examined by means of the corresponding vectors of species loadings and the correlations between species (or size class) density and track density. These are presented for site 3 in Table 4. The 5 per cent analyses strongly contrast *Eremophila* sp (1-2)* and *Maireana planifolia* (1-2) with size classes of *Eremophila leucophylla*, especially classes 1, 3 and 4. The correlation coefficients indicate that the former tend to be abundant in areas of high track density while the latter are favoured where track density is lower although the correlations for smaller size classes are not high. Primary interpretative value, however, attaches to the vectors of species loadings and the sign, rather than the magnitude, of the correlation coefficients. The results are consistent with the classification of *Eremophila leucophylla* as a decreaser while both *Maireana planifolia* and *Eremophila* sp. tend to increase with grazing disturbance in this site.

Species loadings for the one per cent analysis lead to an interpretation identical to the above for the three major species but provide additionally an opportunity to examine the response of minor species. The loadings and correlations for *Maireana villosa* (2-3) and *Eremophila clarkei* (2-3) suggest a negative response to grazing and tentative classification of these species as decreasers. Such a classification is probably spurious for *Eremophila clarkei* as inspection of the primary data and photo overlays reveals a highly localised population, in an area of low track density, consisting largely of juveniles associated with a parent plant. The high positive score for *Eremophila* aff. *leucophylla* (2-4) also suggests a negative response to grazing but its correlation with track density is positive. The anomaly arises due to the occurrence of the maximum score for this species (3) in the first quadrat of an 8 unit block with high track density. The positive correlation is an artefact associated with the blocking of quadrats into larger units and the scale at which track density was recorded.

The high negative loading and positive correlation with track density for *Acacia aneura* (2-4) suggest that mulga increases under grazing in this community. It is interesting to note that this response cannot be explained as an artefact arising from the association of young mulga with mature trees (class 5) since these groups have contrasting correlations with the track density profile and in fact their covariance-block size graph (the appropriate off diagonal elements of the V_S matrices) reaches a peak of negative covariance at block size 8.

Interpretation of species loadings for the first component, and the track density correlations, for sites 4 and 6 led to conclusions identical to those above for the three major species. The analyses are not discussed in detail but species loadings for the 1 per cent analyses, and track density correlations, are presented in Table 5. As for site 3, interpretation of responses for minor species presented difficulties and required reference to the primary data and the photo overlays. On site 4, both *Acacia aneura* (2-4) and *Maireana villosa* (2-3) show relatively extreme loadings but their track density correlations are the opposite of those observed for site 3. This apparently conflicting response for mulga is due to positive association between young mulga and mature trees at all block sizes (except block size 1) in this site. For *Maireana villosa* (2-3), the overlays reveal clumping under the low-hanging canopy of a single tree (*Grevillea*) at the degraded end of the transect. The positive correlation with track density on this site is thus an artefact induced by the virtually complete protection from grazing afforded by this canopy. None of the minor species on site 6 has a loading sufficiently extreme to warrant further investigation.

The second and third components for sites 3, 4 and 6 revealed little useful information concerning grazing responses. It is notable though that the second species vector was unipolar (all elements of the same sign) for the standardised 5 per cent analysis for site 3 and for both of the 5 per cent analyses for site 6. This suggests a considerable degree of overlap in the distributions of the major species or size class groups in these sites and is compatible with the interpretation above that distribution patterns are determined primarily by an externally imposed grazing factor rather than by differential responses to microenvironmental variation within the sites.

---

* Figures in brackets indicate size class groupings. Size class 1 represents seedlings.

Interpretation of the first component for sites 1, 2 and 5 in terms of the track density profiles proved unsatisfactory. Examination of the variance - block size graphs for the size classes entered in the 5 per cent analyses (the appropriate principal diagonal elements of the V_S matrices) revealed that for site 1, the major peak at block size 16 in the λ_S - block size graph (Table 3) was associated with corresponding peaks in the graphs for *Eremophila leucophylla* (2), (3) and (4) and *Maireana planifolia* (1-2). Marked correspondence between first component (5 per cent) pattern and individual size class patterns was evident for *Eremophila leucophylla* (1) and (3) on site 2 and for *Eremophila* sp. (1-2), *Maireana planifolia* (1-2) and *Eremophila leucophylla* (1-4) on site 5. An explanation of these individual patterns will thus largely explain the major aspect of total community pattern for these sites as revealed by the M.P.A.

A tendency for species to aggregate around the relics of dead trees and tall shrubs (*Acacia aneura* and *Acacia linophylla*) had been noted during cordinate extraction. Some aggregation also occurred under the canopies of live mulgas or other shrubs. The influence of this clumping on the distribution of species (or size class) populations in total was examined by counting these clumped individuals, or the number of such clumps, in contiguous quadrats (4 m x 35 m or 16 m x 35 m.) scaled on the overlays. Counts were then subjected to the conventional Greig-Smith analysis of variance. The position of peaks in the resultant variance-block size graphs and their relationship to the pattern of the total population are evident from Table 6. (Peaks are judged subjectively, there being no entirely satisfactory test of significance available except in the case of randomness at all scales). The degree of aggregation around relics and live trees or shrubs is also evident from Table 6.

The influence of old relics and current overstorey elements is clearly the major factor contributing to species (and community) patterns on sites 1 and 5. Distribution of *Eremophila leucophylla* seedlings on site 2 is basically a function of the distribution of class 3 adults (V_S matrices reveal positive covariance at all scales except block size 1 and peak positive covariance at block size 32) so that the distribution of the latter is a major determinant of total community pattern. This is seen to be influenced mainly by the isolated individuals (not associated with relics or living trees) although the marked peak for clumped individuals at block size 2 probably contributes to the secondary peak at block size 1 for the total population and to the slight peak at this block size evident for the first component of the unstandardised 5 per cent analysis.

7. DISCUSSION

The use of M.P.A. in conjunction with a photo interpreted measure of grazing intensity has proved a useful technique for examining species responses to grazing. Significantly, such information has been extracted from sites in which the internal patterning of grazing pressure, and the corresponding changes in vegetative composition, were not obvious in the field. For dominant species, the responses are well defined (within the limited range of grazing pressure encompassed by the sites studied) but the interpretation of such responses for minor species needs to be accepted cautiously. Interpretation of species responses over a wider range of grazing pressure could be easily achieved by the use of extended photo transects radiating, for example, from a watering point. Such transects should also provide clearer evidence of the grazing response of minor species.

In the absence of marked grazing effects, species and community pattern is strongly influenced by the aggregation of shrubs around the relics of previous populations of trees and tall shrubs and, to a lesser extent, under the canopies of living individuals. Such aggregation is thought to be associated with soil nutrient patterns induced by foliar leaching and litter decomposition, but no soil chemical data are available to support this hypothesis.

No conclusive evidence for the existence of a characteristic representative area in this community has been produced. Some evidence for a fundamental pattern, now of minor importance in determining total community pattern, is available, however, and may represent the pattern of earlier generations of large woody species and environmental modifications induced by them.

8. REFERENCES

1. Carneggie, D.M. and Reppert, J.N. 1969. Large scale 70 mm aerial colour photography: Numerous potential uses exist for range inventory and range management. Photogrammetric Engineering 35 : 249-257

2. Carneggie, D.M., Wilcox, D.G. and Hacker, R.B. 1971. The use of large scale aerial photographs in the evaluation of Western Australian rangelands. Tech. Bull. No.10, Dept. of Agric. of Western Australia.

3. Driscoll, R.S. 1969. Aerial colour and colour infrared photography - some applications and problems for grazing resource inventories. In Aerial colour photography in the plant sciences. Aerial colour photography workshop (Univ. Fla., Gainesville, March 5-7, 1969) Proc., 140-149.

4. Driscoll, R.S., Reppert, J.N., Heller, R.C. and Carneggie, D.M. 1970. Identification and measurement of herbland and shrubland vegetation from large scale aerial colour photographs. Proc. XI Int. Grassld. Congr., 95-98.

5. Driscoll, R.S., Reppert, J.N. and Heller, R.C. 1974. Microdensitometry to identify plant communities and components on colour infrared aerial photos. J. Range. Manage. 27:1:66-70.

6. Goodall, D.W. 1961. Objective methods for the classification of vegetation IV. Pattern and minimal area. Aust. J. Bot. 9 : 162-196.

7. Greig-Smith, P. 1952. The use of random and contiguous quadrats in the study of the structure of plant communities. Ann. Bot. 16 : 293-316.

8. Nicholls, A.O. 1977. The multiple pattern analysis program package. Tech. Memo. 77/9, CSIRO, Division of Land Use Research, Canberra.

9. Noy-Meir, I. and Anderson, D.J. 1970. Multiple pattern analysis or multiscale ordination: towards a vegetation hologram? In "Statistical Ecology". Proc. Int. Symp. Statist. Ecol., New Haven, 1969, Vol.3, 207-225.

10. Usher, M.B. 1969. The relation between mean square and block size in the analysis of similar patterns. J. Ecol. 57 : 504-514.

11. Walker, J., Noy-Meir, I., Anderson, D.J. and Moore, R.M. 1972. Multiple pattern analysis of a woodland in south central Queensland I. The original trees and shrubs. Aust. J. Bot. 20 : 105-118.

12. West, N.E. and Goodall, D.W. 1971. Analysis of plant dispersion patterns from low level aerial photographs. Paper presented to the annual meetings of the Ecological Society of America in conjunction with the American Institute of Biological Sciences, Fort Collins, Colorado.

TABLE I. POPULATION DATA FOR SIX STUDY SITES

Species	No. of size classes defined	Total population					
		1	2	3	4	5	6
Eremophila leucophylla	4	1067	915	630	796	307	646
Eremophila aff. leucophylla	4	72	21	29	13	28	5
*Eremophila sp.	2	30	9	194	145	1095	875
Eremophila clarkei	3	38	46	46	97	45	310
Eremophila margarethae	4	6	1	5	9	154	56
Maireana planifolia	2	115	129	125	67	406	428
Maireana villosa	3	44	49	47	91	33	40
**Maireana spp.	2	98	0	7	23	2	8
Acacia aneura	5	85	82	96	119	143	130
Acacia linophylla	4	16	21	40	42	60	69
Prostanthera wilkiana	2	1	0	1	0	0	2
Rhagodia	3	29	5	12	30	14	17

* Postive identification not available at time of writing due to lack of flowering material.

** Includes rare species of *Maireana* difficult to separate in the field.

TABLE II. EFFICIENCY EXPRESSED AS PERCENTAGE OF VARIANCE ACCOUNTED FOR (ABOVE) AND CUMULATIVE EFFICIENCY (BELOW) FOR THE FIRST THREE COMPONENTS OF MULTIPLE PATTERN ANALYSES

Site	5 per cent analysis unstandardised			5 per cent analysis std. by max. score			1 per cent analysis std. by max. score		
	λ_1	λ_2	λ_3	λ_1	λ_2	λ_3	λ_1	λ_2	λ_3
1	48.3	30.6	11.5	47.3	34.3	7.6	36.7	25.8	9.6
	-	*78.9*	*90.4*	-	*81.6*	*89.2*	-	*62.5*	*73.1*
2	82.6	7.8	5.9	62.8	16.7	13.2	41.8	17.1	11.5
	-	*90.4*	*96.3*	-	*79.5*	*92.7*	-	*58.9*	*70.4*
3	65.6	20.0	5.9	49.4	27.3	10.0	28.3	19.6	15.4
	-	*85.6*	*91.5*	-	*76.7*	*86.7*	-	*47.9*	*63.3*
4	73.2	15.5	5.6	68.9	12.1	7.7	62.9	10.1	7.3
	-	*88.7*	*94.3*	-	*81.0*	*88.7*	-	*73.0*	*80.3*
5	66.6	18.4	8.5	42.1	26.6	16.5	30.8	22.5	11.9
	-	*85.0*	*93.5*	-	*68.7*	*85.2*	-	*53.3*	*65.2*
6	74.2	14.9	9.6	78.6	12.1	6.8	62.2	13.8	8.4
	-	*89.1*	*98.7*	-	*90.7*	*97.5*	-	*76.00*	*84.4*

TABLE III. SUMMARY OF PEAKS IN THE VARIANCE (λ_s)- BLOCK SIZE GRAPHS
(FIGURES ARE BLOCK SIZES FOR PEAKS)

Site No	5 per cent unstandardised			5 per cent standardised			1 per cent standardised		
	λ_1	λ_2	λ_3	λ_1	λ_2	λ_3	λ_1	λ_2	λ_3
1	1 4 16*	4 32*	4-8* 32	4 16*	8 32*	8	16	+	16
2	1 8 32*	2-4	8	8 32*	16	2 8*	8 32*	16	2 16*
3	4 16*	8* 32	1 8*	4 16*	8	4 16*	4 16*	+	8
4	++	8	4 16*	+	4 16*	8	++	16	4 16*
5	4 16*	1 16*	+	16	32	8	++	16	16
6	+	1 4 16*	8-16	4 32*	16	16	4 32*	16	8

\+ Linear regression of log λ_s on log spacing significant at $P < 0.05$

++ Regression significant at $P < 0.01$

* Position of major peak

TABLE IV. SPECIES LOADINGS ON THE FIRST AXIS AND CORRELATIONS BETWEEN SPECIES DENSITY AND TRACK DENSITY - SITE 3.

Species and size class	Scores on first axis			Correlation coefficient
	5 per cent; unstd.	5 per cent; std. by max. score	1 per cent; std. by max. score	
E.leucophylla (1)*	2.540	0.254	0.204	-0.16
E.leucophylla (2)	-0.897	-0.016	0.021	-0.23
E.leucophylla (3)	2.860	0.213	0.203	-0.23
E.leucophylla (4)	2.227	0.364	0.322	-0.71
Eremophila sp (1)			-0.550	0.26
Eremophila sp (2)			-0.768	0.58
Eremophila sp (1-2)	-18.044	-0.864		0.51
M.planifolia (1-2)	-7.527	-0.563		0.88
M.planifolia (2)			-0.595	0.85
M. villosa (2-3)			0.289	-0.36
Rhagodia (2-3)			0.063	-0.008
A.linophylla (2-4)			-0.369	0.68
E.clarkei (2-3)			0.272	-0.59
A. aneura (1)			-0.157	0.18
A. aneura (2-4)			-0.418	0.19
A. aneura (5)			0.126	-0.21
Eremophila aff. leucophylla (2-4)			0.213	0.10

* Numbers in brackets indicate size class groupings.

TABLE V. SPECIES LOADINGS ON THE FIRST COMPONENT (1 PER CENT ANALYSIS) AND TRACK DENSITY CORRELATIONS FOR SITES 4 AND 6

Site 4			Site 6		
Species and size class	Loading	Correlation coefficient	Species and size class	Loading	Correlation coefficient
E. leucophylla (1)*	0.738	-0.75	E. leucophylla (1)	-1.351	-0.48
E. leucophylla (2)	1.412	-0.82	E. leucophylla (2-4)	-1.478	-0.55
E. leucophylla (3-4)	0.895	-0.93	Eremophila sp. (1)	1.002	0.78
Eremophila sp. (1)	-0.304	0.66	Eremophila sp. (2)	0.702	0.58
Eremophila sp. (2)	-0.555	0.71	M. planifolia (1)	0.112	0.67
M. planifolia (2)	-0.567	0.70	M. planifolia (2)	0.407	0.53
M. villosa (2-3)	-0.363	0.25	M. villosa (2-3)	0.120	0.25
Rhagodia (2-3)	-0.298	0.71	Rhagodia (2-3)	0.055	-0.09
A. linophylla (2-4)	0.311	-0.40	A. linophylla (2-4)	0.132	0.49
E. clarkei (2-3)	-0.073	-0.46	E. clarkei (2-3)	-0.283	-0.30
A. aneura (1)	0.334	-0.24	A. aneura (2-4)	0.043	-0.41
A. aneura (2-4)	0.556	-0.70	E. margarethae (2-4)	0.142	-0.27
A. aneura (5)	0.599	-0.68			
Maireana spp. (2)	0.183	-0.36			

* Numbers in brackets indicate size class groupings.

TABLE VI. RELATIONSHIP BETWEEN PATTERN OF INDIVIDUALS ASSOCIATED WITH RELICS OR LIVING TREES/SHRUBS AND PATTERN OF TOTAL POPULATION

Site	Species and size class	Block size †						Percentage of population associated with		
		1	2	4	8	16	32	Relics	Trees/shrubs	Total
1	E. leucophylla (2)			*		**		44.8	9.9	54.7
				+		++				
	E. leucophylla (3-4)			*		**		35.6	7.4	43.0
				+††		++				
	M. planifolia (1-2)			*			**	-	-	63.5
				+			++			
2	E. leucophylla (3)		**			*		34.7	9.8	44.5
		+					++			
	E. leucophylla (3) (isolated)						**	-	-	-
5	E. leucophylla (1-4)					**		N/A	N/A	N/A
						++				
	M. planifolia (1-2)					**		N/A	N/A	N/A
						++				
	Eremophila sp. (1-2)			*		**		29.8	6.8	36.6
				+		++				

* Position of peaks in analysis for individuals associated with relics etc.

** Indicates position of major peak.

\+ Position of peaks in analysis of total population.

++ Indicates position of major peak.

† Block sizes for all analyses expressed in terms of the M.P.A. equivalents.

†† Peak for class 3 only. Classes 3 and 4 combined for analysis of individuals associated with relics etc. Total populations of both classes 3 and 4 show major peak of block size 16.

N/A Not applicable. Analysis based on clumps occurring in association with relics rather than counts of individuals.

FIGURE 1. ORDINATION AND TRACK DENSITY PROFILES AT BLOCK SIZE 8 (32 m) FOR SITES 3, 4 and 6.

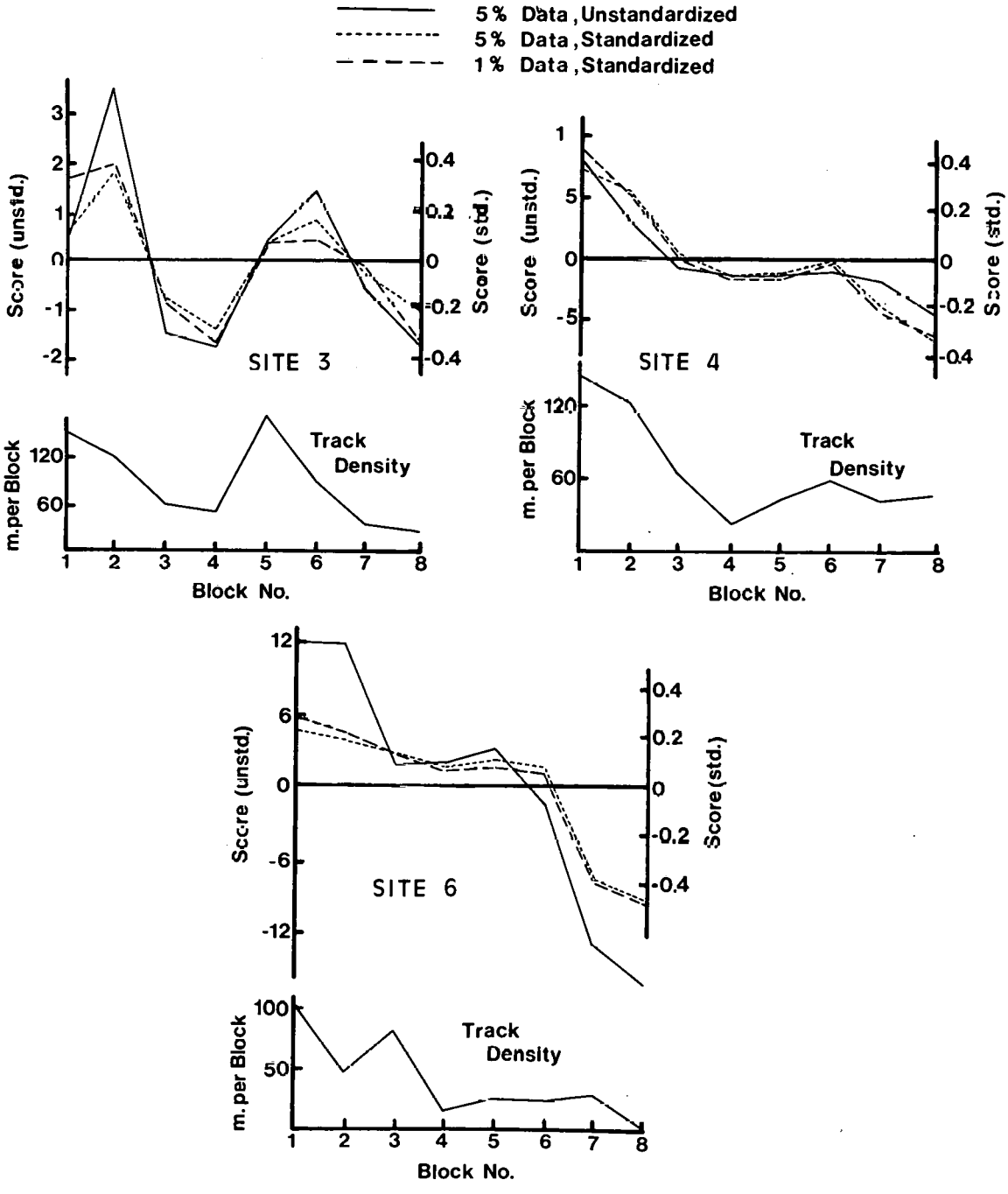

SOME NOTES ON THE EXPERIENCES OF LAPAN (THE INDONESIAN NATIONAL INSTITUTE OF AERONAUTICS AND SPACE) IN THE DEVELOPMENT OF REMOTE SENSING IN INDONESIA

Mahsun Irsyam
Indonesian National Institute of Aeronautics and Space
(LAPAN)
Jakarta, Indonesia

ABSTRACT

LAPAN has started development of indigenous capabilities in remote sensing in 1972. Within the frame of these activities, a number of visible and infra-red sensors, processing and interpretation equipment are available at present. A number of experiments have been carried out using said instruments. This paper reports on those experiments, experiences and problems faced by LAPAN during the conduct of remote sensing activities.

INTRODUCTION

LAPAN (The Indonesian National Institute of Aeronautics and Space) is a Non-Departemental Government Institute carrying the function of assisting the President in resolving aerospatial issues which might bear significance on national policy and to initiate, develop, promote and coordinate aerospace activities for the purpose of national development and national interests in general. In order to carry out said function, the scope of activities comprise aerospace applications, aerospace technology, aerospace research and aerospace studies.

It is in the frame of aerospace applications, that LAPAN carried out remote sensing activities since 1972, which were aimed for developing indigenous capabilities in support of research, inventory and evaluation of earth resources in Indonesia. The development of indigenous capabilities are considered very important to ensure the build-up of the system.

Like in other countries, remote sensing activities in Indonesia are conducted by various user agencies, universities and institutes. Besides LAPAN herself, other agencies are maintaining most of their main activities for interpretation of Landsat imageries for their specific fields of applications. Both types of activities, by LAPAN and by user agencies, are not separately standing but interlinked and in support for each other.

The development of remote sensing by LAPAN is conducted within the framework of the Five Year Development Plan, assigned to the Remote Sensing Project of LAPAN. At present the project has a number of sensor instruments, processing and interpretation equipment, and remote sensing experiment have been conducted, each of which are described in the following paragraphs.

EXISTING RESOURCES

At present LAPAN has the capability and capacity of the following sensors :

- A cluster of 4 Hasselblad Cameras 500 EL/70 mm
- NAC Mini Multiband Camera, Type MK-III
- Daedalus Dual Channel Quantitative Scanner, type DS-1230
- I_2S Mark II Multiband Camera with 4 lenses
- Four Channel Radiometer from DFVLR (W. German Space Agency)

The data collected with those sensors is processed with available equipments :

- Photographic Processing Laboratory, which has the capability of processing, printing and enlarging B & W film and color film
- Diazzo system
- Electronic Processor, which is used to process magnetic tape recorded data collected with the scanner

Available equipment for interpretation are :

- Mirror Stereoscope, viewing desk etc.
- Model 6040 P Color Additive Viewer
- NAC Mini Color Additive Viewer
- Model ZT-4 Zoom Transfer Scope
- Model 401/704 Data Color and Edge Enhancer System

The operational phase of this system development is now accentuated by the acquisition of the new Cessna 206 Stationair PK-UFO single engine by LAPAN.

In regard to the operation of activities and conduct of experiments, a total of 20 university graduates are working with the Remote Sensing Project as full-time personel. This team comprises of physicists, engineers, geographers, geologists, and foresters.

In its present development state, the project includes the acquisition of an Earth Resources Satellite Ground Station, which will provide direct reception of Landsat data. This adds the availability of data recording on magnetic tape, which will be accompanied by facilities for processing.

EXPERIMENTS WITH MULTIBAND CAMERA

As mentioned earlier, LAPAN is now provided with a Cluster of 4 Hasselblad 500 EL/70 mm Cameras, a Mini Multiband Camera and a Mark II Multiband Camera. With said sensors, photographic experiments have been done, using aircrafts and stratospheric balloons, which experiments were aimed to detect areas of critical soils, agriculture and land use in the streams regimen.

The use of stratospheric balloon platforms are allowing the conduct of photographing from stratospheric altitudes, from 25 km up to 40 km. The first of these series were flown in August 1976 on Bali (Bedugul area), in which two Hasselblad Cameras were taken in the payload, each loaded with B & W and Infrared films. The results from the 27 km altitude coverage comprised an area of 120 sq.km per frame. The infrared film produced less successful exposures than expected.

A second experiment used similar stratospheric balloon, in July 1977, launched from East Java, carrying two Hasselblad Cameras and each loaded with normal color film and false color film. The mission was to monitor the extent of critical soils from approximately 27 km altitude. The photographs covered areas of about 120 Sq.km per frame and produced significantly sharp images. On figure 1 an example of the stratospheric balloon is shown.

It should be noted, that stratospheric balloon launchings by LAPAN were not merely for purposes of carrying remote sensing missions, but were aimed to develop balloon technology and its application for other purposes as well. The major merit of stratospheric balloons are their higher ceiling altitudes compared to aircrafts. From their stratospheric heights, the photographic coverage is increased using simple techniques and include relatively lower costs. In this regard it may be reiterated, that remote sensing using balloon platforms will bear specific significance for Indonesia and other developing countries.

The latest experiment during the first part of this year was the photographic aircraft flight to serve the purpose of a study of a river basin and rice cultivation areas in West Java, using the multiband camera and using normal film and B & W infrared film. Results from this study will be reported in this symposium by J.P. Malingreau, Gajah Mada University and University of California, who is present conducting research in Indonesia.

The growing interest of user agencies in using the multiband camera is considered significant. At this time cooperation is under way between LAPAN and the Department of Agriculture, to plan remote sensing operations for forestry applications. It is expected that this type of operational

activity would be increasing and adopted systematically.

EXPERIMENTS WITH SCANNER

The Dual Channel Quantitative Scanner type 1230, used by LAPAN, is provided with 3 detectors which are sensitive in the visible range, and near-and thermal infrared, i.e. Silicon Photodiode (0.38 - 1.1 microns), InSb (3 - 5 microns) and HgCdTe (8 - 14 microns). Data is recorded on magnetic tape during flight and later processed by the Electronic Processor in the laboratory to produce B & W imagery on film.

Experiments are carried out, besides technical tests, to identify land use, thermal water pollution and fresh water occurences in coastal areas. The experiments during the month of June 1976 at 09.00 p.m. using InSb detectors had demonstrated contrasts between temperatures of the electrical power station's waste water and the coastal sea water in the Tanjung Priok harbor of Jakarta (Fig. 2). Other survey was held in Middle Java at the southern coast areas during April 1977 which was to discern the occurences of fresh water outflow along the shoreline.

The potential use of the scanner for other types of surveys are being studied at present, for the detection of historical remnants, critical soil areas and other studies in the field of Oceanology.

EXPERIMENTS WITH RADIOMETER

As a result of a cooperation program between LAPAN and DFVLR (Deutsche Forschungs und Versuchsanstalt fur Luft und Raumfahrt, West Germany) a 4 channel radiometer which has 4 detectros in visible spectrum, i.e. 0,443, 0,525, 0,560 and 0,680 microns, had been designed and built, during which LAPAN has attached one engineer to the German team, and was later donated to LAPAN for its experimental purposes. Beside that also an Infrared Radiometer PRT-5 had been transfered for the same purpose to LAPAN.

A joint experiment had been held to make a survey of the plankton concentrations in the Jakarta Bay during October 1977. Both teams of the DFVLR and LAPAN had carried out the aircrafts overpass while LON (National Institute of Oceanology) did the ground truth on the sea surface. The result of this joint experiment is reported in this symposium by D.P. Praseno, et,al., in a separate paper.

As it is obvious from the geographical spread of Indonesia, with two thirds of its territory occupied by sea, fishery is an important resource in the country. In this regard data is much needed, and tools for an inventory system should be

developed. Remote sensing would be one of the objective assets in that system which could be acquired. Therefore experiments using the radiometer to detect chlorophyll of planktons are expected to provide good support of the management of sea resources. The previous joint experiments will be followed with other surveys within this year using the radiometer and other sensors also.

INTERPRETATION OF LANDSAT IMAGES

Within the participation program with the NASA Landsat-1, about 80% of the Indonesian territory has been covered by the satellite coverage and provided basic support to the multidisciplinary studies. This data file is managed with LAPAN together with the rest of the remote sensing system and disseminated for the user agencies. Mostly the high rate of cloud cover incidence had caused the discrepancy in the total coverage, which only delivered photo coverage with less than 30% cloud covered areas. Among the direct impacts of Indonesia's participation in the ERTS/Landsat-1 are the growth of interest and investigations of Landsat imagery for applications carried out by user agencies, each according their specific fields or disciplines.

In regard with the wide interest in the satellite imaging system, LAPAN has submitted a new proposal of investigations to NASA, i.e. "Participation in the Landsat-C Program", and prepared the organization for the conduct of the participation program. The geographical areas of interest in the investigations cover the whole Indonesia territory for a time period of one year. Participating agencies and investigators are listed in the following :

- LAPAN, Jakarta
- Department of Public Works, Jakarta
- National Institute of Oceanology (LON), Jakarta
- National Coordinating Body for Surveys and Mapping (BAKOSURTANAL), Jakarta
- National Institute of Geology and Mining-LIPI, Bandung
- Padjadjaran University, Bandung
- Department of Agriculture, Bogor
- The Government of the Capital City, DKI Jakarta
- Department of Labor, Transmigration and Cooperatives, Jakarta.

Each agency has its investigation program and LAPAN will give its support to their investigations and included in the cooperation program. Another asset, i.e. a Natural Resources Satellite Ground Station, will be added to the system by LAPAN and being prepared at this time. This Ground Station is considered pertiment to provide direct access of Landsat image coverage, which is continuous, repetitive and comprehensive.

EXPERIENCES AND PROBLEMS

Remote sensing is a new and advanced technology, with a rapid rate of development and application techniques. Besides skilled manpower development, problems of system formation comprised the acquiring and development of instruments and equipments are the major efforts in the development of capabilities in remote sensing. To most university graduates as the main source group of skilled technicians, remote sensing is still a broad new field, which give reason to priority to training programs and literature compilation in the field of techniques and applications of remote sensing which are direct needs. This fact, LAPAN indeed appreciate the excellent opportunities for training for hers scientists and engineers at INPE (Brazil), EROS Data Center (USA), CNES (France) and DFVLR (West Germany). Nevertheless further efforts should be anticipated to continue training programs and international cooperation.

The need for recent information and up to date literature are fervently felt and being compensated gradually during the first phases of remote sensing activities of LAPAN. Participation in international seminars, visits to other remote sensing centers and exchange of publications and information are beneficial for resolving the need of information and literature.

During the first phase of remote sensing programs in Indonesia, problems of "overlapping activities" had been considered a handicap in management. With the lapse of time and the development of specific applications and understanding of the multidisciplinary nature of investigations using remote sensing techniques, it was observed that this problem had decreased and inter agency cooperation could be enhanced.

Another problem which had been experienced by LAPAN during the conduct of activities was that introducing new methods and techniques imposed on existing systems of management had proved insufficient when merely meetings were held, but visual factor should be demonstrated. In this regard the organization of joint experiments, technical workshops and similar efforts would be good support to the formation of cooperation and team work.

R E F E R E N C E S

....., "Remote Sensing Activities of LAPAN", Remote Sensing Project LAPAN 1975

....., "Proceedings of the LAPAN - DFVLR Seminar on Joint Remote Sensing Experiment with Radiometer", Remote Sensing Project LAPAN 1977

....., "Brief Information Concerning Proposed Landsat-C Data Investigation in Indonesia", LAPAN 1977.

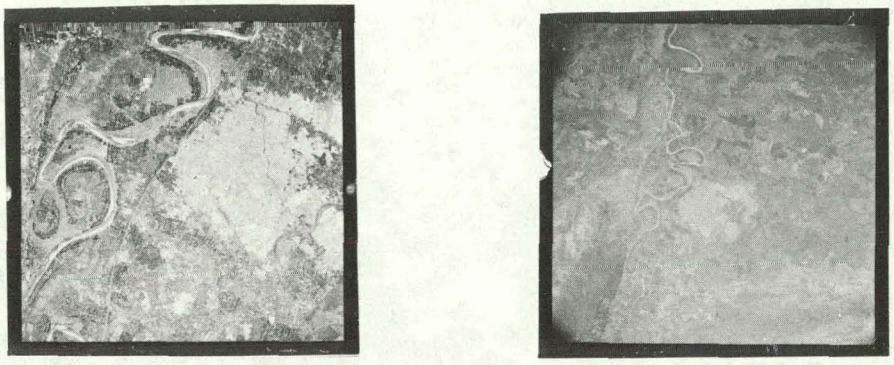

Figure 1. Photographs taken from Stratospheric balloon, altitude 27 km (approx) for monitoring of the extent of critical soils distribution in Middle and East Java. The sensors consisted of Hasselblad Cameras 500 EL/70 mm, f = 150 mm and f = 50 mm

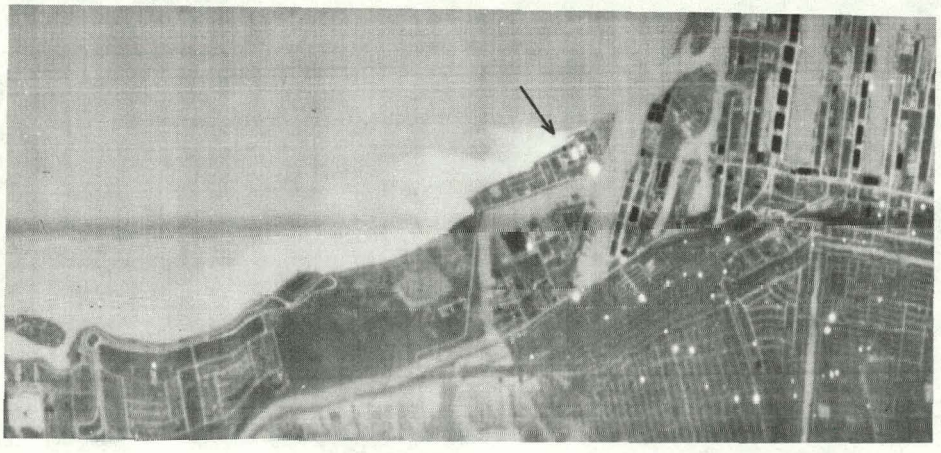

Figure 2. Scanner DS-1230 imagery. Thermal water pollution from Electric Power Station at Jakarta Coastal waters clearly presented in the imagery (arrow)

THIS PAGE

WAS INTENTIONALLY

LEFT BLANK

SONAR IMAGERY OF SEA FLOOR OBJECTS

Dr. Lloyd Breslau

Department of Transportation
United States Coast Guard
Groton, Connecticut, U. S. A.

ABSTRACT

Sonar is the remote sensing technique that is most generally applicable to the subsea environment. Sonar and radar are conceptually analogous in-as-much as both techniques involve pulse generation, two-way transmission through a fluid medium, echo generation by a target, and subsequent echo synthesis to form an image. While grossly analogous, sonar is quite different from radar due to relatively larger wavelengths, smaller transducers, longer propagation times, and a relatively less cooperative medium involving relatively higher signal attenuation, reverberation, and propagation path variability. Side scan sonar, which is conceptually analogous to side looking radar is a powerful tool for obtaining sonar imagery of sea floor objects. This paper will discuss the side scan sonar technique, present several examples of sonar imagery of sea floor objects, and discuss the interpretation of the sonar imagery.

THIS PAGE

WAS INTENTIONALLY

LEFT BLANK

VEGETATION MAPPING OF NIGERIA FROM RADAR

J. W. Trevett

Hunting Technical Services Limited
Borehamwood, Herts., England

1. INTRODUCTION

In 1976 the Federal Government of Nigeria through the Federal Department of Forestry awarded a contract for acquiring radar imagery cover for all Nigeria to Motorola (MARS) Inc., and another contract to interpret the imagery for a vegetation survey to Hunting Technical Services Limited.

The imagery acquisition scale was 1:250,000 with a swath width of 25km using an X band real aperture system. The imagery is taken in two look directions so that there is complete cover with both a north and a south looking direction.

Hunting were provided with mosaics at acquisition scale matched to the sheet layout of the joint Operations Graphics (JOG) series, 2 sets of mosaics gave both look directions. Hunting were also provided with copies of the original strip imagery and this was found to be invaluable for interpretation.

The contract requires that maps be produced at 1:250,000 scale based upon the JOG series to show the vegetation associations and that selected forest reserves be mapped in detail at 1:100,000 and 1:50,000 scale also based upon the radar imagery. Further the consultants were required to train Nigerian staff in the use of radar imagery and to carry out a special research into the use of digital analysis techniques to radar imagery.

The project is due for completion in October 1978, this paper describes the progress on the mapping and the digital analysis to date.

2. PRELIMINARY INTERPRETATION

Before any interpretation was started it was necessary to assemble all existing related maps and any conventional airphotography. This was necessary in order to construct the framework of an interpretation legend and indicate the general direction the study should take. One of the problems with radar imagery is that at the present time there is still a certain amount of uncertainty on how various physical features will record on radar and interpretation without a certain amount of related base information could be less valid and require more extensive ground truth checking.

In this case the Land Resources Division of the UK Department of Overseas Surveys has carried out extensive surveys in Northern Nigeria to produce a series of Land Capability, Soils and other maps and these provided an invaluable first basis for correlation. Nigeria has also been covered by airphotography mainly in central and northern areas although at varying dates and scales, this conventional photography provided an equally essential interpretation guide.

The interpretation of any form of imagery consists of the delineation of boundaries based upon differences in tone, texture and pattern and the subsequent definition of the units so delineated. On radar imagery the delineation of the initial boundaries raises no great difficulty, differences of tone and texture are easy to discern and boundaries readily drawn. It is in the definition of these units that the experience of the interpreter is required,

experience based upon local knowledge, knowledge of similar environments, his own discipline and the ability to read and relate other data sources to the interpreted imagery.

The NIRAD project, because of its size, employs a team of skilled interpreters and this introduces the need to establish clear cut interpretation methods and a standard legend. In the second stage the interpretation is checked by field survey and the results of this field ground truth are used to re-work the interpretation where necessary and at the same time it provides a knowledge of the next area of interpretation.

For this reason the policy on the NIRAD project has been to use the same team for interpretation, ground truth and final interpretation, thus the team can see how their boundaries relate to the ground data and can use this knowledge to improve the future initial interpretation.

The country has been divided into working blocks, related to the main vegetation zones. A block is interpreted, ground truth checked and finally mapped before turning to the next block. By this means the interpretation produces completed areas for the drawing office to work on so that final maps are produced in parallel with the interpretation.

3. STANDARDISATION

To assess what interpretation differences could occur, the same strip of imagery was interpreted by each of the team and then superimposed on each other for comparison.

Six interpreters identified a range of units that varied between 14 units and 20 units. The comparison showed that the broad mapping units were in agreement, the differences occurred in the smaller sub-divisions. This in part resulted from what one interpreter regarded as a valid mapping unit at scale compared with anothers concept of ultimate mapped unit size.

The definition of the mapped unit sizes was discussed between the interpreters and the cartographers, subsequent experience has shown that differing zones introduce different problems in unit size and this problem has to be continually appraised.

Experience has shown that mixed vegetation zones cause the greatest interpretation differences. In an area of combined parkland and farmlands for example, the parkland consists mainly of scattered trees over the cultivated land. The breakpoint between this mixture and pure farmland is a judgement of the density and significance of the parkland cover, some interpreters will tend to map out small farmland units within this mixture others will regard the whole area as conforming to the general mixture definition.

This difference in appreciation of mappable units proved a greater factor between interpreters than the ability to agree on differences of tone and texture. Where differences in interpretation of tone and texture, that is interpretation differences of actual units, occur then these differences are usually a measure of the interpreters applied earth science background and field experience which introduce a bias to his interpretation. As the project progresses and the general interpretation and field experience grows then these differences are equalled out.

4. INTERPRETATION PROCEDURES

A sub-section of this contract calls for revision of the planimetric detail on the JOG sheets within the capability of the radar imagery. In effect this has meant a revision of the drainage systems where errors or changes are apparent and corrections or additions to the principal roads where supported by field knowledge. Villages, railways and some urban areas are particularly difficult to discern and changes in these features have not been identified.

The interpreter compares the mosaic with the JOG sheet and records any changes of planimetric detail on the interpretation overlay at the same time identifying the features to be drawn on the planimetric base used when over-printing onto the mosaic. With two methods of final product, printed on the JOG sheet and printed onto the mosaic this detail is already on the former but selected detail is required for the latter.

The interpreter then indicates units of similar tone and texture and where possible identifies these units as vegetation associations according to an interpretation legend. Interpretation is aided by field experience, field notes for other similar areas on file, interpretation of any existing conventional photography and the study of any existing maps.

When the initial interpretation is completed for each mosaic it is checked against all the surrounding mosaics for correlation of boundaries and similarity of style.

The interpreter will also note particular areas of uncertainty which require field checking and indicate the field traverse routes to be taken over the area covered by the sheet interpreted.

The initial interpretation employed numeric codes to identify units of similar distinctive appearance, the first field check identified these units into mapping vegetation units and named the predominant species in that unit. Subsequent interpretation used this information to identify units in their correct nomenclature to be verified by field checking. New vegetation zones do however introduce new units which have to be identified in the field.

Figure 1 shows an example of the preliminary radar interpretation of part of a mosaic in Northern Nigeria. In reality the interpretation is drawn onto transparent stuble base plastic drawing foil using coloured inks, roads in red, railways, towns, airfields, bridges in black, drainage features in blue. Solid lines denote features visible on SLAR, broken lines detail derived from the JOG sheets.

Numbers denote main units, lower case sub-script is used for sub-division of these units.

5. GROUND TRUTH SURVEY

The country has been divided into 5 blocks of sheets designed to produce a logical block for field work and comprising as far as possible a homogenous vegetation zone.

As the first interpretation of a block is completed so the ground truth survey is undertaken by the interpreters working on the block.

To cover such vast areas, four wheel drive field vehicles are used, fortunately Nigeria has a good road system and road traverses are feasible.

Figure 2 shows a typical project traverse record form with traverse details compiled prior to departure of the field teams, the remainder with verification will be completed in the field.

Where a site is regarded as typical of a particular unit the forms in Figures 3 and 4 are completed.

Extensive use is made of ground photographs to record typical vegetation/terrain schemes to aid other interpreters. In this respect photographic stereo pairs have been found to be particularly useful.

Observation sites are marked on the mosaic overlays and all the field data contained in a special file.

6. THE VEGETATION CLASSIFICATION FRAMEWORK

It is unlikely that any vegetation classification system and its nomenclature will satisfy all users, particularly where finite boundaries are being placed on parameters that form a continuum. Although the nomenclature is of secondary importance, compared with the consistency of the classification and the definitions of its categories, a decision on nomenclature needs to be made.

The Yangambi classification of CCTA/CSA (1956) is one of the best known physiognomic systems for the classification of African vegetation. However, there were a number of objections to the Yangambi terminology, particularly from East African workers (Pratt et al, 1966) who showed why this system, based mainly on West African experience, was not wholly suitable to East and Central African conditions. On the other hand, the system forms the basis of the vegetation studies carried out in north-eastern Nigeria by the Land Resources Division (L.R.D., 1972). They argue that the terms used are in such common usage and so widely recognised in West Africa that their retention is advisable until some universally accepted scheme is available.

The recent publication of the UNESCO/AETFAT vegetation map of Africa, compiled by F. White, appears to fulfill this requirement, at least as a primary framework for classification. Unfortunately, a complete copy of the legend and definitions has only just been acquired by the interpretation team. Thus, for the purpose of data compilation and interpretation, the Yangambi derived L.R.D. nomenclature has been used.

The classification framework based on the UNESCO map legend tested during the field investigation programme. The primary classification unit in this system is physiognomic. Despite some ambiguities in the recognition of physiognomic boundaries, results of interpretation suggest that an acceptable level of consistency can be achieved in mapping physiognomic form.

Floristic, geomorphological and ecological categories are used in the classification system. Landform units are separated from vegetation units to avoid confusion and inconsistency by the mixing of terms and will be described on a parallel key. Floristic sub-divisions of the primary physiognomic units which cannot be mapped will be listed in the key and described in more detail in the text of the report. Such descriptions are necessary in order to link the mapping units with previous land-use and vegetation studies.

The correlation of field observations in northern Nigeria with the interpreted radar units indicates that many boundaries did not relate to significant vegetation differences in a consistent manner. The discrepancies were caused, for the most part, by the sparse vegetation cover occurring in the Sahel and Sudan zones allowing a large proportion of backscattered energy from bare soil and rock. In addition, the relatively low moisture content of the vegetation and soil at the time of over flight will probably have increased the soil penetration by the X-band microwave energy, thus further complicating the interpretation of the returned signal.

Many of the radar mapping units in northern Nigeria represent varying proportions and patterns of different physiognomic vegetation types. Of these types, only dry grassland and aquatic grassland have unambiguous radar signatures. However, in dry grassland in the uniqueness of the signature is due to the specular reflecting properties of the smooth black clay soils (kirki clays) which support a sparse cover of *Sorghum aethiopicum* grass. Backscattered energy due to isotropic reflection from the grass is insufficient to modify the signature from the soil.

The consistent recognition of dry grassland has enabled relative proportions of grassland to other physiognomic types to be mapped only where clay soils occur. The isotropic reflecting properties of a sandy surface are similar to those of dense shrub and grass cover. Thus, higher returns (i.e. light tones) on the radar imagery can be either:

(a) sand island with sparse vegetation cover

(b) sand island with a dense vegetation cover

(c) a clay plain with a very dense thicket

The vegetation cover in (a) and (b) can either be grass, shrub, woodland or a combination of all three. Only by field checking can the physiognomic form of the vegetation be determined unequivocally at any point and it has not been possible to give the proportions of say, shrubland to grassland or shrubland to woodland, numerically.

The method of determining to which category a particular mapping unit belongs involves the correlation of field data with all available contextural information in the form of natural resource maps, reports and aerial photography. However, the final mapping units delineated are determined by the boundaries visible on the 1:250,000 radar imagery. Vegetation boundaries which exist in reality but are not recognisable on the radar cannot be mapped. Conversely, a number of interpreted units may have no relevant vegetative significance and merely reflect changes in soil or geomorphology. In these instances radar units mapped in the preliminary stage may be amalgamated on the final map.

It is clear that the objective and consistent interpretation of single season radar imagery of northern Nigeria is precluded by the large number of ground variables. The effect these variables have is understood in relative terms but cannot be quantified by the interpreters.

Thus a large measure of subjectivity is present in the interpretation and mapping of the northern region. This is regretable but unavoidable. These problems are not so pronounced in the southern region where the dense vegetation cover (irrespective of physiognomic form) prevents all but a very small proportion of backscattering from the ground. The radar signatures in the south arise mainly from differences in the roughness of the canopy and the nature of the scattering surface.

Landform units have been separated from the vegetation units on the map and in the legend to avoid confusion and inconsistency by the mixing of terms. Relevant information on the geomorphology and soils of the area covered by each mosaic are given in a separate sketch map accompanying the legend. The names of existing forest reserves are also presented on a separate sketch map, although the actual reserve boundaries will be drawn to scale on the map sheets.

7. THE MAP LEGEND FRAMEWORK

Formation	Sub-formation	Examples of Floristic Dominants/Land Use
Grassland	Dry Grassland Grassland Aquatic Grassland Montane Grassland Shrub Grassland Wooded Shrub Grassland	
Grassland/Shrubland Transition	Dense Shrub Grassland	
Shrubland and Thicket	Non-Thorny Thorny Mixed	*Combretum, Guiera* *Acacia* spp.
Wooded Shrub Grassland Woodland Transition	Wooded Shrub Grassland with patches of woodland	

Formation	Sub-formation	Examples of Floristic Dominants/Land Use
Woodland	Broad leaved	*Isoberlinia/Daniellia*
	Thorn	
Woodland Mosaics and Transitions		
Forest	Primary/High	Logged
	Secondary	Small holder rubber
	Swamp	
	Mangrove	
	Montane	
	Riparian/Riverine	Raffia
Farmland	Sahel & Sudan	Mapped at two levels
	Guinea	<60% intensity
	Derived Savanna	
	Forest	30-60% intensity
	Forestry Plantations	(Terminalia, Teak, (Cmolina, etc
Plantations and Agricultural Projects	Crop Plantations	Rubber/Oil Palm
Projects		Cocoa/Coconut etc.
	Irrigation/Project	Wheat, rice, cotton
	Mechanised Farming Project	
	Rainfed Agricultural Project	

8. GENERAL COMMENTS ON SIGNATURES AND GROUND CORRELATION (NORTHERN SECTOR)

The most significant vegetation signatures identified on the sheets studied were from:

(1) annual crops
(2) fallow, including shrubland
(3) plantations
(4) closed woodland
(5) grassland

Each type can be subdivided by topography into

(a) Upland, and
(b) Valley sites

8.1 Annual Crops and Fallow Land

Annual agricultural crops planted on a large scale include millet, guinea corn and maize, though it has not been possible to discriminate between these or other crops such as rice, cotton and groundnuts.

Fallow areas are extensively grazed. The area of close woodland in the northern sector is very limited, and even where identified was subject to heavy grazing and uncontrolled cutting for poles and fuelwood.

The actual canopy cover of tree farmland may in some cases be greater than that of open woodland. The impression has been gained that scattered trees have little significance on radar signatures in the Sudan zone (leaf width is less than 3 cm in the majority of dominant species).

Stands of trees with continuous canopy show up clearly, usually with lighter tones than even annual crops (in full leaf before harvest) with scattered trees. Probably a similar signature will be given by large units of crops of the same species without tree cover - as in a large mechanized agricultural development area.

Similarly, an area of improved grazing will have a uniform signature of light tone.

Normal farmland is distinguished by a texture that can be associated with the discontinuous, patchy nature of most traditional forms of farming, due to small field separation by hedgerows or fallow strips, mixed crops, differing sowing and harvesting times and, perhaps, by significant groupings of fruit trees. Blocks of fallow within farmland of ca. 25 ha in extent (0.2 cm square on the mosaic sheet) or even less, have been identified.

8.2 Woodland

Limited areas of closed woodland occur in the northern sector. These include riparian vegetation, since it was found to be impossible to discriminate between patches of the characteristic woodland of moister depressions in the upland areas and the sparse and relatively infrequent occurrences of riparian vegetation characterized by *Diospyros mespiliformis* and *Mitragyna inermis*, in the areas visited.

Most closed and predominantly xerophytic woodlands produce a light canopy not readily distinguished from the shrub and tree shrublands, on the imagery. A grass cover usually develops which is only replaced by thickets on better drained areas, suggesting that such types should not, in fact, be classified as woodland, but rather as wooded grassland.

8.3 Grassland

The radar signature for grass varies according to the density of the grass cover, the soil type and microrelief of the soil surface. In northern Nigeria, the grass cover is sparse, particularly during the dry season when the majority of the imagery was acquired. This soil type and microrelief primarily determine the strength of the 'returned' signal. For example, the areas of sparse dry grass cover on the fine clay soils in the Chad Basin have a very distinct dark grey to black signature. The level black clays appear to act as a very good specular reflector and appear black on the image. The low density of grass cover and physiognomic properties of the wild sorghum grass, (*Sorghum aethiopicum*) prevent any significant signal scattering.

Where sandy soils occur, density of shrubs and grass communities, other than Sorghum, tends to increase but rarely exceeds 20 per cent in areas mapped as shrub grassland. The high return from the uneven sandy surface appears to dominate the radar signature, giving light grey and white tones.

Generally, it was not possible to differentiate the radar signatures of dry grass cover and shrubland or thicket where they occur together on sandy soil. Thus, the mapping unit "shrub grassland" consists of a mosaic of two radar signatures; 1, areas of light tone representing a mixture of grass and

shrub communities on sand: 2, the more extensive areas of dry grassland on clays with a darker tone. Occasionally it is possible to recognise on the radar Acacia thorn thicket growing on clay soils. The radar return is moderately strong despite the fact that Acacias possess very small bipinnate leaves and many of the Acacias were leafless at the time of overflight. This suggests that the radar return is coming from the Acacias' dense tangle of randomly orientated stems, branches, and spines.

The aquatic grassland on Lake Chad is easily identified on the radar by its very distinctive signature and location. The boundary between the grassland and the shrub grassland follows the shoreline and confirms the strong correlation between vegetation and geomorphic boundaries in the Chad Basin.

8.4 Special Problems

Tones for intensively cultivated areas on some strips were darker in tone than fallow, in contrast the tonal pattern occurring on the other mosaics checked.

This apparent inconsistency should be distinguished from the change in tones, or even reversal of tones, between two strip of the same area acquired at different dates. This is more easily explained by seasonal differences in the physiognomy of the vegetation. It would found impossible to account for the differences between strips, which were both acquired in apparently the same season, without:

(a) knowledge of the date and climatic conditions at the time of acquisition and,

(b) knowledge of the crops grown in the different regions and normal harvesting times.

To return to the general point mentioned earlier, the strongest signatures are given by annual crops in full leaf. After harvest and drying of the leaves and stems of cereal crops, the signature is expected to alter to give darker tones. After clearing and burning the signature will be that of bare soil in many cases and will depend on surface moisture and roughness. Signatures from closed woodland would be expected to change less with season and should be used in cross-correlation between mosaics or strips. However, most long term fallow areas such as forest reserves have open canopies so that surface soils characteristics (grass cover, trampled areas, compacted surfaces, burnt grass layer, etc) may be dominating the reflectivity pattern.

The foregoing comments on the legend and the relationship of the radar signal to the ground truth apply only to the northern area of Nigeria. The ground truth for the central and southern areas are still in progress and observations on these areas will not be available until the publication of a final report on October/November 1978.

These remaining areas cover the more densly vegetated and high forest zones of Nigeria and will therefore introduce problems in separating forest types, of distinguishing rubber and oil palm plantations and coastal vegetation types.

Two figures are included to demonstrate the interpretation of a central and coastal area.

Figure 5 covers an area to the south east of Benin City, Bendel States and in an example of the interpretation of imagery in the high forest zone.

Figure 6 is an example of coastal imagery, the area falls into two distinctive radar signatures and coastal dunes and older beach ridges and the saline coastal swamp and riverflood plains with mangroves.

The legend is continually being strengthened and extended as new zones are interpreted and checked.

9. MAPPING

The consultants are required to prepare all the fair drawing work including separations for colour printing of the 1:250,000 series. The printing is being undertaken by the Nigerian Federal Department of Forestry within their own facility.

In order to allow the maximum flexibility of presentation the masters are prepared in such a way that printing can be carried out using the JOG sheets as a base or a half-tone copy of the radar mosaic.

The complexity of the legend demanded the use of colour but this had to be fairly simple if the mosaic was still to show through. The use of subtle tone differences of colour complexes would have worked on the map base but the use of a tone underprint would result in slight apparent colour changes which could lend to confusion.

The system adopted has been to use a distinctive colour for the principal formation with over-printed screen symbols for the sub-formation. This permits a fairly extensive legend to be devised which is distinguishable over both base medium. It does however raise some problems when the interpreters wish to introduce complexes involving more than one mapping unit. In effect it has placed a stricter constraint on the interpreters and forced a clear cut decision on units in certain cases, in others the colour for the dominant formation has been used with a distinctive symbol overprinted to denote a mixture.

The original intention has been to show geomorphological units on the main map and to name forest reserves but it became apparent that such a practice would lead to confusion in reading the main map subject. A series of smaller maps at the bottom of each sheet have been included to record forest reserve names, geomorphology, administrative units and eco-climatic zones.

The completed mapping will produce a series of 66 sheets covering the whole of Nigeria, such a comprehensive series of vegetation maps based as it is upon radar interpretation and field checking, is believed to be a unique achievement.

10. DIGITAL ANALYSIS

The use of digital analysis in the interpretation of radar is perhaps a new departure and because of the uncertainty of the possible application this segment of the project is being undertaken as a research project on specific forest reserves.

The initial study involved the digitising of a segment of a radar image and applying various standard density slicing techniques. It soon became apparent that this revealed no units compatible with the interpreted vegetation units and alternative diagnostic systems were investigated.

Image density or tone is only one of a number of parameters, which include texture, shape and pattern, used by interpreters. Of these parameters, texture, which may be defined as the local spatial relationship of grey tones of an image, is of particular importance in the interpretation of radar imagery. The Image Analysis Group, Harwell, who are undertaking this element of the project, have therefore concentrated their efforts on developing various analytical tools for the characterisation of textural features.

One of the principal problems involved with texture measurement is that it is by definition an extended property. That is, because it involves the environment surrounding a given pixel, it can only be defined at an equivalent resolution

somewhat lower than that of the original image. This degradation is itself a function of the longest spatial wavelength of interest since all the methods to be described need to sample over an area of at least that size around each point. This effect should always be borne in mind when comparing the results of spatial texture processing with more familiar spectral point-by-point processing on multi-channel imagery.

Two basic methods of quantifying texture exist, distinguished usually by the terms "first" and "second order" statistics. In the former case the immediate environment of each pixel is examined within a 'window' of variable size which surrounds it, and various parameters are computed which measure in different ways the variability of the pixel intensities. The results are then taken as a measure of the texture at the central pixel. In this way a point map of such properties is constructed which can be compared directly with the original image. Second order methods generally look at a much larger portion of the image, normally selected to have approximately homogeneous properties, and calculate a mean value for a number of possible measurements which have very high statistical significance because of the large number of pixels involved. In addition, there are methods which compute power spectra for large area samples and, taking the Fourier transform as an example, produce a complete spectrum in the frequency domain. This represents the spatial wavelengths present in the area processed as a function of both frequency and direction.

The choice of approach is a difficult one and depends on the type of output information required and computational efficiency. For the present research a number of different implementations have been developed to enable a comparison of their various merits to be made.

It is not possible at this stage to go into the detailed research at present taking place to do so would be premature and would require a separate detailed paper of its own. Some of the conclusions reached so far may however be of interest to other researchers in the subject.

The results of the digital analysis conclusively demonstrate that textural information contained in the radar imagery can be separated into units with boundaries which broadly correlate, in terms of shape and position in the image, with those units identified visually by the earth scientist and predicted to contain vegetation of like physiognomic form.

The digital methods of texture analysis each discriminate textural classes by detecting subtle and statistically significant differences in the spatial relationships between the picture elements as pixels, which make up the image.

Of the two basic methods used to quantify texture, the first order methods appear to reinforce the visual interpretation carried out by the earth scientist, and second order methods offer the possibility of discriminating quantitatively between areas on the image with visually similar textures.

The first order methods of quantifying texture discriminate similar broad textural classes to those recognised by the human interpreter using non-digital methods. However, in the case of the Sapoba Forest Reserve image, the local operators used, namely Laplacian, average and auto-correlation, do not give information which can discriminate the rubber plantation from the older taungya areas. The availability of a cross-polarised channel may resolve this type of ambiguity although the problem may be more fundamental. These textural properties of the two units, as quantified digitally, may indeed be inseparable but there are additional image characteristics, both textural and tonal, which can be used in image classification. In the present case, contextural information such as that provided by shape and radar tree shadow, enable the human interpreter to make subtle distinctions. For example, the discrimination of an area of tree shadow with low density using the present first methods does

not convey to the computer information about the two units on either side of the shadow area, in the same way as it does to the human interpreter. Similarly valley shadow will have similar textural and gross tonal properties to tree shadow, and so will be grouped in the same class using digital methods. The shape and environment of these two homogeneous areas of low intensity usually permits their separation and significance to be established by the human interpreter. Thus first order methods can separate areas of homogeneous texture and provide a quantitative measure of the same. However the units so delineated do not all have the same vegetation and land use significance, and thus classification using these measures alone is ambiguous.

Clearly it will be necessary to include the parameter of shape and the related contextural data if a completely digital method of classification is to succeed. On the other hand, second order methods, such as the co-occurrence measures used, appear to offer the possibility of discriminating between textural groupings which are visually similar and cannot be consistently separated by the human interpreter. This is because a large area can be sampled to produce a numerical measure of texture which has high statistical significance.

The next stage of the research will be concerned with a more thorough evaluation of the results from the Sapoba Forest Reserve, and the design of an experiment to test the suitability of these processing methods for mapping vegetation in another forest reserve, having first established the textural parameters of a number of training sets in a similar reserve. This exercise will be carried out in the Oluwa and Omo Forest Reserves which have been designated priority areas for more detailed mapping.

Field checking will be carried out in the Omo Reserve, for which a large amount of ground data exists, to provide data for the digital training sets. The first and second order local operators can then be applied to imagery of the adjacent Oluwa Forest Reserve under the interactive control of HTS interpreters, and units with similar textural properties to those of the training sets identified. The resultant digital classification will then be checked in the field.

Although the results of the digital analysis to date are encouraging, it must constantly be borne in mind that computer assisted digital methods of image interpretation must provide the interpreter with information (at a viable cost) that other methods cannot provide.

ACKNOWLEDGEMENT

The maps, mosaics and reports used in the preparation of this paper are the copyright of the Federal Ministry of Agriculture and Rural Development, Federal Department of Forestry Nigeria and I should like to express my gratitude to the Director Mr. Oseni for permission to use material from the radar survey project.

It was his foresight which perceived the application of radar to the needs of his department and the success of the project to date owes much to his continual cooperation and encouragement.

Figure 1

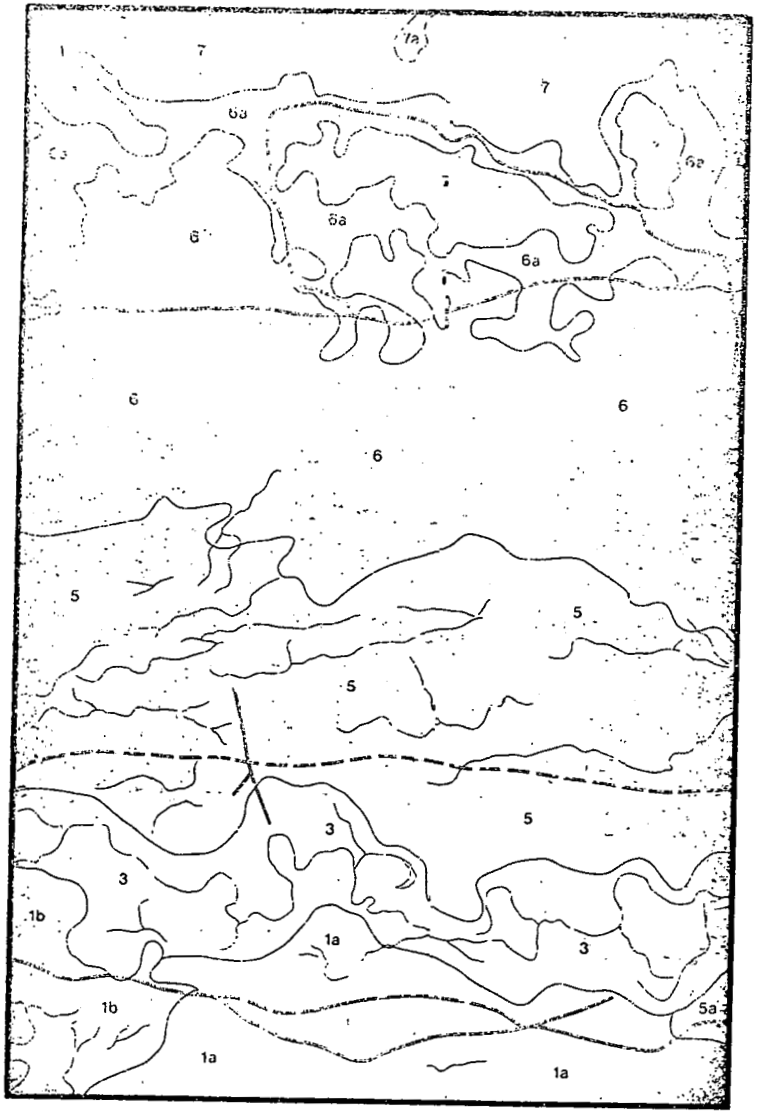

VEGETATION

Parkland \ Tree and Shrub Savanna mosaic 1a

Shrub Savanna 1b

N. Alluvial complex \ Grassland \ Shrub Savanna mosaic 3

Tree and Shrub Savanna \ Grassland mosaic 5

N. Alluvial complex \ Palmbush \ Scrub mosaic 6

N. Alluvial complex 6a

Parkland \ Grassland \ Tree and Shrub Savanna mosaic 7

Farmed Parkland 7a

TOPOGRAPHY

Roads (apparent on Imagery) .....

Roads (added from J.O.G. maps) .....

Rivers (apparent on Imagery) .....

Rivers (added from J.O.G. maps) .....

Lakes .....

Rock outcrop .....

Settlement .....

Radar Mapping Units (R.M.U.) .....

R.M.U.'s (with indistinct boundaries) .....

Edge of Forest reserve .....

Tree shelterbelts .....

NIRAD PROJECT TRAVERSE FORM.

Traverse: 21/2 State: BAUCHI Mosaic: ND32-3 Observer: G.Deane Date:

AZARE - ZIGAU

1.	2.	3.	4.	5.	6.	7.	8.	9.	10.	11.
Speedo km.	Ref. point	SLAR		MAPPING		UNIT		VEGETATION		
		No.	Width km.	Cross boundary	Tone	Texture	Pattern	Interpreted	Ground checked	Classification
	AZARE + 0	1	3	0	6	coarse	matrix	FP		
		1C	4.5	3	6 with 5/7	fine & dark mottles	linear?	SS with some FP		
	KUJURU F.R.+ 7	4	+ 2 from road	-	4/5	fine	clear boundaries	Combretum, Lannea T & SS		
		1	5.5	7.5	6	course	matrix	FP		
	DALLI F.R.+ 13	4	6.5	13.0	4/5	fine	clear boundaries	T & SS Guiera, Vitex		
		1	5.5	19.5	6	coarse	matrix	FP		
	SHIRA+27.5 SARKIN DUTSI HILL	1C	2.5	25.0	6 with 5/7	fine & dark mottles	linear?	SS and some FP		
		1	5	27.5	6	coarse	matrix	FP		
	ROAD + 35 JUNCTION	3	5	32.5	5 with 6 & 4	medium coarse		Savanna Woodland		
		7	2.5	37.5	6/7	fine	straight boundaries	plantation?		
	ZIGAU	END		40.0						

Offsets and headings to be indicated in column 2 and underlined in red.

FIGURE 2

1931

FIGURE 3 VEGETATION RECORD

VEGETATION RECORD:

LOCATION: OBSERVER: DATE:

Observation of region

1. PATTERN

Indicate regional vegetation pattern on chart and describe:

AREA UNDER REFERENCE

PATTERN SKETCHED SCALE

Scale

	1 cm	$1cm^2$
1:10k	100m	1ha
1:100k	1 km	$1km^2$
1:250K	2.5km	$6.25km^2$

MATRIX

ELEMENTS WITHIN

NONE

RANDOM

REGULAR

CLUSTERED

LINEAR

OTHER

Indicate whether matrix or element at local site

Observation of local site

PHYSIOCNOMIC TYPE

DISTURBANCE CLASS

CHARACTERISTIC DOMINANTS

CHARTERS VEGETATION TYPE

	EMERG.	MAIN	LOWER	GROUND
HEIGHT CLASS				
COVER PER CENT				
CANOPY TYPE				
CANOPY DENSITY				

PROFILE

Height Scale

PHOTOGRAPH REFERENCE

FIGURE 4 TERRAIN CLASSIFICATION

TERRAIN CLASSIFICATION - REGIONAL DESCRIPTION

SAMPLE AREA NO: OBSERVER: DATE:

LOCATION:

MAP REF: SLAR REF: PHOTO REF:

LANDSAT REF: ELEVATION: RAINFALL:

LANDUSE: EXTENT OF AREA UNDER REF:

GEOLOGY	
LANDFORM	
TOPOGRAPHY	
DISSECTION	
SOILS	

SITE DESCRIPTION

SLOPE: MICROTOPOGRAPHY:

EVIDENCE OF EROSION: NATURE OF SURFACE:

DRAINAGE:

SURFACE: SUB-SURFACE:

SOIL DESCRIPTION: BORE ☐ PIT ☐ SECTION ☐

HORIZON	DEPTH CM	COLOUR	MOTTLES	CONSIST.	TEXTURE	OTHER PROPERTIES

Figure 5

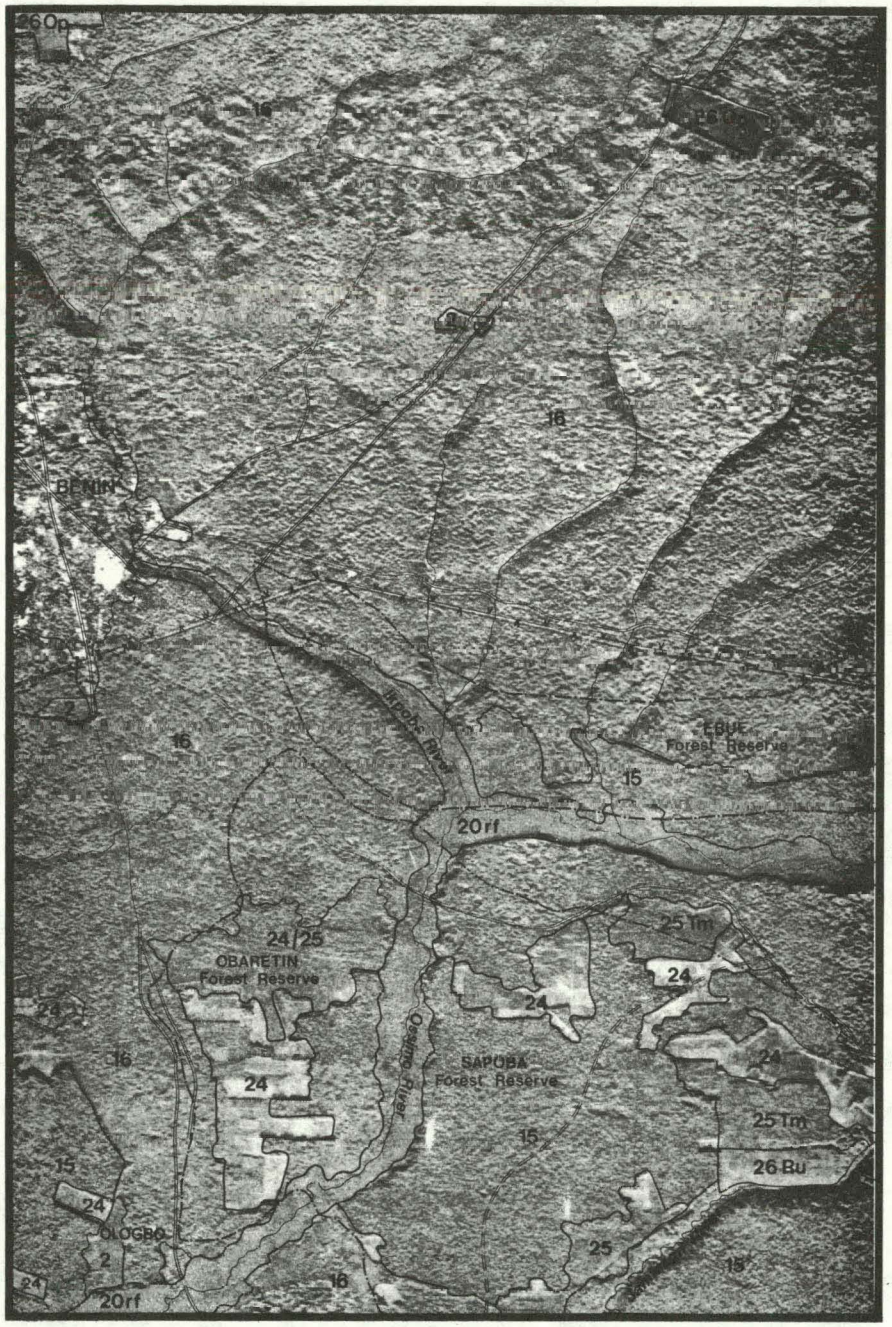
60p
16
BENIN
18
Ibropa River
EBUE
Forest Reserve
15
20rf
24/25
OBARETIN
Forest Reserve
25 Tm
24
Osiomo River
SAPOBA
Forest Reserve
26 Bu
OLOGBO
20rf

Figure 6

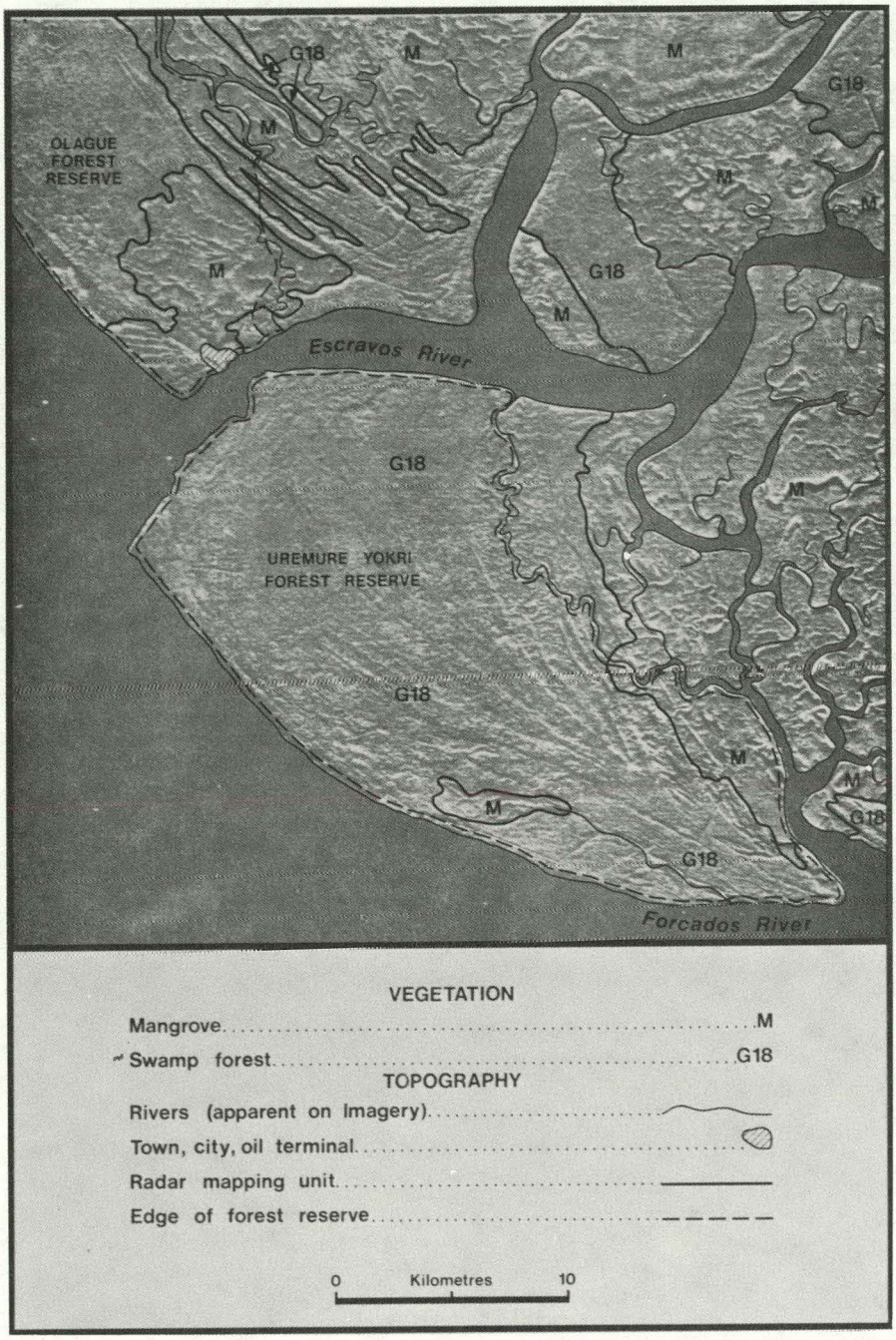
G18
M
OLAGUE
FOREST
RESERVE
Escravos River
UREMURE YOKRI
FOREST RESERVE
Forcados River
VEGETATION
Mangrove ..... M
Swamp forest G18
TOPOGRAPHY
Rivers (apparent on Imagery)
Town, city, oil terminal
Radar mapping unit
Edge of forest reserve
0 Kilometres 10

THIS PAGE

WAS INTENTIONALLY

LEFT BLANK

SPECTRAL CHARACTERISTICS IN UV-V-IR OF MATERIALS IN REQUENA AND LA ESPERANZA DAMS AND THEIR DETECTION BY REMOTE SENSING

P. Ruiz Azuara and L. Lemus Hidalgo

Laboratorio Interdisciplinario. Facultad de Ciencias
Universidad Nacional Autónoma de México
México, D.F. MEXICO

ABSTRACT

The spectral characteristics of some materials which were reported in the chemical analysis as possible compounds in an early study of total suspended solids realized by remote sensing in the Requena Dam had been studied using ultraviolet, visible and infrared spectroscopies. Three regions of the electromagnetic spectrum in which some of these materials can be distinguished in aqueous solutions had been found. They are: .2-.36 μ, 6.5-8.5 μ and 8.5-10.5 μ. Assuming additivity these results can be used for to interpret in a first approximation the spectra of water samples that were taken in La Esperanza Dam. The problems related with the use of the partial transmissibility as a selective indicator in water quality studies by remote sensing were discussed.

1. INTRODUCTION

One of the most important water quality indicators is the concentration of suspended solids. In other paper (Ruiz-Lemus, 1977) was studied the problem of total suspended solids detection by remote sensing using aerial photography with Ektachrome infrared film of 35 mm. in the Requena Dam. A linear relationship between the infrared film transmissibility and the total suspended solids concentration obtained from chemical analysis of the water samples was suggested.

The spectral properties of the different materials detected were not considered. However, some of them absorb certain wavelengths of the electromagnetic spectrum.

In this paper the spectral characteristics of some materials detected in water samples of the Requena and La Esperanza Dams, both located in Edo. de Hidalgo,MEXICO, are reported. The differences between them were analyzed with ultraviolet, visible and infrared spectroscopies. The sample transmissibility depends, essentially , of : the transmissibility and concentration of their constituents, the sample size, the distilled water spectrum and, naturally, the wavelength of the incident radiation.

For remote sensing studies to obtain water quality indicators is a very complex problem. With relation to the water color in lakes, the visible region of the electromagnetic spectrum had been discussed (Scherz-Van Domelen, 1975).

In the present work were also analyzed two non-visible regions: ultraviolet and infrared. The object of this study was to find wavelengths in these regions of the electromagnetic spectrum in which we can distinguish some materials from the others.

2. ULTRAVIOLET-VISIBLE-INFRARED SPECTRA

2.1 Partial Transmissibility

Using very small samples the spectra in UV-V-IR of transmissibility (or absorbance) corresponding to several constituents detected in water samples of Requena and La Esperanza Dams were obtained in aqueous solutions with different concentrations. In the Table I are shown the possible chemical compounds reported by the laboratory analysis made in the Geology Institute,UNAM. They are: sodium chloride (NaCl), sodium bicarbonate ($NaHCO_3$), sodium sulfate (Na_2SO_4), sodium nitrate ($NaNO_3$) and others.

The range of total solids concentration is 240-300 mg/l, except in the sample point III from Requena which corresponds to D.F. wastewater and has higher concentration, around 700 mg/l. Then, were selected concentrations between 100 and 500 mg/l for to obtain the spectra of the different compounds. When the aqueous solutions were saturated the corresponding spectra were not made.

For to clarify we will present separately the spectra corresponding to the three regions ; UV, V and IR.

a) Ultraviolet Region

The UV spectra of NaCl, Na_2SO_4, $NaNO_3$ and $NaHCO_3$ are shown respectively in the figures 1-4 (made in the Biology Institute,UNAM). The distilled water spectrum was used as reference. In the figures 1-4 can be compared the absorbance of the four compounds studied. Sodium chloride presents a peak at 204 nm., sodium sulfate at 220 nm., sodium bicarbonate at 224 nm. and sodium nitrate presents an absorption band between 188-360 nm.. In the figures 1-3 are shown spectra corresponding to a concentration of 100 p.p.m.. For the last compound in the figure 4 is shown the spectrum at 500 p.p.m. because it is similar to the others for 100 and 250 p.p.m.

b) Visible region

The spectra in this region of the electromagnetic spectrum for the four substances showed the same behavior: nonabsorbance. These materials are transparent in the visible region. Then, is no necessary to show the figures corresponding.

c) Infrarod region

In the infrared region the water has a very strong absorptivity and "its extremely troublesome because of its opaqueness and tendency to attack cell windows" (see Szymanski, 1964). In our case, were used special cell windows of AgBr for to avoid the second effect.

The characteristic frequencies of groups $SO_4^=$, HCO_3^- and NO_3^- are known (see Szymanski,1964) but the problem in this work is to know their behavior in presence of water, i.e. in aqueous solution.

The spectra are shown in the figures 5-8 for the IR region. Also the distilled water spectrum appears as reference. The water absorption effect is dominant specially for the NaCl spectrum shown in the figure 5, but we can observe regions in which the solutions with the different substances have lower transmissibility than the water. These regions correspond to absorption peaks of these substances in an adequate solvent.

In the figure 6, for 100 and 250 p.p.m. of sodium sulfate, a strong absorption band is observed at 1100 cm^{-1} where there is a characteristic band for the group $SO4^-$. The $NaNO_3$ solution (figure 7) has an absorption peak cen-

tered at 1375 cm^{-1} corresponding to a characteristic band of the group NO_3^-. For the highest concentration, 500 p.p.m., also there is a weak peak at 1050 cm^{-1}. Similar behavior shows the sodium bicarbonate (figure 8) but the peak is around 1350 cm^{-1} and it has also other small at 1010 cm^{-1}. There are characteristic bands for HCO_3^- at 1400 cm^{-1} and 1000 cm^{-1}. The NaCl solution has in its spectrum a very weak peak at 1015 cm^{-1} for 250 p.p.m. which present also the distilled water spectrum.

As we expected, in spite of the water effect due to its strong absorptivity it is possible to find differences between the IR spectra of different compounds in aqueous solution.

2.2 Regions of interest.

To compare these spectra for several sodium compounds; chloride, sulfate, bicarbonate and nitrate, using as reference the distilled water spectrum had been found spectral zones of interest in which can be distinguished some materials.

The highest differences between the partial transmissibility of several compounds in aqueous solution and the distilled water spectrum in IR are:

a) 40 % for $NaHCO_3$ at ν= 1350 cm^{-1}
b) 36 % for Na_2SO_4 at ν= 1100 cm^{-1}
c) 35 % for $NaNO_3$ at ν= 1375 cm^{-1}

The wide of these peaks determines the following zones:

i) .2 - .36 μ (including the four compounds studied)*
ii) 6.5 - 8.5 μ ($NaHCO_3$)
iii) 6.7 - 8.3 μ ($NaNO_3$)
iv) 8.5 -10.5 μ (Na_2SO_4)
v) 9.5 -10.3 μ ($NaHCO_3$, $NaNO_3$ and NaCl)**

Due to three of them are superposed had been obtained three regions of interest. They are: .2 - .36 μ, 6.5 - 8.5 μ and 8.5 - 10.5 μ. One is in the ultraviolet and two are in the infrared.

Using the values of the transmissibility in the infrared region that are shown in the figures 5 - 8 were prepared graphs of the partial transmissibility vs. concentration for to compare different substances at certain wavelength. Such graphs are shown in the figures 9 - 12. With them can be selected the most useful wavenumber for pairs of substances easier than in the original figures. Besides of the wavenumbers mentioned before, i.e. 1000, 1100 and 1350, in these figures appear also other wavenumbers as 1500, 1800, 2100 and 2500. Some of them coincide with atmospheric windows.

From figures 9 - 12 we can see, e.g. that sodium chloride and sodium bicarbonate transmissibilities differ more at 1350. For nitrate and sulfate the most useful wavenumber is also 1350.

We would like to remark that as show the figures 5 - 8 in all IR spectra the initial transmissibility at 4000 cm^{-1} was chosen with the same value. In these curves we were not interested in a quantitative study of the relationship between transmissibility and concentration but in to detect differences between distilled water and the dissolved material spectra at several concentrations.

* See differences between its peaks in Table II.
** In the concentrations indicated in Table II.

2.3 La Esperanza Dam Samples and their interpretation

La Esperanza Dam is located in Tulancingo, Edo. de Hgo., Lon. W. 99° 22' Lat. N. 20° 09' 25". This dam is used as the agricultural water supply for the surrounding district (Distrito de Riego 28, Tulancingo, Hgo.). The main tributary is The Chico River.

The spectra of two water samples M I and M II which were taken in La Esperanza Dam are discussed in this section. Their possible compounds are shown in Table I. There is no sodium bicarbonate but the same functional group is in $Mg(HCO_3)_2$ and $Ca(HCO_3)_2$ and this last substance has concentrations around 100 p.p.m. in these samples.

a) Expected Spectra assuming additivity

If additivity is assumed between the transmissibility of the different constituents, then the total transmissibility, i.e. the water sample transmissibility, can be expressed as

$$T_s = \sum_i a_i \cdot T_i$$

where i denotes each constituent including also water as one of them and T_i means the partial transmissibility of the constituent i. The coefficients a_i depend of the concentration of the constituent i.

The additivity in the transmissibility implies that the compounds are not interacting between them. In a dilute solution this consideration is reasonable.

Then, using the spectra of constituents (see section 2.1 a) in a first approximation can be expected the following:

i) An absorption peak between .2 and .22 μ.

ii) Transparency in the visible region.

iii) No great differences with respect the distilled water spectrum in the infrared region except a weak peak around 9.9 μ.

b) Samples Spectra

i) Ultraviolet spectra

The UV spectra for the sample points M I and M II (made in the Chemical Sciences Faculty,UNAM) are shown in the figures 13 and 14. Both present an absorption peak around 210 nm.

ii) Visible spectra

The visible spectra (made in the Chemical Sciences Faculty,UNAM) report that both samples are transparent in this region.

iii) Infrared spectra

The IR spectra for M I and M II are shown in the figure 15. There are no great differences with respect to the distilled water spectrum. Only a weak peak at 1015 cm^{-1} appears.

Were detected also greasses and oils due to petroleum pollution in The Chico River. They are residues from an incident that happened some months before to the sampling day. The extractable (with $CHCl_3$) spectra are shown in the figures 16 and 17.

In general terms the samples spectra show the expected behavior.

3. PARTIAL TRANSMISSIBILITY AS A SELECTIVE INDICATOR OF WATER QUALITY BY REMOTE SENSING

The results of preceding sections suggest that the partial transmissibility could be useful for to detect by remote sensing specific pollution in water bodies. As shows the Table II the peaks of the nitrates, sulfates and carbonates (or bicarbonates) occurs at different wavelengths in IR. Then, in principle these constituents are perhaps distinguishable at certain wavelengths. Due to the bands are wide some of them are superposed in several regions. This fact raises difficulties that must be considered. In water bodies that have specific pollution, i.e. that one substance has higher concentration than the others, the superposition of the corresponding bands must be less important. For example, in La Esperanza Dam samples where carbonates concentration is higher than the other compounds, the peak at 9.9 μ is due to their presence because the NaCl concentration is too low for to get this effect. The same situation can be expected for water bodies highly contaminated as the D.F. wastewater in Requena (sample point III in Table I) where the concentration of carbonates and bicarbonates reachs 500 p.p.m.. Then, it is clear that the partial transmissibility is a natural selective indicator of suspended solids in aqueous solution in the nonvisible regions studied, specially in IR. Now the problem is to know if it can be used in remote sensing studies. This is a very complex problem because implies other effects which must be considered.

The atmospheric absorptivity, for example, has great importance for aircrafts and satellite detection. The regions of interest that had been found in this work can be compared in the Table II with the atmospheric windows. The atmosphere filters several wavelengths but not all. The free wavelengths for remote sensing , λ_F, are shown in the Table II. The partial transmissibility can be used for to detect nitrates in UV and sulfates in IR because there are atmospheric windows coinciding with peak values. Also there are two more regions in which the carbonates (or bicarbonates) are with nitrates and sulfates respectively (see Table II).

Now, it is necessary to get an adequate sensor to detect these substances by remote sensing. That is another big problem. We found only the band 13 of Skylab . Using it could be detected sulfates from 10.3 to 10.5 μ and bicarbonates and sulfates between 10.2 and 10.3 μ. if the water temperature is such that does not produce interference.

Other two effects that might be important are the radiation transfer in the interface air-water (presence of greases,oils,etc) and the bottom backscatter.

In summary, this work suggests that the partial transmissibility can be considered as a useful selective indicator for remote sensing of water bodies highly contaminated in the regions found with the adequate detectors when the others effects mentioned are small.

REFERENCES

1. Ruiz Azuara P. and Lemus Hidalgo L. Proceedings of the Eleventh International Symposium on Remote Sensing of Environment, 495-504, 1977.
2. Scherz J.P. and Van Domelen J.F. Proceedings of the Tenth International Symposium on Remote Sensing of Environment, 447-460, 1975.
3. Szymanski H.A. IR Theory and Practice of Infrared Spectroscopy. Plenum Press, 1964.

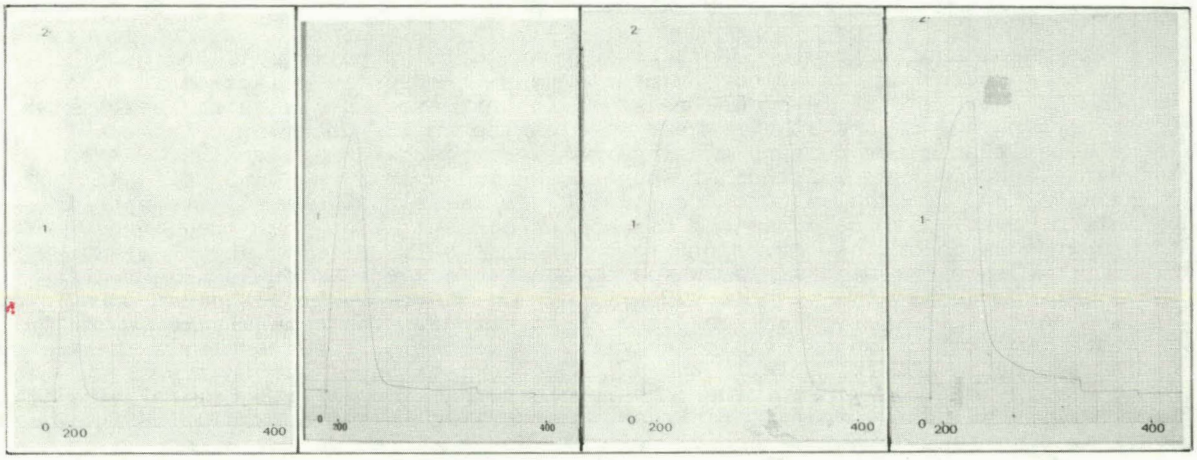

Figures 1-4. UV SPECTRA OF NaCL, Na_2SO_4, $NaNO_3$ and $NaHCO_3$.

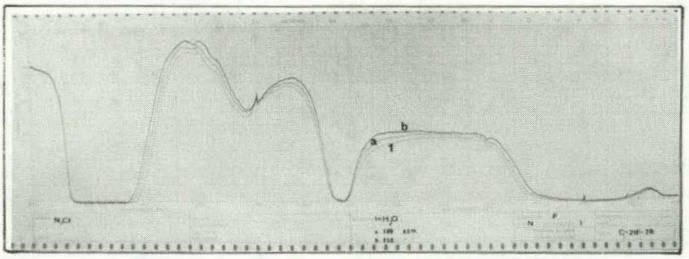

Figure 5. IR SPECTRA OF NaCl.
a. 100 p.p.m. b. 250 p.p.m.
(1. Distilled Water reference)

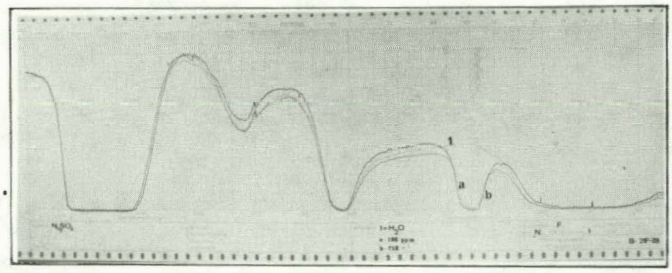

Figure 6. IR SPECTRA OF Na_2SO_4.
a. 100 p.p.m. b. 250 p.p.m.
(1. Distilled Water reference)

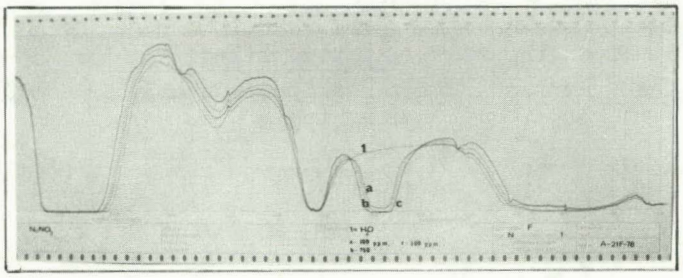

Figure 7. IR SPECTRA OF $NaNO_3$.
a. 100 p.p.m. b. 250 p.p.m.
c. 500 p.p.m. (1. Distilled
Water reference)

Figure 8. IR SPECTRA OF $NaHCO_3$.
a. 100 p.p.m. b. 250 p.p.m.
(1. Distilled Water reference)

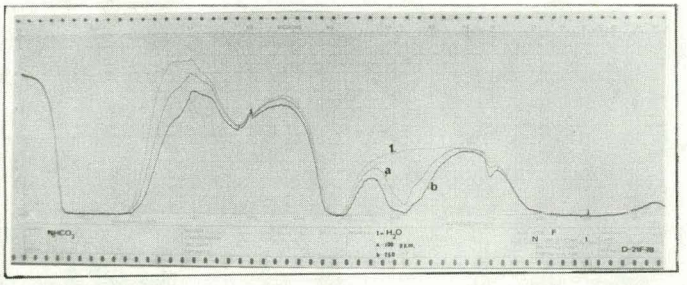

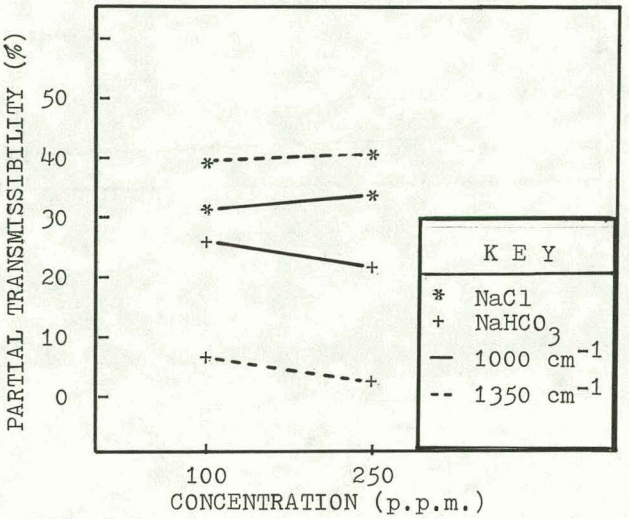

Figure 9. PARTIAL TRANSMISSIBILITY OF NaCl AND $NaHCO_3$ AT ν=1000, 1350 cm^{-1}.

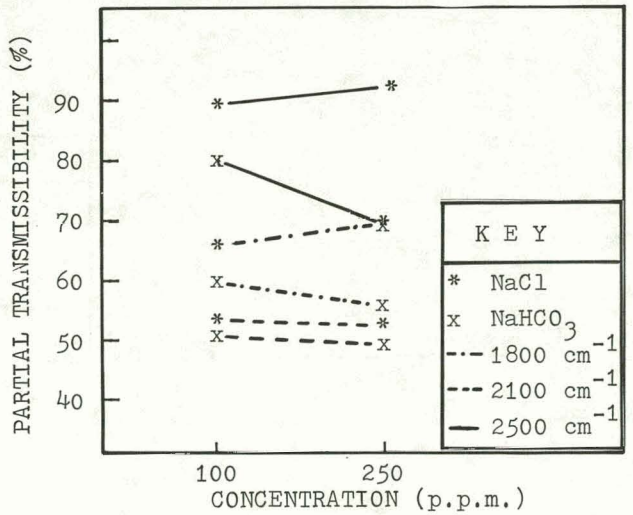

Figure 10. PARTIAL TRANSMISSIBILITY OF NaCl AND $NaHCO_3$ AT ν=1800,2100,2500 cm^{-1}.

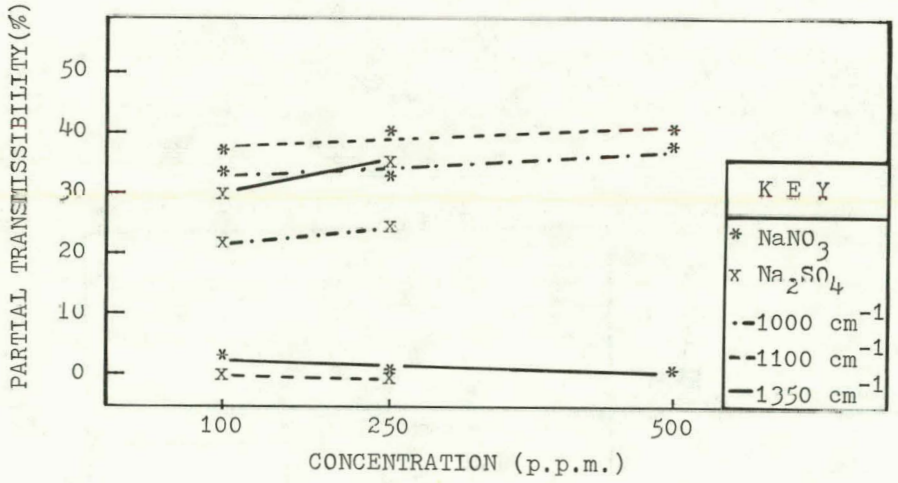

Figure 11. PARTIAL TRANSMISSIBILITY OF $NaNO_3$ AND Na_2SO_4 AT ν=1000,1100,1350 cm^{-1}.

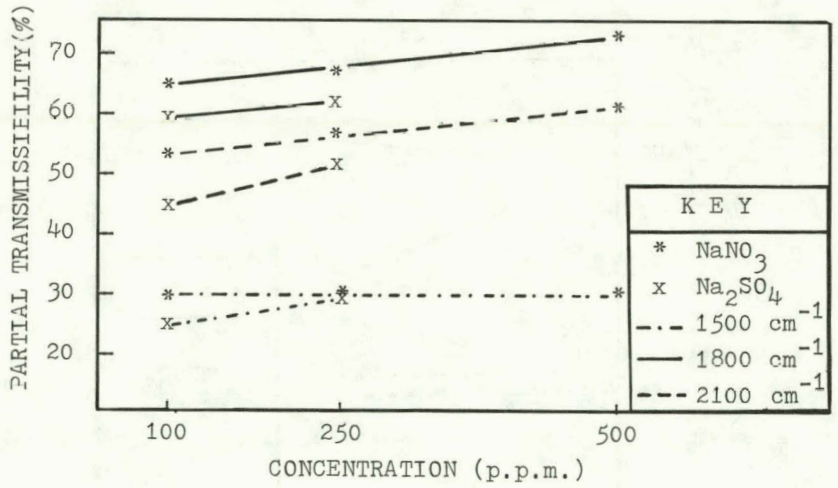

Figure 12. PARTIAL TRANSMISSIBILITY OF $NaNO_3$ AND Na_2SO_4 AT ν=1500,1800,2100 cm^{-1}.

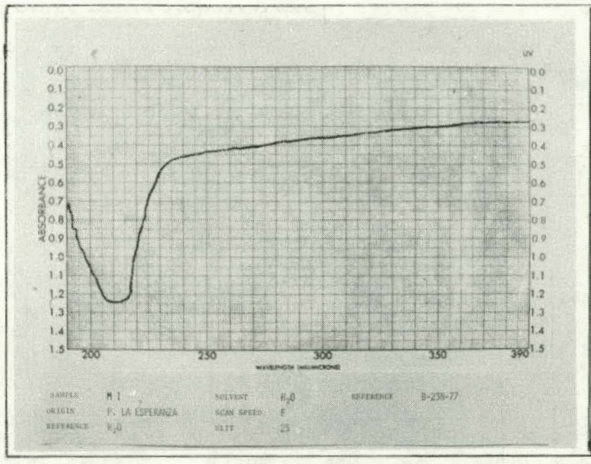

Figure 13. UV SPECTRUM OF SAMPLE M I

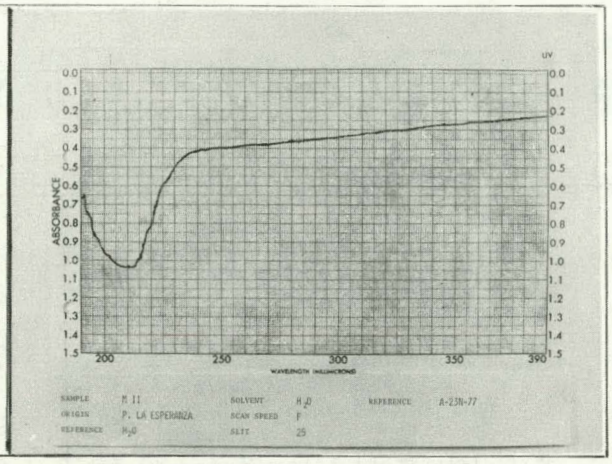

Figure 14. UV SPECTRUM OF SAMPLE M II

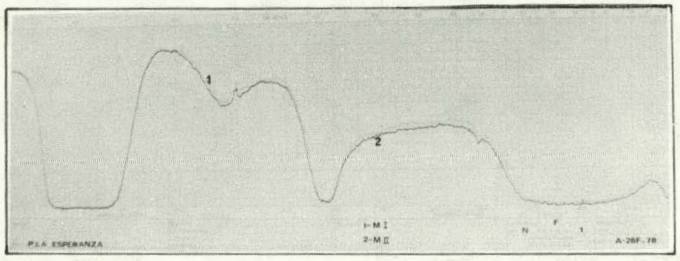

Figure 15. IR SPECTRA OF SAMPLES M I AND M II

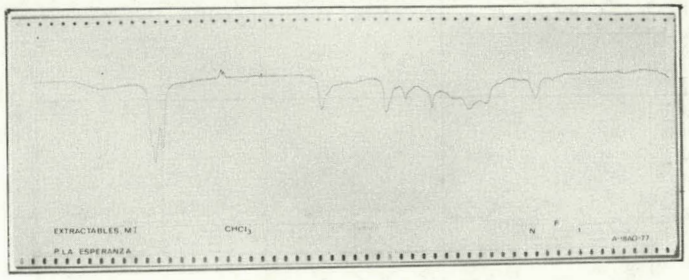

Figure 16. IR SPECTRUM OF EXTRACTABLES AT M I

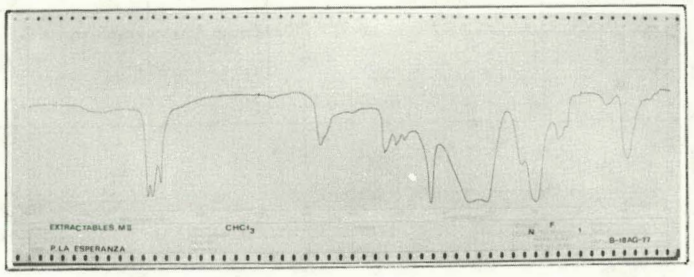

Figure 17. IR SPECTRUM OF EXTRACTABLES AT M II

TABLE I. COMPOSITION OF WATER SAMPLES(mg/l)

CHEMICAL COMPOUND	D A M R E Q U E N A				DAM LA ESPERANZA	
	I	II	III	IV	M I	M II
NaCl	14.35	15.85	72.38	63.23	34.82	23.07
Na_2SO_4	25.53	21.89	23.10	-----	10.65	38.96
$NaHCO_3$	17.38	34.13	250.93	-----	-----	-----
$NaNO_3$	1.21	1.21	1.21	1.21	25.35	19.61
KCl	12.40	10.49	38.16	11.45	11.45	15.26
$Mg(HCO_3)_2$	55.22	83.56	167.11	32.24	22.88	33.83
$Ca(HCO_3)_2$	154.22	123.24	123.24	3.08	107.65	86.10
TOTAL SOLIDS	242	270	688	284	303	280

TABLE II. SELECTIVE ABSORPTION

SUBSTANCE	ABSORPTION BAND(μ)	PEAK(μ)	ATM. WINDOW(μ)	λ_F(μ)	C_{MIN}	ZONE
NaCl	.184 - .220	.204	---	--	100	ULTRAVIOLET
$NaHCO_3$	.188 - .250	.224	---	--	100	
Na_2SO_4	.192 - .236	.220	---	--	100	
$NaNO_3$	.188 - .360	*	.3 - .75	.3 - .36	100	
NaCl	9.7 - 10.0	9.85	---	--	250	INFRARED
Na_2SO_4	8.5 - 10.5	9.1	8.0 - 9.2 10.2 - 12.4	8.5 - 9.2 10.2 - 10.5	100 100	
$NaNO_3$	6.7 - 8.3 9.4 - 10.0	7.3 9.5	8.0 - 9.2 ---	8.0 - 8.3 --	100 500	
$NaHCO_3$	6.5 - 8.5 9.5 - 10.3	7.4 9.9	8.0 - 9.2 10.2 - 12.4	8.0 - 8.5 10.2 - 10.3	100 100	

* Full band

λ_F Free wavelengths for Remote Sensing

C_{MIN} Minimum concentration studied that presents peak (in p.p.m.)

JAPAN'S RECEIVING AND PROCESSING FACILITIES FOR LANDSAT DATA

Y. HARUYAMA
Y. YAMAMOTO

NATIONAL SPACE DEVELOPMENT AGENCY
OF JAPAN (NASDA)
TOKYO, JAPAN

ABSTRACT

Japan's receiving and processing facilities for Landsat data are now under construction, aiming to be completed by the end of 1978.
The facilities are located in the middle part of Saitama Prefecture (36°00'N, 139°21'E), about 50 Km northwest of Tokyo, and consist of four systems; receiving system, recording system, data processing system and photographic processing system.
The facilities will be able to correct radiometric and geometric distortions existing in incoming Landsat image and then will be able to produce computer compatible tapes, films and papers.
These output products will be available by adjacent countries with reasonable prices for international cooperation.
The system construction, the processing method and output products of the facilities will be reported.

1. Receiving system

The receiving system (shown in Fig. 2) is for receiving and demodulating the radio signals of the MSS, RBV and USB telemetry data transmitted from Landsat.
The antenna is a X-Y mount structure not to loss signals near zenith and a unti-backlash structure that is useful to X-band frequency of Landsat D.
The program tracking unit can operate automatically each equipment in the receiving and recording systems in addition to calculating the pointing angle for the antenna at intervals of 50 msec from NASA orbital constants.
Feed is the single-born monopulse type achieving the antenna pattern $G(\theta) = 32 - 25 \log_{10} \theta$ dBi $(3° < \theta \leqq 48°)$ to avoid radio interference from terrestrial radio communication systems.
The total system noise temperature is 120°K or less at spacecraft elavation angle of 5 degrees under fair weather condition.
The specifications of this system are as follows:

(a) Antenna

Structure	10 m in diameter, Cassegrain-type, X-Y mount (Y over X, X-axis east and west)
Surface tolerance	0.5 mm rms
Range of performance angle	X-axis $\pm$ 90°, Y-axis $\pm$ 86°
Frequency range	2,200 ~ 2,300 MHZ
Gain	44.4 dBi or more at 2,250 MHZ including feeder loss
Feed	single-horn monopulse
Pattern	$G(\theta) = 32 - 25 \log_{10} \theta$ dBi $(3° < \theta \leqq 48°)$ -10 dBi $(\theta > 48°)$ where θ : angle from the main beam direction
Sidelobe level	14 dB minimum below sum channel peak
Difference channel	null depth

	35 dB minimum below sum channel peak
Polarization	RHC and LHC (axial ratio: 1.5 dB maximum)
V.S.W.R.	1.2 dB maximum for sum channel (at input point of low noise amplifier)
Angular deflection	0.035° rms maximum in 15 m/sec wind.

(b) Tracking control unit

Velocity	X-axis 2 deg/sec, Y-axis 1 deg/sec
Acceleration	X-axis 2 deg/sec^2, Y-axis 1 deg/sec^2

(c) Low noise amplifier

Noise temperature	Sum channel 55°K or less, Difference channel 360°K or less
Gain	Sum channel 45 dB ± 3 dB Difference channel 30 dB ± 3 dB

(d) Program tracking unit

	CPU Equivalent MELCON - 70/20, Memory 16 KW Disk 123 KW

(e) MSS/RBV receiver

	IF frequency 70 MHZ (nominal) IF bandwidth 30 MHZ ± 1 MHZ

(f) USB telemetry tracking receiver

	IF frequency 70 MHZ (nominal) Tracking range ± 150 KHZ Phase lock loop bandwidth 1000 HZ ± 20 %
Locking threshold	-130 dBm or less (at input point of low noise amplifier)

2. Recording system

The recording system (shown in Fig.3) is for recording the video signals from the receiving system on high density digital tape (HDT) or quick-look film. This system performs

(1) sync pulse extraction, video restoration and analog to digital conversion for RBV signal
(2) bit synchronization for MSS signal
(3) PSK demodulation and bit synchronization for USB telemetry signal

and then makes two kinds of HDTs recording RBV sensor data or MSS sensor data, USB telemetry data, IRIG-A station time code and voice annotation.
This system can also generate simulated MSS, RBV and USB telemetry test signals.
The quick-look unit performs simplified processing of MSS or RBV data to display them onto the CRT, whereby the receiving status can be monitored and photographed on 70 mm black-and white film by use of a camera.
The specifications of this system are as follows:

(a) MSS bit synchronizer (equivalent AYDIN MONITOR 319)

Input code	NRZ-L
Bit rate	15.062 Mbps (nominal)
Bit error rate	1×10^{-5} maximum with SNR = 10.6 dB (random data without jitter)
Sync acquisition time	Within 100 bit periods for SNR $\geqq$ 10 dB

(b) USB telemetry PSK demodulator (equivalent AYDIN MONITOR 329)

Input signal code	2 phase PSK
SNR	Lock retained to 0 dB

(c) USB telemetry bit synchronizer (equivalent AYDIN MONITOR 336)

Bit rate	1 bps to 5 Mbps for all PCM codes
Sync acquisition time	Within 100 bit periods for singals with 50 % transition density and SNR $\geqq$ 15 dB
Output code	Bi ϕ - L

(d) SPEVOR (Sync pulse extraction and video restoration)

Input data	Video bandwidth 3.2 MHZ (analog), Filter (-20 dB at 3.2 MHZ) is inserted.
Output signal	Horizontal sync pulse, Vertical sync pulse, Clock (3.2 MHZ), Frame identifying signal, Video signal (analog)

(e) RBV digitizer (equivalent COMPUTER LAB 3808)

Input video bandwidth	0 - 3.2 MHZ
Sampling rate	6.4 M samples/sec
Number of bits per sample	
Output data	39.96 Mbps serial NRZ-L

(f) MSS high density digital tape recorder (equivalent MARTIN-HONEYWELL 96)

Tape speed	90, 45, 22-1/2, 11-1/4, 5-5/8 ips
Track assignment	Servo reference ... track 1 IRIG-A time code ... track 2 MSS data ... track 3 thru 12 (direct recording, serial-in serial-out) USB telemetry data ... track 14 (FM recording) Voice annotation ... edge A Not used ... track 13, edge B
Tape width	1 inch
Bit error rate	1×10^{-6} or less

(g) RBV high density digital tape recorder (equivalent MARTIN-HONEYWELL 96)

Tape speed	120, 45, 22-1/2, 11-1/4, 5-5/8 ips
Track assignment	Servo reference ... track 1 IRIG-A time code ... track 2 RBV data ... track 3, 5, 7 thru 21, 23, 25, 27 (direct recording, serial-in serial-out) USB telemetry data ... track 26 (FM recording) Voice annotation ... track 28 Not used ... track 4, 6, 22, 24
Bit error rate	1×10^{-6} or less

(h) Quick-look unit

Input data	MSS data (15.06 Mbps serial NRZ-L) in real time or playback mode, RBV data (14.99 Mbps serial NRZ-L) in playback mode
Items of correction	Distortion due to earth rotation, Distortion due to aspect ratio
Annotations on film	Orbit number, Frame number, Satellite number, Exposure time, Gray scale (10 steps)
Film	70 mm, black-and-white
Resolution of CRT	MSS 1024 lines x 1024 pixels, RBV 1024 lines x 922 pixels

3. Data processing system

The Data processing system (shown in Fig. 4) consists of two subsystems of image data processing and product generation.
The image data processing subsystem is for making radiometric and geometric correction of raw image data and for making original computer compatible tape (CCT)
This subsystem has three processing methods of bulk correction, precision correction and ocean mode.
The bulk correction is made accounting for the attitude data (pitch, yaw and roll) and the ephemeris data (X, Y, Z, $\dot{X}$, $\dot{Y}$, $\dot{Z}$) of spacecraft as function of time.
The precision correction updates Kalman filter using ground control point (GCP) data in addition to both the attitude and the ephemeris data.
The ocean mode is made using GCP from adjacent scenes when the scene has no GCP.
The application sofrware in this subsystem performs

(1) computation of ephemeris data from NASA orbital constants
(2) reading both MSS and USB telemetry data from HDT
(3) processing USB telemetry data and generation of attitude data
(4) determination of framing parameters
(5) generation of radiometric correction tables
(6) computation of geometric correction coefficients
(7) computation of tick mark locations and precise framing parameters
(8) resampling on map coordinate
(9) generation CCT

The product generation subsystem is for copying CCT and for making original film (both black-and-white (B/W) and color) by laser beam image recorder.
The following are major functions and specifications of this system:

(a) Processing accuracy

Radiometric error	± 1 quantum level maximum
Geometric error	1 Km rms maximum, bulk corrected (no GCPs)
	160 m rms maximum, precision corrected (6 GCPs)
	80 m rms maximum, precision corrected (16 GCPs)
Registration (scene to scene)	
	40 m rms maximum, precision corrected (16 GCPs)

(b) Throughout rate — 185 MSS scenes in 103 hours minimum, precision corrected (10 GCPs)
200 MSS scenes in 103 hours minimun, bulk corrected (no GCPs)

(c) Resampling method — Nearest neighbor, Bilinerar, Cubic convolution

(d) Map projection — Universal transverse mercator (UTM), Hotine oblique mercator (HOM)

(e) GCP correlation method — Manual, Automatic using SSDA

(f) Resampling interval — variable

(g) Radiometric correction method — Use of calibration wedge data transmitted from spacecraft

(h) Geometric correction items — Change in altitude of spacecraft, change in altitude of spacecraft (roll, pitch and yaw), change in velocity of specacraft, distortion due to earth rotation, band to band offset, distortion due to finite scan time, mirror scan nonlinearity, line length, data aspect ratio, earth curvature, finite sensor detector/ detector sampling interval

(i) Scene framing — Worldwide reference system (WRS)

(j) CCT format

Recording format	Band sequential (BSQ), Band interleaved by line (BIL), Band interleaved by two pixels (BIP_2)
Recording density	800 BPI, 1600 BPI
Recording code	NRZ-1 for 800 BPI, PE for 1600 BPI
Number of tracks	9 tracks (8 data bits + 1 parity bit)
Parity check	Odd

(k) Film format

Film	70 mm, B/W, color
Image size	55.1 mm x 50.7 mm (nominal)
Information on film	Registration marks (4 corners), Tick marks (latitude and longitude at intervals of 30 arc minutes), Gray scale (16 steps)
Alphanumeric annotation	Day, month and year of exposure, Latitude and longitude of image center, Path and row number, Latitude and longitude of madir, Sensor and spectral band, Sun angle, Type of correction, Agency and spacecraft code, Frame identification number

4. Photographic processing system

The photographic processing system is for developing original 70 mm films (latent image) and also for enlarging and copying films and papers in addition to color composition.
This system consists of the B/W film processor, the B/W paper processor, the color film processor, the color paper processor, the B/W contact printer, the color contact printer, the B/W enlarger, the color enlarger, the color composite printer and the inspecting device (the color viewer, the dinsitometer etc.).
Both film and paper are available in B/W and color.

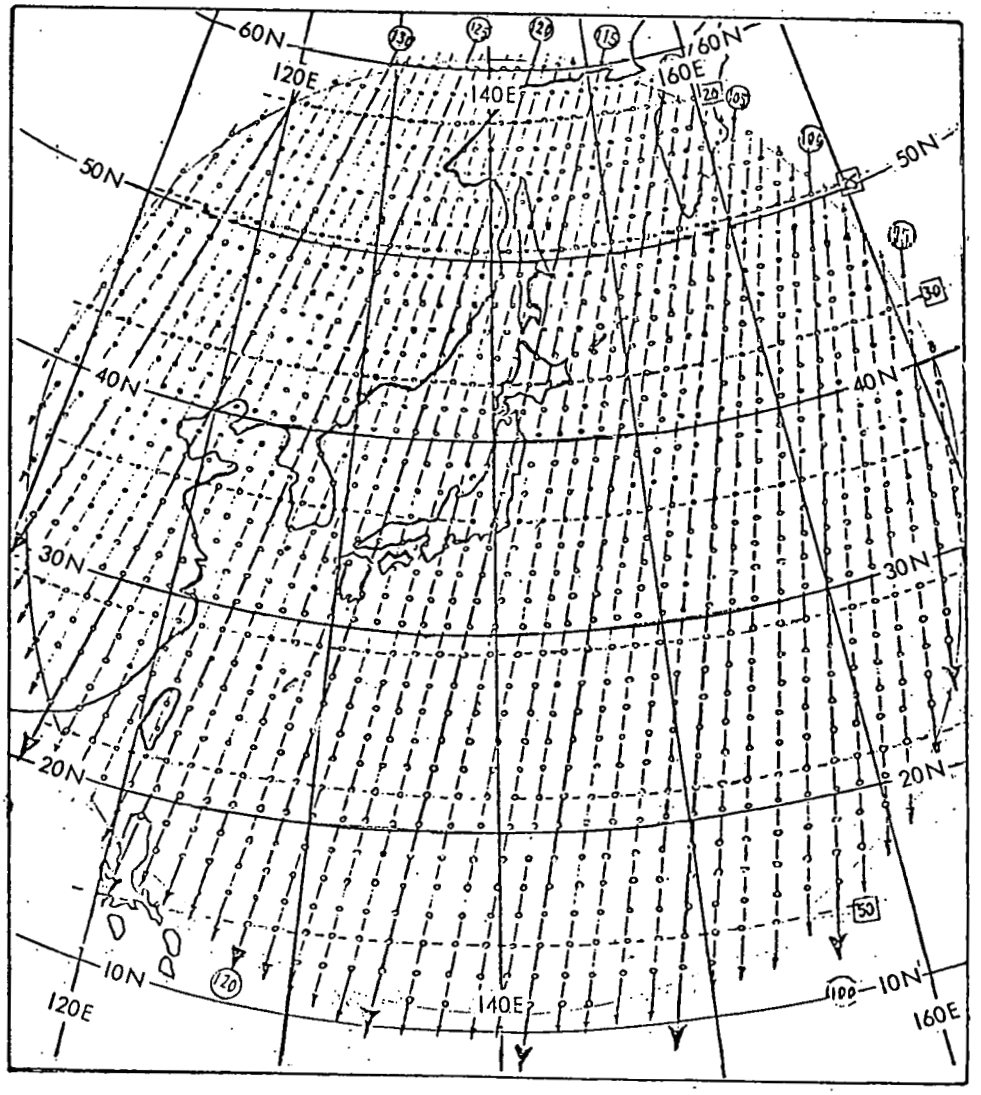

Fig. 1 The Landsat pass over and around Japan together with the area covered by the antenna at 35°N and 140°E. The numbers in ○ and □ are those of worldwide reference system.

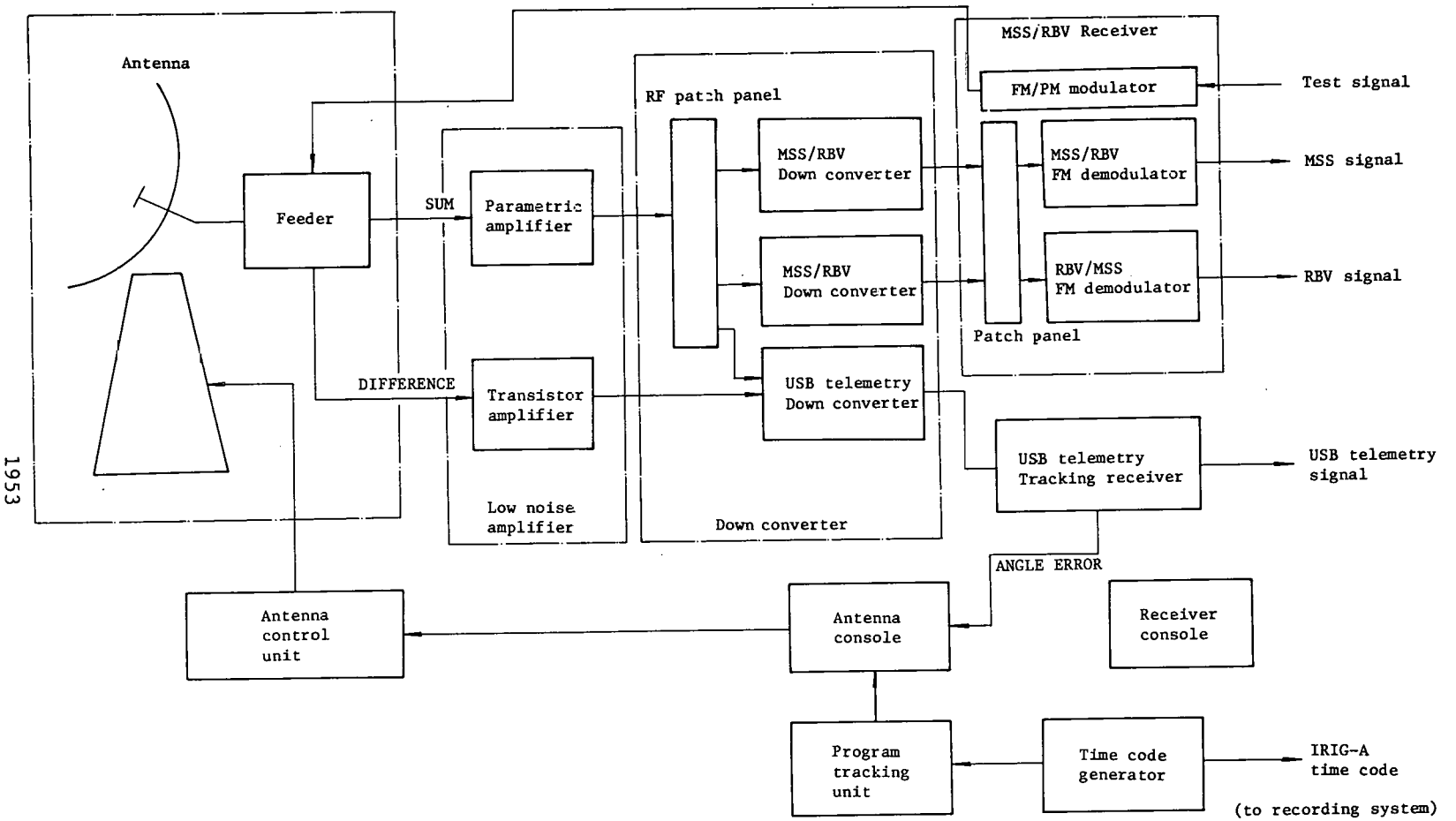

Fig. 2 RECEIVING SYSTEM block diagram

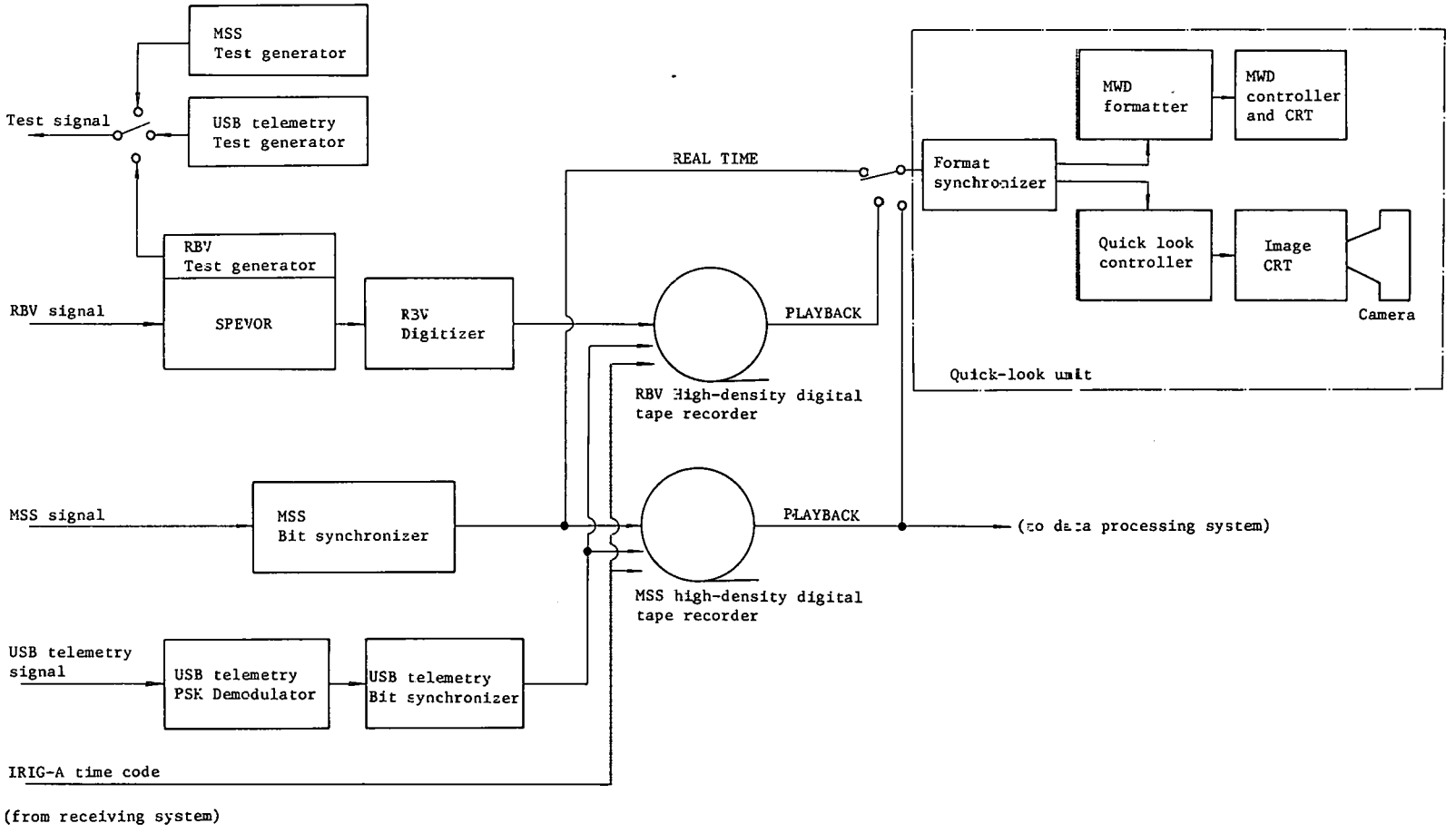

Fig. 3 RECORDING SYSTEM block diagram

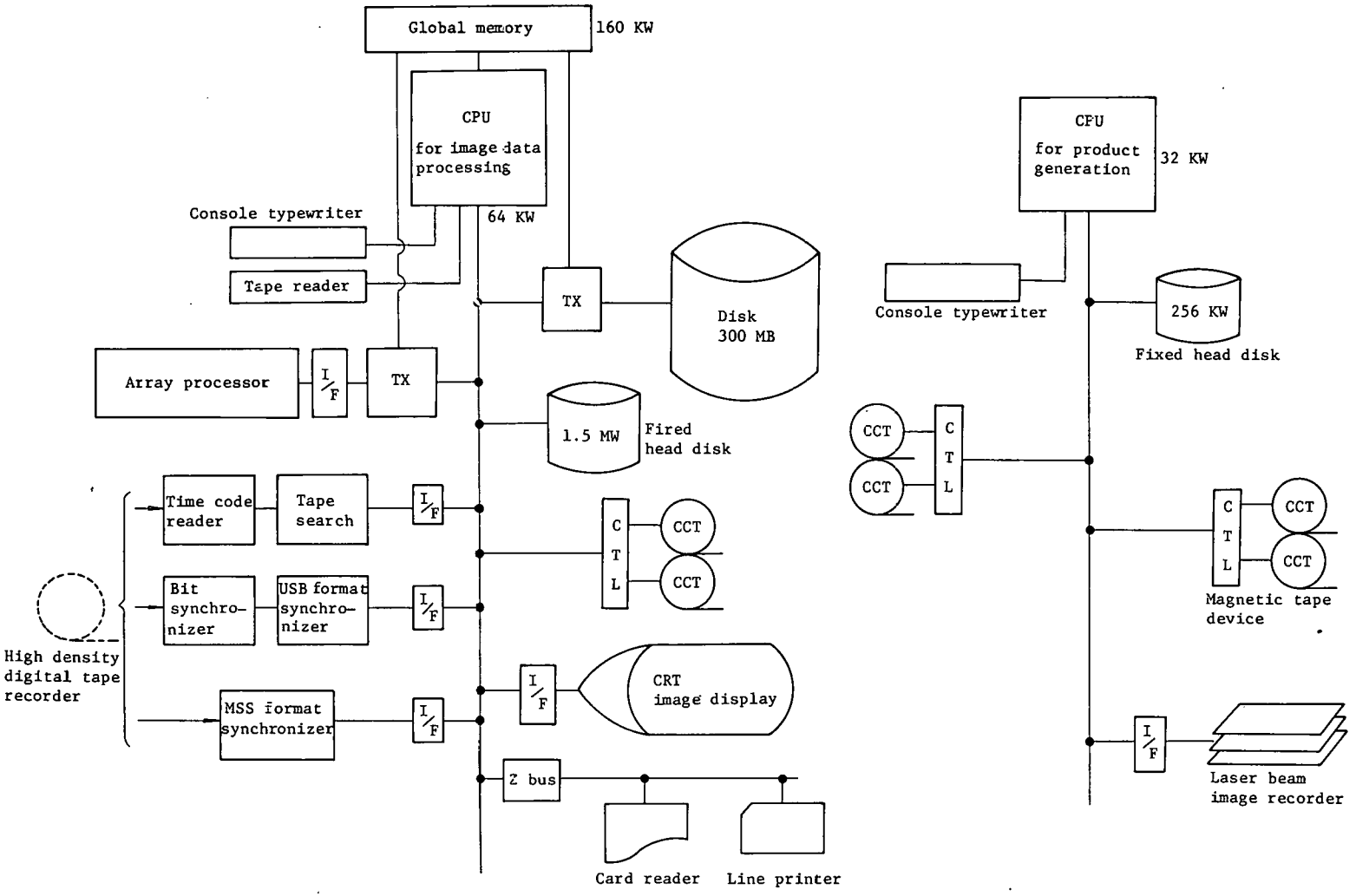

Fig. 4 DATA PROCESSING SYSTEM block diagram

THIS PAGE

WAS INTENTIONALLY

LEFT BLANK

APPLICATION OF TEXTURE ANALYSIS AND IMAGE ENHANCEMENT TECHNIQUES FOR REMOTE SENSING

Joji IISAKA * Eiichi NAKATA ** Yoshinori ISHII ***

Makoto IMANAKA ** Yoshinori MIYAZAKI ***

* Tokyo Scientific Center
IBM Japan, Ltd.
1-11-32 Nagata-cho, Chiyoda-ku
Tokyo, Japan

** Waseda University
School of Science and Engineering
2-26-8 Nishi-waswda
Schinjuku-ku, Tokyo, Japan

*** Tokyo University
Department of Mineral Development Engineering
7-3-1 Hongo, Bunkyo-ku
Tokyo, Japan

ABSTRACT

This paper deals with two processing types, image enhancement and pattern recognition --- especially based upon textural feature. Texture analysis was applied to aircraft MSS data of OTOINEPPU, northern part of HOKKAIDO to classify local forest zone by textural feature. Compared with spectral analysis, this method proved itself to be more useful and worthy of efficiency.

In applying image enhancement techniques, the Middle Area of Japan was selected as the test site where one of the famous Japan's macrostructures, Fossa Magna, exists. We tried to obtain large linear feature and also piecewise linear approximations to lineaments or segments of linearments using above-mentioned filters and differencial filters.

1. INTRODUCTION

There are various feature types with LANDSAT or aircraft imagery data according to one's aim and/or various conditions. We can specify spectral feature, textural feature, structural feature and so on, as an example of them in remote sensing. These features are enhanced through some processing techniques such as stretching techniques, and are used for pattern recognition etc.

But the selection of useful processing is dependent upon what purpose we are going to apply. Some features, for example, linear features and textural features are not quantitatively well defined in practice. There are, of course some theoretical idea for its application in past, but it is open to question in its actual use. This is because there are some problems with respect to its processing time, core size, etc. On the basis of considerations of these background, we used spatial lattice filter which has many advantages as one of methods to enhance textural feature. Next we applied it to enhance global geological feature and could get good results as to precise lineaments which was detected by local operator of differential filters.

o FOREST TEXTURE

We tried at first to classify forest in detail according to species such as needle leaf, broad leaf, etc with multi spectral scanner data acquired by aircraft. Classification of forest may be difficult only by spectral feature so far as we use only one season MSS data, for forest will indicate similar pattern of plant reflection no matter what species of plant may appear. So we feel keenly the necessities of considering textural features which are connected with an arrangement or sparsity of trees, apart from the previous classification based upon mainly spectral features. There are so many methods for texture analysis and some of them will be discussed in section 2 later. Most of these methods are not necessarily practical with regard to CPU time and so on. So we conceived some spatial lattice filter to verify its effectiveness by applying it to forest classification in fact in comparison with ground truth of field works, while we tried two other methods, previous spectral classification and noted Haralick method, comparing them with our own . It was found consequently that the spatial filter is very effective in both the points of processing time and correctness of classification.

o GEOLOGICAL LINEAMENT

In the second place, this spatial filter was applied to LANDSAT data to enhance global geological feature. On this preliminary stage, three LANDSAT images, OSAKA, ISE, and TAKAYAMA, were processed digitally to make a mosaic scene. From this stretched mosaic scene, we can see distinct Median Line and Fossa Magna which are main Japan's macrostructures, and small piecewise lineaments from a macroscopic and tectonic standpoint.

Spatial lattice filter was applied to this mosaic scene to extract global texture. We can say that the map obtained through this filter processing show us the geological areas of approximately same textural pattern on global surface. In other words, it may be possible to use this map for searching candidate areas of our concerned geological lineaments.

We selected YAKEDAKE on this map as a detail survey area which is one of potential geothermal areas of Japan to enhance small piecewise linear features. We applied differential filters at first which is one of traditional methods to enhance edges or lines. Gradiant and Laplacian were applied as this differential filters, and final imageries of this filter processing was obtained by multi-channel imageries could indicate very fine and detailed linear features compared with single-channel imageries.

2. TEXTURE ANALYSIS

2-1) FOREST CLASSIFICATION

For the protection of the forest resources, or for the management of them, it is important for us to get the timely and accurate information of the global geographical distribution of plants in forest.

The investigation of the forest only by field work is useful to get local information, but it is difficult to grasp in general. However, present-day, we could get the timely global imformation of forest through the use of remote-sensing technique.

By the two demensional investigation through remote-sensing addition to one dimensional investigation through mankind work, it is possible to get the more useful imformation of the forest.

We tried to draw up the forest classification map using the remote-sensing techniques, one of which is classification by spectral feature, and another by texural feature.

Forest classification using low altitude aircraft M33 data encounters the following problems.

1) illumination fluctuation dependent on slope.

2) shade change of tree height and/or species.
3) sparsity of tree

In the case of forest classification, these problems connected with low altitude data and tree property will disturb our classification work especially only with spectral feature. But it may be possible to cope with such peculiarities with use of differences of textural feature.

Then we applied this texture method to the forest area located at OTOINEPPU , northern part of HOKKAIDO, and tried to classify this forest into several categories such as needle-leaf, broad-leaf and mixture ,etc and each group into two categories, thin wood and thick forest.

We used three different ways for classification with the aim of evaluating effectiveness of each method.

* spectral feature extraction

* textural feature extraction
  space filter processing
  Haralick method
    (spatial grey tone co-occurrence probabilities)

We must here-upon take it into consideration that textural feature extraction is very susceptible to relative scale of original image data and filter size. Then we prepared original imagery with two different scale, 1/1 and 1/2.
Fig.2 shows flow chart describing how our work was done with three above mentioned methods.

Fig.3 shows the ground truth map of the area of this study. We compared the classified results using this map.

2-2) TEXTURAL FEATURE EXTRACTION

Spatial enviroments can be understood as being spatial distributions of various area-extensive objects having characteristic size and reflectance or emissive qualities. The spatial organization and relationships of the areaextensive objects appear as spatial distributions of grey tone imagery taken of the environment.

We call the pattern of spatial distributions of grey tone, texture.

There have been seven basic approaches to the measurement and quantification of image texture:

autocorrelation functions	(Kaizer, 1955)
optical transforms	(Lendaris and Stanley, 1970)
digital transforms	(Gramenopoulos, 1973: Hornung and Smith, 1973 Kirvida and Johnson, 1973)
power spectrum	(R. Bajcsy, 1972)
edgeness	(Rosenfeld and Thurston, 1971)
structural elements	(Matheron, 1967 , Serra, 1973)
spatial grey tone co-occurrence probabilities	(Haralick et al., 1973)

The first four of these approaches are related in that they all measure spatial frequency directly or indirectly. Spatial frequency is related to texture because fine textures are rich in high spatial frequencies while coarse textures are rich in low spatial frequencies. An alternative to viewing texture as spatial frequency distribution is to view texture as amount of edge per unit area.

We applied a technique of space filtering proposed by J. Iisaka for textural classification of forest to reduce the processing time. The basic idea of a space filter is as follows:

Let s(i,j) be the value of a picture element (i,j). Applying filter function F, response S'(i,j) becomes :

$$S'(i,j)=F \oplus S(i,j)$$

Here , we introduce reticle type masks as Fig.4 Let F be a k x k matrix and matrix elements Fem = 1 or 0 according to the mask type as shown in Fig.4 . Using various type of masks, we obtain various response values for picture elements (i,j). A number of response values can be generated as additional channel data besides spectral channels. The above filtering techniques are a kind of space filtering.

Let the input message spectrum be G(fx,fy) and R(fx,fy) be a transfer function at the field stop. The output message spectrum U(fx,fy) = K* R(fx,fy) * G(fx,fy) . The massage signal from an object is maximized when an optimal filter and a power spectrum density of background scene are known.

An attempt was made to clarify the effect of a space filter by simulating the system, using several types of mask patterns as shown in Fig.5 . Clustering algorithm was applied to classify the textural zone of test patterns. As the reticle itself has an effect of a spatial low pass filter, spatial resolution is degraded.

Another texture method which we applied is Haralick's method. He measures the spatial dependence of grey tones in co-occurrence matrix for each fixed distance and/or angular spatial relationship and uses statistics of matrix as measures of image texture.

The co-occurrence matrix $P=(p_{ij})$ has its $(i,j)^{th}$ entry P_{ij} defined as the number of times in which grey tone i and grey tone j occur in resolution cells of a subimage having a specified spation, such as distance 1 neighbors.

We used the following five functions which calculate statistics mentioned.

FUNC1	computes the sum probability feature of the image.
FUNC2	computes the gradient entropy feature of the image.
FUNC3	computes the entropy feature of the image.
FUNC4	computes the gradient feature of the image.
FUNC5	prepares normalized lex arrays which have been equal probability quantized according to their diagonal elements. (lex array containing count over all grey levels neighbor ; 0-degree , 45-degree , 90-degree , 135-degree)

2-3) RESULTS

We used smooth-processing to exclude the noisy data from output data. Photo.2 - Photo.4 show this results of forest classification in the case of 1/2 scale data.

These pictures show the following things.

1) In general , we could get fine classification and good correspondence to ground truth at 1/2 scale rather than original scale.
2) Shifting area appeared on the boundary of each forest distribution in case of filter processing (Haralick , space filter)
3) Spectral feature extraction made much erroneous classification than space filter method as to illumination fluctuation caused by geological slope.

TABLE 1 shows the performance of each method.
This performance table indicates the percentage of erroneous categories which were misclassified mostly by each classified category. And the average performance of this training area classified proved to be about 60 % .
This table indicates that spectral feature extraction made incorrect classification at about 30 % , and at about 20 % in case of Haralick method.
Space filter method made least mistaken categorization.

We can find the following two tendencies with this table.
In the first place, classification of thick and sparse tree was well done in general. Secondly, it seems to be difficult to classify forestry into each forest zone such as needle-leaf, broad-leaved and mixed tree. This is because each forest zone can't be fixed the boundary on account of natural botanic character. This fact suggests us the formidable problem that we should select the most fitted threshold on classification to correspond to distribution map of each forest zone acquired through ground-field, what is called ground truth.

In summary, application of textural analysis method to forest area yield these results.

1) Space filter is useful for extracting local feature of ground covering objects as well as spectral characteristics.
2) there is an optimal window size of a filter and a filter type for each class to be classified.
3) It is possible to classify the forest into two groups, thick and sparse tree by textural featurs.
4) In the case of classification into three groups, needle-leaf, broad leaved and mixed tree, the boundaries among them change continuously.
If the ratio of constitution of composite tree is defined clearly, it will be possible to classify forestry more correctly by space filter method.

N : needle-leaf tree
M : mixture
L : broad-leaf tree
B : bamboo

(Y : thin wood)

Fig.3 The ground truth map of the area of this study.

3. IMAGE ENHANCEMENT FOR LINEAR FEATURE

3-1) LINEAR FEATURE

A class of important features in satellite imagery are the linear features. There are many kinds of linear features; for example, roads, rivers, bridges, vegetation alignments, as well as geologically significant features such as faults and joints. Lineaments are linear features which are inferred to be surface manifestations of fractures, faults or joints in the earth's crust.

Finding lineaments is of interest not only because of their geological significance, but also because of their usefulness to areas such as environmental geology, mineral exploration, and in the identification of hazards.

Fig. 6 shows the structural outline of the Japanese Islands (Median Line, Fossa Magna) and the direction of natural remanent magnetization (NRM) of Cretaceous rocks. It is interesting to note that magnetizations for the Cretaceous formations are characterized by the fact that the direction of magnetization for the north-eastern Japan is markedly different from that for the south-western Japan. The fact seems to support an idea that the Honshu Island (the Mainland of Japan) was subjected to a bending some time in the early Tertiary. The shape of Japanese island is indeed bending in the middle part of Honshu Island, and it is further interesting that one of the famouse Japan's macrostructures, Fossa Magna, is located near the bending area.

Recent advances indicate that satellite-acquired imagery can be effectively used for many geological tasks. The wide area coverage in a single image of LANDSAT data, for instance, is particularly advantageous for the detection and mapping of lineaments. This improvement in detecting linear features is important in finding new areas to explore for fracture controle mineral deposits in assisting in relating earthquakes to their causes through understanding basic tectonic relationships and in noting potential hazards in minining and construction.

LANDSAT mosaics are ideal for getting a perspective on the tectonic framework of large regions of the crust. On the basis upon above-mentioned palaeomagnetic study, we made a mosaic with three LANDSAT imageries (Fig. 7) Thus, through-going lineaments that continue for hundreds of miles can be integrated into a unified network which reflects the influence of fractures in an ancient basement or results from stress systems developed from more recent plate tectonic movements. Seen in a broad context, where diversities of topography and surface geology tend to be filtered out, a new synthesis of structural data emerge.

Median Line and Fossa Magna can be seen to intersect at the right upside of Fig. 7. If we allow 20 m.y. for the 60 km of relative displacement along the Fossa Magna fault zone, then the minimum average rate of movement would be about 3 km per m.y. .

3-2) APPLICATION OF TEXTURE ANALYSIS TO GEOLOGICAL FEATURES

Texture analysis was applied to the former mosaic scene (Fig. 7) using spatial lattice filter. Firstly, nine categories were selected as training areas in mosaic scene and one of categories which seemed to be most meaningful for geology was shown in Fig. 8 after post-processing. Fig. 9 shows the map of the active faults of Middle Japan. The map of Fig. 8 indicates the geological areas which were classified as approximately same textural pattern. Thus, Fig. 8 is considerably different from Fig. 9 on the points that the former implies two dimensional information and the latter implies linear information as usual.

In LANDSAT image mosaic of Fig. 7, black areas of Fig. 8 correspond to North, Middle and South Alps of Japan which are orogenic ranges over 3000m altitude and show very complicated texture. But it is interesting fact that mountainous district called HAKUSAN which is located west of North Alps of Japan is classified as different category in Fig. 8, while Fig. 7 shows there

are many linear features at HAKUSAN similar to that of Alps of Japan.

Such geological textural maps as Fig. 8 is useful for searching candidate area of detailed survey, or for changing our viewpoint from usual photogeometry to textural analysis.

3-3) LINEAR FEATURE ENHANCEMENT

Edge is considered to be the place where brightness changes suddnly, and it is most natural to calculate differencial value of brightness to detect edge or line.

Gradient of image b(x, y) has two elements as vector.

$$\nabla b(x, y) = \frac{\partial b(x,y)}{\partial x} u_x + \frac{\partial b(x,y)}{\partial y} u_y$$

Laplacian can be also used to edge detection in correspondence to Mach phenomenon. Laplacian is scalar and is expressed as

$$\nabla^2 b(x, y) = \frac{\partial^2 b(x,y)}{\partial x^2} + \frac{\partial^2 b(x,y)}{\partial y^2}$$

It is necessary to remove noisy data from original differential result in order to make it plain. We set up the threshold of $\mu + 2\sigma$, and make the data into two tone, black and white.

Fig. 10 shows this case of two valued gradient map. Although the spatial resolution of this map is more than about 1 km, Median line is seen as a global and basic tectonic feature. Generally speaking, Fig. 10 is a similar map as Fig. 8, but it is adequate that Fig. 8 and Fig. 10 are completely different at HAKUSAN district, just like we described before.

The above-mentioned enhancement was done toward band 7 only. The LANDSAT data has four channels actually, and it means loss of information not to use other multi-channel datum. So we applied the former differential operators to YAKEDAKE which had been selected under Japan's new energy research program, what is called "Sunshine Project", one of potential geothermal areas characterized by conspicuous geothermal anomaly, especially with fumarole and hot-springs of boiling temperature. Original composite image is shown in Fig. 11 with original scale and its location in Fig. 12. YAKEDAKE is at the center just to the right in Fig. 11.

Fig. 13 shows the result of gradient and fig.14 shows that of laplacian. Fine linear features are extracted on account of multi-channels datum. So far as Fig.13 and Fig.14 are concerned, simple gradient is more effective for linear feature detection than laplacian.

We subsequently applied same gradient filter to multi-channel datum of TAKAYAMA district (Fig.12) with changing scale factor for input image such as 1/5 and 1/10 reduction with an intention of verifying how much the scaling factor has an effect on filtered results. The example of 1/5 reduction is shown in Fig.15 and 1/10 in Fig.16 . It was found that most of fine linear features were lost due to high reduction. This fact means that we must select the appropriate scale factor in correspondence to lineament criterion with which we are concerned at study site of image.

3-4) SUMMARY

3 x 3 different filters were used in this study as local operators. This filters have following weak points:

1) susceptible to noise
2) no consideration for texture
3) no use of global information

Therefore, it is desirable to use this differential filters with textural

feature analysis as did in this study to avoid above 2) and 3).

It is also necessary to fit operators and/or threshold for desirable lineament extraction, and post-processing is needed still more to delineate lineaments. This post-processing must be studied deeply and improved in future. Although differential filtering has above shortcoming, it is possible to enhance linear features with multi-channel data and low reduction scale imagery.

4. CONCLUSION

We conceived the spatial lattice filter and compared its results with other methods. So far as performance of classification is concerned, our spatial lattice filter proved very fruitful. With regard to CPU-time, it became clear that spatial lattice filter processing took only 60% of time that was needed with Haralick method in general. There are some points to be improved such as the most fitted selection of filter operator and of filter size.

We tried to enhance geological linear features with following strategy.

1) apply spatial lattice filter to global image as texture analysis.
2) search candidate area for detailed survey using above map of textural pattern
3) apply differential filters, that is , Gradient and Laplacian, to multi-channel image as local operators
4) divide the differential data into two tone, black & white to make its image plain.

Thus, we could get fine and small linear features from LANDSAT MSS data. But we felt keenly the necessity of post-processing to delineate lineamens finally.

5. REFERENCES

1) G.J. Vanderbrung, "Line Detection in Satellite Imagery", IEEE Trans. Geo. Volge-14 No. 1 (1976) p (37).

2) Roger W. Ehrich, "Detection of Global Edges in Textured Images",IEEE Trans. Com. Vol. C-26 No. 6 (1977) p (589).

3) T.G. Long Shaw, R.P. Viljoen, and M.C. Hodson, "Photographic Display of LANDSAT -1 CCT Images for Improved Geological Definition", IEEE Trans. Geo. Vol. GE-14 No. 1 (1976) p (66).
4) J. Iisaka, "Synthetic Approach to Pattern Recognition for Remote Sensing", Tokyo Scientific Center Reports GE18-1858-0 (1977).
5) R.M. Haralick and W.F. Bryant, "Documentation for Textural Pattern Recognition Techniques: Final Report", NASA-C-150998 (1976)
6) J. Iisaka et al, "On the Data Processing of Aircraft MSS Data and Application for Detection of Temporal Changes in Urban Area", Lecture Note of US-Japan Seminar on Remote Sensing (1976) (Washington).
7) R.Bajcsy, "Computer Identification of Textured Visual Scenes", Stanford Artificial Intelligence Laboratory Memo. AIM-180 (1972)
8) ARTHUR HOLMES, "Principles of Physical Geology", Thomas Nelson Ltd., 1288 p.
9) H.Th. Verstappen, "Remote Sensing in Geomorphology", Elsevier Scientific Publishing Company (1977)

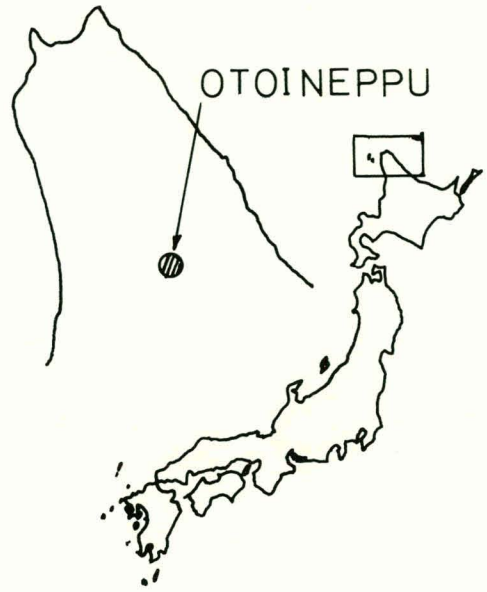

Fig.1 Location of OTOINEPPU forest

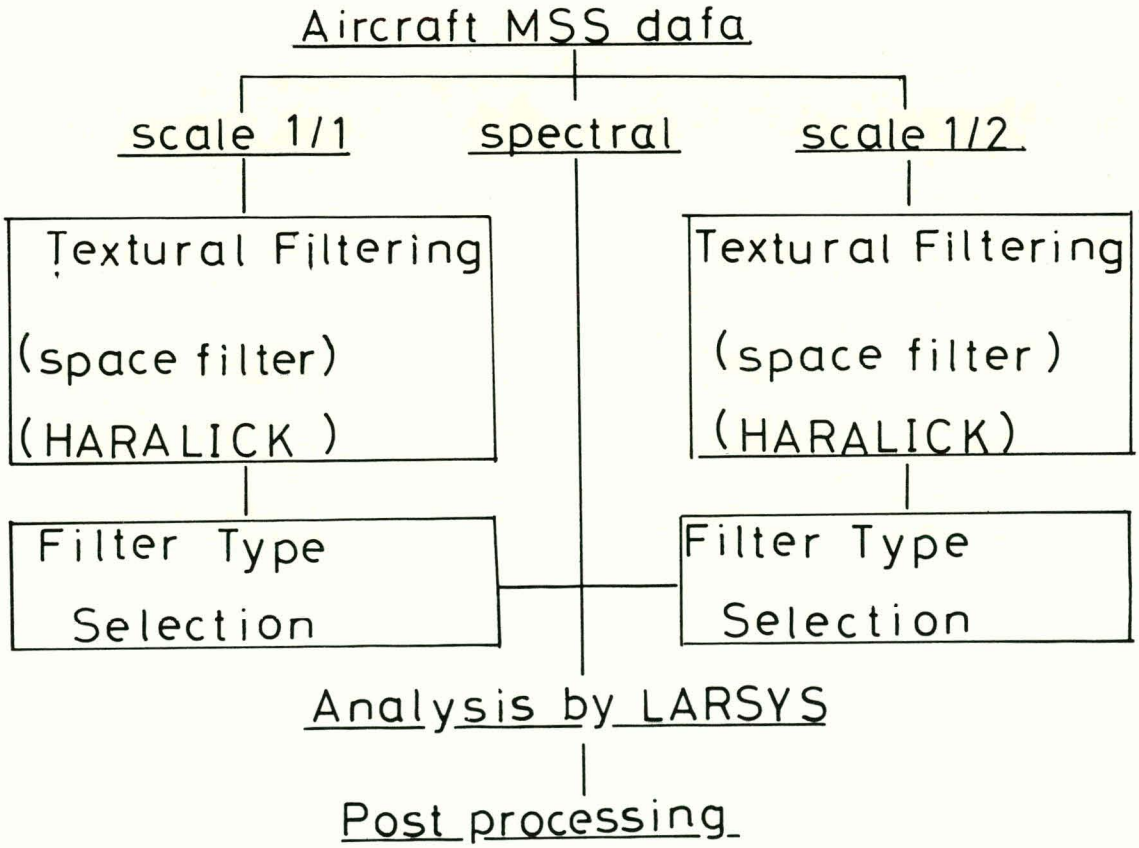

Fig.2 The flow chart of this study

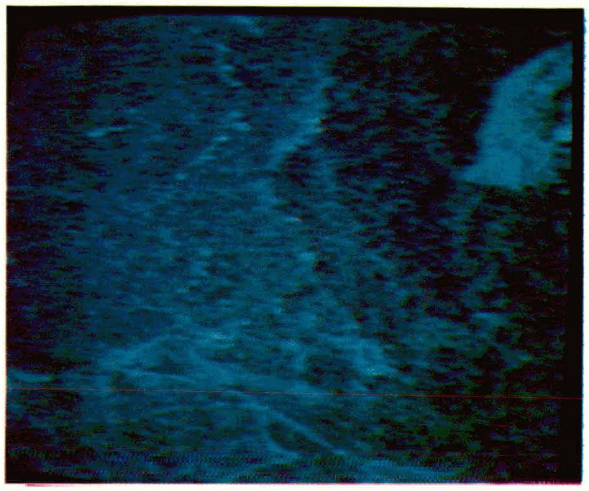

Photo 1

Original Aircraft MSS Data Image

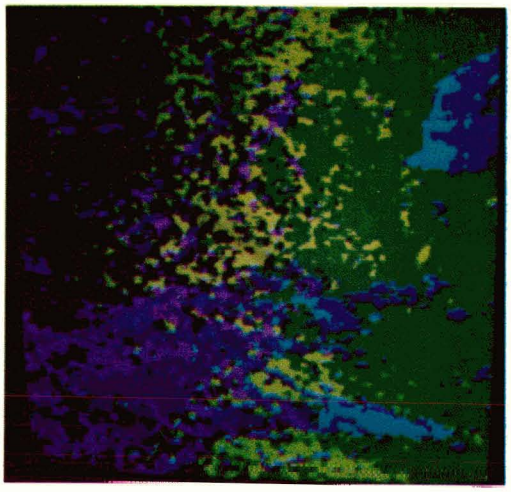

Photo 2

Result of Spectral Classification (1/2)

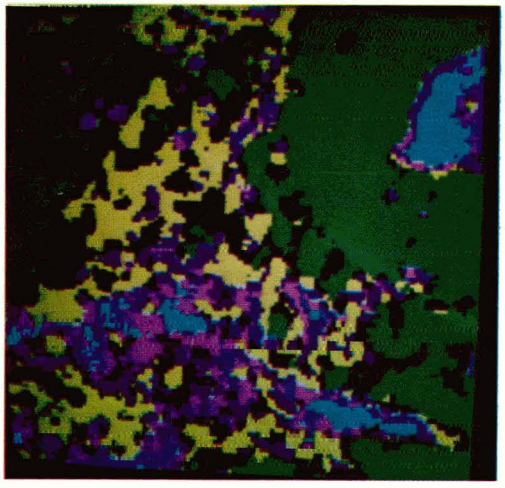

Photo 3

Result of Textural Classification (Space Filter ; 1/2)

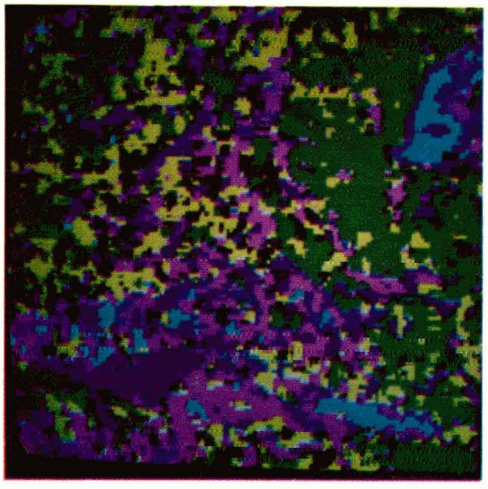

Photo 4

Result of Textural Classification (Haralick's Method; 1/2)

(Post Processing ; Regrouping of classified result according to major population)

1966

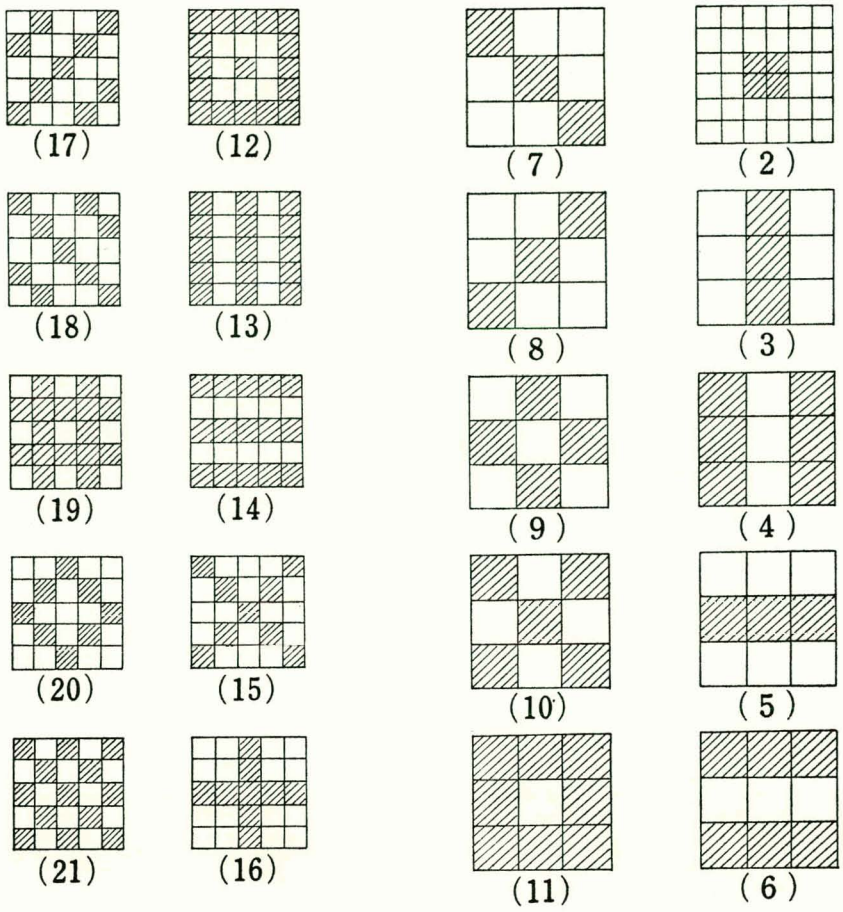

Fig.4 An illustration of space filters

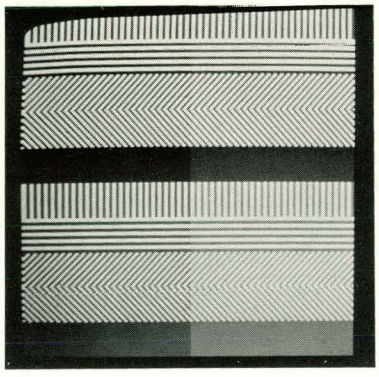

Fig.5 (a) Test pattern
(Simulated in a computer)
The textural zones are well classified

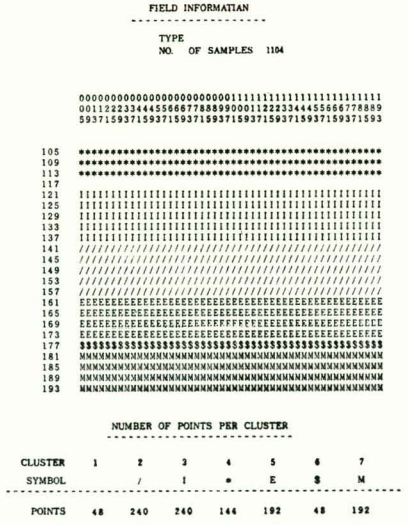

Fig.5 (b) Classified results of test pattern by applying space filters ; type 2,4,6,7,8

TABLE 1 Performance of the each method
(1/2 scale data)

	space filter	spectral	HARALICK
L	N(8.3)	N(33.3)	N(27.8)
LY	MY(20)	Z(30.0)	MY(23.3)
M	——	N(45.8)	N(26.7)
MY	LY(11.1)	NY(31.1)	NY(24.4)
N	L(27.8)	L(33.3)	L(27.8)
NY	L(30.0)	N(30.0)	MY(25.8)
B	——	MY(30.0)	LY(38.8)

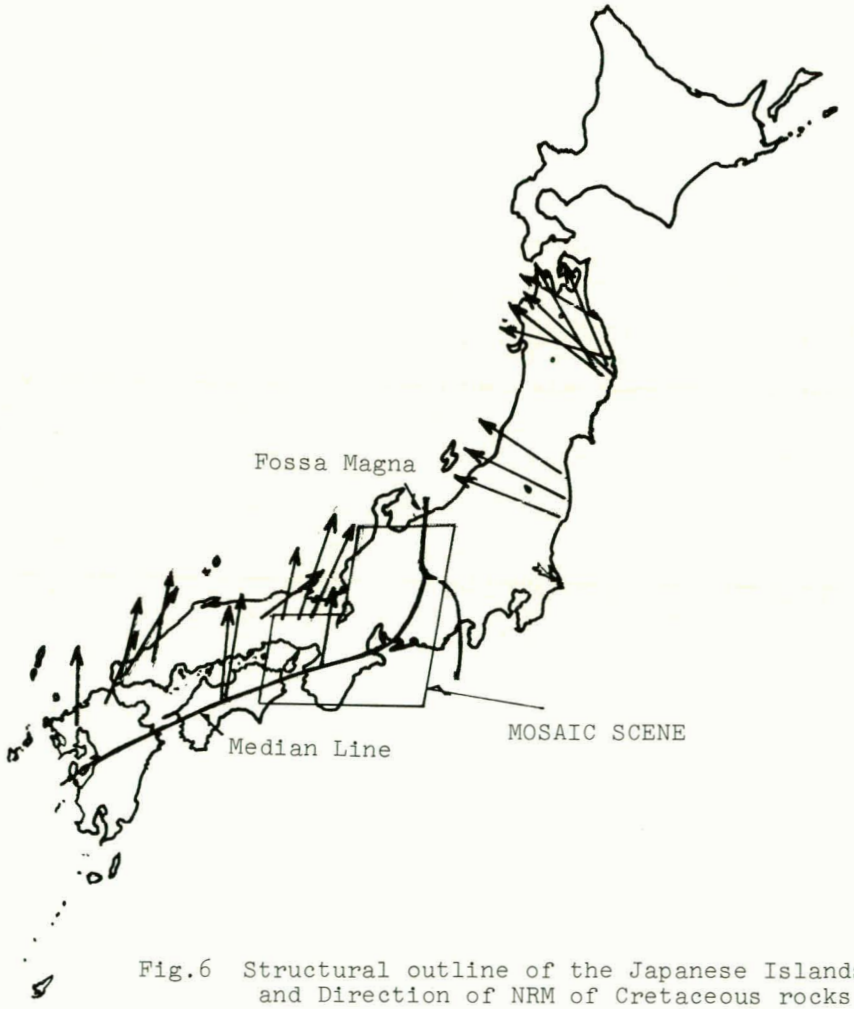

Fig.6 Structural outline of the Japanese Islands and Direction of NRM of Cretaceous rocks.

Fig.7 LANDSAT image mosaic of
OSAKA, ISE, and TAKAYAMA

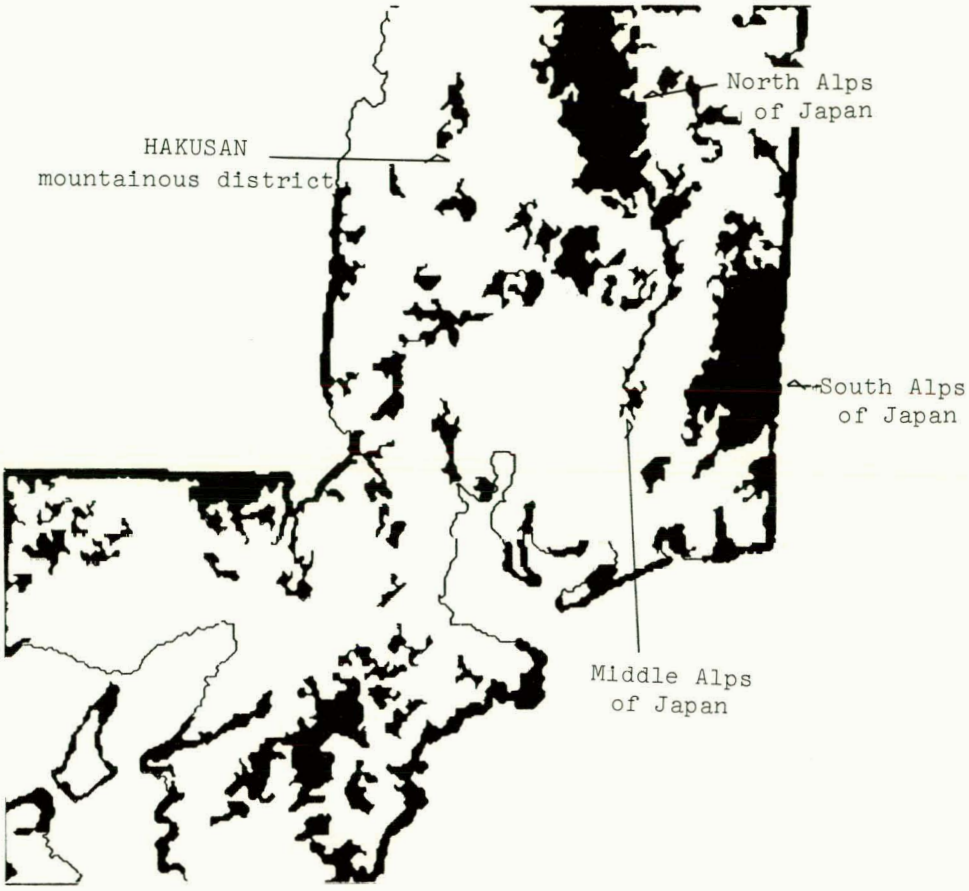

Fig.8 Map of textural analysis
with spatial lattice filter

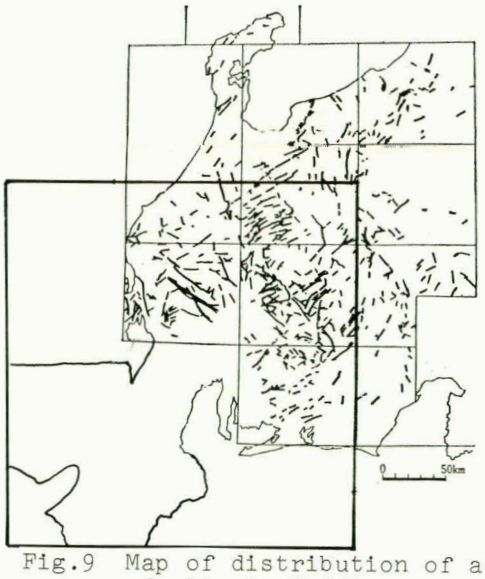

Fig.9 Map of distribution of active faults in Middle Japan
(after MATSUDA.OKADA,1968)

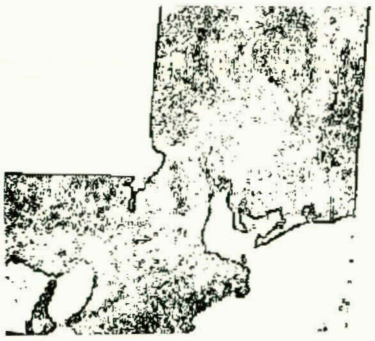

Fig.10 Two valued map of Gradient

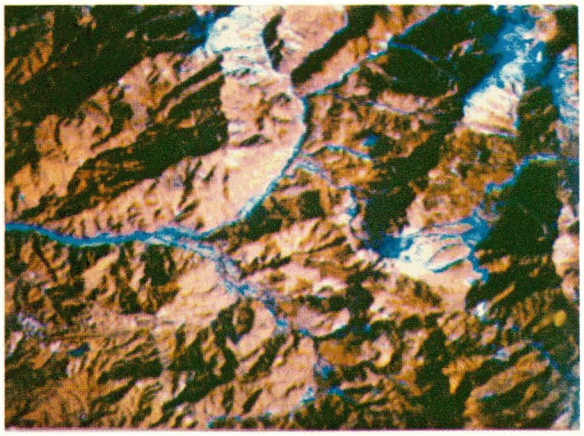

Fig.11 Original image of YAKEDAKE

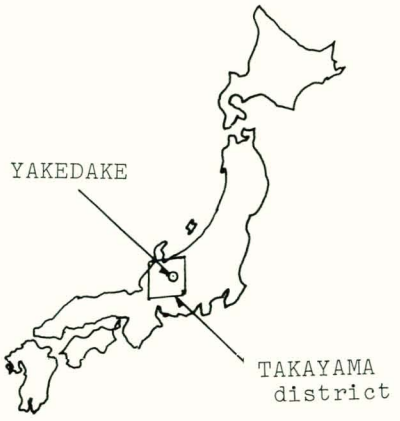

Fig.12 Location of YAKEDAKE and TAKAYAMA district

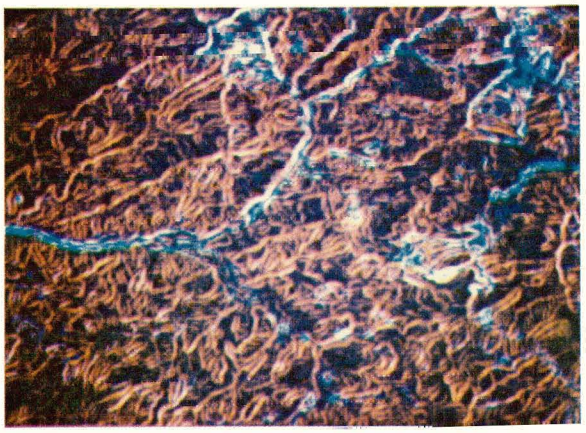

Fig.13 Gradient image of YAKEDAKE

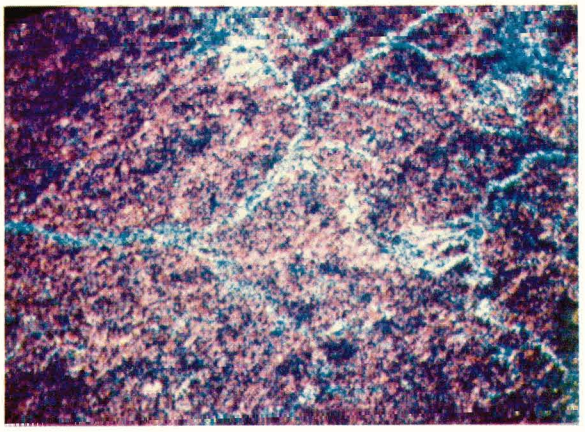

Fig.14 Laplacian image of YAKEDAKE

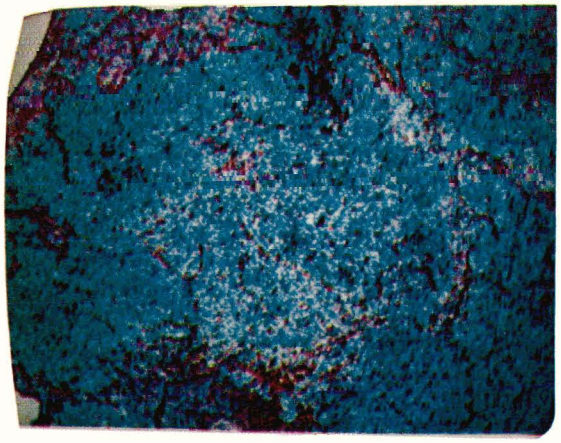

Fig.15 Gradient image of TAKAYAMA in 1/5 reduction

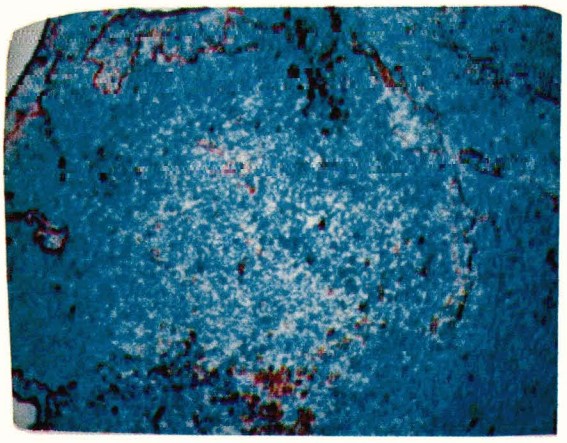

Fig.16 Gradient image of TAKAYAMA in 1/10 reduction

THIS PAGE

WAS INTENTIONALLY

LEFT BLANK

AN ECONOMIC WAY OF DATA HANDLING AND REPRODUCTION OF LANDSAT DATA

Suvit Vibulsresth[1]
Vaschrin Booncong[1]
Joseph O. Morgan[2]

[1]Thailand National Remote Sensing Program
National Research Council
Bangkok, Thailand
[2]U.S. Geological Suryey, Restcn
Virginia, U.S.A.

ABSTRACT

An economic way of data handling and reproduction of the Landsat data was designed and implemented at the Thailand National Remote Sensing Program, National Research Council. Effective low cost procedures which are appropriate for use in other developing countries are presented. The discussion is centered around the reproduction of black and white imagery at 1:1 million, 1:500,000 and 1:250,000 scale and the diazochrome color composite transparencies at 1:1 million xcale. The system enables Thailand to provide all the required data at the quality and quantity needed by user agencies and can be expanded to meet the regional requirements.

1. INTRODUCTION

For a developing country with scarce resources like Thailand, the most economical way of utilizing the satellite remote sensing data must be envisaged. Based on this thinking the Thailand National Remote Sensing Program (TNRSP) of the National Research Conuncil made a decision to undertake the production of black and white Landsat photographic data products for nation-wide use. The intent was to conserve available project funding by ordering only 70 mm negative images of Landsat scenes on a routine or standing order basis from the EROS Data Center and to master the techniques of contact printing and enlarging to professional standards, so that the delivery of data products could be expedited and purchases of the more costly data products from EROS Data Center can be minimized. The plan includes initiation of color reproduction at a later date.

A logical approach toward meeting this requirement is to set acceptable standards of photographic quality and control, and to select equipment and develop procedures to meet the requirements within a limited budget. It is also necessary to consider availability, from local commercial sources and by mail order, of necessary materials and supplies, and to utilize equipment already in hand to the maximum practical extent.

Black and white paper prints at scales of 1:1 millon, 1:500,000 and 1:250,000 as well as diazochrome color composite transparencies at 1:1 million scale are currently being produced, using equipment furnished by US Operations Missions (USOM) through project contributions and by direct purchase under a Participating Agency Service Agreement (PASA) with the U.S. Geological Survey. Expendable supplies such as print paper and processing chemicals, as well as some hardware items, have been purchased with Tahi government funds allocated to the project. The purpose of this paper is to summarize what has been accomplished and to present some procedures and recommendations which might be useful to other developing countries in the data handling and reproduction of Landsat data at low cost.

2. SOURCE OF DATA

Countries without a ground receiving station must, at present, purchase Landsat data products from EROS Data Center at Sioux Falls, South Dakota in the United States. The process of film generation from High Density Digital Tape (HDDT) to 70 mm negative transparencies which are supplied to users is illustrated in Figure 1. TNRSP has opened an account with EROS Data Center and during the active life span of the tape recorder on Landsat-2, a standing order was placed with EROS Data Center which would then supply to TNRSP all the 70 mm negative transparencies of Landsat imagery taken over Thailand on a routine basis as the imagery became available. This system was very effective as it shortened the length of time between the date the imagery were taken and the date the imagery were received at TNRSP.

The data products which were planned to be generated in Thailand are listed in Table I. However, at the initial stage, only products 1,2,3, and 8 are being produced to users on a production scale; whereas other products are produced on special request.

TABLE I.

LANDSAT DATA PRODUCTS TO BE GENERATED IN THAILAND

Data Product No.	
1	1:1 m scale positive paper print (+5), made by enlargement (3.369X) from EROS 70 mm (-4)
2	1:500,000 scale positive paper print (+5), made by enlargement (6.738X) from EROS 70 mm (-4)
3	1:250,000 scale positive paper print (+5), made by enlargement (13.476X) from EROS 70 mm (-4)
4 (a)	70 mm positive film (+5) made by contact printing from EROS 70 mm negative (-4), for archival storage. To be used only for making negative copies (70 mm-6) in case of loss or damage of original 70 mm (-4)
(b)	70 mm positive film (+5) for use in 4 channel viewer, made as above
5 (a)	70 mm negative film (-6), to be made from product No.4 (a) 70 mm (+5), when necessary
(b)	70 mm negative film (-6) to be supplied to user. Made from Product No.4 (b)
6	240 mm (1:1 m scale) positive film (+5), made by enlargement (3.369X) from EROS 70 mm (-4). For use in diazochrome production and for other users as needed
7	240 mm (1:1 m scale) negative film (-6), made by contact printing from product No.6. For use in diazochrome production and for other uses as needed
8	240 mm (1:1 m scale) diazochrome color composite transparencies made by contact printing from product No.6

3. PROCEDURES FOR DATA HANDLING

Some procedures for logging, inspection, and reproduction of incoming data products have been developed, and the master files at TNRSP are in good order. Basically, the work flow of data handling can be divided into three sections, as illustrated in Figure 2. The Data Processing Section receives data products from EDC or other sources and the inspection of cosmetic and electronic defects are performed in the Data Control Unit which refers all the problems to System Analysis. Then the relevant data are recorded on a master file card, and the master data products logged in and kept in the Data Room. The Data Control Unit also receives requests for photographic products from the users through the User Section which interfaces with the users. When prints are required, a work order card is filled in and negatives and cards are selected from the file. The work order card, the negative and the card are then sent to the photolaboratory for reproduction. The photolab would then make contact printing, or enlargement, or microfilms/microfiches (to be initiated later) as required. The outputs are sent back to the Standard (or Quality) Contral Unit for inspection together with negatives and cards. The Standard Control Unit would inspect prints or diazochromes, and reject them if they do not meet the required standards. If the outputs pass the inspection, they are sent to User Section to be shipped to users. If they are rejected, the outputs are sent back through User Section to the Data Control Unit which would recheck densitometry, filter selection, exposure selection, etc. for rework. Examples are shown in Figure 3.

4. PROCEDURES FOR DATA REPRODUCTION

When the master negative transparencies were received from EDC, density of the first (most dense) step on the annotation gray scale, and the 15th or last (least dense) step, were measured using a TD-504 densitometer with 1 mm aperture plate. These values, called D(1) and D(15), were recorded on the master file card. Then measurement of the density of the lightest area (least dense) and the darkest area (most dense) within the image were made and recorded on the master file card as D(min) and D(max) respectively. D(1) and D(15) values should fall within the limits set by NASA or EDC, edpending on which data product was measured. From the scene D(min) and D(max) ΔD and D(mp) (md = mid - point) were calculated.

$$D = D(max) - D(min)$$

$$D(mp) = \frac{D(max) + D(min)}{2} = D(min) + \frac{\Delta D}{2}$$

These values were recorded on the master file card, and the cards were filed with the image.

Polycontrast filter is determined from the value of the density range of the negative which should be based on experience with the paper to be used. The exposure time is in turn determined by the values of mid-point density and Polycontrast filter number. These values serve only as guidelines and in actual practice, experience of the photolab technician is the most important factor in obtaining good quality prints.

Figure 4 shows the flow chart for the photographic reproduction process at TNRSP. A negative cleaning station is provided because negatives cannot be cleaned properly under the lights normally provided in a printing dark-room, and because the printing technician should not be required to switch on the white lights except when he needs them to check the quality of the prints. Dust dirt and fingerprints anywhere in the optical train of the enlarger or contact printer will degrade the print and will make it less useful to the interpreter. Materials used at the negative cleaning station and pass-through are listed below:

1. Work table or desk, located at the pass-through on the outside of the darkroom.
2. Chair or lab stool
3. Tensor lamp
4. Fluorescent lamp
5. Small light table
6. Kodak static cleaner
7. Transformer, step-down, 220/110V
8. Magnifying glass, 2-3X, mounted on base
9. White gloves
10. Blower brush
11. Photo chamois
12. Lens tissue
13. Film cleaner (carbon tetrachloride)*
14. Glass cleaner (Windex)
15. Q-tips
16. Soft cotton
17. Distilled water
18. Acetone*
19. Tack Cloth

* These chemicals should be used sparingly and with caution. Avoid prolonged exposure.

The cleaning station is provided with three different kinds of light sources to assist the operator in seeing different kinds of particles and stains on the transparency and the negative carrier glass:

Tensor lamp. Small dust particles may be seen most easily under this light source.

Fluorescent lamp. This may be better than the tensor lamp for showing fingerprints and other kinds of large area stains.

Light table. Scratches,pinholes and dark particles or strands of lint or hair that do not reflect much light may be seen best when the transparency is held over the light table. Scratches, pinhole defects, and emulsion tears should be noted on the envelope or work order card, but they cannot be removed by cleaning. Great care should be used in cleaning to avoid adding more scratches or other permanent defects.

Procedures for cleaning the negative carrier, and the negatives, as well as the loading of the negative carrier can be found in the reference.

Figure 5 shows the set-up of the pass-through and the negative cleaning station.

5. EQUIPMENT

The primary equipment for enlargement from Landsat 70 mm negatives is a Beseler Model 45 MCRX enlarger purchased under the USOM/USGS PASA. The machine has been set up for printing at the three most frequently requested scales (1:1 m, 1:500 k, 1:250 k), using one lens (135 ElNikkor) for all scales. Ancillary equipment includes an adjustable steel stand, a heavy vibration isolating concrete pad, two vacuum operated printing easels, and a vacuum pump. The stand, mounting pad, and vacuum easels were designed and fabricated locally. An electrical junction box with all necessary outlets and switches for enlarger and safelight operation was also fabricated locally.

In practice, since the request for 1:250,000 scale print has been very large, the Beseler enlarger has therefore been set to enlarge only at 1:250,000 scale. One Omega enlarger was dedicated to enlarging at 1:500,000 and 1:1,000,000 scale. Furthermore, another Omega enlarger complete with one Apac motor driven roll paper transport printer with timers and automatic knife cut-off assembly for paper widths up to 9½ inches was set-up for enlargement at 1:1,000,000 scale on a production basis.

Figure 6 shows the Beseler enlarger in the position for enlargement at 1:250,000 scale(a), wall-mounted printing easel with adjustment capability(b), heavy vibration isolating concrete pad(c), and the set-up for 1:500,000 scale enlargement(d). Figure 7 shows how to calibrate the enlarger with a three point adjusting screw.

For production o diazochrome color composite transparencies, a specially designed room with a hood, a cleaning station and a pass-through was designed and constructed. The equipment consists of Arkwright diazo-printers and developers. The need for diazochrome color composite transparencies has been very great and the technician has learned how to produce different kinds of composites for interpretation of special categories of interest to users.

Total investment in photographic equipment at TNRSP is around U.S. $ 50,000 and only four technicians are needed to handle the work under the supervision of an engineer.

6. CONCLUSION

An economic way of data handling and reproduction of Landsat photographic data has been presented. The current system has enabled Thailand to provide Landsat data to researchers and users both within the Thai government agencies and international organizations with almost the same quality as those obtained at the EROS Data Center, but at a much lower cost. Major users amount to forty at present and the current annual output is approximately 3000 black and white paper prints at scales of 1:1 million, 1:500,000 and 1:250,000 as well as 2,000 diazochrome color composites at 1:1 million scale. Research and development is being continued to upgrade TNRSP capability further in providing good quality products to users, especially in the color reproduction and in the printing of different bands on the same paper to obtain special effects which may be useful to interpreters. The system can be easily expanded to meet the regional requirements.

7. REFERENCE

TNRSP Technical Note No.760602, "Handling and Reproduction of Landsat Imagery", by Joseph O. Morgan, National Research Council of Thailand.

Figure 1. Landsat 70 mm Film Data Products

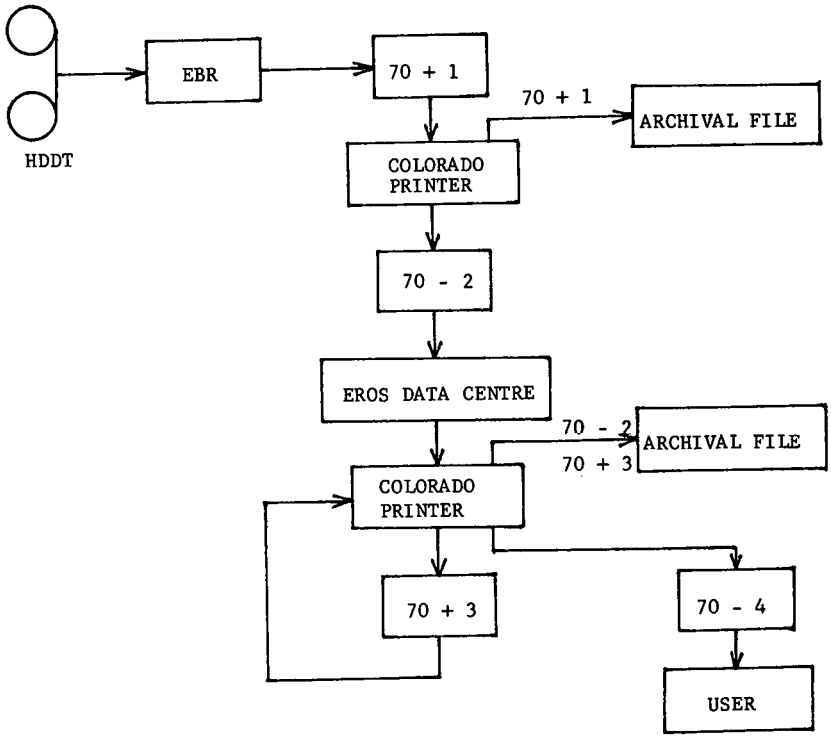

Product	Disposition	How Produced	Annotation Gray Scale Density Range	Tolerance	Remarks
70+1	Goddard Archive	Electron Beam Recorder Versamat processor	0.1 - 2.1	0.1+0.06 -0.03 2.1±0.1	1st Generation Positive Transparency, 70 mm.
70-2	Sent to EDC	Goddard Colorado printer	0.4-2.4	±0.2	2nd Generation Negative Transparency, 70 mm.
70+3	EDC archive and working roll. Also sent to user	EDC Colorado printer Versamat processor	0.4-2.4	±0.1	3rd Generation Positive Transparency, 70 mm.
70-4	Sent to user	EDC Colorado printer Versamat processor	0.1-2.1	±0.1	4th Generation Negative Transparency, 70 mm.

Figure 2. Work Flow of Data Handling at TNRSP

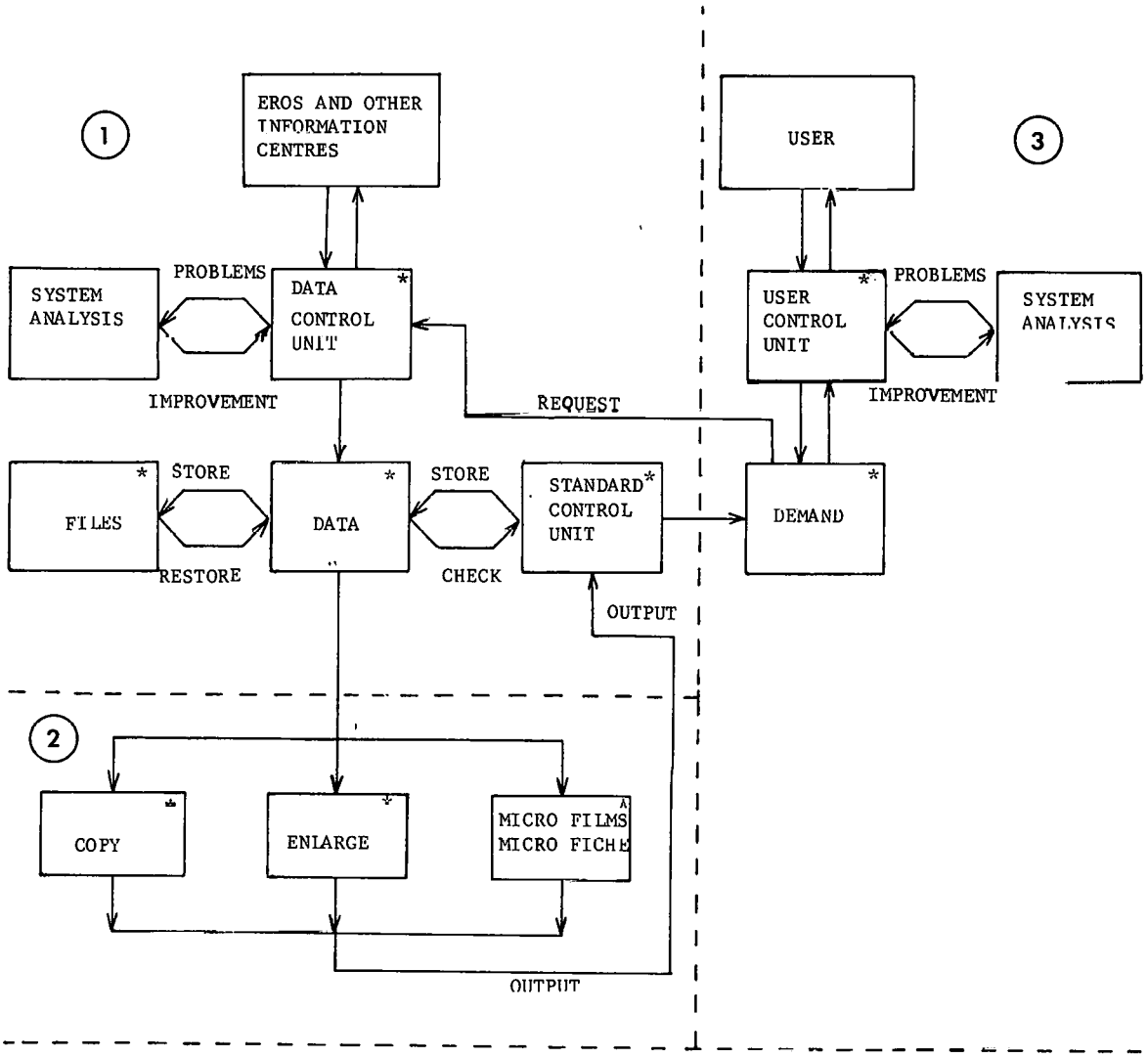

Notes

1 Data Processing Section

2 Technical Reproduction Section

3 User Section

* Communication via control cards

Figure 3. Examples of Work Order Card and Control Card

TNRSP

WORK ORDER

Card No. 13

Thailand National Remote Sensing Program
Photo Reproduction Service

DATA PRODUCTS REQUIRED

Black & White

- [ ] Contact print
- [X] Paper
- [X] Positive
- [X] Enlargement
- [ ] Film
- [ ] Negative

Color Composite

Band	4	5	6	7
Color				

Scale

- [ ] 1:3.369m
- [X] 1:500k
- [ ] Other _____
- [ ] 1:1m
- [ ] 1:250k

Number required
Each [3] Total [60]

Remarks: _____

DATA PRODUCTS FURNISHED

- [X] 70-
- [ ] 240-
- [ ] 480-
- [ ] Other _____
- [ ] 70+
- [ ] 240+
- [ ] 480+

No. [80]

CONTROL INFORMATION

		Initial
Date ordered	780412	Malinee
Date needed	780415	Malinee
Date completed	780415	Prasan
Inspection:		
No. accepted	60	Malinee
No. rejected	–	

Comments: _____

TNRSP

FILM CONTROL CARD

File No. 02 Row 01 Column 02

Card No. 75 — 02 — 01

Date of Exposure, Year 1975 Month Feb.

Date Received	Thailand ID	NASA ID	Cloud %	Sun Elev.	Syn Azim.	Product / Generation / Band / Total																Remark L = Lost D = Damage O = Others
						70+				70-				240+				240-				
						4	5	6	7	4	5	6	7	4	5	6	7	4	5	6	7	
771005	750209-3-6	E-2018-02493	40	42	126	1	1	1	1	2	2	2	2	1	1	1	1					
771005	750227-3-6	E-2036-02493	30	45	119	1	1	1	1	2	2	2	2	1	1	1	1					

Figure 4. Flow Chart of Photographic Reproduction Process at TNRSP

Fig. Flow of processing method for LANDSAT imagery at TNRSP

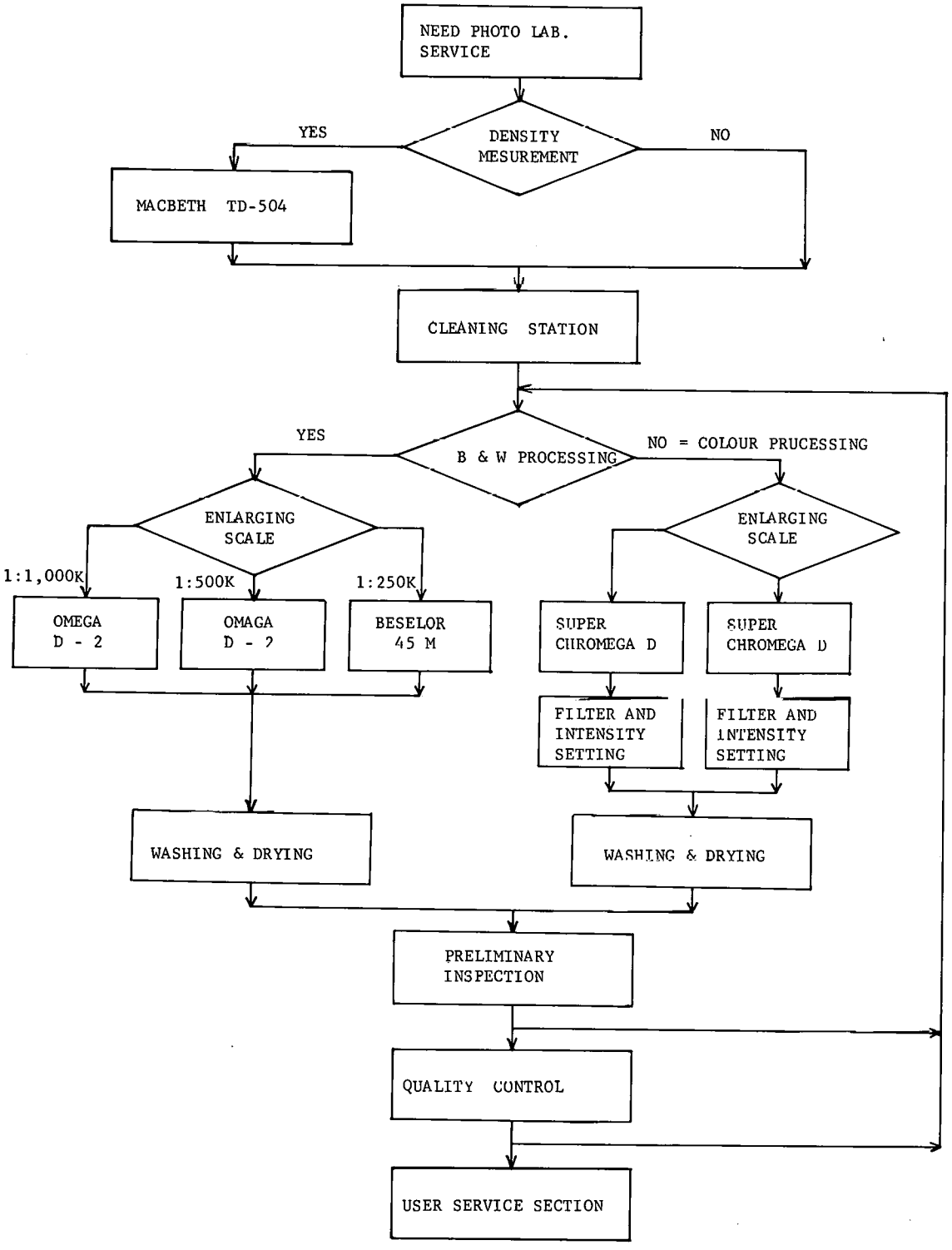

Figure 5. Pass Through and Negative Cleaning Station

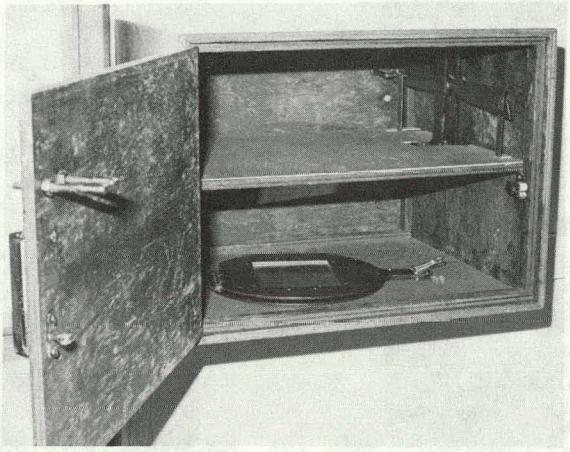

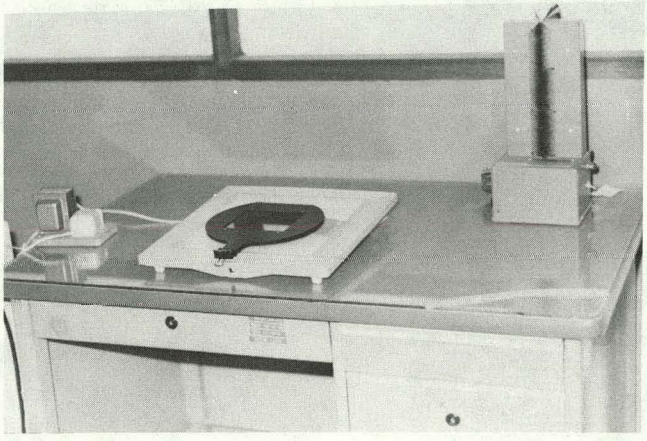

Figure 6. Photolaboratory Equipment and Set-up

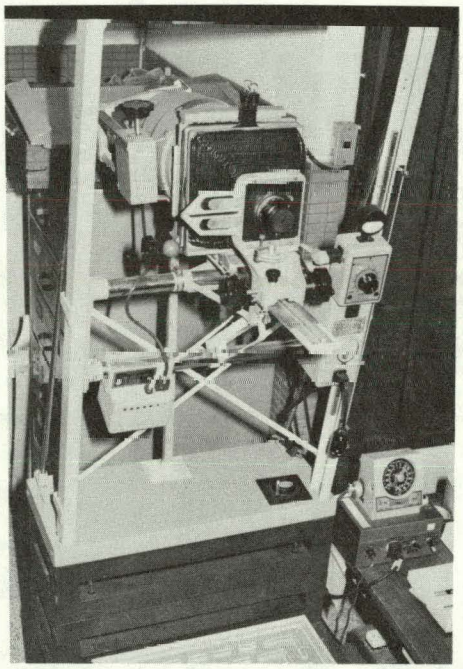

A

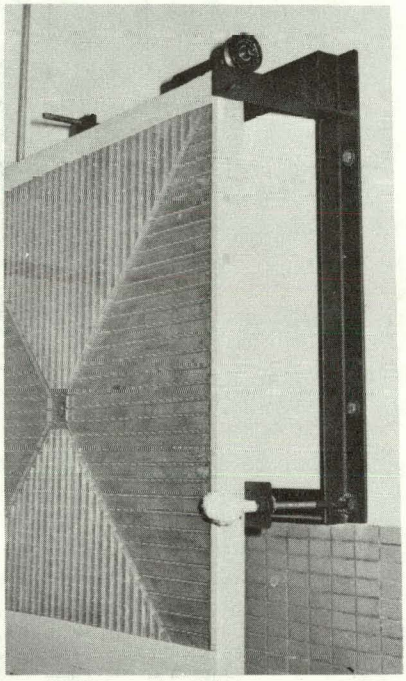

B

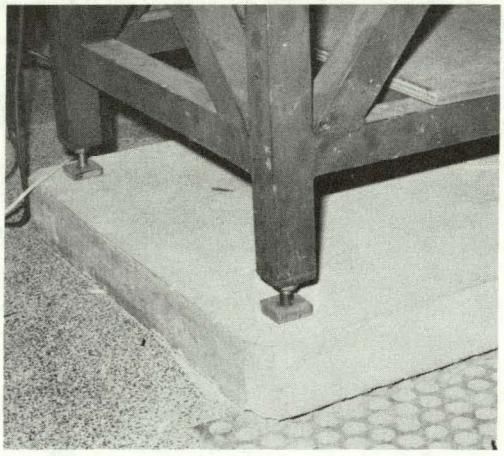

C

D

1982

Figure 7. Calibration of Enlarger

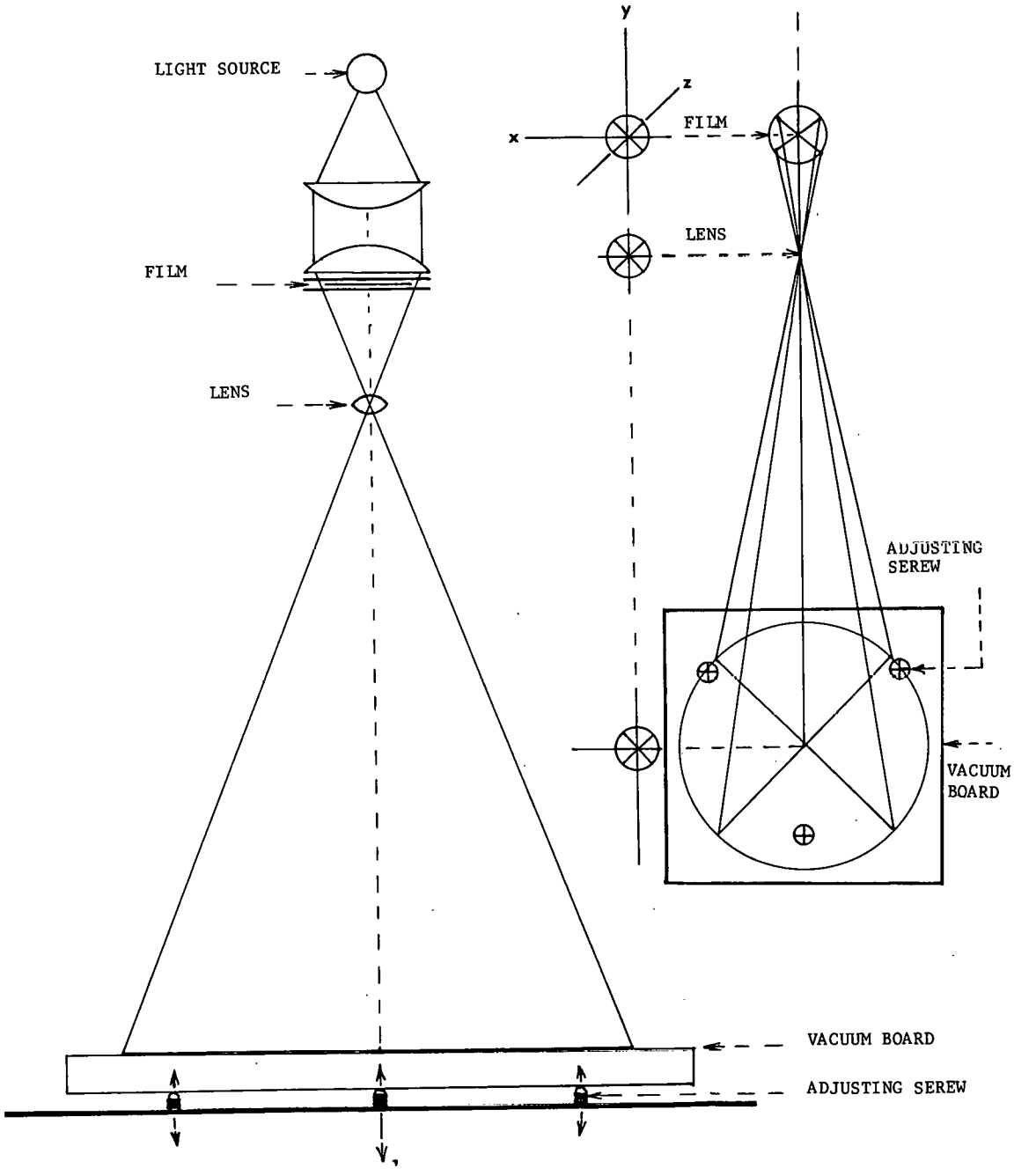

THIS PAGE

WAS INTENTIONALLY

LEFT BLANK

LANDSAT-DIGITAL DATA AS A TOOL IN QUATERNARY GEOLOGICAL MAPPING IN THE COASTAL PLAIN OF THE MALAYSIAN PENINSULA*

A. E. Prelat, R.J.P. Lyon

Stanford Remote Sensing Laboratory
School Applied Earth Sciences
Stanford University, Stanford, California 94305

and

E. A. Van de Meene

Geological Survey of Malaysia
Ipoh, Malaysia

ABSTRACT

The Geological Survey of Malaysia has begun a systematic mapping of the coastal plain of the Malaysian peninsula. The present research was conducted to evaluate the use of LANDSAT digital data to assist the geologist in quaternary mapping. The study was carried out at the Stanford Remote Sensing Laboratory during a 10-day period with the assistance of a geologist with recent field experience in this area of Malaysia. The Remote Sensing Interactive System (STANSORT) was used to view selected channels and ratios on the 3-color Grinnell TV display, make simulated-grey level pictures ("Dotprints") on a Printronix matrix printer, and scene classification.

The supervised classification technique, known as Discriminant Analysis, was applied based on the knowledge of the geology. A number of soil units were selected from the geological map to define training groups, and then the rest of the study area was classified into the pre-selected categories.

The results indicated that the LANDSAT information in combination with geological knowledge improved the interpretation and quality of maps with appreciable time savings.

1. INTRODUCTION

The Geological Survey of Malaysia has begun a systematic mapping of the coastal plains of the Malaysian peninsula. The aim of this mapping is the production of mapsheets on a scale one inch to the mile (1:63 360). At the present mapping is done mainly with the help of hand-drilling. Besides this traditional way of mapping other methods are being tested, as, for example, geophysics. The present report describes the use of LANDSAT digital data to assist the geologists in the mapping of the Quaternary terrain in the coastal plain of the Malaysian peninsula. The present analysis was conducted at the Stanford University Remote Sensing Laboratory during a 10-day visit by Drs. E. A. Van de Meene from the United Nations, Ipoh, Malaysia, in August, 1977.

Previous experience had shown that the interpretation of LANDSAT digital data in areas covered by vegetation is most effective when the natural vegetation has not been disturbed by human activity. Differences in vegetation usually show differences in the soil which, in turn, can be indicative of the source material. In West Malaysia, large tracts of land consisting of different soil types are now covered by rubber and oil-palm estates which makes difficult the detection of differences in source material. In consequence, the LANDSAT digital data have to be processed by numerical classification techniques to produce more reliable geological information by accentuating the minimum differences among different types of materials.

* The present study is a joint research project between the Committee for Coordination of Joint Prospecting for Mineral Resources in Asian Offshore Areas (CCOP), United Nations and Stanford University.

The interactive computer program used for this study provided an extremely rapid, flexible and low cost processing of the LANDSAT digital data.

2. GENERAL PROCEDURE

The study of the area was based on the analysis of the LANDSAT computer compatible tape 1184-03035, exposure dated January 23, 1973. Although the quality of the tape is good, partial cirrus cloud coverage made the analysis in certain areas difficult. The brightness of Channels 4,5,6, and 7 and the ratios 7/6, 7/5, 7/4, 6/5, 6/4, and 5/4 were used as raw data for input to the STANSORT programs (Honey, Prelat & Lyon, 1974),(Lyon, 1976). The STANSORT system developed at Stanford University has been designed for the analysis of satellite CCT's, digitized aircraft film products, and line-scanner data tapes. The portions of the system utilized for the present analysis were (1) the production of Dotprint maps and the TV display to produce color images, (2) the numerical classification techniques.

Step 1 was the generation of a series of Dotprint maps at orthogonal scale 1:63 360. This specific scale was selected to match that of the geological map. The main purpose of the Dotprints was to outline the area of investigation and at the same time recognize features like roads, rice fields, water bodies, etc., to facilitate the geographic location and precise extraction of pixel coordinates in the LANDSAT digital tape (Ballew and Lyon, 1977). Figure 1 is an example of a Dotprint for Channel 7 at scale 1:63 360. In the figure, the streams, tailing ponds, and rice fields are clearly recognized. On Dotprints based on the ratio 7/5 features such as roads and railroads may be identified. The 3-color Grinnell TV display was used to view selected channels and ratios.

Step 2 in the analysis was the selection of training areas for input to the numerical classification techniques. This selection was based on the prior geological knowledge of the area which has been partly mapped at scale 1:63 360. One drawback in the present analysis was that the mapping was quite general, and in consequence, each training area contained more than one type of material, making it difficult to have homogeneous groups to use in the classification procedure.

3. NUMERICAL CLASSIFICATION TECHNIQUES

Ten different training groups were selected using the geological knowledge of the area for the application of the supervised classification known as discriminant analysis. The groups are listed below with the corresponding number of pixels (1 pixel = 60 x 80 m) extracted from the LANDSAT digital tape.

IDENTIFICATION NUMBER	GROUP NAME	NUMBER OF PIXELS
1	"Outcrop"	84
2	Sand	100
3	Sandridges	92
4	Mangrove	100
5	Thin peat on clay	100
6	Water	19
7	Tailings	81
8	Clayey sand and sandy clay	100
9	Clay	100
10	Thick peat	100

The brightness of the four LANDSAT channels and six ratios were recorded at each pixel location and subsequently used on the classification analysis. The relationship among the training groups was defined by using a cluster analysis procedure (for mathematical background, see Davis, 1973). Below is the dendrogram showing the result of cluster analysis, which displays the relationship among the training groups.

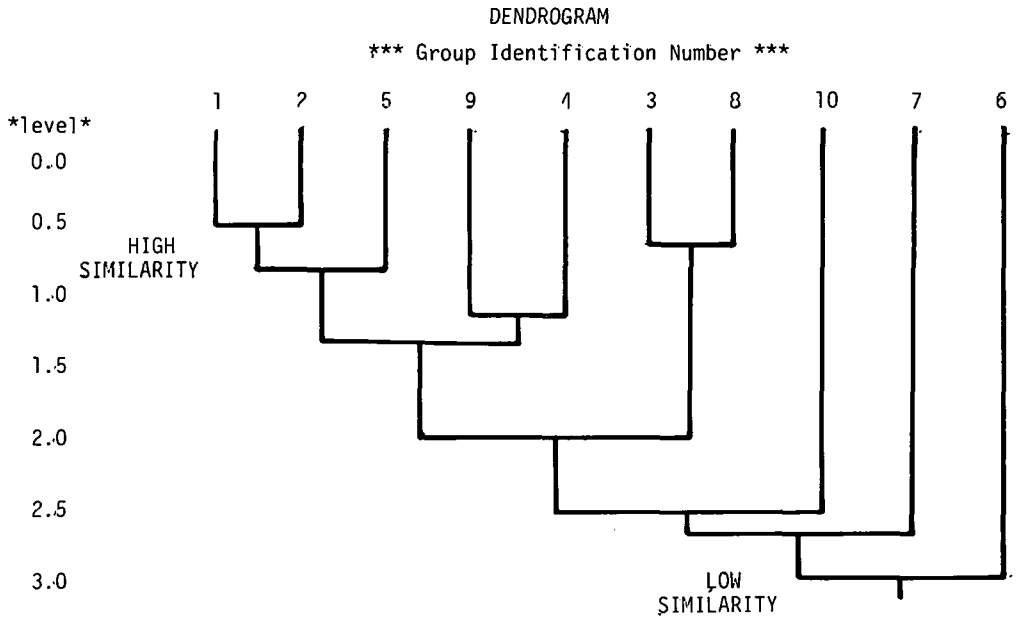

In the dendrogram the groups are connected at different levels, the low levels indicating a high degree of similarity, and the large levels a low degree of relationship. For example, 1 (outcrop) is connected to 2 (sand) at a level of 0.50 indicating a high degree of mutual similarity. The correlation between 1, 2, 5, 9, 4, 3 and 8, on one hand, with 10, on the other, is 2.50. indicating a low degree of similarity.

Analysis of the dendrogram indicates that water (6), tailings (7) and the thick peat (10) form individual homogeneous groups and are quite different from the rest. On the other hand, the outcrop (1) with sand (2), and sandridges (3) with clayey sand and sandy clay (8) are closely associated.

A sequential discriminant analysis, based on the relationship presented in the dendrogram, was used to classify the study area (Ballew, 1977). First, a discriminant function was calculated between water and the rest of the groups; a second discriminant function was calculated between tailing and the rest (but without water); a third function was established between the thick peat and the rest (but without water and tailing), and so on. For practical purposes the outcrop, thin peat on clay and sand, were merged into one group.

4. RESULTS

The statistical results of the sequential discriminant analysis were used to produce the classification maps shown in Figures 2 and 3. Figure 2 shows the output of the classification of the sequential discriminant analysis procedure based on the training groups selected. In the figure, the water bodies (black), thick peat (grey), and the tailing (white) can be easily

recognized, but the sandridges (medium grey) are not clearly identified. The rest of the classes were coded with the same symbol (light grey). In part of the map, the non-peaty areas are classified as peat. Figure 3 is a Dotprint classification map based on a new training set with a larger number of samples for clay (500 pixels), peat (240 pixels), and clayey sand and sandy clay (500 pixels). For identification purposes the results have been coded with only two symbols. The main soil of geological interest in the figure is located between Port Weld and Taiping (area inside dotted line), and had not been recognized as a unit during the field work. Apparently it is an older unit of the sand. This will be confirmed by further field work in the area. It is interesting to note that now the same area can be identified using Dotprints of the ratios 7/5 and of 6/4.

The TV display was used to produce a series of images using the different channels and ratios, with the red, green, and blue color-guns. A series of color slides were taken to document the analysis. The thick peat, tailings, hilly areas, streambeds, and mangrove swamps were clearly recognized. The mangrove swamps showed different patterns which might be related to sedimentation systems. The delineation of the peat area was clearly defined by using channel 5 coded with green. Figure 4 shows a Dotprint of channel 5 at scale 1:63 360 with details of the peat area. Using the TV display was possible to separate the mangrove swamps from the peat with the combination channel 5 and ratio 7/5. The most useful LANDSAT parameters to study the geology in the area were channels 5 and 7 and their ratio 7/5. Vegetation areas were enhanced by the ratio 6/4.

5. CONCLUSIONS

The main purpose of the present analysis was to evaluate the LANDSAT information to assist the geologist in Quaternary mapping in West Malaysia. The results indicated that the use of LANDSAT digital data in combination with the geologic and topographic information can improve the interpretation and quality of the maps. The LANDSAT information was mainly useful to delineate the peat body and recognize different patterns in the mangrove areas which can be related to sedimentation systems. On the other hand, some units like clay and clayey sand and sandy clay were difficult to separate from each other, and the classification of sandridges was not satisfactory. To overcome this problem a better selection of training groups must be achieved based on more detailed geological knowledge. Further, a new area was defined as a potential soil unit which must be checked in the field.

In conclusion, it was rewarding to start the evaluation of the LANDSAT digital data as a tool for Quaternary mapping in West Malaysia. A new set of training groups have been already selected by more detailed field work. This set will be used to produce more precise classification maps by the sequential discriminant analysis technique.

6. REFERENCES

Ballew, G. I. (1977). Alteration Mapping at Goldfield, Nevada, by Cluster and Discriminant Analysis of LANDSAT Digital Data: Proceedings of the Eleventh International Symposium on Remote Sensing of Environment, 25-26 April, 1977, ERIM, Ann Arbor, Michigan.

Ballew, G. I. and Lyon, R. J. P. (1976). The display of LANDSAT Data Large Scales by Matrix Printer: Photogram. Eng. and Rem. Sens., 43, No. 9, September, 1977.

Davis, J. C. (1973). Statistics and Data Analysis in Geology. John Wiley & Sons, 550 pp.

Honey, F. R., Prelat, A.E., and Lyon, R. J. P. (1974). STANSORT: Stanford Remote Sensing Laboratory Pattern Recognition and Classification System: Proc. Tenth Int. Symp. Remote Sensing Environment, Ann Arbor, Michigan, pp. 897-905.

Lyon, R. J. P. (1976). Evaluation of the ERTS Multispectral Signatures in Relation to Ground Control Signatures Using a Nested Sampling Approach: Final Report, Contract NAS5-21884(UN-142) to NASA, October, 1976, 258 pp. (Chapter 2.2.1.STANSORT: Philosophy and Operational Use, pp. 17-44 by F. Honey).

Figure 1. Dotprint of channel 7 at scale 1:63 360. The Dotprint shows the tailing ponds (T), rice fields (R), and streams (S).

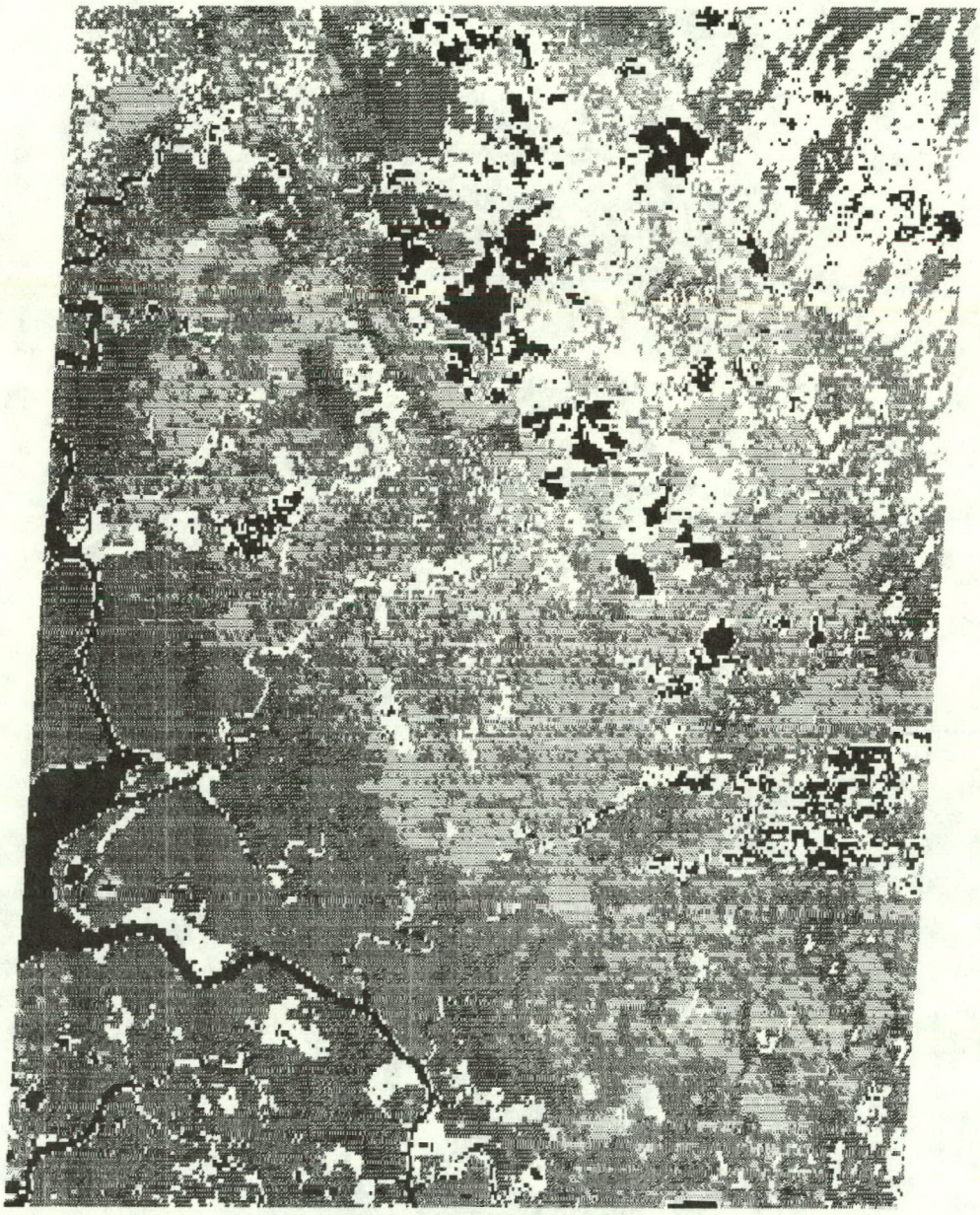

Figure 2. Dotprint classification map at scale 1:62 500. The map shows the peat (grey), tailings (white), sandridges (medium grey), and water (black). The rest of the classes were coded with the same symbol (light grey).

Figure 3. Dotprint classification map at scale 1:62 500. The area inside the dotted line apparently is an older sand unit not recognized during the field work.

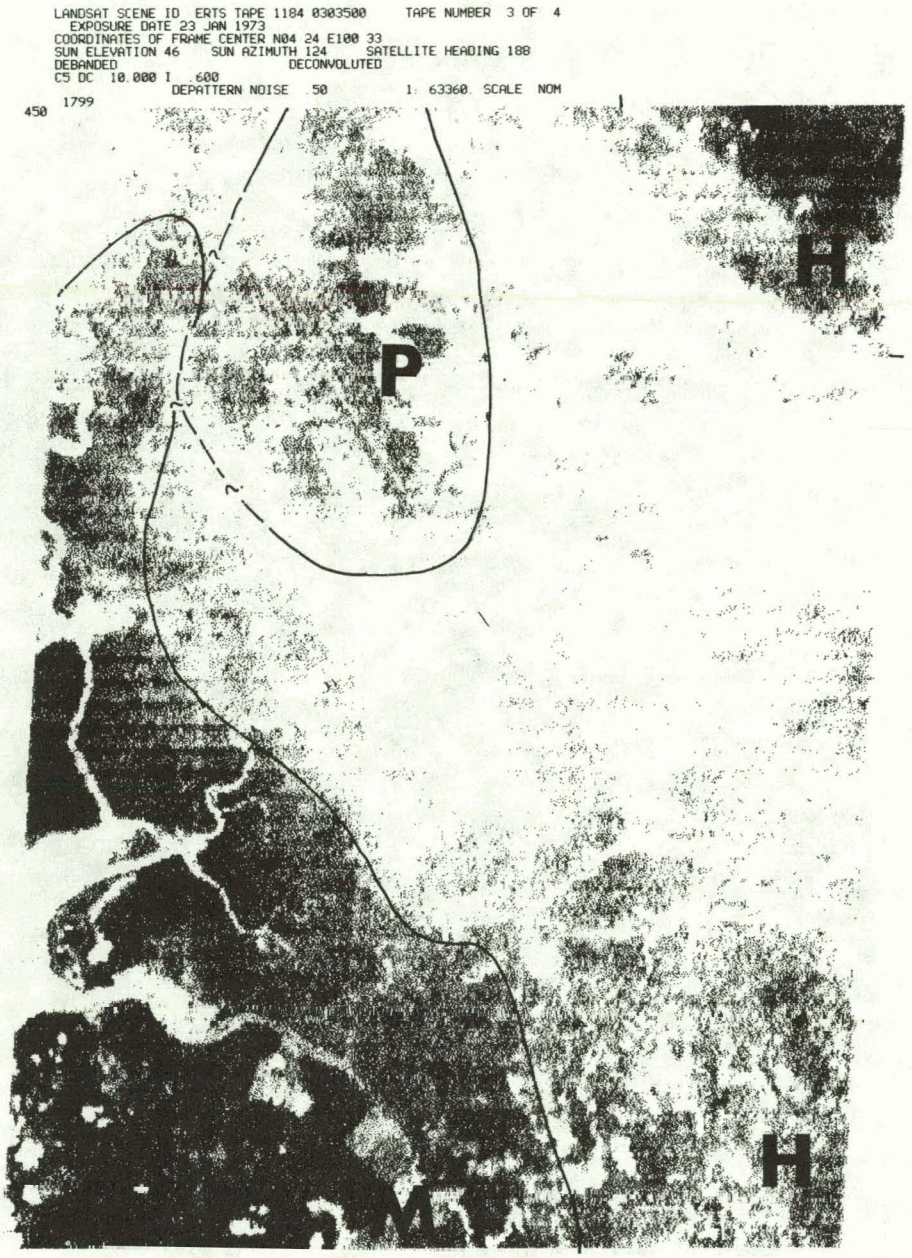

Figure 4. Dotprint of channel 5 at scale 1:63 360 showing the peat area (P), and the mangrove (M) and hills (H).

ZONE OF MINERALIZATION IN THE NORTHERN PART OF SOUTH SULAWESI AND ITS STRUCTURAL CONTROL, AS OBSERVED FROM LANDSAT IMAGERY

SUWIJANTO

Indonesian Institute of Sciences
Jakarta, Indonesia

SUMMARY

Study of LANDSAT imagery in mineral exploration has been done in conjunction with the fast field activities for base metal discoveries in South Sulawesi.

LANDSAT-1 imagery of Gulf of Bone taken in October 1972 covered most of the mineralized zones in the western part. Based on tone, texture and topographic expressions, several geological informations could be extracted from the four MSS bands as well as from color composites. Aerial photographs were used to get more detail informations for areas where ore deposits were reported and assumed to exist.

The granitic masses of Mamasa in the southwest and Kumbano in the northeast could clearly be separated from sediments and volcaniclastics in the surrounding. Distribution of mineralized zones were found along the margins and were mainly associated with stocks and other small-scale intrusions. On the imagery, they were shown in a more rigid broken isolated hills and circular features.

As far as structure is concerned, one could clearly identify two sets of lineaments running in a NNW-SSE and NE-SW directions, which were very prominent for the region. The NNW-SSE lineaments were regarded as faults which some of them indicated left lateral movement, while the NE-SW trends were formerly unrecognized. Plotting all of the ore findings on the imagery revealed that the distributions were likely confined along the NE-SW lineaments, especially when two sets intersect each other.

THIS PAGE

WAS INTENTIONALLY

LEFT BLANK

A STUDY OF AIRBORNE GAMMA-RAY SPECTROMETRY FOR GEOLOGICAL MAPPING

V. R. Slaney

Geological survey of Canada

ABSTRACT

Airborne gamma-radiation surveys are not easily correlated with published geological maps. This is particularly true in the swampy, glaciated terrain of the north-western Precambrian Shield, with its numerous lakes. To investigate the applicability of such surveys as aids in geological mapping, high sensitivity gamma-ray data were collected over 8000 km^2 in the Hearne Lake area of the Northwest Territories of Canada. Hearne Lake itself lies 75 km southeast of Yellowknife. The area chosen had been mapped geologically at a scale of 1:125,000. Rocks are exposed in about 60% of the region, the remaining area consisting of water and overburden of glacial origin.

The high sensitivity gamma-ray survey was flown at a nominal height of 120 m above ground with a line spacing of 2.5 km and at an average speed of 190 km/hr. The spectrometer had three channels to measure ground concentrations of potassium, uranium and thorium, and one broader total count channel to measure overall ground radioactivity.

Twelve flight lines were selected as test lines, since they crossed most of the major rock types known to exist in the area. Colour air-photographs were used to identify outcrops of each rock type and the distribution of overburden, swamp and water. Since each individual intrusion was regarded as a separate lithologic unit, there were 24 of these units within the area of the test lines but only 17 of them were sufficiently exposed to provide reliable radiation signatures. The average and standard deviation of the potassium, uranium and thorium contents, as well as that of total radioactivity, were calculated for those measurements taken over outcrop. Similar calculations were performed on the three radio-element ratios; uranium/thorium, uranium/potassium and thorium/potassium.

Using a maximum likelihood technique, it was found that by grouping the seventeen lithologic units into nine rock classes, approximately 80 percent of the 1730 airborne measurements within the test lines could be correctly identified. A test was introduced to confirm that each classified data point lies within the normal population bounds of its class. Because of this test, 2 more classes were identified. Water is also represented as a separate class. In studying individual radiometric parameters, the total count channel was found to reflect best the geology, followed by the potassium and thorium channels. Only minimal classification success was obtained utilizing the uranium channel and the uranium/thorium ratio, due to their relatively large standard deviations in all rock classes.

When the classification procedure was extended to the whole survey area, many rock units were found to have quite variable radiation patterns. In a few cases, similar rocks, located in different parts of the area, were found to have different radiometric signatures. Zones of anomalous high radioactivity were often found to cross lithological boundaries and may be considered useful

indicators for uranium exploration.

The study shows that airborne gamma-ray data can be analyzed and displayed in a simple format to provide both mapping and exploration geologists with information not readily obtainable from the original data. The technique described appears to be most usefully applied to areas where outcrop is extensive. Further studies are needed in areas where overburden obscures the lithology.

1. INTRODUCTION

The Geological Survey of Canada began investigating airborne spectrometric methods in 1968 (Darnley and Fleet, 1968, Darnley, 1975). It was always hoped that the airborne spectrometer would be useful to mapping geologists as well as to geologists concerned with exploration for radioactive minerals. Exploration geologists, interested mainly in anomalous concentrations of eUranium, were from the start, enthusiastic supporters of the programme Mapping geologists showed less interest, partly because the correlation between published geological maps and the radiation maps is frequently poor, and partly because of the very large numbers of maps that have to be examined for each area of investigation. There are two reasons for the poor correlation between geology and radiation maps in Canada. Lakes and swamps are very common and water attenuates the radiation signal. Large parts of Canada are also covered by an overburden usually only partially derived from the lithology beneath the cover. Almost invariably, the overburden is at least moist. Airborne radiometric surveys in Canada are normally published as flight line profiles (one map per flight line) and as individual contour maps showing the distribution of potassium, equivalent uranium, equivalent thorium and total (integral) count rates as well as maps of the three ratios eU/eTh, eU/K and eTh. The contour maps are smoothed to reduce statistical noise and to allow the automatic contouring programme to work more effectively (Cameron et al, 1976). The study of a single topographic map sheet may involve the examination of more than 45 separate radiation maps.

This study considers a part of the Canadian Precambrian Shield (Figure I) where the rocks are exposed over 60% of the area. The aim was to try to establish radiometric signatures for the different rocks occurring within a limited test area, and to use these signatures to identify the same rock types where they occur outside the test area. Further, if such rocks could be defined by some norm it might be possible to delimit areas where the patterns of radioactivity were anomalous to that norm. The results of the investigation would be recorded on a single map.

Beginning in 1976, the basic methodology was established and a first classified radiation map produced early in 1977 (Newton and Slaney, 1978). The present work incorporates most of what was done for the previous study together with improvements and additions developed over the past year.

The Gamma Spectrometer used for this survey has been described on a number of occasions (Darnley, 1970). Table I lists the most important characteristics of the aircraft, the spectrometer system and the airborne survey itself. For a review of the basic principles of the gamma spectrometer, reference should be made to Grasty (1976a).

2. THE SURVEY AREA

The Hearne Lake area, located some 45 km south-east of Yellowknife in the Northwest Territories of Canada (Figure I), was chosen for a number of reasons. It lies within the Precambrian Shield, the environment most favoured for uranium exploration in Canada; an airborne gamma-radiation survey was completed in 1971 (Grasty and Richardson, 1972); 1:15,000 colour airphotos are available (Slaney, 1971); the lithology is very well exposed; the area was remapped between 1971 and 1973, so that a draft map at 1:125,000 scale of the area (Henderson, 1976) was available.

The survey area is 110 x 75 km in size and occupies the western-most two-thirds of map sheet 85I.

The region was glaciated in Quaternary times. The present day surface forms a peneplain which rises from around 200 m above sea-level in the southwest to 300 m in the northeast. Relief in any part of the area rarely exceeds 100m. The landscape consists of low rounded hills of bare rock separated by hollows floored with glacially-derived material, usually with an organic cover of peat or bog. Lakes are so frequent as to occupy between 15% and 20% of the

total area. Trees are sparse and poorly developed since the northern limit of tree growth is less than 60 km to the north.

A number of reports are available which describe different aspects of the geology (Davidson, 1972, 1978; Henderson, 1972, 1976). The whole area will be described in detail in a forthcoming report by Henderson. A somewhat simplified version of Henderson's geology map is reproduced as Figure 5.

Archaean rocks of the Yellowknife Supergroup are described as a very thick unit of greywacke and mudstone and a volcanic sequence which includes both acid and basic lavas and tuffs. The volcanics only occur near the base of the greywacke sequence in the northeastern part of the study area. A number of granitoid bodies, including granite, granodiorite and adamellite intrude rocks of the Yellowknife Supergroup in the northeast, northwest and south-western quadrants of the area. The intrusives are surrounded by wide aureoles of metamorphism within which the sediments have been converted to schists. In the southeast is a complex of alkaline intrusives, including syenites, anorthosites and granite, which belong to a younger, probably Proterozoic, magmatic cycle (Davidson, 1972).

3. CLASSIFICATION PROCEDURES

3.1 TEST LINES

Twelve lines or part lines were selected for detailed examination because they crossed 10 of the 12 major rock types known to be present. The test lines were located on 1:15,000 scale colour aerial photographs, which were then examined stereoscopically to distinguish those portions of the lines where each rock type cropped out. Henderson's (1976) geological map was used to provide a rock code for each outcrop. In addition since many of the rock types occur in several different parts of the map area, and to help with the analysis of the outcrop information, every occurrence of each rock type was given a separate coding. Thus, 24 lithologic units were created. The coded outcrop information was transferred onto a topographic map and the coordinates for each outcrop were calculated. This permitted the location and identity of each outcrop to be added to the magnetic tape containing the radiation data. Seven of the coded units were found to contain too few data points to establish spectral signatures. The 7 were dropped from the listing which then contained 17 unit names. This first stage in the investigation was completed by calculating the means and standard deviations for each of the 17 litho-radiation units. A complete spectral signature consists of 7 means (Total count, K, U, Th, U/K, U/Th) and the 7 corresponding standard deviations.

3.2 CLASSIFICATION ALGORITHM

The aim of the classification technique is to allocate each unknown set or partial set of radiation data to whichever spectral signature the unknown data set most closely resembles. The algorithm described here is based on the well-established Maximum Likelihood Decision Rule (Shlien and Goodenough, 1973).

If all radiation measurements from a particular rock unit follow a normal distribution, the probability, $P(x)$ of an individual measurement occurring within its range $(x_1, x_1 + dx)$ is given by,

$$P(x) = \frac{1}{\sigma\sqrt{2\pi}} e^{-\frac{(x - \bar{x})^2}{2\sigma^2}} dx$$

where $\bar{x}$ is the mean radiation measurement for that particular rock group and σ its standard deviation. If there are individual gamma-radiation measurements (potassium, uranium, thorium etc.) for each rock group that are uncorrelated, then the probability of a particular set of measurements occurring within its range, $P(x_1, x_2, \ldots x_n)$, $(x_1, x_1 + dx_1)$, $(x_2, x_2 + dx_2)$ etc., is given by,

$$P(x_1, x_2, \ldots x_n) = P(x_1)\, P(x_2) \ldots P(x_n)$$

$$= \frac{1}{\sigma_1\, \sigma_2 \cdots \sigma_n\, (\sqrt{2\pi})^n} e^{-\frac{(x_1 - \bar{x}_1)^2}{2\sigma_1^2} - \ldots - \frac{(x_n - \bar{x}_n)^2}{2\sigma_n^2}} dx_1 \ldots dx_n$$

where $\bar{x}_i$ and σ_i are the means and standard deviations for a particular rock group, i.

For a particular set of gamma-radiation measurements, the most probable rock group to which those measurements belong will be the one in which, $P(x_1, x_2 \ldots x_n)$ has a maximum value.

The application of this algorithm requires a solution to two problems - to decide which elements or ratios or combination of both, to use in the classification procedure. Table II is a matrix of the correlation coefficients of the seven channels of information. The 1730 radiation readings from the test lines are used to produce the table. While the degree of correlation between the different elements and ratios is quite variable, it was not feasible to use the matrix to decide which element or ratios or combination of both would be most efficient. Many of the spectral signatures determined so far are not unique. Many of them are nearly identical or overlap with one or other classes in one or several of the data channels. The class spectra have to be combined in some way to develop a smaller list of spectra, reasonably distinct from each other in at least one of the channels. Both problems were solved in the following way:

By applying the algorithm to the test line date with geological information, a cross-tabulation table was prepared which showed how many data points were correctly classified and how many were not. The table also showed where the wrongly classified data was being allocated, and the percentage of successfully classified data points for each class and for the test lines as a whole. The table was repeated 127 times to investigate all of the possible combination of elements and ratios that could be used to classify the data. The elements and ratios used to produce the table with the highest percentage of successfully classified data points were also used to carry out the spectral grouping process. The first classification table contained 17 rock spectra. The rock type with the lowest percentage of correctly classified values was combined with the rock type with which it was most closely identified. Another classification table was prepared with 16 spectral classes, using the same elements and ratios in the algorithm. Once again, the spectrum with the fewest identified data points was chosen to be combined with that which it most closely resembled. New means and standard deviations were calculated for each new grouping. In this way, the number of spectra was reduced one by one until a stage was reached at which a further reduction in the number of spectra would not result in a significant increase in the percentage of successfully identified points. The exercise to determine the most useful combination of elements and ratios for the classification was repeated with 18 classes and again when the number of spectral classes was reduced to 9, at which point the grouping was ended. The final test line classification table showing the nine final classes is reproduced as Table III. It shows that 78.87% of the test line data were allocated correctly within the 9 spectral classes. The success rate for individual classes ranges from 66.7% to 95.1%. A combination of the total count, potassium, U/K and Th/K channels were most successful for classifying the data at both the 18 and the 9 spectra levels. This was also the combination used to classify the whole survey area. Table IV shows how the percentages of correctly classified data varies according to the several elements and ratios used in the classification routine. If each of the 7 channels were completely uncorrelated, optimum success would be achieved by using all the elements and all the ratios to classify the data. Evidently there is sufficient correlation between the channels to make it very difficult to predict which ones to use with the algorithm. Before extending the classification routine to the full survey area, the classifying routine was modified to ensure that each classified value actually lay within a reasonable distance of the mean of the class in which it was classified. The 'reasonable' distance was set at 2.6 σ above and below the mean, which would ensure a 99% probability that, for the channel tested, the data are derived from that population to which they are classified. Because four independent tests are involved, rejection by any one test means that the data point is reclassified as '000' i.e. it becomes an unclassified data point. Thus there is a 96% probability (0.99^4) that any classified data point will have integral, potassium, U/K and Th/K values within 2.6 σ of the means which define its class.

Early 1:50,000 scale computer printout maps of classified data from the whole survey area showed a fairly large portion of the north-east quadrant of the survey area as class 000, i.e. unclassified. Histograms were prepared for these points which indicated that the 000's here represented 2 quite distinct classes. These 2 classes (coded as MAR and VLO) were added to the class listing. The statistics relating to the final list of 11 classes are contained in Table V. The degree to which the classes are separated is shown graphically in Figure 2. While the integral and potassium channels are the most highly correlated it is also evident that these two channels do separate most efficiently, class YS (by far the largest class of all) from the other classes. One more modification was made to the class list. To improve the sensitivity of the classification, class YS was split into 3 equal sized subclasses. (YSA, YSB, YSC), using the integral channel. Details are included on Table V. Water is also recognized as a class. All data points where the potassium channel contains less than 100 counts, are classified as water.

The whole area was again classified and a computer printed map at 1:50,000 scale produced. A small portion of the map with geological boundaries superimposed, is reproduced as Figure 3.

4. COMPARISON OF GEOLOGY AND RADIOMETRIC MAPS

Reference should be made to Figure 4 (Geology) and 5 (Radiometric Map).

4.1 N.W. PLUTONIC COMPLEX

There are eight separate intrusives in this northwest quadrant, all of which are described as porphyritic, biotite adamellite. All but two of the intrusives can be recognized on the radiation map. The boundaries of these 6 intrusives on the radiation map match those on the geology map quite closely except in a few local areas where swampy valleys occur. One of the two missed intrusives is small and is not crossed by a flight line. The other is largely obscured by drift. The two largest of the intrusives, (Duncan Lake and Sparrow Lake), are characterized as class G3 although the borders of the intrusives are more highly radioactive as is shown by the presence of classes G2 and G4. The Wedge Lake intrusive is particularly interesting because it has quite different radiation characteristics (G3X) to any other part of the survey area.

4.2 S.W. PLUTONIC COMPLEX

Most of the southwest quadrant of the area is underlain by granodioritic rocks intrusive into the sediments of the Yellowknife Supergroup. The largest granodiorite is subdivided by several curvilinear features, mostly lake filled valleys, but no consistent lithological differences have been recognized between the areas separated by these sutures. The most important feature of the radiation pattern here is that the granodiorite is normally indistinguishable from the mudstones and schists of the surrounding Yellowknife Supergroup. These are a number of exceptions to this. A dome shaped area, separated from the main granodiorite body by curvilinear sutures, becomes prominent on the radiometric map because of a marked increase in the proportions of class G3C (very low U/K ratio). Three of the eight separate intrusions of granodiorite in the south-central part of the survey area also show this increase in class G3C.

The southeastern tip of the main granodiorite body (also partly bounded by a suture) is different because of the presence of numerous scattered YSC data points which indicate a significant increase in regional radiation levels. There are also 9 small occurrences of classes G3, G4, G2 and YSC. All of these indicate higher radiation sources, believed to be small intrusions or pegmatites. None of these can be correlated with features on the geological map. At Matonabee Point, on the shoreline of Great Slave Lake there is an adamellite correlated with the plutons in the northwest quadrant. The rock is classified as G2 and G4, both of which are significant because of their relatively high uranium content (6-7 ppm).

4.3 SOUTHEAST PLUTONIC COMPLEX

This alkaline complex is regarded by Davidson (1972) as being quite distinct from all other parts of the area. The greater part of the complex between Great Slave Lake and Blachford Lake is a hornblende granite with a core of hornblende syenite. The syenite is indistinguishable from the northern half of the granite. Most of the southern half of the hornblende granite is characterized by radiation levels similar to that of the Yellowknife Supergroup sediments. Two portions of the granite are highly anomalous. One of these, labelled G3X, lying close to the syenite contact, is described by Davidson (1972) as a quartz breccia containing uranium mineralization. The second area, labelled S, G3X, follows the shoreline of Great Slave Lake for a distance of 9 km and is presumed to be related to the extensive regional fractures that mark the edge of the lake. To the west of the hornblende granite there is a group of granites, syenites and anorthosites. The anorthosite with a predominance of G3C values, has a similar character to G3C-rich parts of the southwest granodiorite complex. The granites and syenites have a similar radiation pattern to the south-east tip of the southwest granodiorites.

To the west there is a narrow gabbro dike, which follows a lake-filled valley and so cannot be recognized. To the west again, there is an adamellite with a very similar radiation pattern to that of the adamellite in the northwest quadrant. In the north the granite is mostly class G3, becoming more highly radioactive (G2, G4) towards Great Slave Lake.

4.4 NORTHEAST PLUTONIC COMPLEX

The central core of this complex, is a massive adamellite characterized by the presence of scattered YSC values in a background of YSB, VLO and MAR. The western boundary of the radiation pattern follows that of the geology quite closely in the N.W. but extends beyond the

known lithological boundaries to the southeast and to the north to include a series of mixed migmatites, tonalites and diorites. The mixed gneiss which crops out to the northwest of the Morose Lake adamellite has two distinctive radiation patterns. The eastern half of the gneiss has a radiation pattern that is very like the mudstones of the Yellowknife Supergroup. The western half (VLO(MAR)) is quite unlike any other part of the survey area. The Redout Lake granite underlies most of the southern portion of the northeast complex. The rock is described by Davidson (1972) as being structurally complex and variable in composition. This being so, it is surprising that the boundaries of the Redout granite and the corresponding radiation pattern (G2, G3, G3X) fit each other so well.

From Detour Lake, a spine of foliated muscovite-biotite adamellite extends southwards into the rocks of the Yellowknife Supergroup. This adamellite is correlated on the geology map (Figure 4) with the adamellites of the northwest complex. As happens with some other adamellites, the Detour Lake adamellite appears to be zoned, the southern tip carrying the highest uranium values (G2(G7)) and the northern part (YSC) lower quantities of uranium.

The southern part of the Detour Lake adamellite and portions of the Redout granite both contain radiation classes that may indicate areas of economic interest. Two other parts of the northeast complex both with similar radiation patterns (G2(G3X)) may also be of interest for exploration. One area is located east of the Morose Lake adamellite and is centred on an adamellite of the northwest complex variety; the other is also centred on an adamellite at the northeast corner of the survey area.

4.5 YELLOWKNIFE SUPERGROUP

The acid and basic volcanic rocks occur only around the margins of the northeast plutonic complex. Along the western edge of this complex, only basic rocks occur and these are delineated very precisely by the class MAR. West of the Detour Lake granite, the basic rocks appear to be mixed with more acid rocks since the volcanics are designated by a mixture of MAR and VLO. Here, too, an area known to be underlain by acid flows alone, has been classified as YSC. East of the Detour Lake granite, the mixed acid and basic flows indicated on the geology map is classified as YSC (VLO) suggesting that the rocks here are mainly acid in composition.

Throughout most of the north and central parts of the area the mudstones and schists are mostly classified as YSA with scattered YSB and VLO. MAR occurs mostly in areas of marsh or immediately adjacent to lakes. South of Campbell and Hearne Lake there is a marked increase in the numbers of YSB data points. This increase in YSB can be traced westwards into the southwest granodiorites, and then northwards along the western margin the northwestern pluton complex. The advent of YSB indicates a modest regional increase in radioactivity levels. An earlier classification of this area (Newton and Slaney, 1977) based on the elements K, U, and Th alone indicated a regional increase of 1 to 2 ppm thorium and 0.5 to 1.0% potassium in this southern area. The reason for this regional increase is not known. A few small areas occur within the sediments where data values representing increased levels of radiation are found. The three largest of these occur adjacent to Campbell and Hearne Lakes and are believed to represent pegmatites or other small intrusions. None of these features appear on Henderson's compilation.

5. SUMMARY OF RESULTS

Eleven radiation signatures (plus a water signature) have been established by analysing airborne gamma-ray data from a limited number of test lines where the geology is known. Using these 11 signatures and an algorithm based on the Maximum Likelihood Decision rule, the whole study area has been classified and compared with a map of the geology. None of the radiation spectra can be related uniquely to any one rock type. All rock types are represented rather by patterns of different spectral classes. More than 20 spectral patterns occur within the radiation map, most of which can be related to one or more rock types. The boundaries of the spectral patterns often coincide closely with those of the geology map except where overburden or swamp obscures the contact. Spectral patterns often repeat where the same rock recurs, thus agreeing with the geology as mapped. In some cases the contrary happens, indicating that geochemical differences exist between rocks given the same identification. Many of the plutonic intrusions are inhomogeneous. Such evidence might indicate the need for further field or petrological investigations. Some classes are, by definition, more radioactive than others, e.g. classes G2, G4, G7 and G3X all have mean eU contents of 5.5 to 7.0 ppm. The only published occurrence of uranium mineralization in the area is located in a quartz breccia zone classified as G3X. Possibly other areas of G3X as well as G2, G4 and G7 deserve investigation for signs of uranium mineralization.

The techniques used in this study are best applied in areas where outcrops are extensive, and the overburden minimal. This would include large portions of the Canadian Precambrian Shield and much of the Arctic Islands. A geologic map and airphotos at 1:30,000 scale or larger are essential aids, preferably acquired about the same time of year as the gamma-ray survey data. The spacing of the survey lines should not be greater than 2.5 km; the closer the lines, the better the results will be.

6. REFERENCES

Cameron, G.W., B.E. Elliott, and K.A. Richardson. 1976. Effects of Line Spacing on Contoured Airborne Gamma-Ray Spectrometry Data. Paper IAEA-SM-208/2, in Exploration for Uranium Ore Deposits, pp. 81-92, International Atomic Energy Agency, Vienna.

Darnley, A.G. and M. Fleet. 1968. Evaluation of Airborne Gamma-Ray Spectrometry in the Bancroft and Elliot Lake Areas of Ontario, Canada. 5th Symp. Rem. Sens. Envir., Ann Arbor, Mich., pp. 833-853.

Darnley, A.G. 1970. Airborne Gamma-Ray Spectrometry. Can. Min. and Metall. Bull. 63, pp. 145-154.

Darnley, A.G. 1975. Geophysics in Uranium Exploration. in Uranium Exploration '75, Geol. Surv. Can., Paper 75-26, pp. 21-31.

Davidson, A. 1972. Granite Studies in the Slave Province. Report of Activities, Geol. Surv. Canada, 72-1, Part A, pp. 109-115.

Davidson, A. 1978. The Blachford Lake Intrusive Suite: An Aphebian Alkaline Intrusive Complex in the Slave Province, Northwest Territories. Geol. Surv. Can., Paper 78-1A, pp. 119-127.

Grasty, R.L. 1972. Airborne Gamma Spectrometry Data Processing Manual. Geol. Surv. Can., Open File No. 109.

Grasty, R.L. and K.A. Richardson. 1972. Gamma-Spectrometer Survey of an Area North of the Great Slave Lake and the Islands of the East Arm of the Great Slave Lake, Northwest Territories. 7 maps and profiles, Open File Report No. 124, Geol. Surv. Can.

Grasty, R.L. 1976a. Applications of Gamma Radiation in Remote Sensing. in Remote Sensing for Environmental Sciences, Ed. E. Schanda, Springer-Verlag, N. York.

Henderson, J.B., M.P. Cecile, and D.C. Kamineni. 1972. Yellowknife and Hearne Lake Map Areas, District of Mackenzie. Report of Activities, Geol. Surv. Canada 72-1, Part A, pp. 117-119

Henderson, J.B. 1976. Yellowknife (85J) and Hearne Lake (85I) Map Areas, District of Mackenzie, N.W.T. Compiled at 1:125,000, Open File 353, Geol. Surv. Can.

Newton, A.R. and V.R. Slaney. 1977. Geological Interpretation of an Airborne Gamma-Ray Spectrometer Survey of the Hearne Lake Area, N.W.T. Geol. Surv. Can. Paper 77-32.

Richardson, K.A. 1976. Canada's Uranium Reconnaissance Program. in Uranium Geophysical Technology Symposium (Abstract), Bendix Corp., Grand Junction, Colorado, Sept. 14-16, 1976.

Shlien, S. and D. Goodenough. 1973. Automatic Interpretation of ERTS-A Imagery Using the Maximum Likelihood Decision Rule. Canada Centre for Remote Sensing Research Rep. 73-2.

Slaney, V.R. 1971. Colour Aerial Photography of Hearne Lake (85I) and Yellowknife (85J) Map Sheets. Geol. Surv. Can. Open File 100.

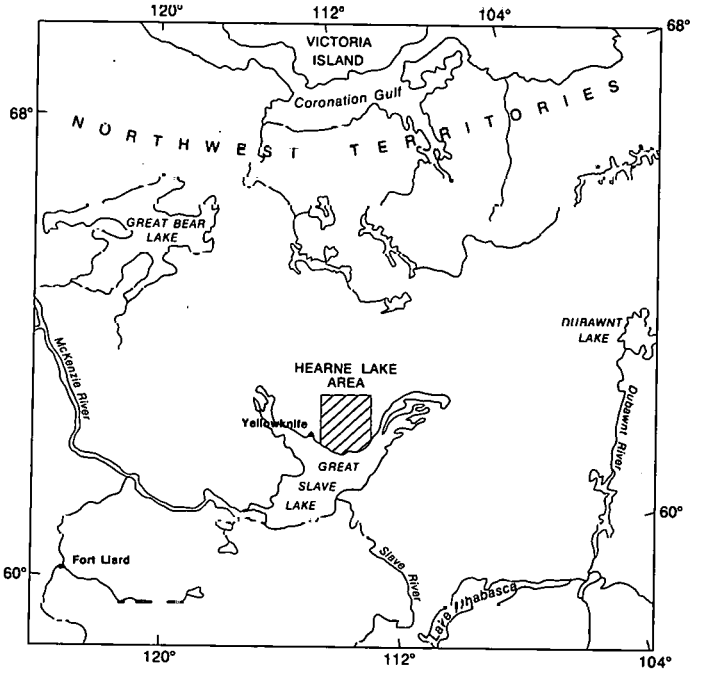

FIGURE 1 LOCATION OF HEARNE LAKE AREA

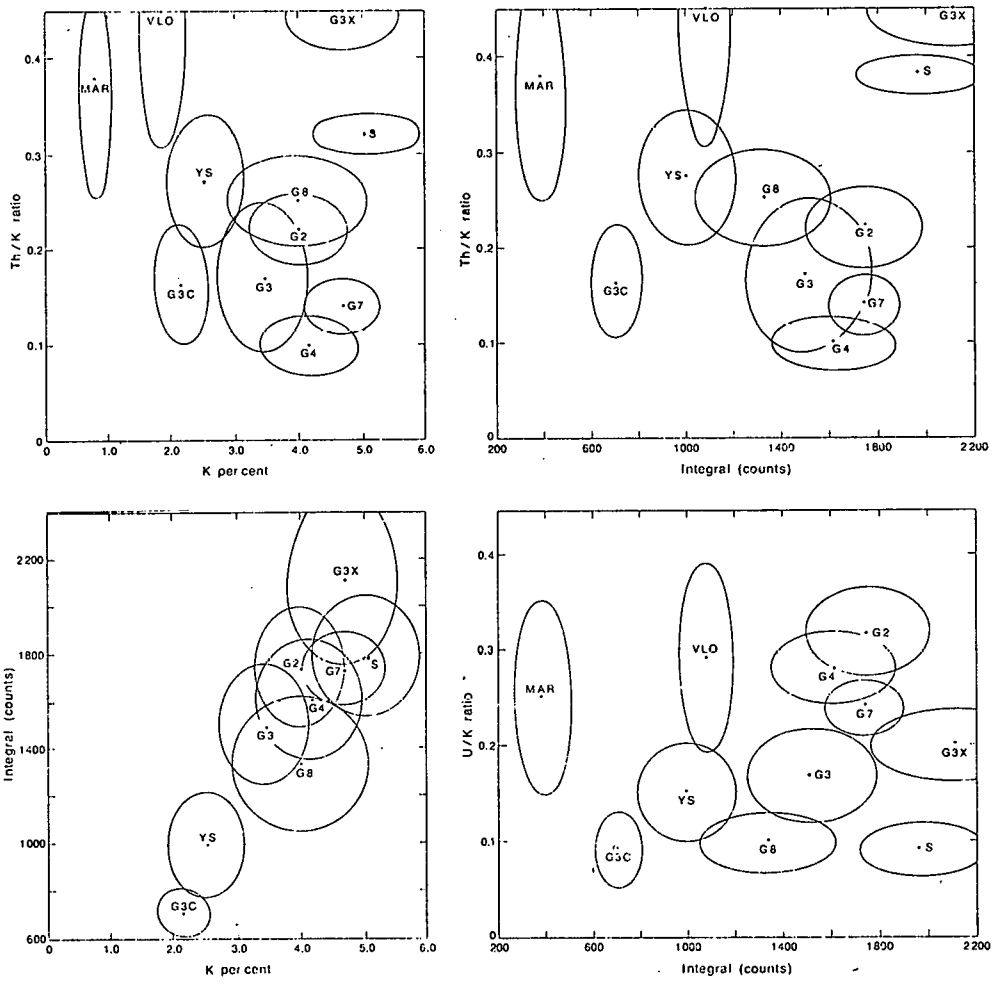
VLO
G3X
MAR
S
YS
G8
G2
G3C
G3
G7
G4
Th/K ratio
K per cent
Integral (counts)
U/K ratio

FIGURE 2

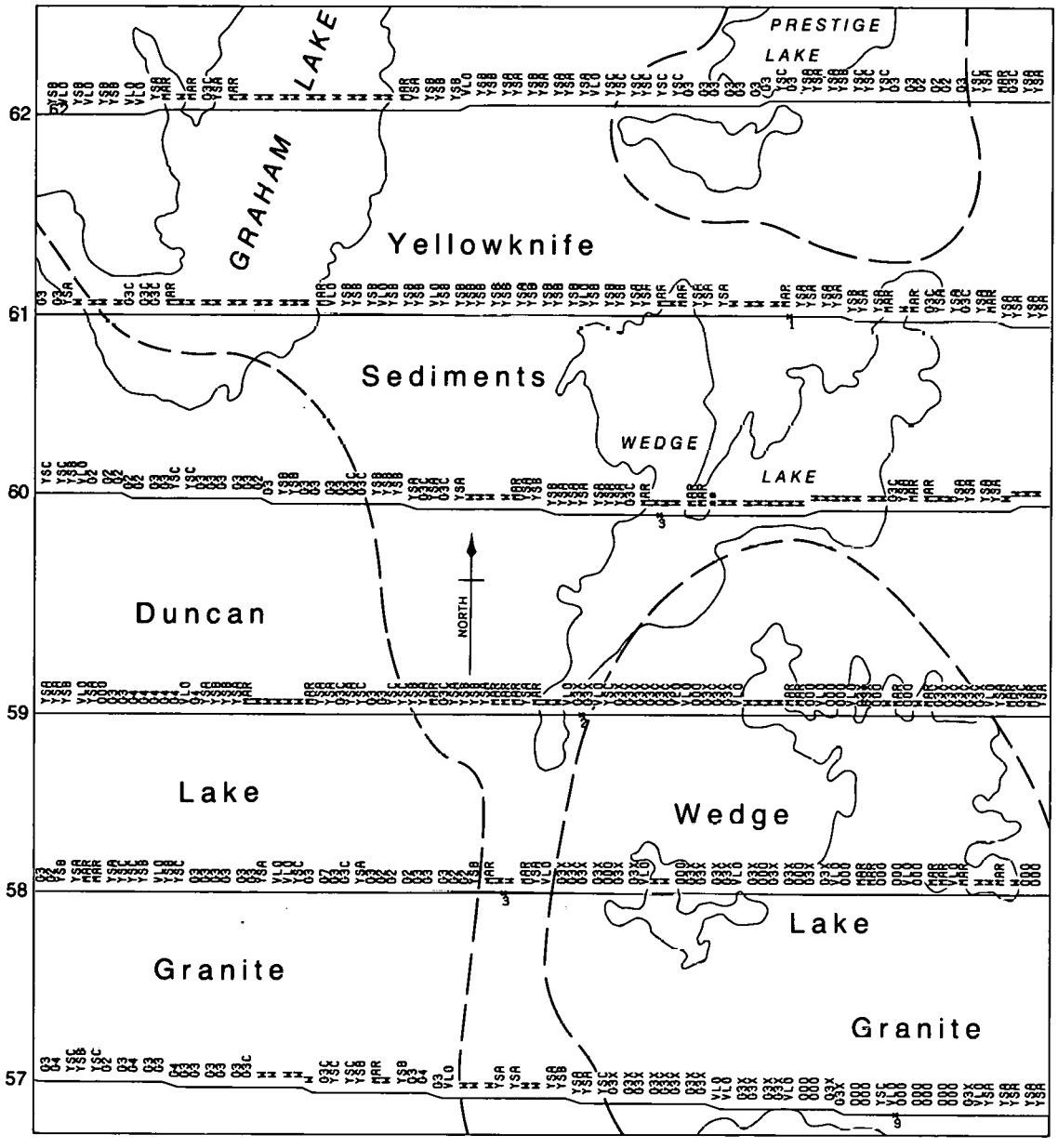

FIGURE 3 PARTS OF THE NORTHWEST IGNEOUS COMPLEX

COMPUTER CLASSIFIED PRINTOUT WITH GEOLOGICAL ANNOTATION

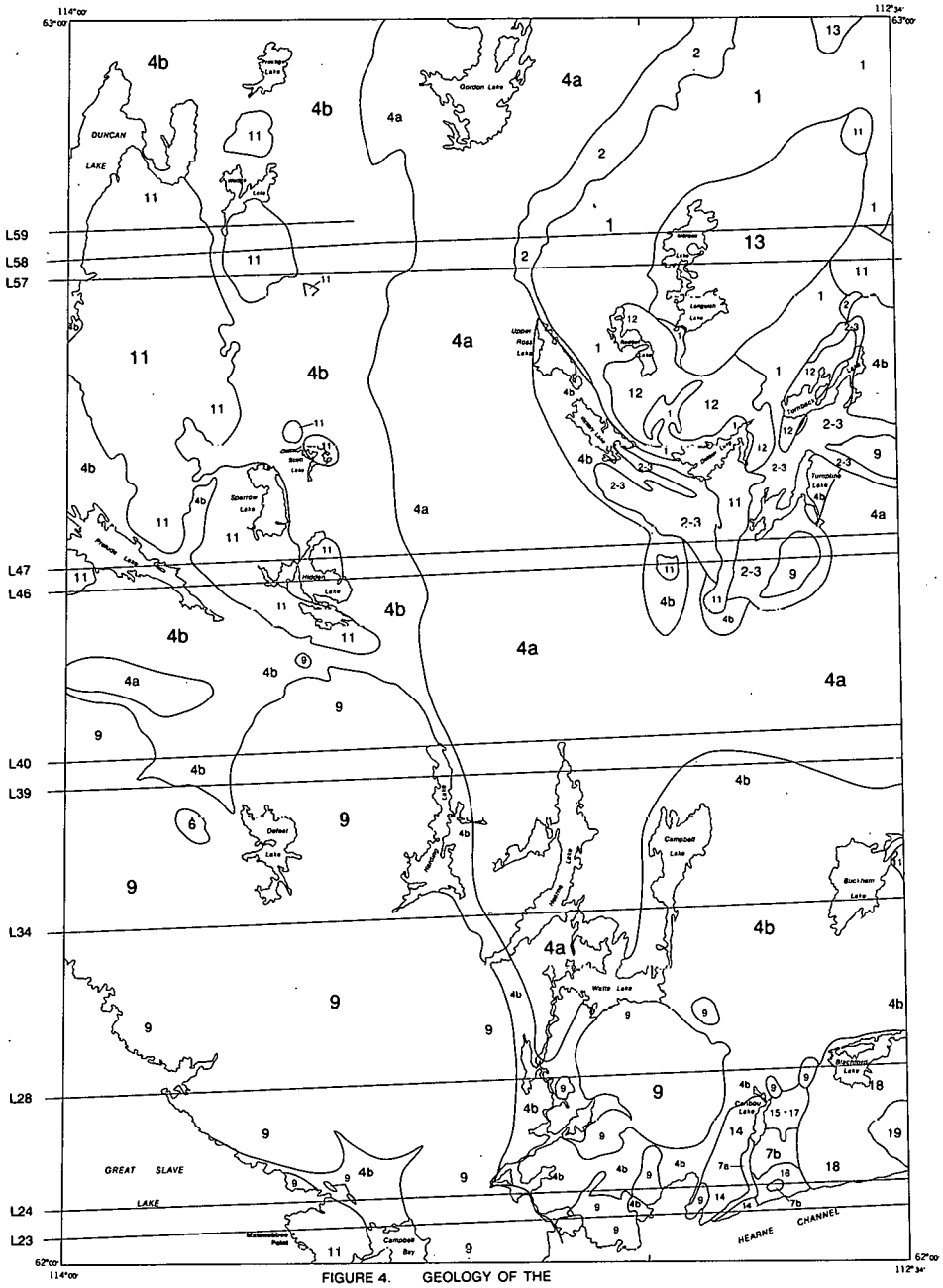

FIGURE 4. GEOLOGY OF THE HEARNE LAKE AREA
DISTRICT OF MACKENZIE
NORTHWEST TERRITORIES

Kilometres 6 0 6 12 18 Kilometres
Miles 4 0 4 8 Miles

Simplified geology from Geological Survey of Canada, Open File No. 353, June 1976, 1:125,000
Compiled by J.B. Henderson

19 Syenite, hornblende
18 Alkali granite, coarse grained, hornblende
17 Granite, fine grained, hornblende, biotite
16 Quartz syenite, hornblende
15 Syenite, hornblende
14 Adamellite, coarse, porphyritic, biotite
13 Adamellite, coarse, porphyritic, muscovite, biotite
12 Granite, medium fine-grained
11 Adamellite, medium grain, biotite, muscovite
9 Granodiorite
7b Anorthosite
7a Gabbro
6 Amphibolite pluton

YELLOWKNIFE SUPERGROUP

4b Psammitic, pelitic schists
4a Graywacke, mudstone
2-3 Mafic and felsic volcanic rocks
2 Mafic volcanic rocks
1 Mixed diorite, tonalite,

L47—— Test line for gamma ray analysis

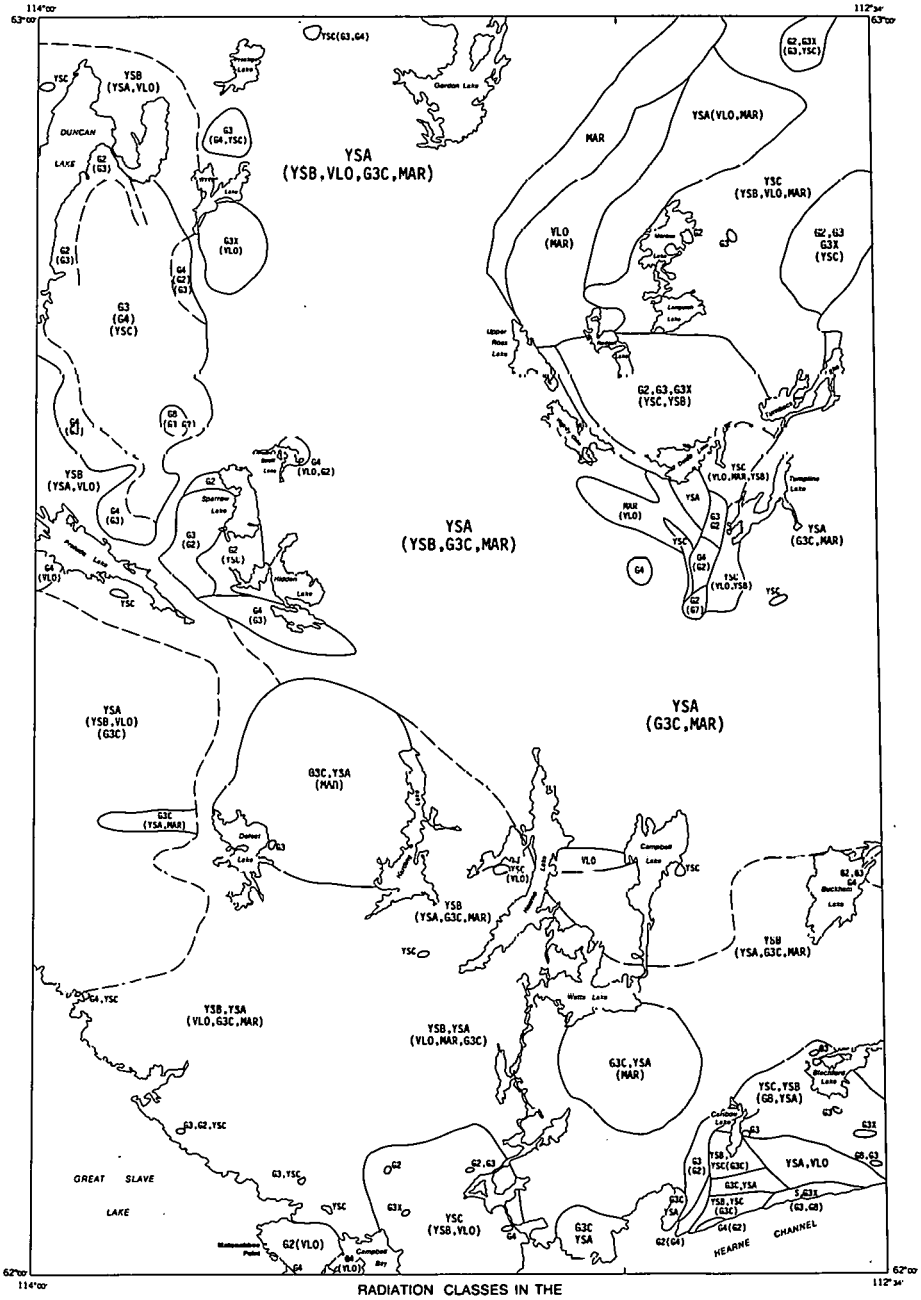

RADIATION CLASSES IN THE
HEARNE LAKE AREA
DISTRICT OF MACKENZIE
NORTHWEST TERRITORIES

Kilometres 0 4 8 12 16 Kilometres
Miles 0 4 8 Miles

G3 Dominant class

G3(G4,YSC) Predominantly G3, with minor G4 and YSC classes

The classes are described in Table 5

FIGURE 5

TABLE I

Geological Survey of Canada Airborne Gamma-Ray System

Aircraft - Short Bros. Skyvan

Survey Airspeed - 190 ± 30 km/hr.

Mean Flying Height - 120 m

Line Spacing - 2.5 km

Gamma-Ray Spectrometer - designed by Atomic Energy of Canada Ltd.

Detectors - 12 NaI(Tl) crystals, diameter 230 mm x 130 mm thick, 50,000 ml total volume

Channels - 0.41 - 2.81 MeV, Integral

1.37 - 1.57 MeV, Potassium (^{40}K)

1.66 - 1.86 MeV, eUranium (^{214}Bi)

2.41 - 2.81 MeV, eThorium (^{208}Tl)

Integration Time - 2.5 secs, K, eU, eTh; 0.5 secs Integral

Record - magnetic tape, strip chart

Data Corrected For - background, aircraft-terrain distance, spectral stripping

Data Release - Geological Survey Open Files, Geophysical Map Series (paper prints and microfiche), Magnetic Tapes (on request). For each topographic map sheet - 7 contoured maps (Integral, eU, eTh, K, eU/eTh, eU/K, eTh/K). Approximately 40 flight line profiles (one map per line).

TABLE II

Number of Observations = 1730

	Mean (Counts)	St. Dev.	INT	K	U	Th	U/K	Th/K	U/Th
INT	1119.358	355.016	1.000						
K	390.185	127.350	.926	1.000					
U	62.580	35.400	.834	.734	1.000				
Th	97.399	45.766	.722	.538	.397	1.000			
U/K	.157	.058	.385	.190	.768	.118	1.000		
Th/K	.255	.084	.059	-.207	-.132	.661	.006	1.000	
U/Th	.723	.538	.272	.333	.596	-.319	.561	-.614	1.000

Correlation Coefficients Between the Elements and Ratios of the Radiation Data from the Test Lines

Int. K / U/K Th/K	Distribution of Data After Classification									Number of Samples	Total Wrongly Classified	Percent Correct
	G2	G7	G8	S	G3	YS	G4	G3C	G3X			
Classes Based on Known Geology G2	23	0	0	0	3	1	2	0	0	29	6	79.3
G7	2	16	0	0	1	0	5	0	0	24	8	66.7
G8	0	0	14	2	0	3	0	1	0	20	6	70.0
S	0	0	1	11	0	0	0	0	0	12	1	91.7
G3	18	10	8	3	171	15	10	0	7	242	71	70.7
YS	19	0	83	7	44	1045	2	113	3	1311	266	79.7
G4	1	0	0	0	1	0	14	0	0	16	2	87.5
G3C	0	0	0	0	0	2	0	26	0	28	2	92.9
G3X	0	0	0	0	1	1	0	0	39	41	2	95.1
							T O T A L S			1723	364	78.87

TABLE III Test Lines Classified and Correlated with Geology

9 Classes

I+K+U+Th	67.6	69.5	72.7	68.0	75.6	71.3	72.8	75.3
K+U+Th	68.3	68.0	72.8	67.4	75.0	68.7	73.3	75.0
I+U+Th	63.3	65.9	70.3	62.3	74.2	65.9	70.0	72.0
I+K+Th	60.7	71.5	64.8	65.4	75.9	72.1	69.5	76.0
I+K+U	66.4	65.6	75.9	68.1	76.8	70.8	75.7	77.1
Th+U	57.5	56.6	68.3	56.1	66.0	57.0	65.1	63.4
K+Th	54.8	69.2	61.5	63.2	74.9	70.3	67.2	73.0
K+U	60.0	57.2	76.0	66.6	78.2	64.8	76.7	72.8
I+Th	57.2	67.1	63.7	62.1	75.0	68.0	68.1	72.6
I+U	63.6	62.3	74.9	64.0	73.2	61.4	73.4	70.0
I+K	60.3	66.9	68.9	67.1	78.9	72.8	74.2	77.7
Th	5.7	42.4	54.4	52.5	58.9	52.8	59.2	58.1
U	9.6	45.3	35.8	47.9	57.9	53.6	54.8	56.4
K	44.4	58.9	66.2	63.5	75.0	67.3	71.4	72.2
I	58.2	62.5	69.0	63.7	76.0	64.3	72.3	71.4
Nil	0.0	26.6	15.8	36.7	44.6	43.8	42.9	47.9
	Nil	U/K	Th/K	U/Th	U/K+Th/K	U/K+U/Th	U/Th+Th/K	U/Th+U/K+Th/K

TABLE IV Percentages of Correctly Classified Test Line Data Using All Combinations of Elements and Ratios

TABLE V - CLASS STATISTICS

Class	Integral (Counts) Mean	S.D.	Potassium (%) Mean	S.D.	eUranium (ppm) Mean	S.D.	eThorium (ppm) Mean	S.D.	eU/K(x10^4) Mean	S.D.	eU/eTh Mean	S.D.	eTh/K(x10^4) Mean	S.D.
G2	1739	243	4.00	0.71	7.11	1.56	13.08	2.43	1.79	0.32	0.56	0.17	3.33	0.62
G7	1729	148	4.65	0.57	6.70	.91	9.91	2.53	1.45	0.20	0.72	0.20	2.12	0.44
G8	1335	275	3.98	1.09	2.27	0.74	14.58	3.72	0.59	0.19	0.16	0.05	3.78	0.78
S	1794	256	5.05	0.82	3.11	0.89	23.69	3.80	0.62	0.18	0.13	0.04	4.71	0.31
G3	1483	265	4.21	0.67	4.42	1.33	10.73	5.29	1.06	0.29	0.51	0.31	2.55	1.17
YSA*	761	127	1.97	0.39	1.66	0.62	7.15	1.87	0.86	0.32	0.25	0.11	3.71	0.98
YSB*	978	50	2.54	0.26	2.18	0.65	9.91	1.90	0.87	0.29	0.23	0.09	3.95	0.90
YSC*	1220	160	3.07	0.43	3.09	1.12	13.52	2.68	1.01	0.35	0.24	0.12	4.46	0.99
G4	1613	256	4.13	0.76	7.02	1.63	6.18	1.53	1.71	0.26	1.20	0.40	1.53	0.43
G3C	704	102	2.14	0.38	1.19	0.52	5.17	2.11	0.57	0.24	0.34	0.48	2.39	0.90
G3X	2112	353	4.69	0.84	5.64	1.23	31.28	6.42	1.22	0.24	0.18	0.04	6.68	0.69
VLO	1120	90	1.86	0.34	2.73	0.91	13.67	2.56	0.29	0.10	0.20	0.09	0.45	0.15
MAR	380	100	0.81	0.22	1.09	0.73	3.33	1.33	0.25	0.10	0.33	0.24	0.38	0.13

*YS divided into 3 subclasses using Integral Count - YSA = 434-890; YSB = 891-1070; YSC = 1071-1546 counts

Factors used to convert instrument counts are as follows: 1%K = 134 counts, 1 ppm eU = 22 counts, 1 ppm eTh = 9 counts

THIS PAGE

WAS INTENTIONALLY

LEFT BLANK

RESOURCES ENGINEERING INVESTIGATIONS - AN APPROACH AND OUTPUT APPLICABLE TO 'CHANDRAPUR PROJECT'

A. Parthasarathy
Centre of Studies in Resources Engineering
I.I.T., Bombay, India

ABSTRACT

The basic concepts, methodology and the interpretative means specially relevant to the various disciplines are to be used in exploration, assessment and utilisation of natural resources. 'Chandrapur Project' presently described is a multidisciplinary project. The project pertains to the study of natural resources in an area of nearly 6000 sq. kms in parts of Chandrapur District, Maharashtra State, India.

The region is largely covered by forests and is endowed with mineral resources not fully explored and utilised. Ground and surface water potential of the region are to be fully assessed and the region is to be put to optimal landuse development for the fuller economic growth of the area.

Project involves use of satellite imageries and aerial photographs followed by ground check, geological, hydrologic, geotechnical and pedological investigations. With the help of the maps prepared from field and laboratory data relevant to this integrated approach pertaining to Resources Engineering studies and the results obtained, the work in progress is briefly presented in this paper.

INTRODUCTION

Exploration, assessment and proper utilisation of natural resources call for an application of wide range of methods in the field and laboratory. The 'Chandrapur Project' presently described is a multidisciplinary project. The basic data are obtained by the use of remote sensing techniques for studies relating to minerals, water and soils and the data are also obtained through field and laboratory work on the materials by application of techniques normally used in ground engineering and earth sciences. An attempt is made to arrive at an optimal use of natural resources. Such an integrated approach is considered relevant for achieving economic growth and development at a rapid pace in particularly in such unexplored, backward and rural areas and hence the technology that is developed in this context would be of immense value.

PROJECT AREA

Chandrapur district in Maharashtra State (India) covers an area of nearly 25,600 sq. kms and the region is known for its mineral riches and forest reserves. This district accounts for a large portion of state's mineral and forest reserves, and the ground water potential of the area has been estimated in terms of annual ground water recharge of 2300 million cubic metre and nearly this accounts for 11% of the recharge amount for the entire state. As against this, the extraction is hardly 2%. There are several hundreds of square kilometres of area within the region that need to be fully explored for its mineral and water resources for industrial development and optimal landuse planning. (I.C.A.R. 1977). The area covered under this project is nearly 6000 sq. kms.

At the first phase of investigation, an area of nearly 1000 sq. kms is being critically examined for the mineral resources, hydrologic conditions,

soils, forests and vegetation, using landsat imageries and aerial photography followed by ground check and detailed field investigations. An inter-disciplinary team of scientists and engineers are working on this project applying modern technological methods in an integrated manner.

With the help of the maps prepared from field and laboratory studies and based on the results obtained, the salient aspects of the work in progress is briefly presented in this paper.

The project area is covered by three Landsat imageries in parts and together with the aerial photographs available, the recognition of major lineament features and topographic expression have been made out.

GEOLOGY, GEOMORPHIC FEATURES AND MINERAL RESOURCES

The area falls on the water divide between Pranhita river on the west and Indravathi river on the east (Fig. 1). To the south a few kilometres away is the Godavari river (not shown in figure) linking the two above mentioned rivers. The black tone represents forested quartzite ridges. The grey tone on the east and south east represents shale, limestone plains. The slightly paler grey to the S.W. stands for sandstone platean and limestone plains. (V. Subramanian and A. Parthasarathy, 1977). Detailed microdensitometric studies in areas of tonal contrasts to correlate the spectral signatures with the lithologic boundaries and variations are under progress.

The photogeological map prepared for the area shows the presence of Archaean gneisses in N.E. corner of the area (toposheet 65 B/1). Southwest of this, are the sedimentaries (Pakhals) - quartzite ridges marking a N.W.-S.E. syncline plunging S.E. and the shales and limestones are to the S.E. Southwest of these are the sandstones and limestones (Gondwanas). The major structural features on the area that can be made out in the region is the faulted zone trending nearly N.W.-S.E. between the Gondwanas and Pakhals. The hard rock areas and region covered by sedimentaries and alluvium are investigated for mineral resources, ground and surface water potential and soil cover characteristics, and geotechnical properties.

To achieve this purpose, interdisciplinary approach to understand fully the natural resources of the area, based on the remote sensing data has been attempted.

Geomorphology as a parameter effectively integrates geology, soils, hydrology, vegetation and landuse. Application of geomorphic techniques in the field, for the study of a region for natural resources is hence imperative. Landscape patterns that recur are recognisable through interpretation from imageries and airphotos. Distinctive land systems can be further recognized and these are the results of harmonious grouping for landforms, bed rock structures, soils, vegetation and hydrologic conditions. Individual component units such as plains, plateaus have been distinguished in these land systems by the application of geomorphic techniques on representative sample site. For the region under investigation, various geomorphic features such as ridges (quartzites), residual hills, erosional pediments, limestone pavements, domal summit, ridge crest lines, stream orders, valley head slopes, valley side slopes, spur end slopes have been identified and geomorphic map prepared using international symbols. Such a map is significant, as with this as a base, soil and geologic data can be critically evaluated for their use. The geomorphic units recognized in the area fall under Archaean gneissic land systems, Purana quartzite and shale-limestone land system, Gondwana sandstone, shale land system, shale-limestone plains, quartz ridges, sandstone platean and gneissic plains are the major units observed with the characteristic soil and slope characteristics, and drainage associations. (S. Viswanathan et al 1977). Thus, from the geomorphic features of the area and soil cover it has been inferred that the ridges and valley provinces - quartzite land system has largely soil cover of coarse sandy material. The rolling ground of the shale land system is predominantly having clayey soil and at places sandy. The plains

comprising limestone land system has a cover of coarse to fine black sandy soil with calcareous material.

The geological map (part of area covered by Toposheet 65 B/1) based on field observations, shows in the central region, the Proterozoic formation - Pakhals, shales, limestones and quartzites with steep dips and major N.W. - S.E. trends (Fig. 2). Resting on these are the Gondwanas - limestones, sandstones and conglomerates (Oxfordian and Kimmeridgian). Archaean gneisses and granites are exposed sparsely in this region. However the Archaeans are well exposed to the north and N.E. parts of this area. Certain sporadic occurrence of graphite and sillimanite occur in the schistose and gneissic rocks. Limestones are predominant in this area and the barytes that occur in limestones and shales and their contacts are being investigated. Barytes occur as fracture, breccia and joint fillings in limestones and as boulders associated with shales. Geochemical studies on limestones have shown a wide range of types, with values of CaO ranging from 25-50%, MgO 5-10% and amount of insoluble residues vary considerably. Limestones of the area form 5 units and are grouped as (1) mixed rocks with carbonates, (2) impure dolomitic limestones, (3) impure limestones, (4) limestones. The good quality limestone in this area occur close to Mangigudam and they are being further examined for reserves and quality for their industrial use and application.

Preparation of macro-level land unit map form a prime requisite in resources investigation, and land resources map serve as a sound basis for integrated planning for optimal exploitation of land resources using airphotos of the area combined with field checks. Various units have been recognized and each of these units, is characterised in terms of lithology, physiographic division, landuse and soil composition. Each unit roughly corresponds to Integrated Resources Unit (IRU) and these units occur in a repetitive pattern. The map prepared is being utilised for choosing representative sites for intensive studies for geotechnical purposes, thereby reducing the number of study sites to the minimum needed and each such unit corresponds to minimal integrated resources unit (MIRU). Land unit map is also a basic soil and landuse map useful for agriculture and forestry.

HYDROLOGIC AND GEOTECHNICAL STUDIES

Realising that a rational policy for water resources planning and development of the region has to take into account the demand of its availability for the predominant occupational activity of the region viz. agricultural in a few and scattered tribal villages, in the otherwise predominantly forested areas, the hydrologic studies have been initiated.

The drainage network analysis reveals the dendritic branching of the streams to be predominant, forming radial and parallel patterns at places. The N.W.-S.E. trends of the rocks had influenced the stream courses and an occasional barbing is noticeable.

The ground water contour map has been prepared from the water levels observed in the existing open, shallow (> 20 m) dug wells (or the piezo-metric levels). Also the surface drainage pattern and geological features (structural aspects) were given due consideration in drawing the ground water contour map. It is evident from the map that the ground water table fluctuates in the range of 0-6 m. between post and premonsoon periods (1976 Oct.-1977 May) and works out to a recharge rate of approximately 6% of the mean annual rainfall. Detailed resistivity survey is in progress in the region.

Based on storage and transmissivity data to be obtained subsequent to drilling and conducting pumping tests, digital and analog modelling of the aquifers are to be worked out for water resources development. The hydrological data pertaining to the rivers, in terms of discharge and storage of rivers have been obtained and are being used to assess safe yield of surface water.

The major soil associations of the area have been demarcated based on genetic factors. These have been linked to the representative soil profiles examined in the field and further distinguished from laboratory work. The soils have been classified using the unified system. The suitability for engineering purposes is being determined. This coupled with strength data are useful in engineering landuse planning and performance prediction of the structure provided on these soils. Different soil units recognized on the parent rock materials of limestones, quartzites, sandstones, and shales and the depth to different horizons up to bed rock have been determined. It can be said in general that 'A horizon' consisting of mostly clayey sand varies in thickness from 20 cm - 1 metre; 'B horizon' 120 cm - 150 cm in thickness as seen from the profiles attached. B horizon is generally silty sand but is occasionally mixed with high percentage of gravel. Though the soil is residual in nature over a large area transported soils are observed in certain areas traversed by rivulets (Fig. 4).

An integrated map (Fig. 3) has been drawn showing the geomorphic provinces of the area under study incorporating as well, the data on the soil series pertaining to the above. Correlative trends if any, are to be critically examined using geomorphic features, geotechnical soil profiles and bed rock characteristics for engineering applications; combined particularly with pedological data, studies will be significant in landuse development.

It may be relevant to mention that attempts are being made to process data available in CCTs pertaining to this area (information collected by landsat) for generating thematic maps that can be correlated with special purpose maps obtained by integrated resources engineering studies. Computer print out map with ground data check for the region is being prepared. Preparation of scaled map and pattern recognition studies are in progress.

In conclusion, it may be said that the 'Chandrapur Project' (the results of the preliminary studies are presented in this paper) is an experimental study taken up at the centre for integrated resources engineering investigations not only to assess and utilise the natural resources through the application of modern methods of study such as remote sensing but also develop technology that is relevant and significant for achieving economic growth and development of hitherto undeveloped regions.

ACKNOWLEDGEMENTS

The author is grateful to Prof. A.K. De, Director, I.I.T. Bombay and Prof. R. Mallikarjunan, Head, Centre of Studies in Resources Engineering for all the encouragement given to this work. Thanks are due to my colleagues at the centre for their valuable suggestions and particularly to Dr. S. Viswanathan, Dr. V. Subramanian, Dr. G. Venkatachalam, and Dr. Pavate for their help in the preparation of maps presented.

REFERENCES

1. Indian Council of Agricultural Research, New Delhi, 1977, Report on 'Chandrapur District (Maharashtra), Resources Inventory - Programme for Integrated Rural Development.

2. V. Subramanyam and A. Parthasarathy, 1977, 'Some select mineral occurrences in parts of western and central India as reflected on space imageries and air photographs', Symposium on Remote Sensing for Hydrology, Agriculture and Mineral Resources - Abstract, ISRO Ahmedabad, 1977.

3. S. Viswanathan, V. Subramanyam, A. Parthasarathy, K.C. Sahu and G. Venkatraman, 'Integrated geomorphic studies and mineral resources evaluation of the area around Sironcha, Chandrapur District, Maharashtra State', National Seminar in Resources Engineering and Technology, CSRE, I.I.T Bombay, 1977.

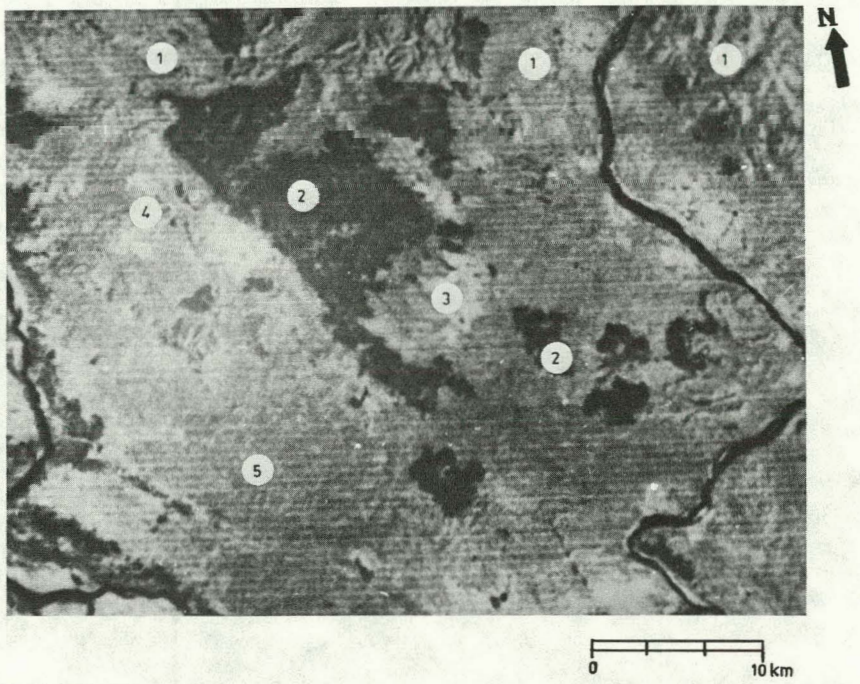

FIGURE.1. PART OF LANDSAT IMAGERY-SIRONCHA AREA BAND-7.

(LANDSAT IMAGERY OF BAND 7. COLLECTED ON 26th FEB. 73, CENTERED AT 19°00'N LATITUDE, 81°00' E LONGITUDE, DIMENSIONS ARE 185 km X 185 km).
1) ARCHAEAN GENISSESS. 2) PAKHAL QUARTZITES. 3) PAKHAL SHALE-LIMESTONES.
4) GONDWANA CONGLOMERATE-SANDSTONES 5) GONDWANA SANDSTONE-LIMESTONES.

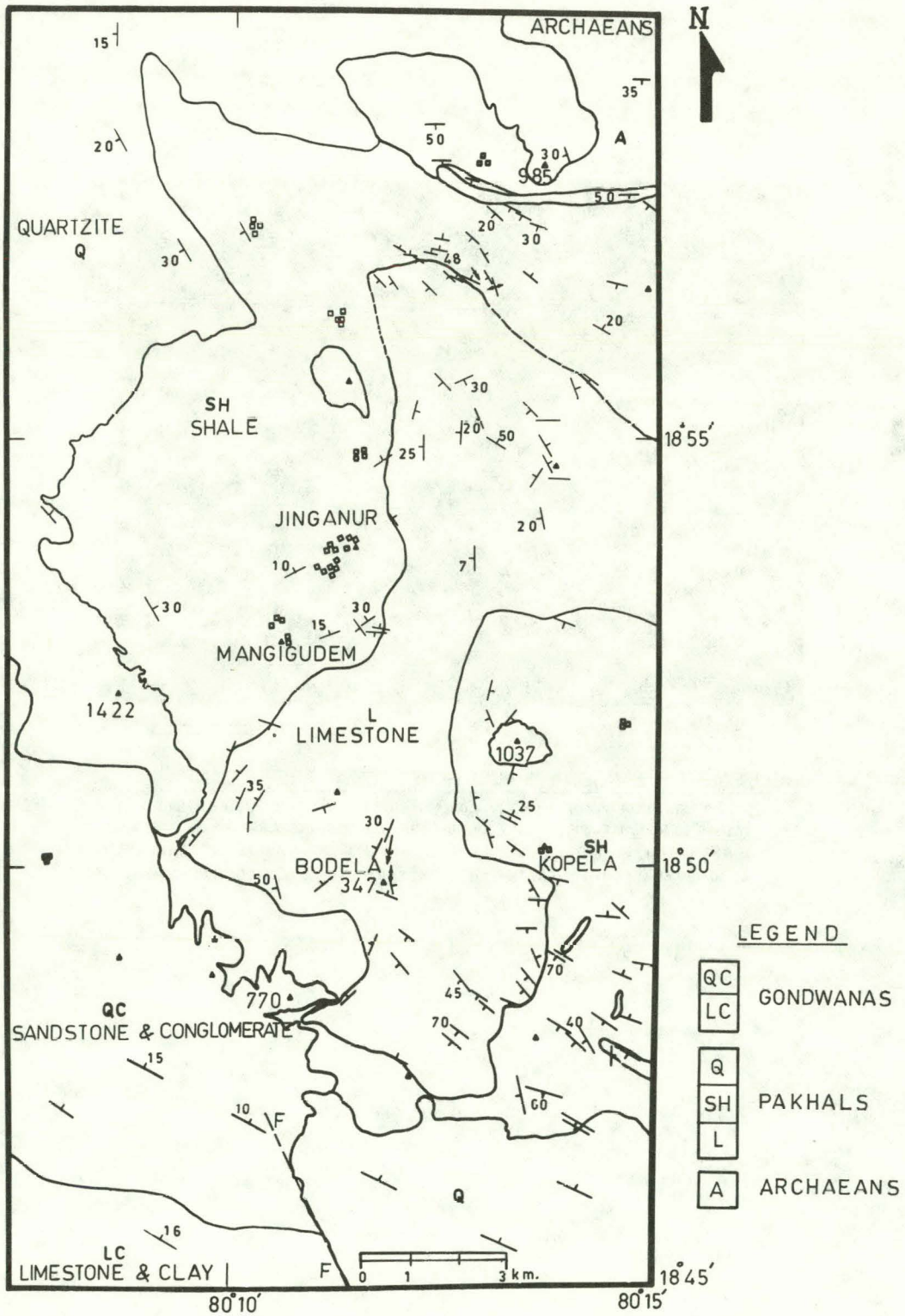

FIGURE.2. GEOLOGICAL MAP (PART OF SIRONCHA AREA).

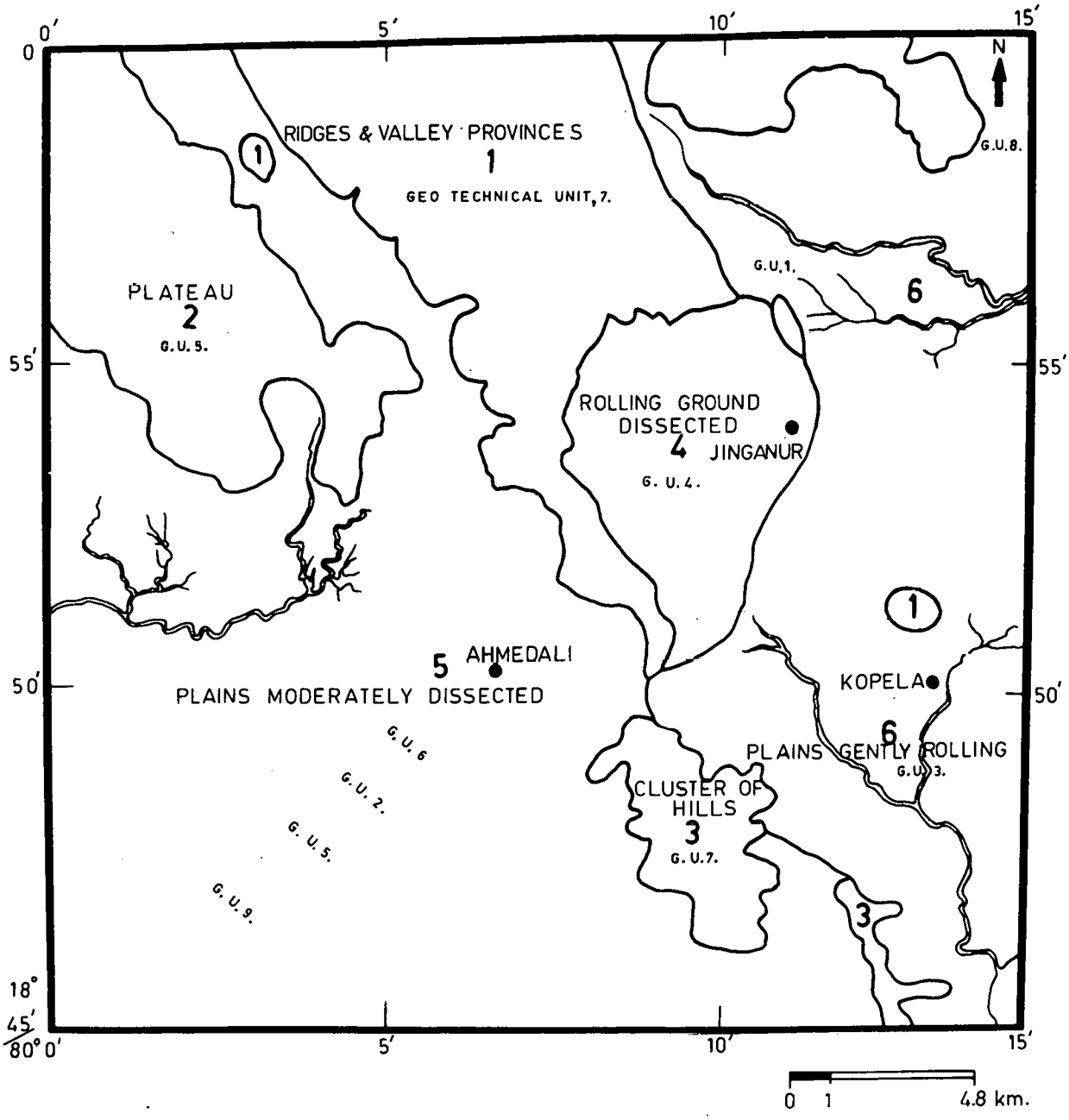

FIGURE.3. GEOMORPHIC PROVINCES AND GEOTECHNICAL UNITS.

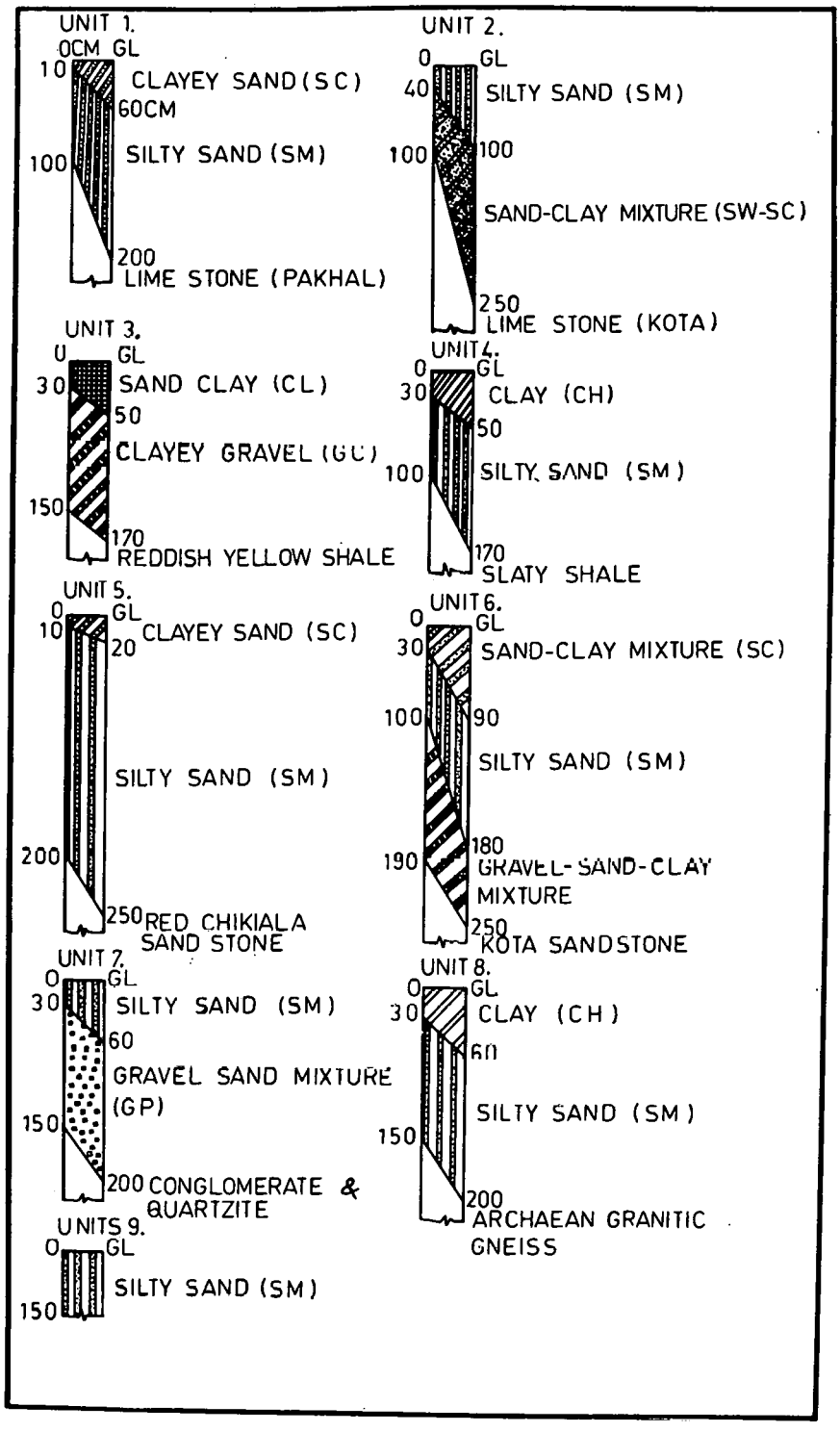

FIGURE.4. GEOTECHNICAL UNITS.

PHOTOGRAPHIC REMOTE SENSING AT CHIBA UNIVERSITY
(a) STUDIES OF KUMANO RIVER WATER AND
(b) ANALYSIS OF CONCRETE MOISTURE BY SIMULATION

Hidesaburo Genda
Hiroshi Okayama
Takashi Ishiyama

Division of Remote Sensing Image Processing,
Institute of Color Technology,
Chiba University.
1-33 Yayoi-cho, Chiba-shi 280, Japan

Kaname Takeda

National Institute of Resources,
The Science and Technology Agency.
2-1-1 Kasumigaseki, Chiyoda-ku, Tokyo, Japan

ABSTRACT

Image processing of an area photograph of the Kumano river water system in Japan is carried out by the use of a photographic technique of extraction of equidensity. The minimum extraction density range $\Delta D = 0.05$ is obtained by giving the film an exposure Epn which satisfies Log $Ep.n = \sum_{n=1} 0.05 \cdot n$. The result is displayed in faulse color and compared with that of ground truth.

Secondly, it is of great interest to assess the concrete, which is widely used as building material, by means of remote sensing. The variance by different curing conditions of the concrete is observed by the photographic measurement and the measurement of the degree of polarization by use of a remote sensing simulator and thereby the concrete moisture is estimated.

1. INTRODUCTION

Photographic, analog and digital processes are well known as the process of the image obtained by remote sensing. There are pattern recognition and classification, extraction of the density and contour, etc. as a measure of image analysis. These classification and extraction are carried out by the above-mentioned ways of processing.

The photographic, analog and digital processes of images are carried out by our research group. It is generally admitted as a beginning of remote sensing using a camera when Gaspard Felix Tournachon[1] took a photograph with a glass plate camera over Paris from a captive balloon in 1858. An aerophotograph was taken in 1909 for the first time. Fifty years after the recording of an image was realized by Daguerre in 1839, the emulsion was coated on a clear film by G. Eastman in 1889, and thereafter the photographic silver halide emulsion was industrialized. Recently there are infrared films which have a sensitivity as high as 1,300 nm of infrared region. Since Kodachrome was marketed in 1935, about ten sorts of color film for remote sensing have been manufactured.[2]

Advantages of using a camera as a sensor are; simple operation, immediate and two-dimensional record of an image on the film, high resolution image, and less strain of the photographic image than that of MSS or RBV. Therefore a camera is important as a sensor in the remote sensing field.

This paper presents the latest results of our research group in Chiba University. The research was projected by the National Institute of Resources in the Science and Technology Agency of Japan in 1975. The photographic remote sensing is applied to the studies of the Kumano river water and to the analysis of the concrete moisture.

2. EXPERIMENT

Visual looking as an image of the information obtained by remote sensing is very important for the understanding of the information. In this paper, the results of the photographic analysis of the area photograph of the water system are compared with those of ground truth and the analysis of concrete moisture by the use of a camera and a remote sensing simulator is performed.

2.1 STUDIES OF KUMANO RIVER WATER

Belonging to the temperate zone, Japan has four seasons of spring, summer, autumn and winter, and is blessed with abundant water resources due to much rainfall compared with other countries all the year round. But this large rainfall is discharged immediately into the sea, as the rivers incline steeply. A great deal of soil flow into multipurpose dams through steep incline of rivers because of the deforestation of mountains, and as a result the pondage decreases. When the soil flows into the storage of water, the water becomes turbid and unsuitable for drinking. Thus the water resources play an important role in making the human environment and there is a necessity for many investigations for its estimation.

2.1.1 IMAGE PROCESSING

The aerial sensing of the Kumano river water system of the Kii Peninsula in Japan was carried out twice on December 21, 1976 and October 16, 1977. The Kii Peninsula is the area of the largest rainfall in Japan, which is 4,000 mm a year. It will be advantageous to make good use of the abundant water resources.

The purposes of our remote sensing are to investigate the diffusion of the turbid water and cold water discharged from the Kumano river system, their distribution patterns, the vegetation of the drainage area of the Kumano river system, and the land use, and it was done by the use of an aircraft.[3,4] An M^{2}S of Bendix Co. and an Wild RC-10 camera with an Aerocolor Negative 2445 of Eastman Kodak Company and a Hasselblad 500EL camera with an Aerochrome 2443 of Eastman Kodak Company were used as sensors loaded on the aircraft in this remote sensing. The ground truth was done in some places on the weather, temperature, wind and velocity of wind, turbidity and transparency of water, etc. simultaneously with the aerial sensing.

In this paper color equidensitographs of remotely sensed imagery of Kazaya Dam of the Kumano river system are obtained by photographic density slicing processing and compared with the water resources information obtained by ground truth. An aerial photograph of Kazaya Dam taken with Aerocolor Negative 2445 is shown in Fig. 1. Color equidensitographs of aerial sensed imagery on Kazaya Dam on December 21, 1976 and October 16, 1977 are obtained by photographic density slicing, with a density resolution of D = 0.05 as shown in Fig. 2 and Fig. 3, respectively. The block diagram shown in Fig. 4 is the procedure of the photographic density slicing processing.

Aerocolor Negative 2445 was used as an original negative required for density slicing processing. The information within the visible band is contained in this aerial color photographic film[5]. In order to extract only the green band which has the most information on water among the 3 bands in aerial color photographic film, it is processed by color separation with Wratten Filter No. 99 on a Separation Negative Film[6].

The working positive film having green band's information is shown in Fig. 4-(b). The nagative image "N" is obtained by processing after exposing the working positive film and Kodaline Reproduction film of lith type of Eastman Kodak Company laid one over another, as shown in Fig. 4-(c). If the exposure of the obtained image "N" is En and extraction density range Dw = 0.05, in order to obtain the negative images $N_1 \sim Nn$ from the working positive film, exposure "En" should satisfy Log ENn = $\sum_{n=1}^{n}$ 0.05·n and this amount of exposure must be given to Kodalice Reproduction film. Thus the tone separated negative images from N_1 to Nn are obtained corresponding to density range of the working positive film. As the next step, the images $N_1 \sim Nn$ shown in Fig. 4-(c) contacted with Kodaline Reproduction film are exposed and processed and thereby the positive masks from P_1 to Pn are obtained. It is shown in Fig. 4-(d). Here the exposure to obtain $P_1 \sim Pn$ is fixed. As shown in Fig. 4-(e), the "Ni" shown in Fig. 4-(c) and "Pi" shown in Fig. 4-(d) are laid face to face for exposing and processing and the first order positive "Pi" shown in Fig. 4-(f) is obtained as equidensitograph. By making P_1 to Pn, the tones of the working positive film image are sliced from the minimum density to the maximum density within the density width ΔDw = 0.05 and n sheets of P are obtained. Next, for the color display of Pn sheets of equidensitographs as a sheet of photograph easier to recognize, the first order negative "N" must be made from Pn as shown in Fig. 4-(f). These are obtained by contacting P with Kodaline film and processing after exposing as shown in Fig. 4-(g). A color equidensitograph is obtained by processing the lst order negative N through these 6 steps by contact exposing with several color lights to color photographic paper as shown in Fig. 4-(h).

Kodaline reproduction film are processed by use of an automatic processor Supermatic Model 242A of Eastman Kodak Company in order to make rapid and precise reproduction of image. The two aerial photographs on Kazaya Dam in Figs. 2 and 3 show the color equidensitographs displaying the intensity distribution of reflection from a scene. Color equidensitographs are color coded in order of low density of the original negative; green, black, red, cyan, yellow, blue, magenta, on the photograph of 1976, and black, blue, orange, white, yellow, magenta, cyan, red, green, light green on the photograph of 1977.

2.1.2 IMAGE ANALYSIS

The measuring points of water quality of water area of Kazaya Dam, from P6 to P12, which is an object of data analysis, are shown in Fig. 5. The values of ss and turbidity on measurement points are shown in Table I, but the ss is measured only in 1977. There is little difference in turbidity as far as the data in 1976 are concerned, if P10 is regarded as singularity. But the results of a density slicing show some difference in photographic density. It is regrettable that the data of turbidity at P8 and P9 in 1976 are lacking. The data in 1977 show scattered values regardless of the position of the measurement points. There are some mutual relations between the results of density slicing and ground data with regard to turbidity but none with regard to ss.

2.1.3 CONCLUSION

Photographic remote sensing was carried out on the Kumano river water and the results were displayed in color equidensitographs. In this experiment color aerial photographs were processed by use of green band color separated from them. The results were compared with those of ground truth. However, a multiband processing of photographic images is needed to obtain a clearer relationship between the values of turbidity and ss obtained by ground truth and the density-sliced images.

It is also necessary to discuss the relations between the turbidity and the water depth in the study of turbidity. The negative density at the embankment of the dam is larger than the other places due to the reflection of the sun light.

Measurement points of ground data should be more carefully selected as a part of the measurement points of the water quality is situated near the shadow

of the mountain. The density width of the density resolution must be narrower for the image analysis of the details.

2.2 ANALYSIS OF CONCRETE MOISTURE BY SIMULATION

Ferro-concrete is widely used as building material due to the advantages in durability and strength. The properties of concrete depend greatly on the selection of materials or their mixing ratio. Since concrete is a mixture of cement, sand, gravel and water in a certain ratio, the durability of a ferro-concrete building is dependent on this ratio. For the purpose of estimating the durability of a ferro-concrete building by remote sensing, the authors have made fundamental studies of concrete moisture by simulation.

2.2.1 MEASUREMENT OF CONCRETE MOISTURE

The dryness and moisture of concrete give a notable influence on the hardening of cement and the strength of concrete. It is generally known that concrete gets over 80% of the strength to be reached in a year of material age when it ages 28 days. Therefore the semipermanent durability of a concrete building is determined during the 28 days of material age. However the assessment of concrete moisture during the 28 days by remote sensing has been done in few papers.

Then we obtained the relationship between the results obtained by the photographic measurement using an infrared film and those by a remote sensing simulator[7] equipped with a polarimeter which was made by the authors. The experiment was carried out for the first five days of the 28 days of material age. The components of the concrete used for measurement are shown in Table II. As concrete is used actually under various conditions, the establishment of some different conditions is necessary in experiment. In our experiment the water quantity at the time of mixing of cement is set to be 650 cc and 500 cc. The curing conditions after mixing are also shown in Table II. The curing conditions are; to put in the water at the constant temperature (20°C) and to leave in the room of constant temperature (20°C, 40°C and -7°C). The concrete which had been under these conditions was let alone in the room for measurement one hour before the measurement.

As is shown in Fig. 6, the photographic measurement was done by setting a sample of concrete on the stage. The film which was used in this experiment was Kodak Aerographic Infrared film 2424 and the camera was Hasselblad 500EL/M with Planer f = 80 mm of Zeiss and Wratten 88A filter. The four flood photo-reflecter lamps (300W) were used to illuminate the sample. To estimate the intensity of reflected light from the concrete a step tablet was photographed with the concrete of the sample as a reference. The exposed film was developed with Kodak Versamat M11C with chemicals 885.

The measurement of the concrete moisture was done immediately after the photographic measurement. The photomultiplier in the simulator was R889 of Hamamatsu T.V. Co., and Wratten filter No. 25 was attached on the photomultiplier. The moisture is estimated by measuring degree of polarization of the scattered light from the concrete.

2.2.2 EXPERIMENTAL RESULTS

When 1 kg of cement and 2 kg of sand are mixed to make concrete as is shown in Fig. 6, the standard water quantity is 650 cc. In our experiment the water quantities were 500 cc and 650 cc.

The results obtained by the photographic measurement are shown in Fig. 7 and Fig. 8. The measurement values are normalized letting the value of measurement of the first day of mixing of the cement be unity. From Figs. 7 and 8 the relative reflectance of the concrete after mixing of the cement increases as the day proceeds. And it is of great interest that even the relative reflectance of the sample which is curing in water at a constant temperature as the day elapses when the water quantity of the mixing is 650 cc, as is shown in Fig. 8. When the water quantity of mixing is 500 cc, the increase of the reflectance is less than that of 650 cc.

The experimental results of degree of polarization using the remote sensing simulator are shown in Figs. 9 and 10. These experimental results are also normalized letting the value of the first measurement be unity. In the sample with water quantity of 650 cc, the results obtained from the photographic measurement show in Fig. 8 that daily variations of reflectance of the curing sample in water are less than those under other curing conditions, while the measurement results of degree of polarization in the condition in Fig. 10 show that the daily variations of degree of polarization of the sample decrease largely. Perhaps it may be attributed to the decrease in moisture in the concrete and to the variation of composition of the surface, while in the sample with water quantity of 500 cc the variations of the degree of polarization of the curing sample in the water were hardly detected. And the surface of the concrete becomes rough compared with the sample with water quantity of 650 cc.

From these results it is noted that the nature of concrete is varied with the water quantity in the mixing of cement. The curing condition of concrete gives a different moisture in the concrete and influences the nature of the concrete.

3. CONCLUSION

In the analysis of concrete moisture by simulation, the moisture is estimated by the photographic measurement and the measurement of degree of polarization by the use of remote sensing simulator. In the photographic measurement the increases in relative reflectance are observed, while from the measurement of degree of polarization by remote sensing simulator the decreases in degree of polarization as the day elapses are measured. The decrease in degree of polarization shows the decrease in moisture as well as the variation of the state of the roughness of the concrete.

Though our experiments did not obtain the relationship between moisture and strength, if it is found out, the strength of a concrete is easily estimated by the photographic measurement of concrete. Therefore this method will have a very large utilizing area for remote sensing.

REFERENCES

1) Frank J. Janza et al., 'Manual of Remote Sensing' Vol. 1, p. 27 (American Society of Photogrammetry, 1975).
2) Norman L. Fritz, Photogrammetric Engineering and Remote Sensing, 42, 525 (1976)
3) The interpretation and analysis of water resources information by multispectral data, National Institute of Resources, The Science and Technology Agency Report, 1977.
4) The interpretation and analysis of water resources information by multispectral data, National Institute of Resources, The Science and Technology Agency Report, 1978.
5) Kodak Aerial Films and Photographic Plates, Kodak Publications No. M61, D-24.
6) Robert G. Reeves et al., 'Manual of Remote Sensing' Vol. 2, p. 1487 (American Society of Photogrammetry, 1975).
7) H. Genda and H. Okayama, Appl. Opt., 17, March (1978).

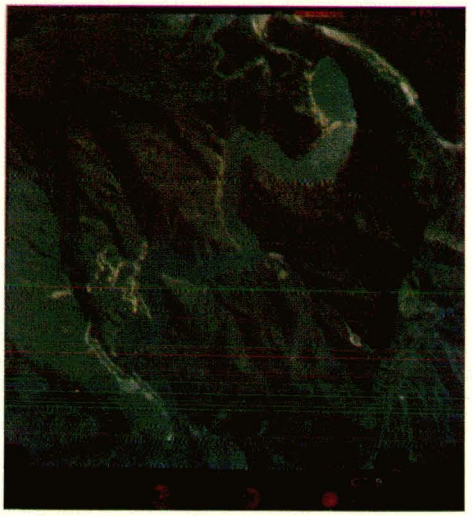

Fig. 1. Aerial photograph of Kazaya Dam.

Fig. 2. Color equidensitograph of aerial sensed imagery on Kazaya Dam on December 21, 1976.

Fig. 3. Color equidensitograph of aerial sensed imagery on Kazaya Dam on October 16, 1977.

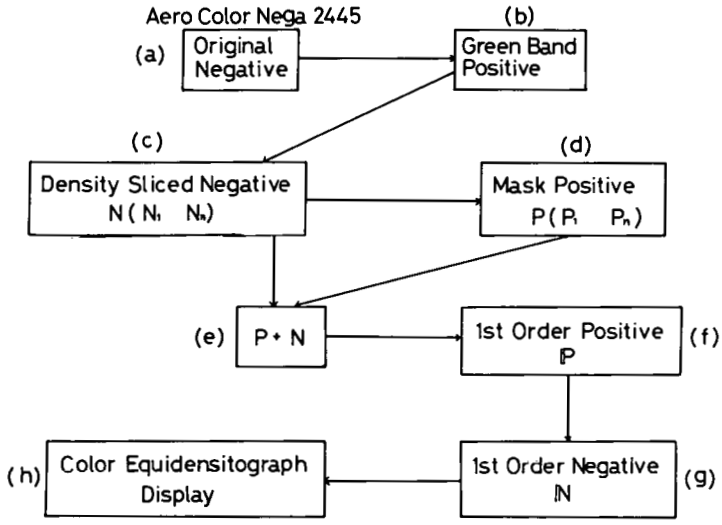

Fig. 4. The block diagram of photographic density slicing process.

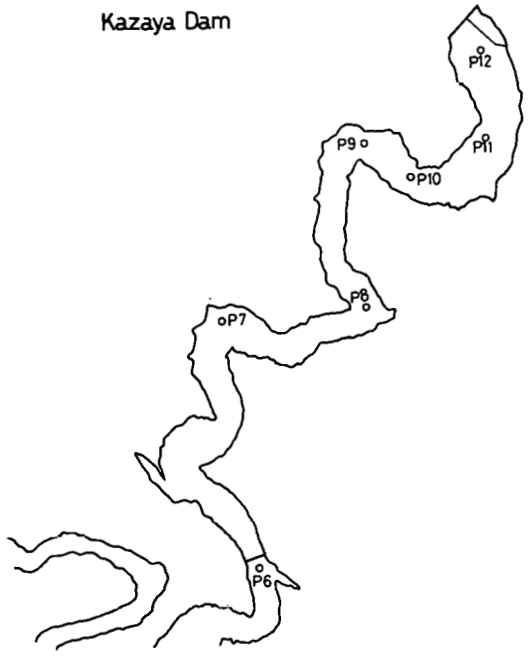

Fig. 5. Measurement points of water quality of water area of Kazaya Dam.

	1976		1977	
	Turbidity	SS	Turbidity	SS
P6	13.0		0.60	0.25
P7	13.0		0.50	0.23
P8			1.00	0.07
P9			2.10	0.43
P10	250.0		1.40	0
P11	15.0		0.75	0.13
P12	10.5		0.70	0.07

(ss: ppm)

Table I. Values of ss and turbidity on measurement points.

Sample

water	650cc
cement	1000 g
sand	2000 g

water	500cc
cement	1000 g
sand	2000 g

Condition
- constant (in water)
- room temp.
- high temp. (41°C)
- low temp. (−7°C)

water : 20 C
cement: Mitsubishi Mining And Cement Co. Ltd.
sand : JIS Standard Sand

Table II. Components and curing conditions of concrete.

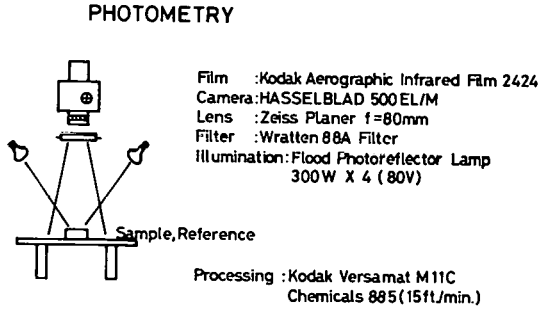

Fig. 6. Experimental system for photometry.

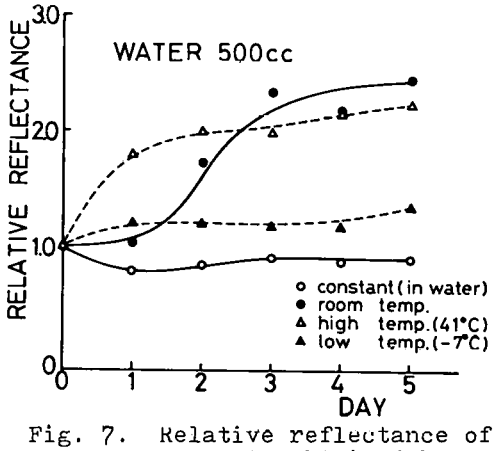

Fig. 7. Relative reflectance of concrete obtained by photometry.

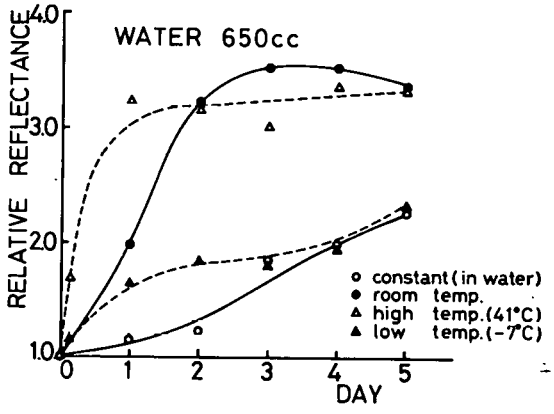

Fig. 8. Relative reflectance of concrete obtained by photometry.

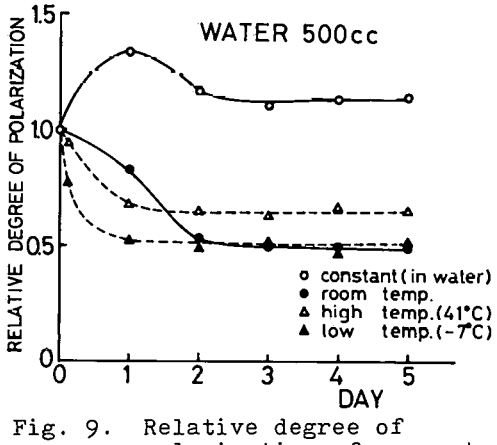

Fig. 9. Relative degree of polarization of concrete obtained by a remote sensing simulator.

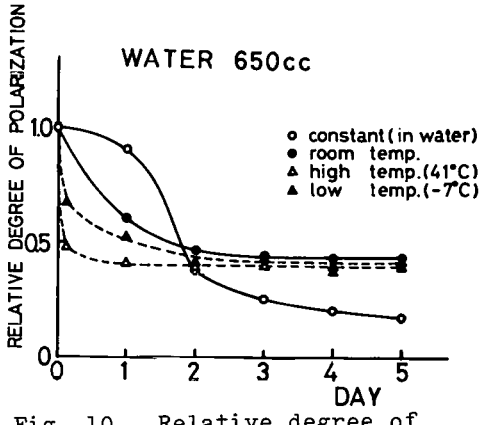

Fig. 10. Relative degree of polarization of concrete obtained by a remote sensing simulator.

MULTI LEVEL INVENTORY AND MONITORING OF WETLANDS ON THE SWAN COASTAL PLAIN, WESTERN AUSTRALIA

F.R. Honey[1], P.T. Hick[1] and D.R. Blatchford[2]

1 CSIRO, Division of Land Resources Management, Floreat Park, Western Australia.

2 Geography Department, University of Western Australia, Nedlands, Western Australia.

ABSTRACT

There are several conflicting demands upon the wetlands of the Swan Coastal Plain, Western Australia, particularly near the rapidly developing state capital, Perth. Planning fauna and flora reserves, utilizing groundwater resources, development of urban and industrial areas, and areas for leisure and recreation requires detailed knowledge of the extent and nature of the wetlands. Additionally, a scheme is required for the routine, inexpensive monitoring of the wetlands at a level of detail determined by the particular application.

A comparative study of the levels of detail obtainable using LANDSAT imagery, aerial photography, ground survey and combinations of the three was undertaken. Analysis of LANDSAT imagery was performed both by photo interpretation and by computer analysis of the CCT data. After detailed cluster analysis and selection of appropriate signatures for vegetation, wet mud areas and areas subject to inundation, thematic maps were produced at a scale of 1:25,000 for comparison with the air photo interpretation and ground survey results.

Aerial photography at scales ranging from 1:15,000 to 1:40,000 in panchromatic black and white, colour and colour infrared was used for mapping in more detail the vegetation associations in the wetlands. Ground survey indicated a strong correlation between the permanence of the wetland, depth and salinity and the vegetation species in and around the wetland. The various species could be mapped easily from the colour and colour infrared photographs.

Ground survey was required for extracting detailed information on the suitability of the wetlands as breeding, feeding and resting sites for water fowl. Samples were taken for analysis to determine chemical composition.

Maps illustrating the results of the three survey methods are presented, and conclusions drawn of the suitability of each of the techniques for the different requirements in a monitoring scheme.

1. INTRODUCTION

The Swan Coastal Plain, situated on the lower western coast of Western Australia (Fig. 1) is a strip approximately 25 km in width extending from lat. 31°30' to 35°30'S, bounded on the east by the Darling and Dandaragon plateaus and to the west by the Indian Ocean. Perth, the state capital with a population of 800,000 is sited approximately at the centre of the plain, on the estuary of the Swan River. The geomorphology of the region has been described in detail by McArthur and Bettenay (1960). Broadly, the plain consists of sedimentary materials, with units derived from fluvial, aeolian and marine deposits. Three dune systems occur on the plain, and control significantly the location and nature of the wetlands. The oldest system, the Bassendean dunes, originated as Pleistocene accumulation of beach sands. Subsequent leaching resulted in grey siliceous, infertile sands. The Spearwood system is younger than the Bassendean system, of late Pleistocene age. These dunes have been less leached than the Bassendean dunes consisting of yellow siliceous sands with appreciable iron content. The youngest system, the Quindalup dunes, consists of calcareous dune sands along the western extremity of the plain.

The lake systems and inlets of the plain are, in general elongate and aligned in an approximate N-S direction, paralleling the coastline and suggesting a relationship to the interdune depressions of the three dune systems. The wetland system in general represents a surface expression of the groundwater table in the unconfined aquifer. As a consequence, the wetlands are sensitive to change in the water table, and to pollution of the water by waste disposal or fertilizer application in surrounding areas.

These wetlands are a valuable, and in some instances, diminishing resource. Pressures due to the increasing population around Perth are creating conflicts between development requirements, such as urban, industrial, agricultural and transportation needs, conservation requirements for waterfowl management, and recreational requirements, ranging from passive recreation to water sports. In recognition of these conflicting demands, and as part of the Australian responsibility under the Ramsar Convention, the Western Australian Environmental Protection Authority (EPA) established the Wetlands Advisory Committee to review and advise the E.P.A. on the desirable allocation of wetland reserve resources and the adequacy of their management. This committee recognized the need for an inventory of wetland resources on the coastal plain, and for a method of monitoring these wetlands to assess the effects of development around them. Various levels of detail were needed for the inventory phase, and an assessment was made, on some specific wetlands, of the capabilities of several remote sensing techniques.

2. INFORMATION REQUIREMENTS FOR WETLANDS INVENTORY

Before evaluating the various remote sensing techniques available, it was necessary to determine:

(i) the parameters which are significant in classification and monitoring of wetlands,

(ii) which of these parameters can be measured both directly and indirectly by remote methods and

(iii) which parameters the various resource planners and managers must monitor.

Several classification schemes for wetlands are in use, the most fundamental of which is perhaps that of the United States Fish and Wildlife Service (Shaw and Fredine 1956), which describes twenty wetlands classes. A more refined system has been described by Marchant (1978). This system presents a hierarchical scheme, sorting classes on areal extent, salinity and percentage of vegetation cover of the wetland. Marchant has found that all of the wetlands he has studied on the Swan coastal plain can be classified using this scheme. An additional parameter which should be considered in water depth, a factor which is important for waterfowl, recreation and water resources.

The parameters which we must measure to utilize these classification schemes, and to provide additional information on the condition of the wetlands are

(i) Areal extent of the entire wetland

(ii) Permanence of the wetland

(iii) Depth

(iv) Proportion of wetland covered by vegetation

(v) Types of vegetation

(vi) Salinity

(vii) Turbidity

(viii) Presence of pollutants

(ix) Dissolved oxygen levels and biological oxygen demand (BOD).

Of these parameters, (i), (ii), (iv) and (v) can be measured directly by remote techniques, whilst (iii) and (vi) may be estimated in some cases by indirect means, such as vegetation association. Blatchford (1977) describes vegetation associations which may be used to indicate depth and salinity. Turbidity (vii) may be determined qualitatively by aerial photography and satellite imaging. Precise measures of turbidity, salinity, depth, presence of pollutants and dissolved oxygen levels and B.O.D. require extensive sampling of wetland areas are, as are a consequence, expensive.

The conflicting demands for the wetlands which will require different levels of detail are:

(i) Reserves for flora and fauna conservation, particularly waterfowl; requires knowledge of the area, permanence, percentage of vegetation cover, vegetation types, salinity of water and food sources.

(ii) Recreation reserves; requires less detailed information on area, depth, permanence, vegetation cover, salinity and eutrophic levels, particularly for passive recreation.

(iii) Water resources; the shallow aquifer is pumped both by the pumping water supply authority, and by private pumping. Subsequent variations in the groundwater table, both periodic and permanent, can cause a change in this type of wetland, and its suitability for conservation and recreation. Parameters which need monitoring are areal extent, depth and vegetation condition.

(iv) Urban development which requires clearing of vegetation around wetlands and some filling of swamp areas can influence local water table levels, and cause pollution of remaining wetlands from lawn and garden fertilizers and stormwater runoff. As this development is irreversible, a pre-development inventory of the extent and nature of the wetlands to ascertain which areas should be reserved is essential, and subsequent monitoring to assess the effects of development is desirable. Parameters necessary for this inventory are area, depth, vegetation cover and type, and salinity. For monitoring purposes, vegetation cover and type, turbidity and chemical composition must be measured.

(v) Industrial development - similar criteria to urban development, with more potential for pollution and hence a greater need for monitoring of chemical composition.

(vi) Waste disposal. Wetlands are traditionally considered as ideal sites for sanitary landfill. This may be appropriate for some wetlands with low conservation and recreation potential. Before designating a wetland as a waste disposal area, it should be assessed by comparison with all other wetlands in the area to determine its potential, and need for its conservation. Parameters necessary are area, vegetation cover and type, depth and salinity. Monitoring of surrounding wetlands will become necessary after filling is commenced to determine the effect of disposal.

(vii) Agriculture. Some wetland areas under private ownership are considered un-productive to the farmer. They may then be drained or filled. Large areas of the wetlands on the Swan coastal plain have been drained for agriculture. Knowledge of the number, area and class of wetlands under private ownership is essential to the management of the wetlands over the entire plain. This requires a complete inventory with estimates of area, depth, vegetation cover and type, and salinity. Increases in phosphate and nitrate levels in the groundwater in agricultural areas may also affect the eutrophic levels of surrounding wetlands. Periodic monitoring of chemical composition is desirable.

(viii) Transport - similar criteria to urban and industrial development.

3. REMOTE SENSING LITERATURE SURVEY

Examples may be found in the literature of all aspects of remote sensing of wetlands and coastal marsh areas. Early work on the application of aerial photography is described by Olsen (1964). Examples of the application of colour and colour infrared photography are presented by Seher and Tueller (1973), Anderson and Webber (1973), and Klemas et al. (1974). Airborne scanner techniques, coupled with aerial photography are outlined, for thermal scanners, by Reimold et al. (1973) and for multispectral scanners by Wezernak and Lyzenga (1975). Examples of studies using aerial photography and satellite imagery are provided by Anderson et al. (1973) and Gammon et al. (1977). The use of vegetation association and remote sensing for marsh areas to define mosquito breeding habitats is described by Arp (1975).

4. TECHNIQUES AVAILABLE FOR THE STUDY

A range of information gathering techniques are available to the planner and manager within Western Australia, from Landsat imagery and aerial photography to facilities for detailed chemical and biological sampling and analysis.

Landsat imagery is applied in two ways by by photo interpretation and by computer analysis of the CCT data.

The types of photographic Landsat products utilized are 70 mm black and white negative transparencies of band 7, 1:1,000,000 scale standard black and white and colour composite prints and transparencies and 1:250,000 scale prints, either standard EROS products or computer enhanced products available from EROS or from the CSIRO Division of Mineral Physics which have been enhanced to specifically delineate wetlands. The 70 mm products provide a rapid inexpensive means of mapping water areas by back projection of the band 7 negatives onto a ground glass screen at scales up to 1:100,000.

The CSIRO Division of Land Resources Management has available a set of interactive programs for the analysis of Landsat CCT data on a DEC-10 computer. The types of processing which may be performed are:

Histogram

Haze removal

Density slicing

Contrast enhancement

Filtering and destriping

Ratioing

Cluster analysis (modified parallelepiped)

Thematic mapping

Using these programs, it has been demonstrated that it is possible to

(a) Delineate wetland areas, both open water and areas which are subject to inundation.

(b) Broadly classify the wetland vegetation into categories of emergent vegetation in water.

(c) Estimate the percentage of vegetation cover of the wetland.

(d) Detect algal blooms at the surface. Summer and winter coverage is available for several overpasses of Landsats 1 and 2. More imagery will be available when the Australian receiving facility becomes operational.

Aerial photographic products are black and white panchromatic, at scales ranging from 1:50,000 to 1:15,000, and colour and colour infrared photography of specific areas at scales of 1:25,000 to 1:15,000. No routine wetlands monitoring system using aerial photography has been initiated. Most of the available photography has been taken for other purposes.

Using the available photography it is possible to measure wetland areas, percentage of vegetation cover, classify in detail vegetation units and any yalgal blooms and estimate turbidity. The detailed mapping of vegetation, and the vegetation associations observed provide some knowledge of depth and salinity of the lakes, and yield valuable information on availability of feed for waterfowl.

To illustrate the capabilities of the techniques, two examples were taken, Lakes Jandabup and Mariginiup, two lentic wetland areas 23 km north of Perth. These lakes are in an area which has increasing urban development, and which is subjected to heavy pumping for groundwater. They display many of the characteristics which may be measured directly by remote means, such as area, percentage vegetation cover and vegetation type.

5. MAPPING AND INTERPRETATION

5.1 AERIAL PHOTOGRAPHY

Black and white aerial photography for the area was available at low cost from the Western Australian Department of Land and Surveys at scales ranging from 1:11,000 to 1:40,000. Total area, area of water, areas of emergent and peripheral vegetation and boundaries between different vegetation communities may be mapped accurately. However, species comprising the vegetation communities can not be identified with any confidence. This implies that black and white aerial photographs can not be used to obtain quantitative information on the plant species and the environment affecting their distribution, for example water depth and salinity. A reproduction of a black and white aerial photograph of lakes Mariginiup and Jandabup is presented in Fig. 2.

Colour and colour infrared aerial photography of the Swan coastal plain is, as a result of the greater cost, less readily available than black and white. The coverage is sparse, and no sequential photography is available. Colour and colour infrared photography was available for lakes Mariginiup and Jandabup as part of the survey for the Wetlands Advisory Committee.

The amount of general information discernible from colour aerial photography is considerably greater than that available from black and white photography. For assessment of waterfowl habitat quality, the greater ease and accuracy of vegetation mapping and interpretation was the principal advantage in using colour aerial photography. Colour infrared photography complemented the colour photography in areas where identification of species was difficult. A limitation in the suitability of the colour infrared for classification purposes what the strong influence the vegetation vigor had on the magenta shades. This aspect obviously is valuable however in monitoring wetland condition trends. An example of the detailed vegetation species classification obtainable from colour and colour infrared photography is illustrated for Lake Mariginiup in Figs. 3 and 4 (Blatchford 1977).

5.2 SATELLITE IMAGERY

Location of water areas on Landsat imagery may be achieved in two ways. If the water areas are large enough, they may be readily identified on the photographic product. The most economical and rapid technique for mapping these areas is to back project the 70 mm negative transparencies onto a ground glass screen. Wetland areas with little or no surface water require colour composite material for identification of the more vigorous vegetation usually present in and around wetlands.

The second approach, computer analysis of the Landsat digital information on the CCT's, allows mapping of pixel sized areas of water, and more refined analysis of signatures to enable some discrimination of the types of vegetation (emergent, peripheral, areas subject to flooding) in and around the wetlands. It is possible to initiate a semi-automated scene search and mapping operation using signature analysis.

The examples considered here, Lakes Mariginiup and Jandabup have been located on a summer Landsat scene E-1149-01370, 19 December, 1972 and a winter scene, E-2523-01182, 28 June, 1976. Band 7 shadeprints, density sliced emphasize water and wetland areas are presented in Fig. 5a and b for the summer and winter scenes respectively. A cluster analysis was performed on each of the areas, with the total area being clustered initially, then concentrating on the wetlands themselves to establish signatures more representative of the open water and wetland vegetation we wished to map. A cluster result for the Lake Jandabup from scene 1152-01370 is presented in Figs. 6a and b. From the cluster analysis results signatures on themes were extracted which were characteristic of open water, emergent vegetation, thick emergent vegetation and peripheral vegetation, these were input to the program and a thematic 'map' prepared (Fig. 7). A similar exercise was carried out on the winter scene. From these two analyses, areas of the wetlands, percentage vegetation and some vegetation categories could be calculated and compared with results from photo interpretation.

Satisfactory themes can then be input to a program which produces a geometrically rectified map on a plotter. An example of typical plotter output is presented in Fig. 8 for a wetland area south of Perth.

6. COMPARISONS OF RESULTS

Using aerial photography, an estimate of the area of the lakes, area of vegetation, vegetation boundaries and classification of species could be obtained, particularly for the areas where colour and colour infrared photography was available.

Using Landsat imagery, wetland area, area of open water, and some broad vegetation classifications (emergent vegetation, peripheral vegetation) could be extracted.

Unfortunately, the times of the satellite imagery and aerial photography did not correspond. However, some evaluation may be made on estimation of area and of the percentage of open water.

From the aerial photography of September 1972, the total area of Lake Jandabup was measured as 327.04 ha, with 46.58% open water. From the Landsat scene E-1149-01370, December 1973, the area water was estimated to be 303.95 ha, with 53.63% open water, and from the scene E-2523-01182, June 1976, the total area was 267.43 ha, with 50.25% open water. No attempt has been made to correct 'edge pixels' caused by the sampling grid of the satellite. The classes used were from training areas within the wetland. It would be possible, if necessary, to develop a 'boundary class' which would increase the total area, and decrease the percentage of water, or to establish a signature for the area bounding but outside the wetland, then by analysis of the 'boundary pixel' signatures, estimate the proportion of wetland contained in each boundary pixel and hence arrive at a more accurate figure for the total area.

The difference in area between the two results from Landsat can perhaps be accounted for by the different seasons. The winter (southern) of 1973 had an above average rainfall. This would tend to increase the area of the wetland as observed from Landsat, as perennial grasses would remain in lush condition for longer periods, and could be included in the peripheral vegetation class. For 11 December 1973, the surface of Lake Jandabup was 45.594 metres above the Australian height datum (A.H.D). The period before the June 1976 overpass had below average rainfall, resulting in a lowering of the water table, as evidenced by the height of the surface relative to the A.H.D. of 45.062 metres, a drop in level of 0.532 metres. Boundary areas would be dry, some peripheral vegetation not being included in the signatures resulting in a lower total area.

7. CONCLUSIONS

Routine monitoring of wetlands using Landsat can be performed, provided careful consideration of environmental factors which will affect wetland areas are considered, and provided reliable signatures can be established, and proportions estimated for the boundary areas. Landsat monitoring should prove effective for the periodic assessment of wetlands on a regional basis. For more detailed information on the condition of the wetlands, and for more accurate estimates of their areas to assess the effects of development activities, aerial photography is essential. Some use can be made of the vegetation associations in assessing qualitatively the salinity and depth of wetlands. For more quantitative measurements, ground sampling and survey is required.

8. REFERENCES

1. Anderson, R.E. and Webber, F.J. 1973. Wetlands mapping in New Jersey. Photogramm. Eng. 39, p. 353.

2. Anderson, R.R., Carter, V., McGinness, J. 1973. Application of ERTS data to coastal wetland ecology with special reference to plant community mapping and typing and impact of man. Proc. Third Earth Resources Technology Satellite-1 Symp. Washington Ece. 10-14, 1973, p. 1225.

3. Arp, G.K. 1975. The reationale for attempting to define salt marsh mosquito breeding areas in Galveston County by remote sensing the associated vegetation. Proc. NASA Earth Resources Survey Symp.

4. Blatchford, D.R. 1977. The use of remote sensing techniques for assessing waterfowl habitat suitability. Honours Thesis, Department of Geography, University of Western Australia 1977.

5. Gammon, P.T., Malone, D., Brooks, P.D. and Carter, V. 1977. Three approaches to the classification and mapping of inland wetlands. Proc. Eleventh Int. Symp. on Remote Sensing of Environment, Ann. Arbor, Michigan April 25-29, 1977, p. 1545.

6. Klemas, V., Daiber, F.C., Bartlett, D., Crichton, O.W. and Fornes, A.O. 1974. Inventory of Delaware's Wetlands. Photogram. Eng. 40, p. 433.

7. Marchant, N. 1978. Wetland Classification Scheme, Western Australian Herbarium Research Notes. No. 2, 1978 (in press).

8. McArthur, W.M. and Bettenay, E. 1974. Development and distribution of soils on the Swan Coastal Plain, Western Australia. Soil Publication No. 16. Commonwealth Scientific and Industrial Research Organization, Australia 1974.

9. Olsen, D.P. 1964. The use of aerial photographs in the studies of marsh vegetation. Maine Agr. Exp. Sta. Tech. Bull. V13, p. 62.

10. Reimold, R.J., Gallagher, J.L. and Thompson, D.E. 1973. Remote sensing of tidal marsh. Photogram. Eng. 34, p. 477.

11. Seher, J.S. and Tueller, P.T. 1973. Colour aerial photos for marshland. Photogram. Eng. 39, p. 489.

12. Shaw, S.P. and Fredine, C.G. 1956. Wetlands of the United States. Circular 39, Fish and Wildlife Service, United States Department of the Interior 1956.

13. Wezernak, C.T. and Lyzenga, D.R. 1975. Analysis of Cladophora distribution in Lake Ontario using remote sensing. Remote Sensing of Environment 4, p. 37.

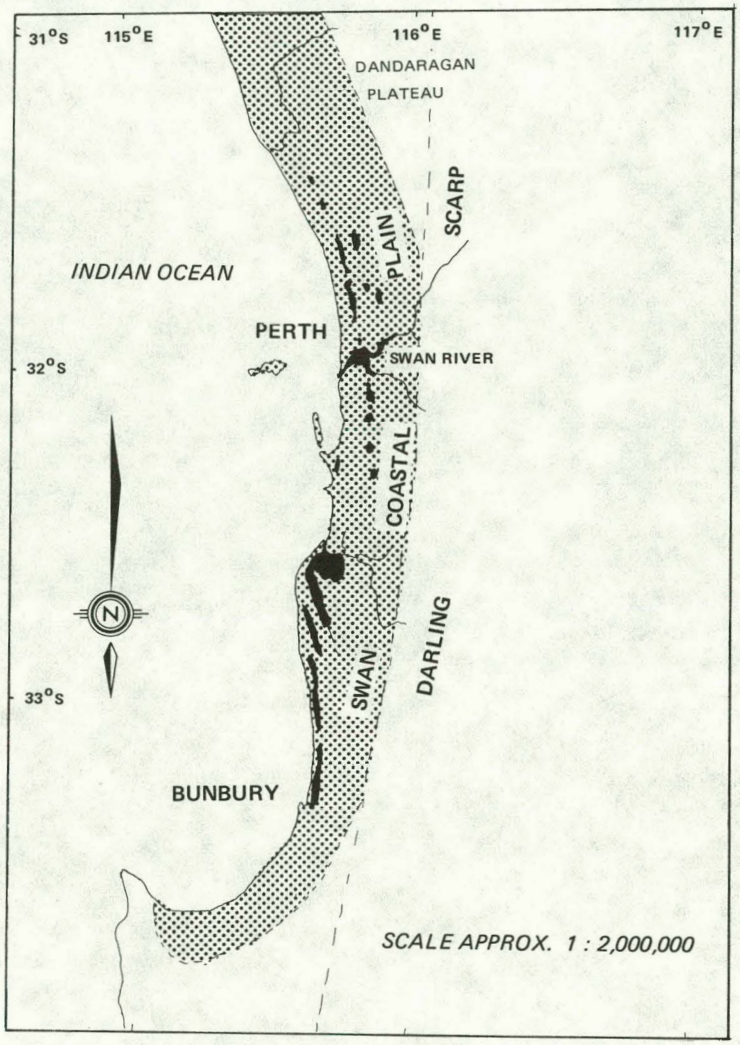

FIG. 1 LOCALITY MAP, SWAN COASTAL PLAIN.

FIG. 2 REPRODUCTION OF PANCHROMATIC BLACK AND WHITE AERIAL PHOTOGRAPH OF LAKES MARIGINIUP AND JANDABUP.

FIG. 3 VEGETATION CLASSIFICATION MAP, LAKE MARIGINIUP, FROM COLOUR AERIAL PHOTOGRAPHY (BLATCHFORD 1977).

Key to Fig. 3

1. Cladium junceus
2. C. articulatum; dense stands, located shorewards, roots exposed during late summer
2a. C. articulatum; dense/vigorous stands
2b. C. articulatum/open water; open stands
2c. C. articulatum; closed stands bordering open water
2d. C. articulatum; old stand
2c. C. articulatum; medium age stand
3. Eliocharis spp.
4. Scirpus prolifera, S. maritimus, C. articulatum, Leptocarpus canis, Typha orientalis meadow
5. C. articulatum and S. prolifera
6. Surface water with open stand of C. articulatum
7. C. articulatum, T. orientalis
8. L. canis, C. articulatum, C. junceum, S. prolifera
9. T. orientalis, J. maritimus, C. articulatum
10. Astartea fascicularis
11. Cleared

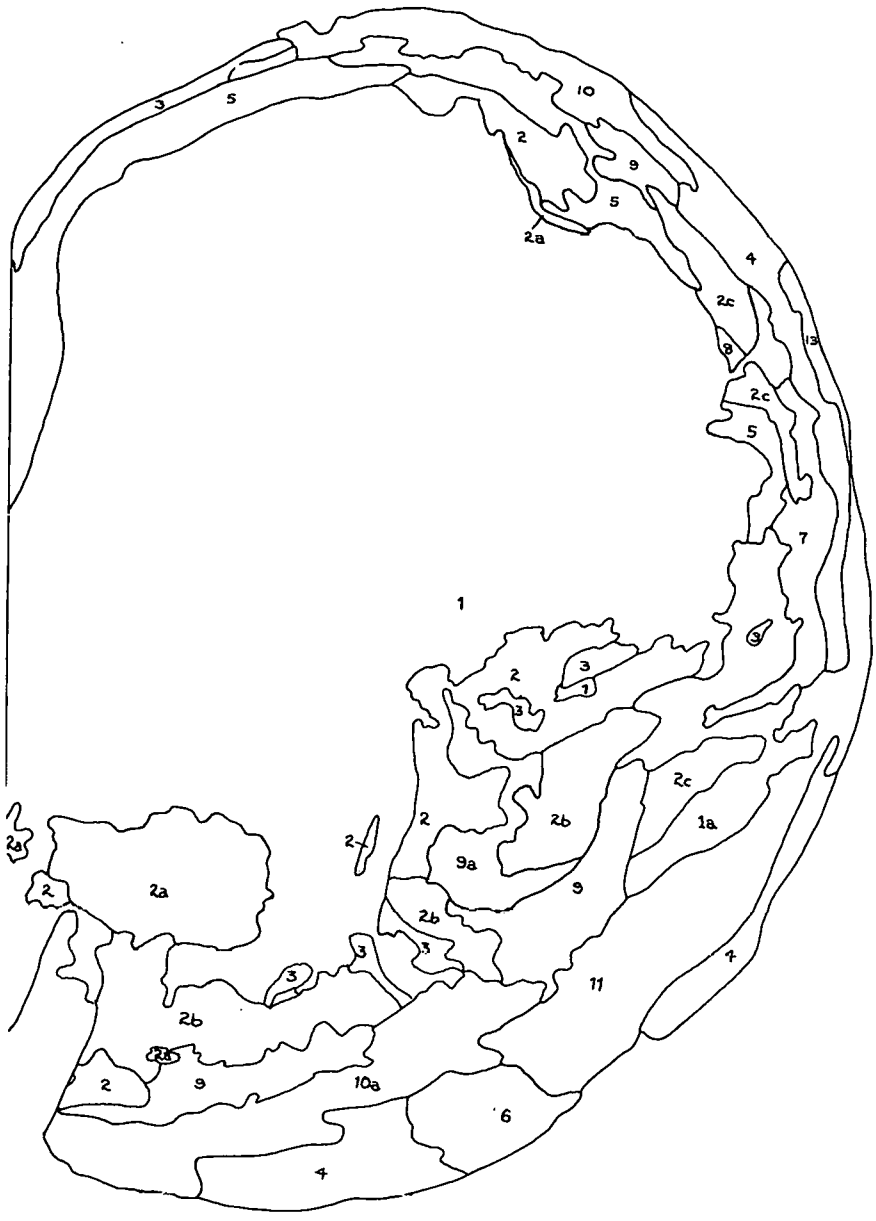

FIG. 4 VEGETATION MAP, LAKE MARIGINIUP, FROM COLOUR INFRARED PHOTOGRAPHY (BLATCHFORD 1977).

Key to Fig. 4

1. Open Water
2. *Cladium articulatum* (closed)
2a. *C. Junceum*
2b. *C. Junceum* (open and shoreward)
2c. *C. articulatum* (medium density)
3. *Eliocharis* spp.
4. Cleared
5. *C. articulatum* (mature)
6. *Leptocarpus canis*, *C. articulatum* and *Typha orientalis*
7. *C. articulatum* and *Scirpus prolifera*
8 Bare mud
9. Mainly open water
9a. Water and significant amounts of *C. articulatum*
10. *Typha orientalis*
10a. *T. orientalis*, *C. articulatum*, *S. prolifera* and *Leptocarpus canis*
11. *L. canis*, *C. articulatum*, *C. junceum*, *J. maritimus*, *S. prolifera*

(a)

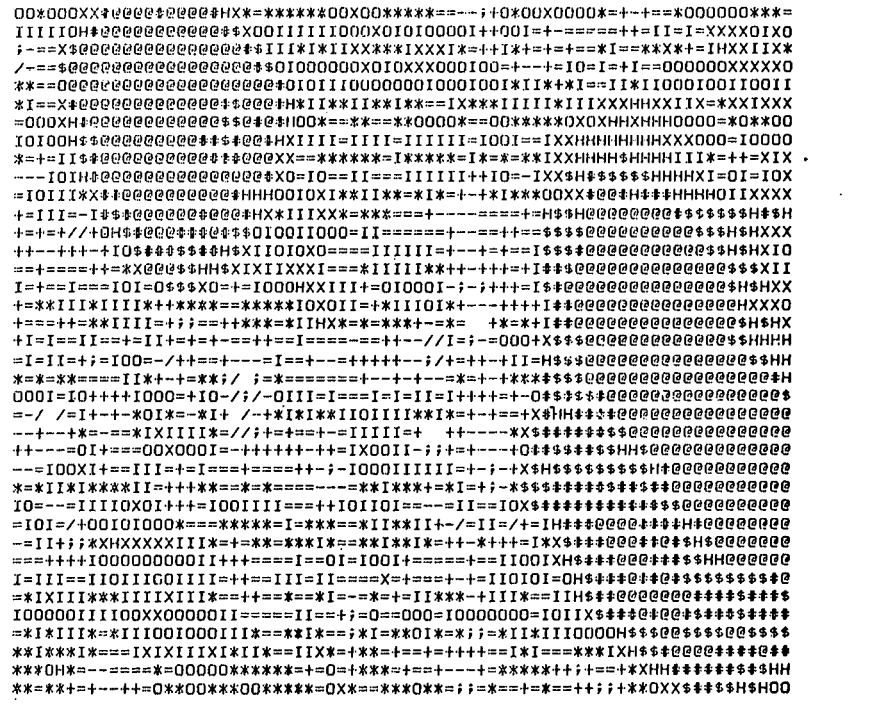

(b)

FIG. 5 DENSITY SLICED BAND 7 SHADEPRINT FOR LAKES JANDABUP, MARIGINIUP.
(a) E—1149-01370
(b) E—2523-01182

(a)

(b)

FIG. 6 CLUSTER ANALYSIS RESULTS FOR LAKE JANDABUP, E—1149-01370
(a) TRAINED ON WHOLE AREA, INCLUDING AGRICULTURAL
(b) TRAINED ON LAKE JANDABUP

FIG. 7 THEMATIC MAP OF LAKE JANDABUP. E—1149-01370

W = WATER AREA
/ = EMERGENT VEGETATION
X = THICK EMERGENT VEGETATION AND PERIPHERAL VEGETATION
T = TREES

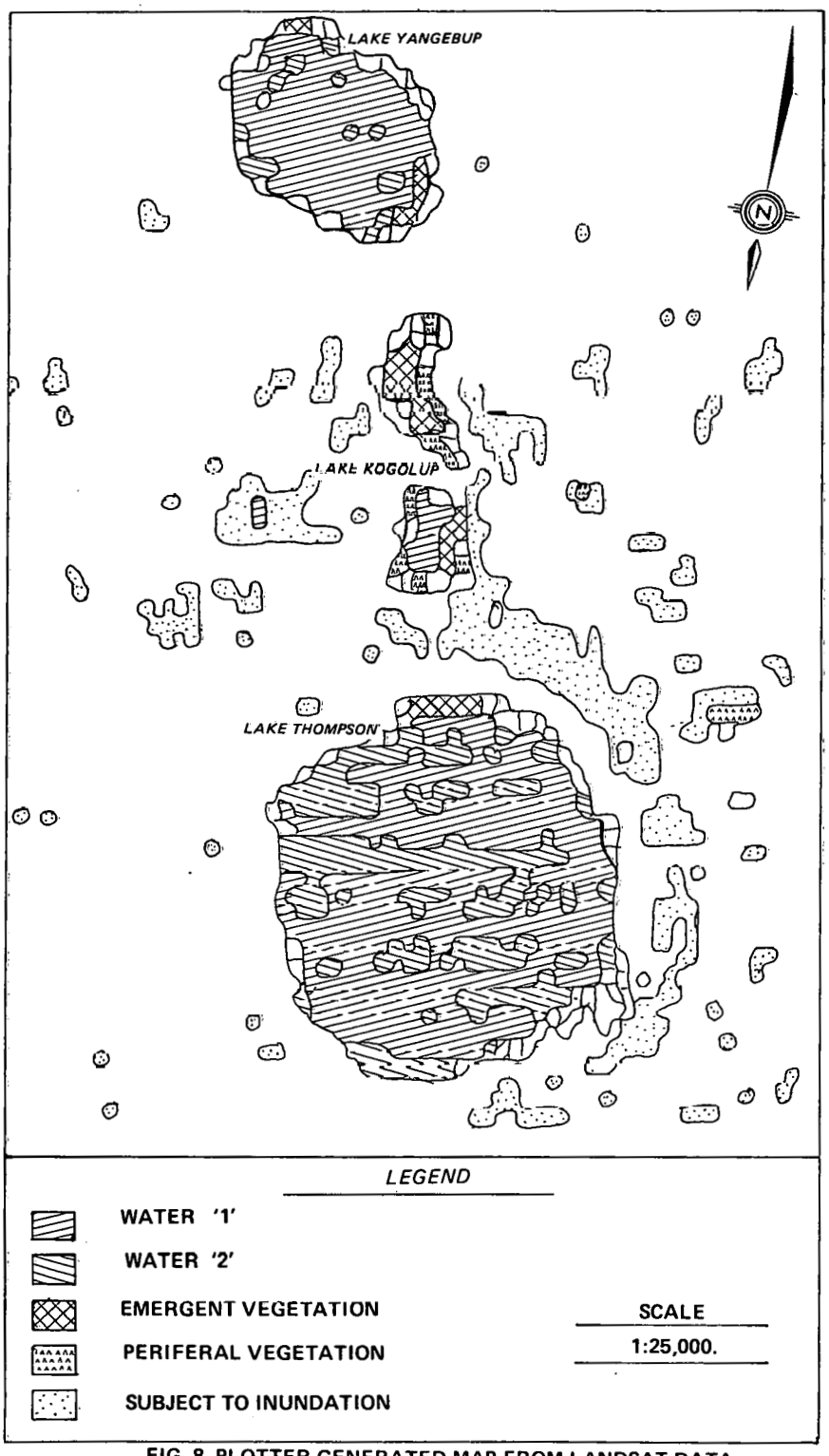

FIG. 8 PLOTTER GENERATED MAP FROM LANDSAT DATA, WETLAND AREA SOUTH OF PERTH.

THAILAND'S LITTORAL MUDFLATS AS INTERPRETED FROM LANDSAT IMAGERY

Nissai Sriplung

Applied Scientific Research Corporation
of Thailand
Bangkok 9, Thailand

ABSTRACT

An investigation was conducted to determine the littoral and sublittoral mudflats of Thailand based on Landsat imagery. The interpreted map was verified by ground truth survey using cars, boats and helicopter. A combination scheme of diazochrome color composite transparencies was conceived which yields best results for mudflat identification. The study showed an area of 910 km^2 and 3700 km^2 for Thailand's littoral and sublittoral mudflats respectively.

1. INTRODUCTION

It is generally known that the littoral mudflats are economically important to countries like Thailand as they are excellent habitats for some marine species such as molluscs, mud clam, Anadara granosa, etc; which provide a certain amount of food supply to the population. Unfortunately, the industry situated along the coast of Thailand, allhough they may be of importance to the economy of the country, has put its waste into the surrounding areas, causing sea water pollution. This, of course, affects the ecosystem of those marine species in the area. Therefore a certain policy on coastal environment including the mudflats should be considered by agencies concerned.

However, in order to maintain and conserve the mudflats for control and planning purposes, a preliminary study involving the mapping of the size, the monitoring of change in time and space, must be attempted. It is the intention of this study to initiate an economic method for mapping and for monitoring of mudflats using Landsat imagery obtained during 1975-1977.

2. PREPARATION OF IMAGERY

Landsat imagery taken at the time of low tide based on hydrographic data were selected for interpretation. For instance, the imagery of NASA ID E-2163-02552 taken at 0255 U.T. on July 4,1975 which covers the eastern coast of Thai Gulf was chosen as the maxima of low tide and high tide of that day occurred at 0014 U.T. and 1552 U.T. respectively (Royal Thai Navy, 1975). So the mudflats shown on the imagery was almost the maximum extent of the area. Table I contains the details of the imagery selected for the study.

It has been found, in general, that the distribution of sediment laden waters or turbid waters, appear rather clearly in Landsat MSS band 4 and band 5 whereas mudflats may be seen clearly in MSS Band 6 and Band 7 as light grey tone in black and white imagery. In addition, false color composite imagery were also produced using diazochrome films. For standard combination of band 4(yellow), band 5(magenta), and band 7(cyan), the sea water would appear as dark blue, mudflats as light grey, mangrove forest as bluish red, heavy sediment as heavy tone of white colour and less turbid water as light tone of white colour. Novmally, the grey tone of mudflats can be obscured by white tone of the high concentration of sediment. However, a better colour combination scheme which would enhance the mudflats by using band 4 as yellow, band 5 as orange and band 7 as cyan, was attempted. The mudflats in this new combination-appear as light blue, mangrove as yellowish green, and sediment as bluish white.

Figure 1 shows the false colour composite imagery using the standard combination of colours (a) compared with the new scheme(b).

3. IMAGE INTERPRETATION

From the imagery prepared at the Thailand National Remote Sensing Program (TNRSP) the whole Thailand coastal zone around the gulf was identified for mudflat and mangrove areas. Figure 2 shows examples of the results of identification. The ground truth survey was also conducted to verify the imagery interpretation. When the ground truth data were compared with the imagery, it is found that the actual area of mudflats at lowtide is normally larger than the area estimated from the imagery. This is due to the fact that many imagery were taken at the time close to low tide but not exactly at low tide.

4. RESULTS AND DISCUSSION

The study showed that the total areas of Thailand's littoral and sublittoral mudflats are approximately 910 km^2 and 3700 km^2 respectively. The slope angle of mudflats can be related to the width of the area exposed in the imagery at low tide. Figure 3 explains the relationship between the slope angle which could be roughly estimated if the width of the mudflat is known at a particular point.

The distribution of sediment is, however, found to be highly coherent to the coastal environments such as tides and wind. The distribution patterns are clearly different between low and high tides depending on the fluid motions of the area. Figure 4 shows the different sediment distribution patterns corresponding to different tidal stages.

REFERENCE:

Royal Thai Navy, 1975. "Tide Tables". Hydrographic Department, Royal Thai Navy, Bangkok

TNRSP Technical Note No. 751003, "Distribution of Mangrove Forest As Revealed By the Earth Resources Technology Satellite (ERTS-1) Imagery", National Research Council, October, 1975

ACKNOWLEDGEMENT

The author wishes to thank Mr. Suvit Vibulsresth and Dr. Sasithorn Aranuvachapun of the National Research Council for there helpful discussion.

TABLE I IMAGERY SELECTED FOR THE STUDY

NASA ID	DATE	THAILAND ID	LOCATION
E 2053 - 02442	16 MAR 75	2-8	KLONGYAI,TRAD
E 2162 - 02494	3 JULY 75	3-7	CHANTABURI TO TRAD
E 2163 - 02552	4 JULY 75	4-7	CHAOPHYA RIVER TO SATTAHEEB
E 2164 - 03111	5 JULY 75	5-7	THACHIN RIVER, MAEKLONG RIVER, PHETCHABURI
E 2164 - 03011	5 JULY 75	5-8	HUA HIN, PRACHAUB KIRI KHAN
E 2164 - 03020 E 2182 - 03014	5 JULY 75 23 JULY 75	5-9	CHUMPORN, SURATTHANI, RANONG
E 1204 - 03142	12 FEB 73	5-10	PHANGNA , KRABI
E 1168 - 03142	7 JAN 73	5-11	PHUKET
E 2163 - 02564	4 JULY 75	4-10	SURAT, NAKHON SRI THAMMARAT
E 2163 - 02570	4 JULY 75	4-11	TRANG, SATUN
E 2162 - 02512	3 JULY 75	3-11	SONGKHLA, PATTANI

Figure 1. False Colour Composite Imagery Using Standard Combination Showing No Mudflats (a) and New Combination Showing Mudflats(b)

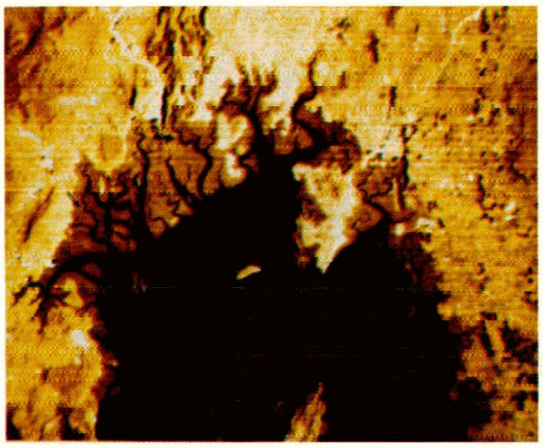

(a)

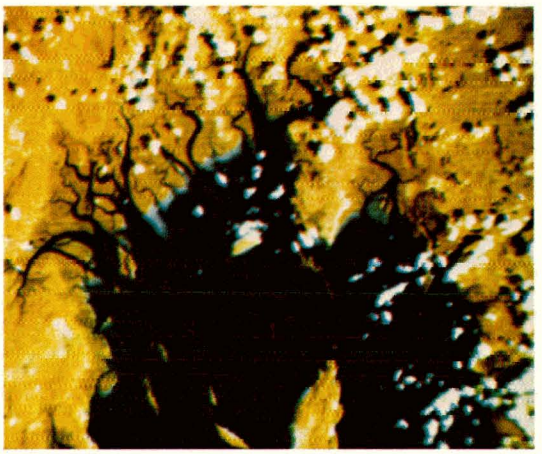

(b)

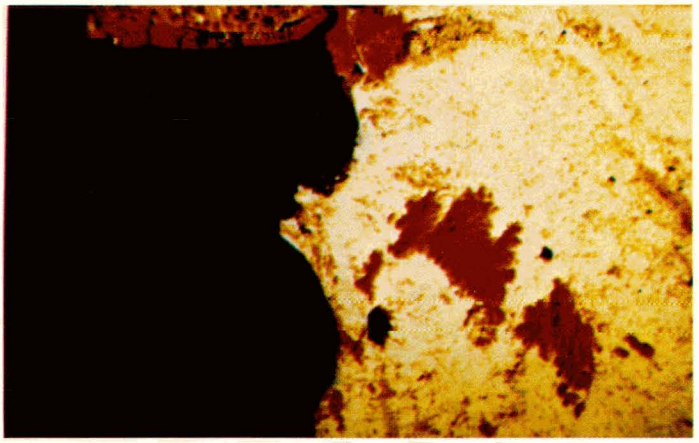

Figure 4.

Different Sediment Distribution Patterns Corresponding to Different Tidal Stages

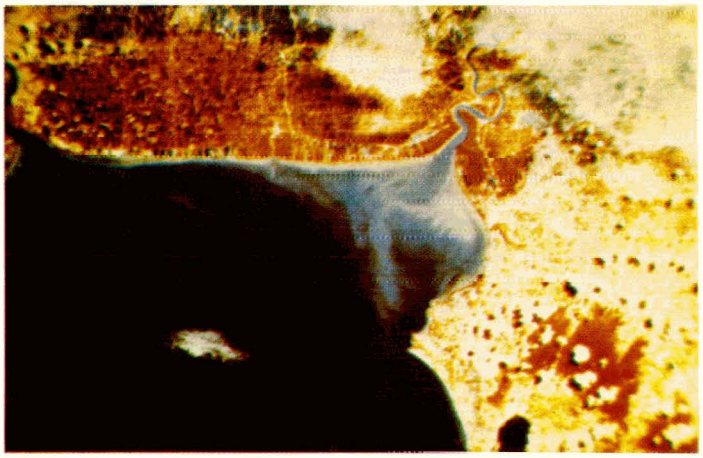

Figure 2. Examples of the Results of Identification

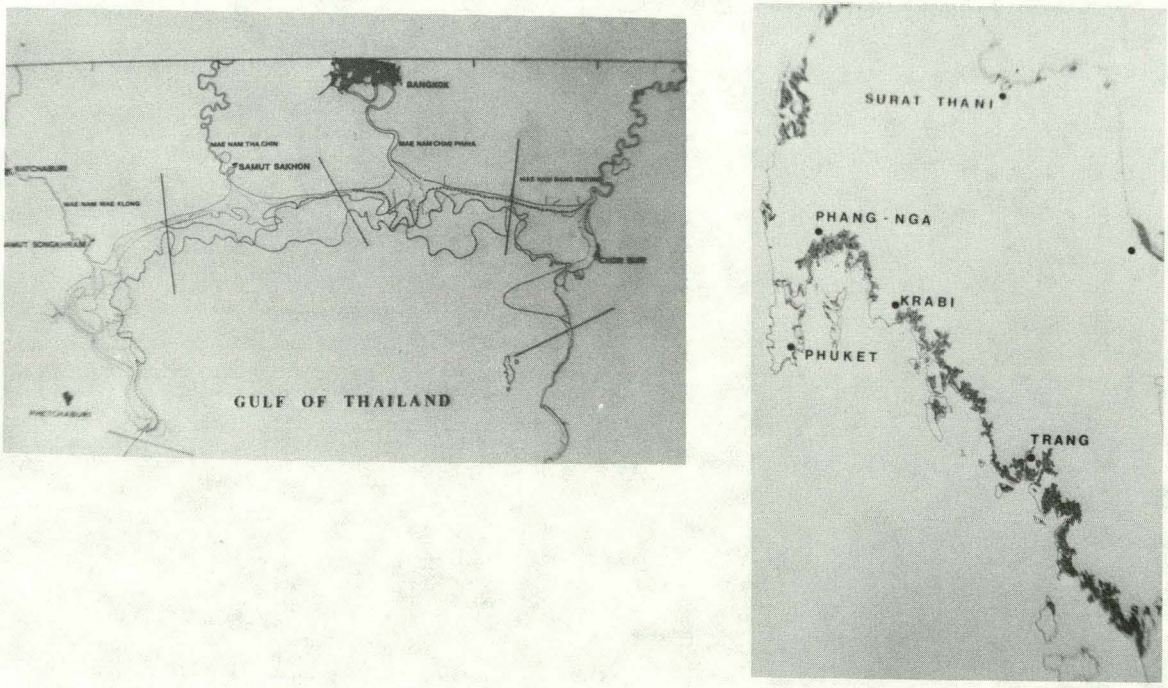

Figure 3. Relationship Between the Slope Angle and the Width of Mudflats Exposed During Low Tide

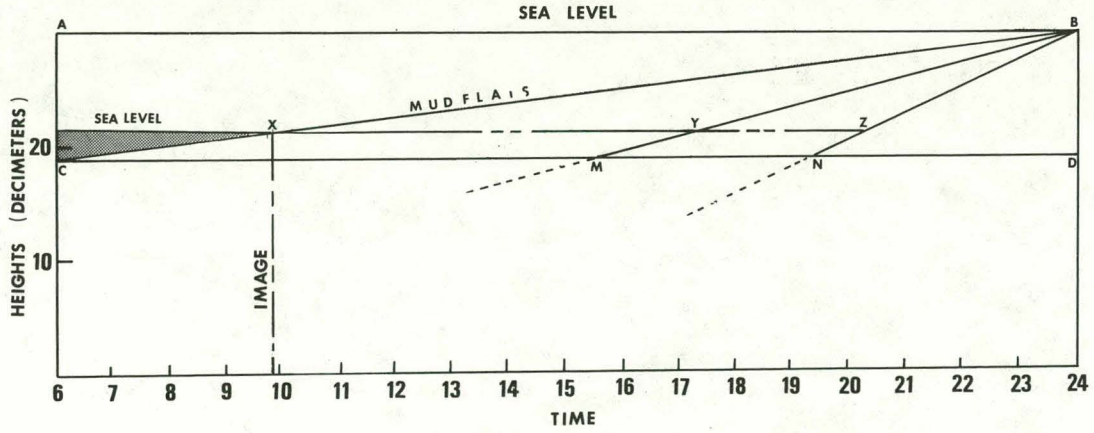

THIS PAGE

WAS INTENTIONALLY

LEFT BLANK

CORAL REEF MAPPING USING LANDSAT DATA: FOLLOW-UP STUDIES

Ricardo T. Biña

Natural Resources Management Center
Quezon City, Philippines

Kent Carpenter

Bureau of Fisheries and Aquatic Resources
Manila, Philippines

Wolfgang Zacher

University of the Philippines
Quezon City, Philippines

Robert Jara and Jose Bernardo Lim

Natural Resources Management Center
Quezon City, Philippines

ABSTRACT

This paper reports on additional techniques for mapping and interpretation of coral reef imageries based on the digital processing of LANDSAT data using the Image 100 Multispectral Analysis System. Major physiographic zones and bottom cover types of Apo Reef (Mindoro Island, Philippines) were categorized and mapped using combinations of unsupervised and supervised modes of digital processing. Categories were checked by actual ground survey. The advantages and limitations of LANDSAT 1 and 2 data for inventory and monitoring of coral reefs are discussed.

INTRODUCTION

The stenotypic nature of most coral reef organisms makes them particularly vulnerable to environmental changes. This vulnerability makes strict resource management of coral reefs necessary to insure their growth and survival. The vast distribution and often inaccessible locale of coral reef areas in the Philippines, however, renders systematic ground sampling for inventory and monitoring difficult. It is desirable therefore, to develop alternative or supplementary surveying techniques using remote sensing technology.

The use of digitally-processed LANDSAT imageries in thematic mapping of coral reefs has been demonstrated by Smith et. al. (4,5). Availing of aerial photographs as the source of ground truth, the study identified and mapped the major physiographic features of a reef surface through supervised four-band multispectral scanner (MSS) classification. Evaluation shows, however, that for an effective inventory and environmental monitoring of coral reefs, more information regarding bottom cover composition and bathymetry are necessary.

In conjunction with projects of the Philippine government on coral reef resource management, studies are now being conducted to determine the extent of useful information derivable from LANDSAT coral reef imageries through digital analysis. These studies include the following investigations: (1) development of techniques for extraction of maximum bottom cover and

bathymetric information within the limits of LANDSAT MSS band penetration using both supervised and unsupervised modes of classification; (2) development of techniques for interpretation and verification of digitally-produced categories; and (3) determination of the most efficient method of ground surveying of coral reefs for LANDSAT imagery interpretation.

This paper reports on the initial results of these investigations, giving emphasis on procedures for unsupervised digital mapping and interpretation based on ground truth.

DESCRIPTION OF THE STUDY AREA

The test site for this study was Apo Reef, an atoll located west of Mindoro Island (Fig. 1). Apo reef was selected because of its extensive reef area and accessibility for ground truth operations. The LANDSAT data used was from Scene No. 1153-01464, taken in December, 1972 at low, low water.

The physiographic features of Apo Reef appear to be the result of a complex combination of wind and current actions. Wind directions are strongest from the northeast and southwest, depending upon monsoon seasons. Although adequate oceanographic information are lacking, prevailing currents can be said to originate from the northwest. This is supported by the definite open back-reef characteristics of the southeast portion of the atoll. This southeast foul ground area of the reef is the only extensive shallow area with a seaward exposure. Submerged knolls characterized by sharply sloping southeast faces and gently sloping northwest faces, are numerous in the southeast foul ground area. The north, east, and southwest seaward slopes are steep, originating from shallow reef margins and dropping rapidly to depths of over 100 fathoms.

A deep west-to-east channel divides the Apo atoll into two separate lagoon systems. The southern margin of the north lagoon shows open back-reef characteristics, while the northern lagoon has limited access channels in its southwest corner opening to the west and south. The southern lagoon is generally more turbid and has a higher organic content in its sediments than the south lagoon.

Apo Reef exhibits the widely varying habitat types and biotic assemblages characteristic of atolls. Coral diversity is very high, making attempts to characterize the different coral communities according to a particular species, futile. Seaward shallow reef margins have generally high hermatypic coral cover, except in areas where alcyonarians dominate the coral community. The inner lagoon slope is often ill-defined. Large, branching acroporans are common on lagoon slopes and on the numerous mounds dotting the sandy lagoon floor. Gorgonians dominate the coral fauna of the southeast foul ground area of the northern lagoon and inside the channel opening up the southern lagoon to the southwest.

GROUND TRUTH METHODS

Four methods were used to obtain ground truth data on Apo Reef, namely: transects, "bounce" dives, underwater sled transects, and shallow surface reconnaissance. Employing Scuba and snorkeling equipment, the underwater investigation collected the following ground truth data: visually estimated percent bottom cover of rock, coral, and sand; predominant coral types; conspicuous flora and fauna; physiographic features; time; and depth. Position was determined by surveyor's compass.

Transects were used primarily on narrow reef flats. Graduated nylon lines were placed perpendicular to the shoreline extending down to depths of around 20 meters. Data for each predetermined length-interval were recorded. To establish the horizontal continuity of bottom cover zonation, additional transects were placed parallel to each other at a 100-m distance.

"Bounce" dives were resorted to on reef expanses where pre-determined diving points were located based on the evaluation of LANDSAT imagery. The "bounce" dives were simply short-duration dives in which divers recorded information in the immediate vicinity of the dive site.

Timed-sled transects were utilized for coverage of extensive reef-flats, lagoon areas and areas between transects and "bounce" dive points. This method employed a two-diver sled towed in a straight line by a motorboat between two fixed points. To orient the data spatially along the transect, the motorboat traveled at a constant speed and time was recorded during data collection. The sled was maneuvered close to the bottom and depth was recorded with a submersible depth gauge.

For extensive shallow reef areas, surface reconnaissance was used. When an easily recognizable bottom type was viewed from the surface, position was recorded and data were collected in the immediate area using snorkeling gear. This method was useful both in point identification of bottom types, and along a continuum between two fixed points.

METHODS USED IN DIGITAL ANALYSIS

Digital analyses and processing of the Apo Reef LANDSAT imagery were performed using the Image 100 Interactive Multispectral Image Analysis System. It is a computer-aided system in which the different processing and analytical functions, i.e. band ratioing, parameter modifications, feature training, spectral signature acquisition and input, clustering color-coding, image and theme superposition, synthesis, etc., are either built-in hardware functions or stored software which can be selected and executed by push-button operations.

False-color composites of MSS 4, 5, 6 and 7 LANDSAT imageries of Apo Reef (Fig. 2) were derived from the LANDSAT CCT and displayed on the TV monitor screen at a scale of about 1:50,000. Target areas for analysis were specified to the computer through an electronic cursor display. Results of digital classification were also displayed in the TV screen in the form of false-colored thematic maps which can be superposed with the video image. Based on the analyst's options, such thematic maps could be altered and modified using appropriate function programs or switches. Classified imageries were photographed from the video screen and printed in alphanumeric and binary theme print forms via the line printer.

Unsupervised Mapping of Major Physiographical Features

Prior to detailed mapping of coral reefs, it was found desirable to first map out the major bottom cover and bathymetric variations of the reef's surface. This is to aid in the interpretation of the more detailed categories, and also to provide qualitative and quantitative information on the reef's major structure.

By digital ratioing of the two most penetrating bands (MSS 4/MSS 5), a set of signals related to depth changes (3) was obtained. These signals were digitally superposed with the raw MSS 4 and MSS 5 data to obtain a digital image with pixels characterized by bottom-related and depth-related signals. This "depth-enhanced" data set was used as input in the execution of an automatic clustering algorithm which uses a combination of maximum likehood and Euclidian distance functions. Results were displayed in the video screen in the form of a false-colored thematic map.

Stratified Mapping of Bottom Cover Types via Unsupervised and Supervised Digital Classification

Polcyn et al. (3) has demonstrated that the band signals defining underwater features of an imagery are the sum of signals due to bottom reflection and signals due to sea-surface and atmospheric influences. The former contain depth and/or bottom-type information while the latter are considered as background signals. For submerged features, the same background signals are

the only data on channels with little or no water penetration (MSS 6 and MSS 7). Hence, in a four-band data set, not all the four MSS bands are useful. The number of significant channels defining a pixel of a reef imagery would be a function of water depth as a result of differences in water attenuation coefficients among the four MSS bands. In the case of Apo Reef imagery, for example, the four-band data set would be useful in defining variations in surface feature of emergent and very shallow areas, but not so in deeper portions where no bottom reflections could be derived from MSS 6 and MSS 7. These considerations suggest that to obtain the maximum digital information from an imagery with combined emergent and submerged features, the number of MSS channels to be used in digital mapping should be a function of significant bands defining each pixel in the imagery. This means separate digital mapping for different portions of the imagery. Moreover, it would be necessary to eliminate the background signals from every pixel to avoid false classification.

To determine the appropriate number of MSS channels for the digital processing of the different portions of the Apo Reef imagery, each pixel in the image was assigned to a "band zone." A band zone defines which band data are significant in a given pixel. Band zone mapping was accomplished by first determining the level of background signal. This was done by scanning on deep water where there was no bottom-reflected signals. The obtained signal values were then subtracted from the four band data set. All the pixels in the four-band imagery were then digitally sorted into four color-coded categories. The categories (band zones) represent pixels with band signals above the background signal level in the following spectral regions: MSS 4-7 (Zone 1), MSS 4-6 (Zone 2), MSS 4-5 (Zone 3) and MSS 4 (Zone 4). Each band zone was then digitally classified into spectral clusters via the previously mentioned clustering algorithm using the corresponding number of channels. The spectral data set for each zone was specified to the computer using the electronic cursor display.

To synthesize the derived spectral clusters into bottom-cover categories and correlate them with the ground data, the band signal counts of bottom-cover types identifiable from the imagery (with depths verified via ground survey) were read directly from the cathode ray tube terminal using the electronic cursor. The probable band signal counts of these bottom-cover types corresponding to depth changes were then approximated using Polcyn's (3) equation:

$$z = \frac{1}{\alpha i\ (\text{Sec}\ \theta + \text{Sec}\ \phi)} \ln \frac{\Delta Voi}{\Delta Vi}$$

$$\text{or}\quad \Delta Vi = \frac{\Delta Voi}{e^{z\,\alpha i\ (\text{Sec}\ \theta + \text{Sec}\ \phi)}} \qquad (1)$$

$$\text{and}\quad Vi = \Delta Vi + Vbi \qquad (2)$$

where z = water depth
αi = attenuation coefficient of an MSS band
ΔVoi = band signal count of a bottom type at zero depth (background signal subtracted)
ΔVi = band signal count of a bottom type at Z depth (background signal subtracted)
Vbi = background signal count
Vi = actual image band signal count

To calculate for the expression $\alpha i\ (\text{Sec}\ \theta + \text{Sec}\ \phi)$, a point in the imagery whose depth and bottom type were actually determined by ground survey was located using the electronic cursor and the corresponding band signal count (Vi) was read. The background signal count values (Vbi) were then subtracted from Vi to obtain ΔVi. Similar procedure was used for ΔVoi for each bottom cover type. From the derived constant and using Equations 1 and 2, band signal counts of a bottom cover type for every given depth interval for MSS 4 and MSS 5 were derived and tabulated. Each spectral cluster derived from the clustering algorithm was then assigned to a bottom type category by matching its mean band signal counts with the derived bottom cover depth-signal values. The synthesized clusters were color-coded and superposed with the video image to produce a thematic map showing variations in bottom cover within a given depth-

range. Accuracy of the thematic patterns were then checked against ground truth data.

RESULTS

Figure 3 indicates the major physiographical features of the reef represented by coded thematic clusters derived from the digital clustering of combined MSS 4, MSS 5 and ratio of MSS 4/5. Figure 4 shows the "band zones" or areas in which the band signals in each channel are above the background signals. Figure 5, 6, 7 and 8 show the bottom type categories stratified according to band zones after application of the unsupervised clustering program. Each cluster represents a synthesis of several clusters combined after interpretation and correlation with ground truth data. The mean band signal counts of each cluster are shown in Table 1. Table 2 shows the derived band signal counts in MSS 4 and MSS 5 of each bottom cover category in different depths based on Polcyn's (3) depth-band signal function. The values were used to verify the bottom cover category of each cluster in Figs. 5 to 8.

DISCUSSION

The unsupervised clustering of the combined MSS 4, MSS 5 and ratio of MSS 4/MSS 5 data (Fig. 3) demonstrates that the major physiographical features of coral reefs can be thematically mapped without providing a training set. Since the ratio of MSS 4 and MSS 5 are related to depth changes, relative depth-bottom categories can be approximated by inspecting the band signal counts of each cluster and comparing them with previously processed imageries verified by ground truth (assuming radiometric corrections are made). Such an approach should be useful in pre-mapping unsurveyed reef areas to pinpoint features of interest for detailed surveys and for establishing survey stations.

The categories in Fig. 3 represent only the major structural features of the reef and do not show the variations in bottom cover within each category. This is to be expected since band ratioing tends to obscure minor spectral variations among pixels. To map in detail the variations in bottom cover, it would therefore be necessary to go back to the original four-band data sheet.

Two general approaches can be considered in mapping bottom cover categories from LANDSAT imageries namely, the supervised and the unsupervised approaches. The supervised approach using training sets is useful in pinpointing features of interest, e.g. corals and algal rims. This approach, however, could be extremely tedious if one desires to map the maximum details within the limits of the LANDSAT resolution. Such task would require a large number of training sets and precise cursor sizes to ensure spectral uniformity. To be able to do so would also require a synoptic and detailed knowledge of the test area which can only be obtained through intensive ground survey.

The unsupervised approach using clustering algorithms and the whole data set, as demonstrated in this paper, can conveniently classify the imagery into as many categories as statistically feasible without inputting a training set. However, this approach is easily susceptible to miscategorizations in the absence of preprocessing treatment of the data. For underwater features, unsupervised digital misclassification can be expected since different bottom types at different depth locations could have the same band signals. This misclassification can be greatly minimized though by stratified mapping using the appropriate band combinations as shown in Figs. 5, 6, 7 and 8. By segregating pixels according to their significant band data (Fig. 4) and classifying them separately, the probability that pixels belonging to different band zones are clustered together is eliminated. Thus in Figs. 5, 6, 7 and 8 each group of clusters are limited to within the depth range of the least penetrating channel so that bottom cover categories within the emergent areas (Fig. 5), the very shallow areas (Fig. 6), depths between 1-3m (Fig. 7), and depths between 3 - 9m (Fig. 8) are well-defined.

The band zone map (Fig. 4) is useful in stratifying bottom cover categories and also serves as a reference point in interpreting the major physiographic zone categories (Fig. 3). Each category in Fig. 3 was verified aside from the ground data, by superposition with the band zone map and noting the location of overlap. In this way the depth range of each category, based on the depth penetration of each MSS band, was established. The band zone map in itself gives information on the gross morphological features of the reef, including the approximate depth ranges of the reef's surface. As shown in Fig. 4, areas of abrupt drop, gradual slopes, intertidal zones (zone 1 and zone 2), shallow and deep lagoons are well-delineated. For ground surveys, this information can save several man-hours in locating study stations and routes for watercraft. The band zones likewise indicate the quality of radiant energy received by different areas in the reef and should prove very useful for radiance productivity studies.

The area and number of band zones in an imagery will depend on the tidal state in which the scene was taken, as well as the extent of emergence of the reef's surface from the highest tide line. A temporal comparison of the band zones of the same reef area should therefore delineate the areas which are subject to light quality changes ("interspectral zones") and which have to be taken into account in attempts to map bottom features based on LANDSAT imageries. It should be noted that categories in each band zone in Fig. 4 are extant only with the tidal conditions at the time the LANDSAT scene was taken. Analysis of temporal imageries should reveal the more stable features (1).

Another problem inherent in the unsupervised clustering concerns the interpretation and categorization of the numerous digitally-produced patterns, unless one is thoroughly familiar with the conditions existing in the study area. In the initial classification, for example, more than thirty clusters were obtained. To interpret these clusters and synthesize them into meaningful categories, the spectral signatures (or band signals) of each cluster were examined and correlated with existing data. From these inspections, the following classes of clusters were observed:

1. Clusters representing homogenous bottom units, i.e. hermatypic corals, calcareous rocks and sand.

2. Clusters representing mixes of bottom units, e.g. coral-rock, rock-sand, etc. These are further subcategorized into clusters according to percentage of mixes.

3. Clusters representing the same bottom unit but are subcategorized according to color tone, e.g. pure white sand vs. silty-sand, bare calcareous rock vs. algal-covered rocks.

4. Clusters representing the same bottom unit but with spectral difference due to depth locations.

The number of cluster classes mentioned above points to the complexities involved in the detailed mapping of submerged features based on LANDSAT digital data. It also emphasizes the wide variations in reef community structures and the number of training sets required for supervised classification.

Resolving the above-mentioned clusters into meaningful categories can be made easier by matching each cluster's mean band signals with the values in Table 2. By this approach, clusters representing the same bottom type can be grouped together irrespective of depth. The efficiency of this method, however, depends in the acquisition of a set of ground data which should either show the attenuation coefficient in water for each band at several points in the imagery or identify the representative bottom types with known depths in the imagery. The former requires real-time *in situ* investigation which on the operational standpoint is not practical, especially when several LANDSAT scenes are involved. The latter does not require real-time ground truth, assuming that bottom types in a reef area do not appreciably change within a certain number of years (unless disturbed by human activities or storms). To obtain the latter set of information, the transect method would be the most practical to employ. The problem of locating the transect can be facilitated by first per-

forming clustering classification on the imagery and then determining points in the imagery which contain clusters showing progressive spectral changes and points in the imagery with clusters showing wide variations in spectral signatures.

An alternative procedure which can be considered in the future is to locate homogenous bottom units, e.g. corals, calcareous rocks, sand, etc., and establish their spectral signatures in two MSS bands at different depth locations. A mathematical model then could be constructed which will predict spectral signature changes for various percentage combinations of these bottom units. Pixels with such spectral combinations can then be clustered together.

Inspection of the band signal counts given in Table 1 and Table 2 shows that spectral distinction among the bottom features is possible only when at least two MSS bands are used. As can be observed, different bottom features at different depths would have the same counts in either MSS 4 or MSS 5. However, when the signals in both channels are taken together, the spectral differences among the bottom features become apparent.

Since classification accuracy is a function of the number of MSS bands, the maximum depth in which bottom type can be identified from LANDSAT imageries is limited to that point where its MSS 5 band signals fall just above noise level. This threshold depends on the bottom-cover reflectivity. Thus, for Apo Reef imagery, coralline sand, which has the maximum bottom reflectivity, can be confidently recognized up to 3.5 m depth using both MSS 4 and MSS 5. For the remaining bottom types the recognition thresholds lie above 3 m using the same band combinations. Beyond these threshold levels, where only MSS 4 data are significant bottom type identification is severely diminished unless one can deduce information from the spatial relationships of gray tones.

The recognition thresholds will vary according to the background signal levels as well as the clarity of sea water. With less atmospheric interference and with clearer water, the recognition threshold could still be extended if a high-gain mode setting for MSS 4 and MSS 5 is used. Since the low-gain mode setting was predominantly used in LANDSAT 1 and 2 coverage, this study, through the derived values in Table 2, has more or less bracketed the limits in which we can derive useful information from LANDSAT 1 and 2 data. For coral reef inventory and monitoring, where more exact recognition of bottom type is required, LANDSAT 1 and 2 data appear useful to depths of only about three meters. On the other hand, through MSS 4, simple detection of reefs with predominantly coral-rock structure is possible up to 9 m. As shown in Table 2, the maximum depth detectable in MSS 4 is 14.5 m for white-sand bottom, which agrees with the observations of other workers (2). Within this depth, range, therefore, LANDSAT MSS 4 should be useful in detecting submerged reef areas.

The limitation in terms of depth coverage, is compensated by the ability of LANDSAT 1 and 2 data to generate useful synoptic information over a large area. The bottom feature delineation within the recognition thresholds allows for habitat identification which could be used to predict adjacent deeper bottom types. This information is valuable when considering the time and effort required to obtain the same information through conventional ground surveys.

For environmental monitoring, the 3-m bottom recognition limit would be sufficient to indicate gross changes on the reef's surface. The fact that the spectral population can be resolved into finer categories via stratified classification at a distance of 2 to 4 MSS signal counts suggests that spectral shifts due to biotic changes, such as massive coral destruction or unusual growth of algal mats, could be detected.

CONCLUSION

These preliminary results demonstrate the feasibility of unsupervised and automatic digital mapping of major physiographic structures and bottom cover variations of coral reef using LANDSAT imageries, provided that data inputs are pre-treated using the described procedures. The main advantage of this method is that previously identified training sets which are difficult to define in the imagery are not necessary to produce a total classification of the study area. Thus, a digitally produced thematic map of the study area can be prepared prior to a ground survey. This map would then be the basis for plotting sampling points and designing the sampling techniques to be used. Final class assignment and synthesis of the digitally-produced patterns into concrete categories, however, still require the analyst's supervision based on the outcome of ground investigation and analysis of the spectral signatures of each pattern.

Since the band signals of a bottom feature depend on tidal conditions as well as atmospheric state and oceanographic influences, temporal analysis would be necessary in order to make a permanent bottom-feature map of reef areas. Likewise ground truth data are also necessary for each imagery to be analyzed. This brings to task the value of LANDSAT data in mapping and monitoring reef areas where no ground information are available and which are too isolated to be investigated. One approach to this challenge, which would be the subject of our succeeding investigations, is to determine the relationships among the spectral signatures of the different bottom types, particularly of corals, against other substrates, and the relationship between MSS 4 and MSS 5 signals for each bottom type. Hopefully, some coefficient values would then be generated which could be used in recognizing bottom features or imageries without ground data.

Despite the limited water penetration range of LANDSAT bands at low gain mode, LANDSAT imageries are still very useful for obtaining coral reef inventory and monitoring data. The synoptic information the imageries provide within the limited depth range compensate for the number of man-hours and cost to obtain such information through conventional methods.

LANDSAT C and D higher data resolution and additional bands may prove more versatile in the delineation of bottom types. This advanced capability will be studied to determine its usefulness in monitoring and inventory of coral reefs.

ACKNOWLEDGEMENTS

The authors wish to acknowledge the participation and contributions of following persons in the ground survey operations: Mitchell Colgan, W. Einziger (UP Marine Science Center), P. Castañeda, H. Demarest, M. Davis, J. Ordoñez, R. Estudillo, M. Keeney, R. Deanon, V. Corpuz, S. Mohamed Ali Jr. and V. Albaledejo (BFAR Coral Research Project).

REFERENCES

1. Middletown, E. M. and J. L. Barker, 1976. Hydrographic charting from Landsat satellite: A comparison with aircraft imagery. GSFC Preprint No. x-923-76-111.

2. Polcyn, F. C. and D. R. Lvzenga, 1973, Calculations of water depth from ERTS-MSS data. Symp. on Significant Results Obtained from ERTS-1, 1B: 1433-1441.

3. Polcyn, F. C. and D. R. Lyzenga, 1975. Final Report Bathymetry and Shoal Detection with ERTS: NASA CR-ERIM 193300-51-F, April 1975.

4. Smith, V. E., R. H. Rogers and L.E. Reed, 1975a. Automated mapping and inventory of Great Barrier Reef zonation with Landsat data. Ocean 75 Conference Record, Institute of Electrical and Electronic Engineers, Inc., New York, 952.

5. Smith, V. E., R. H. Rogers and L. E. Reed, 1975b. Thematic mapping of coral reefs using Landsat data. Proc. 10th Int'l. Symp. on Remote Sensing of Environment, Vol. 1, p. 585.

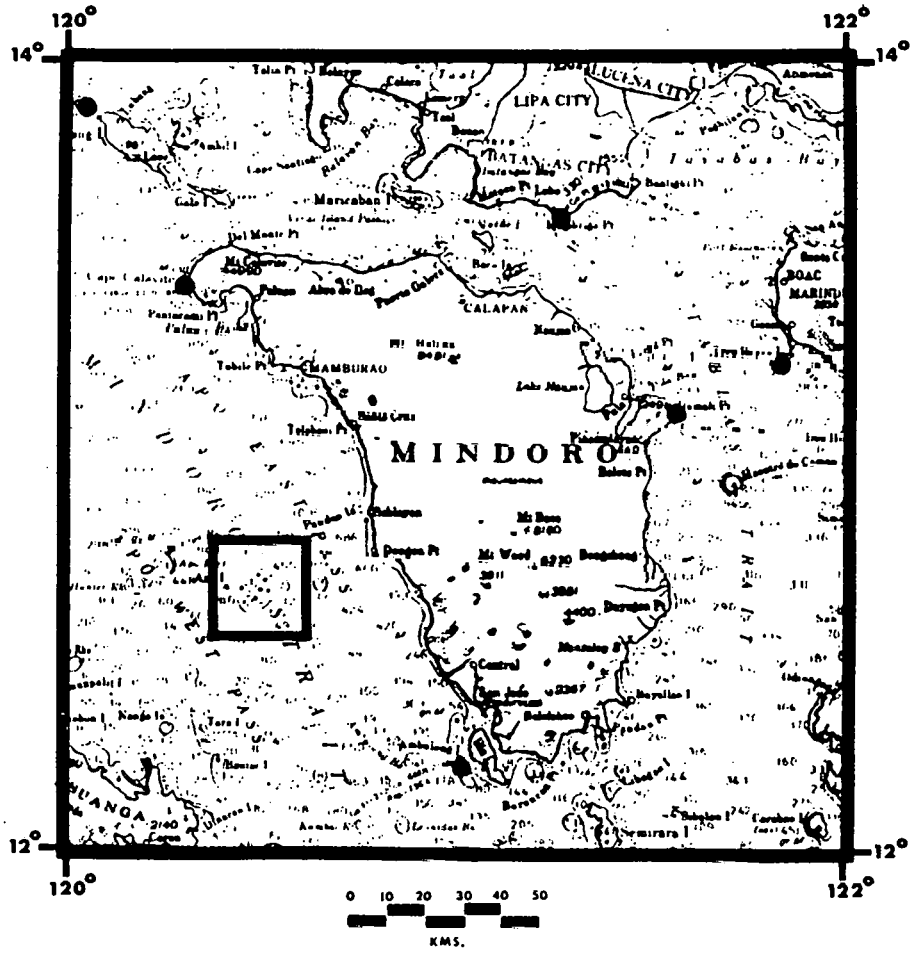

Fig. 1. Map showing location of study site.

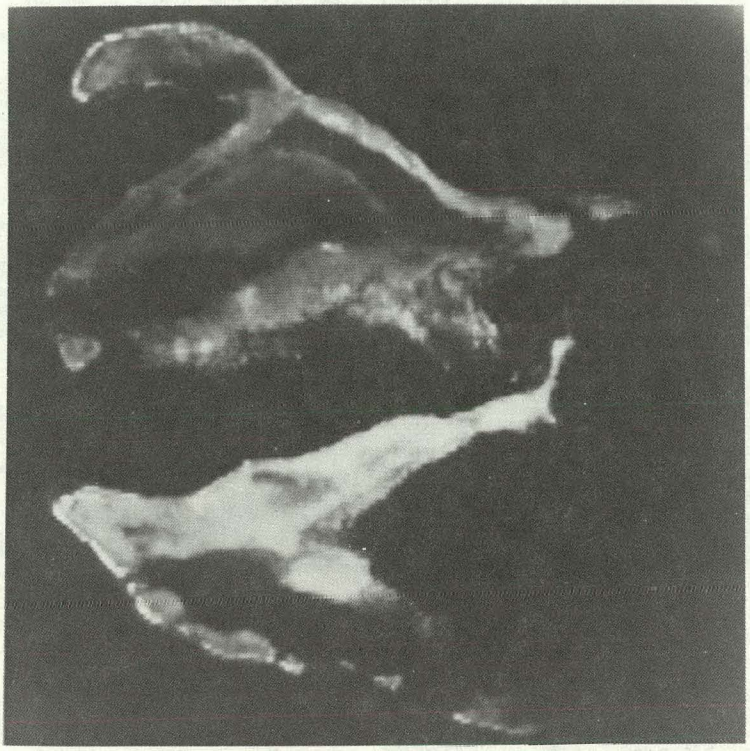

Fig. 2. Three-band composite image of Apo Reef.

Fig. 3. Categorized image of Apo Reef via unsupervised classification using combinations of MSS 4, MSS 5 and ratio of MSS 4/MSS 5 data. Categories represent the major physiographic features of the reef.

Legend:

0 - Reef ramparts and outer slopes and pinnacle reefs at 3-9 m. deep
\+ - Deep sandy lagoon (5 - 9 m)
* - Active coral reef flat
. - Sandy reef flat (3 - 5 m)
< - Coral rubble, sand and coral patches
3 - Shallow sandy flat with rubbles (1 - 3 m)
1 - White-sand covered inner slope (0 - 1 m)
8 - Emergent ridges

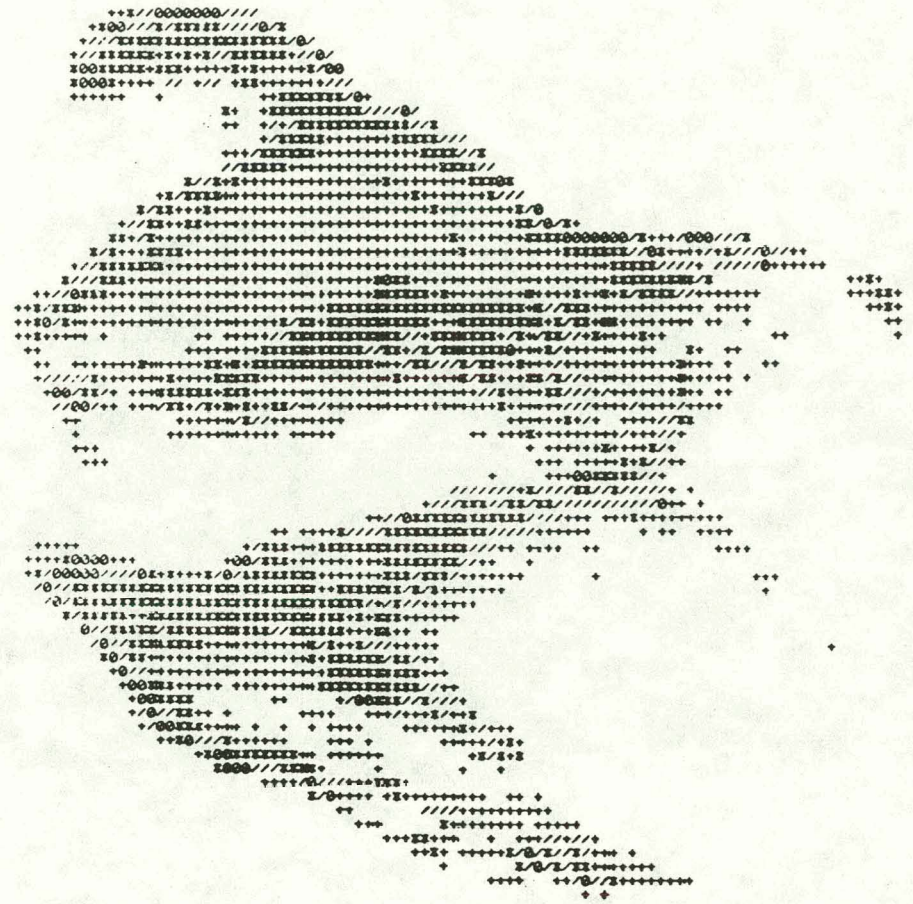

Fig. 4. Band zone categories of Apo Reef image showing areas in which the band signals in each channel are above the background signals.

Legend:

Band Zone 1	(0)	-	Pixels with 4-channel signals (MSS 4, MSS 5, MSS 6 and MSS 7).
Band Zone 2	(/)	-	Pixels with 3 channel signals (MSS 4, MSS 5 and MSS 6).
Band Zone 3	(*)	-	Pixels with 2-channel signals (MSS 4 and MSS 5)
Band Zone 4	(+)	-	Pixels with 1-channel signals (MSS 4).

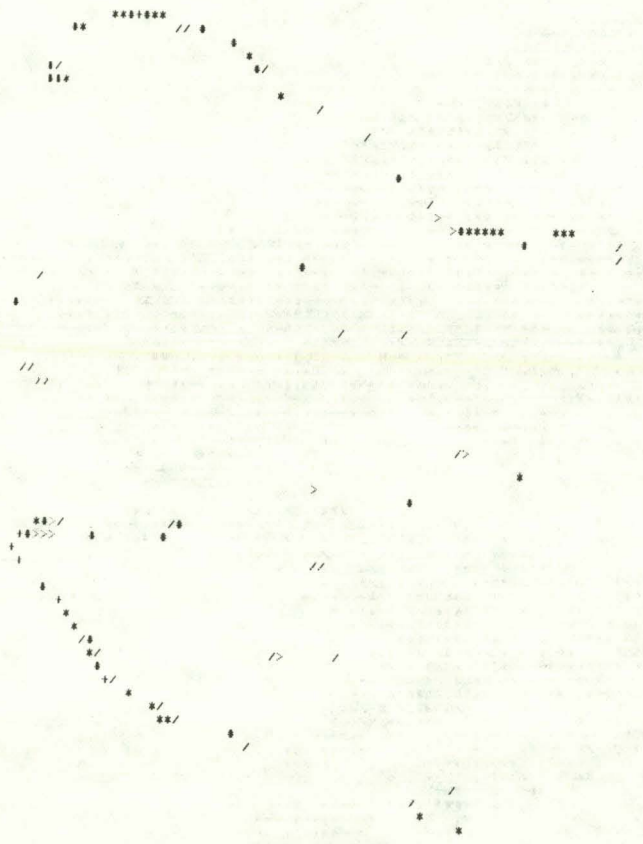

Fig. 5. Band Zone 1 categories representing reef bottom covers in intertidal and emergent areas.

Legend:

/ - Exposed high-density corals
* - Coral-rock mixes
\# - Rock-coral mixes
\+ - Emergent calcareous rocks including islet and bluffs
\> - Rock-coral-sand patches

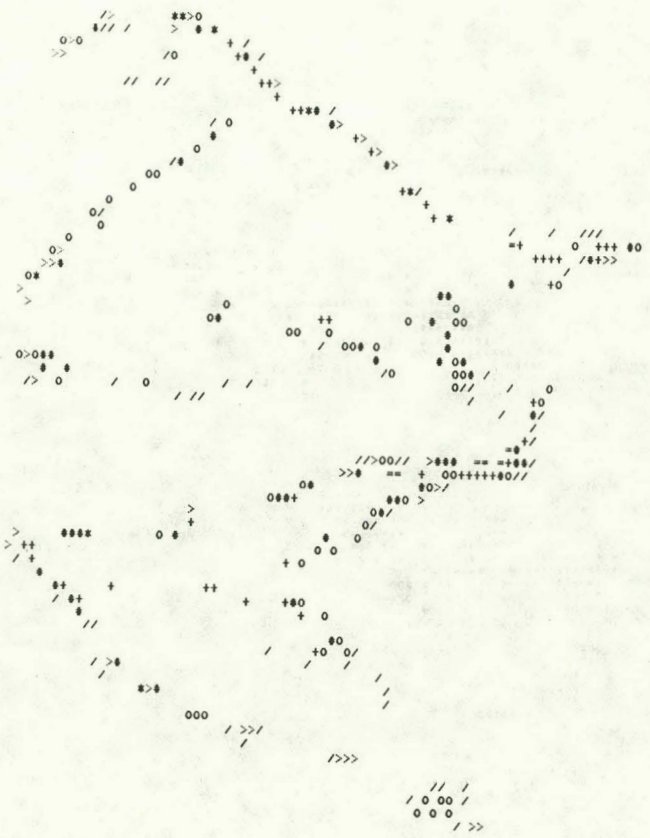

Fig. 6. Band Zone 2 categories representing bottom covers in very shallow (0.5m) areas.

Legend:

/ - High-density corals (90%) consisting mostly of table corals located at reef edge.
0 - Rock-coral (60% rocks, 40% corals)
> - Coral-rock (60% Corals, 40% rocks)
* - Rock-coral-sand patches (30% Coral, 30% rocks and 30% sand)
# - Calcareous rocks (90%)
+ - Rock-sand-rubbles at the edge of inner slopes
= - Coralline Sand patches

Fig. 7. Band Zone 3 categories representing bottom covers from 0.5-3 m.

Legend:

- / - High density corals (70-90%) in outer slopes (1-2m)
- 0 - Coral-rocks (60% Coral, 40% rocks) in inner and outer slopes (1-2m)
- . - Very shallow, almost emergent calcareous rocks (0-1m)
- * - Rock-coral-sand-rubbles along the inner lagoon slopes and foul ground areas (2 - 3 m)
- # - Sand and coral rubbles along inner slope of lagoon and foul ground areas (2-3 m)
- + - Rock-sand-rubbles (0.5 - 1 m)
- = - White sand flat (0.5 - 1 m)
- > - White sand flat (0-0.5 m)

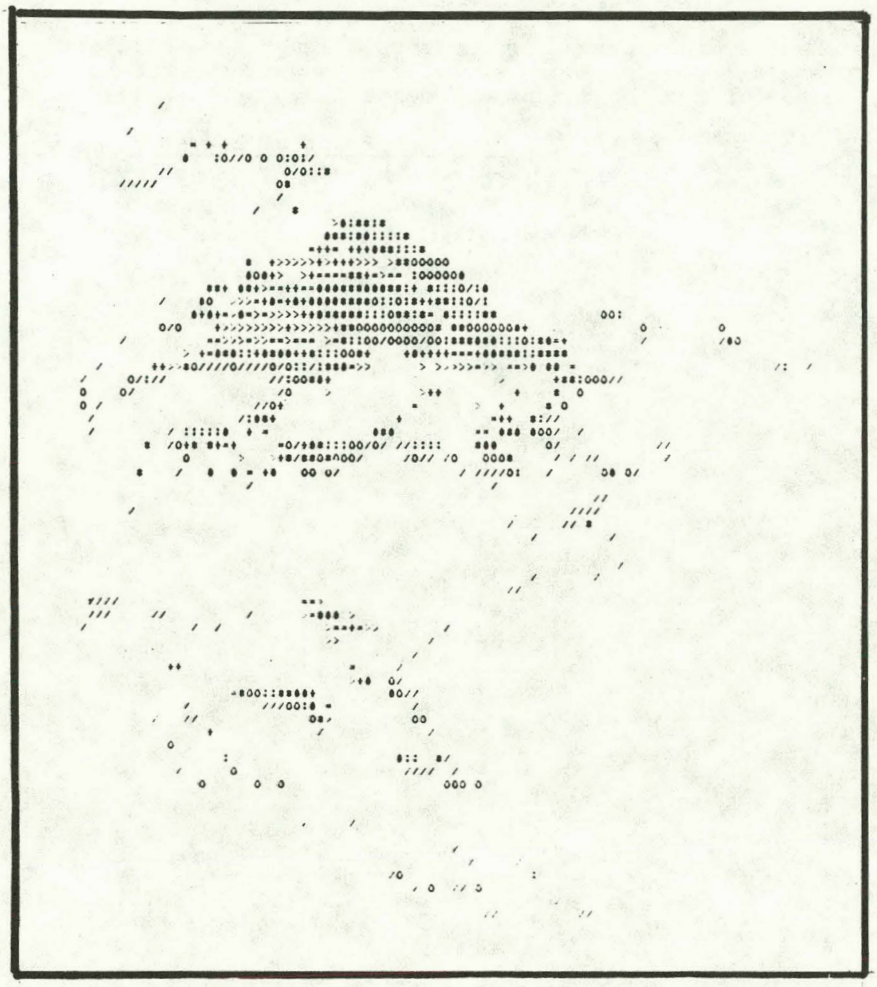

Fig. 8. Band Zone 4 categories representing areas from 3-9 m. deep.

Legend:

/ -
0 - Mixed depth-bottom categories of deep lagoons, ramparts and
: - pinnacle reefs (5 - 11 m)
* -

-
+ - Sandy bottom of lagoon subcategorized according to depth in-
= - tervals from 3 - 5 m.
> -

TABLE I

Mean band signal (counts) of clusters derived from unsupervised classification of Apo Reef Landsat imageries. MSS bands used for each band zone are denoted by asterisk (*).

Band Zone	Cluster No.	Map Symbol	Spectral Bands MSS 4	MSS 5	MSS 6	MSS 7
			*	*	*	*
	1	/	32	20	15	7
	2	*	33	23	20	8
1	3	#	37	25	18	6
	4	+	35	26	26	16
	5	>	44	30	20	8
			*	*	*	
	1	/	29	14	8	2
	2	0	37	18	8	2
	3	>	32	20	8	4
2	4	*	37	24	12	4
	5	#	44	23	9	2
	6	+	54	24	8	2
	7	=	62	26	8	2
			*	*	*	
	1	/	26	12	6	2
	2	0	32	13	6	2
	3	°	34	24	6	0
3	4	*	38	12	4	0
	5	#	43	13	4	0
	6	+	48	16	4	0
	7	=	54	18	4	0
	8	>	60	22	6	0
			*			
	1	/	26	8	4	0
	2	0	20	8	4	0
	3	:	30	8	4	0
	4	*	32	8	4	0
	5	#	34	8	4	0
	6	+	36	8	4	0
	7	-	38	8	4	0
	8	>	40	10	4	0
	Background signals:		21	11	8	4

TABLE 2

Band signal-depth relationship derived from Polcyn's depth-signal model vs. ground-truth derived bottom type.

Bottom Type	MSS 4 Signals (Counts)	Depth (m)	MSS 5 Signals (Counts)	Depth (m)
High Density Coral (75%-90% corals)	29 - 28	0.0 - 0.5	14 - 13	0.0 - 0.5
	27 - 26	0.5 - 2.0	12 - 11	0.5 - 2.5
	25 - 24	2.0 - 4.0	10 - 0	2.5 -
	23 - 22	4.0 - 8.0		
	21 - 0	8.0		
Coral-Rock (predominantly coral than rock)	32 - 30	0.0 - 1.0	20 - 17	0.0 - 0.5
	29 - 28	1.0 - 2.0	16 - 15	0.5 - 1.0
	27 - 26	2.0 - 3.0	14 - 13	1.0 - 1.5
	25 - 24	3.0 - 5.5	12 - 11	1.5 - 3.0
	23 - 22	5.5 - 9.0	10 - 0	3.0 -
	21 - 0	9.0 -		
Coral-Rock-Sand Mixes	37 - 36	0.0 - 1.5	24 - 21	0.0 - 0.5
	33 - 32	1.0 - 1.5	20 - 17	0.5 - 1.0
	33 - 32	1.0 - 1.5	16 - 15	1.0 - 1.5
	31 - 30	1.5 - 2.5	14 - 13	1.5 - 2.0
	29 - 28	2.5 - 3.0	12 - 11	2.0 - 3.5
	27 - 26	3.0 - 4.5	10 - 0	3.5 -
	25 - 24	4.5 - 7.0		
	23 - 22	7.0 -10.0		
	21 - 0	10.5		
Calcareous Rock	44 - 42	0.0 - 0.5	23 - 19	0.0 - 0.5
	41 - 40	0.5 - 1.0	16 - 15	1.0 - 1.5
	37 - 36	1.5 - 2.0	14 - 13	1.5 - 2.0
	35 - 34	2.0 - 2.5	12 - 11	2.0 - 3.5
	33 - 32	2.4 - 3.0	10 - 0	3.5 -
	31 - 30	3.0 - 3.5		
	29 - 28	3.5 - 4.5		
	27 - 26	4.5 - 6.0		
	25 - 24	6.0 - 8.5		
	23 - 22	8.5 -12.5		
	21 - 0	12.5 -		
Rock-Coral (predominantly Rock)	37 - 36	0.0 - 0.5	18 - 15	0.0 - 0.5
	35 - 32	1.0 - 1.5	12 - 11	0.5 - 1.5
	33 - 32	1.0 - 1.5	12 - 11	1.5 - 3.0
	31 - 30	1.5 - 2.5	10 - 0	3.0 -
	29 - 28	2.5 - 3.0		
	27 - 26	3.0 - 4.5		
	25 - 24	4.5 - 7.0		
	23 - 22	7.0 -10.5		
	21 - 0	10.5 -		
Rock-Sand-Rubbles	54 - 50	0.0 - 0.5	24 - 21	0.0 - 0.5
	49 - 46	0.5 - 1.0	20 - 17	0.5 - 1.0
	45 - 44	1.0 - 1.5	16 - 15	1.0 - 1.5
	43 - 42	1.5 - 2.0	14 - 13	1.5 - 2.0
	41 - 38	2.0 - 2.5	12 - 11	2.0 - 3.5
	37 - 36	2.5 - 3.0	10 - 0	3.5 -
	25 - 34	3.0 - 3.5		
	33 - 32	3.5 - 4.5		
	31 - 30	4.5 - 5.0		
	29 - 28	5.0 - 6.0		
	27 - 26	6.0 - 7.0		
	25 - 24	7.0 - 9.5		
	23 - 22	9.5 -13.5		
	21 - 0	13.5 -		

(con't Table 2)

	MSS 4 Signal (Counts)	Depth (m)	MSS 5 Signal (Counts)	Depth (m)
Coralline Sand	62 - 58	0.0 - 0.5	26 - 21	0.0 - 0.5
	57 - 54	0.5 - 1.0	20 - 17	0.5 - 1.0
	53 - 50	1.0 - 1.5	16 - 15	1.0 - 1.5
	49 - 46	1.5 - 2.0	14 - 13	1.4 - 2.0
	45 - 42	2.0 - 2.5	12 - 11	2.0 - 3.5
	41 - 40	2.5 - 3.0	10 -	3.5 -
	39 - 38	3.0 - 3.5		
	37 - 36	3.5 - 4.0		
	35 - 32	4.5 - 5.0		
	33 32	4.5 - 5.0		
	31 - 30	5.0 - 6.0		
	29 - 28	6.0 - 7.0		
	27 - 26	7.0 - 9.0		
	25 - 24	9.0 -11.5		
	23 - 22	11.5 -14.5		
	21 - 0	14.5 -		

α_4 (Sec θ + Sec $\emptyset$) = .26

α_5 (Sec θ + Sec $\emptyset$) = .77

THE APPLICATION OF REMOTE SENSING IN MARINE RESEARCH IN INDONESIA

D. P. Praseno

National Institute of Oceanology
Indonesian Institute of Sciences
Jakarta, Indonesia

Z. Soejoeti
Indonesian National Institute of Aeronautics and Space
Jakarta, Indonesia

Dijardjana
Indonesian National Institute of Aeronautics and Space
Jakarta, Indonesia

ABSTRACT

Indonesia is in the beginning of using remote sensing in oceanography. Some satisfactory results have been obtained from aerial photography and satellite imagery. The best results were mainly obtained from coastal regions.

Other sensors - the radiometer and thermal scanner - are presently being tested. The technique and preliminary results are discussed in this paper.

INTRODUCTION

The Indonesian archipelago consists of over 13,000 islands with more than 61,000 km of coastline. The Indonesian waters cover two-thirds of the Indonesian territory. In order to realize return from maritime opportunities, Indonesia is devoting considerable attention and efforts to scientific surveys and research in the marine environment.

In recent years Indonesia has started to utilize the remote sensing technique to complement the conventional types of surveys and research on marine environment by using research vessels. A few examples of satisfactory results are given here. Aerial photography with a multispectral camera was used in the study of coastal waters in Bali. LANDSAT imageries were used in studies of sediment transport in the Jakarta Bay, the Surabaya Strait, and the coastal zone studies in South Sumatera.

Other sensors are tested by the Indonesian National Institute of Aeronautics and Space

(LAPAN), such as radiometer for the detection of chlorophyll concentrations in the upper layers of the sea and a thermal scanner to monitor pollution in the marine environment.

AERIAL PHOTOGRAPHY

In 1973-74 a project was carried out to study the possible applications of remote sensing in oceanography, A MK-8 multispectral camera was used to collect data of coral conditions, freshwater discharge, and distribution of mangrove forests. A BW panchromatic aero 2424 film was used which is also sensitive to IR radiation (DARMOYUWONO 1976). The camera has four lenses, each equiped with four different filters. The filters were IR, red, blue, and green. Results were reported in several papers.

PRASENO and SUKARNO (1977) reported damage of coral roof in the Sengkidu waters, east coast of Bali. The destruction of reef was mainly caused by intensive mining by local people for construction material. Damage of the reef has caused beach erosion due to current and wave actions, The area of destructed corals and beach erosion was clearly shown in aerial photographs (figure 1).

DARMOYUWONO (1976) studied water conditions in Padang Bay, east coast of Bali. Sedimentation and sediment transport in the bay was clearly seen in the red band. Areas affected by the sediment showed poor coral growth, otherwise coral is seen in good condition.

Using the blue band, DARMOYUWONO (1976) studied patches of eel grass at the bottom of the sea. Bottom features could clearly be seen in clear water. Water depths in the bay doesnot exceed a depth of 2 m. The same diapositive was analyzed with an enhancer. More details could be observed by density contouring.

Another result which was not reported is the ability of the multispectral camera to map mangrove forests. The area, especially within the intertidal zone, is very important to fisheries. The water between the mangrove trees are usually used as nursery ground for many fish and crustacean larvae. Attached to the roots of the mangrove trees are several species of mollusks.

SATELLITE IMAGERY

A combination of two types of data, aircraft and satellite, was used in the study of coastal zone development (SOEUR et al 1975). The data were used to provide basis for the study of landforms, sediment and erosion sites, landuse dynamics, and albedo mapping in the Musi-Banyuasin area of South Sumatera. The study is meant as basis to develop National strategy on the multiple resource use management of coastal low land swamps, rivers, and estuarine areas.

LANDSAT data was also used in pollution studies (PRASENO 1975). The Jakarta Bay is greatly influenced by several types of pollutants. The study of water circulation systems in the

bay helps to ascertain affected areas. Sedimentation and sediment transport in marine environment is also important in harbor areas. The Surabaya Strait, east Jawa, is a very narrow passage to the harbor of Tanjung Perak. Aggradation endangers traffic to and from the harbor. LANDSAT imageries provide a system to monitor conditions of the passage (figure 2).

RADIOMETER

The radiometer was designed and constructed by the Deutsche Forschungs und Versuchtanstalt für Luft und Raumfahrt (DFVLR) in co-operation with the Indonesian National Institute of Aeronautics and Space (LAPAN). The instrument has four channels which detect upwelled electromagnetic energy in the 443, 525, 560, and 680 nm bands. It has a focal length of 10 cm, 3 cm collector lens, and a field of view of 6^{o}. Another set of detectors within the instrument is placed facing upwards with afield of view of 180^{o} to measure the incoming irradiance.

Upwelled energy from the sea is converted to electric signals. These signals contain among others informations about chlorophyll concentration. The incoming irradiance is also converted to electrical signals and used as reference in the multiplexer input system. The AC signals are converted to DC using a low pass active filter. After passing a 16 channel multiplexer each input signal is placed into different time intervals. A/D converter system and serial/parallel register converts multiplexer output signals into digital code pulse and records them on magnetic tape.

Chlorophyll characteristics in clear ocean water is shown in figure 3 and figure 4 (DUNTLEY). An increase in chlorophyll concentration is recorded as an increase in the absorption of the red (680 nm) and blue (443 nm) bands, and an increase in reflection in the green (560 nm) spectrum. In the yellow-green region there will be nochange by increase in chlorophyll concentration. The 680 nm spectrum is mostly absorp by water molleculs and is not directly used to detect chlorophyll, but is important for measuring water turbidity.

The determination of chlorophyll concentration is made in several ways. It can be calculated by using the formula :

$$Y = a + b \log X ;$$

in which Y is the ratio between signal-1 and signal-2,
a and b are constants, and
X is the chlorophyll concentration.

The ratio between reflectance recorded by detector-1 and that recorded by detector-2 (R1/R2) or R1/R3 or R2/R3 as a function of chlorophyll concentration is plotted in figure 5. Also the difference (R1 - R2) or (R1 - R3) or (R2 - R3) as a function of chlorophyll concentration is plotted in figure 6,

The radiometer was tested in the Jakarta Bay lead by Messrs. V. AMANN and G. MIOSGA. Results showed higher values obtained by the radiometer in comparison to ground truth. The chlorophyll concentrations obtained from ground truth were only measured at the surface of the sea. Since the mission was flown in the afternoon (1.30 p.m) phytoplankton might be concen-

trated in deeper layers. Another explanation of the radiometer's high value is the possibility of non-chlorophyll reflectance which was recorded by the detectors. The bay water is highly influenced by freshwater discharge coming from many rivers, and carrying many types of pollutants.

THERMAL IR SCANNER

In 1976 LAPAN received and began to operate a thermal IR scanner. The sensor is a dual channel IR scanner type DAEDALUS which is a quantitative line scanner system. The equipment consists of two subsystems; respectively an airborne subsystem unit and a ground subsystem unit. The detectors are composed of an InSb sensor working in 3 - 5,5 micrometer region and a HgCdTe sensor working in the 8 - 14 micrometer region. The detectors are mounted in an end-looking, metal cased vacuum dewar which has sufficient liquid nitrogen coolant that has a capacity of approximately 6 hours of operation before refueling.

In the marine environment the scanner is used, among others, for the detection and monitoring of pollution. Biochemical processes of sewage causes increase in sea surface temperature. Different temperatures may also be caused by oil pollution due to the process of evaporation. However, the ability of IR imagers to respond to signals generated either by changes in temperature or by changes in emissivity may give rise to ambiguities in image interpretation. These ambiguities can be reduced to some extent by the acquisition of correlative or ground truth data.

Water is generally considered to be a blackbody radiator in the IR region at normal terrestrial temperatures (CONROD and BLYTHE 1971). According to STEFAN BOLTZMAN's law, blackbody radiates energy in the form of : $W = \sigma T^4$, which describes the total emitted energy of a blackbody as proportional to the fourth power of temperature. The temperature may be determined by comparing thermal image densities with grey scale generated by independent calibration technique or by using an on board blackbody reference device.

Both positive and negative transparancies have tones varying from a very dark to a very bright level. On positive transparancies or paper prints the very dark level indicates a very low temperature, and a very bright level indicates a very high temperature. By knowing the densities of each grey level of the terrain, the temperature difference can be determined.

Blackbody radiant emmittance as a function of wavelength at various temperatures is plotted in figure 7. Temperature differences in water are best measured using the 8 - 14 micrometer wavelength. This region offers the highest emittance levels. On the other hand the percentage change in radiance energy is greater in the lower wavelengths. This will offer higher contrast in the end product imagery.

The scanner was tested in the Jakarta Bay area. During a night mission on January 23,1977 thermal pollution was observed caused by hot water discharge coming from water outlet of a power plant (figure 8). East of the harbor oil pollution some temperature differences with

the surroundings (figure 9). During a morning mission on April 19, 1977 over Muara Angke freshwater is seen entering the sea (figure 10). The river water may carry several kinds of pollutants, and have different temperatures than the sea water. By studying distribution patterns, current systems in the bay can be monitored. Also areas affected by pollution.

CONCLUSION

1. Remote sensing data in oceanography can complement conventional obtained data.
2. Multispectral photography is proven useful in oceanography, especially in coastal regions. The blue band is able to penetrate sea water to several meters and can be used to study bottom features. Admospheric noise may sometimes interfere. The green band is also useful for the study of the coral reefs, benthic flora, and sediment transport (water circulatory patterns). The IR band is good for mapping purposes and for the study of mangrive forests in the intertidal zone.
3. LANDSAT imagery is found useful, especially for monitoring puposes. Repeated coverages enable the study of changes of the environment.
4. The radiometer may develop into a useful tool to detect upwellings in the ocean.
5. The thermal scanner is found a perfect tool for pollution studies, and might also be useful in detecting thermal differences in upwelling regions.

REFERENCES

CONROD, A. C. and R. BLYTHE 1971. Infrared imagery of polluted water: The need for multispectral scanner. Bendix Technical Journal 4(3): 29-34.

DAEDALUS ENTERPRISES INC. Instruction manual Daedalus DS-1230 Basic Dual Channel Quantitative line scanner system, vol.1.

DARMOYUWONO, K. 1976. The applications of remote sensing for detection and monitoring of pollution in the marine environment in Indonesia. Paper presented at the Seminar on marine pollution, Jakarta 26-28 July 1976: 27 pp. (in Indonesian).

DUNTLEY, S. Q. Detection of ocean chlorophyll from earth orbit.

PRASENO, D. P. 1975. A study on pollution in the Jakarta Bay and its vicinity based on ERTS-1 imagery. Proc.Joint UN/FAO Regional Seminar on Remote Sensing Applications, Part II: 241-250.

PRASENO, D. P. and SUKARNO 1977. Observation on beach erosion and coral destruction by remote sensing techniques. Marine Research in Indonesia 17: 59-68.

SOBUR, A. S.; R. J. CHAMBERS; J. DAMOPOLII; S. HADI; A. J. HANSEN 1975. Remote sensing application for environmental and resource management studies in Musi-Banyuasin coastal zone, South Sumatera. Proc.Joint UN/FAO Regional Seminar on Remote Sensing Applications, Part II: 251-280.

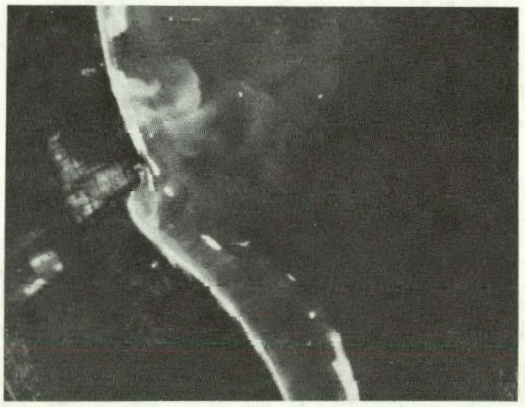

Figure 1. Beach erotion and coral destruction observed with a multicpectral camera, green band

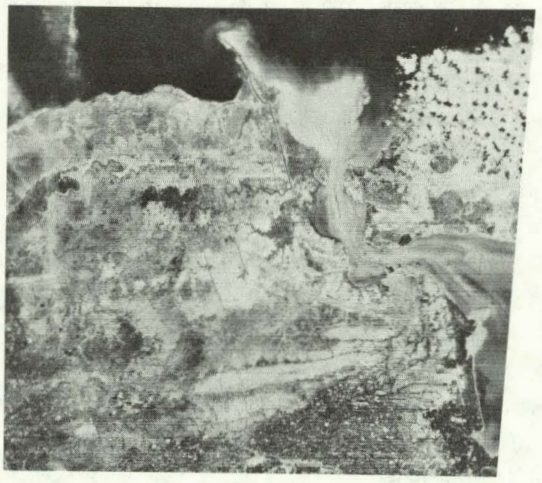

Figure 2. LANDSAT imagery of Surabaya strait showing sedimentation and sediment transport channel.

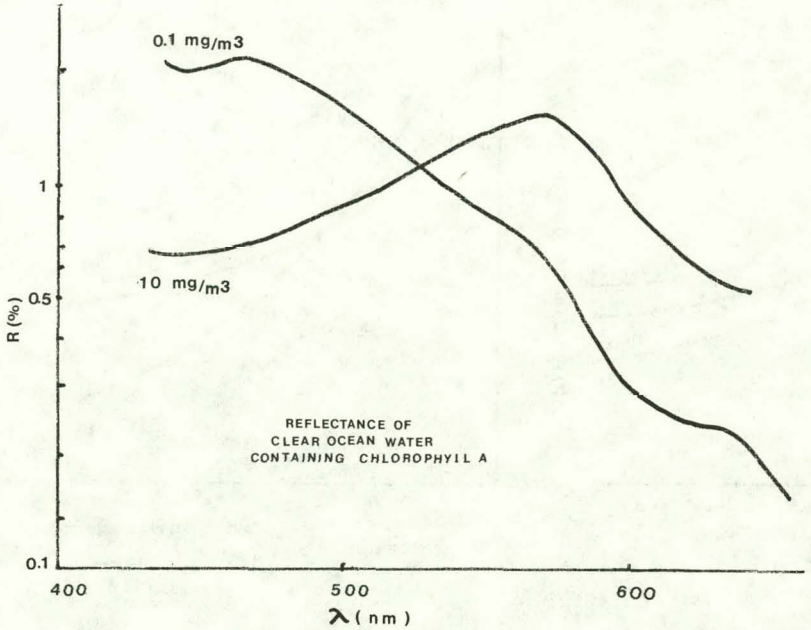

Figure : 3

(DUNTLEY)

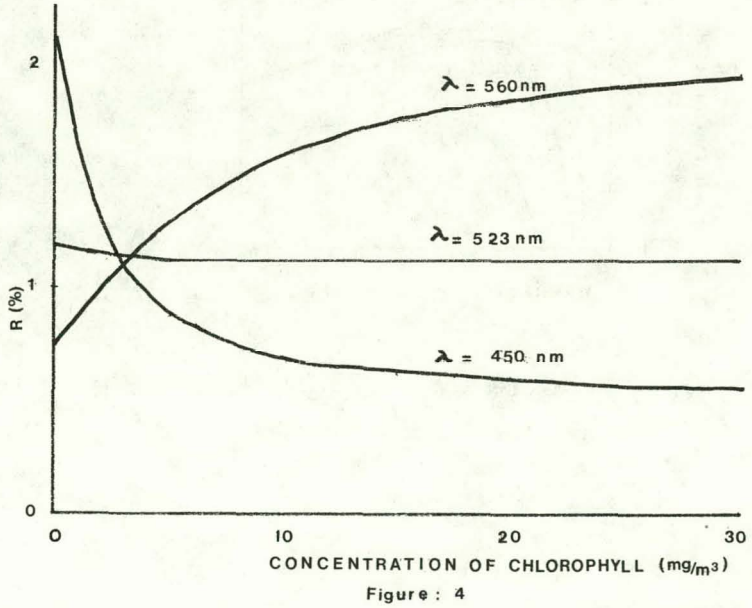

Figure : 4

(DUNTLEY)

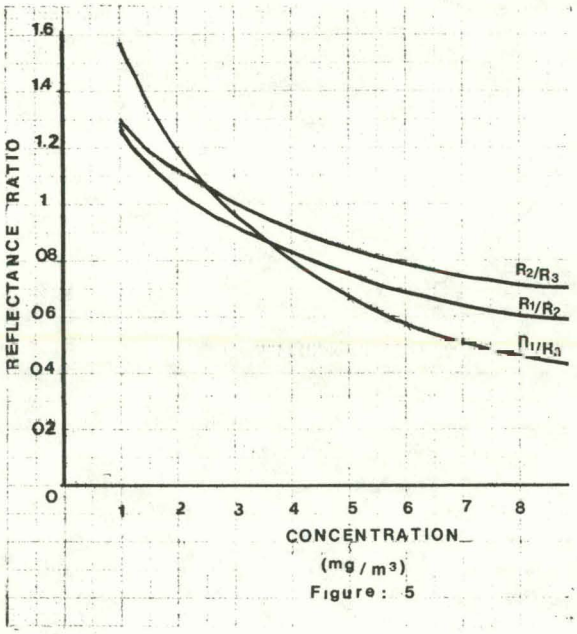

Figure: 5

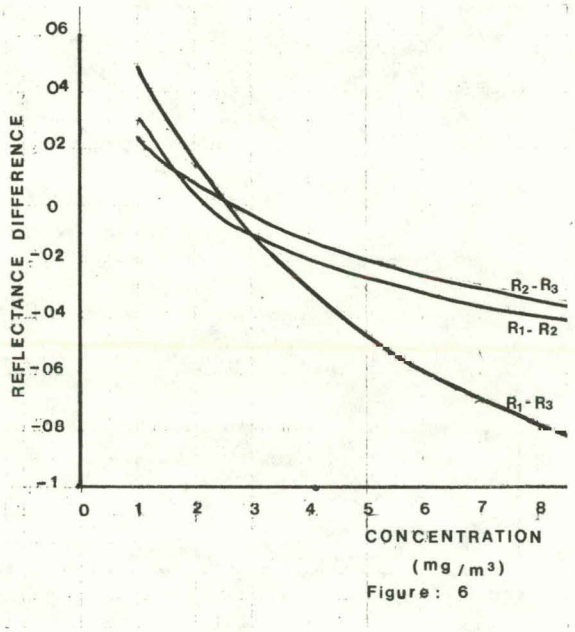

Figure: 6

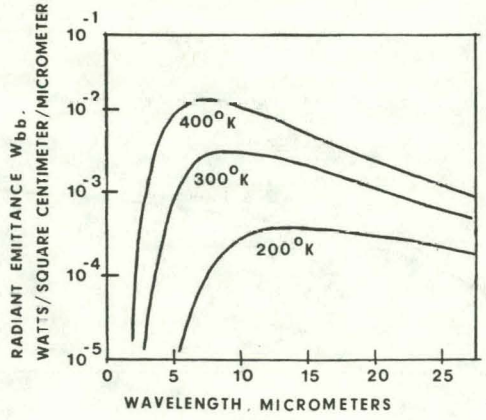

Figure 7. Blackbody radiant emittance as a function of wavelength

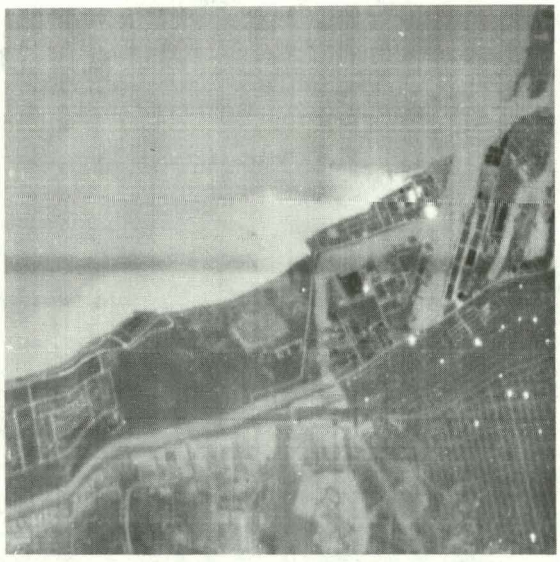

Figure 8. Thermal pollution was observed caused by hot water discharge coming from water outlet of a power plant in the Jakarta Bay area.

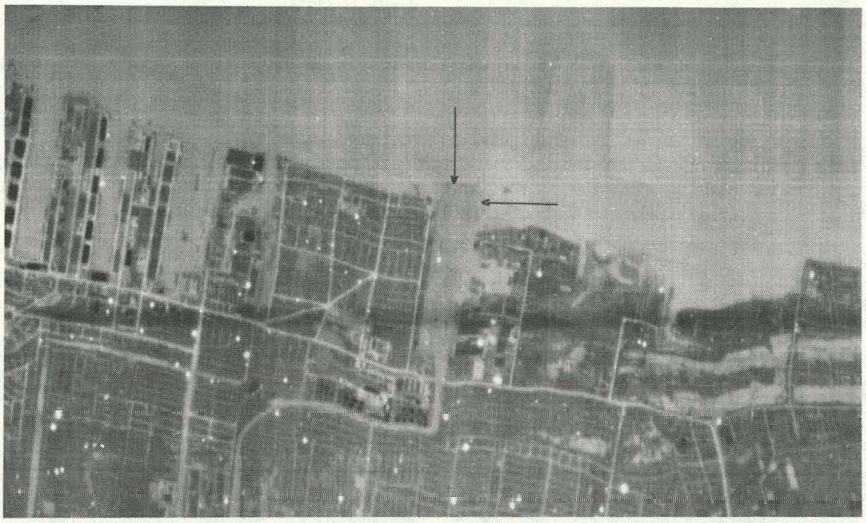

Figure 9. East of the harbor oil pollution some temperature difference with the surrounding.

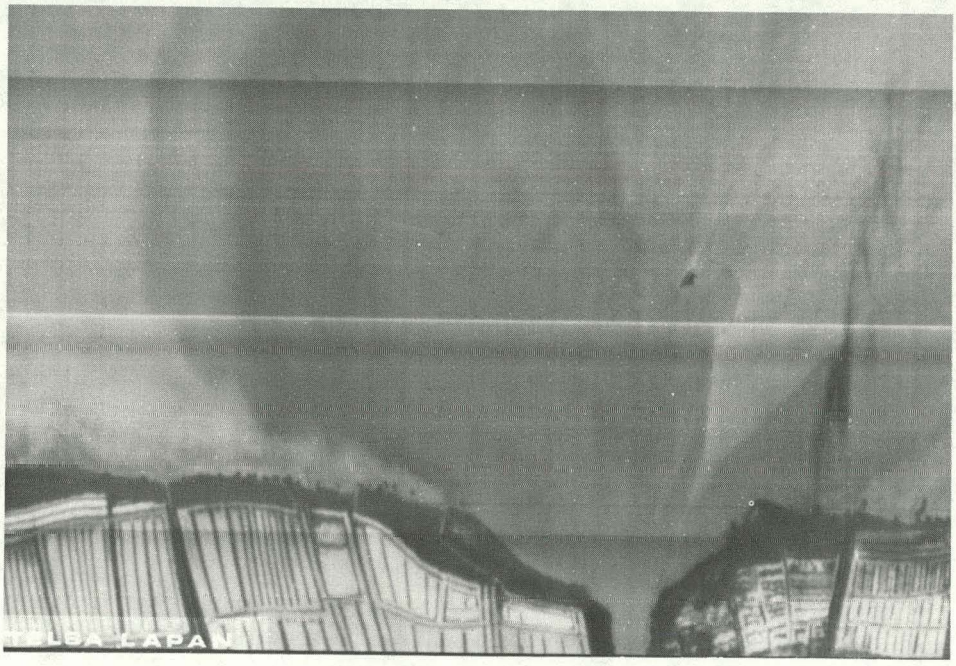

Figure 10. Fresh water is seen entering the sea in the Muara Angke.

THIS PAGE

WAS INTENTIONALLY

LEFT BLANK

THE APPLICATION OF REMOTE SENSING TECHNIQUES TO FOREST VEGETATION SURVEYS IN TROPICAL AREAS AND URBAN FRINGE LAND USE PROBLEMS IN COSTA RICA

Timothy K. Cannon, Richard A. Ellefsen, Kenneth B. Craib

Resources Development Associates
Los Altos, California USA

Jorge Crespo

Instituto Nacional de Vivenda y Urbanismo
San Jose, Costa Rica

ABSTRACT

The capability of various remote sensing techniques was evaluated for the determination of forest land cover and urban expansion within the nation of Costa Rica. The relative effectiveness, various scales and types of aerial photography, and LANDSAT satellite data were compared and evaluated. Conclusions were that aerial photography must be relied on for management data base compilation whereas LANDSAT data can provide immediate national data and can provide a monitoring base.

1. INTRODUCTION

The use of land for agricultural purposes has been the economic backbone for Costa Rica for several centuries. As Costa Rica's industrial and economic base grows, increasing pressures are put upon agricultural and range land and, in turn, upon the forest lands of the nation. Thus, prime agricultural areas are being threatened by urban expansion and areas predominantly suited to forestry due to location, topography, and/or soils are being converted to marginally productive range and agricultural uses.

Resources Development Associates (RDA) has completed an analysis and demonstration project aimed at evaluating the potential of remote sensing technology to provide information needed for mitigating these expansion problems within Costa Rica. In order to attack this broad-based information assessment problem, a project was initiated under the auspices of USAID/Costa Rica and the Government of Costa Rica. The project was divided into two primary components, a forest resources sector and an urban land-use sector. Both sectors investigated similar techniques and technologies and the evaluation of both sectors was presented in February 1978 to the Costa Ricans in the form of a workshop and demonstration. The result of this information has been the initiation of a pilot project within the country to begin implementation of conclusions and techniques recommended within this project.

2. FOREST RESOURCES SECTOR

The intent of the forestry sector of the project was to evaluate remote sensing products and techniques including both multi-scale, multi-film aerial photographic visual interpretation techniques and LANDSAT visual and digital analysis techniques for providing a forest cover data base. In addition, the suitability of these products and techniques for subsequent monitoring of forest cover was examined. Costa Rica has a total land area of 51,000 square kilometers with forest clearing being estimated at about 50,000 hectares per year. The latest estimates (Coberture de Bosgues, 1977) indicate less than 33% of the area of Costa Rica is presently in forest cover. Forest cover is defined as areas having more than 80% of a unit area in tree cover. However, the accuracy of the estimates in regard to spatial placement of this forest cover, total amount, and especially rate of clearing is unknown at this time. The forest land clearing problem is resulting primarily from the conversion of forested land to rangeland with these areas being located on either

government-owned land or private lands designated as forest reserves. The resultant clearing has created a major erosion problem with many watersheds being destroyed due to the loss of water-holding capacity as well as some suspected regional impact on climate.

In order to efficiently combat this problem before irreversible damage is done to the resource base, timely information concerning the extent and location of the forest resources has to be known. In addition, rates of change and areas of greatest change should be located. Traditional ground surveys have been ruled out due to the extreme amount of time and money required to mount such an effort. The time factor would dictate that a majority of the forest would probably be gone by the time the information has been gathered, thus negating any realistic use of the information in solving the problem.

Two study areas were chosen within this project, one being an area in the region of Volcán Poás and the other near the Tarcoles River, located on the Pacific coast south of the Gulf of Nicoya. The Poás test area encompassed several life zones (Holdridge, et. al., 1972), including tropical montane rain forest, tropical lower montane rain forest, and tropical lower montane wet forest. This area was chosen as an example of the problems and the character of the high forests located in the interior mountains of the country. The Tarcoles test area encompassed tropical dry forest, pre-montane moist forest, and tropical moist forest. This area characterizes the Pacific lower slopes. The Poás and Tarcoles test areas represented varied geology, soils, forest, and potential problems arising from pressures created by expanding settlements.

Aerial photography was obtained by providing film and training for the Instituto Geografico Nacional (IGN), who supplied the plane, pilot, and camera for the photographic mission. The development of the film took place in USA facilities. Procurement and development was done in the United States because at that time color and color infrared film and developing processes were not available in Costa Rica. Film types evaluated were: black and white panchromatic, natural color, and color infrared. All film was of the 9 x 9 inch format using a Zeiss camera with a 152 mm focal length lens flown at varying altitudes. Scales evaluated ranged from 1:20,000 to 1:40,000. Imagery obtained at lower altitude was judged to be too costly on a national basis, whereas in-country capabilities for higher altitude photography was not available. Through the use of sensitivity wedges that were exposed before shipment of the film and developed after the film returned to the USA, film handling problems and techniques were evaluated. Each one of the film types were evaluated qualitatively for ease of interpretation, accuracy of delineation of cover types, and ability to distinguish forest associations. Areas were also mapped in each of the test sites for subsequent comparison to satellite data.

The results of this stage of the forest resources sector are; color and color infrared photography can be recommended over black and white photography due to the combination of the facts that the country obviously had the capability of obtaining high quality color and color infrared photography, and the ease, speed, and accuracy of interpretation were increased with the use of either one of these film types over black and white. The cost of obtaining color and color infrared film is of little significance compared to the total image acquisition program costs. Detailed examination of the color and color infrared film revealed that, unlike United States' experience, the color film was actually able to differentiate more tree association types than the color infrared. In addition, at medium altitudes, the color infrared and its use of blue blocking filters produced a much more sharp and clear product than did color at those same altitudes. Color film was deemed superior at low altitudes (3,500 meters agd and below).

This information, coupled with on-site visits, formed the basis for the evaluation of the satellite data. The investigation and demonstration of satellite information utilized primarily a March 3, 1975 LANDSAT frame over the central part of Costa Rica. This LANDSAT frame contained the two test

areas with a minimum amount of cloud cover. Visual techniques relied upon the interpretation of forest cover from 1:500,000 and 1:250,000 black and white, and color composites generated by the EROS Data Center. It became readily apparent that sufficient detail was not available from visual techniques for cover type mapping of either test area. The digital processing portion utilized the ESL, Inc. data facilities and software programs. A computer compatible tape for the LANDSAT frame previously mentioned was obtained from the EROS Data Center and placed on the ESL system. Using both unsupervised and supervised training techniques on the interactive system, cover types for forest land, agriculture, rangeland and other categories (including no information due to cloud cover and shadow, bare ground, water) were determined. Using a maximum likelihood classifier both test areas were classified and mapped. Both ground information and aircraft photography were used in the selection of training areas. Data formats investigated included line printer output at 1:25,000 and 1:50,000 scales, electrostatic printer at both scales, and film recorder products. Final data format was considered important in this case because on a long-term working basis a great deal of the expense incurred for such a system as well as the utility revolves around the final format chosen.

Regardless of the data format, the information from classification of digital data revealed that in the Tarcoles test area the range and brushland as well as agriculture, bare ground, and water classes could be easily and accurately identified and separated from the areas in forest cover. In addition, areas that had tree cover of less than 80% (these primarily being brushland and rangeland) could be accurately assessed and an estimation of the tree cover for these areas could be made. Although these areas did not contain what would be considered commercially suitable or exploitable forest resources, the amount and composition of tree cover was considered signficant. A tentative Level I and Level II classification scheme that was compatible with the urban sector was formulated. It should be noted that, differing from Anderson's classification system (Anderson, et. al., 1976), areas in pasture were extracted from agricultural areas and put into a rangeland classification. This was justified due to the fact that pasture and rangeland are actually producing and being utilized for similar purposes and the fact that between these two uses a majority of the misclassification occurs. In the Poás test area, similar results were obtained with the exception that agriculture and rangeland were less efficiently separated. However, the distinction between these two uses and forest land remained at a high level. No conclusions should be drawn from this work concerning agriculture and range classification since the project's primary intent was not to evaluate the differentiation between these two classes and as such, the training samples did not concentrate on these areas. Unfortunately, coffee as an agricultural product did not occur in large amounts in either training site, therefore effectiveness of the LANDSAT data to differentiate between natural forest and coffee land was not fully evaluated. It is our fear that confusion will result from misclassification of coffee and forest land in some areas due to very similar spectral response of these two cover types.

Examples of the photographic mapping and the digital mapping can be seen in Figures 1 and 2. Figure 1 shows an electrostatic grey print with the grey levels classified and labeled, and line drawings showing corresponding photographically derived information. This figure demonstrates the fact that the satellite system was able to capture, in many cases, both the character of the cover type; i.e., the increasing amount of tree canopy as one goes from pasture to rangeland to brushland to forest, and to accurately delineate major areas of forest land and spatially locate them. Although it was concluded that LANDSAT was not feasible for a final data base preparation for resource management, the satellite derived product was effective at both providing a monitoring tool, once the data base had been established from aerial photographic products, and for giving an immediate assessment of the forest status in Costa Rica. This is especially warranted due to the fact that the foresters in Costa Rica desire immediate mapping of the forest that precludes the use of

photography due to the extended time element in data acquisition. Data formats were also demonstrated to be effective at 1:25,000 and 1:50,000 scale, although use of the line printer resulted in data compression as the data were aggregated. However, government foresters in Costa Rica advised that even a 1:200,000 scale would be desirable for initial planning purposes.

3. URBAN LAND-USE SECTOR

Large areas of agricultural land, especially those devoted to raising an export coffee crop, have been converted to urban uses as the city of San Jose, Costa Rica has undergone rapid expansion in recent years. The typical urban expansion characteristic of "leap-frogging" has further placed undeveloped parcels in such jeopardy that they are no longer being intensively managed for agriculture. The conversion of agricultural land to high value commercial-industrial development is defensible as being vital to the country's economic growth but discontiguous housing developments especially those placed a few kilometers beyond the periphery of the contiguously built-up areas, pose the dual problem of removing valuable land from production while requiring the provision of expensive urban services. Of concern also is the engulfing and subsequent loss of distinctiveness of surrounding satellite communities and the visual green belts which traditionally have separated them from San Jose.

To provide Costa Rican policy makers with information necessary for treating this problem, a demonstration land-use inventory project was conducted. Goals of the project were:

1. To delineate the boundary of the contiguously built-up area for a selected sample area of the Meseta Central extending from the western edge of San Jose to the international airport, some 12 kilometers away
2. To classify and map both urban and non-urban land uses in areas near cities
3. To provide details on the stages of land-use change in the rural-urban fringe areas
4. To test possible ways of monitoring and forecasting future urban growth.

For these purposes, the project employed and evaluated: vertical air photography in black and white, natural color, and color infrared: oblique 35 mm color photography; and LANDSAT digital data processed by computer.

A prerequisite step to mapping was the development of a land-use classification scheme commensurate with project goals. For the air photo interpretation mapping, this involved modification of the system developed by Anderson, et. al. (1976) plus the addition of a Level III classification subdivision to plot degrees of residential building density and a Level IV to indicate the condition of agriculture in the rural-urban interface area (see Figure 3). To accomplish this it was necessary first to delimit the boundary of the contiguously built-up area. The rationale supporting the method used in the United States by the Census Bureau (Murphy, 1974) was employed in a boundary determination based on the contiguity of urban land uses as observed on the air photographs. Nearby urban enclaves were attached and narrow embayment mouths were closed. In between, the boundary followed major natural or cultural linear features.

The essential detail of the classification system further required a large mapping scale, one where the minimum mapping unit could be as small as one hectare. Since the project's goal was to demonstrate potential general utility within the country, the universal 1:50,000 scale maps were selected as map bases. In order to meet requirements imposed by the level of detail of classification system, map sheets were quartered and enlarged, through

photographic processes, to 1:25,000. Each of these was prepared as a new map complete with marginal locational grid data and enlarged bar scale.

Polygons of land use were plotted directly on matte plastic material overlaying 9 x 9 inch air photo transparencies (either natural color or color infrared) of approximately a 1:20,000 scale. Photographic enlargement on clear film material was then employed to transfer the polygons to a map composite scribe guide at the 1:25,000 scale.

All polygons were then scribed, each with their identifying codes. By superimposing the scribed land-use color separation sheet over the negative of the base map, a two-color proof sheet was prepared, a black and white example of which is shown in Figure 4; the final step, making printing plates, was not done.

To test the potential for using digital LANDSAT data, a 326 by 139 pixel area was mapped using the Interactive Digital Image Manipulation System (IDIMS) of ESL, Inc. Supervised training fields, sampling the known cover types, were selected on a CRT screen. These, augmented with random samples, were then clustered and evaluated. Thirty-nine clusters, sufficiently separated in measurement space, were then employed to classify the entire test window. Upon comparison to the air photographs (serving as ground truth) these cluster classes were grouped into six land-use/land-cover classes (see Figure 5).

The demonstration map products were:

1. The base-line land-use inventory derived from air photo interpretation
2. Computer processed LANDSAT digital data
3. Sample area measurements for both
4. Comparison of their aggregated data
5. Post-processing manipulation of the computer/LANDSAT maps.

The base-line inventory is a conventional land-use map. It has a high level of accuracy made possible through the use of supporting contemporary low altitude oblique photography and ground checking. The digital map (Figure 6) presents a clear separation between rural and urban land uses.

To evaluate the performance of the digital map product, areas of all land uses by both methods were measured for the administrative reporting unit of Distrito Cinco Esquinas and compared in a matrix (Figure 7). Total urban and non-urban aggregations were nearly the same and would be more so were it not that the photo interpretation of 1977 imagery correctly records more urban development than existed in 1975, the date of the LANDSAT data.

The demonstration products from the computer processing of LANDSAT digital data consisted of:

1. Scaled and geometrically corrected line-printer output
2. Film recorder output
3. Electrostatic grey level printer output at various degrees of enlargement.

Using a version of the latter with an approximate scale of 1:12,250, in which each pixel measured nearly one centimeter on a side, a delineation was made of the urbanized area to the west of San Jose. Adapting rules developed by the U. S. Census in their Urbanized Area Delimitations to account for exclaves and embayments, lines were drawn around contiguous pixels representing urban classes (see Figure 8). Distinctively demarcated were:

1. The central city and its contiguous urban periphery
2. The old satellite communities
3. Outlying urban nuclei containing at least ten hectares.

Areas separated by but the length of two pixels (160 meters) were retained as individual units while those more proximate were combined. Clearly where gaps between urbanized units are only a few hundred meters wide, little additional urban development would be required to close them. Future urban expansion could be monitored through analysis of maps made from a sequential series of LANDSAT passes.

4. CONCLUSIONS

The design of the project as implemented in the test area has proved to be sound. The classification system has adequately accounted for land cover and use, and provided potentially valuable information for planning purposes. Within the forest sector, color and color infrared photography proved to be most valuable with color being superior at low altitudes and color infrared at medium and high altitudes. The LANDSAT information proved to be effective for the gathering of timely and immediate data and as a monitoring system whereas photographic products must be relied on for long-term management data. Within the urban sector, a good match was achieved between the classes and the map scale of 1:25,000. Extension of the system to other urbanized areas within the country seems feasible and will result in achieving an essential base-line inventory. Computer processed LANDSAT digital data also shows promise especially when directed to the monitoring of expanding urban peripheries.

References

Anderson, James R., Ernest E. Hardy, John T. Roach, and Richard Witmer, 1976, A Land Use and Land Cover Classification System for Use with Remote Sensor Data, Geological Survey Professional Paper 964, Washington.

Direccion General Forrestal, Ministerio de Agricultura Y Ganaderis, 1977, Coberture De Bosques De Costa Rica, San Jose, Costa Rica, map.

Holdridge, L. R., W. C. Grenke, W. H. Hatheway, T. Liang, and J. A. Tosi, Jr., 1971, Forest Environments in Tropical Life Zones, A Pilot Study, Pergamon Press, New York.

Murphy, Raymond E., 1974, The American City, McGraw-Hill, pp. 20-26.

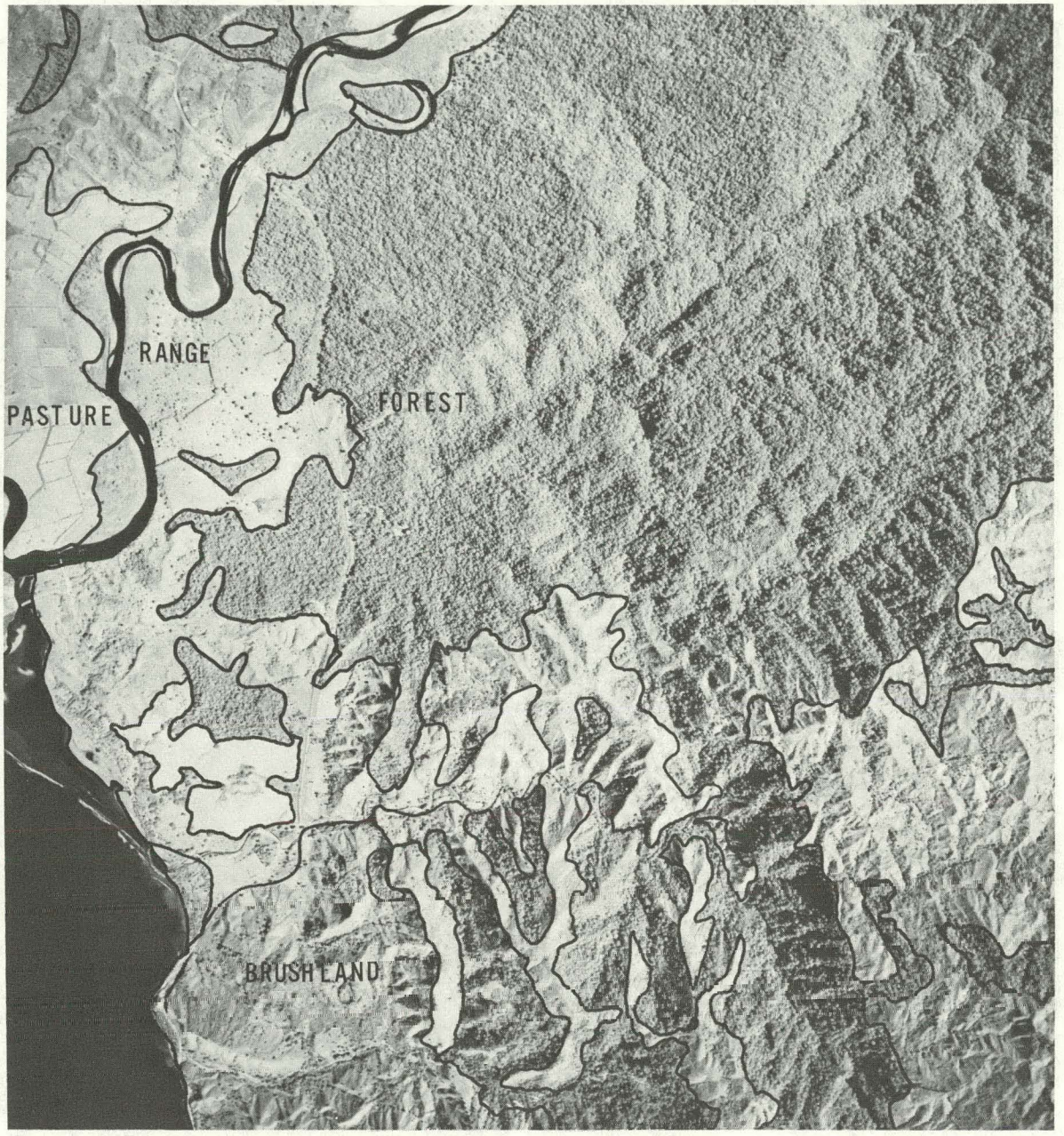

Figure 1 - B/W Infrared, 1:50,000 Aerial Photograph, Tarcoles Test Area

This figure is a black and white print of a color infrared photograph showing the Pacific coastline and the Tarcoles River. Several large cover types are labeled for identification. This figure should be compared to Figure 2.

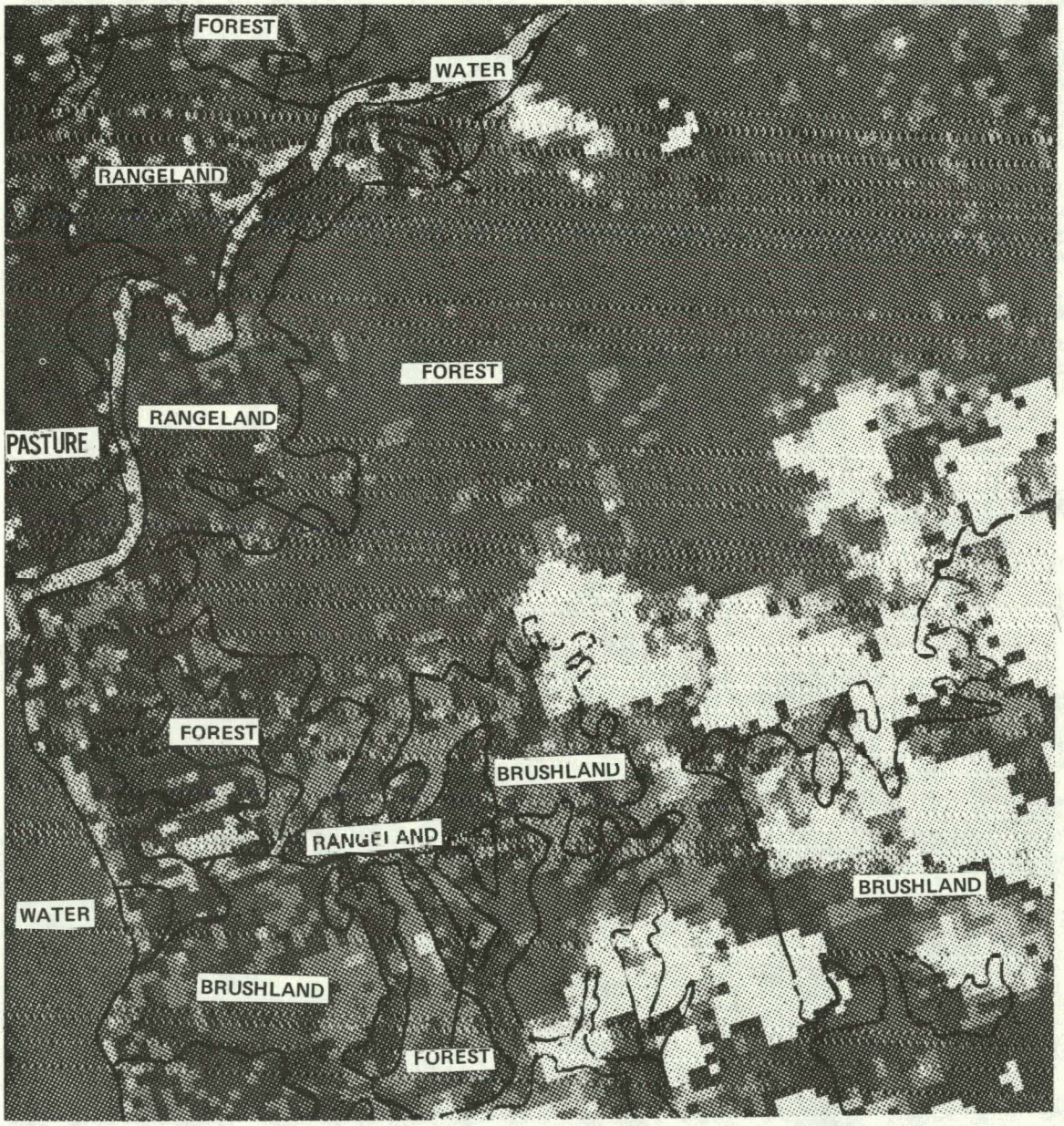

Figure 2 - Electrostatic Greyprint, LANDSAT Classification, Tarcoles Test Area

This figure demonstrates the ability of the satellite to identify and locate major land cover classes. Lines indicate photographic cover types from Figure 1.

Land-Use Classification System for Air Photo Interpretation Mapping

Class Number	Class
	URBAN
111	Residential (low building density)
112	Residential (medium building density)
113	Residential (high building density)
12	Commercial and services
13	Industrial
14	Transportation, communications, and utilities
15	Industrial and commercial complexes
16	Institutional
171	Recreation
1721	Coffee (viable)
1722	Other agricultural land (viable)
1731	Coffee (abandoned)
1732	Other agricultural land (abandoned)
174	Vacant land in transition
	NON-URBAN
211	Sugar Cane
212	Field Crops
213	Other (including small, fenced pastures)
221	Coffee
222	Bananas
223	Palms
224	Greenhouses
23	Agricultural Structures
3	Rangeland (grass)
4	Forest Land
51	Streams, canals
52	Lakes
53	Reservoirs
72	Beaches
74	Bare, exposed rock
75	Strip mines, quarries,

Figure 3. LAND-USE CLASSES DERIVED FROM AIR PHOTO INTERPRETATION

Land Uses & Land Covers Derived from Computer Processing of Landsat Data

Urban

- Old Central City
- Dense Concentration of Small Buildings (mostly residential)
- Light Concentration of Small Buildings (mostly residential)
- Large Buildings and Contiguous Buildings (mostly commercial-industrial)

Non-urban

- Coffee
- Other Agriculture

Figure 5. LAND-USE AND LAND-COVER CLASSES DERIVED FROM COMPUTER PROCESSING OF LANDSAT DATA.

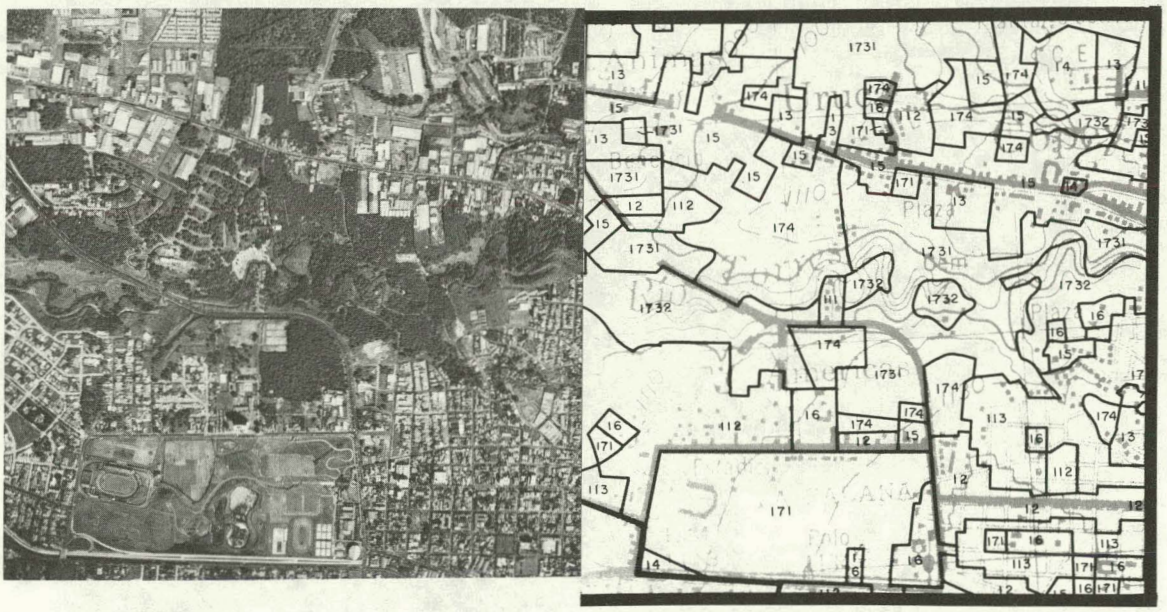

Figure 4. LAND USE FROM AIR PHOTO INTERPRETATION

Land-use polygons overlie the base map. Central San Jose is in the southeast corner, abandoned coffee land occupies the center, and an industrial-commercial strip is seen in the north.

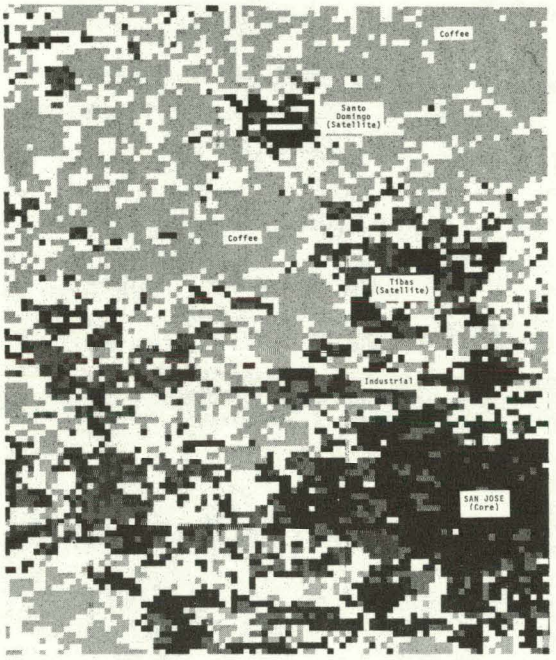

Figure 6. URBAN-RURAL SEPARATION FROM COMPUTER-PROCESSED LANDSAT DATA

	PHOTO INTERPRETATION	URBAN: Old Central City	URBAN: Dense Concentration Small Buildings	URBAN: Light Concentration Small Buildings	URBAN: Large Buildings Contiguous Buildings	NON-URBAN: Coffee	NON-URBAN: Mostly Grass	TOTAL HECTARES	
URBAN	(12) Commercial, Services	X						4.3	96.3
	(16) Institutions	X						1.5	
	(113) High Density Residential		X					28.6	
	(112) Med. Density Residential			X				14.0	
	(15) Commercial, Industrial				X			8.4	
	(13) Industrial				X			30.4	
	(14) Utilities, Transport				X			9.1	
NON-URBAN	(221) Coffee					X		52.9	194.4
	(1721) Viable Coffee					X		11.0	
	(1731) Abandoned Coffee					X	X	64.8	
	(1732) Abandoned Other						X	13.0	
	(174) Vacant						X	48.3	
	(171) Recreation						X	4.4	
	TOTAL HECTARES	12.9	42.3	18.4	11.4	111.0	108.6	304.6	
		85.0				219.6			

Figure 7. PHOTO INTERPRETATION-LANDSAT RESULTS COMPARISON

Figure 8. URBANIZED AREA DELIMITATION
Central city is in white hatching, satellite towns are in white cross hatching, and new urban nuclei are indicated by black hatching

AUTOMATIC CLASSIFICATION OF REFORESTED PINUS SPP. AND EUCALYPTUS SPP. IN MOGI-GUAÇU, S.P., BRAZIL USING LANDSAT DATA

Y. E. Shimabukuro, P. F. Hernandez, N. F. Koffler and S. C. Chen

Instituto de Pesquisas Espaciais (INPE)
Conselho Nacional de Desenvolvimento Científico e Tecnológico (CNPq)
12.200 - São José dos Campos, S.P. - Brazil

ABSTRACT

Single date Landsat (computer compatible tapes) (CCTs) were processed, by Image-100 to classify Pinus and Eucalyptus species and their age groups. The study area Mogi-Guaçu is located in the humid sub-tropical climate zone of São Paulo State. Prominent Pinus species are P. elliottii and P. taeda. Eucalyptus species are E. alba and E. saligna. The ages of these tree types range from 8 months to 20 years. The study area was divided into ten preliminary classes and feature selection algorithm was used to calculate Bhattacharyya distance (B-distance) between all possible pairs of these classes in the four available channels. The classes having B-distance values less than 1.30 were grouped together resulting in four classes: 1) class PE - P. elliottii, 2) class PO - Pinus species other than P. elliottii, 3) class EY - Eucalyptus spp. under two years, and 4) class EO - Eucalyptus spp. more than two years. For classification, single cell signature acquisition option was used. The low percentages of correct classification for class PO was due to its relatively small area (a total of 1.44 km²) while for class EO error was caused by the similar signature responses of cerrado, gallery forest and heterogenous P. elliottii plots in the study area. The percentages of correct classification ranged from 70.9% to 94.12%. Comparisons of acreage estimated from the Image-100 with ground truth data showed agreement. The Image-100 percent recognition values for the above four classes were 91.62%, 87.80%, 89.89% and 103.30%. Greater precision of area estimation could have been obtained if the ground truth data based on the seedling area at planting time had been up-dated.

1. INTRODUCTION

Landsat is one of the potential tools which is meeting the increasing demands of government agencies and private industry for timely and precise inventories of forestry data. In the past few years various researchers have tested the possibility of identifying forest plant communities using Landsat data by conventional or automatic classification techniques. Sayn-Wittgenstein (1972) used a color composite of MSS band 4, 5 and 6 to separate coniferous forest (mostly spruce), hardwood (mostly poplars) and areas covered by willow and alder. López-Cuervo (1973) visually analyzed Landsat enlarged images and identified Pinus and Eucalyptus at the generic level according to their tonal differentiations. Gimbarzevsky (1974) also confirmed the separability of coniferous and deciduous forest using Landsat imagery. Lee et al. (1974) observed that

Landsat imagery could be used to distinguish forested and non-forested lands. Difficulties were encountered in separating coniferous species, even though age difference was recognized. Kalensky and Scherk (1975) reported that overall Image-100 classification accuracies for coniferous forest, deciduous forest and non-forested land ranged from 67% to 81% for single date imagery while for multidate imagery consistently above 80%.

The objective of this study was to classify Pinus and Eucalyptus species and their age groups, using the Image-100 automatic classification system.

2. STUDY AREA AND DATA SOURCES

São Paulo State contributes more than 50% of the paper and cellulose produced in Brazil. The state has an artificially reforested area of 6,144 km^2 predominantly in pine (22.15%) and eucalypt (76.48%). The study area Mogi-Guaçu is located at 22°15' S and 47°10' W (Fig. 1) and is a representative of pine and eucalypt plantations common to the region. This area includes the Campininha pine experimental station of the Forestry Institute of São Paulo State (IFSP) and the Santa Terezinha eucalypt plantation of the Champion Cellulose & Paper Company (CCP). The major Pinus species in Campininha are P. elliottii and P. taeda. Other species such as P. caribaea, P. bahamensis, P. oocarpa and P. palustris are also planted in small areas. The prominent Eucalyptus species in Santa Terezinha are E. alba and E. saligna. The tree age range from 8 months to 20 years.

Landsat multispectral scanner CCTs of September 13, 1975, orbital number 178, were processed for the classification of Pinus and Eucalyptus species and their age groups by the Image-100 system.

"Ground truth" information and forest cover maps (Fig. 2) were provided by IFSP and CCP and used for supervised classification and accuracy analysis. Spot field checks to verify the ground truth were also carried out.

3. IMAGE-100 ANALYSIS PROCEDURES

3.1 FEATURE SELECTION

Prior to the supervised signature extraction and classification, the CCTs were corrected radiometrically. A preliminary analysis of the study area was carried out through for B & W imagery and a false color composite displayed on the image monitor at an approximate scale of 1:82,000. The following ten preliminary classes were derived for the Image-100 study.

PE_a - P. elliottii over 13 years.

PE_b - P. elliottii under 13 years.

OP - Pinus species other than P. elliottii and P. taeda.

PT - P. taeda.

$E_{8mo. \sim 2yrs.}$ - Eucalyptus spp. from 8 months to 2 years.

$E_{2yrs. \sim 4yrs.}$ - Eucalyptus spp. from 2 to 4 years.

$E_{4yrs. \sim 7yrs.}$ - Eucalyptus spp. from 4 to 7 years.

$E_{7yrs. \sim 20yrs.}$ - Eucalyptus spp. from 7 to 20 years.

$RE_{< 2yrs.}$ - Regrowth Eucalyptus spp. under 2 years.

$RE_{2yrs. - 9yrs.}$ - Regrowth Eucalyptus spp. from 2 to 9 years.

Bhattacharyya distance (B-distance, Marill and Green, 1963) between these ten preliminary classes was calculated using INPE's feature selection algorithm. This algorithm assumes that each class has a multivariate Gaussian distribution. In this operation, 40 to 50 training samples of each class were deline-

ated on the image monitor by the electronic cursor which was adjusted to the minimum size equivalent to a 4 pixels/sample. Then the B-distance value was calculated in the four available channels. The results of the B-distance values for the preliminary Pinus and Eucalyptus classes in four channels are presented in Tables I and II. The separability of the preliminary classes was defined according to the values of B-distance. Using the curve of Swain and King (1973) the estimated probability of correct classification is > 0.85 for the value of B-distance > 1.30. Thus those classes having B-distance values less than 1.30 were grouped together to form four classes as follows:

PE --- P. elliottii.

PO --- Pinus species other than P. Elliottii.

EY --- Eucalyptus spp. under two years.

EO --- Eucalyptus spp. over two years.

Table III lists the "B-distance" values of classes PE, PO, EY and EO in four spectral channels.

3.2 SIGNATURE EXTRACTION AND CLASSIFICATION

Single cell signature acquisition of the Image-100 was used for classification. This option creates a four-dimensional parallelepiped; each of the sides of which corresponds to the signature limits of the training areas in each channel. Training samples, independent from the test area, were selected from each of the four classes (PE, PO, EY and EO) using the electronic cursor. The limits of the histograms of the training areas were modified in the four spectral channels until a satisfactory classification was obtained. The final classification result is presented in an alphanumeric printout as shown in Fig. 4.

4. IMAGE-100 PERFORMANCE

4.1 PIXEL CLASSIFICATION ACCURACY

After classification, the electronic cursor was again positioned on the image monitor. The "alphanumeric theme print" was executed for a cursored area of approximately 50 km^2. This printout was compared pixel by pixel with the IFSP and CCP's forest cover maps to produce a confusion matrix (Table IV). This table shows the number of pixels classified according to its "true" class and Image-100's "chosen" class in the cursored area. The percentages given in parenthesis were calculated based on the total number of classified pixels in each class. Histogram modification thresholding in the four spectral channels tends to increase errors of omission and decrease errors of commission. Thus, percentages of correct classification which take into account errors of omission were not high. To give a more realistic view of the Image-100's pixel classification accuracy the following formulas were used to calculate the percentages of correct classification and errors of commission.

$$\text{Correct Classification (\%)} = \frac{\text{No. of correctly classified pixels in class A}}{\text{Total no. of pixels in the test area of class A}}$$

$$\text{Error of Commission (\%)} = \frac{\text{No. of pixels classified as class A but actually belonging to another class}}{\text{Total no. of pixels in the test area of non-A classes}}$$

4.2 AREA ESTIMATION ACCURACY

The Image-100 estimated class areas were compared to their corresponding "ground truth" data provided by IFSP and CCP. The percentage of the estimated areas on ground truth data are presented in Table VI.

5. DISCUSSION AND CONCLUSIONS

For the study, sufficiently large test areas of eucalypt trees less than thirteen years old and trees over thirteen years old were further separated geographically into two classes, PE_a and PE_b, although a "B-distance" value of 0.22 indicated that no satisfactory separation was possible. P. taeda and the class OP were readily separable from P. elliottii but unseparable from each other (Table I). The morphological similarity among the Eucalyptus species made their differentiation difficult, although Image-100 successfully classified Eucalyptus under two years from the other preliminary age groups (Table II). This separability was due to the distinct spectral characteristics of the homogenous young Eucalyptus which aided the Image-100 identification.

For classification a hyperparallelepiped signature file was constructed for each of the classes PE, PO, EY and EO using a "single cell signature acquisition" program. The separability of these four classes was most easily observed on "N-dimensional histogram two-dimensional print" (Fig. 3).The longer distance between genera Pinus and Eucalyptus confirmed their higher separability than species and age classes. The percentages of Image 100's correct classification for the classes PE, PO, EY and EO were found to be 89.14%, 79.26%, 94.12% and 70.99% respectively. These percentages were relatively lower compared to those calculated using the total number of pixels from each class classified as the denominator (Table V). The lower percentage of correct classification was obtained from the class EO (70.99%). It was caused by cerrado, gallery forest and heterogeneous P. elliottii plots of the area which gave a similar spectral responses as class EO. The highest percentage of correct classification was found for class EY (94.12%). It may have been due to the homogeneity of the eucalypt under two years old.

In the area estimation study the misclassified pixels shown in Table IV accounted for the low pixel classification accuracies of Table V and gave area estimations of 17.28, 1.44, 4.00 and 22.51 km² for the classes PE, PO, EY and Eo respectively (Table VI). The above areas estimated by the Image-100 when compared to the same ground truth areas gave recognition values (RVs) of 91.62%, 87.80%, 89.89% and 103.30%. The 3.30% overestimation of class EO was due to a high proportion of misclassified pixels (13.61%) which had produced spectral signature similar to class EO. The overall area weight difference of 6.31% was achieved. The results of the Image-100 area estimations were encouraging, considering that the machine classification was carried out at the species level, for pine, and based on age groups, for eucalypt.

The ground truth provided by IFSP and CCP agencies were based on the seedling area at planting time. These data represented "theoretically reforested areas" under "optimum conditions" without damage and mortality. In the field check, various plant-failure areas were observed. The recognition value could have been greater if the ground truth data had been up-dated annually.

The following significant results were obtained from automatic classification of reforested areas of pine and eucalypt:

Based on "B-distance" values the following spectral separations were achieved:

1. P. elliottii was separated from the other pine species.
2. Eucalyptus spp. under two years old were separated from Eucalyptus spp. more than two years old.
3. Clear distinctions were made between pine and eucalypt.

Based on Image-100 area estimations, accuracies ranged from 87.80% to 103.30% for the four classes defined (PE, PO, EY and EO) when compared to the same information provided by forestry agencies.

These results point to the operational potential of computer automated processing of Landsat data to recognize tree species and calculate standing volume, especially in remote regions where ground and aerial surveys are often costly.

Before the methodology used in this study can be applied on an operational scale, more consideration should be given to signature extention to other geographical regions, and to spatial differences between areas of natural and artifical reforestations.

REFERENCES

Gimbarzevsky, P., 1974. ERTS-1 imagery in biophysical studies: Proceedings, Second Canadian Symposium on Remote Sensing, Ottawa, V. 2, P. 391.

Kalensky, Z. and L. R. Scherk, 1975. Accuracy of forest mapping from Landsat computer compatible tapes: Proceedings, Tenth International Symposium on Remote Sensing of Environment, Environment Research Institute of Michigan, Ann Arbor, Michigan, V. 2, P. 1159.

López-Cuervo, S., 1973. A study of agroforestry natural resources: Proceedings, First Panamerican Symposium on Remote Sensing, Panama City, EROS Data Center, Sioux Falls, P. 86.

Lee, Y. J., E. T. Oswald, and J. W. E. Harris, 1974. A preliminary evaluation of ERTS imagery for forest-land management in British Columbia: Proceedings, Second Canadian Symposium on Remote Sensing, Ottawa, V. 1, P. 87.

Marill, T. and D. M. Green, 1963. On the effectiveness of receptor in recognition systems: IEEE Trans. on Information Theory, V. IT-9, P. 11.

Sayn-Wittgenstein, L., 1972. A first look at Canadian ERTS experiments in forrestry: Proceedings, Earth Resources Technology Satellite-1 Symposium, Goddard Space Flight Center, Beltsville, Maryland, P. 48.

Swain, P. H. and R. C. King, 1973. Two effective feature selection criteria for multispectral remote sensing: LARS Information Note 042673, Laboratory for Applications of Remote Sensing, Purdue Univ., W. Lafayette, India.

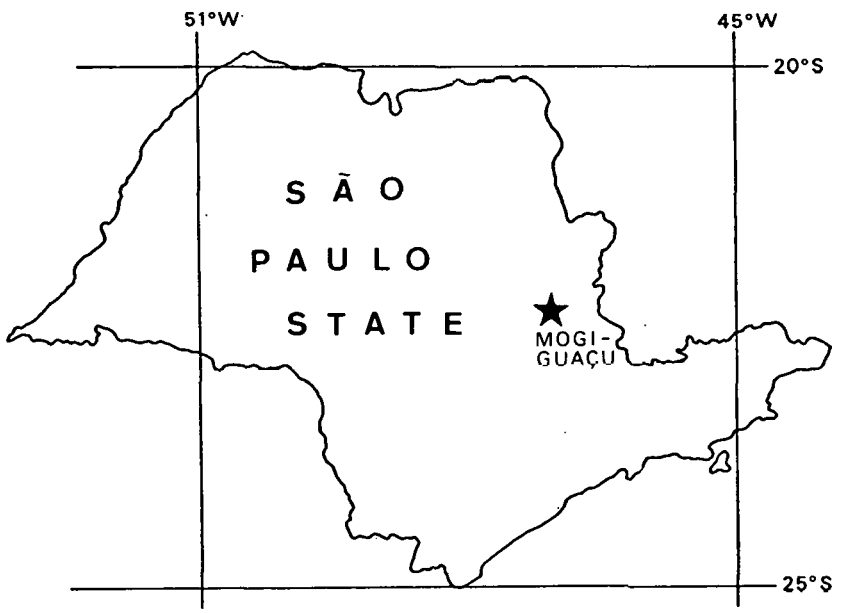

Figure 1. LOCATION OF STUDY AREA IN MOGI-GUAÇU, SÃO PAULO STATE

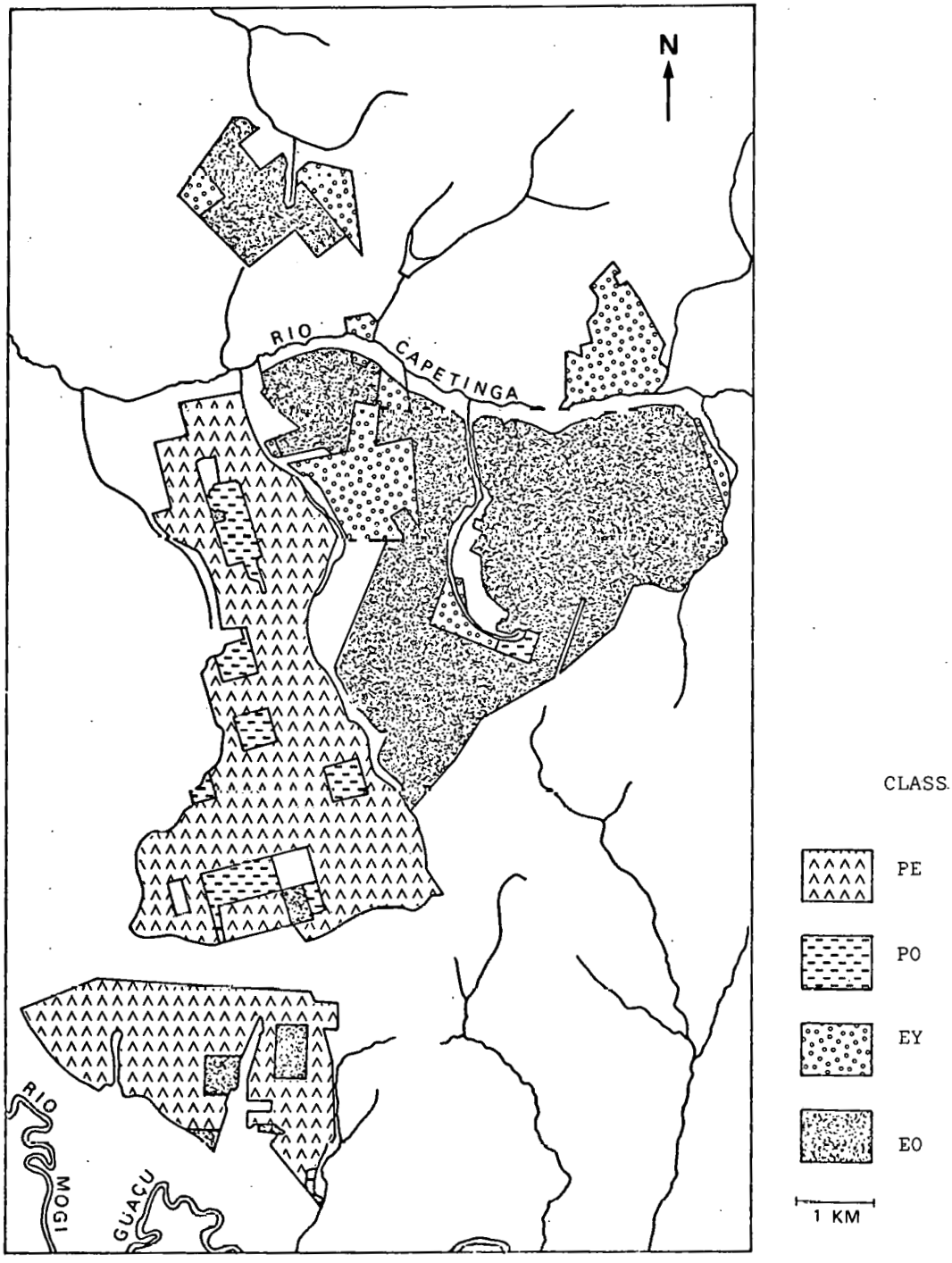

Figure 2. FOREST COVER TYPES OF CAMPININHA AND SANTA TEREZINHA

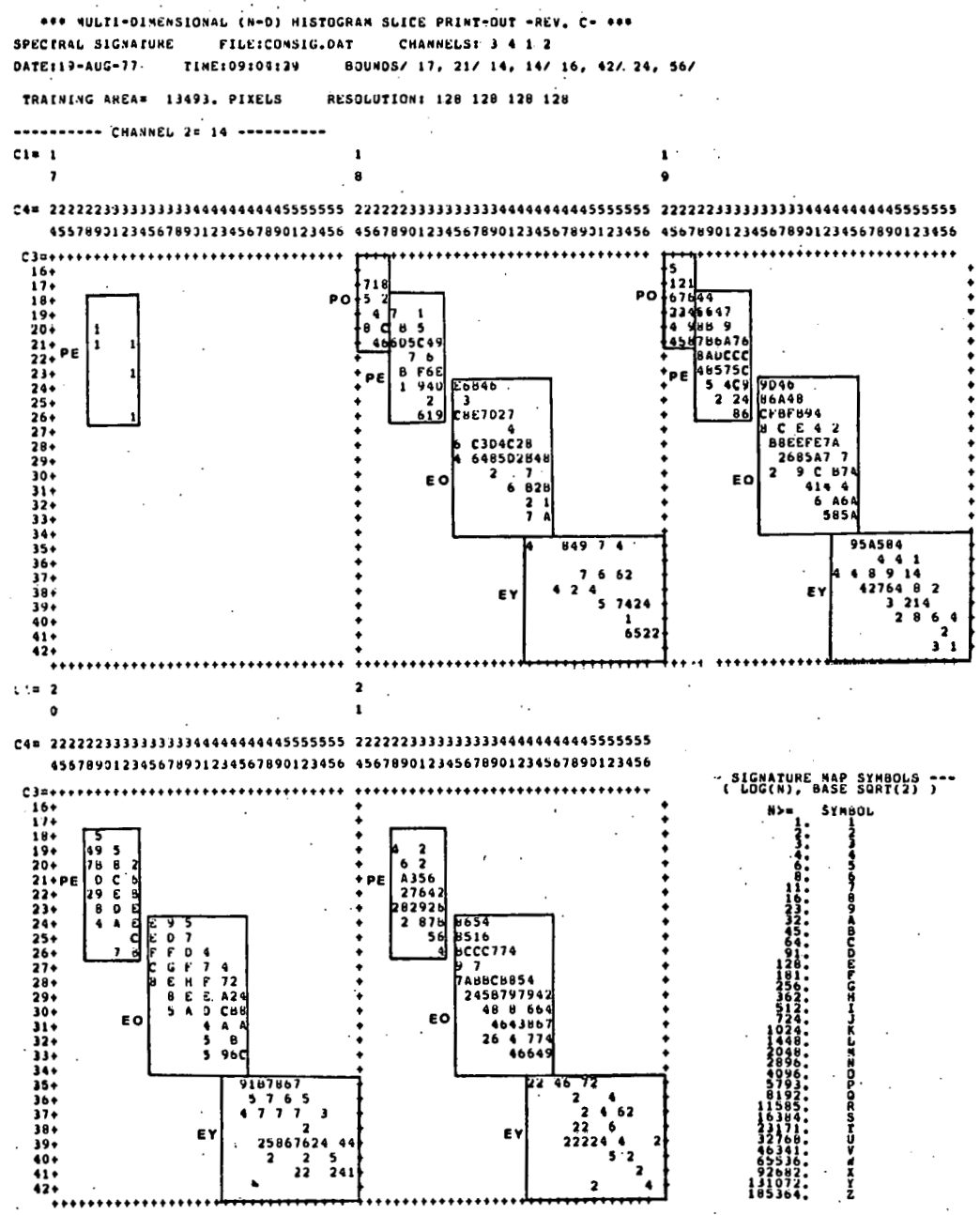

Figure 3. AN EXAMPLE OF "N-DIMENSIONAL HISTOGRAM TWO-DIMENSIONAL PRINT"

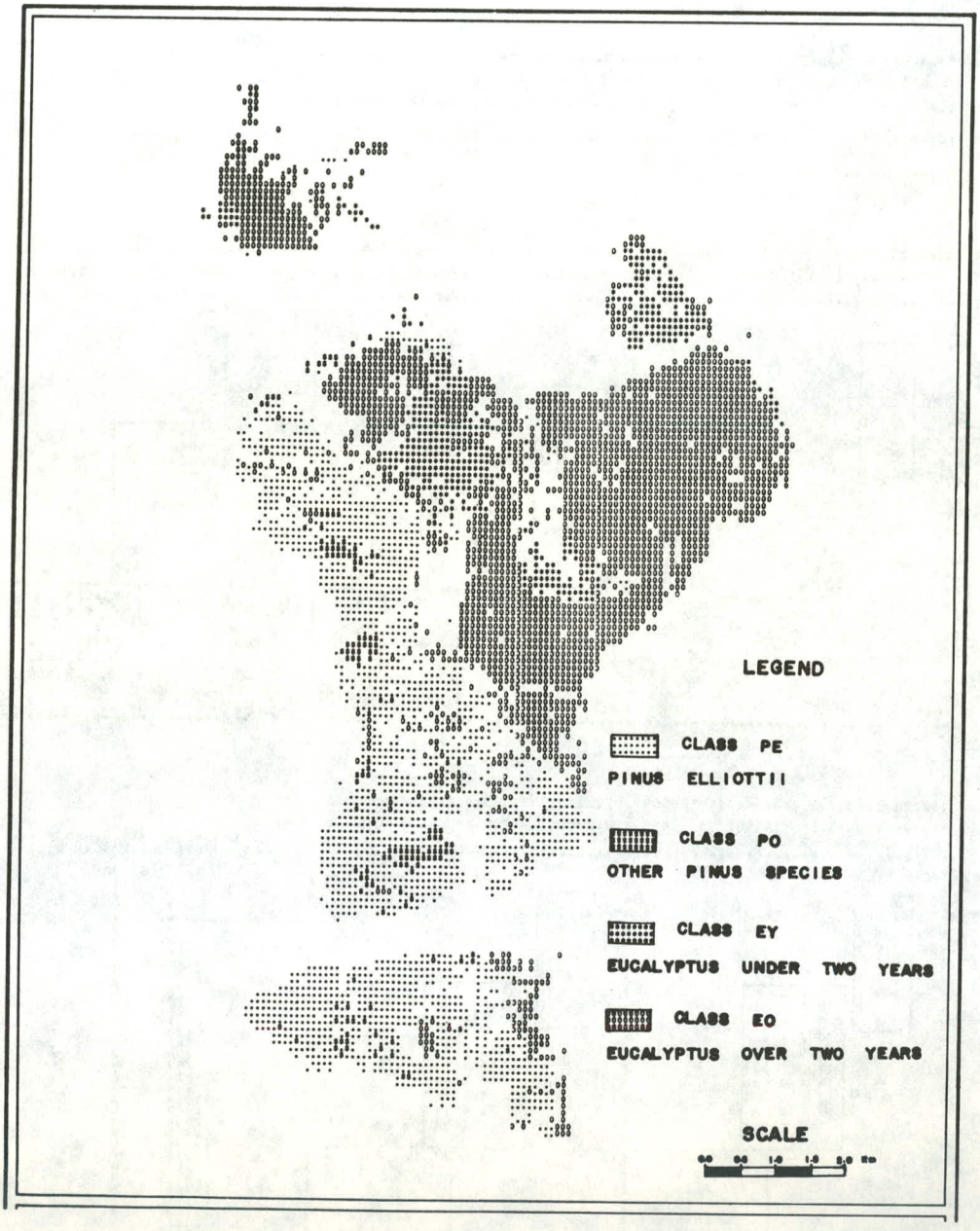

Figure 4. ALPHANUMERIC PRINTOUT OF THE CLASSIFIED MOGI-GUAÇU STUDY AREA

CLASS / CLASS	PE_b	OP	PT
PE_a	0.22	1.92	1.70
PE_b		1.79	1.37
OP			0.67

TABLE I. B-DISTANCE VALUES OF PRELIMINARY CLASSES OF PINUS IN FOUR SPECTRAL CHANNELS

CLASS / CLASS	PO	EY	EO
PE	1.78	2.00	1.99
PO		2.00	2.00
EY			1.90

TABLE III. B-DISTANCE VALUES OF CLASSES PE, PO, EY AND EO IN FOUR CHANNELS

CLASS / CLASS	$E_{2yrs. \sim 4yrs.}$	$E_{4yrs. \sim 7yrs.}$	$E_{7yrs. \sim 20yrs.}$	$E_{< 2yrs.}$	$RE_{2yrs. \sim 9yrs.}$
$E_{8mo. \sim 2yrs.}$	1.99	1.99	1.98	1.94	1.98
$E_{2yrs. \sim 4yrs.}$		0.41	0.23	0.51	0.31
$E_{4yrs. \sim 7yrs.}$			0.63	0.70	0.49
$E_{7yrs. \sim 20yrs.}$				0.56	0.55
$RE_{< 2yrs.}$					0.23

TABLE II. B-DISTANCE VALUES OF PRELIMINARY CLASSES OF EUCALYPTUS IN FOUR SPECTRAL CHANNELS

CHOSEN CLASS / TRUE CLASS	PE	PO	EY	EO
PE	5730 (92.26%)	30 (5.19%)	0	449 (6.18%)
PO	359 (5.78%)	535 (92.56%)	0	40 (0.55%)
EY	0	0	1713 (91.21%)	195 (2.69%)
EO	24 (0.38%)	0	155 (8.25%)	6272 (86.39%)
NO CLASS	98 (1.58%)	13 (2.25%)	10 (0.53%)	304 (4.19%)
PROPORTION OF MISCLASSIFIED PIXEL	7.74%	7.44%	8.79%	13.61%
PIXEL TOTAL	6211	578	1878	7260

TABLE IV. CONFUSION MATRIX

CLASS	CORRECT CLASSIFICATION (%)	ERROR OF COMMISSION (%)
PE	89.14	2.11
PO	79.26	0.15
EY	94.12	0.61
EO	70.99	2.08

TABLE V. SUMMARY OF CORRECT CLASSIFICATIONS AND ERRORS OF COMMISSION

CLASS	AREA (KM^2)		R.V.* (%)	RELATIVE DIFFERENCE (%)
	GROUND TRUTH	IMAGE-100 ESTIMATED		
PE	18.86	17.28	91.62	- 8.38
PO	1.64	1.44	87.80	- 12.20
EY	4.45	4.00	89.89	- 10.11
EO	21.79	22.51	103.30	+ 3.30
OVERALL AREA WEIGHTED DIFFERENCE				6.31

* RECOGNITION VALUE = $\frac{\text{IMAGE-100 ESTIMATED AREA}}{\text{GROUND TRUTH AREA}} \times 100$

TABLE VI. COMPARISON OF IMAGE-100 ESTIMATED AREAS WITH "GROUND TRUTH" DATA

THERMAL INFRARED REMOTE SENSING OF SOIL MOISTURE: WHAT CAN BE EXPECTED FROM HCMM DATA?

Ferdinand J. Bonn

Département de géographie
Université de Sherbrooke
Sherbrooke, Québec

ABSTRACT

The Heat Capacity Mapping Mission (H.C.M.M.) Satellite, to be launched by N.A.S.A. in April 1978 will map thermal patterns of the earth's surface, especially thermal inertia. Thermal inertia of soils is related to soil moisture content, and this gives H.C.M.M. the potential of mapping soil moisture. However, certain restrictions exist, especially in vegetated area, as shown by the experiments made in Sherbrooke, in comparing remotely sensed and ground truth data.

Soil moisture is a very important factor in many areas of the world. It influences crop production in agricultural areas, timber production in forest areas, resistance to soil erosion in arid or semi arid areas, flood prediction and even stability of slopes in many regions. A good knowledge and monitoring of soil moisture can thus be an important decision making factor for agriculture and resources management. Most soil moisture measurements and studies are made at a few specific places: experimental farms, agricultural and forestry research stations, etc, and the areal extension of these measurements is generally done by deduction, if sufficient knowledge of soil types and drainage conditions in the area of interest is provided. However, the irregularity of precipitations and the lack of a dense network of measuring stations in many areas make it very difficult to obtain accurate soil moisture maps for almost any part of the world

Remote sensing techniques have the potential to increase our ability to map soil moisture, because soil moisture affects emitted and reflected radiation in many areas of the electromagnetic spectrum. Soil moisture affects reflectivity in the visible and near infrared channels, as observed by different authors, but there is no direct relation between soil moisture and reflectivity, due to the great variations in soil colour which are not necessary related to moisture. Soil moisture affects reflection and emission in the microwave range, due to the dielectric properties of water, but passive microwave as well as S.L.A.R. data are still not available

on a large basis.

Thermal infrared remote sensing in the 8-14 spectral range measures the upgoing component of the thermal radiation emitted by the earth. This component is a part of the net radiation, which can be expressed the following way:

$$R_N = R_S\ (1-\rho) + R_L - R_T \qquad (1)$$

where R_N is the net radiation

R_S the incident solar radiation (direct and diffuse) of short wave lengths (visible and near infrared)

R_L is the incident longwave (thermal) radiation

R_T is the thermal radiation emitted by the earth, measurable by thermal infrared remote sensing

ρ is the albedo of the earth surface.

The energy balance at the earth's surface is generally expressed the following way:

$$R_N = L\,E + G + H + P + M \qquad (2)$$

Where L E is the energy used in evapotranspiration

G is the energy transmitted to the soil by conduction

H is the energy transmitted to the air by convection

P is the energy used by photochemical processes in the vegetation (photosynthesis)

M is the energy used for other metabolic processes in the vegetation.

The terms P and M, which are small compared to the others, are often neglected in budget calculations. The term G is the main generator of soil temperature variations, and these variations are dependant of soil thermal parameters, as described in TABLE 1.

If we assume that the soil is a homogenous and isotropic media, and that heat exchanges in the soil are done essentially by conduction (which is true for water contents below field capacity) the relation between temperature, depth and time is given by

$$\frac{\partial T}{\partial t} = a\,\frac{\partial^2 T}{\partial z^2} \qquad \text{(Rose, 1966)} \quad (3)$$

where T is the temperature, T the time, z the depth and a the diffusivity, as defined in TABLE I.

Specific heat per volume unit of soil depends on the water content, and can be calculated by using a formula due to De Vries (1952), which gives a 5% error margin:

$$\rho C = 0.46\,\theta_m + 0.6\,\theta_o + \theta_w \qquad (4)$$

where θ_m, θ_o and θ_w are the volumetric contents of the soil in mineral matter, organic matter and water respectively.

It is to be noted that

$$\theta_m + \theta_o + \theta_w + \theta_a = 1 \qquad (5)$$

where θ_a, volumetric content of the soil in air has little influence on ρC, because the air has a volumetric heat capacity of only 0.00029, but an important one on the conductivity, k, due to the low conductivity of air (0.00006) compared to water (0.0014). An increase of water content will then, according to Rider (1957) increase both the heat capacity and the conductivity, water replacing air in the soil empty spaces.

Thermal inertia being the square root of the product of the conductivity by the volumetric heat capacity will thus increase greatly when the volumetric content of water increases.

Soil moisture variations, by affecting thermal inertia, will affect the rapidity of temperature changes in the soil, and thus the attainable daily temperature ranges. The Heat Capacity Mapping Mission Satellite, to be launched by N.A.S.A. in April 1978, will monitor diurnal temperature ranges of the earth surface, by measuring thermal infrared emission at predawn and in the early afternoon. Nominal resolution will be 0.5 km at nadir, with a swath width of 700 km. The radiometer will have two spectral channels:

1) a visible and near infrared channel, which will be used to measure the albedo
2) a thermal infrared channel (10.5 - 12.5μm), which will be used to measure black body temperatures of the earth surface.

Repetitive coverage of the same areas will occur at 5-6 days intervals, which should be sufficient to monitor soil moisture variations. According to the H.C.M.M. data users bulletin #1, the data will be available in the following forms:

- day temperature
- night temperature
- albedo
- day-night temperature difference
- apparent thermal inertia

The two latter outputs will be available on special request, after examination of the first three by the investigators. The apparent thermal inertia will be obtained from the data of day and night orbital passages by using the following algorithm:

$$P \text{ (apparent)} = \mathcal{K} \frac{1-\alpha}{\Delta T}$$

where P is the thermal inertia
$\mathcal{K}$ is a constant coefficient, to be defined
α is the surface albedo
ΔT is the day-night temperature difference

In desert areas, or in areas with a low vegetation cover, the thermal inertia mapped this way can be used to map volumetric water content in the soil; this knowledge should be completed by a good knowledge of the physical properties of the soil especially the grainsize distribution (texture), because the same volumetric water content can mean very different moisture availability for the vegetation, according to the soil texture (Duchaufour, 1965). Per example, a volumetric water content of 10% can mean saturation for a sandy soil or severe drought conditions

for a clay. (Figure 1). The usable water reserve, which is comprised between the field capacity (p F 2.5) and the wilting point (p F 4.2) is maximum for a soil with a silty texture, and decreases if the texture gets more towards sand or clay. A good knowledge of the soil texture of the investigation area is thus necessary.

The use of H.C.M.M. data in areas where the vegetation cover is inexistant or low in percentage should then be successful for soil moisture studies as previous works have shown for geologic applications in desert areas (Kahle, 1975) because the correlation between true surface temperature and remotely sensed blackbody temperature is high on bare soil (Figure 2)

On areas with a dense vegetation cover, even in case of grassland, the correlation between remotely sensed black body temperature and surface temperature is much lower than on bare soil areas, and the regression lines vary according to the seasons (F. Bonn, 1977). However, it is possible to estimate the soil surface temperature by using correction equations, which should be established experimentally in the area of interest. Table II gives such correction equations, as established in the Sherbrooke area on a glacial till.

Vegetation cover affects not only the outgoing radiation, but also the soil thermal properties and profiles, as shown in table III. This influence is a double one: 1) a general damping effect of external temperature variations reduces the temperature ranges on vegetated areas 2) the spectral selection of sunlight made by living plants, due to the high reflection of near infrared radiation by chlorophyllian activity affects the soil surface temperature, by reducing the daily maximums during the vegetative season. (F. Bonn, 1976). On the other hand, the presence of vegetation accelerates the drying of the soil, by accelerating evaporation. (C. Jalbert, 1973). This tends to reduce the thermal inertia, and thus to increase the attainable temperature ranges.

The interaction between vegetation, climate and soil constitutes a very complicated system by itself, and using thermal infrared measurements to monitor changes within that system can help to understand the existing relationships, but can also be misleading if we want to isolate just one component (such as soil moisture) in that complicated system. A valid interpretation of soil moisture variations from H.C.M.M. data must then be based on a good knowledge of ground conditions and energy exchanges in the area of interest. Ground truth stations measuring soil, grass level and air temperatures at the satellite overpasses are necessary, completed if possible by radiation measurements in the visible, near infrared and thermal infrared spectral ranges, along with soil moisture profiles.

ACKNOWLEDGEMENTS.

This research has been supported in part by grants from the National Research Council of Canada, the Quebec Department of Education and the University of Sherbrooke.

REFERENCES.

Auding, F. & Kanth, R. (1970). Estimation of Sea Surface Temperature from Space, Remote Sensing of Environment, 1, pp. 217-220.

Bonn, F. & Clément, P. (1972). Utilization of Thermal Infrared Ground Measurements for Determination of Adequate Surveying Periods in Remote Sensing 8th International Symposium on Remote Sensing of Environment, Ann Arbor, Michigan, U.S.A., 2-6 October 1972, pp. 709-714.

Bonn, F. & Clément, P. (1974). Les installations expérimentales extérieures de géographie physique sur les terrains de l'Université de Sherbrooke, Université de Sherbrooke 68 p.

Bonn, F. (1975). Répartition de l'énergie dans le milieu écologique, Thèse Doctorat 3e cycle, Université Louis Pasteur, Strasbourg, France, 202p.

Bonn, F. (1976). New information on the relationships between vegetative cover and soil thermal regime, obtained by use of remote sensing devices. Proc. Comm. Geogr. Data Sensing and Processing, Moscow, pp 35-40.

Bonn, F. (1977). Ground truth measurements for thermal infrared remote sensing. Photogr. Eng. and Rem. Sens. vol 43, no 8, pp 1001-1007.

Buettner, K.J.K. & Kern, C.D. (1965). The Determination of Infrared Emissitivities of Terrestrial Surfaces, Journal of Geophysical Research, Vol. 70, no 6.

Cihlar J. and McQuillan A.K., (1977). Applications of satellite thermal infrared measurements to Earth's resources studies. Remote Sensing Science and Technology, Symp., Ottawa, 1977.

Clément, P. & Gadbois, P. (1971). Comparaison et interprétation des résultats de deux parcelles expérimentales d'érosion (1969-1970), in Research Methods in Pleistocene Geomorphology, E. Yatsu & A. Folconer, ed., Guelph, Ontario.

De Vries, D.A. (1952). The Thermal Conductivity of Granular Materials, Bulletin de l'Institut International du Froid, Annexe, 1952-1, 115.

Hadni, A. (1967). Elements of Modern Physics Applied to the Study of the Infrared, Pergamon.

Jalbert, C. (1973). Compte-rendu d'observations sur les fluctuations de l'humidité disponible du sol, Mémoire Bacc. spécialisé, Département de géographie, Université de Sherbrooke.

Kahle, A.B., Gillespie, A.R., Goetz, A.F. & Addington, J.D. (1975). Thermal Inertia Mapping, 10th International Symposium on Remote Sensing of Environment, Ann Arbor, Michigan, October 6-10, 1975.

Lajeunesse, M. & Bareilhe, B. (1974). Interprétation de traverses à l'infrarouge thermique dans le bassin de la rivière Eaton (Québec), Communication au 42e congrès de l'ACFAS, Univ. Laval, 8-10 mai 1974.

Mattson, R.B. (1969). Thermal Pattern in the Landscape Recorded with Infra-Red Technique and Simulated in Model Experiments. Geografiska Annaler 51A, # 4.

Platt, R.B. & Griffiths, J.F. (1965). Environmental Measurement and Interpretation, Reinhold, 235 p.

Pouquet, J. (1969). Géomorphologie et ère spatiale, Zeitschrift (für Geomorphologie, 13, # 4, pp. 414-471.

Pouquet, J. (1972). Résultats obtenus avec un radiomètre opérant dans la bande spectrale 10,5 - 12,5 microns, Revue de Géomorphologie Dynamique, I XX1, 1.

Rider, N.E. (1957). A note on the physics of soil temperature, Weather, 12,241.

Rose, C.W. (1966). Agricultural Physics, Pergamon, 230 p.

Tricart, J. & Husson, A. (été 1972). Quelques apports des enregistrements infrarouges à la connaissance du milieu physico-géographie, Annales de Géographie.

Table 1. Thermal Parameters Used in Soil Thermal Studies

Parameter	Symbol	Description	Units
Thermal conductivity	k	Quantity of heat flowing through a 1 cm thick layer during 1 second when there is a 1°C temperature difference.	cal $cm^{-1}s^{-1}{}^{o}C^{-1}$
Specifid heat	C	Quantity of heat necessary to raise the temperature of 1 g by 1°C.	Cal $g^{-1}\ {}^{o}C^{-1}$
Density	ρ_C	Weight-per-volume unit	g cm^{-3}
Volume heat capacity	ρC	Quantity of heat necessary to raise the temperature of 1 cm^3 by 1°C.	cal $cm^{-3}\ {}^{o}C^{-1}$
Thermal diffusivity	a	$a = k/\rho C$	$cm^2 sec^{-1}$
Thermal inertia	P	$P = \sqrt{k\rho C} = \rho C\sqrt{a}$	cal $cm^{-2}s^{-\frac{1}{2}}{}^{o}C^{-1}$

Table II. Correlations Between Radiation Temperatures (T_{BB}) and Surface Temperatures (T_s)

$T_{BB} = a + b\ T_s$ T_{BB} AND T_s IN °K

Period	Grass-covered plot			Bare plot		
	a	b	r	a	b	r
May 1971	-150	2.42	0.86	-79	1.27	0.92
May 1972	-173	1.62	0.91	-34	1.12	0.94
May 1973	-186	1.65	0.79	-30.4	0.85	0.97
June 1973	-101	1.34	0.82	-21.2	0.92	0.97
July 1971	- 59	0.78	0.90	-80	1.27	0.93
July 1972	-157	1.54	0.90	- 1.30	1.00	0.96
July 1973	-189	1.64	0.82	-78	1.25	0.95
August 1972	-202	1.68	0.84	-12	1.03	0.92
August 1973	-226	1.78	0.82	-17	1.05	0.94
Sept. 1971	- 35	1.12	0.94	-19.6	0.92	0.91
Sept. 1972	-282	1.97	0.89	-179	1.29	0.95
Nov. 1972	- 43	1.13	0.54	42.8	0.83	0.62
Mean		1.55	0.84		1.06	0.92
Standard deviation		0.38			0.14	

Table III. Mean diffusivity (a) between 0 and 30 cm depth and speed of penetration of heat flow, on vegetated and bare plots (VP and BP).

Period (1972)	Mean a ($cm^2 . s^{-1}$)		Speed (cm/h)	
	VP	BP	VP	BP
May	0.0025	0.0056	2.15	3.23
July-August	0.0026	0.0068	2.19	3.56
September	0.0023	0.0068	2.09	3.57

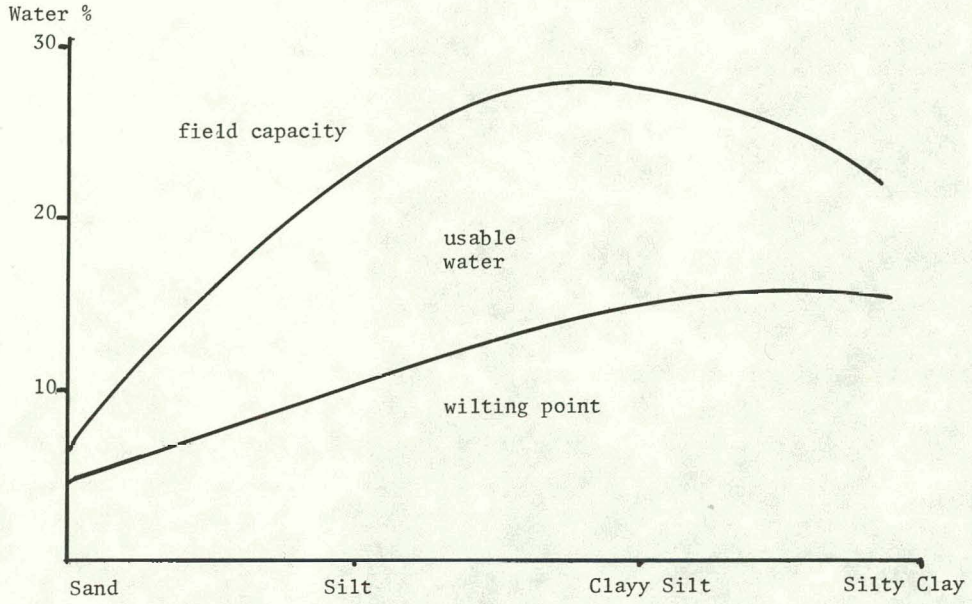

Fig 1 Relation between usable water and soil texture (after Duchaufour, 1965)

Fig 2 Correlation between soil surface temperature and emitted thermal infrared radiation, during August.

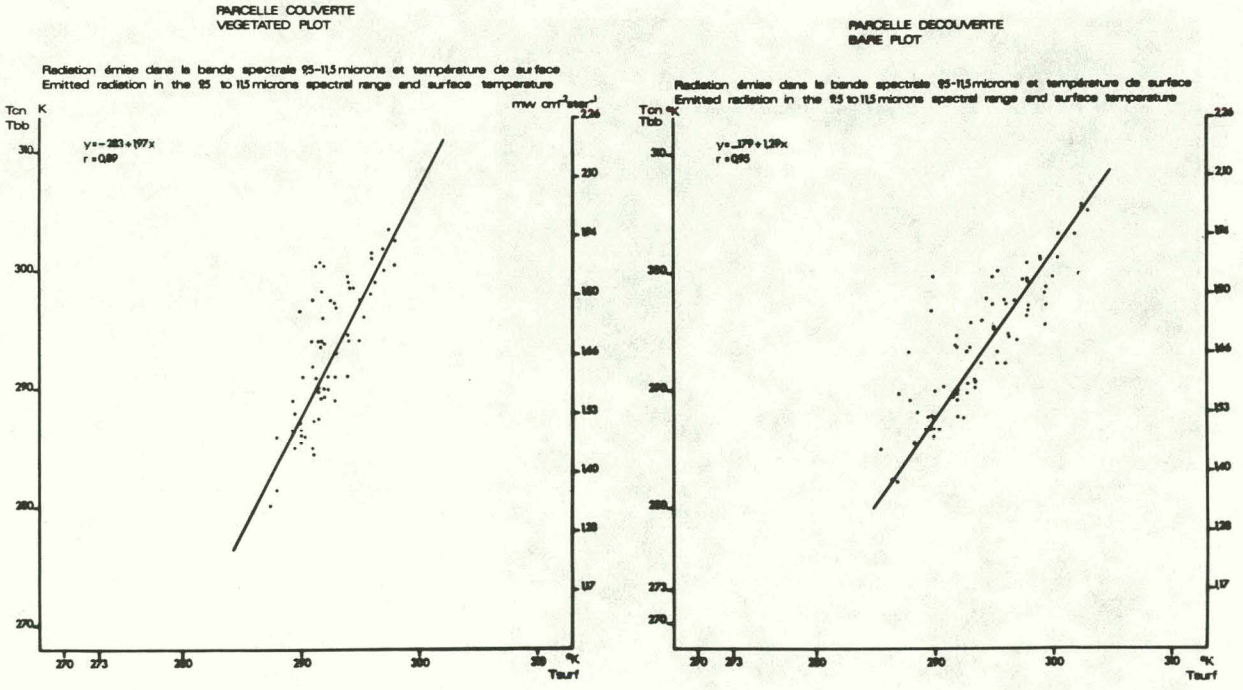

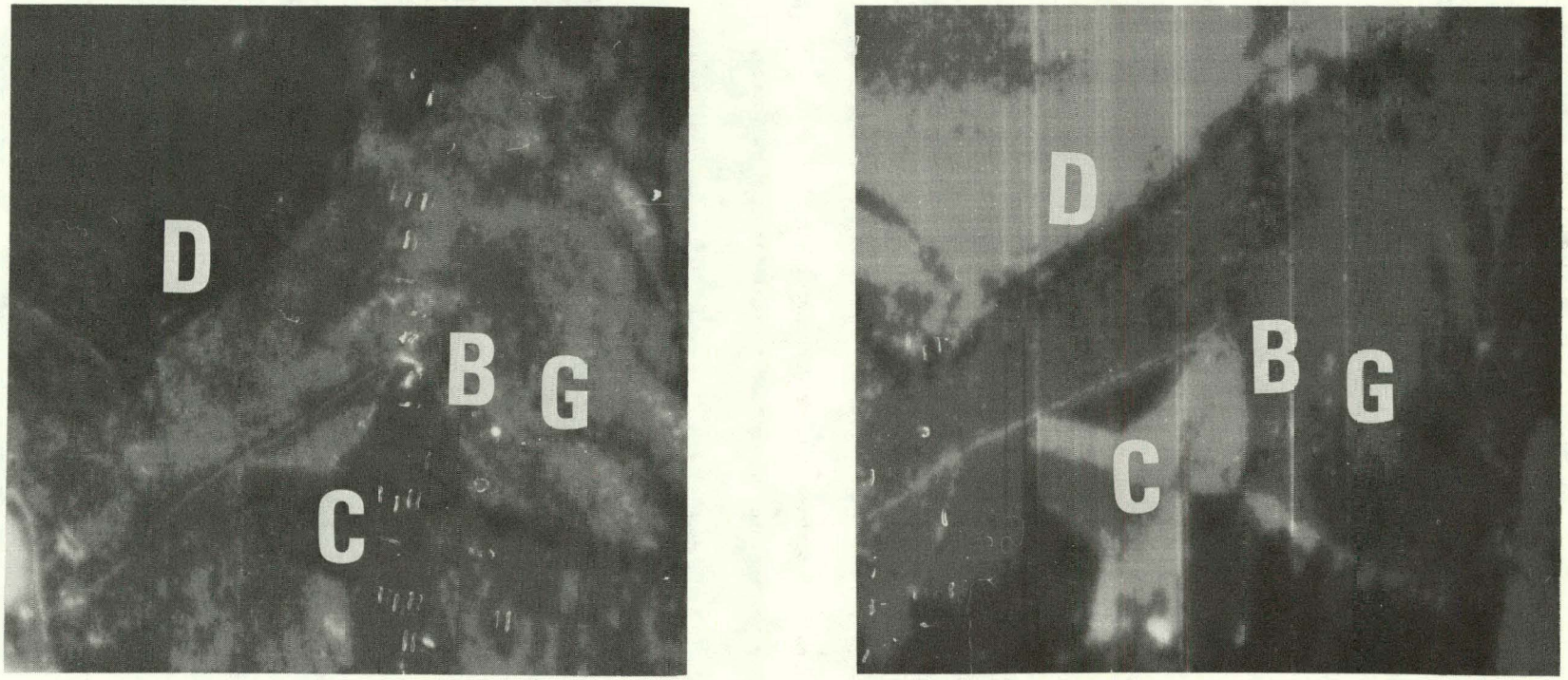

Fig 3 Day (left) and night (right) thermography over the Sherbrooke test site, in June

D: Deciduous
C: Coniferous
G: grassland
B: bareground

GRASSLAND AND FORESTRY APPLICATIONS FROM NEW ZEALAND LANDSAT DATA

G. Ross Cochrane

Geography Department, University of Auckland
Auckland, New Zealand

ABSTRACT

Vegetation is New Zealand's key economic resource. No country in the world is so heavily dependent upon pastures for its economic prosperity. Over 80 percent of its export earnings are derived from pastures: New Zealand grassland farming (with nil or minimal dependence upon other crops) has a worldwide reputation for its efficiency and productivity. Forestry products, particularly from New Zealand's exotic conifer plantations, constitute the second most important source of this country's export earnings. Almost all the country's electrical energy is generated from hydro-electric stations. Maintenance of plant cover in catchment areas of this predominantly hilly to mountainous land is vital for water regulation and protection of productive lowlands. Any techniques that can contribute towards better monitoring or management of New Zealand's grasslands and forests is of vital importance both to New Zealand, as a producer, and also to a fibre and food-hungry world with a rapidly increasing population and decreasing resources.

A sampling model that has proved useful involves three stages of analysis: 1) LANDSAT data at small scales (1:1,000,000) for broad large area survey; 2) substage aircraft photography of selected representative sample areas at intermediate scales (1:15,000); and, 3) field survey at sample sites within the former for the most detailed studies to calibrate spectral reflectances with forest or pasture composition, productivity, vigour, incidence of disease or other physiological stress factors, role of management, influences of fertilizers and soil conditions, felling, logging and silvicultural practices, or other relevant aspects.

In addition, a range of analytical techniques--photographic, optical, electronic, and digital methods--can be applied to LANDSAT data for deriving a range of information in applied problems of forestry survey and management and for rapid or repetitive assessment of pastures at different scales. Examples of each of the four analytical methods are given.

An analysis of the relative cost and usefulness of each of these four methods, related to the degree of technological development available to potential users, has relevance to others than in the specific New Zealand context. Inferences are made concerning possible contributions to data analysis that may be expected from LANDSAT-III thermal band and the higher resolution panchromatic photographic imagery from this satellite.

INTRODUCTION

As pastures are New Zealand's most valuable national resource it is important to have as full and complete information about these as is possible. Details of area covered, regional variations, composition, vigour, seasonal productivity, influences of management policies, problems of pastures on drought-prone soils, and pests, diseases and weeds should be known at national, regional, county, local and individual farm scales for optimum planning, management and production. Ultimately, the most detailed information can only be achieved from measurement at the field level. However, it is not practical, nor economic, to obtain all information at this level. At the opposite extreme, broad synoptic surveys of pasture areas, gross floristic composition, regional differences, seasonal variation in growth, and soil influences upon pastures--all recognizable from satellite (LANDSAT) imagery--provide other useful parameters.

Similar criteria apply to forests. Surveys defining indigenous broadleaf podocarp from exotic softwood (conifer) forests and, particularly in the latter case, differentiating between forest blocks on the basis of species, age classes, clear fell, newly planted areas and current felling can be derived from LANDSAT to augment field information.

Reflectances of electromagnetic energy from pastures, forests and other landscape features can be recorded on remote sensors such as satellite multispectral scanners (MSS) and aerial single lens and multispectral cameras. Such reflectances from pastures is a complex integrated response from the plants and the soil background. For most New Zealand forests the role of soil reflectance is masked by the vegetation canopy.

Thus although pasture areas are relatively uniform, and are often less heterogeneous than many other forms of land cover, pasture analysis is complex due to the inherent biological properties of vegetation, soil characteristics, and because pastures are dynamic. There are constantly changing conditions resulting from grazing management, seasonal weather, soil moisture status and soil nutrient content and mineral availability. Remote sensing applications attempt to interpret the variety and complexity through an understanding of plants and soils and their interactions with the electromagnetic spectrum.

LANDSAT DATA

LANDSAT imagery provides large area synoptic views portraying geologic, ecologic and land use/land cover patterns that have been obtained under uniform altitude, lighting and angle of view for any one image. They are unrivalled for broad scale comparative purposes and are vastly superior to photo mosaics from aerial photography taken under a wide range of lighting, time, altitude and angles. Tonal contrasts (i.e., spectral reflectances), on LANDSAT images, therefore, represent real differences not differences due to variations in light, time, season, angle of view, altitude, film processing and photographic printing that are inherent in aerial photographs or photo mosaics of large areas. The large area coverage and relatively frequent repetitive or temporal survey facilitates recognition of areas and zones of importance of temporal patterns of change. This "highlighting" of areas of interest provides important economies of time for broad scale surveys and for monitoring progress or change. The multispectral properties of LANDSAT imagery provide a mapping tool not normally available from aerial photography.

LANDSAT DATA AND LAND USE REQUIREMENTS

Some critics condemn LANDSAT 1:1,000,000 imagery as too broad, coarse and generalised. This is not a valid criticism as there are analytical procedures enabling surveys at increasingly larger scales to be carried out with increased information and detail to be gained.

LANDSAT data can be used at different scales for a wide range of applied

applications including pasture surveys (Carneggie, De Gloria and Colwell 1974, Poulton et al. 1975, Myers, et al. 1975) employing any one or combinations of the following four techniques: photographic, optical, electronic, or digital.

LANDSAT data can fill a constant need of many people for basic land use information which is current, detailed and in a form which can be readily referred to, handled easily, is relatively cheap, and can be shared in discussion with others--farmers, foresters, woodsmen, contractors, engineers--who may not have the interpretive skills or experience to analyse digital print-out data.

LANDSAT imagery presented in a large-scale photographic format meets these requirements. A constant feature of much of the New Zealand landscape is change, both seasonal change in pasture productivity and longer term change. In many areas new scrub and brushland is being cleared for pastoral farming or for planting with exotic forest plantations. Within existing areas of grassland and forestry activities substantial changes are occurring which will have long-term implications for farm and forest industries. One of the most obvious is the ongoing replacement of exotic tree species such as Pinus ponderosa, P. nigra and miscellaneous other species with P. radiata, and subsequent different management/silvicultural regimes being practiced.

On the fringes of agricultural development, especially in hill country, pasture quality is an everchanging factor. New areas are being cleared for sowing to grass, whilst areas of scrub, bracken fern or native tussock grass may be grazed whilst yet other areas of pasture may be reverting back to scrub or fern or secondary forest. For agricultural planners and advisors as well as for individuals the pasture/scrub interface is an important one. LANDSAT data can provide up-to-date information or subsequently monitor change, progress or decline of pasture area and quality.

In the areas of grassland farming in the Volcanic Plateau, the most significant development has been the move towards a greater dependence upon lucerne as a supplementary feed crop in this "drought prone" area. During summer months the free draining pumice-volcanic ash soils dry out readily and pasture productivity declines. Lucerne also serves as a cash crop and its extension is additionally a partial counter to the ravages of grass grub pests on permanent pastures. Lucerne is not attacked by grass grubs.

The increased area of lucerne in the last eight years, the rate of adoption, and areal increase has important agricultural implications. For example, in the study of the viability of a lucerne processing factory or factories in the area, up-dated information is needed on the location, total area and quality of productivity of lucerne stands. LANDSAT data, in its several formats, gives an accurate measure of all of these criteria at scales where individual properties can be identified, but local and regional patterns can still be readily recognised. For a period considerable subsidies were being paid in this area for lucerne establishment. Regular imagery provides an ideal basis for policy making and for subsequent monitoring, i.e., checking on its application.

Currently lucerne stands in this area are being threatened by diseases and pests. The logistics of any control or eradication programmes depend upon accurate information about the location of lucerne and its quality. LANDSAT data has the potential to provide such information.

PHOTOGRAPHIC TECHNIQUES

Standard photo interpretation techniques using LANDSAT black and white single band imagery of New Zealand scenes at 1:1,000,000 scale and enlargements up to 1:100,000 provide useful practical working maps. Tonal contrast is the major differentiating criterion for small scale imagery. As spectral signatures of pastures commonly vary with different wavelengths, use is made of this by comparing photographic tones on different LANDSAT bands. The added dimensions thus provided enable an interpreter to analyse the patterns with a greater surety

than is possible even on much larger scale conventional aerial photography. Thus, comparison of the differential spectral reflectances on standard single band New Zealand LANDSAT imagery can be used to separate indigenous grasses (tussock), exotic pastures, and field crops; to differentiate between highly productive and less productive pastures; and to separate exotic forest plantations of different species. Single band LANDSAT images are less effective for differentiating major communities within indigenous forests because spectral band contrasts between such communities are very subtle. Enlargements are practical up to a 1:100,000 scale. Such enlargements of pasture areas can be a valuable, easily handled, management record for Ministry of Agriculture surveys, agricultural extension and advisory officers, for county planners, and individual farm owners. They can provide useful working tools for foresters recording areas of different exotic forest species, clear fell, newly cleared and newly planted areas.

Preliminary studies of single band LANDSAT images covering most of the pasture areas of New Zealand--Southland, Otago, Canterbury, Westland, Marlborough, in the South Island; and Wairarapa, Manawatu, Volcanic Plateau, East Coast, South Auckland, and Northland peninsula, in the North Island--show conclusively that they provide a range of information about pastures that is difficult or in some cases impossible to obtain from conventional aerial photography.

MULTITEMPORARY IMAGERY

Comparison of LANDSAT-II scenes, E-2282-21525, E-2299-21190 and E-2334-21183 on 31 October, 17 November and 23 December 1975 respectively, demonstrate changes in seasonal vigour of pastures in the Wairarapa in the North Island and the Marlborough area in the South Island. These changing patterns are recognisable from inspection of single band imagery, but are much more readily obvious when using colour composites. Seasonal changes in Canterbury pastures on the extensive plains east of the Southern Alps in the South Island are also clearly seen from inspection of LANDSAT imagery of winter (E-2192-05311, E-2192-21272), spring (E-2265-213211, E-2232-21252), and summer (E-1502-21362, E-2355-21190 and E-2390-21240). Seasonal pasture change and variations in pasture quality and composition are also well illustrated in LANDSAT imagery of Otago (E-1503-21421, E-2787-21172, E-2805-21163, and E-2805-21165).

This is a region of basin and range topography, of uplifted mountain ranges (horsts) with extensive, down-faulted valleys (graben) between, deeply filled with Tertiary, Quaternary and recent alluvial materials. Soils and drainage characteristics vary, as do farming practice. Irrigated lucerne, sown exotic pastures and coarser mixed exotic-indigenous pastures on parts of the great alluvial valleys contrast with modified indigenous tussock on lower slopes aerially oversown with exotic grasses and clovers, and with indigenous tussock on the higher mountain slopes and summits.

Tonal contrasts on LANDSAT imagery portray these differences while multitemporal imagery monitors seasonal change--spring growth, progressive drying during summer, and influence of winter snow cover. Seasonal coverage with LANDSAT imagery is not as good as the above areas for other parts of New Zealand but there is imagery for most of the country.

MULTISPECTRAL IMAGERY

Multispectral analysis of (E-2787-21172) of LANDSAT MSS Bands 4, 5, 6, and 7 photographic images of North Otago and the McKenzie Basin of the South Island of 19 March 1977 and image scene, E-2805-21163, eighteen days later (6 April 1977) are excellent examples of the use of satellite remote sensing for pasture analysis. Comparison of these images shows pasture variations resulting from differences in soils, in pasture composition, and farm management that are not possible to recognise even from large scale aerial photographs.

Differences in spectral reflectances of pastures recorded on each of bands 4, 5, 6, and 7 reflect variations in sward density, and particularly vigour of

plants and soil moisture availability. These can be seen clearly on LANDSAT E-2334-21123 of 22 December, 1975 for the areas south of Lake Rotorua, the Galatea Basin and much of Hawkes Bay and East Coast. Farm units in the area south of Rotorua are the same general size, farming enterprise is the same, and soils are derived from recent volcanics, but the western half are on soils derived from Rotomahana mud and the eastern half from Tarawera lapilli. Soils formed on the latter are porous with poor moisture retaining capacity and dry out rapidly during dry periods in the summer months. Soils on the former maintain more productive pasture swards because of better soil moisture retentivity.

Pastures on the heavier textured alluvial soils in the Galatea Basin remain green when the swards on the predominantly pumiceous, free-draining soils formed on Taupo ash over most of the basin become drought stressed. The relatively narrow LANDSAT multispectral bands record such contrasts over wide areas at a single point of time. Collectively they provide a wider range of information about pastures than can be achieved from conventional aerial photography, even at larger scales.

Knowledge of land use change, particularly of pastures and forests, is important to the economy of New Zealand. LANDSAT imagery can provide a record of the extension of farming and forestry activities on the margins of presently settled areas and of the changing land use patterns within settled areas more readily than is currently available by other methods. An example of complimentary land use/land cover information, of the type required, built up from analysis of the four separate band images of LANDSAT scene (E-2334-21123) follows.

Table I summarises some of the differences between LANDSAT MSS bands found useful in multiband analysis for differentiating pastures and agricultural crops in the Taupo area. Comparison of Figure 1 and 2 showing the Poronui and Loch Inver stations (ranches) and forest and scrub areas east of Lake Taupo, illustrate that each band can contribute information that collectively facilitates pasture mapping.

Figures 1 and 2, showing Bands 5 and 6 respectively, should be compared noting the very different boundaries that appear. Category F (sown exotic pastures) is most clearly separated from adjacent areas of tussock, fern, scrub and cleared areas on the near infrared Bands 6 or 7. Used in conjunction with Band 5, which clearly shows the pasture-scrub interface, area C (tussock grass) can be readily mapped.

Areas B and E, or fern, scrub and some tussock, cannot be separated from pastures, lucerne or cleared areas on Bands 4 and 5 (Figure 1). The boundaries are strong and clearly separate this entity from pastures and lucerne on Band 6 (Figure 2).

New Zealand has over 400,000 hectares (1,000,000 acres) of exotic forests, the world's largest area of man-made conifer plantations. The greatest area of these are concentrated in the central North Island and are contained within the area covered in a single LANDSAT frame (E-2334-21123). The country's exotic forest industry is characterized by extensive blocks of even-age, single species, sustained yield, short rotation (15-25 years), high annual incremental growth, conifer forests. The industry is highly mechanised and efficient. It provides a diversity of products: round log for export, and timber, posts, props, structural timbers, pulp, paper, plywood and particle (chip) board products for domestic and export markets.

Conventional panchromatic aerial photography at intermediate to large scales has played an important role in planning and management. A new dimension is provided with LANDSAT data. By the use of three or four multispectral band LANDSAT images, patterns of land cover suites can be built up to define forestry boundaries. In determining the boundary between exotic pine species and indigenous forests one benefits from an analysis of Band 4 in respect to Pseutosuga menziesii--indigenous forest (bush), Band 5 for Pinus radiata--bush, and Band 7

for Pinus ponderosa--bush interface. In forest analysis Band 4 has proven to be the most generally useful band. However, it is necessary to reinforce signature classification (i.e., identification decisions) by comparisons with other bands. Table II summarizes the usefulness of LANDSAT bands for forestry analysis in the central volcanic plateau area of the North Island in New Zealand. Simple enlargement of one or more bands or portions of areas provide useful working tools for mapping, management and planning purposes at small to medium scales. For example, monitoring silvicultural practices: clearing, regrowth progress, thinning, and for management purposes: felling, logging, road construction. Used in conjunction with (a) available aerial photography, or (b) photography, flown for selected sample areas, and (c) ground truth data, LANDSAT photographic images can be important for updating information, map revision, and as a basis for planning decisions.

OPTICAL PROCESSING

Projection of single 70 mm LANDSAT transparencies or colour composites can provide superior enlargement to that possible from photographic enlargement alone. Different filters, a range of light intensities and varying combinations of both positive and/or negative transparencies provide a wide variety of processing alternatives.

LANDSAT COLOUR COMPOSITE PHOTOGRAPHS

Colour composite LANDSAT photographs combine into one image the advantages of data from two, three, or four separate multispectral bands with the added merit of the grey tones on the original bands being portrayed as colour tones. Such tonal contrast often "highlights" areas of interest that may require more detailed evaluation by second or third-stage sampling. In studies of New Zealand LANDSAT colour composite imagery, colour tones greatly facilitate differentiation of exotic forest species, ages classes of planting of exotic forests, variations in pasture quality and vigour, separation of tussock grassland from exotic pasture, recognition of different categories of scrub communities (Cochrane & Batty 1977), and broad differentiation of major indigenous forest communities (Batty & Cochrane 1977). Some of the boundaries could not be detected as discrete areas of grey tones on the black and white single band imagery.

High quality colour composite positive transparencies represent the optimum photographic working tool for mapping. Enlarged colour composite prints are also useful but to a lesser degree because there is some loss of colour tone and colour fidelity during printing (Batty & Cochrane 1977, Cochrane & Batty 1977).

Carneggie, De Gloria and Colwell (1974) used LANDSAT 1:1,000,000 colour composites to monitor phenology of California pastures, and equated these against productivity using radiance measurements and biomass productivity from clip quadrats. The practical utility of such information on a state-wide basis requires no stressing.

Such patterns of seasonal productivity have similar parallels in much of New Zealand. Sequential imagery of Canterbury, Marlborough, Wairarapa and Otago, although not available as regularly as in the Californian study, provide examples for the potential adoption of such methods of pasture survey. Preliminary sequential surveys on a qualitative basis for Marlborough-Wairarapa, for Otago and Canterbury clearly demonstrate relationships between rates of pasture drying off and gravelly soils, loams, loess and alluvial soils. Similar patterns, present elsewhere, have yet to be investigated between short rotation and permanent pastures and soils.

Ability to differentiate classes increases with larger scales. Exotic forest categories and many indigenous forest communities become more easily distinguishable on simulated colour-infrared-colour composites. Several categories of pasture can also be mapped. Figure 3, derived from enlarged LANDSAT colour composites of Aupouri Peninsula, North Island, shows 27 categories of land use/

land cover. The total area covered only 80 mm x 20 mm on a standard LANDSAT 1:1,000,000 image. Five different age classes of young conifers were mapped on the basis of subtle tonal contrasts. Exotic pastures, especially where closely associated with distinctive soils that seasonally influence productivity (e.g., peats, sands, clays, alluvials, volcanic ash and pumice) can be mapped more confidently using colour composite imagery.

Although some interpretation problems are present, enlarged LANDSAT colour composites of a complex area of indigenous forests in Westland, South Island proved useful for mapping several categories of major forest communities as well as scrub, swamp and cut-over areas (Batty and Cochrane 1977).

Combinations of both positive and negative transparencies of two bands only, 4 and 7 and 5 and 7, proved more valuable for pasture-crops discrimination and forestry and other land use and for suspended sediment detection (a measure of erosion of catchment areas) than conventional simulated colour infrared colour composites using Bands 4, 5 and 7.

Advantages of optical analytical processing are the superior enlargement possible, thereby providing a more flexible range of scales to be used; the colour enhancement of multispectral differences; and the versatility of the combinations that are possible. Simple projection is not difficult but a colour additive viewer is an expensive piece of equipment. Establishing accurate congruency of each image is most important: it can be time consuming but is absolutely necessary if optimum results are to be achieved.

ELECTRONIC PROCESSING

Isodensitometer instruments electronically scan a single LANDSAT transparency, registering areas of equal density, to produce an increased range of areas of equal film density from that detectable by the human eye. These densities are measures of equal spectral reflectances reproduced as tonal contrasts on LANDSAT film.

A colour isodensitometer provides quick flexible density slicing, colour enhancement and variable magnification, all of which can greatly increase the range of information extractable from LANDSAT transparencies. This electronic density slicing provides many more categories than can be recognised in normal photo interpretation or without optical processing by additive viewers. Inherent in all density slicing procedures there is a loss of sharp detail but there is an increase in another form of information, patterns of densities. Large areas can be rapidly scanned, or a selected smaller area can be enlarged to scales ten times greater than is possible with photographic enlargement.

Controls on many isodensitometers allow quantitative measurements to be made, from a digital readout panel, of areas portrayed on the viewing screen. Once a pattern has been established selective control buttons can be used to exclude all but the desired colour or colours to produce thematic maps, e.g., of the extent of indigenous tussock grassland.

Results from colour isodensitometer analyses of New Zealand LANDSAT images for pasture and exotic forestry studies have been less productive than from use of colour composites. Conversely, colour isodensitometer imagery has proven a useful practical tool for mapping the complex patterns present in indigenous forests. Used in conjunction with colour composites mapping of indigenous forest communities in difficult country has been moderately successful (Cochrane et al. 1976, Batty and Cochrane 1977). Attempts to accurately plot and measure areas of lucerne has not been successful. Nor has a high degree of success been achieved in exotic forest species analysis. Primarily information is restricted to one band. Contrasts are less obvious than when using multiband analysis. On the other hand for broad land use classification good results have been achieved. Cochrane et al. (1976) compared LANDSAT colour isodensitometer patterns of an area in east Taupo to a land capability classes map derived from lengthy photo

interpretation and extensive field work. Close correspondence was found. The isodensitometer map was produced in a matter of minutes only, the other took many months. Colour isodensitometer analyses of Band 4 imagery have proven to be an excellent technique for recognising variations in densities of suspended sediments in both fresh water lakes (Campbell and Cochrane 1977) and in coastal waters (Cochrane and Male 1977).

DIGITAL PROCESSING

Digital processing offers the most promise for extracting maximum information from LANDSAT data. It is the most versatile. Currently it is also the most expensive in the short-term sense.

DIGITAL: two main approaches have been tested; (1) digital enhancement of imagery and (2) digital analysis of radiance values. Digitally enhanced images in both black and white single band (PHOTOWRITE) and colour composites (GE 100) provide superior information, at a range of scales, to that possible from standard products. Digital analysis of radiance values to produce line printout patterns at larger scales than is practical from any of the former three methods produces information of importance in practical forestry management.

Changes will be required in mapping outlook and new techniques learned if full advantage is to be taken of the enormous potential provided by CCTs for mapping. A familiarity with such techniques will be a prerequisite if maximum use is to be made of resources surveys from the five band sensor of LANDSAT-III and from the future space programmes of LANDSAT-D, SEASAT, and SPACE SHUTTLE.

LANDSAT COMPUTER COMPATIBLE TAPES

LANDSAT computer compatible tapes are a first generation product with pixel resolution not degraded by multiple copying as is the case with photographs. Thus, many small differences in radiances of targets can be distinguished on CCTs but not on photographic products. Thematic mapping by cluster analysis enables desired categories--exotic pasture, tussock, stressed pasture, scrub, forest, etc.--to be mapped automatically by computer. As each pixel represents the scene radiance from a surface area of 79 x 59 metres, considerable detail can be extracted at quite large scales. Currently in pasture and forestry studies only broad land use/land cover classes have been mapped by the author using digital analyses of radiance values (Strachan and Cochrane 1977). More detailed analyses have been focused upon mapping suspended sediments (Cochrane and Male 1977, Campbell and Cochrane 1977, Male and Cochrane 1977). The greatly increased detail and larger scales achieved in those studies augers well for similar techniques applied to detailed forestry and pasture analyses.

Again economics in mapping can be achieved by using a three-tiered sampling method. Selected representative areas recognized on the computer maps can be compared with recent aerial photographs and ground sampling carried out within the photo sample area for verification or establishing quantitative data.

A range of very sophisticated hybrid systems welding advantages from optical, electronic, and digital processing, the speed and diversity of automatic computer processing, and the versatility and flexibility of interfacing a human operator at desired stages are completely revolutionising mapping from LANDSAT data. Currently none of these hybrid data processing systems are available for use within New Zealand.

Digitally enhanced (PHOTOWRITE) images in black and white of Bands 4, 5, and 6 of the central Taupo area and a GE 100 colour composite of the Christchurch urban area have been compared with conventional LANDSAT products. Both forms provide superior information. These have been entirely experimental. Currently such data are not available on an operational basis. Later in 1978 it is hoped a PHOTOWRITE facility will be available for New Zealand users centred in Lower Hutt at the Physics and Engineering Laboratory (PEL) of the Department

of Scientific and Industrial Research (DSIR).

FUTURE APPLICATIONS

Receipt of LANDSAT I data of New Zealand was minimal and that of LANDSAT II data of New Zealand has been very sporadic. With the successful launching on 5 March 1978 of LANDSAT-III, it is hoped that data acquisition will be more regular. In addition to the four band MSS used on LANDSAT I and II, LANDSAT-III has a fifth sensor band monitoring emissive radiation in the 10.4-12.6 μm wavelength band. Capability for daytime and nighttime monitoring of thermal differences but at coarser resolution (240 m) should prove useful in pasture analysis. Particularly this should augment pasture information related to gravel and sandy drought prone soils, and to peat and alluvial areas with higher soil moisture and relevant pasture characteristics.

It is also planned to provide photographic coverage at a scale of 1:500,000 with resolution to 40 metres to augment the standard MSS imagery. Such resolution closely approximates the threshhold for detailed discrimination of features giving details equivalent to that obtainable from medium altitude photography. Thus, the utility of LANDSAT data for pasture analysis and forestry applications promises to improve. For many areas a substantial decrease in dependence upon the second tier of sampling--aircraft photography--is likely. Refinement of analytical procedures coupled with improved collection of ground data offer promising prospects for remote sensing applications in pasture and forestry analysis in New Zealand in the near future.

SUMMARY

A wide range of methods can be employed for mapping from LANDSAT data. These fall into four broad categories: photographic, optical, electronic, and digital, each of which has advantages and limitations particularly with respect to the range of scales for which it is practical. Broadly speaking the amount of detail that can be derived increases from photographic processes through optical and electronic to the maximum from digital analytical procedures. For optimum results from all of these analytical procedures dependence (to a greater or lesser extent) is required upon a systematic substage sampling programme. There can be no escaping the important role that ultimately some ground control or field sampling is a vital component in analysis of LANDSAT data.

Regardless of the degree of technological sophistication present in a country one or more of these analytical techniques can be applied to provide better information.

REFERENCES

Batty, J. & Cochrane, G. Ross 1977. Thematic mapping in Westland, South Island, New Zealand, from LANDSAT colour composites: a preliminary survey. DSIR PEL LANDSAT-II Investigation Programme No. 28230. Final Report, Part 18, Section 3.

Campbell, G.H. & Cochrane, G. Ross 1977. Lake Taupo suspended sediment study: a preliminary statement. DSIR PEL LANDSAT-II Investigation Programme No. 28230. Final Report, Part 18, Section 7.

Carneggie, D.M., De Gloria, S.D. and Colwell, R.N. 1974. Usefulness of ERTS-I and range conditions in California's annual grasslands. Remote Sensing Research Programme School of Forestry and Conservation, University of California, Berkeley.

Cochrane, G. Ross & Batty, J. 1977. Thematic mapping: land use and vegetation mapping of the Aupouri Peninsula, Northland, New Zealand, from LANDSAT. DSIR PEL LANDSAT-II Investigation Programme No. 28230. Final Report, Part 18, Section 1.

Cochrane, G. Ross and Male, A.G.R. 1977. Regional and seasonal patterns of stream sediment discharges along N.Z. coasts from SKYLAB and LANDSAT imagery. Proc. N.Z. Ecol. Soc., 23: 13-20.

Cochrane, G. Ross, et al. 1976. Geographical applications in LANDSAT mapping: land use mapping and environmental studies. DSIR PEL LANDSAT-II Investigation Programme No. 28230, Third Quarterly Report, Part 6, 41 pp.

Male, A.G.R. & Cochrane, G. Ross 1977. Analysis of suspended sediment patterns in the Firth of Thames. DSIR PEL LANDSAT-II Investigation Programme No. 28230. Final Report, Part 18, Section 2.

Myers, V.I., et al. 1975. Crops and soils. Chapter 22 in L.W. Bowden (ed.) Manual of Remote Sensing, Vol. II (Am. Soc. Photogram., Virginia).

Poulton, C.E., et al. 1975. Range resources: inventory, evaluation and monitoring. Chapter 18 in L.W. Bowden (ed.) Manual of Remote Sensing, Vol. II, (Am. Soc. Photogram., Virginia).

Strachan, C.M. & Cochrane, G. Ross 1977. Large-scale mapping of vegetation from a LANDSAT-II image of East Taupo: a preliminary survey. DSIR PEL LANDSAT-II Investigation Programme No. 28230. Final Report, Part 18, Section 2.

TABLE I. USEFULNESS OF BANDS 4, 5, AND 6 FOR DISTINGUISHING PASTURE LAND COVER AT SMALL SCALES

1-5 Rating:
1 = very good
2 = good
3 = moderate
4 = poor
5 = very poor

CATEGORIES	BANDS 4	5	6 or 7
Exotic pasture from tussock	4	4	1
Exotic pasture from crushed scrub	4	3	1
Exotic pasture from scrub	4	3	1
Exotic pasture from swede crop	1	1	4
Exotic pasture from lucerne	4	3	3

TABLE II. USEFULNESS OF LANDSAT BANDS 4, 5, AND 7 FOR DISTINGUISHING FOREST AND SCRUB (SHRUBLAND)

1-5 Rating:
1 = very good
2 = good
3 = moderate
4 = poor
5 = very poor

CATEGORIES	BANDS 4	5	7 or 6
Pseutosuga menzeisii from indigenous forest (bush)	2	4	4
Pseutosuga menzeisii from scrub	1	1	5
Pseutosuga menzeisii from Pinus ponderosa	2	2	4
Pseutosuga menzeisii from Pinus radiata	2	3	4
Pinus radiata from bush	2	1	4
Pinus radiata from scrub	1	1	5
Pinus radiata from Pinus ponderosa	2	1	4
Pinus ponderosa from scrub	2	2	1
Bush from scrub	1	2	5

FIGURES 1 & 2. BANDS 5 & 6 of 70 Km wide area of East Taupo. I, Poronui, II Loch Inver. Cover classes: A lucerne, B fern, C tussock, D new grass, E tussock & scrub, F exotic grass, G scrub, H cleared, I burned, J radiata pine, K ponderosa pine, L pine & fir, M bush.

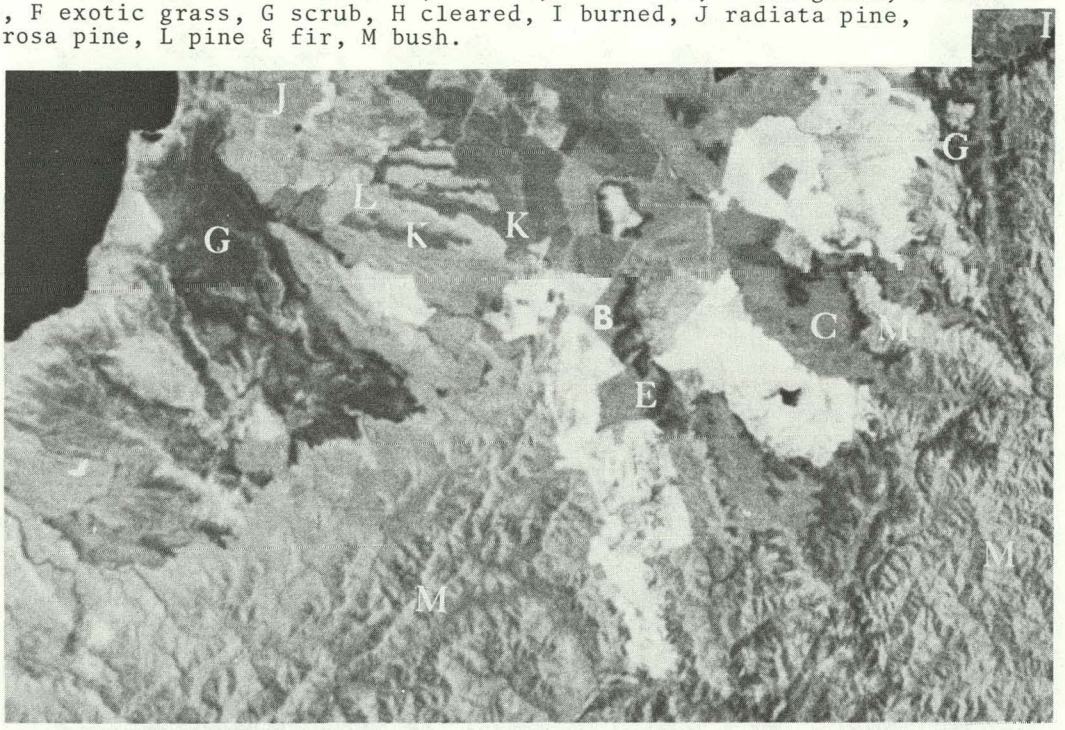

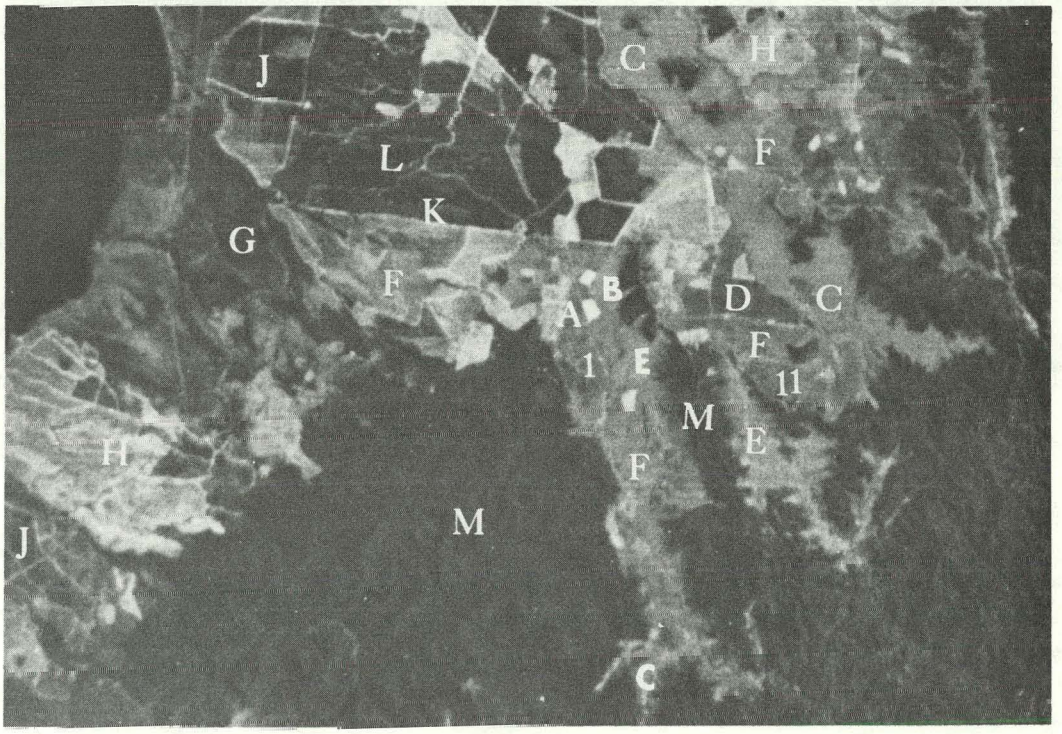

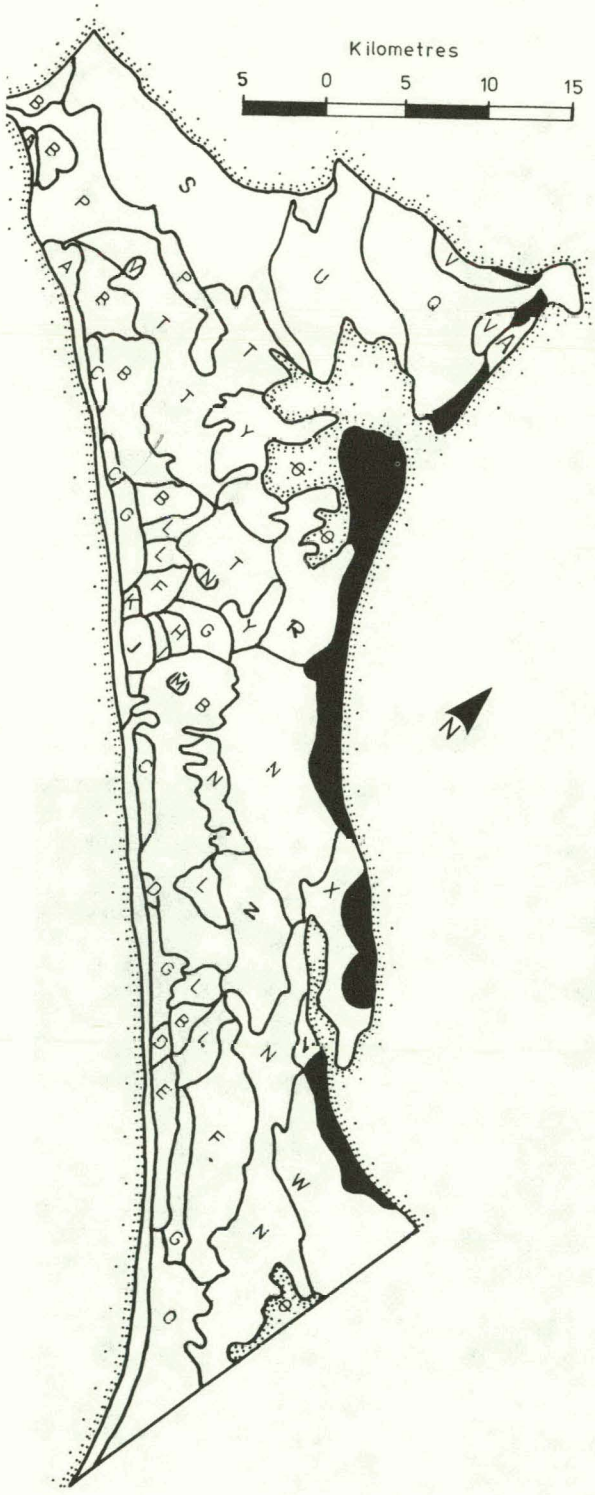

Figure 3. LAND USE/LAND COVER CLASSES AUPOURI PENINSULA

Categories	Symbol
EAST COAST PARENGARENGA SAND:	Black
WEST COAST SAND: UNSTABLE DUNES:	
Intertidal and salt flats	A
Unvegetated dunes, shifting sand	B
Foredunes with marram grass	C
Foredunes with Scirpus sedge	D
Foredunes with flax	E
Dunes with lupins	F
Dunes with pines, age undefined	G
Dunes with pines, planted 1971	H
Dunes with pines, planted 1973	I
Dunes with pines, planted 1972	J
Dunes with pines, planted 1974	K
MORE STABLE DUNES:	
Marram association	L
Coastal forest	M
Established pasture	N
Established pine	O
NON SAND AREAS:	
Developed pasture on volcanic soils	P
Developed pasture on other soils	Y
SCRUBLAND:	
North cape type	Q
Parengarenga type	R
West coast highland type	S
West coast lowland type	T
Gumland type	U
Mt. Camel type	X
Ngataki type	Z
MANGROVE ASSOCIATIONS:	Θ
FRESH WATER SWAMP:	
Manuka-swamp associations	V
Wiwi-raupo associations	W

Figure 3. LAND USE MAP OF AUPOURI PENINSULA, NORTHLAND, NEW ZEALAND, DERIVED FROM LANDSAT COLOUR COMPOSITE (E-1648-21420)

VOLCANIC GAS ERUPTION VELOCITY SENSOR USING A SPATIAL FILTER

Suteo Tsutsumi, Kohji Takemura, and Yasumasa Itakura

Department of Electronics Engineering, Kyoto Institute of Technology, Matsugasaki, Sakyo-ku, Kyoto, 606, JAPAN.

ABSTRACT

Quantitative informations about temperature, concentration and escaping velocity of the volcanic eruption from the craters will or may provide some parameters necessary to estimate the grade of volcanic activity or the heat energy stored in the volcanic area. This paper describes some experimental results for application to remote sensing of the escaping velocity of the volcanic gas, smoke or steam jet by the use of a phase locked loop followed after the balanced modulator and a spatial filter such as a plus-minus strip-formed detectors' linear array with either a silicon photovoltaic detector or a pyroelectric detector.

INTRODUCTION

This paper is to propose a passive type of volcanic gas eruption velocity sensor, which is based on the optical image-velocity sensing technique[1] by the use of a plus-minus strip-formed detectors' linear array, and to describe both a signal processor making it possible to improve the measurement accuracy and some experimental results exhibiting the feasibility of the measurement. The sensor can be provided with a versatility by using the detector either sensitive to the emission or scattering reflection from the volcanic gas, when it should be utilized at least within the wavelength region of the atmospheric windows because of remote sensing. In general, in the nighttime the pyroelectric detector would be utilized and in the daytime the silicon photovoltaic detector (Si detector) would be utilized. These passive types of velocity sensor have some points of excellence such as low cost, simple construction, etc., compared with the active type of laser radar system.

MEASUREMENT AND ITS ACCURACY

1. PRINCIPLE OF MEASUREMENT

Figure 1 shows the typical optical construction of the proposed sensor. The heart of the sensor is the spatial filter, which is composed of a half mirror M, one detector D_1 laid behind a reticle r_1, and another detector D_2 laid behind the same but only one-slit shifted reticle r_2. Outputs of the detectors D_1 and D_2 are differentially connected with the following amplifier, whose output is available as the output signal of the sensor.

Both of the reticles, each placed at the image-plane of the objective lens, are respectively the parallel fence reticles with the alternately transparent and opaque bars of equal width a and the field-of-view $A \times B$, through which every outgoing radiation should be gathered on to the corresponding detector. Thus, as sketched in Fig.2, such a plus-minus strip-formed detectors' linear array as required is obtained.

Supposed that the optical image of the volcanic gas and smoke, rising with an angular velocity Ω_y in y direction, is formed on the image-plane of the sensor, the output signal v(t) is given by

$$v(t) = \int\int_{-\infty}^{\infty} r(x,y) \cdot s(x, y-\Omega_y t)\, dx\, dy \tag{1}$$

where s(x,y) is an input scene, a two-dimensional spatial radiance distribution of the volcanic gas and smoke, and r(x,y) is the response function of the spatial filter, i.e., the plus-minus strip-formed detectors' linear array. Taking the Fourier transform, Eq.(1) gives

$$V(f) = \frac{1}{\Omega_y} \int_{-\infty}^{\infty} R(f_x, f/\Omega_y) \cdot S(f_x, f/\Omega_y)\, df_x \tag{2}$$

where

$$f = \text{temporal frequency in Hz} = f_y \cdot \Omega_y \tag{3}$$

Considering the fact that the input scene is not deterministic but random in shape and radiance distribution, it would be adequate to deal with Wiener spectrum $W(f_x,f_y)$ instead of the message spectrum $S(f_x,f_y)$ in Eq.(2). The output spectrum U(f), then, reduces to

$$U(f) = \frac{1}{\Omega_y} \int_{-\infty}^{\infty} |R(f_x, f/\Omega_y)|^2 \cdot W(f_x, f/\Omega_y)\, df_x \tag{4}$$

The transfer function $R(f_x,f_y)$ of the spatial filter shown in Fig.2, has spatially a narrow bandpass characteristic in y direction, and it is given by

$$R(f_x,f_y) = \frac{AB}{2} \operatorname{sinc}\left(\frac{\pi A f_y}{2n}\right) \cdot \frac{\sin(\pi A f_y)}{n \cdot \sin(\pi A f_y/n)} \cdot \operatorname{sinc}(\pi B f_x) \tag{5}$$

where

$$\operatorname{sinc}(z) = \sin(z)/z$$

n = number of pairs of strip-formed detector included in a linear array.

If we assume that the Wiener spectrum $W(f_x,f_y)$ of the input scene is a white noise, i.e.,

$$W(f_x,f_y) = W_0 \tag{6}$$

then, Eq.(4) reduces to be from Eqs.(5) and (6)

$$U(f) = \frac{A^2 B W_0}{4} \left[\sin\left(\frac{\pi A f}{2n\Omega_y}\right) \cdot \frac{\sin(\pi A f/\Omega_y)}{n \cdot \sin(\pi A f/n\Omega_y)} \right]^2 \tag{7}$$

Equation (7) is plotted in Fig.3, when n = 25. Obviously from Fig.3, the narrow-

band signal has the center frequency f_0 and the half power band-width B_n, respectively, as follows:

$$f_0 = n \cdot \Omega_y / A \quad \text{Hz} \tag{8}$$

$$B_n = \Omega_y / A = f_0 / n \quad \text{Hz} \tag{9}$$

Equation (8) indicates that the center frequency f_0 is proportional to the angular velocity Ω_y results in that of the center frequency f_0, i.e.,

$$\Omega_y = \frac{A}{n} f_0 \tag{10}$$

It is obvious, in this case, that the linear velocity V_y can be evaluated by the knowledge of the distance L between the input scene and the sensor as follows:

$$V_y = L \cdot \Omega_y \tag{11}$$

In our experiments, the distance ranges from about 50 m to about 3 km. The typical examples of the Wiener spectra as the input scene are illustrated in Fig.4.

2. MEASUREMENT ACCURACY

The accuracy of the velocity measured by the proposed sensor is considered to be influenced by several kinds of errors in the process of making the frequency measurement. The first type of errors is derived from the hardware realizability in the part of the sensor, e.g., errors based on the finite bandwidth of the spatial filter and on the system noise such as detector noise. The second type of errors is derived from the physical natures in the part of the object as input scene,e.g., errors based on the random spatial radiance distribution of the object and on the nonuniformity of the spatial velocity distribution of the object.

(1-1) Errors due to finite bandwidth

The measurement accuracy of the instantaneous velocity is inversely proportional to the value of the factor $Q = f_0/B_n = n$. Under condition that n is constant, the further improvement of the measurement accuracy is accomplished by averaging the results obtained in a longer observation time-interval T. Assuming that both an occuring event for one cycle generated at the sensor output is independent upon that for another one cycle generated there and the object velocity can not be considered to vary during the time-interval T, the resultant measurement accuracy should be given by[2]

$$\varepsilon = \frac{1}{2\sqrt{3}\, n \sqrt{T \cdot f_0}} \tag{12}$$

This effect is accomplished by the low pass filter or the PLL circuit. Given n = 25 and T = 1sec, this kind of error will be of 1 [%] or below for $f_0 \geqq 2$ Hz.

(1-2) Errors due to system noise

The system noise generated in the detector and preamplifier deteriorates the accuracy of the frequency measurement. However, in general, the use of a

PLL circuit as a tracking filter is able to decrease practically the noise to the negligible level.

(2-1) Errors due to randomness of spatial radiance distribution

The randomness of spatial radiance distribution included within the sensor's field-of-view causes the amplitude of the output signal to vary at random. This leads to the miss count when the frequency measurement is made by the frequency counter. It is clear that the employment of the PLL circuit is also effective in reducing this kind of error.

(2-2) Errors due to spatial nonuniformity of velocity distribution

The spatial nonuniformity of the escaping velocity distribution of the volcanic eruption included within the field-of-view would yield the output signal having a composite spectrum. In this case, the spectrum analyzer may be significantly effective as far as the frequency measurement is concerned. However, we have done without the use of the spectrum analyzer in the field test for the normal volcanic eruption, though we have had a problem as for the extensiveness of the field-of-view.

In the daytime, Si detector had better be employed, because it provides larger output available and lower cost to setup, compared with pyroelectric detector which ought to be employed in the nighttime. In order to decrease the error described in Eq.(12), how to share the values of n and T is a very important problem.

We have already pointed out that the employment of the PLL circuit was very useful for processing the output signal from the view point of noise depression, etc.. To equivalently extend the capture range of the PLL circuit, the frequency of the sensor's output signal was up-converted by the use of a balanced modulator.

EXPERIMENTAL RESULTS AND DISCUSSION

1. MEASUREMENT BY THE SENSOR WITH SILICON DETECTOR

The speeds of intermittent eruptions continuing to occur at the active volcanoes, Mts. Aso and Sakurajima in Kyushu, Japan, were measured at the distance about 200 m and 2.8 km far from there, respectively. Figure 5 shows the optical configuration of the sensor used for the measurement in the daytime. Figures 6 and 7 reveal two different types of eruptions: the less active and the active. The former seems to be mainly erupting the steam and the latter seems to be belching forth masses of steam, gases, cinders and ashes.

Figures 8 and 9 show the typical results analyzed for Aso and Sakurajima active volcanoes, respectively: the occurrence frequency vs the escaping velocity. Note that an event that the escaping velocity averaged for the integration time of 1 sec had been obtained from the output signal is regarded as one unit of the frequency. Therefore, the area under these curves analyzed for each eruption is related to the grade of the respective volcanic activity. The parameters shown in the upper right portions of the figures denote the observation time-interval for which results were analyzed.

Figure 8 shows that the escaping velocity of about 1 m/sec is the most frequent one. This means the low volcanic activity at this time. Figure 9, on the contrary, represents that the escaping velocity ranges from 4.5 m/sec to 15 m/sec. The most frequent velocity also varies from time to time.

2. MEASUREMENT BY THE SENSOR WITH PYROELECTRIC DETECTOR

The speeds of the steam jet, whose temperature was about 370 K, erupted from the bored wells located in Takenoyu and Otake areas in Kyushu, Japan, were measured at the distance about 50 m and 150 m away from there, respectively. Figure 10 shows the optical configuration of the sensor used for the measurement day and night: n = 4 and F-number = 1.5. Figures 11 and 12 show the views of the steam jet in Takenoyu and Otake, respectively.

Figures 13 and 14 show the spectra of the output signals for Takenoyu and Otake, respectively. Comparison of the spectra (a) of the signal plus noise with those (b) of the noise alone made it possible to estimate the steam jet velocity for Takenoyu and Otake as 127 m/sec and 63 m/sec, respectively.

The measurement at such a short distance as in Takenoyu and Otake areas brings about the deterioration of the signal-to-noise ratio, since the pyroelectric detector has the responsivity performance inversely proportional to the frequency and the Wiener spectrum of the object has the spatial frequency characteristic inversely proportional to the squared spatial frequency as shown in Fig.4. Therefore, it should be noted that if this sensor will be used to measure the eruption velocity of the steam or the water vaper at the distance about 3 km then we are able to find directly the required frequency from the sensor's output signal without the technique of the Fourier transform.

CONCLUSION

It has been shown that the passive type of the optical image-velocity sensor was available successfully in measuring the escaping velocity of the volcanic gas or smoke from such a distance as 3 km. Although a pyroelectric detector makes it possible to measure the escaping velocity of the gas or smoke day and night, a Si detector is favourable to use for the daytime measurement from the point of view of the sensor's signal-to-noise ratio.

Adoption of the PLL circuit followed after the balanced modulator will be useful to improve the measurement accuracy and yet process the signal automatically. It is worth to point out that a simultaneous measurement of the temperature of the volcanic gas or smoke will make it possible to estimate the released heat flow in co-operation with the sensor proposed here. This investigation was aided in part by grants from the Research Comittee of "A Feasibility Study on Volcanic Energy Utilization, Japan".(3)

REFFERENCES

(1) J.A.Ator, JOSA, Vol.53, No.12, 1963.
(2) S.Tsutsumi, Y.Itakura, & T.Takagi, Proceedings of the 10th Symposium on Remote Sensing of Environment. Vol.1, p.637, 1975.
(3) S.Tsutsumi, Research Comittee Reports of Feasibility Study on Volcanic Energy Utilization in Sunshine Project, Japan, 1974-1977.

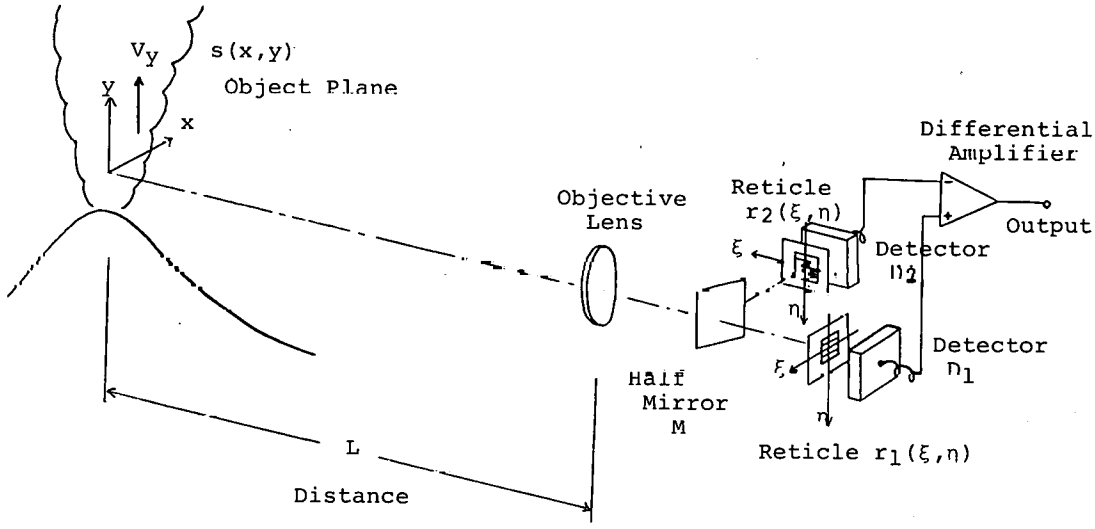

Figure 1. OBJECT AND TYPICAL CONFIGURATION OF THE SENSOR

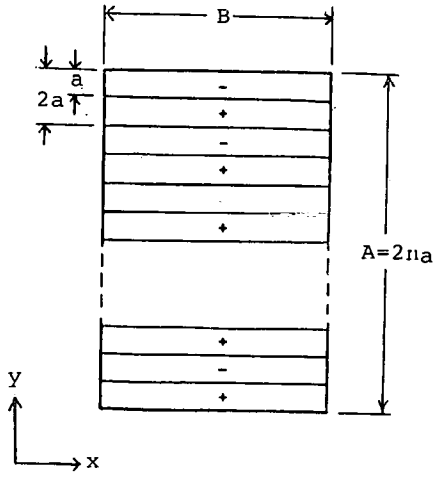

Figure 2. PLUS-MINUS DETECTORS' LINEAR ARRAY AS THE SPATIAL FILTER

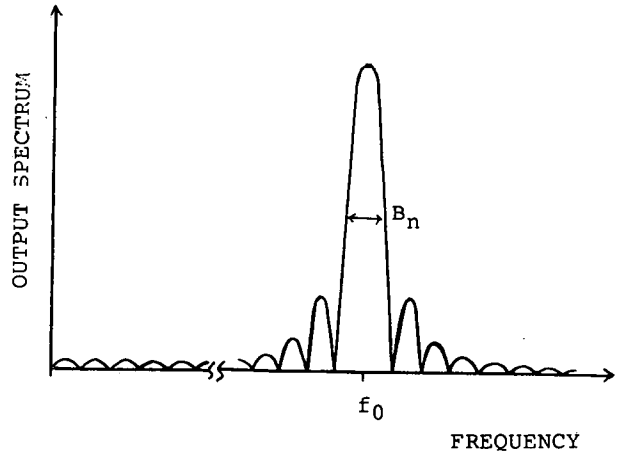

Figure 3. SIGNAL SPECTRUM PASSED THROUGH THE SPATIAL FILTER

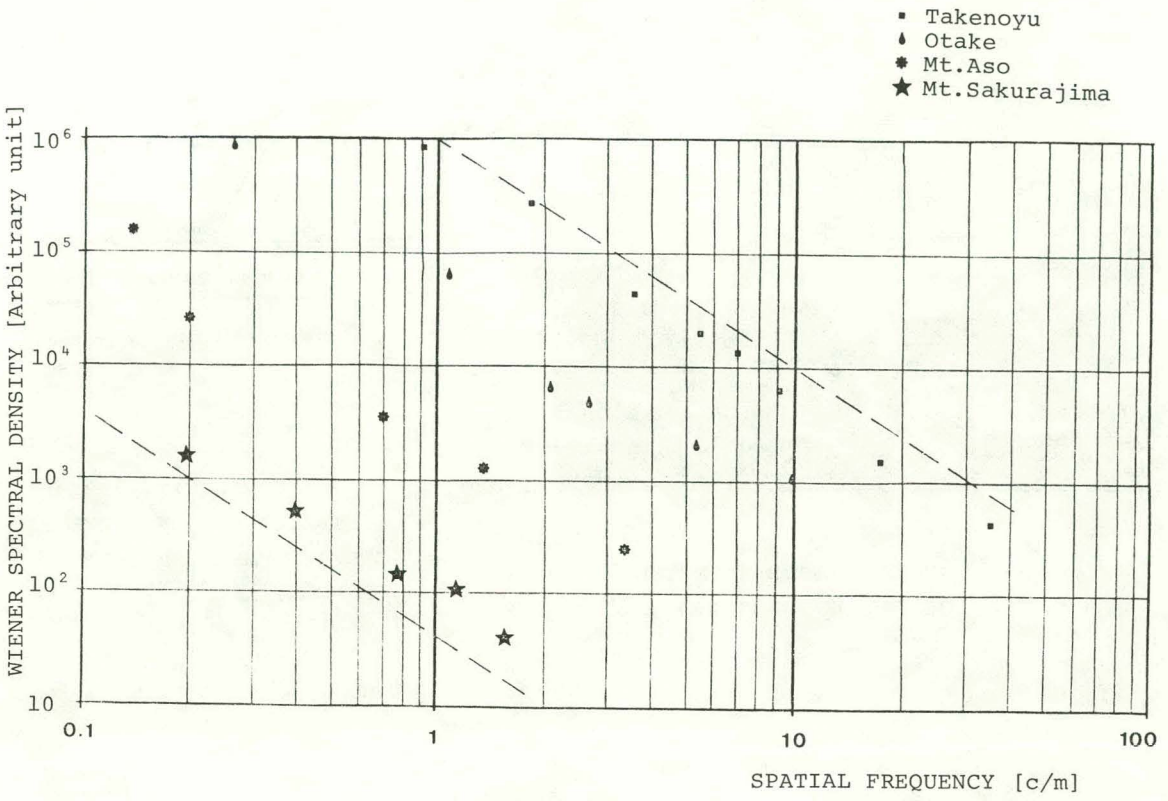

Figure 4. TYPICAL WIENER SPECTRA OF THE OBJECTS

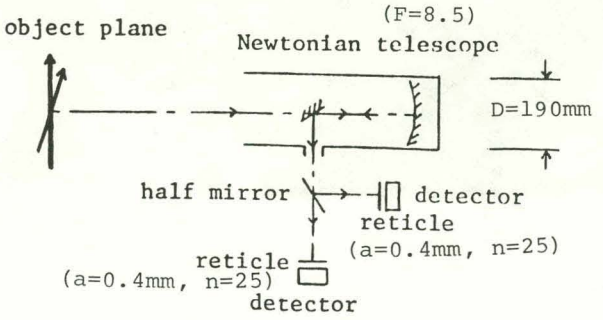

Figure 5. OPTICAL CONFIGURATION OF THE VELOCITY SENSOR USED, WITH SILICON DETECTOR

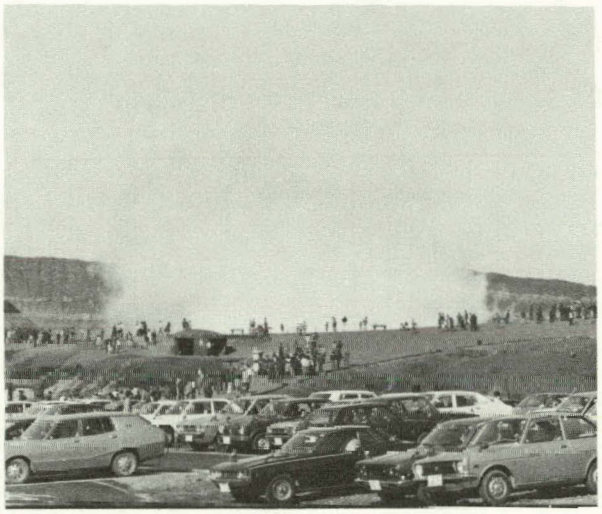

Figure 6. STEAM ERUPTED FROM THE CRATER OF MOUNT ASO

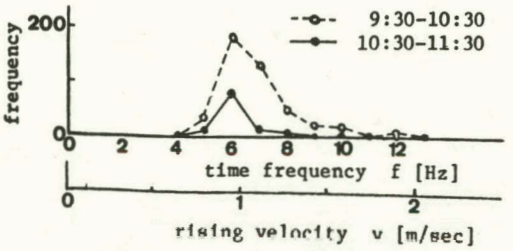

Figure 8. ESCAPING VELOCITY SPREAD-DISTRIBUTIONS OF THE STEAM ERUPTED FROM THE CRATER OF MOUNT ASO

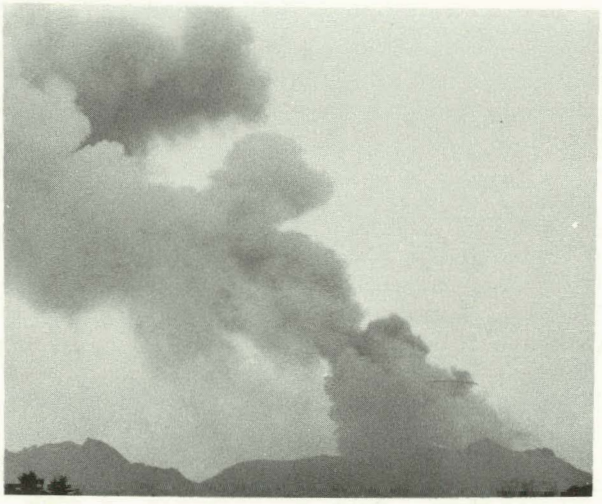

Figure 7. COLUMN OF SMOKE AND GAS ERUPTED FROM THE CRATER OF MOUNT SAKURAJIMA

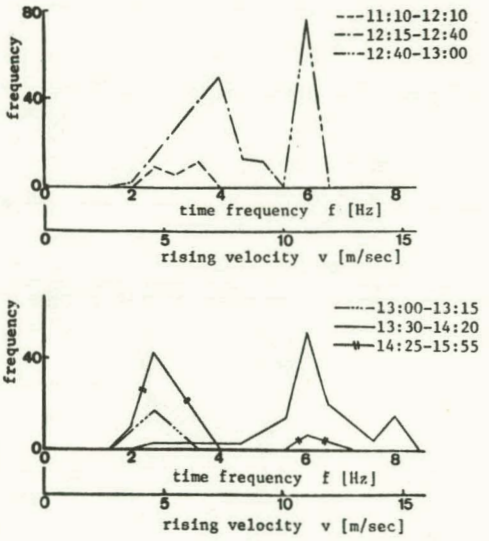

Figure 9. ESCAPING VELOCITY SPREAD-DISTRIBUTIONS OF THE SMOKE AND GAS ERUPTED FROM THE CRATER OF MOUNT SAKURAJIMA

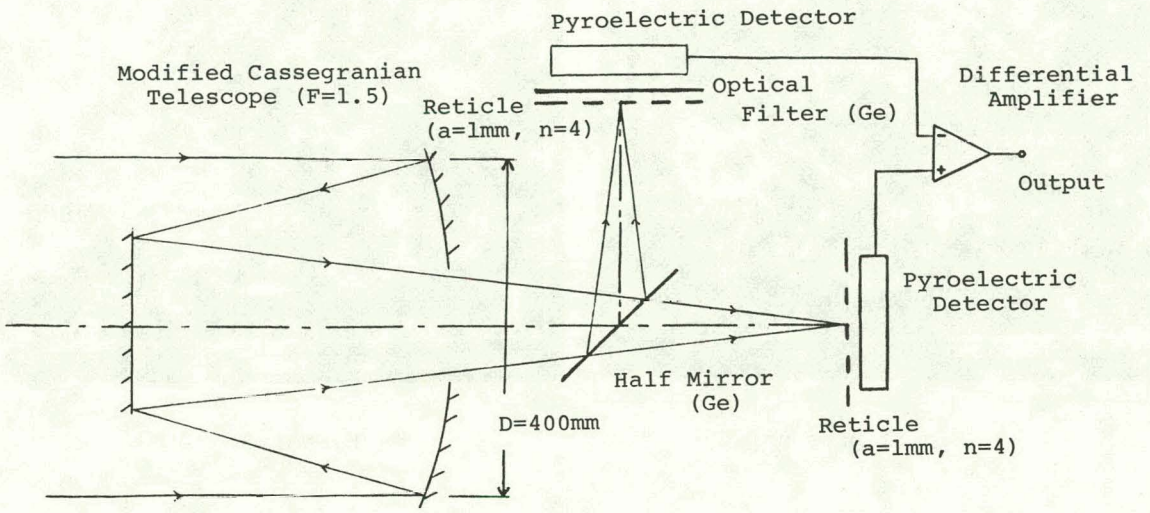

Figure 10. TYPICAL CONFIGURATION OF THE SENSOR WITH PYROELECTRIC DETECTORS

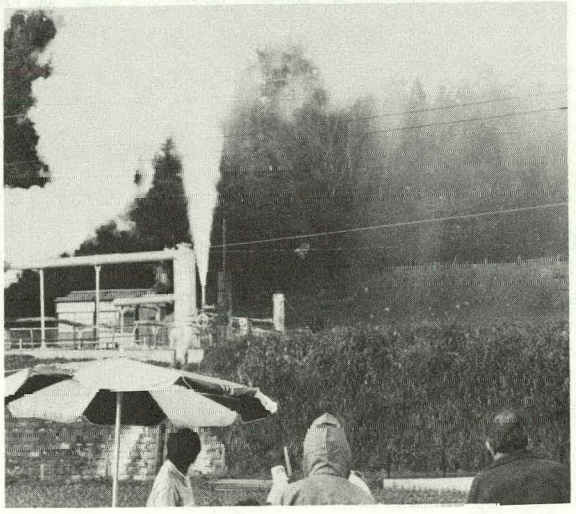

Figure 11. STEAM JET ERUPTED FROM THE BORED WELL AT TAKENOYU

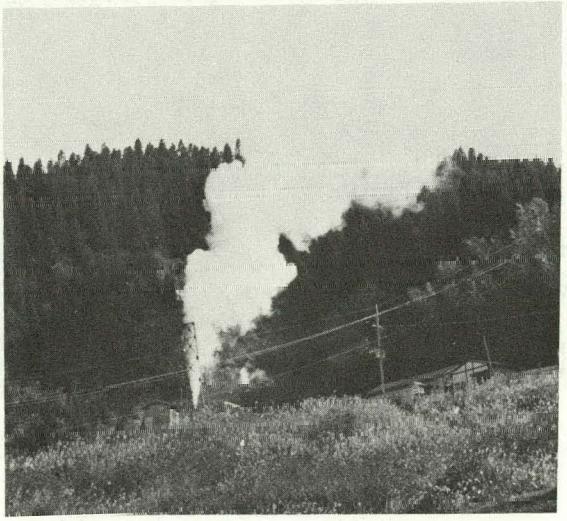

Figure 12. STEAM JET ERUPTED FROM THE BORED WELL AT OTAKE

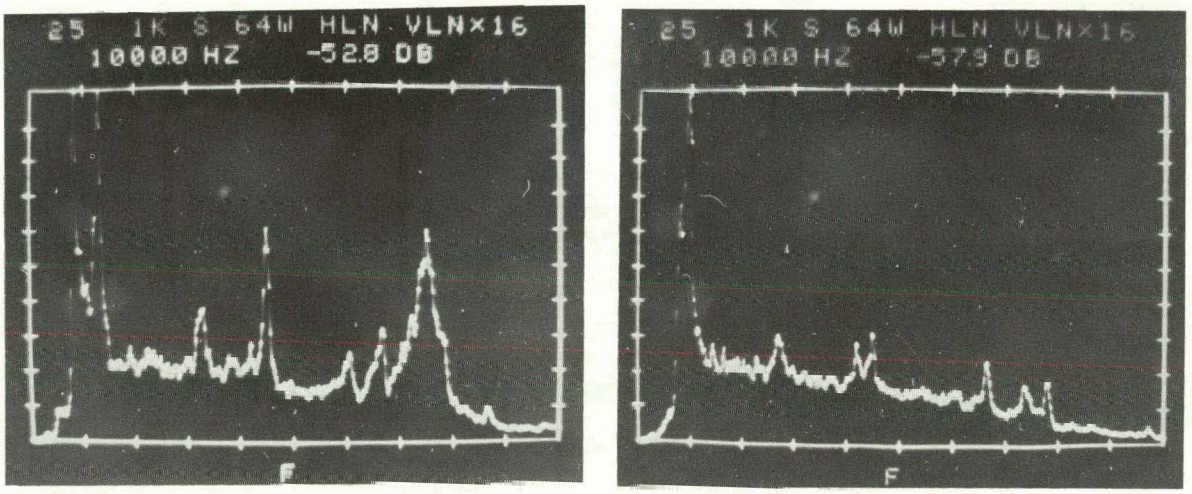

(a) Signal plus noise

(b) Noise

Figure 13. OUTPUT SPECTRA ANALYZED FOR THE TYPICAL SIGNAL OBTAINED AT TAKENOYU

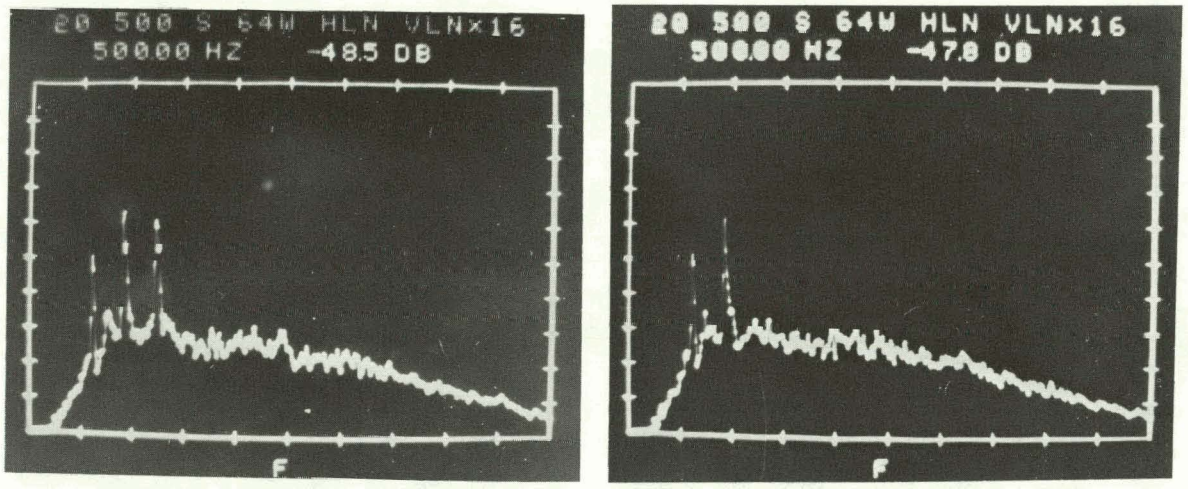

(a) Signal plus noise

(b) Noise

Figure 14. OUTPUT SPECTRA ANALYZED FOR THE TYPICAL SIGNAL OBTAINED AT OTAKE

AUTOMATIC COLLECTION OF ENVIRONMENTAL GROUND TRUTH DATA IN CHILE BY EMPLOYING EARTH ORBITING SATELLITES.-

Mauricio Araya F.

Civil Engineer of Geodetic Department, Faculty of Physics and Mathematics Sciences, University of Chile. Beaucheff 850, Casilla 2777. Stgo. Chile.

ABSTRACT

This paper explains the main aspects of Chilean experiences to collect environmental ground truth data from remote sites, by employing Satellite Data Collection Systems (DCS). This technology employs several automatic sensing stations called Data Collection Platforms (DCPs); the DCPs send the data obtained by the sensors conected to them to the space, where a satellite relays the information to a ground receiving station for the final distribution of the data to the users. The results obtained in the Chilean DCS Experimental Plan have been very succesful and it looks very possible the operational employment of Satellite DCS in Chile, in the next future. The main theoretical and practical aspects of Satellite DCS are presented in the first part of this paper. The second part is related with Chilean DCS Program. Finally, the conclusions and Bibliography are included.

1. INTRODUCCION

The motive of this paper is to show, trough Chilean experiences, how useful can result the adequate employment of remote sensing techniques for a country. It is usual to think that this technology is very expensive. Really it depends on how the problem is focused. Due to the different realities of the countries, it is not convenient to exactly employ the same methods and equipments succesfully employed in another country. Normally, it is necessary to emphatize some system, method or equipment to solve that specific problem. It is very important that the remote sensing specialist be able to exactly realize about the nature of the problem he is solving, the infrastructure that he can employs and the new tools that he will need. In this way, in according to the national reality, the employment of remote sensing techniques will result an effective, economic and rapid technology to solve problems related with natural resources.

For instance, in the Chilean situation, the employment of Satellite DCS appears very convenient. It solves many urgent problems to collect environmental ground truth data mainly from Los Andes Ranges of Mountains, Pacific Ocean, extreme North and South of the country. The urgency and advantages of having DCA appers very clear. Besides, the cost to furnish this system is very low due to the infrastructure existing in the country. Howewer it is much more expensive and difficult to have a LANDSAT image receiving station in Chile. It is more urgent and cheaper to improve the existing meteorological images stations (APT) to receive high quality meteorological images from GOES and NOAA satellites. In the other hand, due to the Chilean topography, the agriculture is practiced in small valleys, etc. Then, for detailed studies (such as agricultural census), it is more convenient to emphatize the existing capability to take multispectral photographies from airplanes rather than satellites. Of course, satellite images (LANDSAT mainly) are excellent for regional planing purposes but, at least by now, it should not be so necessary to receive them in a real-time way. In relation with digital interpretation of satellite and airplane images, it could be possible to employ the computing capability already existing (such as the IBM-370 of our Faculty).

As it is possible to realize, the adequate proportion to employ the different systems, equipement and observation levels (spatial, aereal, ground) of remote sensing techniques, is a key element to obtain the maximum benefits. The scientific research must exist in every country to obtain these results. For this reason our Faculty through Geodetic Department, is very interested to develop studies and experiences to determine the more convenient systems to be employed in Chile.

In relation with Satellite DCS, it is necessary to say that this system looks to accomplish very well the requirements to collect ground truth data from remote sites in Chile. It is usual that researchist doesn't obtain all the information that he would need (in quantity and regularity or frequency). This is due to the difficults to reach to the adequate sites. The expeditions are normally very expensive and riskful and sometimes it is quite impossible to arrive to the desired site. The environmental ground truth data is collected along the country for several purposes: water resources management (irrigation, hydroelectric generation, water supply); navigation; meteorological forecast; volcanic and seimic activity surveillance; forestry; environmental pollution; etc. This information is employed in conventional jobs or projects related with remote sensing. Satellite DCS is a very promising tool to solve these data collection problems in Chile.

2. MAIN ASPECTS ON SATELLITE DATA COLLECTION SYSTEMS

A Satellite Data Collection System (DCS) comprises several automatic sensing stations (Data Collection Platforms, DCPs) that send their information to a satellite. The spacecraft receives the data sent from the DCPs and relays it to a ground receiving station, where the information is treated to be finally distributed to the users (Figure 1).

A Data Collection Platform (DCP) is a small field radio set with a microprocessor. The user can program the DCP in according to his necessity and to choose : the times for the update interval (lectures of sensors connected to DCP) and the transmission interval (DCP sends data to the space); the type (analog and /or digital) and number (normally up 8) of sensors to be employed; the satellite to be used; etc. The DCP model employed in Chile is convertible type, wich is compatible with LANDSAT and GOES satellites. It is very small and light (30 cm. diameter x 40 cm. high; 5 kg.). The batheries are 12 Vdc and they are recharged by solar panels. The DCP can operate under rough environmental conditions: -30°to + 50°C; 0- 100 % air humidity; 0 - 7,000 meters over sea level. It is usual to visit the installation site every 6 months because few failures are produced. It is possible to work with analogic (0 - 5 Vdc inpust to DCP) and digital sensors. Each analogic input employs 8 data bits and 16 data bits are used for each digital input. In the LANDSAT mode, up 8 analogic sensors can be employed (or combination up 64 bits). In the GOES mode, it is possible to connect up 8 analogic sensors and 4 digital sensors to the DCP. It is usual to employ analogic sensors because they are easier and cheaper to be made. Figure 2 shows a general installation scheme of a DCP. Really, it depends on the characteristics of the installation site, the precautions to be taken to assure a correct performance of DCP and sensors when the user leaves the installation site. Normally it is possible to employ existing facilities to install DCP, sensors, antena, solar panel, etc.

The satellite is the link among DCPs and ground receiving station and the spacecraft only relays DCP messages when there is mutual visibility among DCP-satellite-receiving station. Then, their orbiting characteristics are very important. When a geostationary satellite is employed (GOES), there is permanent mutual visibility and it is possible to exactly program the DCP update and transmission intervals in according to user requirements. If a polar orbiting satellite is employed (LANDSAT), the flexibility and capability to relay a great deal of information, is considerably reduced. The satellite only enters to the mutual visibility zone some few minutes of certains orbits per day (normally every 12 hours). Some satellites have the capability to record DCP messages on board and to relay the data when a receiving station is visible (Tiros-N). Some satellites can locate moving DCPs (buoys or balloons) by Doppler effect (Nimbus,

Tiros-N). At present, for Chilean situation, LANDSAT/DCS and GOES/DCS look to be the more useful systems to be tested. In the next future, some system to locate moving DCPs should be tested (Nimbus or Tiros-N).

The ground receiving station receives the data relayed by the satellite and prepares it to be distributed to the users. Normally, a ground receiving station has a passive rol. But sometimes, such as in GOES/DCS, it is possible to interrogate the DCPs trough a command sent to the satellite by the station. This would be a ground receiving/command station. The data is distributed to the users in according to the urgency required and the link means with the station. So, it is possible to employ telex, telephone lines, remote computer terminal, special or regular mail. It is usual, when no urgency is required, to send to the user a computer printout with all the information sent by their DCPs. The action range of a ground receiving station depends on several aspects such as: electronic and mechanical characteristics; geographic location; local topographic conditions; type of satellite employed (geostationary or polar orbiting).

2.1. BASIC CHARACTERISTICS OF LANDSAT/DCS.

LANDSAT serie is operated by U.S. National Aeronautic and Space Administration (NASA). There are three orbiting spacecraft: LANDSAT-1 (July 1972), LANDSAT-2 (Jannuary 1975), LANDSAT-3 (March 1978). At present, LANDSAT-3 relays DCS data. These satellites have near polar and circular orbits, at 900 km altitude, completing 14 orbits per day. The orbital ground trace coincides every 18 days, to take multispectral images over earth surface. These images are presented as squares covering 185 x 185 km, with a spatial resolution of aprox. 80 meters. Normally it is employed the Multispectral Scanner (MSS) that obtains images in 4 spectral bands (two visible, two near infrassed and, in LANDSAT-3, one more in thermal infrared). Really, this is the main purpose of this satellite. DCS is only an experimental system but it works very well. There is one single DCS channel per satellite (401.5 MHz).

The satellite crosses the mutual visibility zone aprox. every 12 hours, for 1-2 orbits (figure 3). Because the spacecraft only remains in this zone about 5-15 minutes, it is necessary that the DCP sends a message very continued. So, the DCPs normally send a message every 90 or 180 seconds. The transmission of the data takes only 38 miliseconds. Each message contains 64 data bits, plus DCP ID, initial and end flags. It is necessary to determine the minimun number of messages relayed by the satellite every 12 hours, and so it is possible to select an adequate update interval. For instance, if 8 messages can be relayed every 12 hours (for orbit), an adequate update interval could be 2 hours. In this way, every 12 hours, 6 different messages (recorded in DCP memory) would be relayed by the satellite (corresponding to lectures done every two hours). This information is enough for several purposes but when more real time and more continued data is required, LANDSAT/DCS is not enough. This is a random access system and it assures to receive a DCP message, at least once every 12 hours, if 1000 DCPs are working in an area such as North America.

2.2. BASIC CHARACTERISTICS OF GOES/DCS.

The GOES serie is operated by U.S. National Oceanic and Atmospheric Administration (NOAA). These are geostationary satellites, at approx. 36.000 km. altitude, over Ecuator line. The operational system employs two satellites to 75° W and 135°W. There is one spare orbiting satellite and one spare satellite on earth which can be launched within 30 days. This is an operational system. Each satellite has 100 channels for self-timed DCPs (401.7 - 401.85 MHz, approx). and 100 channels for interrogable DCPs (401.85 - 402.0 MHz, approx,). Because the satellite is always in the mutual visibility zone (figure 4), the self-timed DCPs can be programmed to read the sensors and to send the data, as the user needs. It is possible to select update intervals multiple of 6 or 15 minutes increments (1 to 255 increments). The transmission intervals can be selected from any multiple of 15 minutes increment (1 to 255 increments). The interrogable DCPs are normally interrogated following a fixed schedule (for instance, every 3

hours). but in an emergency situation the DCP or DCPs can be interrogated at any instant. Every DCP message can contains up 2000 data bits. The DCP transmission rate is about 100 bits/seg in the GOES mode and 5000 bits/seg. in the LANDSAT. When a convertible DCP model (self-timed) is employed, it is necessary to change the antena and to program again the DCP microprocessor, in according to the new satellite wich will relay the DCP data. An interrogable DCP has a higher power consumption because a receptor must always be activated. In general, the main power consumption is done when a sensor lecture is being done or when a message is being sent. Normally, only a clock is always energized (self timed DCPs).

2.3. ANOTHER TYPES OF DCS AND FINAL COMMENTS.

There are more satellites that relay data from DCPs. But their characteristics can be assimilated to geostationary or polar orbiting systems. Nimbus and Tiros-N are the last type and some commercial geostationary satellites are being tested (COMSAT). It is necessary to realize about the most convenient (and cheap an easy to furnish) DCS system for every country. In Chile, it was better to begin with LANDSAT and GOES DCS.

Finally, it is necessary to say that Satellite DCS is very adequate to collect data from remote sites. It is a system very flexible (DCPs can be added or eliminated without problems), economic (a complete automatic station costs no more than U.S. $ 10,000 normally), reliable (failures in DCPs are very limited, ground receiving stations almost always receives correct data), and gives environmental data in a continuedly and near real-time way. However, it is necessary to analyze every future DCP installation and to compare their advantages in relation with existing or conventional methods. This is very important in countries with restricted economic resources. So, in Chile the idea is to install DCPs in those place that urgently require it and when more resources (funding) become available, it will be possible to increase the automation of the sensing net.

3. CHILEAN EXPERIENCES ON SATELLITE DATA COLLECTION SYSTEMS.

3.1. CHILEAN DCS PROGRAM.

In the Faculty of Physics and Mathematics Sciences of the University of Chile, studies and experiences are being developed since 1974, to test Satellite DCS as a future operational tool. The author has created and conducted this Program since 1974, in the Geodetic Department of this Faculty. The valuable aid of U.S. Geological Survey, U.S. NASA and U.S. NOAA has been decisive for the success of this Program. Nowadays this DCS Project is being performed with the participation of Geodetic Department, NASA Division (both institucions belonging to this Faculty) and several Chilean institutions. The Program comprises three stages: a) Study of Antecedents and Feasibility to employ Satellite DCS in Chile; b) Preparation and Development of an Experimental Plan; c) Operational Employment of Satellite DCS in Chile.

In the first stage it was necessary to consider : a) Technical characteristics of Satellite DCS and results obtained in other countries; b) Need of Satellite DCS in Chile (remote sites are very current); c) Interest and convenience for Chilean institution (costs are reasonable); d) Feasibility to employ Satellite DCS in Chile (using existing facilities). All these considerations were satisfactory. Several publications of the author resume this stage. The main areas that need DCS are:

- Hydrology and Meteorology (snow data from mountains, river stage, hidrometeorological data, meteorological data from continental, antartic and oceanic sites, etc.).
- Hydrography and Oceanography (Tsunami Warning System, improvement of navigation in Southern Chilean Straits, oceanic current studies, etc.).

- Vulcanology and Seismology (surveillance system with forecasting purposes because there is a great and continuous seismic and volcanic activity in Chile).
- Environmental pollution (water and air), Forestry (warning of forest fires), and other disciplines.

Because Satellite DCS was convenient for Chile, the Second Stage was begun. The U.S. Geological Survey borrowed three (3) Convertible Data Collection Platforms (CDCPs) for an experimental plan outlined by the author and some Chilean institutions: Dirección General de Aguas (DGA, General Water Survey), Empresa Nacional de Electricidad S.A. (ENDESA, National Enterprise for Electricity Inc.), Instituto de la Armada (IHA, Hydrographic Institute of the Chilean Navy), and Instituto de Investigaciones Geológicas (IIG, Geological Research Institute of Chile). The three DCPs are installed with DGA, ENDESA and IHA. It was not possible to work with IIG in Villarrica Volcano (about 800 km south from Santiago), for a vulcanologic experience, due to funding restrictions. The success of this preliminar experimental plan was possible due to the valuable cooperation of several persons of U.S. Geological Survey, U.S. NASA and U.S. NOAA, specially Mr. Richard W. Paulson (U.S.G.S.) and Mr. William D. Carter (U.S.G.S.). Besides, the personel of NASA Division in Chile was able to receive and to decode LANDSAT /DCS data in the NASA Station in Chile.

During January 1977 the First Chilean Meeting on Satellite DCS was developed, with the attendance of more than 200 Chilean professionals and the participation of Mr. Richard W. Paulson (U.S.G.S.), Mr. Earle Painter (U.S. NASA), and some electronic engineers of the industry that makes the CDCPs. This event , held at this Faculty and organized by the author,marks the end of the theory and the begining of practice experiences on Satellite DCS. Really, this event was scheduled for 1976 but it had to be delayed. During the second part of 1977 the first 3 DCPs were succesfully working. The first results were so promising that some Chilean institutions decide to participate in this experimental plan. In this way, the Instituto Antártico Chileno (INACH, Chilean Antartic Institute) adquired three (3) more DCPs and sensors, wich were installed in Chilean Antartic during February 1978. The DGA acquired five (5) more DCPs for an hydrologic pilot net about 300 - 500 km North from Santiago. It is possible that during 1978, more DCPs be installed by: Empresa Nacional del Petróleo (ENAP, National Enterprise for Petroleum), in Magallanes Strait, for hydrographic studies; Servicio Meteorológico de la Armada (Meteorological Service of Chilean Navy), for a pilot experience near Valparaíso; Compañía Manufacturera de Papeles y Cartones (a cellulose industry about 600 km. south from Santiago), for warning forest fires; IIG or another institution, for vulcanologic experiences in Villarrica Volcano (800 km south from Santiago). The figure 5 shows the existing and planned (1978) DCP installation sites.

As it is seen, Satellite DCS is being tested in several disciplines in Chile and under different environmental conditions. The experimental stage will follow during 1978 and maybe 1979. Then, an operational system should exist. It could be operated by the University of Chile (because U.S. NASA will leave the Tracking Station in 1980) or for some specialized spatial organization of Chilean Government. The main University rol is the research and transference of technology. It is necessary to study, to test and to evaluate (and, if necessary, to develop) new systems or technology. Once it is found convenient for the country, that new tool must be given to existing specialized institutios, for an operational employment. Under this idea the Remote Sensing Office of Geodetic Department is working.

3.2. MAIN ASPECTS ON DCP INSTALLATIONS IN CHILE.

The most important aspects will be considered, in relation with the existing DCP installation sites showed in figure 5. The author and specialized personnel of NASA Division has participed in the DCP installations, besides of personnel of the related institutions..

a) Dirección General de Aguas , DGA (site 1). This DCP was installed during begining August 1977 in El Yeso Dam (site 1 a) because it was not possible to reach to the original selected site in Echaurren Glacier, Negra Lagoon (site 1 b). Anyway, these two sites are separated by few kilometers and are located at about 150 km. South East from Santiago, Los Andes Ranges. In spite of the 3000 meters

over sea level, the environmental conditions are very rough. This experience was selected for snowmelt forecast. DGA must control many hydrometeorological stations along Chile and DGA must elaborate the forecast for irrigation, water supply and hydroelectric generation. In the central zone, the most valuable for agriculture, the irrigation water during the dry summer is produced by snowmelt. Then, it is fundamental to make good forecast of snowmelting. It is very difficult to make the necessary measurements. Only some months of the years it is possible to arrive to the those sites. Anyway, it is very riskful and expensive. Satellite DCS looks to be a very good solution. For this reason, DGA is very interested to check the system for future operational employment. The DCP operated in El Yeso Dam during four months without any failure, in spite of some storms occured during this period, The parameters measured are: wind speed (2 levels), air temperature (2 levels), air humidity (2 levels), snow temperature and solar radiation. Some parameters are measured in different levels to obtain the gradient. The snow temperature sensor will be replaced (hopefuly during the first part of this year) by a snow-water equivalent sensor (snow pillow). This DCP was moved (December 1977) to Echaurren Glacier and it has also been operating without problems. LANDSAT relays data every 12 hours and the recorded information in DCP memory allows to have lectures of sensors every 3 hrs. The DCP can be modified to send messages every 30 second and to receive more data (one lecture every 1 hours, for instance).

b) Empresa Nacional de Electricidad S.A., ENDESA (site 3). The original selected site was in Del Maule Lagoon (site 3 b), for an experience similar to DGA (snowmelt forecast). However, due to the difficult environmental conditions during ending August 1977, it was impossible to reach to this site (Los Andes Ranges, about 400 km South-East from Santiago). Then, the DCP was installed in Rapel Dam, a very important hydroelectric dam wich gives electricity to Santiago zone mainly. The parameters measured are: river stage or level, water temperature, air temperature, air humidity, wind speed, solar radiation. This DCP has been operating since begining september 1977 until now (march 1978) without problems. ENDESA, also needs to make snowmelt forecast ant to obtain real-time data about river stage for the adequate operation of their hydroelectric dams. If this experience is succesful, Satellite DCS could be operationally employed. Besides the more continous and near real time data given by Satellite DCS, sometimes it is much cheaper than conventional means. For instance, a visit to a remote site (by helycopter) costs about U.S. $ 1.500 and if it is considered 6 winter months, in one year the DCP and sensors cost could be payed.

c) Instituto Hidrográfico de la Armada, IHA (site 2). There was not problems to install DCP at Valparaíso during middle August 1977. The DCP and sensors were disposed at the Navy Mole. The parameters measured are: sea level, water temperature, atmospheric pressure, wind speed, air temperature. This installation has operated well until now (March 1978). Only some installation problems with the sensors occured but they were rapidly solved. This is a pilot experience because the idea is to deploy DCPs along Chilean coast and above all in southern straits, to improve navigation.

d) Instituto Antártico Chileno, INACH (sites 4,5 and 6). Three (3) Data Collection Platforms were installed in Chilean Antartic lands during February 1978. Maybe this is the most spectacular experience due to the rough environmental conditions and the very remote installation sites. This experience was financed by INACH and the author and an electronic specialist of NASA División (Mr. Luis Pérez) participated in the installation. The DCPs and sensors were disposed on metalic structures, specially designed (author) and built at the Faculty repair shop. These elements were carried such as single pieces and put together in the site with metalic pins (such as meccano), to form a tower of 1,5 x 1,5 meters basis and 4 meters altitude. One metalic mast was employed to dispose antena and solar pannels and another mast, to dispose sensors (see figure). The DCP, battery and sensor interface were protected into a waterproof (and thermic aislant) metalic box. This experience demonstrates the flexibility of Satellite DCS to arrive to remote sites. It was necessary to travel on airplane from Santiago to Punta Arenas. From that city, a Chilean Navy ship did the trip to Chilean Antartic (more than two days).

In Presidente Frei Basis, the Meteorologic Center of Chilean Air Force, two (2) DCPs were installed in one metalic tower. The parameters measured are: wind speed, wind direction, solar radiation, air temperature, air humidity and snow temperature. At present, both DCPs are working with LANDSAT DCS. To recei

ve more data, the DCPs send a message every 30 seconds and so it is possible to receive, every 12 hours, 12 DCP messages (one lecture every 1 hour). Howewer, the power consumption is increased and solar pannels are not enough. So, a battery charger (connected to the basis) must be used. In the next future (April or May 1978), one DCP will work in the GOES mode. A trained scientific in the basis will do the necessary changes. These DCPs have operated well until now. A power problem occured but it was solved with the battery charger.

In General Bernardo O'Higgins Basis (Chilean Army), one DCP was installed in another metalic tower. The parameters measured are: wind speed, wind direction, air temperature, air humidity, snow temperature, solar radiation and atmospheric pressure. This DCP works with LANDSAT/DCS and every 12 hours, it is received information corresponding to one lecture every 1 hour (transmissions every 30 seconds). There is capability to recharge battery if solar pannels are not enough. This DCP has operated without problems at the date.

Next year these DCPs will be moved to some remote sites, far from Chilean Basis. During this year, experience will be taken to planify the necessary precautions to assure the correct performance of future DCP installation. A combination of solar pannels and wind charger should be employed to keep energy of batteries. Satellite images will be employed to accomplish DCS data (GOES, NOAA, Nimbus, LANDSAT images). The Remote Sensing Program of INACH, developed in cooperation with Geodetic Department will be increased during next years. This only was the begining.

4. CONCLUSIONS.

Satellite DCS is a practic, economic, reliable system for the automatic collection of environmental ground truth data from remote sites. The experiences developed in Chile are very promising and Satellite DCS looks to be a good solution to solve some important chilean problems. The Geodetic Department, following the Faculty politic, is working to check different remote sensing systems and techniques before their operational employment in Chile. This is the best way to obtain the maximun benefits of this valuable technology. Sometimes, a sofisticated and advanced system can result more convenient than conventional means. Satellite DCS looks to be this case, for several applications in Chile.

5. BIBLIOGRAPHY.

- "Use of Earth Satellites for Automation of Hydrologic Data Collection". Richard W. Paulson, U.S.G.S., Reston, Virginia. Seminar on Organization and Operation of Water Resources Services. Ottawa, Canada. July 15-16, 1976.
- "Data Retransmission from Water Survey of Canada Gauging Stations Using The ERTS DCS". Robert A. Halliday, Department of Environment, Ottawa, Canadá. NASA SP-364, Workshop at Wallops Flight Center, Wallops Island, May 30-21, 1973.
- "Hydrologic Applications of ERTS-1 DCS in Central Arizona" Herbert H. Schumann, U.S.G.S., Phoenix, Arizona. 1974.
- "Development and Evaluation of a Prototype Global Volcano Surveillance System Utilizing ERTS-1 DCS". Peter L. Ward, Elliot T. Endo, David H. Harlow, Rex Allen, Dan Marquez and Jerry P. Eaton. U.S.G.S., Menlo Park, California. February 1974.
- "El Sistema de Colección de Datos del Satélite ERTS. Aplicaciones en Hidrología". Mauricio Araya F. Geodetic Department (SERREN), University of Chile. 250 pages, April 1975.
- "Aplicaciones de Técnicas de Percepción Remota en Recursos de Agua". Mauricio Araya F. Thesis work, Faculty of Physics and Mathematics Sciences. 540 pags. December, 1975.
- "Percepción Remota en Recursos de Agua. Situación Chilena". Mauricio Araya F., 90 pages. Presented at the Technical and Scientific Reunnions on Water Resources, U.N. World Water Conference. Mar del Plata, Argentina, March 14-25,1977.
- "Empleo de Sistemas de Colección de Datos por Satélites en Chile". Mauricio Araya F., 90 pages. First Argentinian Seminar on Satellite DCS, organized by Argentinian Spatial Comission, Nobember 15-17, 1977.

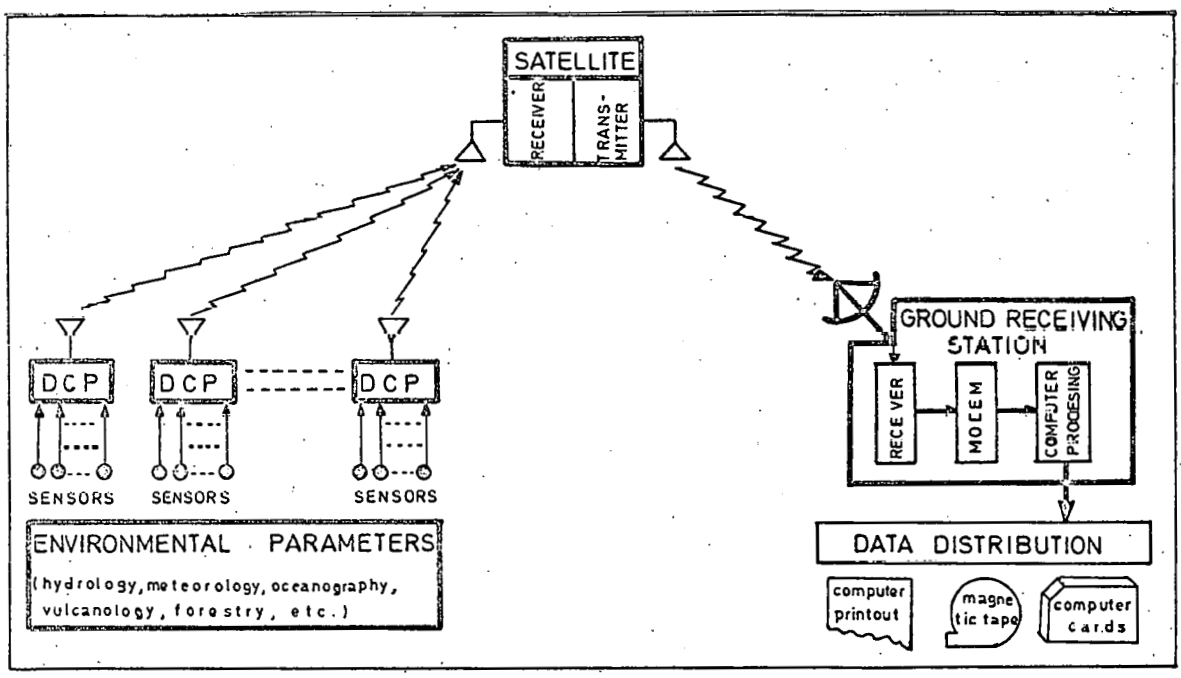

Figure 1. GENERAL SCHEME OF SATELLITE DCS.

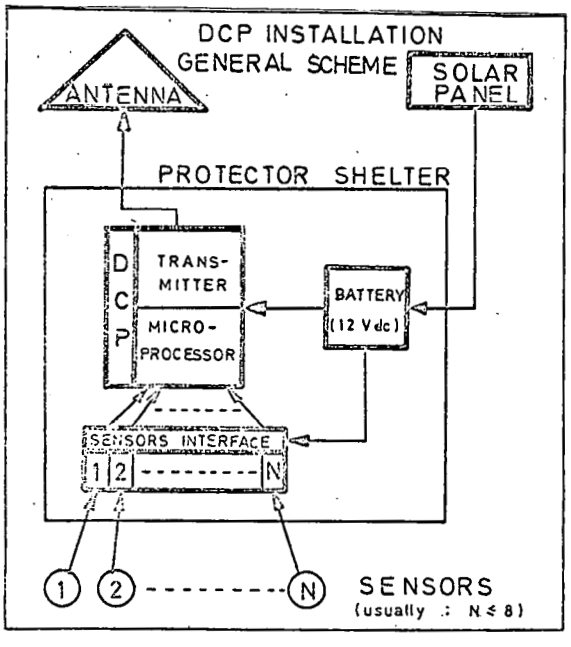

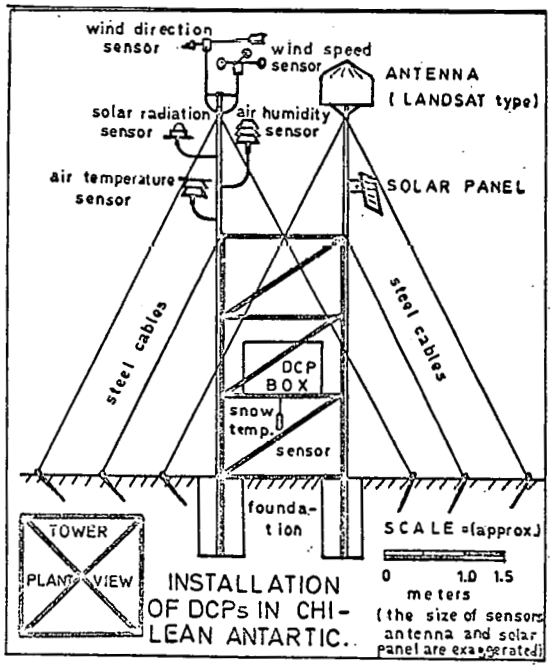

Figure 2. DCP INSTALLATION SCHEME.

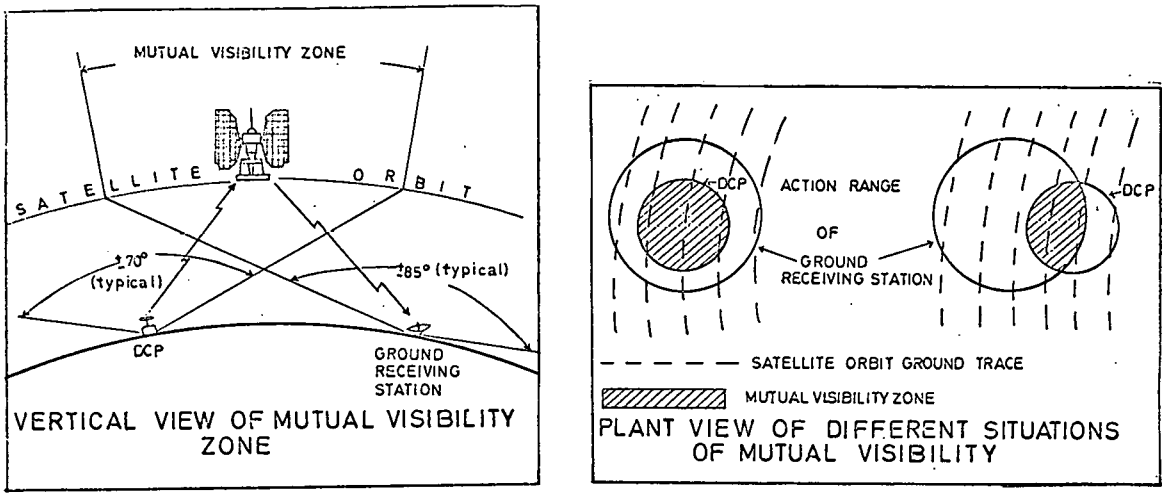

Figure 3. SCHEME OF LANDSAT/DCS.

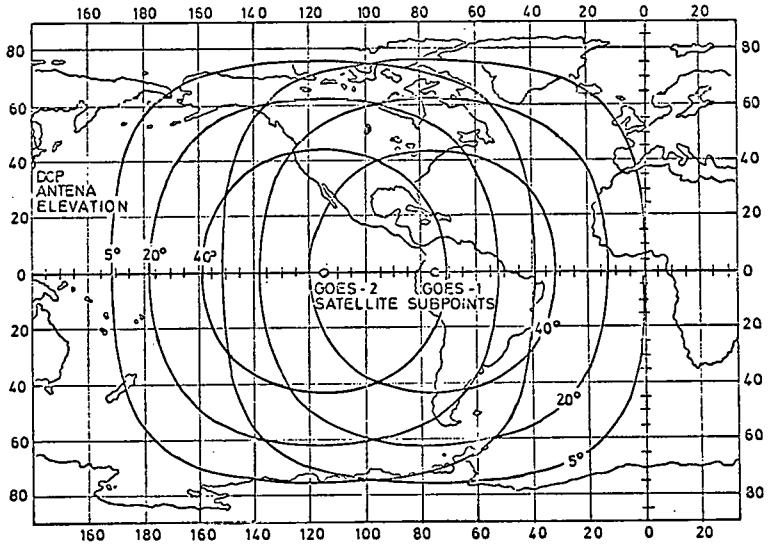

Figure 4. SCHEME OF GOES/DCS.

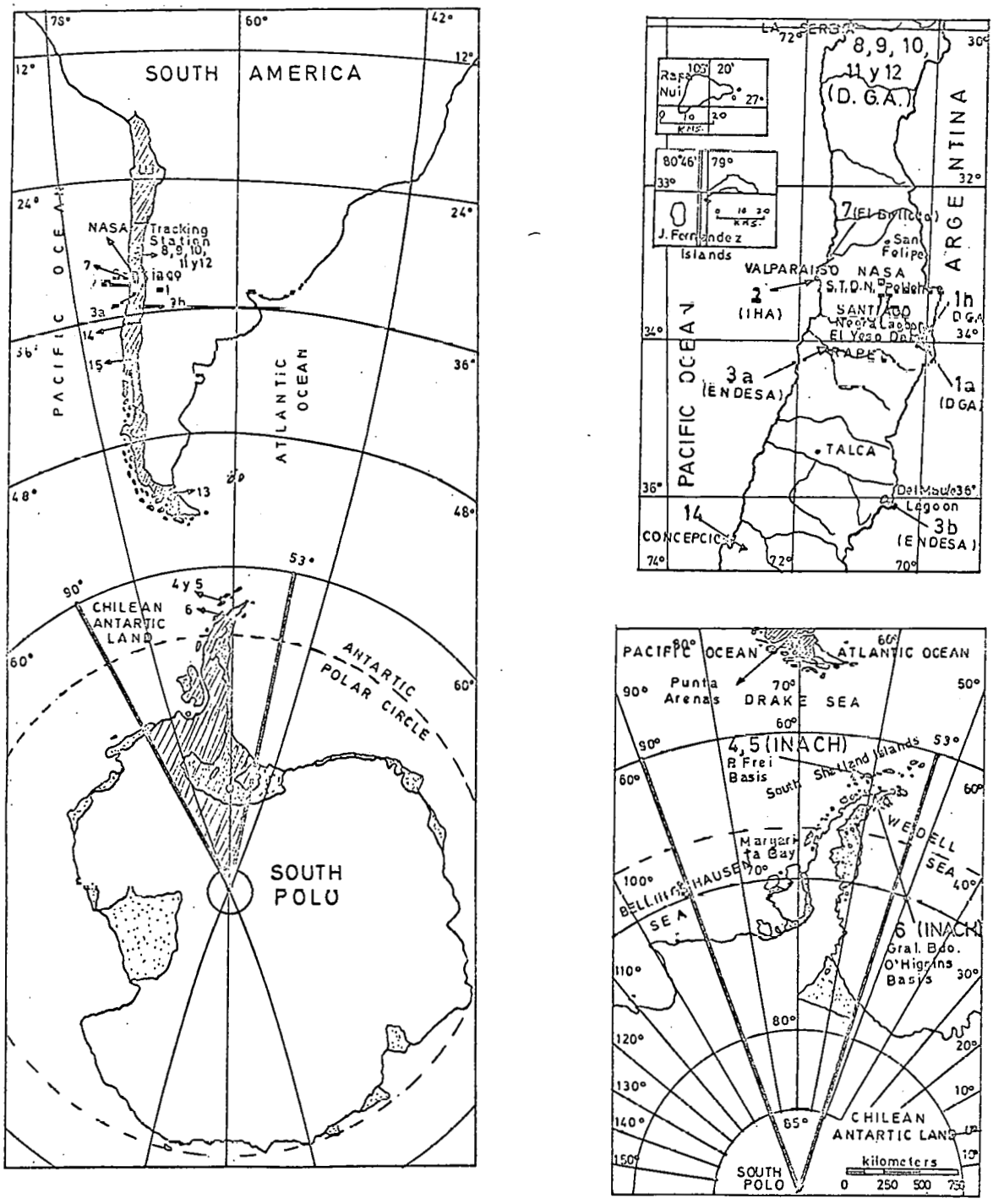

Figure 5. LOCATION OF EXISTING AND PLANNED DCPs IN CHILE.

DESIGN OF DECISION-TREE CLASSIFIER FOR REMOTE SENSING APPLICATIONS

Z. Chen and L. Y. Tseng

Institute of Computer Science
National Chiao Tung University
Hsinchu, Taiwan

ABSTRACT

In remote sensing data processing the classification rules for identifying land cover types are mainly evaluated by two performance factors: the amount of computation time used and the correct recognition rate achieved. A decision-tree classifier is considered in the present paper. The decision tree is formally shown to be embedded in an AND/OR tree that represents all possible classification outcomes. These outcomes are obtained with respect to all feature sets generated by a moderate number of pattern features. A search process in terms of forward and backward procedures is developed to generate the tree. A cost function based on the two performance factors is used to order nodes for expansion. Various types of pointers and tables are set up to link and to store all relevant tree structure data. An alpha-beta procedure is stated to make the search more efficient. Experimental results are included and discussed.

1. INTRODUCTION

In dealing with the cover type classification of the multispectral remote sensing data, the tremendous data volume reflects the importance of the computational efficiency of a classifier in addition to the accuracy requirement. The commonly used single-stage maximum likelihood classifier is found to have defects due to the fact that it ultilizes only one feature set to characterize all cover types (i.e., pattern classes) and that an unknown sample has to be tested against all cover types [1],[2].

A multi-stage classifier can be used instead to reduce significantly the number of tests, while still fulfilling a comfortable accuracy requirement. A decision tree classifier falls under this category.

In a decision tree classifier design nodes correspond to class sets. Each node is expanded with respect to certain feature sets. The descendants of a node are the class subsets which constitute a partition of the class set of the parent node. There are two problems encountered for designing a decision tree classifier. One is the determination of the family of feature sets which will be used in the design process, the other is the determination of the mathematical model of the classifier. Since the number of the possible feature sets in an m-feature classification is 2^m-1 this number is relatively large for a moderate value of m. If each feature set is used to expand a node, the total number of resulting trees is very large. It seems reasonable to reduce the number of trees to some extent. Therefore, often only a portion of these feature sets is used by selecting either those feature sets whose size is equal to a prespecified number [2] or those feature sets deliberately chosen by the user or by some techniques [3],[4]. Meanwhile, the tree is pruned to retain only one "promising" descendant node (in some sense) and discard all of the other descendant nodes for the sake of memory saving. Under the circumstance the optimality of the

classifier design may be harmed. Actually the situation is not always so bad as it might appear. The empirical result reveals that the intrinsic data cohesion leads to only a comfortable number of class groups in the possible feature spaces, if the number of features is moderate, say, 10 or less. Furthermore, as the tree grows, fewer and fewer classes will be grouped in a node. It in turn implies the number of descendants will cease to grow. Therefore, by a careful memory allocation scheme, the entire family of feature sets can be used in the tree generation and the entire tree will be examined.

The mathematical model of the classifier is used to partition a parent node (i.e., a class set) into a number of successor nodes (i.e., class subsets). The complexity of the model has a great influence on the computational efficiency of the classification strategy. Since a multi-stage classification strategy is used here, different feature sets which reveal the well separated class subsets contained in the parent node are chosen for the classification. Hence the structure complexity of the decision boundary surfaces can be relaxed without deteriorating the accuracy of the classifier much, while achieving a simplicity in computation. The hyperplane decision boundary is used for this purpose.

In the present paper the multi-feature, multi-class classification is characterized by an AND/OR tree. For each node expansion a cost will be specified to measure the position value of the node which is defined in terms of the computational time taken to expand the node and the error probability committed by the node expansion. An optimal solution tree is a subtree of the AND/OR tree which has the minimum sum of these costs. A search procedure will be developed with the aid of various types of pointer and tables. This procedure will search the entire AND/OR tree and allows the use of all possible feature sets for the tree generation.

2. DECISION TREE MODEL

A classification decision tree represents an iterative process for partitioning a class set containing all pattern classes into final class subsets each of which contains exactly one class. Obviously this classification tree is only one of the similar trees which illustrate alternative ways of partitioning the set of all classes under consideration. Therefore, the decision tree is embedded in a large tree which will be shown to be an AND/OR tree. Before presenting the AND/OR tree, a presumption is made here that in the classification strategy proposed each node will be expanded into two successor nodes using a discriminant hyperplane in the observation space specified by the feature set chosen. The hyperplane will be given later in the section.

2.1 USE OF AN AND/OR TREE

In the following an m-feature, n-class classification will be described by an AND/OR tree. To begin with, the set of all n classes is taken to be the root node of the tree. The root node is expanded into the derivable successor nodes with respect to all possible feature sets. Each node contains a pair of class subsets representing a dichotomy of the parent node based on a grouping algorithm to be given later. Let the parent class set be denoted by $CS=(C_1,C_2,\ldots,C_n)$ and the pair of class subsets by $CP=\{(C_{i_1},C_{i_2},\ldots,C_{i_s}),(C_{j_1},C_{j_2},\ldots,C_{j_t})\}$, where $n=s+t$. Then the pair of class subsets is called a class pair CP, derivable from the parent class set CS, and the pair of class sizes (s,t) is called a partition pair, PP, of the parent class set. The two partition pairs (s,t) and (t,s) are said to be equivalent. For a parent node of an arbitrary size k, there are k/2 partition pairs, if k is even, and (k-1)/2 partition pairs, if k is odd. On the other hand, for a given partition pair (s,t) with s+t=k, there are at most ℓ possible class pairs derivable from the parent node, where $\ell=\binom{k}{s}$ if $s\neq k/2$, and $\ell=\binom{k}{s}/2$ if $s=k/2$. Totally there are at most $2^{(k-1)}-1$ distinct class pairs for a parent class set of size k. Meanwhile, the total number of distinct class pairs must not exceed 2^m-1, as there are only 2^m-1 different feature sets which can be used for the node expansion. From the above discussion it can be seen that the upper bound of the number of possible class pairs derivable from the parent node of size k is equal to the minimum of $2^{(k-1)}-1$ and 2^m-1. When $k \geq m+1$, the upper

bound is 2^m-1; when the class size k is smaller, the upper bound becomes $2^{(k-1)}-1$. Notice that, when the upper bound is larger at the beginning of the tree generation, due to the fact that the intrinsic cohesion between the classes exists in the various feature spaces, quite often only a comfortable portion of the possible class pairs is derivable from a parent node.

Now let us go back to the node expansion process, the root node has been shown to have a number of descendants. Any one of these descendants can be used as an alternative way of partitioning the parent node. For this reason, they are called OR nodes. Any OR node consists of a pair of class subsets, so it will be expanded into exactly two nodes. These two class subsets have to be classified both, if the parent OR node is to be classified. For this reason, these two descendants are called AND nodes. Up to this stage, a cycle of node expansion is completed which results in a set of OR successor nodes from the root node, and each OR node having two AND successor nodes. In case that the two class subsets thus obtained contain more than one node. The same cycle of expansion can be repeated to expand them into a number of smaller class pairs. The process continues until the n classes are finally partitioned into n terminal nodes each of which contains exactly one class. The classification problem is thus completely represented by an AND/OR tree, as shown in Fig. 1. Every subtree rooted at the start node whose terminal nodes are exactly the n classes is a potential decision tree. Figure 3 illustrates the tree diagram of such a tree.

2.2 GROUPING ALGORITHM

In the AND/OR tree each node corresponding to a class set is shown to be partitioned into a pair of class subsets. A certain grouping algorithm is tacitly employed in the partition process. Before we proceed to propose such an algorithm, we shall temporarily depart the subject to look at the probabilistic distributions of the pattern classes under consideration. A priori knowledge of underlying distributions of the classes is valuable to the design of a good classifier. It is well documented [5]-[6] that the agricultural remote sensing data can be characterized by multivariate normal distributions. This assumption will be kept in this paper.

In the grouping process a feature set is specified first upon which the grouping operation is based. For each of the classes to be grouped, the mean vector Mi and the covariance matrix Σ_i are computed. To measure the separability between two classes, the divergence and the Bhattacharya distance are often used [7]. The Bhattacharya distance, abbreviated as B-distance, will be used here which, in the normal distribution case, is given by

$$B = \frac{1}{8}(M_2-M_1)^T\{(\Sigma_1+\Sigma_2)/2\}^{-1}(M_2-M_1)+\frac{1}{2}\ln\{|(\Sigma_1+\Sigma_2)/2|/|\Sigma_1|^{\frac{1}{2}}|\Sigma_2|^{\frac{1}{2}}\}$$

The large value of B-distance indicates that the two classes are well separated. In the following a grouping algorithm is given.

Step 1. Calculate the B-distance between every pair of classes in the class set under consideration $(C_1,C_2,\ldots,C_s)$ with respect to a given feature set.

Step 2. Choose the two classes with the largest value of B-distance as the initial members of two groups A and B.

Step 3. Pick up one class which is not yet grouped from the list of classes. Calculate the average B-distance between the current class and members of group A. Similarly, calculate the average B-distance between the current class and members of group B.

Step 4. If the ratio of the two average B-distances exceeds a prespecified threshold value, merge the current class to the group with the smaller average distance. Otherwise, postpone the grouping of the current class. Mark the class as one not yet grouped and skip it.

Step 5. Check to see if there is any class that has not been attempted for grouping. If yes, go back to Step 3. If an interation is completed and each

class has been grouped, terminate the process. Otherwise, continue.

Step 6. For those classes that has been postponed for grouping. Recycle Step 3 to Step 5 and check to see if there is any new resultant grouping. If so, recycle again for the left-over. If a recycle ends up with no new possible grouping. It implies that the ratio of the two average distances does not exceed the threshold, go to the next step.

Step 7. Pick up the first one of the remaining classes and merge it to the group having the smaller population size, so the resultant grouping is more balanced. If there are still classes remaining, go back to Step 3 for further grouping. If no class remains, terminate the process.

2.3 A PARTITIONING HYPERPLANE WITH MINIMUM ERROR

After the class pair is determined for a parent node, a partitioning hyperplane will be placed in between the two class subsets derived by the grouping algorithm. The formula for discribing such a hyperplane with minimum error developed in [2] will be used in this case. The formula is briefly restated below. Let the hyperplane equation in the given feature space be given by $A^TF + d = 0$ where F is a feature vector, A^T is the tranpose of a coefficient row vector, and d is a constant. The average error probability for expanding the OR node v is given by

$$E_F(v) = \sum_i Pr(C_i)\varepsilon_F(C_i)$$

where the summation is taken over all classes in the class set at node v, $Pr(C_i)$ is the prior probability of class C_i, and $\varepsilon_F(C_i)$ is the conditional error probability of class C_i that is given by

$$\varepsilon_F(C_i) = \frac{1}{2} \pm \frac{1}{2}erf(x/\sqrt{2})$$

Here $erf(x/\sqrt{2})$ stands for the error function with $erf(x/\sqrt{2}) = \int_{-x}^{x} 1/\sqrt{2\pi}EXP(-y^2/2)dy$. And $x=(A^TM_i+d)/(A^T\Sigma_i A)^{\frac{1}{2}}$ with M_i and Σ_i being the mean vector and the covariance matrix of class C_i. A first-order gradient method can be employed to find a partitioning hyperplane $A^TF+d=0$ with the minimum error value of $E_F(v)$.

3. SEARCH PROCESS FOR THE AND/OR TREE

Previously it was stated that a decision-tree classifier is a subtree of an AND/OR tree. A systematic way of searching for one of such subtrees as the desired decision tree must be developed. In this connection an cost function will be specified to direct the search for an optimal decision tree. It is not necessary to generate the entire tree before the determination of a decision tree is initiated. Instead, only needed nodes will be selected by a combination of forward and backward procedures for expansion. Four types of tables are set up for effective tree searches. An alpha-bata procedure is applied to cut off fruitless node expansions to aid the search process.

3.1 COST FUNCTION

In remote sensing problems the performance of a classifier is mainly evaluated by two factors, the amount of computation time used (i.e., efficiency) and the overall probability of misclassification committed (i.e., accuracy). A linear combination of these two factors is used to measure the goodness of the classifier.

Recall that an OR node corresponding to a class set is expanded to produce two class subsets, called AND nodes. Let an OR node be denoted as v and its two AND descendants as v_1 and v_2. Assume the selected feature set is F and the class set under consideration is CS. Then the performance measure of this node expansion with respect to F is given by

$$g_F(v) = E_F(v) + \alpha P(v) T_F(v) \quad \text{and} \quad P(v) = \sum_{C_i \varepsilon CS} Pr(C_i)$$

where $E_F(v)$ is defined as before, α is a weight constant, and $T_F(v)$ is the classification time, depending on the execution time needed to carry out the operation $A^TF+d \gtrless 0$. The partition cost of the node v is defined to be $g(v)=\min_F\{g_F(v)\}$ among all possible feature sets F's. If v is a terminal node, then $g(v)=0$, as no further partition is required. An optimal solution decision tree is defined to be the potential solution tree that has the minimum sum of all of the partition costs in the solution tree. Let h(v) be the minimal sum of cost for an optimal solution tree rooted at node v. Then (i) if v has $v_1,v_2,\ldots,v_k$ OR successor nodes, $h(v)=\min_i[g(v)+h(v_i)]$. (ii) if v has v_1,v_2 AND successor nodes, $h(v)=g(v)+\sum_{i=1}^{2} h(v_i)$.

3.2 SELECTION OF NODES FOR EXPANSION

In searching for an optimal decision tree, we shall show how to generate the nodes of the AND/OR tree and to allocate the memory storage required. This should be done in such a manner that we will keep the memory size within a manageable range. Otherwise, we shall easily run out of the available memory space.

It will be seen that the node expansion process is an iterative procedure. There are two search procedures, namely, the forward search procedure and the backward search procedure. The forward procedure will cause a nonterminal CS node to expand and the tree will increase its depth. When the tree reaches terminal nodes, the forward procedure can not be applied. Then the backward procedure will be used to look backward along a path in the tree to find the next available nonterminal CS node for the application of the forward procedure. The tree will increase its breadth in this case.

First of all, we shall show how to order the nodes for expansion in generating the tree. A nonterminal CS node is expanded with respect to the 2^m-1 possible feature sets by using the grouping algorithm. The CP successor nodes which correspond to class pairs are divided and identified by the partition pairs. The feature sets that lead to a particular CP node may consist of one feature up to m features. They are divided into m groups according to the feature size. Feature sets in each group will be compared based on the associated estimated error commitments that are given by the average of the Chernoff upper bound ε_u and a lower bound ε_ℓ, i.e., $\frac{1}{2}(\varepsilon_u+\varepsilon_\ell) \approx \frac{1}{2}(\varepsilon_u+\varepsilon_u^2)$. For detailed information of these bounds, please refer to [7]. Therefore, the possible feature sets associated with the particular CP node are reduced to at most m good feature sets denoted by $F_1,F_2,\ldots,F_m$ which are stored in the FS table, as shown in Table I. After these good feature sets are obtained, partitioning hyperplanes are derived for each of these sets and the partition cost functions g_{F_i}'s are computed. The feature set with the minimum g value is the final optimal feature set associated with the CP node. The CP nodes of the same partition pair are sorted by their minimum g values. Furthermore, partition pairs can be sorted in accordance with the minimum g value of its CP descendants.

In the forward procedure a nonterminal CS node is expanded with respect to 2^m-1 feature sets to obtain CP successor nodes, grouped by PP pairs. The CP nodes are sorted, so are PP pairs. Then the first CP node of the first PP pair will be selected for expansion. The two CS successor nodes will be obtained from the CP node. One is called the left son and the other is called the right son. Up to this moment, a stage of forward node expansion is completed. During this expansion process, various pointers are set up to represent the expanded tree structure. Tables CS, PP and CP, as shown in Table I, are used to store the pointers, together with the class information of nodes and cost values associated with the node expansions.

The next stage of forward node expansion will start at the left CS node produced at the end of the last stage. In case it is not a terminal node, the forward procedure will be repeated. This procedure continues until the CS nodes are terminal nodes. Then, no further forward expansion is possible, the backward procedure has to be called for to find a nonterminal CS node available.

The backward procedure is more complicated which will be given as an algorithm stated below.

Step 1. Check the CS node to see whether it is the root node. If yes, the tree search has been completed and stop. If no, proceed to step 2.

Step 2. Check the CS node to see whether it is a left son or a right son of its parent CP. If it is a left son, proceed to step 3. If it is a right son, go to step 4.

Step 3. Look up the CP table of its parent CP and get the right CS son of this CP node. If this CS node is a terminal node, go back to step 1. Otherwise, this CS node will be the starting CS node for the next expansion and stop.

Step 4. The optimal subtree rooted at this parent CP must have been completed. Look up this CP table to see whether there exists a CP brother. If there exists one, proceed to step 5. Otherwise, go to step 6.

Step 5. Get the CP brother and the left CS son of this brother CP will be the starting CS node for the next expansion and stop.

Step 6. Look up the present CP table to get its CS parent, go back to step 1.

During the forward procedure of expanding a CS node, only two copies of memory storage will be used to store CS, PP, CP and FS tables for generating the subtrees rooted at all CP successors. One copy will store the information of the existing optimal subtree obtained so far, and the other copy will be the working storage for generating a subtree which is still under construction. After the current subtree generation is completed, the two subtrees will be compared based on the performance evaluation. The storage for the optimal one will be retained, and the other copy will be released to be used as the working storage of the next possible subtree generation.

By the preceding search process the total AND/OR tree will be fully examined and the truly optimal decision tree will be obtained.

3.3 ALPHA-BETA CUTOFF

In generating nodes by the forward and backward procedure, some fruitless nodes can be cut off by the application of a so-called alpha-beta procedure [8]. An example shown in Firuge 2 is used to illustrate this point. Two terminal nodes a and b will be generated by the forward procedure, the cost at node c is given by $h(c)=g(c)$. At this point node d is also given the backed-up value $h(c)$. Similarly the node e is expanded to obtain the cost $h(e)$. Therefore, the cost $h(u)$ is given by $h(u)=g(u)+h(d)+h(e)$. The backed-up value at node w is an estimated cost of $h(w)$ so $\hat{h}(w)=h(u)$. The search procedure will select the next OR node v for expansion. If $g(v) > \hat{h}(w)$, there is no need to expand OR node v further, so node v is cut off, called an alpha cutoff. On the other hand, if $g(v) < \hat{h}(w)$, the node v is expanded into two AND successors x and y. If $g(x)+g(v) \geq \hat{h}(w)$, there is no need to expand AND node x further, so node x is cut off, called a beta cutoff. Meanwhile if node x is a left AND node, the right AND node y is also beta cut off.

By the application of the alpha-beta procedure the search process may terminate sooner. If the OR nodes and AND nodes happen to be arranged in the ascending order of the cost values, the number of cutoffs will be maximized.

4. EXPERIMENTAL RESULT

The method of the decision-tree classifier design developed above is applied to a twelve-band remotely sensed agricultural data collected by the LARS of Purdue University on a DEC-10 computer. The features chosen correspond to bands 1, 3, 5, 7, 9, 10, 11, 12. 7426 training samples are selected randomly from six classes which is given in Table II. These samples are used to estimate the prior probabilities, mean vectors, and covariance matrices of the classes. The weight coefficient α used in the cost function is set to range from small to large.

Optimal decision trees and their associated feature sets are obtained by making use of the search method with an alpha-beta procedure, Figure 3 illustrates the results of the tree design. On the other hand, 4404 testing samples different from the training samples are selected from the six classes of which prior class probabilities are nearly the same as those of training samples. The recognition rate of the single-stage maximum likelihood classifier is found to be 85.18%. The error is mainly attributed to the overlapping between classes 5 and 6, i.e., non-farm and woods. The classification results of decision-tree classifiers are listed in Table III.

From the preliminary experience of computer simulation, we find that the alpha-beta procedure does speed up the search process significantly. Furthermore, the tree design time can be cut down by discarding those CP nodes corresponding to two class sets whose sizes are widely different. In other words, we throw away the badly unbalanced decision trees. On the other hand, the classification time of the decision-tree classifier is faster than that of a single-stage maximum likelihood classifier, while the recognition rates are close.

5. CONCLUDING REMARKS

It has been shown that a decision-tree classifier can be formulated as a problem of finding an optimal solution tree of an AND/OR tree. Through this framework, the classifier design is more meaningful, as far as the performance is concerned. The decision-tree classifiers finds its application in the remote sensing data processing. Future research work is possible in the area of different partitioning procedures of expanding nodes and different selections of cost function to speed up the decision-tree classifier design.

REFERENCES

[1] H. Hauska and P. H. Swain, "The decision tree classifier: design and potential," Proceedings of Second Symposium on Machine Processing of Remotely Sensed Data, pp. 1A 38-48, 1975.

[2] K. C. You and K. S. Fu, "An approach to the design of a linear binary tree classifier," Proceedings of Third Symposium on Machine Processing of Remotely Sensed Data, pp. A3 1-10, 1976.

[3] A. N. Mucciardi and E. E. Gose, "A comparision of seven techniques for choosing subsets of pattern recognition properties," IEEE Trans. Computers, vol. C-20, pp. 1023-1031, 1971.

[4] B. Chandrasekaran and A. K. Jain, "Independence, measurement complexity, and classification performance," IEEE Trans. Syst., Man., Cybern., vol. SMC-5, pp. 240-244, 1975.

[5] K. S. Fu, D. A. Landgrebe and T. L. Philips, "Information processing of remotely sensed agricultural data," Proc. IEEE, vol. 57, pp. 639-653, 1969.

[6] K. S. Fu, "Pattern recognition in remote sensing of the earth's resources," IEEE Trans. Geoscience Electronics, vol. GE-14, pp. 10-18, 1976.

[7] K. Fukunaga, Introduction to Statistical Pattern Recognition, Academic Press, New York, 1972.

[8] N. J. Nilsson, Problem-Solving Methods in Artificial Intelligence, McGraw-Hill, New York, 1971.

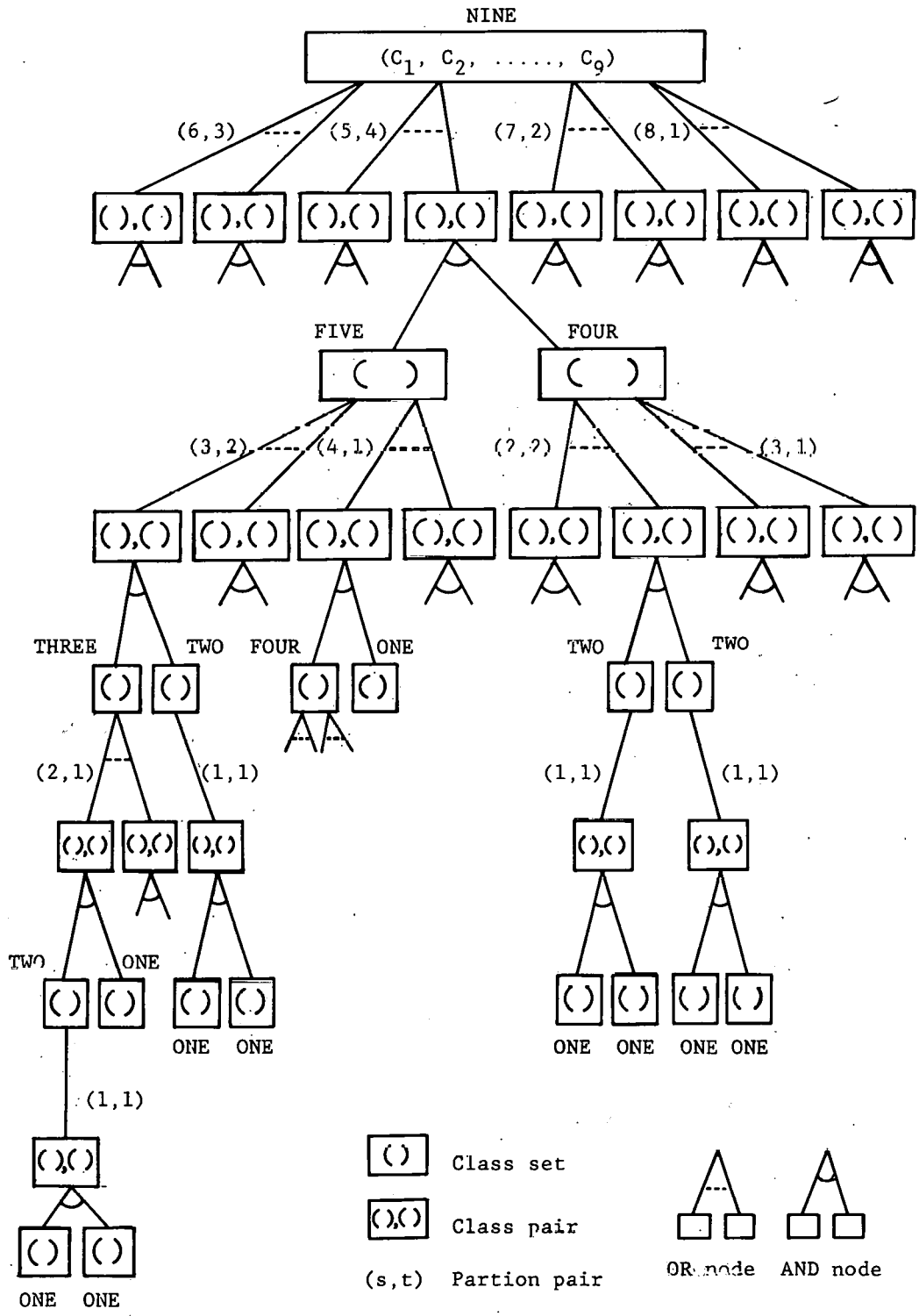

Figure 1. An AND/OR tree diagram (for n=9)

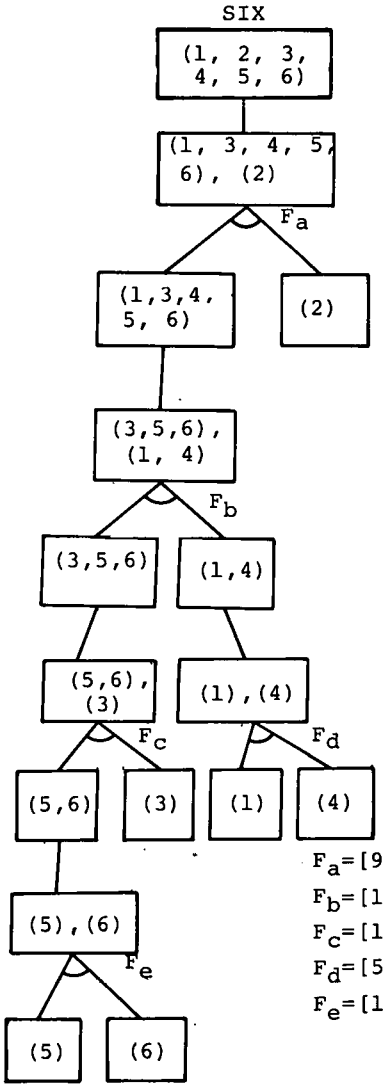

(a)

F_a=[9,11,12]
F_b=[1,3,5,9,10,12]
F_c=[1,3,5,7,9,10,11,12]
F_d=[5,7,12]
F_e=[11]

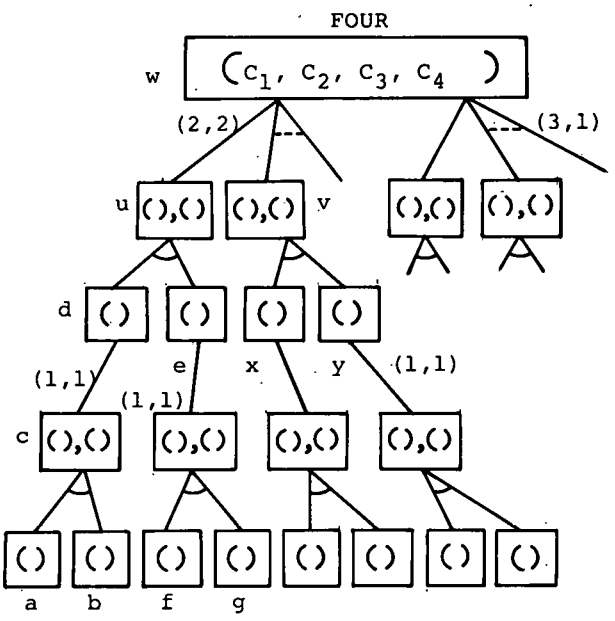

Figure 2. An example of alpha-beta cutoff.

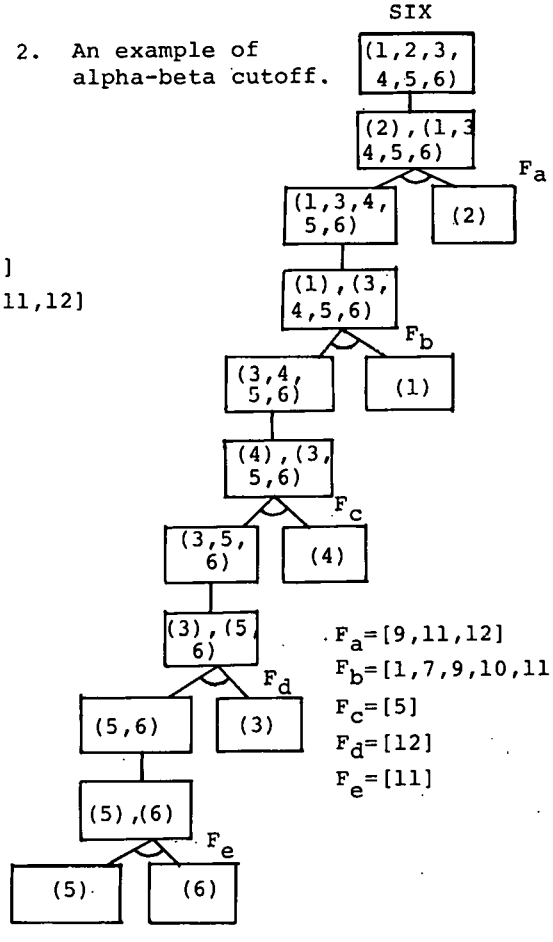

(b)

F_a=[9,11,12]
F_b=[1,7,9,10,11,12]
F_c=[5]
F_d=[12]
F_e=[11]

Figure 3. The optimal decision tree classifiers for n=6, (a) α=3, (b) α=15,30

Table I. Four types of tables.

CS

1	2	3 - 11	12	13	14
No. of classes	L = 1 OR R = 0	Classes	PTR TO FIRST PP	PTR TO PARENT CP	Cost

PP

1	2	3	4	5	6
No. of classes in group 1	No. of classes in group 2	PTR TO FIRST CP	PTR TO NEXT PP	PTR TO PARENT CS	Cost

CP

1	2	3	4	5	6	7	8	9	10
Classes in group 1	Classes in group 2	Best Feature Subset	PTR TO Feature Subset Table	PTR TO Next CP	PTR TO LEFT CS	PTR TO RIGHT CS	PTR TO PARENT PP	Partition cost	Cost

FS

0	1	2	3 - 7	8	9
Size of the Last Feature Subset	F1	F2	.....	F8	Best Estimated Error

Table II. Class types and the prior probabilities.

Class No.	1	2	3	4	5	6
Class Type	Corn	Soybean	Hay	Oat	Non-Farm	Woods
Probability of class	0.32	0.24	0.10	0.03	0.12	0.19

Table III. Classification results.

Classifier	Accuracy (%)	Classification Time per Sample (Sec.)	Weight Coeff. α
Maximum Likelihood	85.18	3.94×10^{-2}	—
Decision Tree (a)	81.56	1.68×10^{-3}	3
Decision Tree (b)	81.11	1.65×10^{-3}	15
Decision Tree (c)	81.11	1.65×10^{-3}	30*

* Decision tree (b) = Decision tree (c).

LAND USE MAP COMPILATION SYSTEM FROM AERIAL MSS DATA

Sotaro Tanaka

Remote Sensing Technology Center of Japan
Uni-Roppongi Building
7-15-17, Roppongi, Minatoku, Tokyo 106 Japan

ABSTRACT

A method of practical land use map compilation system from aerial MSS data is described in this paper. As compared with satellite data, aerial MSS data has greater distortion geometrically and radiometrically, and is more complicated. It is not easy to eliminate completely these two distortions. But by extracting the main factors which cause great distortion and correcting these, it is possible to change original imagery into near ideal imagery status. This paper deals with the factor which causes great distortion and one of the method of correcting it. (Multispectral Scanning)

To discriminate the state of land use from (MSS) data, "Maximun likelihood method" is considered to be one of the most proper one. According to experience, the instrument of a maximun likelihood method named MCP developed by Bendix Co., Ltd. is considered to be sufficient.

A knowledge of the correction method applicable to only one scene is not enough for compilation of land use map in practice. A method of mosaic of aerial MSS data is necessary to be devised. Extending the method of aerial photo mosaic, a method of the aerial MSS data mosaic is set up.

The combination of three techniques (1. Maximun likelihood method, 2. Correction of MSS data distortion, 3. Method of MSS data mosaic) can lead a practical LAND USE COMPILATION SYSTEM FROM AERIAL MSS DATA.

As a result of the system, a land use map of western Tokyo area mosaiced of 80 TV imagery photographs is shown here.

1. PRE-PROCESSING OF AERIAL MSS DATA

The pre-processing of aerial MSS data is devided into two parts. One is the process of eliminating the geometrical distortion and another is the process of eliminating the radiometric distortion.

1.1 GEOMETRIC CORRECTION OF RAW MSS DATA

In general, imagery of aircraft scanner data has much distortion. This is because aircraft flies in the airmass moving comlicately. The movement of aircraft which causes imagery distortion is three dimensional against the surface of the earth, including the change of ground speed, the change of flying height, drifting away from the flight course and swaying of the aircraft itself (pitching, rolling and yawing). Among these, specially the change of ground speed and rolling of the aircraft bring big distortion to the imagery. In usual, scanner have the compensation system to eliminate these two effects. The compensation for the change of ground speed of aircraft is practiced by adjusting the revolutional frequency of the scanner in the ratio of ground speed per flying height. On the other hand, the compensation for the rolling of aircraft is done electrically by using the principle that the rotating gylo inside the scanner continue to keep the initial direction.

However, as far as the MSS data which the author has dealt with so far, the correction

of rolling was sufficient, on the other hand, the correction against flying speed was not, i.e., most data were rather overscanned. Therefore, the correction of overscanning is mentioned as first step as following.

1.1.1 CORRECTION OF OVER SCAN

Over scanned data means the scanner data having excess lines against the flight length. The correction of this can be done by resampling scan line from original data at proper intervals. The interval of resampling is decided by comparing the raw MSS data with the corresponding topographical map.

Along flight direction, select point A, B, which are founded out clearly either on the MSS data and on the topographical map as shown in Figure 1. If point A on the original MSS data of HDDT is numbered m_1, point B is m_2 as well, $m = m_2 - m_1$ means the number of over scanned lines included in the space from A to B. Next, measure the distance between A and B on the topographical map, and let the length suppose ℓ^m. And also supposing the flight altitude H^m and instantanious field of view (IFOV) θ radian, the regular width of one line becomes $d = \theta H$. The number of scan line which should be contained normally between A and B becomes $n = \ell/d$.

In case of this data, the ratio of over scan is m/n. Since, after the process of extracting n lines among the m lines is executed, it is said that the correction of over scan has been finished.

1.1.2 TANGENT CORRECTION

Tangent distortion is one of the geometric distortion of imagery occured in lateral direction. This is not due to the movement of aircraft, but due to the scanner's characteristics of equ-angle scanning against the flat surface of the earth. When imagery containing this distortion, the projected image of the earth looks like a spherical surface. If the surface of the earth is flat enough, tangent correction makes almost orthogonal projective image. The general formula of tangent correction can be lead as shown in Figure 2.

The aircraft tangent correction is the special case of it. It is possible because the altitude of aircraft is low enough compared with the radius of the earth.

1.2 RADIOMETRIC CORRECTION OF RAW MSS DATA

Looking downward from airplane, when the atmosphere contain haze or fog, the clearness of the earth surface is different at the point of just underneath from at the point of oblique direction. This is caused by the reason why haze or fog drifting in the air diffuses the sunlight.

MSS data of the earth surface, in actual, contains both reflected light from the earth surface and diffused light on the way of lightpass. In order to extract the pure information of spectral energy, it is necessary to subtract the diffused light from the total energy reached the scanner.

1.2.1 PARABOLA CORRECTION

Under two assumptions, an actual process for radiometric correction is devised and applied. The process is called parabola correction simply.

Assumption for Parabola Correction:

1. In sufficient long distance taken along flying course, the average distribution of spectral energy reaching scanner depends on mainly the pass radiance.

2. Distortion of spectral energy have parabolic form toward the direction of scanline.

The assumption above is very suitable remarkably in the case that haze or fog exists much. Figure 3 shows the scanning angle of M^2S and Figure 4 shows the mean value of spectral data of M^2S corresponding with this scanning angle. The mean value is against 2,000 lines of the MSS data which scanned at an altitude of 6,000m along Tama river from 11^h 35^m A.M. to 12^h 02^m A.M. on January 22, 1977.

The distortion is approximated considerably well by a parabolic function and its

performance amounts up to 90% in every channel.

1.2.2 CORRECTION ALONG FLIGHT DIRECTION

The radiometric distortion also exists upon the flight direction. The magnitude of it is smaller than one of lateral distortion. To perform the correction, such a method may be available that spectral data on both side of a course are measured and the amount of correction along the course is interporated by a liner function.

2. LAND USE CLASSIFICATION

2.1 CATEGORIES OF LAND USE CLASSIFICATION

Categories of land use classification might be chosen as one likes according to the purpose of its utilization. The area treated here as an exercise is the basin of Tama river, the western part of Tokyo. The purpose of land use map is to make use it for the flood management.

Earth surface have eigen-rate of run-off in accordance with the land use, so by investigating the distribution, the amount of run-off caused by a rainfall will be calculated. Categories of classification are decided, in this example, as following 10 classes.

1. City area
2. Housing lot
3. Factory
4. Golf links
5. Farming area
6. Woody park
7. Tea plant field
8. Forest (Sunny side)
9. Forest (Shade side)
10. Water

2.2 OUTLINE OF MCP

Multi categorical process is an improved model of Maximun likelihood method for multi-spectral analysis developed by Bendix Co., Ltd.. The details are described in references (1). Showing one characteristics of the MCP, it is the performance of discrimination against the number of input channel, as refered in Figure 5. This teaches that four channels spectral data are enough.

Though multi-spectral scanner M^2S collects 11 channel spectral data, the most efficient 4 channels among the 11 channels were extracted and applied, as 3, 5, 8 and 10 channel. Wavelength of each are 0.49μ-0.54μ, 0.58μ-0.62μ, 0.70μ-0.74μ and 0.87μ-1.06μ respectively. Table 1 shows a categorization performance by MCP.

2.3 RELATIVE TRAINING AREA METHOD

——— Compensation of radiometric small differences between the courses ———

In case of collecting data of large area by aircraft, difference of time makes an important problem. As change of sun elevation, reflective intensity from the surface of the earth changes graduately and also the atmosphere takes various condition.

In order to compensate these small differences, it is considered to be necessary to have the absolute spectral reflectance by using such data of sun elevation or direction of the incidence. But this method is under researching now and needs more time for the practical application.

On the contrary, the method by relative training area is practical one. In this method, the MCP coefficient is decided by chosing training area in each course, which can be considered to be the same sort. The only problem is wheather such training area could be chosen equally balanced between courses. Figure 6 shows an example of the spectral signature differences.

3. PROCESS OF MSS IMAGERY MOSAIC

3.1 GEOMETRICAL SMALL CORRECTION (Correction the effect of flying height variation)

Aircraft flies in airmass, and its altitude always changes. Also the ground elevation changes in progress of aircraft. These two facts make the variation of flying altitude against the ground surface complicately along the course. In accordance with simple geometrical

relationship existing between flying altitude and scan angle, the scale of the MSS image changes. Therefore, to coincide scanning image with the topographical map, it is necessary to correct the scale.

The data used for the correction is the variation of flying altitude only. But altitude data acquired by altimeter of aircraft is not sufficient.

After tangent correction, each image on TV monitor is oriented upon the topographical map. Then measuring swath width, the variation of flying altitude, in another word, the scale of scan line length can be calculated. Figure 7 shows a variation of swath width.

3.2 MOST PROBABLE LOCATION OF EACH SCENE UPON THE TOPOGRAPHICAL MAP

——Adjustment for whole mosaic of each image distorted by pitching yawing etc.——

Distortions of image are also caused by pitching,yawing or shift of the aircraft. It is difficult to correct these distortions by simple formula. Therefore,when there exists big distortion in the original data due to such motions,it is almost impossible to repair the image as to coincide with the topographical map.

On the other hand, when aircraft flies with little motion above, these distortions become a little, and each image on TV monitor can be set in most proper position as a whole by adjusting the position and the direction. In actual example, the process was treated as follows.

The picture of each image on TV monitor was taken by camera. Each image has 320 pixels x 240 lines and the size of one pixel has been adjusted to correspond with 15m x 15m on the ground. Hence, one scene becomes 4800m x 3600m area, i.e., 192mm x 96mm on the topographical map scaled 1/25,000. All the scenes were enlarged to this size, arranged on the topographical map and then adjusted slightly about the location and the direction.

4. EVALUATION OF THIS SYSTEM

4.1 ACCURACY OF LAND USE CLASSIFICATION

Performance table gives an evaluation on the accuracy of land use classification. Performance is indicated by the percentage categorized as itself in training area by M-DAS. An example is shown in Table 1. Most performance are higher than 90%. This is good.

It is necessary also to examine the accuracy of land use classification about every place on all cources of the area. Following remarks are known:

City area; All city area, for example, Ome, Hachioji or Chofu city are clearly classified. City area includes waterless pebbled river bed and runways of airport in addition.

Housig lot; Housing lot under construction is classified in this category. The characteristics is specified by strong reflectance, because the ground is digged up. Old housing lot is classified to city area by houses on it.

Factory; This is specified by the strongest reflectance of the big roofs. Small factories are classified to city area also.

Golf links; Golf links are covered with lawn. The cources are clearly discriminated in mountainous area. In addition, most parts of airport are classified to golf links, because the sites of airport are covered with lawn. Figure 8 shows the difference between golflinks and airport.

4.2 ORIENTATION ACCURACY UPON THE TOPOGRAPHICAL MAP SCALED 1/25,000

Geometrical accuracy is measured by the degree which indicate how accurately a scene is orientated on the topographical map. A scene takes 4800m x 3600m area as described above. The residual distortion which remains after the mosaic is about 8mm at the maximum on the 1/25,000 topographical map. This is equivalent to 200m in actual length. However, all positions on whole area are fixed within the residual distortion of this degree. Consequently, when land use map is compiled on fairly large area against the pixel size, for example, 20km x 30km area by 15m x 15m pixels, this geometrical accuracy becomes enough.

5. CONCLUSION AND PROSPECT

The essential portions on the land use map compilation system from aerial MSS data are described above by refering to an actual examination. The flow is shown in Figure 9.

The biggest problem, when compiling land use map from aerial MSS data, exists in the matter that both geometric and radiometric distortion contained in the original MSS data is very large and complexed also. To correct rigorously such aerial MSS data distortion is impossible or if possible it needs the highest labor.

Since, the focus when compiling land use map from aerial MSS data should be concentrated on both items, the accuracy and the cost. In other words, more practical and more fundamental.

The system introduced in this paper is one of the final product created on this basis.

As a prospect, such issues might be pointed out that all the distortions would be corrected automatically. Specially the method is requested which will be able to apply for automatic parabola correction, or automatic elimination of subtle radiometric differences between courses.

At the end of this report, the author exhibits the land use map and the infrared false-color photo mosaic of the south-western part of Tokyo.

6. ACKNOWLEDGEMENTS

First of all, the author is greatful to Mr.Hiroshi Kanda and Mr.Toshio Sagawa. They belong to the River Environmental Division of the Keihin Operation Office of the Construction Ministry and support this work strongly.

Next, the author thanks to assistant professor Ichikawa of Tokyo University, assistant professor Okuda of Yokohama University,assistant professor Dr. Tamai of Tokyo university and also Mr. Takase, who constitute the Committee of the Tama River Basin Survey. The author also thanks to the Social Environmental Room of the Mitsubishi Corporation, Pacific Aero Survey Co., Ltd., NAC and all , who actualized this work.

7. REFERENCES

1) Bendix, BSR 4210, MDAS Technical Description.
2) Association of American Geographers, July 1974, Using Remote sensor Data for Land Use Mapping and Inventory : A User Guide, PB-242.

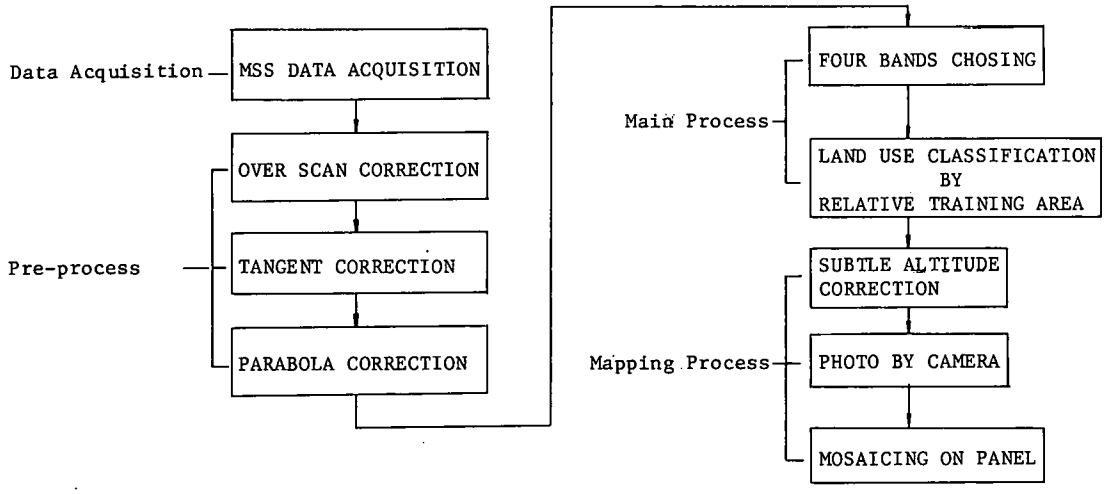

FIGURE 9. FLOW OF LAND USE MAP COMPILATION

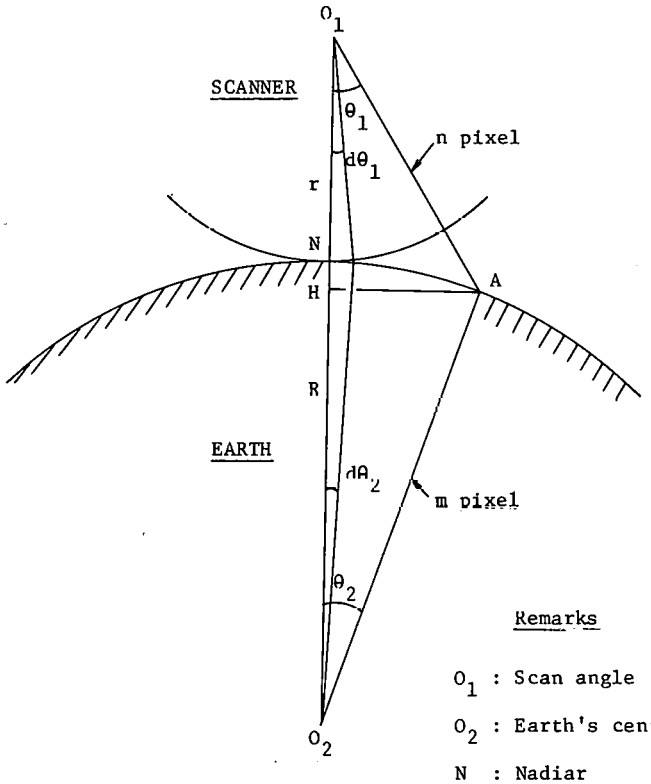

Remarks

O_1 : Scan angle

O_2 : Earth's center

N : Nadiar

II : $O_1O_2 \perp$ AH

r : Scanner altitude

R : Earth's radius

$d\theta_1$: IFOV of scanner

$d\theta_2$: IFOV of corrected image

ds : Pixel length

m : Number of resampling pixel

n : Number of scanning pixel

$$\frac{AH}{O_1H} = \tan\theta_1$$

$$AH = R \sin\theta_2$$

$$O_1H = R + r - R\cos\theta_2$$

$$\frac{R\sin\theta_2}{R + r - R\cos\theta_2} = \tan\theta_1 \quad \cdots\cdots (1)$$

$$ds = r\, d\theta_1$$

$$ds = r\, d\theta_2$$

$$d\theta_2 = \frac{r}{R} d\theta_1$$

$$\theta_1 = n\, d\theta_1$$

$$\theta_2 = m\, d\theta_2$$

$$\therefore n = \frac{1}{d\theta_1} \arctan\left(\frac{R\sin(m\frac{r}{R}d\theta_1)}{R + r - R\cos(m\frac{r}{R}d\theta_1)}\right) \quad \cdots\cdots (2)$$

in case of airplane, r is small against R

$m\frac{r}{R}d\theta_1 \longrightarrow 0$, then

$$n = \frac{1}{d\theta_1}\arctan(m\, d\theta_1) \quad \cdots\cdots\cdots \text{Special case of airplane scanner}$$

FIGURE 2. CONFIGULATION OF TANGENT CORRECTION

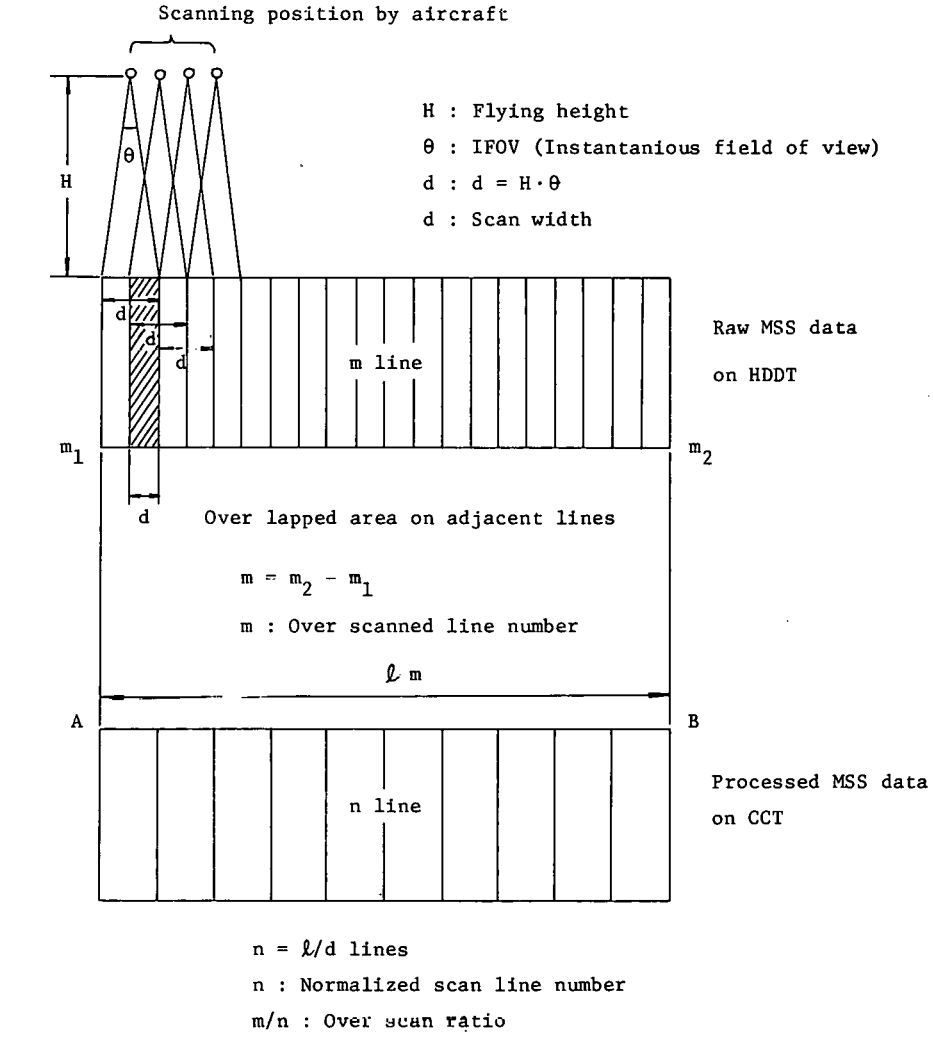

FIGURE 1. CONFIGULATION OF OVERSCAN CORRECTION

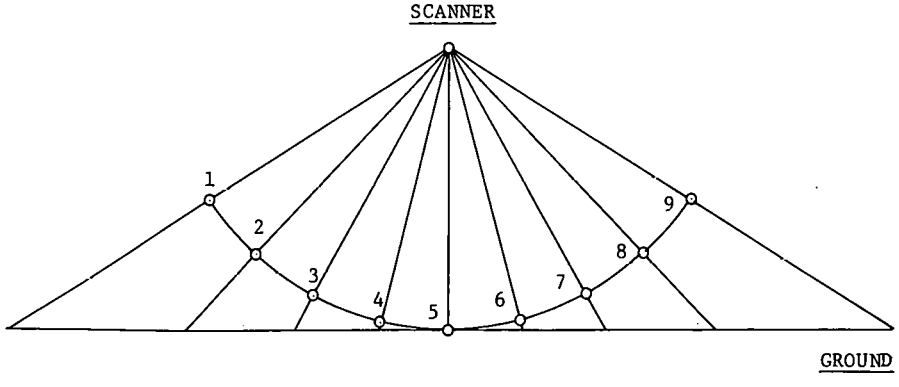

FIGURE 3. SCANNING ANGLE OF M^2S

(Number of 1 to 9 correspond to the number in Figure 4.)

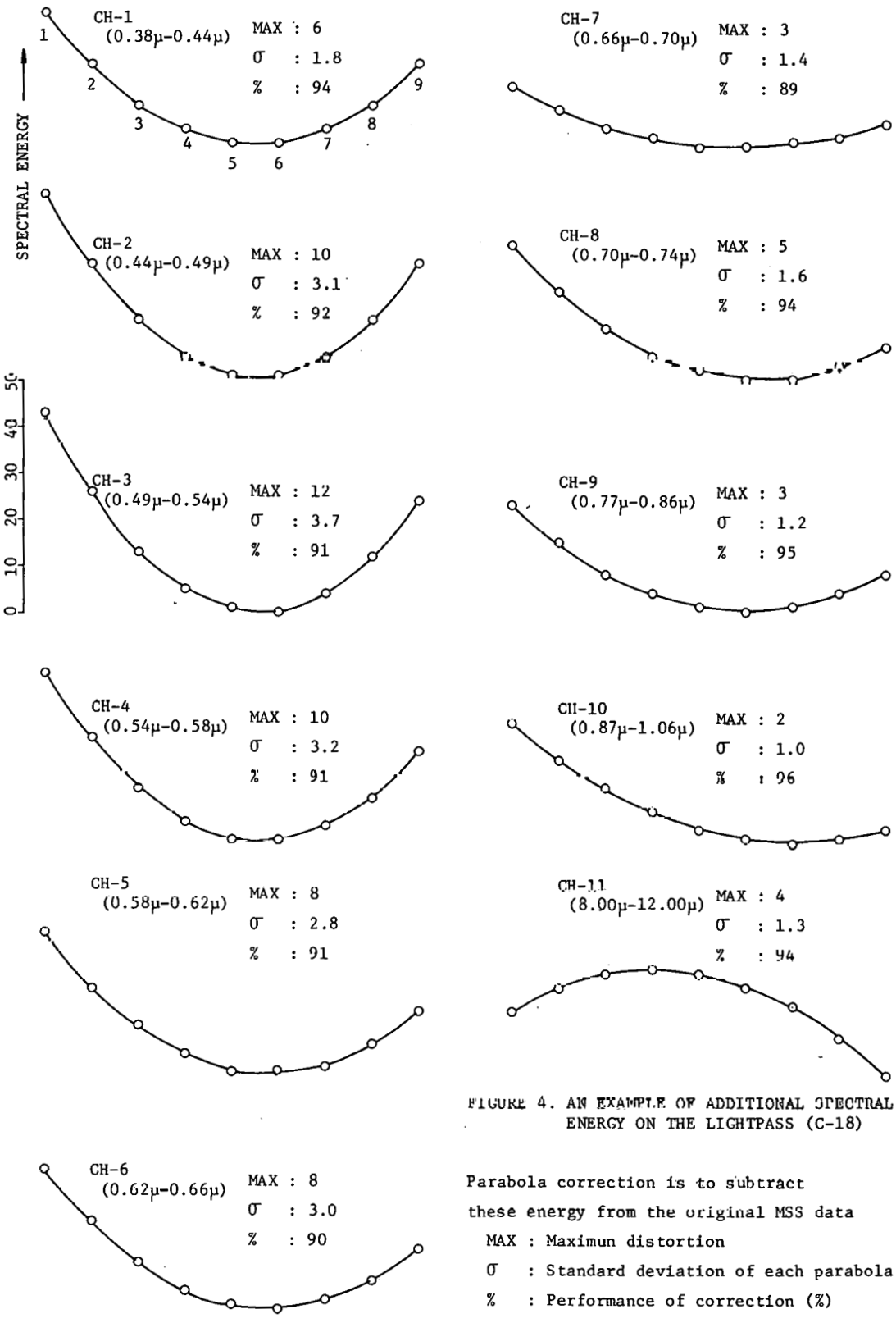

FIGURE 4. AN EXAMPLE OF ADDITIONAL SPECTRAL ENERGY ON THE LIGHTPASS (C-18)

Parabola correction is to subtract these energy from the original MSS data

MAX : Maximun distortion

σ : Standard deviation of each parabola

% : Performance of correction (%)

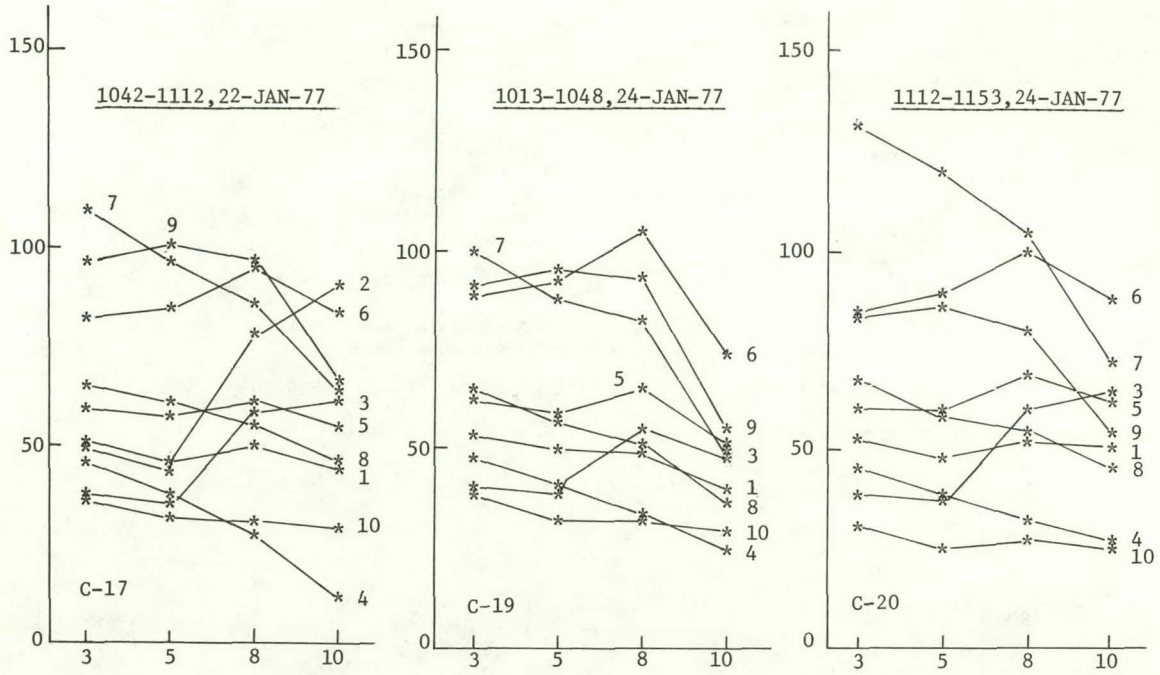

Figure 6. SPECTRAL SIGNATURE FOR LAND USE BETWEEN COURCES

Land Use Classifucation

1. Woody park
2. Tea plant field
3. Forest (Sunny side)
4. Water
5. Farming area
6. Golf links
7. Factory
8. City area
9. Housing lot
10. Forest (Shade side)

Table 1. CATEGORIZATION PERFORMANCE BY MCP (C-17)

TNG SET	PERCENT CATEGORIZED AS GROUP											NAME
	0	1	2	3	4	5	6	8	7	9	10	
1	0.	96.	0.	0.	0.	1.	0.	3.	0.	0.	0.	TAMA BOCHI
2	2.	0.	94.	3.	0.	1.	1.	0.	0.	0.	0.	SAYAMA
3	1.	0.	0.	98.	0.	0.	0.	0.	0.	0.	1.	NARUKI FOREST
4	1.	0.	3.	88.	0.	0.	0.	0.	0.	0.	8.	OUME FOREST
5	0.	0.	0.	0.	100.	0.	0.	0.	0.	0.	0.	SAYAMAKO
6	1.	0.	1.	1.	0.	95.	1.	1.	0.	0.	0.	YOKOTA HATAKE
7	1.	1.	0.	2.	0.	17.	80.	0.	0.	0.	0.	SAYAMA GOLF
8	0.	0.	0.	0.	100.	0.	0.	0.	0.	0.	0.	YAMAGUCHI
9	5.	0.	0.	0.	0.	4.	91.	0.	0.	0.	0.	SHIOFUNE GOLF
10	15.	1.	0.	0.	0.	1.	82.	1.	0.	0.	0.	KOSOGI GOLF
11	3.	2.	0.	0.	0.	5.	0.	85.	4.	0.	0.	HIGASHI OME
12	9.	0.	0.	91.	0.	0.	0.	0.	0.	0.	0.	20 YAMA ONKATA
13	3.	1.	0.	0.	0.	13.	84.	0.	0.	0.	0.	20 GOLF SAGAMI
14	0.	0.	0.	0.	100.	0.	0.	0.	0.	0.	0.	20 WATER YOKOHAM
15	4.	0.	0.	0.	0.	0.	0.	0.	96.	0.	0.	20 KOJO MITSUBIS
16	3.	0.	0.	0.	0.	0.	0.	0.	0.	97.	0.	20 TAKUZO HACHIO
17	0.	0.	0.	0.	100.	0.	0.	0.	0.	0.	0.	20 TSUKUIKO
18	2.	0.	0.	0.	0.	0.	0.	8.	0.	89.	0.	20 TAKUZO SHIROY
19	94.	0.	0.	0.	0.	0.	0.	0.	6.	0.	0.	20 KOJO MITSUBIS
20	0.	0.	0.	0.	100.	0.	0.	0.	0.	0.	0.	TSUKUIKO 20
21	9.	3.	0.	0.	0.	78.	0.	7.	2.	2.	0.	20 HATAKE TSUKUI
22	0.	0.	0.	3.	0.	0.	0.	0.	0.	0.	96.	KOBOTOKE YAMAKAG
23	90.	0.	0.	0.	10.	0.	0.	0.	0.	0.	0.	17 SAKAI JOSUIJO
24	8.	0.	0.	0.	0.	0.	0.	1.	91.	0.	0.	BRIDGISTONE FACT
25	0.	0.	0.	0.	0.	0.	0.	3.	96.	0.	0.	TACHIKAWA HIKOJO

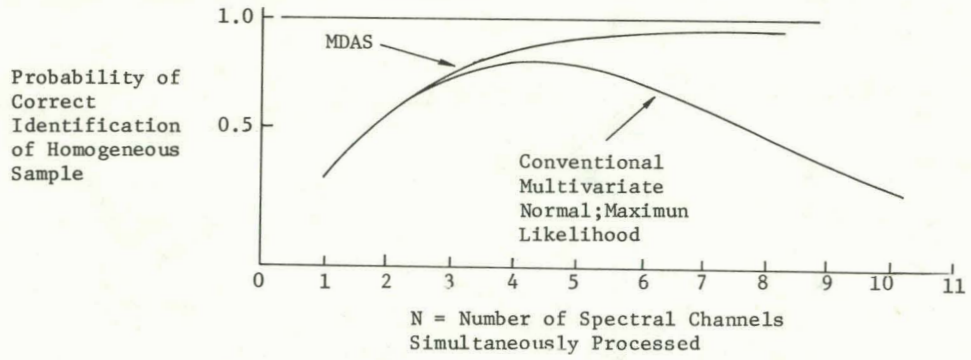

FIGURE 5. PERFORMANCE VERSUS INPUT CHANNELS OF MCP 12819-20[1]

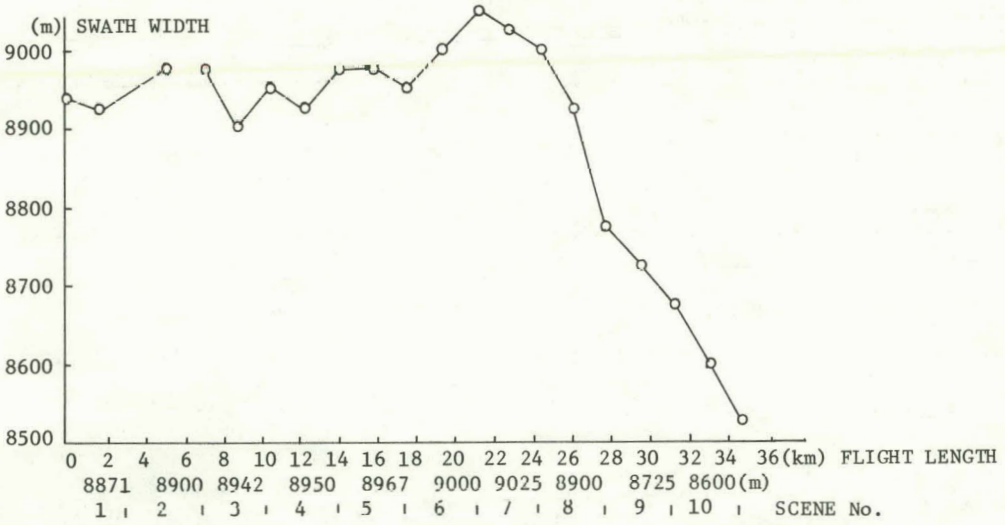

FIGURE 7. VARIATION OF SWATH WIDTH FOR 620 PIXELS AFTER TANGENT CORRECTION

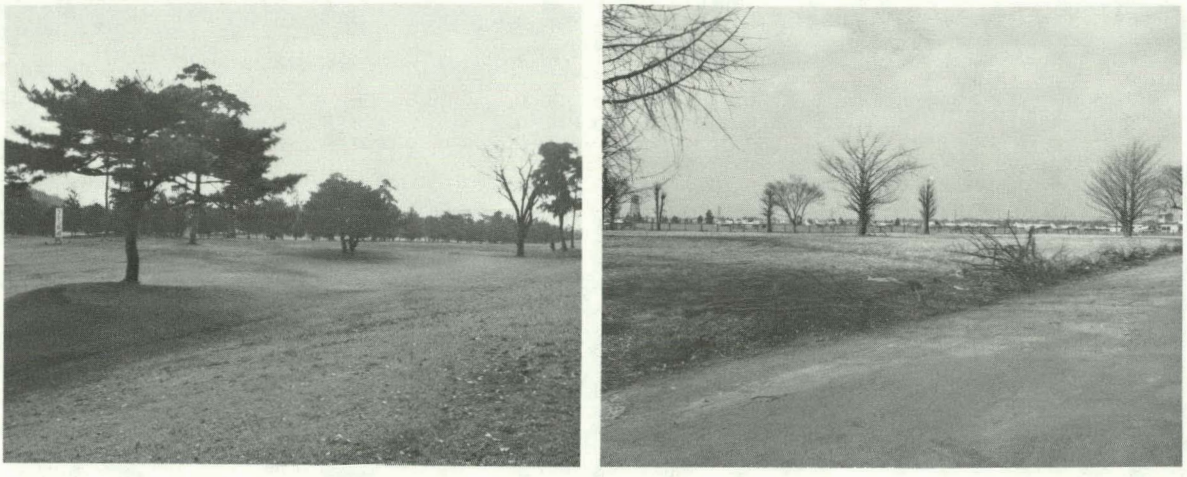

ICU GOLF LINKS CHOFU AIRPORT

FIGURE 8. AN EXAMPLE OF SAME CLASSIFICATION BUT DIFFERENT LAND USE

多摩川流域（府中～青梅間）のリモートセンシングによる赤外擬似カラー写真図

FALSE COLOR MOSAIC
IN
THE TAMA RIVER BASIN

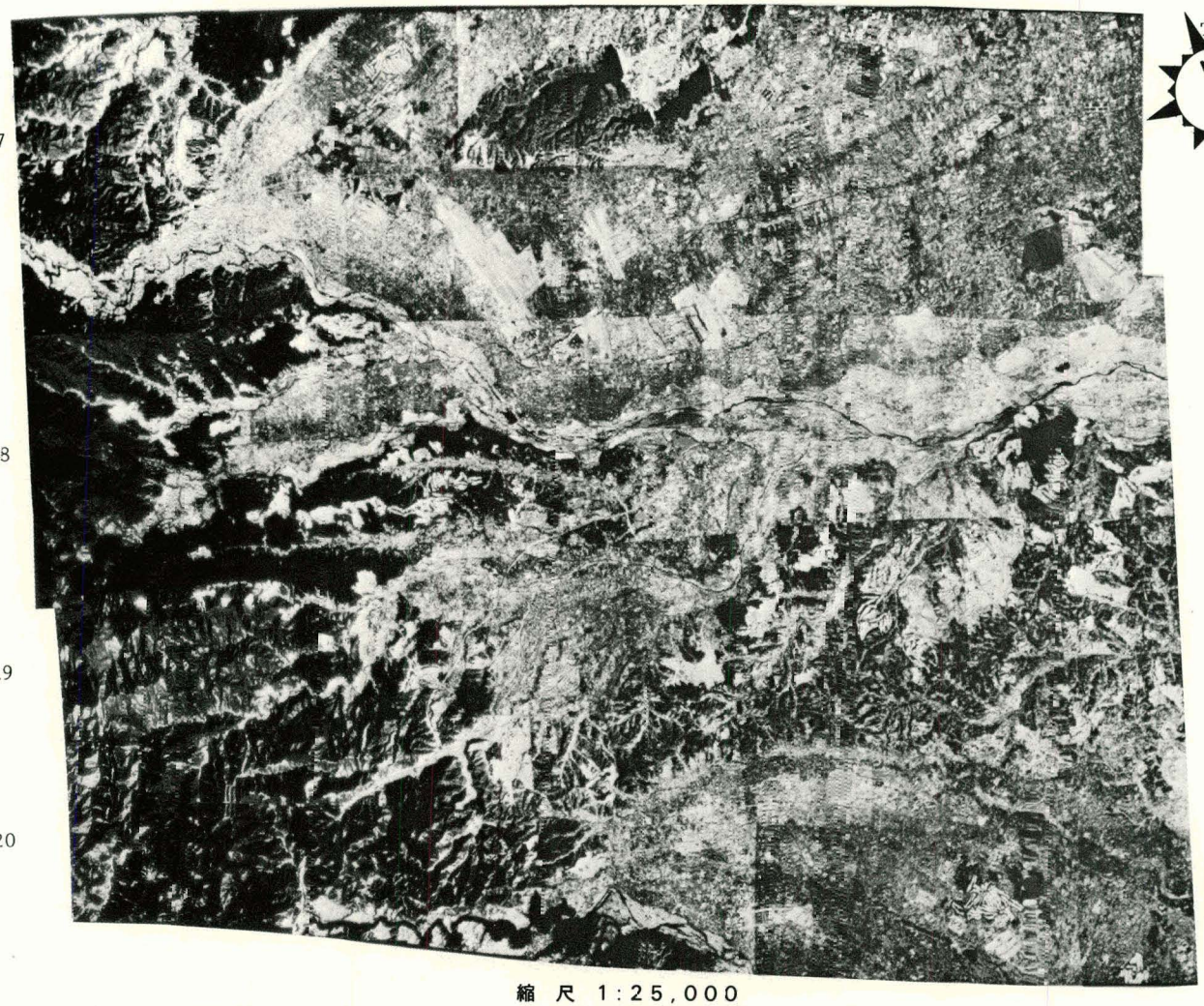

January 1977
by
MINISTRY OF
CONSTRUCTION
&
R E S T E C

縮 尺 1:25,000

0 1 2 3 4 5 KM

撮影　昭和52年1月
製作　昭和52年3月

建設省　京浜工事事務所
財団法人　リモートセンシング技術センター

多摩川流域（府中～青梅間）のリモートセンシングによる土地利用図

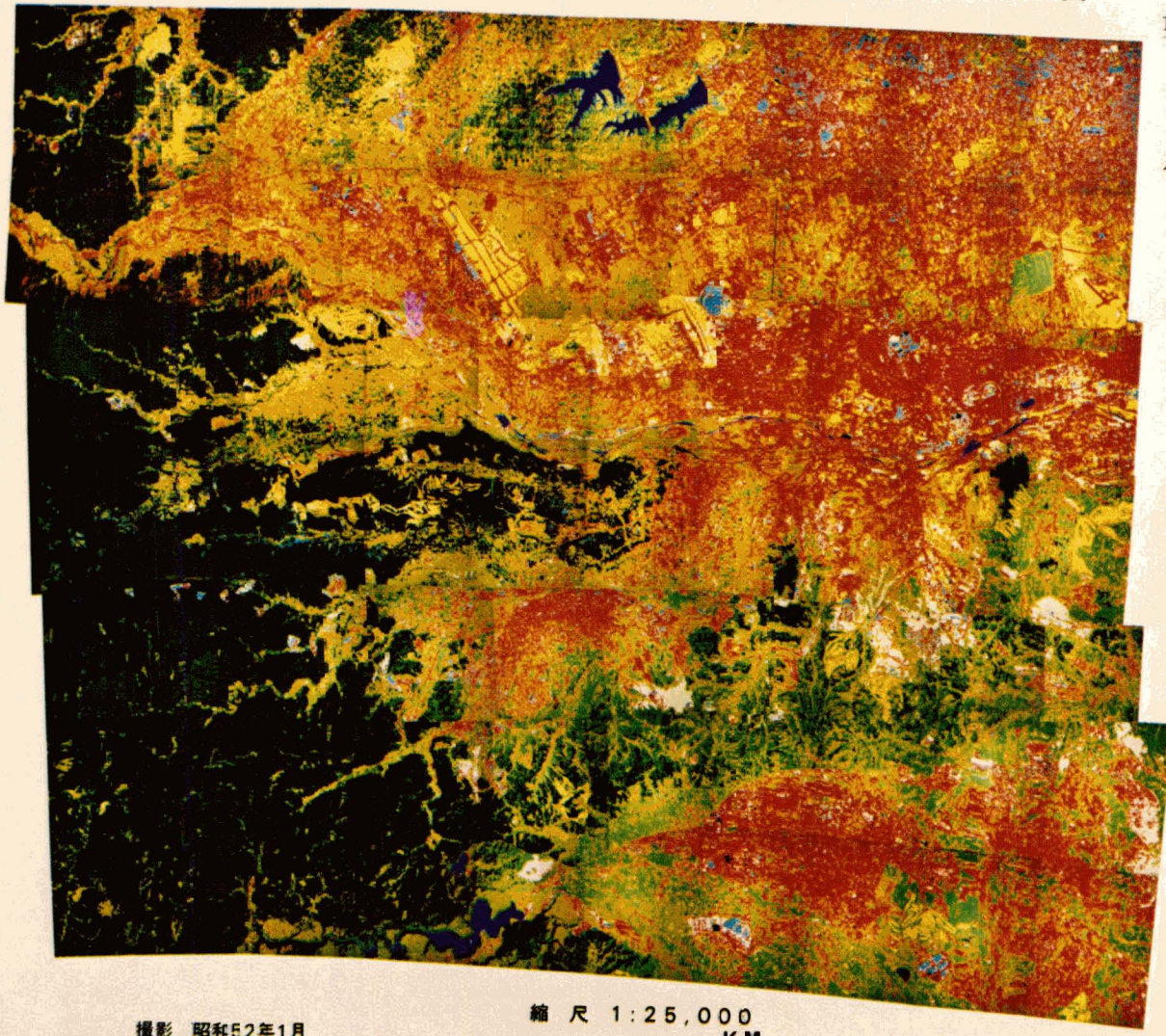

LAND USE MAP
IN THE TAMA RIVER BASIN

N

凡　例　LEGEND

- 市街地 City area
- 宅地造成地 Housing lot
- 工場 Factory
- ゴルフ場 Golf links
- 田畑 Farming area
- 公園緑地 Woody park
- 茶畑 Tea plant field
- 森林（日向部） Forest(Sunny side)
- 森林（日陰部） Forest(Shade side)
- 河川　湖沼 Water

撮影　昭和52年1月
製作　昭和52年3月

縮　尺　1:25,000
0 1 2 3 4 5 KM

建設省　京浜工事事務所
財団法人　リモートセンシング技術センター

January 1977
by
MINISTRY OF
CONSTRUCTION
&
R E S T E C

THE PRODUCTION OF 1:250,000 MAPS OF PRECISION RECTIFIED AND REGISTERED LANDSAT IMAGERY USING THE MDA IMAGE ANALYSIS SYSTEM: INITIAL RESULTS

R. Orth, F. Wong, J.S. MacDonald

MacDonald, Dettwiler & Associates Ltd.
10280 Shellbridge Way
Richmond, British Columbia, Canada
V6X 2Z9

INTRODUCTION

Two features of LANDSAT multi-spectral scanner (MSS) imagery can be isolated to distinguish it operationally from conventional aerial photography. Firstly, the small scale (nominally 1:1,000,000) of a LANDSAT scene provides a continuous image over an area of 185 x 185 km^2. This may be contrasted with a typical 1:50,000 aerial photograph covering an area of 11.5 x 11.5 km^2. Secondly, the digital form of LANDSAT imagery makes it possible to apply computer-based processing techniques to the problems confronting the image analyst. In comparison, aerial photographs require largely analogue techniques due to the film storage medium.

However, despite these distinctions, it is evident that LANDSAT imagery complements conventional aerial photography, especially with regard to scale. This is most graphically illustrated by multistage sampling for national resource mapping, especially suitable for developing countries [1]. Key applications of LANDSAT imagery to date have taken advantage of its synoptic view of the earth, as for example in forest inventory [2] or agricultural crop monitoring [3].

To further extend the complementary use of such imagery to small scale mapping, precision rectified LANDSAT images are highly desirable. Such images, having the effects of spacecraft attitude removed using Ground Control Points (GCP's), are entirely analogous to rectified aerial photographs. Therefore conventional techniques of photointerpretation, planimetric mapping, boundary delineation and map revision that require a photogrammetrically accurate image can be applied in a straightforward fashion to such rectified LANDSAT imagery. The production of rectified LANDSAT imagery accurate to about one pixel (80 m) RMS is necessary for Class A 1:250,000 LANDSAT photomaps. The possible vital importance of such LANDSAT photomaps in countries where little or no recent mapping has been done, has been stressed by Conitz of the Agency for International Development [4].

The digital nature of the rectified LANDSAT image allows a further possibility, namely that of precision image-to-image registration using Registration Control Points (RCP's). Made operationally effective by the 18-day cycle time of LANDSAT, registration of a newly acquired scene to a previously rectified scene makes possible the development of a geometrically consistent set of LANDSAT images on a regional or national scale. Such a data-base is a sine qua non for the identification of changes in an area of interest, as required for example in map revision and multi-temporal analysis.

In the context of these applications, this paper describes the use of the MDA Image Analysis System (IAS) for the production of precision rectified and registered LANDSAT imagery. The introduction is followed by a description of the IAS and its capabilities for general digital image analysis. The use of the system for the production of rectified and registered LANDSAT images is then described, together with an assessment of image accuracy. The final section summarizes this use of the IAS in providing image products and data for application in small scale mapping and resource analysis.

THE MDA IMAGE ANALYSIS SYSTEM

The IAS is a digital image analysis system configured around a standard, high performance minicomputer and peripherals. It may be operated as a stand alone system, remote from any ground receiving station, or incorporated into MDA's Line Scan Receiving and Processing System (LSRPS) [5], to form part of a total low cost ground receiving, processing and analysis system for line scan data [6]. This unique feature may be important for those users wishing to develop an operational capability in two phases. In such a case, during the first phase, application techniques are developed on the IAS using input data from a remote source (e.g. EROS Data Centre, Canada Centre for Remote Sensing). The second phase assures operational use of these techniques, by incorporation of the IAS hardware into a complete ground station system, capable of receiving and analysing line scan data in a timely fashion, not possible when the source of data is remote.

The system software is modular throughout, providing for procedures of image input, radiometric correction, geometric rectification and registration, image classification, and image and data output. An image manipulation module allows the analyst a high level of interaction with the displayed image. This imagery may be derived from LANDSAT, METEOSAT, or any other line scan source. Output products include rectified and registered imagery, thematic images derived from classification, and specially enhanced images (e.g. edge enhanced, principal components) for photointerpretative purposes. At all times, as in the case of photogrammetric instruments, these IAS procedures are based on software that is transparent to the analyst. In what follows, the system hardware is described and then the analysis procedures supported by the software are discussed.

Hardware Configuration

The IAS hardware (Figure 1) comprises a minicomputer, input/output devices, and an interactive colour display for the operator's interaction with the image. These system components include:

- Interdata 7/32 or 8/32 processor with 256 Kbyte memory and 32-bit floating point hardware.
- A 67 Mbyte mass storage disc.
- CRT/Keyboard terminal for dialogue interaction.
- Comtal 30SE digital display with two graphics memories, four function memories, four image memories, one pseudo-colour memory, and trackball cursor control.
- Optronics film recorder.
- 9-track 1600 BPI tape drive.
- Line printer.

The magnetic tape and discs are used for archival and temporary image storage respectively. The Comtal 30SE is used for colour and graphics display, and for presentation of alphanumeric text during various operational modes (viz. during GCP measurement, image-to-image registration and classification). A trackball cursor is provided at the Comtal for operator interaction (e.g. pointing, outlining of training areas, dynamic contrast stretch) with the displayed image.

Software Procedures

The IAS procedures of data input, radiometric correction, geometric correction, image classification, and data output have been developed around the interactive and computational capability of the hardware configuration described above. Easy and effective use of the interactive capability is provided by the image manipulation and display module. A simple block diagram depicting this organization into procedures is shown in Figure 2. Each procedure comprises a module containing a number of software functions. Table 1 lists the specifics of each function on a module by module basis. The objective of these procedures is to supply the image analyst with a comprehensive set of tools, which may readily be expanded upon due to the modular structure. Having selected a procedure, the operator is prompted at the keyboard terminal to enter simple commands, and is in this way guided through any procedure. The precision rectification and registration of LANDSAT imagery, and production of the film product, are described in what follows.

Rectification and Registration of LANDSAT Imagery

Full scene LANDSAT MSS imagery is rectified using GCP's obtained from survey data (e.g. photogrammetric control, or existing map sheets). The rectification process uses a spacecraft platform attitude model [9], wherein the time dependent roll, pitch and yaw, and altitude of the spacecraft are taken into account. The transformation from image pixel/line coordinates to GCP coordinates further takes into account all systematic effects due to sensor geometry, inertial platform motion, earth spheroid and earth rotation. The GCP's are used to provide the best estimates of the way in which the attitude angles varied across the scene, and also an altitude offset from the nominal spacecraft altitude. To provide these estimates, use is made of a Kalman filter, which allows the updating of the attitude and altitude parameters after each GCP is identified and marked. This updating feature also allows the operator to decide whether or not the current GCP identified should be marked, in the following way. Since the current attitude or altitude parameters define the current best estimate of the transformation between GCP coordinates and image pixel/line coordinates, it is possible to calculate where the GCP should be on the image, as opposed to where the operator identifies it to be. The associated difference in distance may be used by the operator to determine the quality of input GCP coordinates, or the precision of identification, and forms a basis for rejection of a GCP. This feature is illustrated in the section below on the production of rectified and registered imagery.

Approximately 10 uniformly distributed GCP's are needed to adequately specify the attitude time series and altitude offset for any single LANDSAT scene. These parameters are used to provide a set of distortion coefficients defining the transformation between the final map coordinates, Universal Transverse Mercator, (UTM) and the raw image. The distortion coefficients depict a piecewise continuous bilinear mapping between 168 rectangular cells in the map coordinate system and the same number of deformed cells in the raw image. A resampling process [10] then uses this mapping to locate pixels in the raw image that correspond to a regular grid of pixels in the output image. The resampling may take the form of nearest neighbour, bilinear or cubic convolution depending on user requirements.

Output to Film Recorder

The resulting rectified image is now ready for final imaging onto film. At this point, the operator decides on the scale of the output image, whether tic marks, UTM coordinate annotation and alphabetic text are to be included. Film gamma compensation is also allowed for. The resulting black and white Optronics image may be either positive or negative, and is on a standard 23 cm x 23 cm format, with 3 films printed for 3 colours. Precision registration marks on each image allow colour composite imagery to be made without misregistration errors. Alternatively, using a colour Optronics film recorder, supplied optionally with the IAS, a single exposed film for colour prints can be produced to avoid the registration step. For the production of monochrome LANDSAT photomaps, a single black and white image would be used.

PRODUCTION OF PRECISION RECTIFIED AND REGISTERED LANDSAT IMAGERY

The previous paragraphs summarize the techniques used to produce precision corrected LANDSAT imagery on the IAS. In this section the way in which the operator interacts with the system to produce such LANDSAT imagery is shown. For this purpose two LANDSAT CCT's were obtained from EROS Data Centre (EDC), Sioux Falls, South Dakota, U.S.A. Both scenes covered the same area surrounding Manila, Republic of the Phillippines, the first imaged by LANDSAT-1 on December 23, 1972 and the second by LANDSAT-2 on April 21, 1976 (Table 2). Together with the CCT's, black and white imagery for all four bands for both scenes were obtained. These photographs perform an important function in GCP selection as explained below.

GCP Selection

Prior to use of the IAS, 20 GCP's were selected using 1:250,000 maps produced by The Phillippine Coast and Geodetic Survey, Republic of Phillippines, in conjunction with the photographic prints mentioned above. Efforts were made to define GCP's at prominent features on the prints, and specifically not in regions of high coral activity, river deltas, and flats etc. as indicated on the map sheets. An identification number, descriptor and location (latitude, longitude, elevation in meters) was generated for each GCP, and a file created on the IAS containing the GCP's. The theoretical accuracy of GCP location determination is 76 m RMS, assuming Class A map accuracy for the 1:250,000 sheets (125 m for 90% confidence interval). This aspect is further discussed in the summary.

Image Input

The first operation on the IAS involved the transfer of the EDC CCT onto the IAS mass storage disc. In this step NASA replicated pixels were removed, and the nominal orbit and attitude data on the Single Image Annotation (SIAT) file read. This latter data is automatically processed to provide initial estimates for the attitude time series, and altitude offset. If SIAT data is not available, as for example on CCRS tapes, the system sets these initial estimates to zero, and generates the orbit data appropriate to LANDSAT-1 or -2. The procedure following the CCT input is the independent of whether SIAT data was present or not.

GCP Measurement, Attitude Model Updating, and Rectification

The operator next invokes the geometric correction procedure, and selects the function of precision rectification from the alternatives (systematic correction, registration, etc.) displayed on the terminal CRT. The GCP measurement now begins, with the operator specifying the identification number of the first GCP chosen from the displayed GCP list (Figure 3(a)). Using the initial attitude and orbit estimates the system extracts a 256 line x 256 pixel region centred on the best estimate of the GCP location in the scene. The image segment is displayed on the upper right-hand quadrant of the Comtal display. Based on the current uncertainties of the attitude and altitude parameters, a box is drawn around the segment centre. This alerts the operator to the fact that the current GCP is most likely to be found within the demarcated area. Figure 3(b) shows the resulting image for the GCP at Talim Pt. as seen by the operator. The GCP coordinates are shown below the image in the lower right-hand quadrant. On the lower left-hand quadrant a menu displays the commands to be entered either to mark the GCP, to select another band (used if the GCP is unrecognizable in the current band), to skip the GCP, or to exit from the program. To mark the GCP, the operator moves the cursor using the trackball to the identified GCP location and types the appropriate keyboard command. This signals the system to enlarge the area around the GCP by a factor of 6, and a zoomed image of a 32 line x 32 pixel area is displayed in the upper left-hand quadrant (Figure 3(c)).

Below the zoomed image the difference between actual GCP coordinates and those estimated from the marked GCP location on the image, is displayed. This difference is resolved along the current spacecraft roll, pitch and yaw axis. Depending on the magnitude of these differences, the operator may decide not to use this GCP, to mark it (with a level of confidence rating), or to redesignate the point. The menu covering these alternatives is displayed on the lower left-hand quadrant. Above this menu is shown the statistics of the Kalman filter for all GCP's used prior to the current one. These statistics are used to monitor the convergence of the attitude model, and for this reason fluctuate less as more GCP's are used. For the first GCP, the RMS deviation is put to zero. Once the operator marks the GCP location on the zoomed image, the Kalman filter and hence the attitude and altitude parameters, are updated. Simultaneously, new confidence levels on these parameters are computed and these are reflected in a change in the size of the box on the 256 x 256 pixel image segment displayed for the next GCP selected. To perform the next selection, the operator may request to display the GCP list. This list will show that all the previously marked GCP's have been removed from the remaining possible points, to avoid duplication of GCP measurement.

An added feature is the designation of all GCP's used as a Registration Control Points (RCP's). In this case the 32 line x 32 pixel image chip surrounding the position of the designated GCP coordinate is stored on disc, together with its coordinates, number and description. For such an RCP, the latitude and longitude coordinates are those computed from the line/pixel coordinates of the marked GCP, and hence may differ from the coordinates in the input GCP list. The RCP coordinates themselves are calculated automatically from the image line/pixel coordinates following the completion of all GCP measurements, using the final best estimates from the attitude model.

The steps outlined above, of GCP selection, marking, refined marking and RCP designation are repeated for each GCP in the list, until the list is exhausted, or the operator is satisfied with the position estimation error, mean and RMS deviations. A sequence of such steps is illustrated in Figures 3(b) to 3(d). Here Figure 3(d) shows the results of the 10th measurement, for the GCP at Sangley Pt. Notice the size of the box is diminished relative to that in Figure 3(b) due to reduced uncertainty in the attitude model.

The Kalman filter mean and RMS deviations for the 10 GCP's used is also seen in Figure 3(d). To provide a reasonable set of RCP's for the registration procedure, 18 GCP's were used altogether. The mean deviation and RMS deviation of these GCP's are discussed below.

With the transformation for mapping between line/pixel coordinates and GCP coordinates now established, the operator may produce a rectified image on the UTM projection. This is most accurately performed using image resampling with the cubic convolution algorithm. The output image (on disc) at this stage is on the UTM projection with a 57 m grid spacing rotated to align with the subsatellite track.

Film Production

In order to produce an image at a user specified scale and annotation, the operator uses as a source the image resulting from resampling to a 57 m grid. A single command invoking the program to produce film output results in a series of prompts to the operator, who must specify the following:

Optronics Spot Size	Scale of Output Image
Line/Pixel Coordinates of Source Image	UTM Tic Mark Separation
	UTM Grid overlaid or not
Positive or Negative Film	Annotation Text size
Contrast Stretch	Annotation Text

Once these parameters have been specified, a latent image is produced on film with the Optronics film recorder in a line by line fashion. The image is scaled using cubic convolution resampling, and all text, registration and tic marks are generated digitally. For colour separation negatives, three images must be generated, unless a colour Optronics film recorder is part of the hardware system. Standard development of the images results in a precision rectified LANDSAT image that can be used for conventional downstream products viz. photomap production, contact prints, etc.

Precision Image Registration

In the production of the rectified LANDSAT scene outlined above, an RCP image chip library was generated. Subsequent LANDSAT frames of the same area may now be registered to this reference library in a manner that further reduces the amount of operator interaction, to speed system throughput. To perform image-to-image registration, the operator repeats the procedure of image input and selects, in the geometric correction procedure, the function of image registration. Having established that an RCP image chip library exists for this scene, the system proceeds in a manner almost identical to the rectification function. The exception is that manual designation of the RCP on the input image is supplemented by an automatic correlation mode. Such correlation is attempted by the system for each RCP entered. Should correlation fail at the first stage (due to cloud cover, radiometric colour inversion, or gross misregistration) the operator is requested to manually designate the RCP position on the 256 x 256 image segment. To assist in this, the 32 line x 32 pixel chip is displayed on the Comtal in the lower right-hand quadrant. Having performed this manual designation, the operator may again elect to automatically correlate, according to the menu on the lower left-hand quadrant. Should manual designation still be necessary the operator is so prompted. This manual marking is now done by flipping between the two zoomed images, and marking corresponding points on each chip. The remaining steps in the sequence (viz. updating the attitude and altitude parameters, examination of RCP estimation error, etc.) are identical to that of the rectification function outlined previously. Likewise, image resampling and film production are identical.

ACCURACY OF PRECISION PROCESSED IMAGERY

In this section, initial results on the accuracy of the images produced during rectification and registration are discussed. While precision measurements on the final film using a monocomparator have yet to be performed, it is possible to present the following results based on statistics from the rectification and registration procedures:

1. Initial and final roll, pitch, and yaw angles, and altitude offset for scene 1153-01463 used for rectification.

2. Mean and root mean square residuals of the GCP's for scene 1153-01463 and of RCP's for scene 2455-01294.

Figures 4(a), (b), (c) show the roll, pitch and yaw angles across the scene prior to and after GCP measurement for scene 1153-01463. The initial attitude values were obtained from the SIAT data as explained previously. The final time series was used to provide the attitude model, and the transformation between line/pixel coordinates and UTM coordinates. The altitude

offset derived from GCP measurements was +1.45 km. Registration of scene 2455-01294 resulted in a similar set of curves, not presented here. Detailed analysis of the intermediate attitude time series showed satisfactory convergence after about 9 GCP's (RCP's) as previously reported [9].

Table 3 shows the mean and RMS residuals for GCP's and RCP's. The mean deviation of marked GCP (RCP) coordinates from actual GCP (RCP) coordinates is defined as

$$(1) \quad m = \frac{1}{N} \sum_{i=1}^{N} \sqrt{(x_i-X_i)^2 + (y_i-Y_i)^2 + (z_i-Z_i)^2}$$

where X_i, Y_i, Z_i refer to the i^{th} GCP (RCP) coordinate and x_i, y_i, z_i refer to the i^{th} GCP (RCP) designated coordinate and N is number of GCP's (RCP's) used.

The RMS deviation is defined by

$$(2) \quad \sigma = \sqrt{\frac{1}{N} \sum_{i=1}^{N} (x_i-X_i)^2 + (y_i-Y_i)^2 + (z_i-Z_i)^2}$$

Since the GCP's were obtained, in this case, from 1:250,000 map sheets (planimetric accuracy: 90% confidence interval = 125 m or one standard deviation = 76 m if Class A map accuracy is assumed), the theoretical residual mean deviation due to the GCP coordinates is 76 m, while the associated residual RMS deviation is also 76 m. These values should be compared with the mean and RMS residuals for scene 1153-01463 used for rectification. The residuals using accurate GCP coordinates and well defined features, will approach 80 m RMS (one pixel accuracy) [9]. However, for the rectification work presented here, the method of measuring GCP coordinates from the 1:250,000 map sheets is estimated as being no better than about 125 m (combining map accuracy with measurement accuracy). Subtracting this effect from the RMS residual for scene 1153-1463 yields an RMS deviation of 85.6 m for the contribution of attitude model uncertainty to the total RMS deviation. This is comparable to one pixel accuracy (80 m for LANDSAT).

For GCP coordinates, 1:250,000 maps form the least accurate of potential sources of data for precision correction of LANDSAT imagery. Significant improvements would result from using 1:50,000 maps (not available for these tests), or aerial photography with identifiable photogrammetric control points. Effective RCP selection depends largely on LANDSAT image clarity, and on the operator's knowledge of the region imaged to avoid the selection of features that can change with time (e.g. rapidly eroding beaches, river deltas, etc.). Despite lack of regional knowledge for the test reported here, registration resulted in subpixel accuracy (i.e. 48.9 m RMS--see Table 3) for the RCP's used. Such subpixel accuracy is vital for multitemporal analysis of LANDSAT images, as would be used in change detection for map revision as discussed in the next section.

SUMMARY

As discussed above, the RMS deviation of the GCP's using the attitude model is contributed to by the accuracy of the GCP coordinates themselves. Once this effect has been roughly accounted for, the remaining RMS GCP deviation intrinsic to the model for scene 1153-1463 is 85.6 m. Comparing this value with the planimetric accuracy specification for 1:250,000 maps, it is evident that Class A map accuracy at a scale 1:250,000 is possible for LANDSAT photomaps. To achieve this accuracy on a routine basis, requires, as shown in the tests reported here, that GCP coordinates be specified to an accuracy of say 25 m RMS to contribute about 4% to the total RMS deviation. Such control is obtainable from Class A 1:50,000 maps, or even more accurately from photogrammetric control points.

The registration of a LANDSAT scene to one previously processed using GCP's has also been discussed in this paper. The RMS residuals at the RCP's were well below one pixel, as required for multitemporal analysis of the images. Key applications for such imagery are change detection for map revision, and multitemporal classification. In both of these subpixel accuracy of registration minimizes the possibility of error when comparing individual pixel gray levels from scenes obtained at different dates. Such comparison techniques underly all multitemporal image analysis. Operationally, this type of image analysis is most effective as a complement to aerial photography. For example, once changes have been highlighted using LANDSAT imagery (at a scale of say, 1:250,000 or smaller), air photo flight lines can be planned to examine only these areas for detailed map revision, with a consequent saving

compared with large area coverage. Again, in multitemporal unsupervised classification, the classified LANDSAT data forms a basis for planning flight lines. These are located in regions that are more likely to contain the item to be inventoried, as indicated by the classification. This again has the effect of considerably reducing the amount of air photo coverage, and affords an excellent example of how LANDSAT imagery can be used operationally to complement aerial photography.

REFERENCES

1. Kalensky, Z.D., Darmoyuwono, K., and Rais, J. - Some Aspects of LANDSAT Ground Receiving Stations for Developing Countries. Intergovernmental Meeting on Remote Sensing and Satellite Surveying, Economic and Social Commission for Asia and the Pacific, Bangkok, June, 1977

2. Nichols, J.D., Harding, R.A., Scott, R.B. and Edwards, J.R. - Forest Inventory of Western Washington by Satellite Multi-stage Sampling. Paper presented at the Fall ACSM-ASP Convention, September 28 - October 1, 1976.

3. Macdonald, R.B., Hall, F.G., and Erb, R.B. - The Use of LANDSAT Data in a Large Area Crop Inventory Experiment. Symposium on Machine Processing of Remotely Sensed Data, LARS, Purdue University, Indiana, June 3-5, 1975

4. Conitz, M. - Photogrammetric Engineering and Remote Sensing, 44, 177-182, (1978)

5. Sloan, D.S., Isherwood, B.C. and MacDonald, J.S. - A Low-Cost System for Reception and Processing of Line Scan Data from LANDSAT and Other Sources. Paper presented at the 11th Annual Symposium on Remote Sensing of Environment, Ann Arbor, Michigan, 25-29 April, 1977

6. Sloan, D.S., and Orth, R. - A Self-Contained LANDSAT Data Reception and Precision Cartographic Image Production System. Paper presented at "Image Processing - Interactions with Photogrammetry and Remote Sensing", International Symposium of Commission III of the International Society for Photogrammetry, Graz, Austria, October 3-5, 1977

7. Strome, W.M., Vishnubhatla, S.S., and Guertin, F.E. - Format Specifications for Canadian LANDSAT MSS System Corrected Computer Compatible Tape. Energy, Mines and Resources, Canada, Research Report 75-3, July 1975

8. Thomas, V.L. - Generation and Physical Characteristics of the LANDSAT -1 and -2 MSS Computer Compatible Tapes. Goddard Space Flight Centre, November, 1975

9. Caron, R.H. and Simon, K.W. - Attitude Time Series Estimator for Rectification of Spaceborne Imagery. Journal of Spacecraft and Rockets, 12 (1) 27-32 (1975)

10. Simon, K.W. - Digital Image Reconstruction and Resampling for Geometric Manipulation. Symposium on Machine Processing of Remotely Sensed Data, LARS Purdue University, Indiana, June 3-5, 1975

TABLE 1

FUNCTIONAL CAPABILITY OF THE IAS

MODULE	FUNCTION
Input	LANDSAT MSS Data CCRS Format CCT[7]
	LANDSAT MSS Data EROS Data Centre Format CCT[8]
Radiometric Correction	Destriping of LANDSAT MSS.
	Haze removal and sun angle compensation.
	User supplied radiometric corrections.
	Manual repair of dropouts.
Geometric Correction	Systematic Correction for LANDSAT Imagery.
	Precision Geometric Rectification of LANDSAT Imagery.
	Precision Image-to-Image Registration of LANDSAT Imagery.
	Registration of 512 pixel by 512 line Images using a two dimensional polynomial.
Image Classification	Unsupervised parametric classification.
	Supervised interactive parallelepiped classification.
	Supervised interactive maximum likelihood decision rule (MLDR) classification with Gaussian statistics.
Output	Edge enhancement.
	Principal components transformation.
	Band ratioing.
	Image Annotation (including tic marks, UTM coordinates).
	Film gamma compensation.
Image Manipulation	Zoom, edge enhancement, ratioing, differencing, boundary delineation, contrast stretch, pseudo-colour and true colour displays, pixel addressing and content retrieval, flipping between images, normalization of two images, subsampled display.

TABLE 2

DESCRIPTION OF PROCESSED SCENES

REGION OF SCENE: MANILA & ENVIRONS, REPUBLIC OF THE PHILLIPPINES

SCENES PROCESSED:

RECTIFICATION	1153-01463	IMAGED ON 23 DECEMBER 1972 (LANDSAT 1)
REGISTRATION	2455-01294	IMAGED ON 21 APRIL 1976 (LANDSAT 2)

MAP SHEETS USED FOR GCP COORDINATES:

PCGS 2511, 2512, 2514, 2515 (Edition 3)
Scale 1:250,000

TABLE 3

GCP/RCP RESIDUALS FOR SCENES 1153-01463/2455-01294

Control Point	GCP Coordinates Latitude N	Longitude+ E	Residuals 1153-01463 m	2455-01294 m
Talin Pt.	13°58'47"	120°36'8"	47.9	*
Ligpo Pt.	13°49'0"	120°54'4"	269.3	*
Saimsim	13°54'34"	120°58'53"	111.4	45.9
Bantigui Pt.	13°41'14"	121°28'11"	176.9	*
Patayan Is.	13°56'40"	121°42'59"	190.4	84.0
Pinacapulan Pt.	13°51'47"	121°53'24"	35.3	*
Fuego Pt.	14°8'1"	120°34'28"	54.8	*
Hooker Pt.	14°23'1"	120°37'7"	84.8	39.7
Sangley Pt.	14°29'44"	120°55'5"	126.7	*
Pier 15-Manila	14°34'45"	120°58'1"	231.6	*
Talim Pt.	14°17'18"	121°14'6"	157.1	61.5
Marcelino Pt.	14°51'8"	121°36'50"	183.3	55.0
Susong Dalaga	14°36'45"	121°36'42"	15.3	15.3
Malazar Pt.	14°12'16"	121°45'13"	65.2	*
Gerardo Pt.	14°14'11"	121°55'49"	105.5	37.7
Balesin Is.	14°23'44"	122°1'57"	176.6	*
Polillo Pt.	14°43'30"	121°54'13"	260.6	18.7
Icol Is.	14°53'3"	121°59'43"	70.5	44.1
		Mean residuals	131.3	44.7
		RMS residuals	151.6	48.9

+ GCP elevations all at 0 m = sea level.

* RCP not used due to cloud cover or poor imagery in scene 2455-01294.

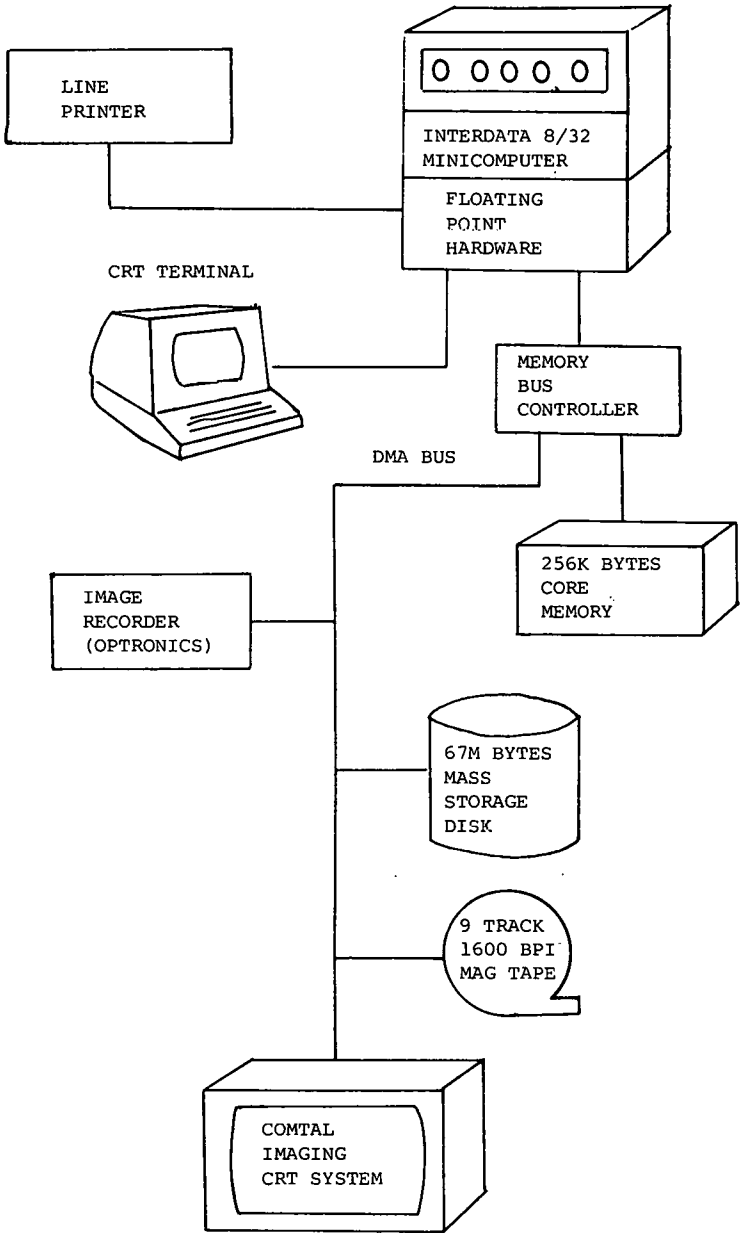

FIGURE 1

MDA IMAGE ANALYSIS SYSTEM HARDWARE

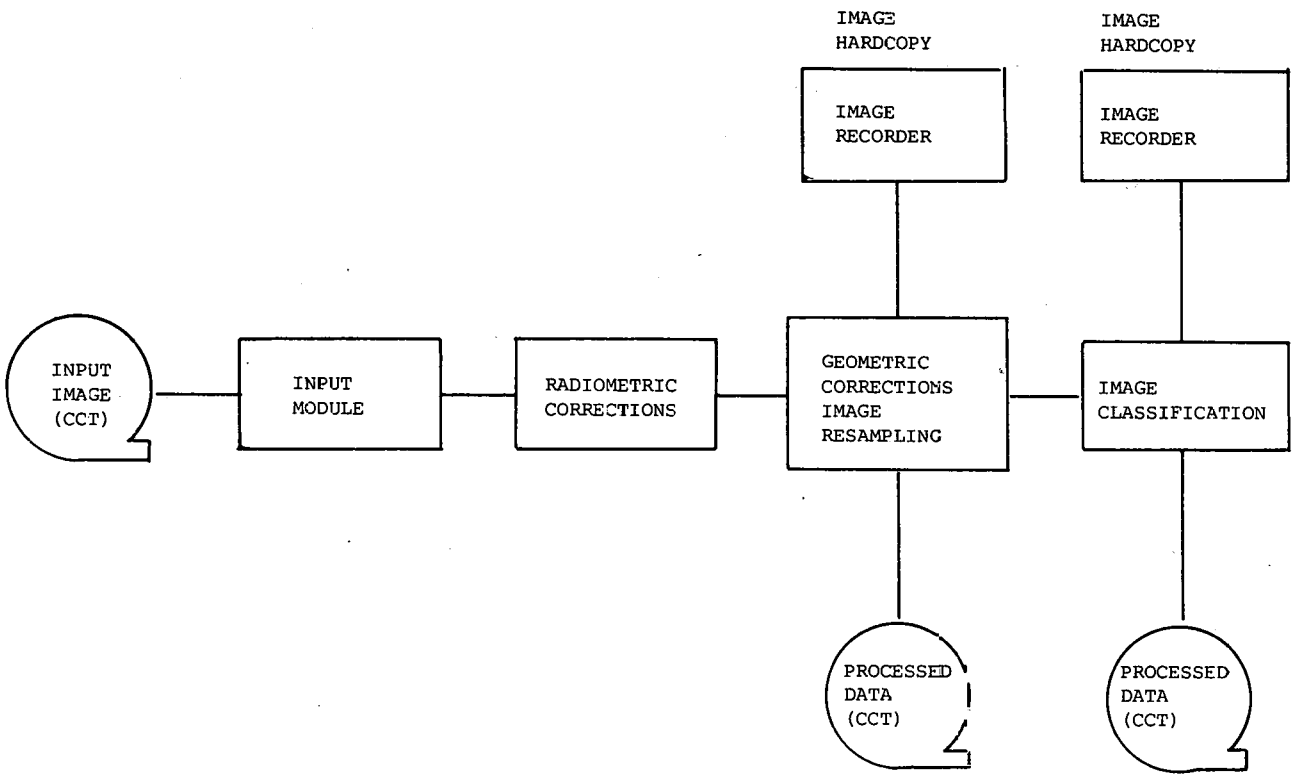

FIGURE 2

FUNCTIONAL FLOW DIAGRAM FOR MDA IMAGE ANALYSIS SYSTEM

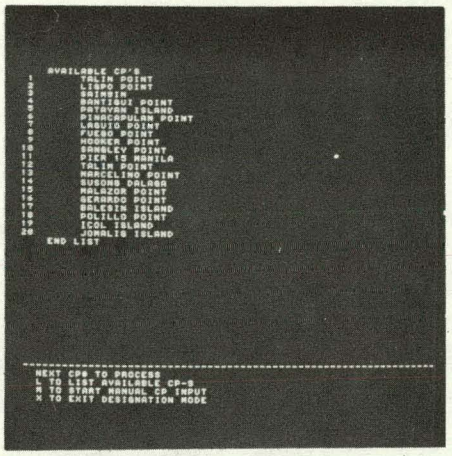

FIGURE 3 (a) GCP LIST DISPLAYED ON COMTAL

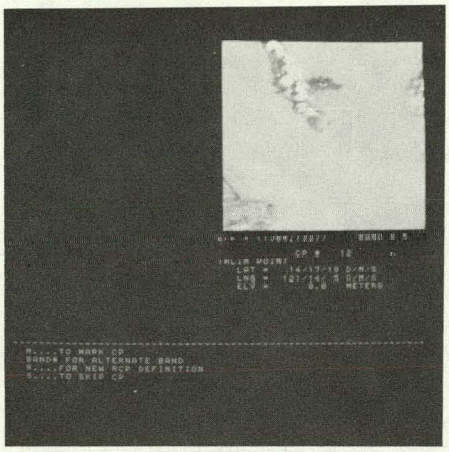

FIGURE 3 (b) 256 LINE X 256 PIXEL IMAGE SEGMENT FOR FIRST GCP, WITH GCP COORDINATES AND MENU DISPLAYED

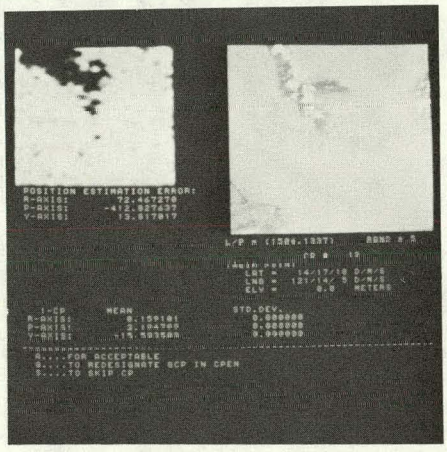

FIGURE 3 (c) 32 LINE X 32 PIXEL ZOOMED IMAGE FOR DESIGNATED FIRST GCP, WITH POSITION ESTIMATION ERROR, KALMAN FILTER STATISTICS, AND MENU DISPLAYED

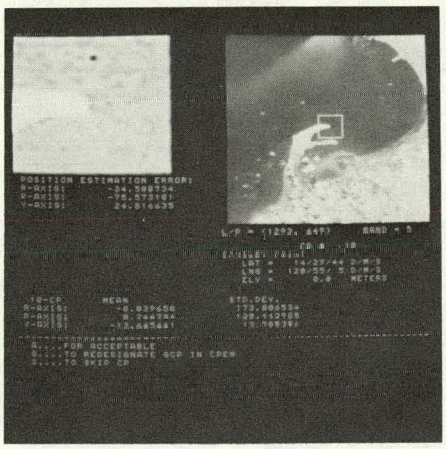

FIGURE 3 (d) COMTAL DISPLAY FOLLOWING UPDATING OF ATTITUDE MODEL AFTER 10TH GCP. NOTICE REDUCED POSITION ESTIMATION ERROR AND REDUCED BOX SIZE IN 256 LINE X 256 PIXEL IMAGE SEGMENT, COMPARED WITH (c)

FIGURE 3

ILLUSTRATION OF GCP MEASUREMENT

FIGURE 4(a) INITIAL (A) AND FINAL (B) ROLL ANGLE TIME SERIES

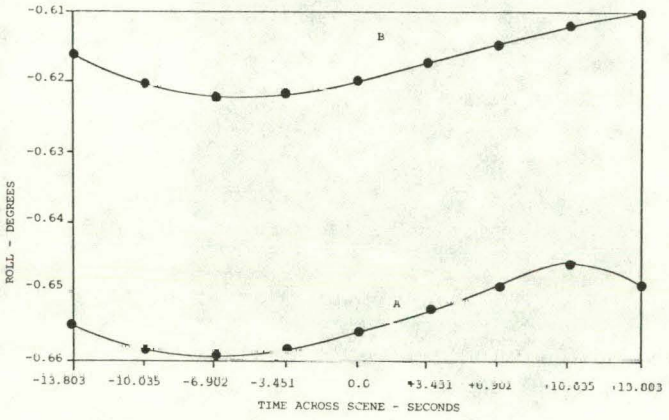

FIGURE 4(b) INITIAL (A) AND FINAL (B) PITCH ANGLE TIME SERIES

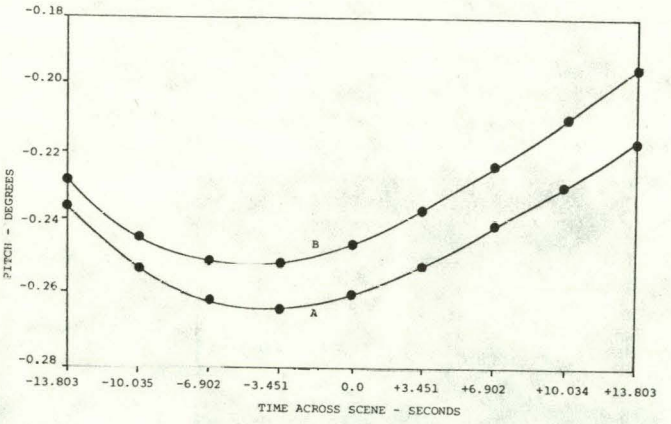

FIGURE 4(c) INITIAL (A) AND FINAL (B) YAW ANGLE TIME SERIES

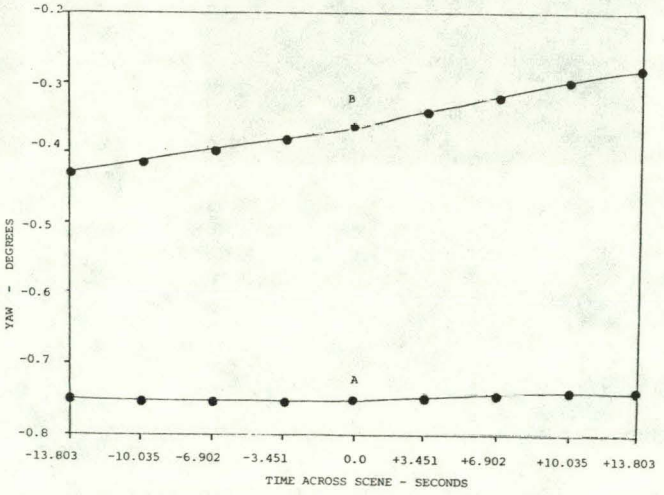

FIGURE 4

ROLL, PITCH AND YAW ANGLES ACROSS LANDSAT SCENE 1153-01463

LANDSAT AND PHOTOGRAPHIC REMOTE SENSING FOR ARID LAND APPLICATIONS IN AUSTRALIA

P.T. Tueller[1], F.R. Honey[2] and I.J. Tapley[3]

[1] Visiting Scientist, CSIRO, Division of Land Resources Management (LRM), Professor of Range Ecology, University of Nevada Reno.

[2] Research Scientist, CSIRO, Division of Land Resources Management, Private Bag, P.O., Wembley, W.A. 6014.

[3] Technical Officer, CSIRO, Division of Land Resources Management, Private Bag, P.O., Wembley, W.A. 6014.

ABSTRACT

Theme extraction (supervised classification) on data from Landsat computer compatible tapes has proven valuable for arid land application in Australia. Suitable themes are established using an unsupervised parallelepiped technique. Mapping can be accomplished with this algorithm at considerable savings in computer costs. Understanding and interpretation of the Landsat 4-band signatures allows for vegetation mapping and other uses throughout a given Landsat scene. Color aerial photographs provide suitable data for interpretation and verification.

1. INTRODUCTION

The arid regions of the world constitute a vast land resource the products of which can support only limited detailed ground inventory and analysis. For this reason arid regions lend themselves very well to study by means of remote sensing and especially to the use of space imagery evaluated by computer. In Australia the arid regions cover over two thirds of the continent. Thirty three percent of its total area lies within the arid zone (Marshall 1948) and 75% within the semi-arid boundaries (Fig. 1; Bowler 1976).

Accordingly our objective has been to study the LANDSAT computer compatible tapes along with aerial photographs and ground data to evaluate their usefullness for classifying several land and vegetation types in the arid regions of Australia. More specifically we have sought to analyze the various 4-band LANDSAT signatures in order to give resource scientists and managers a better understanding of the nature of the signature and what it means in terms of feature identification, interpretation and meaning relative to land use and resource management in the arid regions.

2. REVIEW OF LITERATURE

Numerous authors have developed data and techniques for studying wildlands, including arid rangelands, by the use of the Landsat imagery and computer compatible tapes (Driscoll 1969; Bentley 1973; Carneggie et al. 1974; Poulton 1975, Hoffer 1975, Tueller 1975). Reference is also made to the use of NASA high flight photography, Skylab photography and other large scale photography as a means of supplying ground data for analysis and interpretation of the Landsat imagery. Applications studied include vegetation mapping (Poulton 1975; Tueller 1975; Driscoll and Spencer 1972; Hoffer 1975)

evaluating range vegetation vigor and growth (Haas et al. 1975; Carneggie et al. 1974) preparing inventories of range management sites (Tueller 1975) evaluating erosion (Tueller and Booth 1975; Morrison and Cooley 1973) and assessing range fire damage (Seevers et al. 1973).

Previous work in Australia has primarily involved qualitative photo interpretation techniques for evaluating the usefullness of Landsat 1 and 2 imagery (Dawson 1975; Story et al. 1976 and Graetz et al. 1976). These qualitative investigations suggest the capability of mapping land systems, monitoring condition and mapping certain vegetation types. Graetz et al. (1976) further indicate their feeling that machine-assisted enhancement and interpretation may greatly increase the usable information.

Procedures for computer analyses of the Landsat Computer compatible tapes have been developed by numerous authors and need not be reviewed here - two papers of interest are those of Hoffer (1975) and Smedes et al. (1975). The former describes the interdisciplinary use of computer-aided analysis techniques applied to Landsat MSS data collected over a variety of wildland sites while the latter refers to precautions necessary for the computer mapping of terrain. Goldberg et al. (1975) and Goodenough and Shlien (1974) have compared Landsat computer classification procedures and recommend unsupervised classification wherein the area is first evaluated via a non-supervised approach and then as ground data is related to the spectral classes they are combined for the "modified clustering" analysis. Honey et al. (1974) have described a parallelepiped clustering technique for Landsat computer analysis that is characterized by being highly interactive, extremely rapid, flexible and low cost. Maxwell (1976) indicates the cost to classify a 1,000 square mile region at $2,000 using a stepwise discriminant analysis computer program. Using Honey's parallelepiped method, classifying and plotting the map by the computer would cost only $320, a significant saving.

3. METHODS

Four areas in the Australian Arid Zone were selected for study. These include two areas in Western Australia, Meekatharra and the Pilbara, one area in the Northern Territory, the Burt Plain near Alice Springs and the fourth in Western New South Wales in the general vicinity of Coolibah. The primary reason for their selection was the availability of ground data including aerial photographs that would be useful in our analysis and management questions of importance.

The Pilbara in northern Western Australia is an area of primarily spinifex (Triodia sp.) with occasional wattles, Kanji (Acacia pyrifolia) being one of the most common, and miles of River Gum (Eucalyptus camaldulensis) and Cadjeput (Melaleuca leucadendron) along the numerous intermittent streams. Burning of the closed community of soft spinifex in the summer months will effectively, over the long period, control the spinifex and allow for the establishment of more valuable soft grasses such as the introduced Black Bufflegrass (Cenchrus ciliaris) or Woollybutt (Eragrostis eriopoda). The area is used primarily for free ranging sheep and cattle. Many areas are being intensively mined.

The Meekatharra study site is located in central Western Australia. The vegetation can best be described as mulga scrub, other woodland types, shrublands, spinifex grasslands and other grassland types of extremely local occurrence (Speck 1963). Agricultural activity consists primarily of relatively large (several hundred thousand acre) sheep stations. For example, Meekatharra Shire has some 36 holdings running in total 190,000 sheep and 21,000 cattle. The area also supports thousands of kangaroo and the mulga woodland supplies seasonal habitat for the nomadic emu (Dromaius novaehollandiae). We planned to study emu habitat at Mileura, a station west of Meekatharra for which there is considerable ground data. However, it was not possible to obtain the CCT's from EROS in time for this study.

Our third study site was the rangelands on the Burt Plain northwest of Alice Springs. This area is primarily used for the grazing of cattle (Perry 1962). The Burt Plains represent some of the best range forage for use by cattle stations in arid Australia. Approximately 11 vegetation landform

units are recognized: Hill, gilgai, foothill fan, flood plain, calcareous shrubby woodland, foothill fan - mulga perennial grass, mulga - perennial grass, mulga - short grass, Mitchell grass, savanna woodland, open mulga woodland and spinifex. Emphasis in this study has been given to mulga - short grass, savanna woodland and Mitchell grass.

The final study area in this preliminary investigation was in the Cobar-Coolibah area of western New South Wales. This area is the least zeric and most mesic of the four study areas. Much of the area is referred to as poplar box woodland. Two tall tree species dominate the landscape Eucalyptus populnea (poplar box) and Eucalyptus intertexta. Other species commonly found as a mid tree species include Heterodendrum oleifolium (rosewood), Acacia aneura (Mulga) and Geijera parviflora. Some areas are mulga dominant while others have Callitris columellaris (native pine) either as a dominant or as part of the mid-story. Overgrazed areas have high populations of several shrubs in the sub layer: Dodonaea attenuata, D. lobulata, D. viscosa, Eremophila mitchellii, E. sturtii, Cassia artemisioides and C. nemophila. These increaser species present a woody weed problem.

Ground data available for the four sites consisted of aerial photographs at scales ranging from 1:25,000-1:62,000 with or without overlays with data, overlays prepared for 1:250,000 scale Landsat Prints and ground data keyed to these photos and to complementory planimetric maps. Landsat Computer Compatible tapes used in the study are listed in Table 1. We have used an interactive program for computer analysis of the Landsat imagery developed by one of the authors (F.R. Honey).

Sites were evaluated by first studying histograms of each of the four Landsat MSS bands in order to determine the general ranges in each of the bands. Secondly we developed appropriate shade prints for purposes of evaluating the variability in the data and to determine actual locations on the Landsat scene. The program then provides a modified parallelepiped clustering and classification algorithm. The computer decides the ranges in each of the bands for the signature, building up a table of signatures as the data is scanned.

The algorithm then scans through the pixel array, assigning each pixel to whichever of the previously generated signatures is appropriate or, if the values in each band for the current pixel do not fit into any of the signatures in the table, generating a new signature range, adding this to the table, then proceeding to the next pixel and repeating the search. When all pixels have been assigned, the signatures may be displayed and the operator may then accept the result, or request a change in the tolerance or range of each band. The user may normalize the cluster giving superior separations in hilly terrain but noisier data.

Once the cluster analysis is complete and the Landsat MSS 4-band signatures have been carefully compared a set of themes is developed, the computer then searches the areas of interest and maps according to the theme signatures. These maps constitute an approximation of scene features that may be input to management.

In order to study the Landsat MSS mean digital counts we plotted the mean vectors of the relative reflectance and compared them for each theme. As 4-band signature patterns emerged from the complexity found on these homogeneous wildland sites we began to recognize signatures that were indicative of certain arid land features. Selected signatures were described for future reference.

4. RESULTS AND DISCUSSION

For each study area the unsupervised parallelepiped cluster analysis provided good preliminary classifications of the arid landscapes. When these were compared with reasonably detailed ground information and/or aerial photographs we found good to excellent correspondence with ground features of interest. These cluster analyses of the various test sites within the general region provided numerous fourband signature which were compared and certain ones selected as themes for a supervised classification of the test areas or

on larger areas within the general test site. In some cases the resulting mean digital counts or mean vectors for several signatures were combined as a single signature to map larger areas of similar features.

In actual practice we often found that as we moved the themes to new locations within the test sites certain specific areas would not be covered by any of the existing themes. In such cases we found it necessary to do one of two things. First we would attempt to slightly alter the signatures in terms of their digital range so that they might be separated from other similar signatures that were in fact different on the ground. If this procedure still left gaps in the classification as we moved to new pixel arrays on the landsat scene it became necessary to create a new unsupervised cluster, overlay the theme and cluster arrays on a light table and use the cluster signatures to create new themes to represent the areas of interest. This tended to result in a greater number of themes than we would have desired. However, these themes we feel are quite representative of the heterogeneous wildland sites that we have investigated.

The resulting themes are described as mean reflectance values or mean digital counts and their reflectance ranges. Each theme was given a brief description relative to the ground features portrayed (Tables 2-5). In the Pilbara study area we finalized our classification with 21 themes (Table 2). The majority of the theme signatures were required to portray the variability found along the various intermittent rivers found flowing through this area of spinifex plain. For example, to cover the river sites 13 different signatures were required, four to represent the dry river bottom, river gravels and eroded areas without vegetation and the remainder (9) represent a river vegetation complex. These 9 signatures are indicative of the heterogeneity given to this relatively flat featureless landscape by the river systems.

A depiction of the spinifex plains required four signatures one of which is generally indicative of the bufflegrass areas found on the eroded areas near the major rivers. Two signatures were found for burned spinifex one of which is related to more recently burned areas. The important management implications are (i) the ability to map the river systems from the spinifex uplands and (ii) to evaluate the status of each mapping unit. Mapping of the burned spinifex approximately three times each year would be valuable in determining the success or failure of attempts to summer burn the spinifex plains for several years as a means of affecting a range improvement by enhancing the so-called soft grasses. Numerous other management features could be studied e.g., newly flooded and eroded areas could be monitored along with the resultant changes in the lowland vegetation. Also increases in woodland overstories and changes in scalded/eroded sites could be detected.

For the Meekatharra areas in the Mulga woodland of central West Australia we were able to pixel map the area almost completely with 20 different themes. A water theme was used to map standing water in lakes, stream channels and on clay pans. Associated with this were themes for river gravels, bright wet mud, wet mud and thick woodland areas associated with these areas of water accumulation. Other important themes were those associated with relative levels of vegetation density within the mulga woodland, saltbush sites such as those near Lake Annean and areas with very sparse vegetation and considerable bare soil.

One important differentiation that was made allowed us to separate areas of dark greenstone or basalt with sparse mulga from areas with heavy mulga found in stream channels. On the Landsat scene these areas appeared to have identical tone and texture. The various levels of mulga woodland and bare ground allow the mapping of areas with variable amounts of bare ground. In some instances these mulga separations are indicative of different woody species associated with the mulga. In this case there is obvious potential for evaluating areas of excellent and poor habitat for both emu and kangaroo. For example, large quantities of undesirable woody species in the mulga understory such as Cassia nemophila can be mapped and constitute a relatively poor site for sheep but good to excellent for emu.

On the Alice Springs study area we developed 9 signatures to cover two of the most important rangeland types on the Burt Plains. These were the mulga annual and savannah open woodland. This preliminary classification allowed us to map creek line vegetation, creek line floodout areas and scalded areas with bare soil found within these two plant communities. Also some of the themes indicate our interpretation of relative range condition. These are now being evaluated in a more detailed study of range condition. The theme units very closely follow interpretive vegetation units outlined on overlays of 1:25,000 scale color aerial photographs of the area.

The relative woodland component is quite sensitive to differentiation by the Landsat reflectance data. This is true for both May and November dates at Alice Springs and can prove useful for range conditon mapping and trend evaluations. If data is available within these classification units relative to range productivity then areas of similar forage production can be mapped and the average quantified.

Eleven themes were used for mapping in the Cobar-Coolibah area (Table 5). We found it relatively easy, in the first analysis, to map agricultural fields within the Poplar Box woodland. However, the signature also included grassland areas without mid and overstories of shrubs and trees. Signatures for thick mulga and native pine appeared to be strongly exclusive on 70 by 108 pixel samples. When moving to other sites we found that the native pine signature became less reliable and depicted areas of thick mulga as well as poplar box woodland with considerable shrubs in the understory.

Relatively good signature were developed for areas with heavy eucalypts, sparse woodland vegetation with considerable bare soil and areas with light and moderate shrub understory. Additional ground data will be required to accurately map areas with a known shrub component.

During the course of these investigations we have plotted several hundred 4-band signatures with and without estimated corrections for atmospheric backscatter. As one reviews the shape of these various signatures certain threads of similarity become evident. Selected uncorrected signatures have been plotted in Figures 2-5. Signatures for wet soil and water are very distinctive due to their slope toward the infrared in Landsat MSS channels 6 and 7. There are very few examples of classical forest or thick vegetation signatures with their characteristic high in channel 4, lower in channel 5 and high again in channel 6. Most of variations are a signature low in channel 4, higher in channel 5, higher yet in channel 6 and low in channel 7. Only native pine sites, heavy mulga, and thick poplar box woodland sites even approach this classical shape (Fig. 5). The grassland signature in the arid region is characterized by a flat top produced by equivalence in the 5 and 7 channel digital counts (Fig. 5). Burned spinifex plains (Fig. 2) have a signature with a high peak in channel 6 due to new green growth of post fire spinifex. The normal spinifex plains signature is much lower in the channels 5 and 6. Often differences are very subtle, e.g., the signatures for thick mulga woodland and sparse mulga on dark rock (Fig. 3) are very similar in shape departing primarily in channels 6 and 7. Likewise the comparison of open woodland signatures for sites in good and poor condition shows them to be only slightly different (Fig. 4).

5. CONCLUSIONS

Feasibility has been shown for utilization of the Landsat computer compatible tapes for mapping arid land vegetation resources in Australia. In fact potential has been shown for mapping vegetation and related resources at a level refined beyond that recognised for many uses. A combination of supervised and unsupervised classification is optimum for arid applications. The parallelepiped clustering algorithm is a powerful tool for separating and mapping these resources. Possibly the greatest advantage lies in the cost factor wherein we have found that arid land areas can be mapped at only 1/6th the cost of more computer-time-requiring algorithms such as stepwise discriminant analysis.

Our mapping has been accomplished after the data has been spatially filtered. This procedure of course modifies the grey level of a given pixel by averaging them with the surrounding pixels. The net result is a smoothing which reduces noise and provides maps of vegetation features that are similar to those derived by photo interpreters as they draw lines on aerial photographs.

Aerial photographs provide ground data for Landsat computer applications. Color or color infrared photographs at scales near 1:25,000 are useful for near direct comparisons with the computer grey maps.

The supervised or theme classification is somewhat difficult to use in the arid land context. Large areas of relatively homogeneous desert or woodland vegetation require only a few theme signatures for complete mapping. However when the computer scans an area of much greater heterogeneity such as a stream channel or upland site the number of themes quickly become inadequate and many gaps are left. In these instances it has been necessary to create what might be termed a "complex of themes" in order to adequately map these heterogeneous areas. For example this was required to map the vegetation along the intermittent streams in the Pilbara. These computer generated mapping complexes await further interpretation and comparison with more detailed ground data.

When mapping on a given Landsat scene on a given date atmospheric corrections are not absolutely necessary. As dates and scenes are compared it becomes paramount to make detailed atmospheric corrections. A strong data base for this purpose is not yet available in arid Australia. Winter tapes at low sun angle also give significant shadow effects which tend to obscure ground feed in shrub and tree communities.

Landsat 4-band signatures assume shapes characteristic of specific arid land features to be used in mapping. These signatures when atmospherically corrected tend to hold true over large areas and can be used again and again for arid land applications.

Arid land applications include mapping of discrete plant communities, land forms, standing water, areas of recent inundation and areas of bare soil. Also fence lines, bores and areas in different range condition can be mapped. With further analysis and the use of ratioing techniques we feel it will be possible to monitor range trend, vegetation phenology and areas with active erosion.

6. ACKNOWLEDGEMENTS

The senior author wishes to acknowledge his sabbatical leave from the University of Nevada Reno.

7. REFERENCES

1. Bentley, R.G. 1973. Predicted ephemeral and perennial range quantity and quality during normal grazing season. Goddard Space Flight Center Type III Report. Contract No. S-70243-AG.

2. Bowler, J.M. 1976. Aridity in Australia: Age, Origins and Expression in Aeolian Landforms and Sediments. Earth-Science Reviews 12, 279-310.

3. Carneggie, D.M., DeGloria, S.D. and Colwell, R.N. 1974. Usefulness of ERTS-1 and supporting aircraft data for monitoring plant development and range conditions in California's annual grassland. Remote Sensing Program, School of Forestry and Conservation, University of California Berkeley. Report submitted to the Bureau of Land Management, U.S. Department of the Interior, 53 pp. Contract No. 53500-CT3-266(N).

4. Dawson, N.M. 1975. Rangeland resource surveys for farm and regional development in Queensland. Proceedings of the Seminar. Evaluation and Mapping of Tropical African Rangelands. Bamako, Mali. pp. 83-93.

5. Driscoll, R.S. 1969. The identification and quantification of herbland and shrubland vegetation resources from aerial and space photography. Am. Prog. Report Remote Sensing Applications in Forestry. For. Earth Resources Survey Program. OSSA/NASA, by U.S.F.S. Rocky Mountain Forest and Range Experiment Station, 55 p.

6. Driscoll, R.S., and Spencer, M.M. 1972. Multispectral scanner imagery for plant community classification. 8th International Symposium on Remote Sensing of Environment. Vol. II. pp. 1259-1278. Ann. Arbor. Oct.

7. Gentilli, J. 1972. Australian Climatic Patterns. Nelson, Melbourne. 285 pp.

8. Goldberg, M., Goodenough, D., and S. Shlien. 1975. Classification methods and error estimation for multispectral scanner data. Proceedings 3rd Canadian Symposium on Remote Sensing. pp. 125-143.

9. Goodenough, D., and Shlien, S. 1974. Results of cover-type classification by maximum liklihood and parallelipiped methods. Proceedings 2nd Canadian Symposium on Remote Sensing. Vol. 1, 136-164.

10. Graetz, R.D., Carneggie, D.M., Hacker, R., Lendon, C., and Wilcox, D.G. 1976. A qualitative evaluation of Landsat imagery of Australian rangelands. Aust. Rangel. J. 1, 53-59.

11. Haas, R.H., Deering, D.W., Rouse, J.W. Jr. and Schell, J.A. 1975. Monitoring vegetation conditions from Landsat for use in Range Management, 1975. Proceedings NASA Earth Resources Symposium. Houston, Texas. 507-568.

12. Hoffer, R.M.(Ed). 1974. Natural resource mapping in mountainous terrain by computer analysis of ERTS-1 satellite data. Research Bulletin 919. LARS, Purdue.

13. Honey, F.R., Prelat, A., and Lyon, R.J.P. 1974. Stansort: Stanford Remote Sensing Laboratory Pattern Recognition and Classification System. Proceedings Ninth International Symposium on Remote Sensing of Environment. Ann. Arbor. pp. 897-905.

14. Mabbutt, J.A. 1969. Landforms of arid Australia, in Statyer, R.O., and Perry, R.A.(Eds), Arid Land of Australia. (A.N.U.P., Canberra), 11-32.

15. Marshall, A. 1948. The size of the Australian desert. Aust. Geogr. 5, 168-175.

16. Maxwell, E.L. 1976. A remote rangeland analysis system. J. Range. Mgmt. 29(1), 66-73.

17. Morrison, R.B., and Cooley, M.E. 1973. Applications of ERTS-1 multispectral imagery to monitoring the present episode of accellerated erosion in southern Arizona. Symposium on Significant Results Obtained from ERTS-1. Vol 1: Sect. A. NASA, Washington, D.C.

18. Otterman, J., and Fraser, R.S. 1976. Earth-Atmosphere System and Surface Reflectivities in Arid Regions from Landsat MSS Data. Remote Sensing of the Environment. 5(4), 257-266.

19. Perry, R.A. (Compiler). 1962. Lands of the Alice Springs Area, Northern Territory, 1956-57. CSIRO, Land Research Series No. 6.

20. Poulton, C.E. 1975. A comparative interregional analysis of selected data from Landsat-1 and EREP for the inventory and monitoring of natural ecosystems. Proceedings NASA Earth Resources Symposium. Houston, Texas. 507-568.

21. Poulton, C.E. Schrumpf, B.J., and Garcia-Moya, E. 1971. A preliminary vegetational resource inventory and symbolic legend system for the Tucson-Wilcox-Fort Huachuca Triangle, Arizona. "Monitoring Earth Resources from Aircraft and Spacecraft". NASA, Wasington, D.C. pp. 93-108.

22. Seevers, P.M., Jensen, N., and Drew, J.V. 1973. Satellite Imagery for assessing range fire damage in the Nebraska Sandhills. J. Range. Mgmt. 26(6), 462-463.

23. Smedes, H.W., Hulstrom, R.L. and Panson, K.J. 1975. The mixture problem in computer mapping of terrain: improved techniques for establishing spectral signatures, atmospheric path radiance, and transmittance. Proceedings NASA Earth Resources Symposium. Houston, Texas. June pp. 1099-1159.

24. Speck, N.H. 1963. Vegetation of the Wiluna-Meekatharra Area. Part VII of Lands of the Wiluna-Meekatharra Area, Western Australia. CSIRO Land Research Series No. 7, 143-161.

25. Story, R., Yapp, D.A., and Dunn, A.T. 1976. Landsat patterns considered in relation to Australian resource surveys. Remote Sensing of Environment 4, 281-303.

26. Tueller, P., and Booth, D.T. 1975. Photographic remote sensing techniques for erosion evaluations on wildlands. Final Report to U.S. Deptartment of the Interior. Bureau of Land Management. Contract 08550-CTS-2. 97p.

27. Tueller, P.T., Halvorson, R.M., Lorain, G., and Ratliff, J.M. 1975. Mapping vegetation in the Great Basin from ERTS-1 imagery. Proceedings American Society of Photogrammetry, Washington, D.C. pp. 388-370.

Table 1. Australian Arid Region Tapes used in the study.

Alice Springs	#1102-00311	02 Nov 72
	#1301-00371	20 May 73
Meekatharra	#2108-01175	10 May 75
Bourke	#1145-23360	15 Dec 72
Pilbara	#2073-01214	05 Apr 75
Broken Hill	#2198-23410	08 Aug 75

Table 2. Themes, mean reflectance values and reflectance ranges as signatures for the Pilbara area.

THEMES	Landsat MSS Channel 4	5	6	7
River Vegetation Complex	30.5 *	51	50	20
	28-33	44-58	45-55	18-22
River Vegetation Complex	24	38	45	16
	22-26	33-43	40-50	15-17
River Gravels or Bright Soil	29	55.5	64	25
	27-31	47-64	57-71	23-27
Burned Spinifex	21	45	55	22
	18-24	35-55	50-60	20-24
Bright Spinifex Plains	17	27	30.5	11
	15-19	22-32	26-35	9-13
Brighter Spinifex Plains	20	43	50	18.5
	18-22	36-50	40-60	17-20
Spinifex Plains	16	37	42.5	15
	14-18	30-44	35-50	13-17
Scalded/Eroded	24	58	63	23
	21-27	51-65	56-70	21-25
Buffle Grass or Darker Spinifex	20.5	33	42	15.5
	18-23	26-40	35-49	14-17
Woodland Vegetation	16.5	31	40.5	12
	15-18	24-38	35-46	10-14
River Bottom Eroded	24	43	53	19
	22-26	37-49	97-59	17-21
River Gravels	33.5	45.5	73.5	28
	31-36	60-71	69-78	27-29
River Vegetation Complex	24	44	60.5	25
	23-25	41-47	59-62	24-26
River Vegetation Complex	72.5	36	46	18.5
	21-24	33-39	42-48	18-19
River Gravels or Bright Soil	33	63	70.5	27.5
	32-34	60-66	69-72	26-29
River Vegetation Complex	28	51	55	22
	26-30	41-61	50-60	21-23
River Vegetation Complex	26	45	49	18
	24-28	40-50	44-54	16-20
River Vegetation Complex	23	39	42	15
	21-25	34-44	37-47	13-17
River Vegetation Complex	26	45	44	15
	24-38	40-50	39-49	13-17
River Vegetation Complex	27	46	53	23
	24-30	35-57	48-58	22-24
Bright Burned Spinifex	20	46	62	22
	18-22	40-52	57-67	20-24

* Mean Landsat Digital reflectance with ranges below

Table 3. Themes, mean reflectance values and reflective ranges as signatures for the Meekatharra area.

THEMES	Landsat MSS Channel 4	5	6	7
Thick Mulga Woodland	11*	21	27	11.5
	9-13	16-26	21-33	10-13
Sparse Mulga on Dark Rock	11	20	23	7.5
	9-13	15-25	17-29	6- 9
Whitestone Cobble	15.5	30	38.5	13
	13-18	24-36	34-43	10-16
Sparse Mulga/Considerable Bare Soil	15	36	44	18
	13-17	31-41	40-48	17-19
Intermediate Mulga	12	21	31	14
	10-14	16-26	27-35	13-15
Saltbush or Sparse Mulga	12	23	32	15.5
	11-13	18-28	26-38	14-17
Wet Claypan with large trees	9.5	11	14	6.5
	8-11	7-15	5-23	4- 9
River Gravels	16	39	51.5	18
	15-17	35-43	48-55	16-20
Water	12	17.5	9	1.5
	9-15	9-26	0-18	0- 3
Sparse Mulga Bright Soil	21	40	51	20
	19-23	35-45	45-57	18-22
Wet Mud or Thick Woodland	15	29.5	29	8
	13-17	23-35	21-37	5-11
Sparse Mulga/Considerable Bare Soil	18	39	40.5	18
	16-20	34-44	34-47	15-21
Bright Wet Mud	13	24	19.5	4
	11-15	19-29	13-24	1- 7
Intermediate Mulga	12	22	37	18
	10-14	17-27	29-45	16-20
Sparse Mulga/Considerable Bare Soil	16	32	38	18
	14-18	27-37	30-46	16-20
Sparse Woodland	15	29	28.5	12
	13-17	24-34	23-34	9-15
Thick Mulga	10	13	19.5	11
	8-12	10-16	15-24	9-13
Sparse Woodland	12	28	37	13
	11-13	24-32	32-42	11-15
Sparse Mulga Bright Soil	24	49	60.5	23.5
	21-27	38-60	54-67	22-27
Bright Soil or River Gravels	19	38	47.5	18
	17-21	31-45	40-55	16-20

* Mean Landsat Digital reflectance with ranges below

Table 4. Themes, mean reflectance values and reflectance ranges as signatures for the Alice Springs study area.

THEMES	Landsat MSS Channel 4	5	6	7
Open Woodland Good Condition	48.5*	64	63	28
	46-51	58-70	58-70	26-30
Open Mulga Woodland	43	59	59	26
	41-46	53-65	54-64	24-28
Fair Condition Open Woodland	43.5	65	68.5	29
	41-46	59-71	64-73	27-31
Mulga Woodland in depressions	41	49.5	51	22.5
	38-44	43-55	46-56	21-24
Poor Condition Open Woodland	50	67.5	70	32
	46-54	60-75	64-76	30-34
Poor Condition (Bare) Open Woodland	43	64	60	29.5
	40-46	58-70	56-64	28-31
Scalded Areas Bare Soil	54.5	81.5	74.5	33.5
	44-61	76-87	65-84	31-36
Creek Line Floodouts	52.5	67	64	30
	51-54	62-72	59-69	27-30
Creek Line Tree Vegetation	55.5	71.5	67	32
	54-57	67-76	62-72	30-34

* Mean Landsat Digital reflectance with ranges below.

Table 5. Themes, mean reflectance values and reflectance ranges as signatures for the Cobar-Coolibah study area.

THEMES	Landsat MSS Channel 4	5	6	7
Heavy Eucalypt	36*	41	52.5	19
	32-40	32-50	45-60	18-20
Thick Mulga	33	37	38	17
	30-36	31-43	31-45	15-19
Native Pine	30	30	37	19
	26-34	24-36	29-45	17-21
Sparse Vegetation #2	40	51	50	23
	36-44	44-58	42-58	21-25
Brighter Heavy Vegetation Heavy Shrub	32	40.5	44	19.5
	28-36	36-45	36-52	17-22
Agricultural Fields and Grassland	40	62	63	26
	37-43	53-71	54-72	24-28
Sparse Vegetation/ Considerable Bare Soil	47	66	68	29
	42-52	61-71	64-72	27-31
Moderate Tree Overstory Low Shrub	34	43	52	20.5
	30-38	41-45	44-60	18-23
Sparse Vegetation #1	42	63	62	23
	38-46	56-70	54-70	21-26
Light Shrub Understory	33.5	52.5	51.5	24.5
	31-36	47-58	44-59	23-26
Mod Shrub Understory	32.5	40.5	48	23
	29-36	36-45	43-53	21-25

* Mean Landsat Digital reflectance with ranges below.

FIG. 1.
THE LOCATION OF 7 STUDY SITES WITHIN THE ARID REGION OF AUSTRALIA

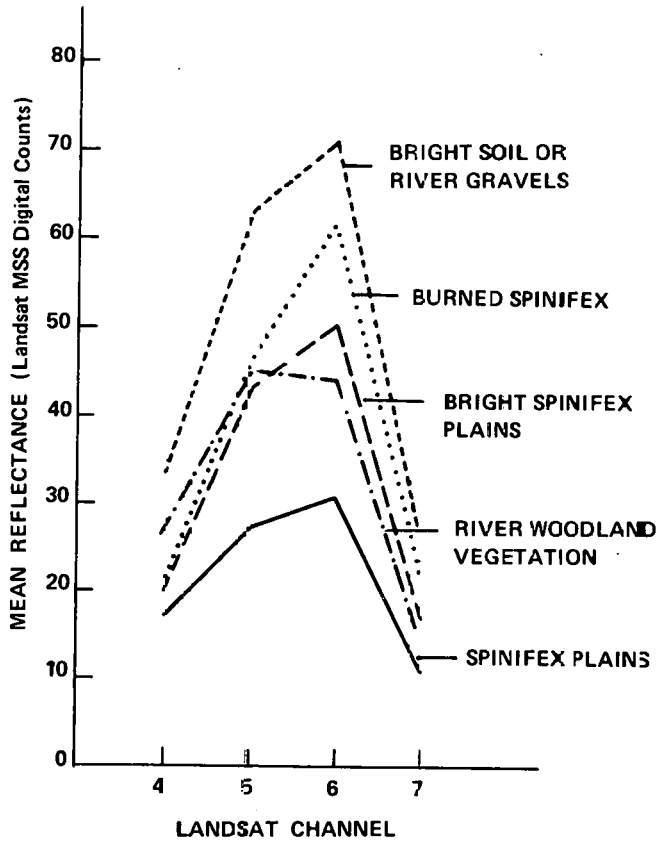

FIG. 2

LANDSAT 4-BAND SIGNATURES FOR SELECTED FEATURES IN THE AUSTRALIAN ARID REGIONS – PILBARA

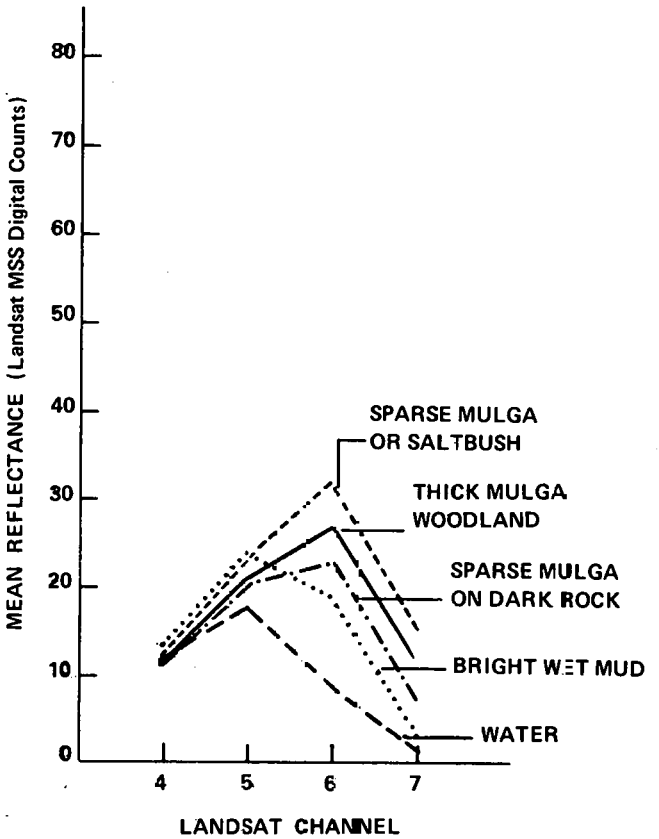

FIG. 3

LANDSAT 4-BAND SIGNATURES FOR SELECTED FEATURES IN THE AUSTRALIAN ARID REGIONS – MEEKATHARRA

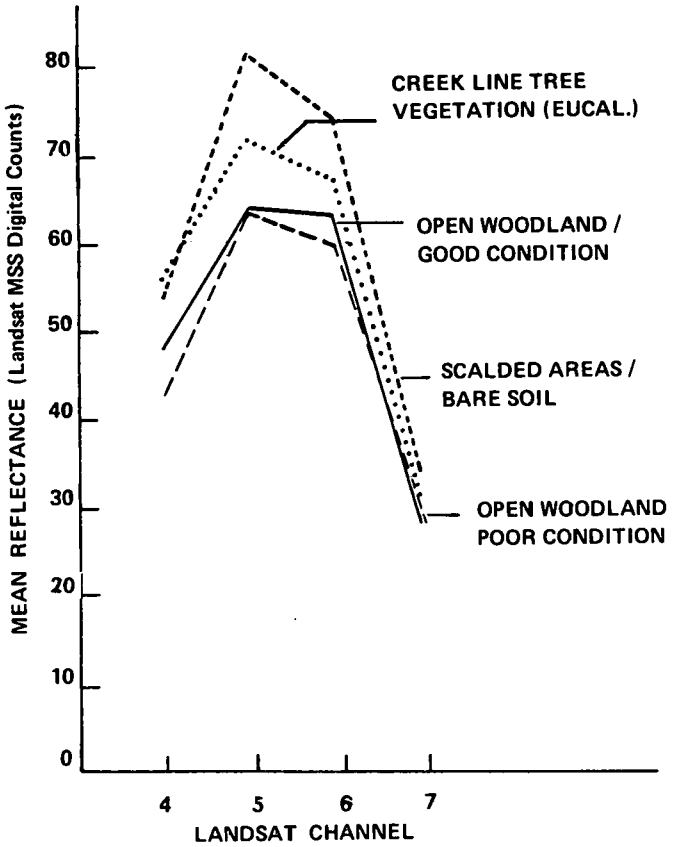

FIG. 4
LANDSAT 4-BAND SIGNATURES FOR SELECTED FEATURES IN THE AUSTRALIAN ARID REGIONS – ALICE SPRINGS

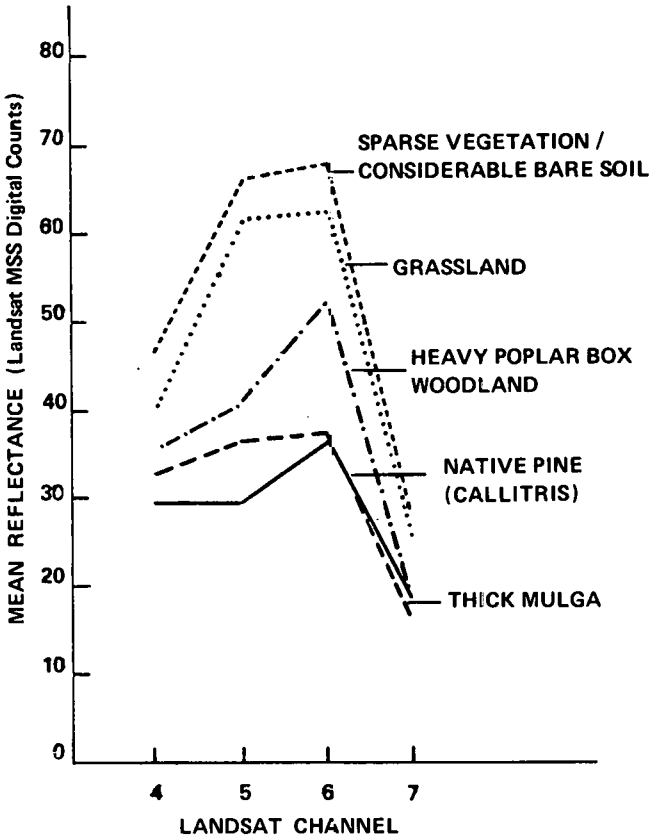

FIG. 5
LANDSAT 4-BAND SIGNATURES FOR SELECTED FEATURES IN THE AUSTRALIAN ARID REGIONS – COBAR – COOLIBAH

THIS PAGE

WAS INTENTIONALLY

LEFT BLANK

A SYSTEM FOR THE COHERENT PROCESSING OF REMOTE SENSING IMAGERY

J. C. Lummaux and S. Braconne

Institut Géographique National
PARIS, FRANCE

ABSTRACT

An image processing system is described which, starting with digital remote sensing data, produces either a thematic interpretation or a general map product. Specific results are described concerning forest fires studies, town planning, revision elements for topographic maps in France and Africa. Finally the advantages are shown of using an interactive image processing system such as the 101 system at the Institut Geographique National particularly the fundamental role played by the display console.

---

1 - Introduction :

The IGN's function is to establish the basic series of topographical maps for France. As a result of its long experience and of the technical facilities at our disposal today, IGN prepares various series of specialized maps in France or abroad and undertakes to establish the cartography of underdeveloped countries.

Remote sensing is one of the means which has been responsible for significant progress. In these domains IGN has perfected a method of analysing and processing images which can be used systematically at every stage of cartographic production.

To do this, it was necessary to design computer programs which could be adapted to any particular problem. An effort was made to keep calculation time, and therefore cost, at a minimum and finally, the result of each program was to produce a printable cartographic document.

The system was perfected with a 101 System made by I2 S. All of the studies that we will treat here were made using this system.

We are going to present the most important programs developed with this system to show some applications both to thematic surveys and to general cartography and finally, we will see to what extent these programs can be introduced into the traditional production of general maps.

2 - Automatic interpretation chain

The system of automatic interpretation was designed to produce printable thematic maps.

To achieve this result, the traditional data processing methods follow a two step process :

- Classification by uniquely statistical methods
- Regularisation

This approach is expensive and inefficient because it requires a very long calculation time. It uses methods which were designed in the past for applications unrelated to image analysis and it does not take into account the structures revealed by remote sensing.

We have thus developed algorithms of classification, regularisation, structure analysis and contour tracing, which are specifically adapted to the findings of remote sensing and which constitute a coherent system in which each stage of the work prepares the following stage so that the calculation time is reduced to a minimum.

a) Classification

Two classification programs (supervised and unsupervised) were developed ; the supervised program was employed especially in making land use maps, while the unsupervised programs were mainly used in preparatory work.

The algorithm use consists of scanning an image and of assigning a point to the class if any, which is spectrally the most numerous in its vicinity ; the degree of proximity can be varied by different thresholds as is most suitable.

A new class has to be created if the point is too far from the classes already existing, either spatially of spectrally (in the part of the image which has already been treated).

This method offers a double interest :

- The result is obtained by a single scan of the image, the priority accorded to vicinity having reduced the number of operations to be performed. Experience shows that neither the initial point of the scanning nor its direction have any appreciable influence on the results.

- The classification obtained shows homogeneous zones because priority is given not to distances in the space of wavelengths but to geometrical proximity. The resulting image is thus easily interpretable.

From this principle a two stage method of supervised classification was derived :

- A choice of test-zones, preferably homogeneous and a non supervised classification within these zones in order to pick out the characteristic centers of the themes.

- Using as a basic the file of centers thus created, classification of the total image using the investigation of vicinity to minimize research time, as was done before.

The advantage of this method is that it greatly shortens the time necessary for calculation.

b) The results of supervised classification are not directly usable in map making for two reasons :

- Confusion between objects of different nature is possible.
- Spatial homogeneity of the classes is too weak.

These problems are resolved by two types of programs :

- A process of elimination which consists of suppressing one class and replacing it by the class which is best represented locally. Thus ambiguous centers can be eliminated.

- A process of regularisation locally modifies the classification of a point if in its vicinity there is a group which is represented beyond the limit that has been fixed as a parameter.

Thus are eliminated any gaps in the interior of the homogeneous zone or any isolated points which can be considerated as "noise", while preserving those which are significant (for example a road which appears sporadically in the middle of a forest).

One obtains thus a mask which is already printable that is to say its contour can be defined for an outline map either used directly in a printing process, or designed on a drawing board.

Other operations upon this thematic mask are possible as well. These involve essentially the analysis of structure.

c) The analysis of structure consists of using the mask thus obtained to define for each componant a group of indications which characterize its size, its shape, its compacity. These indicies then allow one either to measure the surface of a theme or to extract the elements of a determined form (and by that to eliminate impossible shapes).

3 - Tries and results.

a) The first operational tests of the processing system just described took place at the request of the Ministry of Agriculture as part of an exhaustive study of forest fires in the south of France during the year 1976. We had to determine their number, to situate them exactly and for each of them to furnish precise statistics concerning the surface covered.

The following process was used : on the original LANDSAT image (Picture 1 - NIMES), using information furnished by fire-fighting brigades, one or several burnt-out areas were chosen as test zones in order to make a supervised classification of the whole image.

Other carefully selected test zones were added in order to separate as well as possible what resulted from burning from what had a rather similar spectral appearance (for example towns or rock-out croppings). Several tests were made on a small part of the image including a fire damaged zone that had been well studied in order to determine as efficiently as possible the threshold which fixes the distances between classes. Processing was thus initialized and then applied to most important parts of the image corresponding with areas of interest (pictures 2 and 3). In consequence following results could be provided:

1 - An accurate localization of fires
2 - A square measure with a better precision than existing data
3 - As far as programs permit an estimation of the nature of burned growths.

b) This aforesaid method has been also successfully applied to obtain three kinds of mask in Paris country.

1 - Mask of woods without any distinction between species
2 - Mask of inhabited areas, divided into three classes of density of population, from old Paris center to suburban houses
3 - Mask of cultures with generating outlines of great homoneneous fields.

c) Below these processings a few operations are necessary to get in the end a perfect cartographic product : Such as geometric corrections both to put the generated images into a given projection (U. T. M., Lambert) and to correct defects due to recording conditions (systematic errors or random irregularities).

Then a model of the final map is made and the printer is given a trichromatic selection, just fit for use in offset process.

Such a work has been performed to the very end to produce a 1:250 000 scale experimental photomap of Sudan with intensified details (for example rivers). The model was generated on the TV colour screen of the 101 system ; then its three basis colours separated which permits printing without any further reproduction's works.

To project images two different methods are used : a standard digital one interpolation and an orthophotographic one with the aid of a wild OR - 1 machine, which is better cheap for calculation time is more expensive. The last method was used for a Landsat images mosaic of Corsica.

4 - Conclusion

All these operations raise to a maximum utilization of existing instruments and processing up to square in the best way with classical production chains, as also the whole power of 101 system bought by I.G.N. in year 1977, which possibilities are enough supple and iteractive to provide user's wants as to be adapted to other parts of production.

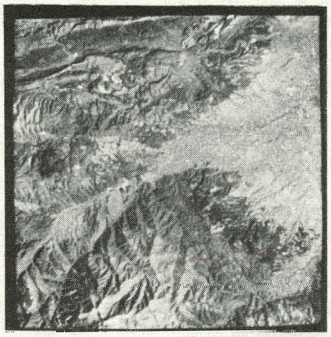

Picture One

Original Landsat view over
South of France

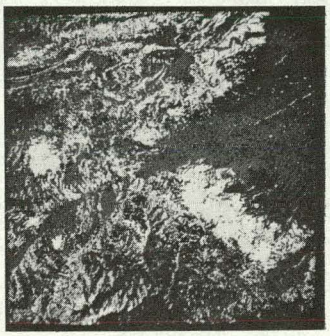

Picture Two

After supervised classification
(test-zones in burnt areas)

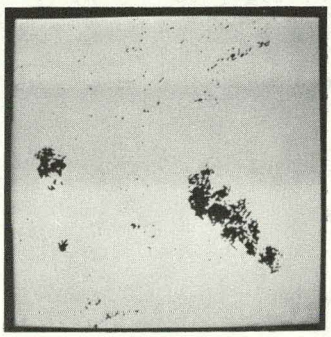

Picture Three

Mask of forest fires theme
after regularisation

All pictures are black and white
photographies of 101 system's color screen

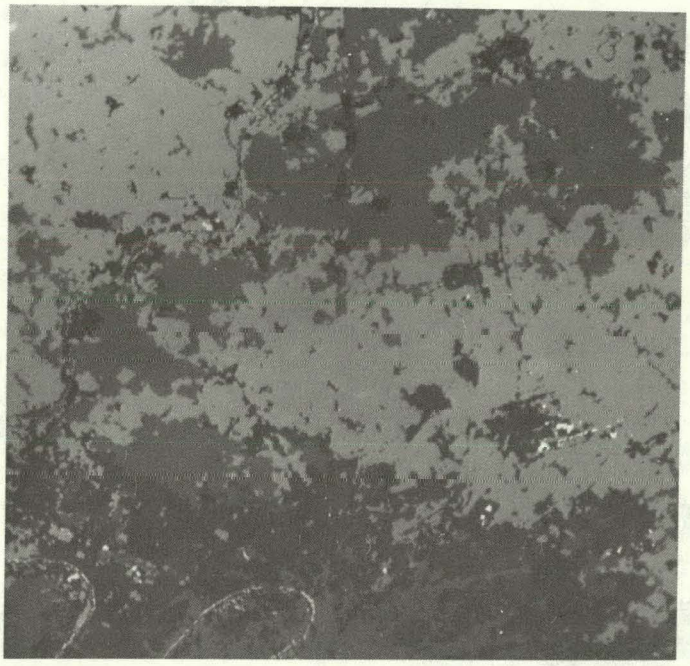

Picture Four

Masks of woods , inhabited areas and cultures

in Paris country

THE VARIED APPLICATIONS OF SATELLITE REMOTE SENSING PRACTICED BY THE FEDERAL INSTITUTE OF GEOSCIENCES AND NATURAL RESOURCES OF THE FEDERAL REPUBLIC OF GERMANY

R. Mühlfeld

Federal Institute of Geosciences and Natural Resources
Hannover, Federal Republic of Germany

The major tasks of the Federal Institute of Geosciences and Natural Resources consist of support for mineral, fuel- and groundwater exploration, as well as investigations into the quality and distribution of soils and improvement of their use for sustained production in agriculture and forestry. Many activities in these fields are connected with technical aid projects in developing countries.

Satellite remote sensing has been used since satellite images were available on the basis of a close cooperation with NASA and the U. S. Geological survey. The aim was to support the above mentioned activities. In consequence satellite remote sensing (mostly as Landsat images and to some extent also Landsat digital data) was applied to a considerable variety of projects, both with regard to disciplines and objectives as well as to geographical regions and climatic conditions.

The most simple but effective use of Landsat images was as a topographical basis for a geological and geochemical study of a 120 000 sqkm area in the Sudan. The available topographic map (scale 1 : 250 000) proved inadequate for the task. A Landsat mosaic showed enough detail for the planning of the field trips (scale 1 : 500 000) and for the indexing of samples (scale 1 : 250 000). Without Landsat a topographic map on the basis of aerial photographs would have had to be prepared at a much higher cost.

Linear structures have been investigated in several different regions. Even in a geolocically well known area like Germany, structural information derived from Landsat could be used as a guide for mineral exploration (HOPPE 1974). A similar study was done in Morocco. In crystalline rocks of the Sahel zone in Upper Volta and Niger, linear structures were mapped as the most suitable locations for groundwater wells.

An investigation of a large region on the Canadian Shield showed some results despite the adverse natural conditions (thick glacial till, heavy forest cover). Information on lithology was very poor. However the linear tectonic features could be worked out in good detail in a northern and southern belt, less completely in the interim area due to the heavy cover of glacial deposits and forests (Fig. 1). Nevertheless, mining geologists could use about one third of the linear structures mapped on Landsat imagery as a guide for mineral prospection within prospective areas.

In the Sahel Zone of Niger and Upper Volta Landsat images have been evaluated for a variety of closely related purposes. The first step was preparation of a geologic map. It shows an improvement of the present knowledge especially in the Precambrian crystalline rocks of the Niger Shield with hints for mineral prospection. In the sediments of the Western Niger Republic indications of hitherto unknown groundwater reservoirs have been found. In both areas the geologic map was an important aid for the pedologic evaluation of the satellite imagery. The result was a combined soil and land capability map. Ten different units could be discriminated (Tab. 1). In addition, observations could be made on population density,

distribution of agricultural activities and damage to the natural environment. A map could be prepared showing overused areas and areas where the natural potential is not fully used. (Fig. 2). These observations can be repeated in short time intervals for monitoring purposes. Thus, satellite remote sensing is a powerful tool for the improvement of living conditions, (planning and control of future developments) and for protection against damage to the natural environment in many developing countries.

The Landsat study of a sedimentary basin in Eastern Asia offered the possibility to follow sedimentary rocks over long distances even under a cover of tropical forests. In this way it was possible to observe changes in thickness and facies of the rocks and to correct an inaccurate stratigraphic correlation. The result was an important change regarding the assessment of the petroleum and gas potential of a rather large area.

In an area of the Argentine Pampa the distribution of salinity in the near surface groundwater was investigated with chemical analysis of many groundwater wells and with geoelectric measurements. It was found that groundwater in areas with a high groundwater table shows a high salinity due to strong evaporation and evapotranspiration. Groundwater in areas with a low groundwater table has a low salinity due to a lack of evaporation. By comparison with Landsat and Skylab images a correlation was established between the vigour of the vegetation and the salinity of the near surface groundwater. With Landsat images it is now possible to extend the investigation over large areas at less cost. The expensive ground survey of waterwells and geoelectrical measurements can be considerably reduced (KRUCK 1976).

Multitemporal evaluation and even more so, monitoring of large areas can be very time consuming. This calls for the use of the computer in classification and mapping. The quality of classification also can in certain cases be improved by computer methods. For these reasons the Federal Institute is developing skills in computer classification techniques. So far experience has been gained in arid and semiarid climatic conditions. In semiarid regions it was possible to discriminate vegetation on irrigated areas from dry farming areas and natural vegetation. The type and intensity of vegetation could also be used to discriminate between rock types and soil units. In arid regions several rock types could be discriminated, even with unsupervised methods.

The projects described in outline above, show a considerable variety in the use of satellite remote sensing. In addition to the specific results obtained, some general experiences have been made with these activities. Information on geology, soils, land use, groundwater, can be derived from Landsat imagery mainly through indirect reasoning. The quality of the results depends largely on the interpreter's understanding of the complete ecology of the area under investigation. Especially important is a knowledge of the composition and seasonal behavior of the vegetation cover, natural vegetation as well as field crops and cultivated forests. This comprehensive approach in Landsat evaluation can be most effectively achieved in multidisciplinary projects. The representatives of the different disciplines involved can support and supplement each other when preparing their specific products.

Multitemporal (multiseasonal) images are in many cases an important aid for evaluation. When vegetation is involved, the time space for the observability of a particular feature may be as short as a couple of days. This underlines the need to increase the number of satellites with technical equipment, compatible with that of the Landsat system. Also the need for real time transmission of the data becomes obvious.

References:

HOPPE, P.: Relationship between the tectonic lineaments and ore districts in the eastern part of the Rhenish Massif compiled from interpretation of ERTS-imagery. - NASA SR No. 328. Type III Report, 1974

KRUCK, W.: Hydrogeological Investigations in the Argentine Pampa using satellite imagery. - Geologisches Jahrbuch A 33, Hannover 1976

Legend

1 Area with good indications of the geological underground on LANDSAT images

2 Area with poor indications of the geological underground due to vegatation cover and/or glacial features

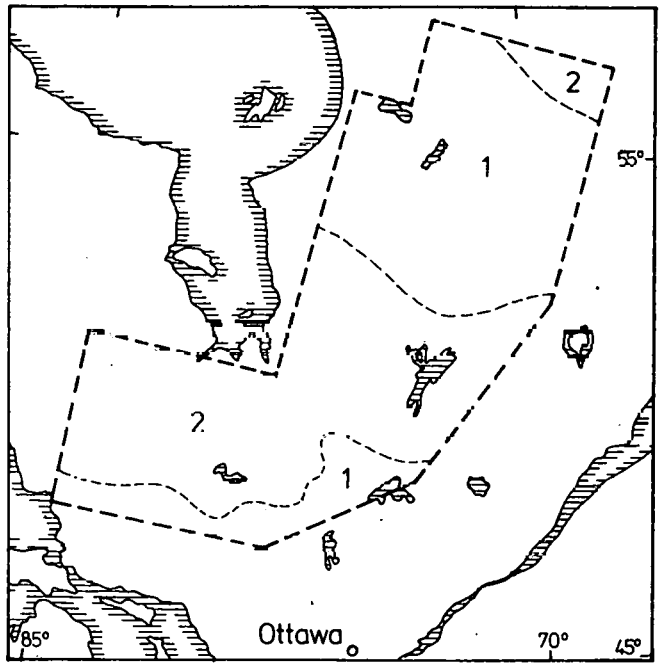

Figure 1. LANDSAT STUDY AREA ON THE CANADIAN SHIELD

Legend

relatively underpopulated

relatively overpopulated

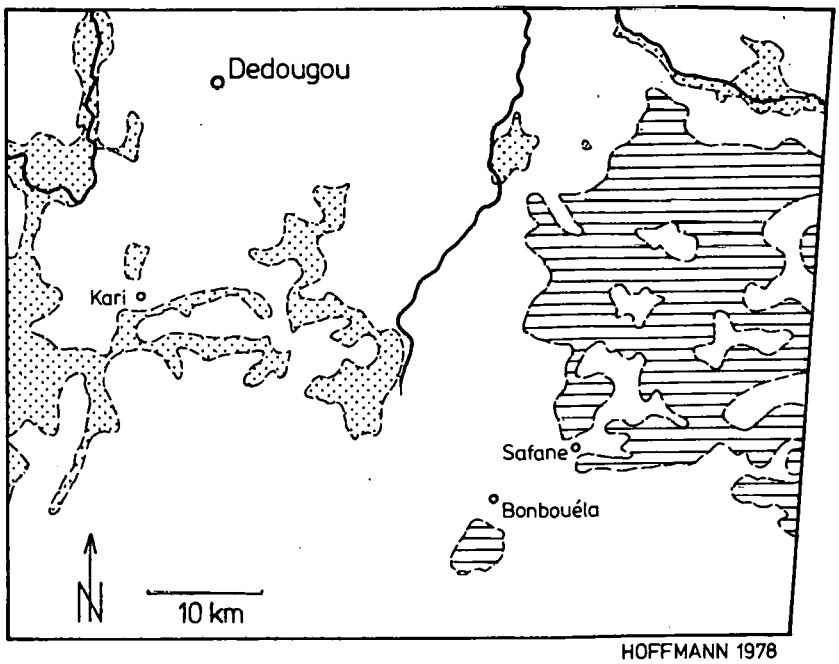

Figure 2. UPPER VOLTA MAP OF POPULATION DENSITY RELATIVE TO SOIL QUALITY (MAP SECTION)

Figure 3.

AREAS OF DIFFERING GROUND WATER SALINITY

75 km SW OF SANTA FE, ARGENTINA

UI - U IV show different salinity of ground water

Soils	Rock Types	Morphology	Potential Land use
1. Raw mineral soils on iron rich layer	plinthite, laterite	peneplain remnants	Not suitable for agriculture and grazing
2. Weakly developed soils	crystalline	rolling country	Limited agriculture only, as shallow foundation grazing use is possible
3. Soils rich in sesqui oxides	crystalline	rolling country	Agriculture possible, in parts a good yield potential, where deeply founded; grazing usage good
4. Hydromorphic soils	crystalline alluvium	broad valleys	Good agricultural area
5. Brown eutrophic soils	crystalline	highlying rolling country	Good agricultural area
6. Raw mineral soils	sandstone	peneplain remnants	Limited grazing use
7. Weakly developed soils	sandstone	rolling country, hilly in parts	Grazing usage, limited agriculture
8. Soils rich in sesqui oxides	sandstone	rolling country	Agriculture possible - good
9. Mixed sesqui oxide and brown eutrophic soils	sandstone	flat	Agriculture good
10. Hydromorphic soils	sandstone	flat	Agriculture good, in parts intensive farming.

TABLE I UNITS OF UPPER VOLTA SOIL AND LAND CAPABILITY MAP

INCREASED VISIBILITY FROM THE INVISIBLE
A COMPARISON OF
RADAR AND LANDSAT IN TROPICAL ENVIRONMENTS

R.H. Gelnett*, L.F. Dellwig** and J.E. Bare***

ABSTRACT

The unique capability of side looking airborne radar in recording terrain data essentially regardless of daylight or weather conditions has been sufficient justification for its utilization in cloud shrouded areas throughout the world, particularly when there is a critical time factor or a need for specific seasonal coverage. In geologic exploration, RADAR imagery has often been considered for utilization only if LANDSAT imagery or aerial photographs are not available. However, imaging in a segment of the electromagnetic spectrum other than the visible and near infrared portions should be expected to provide information supplemental to other kinds of imagery.

A comparison of LANDSAT and RADAR images in several areas substantiates this expectation. Specifically:

1. Because RADAR senses microrelief or surface configuration and dielectric properties of vegetation rather than degree of vigor as in near infrared imagery, any initial classification is supplemented and a level of discrimination not otherwise obtainable is realized.

2. Linear and curvilinear geologic elements identifiable on both LANDSAT and RADAR imagery can be more precisely defined on RADAR imagery. Furthermore, even some major linear features may be well defined on RADAR imagery although not identifiable on LANDSAT imagery. Definition is largely a function of finer resolution and to some lesser degree shadowing.

3. Drainage networks may be more accurately located on RADAR imagery and networks may be expanded to include lower order streams than those identifiable on the LANDSAT image. Such improvement is primarily due to contrasts in the canopy configuration or microrelief of the vegetation.

INTRODUCTION

The imaging of Darien Province in Panama in 1967 by the U.S. Army Corps of Engineers represented the first major effort of any group or agency to utilize a side looking airborne radar (SLAR) for regional mapping in an area which was subject to a yearly cloud cover of 50 to 60 percent and in which the acquisition of aerial photography had not been realized over as much as 30 percent of the area during the previous 15-year period. The success in the development of a series of terrain information maps (Viksne, et al., 1969) and ultimately in the development of a geologic map (MacDonald, 1969) and the consequent demonstration of the value of RADAR in earth studies prompted Westinghouse Aerospace to launch the first commercial imaging system in September of 1967. Until the advent of ERTS (LANDSAT)-1, 23 July 1972, RADAR was the only sensor capable of acquiring small scale synoptic coverage of terrain. Efforts to generate interest in areas in which aerial photography was available, or could be obtained, met with little success, in part because of the high cost of operation of the early SLAR systems. In addition, because of the high cost of mobilization for a mission distant from base, RADAR soon became recognized primarily as a first-look reconnaissance tool. Such was rightly so.

*R.H. Gelnett, Motorola Aerial Remote Sensing, Inc., Phoenix, Arizona 85018.
**L.F. Dellwig, Professor of Geology, University of Kansas, Remote Sensing Laboratory, Lawrence, Kansas 66045.
***J.E. Bare, Remote Sensing Laboratory, Center for Research, Inc., Lawrence, Kansas 66045.

With the launching of ERTS (LANDSAT)-1 and subsequently LANDSAT-2 (22 January 1975) images are now generated which provide small scale synoptic coverage of cloud free portions of the world on a repetitive basis. Because of the financial backing by the U.S. Government and others, the user cost of the imagery is low. As a result, a great deal of experimentation and research utilizing LANDSAT imagery followed with a general user attitude developing that LANDSAT was essentially in competition with RADAR as a prime reconnaissance tool, for with repetitive coverage at a 18-day interval or less, complete coverage should ultimately be generated over any portion of the earth's surface. However, as indicated in a LANDSAT index atlas of the developing countries of the world (World Bank 1976) there remained areas without LANDSAT coverage even after almost four years of imaging and 72 satellite passes over the same area. Excepting a relationship to vegetation type, density or vigor, geologic phenomena are essentially independent of time or season in display. RADAR imagery has thus been considered by many for utilization only if LANDSAT imagery or aerial photography are not available. However, when the time factor is critical, or specific seasonal coverage is needed in cloud shrouded areas, RADAR necessarily becomes the prime sensor.

RADAR and LANDSAT imagery should not be considered competitive because the two are entirely different. The LANDSAT MSS system records data in the visible and near infrared portions of the electromagnetic spectrum whereas RADAR, because of the difference in the nature of properties sensed in the invisible microwave region of the electromagnetic spectrum, provides signatures for terrain elements which may contrast markedly with those of optical devices. Therefore, one should expect a contrast in data content between SLAR and LANDSAT, because they sense different properties of terrain elements and RADAR acquires images at much lower illumination angles compared with solar elevations for LANDSAT. The latter is particularly important for the enhancement of low relief terrain features to a degree not available on LANDSAT imagery.

The justification for a "dual look" and preferred orientation of look direction was early recognized as a capability available only in an airborne SLAR system (MacDonald, et al., 1969). On the other hand, LANDSAT imagery provides four simultaneous frames isolating the green, red, and two infrared bands of the spectrum. Such isolation has been well demonstrated by numerous earth scientists as providing a capability permitting more rapid and effective isolation of data specific to their particular disciplines (Williams and Carter, 1976). Since the imagery from both RADAR and LANDSAT are unique, maximum terrain information of a variety of types is realized through the utilization of both systems when weather conditions permit.

Inasmuch as there is a difference in the nature of the properties sensed in the optical (visible) and microwave (invisible) portions of the spectrum, contrasts in signatures on SLAR and LANDSAT imagery should exist during any given season. Whenever possible, same-season imagery has been used for comparison in this study. Annotation of illustrations has been intentionally omitted so as not to prejudice comparison. All of the SLAR imagery shown herein was acquired by Motorola Aerial Remote Sensing, Inc., with their X-band (3cm) real aperature system. RADAR imagery of portions of Togo and Nigeria, West Africa, are presented at the courtesy of the respective Governments.

VEGETATION

Because RADAR senses microrelief, or surface configuration, and dielectric properties of vegetation rather than degree of vigor as in near infrared imagery, a classification of vegetation unlike that obtained from LANDSAT imagery should be expected to supplement any initial classification and permit a level of discrimination not otherwise obtainable. A smooth surface (relative to wavelength) provides a low return signal (dark) whereas the rough surface provides a strong signal (light), essentially regardless of target size. Thus, contrasting vegetation types can be identified on RADAR by tone signatures.

The effect of water content, leaf and stem configuration is of prime importance. For example, Mangroves in Panama, in an early study utilizing K-band RADARS (MacDonald, 1969), were readily distinguishable on RADAR imagery because of the strong return signal and characteristic texture compared with other tropical vegetation. At the extreme, one of the most prominent vegetation return signals ever recorded was from banana plantations in Guatemala with X-band RADAR (Figure 1.).

In real-aperture X-band RADAR imagery of Togo (west tropical Africa), classification of broad categories of vegetation (Table 1) was possible. Accuracy of classification is somewhat degraded in mountainous areas due to the influence of steep slopes and where woodland canopies become shorter and more open. However, in regions of flat to rolling terrain, the vegetation types in Table I can be easily determined.

TABLE I. VEGETATION TYPES DETECTABLE ON X-BAND RADAR IMAGERY FROM TOGO, WEST AFRICA.

1. Semideciduous Forest
2. Deciduous Woodland
3. Savanna
4. Seasonally Inundated Grassland
5. Marshes and Swamps
6. Cultivated Vegetation:
   a. Oil Palms
   b. Coconut Palms
   c. Teak
   d. Intensive mixed agriculture (corn, millet, cassava, rice, yams, bananas, plantain, beans, and cotton)

Preliminary comparison of RADAR imagery with LANDSAT MSS imagery (bands 5 and 7) suggests that the two sensors can be used as complementary systems, with each contributing information useful in identifying vegetation boundaries. At this writing, LANDSAT frames acquired simultaneously with the RADAR imagery are not yet available due to cloud cover. The frames used for this comparison were acquired during December, 1975, through March, 1976, well into the dry season. The RADAR flights were made during October and November 1977, near the end of the short rainy season and into the beginning of the long dry season. LANDSAT frames with necessary freedom from cloud cover were not available for the Atlantic coast of Togo nor for the area around the town of Lama-Kara in the northeast.

In both types of imagery, zones of intensive mixed agriculture can be detected, although individual fields are generally too small to be resolved. In the RADAR imagery, several kinds of tree crops can be detected. Where stands of mature trees are dense enough, oil palms can be distinguished from coconut palms. The former give a relatively dark, smooth return (Figure 2); the latter, a bright, speckled return (Figure 3). Teak plantations; when the trees are tall enough to cast a RADAR shadow, can also be detected (Figure 4a). Even narrow plantings of mature teak along roads are evident by their characteristic return

signature. In the LANDSAT imagery (Figure 4b), these plantings are but faintly, if at all, visible. LANDSAT coverage of the oil palm plantation and the coconut groves was not available for comparison. Vegetation banding around lakes and lagoons is also apparent in the RADAR images acquired near the coast (Figure 3) where stands of coconut palms border cattail marshes, the latter giving a speckled light gray signature. This is a good example showing the effects of leaf geometry and moisture content contrasts.

In savanna regions, isolated stands of high semideciduous forest are easily detectable (Figure 5a) in the RADAR imagery by virtue of the shadows they cast on adjacent shorter savanna. These stands, comprised of trees of various species and heights, can be distinguished from the previously mentioned teak plantations on the basis of their irregular outlines and rougher texture. While large stands of forest are evident in the LANDSAT images covering the same high forest sites (Figure 5b), it is difficult to separate the small stands from surrounding savanna where the two types are mosaicked, as is the case in much of east-central Togo. The third dimension provided by RADAR is a definite advantage in classifying these vegetation types.

An example of a case in which LANDSAT is more helpful than the RADAR imagery in separating vegetation types can be seen in Figures 6a and 6b, from an area south of the town of Fazao in west-central Togo. In the RADAR image, it is difficult to confidently determine the limits of deciduous woodland, partially because of the amount of topographic relief and partially because the trees have become somewhat shorter and more widely scattered than further south. In the LANDSAT image, however, the woodlands contrast nicely with the adjacent savanna, especially in band 5.

GEOLOGIC ELEMENTS

The capability of detecting subtle scarps and linear or circular geologic elements in all types of terrain is unique to SLAR systems. The degree to which these features can be identified is primarily a function of look direction and depression (illumination) angle, the latter determining the amount of shadowing. Since both are easily controlled with SLAR systems, and once the look direction has been decided, shallow (low) depression angles are desireable in terrain of low relief and steep (high) depression angles are more effective in mountainous terrain. Even in heavily vegetated terrain of low relief, these geologic elements are often identifiable as subtle drainage and microrelief are reflected in the vegetation canopy.

Although a single RADAR look direction may suffice for some survey areas, the interpreter has a tendency to place lineaments, boundaries between geologic units, or stream valleys at the contact between shadow and illuminated zones. These limitations are effectively eliminated by obtaining a second (opposite) look direction of the survey area (Figure 7). This allows the interpreter to place these boundaries in their proper places. Knowledge of depression angle enables the interpreter to establish relative relationships between slopes, the smaller the angle of incidence the stronger the return. Similarly, the width of the slope relative to shadow length will aid in the determination of the dip of a tilted geologic unit, a critical determination in the discrimination between anticlines and synclines. In complexly folded and faulted areas, opposite looks reduce the probability of error, especially in asymetrical or overturned folds (Figure 8).

An outstanding example of the value of shadowing and the resulting 3-D appearance is in the granite porphyry ring-dike complex northwest of Lere, Nigeria (Figure 9). Granite porphyry dikes, many with a ring configuration, are associated with and often enclose granite or rhyolite intrusives. The geologic map of Nigeria of 1974 shows ringing of the enclosed mass of granite except to the southwest and with direct contact between the granite and the granite porphyry dike in the northeast quandrant. Whereas, to the northwest and southeast, an older intruded granite separates the two units. The accentuation of relief

through shadowing on the SLAR image strongly suggests a complete ring dike and the separation of the ring from the intrusive granite core by older intruded granite everywhere except to the southwest. On the LANDSAT image, although the core is defined, the ring is clearly defined only in the southeastern quadrant and outlined to a lesser degree to the southwest.

In a similar manner, to the north of the Benue River and northwest of Dong, Nigeria, a prominent anticline in Cretaceous sandstone, although well defined in overall configuration on the LANDSAT image, provides no expression of thinner resistant units in the core of the structure (Figure 10). Additionally, only the more prominent faults on the southwest end of the structure are defined. Better and more extensive expression of both elements on RADAR results primarily from shadowing and to a lesser degree (especially in the case of the faults) to the utilization of both the north and south look images.

Joint patterns which are more subtle in expression than major linear fracture trends, or folds, are also enhanced through RADAR shadowing which is best achieved with a look direction normal to orientation. Shadowing on LANDSAT imagery may be realized by a decrease in solar elevation, but this cannot be controlled. Under some conditions, as for example in the Petan area of Guatemala, a single joint pattern in limestone on the LANDSAT image may be enhanced but the conjugate system is lacking in expression.

DRAINAGE NETWORKS

Drainage networks are not universally enhanced on any one type of imagery. For enhancement and extension of a LANDSAT derived network to be realized, it is necessary that either (1) the stream occupies a depression and the stream bank vegetation conceals the water surface permitting enhancement through shadowing; (2) bank vegetation is sufficiently high to cause shadowing; or (3) there are contrasts in microrelief of bank and adjacent vegetation to the extent that a unique tone-texture signature outlines the stream course; a contrast that is not often detectable on LANDSAT imagery. Because of the potential dependence on shadow, expansion of drainage patterns may be to some degree "terrain relief" as well as "depression angle" dependent. Southwest of Atakpame, Togo, moist riverain forest with tree heights of up to 120 feet border even minor tributaries, the canopy completely obscuring the stream (Figure 11). The combination of a distinct and easily recognizable tone-texture signature and RADAR shadow from the high trees provides significant definition and expansion of the network beyond that derived from LANDSAT imagery alone.

SUMMARY

The contrast in data sensed by an imaging SLAR and the LANDSAT MSS demands a contrast in pictorial presentation of terrain and vegetation elements. Additionally, both systems have unique capabilities and limitations of operation which permit generation of unique data. Superposition of system capabilities, limitations, and operational mode on natural terrain of varying physical and botanical characteristics results in greater or lesser contribution of data from one or the other sensor for any given area. For maximum terrain data retrieval, SLAR will provide data not otherwise obtainable because of the frequency response on the portion of the electromagnetic spectrum in which such systems operate. Justification of a RADAR mission then, need not necessarily be based on its all-weather-coverage capability. For investigations including vegetation data, it is beneficial to use the unique data provided by both RADAR and LANDSAT in combination.

REFERENCES

Anonymous, 1976, Landsat Index Atlas of the Developing Countries of the World, The World Bank, Washington, 17 pp.

MacDonald, H.C., 1969, Geologic Evaluation of Radar Imagery from Darien Province, Panama, Modern Geology, v. 1, no. 1, pp. 1-63.

MacDonald, H.C., J.N. Kirk, L.F. Dellwig and A.J. Lewis, 1969, The Influence of Radar Look-Direction on the Detection of Selected Geological Features, in Sixth International Symposium on Remote Sensing of Environment, Proc., v. 1, pp. 637-650.

Viksne, A., T.C. Olsen, and C.D. Sapp, 1969, SLR Reconnaissance of Panama, Geophysics, v. 34, no. 1, pp. 54-64.

Williams, R.S., Jr. and W.D. Carter (eds.), 1975, ERTS-1, A New Window in Our Planet, U.S. Geol. Survey Prof. Paper 929, 362 pp.

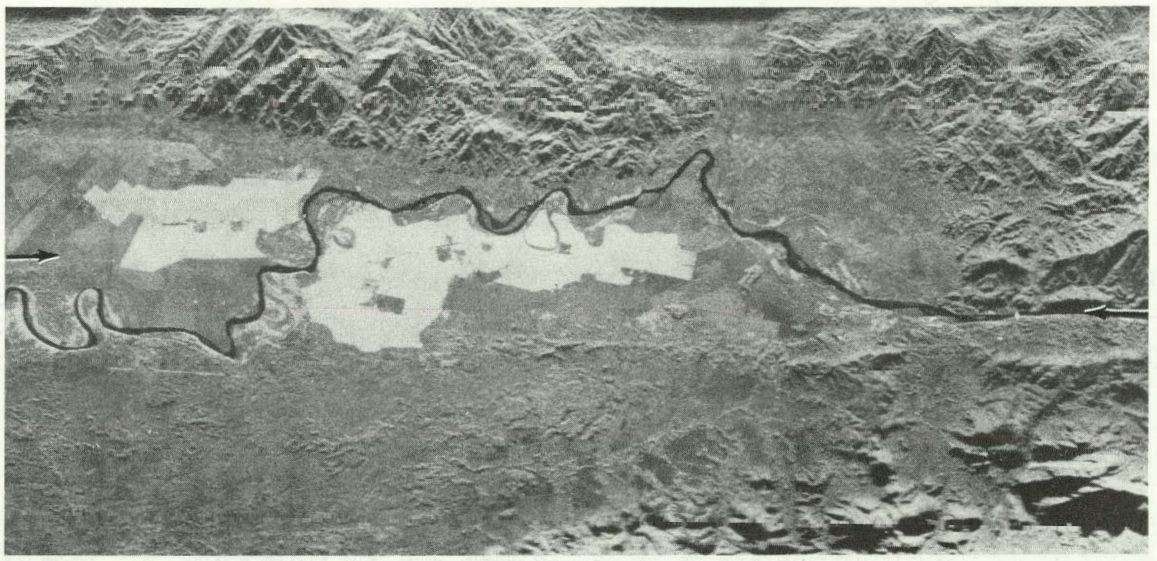

FIGURE 1. BANANA PLANTATIONS ALONG THE MOTAGUA RIVER, GUATEMALA. Banana plantations along the Motagua River are characterized by an exceptionally high return signal. The sharp boundaries between the low plains and adjacent mountains both north and south of the river are along faults. The trace of the Motagua Fault is indicated by arrows.

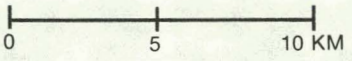

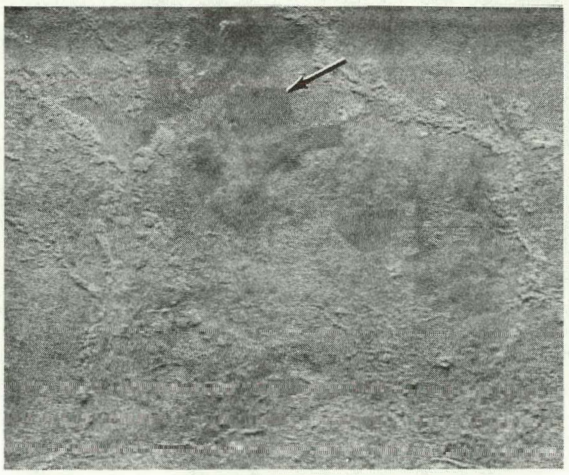

FIGURE 2. RADAR IMAGE OF OIL PALM PLANTATIONS SOUTHEAST OF PIC D'AGOU, TOGO, OCTOBER, 1977.

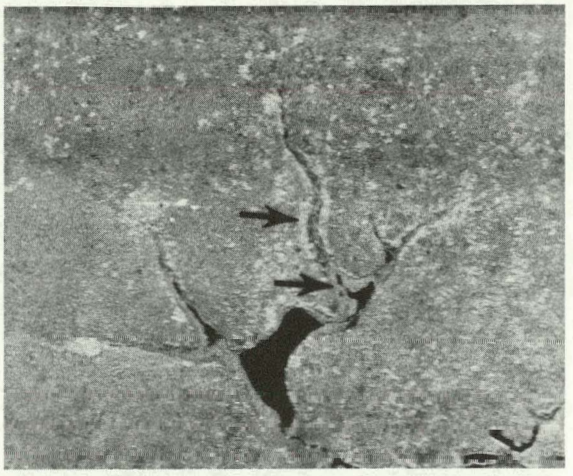

FIGURE 3. RADAR IMAGE OF MARSHES NEAR VOGAN AND ANFOUIN, TOGO. Black areas are open water. Gray zones at water's edge are cattails. Brighter speckled zones bordering the cattails are primarily coconut palms. October, 1977.

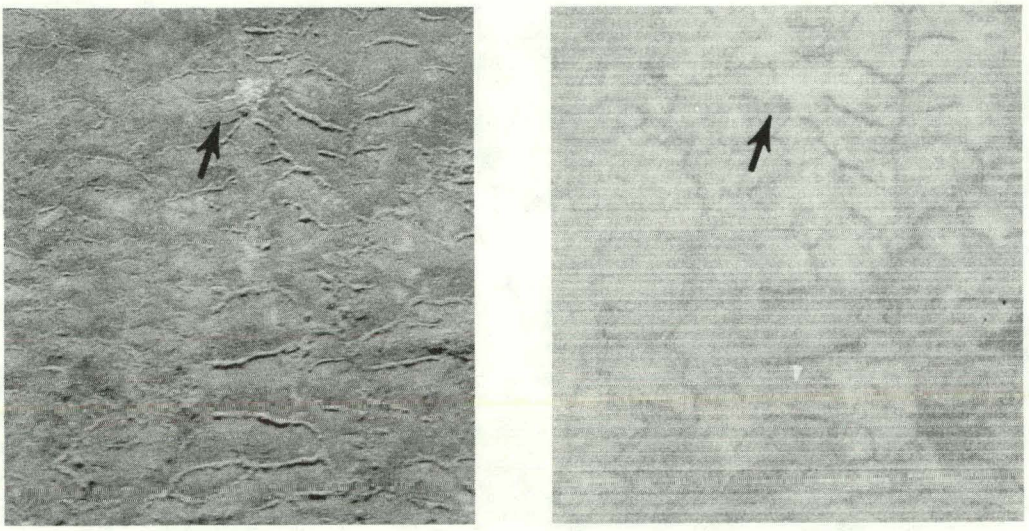

(A) (B)

FIGURE 4. TEAK PLANTATION WEST OF TCHAMBA, TOGO. (A) Radar, October, 1977. (B) LANDSAT, band 5, December, 1975.

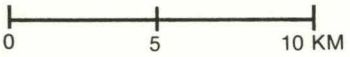

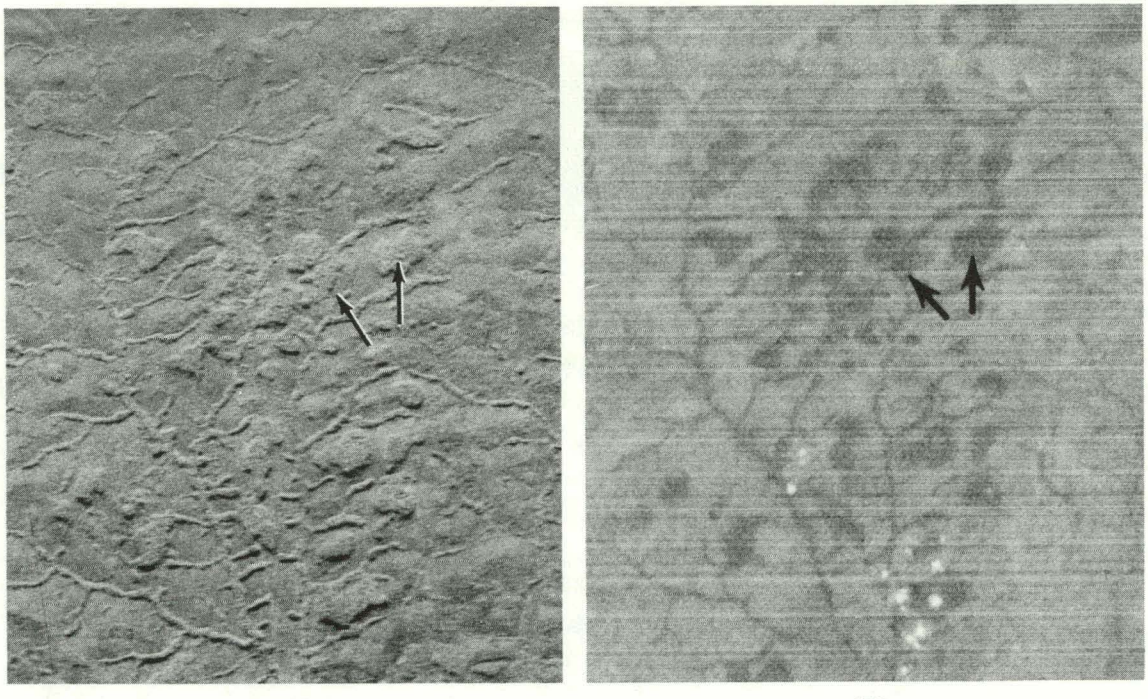

(A) (B)

FIGURE 5. STANDS OF HIGH, SEMIDECIDUOUS FOREST SCATTERED IN SAVANNA. (A) Radar, October, 1977. (B) LANDSAT, band 5, December, 1975.

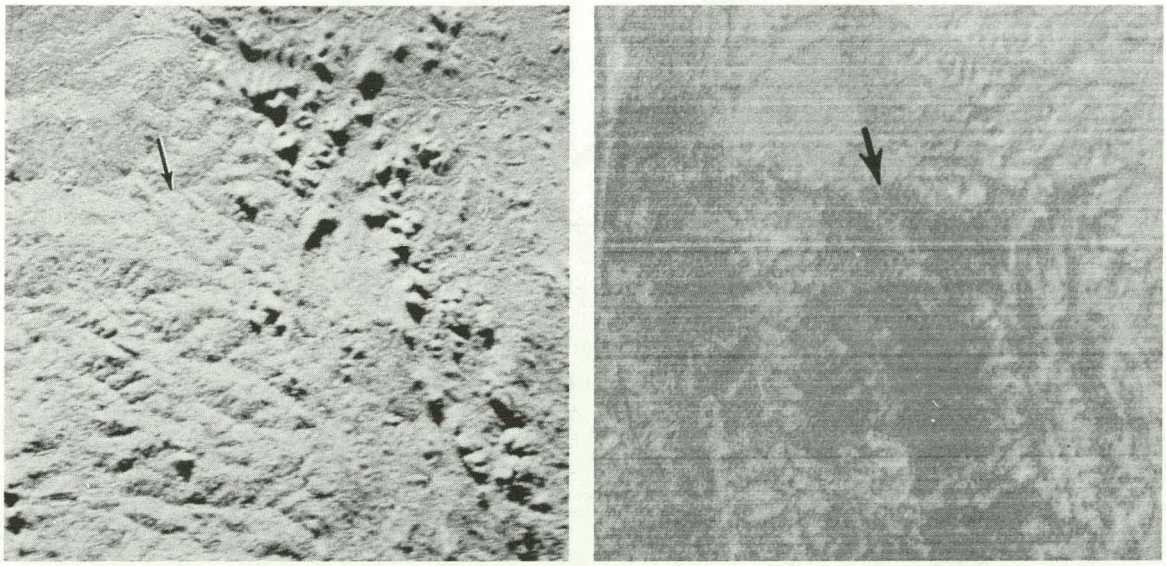

(A) (B)

FIGURE 6. DECIDUOUS WOODLAND GRADING INTO TREE SAVANNA IN HILLS SOUTH OF FAZAO, TOGO. (A) Radar, October, 1977. (B) LANDSAT, band 5, December, 1975. Woodlands medium gray.

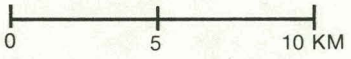

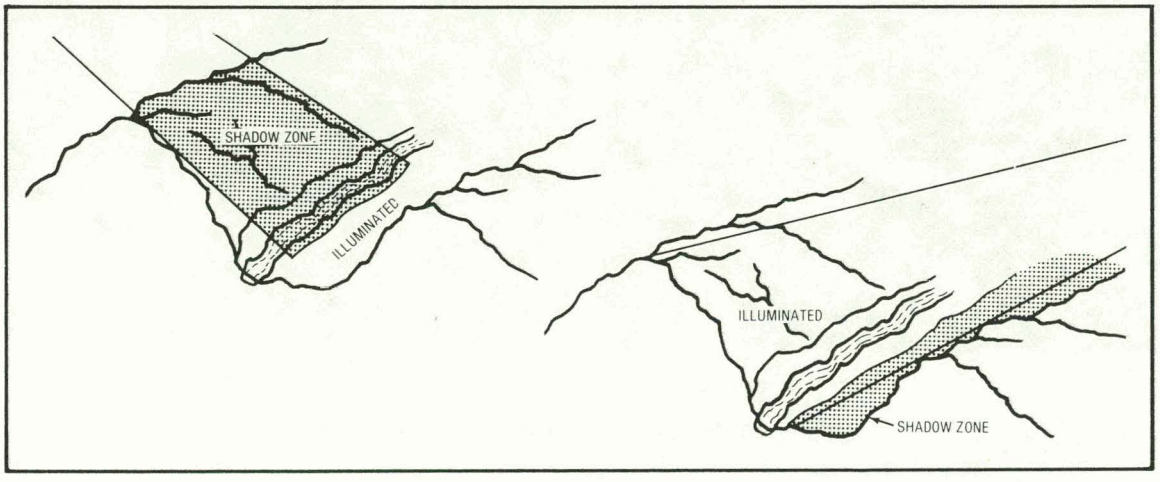

FIGURE 7. SHADOWING OF VALLEY BOTTOM IN HIGH RELIEF TERRAIN. Shadowing may completely obscure valley floor in any one look direction. An opposing look is necessary for the interpreter to accurately define the stream course.

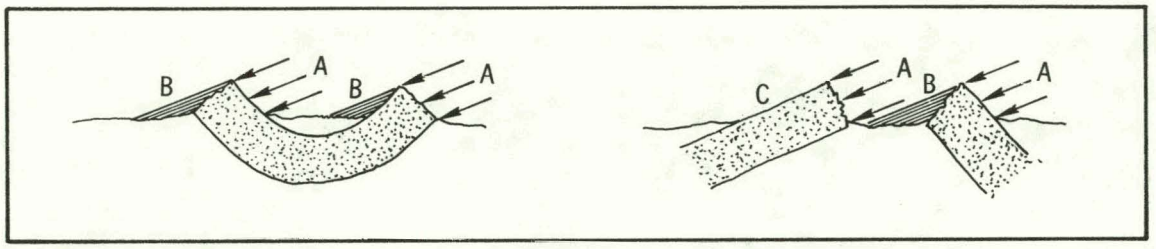

FIGURE 8. SIMILARITY OF RETURN SIGNAL AT SIMILAR DEPRESSION ANGLES FROM AN ANTIFORM AND SYNFORM. As illustrated the return signal is strong from areas in which: (A) the incidence angle is high; (B) absent from shadowed areas; and (C) low to absent on slopes at grazing angle. Knowledge of depression angles along with two opposing looks not only aids in the determination of the nature of the structure but may aid in the determination of the dip of the strata.

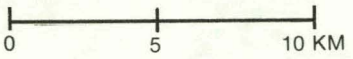

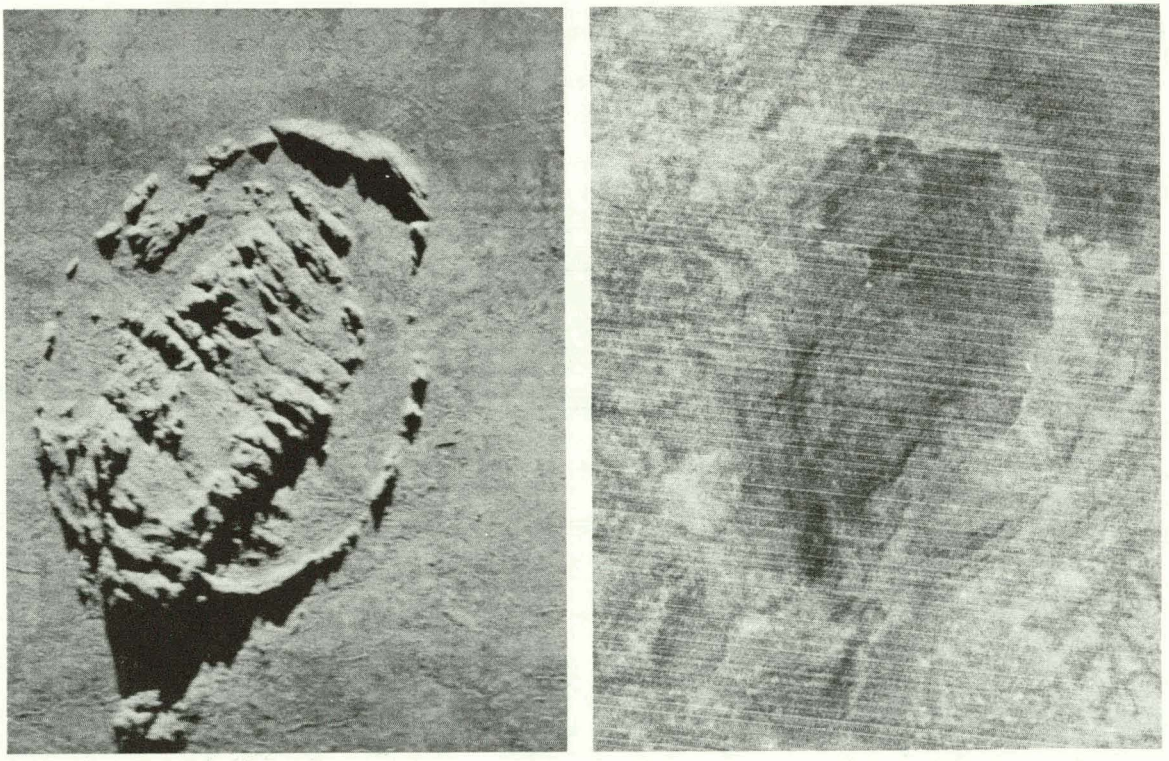

(A) (B)

FIGURE 9. RING DIKE COMPLEX NORTHWEST OF LERE, NIGERIA. (A) Radar image, February, 1977. (B) LANDSAT image, band 5, December, 1975. The topographically high Jurassic granite is separated from the pronounced ring of Jurassic granite porphyry by topographically lower Precambrian basement. Low relief terrain outside of the ring dike is of Precambrian-Cambrian granites.

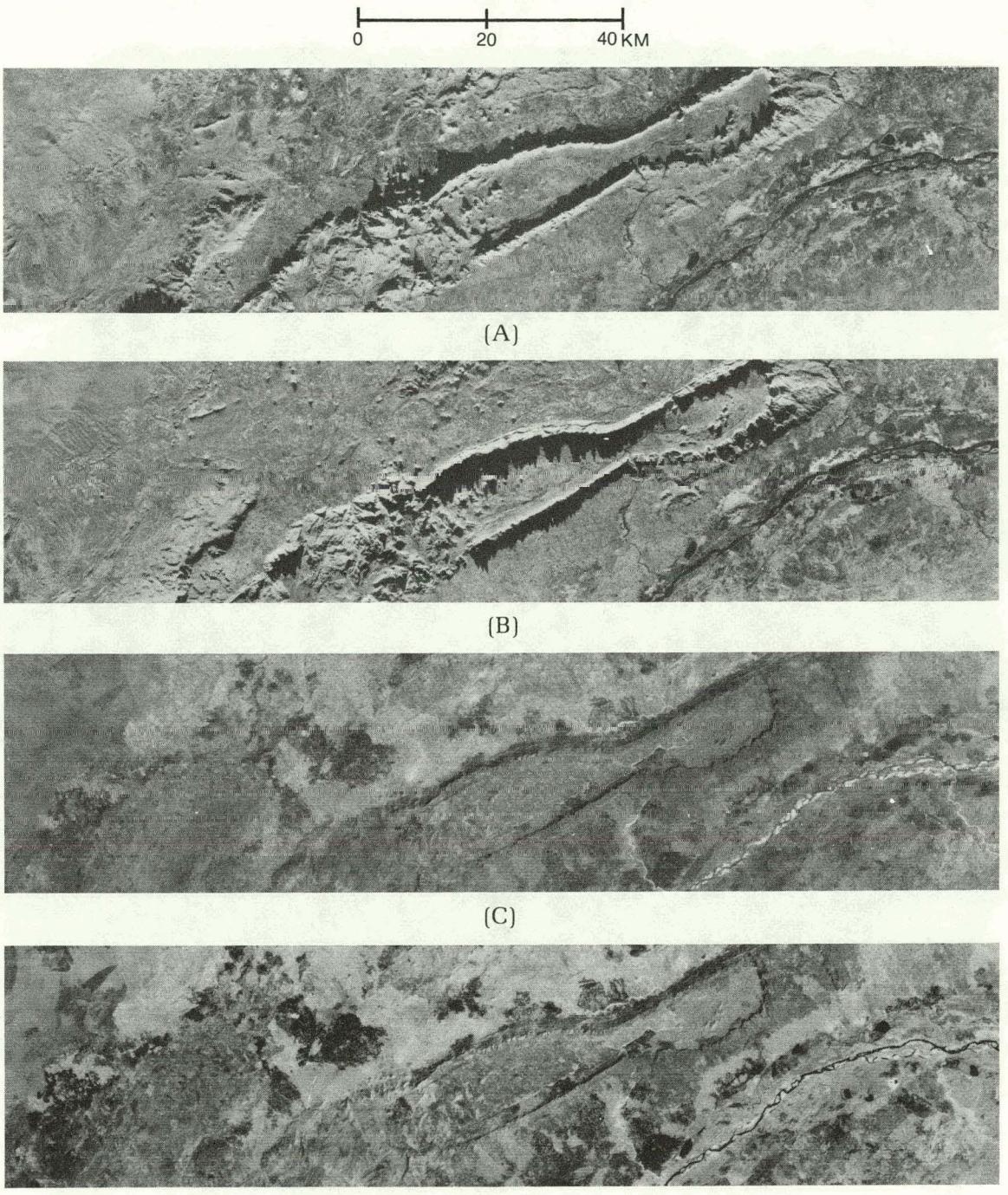

FIGURE 10. ANTICLINE IN CRETACEOUS SEQUENCE NORTH OF THE BENUE RIVER, NIGERIA. Radar image, March, 1977. (A) North look. (B) South look. LANDSAT image, January, 1976. (C) Band 5. (D) Band 7. Primarily through shadowing, both thin resistant sandstone beds within the core of the structure and the complex fracture pattern of the southwest end of the structure are enhanced on the radar image.

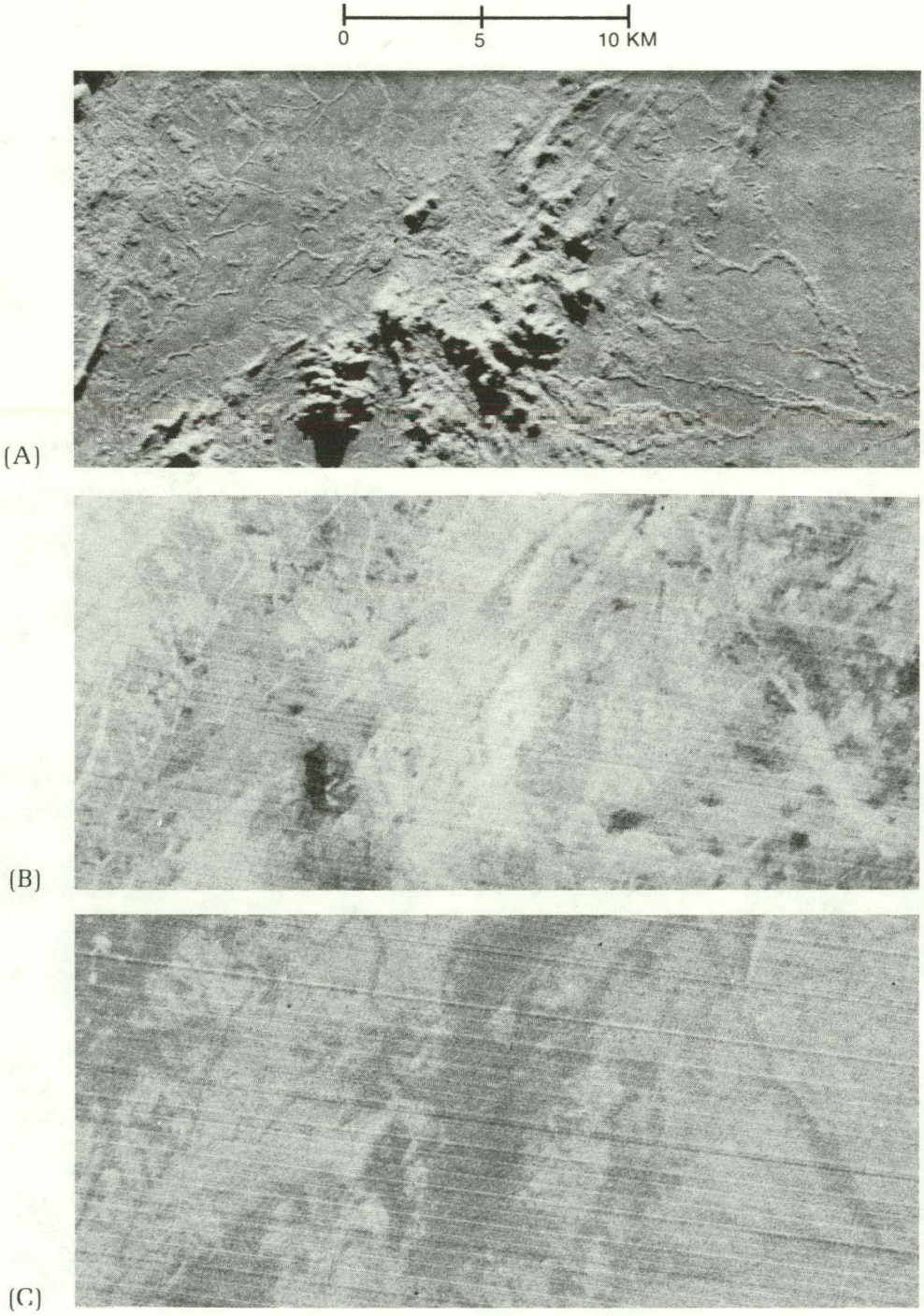

FIGURE 11. DRAINAGE NETWORK SOUTHWEST OF ATAKPAMA, TOGO. (A) Radar image, October, 1977. (B) LANDSAT image, band 5, February 1976. (C) LANDSAT image, band 7, February 1976. The drainage network is defined by moist riverain forest with tree heights up to 120 feet.

REMOTE SENSING APPLICATION FOR GEOLOGICAL MAPPING OF PAHANGAN SHEET, CENTRAL KALIMANTAN, INDONESIA

Turus Soejitno

Geological Survey of Indonesia
Bandung, Indonesia

ABSTRACT

To investigate the geology of the area, several studies have been carried out, i.e. the Landsat study, the airphoto and aeromagnetic studies, ground survey and compilation. In studying the Landsat, two methods have been carried out, the pattern and the spectral analyses. Besides using these methods to complete the geologic map of the area, they also indicate some potential areas of mineralization.

INTRODUCTION

The survey area lies in the central part of Kalimantan, Indonesia and is bounded by latitudes 0° - 1° 00S, and longitudes $112^{\circ}30'$ - $114^{\circ}00$E, with total coverage 18,150 km2 (Fig. 1). Most of the area has not been mapped previously, only a small portion of about 20% which lies at NW-corner of the sheet is covered by some geological data.

Accessibility in the area is very difficult and no roads exist; the area may be reached by small boats following rivers about one week trip from Palangkaraya, the capital of Central Kalimantan Province. The area is mountainous and covered by very dense jungle.

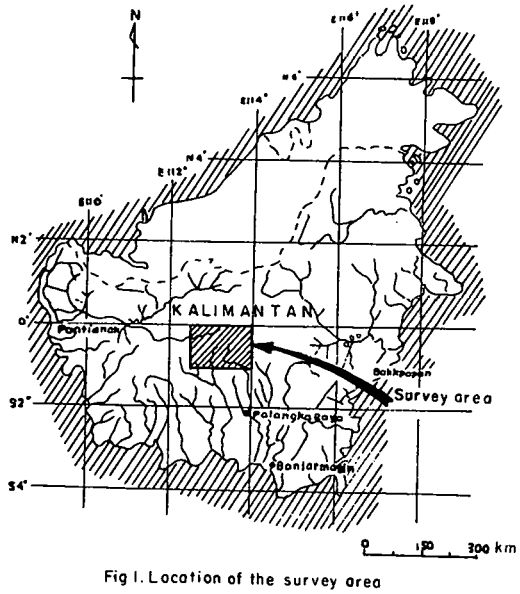

Fig 1. Location of the survey area

LANDSAT IMAGE STUDIES.

a). Landsat image pattern analysis.

The monochrome prints of bands 4, 5, 6, and 7 on the scale of 1 : 250,000 and of bands 5 and 7 on the scales of 1 : 500,000 and 1 : 1,000,000 were used in the study. Those images of small scales are used mainly for observing the large tectonic features and regional relationship of the geology.

The procedure of analysis is a visual method. The Landsat image was laid on the light-table and then it was covered by a tracing paper. The image was examined under a magnification glass and analyzed.

b). Spectral analysis of Landsat images.

Spectral data analysis was carried out by digital processing method which utilizes Computer Compatible Tape (CCT) and by analogic processing method using images which are transformed into film base. The analogic method is further divided into photographic processing (false color composition, additive color composition) and electronic processing (color enhancement, edge enhancement, density measurement).

The existence of the granitic rocks and andesite was clearly identified by spectral analysis. For identifying the granitic rocks, the additive color and color enhancement methods were used. The existence of andesite is characterized by its light tone and protruding topography.

Based on the Landsat studies, the geology of the area was classified into 16 geological units as shown in Table I. The lineament pattern map superimposing interpretative geologic units is shown in Fig. 2. Granites and andesites are mostly distributed in the western part of the sheet, whereas tuffaceous rocks are distributed in the eastern part.

AERIAL PHOTOGRAPHIC AND AIRBORNE MAGNETIC STUDIES.

The total number of the photographs available is 1,400, on a scale 1:40,000. The quality of the photos is not very good, with cloud cover in some places. There is a big difference of scale between the low land and that of the high land.

The largest topographic map which is available in this area is on a scale of 1 : 250,000, but was not sufficiently accurate. Therefore the aerial photographs were used to improve it planimetrically, using the hand teplate method.

The aerial photographs were then interpreted to get more detailed geologic data. Based on this study, the geology of the area was divided into 22 photogeologic units as shown in Table II; the photogeologic map is given as Fig. 3. The intrusive and extrusive rocks are exposed in the southern part of the area. The south-eastern part of the area is predominated by the volcanic sediments and some intrusive rocks. The sedimentary rocks are distributed in the northern part of the area. The structure of the area is mostly trending WSW - ENE. Fold axes are found in the north-western and south-eastern parts, and a strong lineament that is presumably a fault is found in the south-eastern part of the area.

During the aerial photographic survey, airborne magnetic recording was carried out simultaneously. The purpose of this survey was to clarify geological structure, distribution of igneous rocks and occurrence of ore deposits. The data processing is still in progress. The tentative results show that there are agreements between airborne magnetic and aerial photographic studies concerning geological structure and igneous rock distribution.

GROUND SURVEY.

The traverses were carried out mostly following the big rivers, i.e. Kahayan river and some of its tributaries, Kapuas river, upper stream of Katingan river, Melawi river and Juloi river.

The ground survey were carried out to check the result of the remotely sensed data. The geologic sketch maps were made in more detail along the traverses in the scale of 1 : 100,000. The areas bearing ores are also shown in the sketch maps.

The following minerals are found, chalcopyrite, bornite, antimonite, galena, sphalerite, magnetite, pyrite, diamond and gold ores. Primary gold exists, but is more common as placer deposits. Diamonds are also found as placer deposits in the Kapuas river region (south-eastern border of the sheet). Other minerals are found as veins and disseminated deposits. The vein types are mostly associated with quartz veins in the granitic gneiss, whereas the disseminated types are mostly in the bodies of tonalite and granodiorite which intrude the granitic gneiss, andesite and the Tertiary sediment.

COMPILATION.

As the traverses are mostly very far apart, the correlation between the traverses is difficult without using remote sensing. Using the combined methods noted above the tentative geology of the area is as follows (Fig. 4).

The basement of the area is micaceous schist of pre-Carboniferous age. The rock is mostly distributed in the southern part of the area, and some is in north of Juloi river. The Permo-Carboniferous sediments which consist of shale, sandy clay, calcareous rocks and volcanic breccia were deposited unconformably on the basement. Those existing rocks were then intruded by Permo-Triassic granitic intrusive. The schist was recrystalized and the Permo-Carboniferous sediment was metamorphosed into hornfels at the contact aureole with the plutonic rock. Those rocks were overlain unconformably by the Upper-Triassic rocks which consist of clay and sand. In the Jurassic orogenesis took place and was followed by intrusion of granitic intrusive. The Jurassic granitic rocks are present mostly in the area south of this sheet, only some stocks appear in the southern part of this area. During this orogenesis, the Upper Triassic sediments were metamorphosed into slate and quartzite, the Permo-Carboniferous rocks into phyllite and quartzite, and the Permo-Triassic granitic rocks into granitic gneiss. The pre-Cretaceous region became a metamorphosed complex, it is present in the southern part of the area. In the Cretaceous the regionally metamorphosed rocks were overlain unconformably by shale with alternating sandstone. This formation is assigned as the Selangkai formation and developed in Juloi river region. In Tertiary three basins exist, the Melawi basin in the west, the Kutai basin in the east and the Barito basin in the south. In Melawi basin the Tertiary sediments consisting of shale, sandstone and quartz-sandstone were deposited unconformably on the pre-Tertiary rocks. The shale and sandstone of Melawi formation make interfingering contact with quartz-sandstone of Plateau Sandstone formation in this basin. In the Barito basin the Tertiary sediments, which consist of claystone, sandstone, volcanic sediments and intercalations of limestone and quartz-sandstone were deposited unconformably on the older rocks. It is assigned as the Warukin formation. In the Kutai basin the Upper-Tertiary sediments of Pamaluan formation, which mainly consist of shale and sandstone with leaf remains, were deposited conformably on the Plateau Sandstone formation. Andesitic and basaltic intrusions have taken place frequently in pre-Tertiary times. In the investigated area, particularly in the central and south-eastern parts, the volcanic rocks consist of andesite, basalt and dacite and are of Middle-Tertiary age. Small intrusions of tonalite and granodiorite took place probably during Late-Tertiary. They might be following fault zones which are mostly trending WSW - ENE. The mineralization of some area in this sheet may closely relate to these young intrusions.

The occurrence of porphyry copper in Kalimantan is found in Mamut (northern part of this island). Here the mineralization is associated with Tertiary acidic plutonic rocks. It is suggested that this acidic plutonic rocks may be correlated with the tonalite and granodiorite in this survey area.

Based on the whole studies mentioned above reveals that the potential area for mineralization may be extracted within areal coverage of 350 km2 which lies in the middle-southern part of the sheet. Further study of this mineralized area will be carried out, applying other techniques such as geochemistry and detailed geologic study.

CONCLUSION.

Remotely sensed data have offered a new and powerful tool for geological mapping of Pahangan sheet.

UNIT	PHOTOGRAPHIC CHARACTERS		TOPOGRAPHIC CHARACTERS									COMMENT	PROBABLE LITHOLOGY
	TONE	TEXTURE	DRAINAGE			RESISTIVITY	VALLEY	RIDGE	LINEAMENT				
			PATTERN	DENSITY	PARAMETER				DIRECTION	INTENSITY	TYPE		
Q	light	hazy	meander	very rare	permanent	very weak	flat					swamp, oxbow	Quarternary sediments
L	gray	fine	meander	rare	permanent	very weak	flat					densely vegetated	Laterites
B	gray	coarse	dendritic	medium	very short	resistant	V		one	medium	joint	densely vegetated	Basalts (lava+tuff)
S	very dark	fine				resistant			rare	strong	bedding	dipping is almost flat	Coarse sandstone
F	dark	fine				medium			rare	strong	bedding	dip is gentle	Sandstone
C	dark	fine	dendritic	medium	short	medium			rare	weak	bedding	dip is gentle	Finesandstone
H(H')	light	coarse				medium			rare	very strong	bedding	folding is observable	Alternating Shales & sandstone
e	light	fine				very resistant			rare	very strong	bedding		Limestone
E	light	fine				medium			rare	strong	bedding joint		Pyroclastic
T(T')	light dark	hazy				medium	almost flat		medium	weak	joint	characters are variable	Tuffs
N	light	coarse	dendritic	medium	very short	medium			one	medium	joint		Andesites (Lava+tuffs)
D	gray	coarse	partly dendritic	high	short	medium	V		numerous	medium	joint	overlaid by units S & C	Metasediments
M	gray dark	fine	dendritic	medium	short medium	resistant	U		numerous	strong	joint	intruded by units G	Metamorphic rocks
A	very light	coarse				high resistant			rare	weak	joint		Intrusive Andesite
I	dark	coarse				resistant			rare	weak	joint		Intrusive rocks
G	gray	rugged	rectangular	medium	medium long	resistant	V		numerous	strong	joint	characters are variable	Granitic rocks

Table I. CRITERIA OF LANDSAT-IMAGE OF PAHANGAN QUADRANGLE ON BAND 7, CENTRAL KALIMANTAN

UNIT	TEXTURE	TOPOGRAPHIC CHARACTERS								VEGETATION	BEDDING	COMMENT	POBABLE LITHOLOGY
		DRAINAGE			RESISTIVITY		LINEAMENT						
		PATTERN		DENSITY	ROCK	CROSS SECTION	DIRECTION	INTENSITY	TYPE				
Q	smooth	meander		rare	very weak					coarse	none	usually opened timber	alluvium
S-9	finely rugged	dendritic		very dense	weak		rare	weak	fault	medium	vague	opened timber (in E-ern part).	younger sediment
S-8	finely rugged	dendritic		very dense	weak		one	medium	fault	medium fine	vague	opened timber (in W-ern part).	younger sediment
S-6	finely rugged	dendritic		very dense	weak medium		numerous	medium	fault joint	medium fine	vague	opened timber	mudstone, silt
S-11	even	dendritic		medium	weak		one	medium	fault	coarse	none	thinly overlaid on S-3	mudstone or silt
S-5	finely rugged	dendritic		very dense	weak		numerous	medium	fault joint	medium coarse	partly clear	developed in the E-ern part	mudstone, silt
S-1	rough	sub-parallel	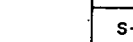	medium	resistant		rare	weak	fault	medium coarse	vague	developed in central part	sandstone or conglomerate
S-3	even	sub-parallel		sparse	very resistant		one	strong	fault	fine	clear		quartz-sandstone
S-2	even partly rugged	sub-parallel dendritic		medium	resistant		numerous	medium	fault + joint	coarse, partly fine	partly clear	partly similar to S-3	sandstone
S-7	coarse	parallel		medium	resistant					medium	clear		sandstone
M	rugged	dendritic		medium dense	medium resistant		numerous	medium	fault, joint	medium	vague	tortuous ridges and valleys	metamorphic rocks
V-2	fine	radial parallel		rare	resistant		rare	weak	fault	fine		slope of the lava flow + dome	lava flow + volcanic neck
V-1	fine	parallel radial		medium	resistant		rare	medium	fault + joint	fine		topography cut	dykes
I-4	rugged coarse	dendritic		medium dense	resistant	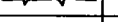	numerous	strong	fault + join-	very coarse		sharp ridges	intrusive rocks
I-3	coarse	dendritic		medium	resistant		numerous	strong	fault + joint	coarse		sub.rounded ridges deep valley	intrusive rocks
I-2	rugged	dendritic sub.parallel		medium dense	very resistant		numerous	strong	fault + joint	fine-medium			intrusive rocks
I-1	finely rugged	dendritic annular		dense	medium		numerous	strong	fault + joint	coarse			granitic rocks
S-4												almost similar with S-5	tuffaceous sandstone
S-10													agglomerate
S-12													sandstone
T												developed in W-ern part	volcanic rocks
I-5												intrusion	younger granitic rocks

Table II. CRITERIA OF AERIAL PHOTOGRAPH OF PAHANGAN QUADRANGLE, CENTRAL KALIMANTAN

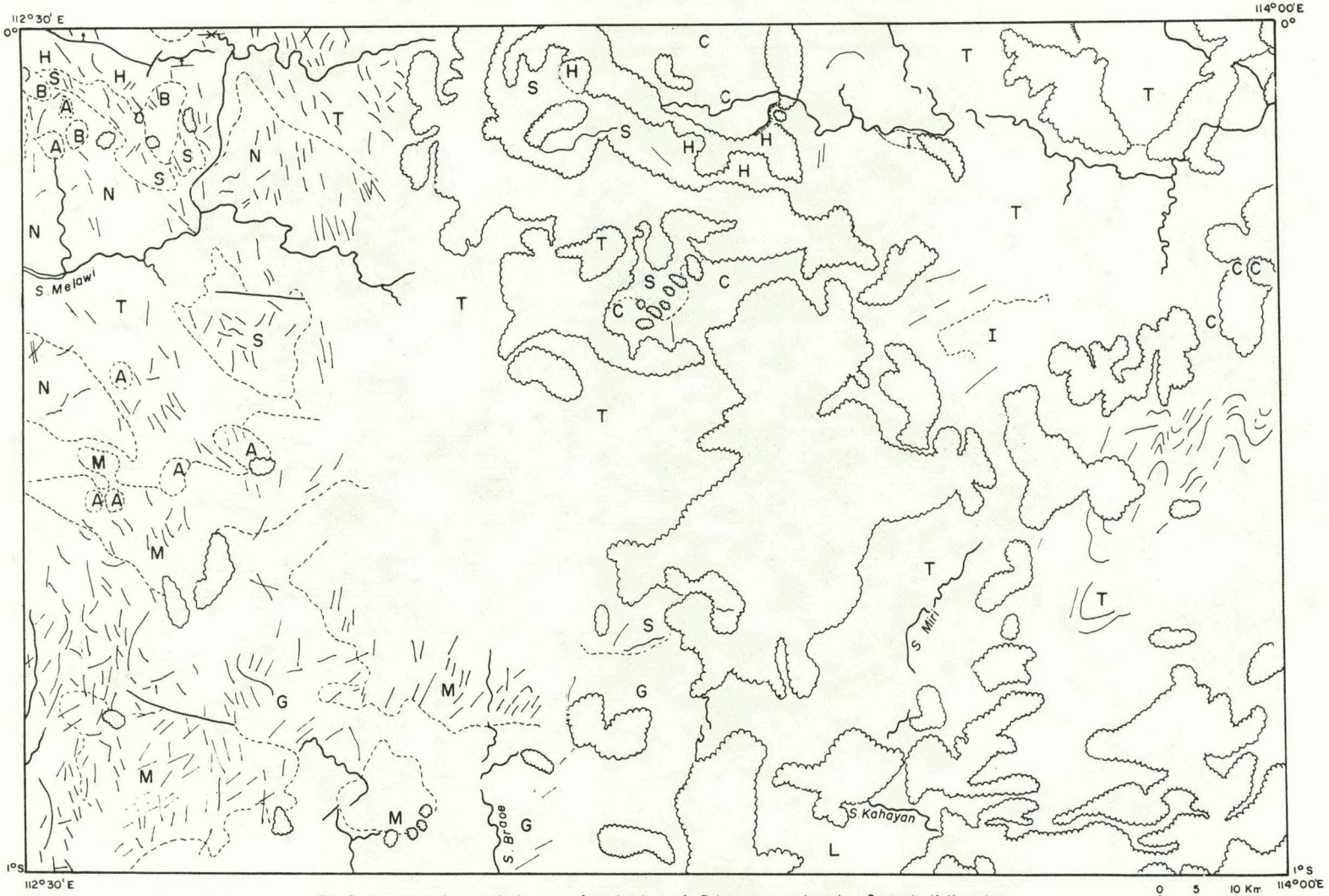

Fig. 2. Interpretative geologic map from landsat of Pahangan quadrangle, Central Kalimantan

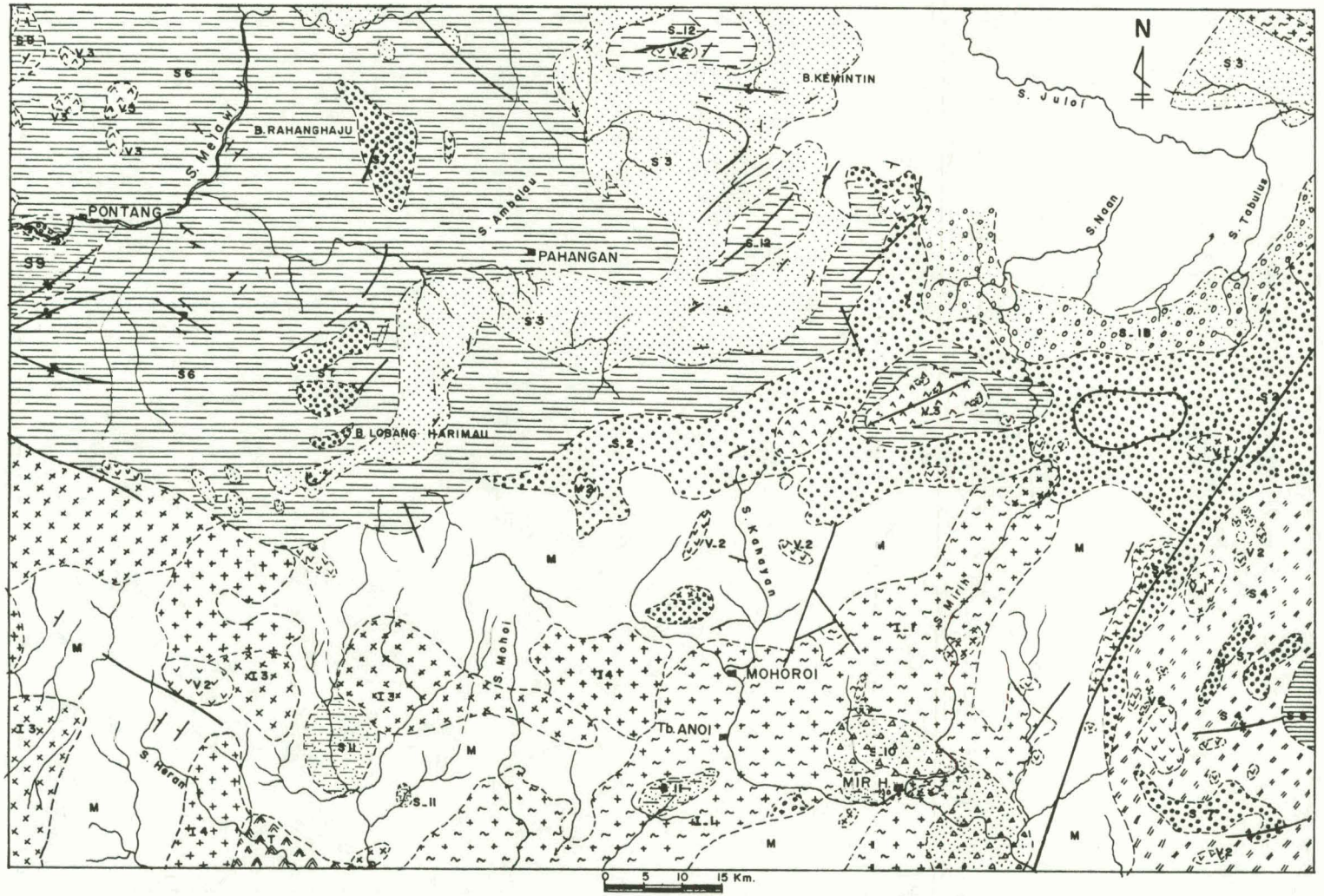

Fig. 3. Photogeologic map of Pahangan quadrangle, Central Kalimantan

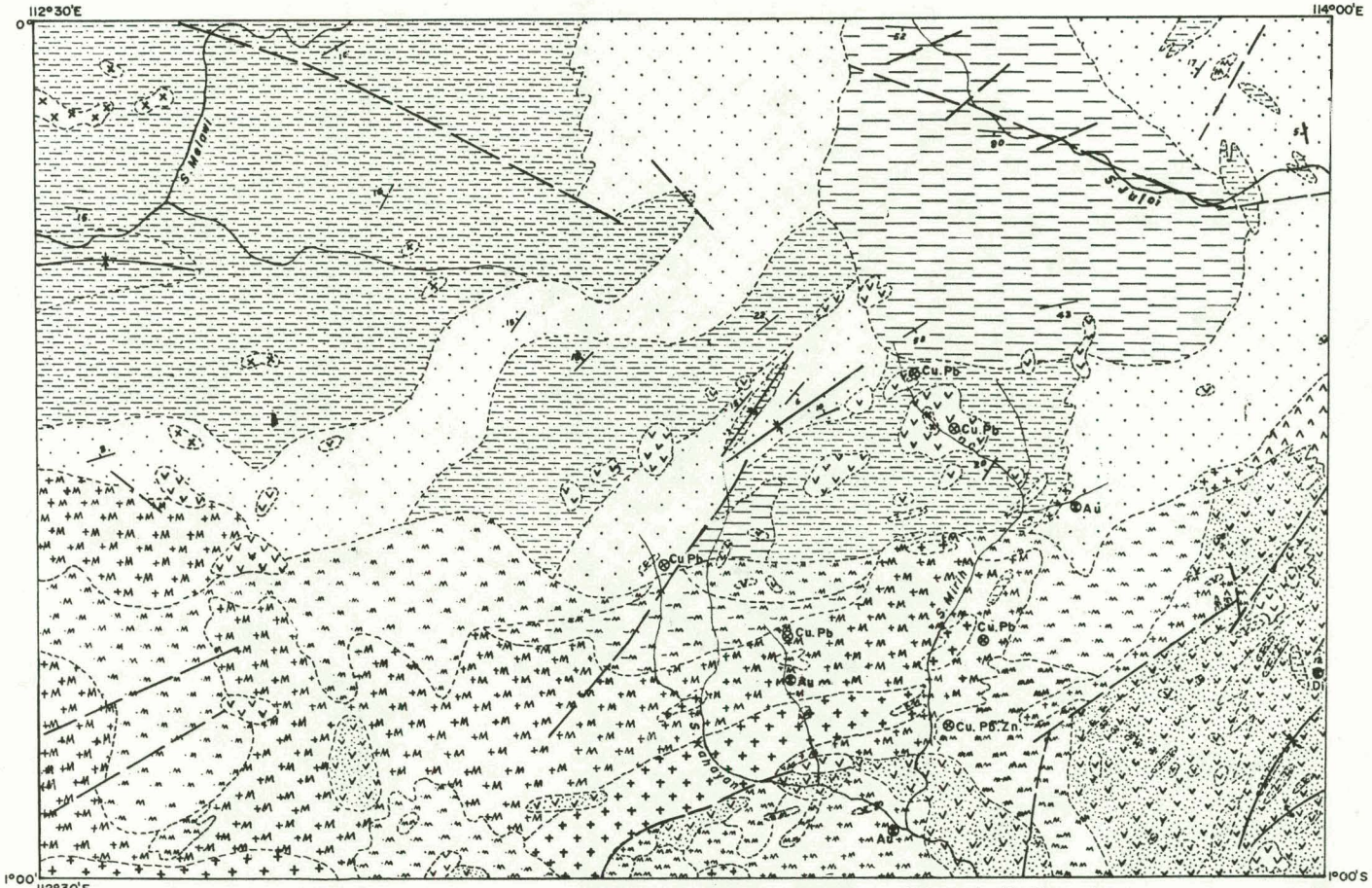

Fig.4. Tentative geological map of Pahangan quadrangle, Central Kalimantan

LEGEND

- Pamaluan formation (Lower Miocene)
- Warukin formation (Oligocene Miocene)
- Plateau sandstone formation (Paleocene - Oligocene)
- Melawi formation (Paleocene – Oligocene)
- Selangkai formation (Cretaceous)
- Slate and quartzite (Triassic)
- Phyllite and quartzite (Permo–Carboniferous)
- Micaceous schist (Pre-Carboniferous)
- Tertiary Tonallite, granodiorite
- Volcanic rocks (andesite, dacite basalt)
- Jurassic granite
- Permo-Triassic gneissic granodiorite
- Prospect location of primary deposits
- Prospect location of placer deposits (Au, gold, Di, diamond).

THIS PAGE

WAS INTENTIONALLY

LEFT BLANK

A B S T R A C T

The goal of this report is to show that: (1) Landsat imagery are an excellent tool to analize and evaluate natural resources, (2) geomorphology is the most appropiate science to investigate natural resources for the development of a particular area.

The study area is located in the Department of Oruro (Bolivia) covered by a Landsat image named COIPASA.

The area under study is dominated by a semiarid climate where different processes such as Volcanic, Eolian, Fluvial and Lacustrin processes have shaped the landscape. Eolian processes mainly, are causing serious troubles due to the enormous areas occupied by sand dunes. Fluvial processes are causing flood, because of the low slope gradient. High evaporation is another important factor in leading soils into salination.

Sparse vegetation all over the area is specially dominated by shrub and grass such as Thola (Lepidophyllum quadrangulare) growing mainly in sandy soils with a high water table. Yareta (Azorella compacta) and Keñua (Polylepsis tomentella). This last mentioned appears specially at the foot of the Sajam peak conforming a typical timber line.

It seems that surroundings of Sajama Payachata and Guallatiri volcanoes are the most profitable areas from the hydrological and land use point of view for agricultural purposes.

Perennial snow covering the before mentioned volcanoes originate many streams with fresh water. Vegetation, mainly Thola has increased. Livestock of Llama (Lama Glama) and Alpaca (Lama Pacos) is widespread where water is concentrated is swamp areas (Paramos).

Material coming from the highest part of the volcanoes, chiefly by denudational processes (sheet erosion) and gravity is deposited at the foot of such volcanoes conforming thick deposits of soils, excellent for Agricultural use.

The southern part of the beforre mentioned area presents completely different morphological conditions. The Lauca river drainage basin is in great part covered by sand dune and flooded areas. These flooded areas become in many cases, deppresions constituted by salty soils where only paja brava grows. No crops are found in these areas because of the high degree of salinity and aridity. The Lauca river forms a delta plain in the neighborhood of Salar de Coipasa, causing serious damage to the Chipaya Village.

GEOMORPHOLOGY AND NATURAL RESOURCES OF THE COIPASA AREA USING LANDSAT IMAGERY

By: Milton Suárez M.
Geological Survey
of Bolivia
Bolivia Erts Program
La Paz - Bolivia
P.O. Box 2729

INTRODUCTION

1. Purpose of the study. Bolivia, a 1.100.000 square-kilometer country approximatelly, was and is essentially a mining country, reason why its mineral resources are more or lees known. However, what happened to the other resources such as soil, water, vegetation, etc? The question is really serious. If Bolivia wants to approach a true development, all its resources must be known. The Bolivia ERTS Program staff is working in this sense since 1973,

in order to inventory natural resources of the whole country using landsat imagery and other remote sensing techniques.

The purpose of this study is to show that landsat imagery is really an excellent tool to make an inventory and to analize all the physical aspect of the Earth specially those connected to natural resources. Geomorphology, the science of the landscape is the most appropiate discipline to investigate natural resources and contribute to the development of a particular area.

1.1. Location of the study area. The area under study is located in the Oruro Department (Bolivia) covered by a Landsat image named COIPASA (Figure N°1) at the Chilean border.

The volcanoe called Sajama of 6.520 m.s.l. (Ahlfeld 1973) is the highest point in Bolivia. Average altitude of the area is 4.000 m.s.l. Most of the rivers have their headwaters in the mountains such as the Lauca, Sajama and Cosapa rivers, which cross a desertic area without incoming themselves into the deposit of sand. They contribute finally their waters to the Coipasa lake. In the study area, all the hydrographic system becomes a closed basin, where the Coipasa lake and the Coipasa Salt Plain are the local base level, without exit to the sea.

1.2. Climate. Unfortunately, it is quite impossible to make an statistical analysis of the climate in the area under study, because of the lack of well distributed meteorological stations. Besides, poor and insufficient existing information is not trusty because there is not a sequential registration of such data since at least 10 years ago.

However, there are many different criteria mainly on Geomorphology, Vegetation and Stratigraphy to confirm that the dominant climate in the area is arid-semiarid climate. In other words, it becomes a mid-latitude desert (Cold and dry), located in the interior of two continental masses; the Cordillera Oriental in the eastern part and the Cordillera Occidental in the western part, Widely sparsed vegetation, sand dunes, fields of sand, show evidence of such type of climate.

The isohyets map (Figure N°3) show that the researched area is within the 50 and 200 mm. Isohyets. The 150 mm. Isohyet coincides with a big difference in relief, the northern part is higher than the southern part, besides both areas are climatologically and geomorphologically different. (Ecological barrier).

The Northern part shows more vegetation, fresher water and deeper soil than the southern part does.

The previous mentioned characteristics are probably due to the increase of relative humidity.

The southern part sand deposits and salted soils indicate an increase of aridity. The predominant wind direction W-E is detected by the presence of barchana and parabolic dunes. The area is probaly greatly influenced by the air masses coming from the Pacific Ocean.

1.2.1. Climatic variation through the time. Some evidences of these changes in the area.

Ochsenius (1975) states: "About 10.000 years B.P. the present Atacama desert was the culmination of a fluvial lacustrine period that had begun at least during the Lower Pleistocene, although interrupted by various dry periods as it is suggested by stratigraphical records of the lacustrine basins". According to the biostratigraphical findings of the Pleistocene megafauna in the Atacama area, Ochsenius 1975, correlates with other species also found in the Bolivia Plateau e.g. Tarija, Ulloma, and Cobrizos. These species had probably come from the Atacama Savanna as it is shown by clear taxonomic affinities.

An stratigraphical record was made in the study area at the foot of the Inca Camacho volcanoe, close to the Escara Village. (Figure N°2).

If we analize the schematic cross section (Figure N°2) we are able to discriminate climatic variation through the time in the investigated area.

Pleistocene volcanic activity is dominant in the area. After this event, the second and third glacial periods are observed in Bolivia, specially in the Cordillera de los Andes, close to La Paz. As Ahlfeld points out (1960), glaciation diminished from North to South, that is why glaciation in the Coipasa area is slightly present corresponding to the fourth period (Wisconsin glaciation).

The Minching lake was formed in the interglacial period (Upper Pleistocene) as confirmed by the finding of the Minching limestone.

Due to the wide specular surface of the lake (90.000 Km^2) strong insolation and high evaporation occurred. This evaporation caused the so called Pleistocene rains, which are evident in the area by the morphological processes such as sheet wash, piedmont glacis, wash plain and so on.

Probably in the interin of the cone glacis and related landforms, the climate was alternating: wet-dry-wet. Finally this climate degraded towards aridity at the beginning of the Holocene, unchaining important eolic actions, as well as the formation of beaches and extensive deposits of evaporites.

There is no doubt that the man had great influence for deteriotation of the climate. C. Ponce Sanjinés (1977) and L. Guerra Gutierrez (1977) agree with the fact that man was present 1.250 years B.C. This criteria is based on C14 dating from Archeological specimens found in the Tiwanacu and Wankarani civilization area.

1.2.2. Vegetation and Land use. Sparse vegetation all over the area is specially dominated by shrub and grass such as Thola (Lepidophyllum quadrangulare) which growsmainly in sandy soils with a high water table. Thola is also characteristic in the border of rivers. Paja brava (Festuca scirpifolia) is developed in flooded areas constituting small depressions, with high evaporation and strongly salted soils.

Yareta (Azorella compacta) constitutes an association of hard cushion in the area. It developed shallow and widely branching root systems which acquire quickly as much moisture as possible during rains and by storing water during the wet season, they are able to survive through the long dry period that ensue. Yareta leaves have a thin film of waxy cover, probably to avoid transpiration, that is why yareta grows either in high aridity saline soils or in the paramo environment.

Keñua (Polypsis tomentalla) appears specially at the foot of the Sajama peak conforming the upper limit of vegetation life (4.700 m.). The Keñua becomes probably a good indicator of the improving climatic conditions, because that is the only place of the study area where Keñua grows.

As it was mentioned in 1.2. more vegetation was observed in the

Northern part than in the southern part (Lauca river basin).

According to Lecarpentier (1971), extremely sparse vegetation is present when the water table is too low and only some phreatophytes survive.

Small increase of vegetation was also observed at the eastern part of the area.

Finally, according to C. Troll (1968, page 29-30) the very slow general growth of plants is due to the lack of thermic seasons and to diurnal temperature climate with minimum temperatures at night, around or below freezing point, throughout the year,

The main activity in the area is livestock of Llama (Lama glama) and Alpaca (Lama pacos) specially where water is concentrated in swamp areas (Paramo) being this Paramo an ecologically appropiate environment. This activity is concentrated in the northern part surrounding Sajama, Cosapa and Tampa Nogachi villages. Agriculture is insipient, however potatoe, oca, quinua, barley and wheat are the most important crops.

Nevertheless, in the southern part (Lauca River basin drainage) no crops are found because of the high degree of salinity, flooded areas, and sand dunes, factors that make the zone be strongly arid.

1.3. General Geology. There is a close relationship between Geology and Geomorfology, reason why it is quite impossible to ignore the importance of Geology particularly lithology as a relievant factor in the evolution and shape of the landscape.

Two types of rocks are present in the area, sedimentary and volcanic rocks, the last ones are covering approximately 80 % of the area, 5 % sedimentary rock and 10 % recent unconsolidated material, filling up the Lauca river basin.

The upper north east part is constituted by sedimentary rocks of Tertiary age, mainly conformed by gypsum, sandstone, claystone (lutite) and conglomerate, interbedded tuff of volcanic origin. Sandstone and conglomerate in many cases are forming hills with sharp ridges and hogbacks. Tuff and lutite have been strongly denudated up to hills of low altitude.

In general, this part is grouping all these formations of the Corocoro Group which age is ranging from upper Eoceno to middle Pliocene (Ahlfeld - Branissa 1960). This sediment was fractured and folded during the Orogenesis of the Pliocene (Ahlfeld et all 1960 p.p. 130).

Concerning the volcanic rocks, they belong to two volcanic periods. The oldest one corresponds to the volcanic activity developed in the Tertiary ephoc, about Miocene (Kussmaul 1973) (Avila W. 1965) represented in the study area by the Pacocagua volcanoe in the neighborhood of Caranga Village (68°40 W - 18°50 S) which lithology is formed by basaltic composition (Avila 1965 pp. 45). At the foot of the previously mentioned volcanoe, there are rocks of basaltic and andesitic composition, conglomerate tuffs and sandstone slightly folded and fractured. The age of this complex is probably Miocene-Pliocene (Avila W. 1965 pp. 54).

The second volcanic activity was developed in the Quaternary epoch at the beginning of the Pleistocene. Most of the volcanic cones in the investigated area are strato volcano (Andesitic-Dacitic lava + Pyroclastic material).

In the northern part (68°30 W - 17°30' S) a large plateau of Ignimbrite appears which composition is mainly riodasitic. It is older than the strato volcanoes, probably 2.5 million years (Servant M. 1977). That

means about the Plio-Pleistocene Age.

In order to have a concise idea on Geology and Lithology of the area under study, the following table will help the readers.

Non-cemented alluvial deposits
(Sands + Gravels + Clays)

Recent eolic Lacustrine deposits
(Silts, + Clays + Sands)

Unconsolidated deposits at the foot of the Volcanic cones.
(Clays + Gravels)

Slightly consolidated deposits
(Gravels + Sands + Clays)

Calcareous material remnants of the Minching Lake (Upper Pleistocene)

Basaltic lava

Andesitic - Dacitic lava + Pyroclastic material

Riodasitic Ignimbrite

Intrusive in general

Folded lavas tuffs

Volcanic-sedimentary Complex
(Sandstones + Conglomerates + lutites + Tuffs)

Sedimentary Complex
(Sandostones + Lutites + Conglomerates)

Gypsum

GEOMORPHOLOGY

2. Brief Introduction. The role of Geomorphology. What direct use may developing countries expect from Geomorphology? "Apart from the indispensable services rendered to topographical mapping, Geomorphological studies, have a variety of highly important application, both in rural and industrial areas. Examples: soil conservation and erosión control, coastal defense, site selection, road construction and many other activities in the field of civil engineering. Knowledge of the morphological situation is also essential for physical planning. In this way, Geomorphology contributes directly to solving problems of the developing countries" (Verstappen Th. 1976-4 ITC Journal).

R.L. Wright 1972 emphasizes how Geomorphology provides a useful basis for land classification, because Geomorphology is strongly linked to study of vegetation, soils and water. Each geomorphological unit is also an ecological unit.

2.1. The Geomorphological map - working Method. The Geomorphological map produced is showing that the Coipasa area was scultured by different processes such as forms of structural origin, volcanic, denudational, fluvial and eolian influence mainly. The influence of other elements was also recognized such as climate, vegetation,man interference, etc. in the evolution and shaping of the landscape. The ITC System of Geomorphological survey was used in the preparation of the Geomorphological map.

The main geomorphological units were identifies based on the following

parameters:

- Relief
- Lithology
- Dissection grade
- Types of slopes
- Types of processes
- Types of erosion
- Vegetation

Each Geomorphological unit is coloured according also to the ITC Coloring system. For instance purple is used for the forms or units of structural origin. Black is used for the linear feature as the geomorphological detail.

2.2. The geomorphological units and their characteristics All the geomorphological units mapped in the Coipasa region will be described as possible following a chronological and genetic order, according also to the legend of the Geomorphological map.

2.2.1. Units of structural origin

Unit (1) described as sharp and sawed parallel ridge hills. Relief amplitude: 4500 m.s.l. Medium dissection. Steep to very steep slopes. Crest lines coincide with water divide which are p perfectly discernible

Rock type. Mainly constituted by sandstone and conglomerates.

Soil. Due to the steepness of slope, soils are absent or meager. However, there are small alluvial and glacis terraces with good soils inside the unit.

Hydrologic situation. None

Vegetation and Land use. Vegetation is sparse. The land is used mainly as grassland.

Unit (2) Hogbacks, Relief amplitude: 4000 m.s.l. High dissection. Steep and concave slopes. Crest line or water divide are discernible.

Rock type. Sandstones and conglomerates mainly.

Soil. Soils are meager due to sparse vegetation and steep slope.

Hydrologic situation. No specific surface and ground water aviable, mainly due to dissection.

Vegetation and Land use. Sparse vegetation it is recommended to have a reforestation scheme. No good for agriculture purposes but good for grazing land.

Unit (3) Highly denudated and dissected structural plateau. Medium to short slopes. Accumulation glacis in formation proce - sses . Cone glacis and other slope smoothing processes.

Rock type. Mainly developed on the Mauri formation, which constituents are clayey sandstone, ignimbrite, conglomerate and lava (Rhyolitic composition)

Soil. There is thick soil especially on the accumulation glacis and other surfaces as a result of pedimentation.

Hydrologic situation. Some springs at the foot of the accumulation and cone glacis.

Vegetación and Land use. Sparse vegetation. Agriculture may exist on the accumulation glacis and other pedimented surfaces.

Unit (4). Slightly dissected structural plateau. Long slopes with NW inclination.

Rock type. Entirely developed on Mauri formation (Clayey sandstone + Ignimbrite + conglomerate + rhyolitic lava)

Soil. Poorly developed.

Hydrologic situation. Water (specially springs) could be possibly found, due to the low dissection and permeability of the constituent materials.

Vegetation and Land use. Mainly as grazing land. However, due to the horizontal terrain and the soil conditions could be used as agricultural area.

Unit (5). Strongly tectonic and fractured hills. High dissection. Very irregular topography. Steep slopes. Volcanic, tectonic and fluvial processes were dominant.

Rock type. Folded Lavas (Andesitic and dacitic composition) and tuff.

Soil. Poorly developed because of the steepness of slopes. However, severe weathering and little erosion may develope deep soils.

Hydrological situation. The area is strongly jointed and fractured, reason why, they may actas aquifers. Springs are also possible to be found.

Vegetation and Land use. Scarse vegetation. Pasture lands.

Unit (5) is showing high density of lineaments, reason why it is recommended for mining exploration.

Unit (6) is named as a monoclinal landscape highly denudated with gentle sloping and long slopes. Sheet wash was also observed.

Rock type. As unit (5)

Soil. Due to gentle sloping, thick soils are expected.

Hydrologic situation. Probably in the lower part, surface and ground water may exist because of a synclinal axe that coincides with the negative topography mentioned above.

Vegetation and Land use. Sparse vegetation. Grazing land.

Unit (7). Monoclinal hills in folded lavas. Steep slopes, Medium to high dissection. Discernible water divide.

Rock type. Lavas of Andesitic-Dasitic composition.

Soil. Poorly developed due to sparseness of vegetation and steep slopes.

Hydrologic situation. Hydrologic situation expected is good because jointing and fracturing is high.

Vegetation and Land use. Sparse to absent vegetation.

Grazing land.

This unit is also excellent for mineral exploration due to its high degree of fracturing.

Unit (8). is described as medium to high dissection Cuesta Landscape, developed entirely in the Mauri formation.

Rock type. Clayey sandstone ignimbrite. Conglomerate and lava of rhyolitic composition.

Soil. Thick soils exist but these are strongly dissected and in many cases eroded.

Hydrologic situation. High dissection diminishes the possibility to find ground water.

Water is found as springs, in the steep slope.

Vegetation and Land use. Sparse vegetation. Grazing land.

Unit (9). Structural plateau in the rounded shaped and slightly dissected Mauri formation. Rill erosion is dominant. Gently sloping and high tectonic.

Rock type. Clayey sandstone, ignimbrite, conglomerate and lava of rhyolitic composition.

Soil. Thin soils, except in the infilled valley as they are probably deep soils.

Hydrologic situation. Good hydrologic situation exists only in the infilled valley.

Vegetation and Land use. Good hydrologic situation exists only in the infilled valley.

Vegetation and land use. Sparse to absent, that is why sheet and rill took place. Grazing land. Reforestation schemes are urgent.

This is another area recommended for mineral exploration due to its high tectonic influence observed in the landsat image.

2.2.2. Units of Volcanic Origin.

Unit (10) is described as Volcanic Cone highly dissected mainly by glacial and fluvial processes. Non identifiable crater. Extremely steep slopes.

Rock type. Strato Volcanoe, alternation of lava and Pyroclastic material.

Soil. Poorly developed or absent in many cases.

Hydrologic situation. Poor hydrologic condition in general but some rivers inside the unit develop wide alluvial plain with good hydrologic situation.

Vegetation and land use. Vegetation is barren in the steep slopes. Agriculture and other activities are also absent.

Unit (11) represented by dissected volcanic cones with relatively steep slopes and identifiable craters. Rill, gully and ravines are present. Radial drainage pattern is their relievant characteristic.

Rock type. Strato volcanoe, the cone is normally formed by hard rock (lava) interbedded with pyroclastic material (ash and some

blocks).

Soil. Thin soils are developed. In the concave slopes relatively deep soils are present.

Hydrologic situation. When the volcanic cone is strongly jointed and fractured at its foot, excellent springs can be expected as it occurs in the neighborhood of Nogachi village.

Vegetation and land use. Usually sparse to absent vegetation. Some cultivations are in the concave slope. (Coipasa Volcanoe).

Unit (12). Medium to highly dissected lava fields. Long and slight steep slopes, specially around the volcanic cone.

Rock type. Andesitic lava.

Soil. Thin and badly developed and highly dissected soils.

Hydrologic situation. Dissection was probably favored by the weathering and jointing where water insumed, reason why it may act as an aquifer or water appears as spring.

Vegetation and land use. Bare to sparse vegetation, no specific land use.

Unit (13) Elongated form lava flows along the topographic slope. Medium to low dissection and gently sloping.

Rock type. Andesitic lava.

Soil. Thin soils.

Hydrologic situation. Because of the gently sloping and weathering at the foot of the slope, springs are expected.

Vegetation and land use. No specific land use.

Unit (14). Parasitic and/or Adventive cones of different sizes in the major cones flank.

Rock type. As strato volcanoe composition.

Soils. Absent. Debris material only.

Hydrologic situation. None

Vegetation and land use. None

Unit (15) Spatter Cones.

Rock type. Andesite lava mainly.

Soil. Absent. Debris material only.

Hydrologic situation. None?

Vegetation and land use. None

Unit (16) Extremely dissected basaltic lava flow with shaped and actually filled valleys. Slightly inclinated and long slopes. Sheet erosion is dominant.

Rock type. Basaltic lava composition, easily identifiable on the image, because of its dark tone.

Soil. Deep soils, specially in the infilled valleys.

Hydrologic situation. Good

Vegetation and land use. Sparse vegetation. Cultivation is better developed in the botton of the infilled valley, but in an insipient form.

Unit (17) Low dissected basaltic lava flow of flat or slightly ondulated shape (like a Basaltic plateau).

Rock type. Basaltic lava composition.

Soil. Thin soils are present.

Hydrologic situation. Springs are present specially at the steeped scarpments. These springs are contributing to the Cosapa river.

Vegetation and land use. Sparse vegetation Pasture land.

Unit (18) Shield volcanoes and/or lava domes.

Rock type. Basaltic lava composition.

Soil. Absent. Except on the relatively flat top, thin soils appear.

Hydrologic situation. None.

Vegetation and land use. None

Unit (19). Lava plateau of extremely high dissection by parallel network. Inclination toward the Cosapa depression.

Rock type. Ignimbrite mainly.

Soil. Badly developed soils. Except in the alluvial plains formed by rivers cutting the plateau.

Hydrologic situation. Surface water in many cases in seasonal streams. Ground water and spring are absent, because of extremely high dissection.

Vegetation and land use. Sparse to absent vegetation. Pasture land. Agriculture activity in a low rate in the alluvial plains.

Unit (20) High dissected lava plateau. Highly eroded and degrada dated top soil. Sheet and rill erosion.

Rock type. Ignimbrite.

Soil. Decapitated soils by sheet erosion mainly.

Hydrologic situation. Surface runoff as overland flow is more important than the infiltration to originate ground water.

Vegetation and land use. None

Unit (21) Slightly dissected lava plateau with gently sloping toward the NE.

Rock type. Ignimbrite.

Soil. Thick soils, due to the relatively flat surface and slight dissection.

Hydrologic situation. Infiltration rate is high due to the permeability of the rock, jointing and flat surface, it may act as

aquifer. At the border of the plateau specially in the scarp - ment zone, water is present as spring.

Vegetation and land use. Sparse vegetation. Agricultural activi ty and pasture land.

Unit (22) Volcanic Caldera. Steep to very steep ridge. Irregu lar surface.

Unit (23) Volcanic neck and other intrusive forms. Usually a lack of drainage pattern.

2.2.3. Units of denudational origin.

Unit (24) Slopes at the foot of the Volcanic Cones (Piedmont Glacis). Very long and gently sloping slopes of 5°(11 %) approximately. Low dissection. Sheet wash is dominant.

Rock type. This accumulation glacis are constituted by clay and gravel and material coming from the volcanic cone.

Soil. Thick soils, probably the most important soils in the stu dy area. Cultivation by mechanized method is possible. Tillage along the contours is recommended.

Hydrologic situation. On the landsat image dark tone is observed, because an increase in vegetation and humid condition exist. All water coming from the volcanic cone insume in the glacis.

Vegetation and land use. More abundant vegetation was observed. Agriculture and grazing activity exist.

Unit (25) Highly dissected slopes at the foot of Volcanic Cones (Piedmont glacis).

Rock type. Same as unit (24)

Soil. Thick soils, but high dissection impede mechanization me - thods.

Hydrologic situation. Due to the high dissection only surface water is expected during the rainy season.

Unit (26) Piedmont glacis remnants. Long, slightly inclinated and slightly dissected slopes with NE inclination.

Rock type. Clay and Gravels.

Soil. Good soils, but sheet wash is more intense and probably the soils are wash down.

Hydrologic situation. A light tone is observed on the image. Ru noff is more important than infiltration due to sparse vegeta - tion.

Vegetation and land use. Sparse vegetation. Agriculture activi- ty and grazing may be the best use of the land.

Unit (27) Erosion surface remnant. Flat surface on the top of the upper Pliocene rocks. Carangas formation.

Rock type. Mainly constituted by gravel and clays.

Soil. Relatively thick soils, where gravel is dominant.

Hydrologic situation. Because of a completely flat surface, in- filtration is rather better than runoff.

Vegetation and land use. Sparse vegetation. Pasture and agricultural activity.

Unit (28) Bad lands developed in the Mauri formation. U shaped and flat bottom filled valley. Very fine drainage network and short steep slopes. Extremely dissected. Gully erosion is dominant.

Rock type. Clayey sandstone, Ignimbrite, conglomerate and rhyolitic lava.

Soil. Eroded and decapitated soils. Deep soils in the infilled valleys.

Hydrologic situation. Surface water during the rainy season only. Moisture is available in the infilled valleys.

Vegetation and land use. Sparse to absent vegetation. In the infilled valley vegetation is rather good. Reforestation schemes are advised.

Unit (29) Badlands developed on gypsum with minor karst phenomena.

Land qualities are the same as in unit (28)

Unit (30) Denudated landscape at a dissected and slightly flat to ondulated level. Medium to long slopes.

Rock type. Slightly consolidated deposits of gravel, sand and clay.

Soils. Thick soils.

Hydrologic situation. Good. It was observed suffosion phenomena

This phenomena means:

large hydrometric gradient, long dry season, less than 4 % of montmorrilonite.

Vegetation and land use. An increase in the vegetation coverage was observed. Agricultural activity and grazing land may be possible.

Unit (31) Residual hills in general, which rise up as an island in the flat areas.

2.2.4. Units of fluvial origin.

Unit (32) Alluvial plains in general.

Rock type. Non-cemented alluvial deposits mainly constituted by sand, gravel and clays.

Soil. In general alluvial plains have thick soils, but in many cases subject to floods.

Hydrologic situation. Hydrologic situation is good. Specially in the Choquecota alluvial plain in the NE corner of the survey area, excellent conditions were observed. - These alluvial plains are probably recharged by rains and floods.

Vegetation and land use. The density of vegetation is increased. Because of the increase of vegetation infiltration opportunities also increases allowing water percolate to the ground water mass being stored therefore for a long period of time. Agricultural activities and grassland.

Unit (33) Flood plain dominated by sand dunes, mainly by barchan type.

Rock type. Unconsolidated material.

Soil. Sandy soils principally.

Hydrologic situation. Huge masses of usually fine grained sand are capable for retention of considerable quantities of water. Sand dune inter-depression with a high moisture content, has been seen.

Vegetation and land use. Sparse vegetation in spots, specially in the interdune depressions.

Unit (34) Delta plain formed specially by the Lauca river in the nearby of the Chipaya village causing serious damage during the rainy season. Several splay or crevases were detected in the Lauca river as to be responsible for the inundations.

Rock type. Unconsolidated material clay sand and silt mainly.

Soil. Thick soils, loam mainly. A crust of salt is formed after evaporation.

Hydrologic situation. It was very interesting to observe dark green grass along the small infilled channels. Springs were observed going down the valley.

Vegetation and land use. Vegetation is represented by grass pasture land.

Unit (35) Eroded and highly dissected alluvial fans.

Rock type. Mainly coarse material such as sand gravel, and boulders.

Soil. Absent

Hydrologic situation. None

Vegetation and land use. Sparse to absent.

Unit (36) Well preserved fans.

Rock type. Gravel, boulders and sand.

Soil. Thin soil, badly developed.

Hydrologic situation. Water is expected specially in the lower part of the fan as seepage manifestation.

Vegetation and land use. Sparse vegetation. Pasture land mainly.

Unit (37) Paramo (Moor). Depressions in the highest parts where water is concentrated in swamp. Troll C, 1968 states that the range of 3.500 m to 4.500 m.s.l. is the altitude where paramo is developed. There is a peculiar type of life forms. (Cuatrecasas 1968).

Soil. Very deep and compact. Soils are grazzy, black to dark brown. Soils are usually saturated by water, retaining the humidity even during periods of reduced rainfall. According to Jenny (1948), the known soils formed in paramos may be classified as "Paramo humus soils"

Hydrologic condition. Excellent. Water is generally supplied to

the paramo by thawing of the perennial snow.

Vegetation and land use. Paramo plant life is active throughout the year; the component species are evergreen.

Humidity and abundant grass species become an excellent grazing land for Llamas (Lama glama) and Alpacas (Lama pacos).

Unit (38) Slightly depressed and temporary flooded areas. High evaporation. High saline soils. Imperceptible slope gradient. (2-3 %) This zone is inundated after intense rains during the sumer season. Although the floods are really caused by the water collected locally, being thus eolian effects specially ablation the responsible factors of the origin of this unit.

Rock type. Clay and silts, as main constituents.

Soil. Thick soils, generally loam. A crust of salt after water evaporation is formed, reason why light tone appears on the Lands at image.

Hydrologic situation. Probably during one or two months after rainy seasons, the phreatic level is high. However during the dry period water table is low.

Vegetation and land use. Sparse to absent, represented by vareta with salt crusting. No specific land use because of many adverse factors.

Unit (39) Permanently waterlogged zone.

Unit (40) Temporary waterlogged zone.

2.2.5. Units of Eolian Origin

Unit (41) Sand fills with well developed sand dunes stabilized by vegetation (Thola).

Soil. Sandy soils dominant. 50 cms of sand covering clayey soils in the neighborhood of Bella Vista were detected.

Hydrologic situation. The Lauca river and other perennial small streams exert some influence. Mainly the small streams coming from the upper part of the mountain insume themselves in the impervious material (sand and sand dunes). Rain water in the rainy season may also contribute to groundwater storing.

Some oasis with grouped vegetation and high moisture content were observed in the eastern part close to the Barras river.

Vegetation and land use. Sparse vegetation, Non-specific land use.

Unit (42) Parabolic sand dunes trapped by vegetation (Thola)

Land qualities are the same as in Unit (41)

2.2.6. Units of Saline origin. (Evaporation + Precipitation)

Unit (43) Salt plains confined to lacustrine basin. This unit is represented by the Coipasa salt plain in the lower southern part of the studied area. K and Li with high p.p.m. content were discovered in this salt plain brines.

Unit (44) Salt plains confined to river beds.

2.2.7. Units of Lacustrine origin.

Unit (45) Flat to slightly inclinated shore line toward the salt plain. Sheet wash is actually dominant.

Soil. Thick soil, but covered by salt crust.

Hydrologic situation. Unknown.

Vegetation and land use. Sparse to absent. Non-specific land use.

Unit (46) Lacustrine terrace belonging to the old Minching lake.

Rock type. Calcareous material.

Soil. Thin soil, badly developed.

Hydrologic situation. Unknown.

Vegetation and land use. None.

2.2.8. Units of Glacial origin.

Unit (47) Perennial snow.

3. CONCLUSIONS.

After this preliminary Geomorphological research of the Coipasa area, conclussions can be as follows:

(1) Geomorphology provides the preliminary land resources surveys, giving the necessary information for future planning and further intensive investigations.

(2) Landsat imagery, due to its regional overview is an excellent tool to inventory natural resources specially in developing countries and unknown areas, where basic information is lacking.

(3) According to their more profitable land qualities, the following Geomorphological units must be investigated as suitable areas:

Unit (24) corresponding to the slopes located at the foot of the volcanic cones. It is recommended that this unit should be investigated for agricultural purposes, because thick soils and abundant fresh water exist, specially in the N-NW part of the study area.

Unit (37) Paramo, due to the abundant fresh water and pasture, is appropiate to increase livestock of Llamas and Alpacas.

Units (2), (9) and (28). These are units that require urgent reforestation schemes, because bad lands (gully erosion), sheet and rill erosion are causing serious damages.

Unit (30) is mainly recommended or suggested for ground water investigation because suffosion phenomena exist.

Units (5), (7) and (9) are areas suggested specially for mineral exploration, because they are strongly fractured tectonically and also connected with some intrusive bodies.

However, there are other units, such as (38), (41) and (42) greatly influenced by soil salination, saline water and sand dunes which do not permit soil fertility. In these units, it is quite important to improve the above mentioned adverse factors.

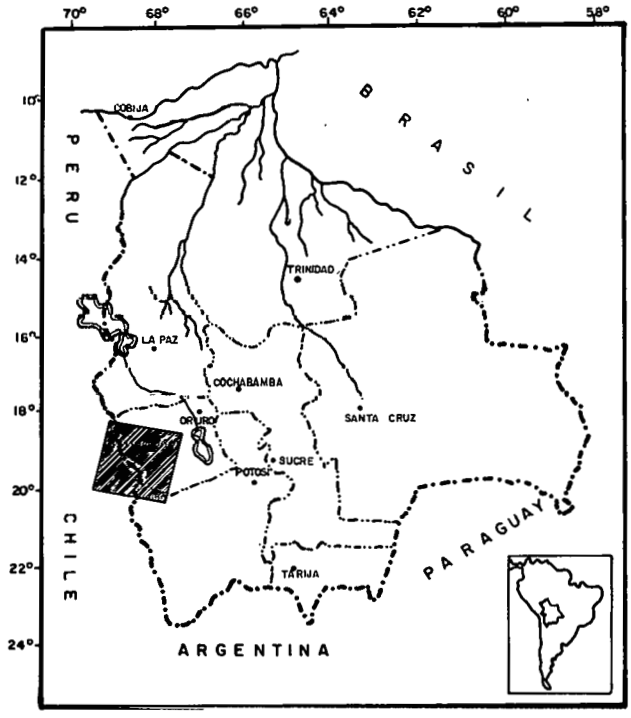

Figure Nº1.- LOCATION MAP

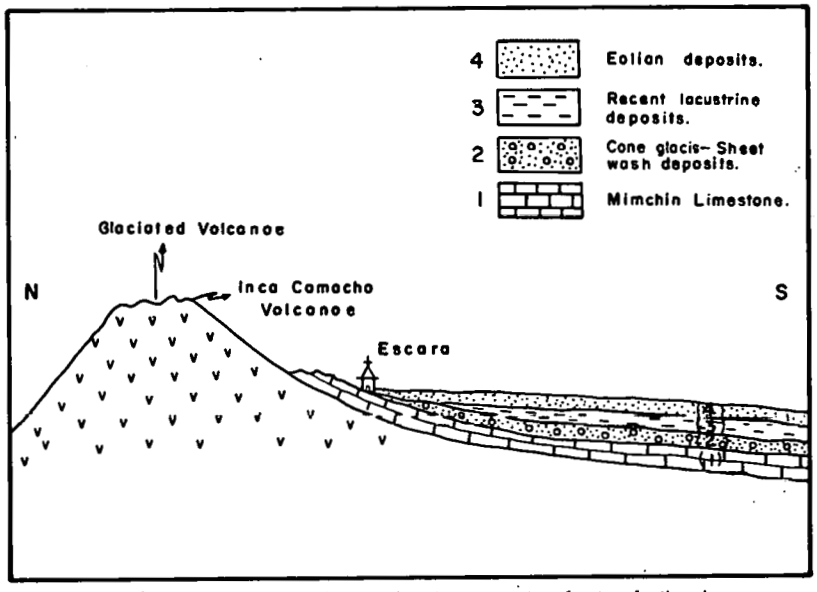

Figure Nº2.- Schematic Cross Section at the foot of the Inca Camacho Volcanoe.

APPROX. SCALE 1:2 000 000

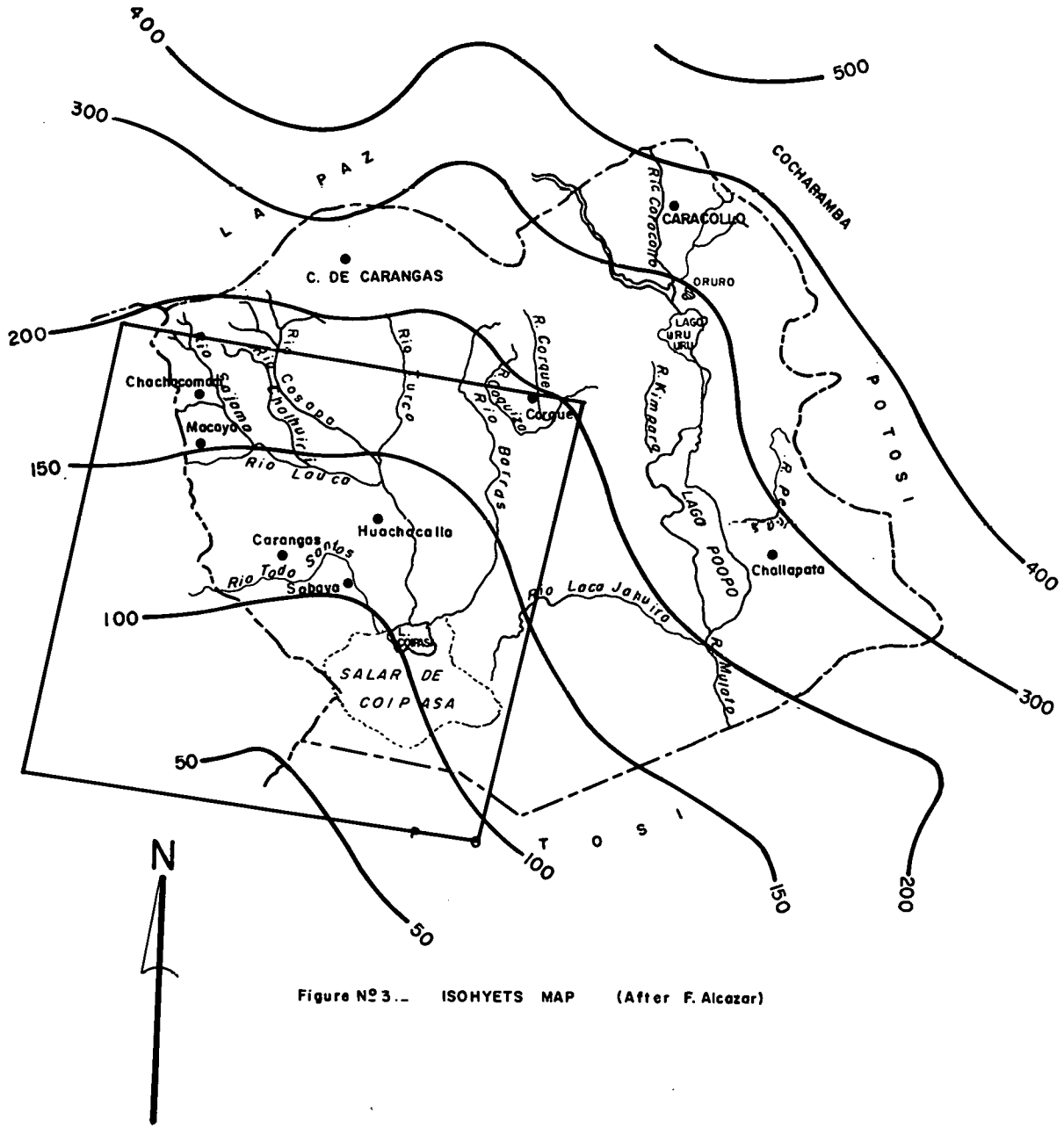

Figure Nº 3.- ISOHYETS MAP (After F. Alcazar)

R E F E R E N C E S

1. AHLFELD F. - 1960 BRANISSA L. Geología de Bolivia
Editorial Don Bosco.
La Paz - Bolivia

2. AHLFELD F. - 1973 Geografía Física de Bolivia
Ed. Los Amigos del Libro
La Paz - Bolivia

3. AVILA S.W. - 1965 Geología del Distrito Minero de Carangas y sus alrededores
Unpublished Universidad Mayor de San Andrés
La Paz - Bolivia

4. CUATRECASAS J. - 1968 Paramo vegetation and its life forms. Proceeding of UNESCO
México Symposium
August 1966

5. FAIRBRIDGE R. - 1968 The Encyclopedia of Geomorphology
Reinhold Book Corporation. New York, USA.

6. GUERRA G.L. - 1977 El arte de la Prehistoria Orureña
Editorial Universitaria
Oruro - Bolivia

7. LECARPENTIER C.- 1973 Geomorphologie et Eaux Souterraines.
Presentation de la Carte Geomorphologique de la Pampa del Tamarugal. Bull. Inst. Fr. Et, and N°2 p. 29-57.
Paris-France.

8. OCHSENIUS C- 1975 The Lacustrine Enviroment of the Atacama and Sahara deserts during the Late Pleistocene. Ecological and climatic importance. Unpublished. Santiago - Chile.

9. OCHSENIUS C. - 1975 Quartenary Biostratigraphy and Biogeographical relations between Lentic Environment of Atacama Desert and Bolivian Plateau. Unpublished. Santiago - Chile.

10. PONCE, S.C. - 1976 Tiwanaku, Espacio, Tiempo y Cultura.
Ed. Los Amigos del Libro La Paz - Bolivia

11. SERVANT M. - 1977 Le Cadre Stratigraphique Du Plio.
Quartenaire de L' Altiplano Des Andes Tropicales en Bolivia. INQUA - 1977 - 1 N°50.

12. TROLL, G. - 1968 Geo-Ecology of the Mountainous Regions of the Tropical Americas. Proceedings of the UNESCO. Symposium, August 1966 México

13. VERSTAPPEN TH.- 1975 ITC System of Geomorphological Survey.
Enschede-The Netherlands.

14. VERSTAPPEN TH.-1976 ITC Journal 1976-4
Enschede-The Netherlands.

15. WRIGHT R.L. - 1972 Principles in Geomorphological
Approach to Land Classification
Berlin-Suttgart - Z. Geomorphie
N.F. 16-4-351-373

IONOSPHERIC AND SATELLITE OBSERVATIONS FOR STUDYING THE DYNAMIC BEHAVIOR OF TYPHOONS AND THE DETECTION OF SEVERE STORMS AND TSUNAMIS

R. J. Hung

The University of Alabama in Huntsville
Huntsville, Alabama 35807, U.S.A.

and

R. E. Smith
NASA/Marshall Space Flight Center
Huntsville, Alabama 35812, U.S.A.

ABSTRACT

Atmospheric acoustic-gravity waves associated with severe thunderstorms, tornadoes, typhoons (hurricanes) and tsunamis can be studied through the coupling between the ionosphere and the troposphere. Reverse ray tracing computations of acoustic-gravity waves observed by an ionospheric Doppler sounder array, show that wave sources observed by an ionospheric Doppler sounder array, show that wave sources are in the nearby storm systems and that the waves are excited prior to the storms. Results show that ionospheric observations, together with satellite observations, can contribute to the understanding of the dynamical behaivor of typhoons, severe storms and tsunamis.

1. INTRODUCTION

Atmospheric acoustic-gravity wave studies can contribute to the understanding of severe weather activity and propagation characteristics of destructive tsunamis. The correlation of atmospheric acoustic-gravity waves and severe storms has been investigated sporadically during the past twenty years. Tepper (1950, 1954) proposed that the pressure jump lines effectively lifted the lowest layers of the atmosphere and appeared to initiate squall line development in convectively unstable air. Matsumoto and Akiyama (1969), Matsumoto and Tsuneoka (1969), and Matsumoto et al. (1967a, 1967b) contended that atmosphric acoustic-gravity waves were responsible for the pulsating tendency of winter and summer convective storms in Western Japan. Recently, Uccellini (1975) proposed that atmospheric acoustic-gravity waves are an important mechanism for triggering severe convective storms. He also suggested that atmospheric acoustic-gravity waves could reveal much about the development of thunderstorms.

In recent years, experimental observations from CW Doppler soundings of the upper atmosphere show that there are ionospheric disturbances apparently associated with severe weather and thunderstorms (Baker and Davies, 1969; Davies and Jones, 1972, Georges, 1973; Prasad et al., 1975; Smith and Hung, 1975; Georges and Greene, 1975; Georges, 1976; Jones and Georges, 1976; Hung and Smith, 1977a; Hung and Smith, 1977b, etc.). These studies reveal that quasi-sinusoidal oscillations, with two harmonics of waves, 3 to 5 minutes and 6 to 9 minutes, are observed when thunderstorms with cloud tops (radar heights) in excess of about 12 Km are present within a radius of several hundred kilometers of the ionospheric reflection points. Malkus (1960) had previously proposed that the convection regions imbedded in the stratiform anvils of the thunderstorms cause the overshooting convective cells which penetrate the tropopause. Saunders (1962), using radar echo observations of a hurricane eye wall, concluded that wall clouds penetrate well above the tropopause. Recent Skylab observations based on stereo-

photographs taken from tropical storm Ellen also showed overshooting turrets above the tropopause in the wall clouds (Black, 1977).

From a fluid mechanics point of view, Lighthill (1952; 1954; 1962; 1967) indicated that gravity waves can be generated by tongues of turbulence penetrating above a turbulent convection zone. This suggests that the overshooting and ensuing collapse of the convective turrets may be responsible for the generation of the atmospheric acoustic-gravity waves.

Atmospheric acoustic-gravity waves associated with hurricanes (typhoons) and severe storms have been studied using a reverse ray tracing computation from the ionospheric observation point, where waves were detected, down to the tropopause, using background wind and neutral atmosphere data. The results show that the waves observed were associated with the hurricanes (typhoons) and severe storms (Hung et al., 1978a; Hung et al., 1978b).

Similar techniques have also been applied to observations of atmospheric acoustic-gravity waves associated with tsunamis. The results show that the technique is useful for tsunami warning systems since at ionospheric heights the propagation speed of the acoustic waves associated with desctructive tsunamis is more than ten times faster than the wave propagation speed of the tsunamis (Najita and Yuan, 1973; Najita et al., 1974).

Results of this study indicate that geosynchronous satellite observations of strong convective cells can be used with ionospheric observations of atmospheric acoustic-gravity waves in a new technique for detecting and predicting typhoons, severe storms and tsunamis.

2. EXPERIMENTAL OBSERVATIONS AND DATA ANALYSIS

Ionospheric and satellite observations are employed in the present study. Our ionospheric high frequency radio wave Doppler array system consists of three sites with nine field transmitters operating at 4.0125, 4.759 and 5.734 MHz. These sites are located in northern Alabama and the Tennessee Valley area. A detailed description of the geographical locations and array systems has been given by Hung et al. (1978a) and Hung and Smith (1978a). The propagation characteristics of atmospheric gravity waves can be determined from the observed electron density fluctuations in the ionosphere. The dynamics of overshooting turrets can be studied by using photographic observations made from Earth-orbiting spacecraft such as geosynchronous satellite, Skylab, Apollo, etc.

Theoretical discussions of group rays of atmospheric gravity waves by Bretherton (1966), Jones (1969), Cowling et al. (1971) and Berlin, et al. (1975) indicate that the geometrical optics approximation seems valid. The wave propagated is assumed to be locally plane so that a local dispersion relation of atmospheric gravity waves, proposed by Hines (1960), is satisfied. Ray tracing, thus, can be carried out by following the group velocity direction in a wind-stratified model atmosphere.

The propagation of wave energy in a lossless transparent medium follows the direction of the group velocity or the ray direction (e.g., Yeh and Liu, 1972), which in general, in an anisotropic medium is different from that of the wave vector. In the reverse ray tracing computation the group velocity is integrated with respect to time from the ionospheric reflection point back down to the tropopause using the wave period, wavelength, and azimuthal direction of wave propagation obtained from the observational data, the initial vertical wave vector computed from the dispersion relation and appropriate atmospheric parameters. The effect of wind is taken into account by considering the time-space transformation given by the Galilean transformations of the displacement vector, time, Doppler-shifted wave frequency, and wave vector. The detailed description of the group ray tracing computation has been given in another article (Hung et al., 1978a).

In the present paper, the neutral wind is treated as constant in each slab of the atmosphere considered. The values of the atmospheric parameters for each altitude are calculated from the U.S. Standard Atmosphere (1962). The profiles of the neutral winds are established using wind profiles above 100 Km altitude

computed from the atmospheric wind model proposed by Kohl and King (1967) faired into wind profiles obtained from meteorological rocketsonde data at Cape Kennedy, Florida.

The reverse ray tracing is started at the altitude of the ionospheric reflection height for a frequency of 4.0125 MHz and continues to a lower limit of 10 Km. For the purpose of the present study the geographic location of the point at which the calculation is terminated is referred to as the probable source. These probable sources are then checked with the actual observations of the severe storms being studied.

2.1 IONOSPHERIC OBSERVATIONS OF GRAVITY WAVES ASSOCIATED WITH HURRICANES (TYPHOONS)

On September 22-23, 1975 when Hurricane Eloise was in the Gulf of Mexico, wave-like fluctuations with wavelengths on the order of 100 Km were observed at F-region ionospheric heights. Doppler observations were subjected to power spectral density analyses and cross-correlation analyses. As an example, Figure 1 shows the power spectral density of the ionospheric disturbances from the transmitters at Muscle Shoals, Alabama to the receivers at Huntsville, Alabama, during the observation time 0200-0340 UT, September 23, 1975. The horizontal phase velocity of the disturbances can be computed from cross-correlograms (for a detailed description see Hung et al., 1978a). As an example, Figure 2 shows cross-correlograms for the same time interval. The azimuthal angle of wave propagation is accurate to within ± 10°, and the horizontal phase velocity is accurate to within ± 10 percent.

During this time period 0200-0340 UT, gravity-waves with a period of 23 minutes, azimuthal angle of propagation of the wave vector of 353°, and horizontal phase speed of 160 m/sec were observed. During the time period 0500-0730 UT, gravity waves with a period of 23 minutes, azimuthal angle of propagation of the wave vector of 344°, and horizontal phase speed of 195 m/sec were detected (Hung et al., 1978c).

Figure 3 shows an example of the trajectory of the computed reverse ray path for the waves observed during the 0200-0340 UT time period on September 23, 1975, in terms of height against horizontal distance while Figure 4 shows the horizontal ray path and the geographical location of the probable source of the waves. The computed location of the wave source is where the storm was located at 0600 UT, September 23, 1975. The calculated traveling time of this wave from the probable source to the receiver at Huntsville, Alabama was 88 minutes; thus, the wave was generated where the storm was located about four hours later.

Figure 5 shows the geographical location of the probable source of the waves which were observed during the 0500-0730 UT time period on September 23, 1975. In this instance, the computed probable source of the wave was where the storm was located at 0730 UT, September 23, 1975, approximately 3.5 hours in advance of the storm.

The probable errors in range in the reverse ray tracing computation due to the accuracy of determination of the azimuthal angle of wave propagation, horizontal phase velocity and wind profiles are estimated to be less than ± 10 Km per 100 Km of horizontal distance. If the probable error of + 10 Km per 100 Km of horizontal distance is taken into account, the wave was generated more than one hour in advance of the storm (Hung et al., 1978c).

2.2 IONOSPHERIC OBSERVATIONS OF GRAVITY WAVES ASSOCIATED WITH TORNADIC STORMS

Using data analysis procedures similar to the analysis of the gravity waves associated with hurricanes (typhoons), analyses of six sets of data from the extreme tornado outbreak of April 3, 1974, showed gravity waves with wave periods of 11 to 15 minutes and 26 to 30 minutes, horizontal wavelengths in the range 100 to 220 Km, and horizontal phase speeds in the range 90 to 220 m/sec (Hung et al., 1978a for details).

Five isolated tornadic storms, two on November 20, 1973 and three on January 13, 1976 were also analyzed. Results are similar to those for the data

from April 3, 1974 with waves with periods of 10 to 15 and 25 to 30 minutes, horizontal wavelengths in the range 120 to 290 Km and horizontal phase speeds in the range 100 to 220 m/sec present (Hung et al., 1978b for details).

Two examples of computed group ray paths of waves (one from the integrated effect of a group of tornadic storms, and the other from an isolated tornadic storm) and the locations of the wave sources are given in this study. Figure 6 shows the computed reverse group ray path of the waves observed during the 2000-2200 UT, April 3, 1974 time period, and the locations and times of four tornado touchdowns where the actual data were provided by the National Severe Storm Forecast Center. The wave traveling time from the computed sources to the receivers at Huntsville, Alabama was 1 hour and 52 minutes; therefore, the signal was excited roughly 2-3 hours ahead of the touchdown of the tornadoes. Figure 7 is a radar summary, provided by the National Weather Service, for the 1935 UT, April 3, 1974 time period, which corresponds to the time when the ionospheric disturbances observed during the 2000-2200 UT time period, at Huntsville, Alabama were excited. It clearly indicates that the tops of thunder storms are significantly above the tropopause in the Indiana area. This example shows that the observed gravity waves are a precursor phenomena due to the integrated effect of a group of tornadic storms which occurred approximately at the same time and place.

Figure 8 shows the reverse ray tracing results for the observed gravity waves associated with the isolated tornadic storm during the 2130-2330 UT, January 13, 1976 time period. In this case, since the wave traveling time from the computed probable source to the receivers at Huntsville, Alabama was 55 minutes and the actual touchdown time was 2245 UT, the signal was excited more than one hour prior to touchdown. The actual tornado touchdown location is well within the $\pm 5^{o}$ accuracy in the determination of the azimuthal angle of propagation of the wave (Hung and Smith, 1978b).

2.3 IONOSPHERIC OBSERVATIONS OF ACOUSTIC WAVES ASSOCIATED WITH TSUNAMIS

Atmospheric acoustic-gravity waves associated with oceanic waves or tsunamis have been observed with similar techniques. Acoustic waves with wave periods of 30 to 200 seconds have been detected at ionospheric heights by a Hawaiian group when destructive tsunamis were generated by earthquakes of the vertical-motion type in relatively shallow water along oceanic margins (Najita and Yuan, 1973; Najita et al., 1974). The propagation speed of the acoustic waves associated with these destructive tsunamis is 3400 m/sec at ionospheric heights, which is more than ten times faster than the wave propagation speed of the tsunamis. By analyzing the ionospheric records and tracing the earthquake-generated Rayleigh wave back to the epicenter, characteristics of the earthquake can be determined. This information can then be used to deduce the probability that the earthquake generated the tsunami.

2.4 SATELLITE OBSERVATIONS OF SEVERE STORMS WITH OVERSHOOTING TURRETS

In addition to the work by Georges (1976); Prasad et al., (1975); Saunders (1962), and Malkus (1960), Vonnegut et al. (1966) using photographs from a U-2 airplane flying over the thunderstorms showed that convective overshooting turrets rose above the anvil cloud and penetrated the tropopause. This may suggest that the penetration of intense updrafts through the tropopause could be the wave generation mechanism. Recent observations made by ATS satellites (Fujita, 1974) and Skylab (Black, 1977) also endorse the suggestion that the growth and collapse of convective overshooting turrets associated with severe storms generate gravity waves.

Recently, Shenk (1974) made extensive analyses of strong convective cells using geosynchronous satellite data and U-2 photographs. When the results of Shenk's analyses are used in the model proposed by Lighthill (1952; 1954; 1962; and 1967), waves with the same periods as those observed by the Doppler array are excited (Hung and Smith, 1978b).

By using photographic enhancement techniques, Black (1977) has successfully determined relative cloud heights of the tropical storm Ellen from Skylab stereographs. Figure 9 shows a Skylab photograph taken at 2018 UT, September 19,

1973 while Figure 10 shows relative cloud heights along the cross-section shown in Figure 9.

3. CONCLUSIONS

Ionospheric Doppler sounder observations during time periods with severe storm activity show a coupling between the troposphere and the thermosphere. Analyses of these observations indicate that acoustic-gravity waves propagating in the ionosphere are clearly related to severe storm activity with the waves apparently associated with tornadoes appearing to be excited where tornadoes touchdown more than one hour later. Results for gravity waves associated with hurricanes show the computed sources of the wave to be located along the track and more than three hours in advance of the location of the storm.

Observations of atmospheric acoustic-gravity waves associated with tsunamis also indicate that a tsunami warning system can be developed by using an ionospheric observation technique.

George (1960) reported that hurricanes tend to move toward the location where the K-instability index is a maximum with a higher index being related to a higher moisture content and a higher temperature. Results of this study seem to indicate that this is the location of the source of the waves. The possibility of using a combination of these facts as a prediction technique will be the subject of future investigations. This study suggests that the analysis of ionospheric Doppler sounder observations of gravity waves together with the study of the growth and collapse of convective over-shooting turrets based on satellite photographs, can contribute to the understanding of the dynamical behavior of hurricanes, severe storms and tsunamis.

4. COMPREHENSIVE SUMMARIES

We have investigated hurricane (typhoon), and severe storm associated acoustic-gravity waves by using a CW, HF radio wave Doppler sounder array. Gravity waves with periods from 21 to 25 minutes, and horizontal phase speeds from 150 to 200 m/sec, were detected when Hurricane Eloise was located in the Gulf of Mexico on September 23, 1975 (Hung and Smith, 1978a; 1978b; Hung et al., 1978c); and another group of gravity waves with wave periods from 10 to 15 minutes and/or 26 to 30 minutes, and horizontal phase speeds from 90 to 200 m/sec, were observed during time periods with tornado activity (Hung et al., 1978a; 1978b). The results are similar for isolated tornadic storms and groups of tornadic storms which occurred approximately at the same time and place.

Identification of the sources of these waves has been attempted. For the case of typhoons (hurricanes) it was found that the computed locations of the sources were along the storm track 3 to 4 hours ahead of the actual location of the center of the storm. For the case of gravity waves associated with tornadoes, it was shown that the wave sources were near where tornadoes touched down more than one hour later. The applicability of the Doppler array to severe storm warning systems has been discussed by Hung and Smith (1978a; 1978b).

Similar techniques have also been applied to the observation of atmospheric acoustic-gravity waves associated with tsunamis. Acoustic waves with wave periods of 30 to 200 seconds were detected by a Hawaiian group when destructive tsunamis were generated by earthquakes of the vertical-motion type in relatively shallow water along ocean margins (Najita and Yuan, 1973; Najita et al., 1974). The propagation speed of the acoustic waves associated with destructive tsunamis is 3400 m/sec, at ionospheric heights, which is more than ten times faster than the wave propagation speed of the tsunamis.

The satellite observations of convective overshooting turrets associated with typhoons and severe storms have been discussed (Black, 1977). This study reveals that satellite observation of wave generation mechanism will contribute to the understanding of dynamical behavior of typhoons and severe storms.

This suggests that the analysis of ionospheric Doppler sounder observations of atmospheric acoustic-gravity waves and group ray tracing computations together with the study of the growth and collapse of convective overshooting

turrets based on satellite photographs, may be used in the development of a technique for the real time detection and prediction of typhoons, severe storms and tsunamis.

ACKNOWLEDGMENT

The authors acknowledge the ray tracing computations made by T. Phan and J. P. Kuo. One of the authors (RJH) also appreciates the support of the present research from NASA/Marshall Space Flight Center through Contract NAS8-31171 and the National Science Foundation/U.S. Army Research Office through Grant NSF/ATM75-15706.

REFERENCES

Baker, D. M., and K. Davies, J. Atmosph. Terr. Phys., 31, 1345, 1969.
Bertin, F., J. Testud, L. Kersley, Planet. Space Sci., 23, 493, 1975.
Black, P. G., in Skylab Explores the Earth, ed. by V. R. Wilmarth, NASA SP-380, pp. 417-461, 1977.
Bretherton, F. P., Quant. J. Roy. Meteor. Soc., 92, 466, 1966.
Cowling, D. H., H. D. Webb, K. C. Yeh, J. Geophys. Res., 76, 213, 1971.
Davies, K., and J. B. Jones, Space Research, 12, 1149, 1972.
Fujita, T. T., Overshooting Thunderstorms Observed from ATS and Learjet, NASA CR-13859T, 1974.
George, J. J., Weather Forecasting for Aeronautics, Academic Press, New York, pp. 673, 1960.
Georges, T. M., Rev. Geophys. Space Phys., 11, 571, 1973.
Georges, T. M., Infrasound from Convective Storms, Part II: A Critique of Source Candidates, NOAA Tech. Rep. ERL 380-WPL49, pp. 59, 1976.
Georges, T. M., and G. E. Greene, J. Appl. Meteor., 14, 1303, 1975.
Hines, C. O., Can. J. Phys., 38, 1441, 1960.
Hung, R. J., and R. E. Smith, Space Research, 17, 205, 1977a.
Hung, R. J., and R. E. Smith, Space Research, 17, 211, 1977b.
Hung, R. J., and R. E. Smith, J. Appl. Meteor., 17, 3, 1978a.
Hung, R. J., and R. E. Smith, Dynamics of Severe Storms Through the Study of Thermospheric-Tropospheric Coupling, J. Geomag. Geoelect., 1978b (in press).
Hung, R. J., T. Phan, and R. E. Smith, Observation of Gravity Waves During the Extreme Tornado Outbreak of April 3, 1974, J. Atmosph. Terr. Phys., 1978a (in press).
Hung, R. J., T. Phan, and R. E. Smith, Ionospheric Doppler Sounder as Remote Sensing for Detection and Prediction of Severe Storms, AIAA Journal, 1978b (in press).
Hung, R. J., J. P. Kuo, and R. E. Smith, in Proc. Hurricane and Tropical Meteorology, pp. 630-635, Am. Meteor. Soc., Boston, Mass., 1978c.
Jones, W. L., J. Geophys. Res., 74, 2028, 1969.
Jones, R. M., and T. M. Georges, J. Acoustic Soc. America, 59, 765, 1976.
Kohl, H., J. W. King, J. Atmos. Terr. Phys., 29, 1045, 1967.
Lighthill, M. J., Proc. Roy. Soc. A., 211, 564, 1952.
Lighthill, M. J., Proc. Roy. Soc. A., 222, 1, 1954.
Lighthill, M. J., Proc. Roy. Soc. A., 267, 147, 1962.
Lighthill, M. J., IAU Symposium, 28, 429, 1967.
Malkus, J. S., in Cumulus Dynamics, Pergamon Press, New York, pp. 65-84, 1960.
Matsumoto, S., and T. Akiyama, J. Meteor. Soc. Japan, 47, 255, 1969.
Matsumoto, S., and Y. Tsuneoka, J. Meteor. Soc. Japan, 47, 267, 1969.
Matsumoto, S., K. Ninomiya and T. Akiyama, J. Meteor. Soc. Japan, 45, 64, 1967a.
Matsumoto, S., K. Ninomiya and T. Akiyama, J. Meteor. Soc. Japan, 45, 292, 1967b.
Najita, K., and P. C. Yuan, Trans. Am. Geophys. Union, 54, 384, 1973.
Najita, K., P. F. Weaver and P. C. Yuen, Proc. IEEE, 62, 1045, 1974.
Prasad, S.S., L. J. Schnack, and K. Davies, J. Atmosph. Terr. Phys., 37, 1357, 1975.
Saunders, P. M., Tellus, 14, 177, 1962.
Shenk, W. E., J. Appl. Meteor., 13, 917, 1974.
Smith, R. E., and R. J. Hung, J. Appl. Meteor., 14, 1611, 1975.
Tepper, M., J. Meteor., 7, 21, 1950.
Tepper, M., Pressure Jump Lines in Midwestern United States, January-August, 1951, Research Paper No. 37, U.S. Weather Bureau, Washington, D.C., pp. 70, 1954.
Uccellini, L. W., Mon. Wea. Rev., 103, 497, 1975.

Vonnegut, B., C. B. Moore, R. P. Espinola, and H. H. Blan, Jr., J. Atmosph. Sci., 23, 764, 1966.
Yeh, K. C., and C. H. Liu, The Theory of Ionospheric Waves, pp. 467, Academic Press, New York, 1972.

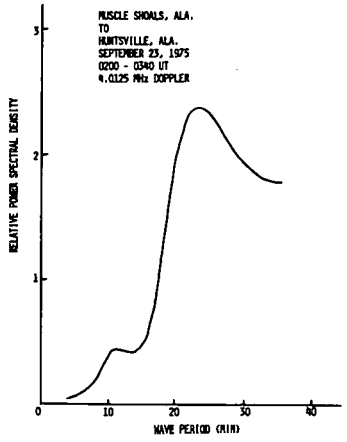

Figure 1. Power spectral density of waves from Muscle Shoals, Alabama to Huntsville, Alabama at 0200-0340 UT, 9-23-1975.

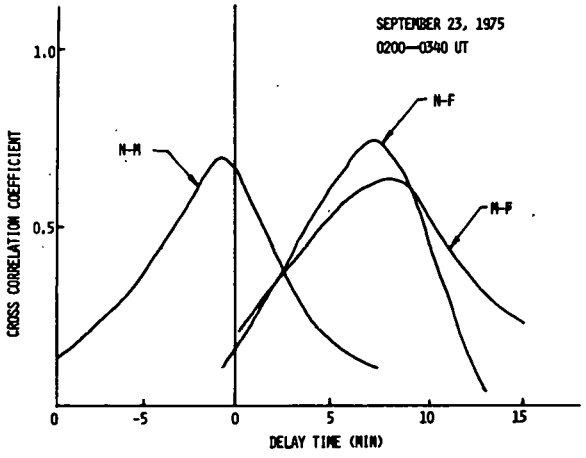

Figure 2. Cross correlograms at time period 0200-0340 UT, 9-23-1975.

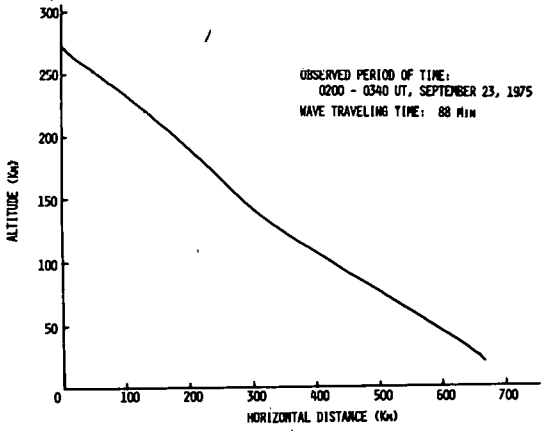

Figure 3. Trajectory of the computed reverse group ray path for the waves at time period 0200-0340 UT, 9-23-1975.

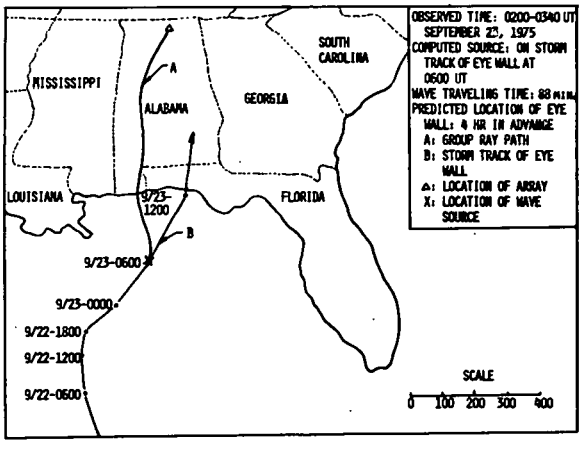

Figure 4. Geographical map of the trajectory of computed source of waves with Hurricane Eloise at time period 0200-0340 UT, 9-23-1975.

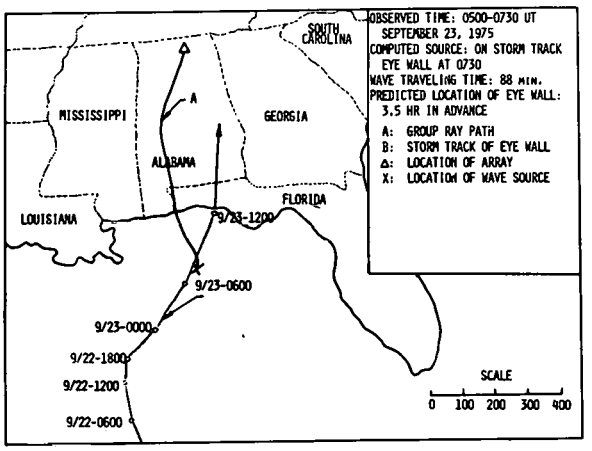

Figure 5. Geographical map of the trajectory of computed source of waves associated with Hurricane Eloise at time period 0500-0730 UT, 9-23-1975.

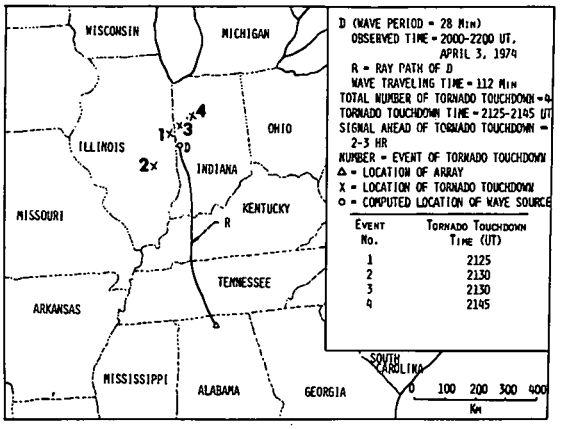

Figure 6. Geographical map of the trajectory of computed source of waves associated with four tornadoes at time period 2000-2200 UT, 4-3-1974, and the locations and times of actual tornado touchdown.

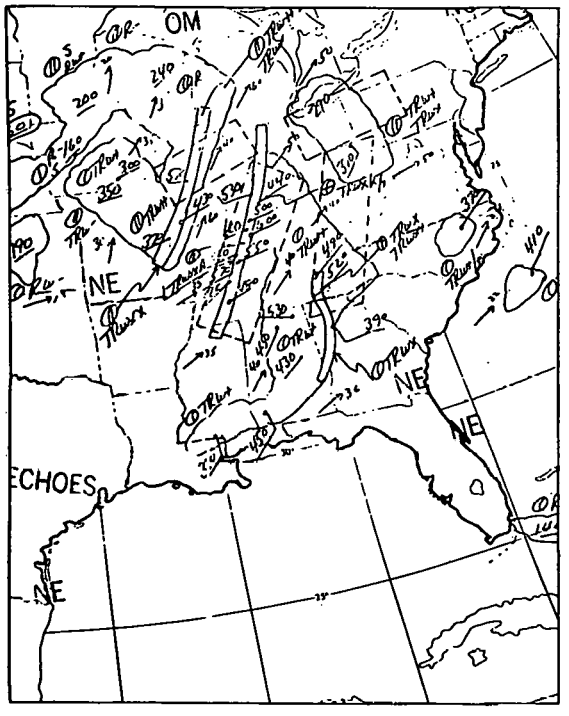

Figure 7. Radar weather summary of the Eastern United States at 1935 UT, 4-3-1974.

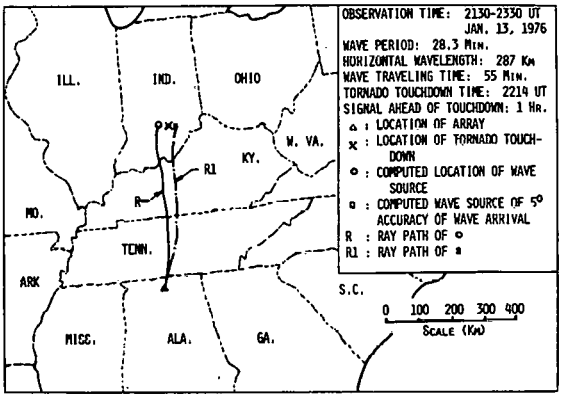

Figure 8. Geographical map of the trajectory of computed source of waves associated with isolated tornado at time period 2130-2330 UT, 1-13-1976, and the location of the actual tornado touchdown.

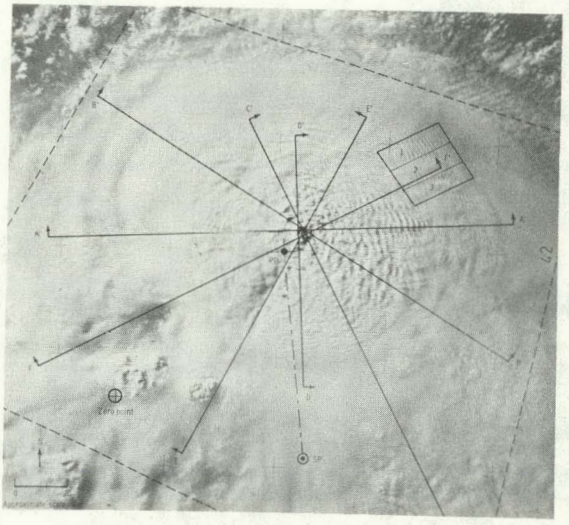

Figure 9. Skylab stereophotograph of tropical storm Ellen taken at 2018 UT, September 19, 1973. The storm was located at latitude 27.3° N, longitude 51.1°W.

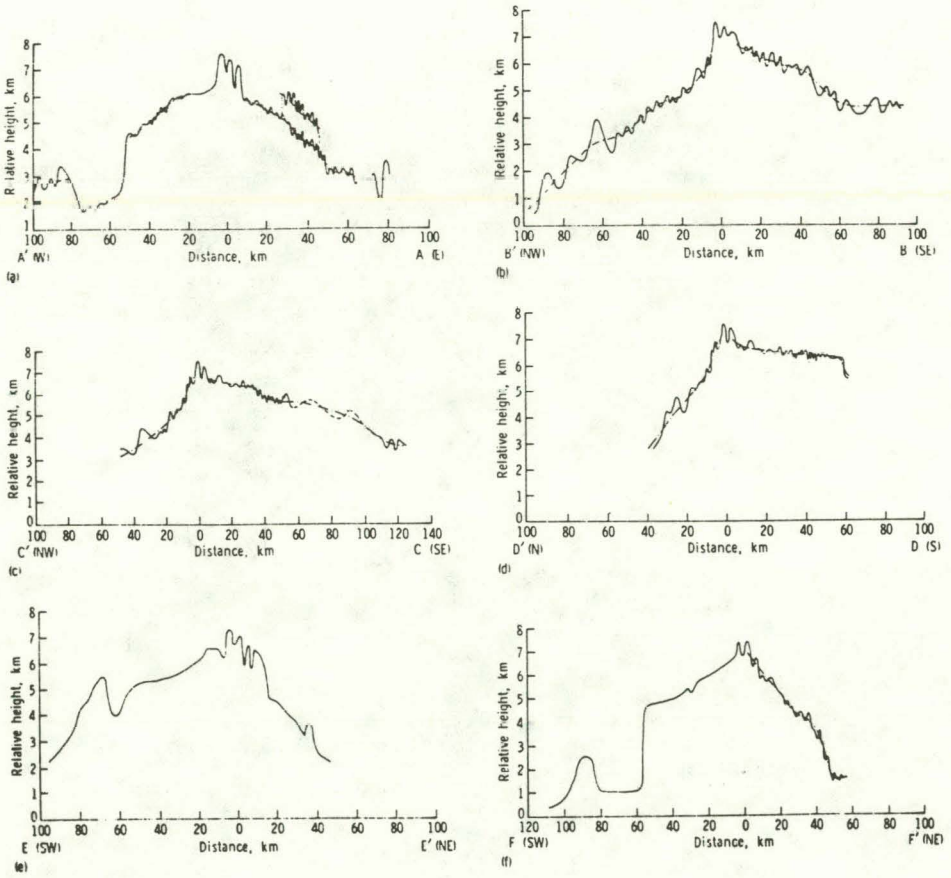

Figure 10. Relative cloud heights of tropical storm Ellen. See Figure 9 for locations of cross-section cutting planes. (a) Section A-A'. (b) Section B-B'. (c) Section C-C'. (d) Section D-D'. (e) Section E-E'. (f) Section F-F'. (from Black, 1977).

THE USE OF LANDSAT DATA TO MINIMIZE FLOODING RISKS CAUSED BY ICE JAMS IN ALASKAN RIVERS

J. M. Miller and T. E. Osterkamp
Geophysical Institute
University of Alaska
Fairbanks, Alaska 99701

ABSTRACT

Breakup of ice in Alaskan rivers in late April or May customarily causes flooding from water backing up behind massive ice jams. Preventive measures normally include dusting the river ice with sand at critical locations in early April at the start of the melting season. To conserve costs of the dusting operations, more effective means are desired to predict the precise locations of the main river channels beneath the ice. Landsat data acquired during the fall freeze-up have been used to predict the locations of the main river channels to optimize the dusting operations performed the following spring. This technique should be operationally useful each year along the major river systems in Alaska such as the Yukon, Tanana and Kuskokwim Rivers which have many villages situated in the flood plain.

INTRODUCTION

Ice jams associated with spring breakup customarily block the flow of some Alaskan rivers for a few days to a week each May. Most of the villages in rural Alaska are located along the rivers, and severe ice jams (Figure 1) cause flooding, property damage, and even loss of life if residents are not evacuated before the river water backs up into the village.

There are four types of ice that grow in lakes and rivers[1]--frazil ice, anchor ice, sheet ice and aufeis. Frazil ice is the dominant form that influences the pattern of freeze-up conditions in the typical Alaskan river. The initial form of frazil ice grows in turbulent water that is slightly supercooled and is observed as thin, circular discs called frazil crystals. These crystals grow, flocculate, form frazil pans and frazil slush-ice, and may eventually evolve into large floes. Freeze-up occurs in many Alaskan rivers when frazil ice--in the form of slush, pans, or floes--jams in river reaches with suitable hydrologic conditions (Figure 2). The initial ice cover may consist of up to a meter thickness of frazil ice, which then consolidates by freezing downward from the surface.

During Alaska's cold winters, the rivers freeze to a depth up to 2 meters and normally are covered with snow. During the spring breakup period, the snow melts before the rivers are ice-free, and the water level rises substantially beneath the ice. Eventually the ice breaks into large floes which drift downstream. These floes may break into small pieces and melt or they may lodge on gravel bars, shoals, and the crenulous meanders of the main river channel thus causing an ice jam. Accumulations of ice sometimes are many miles in length and effectively jam the river and flood the surrounding area.

Customary preventive measures include dusting the river ice and snow with sand or dust (Figure 3) in April prior to the melting season at a location downstream from the more flood-prone villages. In contrast to highly reflective snow, the dust dramatically increases the amount of energy absorbed from the sun by the ice, causes premature melting and eventually an open channel in the ice. (Figure 4) An open river channel is much less likely to experience an ice jam when the ice from untreated areas upstream reaches that point in the river.

Ice dusting is carried out by aircraft based hundreds of miles away from the troublesome areas, so the expense and logistics of preventive measures constitute severe restraints on the program. It is also critically important to deploy the dusting efforts in the most effective manner, since achieving adequate levels of protection by overtreatment must be avoided for economic reasons.

In order to be effective, the dust must be placed specifically on the main channel of the river, but the meanders of the main channel beneath the ice cover compound the problem of targeting the airdrops of dust. Migration of the main channel is rather common so one cannot necessarily base a dusting mission upon the previous year's experience. Further, once the ice cover is formed in the early winter, the accumulation of snow quickly masks the location of the main channels, thus making subsequent reconnaissance very difficult.

Experience to date has shown that late October and early November is the optimum period[2] to define the current location of the main river channels. At this season, slush or frazil ice forms on the rivers and tends to accumulate and freeze in backwater and slow-moving shallows. The processes of frazil-ice accumulation and border-ice growth from the shores tend to "streamline" the river, thus delineating the main river channels (Figure 5).

DATA ACQUISITION

To test the feasibility of Landsat data as a guide to effective dusting operations, two test areas were identified[2] which have historically been flood prone due to the morphology of the flood plain downstream from villages. The selected areas were near Aniak on the Kuskokwim River and near Koyukuk and Galena on the Yukon River. Landsat coverage from previous years in early November of these test areas was searched, but only the Galena site had cloud-free historical coverage available. This was scene 1469-21224 dated 4 November 1973 (Figure 6) upon which we based a tentative conclusion that one should be able to use Landsat data to interpret the conditions during freeze-up and thereby infer where the main channels of major rivers are located.

Visual comparisons were made of 1:250,000 scale prints of the 4 November 1973 scene of all four bands. We concluded that the green visible (MSS Band 4) image was superior for the interpretation of open water, floating frazil ice, rough ice, and snow-covered ice and surrounding terrain. While the infrared bands (MSS 6 and MSS 7) provide more contrast between open water and all ice and snow categories, these images tended to saturate in the photographic highlights from the relatively high reflectances of snow and ice. The infrared images were thus less able to provide information about the conditions of various ice surfaces which is needed to determine the flow patterns of the main river-channels.

The visual interpretation also demonstrated that the spatial resolution of photographic Landsat products was adequate to study ice conditions on the very wide Yukon River (2 km) but only marginally so for medium-sized rivers such as the Kuskokwim or Koyukuk Rivers (0.5 km). To obtain maximum resolution capability, we also plan to evaluate various digital techniques such as digitally-enhanced images, gray-scale line-printer maps, and clustering with 1977 data from the test sites.

Based upon the positive evaluation of historical data for river-ice studies, we requested special data-acquisition efforts for our two sites from 1 November to 20 November 1977. Normally the Landsat sensors are not activated unless the sun elevation is above ten degrees, and at northern latitudes the sun remains lower than ten degrees from mid-October to mid-March. To compensate for the reduced reflectance resulting from very low angles of illumination, we also requested that the satellite be operated in the high-gain mode. To further maximize the amount of data which could be acquired during the relatively short window, we asked that data acquisition be attempted for all passes over the test sites from both Landsat 1 and Landsat 2. With NASA's cooperation, we succeeded in obtaining three data sets from the Koyukuk-Galena area which revealed a sequence of freeze-up events showing many interesting features.

Because there is 60% side-lap coverage on adjacent days at this latitude, we received sequential coverage from Landsat 2 on 10 and 11 November 1977, and from Landsat 1 five days later on 16 November (Figure 7). The 10 November scene of Galena was 70% covered with high cirrus clouds, but the Galena test site itself was totally cloud-free, although it suffered from depressed contrast from cloud shadows over 10% of the site. The 11 and 16 November scenes of Galena were essentially cloud-free, although the extremely low sun-elevation (2°) for 16 November produced a low-contrast image which was of marginal quality for visual interpretation of ice details. Open water was still discernable, however.

The coverage received from the Aniak site was from 11 and 16 November. We discovered that the Kuskokwim River, although here 400 km south of Galena, was completely frozen over and had a rather uniform snow-cover by 11 November. The best window for the Kuskokwim River likely would be from about 15 October to 1 November for future acquisition of Landsat data.

ANALYSIS RESULTS

Analysis of the Landsat data from the Koyukuk-Galena site to date has been restricted only to the visual interpretation of Band 4 imagery from Landsat 2 on 10 and 11 November, and of Band 5 imagery from Landsat 1 on 16 November. There is no Band 4 data available from Landsat 1 because this sensor system failed in March 1977. All Landsat 1 operations were later terminated 6 January 1978, after 5-1/2 years of operation, effectively terminating for the time being the possibility of repeat coverage from two spacecraft. The value of frequent coverage is well demonstrated by this project, and we look forward to a similar nine-day repeat coverage in the future from Landsat 2 and Landsat 3.

An unfortunate difficulty in NASA's capability to produce computer compatible tapes (CCT's) from Landsat digital data has temporarily delayed the arrival of the CCT of the Koyukuk-Galena site. As a consequence, we cannot as yet report any benefits from working with the improved spatial and spectral resolution of digital forms of Landsat data.

The interpretation of the sequence of three Landsat images on 10, 11 and 16 November 1977 proved to be unexpectedly beneficial in understanding the dynamics of the Yukon River. We rather expected that little benefits could be derived from photointerpretation of standard images, but the amount of detail discernable from 1:250,000 scale enlargements proved encouraging. Not only were the details of the areas of open water discernable and diminishing over the six-day period represented by the 3 Landsat scenes, but some rather coarse predictions were possible about the behavior of the main channel of river current based upon texture and brightness of the ice-covered part of the river.

Enlargments of the test areas were used with the Zoom Transfer Scope to produce an overlay at a scale of 1:63,360 of open water on the three days, plus the location of the main channel inferred from Landsat data. The results are shown in Figure 8. This map shows the configuration of the river a few miles downstream from Galena (which would be off the drawing to the right). There

are two critical areas in the river at this test site which are prone to ice jams. One is the fish-hook bend in the river at Bishop Rock and the other is the near right-angle bend in the river about 9 km downstream from the village of Koyukuk. Both of these areas are targets for dusting operations each spring, similar to that illustrated by Figure 3. With the aid of Landsat analyses it is evident that the dusting tracks can be better positioned to coincide with the main river-channel near Bishop Rock, a prominent bluff about 65 meters above the flood plain. Here the farthest downstream dusting was not in the main river-channel.

Several hydrologic features of interest are apparent from the comparison of the three Landsat images with the USGS 15' topographic map. The neck of land east of Bishop Rock is being reshaped by the river channel in two ways. The eastern edge of the neck of land is being eroded away by the current, while the tip of the neck shows deposition. Even without consideration of the open water as an indicator for the main channel, one can infer that the main channel must be very close to the left bank of the neck of land, where erosion of the bank is occurring. This condition is opposite to that of the right bank of the river just upstream from the fish hook bend in the river. Here, comparison of the Landsat images with the map reveals deposition underway such that new shoals and sand bars are forming. The Yukon River is a very turbid river, and suspended sediment tends to be deposited in regions of lesser turbulence. Evidently the right bank of the river upstream from Bishop Rock endures heavy deposition from the evidence of the growing sand bars. This observation would place the main current along the left bank until the tip of the bend in the river. At the tip of the neck, deposition begins which is indicative of the main channel moving into the center of the river. That it does not switch completely to the opposite side of the river is evidenced by the new arc-shaped sand bar at this point. This places the main current at the bend in the center of the river, and this conclusion is supported by Figure 5, an oblique aerial photograph taken during the November 1975 freeze-up cycle.

Open water occurs in a paddle-shaped area just downstream from Bishop Rock largely because of two factors. One is that the river itself is rather severely constricted by Bishop Rock to a narrow neck of water, which increases both the velocity and turbulence of the main channel of current thus inhibiting the formation of an ice cover. This is evident in the 4 November 1973 Landsat image. The second factor is that the constricted river channel at and just above Bishop Rock tends to cause jams of frazil ice which prevent additional ice floes from reaching Bishop Rock and leave the river below them ice free.

The inferred position of the main channel follows along the arcuate left bank for the next eight kilometers (five miles) as shown by the shape of the river bank (without shoals or sand bars), and the difference in ice texture in the 1973 Landsat image. Next, the main channel likely moves to the center of the river, although there is little direct evidence for this assumption. However, at the next inflection point (just past Bishop Rock Island) the channel shifts to the right bank of the river as it makes the turn along the base of Koyukuk Island, which is a truncated former oxbow of the Yukon River. At this point in the river, the left bank is rapidly accreting and the right bank is eroding which is further evidence that the main channel here is along the right bank of the river.

In the mouth of the Koyukuk River, Landsat shows that a large island has formed where the map shows that formerly there was only a small sand bar near the village of Koyukuk. Without the Landsat images, one would be hard-pressed to predict whether the main channel of the Koyukuk River flowed to the east or west side of the new island. However, the evidence of the open water channel along the west bank of Koyukuk Island during the freeze-up cycle is an indication that the main channel probably is not adjacent to the village. In any event, the ice jams that threaten the village each spring do not occur on the Koyukuk River, but rather the Yukon River upstream from the right-angle bend.

A close comparison of the 1977 Landsat images with the 1973 image shows that the first of the two areas of open water in 1977 coincides exactly with the start of the open-water lead in 1973. Apparently an influence that is consistent from year-to-year is at work here. Field observations would be necessary to determine whether the control feature could be bathymetric or perhaps a nearby source of warmer ground water.

At the right-angle bend in the river, in 1977 there is a curious structure to the open-water lead that is not evident in 1973. As one would expect, the main channel tends to follow the outside diameter of the bend, but there is indication of a secondary channel along the inside of the bend--an unexpected occurrence. The reason for the branching of the open-water channel here is unexplained on the basis of available evidence. However, we tentatively postulate an emerging shoal which does one or two things. It may merely divide the main current solely by bathymetric control, or it may serve to ground ice floes moving downstream in the early fall. Once anchored on such a shoal, the ice floe would partially dam and thereby divide the river channel as shown in the line drawing. Here again, depth measurements made in the field might confirm the cause for the branching of the main channel here.

One bit of evidence which favors purely bathymetric control by a shoal, without the damming effect of grounded ice floes, is that the secondary branch in the main channel if linearly extended joins with the leftmost area of open water at the start of the bend in the river. It might be that the tip of the shoal is causing turbulence at the point of the open water in 1977. The effect of the shoal could be both retarded freezing due to turbulence, and a diversion of part of the main current toward the secondary branch of open water.

CONCLUSIONS

An initial and rather cursory analysis of early-winter Landsat imagery shows that satellite data has a rich potential application to river-ice studies. Images acquired during the freeze-up period of early winter can be related to operations to reduce flooding in the spring caused by ice jams during break-up. Visual photointerpretation methods are adequate for large rivers such as the Yukon (2 km wide), but more detailed information would be expected using digital data (which was not available in time for this study).

The best Landsat bands for interpretation of ice features proved to be MSS Band 4, when available, and Band 5 a close second choice. There tends to be uniformly high reflectances from all snow and ice surfaces regardless of texture on the infrared Bands 6 and 7. Further, the infrared bands tended to have similar, low reflectances from both open water and from densely forested terrain. Where the open-water lead bordered a forested river-bank it proved difficult to map boundaries between these two categories from the infrared images.

For the Koyukuk-Galena region along the Yukon River, the optimum time period for acquiring data for delineating the main river-channels appears to be 25 October to 8 November. The optimum time for the medium-sized Alaskan Rivers of central or coastal Alaska, such as the Kuskokwim River, would likely be 15 October to 1 November.

The river maps of the Yukon River near Koyukuk and Galena prepared from Landsat images are being used by the U. S. Army Corps of Engineers to guide their river-dusting operations in April, 1978. This application will minimize the impact of flood risks for two Alaskan villages at minimum cost. These Landsat results should prove especially beneficial this year because there was an absence of aerial reconnaissance of the river during freeze-up. Conventional aerial photography is too expensive to routinely delineate the main river-channels over thousands of miles of Alaskan rivers on an operational basis. Once the cost-effectiveness of this pilot study on the Yukon River has been evaluated after the spring 1978 season, this Landsat-based technique may be extended to include a similar annual reconnaissance of 12 to 15 other flood-prone areas.

ACKNOWLEDGEMENTS

This project was supported by the National Aeronautics and Space Administration, Office of Space Applications, under Grant NGL 02-001-092, and the U. S. Army Corps of Engineers. We especially thank Mr. Robert Meyer, Alaska District, Corps of Engineers for his assistance during this study.

REFERENCES

1. Osterkamp. T. E., Some potential ice problems associated with hydroelectric development in Alaska. The Northern Engineer, Vol. 9, No. 2. 1978.

2. Meyer, R., 1977, private communication.

3. Osterkamp, T. E., Tanana River ice cover, Proc. of the Third International Symposia on Ice Problems, Hanover, New Hampshire. Committee on Ice Problems, IAHR. 1975.

4. Osterkamp, T. E., Frazil ice nucleation mechanisms, Report UAG R-230, Geophysical Institute, University of Alaska, 1975.

5. O'Brien, H. W. and Munis, R. H., Red and near-infrared spectral reflectance of snow. Report AD-A007 732, Cold Regions Research and Engineering Laboratory, Hanover, New Hampshire, 1975.

LIST OF ILLUSTRATIONS

Fig. 1 Spring Ice-Jam

Fig. 2 Ice Floes During Breakup

Fig. 3 Aerial Dusting

Fig. 4 Dust Tracks

Fig. 5 River Ice at Bishop Rock During Freeze-up

Fig. 6 Landsat Image 4 Nov 73

Fig. 7A Landsat Image 10 Nov 77

Fig. 7B Landsat Image 11 Nov 77

Fig. 7C Landsat Image 16 Nov 77

Fig. 8 River Channels and Vicinity Map

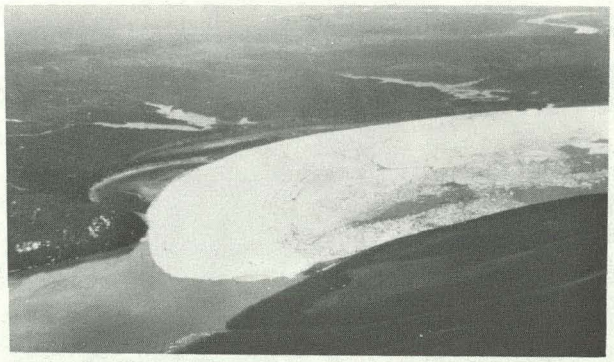

FIGURE 1. SPRING ICE JAM.
Large ice-floe lodged in hairpin bend at Bishop Rock in May 1975. Ice partially dams the river and causes flooding upstream.

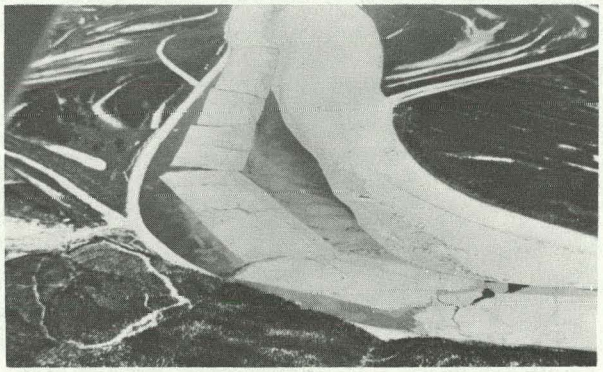

FIGURE 2. ICE FLOES DURING FREEZE-UP.
Large rafts of ice lodged in main channel of the lower Yukon River in November 1975.

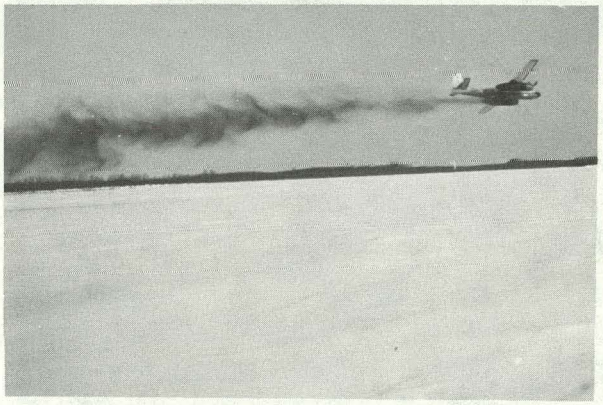

FIGURE 3. AERIAL DUSTING.
A converted B-26 aircraft flying a typical dusting mission in April 1975.

FIGURE 4. DUST TRACKS.
Tracks of dusting plane on river ice near Bishop Rock.

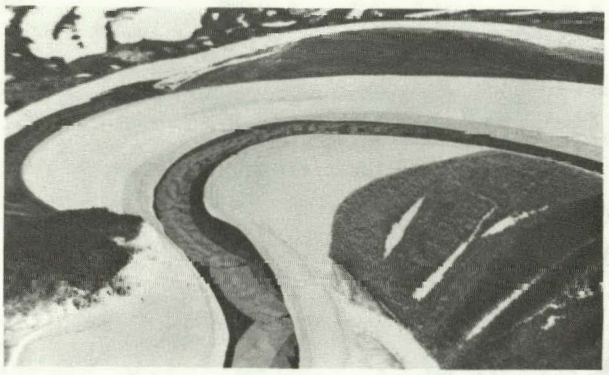

FIGURE 5 (LEFT) RIVER ICE AT BISHOP ROCK. Frazil-ice floes occupy main river channel which is still open 4 November 1975. Streamlines appear where ice floes adhere to shore-fast ice.

FIGURE 6. LANDSAT 4 NOVEMBER 1973. This image depicts river ice conditions earlier in the freeze-up period than the 1977 data of Figure 7 and better delineates the location of the main river channels. The preferred window for satellite data acquisition in this area appears to be 25 October - 8 November. Scene 1469-21224 Landsat 1, Band 4, Sun elevation 9°.

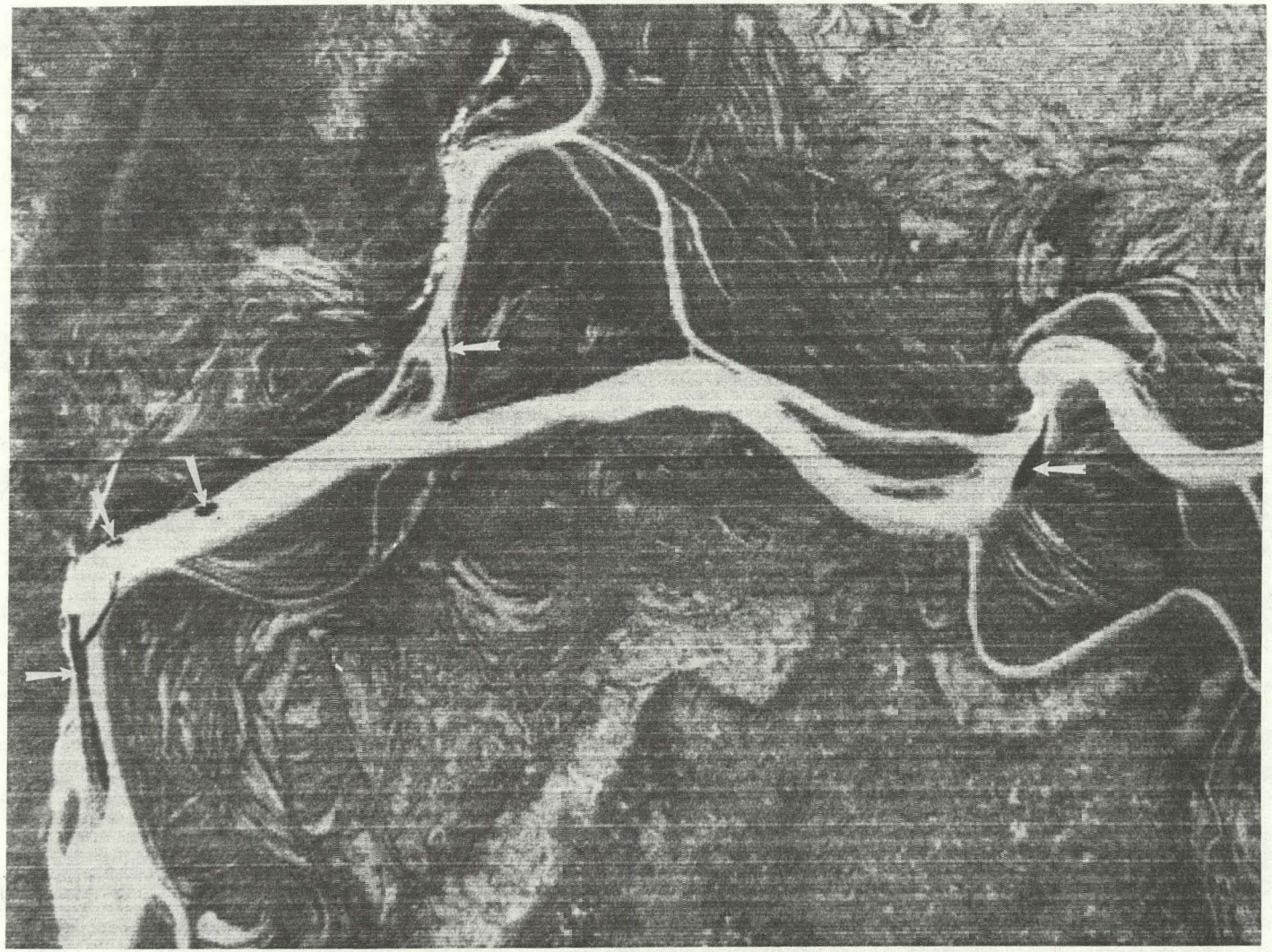

FIGURE 7A. LANDSAT 10 NOVEMBER 1977. Black areas in frozen river channels are open water. Landsat 2 scene 6023-2044 Band 4. Sun elevation 6°.

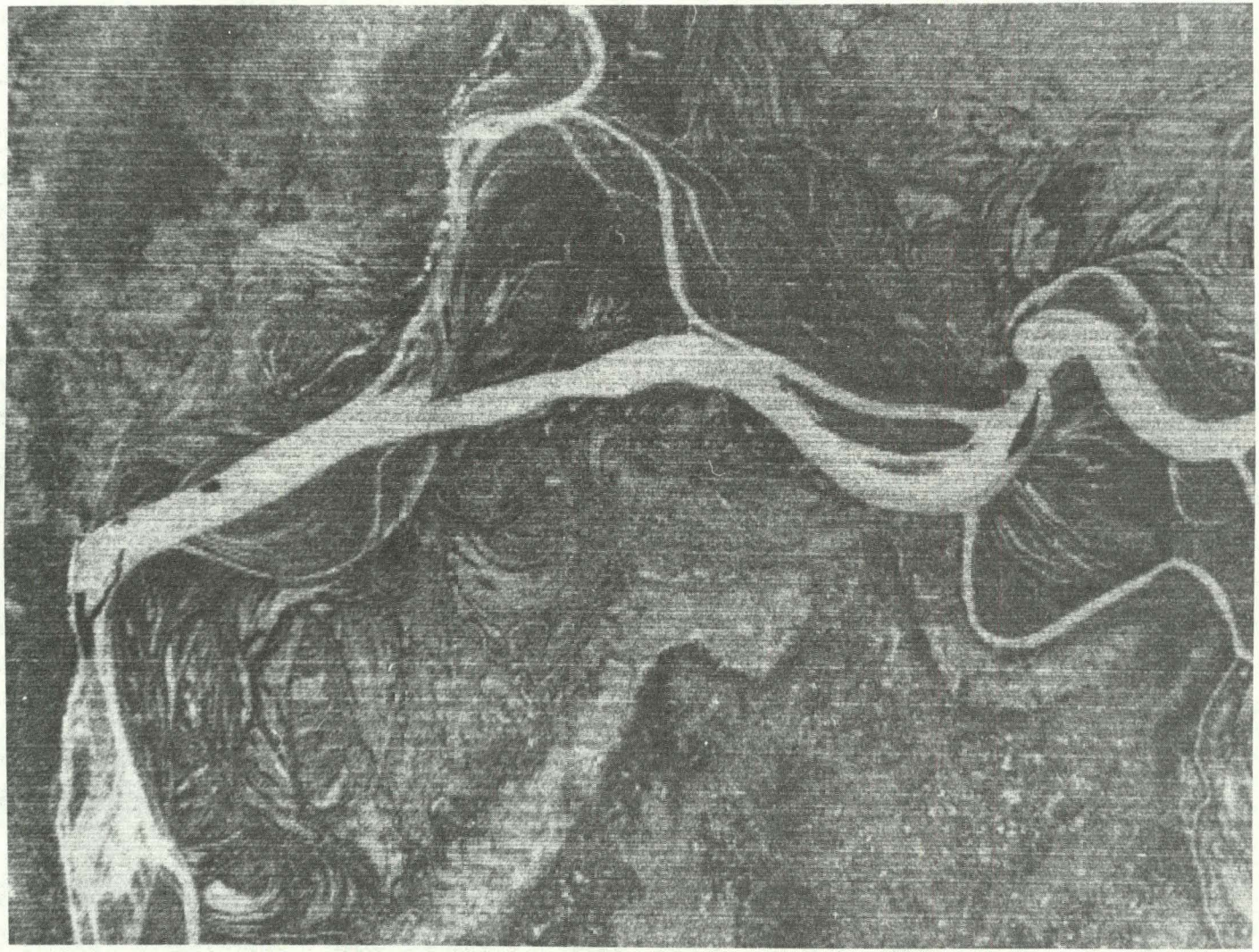

FIGURE 7B. LANDSAT 11 NOVEMBER 1977. Some areas of open water are smaller and there are more texture details visible in the river ice than in Figure 7A. Landsat 2 scene 6024-2055 Band 4. Sun elevation 5°.

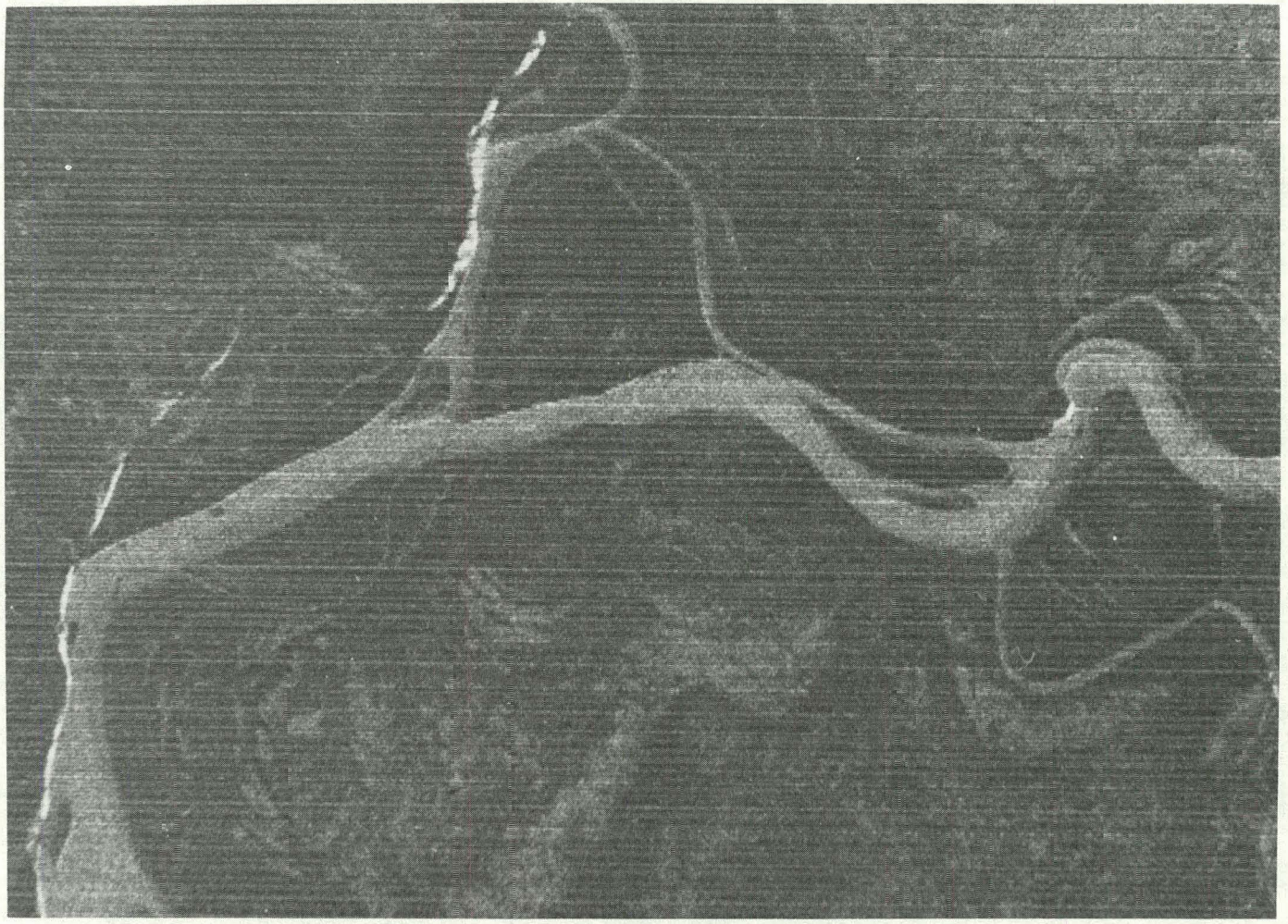

FIGURE 7C. LANDSAT 16 NOVEMBER 1977. Open-water areas in Figures 7A and 7B are almost completely frozen over. Low contrast results from low level of illumination. Landsat 1 scene 5342-19511 Band 5. Sun elevation 2°. (Banc 4 data not available.)

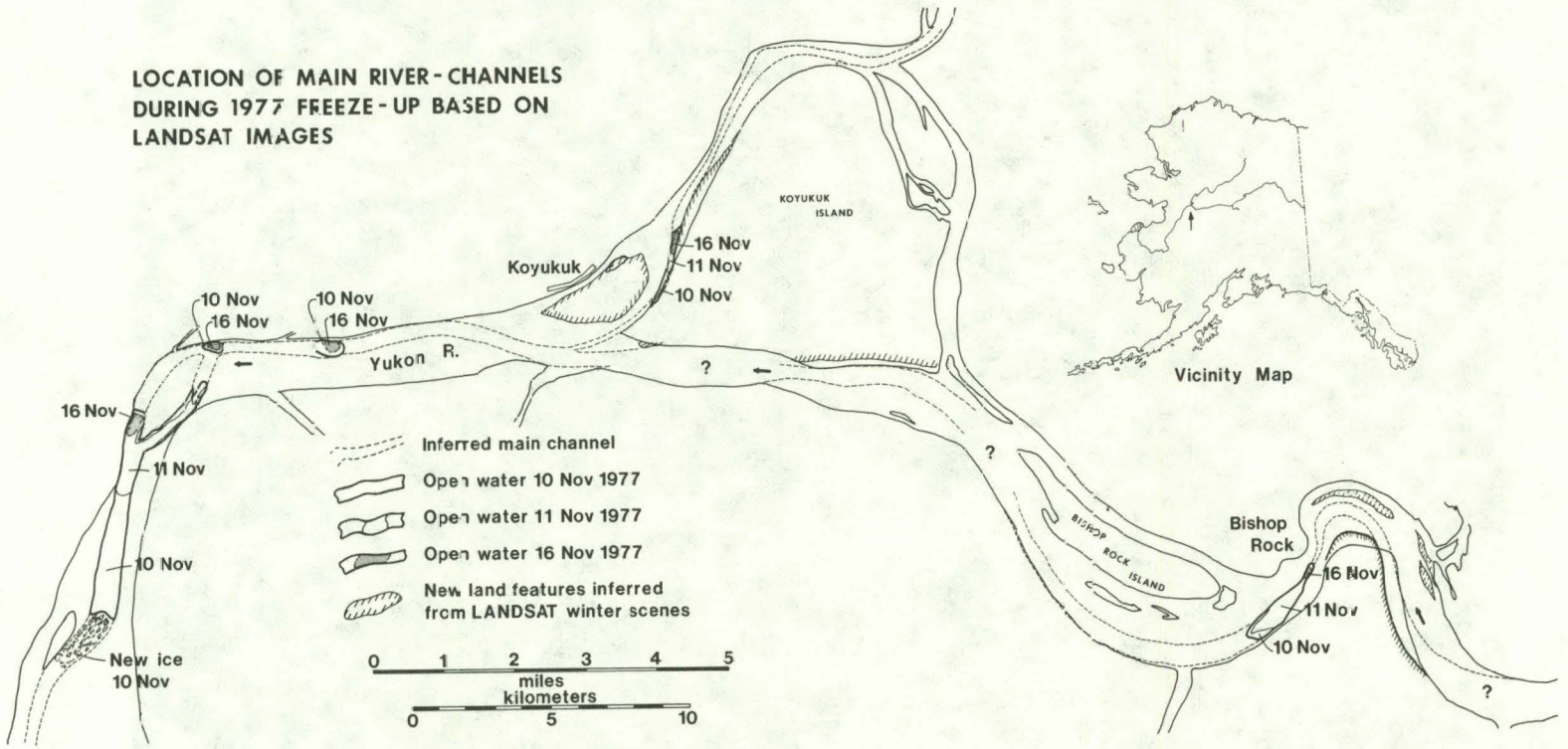

FIGURE 8. RIVER CHANNELS AND VICINITY MAP.

"TELL-US"

A COMBINED SURFACE TEMPERATURE, SOIL MOISTURE AND EVAPORATION MAPPING APPROACH

A. Rosema and J.H. Bijleveld

E.A.R.S. b.v., Engineering Consultants for Environmental Analysis and Remote Sensing,
Delft, the Netherlands

P. Reiniger and G. Tassone

Commission of the European Communities
Joint Research Centre - Ispra Establishment
Italy

K. Blyth and R.J. Gurney

Institute of Hydrology, Wallingford, United Kingdom

ABSTRACT

In the framework of the Tellus Project of the European Communities, an algorithm has been worked out permitting the evaluation of the thermal inertia and of the surface relative humidity of bare and scarcely vegetated soils from remotely sensed day and night surface temperatures. The cumulative daily evaporation can also be calculated by this method.

The algorithm was tested on existing data from a field experiment and was applied in a flight experiment. While the calculated soil moisture agreed satisfactorily with the average moisture content of the top soil layer, the estimated daily evaporation deviated from the measured values due to simplifications inherent in the model.

1. INTRODUCTION

The countries of the European Communities carry out a joint investigation on the applicability of HCMM-satellite thermal imagery for soil moisture and heat budget evaluation in zones of agricultural and environmental interest: the HCMM-Tellus Project. In this framework, a new algorithm has been developed to convert remotely sensed day and night temperatures of bare and scarcely vegetated areas into parameters relevant to soil moisture.

Such an interpretation routine calls for a process, which is the reverse of temperature simulation. For this purpose, and mainly in the U.S., methods have been worked out to calculate the thermal inertia of the soil from the difference between the day and the night temperature to be obtained by means of HCMM [1, 2, 3, 4, 5]. We have discussed this approach [6] which is limited to cases of known or negligibly small evaporation.

It must be noted, however, that in the above approach the available information is not used completely. Only one data point i.e. the day-night temperature difference is used, while two data, the day and the night temperature, are available. Therefore, in principle, two unknowns could be determined. This has been achieved in the "TELL-US" algorithm des-

cribed in the present paper. This algorithm determines the thermal inertia and the surface relative humidity. Moreover, the total daily evaporation is obtained.

2. THE ALGORITHM

The algorithm consists of a main program and of a sub-program simulating the daily course of the surface temperature (Fig. 1). The main program compares the simulated day and night temperatures with the temperatures obtained from the satellite. In one version it adjusts the values of the thermal inertia and the surface relative humidity until agreement between the simulated and the measured temperatures has been obtained.
A second version of the main program produces a look-up table, consisting of the day temperatures, the night temperatures and the daily evaporation totals, for various combinations of thermal inertia and surface relative humidity.

The simulation sub-program solves numerically the finite difference equation which describes transient heat conduction in a homogeneous soil:

$$\frac{dT}{dt} = \frac{\lambda}{C} \frac{d^2T}{dz^2} \qquad (1)$$

(For the meaning of the symbols we refer to the table at the end of this paper)

As a lower boundary, a level in the soil at a depth outside the reach of the daily temperature cycle is taken. For this level the temperature has to be specified. As an upper boundary a level in the atmosphere is taken, where windspeed, air temperature and air specific humidity are measured. The atmosphere and the soil regime are coupled by a continuity requirement: the surface heat balance:

$$I_n + G + H + LE = 0 \qquad (2)$$

$$I_n = (1-a)I + I_\downarrow + \varepsilon I_\downarrow \qquad (3)$$

$$G = \lambda \left(\frac{dT}{dz}\right)_{z=0} \qquad (4)$$

$$H = \varrho c \frac{T_a - T_o}{r} \qquad (5)$$

$$LE = \varrho L \frac{s_a - h.\hat{s}_o}{r} \qquad (6)$$

The atmospheric resistance r depends on the surface aerodynamic roughness, on the windspeed and on the stability of the atmosphere. It is calculated from the integrated Businger-Dyer profile relationships [7].

The simulation sub-program may contain only two unknowns: the surface relative humidity and the thermal inertia. This implies that we have to accept certain physical simplifications. The soil is assumed to be homogeneous and with a constant water content. The surface relative humidity is also assumed to be constant. Accordingly, the values of thermal inertia and surface relative humidity that are produced by the algorithm, should be taken as "effective" values.

One might question why the thermal inertia did not show up in equations (1) - (6). The thermal inertia, defined as:

$$p = (\lambda C)^{\frac{1}{2}} \qquad (7)$$

appears as the soil property that affects the magnitude of changes in surface temperature if differential equation (1) is analytically solved, for simplified boundary conditions and heat balance. Therefore, the observed day and night temperatures depend on the thermal inertia, rather than on the thermal conductivity.

In the present, somewhat more realistic description, our system of equations (1) - (6) included, had to be solved numerically by the explicit finite difference scheme of Dufort and Frankel, applied to a grid which expands with depth. This scheme is used to predict successive temperature profiles. The surface temperature is iteratively solved from the surface heat balance equation after each prediction.

3. DATA ACQUISITION

Table 1 reviews the essential input data, and their determination. The data have been split into local data and regional data. The regional data are to be obtained from the nearest weather station. The local data have to be specified for every ground plot to be interpreted. Of these, the surface temperatures and the albedo may be obtained by means of the HCMM satellite or an airborne scanner. The most cumbersome parameter to be determined is the surface aerodynamic roughness. It can be estimated with existing techniques from the dimensions of the actual roughness elements employing land-use maps, which may be derived from airborne, or even LANDSAT imagery. If the area is not horizontal the slope direction and slope dip have to be estimated from topographical maps.

4. RELATION TO "SOIL MOISTURE"

In terms of soil moisture, the meaning of the thermal inertia and of the surface relative humidity of the soil is not self-evident. While the surface relative humidity depends uniquely on the soil moisture potential at the surface, thermal inertia is a function of the average water content in the top soil. This relation, however, is not unique as it depends also on the soil mineral composition.

5. TEST OF THE ALGORITHM

The TELL-US algorithm has been tested on data from a field experiment of the USWCL at Phoenix, Arizona. On March 3, 1971, a test plot of bare Avondale loam was irrigated with 10 cm of water, and left to dry. We have used the data measured 2, 6 and 14 days after irrigation representing subsequent stages of drying. The soil temperature measured at "1mm depth" was taken to be a good approximation of the surface temperature.

The look-up table produced by the computer program for 2 days after irrigation is plotted as a look-up graph in Figs. 2a and 2b. In Fig. 2a the simulated day-night temperature pairs are plotted for the various combinations of thermal inertia and surface relative humidity, and connected by lines of equal thermal inertia (dashed) and equal surface relative humidity. In Fig. 2b, the total daily evaporation is plotted versus the surface relative humidity. Similar look-up graphs were produced for the other two days of the experiment.

The measured day-night temperature pairs are plotted as crosses in Fig. 2a and the corresponding values of the thermal inertia and surface relative humidity are found by interpolation. Subsequently, the total daily evaporation values are found from the graph 2b. Instead of carrying out this graphical interpretation, the same result may be obtained directly with the automatic search version of the algorithm.

The thermal inertia found on the look-up graphs was translated into soil moisture using the thermal inertia-water content relation shown in Fig. 4. This relation was calculated from

the mineral composition of the soil.

The soil moisture profiles measured gravimetrically 2 and 14 days after irrigation, are plotted in Figs. 3a and b, both for the day and night measurement. The water content calculated by the TELL-US algorithm is indicated by an arrow. The agreement between measured and calculated soil moisture is excellent 2 days after irrigation (Fig. 3a), 14 days after irrigation (Fig. 3b) the calculated soil moisture represents only an "average" moisture content of the top 8 cm of the soil. The data of the 6th day, not shown in this paper, have an intermediate position.

The values of the total daily evaporation as measured by a weighing lysimeter and determined with the TELL-US algorithm are compared in Table II. This comparison is not yet satisfactory as, except for the initial drying stage, the algorithm tends to underestimate evaporation. The reason for this tendency lies in the assumption of a constant surface relative humidity which causes excessive condensation to be simulated for the night.

It may be hoped that after a further improvement of the algorithm calculated evaporation will come closer to values measured with existing field methods.

6. JOINT FLIGHT EXPERIMENT

As part of the pre-launch activities of the Tellus Project, a joint flight experiment was carried out in mid-September 1977 on the Grendon Underwood Experimental Catchment northwest of London, U.K. The application of the TELL-US algorithm was one of the aims of this experiment. At the time of the night-minimum and of the day-maximum surface temperature, a strip 8 km long and 1.6 km wide was scanned from 1000 m altitude with an airborne DS-1250 multispectral scanner having a thermal band between 8 and 14 μm. The night was clear, with no wind and the day was sunny, with a light wind and occasional high altitude clouds.

Simultaneously with the overflight, ground surface temperatures were measured with a PRT-5 radiation thermometer (9.5 - 11.5 μm, 2° FOV) on a 6 ha ploughed field of Denchworth clay. Sixty moisture samples of the top 3 cm of soil were taken in a pattern of four lines across the field, with an additional 10 core samples down to 15 cm depth. Input data for the TELL-US algorithm were obtained from instrumentation installed on the field and from an automatic weather station at a distance of 1.5 km.

First preliminary results of the experiment are presented in Tables III and IV. The field was divided into two parts of about equal size, according to the two distinct temperature classes shown by the daytime scanner image.

The day and night surface temperatures are given in Table III. The airborne surface temperatures were corrected for the effect of the atmosphere using temperature, humidity and pressure data from a tethered balloon 40 km from the site. The night-time correction is less than the day-time correction and has the opposite sign due to a temperature inversion in the first 100 m of the atmosphere at night. While the night temperatures measured by the scanner and on the ground lie in approximately the same range, day-time temperatures measured from the aircraft exceed the ground surface temperatures by a few degrees. This discrepancy may be due to a difference in the temperature distribution on the rough soil surface as seen by the small-angle radiation thermometer on the ground and by the airborne scanner with a resolution element of 2.5 x 2.5 m.

As shown in Table IV, the soil moisture percentage in the 0-3 cm layer seems to be slightly higher in the SE-part of the field, while the 0-15 cm moisture percentage is higher in the NW-part. The thermal inertia and the relative surface humidity in Table IV have been found by interpolation in the corresponding look-up table using the ground measured surface

temperatures. At this early stage of data evaluation it can only be observed that both the thermal inertia and the surface relative humidity evolve in the right direction, i.e. thermal inertia increases with the mean moisture content of the bulk top soil (0-15 cm), whereas surface relative humidity increases with the moisture content in the very topmost layer (0-3 cm).

7. CONCLUSION AND OUTLOOK

It could be shown that by means of the TELL-US algorithm the top-soil water content, the surface relative humidity and the total daily evaporation may be determined from one day- and one night-temperature and standard ground based data. Further experimental work is still needed to test the complete potential of the algorithm. Part of this work is already in progress in the framework of the Tellus Project of the European Communities.

A similar or generalized algorithm might be constructed to cover vegetated surfaces. These algorithms create the attractive prospect of a combined surface temperature, soil moisture and evaporation mapping system on the basis of satellite or airborne thermal imagery. Such data are of high relevance in agriculture, ecology and hydrology. They are useful for irrigation scheduling, prediction of yields, and large scale management of rangelands. They will allow agronomists and ecologists, particularly in arid and semi-arid zones, to follow, analyze and predict processes such as seed germination, early crop growth, drought damage, erosion and desert formation. Such a mapping system could also be used for early warning and fighting of pests, such as the desert locust [8, 9].

ACKNOWLEDGEMENT

We gratefully acknowledge the cooperation of the United States Water Conservation Laboratory, Phoenix, Arizona, and in particular Dr. Ray D. Jackson, for permitting the use of his experimental data in testing the algorithm.

We also thank all the participants in the Joint Flight Experiment for their efforts dedicated to the success of the campaign.

REFERENCES

[1] WATSON, K., "Geologic Applications of Thermal Infrared Images", Proc. IEEE, 63, p. 128-137 (1975)

[2] KAHLE, A.B., GILLESPIE, A.R., GOETZ, A.F.H., ADDINGTON, J.D., "Thermal Inertia Mapping", Proc. 10th Int. Symp. on Remote Sensing of the Environment, Ann Arbor, Michigan, Oct. 1975

[3] PRICE, J.C., "Thermal Inertia Mapping: A New View of the Earth", Rep. X-913-76-121, Goddard Space Flight Centre, Greenbelt, Maryland, June, 1976

[4] KAHLE, A.B., "A Simple Thermal Model of the Earth's Surface for Geological Mapping by Remote Sensing", J. Geoph. Res., vol. 82, no. 11, p. 1673-1680, April 10th, 1977

[5] GILLESPIE, A.R., KAHLE, A.B., "Construction and Interpretation of a Digital Thermal Inertia Image", Phot. Eng. and Rem. Sens., vol. 43, no. 8, p. 983-1000, August, 1977

[6] ROSEMA, A., "Heat Capacity Mapping, is it Feasible?", Proc. 10th Int. Symp. on Remote Sensing of the Environment, p. 571-582, Ann Arbor, Michigan, Oct., 1975

[7] BUSINGER, J.A., WYNGAARD, J.C., IZUMI, Y., BRADLEY, E.F., "Flux Profile Relationships in the Atmospheric Surface Layer", J. Atmos. Sci., 28, p. 181-189, March, 1971

[8] IDSO, B.S., JACKSON, R.D., REGINATO, R.J., "Detection of Soil Moisture by Remote Surveillance", American Scientist, vol. 63, p. 549-557, Sept./Oct., 1975

[9] JACKSON, R.D., REGINATO, R.J., IDSO, B.S., "Wheat Canopy Temperature; a Practical Tool for Evaluating Water Requirements", Water Resources Research, vol. 13, no. 3, p. 651-656, 1977.

DEFINITION OF THE SYMBOLS

C	volumetric heat capacity of soil $[J/m^3K]$
G	soil heat flux at the surface $[J/m^2s]$
H	atmospheric heat flux $[J/m^2s]$
I_l	long wave irradiance $[J/m^2s]$
$I_\uparrow$	long wave emittance $[J/m^2s]$
I	short wave irradiance $[J/m^2s]$
I_n	net radiation $[J/m^2s]$
L	heat of evaporation $[J/kg]$
LE	latent atmospheric heat flux $[J/m^2s]$
T	(soil) temperature $[K]$
T_a	air temperature $[K]$
T_o	surface temperature $[K]$
a	albedo [fraction]
c	heat capacity of air $[J/kgK]$
h	surface relative humidity [fraction]
p	soil thermal inertia $[J/m^2s^{\frac{1}{2}}K]$
r	atmospheric resistance $[s/m]$
s_a	air specific vapour density [dimensionless]
$\hat{s}_o$	specific vapour density at saturation, at the soil surface [dimensionless]
t	time $[s]$
z	depth $[m]$
λ	soil thermal conductivity $[J/mKs]$
ϱ	air density $[kg/m^3]$
ε	long wave emissivity [fraction]

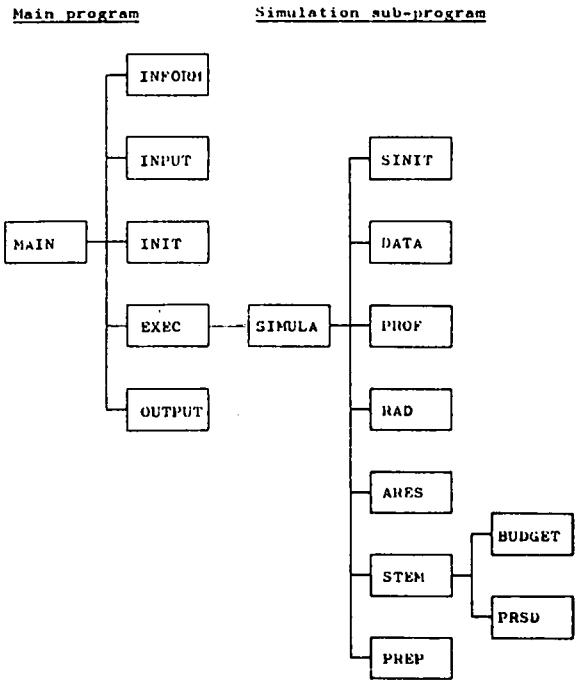

FIG. 1 SUBROUTINE RELATIONAL DIAGRAM

INFORM : general information
INPUT : input
INIT : initialization
EXEC : execution and manipulation of the simulation sub-program, automatic search for the thermal inertia and surface relative humidity
OUTPUT : output
SIMULA : simulation sub-program
SINIT : initialization
DATA : weather data interpolation
PROF : temperature profile prediction
RAD : calculation of irradiation terms
ARES : calculation of the atmosphere resistance
BUDGET : surface heat budget evaluation
STEM : iterative solution of the surface temperature
PRSD : intermediate output facility
PREP : determination of day temperature, night temperature and total daily evaporation.

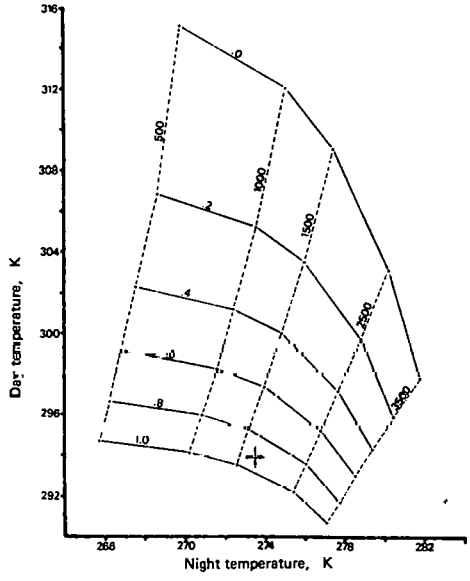

a) Thermal inertia and relative surface humidity

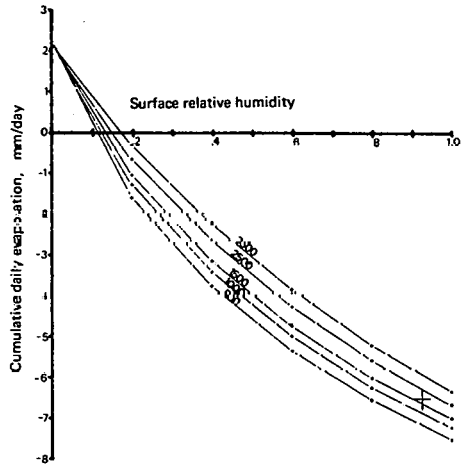

b) Cumulative daily evaporation

FIG. 2 LOOK-UP GRAPH, 2 DAYS AFTER IRRIGATION

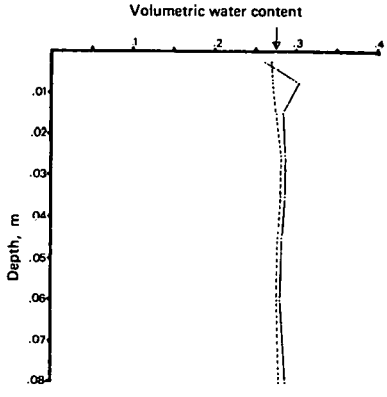

a) 2 days after irrigation

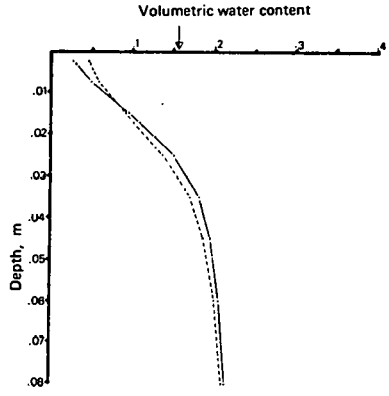

b) 14 days after irrigation

FIG. 3 SOIL MOISTURE PROFILES OF AVONDALE LOAM

———— day)
---------- night) measured

arrow calculated from thermal inertia

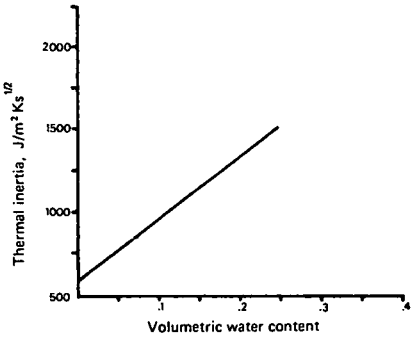

FIG. 4 THERMAL INERTIA - WATER CONTENT RELATIONSHIP FOR AVONDALE LOAM

TABLE I. INPUT TO "TELL-US" ALGORITHM

Datum	How to determine		Remarks
1. Day surface temperature	HCMM/airborne scanning		Time of observation variable
2. Night " "	" " "		" " " "
3. Albedo	" " "		
4. Surface aerodynamic roughness	Estimation from land-use map		If not available, to be derived from LANDSAT imagery
5. Slope direction	Topographical map		
6. Slope dip	" "		
7. Sub-surface temperature	Measurement/Estimation		At 1 m depth
8. Initial surface "	" "		At midnight
9. Solar irradiance	Radiometer	Weather Station	Every hour
10. Wind speed	Anemometer		
11. Air temperature	Dry and wet bulb thermometer		
12. Air specific humidity			

TABLE II. TOTAL DAILY EVAPORATION [mm/day]

Days after irrigation	Measured by lysimeter	Calculated with TELL-US
2	-5.84	-6.48
6	-1.43	-0.59
14	-0.86	+1.63

(+ : condensation)

TABLE III. JOINT FLIGHT EXPERIMENT - MEASURED SURFACE TEMPERATURES OF BARE SOIL

Field	Time	Radiativc Surface Temperature °C		
		Surface	Airborne	Airborne corrected
NW	Night	4.0 ± 0.6*	3.0 - 4.5	2.9 - 4.4
	Day	24.2 ± 1.5	26 - 29	27 - 30
SE	Night	2.4 ± 0.7	3.0 - 4.5	2.9 - 4.4
	Day	23.9 ± 2.2	23 - 26	24 - 27

(* : ± standard deviation)

TABLE IV. JOINT FLIGHT EXPERIMENT - MEASURED SOIL MOISTURE PERCENTAGE AND CALCULATED PARAMETERS RELATED TO SOIL MOISTURE

Field	Soil Moisture Percentage (weight) 0-3 cm	0-15 cm	Thermal Inertia	Relative humidity
NW	9.0 ± 0.9*	32.2 ± 0.7	1700	0.27
SE	10.6 ± 2.2	28.6 ± 1.8	1300	0.32

(* : ± standard deviation)

SEDIMENTATION PATTERN AND LAND FORMATION STUDIES IN THE FENI and LITTLE FENI RIVER ESTUARIES USING LANDSAT IMAGERIES

by

M. A. H. Pramanik, M. U. Chaudhury
and N. H. MacLeod

Bangladesh Landsat Programme
Dacca, Bangladesh

ABSTRACT

This study of land formation in tidal estuaries of the Bay of Bengal was undertaken to make a preliminary estimate of the effects of installing flow regulators in tidal rivers. In 1967, a flow regulator was placed in the little Feni river to provide water for winter irrigation in southeastern Bangladesh south of Comilla and east of Noakhali, near the town of Feni. Each winter the river channel on the seaward side of the regulator has been silted to the extent that excavation is required to re-establish new flow in the spring. The sedimentation process which led to land formation in the coastal areas has, as in the case of Little Feni River, also led to partial closing of the Feni estuary.

Analysis of LANDSAT data of the Little Feni estuary at the Bangladesh LANDSAT Centre for the years 1973 to 1977, indicated that in addition to the closing of the main channel by sedimentation, sixty percent of the open water area in the estuary in 1973 is now permanent land, formed by sediments from the Bay.

In the adjacent, much larger Feni River estuary, there is no regulator at the present time. There is, however, a programme for installation of a regulator very soon. Analysis of LANDSAT data of the Feni River estuary indicates that land that has been formed occupies forty percent of the 1973 open water surface.

From these studies it is clear that the present sedimentation in the Feni and Little Feni estuaries is closing off the river flow to the seas, whether or not a regulator is present. It is likely that regulator placed near the mouth of such deltaic rivers may accelerate the silting up process in the Bay of Bengal.

INTRODUCTION

Land formation and erosion in the southern central coast of Bangladesh has been studied by scientists and governments for a long period, even centuries. As the Bangladesh land surface is primarily composed of the deltas of three major rivers, the Ganges, the Bramahputra and the Meghna, the processes involved in land formation are these of delta formation, with enormous flows of sediment carried into the Bay of Bengal each year.

Since 1972, the ERTS (Landsat) Task Force of Bangladesh has been analysing the coastal land accretion phenomenon using spacecraft imagery from the Landsat earth observations satellites of NASA. This data are supplemented with field data from ship and aircraft and field trips. In 1973, a map of the Bay of Bengal and the Bangladesh coast was published by the Task Force. It shows the current status of land accretion including these regions in which new lands have appeared and are exected to appear in the near future. Ship observations made in 1977 confirmed that some new lands predicted to rise above low tide have in fact done so.

While the deltaic formation precesses are leading to the formation of new areas which can be used for agricultural and forestry purposes apparently equal to about 5% of the present land area of Bangladesh, there are adverse effects as well. As new land accretions extend further in the Bay, secondary river courses are lengthened and sedimentation within the river courses occurs, closing off the flow which is normally available for agricultural production. In Bangladesh, where food production is not yet at a self-sustaining level, the loss of secondary river flow in the deltaic distributaries and of rivers rising in the eastern uplands, are not easily tolerated. Two such rivers are the Feni and Little Feni which rise in the eastern upland.

One of the principal development objectives of Bangladesh is to reach food self-sufficiency by 1985. There are about 80,000,000 people living in Bangladesh on a national territory of about 14 million hectares, one of the most dense populations in the world. At the same time Bangladesh has exeperienced a very low per unit area crop production, one of the lowest in Asia.

With considerable success, two means of attaining food self-sufficiency are being emphasised. First, production is being increased by use of better crop varieties, more fertilizers and particularly irrigation, which permits the productinn of three crops per year in large areas. Secondly, all available land is being brought into production, especially the newly formed lands in coastal zone. Large scale embankments, winter water impoundment for irrigation water and drainage programmes to remove impounded water before the onset of monsoon rains have been developed in recent years.

Most embankment programmes now include sluice gates to control water entry and drainage. These are necessary to maintain ecological balance. Where embankments do not enclose a project area, flow regulators are installed to hold back irrigation water for the command area and release water during monsoon rains. This is the technique used in the Little Feni River estuary and proposed for the adjacent Feni River (see map, Figure 1).

Use of embankments and flow regulators produces changes in both land formation and land erosion processes. In the Feni estuary we find that land formation is the predominate effect. In view of the national objective of food self-sufficiency, the formation of new land is a positive effect, but in this case the new land may also form a barrier to water flow from the irrigation command area. In fact this has happened and some flooding of winter crop has occurred in the command area, denying the farmers their yield.

The problem, then, is to find a solution to conflicting outcomes of engineering techniques used in the Feni estuary, a solution which will provide both increased crop production through irrigation and stablized new land for further agricultural development. Both programmes must proceed in order to meet national objectives - for the Feni River estuary is but one area where this conflict occurs.

This paper provides a preliminary report on examination of Landsat imagery to observe the process of land formation in the Feni estuary since 1973. We do not provide a solution, only a quantitative estimate of the extent of land formation. But this is information that was previousely not available.

SITE DESCRIPTION

In 1967, a flow regulator was placed in Little Feni River to provide water for winter irrigation in southeastern Bangladesh south of Comilla and east of Noakhali, near the town of Feni. Each winter the river channel on the seaward side of regulator has been silted to the extent that excavation is required to re-establish new flow in the spring. The sedimentation process which led to land formation in the coastal areas has, as in the case of the Little Feni River, also led to partial closing of the Feni estuary.

Observations and measurements on the ground since installation of the regulator show that the outfall of the Little Feni - the seaward point at which the channel depth remains constant - has moved seaward about 10 kilometers. The resulting channel filling between regulator and outfall has closed off flow of one river and caused spring flooding in that river, drainage basin.

Sedimentation of the Little Feni channel occurs rapidly each year. After closing, about 4 meters of silty sand are deposited in one month's time in Fall on the seaward side of the regulator. On excavating the channel and opening the regulator in April, the spring river flow erodes the channel to normal depth in about 2 weeks time. However, the accreted land in the flood plain, standing about 2 meters above mean tide level, remains.

METHODS

The analytical method used in this study, a study which must be considered as only preliminary and indicative, was to photo enlarge 1:1,000,000 scale Landsat images to 1:125,000 scale. (9" X 9" black and white negatives from the EROS Data Centre South Dakota, USA, were the original photo data). Tracings of estuary boundaries (shores) in 1973 and 1977 were made on one drawing at 1:125,000 scale (Figure 1). A Bausch and Lomb Zoom Transferescope was used for this purpose. The area of land formation and loss since 1973 was measured using a polar planimeter. The planimeter measurements are reported in Table 1.

RESULTS AND DISCUSSION

Analysis of Landsat data of the Little Feni Estuary at the ERTS (Landsat) Centre for the years 1973 to 1977, indicated that in addition to the closing of the main channel by sedimentation, sixty percent of open water area in the estuary in 1973 is now permanent land, formed by sediments from the Bay (Table 1). Figure 2 is a photographic rendition of the 1973 Landsat data showing the condition of the Little Feni and adjacent Feni River estuaries at that time. Figure 3 shows the 1977 condition. Both are at a scale of approximately 1:125,000.

In the adjacent and much larger Feni River estuary, there is no regulator at the present time. There is, however, a programme for installation of a regulator at a cost ten times that of the Little Feni regulator. It was important therefore to include the Feni estuary in this analysis. In Figures 2 and 3, for 1973 and 1977 respectively, the Feni estuary appears just to the east of the Little Feni. The two estuaries share a common opening to the Bay of Bengal.

The analysis of the Feni estuary indicates that land has formed which now occupies forty percent of 1973 open water surface. While probably only coincidental, the estuarine surface lost in both the Little Feni and the Feni estuaries is about 3500 hectares in both cases.

CONCLUSIONS

As this is a preliminary study, further field observation is required to confirm the findings reported here. Engineers of the Bangladesh Water Development Board, those responsible for design and operation of the Feni regulators, are represented in the ERTS (Landsat) Task Force and have brought this

specific problem to the Task Force for analysis. Further analysis will acquire better understanding and further observations of the sedimentation, tidal and river flow, land use and general phenomena of accretion and erosion in the Bay of Bengal.

Despite the need for further study, it is clear that present sedimentation in the Feni and Little Feni estuaries is closing off the river flow to the seas, whether or not a regulator is present. It is likely that a regulator placed near the mouth of such deltaic rivers may accellerate the silting-up process in the Bay of Bengal.

While it is evident that the sedimentation which forms new land in the estuary and fills the river channels is, in large part, transported by tidal flow, the information reported in this paper does not address the questions of origin of sediments in the Bay of Bengal nor the scale of land formation and erosion in the coastal zone. Earlier reports by Landsat Task Force do contain discussion of these matters. There is little question that the scale and dynamics of Bay of Bengal sedimentation are much too great for engineering structures alone within the estuaries to control.

At the moment, then, only partial solutions may be available to modify sedimentation effects within the Feni estuary. Even so, these partial solutions must be sought out so that development of the estuary may proceed. The overall solution is probably to be found through gaining a quantitative understanding of the water regime in all of Bangladesh - indeed in the total watershed of Ganges, the Bramhaputra, the Meghna, the great rivers which flow into the Bay of Bengal.

TABLE 1

Change in water surface area in the Feni and Little Feni Estuaries between 1973 and 1977*.

Name of Estuary	Water Surface Area (Hectares) 1973	1977	Difference (Hectares)	% loss of water surface or gain of land surface
Feni	8790	5240	3550	approx. 40%
Little Feni	5520	2880	3440	approx. 60%

*These data are polar planimeter measurements of features in Landsat imagery of 1973 and 1977. Data are of accuracy better than 10%.

MORPHOLOGICAL CHANGES
IN THE FENI RIVER AND THE LITTLE FENI RIVER ESTUARIES

SCALE 1:125000

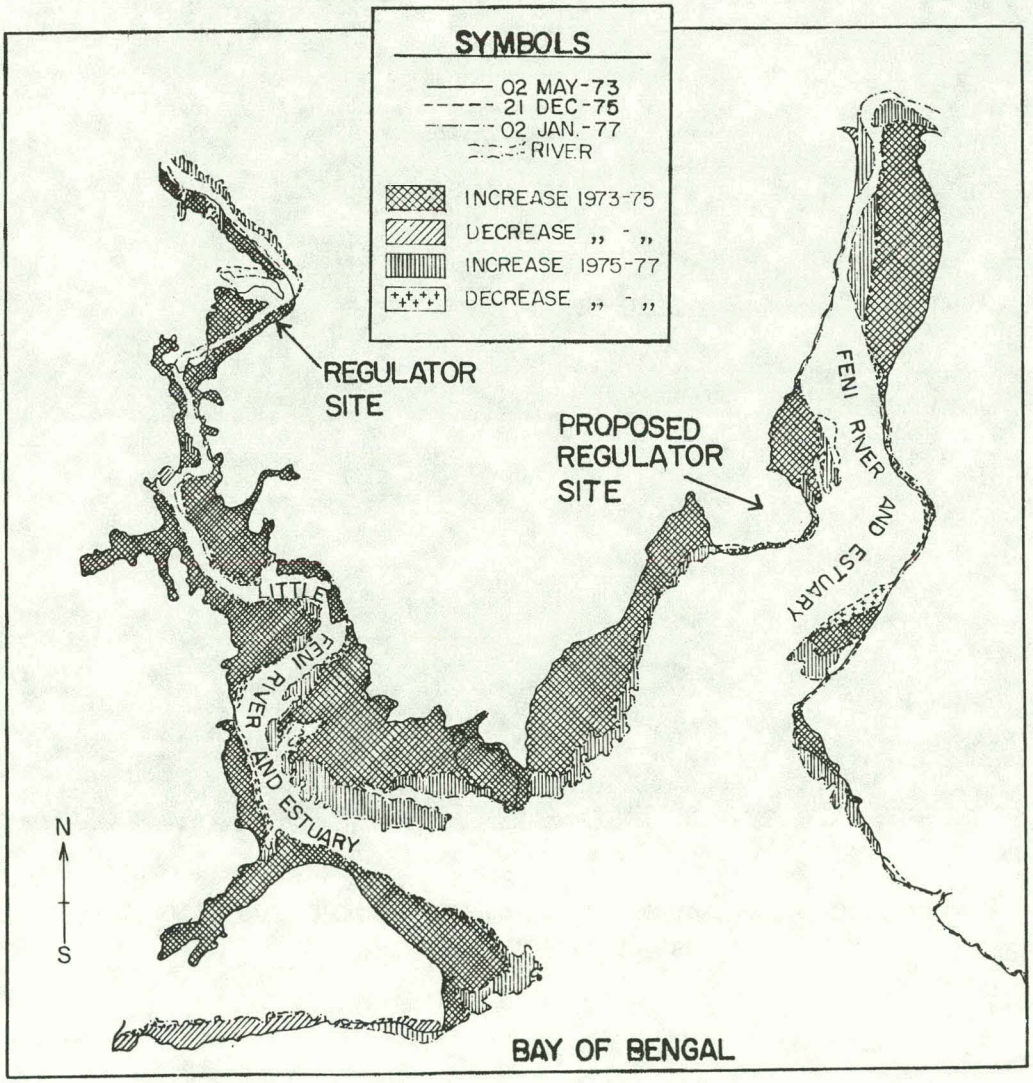

FIG. 1

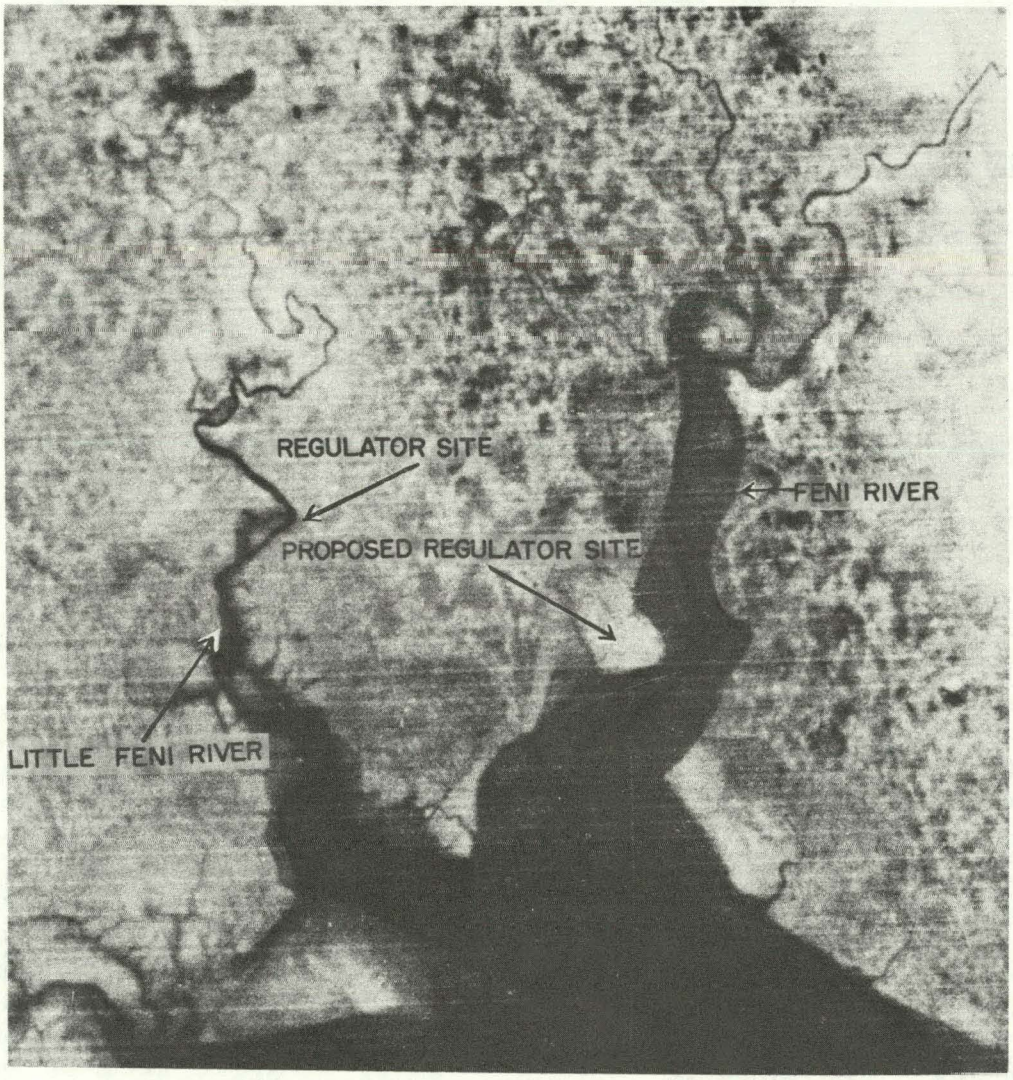

FIG. 2
ENLARGED LANDSAT IMAGE 02 MAY 73 I.D NO. E-1283-03503-7
SCALE 1:190,000(APPROX.)

FIG. 3

ENLARGED LANDSAT IMAGE 02 JAN.77 I.D NO. E-2711-03251-7

SCALE 1:190,000 (APPROX.)

THIS PAGE

WAS INTENTIONALLY

LEFT BLANK

USING INTERMEDIATE REMOTE SENSING TECHNOLOGY PROJECTS FOR NATIONAL DEVELOPMENT IN THE YEMEN ARAB REPUBLIC AND THE REPUBLIC OF SRI LANKA

Harold HAEFNER, Klaus I. ITTEN, Erwin EGLI, Urs GEISER, Rudolf SCHOCH, Hans STEFFEN and Niklaus VOELKE

Department of Geography
University of Zürich
Zurich / Switzerland

ABSTRACT

Four different projects using intermediate-level interpretation techniques are briefly described regarding objectives, data products used, preprocessing and interpretation methods applied and results achieved. They are carried out in the Yemen Arab Republic and in Sri Lanka and are ranging from regional to countrywide levels. The topics are land evaluation and classification, changes in land-use, yield forecasting and demography.

INTRODUCTION

Several remote sensing development projects applying intermediate-level interpretation techniques have been carried out at the Department of Geography, University of Zurich, during the past years (1-6, 15, 16). Some projects which are currently undertaken are realized on behalf of the Swiss Directorate of Development Cooperation and Humanitarian Aid, Berne, within the framework of its bilateral technical assistance programs (7-14).

Main emphasis is always given to land survey studies based on a geoecological concept and reaching from a local to a regional and countrywide level. Accordingly airborne or spaceborne images of various scales are used. The most important programs are listed in the following table.

	country	topic	level	imagery	reference
1	NEPAL	agricultural census	local	b&w airphotos	1/2/4
2	SRI LANKA	rice: acreage and yield	regional	LANDSAT	-
3	LIBERIA	land-use mapping: shifting cultivation	local	b&w IR-airphotos	1/3/4
4	SUDAN	geoecological land classification	regional	b&w airphotos	6
5	ETHIOPIA	changes of rural land-use in arid areas	regional	b&w airphotos LANDSAT	15
6a)	ALGERIA	mapping geology and landforms in arid areas	regional	LANDSAT	5
b)		land evaluation and recent changes in land-use	regional	b&w airphotos LANDSAT	-
7a)	YEMEN ARAB REPUBLIC	land evaluation and classification	country-wide	LANDSAT	10/11/13
b)		population census	regional	b&w airphotos	7/8/9
c)		changes in agricultural land-use	regional	b&w airphotos	12
d)		semicontrolled photomaps 1:25,000 / 1:50,000	regional	b&w airphotos	14
e)		ancient and recent land-use systems	local	b&w airphotos	16

Of these manifolded activities four specific projects shall be discussed briefly regarding objectives, data products used, preprocessing and interpretation methods applied and results achieved.

POPULATION CENSUS

The first Population and Housing Census of the Yemen Arab Republic was carried out in February 1975. The airphoto interpretation project of the Swiss Directorate of Development Cooperation was carried out by our Department accomplishing the following major tasks:

- checking the accuracy of the population figures in selected sample areas;
- estimating the population figures of all areas which were not reached by the official enumerators by airphoto interpretation methods;
- delineating the boundaries of the administrative units (provinces and districts);
- collecting place names and determining the exact location of major villages;
- compiling an adjusted countrywide population databank on the district basis;
- producing the first map on the population distribution and administrative division of the YAR and additional cartographic documents.

One of the most difficult tasks was to estimate the number of inhabitants of all areas which were not reached by the country's enumerators. These areas were mainly situated in the Mashriq, i.e. the northeastern part of Yemen. The objective was attained by means of extended field work and a complete housing census from aerial photographs. During the field surveys the names and locations of settlements and administrative units were determined and recorded on aerial photographs. Furthermore several settlements were selected in which the house types, average house sizes, percentage of empty, abandoned houses, etc., and in random samples the average number of households and families per house unit, family sizes, proportion of emigrants, etc. were recorded (Fig. 1). Based on this information the airphoto interpretation was possible. The dwellings were counted from enlarged film transparencies 1:60,000 using a Bausch & Lomb Zoom Transfer Scope. Applying the sample figures, the approximate number of inhabitants could be determined for the various settlements and the administrative units of the Mashriq.

Approximately 100,000 inhabitants are estimated to live in the Mashriq, an area which covers approx. 47,000 sq km. The previous estimates had ranged between 50,000 and 500,000 inhabitants. The accuracy of the methods applied depends mainly on the quality and scale of the aerial photographs, the dwelling types, the topography and the availability of ground-truth. On average the minimum and maximum estimates of the number of houses counted on aerial photographs differed not more than 10 - 15 % from the most probable number of occupied houses. Therefore the remote sensing methods applied turned out to be quite accurate.

CHANGES IN LAND-USE

The greatest agricultural potentials of the YAR are located in the huge alluvial fans of the Tihamah, the arid coastal plain along the Red Sea. Eight large wadi systems with extensive catchment areas in the mountains drain westwards into the coastal plain and provide good opportunities for spate irrigation. Along the base of the mountain range rainfed agriculture is also possible. But the agricultural land-use depends mainly on the amount of waterflow in the wadis (occurring regularly between April-May and July-September), e.g. on the amount of precipitation in the mountainous area, which varies greatly from year to year. Consequently the land under crop changes constantly, especially along the lower fringe towards the Red Sea, which is farthest away from the outlet of the wadi into the coastal plain. These changes in the quantity of the waterflow and in the extent of irrigated land give rise to substantial local movement of the population,

which uses the land by simple flood irrigation techniques since centuries. On the other hand the big wadi-floods cause severe damages of the earth barrages, irrigation canals and dams, soil erosion, and changes in the course of the wadi channels.

Studies of the changing areal extent of the irrigated crop land, agricultural practices, irrigation systems, use of ground water, amount of erosion, growth of settlements etc. and their relation to meteorological and hydrological data are of greatest importance for planning and development programs.

The test area which was investigated thoroughly is the largest wadi system of the Tihamah, the Wadi Mawr, situated north of Al Hudaydah. It was selected because of the availability of b&w aerial photography from 1953 (1:40,000) and 1973 (1:60,000). Field surveys in 1976 (12) provided the necessary basis for the interpretation of both aerial coverages. Sixteen different land-use categories were distinguished and characterized in a photo interpretation key. The airphotos then were interpreted by analogue techniques and the boundaries of the different land-use categories were transferred onto a map 1:50,000 (prepared by the USGS), using a Zoom Transfer Scope.

The changes which occurred during the twenty years are quite remarkable regarding acreage as well as location (Fig. 2). First, it was possible to determine and measure the maximum extent of the irrigable as well as the rainfed areas. Whilst the allotment of the fields shows a great stability (in accordance with the land-ownership structure), great differences exist in the crop pattern. Abandoned land is connected primarely with damages of the irrigation canals or due to sand accumulations by wind. The size of the wadi channel has diminished considerably in the lower part and its course has changed up to 500 m due to lateral erosion (Fig. 2). The use of ground water by pump irrigation has been introduced during this period and is increasing rapidly. The further development of this irrigation type has to be surveyed carefully to not overuse the ground water supply (12).

The study area shall be surveyed further by LANDSAT-imagery taken shortly after the wadi floods and during the vegetation season, which will provide an excellent basis for monitoring the changes in the future.

LAND EVALUATION AND CLASSIFICATION

About three-fifth of the YAR (110,000 sq km) were studied on LANDSAT-images taken in various seasons to gain a better understanding of the regional structures of the country in regard to their agricultural suitability and potentials. The land evaluation and classification is based on the relief and the landforms, the hydrological network and the density of the vegetation cover, of which almost no information was available. Methods and results therefore may be considered as a good example for producing valuable background information in a short time and at small expenses in developing countries which lack sufficient basic information.

As a first step the following three maps were compiled at a scale of 1:50,000 and then reduced to 1:1,000,000:

- areas of homogenous landform units;
- dynamics of vegetation (Fig. 3);
- hydrographic network and watersheds.

The b&w images in the near IR prove to be suitable for the interpretation of the hydrographic network, the watersheds and the various areas of landform units. The analysis of landforms shows clearly the morphological dynamics resulting from retrogressive erosion in the western and southern mountain escarpments. Water carrying wadis, flooded fields and wet soils can be distinguished from one another. In the visible spectral ranges the salt crusts of the Sabkhah-zone and of the Rub` al Khali can be recognized.

A formal analysis of the crest-lines, divided into three categories, permits the classification of the surface into various areas of homogenous landform units. These correlate closely to the geological and tectonical structures along the Red Sea. In the present study four landform categories were differentiated (plains, plateaus, hills, mountains) which can be further classified according to additional criteria such as stratigraphy, elevation above sea level, etc.

Color composites were used for the interpretation of the vegetation. In order to expose the dynamics of vegetation during a year, there were images available of the dry period (Jan. 1973) and the wet period (Sept. 1972). In the winter half-year mainly the perennial and irrigated vegetation can be distinguished, while in the wet summer period the vegetation of the rainfed farming areas is also visible. Combining the images of both seasons, the rainfed as well as the irrigated fields and the areas of permanent vegetation can be differentiated. A key for interpretation was worked out according to the intensity of the color, the texture, the dynamics of vegetation extent and the geographical location of the cultures: a) vegetation of mainly ephemeral plants; b) vegetation of ephemeral and perennial plants; c) pump and spring irrigated fields; d) flood irrigated fields; e) non arable land with low vegetation density (Fig. 3).

As a second step the analytical data sets were fused into a synthetic map in order to determine uniform regions in a synoptic view (Fig. 4). The catchment areas of the Red Sea, the Gulf of Aden and the Rub` al Khali divide the land surface of SW Arabia into three main parts. They can be broken down further into areas of similar landforms and land-use. This division provides an excellent insight into the grouping of various agricultural regions according to the differences in climate and topography since these decisively affect vegetation and thereby the agricultural situation of the region. Together, the various maps provide a good basic information concerning the agro-potential of the individual regions and serve as background information for forthcoming agricultural inventory and planning programs.

RICE YIELD FORECASTING THROUGH PADDY AND TANK SURVEYS

One of the major problems in the Republic of Sri Lanka is the forecasting of food production and the corresponding import planning. Because about one-fourth of the consumed rice has to be imported, the government strives for self-sufficiency.

Rice yield varies very much from one year to the other. The harvest depends mainly on the starting time and the amount of rainfall from the northeast monsun e.g. the availability and the management of the irrigation water, besides proper fertilizing techniques.

Only at a very late stage in the season - often after harvest - the first yield estimation figures reach the planning ministry. Therefore means and ways to provide earlier rice yield forecast figures had to be studied. Aerial surveys of the dry zone paddy areas, several times during the growing season, was out of question for financial reasons. As LANDSAT provides possibilities to cover such areas every 18 days, this was sought to be the appropriate means for surveying.

Because we deal with forecasting, the timeliness of the data is a major concern. For that reason, and due to the general concept of utilizing intermediate-level technology, photographic products and analog interpretation methods were favoured.

The timelag from aquisition of the imagery until having it in the hands was cut down to one month through a standing request order for 1:1,000,000 positive transparencies.

For two test-sites, the "Kantalai" and the"Pallang Oya" region in eastern Sri Lanka, base maps at a scale of 1:100,000 containing all land-use units were drawn. They are currently updated to the agricultural growing status at each LANDSAT

overflight as an accurate ground truth for the later comparison with the satellite data. At the same time, data on the water level in the irrigation tanks are gathered, because a survey of these tanks is also carried out by satellite imagery interpretation.

The images are enlarged to the base map scale and photographically enhanced for good contrast within the test areas. Diazo color composites and enlargements on Cibachrome serve as means for a detailed comparison.

As shown in Fig. 5 the tanks are easily discernible in either LANDSAT band 6 or 7. Growing paddy cannot be identified in one step as it appears in the figure, because incidently abandoned fields get flooded also. The main information on paddy lies in the change of brightness in band 5 and 7 during the growing season. Best results were achieved until now with a multitemporal color composite of channel 5, combining images from the beginning of cultivation, two months later, and before harvest.

Especially enhanced images are treated in a Datacolor Edge Enhance and Density Analysis System to measure the area under paddy, whereas the surveying of the tanks can be achieved by using band 7 bulk enlargements. Regional masks are prepared in such a way, that in combination with the satellite image enlargement, paddy acreage figures in respect to the total area of the region are obtained.

The major problems encountered are, that different regions start paddy cultivation at different times. In the tank survey, sedimentation in the reservoirs and evaporation losses cause difficulties. Besides, the general weather condition often prevents a successful imaging during the monsun period, due to heavy cloud cover, and therefore is a limiting factor.

The quality of the 1:1,000,000 bulk products necessitated contrast-enhanced rewriting from the tapes on a Photomation System. This was also done for a general land-use survey study, where it was tried to establish a land-use category catalogue for the updating of earlier land-use maps with new LANDSAT-imagery.

In a final step, average acreage-yield figures as well as the data on available irrigation water will be combined, to reach the major scope - an early regionwise rice yield forecast - for the better management of the countries resources.

CONCLUSIONS

Remote sensing technology and in particular repetitive coverage as obtained from LANDSAT provides an excellent base for the preparation of the necessary background information in a short time and at small expenses, and to monitor rapidly changing surface phenomena. This kind of information is essential in developing countries to improve the knowledge on the local natural resources and to expand the food basis, to initiate appropriate planning and developing programs, and to monitor hazards such as floods, droughts and pests. Intermediate-level technology may be considered as the most suitable method for most of these tasks because it is easy to install and handle. Therefore it may be stated that photographic products, which are familiar to everyone, will still remain the most important data source in the future.

REFERENCES

1. BOESCH H. et al: Contributions to land-use survey methods. The World Land Use Survey, Occasional Papers No. 10, 1971.

2. SCHMID R.: Zur Wirtschaftsgeographie von Nepal. Ph.D. Thesis, University of Zurich, 1969.

3. KOCH P.H.: Die Shifting Cultivation und ihre Luftbildauswertung. Ph.D. Thesis, University of Zurich, 1970.

4. HAEFNER H.: Methods and examples of air photo interpretation for land resources studies. Proc. UN Seminar on Photogrammetric Techniques, Swiss Federal Institute of Technology, Zurich, 1971.

5. GEISER U.: Quantitative geologisch-geomorphologische Interpretationen mit ERTS-1-Multispektralaufnahmen. Untersuchungsgebiet: Hoggar-Massiv, Südalgerien. M.A. Thesis, Dept. of Geography, Univ. of Zurich, 1975 (unpublished).

6. STREBEL B.: Landschaftsökologische Aufnahmen im Südsudan. M.A. Thesis, Dept. of Geography, Univ. of Zurich, 1974 (unpublished).

7. STEFFEN H. + GEISER U.: Databank of Yemen's Population and Housing Census 1975. Preliminary Report No. 5, Dept. of Geography, Univ. of Zurich, 1977.

8. STEFFEN H. et al: Major findings of the Population and Housing Census of February 197 and the results of supplementary demographic and cartographic surveys. Final Report, Dept. of Geography, Univ. of Zurich, 1978 (in print).

9. GEISER U. + STEFFEN H.: Population distribution, administrative division and land use in the YAR. Map 1:500,000, Dept. of Geography, Univ. of Zurich, 1977.

10. SCHOCH R.: Regionale Gliederung der YAR mit Hilfe von LANDSAT-Satellitenbildern. M.A. Thesis, Dept. of Geography, Univ. of Zurich, 1977.(unpublished)

11. SCHOCH R.: Land evaluation and classification from LANDSAT-imagery in the YAR. Map 1:1,000,000, Dept. of Geography, Univ. of Zurich, 1978.

12. EGLI E.: Landnutzung und Landnutzungsveränderungen in der Region Wadi Mawr, YAR. M.A. Thesis, Dept. of Geography, Univ. of Zurich, 1978 (unpublished).

13. HAEFNER H. + SCHOCH R.: Land evaluation and classification from LANDSAT-imagery in the YAR. Proc.COSPAR-Nordberg Mem. Symposium, Tel Aviv, 1977.

14. STEFFEN H.: Herstellung von Luftbildkarten in unvermessenen Gebieten, ausgeführt in Hajariyah, YAR. M.A. Thesis, Dept. of Geography, Univ. of Zurich, 1974 (unpublished).

15. STREBEL B.: Kakteenbauern und Ziegenhirten in der "Buknaiti Are" (Nordäthiopien). Ein Planungsbeitrag zur Agrarentwicklung in ariden Berggebieten. Ph.D. Thesis, University of Zurich, 1978 (in print).

16. SCHOCH R.: Die antike Kulturlandschaft des Stadtbezirkes Saba' und die heutige Oase von Ma'rib in der YAR. in: Geographica Helvetica, No 3, Zurich, 1978 (in print).

Fig. 1: Example of ground survey for population census:
The village of Mawsāṭ, Barat Highlands, YAR.

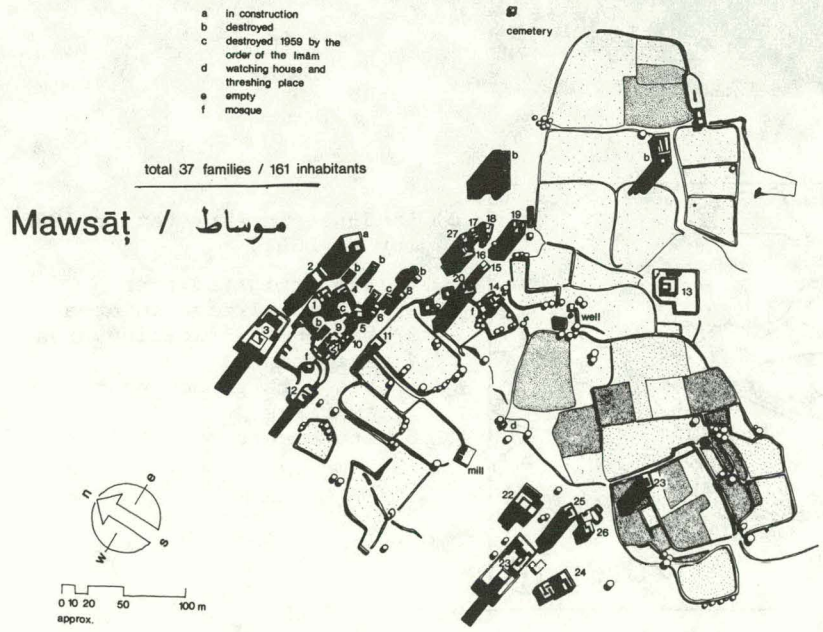

above:
Enlargement of aerial photograph (from 1:60,000 to 1:15,000), February 1973.

left:
Scetch-map showing results of housing count (map by W. DUBACH)

Fig. 2: Example of land-use changes in the Wadi Mawr, YAR, 1953-1973

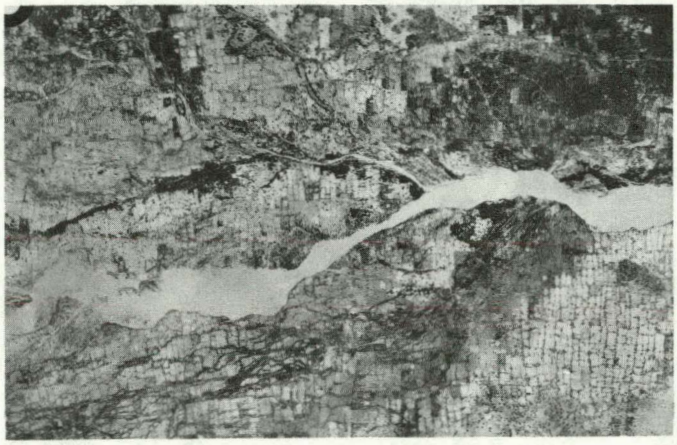

a) Situation in December 1953.
Scale approx. 1:60,000.

b) Situation in January 1973.
Scale approx. 1:60,000.

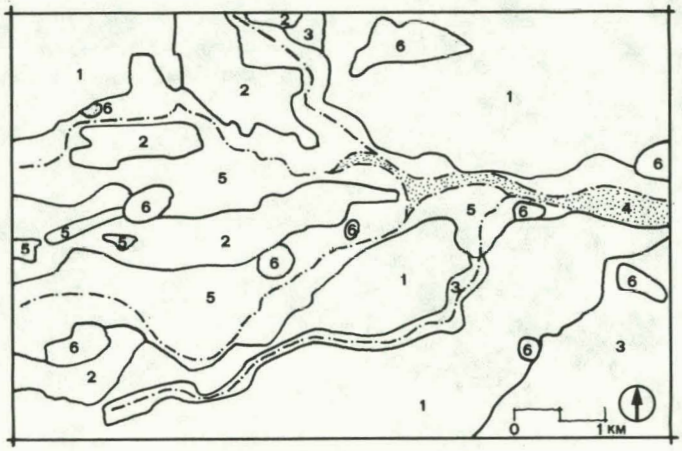

c) Land-use interpretation 1973
(by E. EGLI)

1 1973 irrigated area
2 1973 not irrigated area
3 abandoned irrigation area
4 wadi channel
5 area with predominantly tamarisks
6 settlements

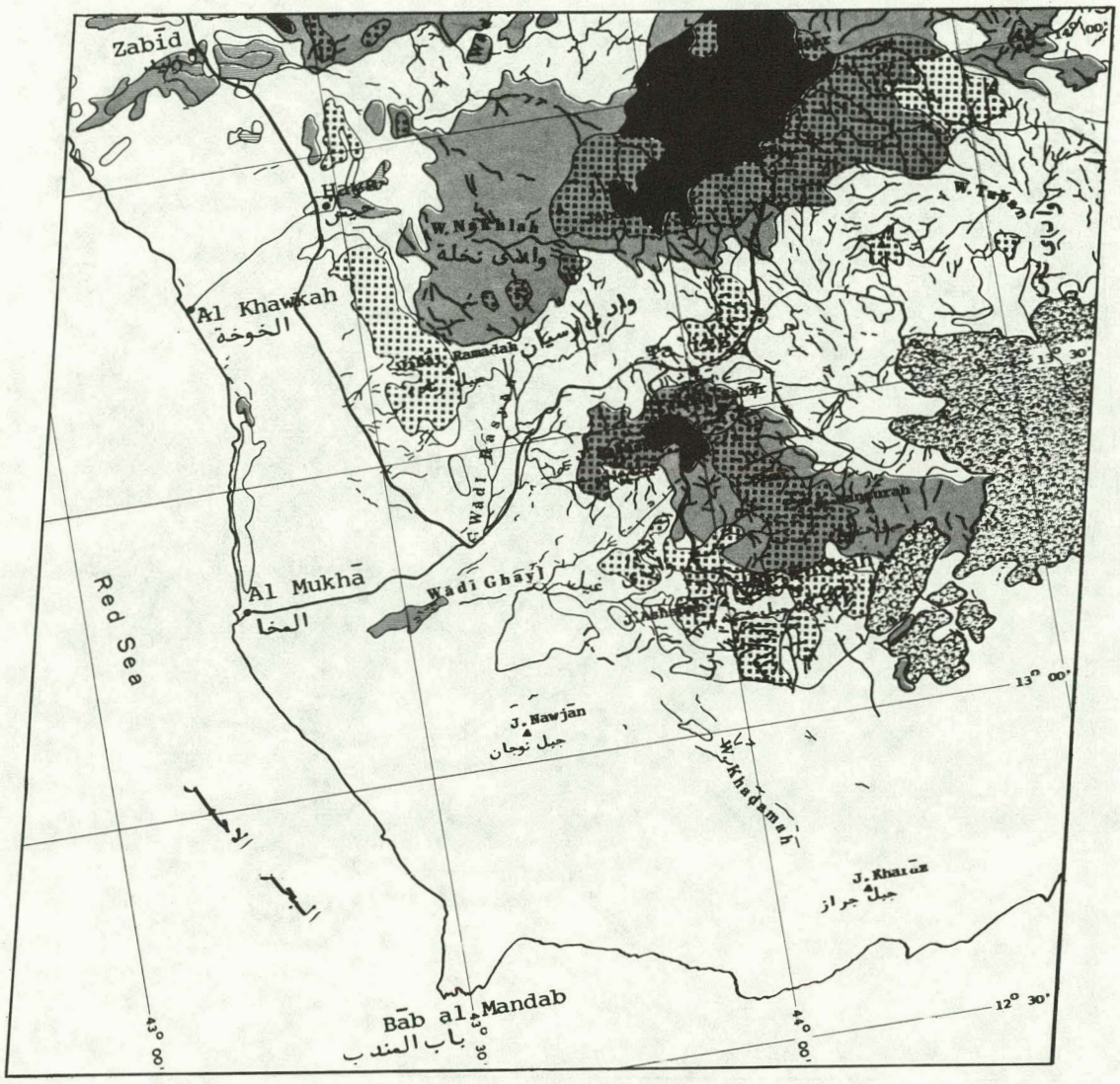

Fig. 3: Dynamics of vegetation growth as interpreted from imagery of dry season (Jan. 1973) and wet season (Sept. 1972). (Int. by R. SCHOCH)

Extent of rainfed areas in the wet period:

- low density vegetation
- medium density vegetation
- high density vegetation

Extent of rainfed areas in the dry period:

- low density vegetation
- medium density vegetation

Pump-, spring- and flood-irrigated fields:

- low to medium density vegetation
- high density vegetation

- intensive vegetation in the wadi channels
- clouds

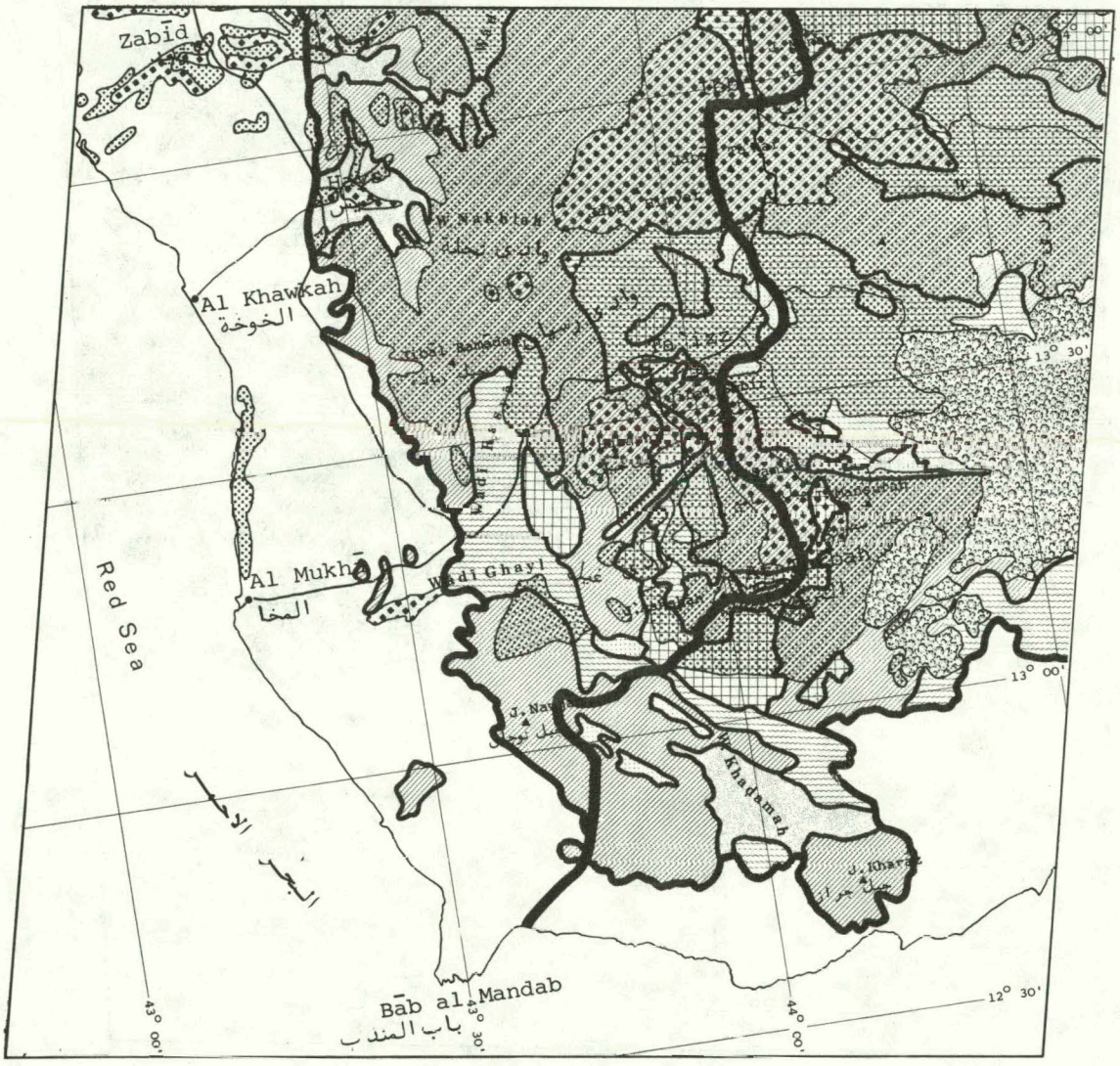

Fig. 4: Synthetic land classification compiled from LANDSAT-imagery (Int. by R. SCHOCH)

Delineation of land facet units

- land region
- land system
- land facet
- vegetation delineation

Units of land facets

- sand plain
- large valley bottom
- intramountainous plain
- plateau
- hilly area
- mountainous area
- low density vegetation
- high density vegetation

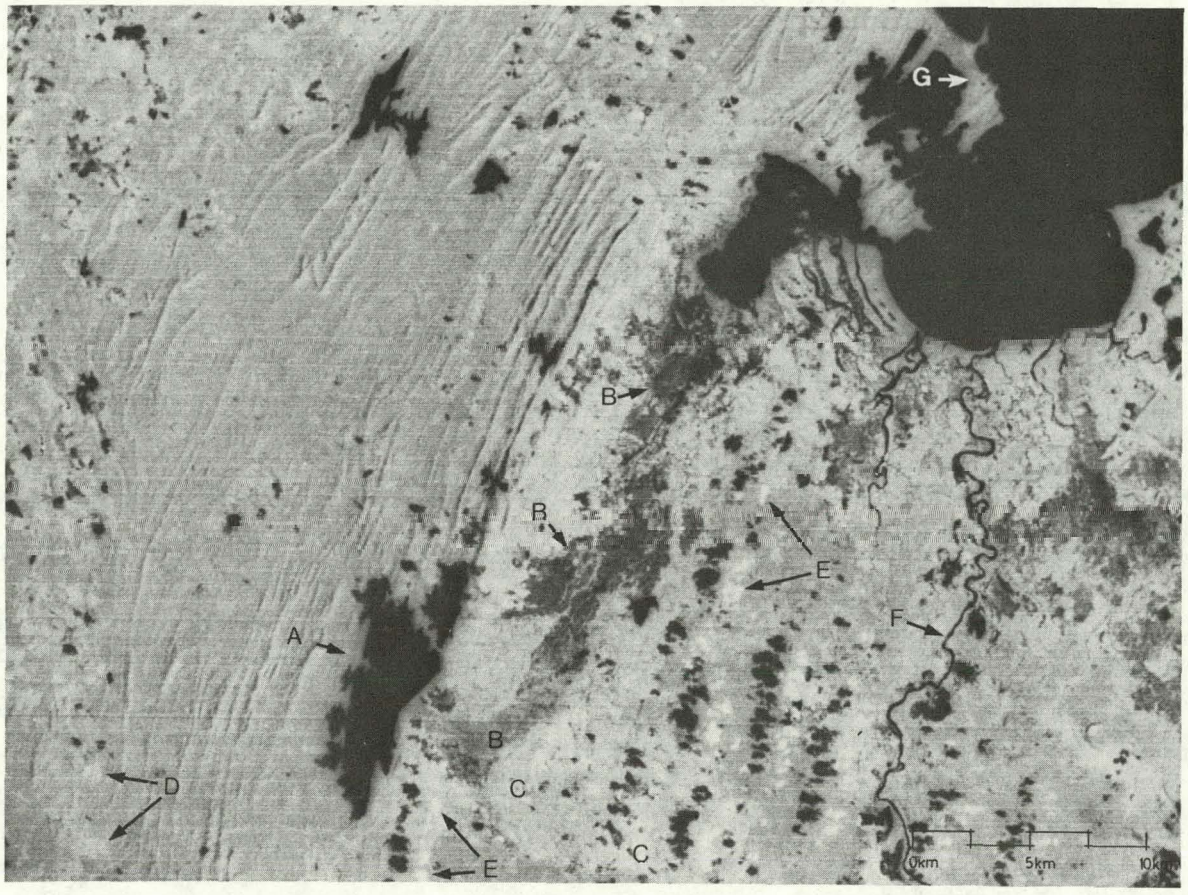

Fig. 5: Paddy and tank survey test area "Kantalai" in the Trincomalee District in northeastern Sri Lanka. LANDSAT-1 band 7 of Dec. 15, 1977, area approx. 1,900 km^2.

A = Kantalai Tank, completely filled in present monsun period

B = associated irrigation area, paddy incl. abandoned fields (best paddy field distinction on color composit of bands 5: early in the season / 2 months later / before harvest)

C = sugarcane plantations

D = forest clearcuts through "Chena Culture" (shifting cultivation)

E = scattered cumulus clouds, which can easily be separated due to their shadow

F = Mahaveli River

G = City of Trincomalee at Koddiyar Bay

THIS PAGE

WAS INTENTIONALLY

LEFT BLANK

LAND USE INVENTORY OF NORTH THAILAND USING LANDSAT IMAGERY

Manu Omakupt

Department of Land Development

Bangkok, Thailand

ABSTRACT

The need for an accurate and up-to-date land use information by an airborne or satellite sensor is especially significant when repetitive surveys are required. Remote sensing technique now provides a hitherto unavailable capability for detecting and mapping land use features and monit ring dynamic events of an area, in a repetitive and temporal basis. Land use inventory in Thailand has been undertaken by the Department of Land Development, Ministry of Agriculture and Cooperatives as an important application program of remote sensing from satellites. The program is first being focused upon mapping and determination of the major types of land use in North Thailand. The results are discussed.

1. INTRODUCTION

Remote sensing has become accepted by most geoscientists as a very useful tool, if properly applied in support of doing ground surveys. In many cases, remote sensing technology has produced useful results without actual ground validation. This aspect of remote sensing, the need for accurate and up-to-date land use map and land cover by an airborne or satellite sensor, is especially significant when repetitive surveys are required of inaccessible or dynamic areas and in hazardous environments. The changes of natural events need to be detected rapidly and repeatedly for meaningful results. Satellite imagery have been used by the Department of Land Development to map land use in Thailand since 1973. It was found that Landsat imagery are very useful for regional land use mapping and for monitoring the changes of land use features.

North Thailand is consisted of mountain ranges, much of the land is hilly and rolling to undulating topography. Sixteen provinces in the region cover 107,011 square kilometers or 106,256,875 rai,* which is about 1/3 of the whole country. Approximately 25 percent of the area is under cultivation along the valley and in the plain of the lower north. The pressure of land holdership becomes more and more serious problem, because of the rapidly growing population. Shifting cultivation is highly extend throughout the area, especially in the watershed areas. Many problems are becoming more aggravating in this region, such as land holding per family is decreasing (the recent average is 6-7 rai/family), low income farmer on the increase, shortage of food and agricultural land, forest deterioration, soil erosion, drought and etc. These problems must be solved carefully and urgently. So there is growing realization of the need to attain a more balanced regional development in Thailand and more crop diversification aimed at maximizing farmers' income. In order to plan for these needs, land appraisal is required to assist the planners, for preparing long term development plans. Agricultural development and appropriate land use planning program are required side-by-side in order to cope with this. Remote sensing techniques will assist in giving the reliable and up-to-date land use information which is neccessary for the proper land use planning.

* rai is a Thai unit for area measurement and is equal to 1,600 square meters (1 Km^2 = 1,600 rai)

2. OBJECTIVES

Since the changes in land use occur at highly variable rates from place to place. Various users always need the existing land use data which must be timely, relatively inexpensive, and appropriate for widely varying needs at national, regional, provincial or local levels. The Department of Land Development has carried out a land use mapping program since 1971. With the introduction of Landsat imagery into Thailand, the program has been intensified to enable updating of existing land use map in a reasonable time and to differentiate various types of crops with the aid of Landsat imagery. The objectives of this study are :-

1. To survey and map land use of North Thailand at the scale of 1:500,000 by using Landsat imagery.
2. To produce maps showing existing land use informations.
3. To evaluate the cost, time, and the result of this survey compared with other types of survey.
4. To provide the data obtained from the study available for the users.

3. MATERIALS AND EQUIPMENTS

1. Black and white Landsat imagery at scale 1:500,000 and 1:250,000 both in band 5 and band 7
2. Color composite tranparency films, at scale 1:1,000,000
3. Topographic map, series L 1501, at scale 1:250,000.
4. Magnifying glasses, compasses, 35 mm. camera, data recording sheets, and other drawing materials and equipments.

4. PROCEDURE

Thirteen frames of black and white prints at 1:500,000 and 1:250,000 scale of Landsat-2 imagery of band 5 and band 7, and diazochrome transparencies of 1:1,000,000 scale supplied by the Users Service of Thailand National Remote Sensing Program were used in the study. Planimetric details from topographic maps at 1:250,000 scale, were transferred to a transparency sheet for ground control purposes.

Direct visual interpretation was performed based on texture, gray tone, size and shape, temporal change, topography, and other environmental features. Five first level categories and seven second level categories were distinguished on the Landsat imagery. They are :-

Urban land (U)
Agricultural land (A)
1. Horticultural land (A 1)
2. Perennial crop land (A 2)
3. Field crop land (A 3)
4. Paddy land (A 4)
5. Pasture and range land (A 5)
Forest land (F)
1. Dense forest (F)
2. Cut forest (F')
Water body (W)
Miscellaneous land (M)

Ground truth observations were carried out during August-October 1976 for test areas. Similar or uniform tones were taken as representatives of land use types in the area. Each field check-point was recorded in data recording sheet and photographs of the area were also taken.

The land use classification scheme developed during Landsat-1 investigation was used in the present study.

5. RESULTS

The results of the study (table 1) enable classification of land use patterns in North Thailand as follows :

(1) Urban land (U) : Only big towns or cities were recognized as very light gray or white toned signature. There exist somewhat different features for the same class according to the location of features adjacent to an urban unit, the shape, size, and their cultural features, patches of wood or fields within the area).

(2) Agricultural land (A) : There are five distinguished categories identified as agricultural land as listed below.

2.1 Horticutural land (A 1) : Truck cropping are dominant in this unit. According to general practice, farmer always grow various crops mixed together such as corn, sugarcane, bananas, and small fruit trees. Those fields are not uniform, size and shape vary from place to place. Most of the fields are too small to be indicated on the map. Light to intermediate gray tones are indication of mixture of crops. Location (low land that is surrounded by rice field and perennial crop) is very important for identification and experience of interpreter is needed.

2.2 Perennial crop land (A 2) : Orchards and trees (coconut, tea, etc.) are dominant in the field. Apparently, quite even intermediate to darker gray tone signature and fine texture are shown on the images.

2.3 Field crop land (A 3) : Large field of even-toned intermediate gray signature are delineated on the photos as A 3 category. Those fields are corn, sorghum, sugarcane, tobacco, soybean, cotton, cassava, and pineapple.

2.4 Paddy land (A 4) : Landsat imagery that were used in the study were taken in the dry season. Most of the paddy field appeared as light and even gray toned, or even terrain. Moreover, those located in the irrigated areas or depressed areas appeared as darker tone. In this area crop rotation or double cropping are active after rice season.

2.5 Pasture and range land (A 5) Signature is even gray toned; dark gray-toned mottles are scattered through the area. Those mottles represent trees that were left in the field.

(3) Forest land (F)

3.1 Dense forest (F) : Darkness and evenness of tone, uneven terrain signatures appeared on the imagery which indicates the dense forest areas. Gray tone show a little difference according to the type of forest. Evergreen forest appeared as darker tone while deciduous forest appeared as lighter. One of the significant features of this unit is substantial areal extent (small isolated wooded areas were excluded from this category but equally small clear-cut areas were ignored and thus included) and softening of ridge and drainage feature contours by vegetation cover.

3.2 Cut forest (F') : The forest areas have been cut and left dominantly second growth forest which include some agricultural and swidden land. Signature is variable intermediate gray tones (indication of stages of regrowth), variably shaped but sharply defined outline, absence of clumps of mature trees, no fixed shapes and rugged boundaries separating forest and clearings.

4. Water body (W) : Very fine texture, solid darkness and evenness of tones signature is recognized. Gray tone may vary as the depth of water varies or the quality of water is changed.

5. Miscellaneous land (M) : Signature is variable darkness and intermediate tones. identification of a surface undesirable for or incapable of use in the same sense as above. This category is composed of idle land, poorly drained areas (swamps, oxbows).

TABLE I. Land use types of North Thailand

Land use type	Symbols	Area		Percent
		rai	sq.km.	
Urban land	U	181,250	290	0.17
Horticultural land	A 1	17,500	28	0.02
Perennial crop land	A 2	198,907	318	0.19
Field crop land	A 3	10,686,250	17,098	10.06
Paddy land	A 4	19,536,719	31,258	18.39
Pasture and range land	A 5	133,188	195	0.11
Dense forest	F	62,777,966	100,444	59.10
Cut forest	F'	11,750,157	18,800	11.10
Water body	W	612,500	980	0.58
Miscellaneous land	M	373,438	597	0.45
TOTAL		106,256,875	170,011	100

TABLE II. Comparison of time, cost, and manpower between two types of survey

Items	Using Landsat imagery	Cost (baht)**	Using aerial photographs	Cost (baht)
Time (field checks)	60 days	-	210 days	-
Manpower	4	36,400.-***	20	285,500.-***
No. of imagery	39 frames*	5,200.-	3,652 photos	36,520.-
Cost/km.^{2}	-	0.24	-	1.89

* cost 60 baht/frame at 1:500,000 scale and 170 baht/frame at 1:250,000 scale

** baht is Thai unit of money, 20 baht = U.S $ 1

*** cost of perdium and other expenses

TABLE III. Comparison of the results of both surveys

Symbols	*Area from Landsat imagery (rai)	%	**Area from aerial photograph (rai)	%	Difference (rai)	%
U	181,250	0.17	1,293,729	1.22	1,112,479	1.05
A 1	17,500	0.02	45,235	0.04	27,735	0.02
A 2	198,907	0.19	331,330	0.31	132,423	0.12
A 3	10,686,250	10.26	5,883,539	5.54	4,802,711	4.52
A 4	19,356,719	18.39	18,313,427	17.24	1,223,292	1.15
A 5	122,188	0.11	93,501	0.05	28,687	0.06
F	62,777,966	59.10	79,840,580	75.18	5,312,447	4.98
F'	11,750,157	11.10	79,840,580	-	-	-

Symbol	*Area from Land imagery (rai)	%	**Area from aerial photograph (rai)	%	Difference (rai)	%
W	612,500	0.58	341,407	0.32	271,093	0.26
M	373,438	0.45	114,127	0.1	259,311	0.35

* Survey was done in 1976

** Survey was done in 1973

6. CONCLUSION AND DISCUSSION

The land use map of North Thailand at scale of 1:500,000 based on photo-interpretation of Landast-2 imagery has been produced. This land use map is being used in the land development planning program and other related projects by government planning agencies. It has been found out from this study that band 5 of Landsat MSS imagery provides maximum information and best discrimination of vegetation. Experience leads to the conclusion that small scale satellite imagery can be used in the broad land use survey with highly reliable results. Moreover, it is more economical, involving less time and less expense when compared with other surveying methods. Satellite survey is most suitable in the studying and mornitoring of land use changes which tend to occur rapidly. It is also very useful in the survey to obtain up-to-date information in land cover types. The Department of Land Development is working on other areas of Thailand in the program to produce land use maps of the whole country based on Landsat imagery. With the added capability to process Landsat CCT's in Thailand at the Asian Institute technology, the Department of Land Development is cooperating with other groups in an affort to produce computer processed land use maps and in the evaluation of the results.

REFERENCES

Thailand National Programme of the Earth Resources Technology Satellite, SR.No. 9620, Type III Final Report for period November 1972-March 1974, May 1974.

Thailand National Programme of the Earth Resources Technology Satellite, G28080, Type III Final Report for period June 1975 - July 1977, July 1977.

Country Report of Thailand for the Intergovernmental Meeting on Remote Sensing and Satellite Surveying, 7 - 13 June 1977, at ESCAP, Bangkok.

LAND USE CLASSIFICATION

URBAN LAND (U)

- U 1. Residential land
  - U 1.1 City, Town
  - U 1.2 Village (strip land clustered settlement)
- U 2. Commercial land
- U 3. Institutional land (school, hospital, park, temple)
- U 4. Transportational land (railroad yard, bus station, airfield, etc.)
- U 5. Industrial land
  - U 5.1 Mine and dump
  - U 5.2 Factory

AGRICULTURAL LAND (A)

- A 1. Horticultural land
  - A 1.1 Truck crop land
  - A 1.2 Ornamental plant garden
  - A 1.3 Vine yard
  - A 1.4 Other horticultural land
- A 2. Perennial crop land
  - A 2.1 Orchards
    - A 2.1.1 Mixed orchard
    - A 2.1.2 Citrus orchard
    - A 2.1.3 Durian orchard
    - A 2.1.4 Rambutan orchard
    - A 2.1.5 Longan orchard
    - A 2.1.6 Litchi orchard
    - A 2.1.7 Mango orchard
    - A 2.1.8 Custard apple orchard
    - A 2.1.9 Jujube orchard
    - A 2.1.10 Peach orchard
    - A 2.1.11 Apple orchard
    - A 2.1.12 Other orchard
  - A 2.2 Rubber plantation
  - A 2.3 Coconut plantation
  - A 2.4 Banana plantation
  - A 2.5 Kapok plantation
  - A 2.6 Coffee plantation
  - A 2.7 Tea plantation
  - A 2.8 Miang tea plantation
  - A 2.9 Oil palm plantation
  - A 2.10 Mulberry plantation
  - A 2.11 Pepper plantation
  - A 2.12 Bamboo plantation
  - A 2.13 Sugar palm plantation
  - A 2.14 Raintree plantation
  - A 2.15 Other plantation
- A 3. Field crop land
  - A 3.1 Corn field
  - A 3.2 Sugar cane field
  - A 3.3 Cassava field
  - A 3.4 Cotton field
  - A 3.5 Tobacco field
  - A 3.6 Pineapple field
  - A 3.7 Beans and peanut field
  - A 3.8 Fiber crop (kenaf, jute)
  - A 3.9 Melon field
  - A 3.10 Castor bean field
  - A 3.11 Sorghum field
  - A 3.12 Sesame field
  - A 3.13 Upland rice field
  - A 3.14 Potato field
  - A 3.15 Mint field
  - A 3.16 Chili field

A 3.17 Other field crop land

A 4. Paddy land
- A 4.1 Broadcast rice field
  - A 4.1.1 One crop only
  - A 4.1.2 Double cropping with second crop
- A 4.2 Transplanted rice field
  - A 4.2.1 Rainfed, one crop only
  - A 4.2.2 Rainfed, double cropping wiht second crop
  - A 4.2.3 Irrigated, one crop only
  - A 4.2.4 Irrigated, double cropping
  - A 4.2,5 Irrigated, double or triple cropping in rotation with other crops

A 5. Pasture and range land
- A 5.1 Improved pasture and range land
- A 5.2 Unimproved pasture and range land

A 6. Swidden land
- A 6.1 Noncyclical swidden land
  - A 6.1.1 Upland rice in rotation or association with other crops
  - A 6.1.2 Corn or opium in rotation or association with other crops
  - A 6.1.3 Other swidden crop land
- A 6.2 Cyclical swidden land
  - A 6.2.1 Upland rice field
  - A 6.2.2 Other crop field
  - A 6.2.3 Bush fallow

FOREST LAND (F)

F 1. Evergreen forest
- F 1.1 Tropical evergreen forest
  - F 1.1.1 Hill evergreen forest
  - F 1.1.2 Dry evergreen forest
  - F 1.1.3 Moist evergreen forest
- F 1.2 Coniferous forest
- F 1.3 Mangrove forest

F 2. Deciduous forest
- F 2.1 Mixed deciduous forest
  - F 2.1.1 Mixed deciduous forest, with teak
  - A 2.1.2 Mixed deciduous forest, no teak
- F 2.2 Dry dipterocarp or deciduous dipterocarp forest
- F 2.3 Scrub forest

F 3. Beach (Littoral) forest

F 4. Swamp forest

F 5. Forest plantation
- F 5.1 Teak plantation
- F 5.2 Pine plantation
- F 5.3 Other plantation

REMARK : put (---------) on every category that forest is disturbed

WATER BODY (W)

W 1. Reservoirs, lakes, ponds

W 2. Fish ponds

W 3. Shrimp ponds

MISCELLANEOUS LAND (M)

M 1. Salt flats

M 2. Marsh and swamp

M 3. Rocky land (stony, rock out crop)

M 4. Waste land (sand dune, river or coastal waste land)

M 5. Other miscellaneous land (currently unused land that is not classified as above)

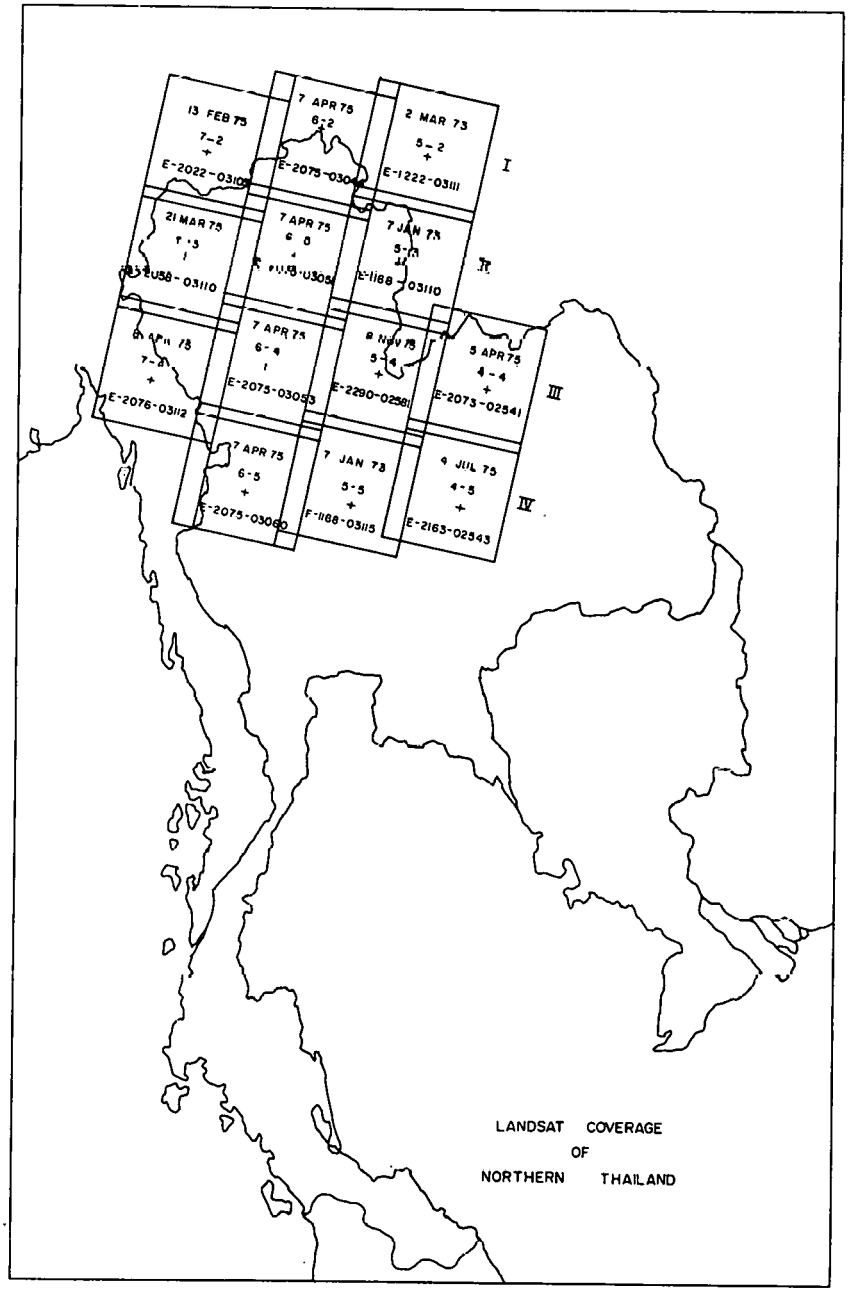

Figure I. Index showing Landsat coverage of North Thailand
(Numbers in the middle are Thai registered numbers)

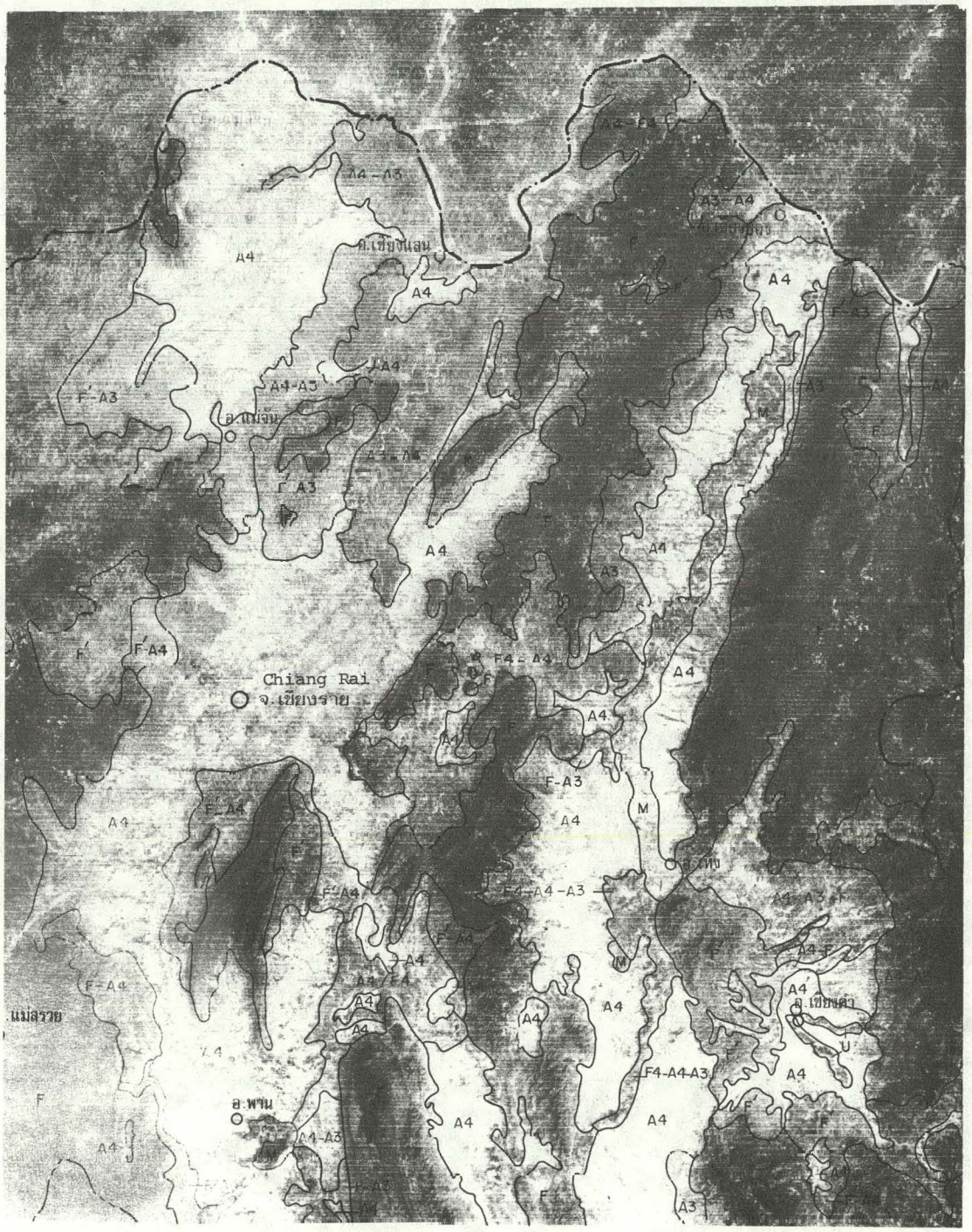

Figure II. Landsat imagery frame 6-4 and 5-4, showing land use type of North Thailand

Figure III. Landsat imagery frame 6-2, showing land use type of North Thailand

U. S. COAST GUARD UTILIZATION OF REMOTE SENSING TECHNIQUES FOR OCEAN SURVEILLANCE

LCDR J. R. WHITE, LCDR D. R. FREEZER, Mr. R. R. Vollmers
USCG, Washington, D. C.

Summary

The U. S. Coast Guard performs a number of missions, e.g. pollution surveillance, search and rescue, ice reconnaissance, and enforcement of laws and treaties, which require large scale ocean surveillance. Evaluation of numerous types of sensor systems has shown that these missions can be performed more effectively by using sensor-equipped aircraft. This paper will discuss some recent Coast Guard research and development programs in remote sensing.

Pollution Surveillance

The U. S. Coast Guard has been actively involved in remote sensing of pollution for many years. This interest became more pronounced in 1971 when the Office of Research and Development was tasked with developing a supporting surveillance system to insure proper enforcement of the Federal Water Pollution Control Act, as amended, pertaining to the discharge of oil and hazardous substances into the navigable waters of the U.S. An airborne, real time, all weather, day/night system that could detect, quantify, identify, and map the extent of coverage of harmful discharges of oil and hazardous substances was required. This led to the development of the Airborne Oil Surveillance System[1,2] (AOSS I and AOSS II).

AOSS II

AOSS II (an updated version of AOSS I) was installed in a Coast Guard HC-130B aircraft by Aerojet Electrosystems Co., of Azusa, California and became operational in April 1977. Several sensors (Side-Looking Radar, Infrared/Ultraviolet Line Scanner, Aerial Reconnaissance Camera and a Passive Microwave Imager) are combined with a real-time control and display console to produce a fully integrated, all weather, day/night remote sensing system. The addition of a multi-spectral surveillance system to a standard HC-130B has increased its surveillance productivity by fourfold. Table 1 presents the results of some recent Coast Guard ocean surveillance patrols. A standard, non-sensor equipped, HC-130B would have to fly four times the number of hours, or approximately 90 hours, to cover the same area. Never before in Coast Guard history has a single aircraft imaged as much territory in as short a time.

AIREYE

In January 1977, the Coast Guard contracted with Falcon Jet Corporation to purchase 41 Falcon 20G jet aircraft. These aircraft, designated HU-25A, will serve as the replacement for the aging HU-16E Grumman Albatross as the Coast Guard's Medium Range Surveillance (MRS) aircraft. Delivery is scheduled to begin in July 1979 at a rate of one aircraft per month. Table 2 lists the HU-25A characteristics.

Because of the success of AOSS I and AOSS II, it was decided to include a remote sensing system on six of the aircraft for the Coast Guard's marine environmental protection mission. The system is called AIREYE, which originated from the pronunciation of the acronym ARI which stands for Airborne Remote Instrumentation. To provide the greatest flexibility, all 41 of the MRS aircraft will be configured to accept the various sensors comprising AIREYE. These sensors include a side-looking airborne radar, an infrared/ultraviolet line scanner, an aerial reconnaissance camera, an airborne data annotation system, and a control, display and record console. It will be designed to permit removal and installation in another aircraft in a four hour period. As much as possible, each sensor will be capable of operating in a stand alone mode.

The AIREYE system is based to a large extent on AOSS II; however, the use of a much smaller aircraft than the HC-130B has necessitated a considerable reduction in size and weight. AOSS II weighes 2366 kg and has an internal volume of 3.75 cubic meters. AIREYE will be limited to 720 kg and internal volume of 2.25 cubic meters. This is being accomplished by the elimination of separate power supplies, equipment pallets, and a judicious selection of sensor and auxiliary equipment.

The side-looking radar will have several improvements over the one used in AOSS. These include a higher power transmitter, 200 KW instead of 45 KW, and a dry film silver radar processor instead of the wet chemical processor. Other SLAR characteristics are listed in Table 3.

The infrared/ultraviolet line scanner will have three channels. Two channels will generate infrared video in the 8.0 to 13.0 micron spectral band. One of these will have a detector angular resolution of 2.5 milliradians and a noise equivalent temperature difference of 0.2° K or less. This is similar to the RS-18 line scanner on AOSS. Experience with AOSS showed that the sensitivity of the RS-18 was marginal and that it was not always possible to differentiate between pollutants and natural effects recorded on the infrared images. For these reasons, the second infrared channel, although in the same spectral region, will have a higher sensitivity. It will have a detector angular resolution of 14.0 milliradians and a noise equivalent temperature difference of 0.02° K or less. The ultraviolet channel records radiation in the 0.320 to 0.400 micron band. It is the same as AOSS except the ultraviolet sensitivity will be improved by a factor of 10.

The aerial reconnaissance camera will be a KS-87B camera which is presently in Department of Defense inventory. It is a pulse operated frame camera containing interchangeable lens cones, high speed focal plane shutter, integral automatic exposure control (AEC), data recording and forward motion compensation (FMC). The film handling system will be a combination cassette-magazine drive capable of pulse or pulsed FMC operation with full 150 meter standard film spools. It will produce high quality nominal 11.5x11.5 cm. format pictures on 12.7 cm. roll film.

The airborne data annotation system will be an AN/ASQ-154 which is also in Department of Defense inventory. It will provide alphanumeric annotation on sensor imagery including time, date, latitude, longitude, altitude, drift, heading, pitch, roll, speed, aircraft number and mission number.

AIREYE will provide several advantages to operations with the HU-25A aircraft:

a. AIREYE's search swath width for the detection of hard targets will improve track spacing while maintaining a probability of detection of 90% or more.

b. AIREYE will detect oil and other pollutants day or night in most weather conditions.

c. AIREYE will map all targets including points of land and navigational aids. Whole fleets can be mapped. When geographic points are included, positioning data becomes indisputable.

d. AIREYE will provide real-time, annotated, hard copy imagery for prosecution of polluting vessels.

To identify polluting vessels at night, the Coast Guard, through the Naval Air Development Center, is also developing an Active Gated Television (AGTV) for later incorporation into the AIREYE system. The AGTV will have a low power (one or two watts), room temperature, pulsed laser illuminator. It will be mounted in a turret with a stabilized pointing system. In the passive mode, it will function as a low light level television and have a maximum diagonal field of view of 18°. It will be capable of detecting 320 candella deck lights at a range of 21 Km. As the aircraft approaches the ship at approximately 150 meters altitude and a speed of 250 Km/Hr the field of view is reduced to a minimum of 2°. At a slant range of 4 Km, the AGTV is switched to the active mode and at this range small ships (6x18 meters) can be observed. At a slant range of 700 Meters, 30 cm. high letters can be resolved and 15 cm. high are readable at 300 Meters. Because the AGTV is a short range identification sensor, the imagery will be recorded on a video tape and a disc recorder. This will enable the operator to play back the passes on the ship and freeze a frame to identify it. The AGTV will be fully integrated into the AIREYE system. In addition to the active and passive operation, it will have both computer and manual modes for target acquisition and tracking.

Search and Rescue Sensors

Other recent Coast Guard Research and Development projects in the area of Ocean Surveillance have concentrated on improving helicopter search and rescue (SAR) techniques. Present efforts to make Coast Guard helicopters more efficient in the conduct of SAR cases are directed toward development of a Forward Looking InfraRed (FLIR) sensor for the Coast Guard Short Range Recovery (SRR) helicopter, and development of a Wide Area Illumination System

(WAILS) for potential use on all Coast Guard helicopters. The FLIR will have a 30^{o}x40^{o}field of view (FOV) for conducting wide area searches and a 10^{o}x13.3^{o} FOV for searching for smaller objects in a more confined area or for seeing greater detail on a target. The FLIR will operate passively in the 8 to 14 micron range and will be trainable in azimuth and elevation with sufficient thermal sensitivity and resolution to be a very powerful remote sensor for use in all Coast Guard missions.

WAILS is an airborne high pressure sodium vapor arc illumination system with an output of approximately $6.0x10^{5}$ lumens. The system is being designed for use on Coast Guard helicopters to replace point source illumination devices. WAILS will provide illumination of at least 0.2 lux over an area of at least $7.2x10^{5}$ square meters on each side of the helicopter with the helicopter operating at an altitude of 150 meters and with illumination directly under the helicopter to a distance of 0.8 km to each side of the helicopter. The azimuthal beam spread will be at least 80^{o} but not more than 120^{o}. The centerline of the beam in azimuth shall be perpendicular to the axis of the helicopter. By comparison, present point source illumination devices such as short arc xenon lamps illuminate, as a maximum, 55 meter diameter circle whereas WAILS will effectively cover a $14.4x10^{5}$ square meter area. This increased capability for night search will result in a significant reduction in lives and property lost due to more timely search efforts.

Foreign Fishing Vessel Surveillance

With the recent expansion of the Fishery Conservation Zone (FCZ) to include all waters within 200 miles of the U. S. Coast, came the problem of locating and providing positive identification of licensed fishing vessels in U. S. Waters. The problem of electronically "tagging" licensed fishing vessels in order that they can be positively identified without the need of a close visual inspection is a very important one if the Coast Guard is to efficiently patrol the FCZ. A semi-active transponder called the Retro-Directive Array (RDA) shows great promise in being able to act as an electronic license plate aboard licensed vessels, with the expectation that a single RDA issued to each vessel would be compatible with all Coast Guard shipboard and aircraft X-band search radars. The RDA is presently being developed through Calspan Corporation and the Naval Air Development Center and it is expected that a disk only 40 cm in diameter and 4 cm thick will act as a modulated corner reflector providing 360^{o} azimuthal and 40^{o} elevation coverage. The RDA lends itself to remote sensing problems using ships or aircraft because it is an essentially passive device requiring very low power and is capable of receiving any X-band radar pulse, modulating it with an appropriate fixed or tunable code, offsetting it by 20 MHz to avoid loss in sea return, and bounding it back in the direction from which it came. Other potential future uses of such a device include remote sensing of icebergs being tagged and tracked and many other similar tasks.

References

1. Edgerton, A.T., J.J. Bommarito, R.S. Schwantge, and D.C. Meeks. Development of a Prototype Airborne Oil Surveillance System. U.S. Coast Guard report #CG-D-90-75

2. Maurer, A., and A.T. Edgerton, and D.C. Meeks, 1977. U.S. Coast Guard Airborne Oil Surveillance System Status Report. Proceedings 1977 Oil Spill Conference. American Petroleum Institute, Washington, D.C.

Mr. Martin S. Roden

TABLE 1 AOSS II OPERATIONS

DATE	AREA PATROLLED	FLT HOURS DAY	FLT HOURS NIGHT	FLT HOURS TOTAL	MILES FLOWN (NM)	AREA MAPPED (NM)2	ALTITUDE (FT)	SHIPS BOATS DETECTED	OIL SPILLS DETECTED	WEATHER CONDITIONS
5/26/77	Elizabeth City, NC to Dry Tortugas	4.6	2.8	7.4	1110	29,970	2500	342	12	5000 Ft. Overcast 2NM Visibility 2 Ft. Seas
5/27/77	Miami, FLA to Elizabeth City, NC	4.1	-	4.1						Clear to 15NM Calm Seas
6/1/77	Elizabeth City, NC to Key West, FLA	3.7	3.4	7.1	965	26,055		460	2	1 to 5 Miles in Haze 2-3 Ft. Seas
6/2/77	St. Petersburg, FLA to Elizabeth City, NC	3.6	-	3.6	556	15,012				1 to 5 Miles in Haze 2-3 Ft. Seas
	TOTAL	16.0	6.2	22.2	3262	88,074		802	14	

Table 2

HU-25A Characteristics

Length	17 Meters
Wing Span	16 Meters
Height	5.4 Meters
Wing Area	40.5 Sq. Meters
Engines	2 Garrett ATF 3-6
Maximum Take-off Gross Weight	14,500 Kg
Internal Cockpit/Cabin Volume	21 cu. m.
Endurance - Approximately 4 hours at	320 Km/Hr
Dash Speed	670 Km/Hr

Table 3

AIREYE	SLAR	Specifications
Transmitter Power		200 KW peak
Pulse Width		0.2 micro seconds
Pulsed Repetition Frequency	Combined	1500 pulses per sec.
	Each Side	750 pulses per sec.
Frequency		X band
Antenna		8 feet vertically polarized - Yaw stabilized $\pm$ 3°
Azimuthal Beamshape		$\pm$ 1.0° maximum
Elevation Beamshape		CSC2 pattern
Total System Loss		12db

THIS PAGE

WAS INTENTIONALLY

LEFT BLANK

AN ECOLOGICAL APPROACH TO RESOURCES INVENTORY; THE PHOTOMORPHIC ANALYSIS OF A LANDSAT IMAGE OF CENTRAL JAVA

Jean-Paul Malingreau and Priyadi Santoso

University of California/Gadjah Mada University
and Institute of Ecology
Yogyakarta, Indonesia

SUMMARY

The central portion of the island of Java is one of the most densely populated rural area of the Indonesian archipelago. Land and water resources are submitted to intense exploitation and the increasing pressure exerted by a growing population brings along its inevitable land degradation sequels. Very contrasting situations can be found over short distances in terms of resources endowment resulting in a patchwork of agricultural systems ranging from the most productive to the most desolated ones. An increasing concern for exercising more control over environmental processes associated with intense land utilization of that sort has prompted many a resources scientist to search for more appropriate methods of data collection and evaluation. This paper presents an attempt at analyzing a satellite image of Central Java in view of determining the usefulness of the photomorphic approach (McPhail 1971) for an integrated study of the landscape.

The LANDSAT 1 image of October 18, 1977 (E-1067-02145) covering that region presents an intriguing variety of tones and textural patterns. These image characteristics are produced by the combination of soil, rock, vegetation and water reflectance properties. The respective proportion of each of these image forming elements is thought to be an expression of the actual land utilization. Assuming that the image presents an objective integrated view of the land, it follows that the analysis has to be performed on the base of intrinsic "image units" rather than by individual resources related topic. In order to test this level of congruence between the form as seen on the image and the conditions of the land, the photomorphic approach has been adopted.

According to this approach, image units are first delineated on a color composite enlargement (1/500,000). Resources related information is then collected for each of the unit of interest (secondary data and field observations). This information pertains to the geology, physiography, soils, hydrology, climate, land cover and land use, and the settlement patterns of the area. The data are assembled in tables per image units and analyzed in view of determining which element, group of elements or condition of the environment is the major image forming agent. Once this link between the image and the ground features has been established, a more detailed analysis of representative units is conducted for assessing the significance of the 'image unit' entities in terms of resources utilization.

The photomorphic units are found to bring new insights into the complexity of the relationships existing between major environmental factors such as water availability, physiographic setting, soils, and the adopted land utilization pattern. Thanks to the synoptic characteristic of the imagery, it is possible to reference these units in a spatial framework over which significantly variable conditions can be found. Additionally, when watershed boundaries are drawn on the imagery, inferences can be made regarding the potential effects of farming practices as adopted in the defined image units within a whole basin resources management context. The paper also shows how a dry season image of this sort is useful for refining typological criteria of classification and mapping of agro-ecosystems under their various forms.

THIS PAGE

WAS INTENTIONALLY

LEFT BLANK

REMOTE SENSING APPLICATIONS TO WILDLIFE MANAGEMENT IN THE U.S. FISH AND WILDLIFE SERVICE

A. D. MARMELSTEIN

U.S. Fish and Wildlife Service
Washington, D.C.

ABSTRACT

Remote Sensing as a tool in wildlife management can be applied to various aspects of this discipline at the regional/national/international perspective. In the U.S. Fish and Wildlife Service (FWS), aerial and orbital imagery are being utilized in both research and operational modes to address data requirements generated by environmental impact assessment, baseline ecological analysis, and wildlife resource management. As an example of remote sensing applications in each of these categories, this paper will discuss relevant features of the National Wetland Inventory, ecological analysis of the lands under energy related development in the northern Great Plains, and assessment of nesting success of Arctic breeding geese.

INTRODUCTION

The U.S. Fish and Wildlife Service (FWS) serves two principle functions. These are acting as the Federal management authority for migratory species (for example, waterfowl), and providing a central source of ecological expertize and information related to wildlife and their habitats. A growing responsibility of the FWS relates to species identified as Endangered or Threatened by the Federal Government. Much of the data and information with regard to these responsibilities is in respect to the status of populations and the amount, extent and condition of their habitat. Remote Sensing technology has been utilized in many, varied applications to obtain the data upon which management of wildlife resources is predicated. Visable, thermal, and telemetric means have all demonstrated acceptable capability, under given conditions, to monitor populations and related parameters. However, the major, and most reliable, application of this technology involves its use in defining certain parameters pertaining to habitat determination.

Habitat in its ecological or wildlife management context has nearly as many definitions as there are professionals in these two disciplines. Without contributing further to the controversial usage of the term, certain data elements common to most usages of "habitat", and available from remote sensing

techniques, can be identified. These include vegetation (composition, stratification, density, closure, etc.) or other surface features, slope, and aspect. Several derived data elements are also most logically obtained by remote sensing techniques, largely due to the facility with which they can be obtained from the vertical perspective. Included here are such things as edge (length of interface between two vegetative/surface types), interspersion (heterogeniety of vegetative/surface feature types), and distance to nearest cover, water, feed, etc. This paper will discuss use of remote sensing technology in three specific applications under the general category of "Habitat", relating to environmental impact assessment, baseline ecological analysis, and wildlife resource management. Specifically, the analysis of fish and wildlife habitat as a basis for impact assessment and reclamation requirements on the lands subject to energy related development in the northern Great Plains will be discussed. The National Wetland Inventory as an example of ecological baseline analysis will also be discussed. Monitoring of nesting habitat of Arctic breeding geese will demonstrate the use of remote sensing techniques in management of specific wildlife resources.

Appreciation is extended to Dr. H. D. Parker, Dr. H. R. Pywell, and Mr. H. M. Reeves of the U.S. Fish and Wildlife Service for their contributions to, and critical review of, this paper.

Environmental Impact Assessment - Energy Development in the Northern Great Plains

Vast acreages of strip-mineable coal underlie the rolling grassy/scrub vegetation of the northern plains States. Much of this area is under stewardship of the Federal Government. It is also home to some of the last remaining large, highly visible populations of Pronghorn Antelope, as well as other large mammals such as Mule Deer and Elk, and numerous small mammal, reptile and bird species. Disruption to the surface vegetative communities threatens to greatly alter the complex ecosystems which support these populations. The problems faced by land managers begin with the paucity of knowledge of the structure and distribution of faunal habitats. Such knowledge must be obtained before other problems, such as lease withdrawals, population management, and stripped-land reclamation can be faced. FWS is investigating the use of Landsat imagery and multi-scale aerial photography as sources of data to fill, at least partially, the existing information gaps. Data obtained from these sources is useful at several levels of detail (detail in the sense of planes of data, rather than specifics of the imagery; for example, regional versus local).

Digital analysis of Landsat imagery has been utilized to gain a regional perspective of wildlife habitat and land cover in important energy development areas. Neither the spectral (or more conveniently,thematic) nor spatial (actual rather than theoretical) resolution of this data lend themselves to other than regional overview of wildlife habitat. We have found that the diversity of vegetative types, their condition, density and heterogenity preclude detailed analysis from Landsat. The broad spectral bands available simply do not, of themselves, provide sufficient data to reliably separate vegetation into other than broad classes. However, for those areas where even this broad segregation

of classes, and the distribution of such classes, is lacking, Landsat is invaluable for providing regional perspective. This is not inconsistant with the findings of others. On the other hand, Landsat does provide sufficient resolution of bodies of water and cultural land-uses such as agricultural/urban areas to satisfy even detailed levels of analysis.

Using Landsat, we have been able to produce computer classified maps of broad vegetational classes within test sites established as representative of the Western energy lands. Landsat imagery can provide reliable separation of such broad classes as Mixed Broadleaf Riparian, Mesic Grassland, Upland Grassland, etc. The principle value of such information lies in its use in defining areas where more detailed information is required. In other words, Landsat can be utilized to stratify a given area on the basis of broad, vegetatively derived habitat components. For those strata known to be of greater importance, for any of a number of reasons such as vulnerability, rarity, etc., more detailed analysis, based on aerial photographic methods, can be specified.

Conventional color infrared photography, obtained at mid (about 1:30,000) to large (about 1:12,000) scale can be utilized to more specifically delineate habitat units within any given area. When supported by appropriate ground-obtained data, aerial infrared photography has repeatedly shown its utility this application. The problem faced by FWS is not assessing the validity of of this data source, but rather the large geographic areas which require such detailed analysis. In many cases, repeated analysis of multi-data photography appears to be the only practical source of data pertinent to both pre-developmental analysis as well as monitoring of post-developmental impacts and reclamation efforts. Given this requirement, we are undertaking an analysis of digital and digitally assisted interpretation of color infrared aerial photography.

For this purpose, subsets of selected photography of representative environments are being analyzed by conventional, manual techniques for the basic data relevant to habitat analysis. The same subsets of photography, subjected to density slicing, are then provided to the photo-interpreter for analysis. These subsets are also subjected to complete classification by computer following scanner digitization. Results of all three approaches are being compared with respect to both detail and accuracy of data produced, as well as cost-effectiveness (and timeliness) of the analytical technique.

Comparison of the results from manual photo-interpretation and image density analysis with ground truth information were made directly through the use of a composite mapping system and cellularization procedures. A direct cell-by-cell comparison of digital multi-spectral analysis was not performed because of the increased spacial resolution of the digitized photography as compared to the manually generated data. In this case aerial estimates of of the land cover categories were compared with ground truth estimates.

Analogue image density analysis was not found to provide an acceptable technique for extracting land cover information from the CIR frames. The broad-band filters required for the image analyzer resulted in overlapping spectral characters of several habitat/land cover classes.

Results of multi-spectral analysis generally yielded acreage estimates which agreed to within 5 to 20 percent of ground truth estimates. However,

of the 6 frames analyzed one frame yielded an error rate of 50 percent, due to confusion between big sagebrush, xerophytic shrub, ash/forb, and mid-tall grass. The amount of bare soil in each type no doubt contributed to the confusion of spectral signatures. The general impression at this point in our analysis is that the subjective judgment of human interpreters familiar with the area involved remains a critical factor which is difficult, if not impossible, to duplicate with computer assisted analysis.

Baseline Ecological Analysis - The National Wetland Inventory

Wetlands are among the most ecologically diverse of environments; as the interface between the terrestrial and aquatic/marine provinces, they are also among the most biologically productive. More ominously, they are among the most highly desired physical sites for recreational/industrial development. Consequently, wetland environments, while supporting large populations of fish and wildlife species, and serving as the most crucial habitat components for many of these species, have been converted (or "developed") at an alarming rate. Such conversion to recreational communities, and commercial/industrial harbors and facilities generally, if not invariably, results in a near sterile environment of little or no value to the once diverse community of fish and wildlife the area supported.

Recognizing the biological importance of wetlands, their diverse nature, their rate of exploitation, and the relative lack of knowledge concerning the abundance and distribution of this national resource, the United States Congress has mandated the FWS to inventory and map the wetlands of our country. To do so, innovative technology has been brought to bear on the incorporation of aerial photographic data into thematic wetland maps.

The National Wetland Inventory (NWI) has been designed, and is being executed to meet a wide variety of needs, and a large community of users, at the regional and national perspective. Its goals, objectives, and procedures have been described elsewhere (Montanari and Wilen, 1977) and will not be repeated here. This discussion will treat of the techniques being utilized by the NWI to produce medium (1:100,000) scale maps and a digital data base using existing mid (1:60,000) to small (1:130,000) scale photography.

Due to the nature of wetland environments, their diversity and complexity, as well as the geographic extent of their occurrence, it was recognized early on that stereo interpretation of aerial photography, supported by ground obtained confirmational data, would provide the most effective and reliable source for basic vegetative delineation of wetlands. The problem faced by NWI was the almost universally identified requirement for thematically detailed and accurate maps as a principle product of the inventory. Classically available techniques for transcribing interpreted data from photographs to available topographic maps - by other than photogrammetric means - invariably entrained inaccuracies unacceptable to NWI, especially in view of the additional requirement to produce a digital map base, available for compositing with other digital map bases. By contrast, available photogrammetric means, coupled with subsequent digitisation, were both too costly and too time and manpower intensive. To solve this impasse, development of a digital technology to proceed directly from interpreted stereophotography into a rectified and orthogonally correct computerized map base was undertaken.

This digital technology, subsequently named WAMS (Wetland Analytical Mapping System), is described in detail in a recently presented paper (Niedzwiadek, Greve and Pywell, 1978). What follows is a brief synopsis of this system. WAMS is composed of three subsystems, as follows:

Triangulation Subsystem - using available or obtained, map or geodetic control, camera calibration parameters, and the relevant stereo-pair of photography, an algorithm providing rectification and orthogonal correction is computed for any given pair of stereo-photographs.

Digitizing Subsystem - using the previously generated correction algorithm, the stereo-pair (having undergone separate interpretation and delineation of wetland types) is processed to reduce the intepreted data to a rectified, orthogonally correct digital map.

Data Base Subsystem - having generated a digital map, this subsystem performs the ordering and storing of each data set according to a specific reference system.

The cornerstone of the WAMS is an instrument entitled APPS (Analytical Photogrammetric Positioning System), a stereo comparator which determines photocoordinates relative to the plane of the instrument to within 10 micron accuracy. The APPS presents the operator with a floating dot which, when placed in the apparent ground plane of the stereo image, calibrates the instrument to the stereo-pair. Known photo identifiable points are utilized as control points to generate the correction algorithm for that stereo-pair. The floating dot is then utilized as the stylus in either point or continuous mode to generate the arc-segments of the digital map base. The associated software rectifies and orthogonally corrects each arc-segment, converting it from photo-base to geodetic (or map) base. In this manner an accurate wetland map base is prepared in digital form. At any later time these maps can be plotted to map accuracy on an available map base of choice.

Wildlife Resource Management - Monitoring Habitat Condition and Nesting Success of Arctic Breeding Geese

The FWS is mandated by Congress as the primary management agency for migratory waterfowl. Each September, the Service issues regulations governing the daily and seasonal limits, times and lengths of seasons, harvest quotas, and other limitations for hunters of waterfowl in each of the major Flyways. For Arctic nesting geese, of which some 80% of the annual harvest occurs in the U.S., these regulations are largely predicated on population status and on nesting success the previous Spring. The principle environmental determinant of nesting success each year is rate of snow and ice disappearance from the Arctic nesting grounds. The nesting season is very short; lack of nesting sites within a critical two to three week period results in absence of nesting for the season. Unlike ducks breeding further south, there is no opportunity for renesting if the first attempt is unsuccessful. Inadequate knowledge concerning breeding success in past years has resulted in both underestimates and overestimates of fall flight. The latter circumstance has created population crises for some species when hunting was not adequately restricted, resulting in highly restricted or closed seasons in following years. Use of Landsat-MSS

and NOAA-VHRR imagery to assess snow and ice conditions in nesting areas has greatly increased the accuracy of fall flight forcasts. These applications have been discussed in detail in previous papers (Reeves, Cooch and Munro, 1976; and Reeves, Munro and Marmelstein, 1975).

Neither the Landsat-MSS nor the NOAA VHRR provide sufficient resolution to allow direct assessment of specific nesting sites. However, geese frequently use the same areas year after year and often concentrate their nests in colonies. Given knowledge of the location of nesting areas or colonies, the satellite imagery can be interpreted to gain a general understanding of snow and ice disappearance from these traditional nesting areas. For example, much of the lowlands of Hudson's Bay and James Bay are recognized to be goose nesting habitat. Suitability of that habitat in any given season is determined by recession of snow cover from the lowlands. Both the VHRR and MSS solar IR band are excellent for this purpose. Satellite imagery thus allows examination of habitat conditions over wide, inaccessible areas which cannot be economically visited on the ground or observed in a timely manner from aircraft.

At present, the principle limitation on the use of VHRR and MSS data is the suseptibility of both sources to cloud cover interference. Neither imaging system has any real capability to penetrate cloud cover. Unfortunately, at the season in question, cloud cover is a frequent attribute. In order to counter this detriment, FWS is initiating an experiment in cooperation with NASA to determine the feasibility of utilizing an imaging radar system to perform the necessary ice and snow assessment on the Arctic breeding grounds. The instrument of choice will be the L-band synthetic aperture radar (SAR) to be carried by SEASAT-A. This satellite system is due for launch in May 1978. Pending orbital insertion and instrument verification, imagery of selected, known nesting sites will be obtained during the 1978 or 1979 breeding season. The high resolution (25 meter), essentially all-weather SAR imagery will be compared to the now conventional VHRR and MSS data to determine its utility in habitat asessment. As in the past, this information, when combined with supporting information such as disribution of populations among available nesting areas, breeding behavior, breeding population size, age structure, and migration affinities of fall flights into various flyways and harvest areas, etc., will be used for developing the annual harvest regulations.

REFERENCES

Montanari, J. H. and B. O. Wilen. 1977. Techniques Developed and Presently Being Used to Conduct the National Wetland Inventory. In Proceedings of the National Wetland Protection Symposium.

Niedzwiadek, H. A., C. W. Greve, and H. R. Pywell. 1978. The Wetlands Analytical Mapping System. In Proceedings of the Annual Convention, American Society of Photogrammetry, Washington, D.C.

Reeves, H. M., F. G. Cooch, and R. E. Munro. 1976. Monitoring Arctic Habitat and Goose Production by Satellite Imagery. Journal of Wildlife Management, 40: 532-541.

Reeves, H. M., R. E. Munro, and A. D. Marmelstein. 1975. USFW Activities in Application of Satellite Imagery to Goose Management. Workshop on Remote Sensing of Wildlife, Quebec. J. D. Heyland, ed.

THIS PAGE

WAS INTENTIONALLY

LEFT BLANK

EXPERIMENT TO EVOLVE METHODS FOR SEPARATION AND IDENTIFICATION OF AGRICULTURAL CROPS FROM MULTISPECTRAL INFORMATION

R.S. Ayyangar

National Remote Sensing Agency
No. 4, Sardar Patel Road,
Secunderabad 500 003
INDIA

ABSTRACT

Spectral separation and identification of crop species and their growth stages was studied under Indian Agricultural system from the multispectral data of airborne multispectral scanner with the aid of highly interactive computer system. The results indicated that by careful consideration of multispectral responses of the crops with respect to variation in growth, it is possible to identify crop species and their growth stages. Attempt made to select best channel combination of the eleven band information to obtain maximum separation and accurate identification of crops in computer analysis is also discussed.

1. INTRODUCTION

In recent years, satellite remote sensing has been reported to be successful for agricultural resources inventory (Mercanti, 1973) and techniques have also been developed to identify and estimate cropland acreage to approach or exceed the 90 percent accuracy level for major crops in many areas (Bauer and Cipra, 1973 ,Baumgardner et al, 1973, and Carlson and Aspiazu, 1975). However, the techniques so far developed for satellite remote sensing of agriculture are not free from constraints and very often meet with some challenging situations. For example, Indian Agriculture characterised by small cultivated fields and farm holding (on the average around 5.7 acres), multiple cropping, variation in farming practices etc., poses a challenge to satellite remote sensing because of spatial resolution. Nevertheless, attempts are being made to develop a suitable remote sensing technique appropriate to the needs of Indian agriculture.

Aerial photography (Panchromatic and infra-red), as one of possible remote sensing techniques has been attempted in recent years to evaluate Indian agricultural resources. The results obtained were though encouraging, the data analysis is slow and laborious as the aerial photography involves visual interpretation. Further, analysis of results of similar nature of work has led to the conclusions that attempts to differentiate crop types solely on the basis of tone or colour in broad spectral bands of the 0.4 to 0.9 um wave length region may not be particularly successful (Colwell, 1972). Other identifying parameters, or perhaps different or narrow spectral bands, appear to be necessary. In this context, multispectral scanners score over aerial photography

Multispectral scanners are capable of collecting spectral information on narrower bands in various regions of electromagnetic spectrum(ultra violet, visible, and reflected and thermal IR) and the data obtained can be analysed rapidly with the aid of a suitable computer. Computer processing of multispectral scanner data for identification of agricultural crops has been attempted in USA by LARS(1968) , Marshall et al (1969), and Nalepka(1970), In India, however, reports on such types of attempts are yet to be published.

Considering the potential of multispectral data collection and data analysis, it appears that airborne multispectral scanners may prove useful in solving some of the constraints imposed on remote sensing of Indian agriculture. This paper, attempts to discuss the separation and identification of agricultural crops from the spectral data of airborne multispectral scanner with the aid of highly interactive computer system.

2. METHODOLOGY

2.1 EXPERIMENTAL SITE AND CROPS

The experiment was conducted in southern part of India during the major cropping season (June-December) of 1977. The crop species mainly comprised sugarcane (Saccharum officinarum), Rice (Oryza Sativa) and patches of finger millets (Elucine coracana) scattered around the area. The crop existed in various stages of growth at the time of collection of spectral information because of variation in planting time. For instance, growth stages of rice crop varied from freshly planted rice to booting stages. Similarly, sugarcane from planting to maturity stage, in addition to ratoon sugarcane.

2.2 SPECTRAL INFORMATION

An eleven channel, Bendix Modular Multiband Scanner(M^2S) was used for collecting the digital multispectral information. The eleven spectral band data were collected and recorded, ten in visible and reflected near infra-red portion of the spectrum and one in the thermal infrared region. The spectral regions covered by M^2S used in the experiment are presented in Table I. The spectral information was collected and recorded on High density digital tape (HDDT) on a clear sunny day from an altitude of 1000 meters above ground level in the last week of September, 1977. The air borne spectral data was simultaneously supported by ground truth information.

2.3 GROUND TRUTH

The ground truth information included both visual and biological parameters consisting of condition of the field, nature of crop (crop species, growth stage, height, color, etc)., and other relevant information which would aid interpretation.

2.4 DATA ANALYSIS

The spectral information recorded on HDDT was converted into computer compatible tape format (CCT) with the help of the Bendix Multispectral Data Analysis System(MDAS). The MDAS, an interactive data processing system for analysing earth resources multispectral data, is designed to accept data from both satellite and airborne multispectral scanners for processing.

For analysis, the CCT containing raw spectral data was displayed on a color moving window (MW) of MDAS and the area, from where the training sets for training the computer for identifying spectral classes were selected based on the ground truth information. In general, each training set represented a single class. However, in some cases, more than one training set was used to represent a class. Thus, computer was trained interactively by the investigator to derive a set of optimum processing coefficient to be used by multivariate normal or maximum likelihood algorithum to process the data into categorized tapes from which symbolized output was generated using Gould Printer/Plotter based on PDP 11/04 computer system.

The data was also analysed in various channel combinations using the same training sets and classes to arrive at the best combination of channels to distinguish spectral classes.

3. RESULTS AND DISCUSSION

Crop identification has long been recognised as one of the potential applications of remote sensing. Infact, accurate identification of crop species is a prerequisite to derive at crop production estimates. This information is of substantial value to a developing country like India for efficient management of the agricultural resources.

Identification of crop species from remotely sensed spectral information is feasible if adequate ground truth and suitable computer processing system are available. The data presented in Figures 1,2,3 and 4 are the results obtained from the analysis of airborne scanner data on an interactive computer system with the support of ground truth.

Spectrally, 23 separable classes of agricultural importance have been identified. For the purpose of clarity in illustration, some of the common classes were merged into one single class. For example, water classes, rice classes and sugarcane classes were merged into one single class as Water, Rice (2-5) and sugarcane respectively (Fig. 1,2,3 and 4) . However, Rice-1 was treated as separate class from other rice classes (Fig. 1) as the spectral signature of rice-1 was not clearly distinguishable from weed class (Water Hyacinth). In such instances, temporal data or inclusion of thermal information in the multispectral analysis may prove useful. Nevertheless, in this case, it was possible to interpret rice-1 from Weed because of circumstantial evidences such as location and other surrounding features.

Matured sugarcane crop around the experimental site is normally harvested in the month of July and the harvesting continues until end of March or April at regular intervals to supply sugarcane to the nearby sugar factory. The cut crop is allowed to grow again for one or more seasons with proper management and such crops are referred to as sugarcane ratoon. The ratoon crop initially is erratic in growth due to variation in cultural practices and environmental factors but with proper management, after three or four months it may attain uniform growth. Since the spectral information in this experiment was collected in the month of September, spectrally separable sugarcane harvested (July, August and September) classes could be identified (Fig. 1). In addition, fields which exhibit mixture of spectral signatures of all the three sugarcane harvested classes were also noticed indicating the variability of sugarcane ratoon crop (in set in Fig. 1,2,3 and 4).

Agriculture is highly dynamic in nature because of constant physiological changes in crop plants with time. As a result, the spectral responses can vary throughout the growing season. By careful consideration of multispectral data, this can be utilised effectively to aid identification of crops and their growth stages. Fig. 3 and 4 illustrate such type of observations.

Rice fields were transplanted around the experimental area in the middle of July and continued upto the end of September. The variation in planting time has resulted in difference in growth stages of rice plant, ranging from active tillering stage to booting stage. In figure 3, five rice classes which were spectrally separable are shown. Each class represents a stage of rice growth. Rice-1, at booting, Rice-2, at maximum tillering, Rice-3, at mid tillering, Rice-4, at active tillering and Rice-5, at initial stage of active tillering. The above classes of rice, based on growth stages, are clearly noticeable in Fig.3 in places where the plant growth was uniform. However, due to variation in plant growth, in some areas, mixture of spectral signature of rice classes can also be observed. The growth variation, especially during the tillering stage of rice plant is attributed to soil fertility differences, cultural and environmental factors.

Similar to rice classes, based on plant growth, spectrally identifiable sugarcane growth stages are presented in Fig.4. Four stages of sugarcane could be recognised in addition to harvested sugarcane fields. Sugarcane-1 represents a crop of 7 months old, sugarcane-2, 5 months old, Sugarcane-3, 3 months old and Sugarcane-4, 2-2½ months old.

Identification of crop growth stages and growth variation is important in yield prediction and forecast. Growth stage would indicate the time at which crop would be ready for harvest which is essential for planning harvest operations, marketing, storage, etc., Irregularities of development stages (two or more spectral classes indicative of different growth stages) observed in some fields (fig. 3 and 4) reveal uneven crop growth condition as a result of poor crop management. While predicting yield, enough care should be exercised to take into consideration such irregularities of growth.

As discussed earlier, multispectral scanner collects spectral information on all eleven channels (Bands). Thus, offers scope for choice of channel or band combination in the computer data analysis to achieve accurate spectral identification of classes with minimum channel combination. Although, it is not impossible to use all the eleven channel information in the computer analysis to distinguish spectral classes, cost of analysis would increase proportionately with the increased number of channels. Therefore, attempts were made to select best combination of channels to achieve maximum spectral separation and accurate identification of classes. Preliminary attempts in this direction indicated that maximum separation of spectral classes to an accuracy level of 95 Percent could be achieved with combination of five M S channels(Bands). The five channels considered in the study were, 3,4,6,8 and 9 with respective peak wave length 0.515μ , 0.560 μ, 0.640 μ, 0.720 μ and 0.815 μ. To confirm these observations and to study the effect of further reduction in number of channels on the accuracy of spectral identification of classes, computer classification with four channel combination 3,4,6 and 9 (0.515μ , 0.560 μ, 0.640 μ , and 0.815μ) and 3 channel combination 4,6 and 9 (0.560μ , 0.640μ , and 0.815μ) were compared with five channel (3,4,6,8 and 9) combination. The data presented in Fig. 1 and 2 are the results of analysis of five band combination and three band combination respectively.

Comparison of Fig. 1 and Fig. 2 would clearly indicate that classification obtained with five bands is better than that of classification obtained with three band combination. With five band combination, identification accuracy to an extent of 95 percent could be achieved and the delineation of spectral classes were clear. With three band analysis, misclassification seems to be increasing indicating that three band combination may prove useful for general categorization. However, when more details are required about a class, as illustrated by the Rice classes based on growth stages (Fig. 3) , more than three bands may be needed. The four band combination of analysis (channels 3,4,6 and 9) , not presented in this paper fully supports this observation and it stands between five band combination and three band combination in computer analysis of classes.

4. CONCLUSIONS

Identification of crop species from remotely sensed multispectral information is possible if adequate ground truth and suitable computer system are available under Indian agricultural system.

Dynamic nature of agriculture resulting in variation of spectral responses of crops throughout the growing season can be taken to advantage by careful consideration of multispectral data to aid identification of crops and their growth stages.

Multispectral scanners offer scope for choice for channel or band combination in the computer analysis to achieve accurate spectral identification of classes with minimum band combination. Spectral information from atleast, three bands may be required for broad identification of categories.

ACKNOWLEDGEMENT

The author wishes to express his appreciation to the National Remote Sensing Agency, (NRSA) Secunderabad, India, for providing facilities during the conduct of the experiment. Special acknowledgement is made to Wg.Cdr. K.R. Rao, Director, NRSA for his constant encouragement and support during the study. The author also wishes to thank Scientists, Engineers and Technicians of various departments of NRSA for their technical assistance

REFERENCES

1. Bauer, M.E., and Cipra, J.E., 1973. Identification of agricultural crops by computer processing of ERTS MSS data. Proc. Symp. Significant results obtained Earth Resources Technol. Satellite-1, 1973 NASA SP- 327, PP. 205-212.

2. Baumgardner, M.F., and Henderson, J.A. and LARS staff, 1973. Mapping soils, crops and range lands by machine analysis of multi-temporal ERTS-1 data.Proc. Earth Resources Technol. Satellite Symp. 3rd,1973 NASA SP-351, PP. 205-224

3. Colwell, J.E., 1972. Use of Remote Sensing in the inventory of agricultural crops. The University of Michigan, Willow Run Laboratories.

4. LARS, 1965 Laboratory for Agricultural Remote Sensing, Purdue University, Annual Report, Vol. 3, 1968.

5. Marshall, R.E., Thomson, N.S., Thomson, F., and Kriegler,F., 1969. Use of Multispectral recognition techniques for conducting rapid, wide wheat surveys. Proc. Sixth International Symposium on Remote Sensing of Environment, University of Michigan.

6. Mercanti, E.P., 1973, ERTS-1 Teaching us a new way to see. Special report on ERTS-1 Experiments, Astronautic and Aeronautics, September, 1973. PP. 36-63.

7. Nalepka, R., 1970. Investigation of multispectral discrimination techniques, University of Michigan, Willow run Laboratories, Final Report, 2264-12-1.

TABLE I SPECTRAL REGIONS OF ELEVEN CHANNEL MULTISPECTRAL SCANNER

Visible Channel (Band)	Wave length (μ)	
	Center	Band Width
1	0.410	0.060
2	0.465	0.050
3	0.515	0.050
4	0.560	0.040
5	0.600	0.040
6	0.640	0.040
7	0.680	0.040
8	0.720	0.040
9	0.815	0.090
10	1.015	0.090
Thermal channel(Band)		
11	11.0	2.5

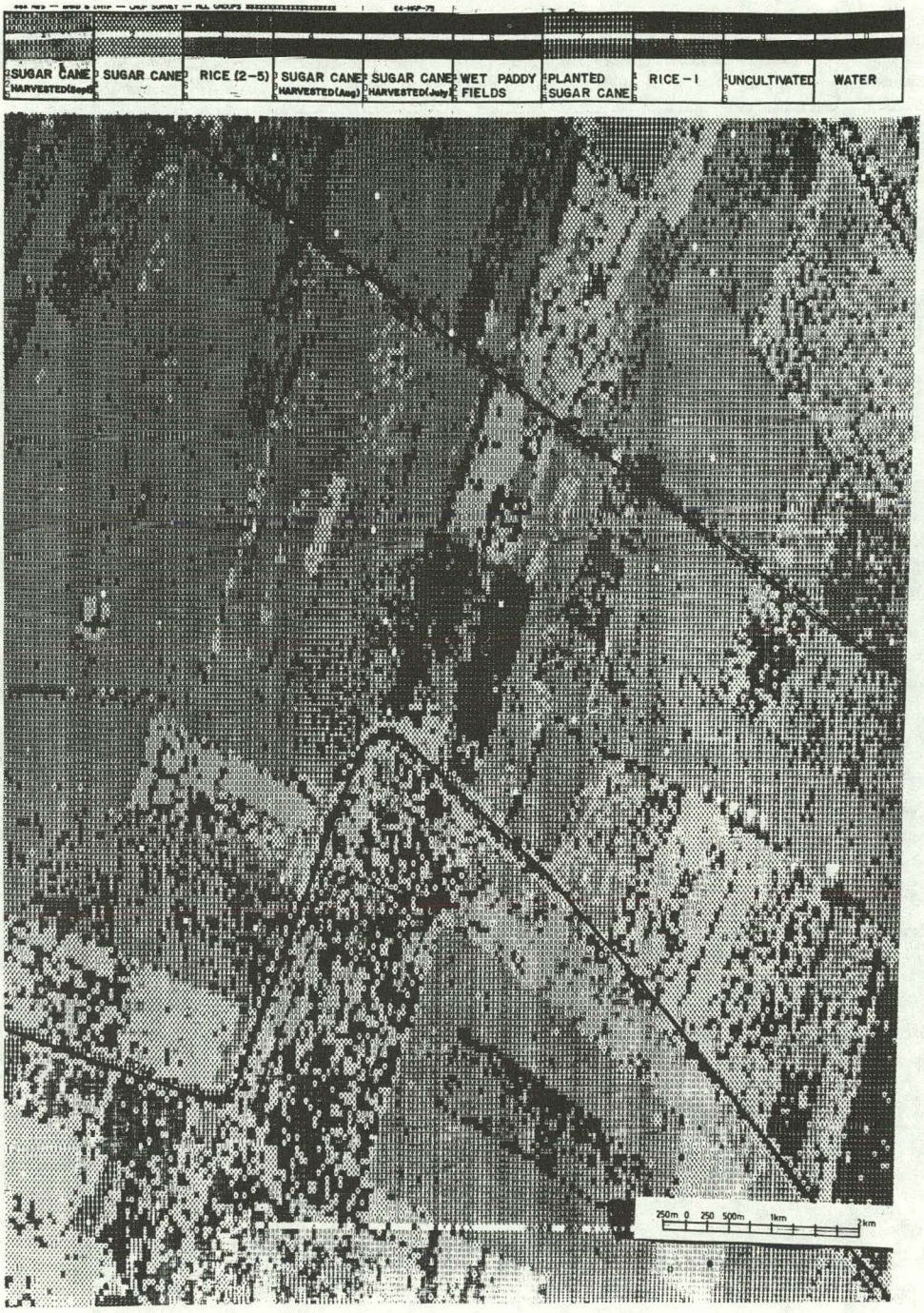

FIGURE 1. COMPUTER CLASSIFIED, GOULD 5100 PRINTER/PLOTTER GENERATED OUTPUT SHOWING SOME IMPORTANT AGRICULTURAL CATEGORIES OBTAINED WITH FIVE BAND (3,4,6,8 and 9) COMBINATION OF M^2S.

FIGURE 2. COMPUTER CLASSIFIED, GOULD 5100 PRINTER/PLOTTER GENERATED OUTPUT SHOWING SOME IMPORTANT AGRICULTURAL CATEGORIES OBTAINED WITH 3 BAND (4,6, and 9) COMBINATION OF M2S.

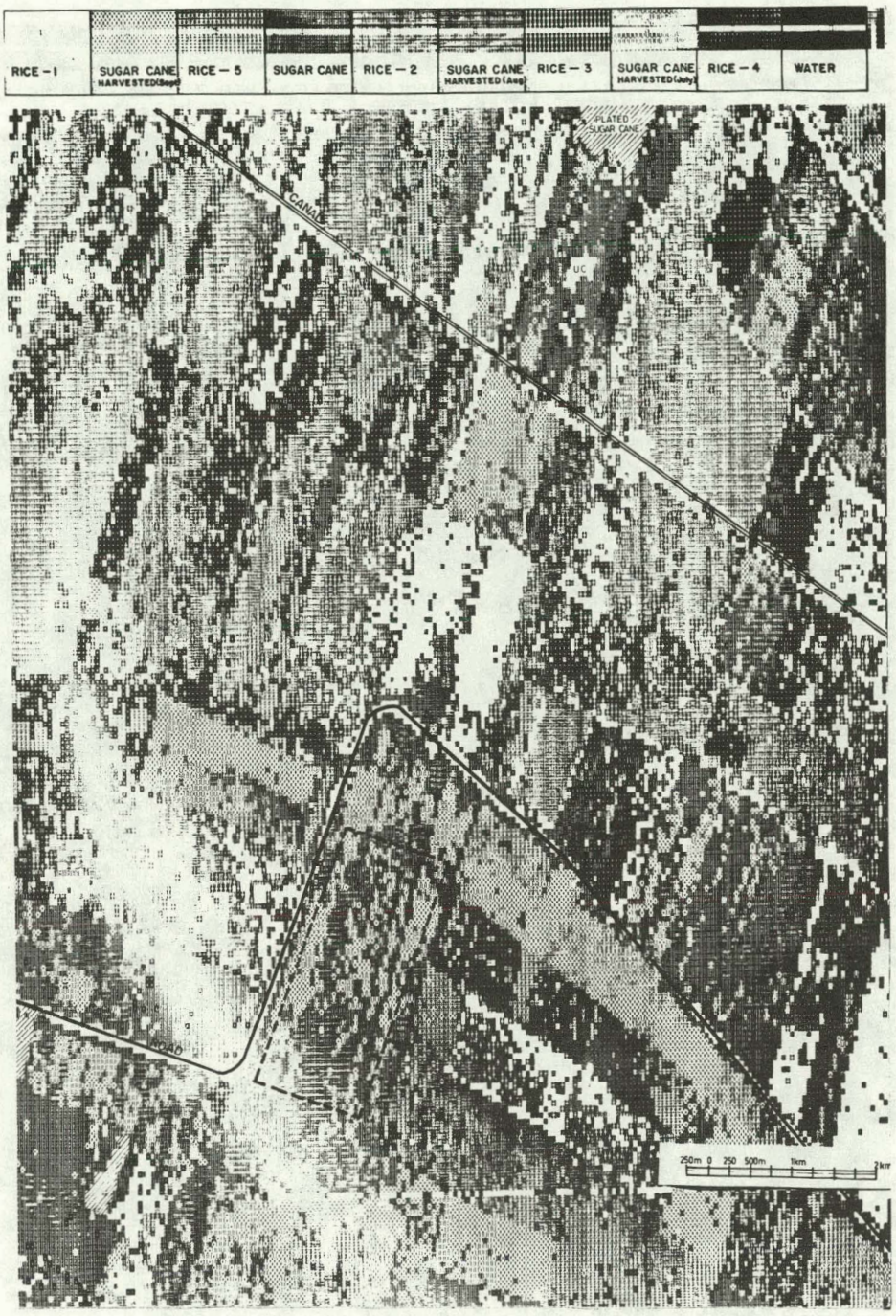

FIGURE 3. COMPUTER CLASSIFIED, OUTPUT SHOWING RICE CLASSES BASED ON GROWTH STAGES OBTAINED WITH FIVE BAND (3,4,6,8 and 9) COMBINATION OF M2S
Rice-1, at Botting. Rice-2, at Maximum tillering. Rice-3, at Mid tillering. Rice-4, at active tillering. Rice-5, at initial stage of active tillering.

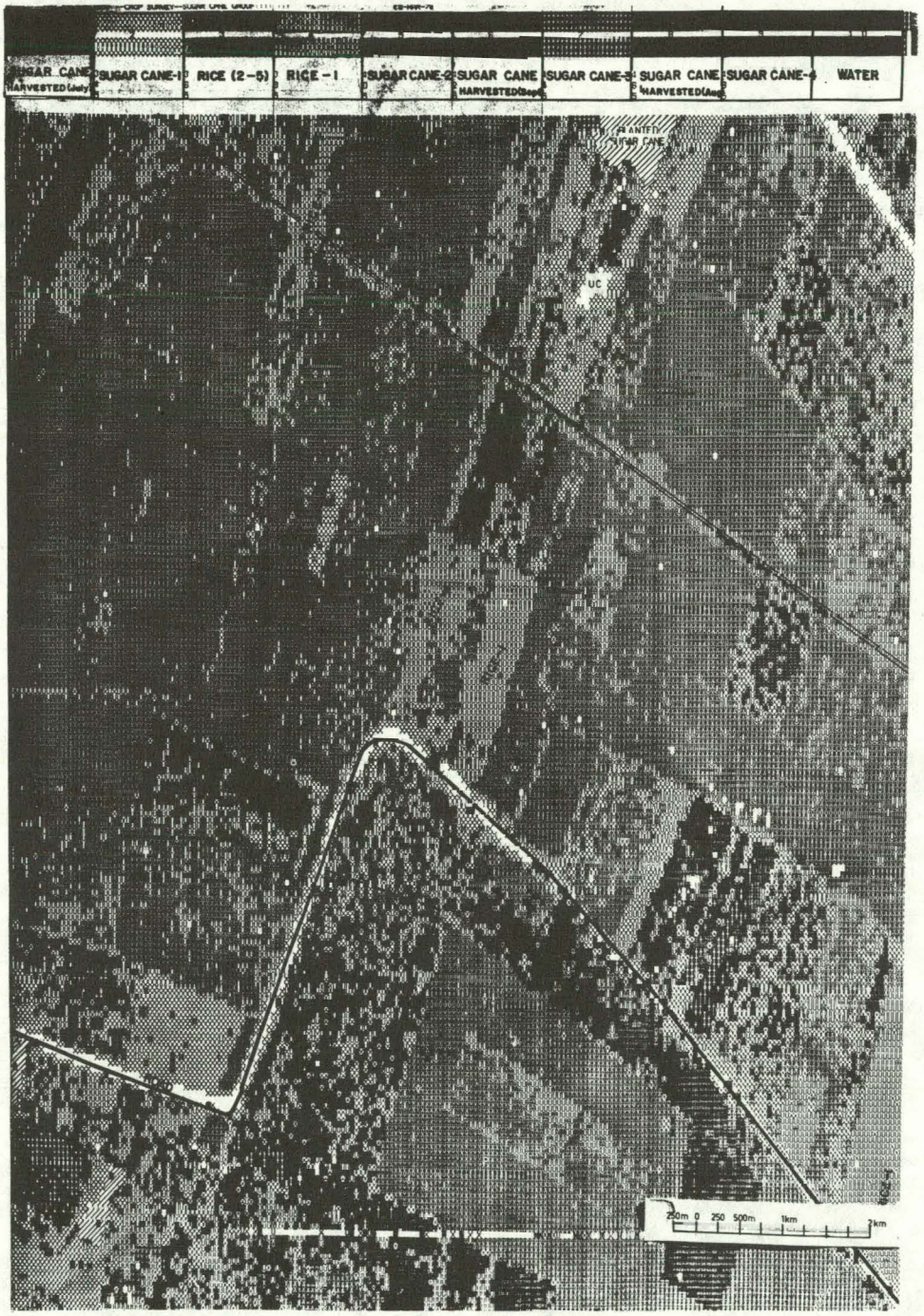

FIGURE 4. COMPUTER CLASSIFIED, OUTPUT SHOWING SUGARCANE CLASSES BASED ON GROWTH STAGES OBTAINED WITH FIVE BAND (3,4,6,8 and 9) COMBINATION OF M2S.
Sugarcane-1, 7 months old, Sugarcane-2, 5 months old.
Sugarcane-3, 3 months old. Sugarcane-4, 2-2½ months old.

DETERMINATION OF SPECTRAL SIGNATURES OF VEGETATED SURFACES BY RADIOMETRIC GROUND MEASUREMENTS

Werner Fischer

Institut für physikalische Weltraumforschung
der Fraunhofer-Gesellschaft
Heidenhofstr. 8, D-7800 Freiburg i. Br.
Fed. Rep. of Germany

ABSTRACT

Spectroradiometric measurements with narrow bandwidth were made in the wavelength range from 400 to 1100 nm. The dependence of the spectral reflectance factor $R(\lambda)$ on solar and observational zenith and azimuth angles for young and ripe wheat, vine, spruce and feeding turnips was investigated. As a result it was found, that the shape of the $R(\lambda)$-curve of young wheat in contrast to ripe wheat depends strongly on the measuring geometry.

1. INTRODUCTION

In the frame of the first German Remote Sensing Program we carried out in 1976 in collaboration with Prof. Hildebrandt (University of Freiburg) ground measurements of selected agricultural and forest canopies, in order to determine their spectral reflectance factor |1,2| in the wavelength range from 400 to 1100 nm. Simultaneously aircraft measurements using a multispectral scanner (M^2S) were also made by the Deutsche Forschungs- und Versuchsanstalt für Luft- und Raumfahrt (DFVLR Oberpfaffenhofen), for which we supplied partially the ground truth in the Freiburg test site. In 1977 systematic ground measurements were continued, in order to study the dependence of the spectral signatures on the geometrical parameters (solar and observational zenith and azimuth angles).

By means of precise spectroradiometric measurements we intend to investigate the possibility to detect previsual vegetation damages or diseases. Requirement for that is the reliable knowledge of the spectral signatures of healthy plants. The spectral reflectance factor often depends differently according to the kind of plant and their canopy on the measuring geometry. Therefore the study of these dependences for some selected species is carried out at the beginning of our investigations. KRIEBEL |3,4|, for instance, measured such angular dependences for other species.

In Europe with its small areas of homogeneous vegetation, aircraft scanner recordings with a scanning angle of $\pm 50^{\circ}$ are of great importance. Ground truth with this scanning range is therefore necessary.

As one is not certain, whether it is sufficient to consider only small wavelength intervals, we scan continuously the visible and near infrared spectrum with a narrow band width. By means of such data it will be possible to optimize

positioning (pitch) and widths of the spectral bands for multispectral scanners. It is known that the optimal values will vary from application to application.

2. EQUIPMENT

We utilized a high sensitivity spectroradiometer (EG & G Mod. 585) modified by a remotely controlled filter wheel. The instrument has a sharply limited and uniformly weighted field of view of 10°. In the monochromator two interchangeable gratings allow the wavelength ranges from 400 to 850 nm and from 700 to 1100 nm to be scanned continuously with a band width of 5 and 10 nm, respectively. However, other band widths can be adjusted. The detector head contains a highly sensitive photomultiplier, which is kept at $-20^{\circ}C$ by thermoelectric cooling.

The instrument is mounted during the measurements at the end of the 18 m long jib (Fig. 1), which is fixed to the trailer of our campaign vehicle. This arrangement provides a maximum field of view of 3 m diameter. The jib can be turned about two horizontal axes (Fig. 2). In the first measuring mode it is turned perpendicular to the vehicle's direction. Then one can measure at different zenith angles (e.g. 0°, 15°, 30°, 45°) and two fixed azimuth angles having 180° difference, without a shift in the observed spot. In the second measuring mode the jib is inclined at about 45° in a plane parallel to the vehicle's direction. Then it is possible to turn the radiometer (with constant observational zenith angle, e.g. 30°) about a vertical axis, so that the radiometer's optical axis scans through all azimuth angles (360°). In this case naturally the radiometer does not point at the same spot.

For measuring the hemispherical irradiation from the sky and the sun we utilize a specially developed integrating sphere instead of a reference panel, which is commonly used. This has the following advantages: better observance of the cosine-law; less sensitivity to dust; convenient and quick handling (bajonet coupling).

The method of measurement and further details are given elsewhere [5,6].

3. RESULTS

A preliminary evaluation of some of our measurements, carried out in 1977, and one measurement of 1976 led to the following results:

Wheat
27 May 1977 (Fig. 3,4,5):

On this day the observed wheat field of practically homogeneous growth had only green leaves of about 15 cm height. Accordingly the curve of the spectral reflectance factor $R(\lambda)$ has the shape, which is typical of green plants (Fig.3): first maximum at 550 nm (green), minimum at 675 nm (red), spectacular increase between 700 and 750 nm. For this young wheat R(800) is more than ten times greater than R(550).

Fig. 4 shows at three selected wavelengths the variation of R due to different observational zenith angles (θ_r). The azimuth difference ($\Delta\phi$) between the direction of observation and the sun is near 0° and 180°, respectively. The solar zenith angle (θ_i) is small and practically constant. R(800), which is representative of the near IR plateau until 1100 nm, has almost the same value for $\theta_r = 30^{\circ}$ and 45° at both azimuths. Only for $\theta_r = 0^{\circ}$ (vertical) and to some extent for $\theta_r = 15^{\circ}$ there exists a small decrease down to the 50 %-line due to greater portions of shadow and soil in the field of view.

In contrast to R(800), R(550) and especially R(675) show a great difference between $\Delta\phi \simeq 0^{\circ}$ and $\Delta\phi \simeq 180^{\circ}$. For the range near $\theta_r = 30^{\circ}$ ($\Delta\phi \simeq 0^{\circ}$) with $\theta_i = 28^{\circ}$ a retroreflection effect occurs, obviously due to the orientation of the leaves, whose inclination is about 60° to the vertical. In Fig. 5, at the same three wavelengths the variation of R due to different observational azimuths ϕ_r (from North-East to South-West) is shown. The observational zenith

angle is kept at $\theta_r = 30^o$ (const.). The changes in solar angles θ_i and ϕ_i are only moderate. (Pay attention to the different scales in comparing Fig 5 with Fig. 4) R(800) is fluctuating only between 42 % and 55 %. However, between $\Delta\phi \simeq 0^o$ ($\phi_r = 45^o$) and $\Delta\phi \simeq 180^o$ ($\phi_r = -135^o$) R(675) shows a dynamic range of 3.5.

According to Fig. 4 and 5 it is obvious, that the shape of R(λ)-curves (Fig. 3) for young wheat depends strongly on the measuring geometry.

3 Aug. 1977 (Fig. 3,6):

The same wheat field was now equally yellow (shortly before the harvest). R(λ) has changed significantly since the end of May. The measuring geometry remained practically the same (Fig. 3).

Fig. 6 shows at the three wavelengths the variation of R due to different observational zenith angles (compare Fig. 4). The solar zenith angle and the azimuth difference during the measurements were almost the same like in May. However, R(550) and R(675), when exactly normalized, would practically merge with the R(800)-line. In this case the shape of the R(λ)-curve (Fig. 3) does not depend on θ_r. Between $\theta_r = 0^o$ and $\theta_r = 45^o$ ($\Delta\phi \simeq 180^o$) R(800) has a maximum fluctuation of only $\pm$ 1 % (abs.) or $\pm$ 6 % (rel.) around the 0^o-value, i.e. the ripe wheat field in this angular range is a quasi-Lambertian surface.

Additionally six vertical measurements ($\theta_r = 0^o$) were carried out in course of three hours (symmetrical to the solar culmination), when θ_i and ϕ_i changed from 30.5 to 37^o and from -36^o to 44^o, respectively (no Figure). Within this time R(800) had a maximum fluctuation of only $\pm$ 0.5 % (abs.) or $\pm$ 3 % (rel.).

Vine
12 and 28 Sep. 1977 (Fig. 7,8,14):

The rows of vine were oriented to (almost) South-East ($\phi = -50^o$) in a horizontal terrain. Since the measurements in the two different wavelength ranges were made on different days, the corresponding curves are shown separately in Fig.7. With $\phi_i = 40^o$ (≃ South-West) the sun ($\theta_i \simeq 57^o$) was shining perpendicular to the rows, i.e. small variations of ϕ_i in this range did not lead to great changes of the shadow and soil portions in the field of view.

In Fig. 8 at the three wavelengths R shows a strong dependence on θ_r. The variation of R(800) on the shadow side ($\Delta\phi \simeq 150^o$) is relatively small compared with R(550) and R(675). Inversely, on the illuminated side ($\Delta\phi \simeq 40^o$) R(800) has the larger increase.

Fig. 14 shows for vertical observation ($\phi_r = 0^o$) the dependence of R(800) and R(970) on θ_i, which varies from 44^o to 62^o. In the range, where the influence of ϕ_i-variations is small (ϕ_i near 40^o, see above), R(800) and R(970) have a similar and almost constant gradient with increasing θ_i.

Spruce
2 June 1977/Bärental (Fig. 9,10,11,15):

The measurements were carried out at the border of a rather homogeneous spruce forest (Fig. 1). The trees had a height of about 10 m and showed light-green sprouts at the ends of the branches. The R(λ)-curve (Fig. 9) has a similar shape like that of green leave plants. But it has lower values.

In Fig. 10 R shows for all the three wavelengths almost the same dependence on θ_r. At θ_i between 29^o and 43^o, the shadow portion for $\theta_r = 30^o$ and 45^o ($\Delta\phi \simeq 140^o$) is relatively large.

Fig. 15 shows the similar dependence of R(550), R(675) and R(800) on θ_i for vertical observation. The gradient is small and is almost constant.

12 Oct. 1977/Neuglashütten (Fig. 9,11):

The measurements were made at another place as in June, but both forests had comparable characteristics. The solar zenith angle had now larger values (56^{o} to 60^{o}). The shape of the R(λ)-curve (Fig. 9) is only slightly different from that of the June-measurements.

The two sets of measurements (Fig. 11 and 10) show significantly different dependences of R on θ_r at the three wavelengths. Between $\theta_r = 15^{o}$ and 30^{o} ($\Delta\phi \simeq 60^{o}$) the two measurements show different gradients.

Feeding Turnips
7 Oct. 1976 (Fig. 12,13,16):

The feeding turnips covered completely the ground with their still green leaves. Accordingly the shape of the R(λ)-curves (Fig. 12) shows the typical pattern. For retroreflection conditions ($\theta_r \simeq \theta_i$, $\Delta\phi$ near 0^{o}) the near IR plateau reaches more than the double value (about 65 %) as against $\theta_r = 0^{o}$ due to the glossy leaves at their corresponding orientation. θ_i was large (54.5^{o}) during the measurements.

Fig. 13 shows the dependence of R(550, R(675) and R(800) on θ_r. At the opposite side of the sun ($\Delta\phi \simeq 180^{o}$) a glossy effect obviously does not occur. R(970) (no figure) has almost the same shape like R(800).

In Fig. 16 for vertical observation the dependence of R(800) and R(970) on θ_i is shown within a small range from 54^{o} to 56^{o}. In contrast to vine and spruce the gradient is negative for increasing θ_i. The absolute and relative gradients are 0.72 % per degree and 2.0 % per degree, respectively.

4. FUTURE WORK

From spring 1978 (in the frame of a new remote sensing program) we will be able to measure irradiation and reflection simultaneously using two separate spectroradiometers (EG & G Mod. 555). Then it will be possible to measure more systematically and with still better accuracy. With the application of microprocessors the result will be available immediately after the measurement.

As we are in a position to measure at all observational angles common to multispectral scanner imagery, we plan to compare the scanner data with our ground-based results and to study the influence of the intervening atmosphere. In connection with this it must be investigated, whether spectral signatures can be obtained from air and space borne scanner data with comparable reliability.

5. ACKNOWLEDGEMENT

The author is thankful to his colleagues H.-J. BOEHNEL, G. KNOLL, Ch. MÜNTHER and S. RAMAKRISHNAN of the Institute and A. KADRO of the University of Freiburg for discussions and help.

6. REFERENCES

|1| International Lighting Vocabulary, CIE Publication Nr. 17 (1970)
|2| Radiometric and Photometric Characteristics of Materials and their Measurement, CIE Publication Nr. 38 (1977)
|3| K.T. KRIEBEL, Remote Sens. Environ. 4, 257-264 (1976)
|4| K.T. KRIEBEL, Appl. Optics 17, 253-259 (1978)
|5| A. KADRO and W. FISCHER, Proceed. Symp. S 6.05 Remote Sensing, XVI IUFRO World Congress, Oslo, June 1976
|6| H.-J. BOEHNEL, Symposium Flugzeugmessprogramm, BMFT-Forschungsbericht W 78-04 (1978)

Fig. 2

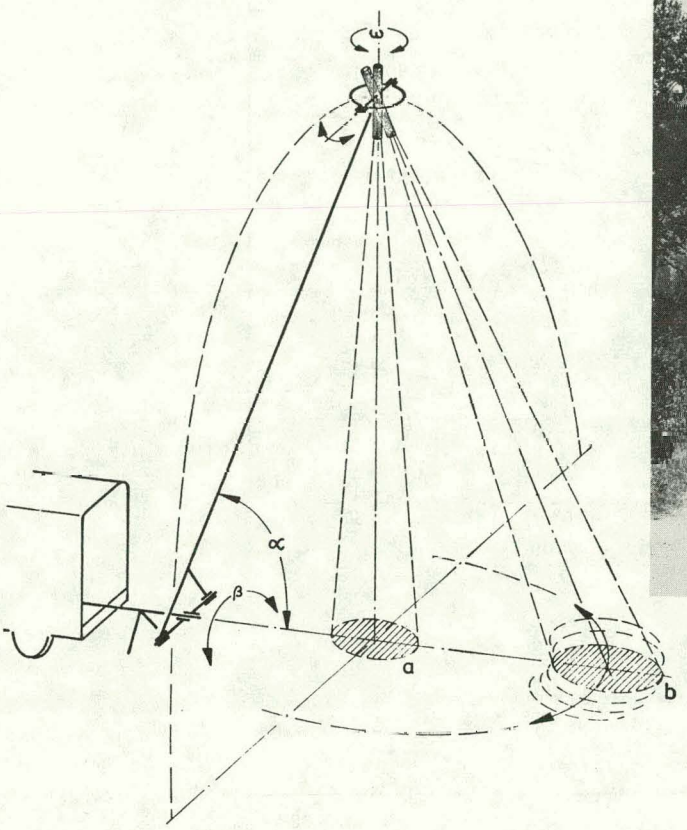

Fig. 1

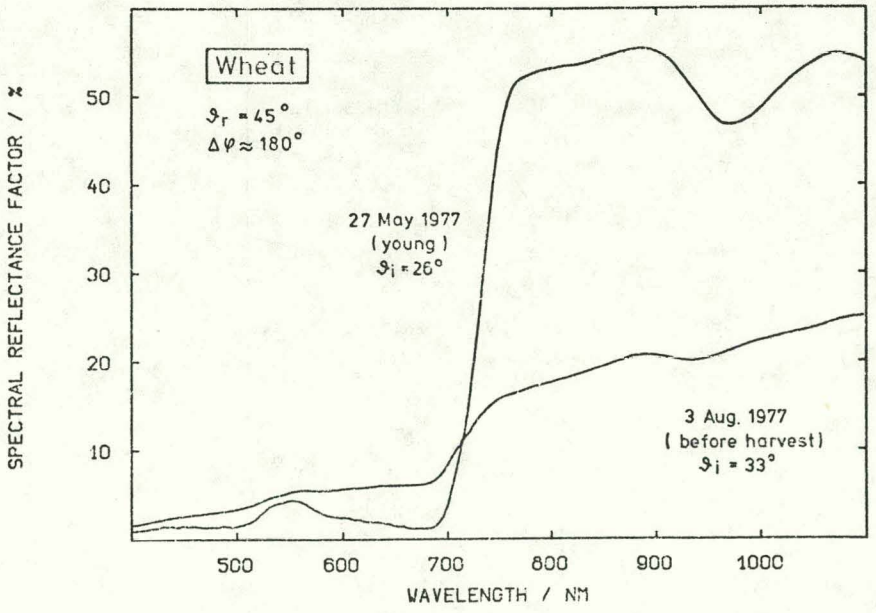

Fig. 3

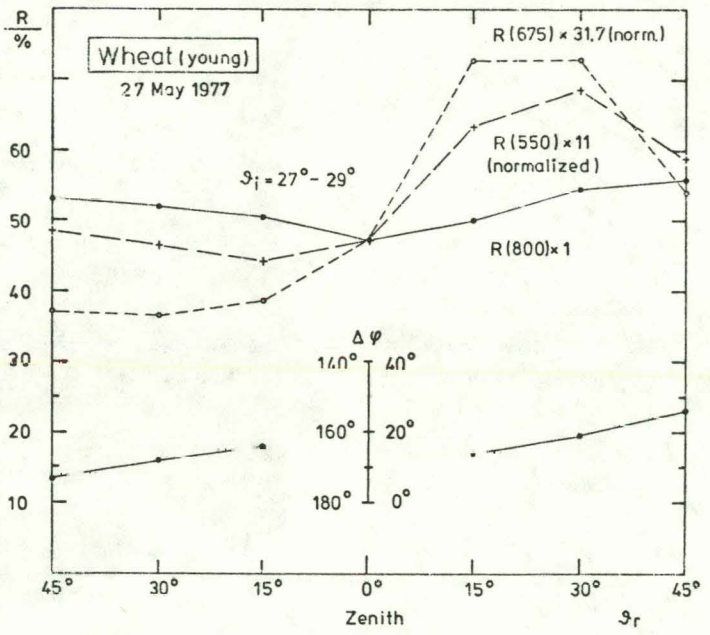
R
%
Wheat (young)
27 May 1977
R (675) × 31.7 (norm.)
R (550) × 11
(normalized)
ϑi = 27° - 29°
R (800) × 1
Δ φ
140° 40°
160° 20°
180° 0°
60
50
40
30
20
10
45° 30° 15° 0° 15° 30° 45°
Zenith
ϑr

Fig. 4

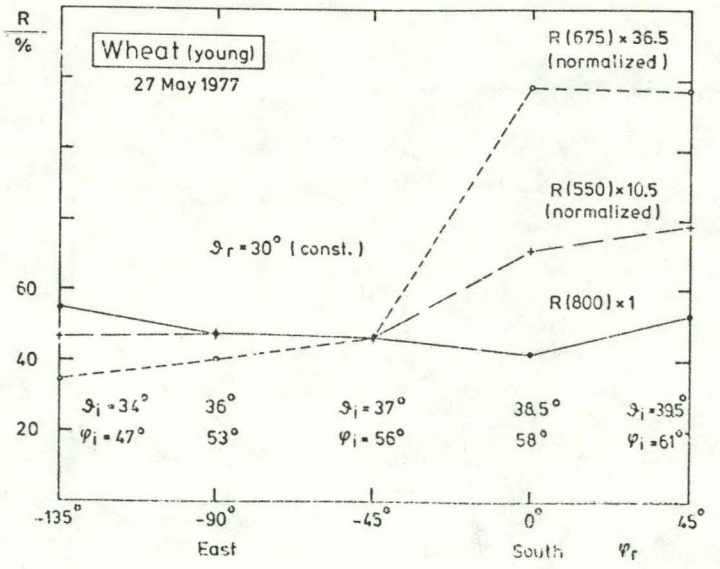
R
%
Wheat (young)
27 May 1977
R (675) × 36.5
(normalized)
R (550) × 10.5
(normalized)
ϑr = 30° (const.)
R (800) × 1
60
40
20
ϑi = 34° 36° ϑi = 37° 38.5° ϑi = 39.5°
φi = 47° 53° φi = 56° 58° φi = 61°
-135° -90° -45° 0° 45°
East
South
φr

Fig. 5

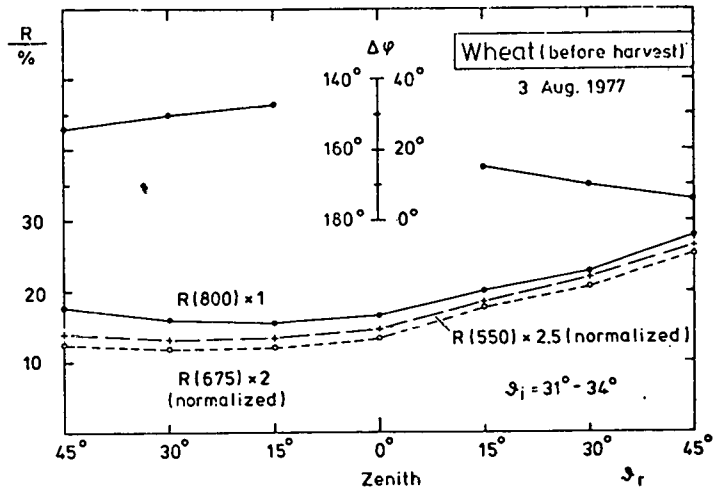

Fig. 6

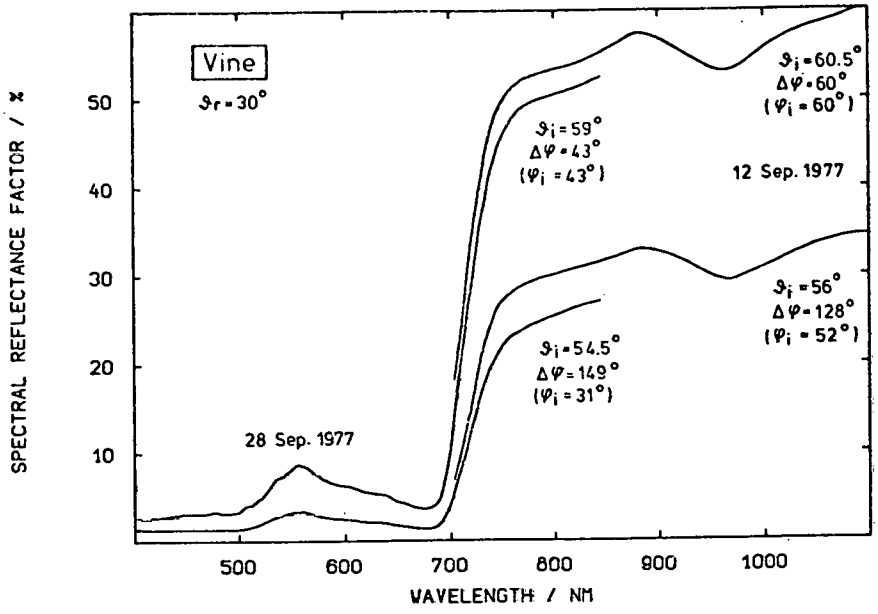

Fig. 7

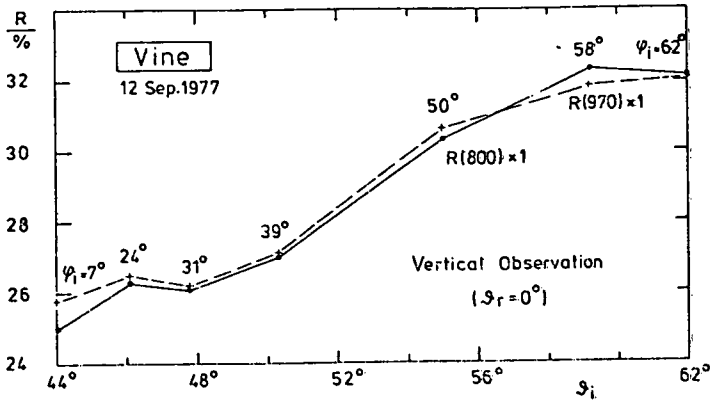

Fig. 14

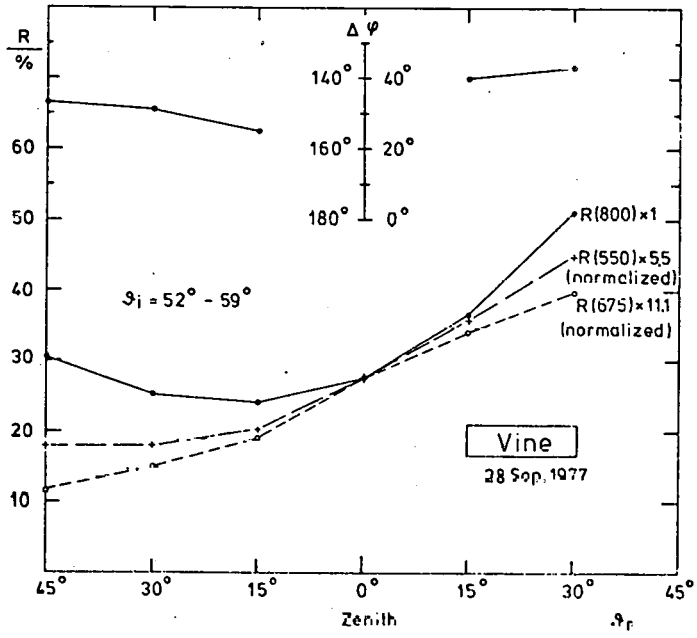
R
%
Δ φ
140°
40°
160°
20°
180°
0°
R(800)×1
+R(550)×5,5
(normalized)
R(675)×11,1
(normalized)
ϑi = 52° - 59°
Vine
28 Sep. 1977
60
50
40
30
20
10
45°
30°
15°
0°
15°
30°
45°
Zenith
ϑr

Fig. 8

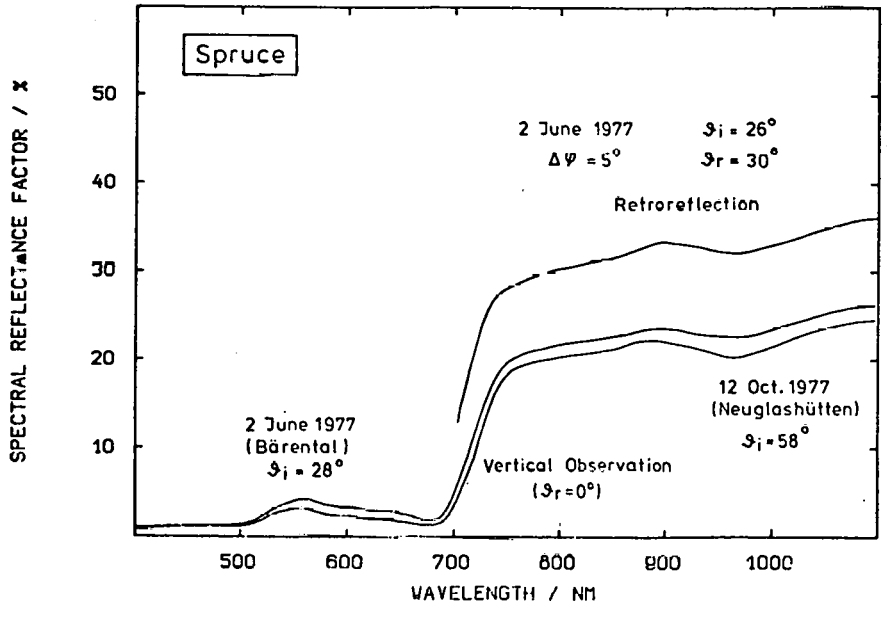
SPECTRAL REFLECTANCE FACTOR / %
Spruce
2 June 1977
Δφ = 5°
ϑi = 26°
ϑr = 30°
Retroreflection
12 Oct. 1977
(Neuglashütten)
ϑi = 58°
2 June 1977
(Bärental)
ϑi = 28°
Vertical Observation
(ϑr = 0°)
50
40
30
20
10
500
600
700
800
900
1000
WAVELENGTH / NM

Fig. 9

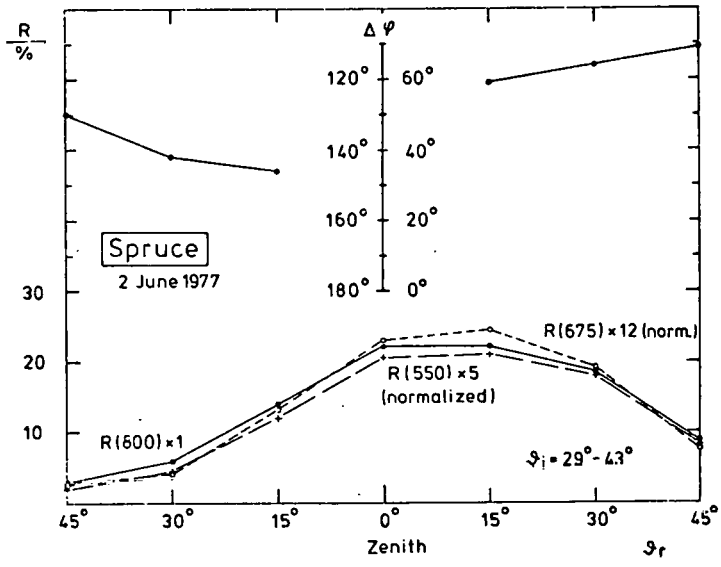

Fig. 10

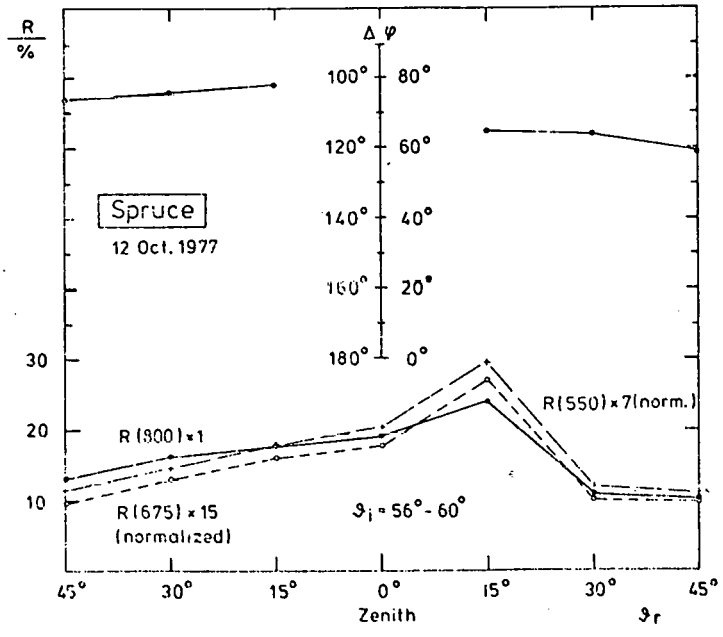

Fig. 11

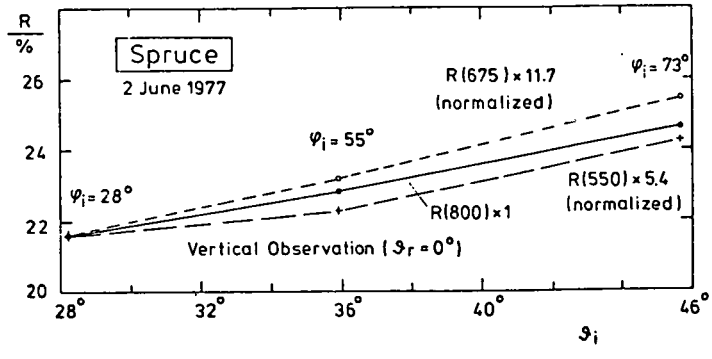

Fig. 15

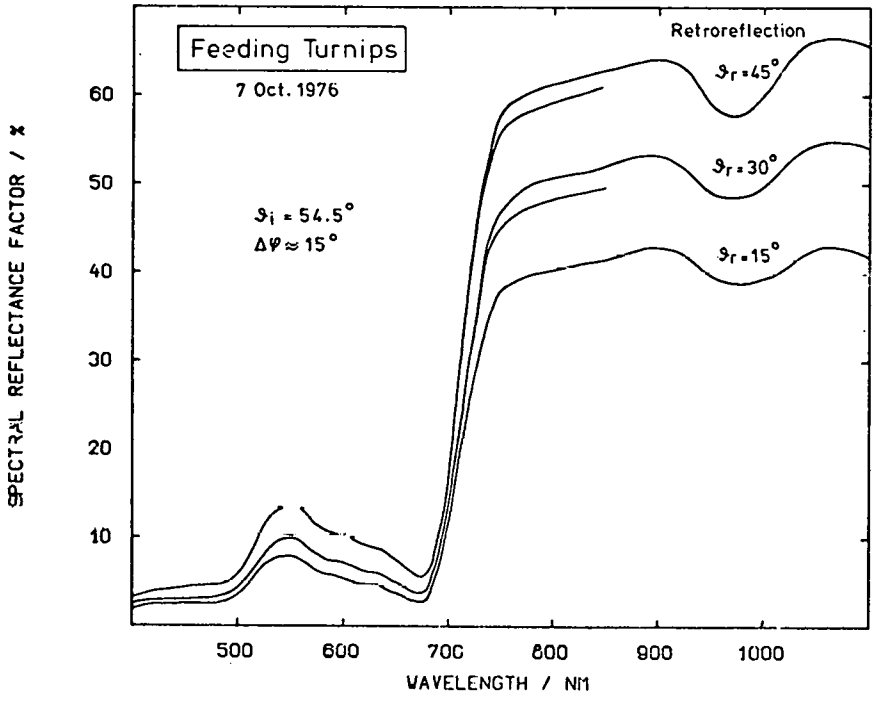

Fig. 12

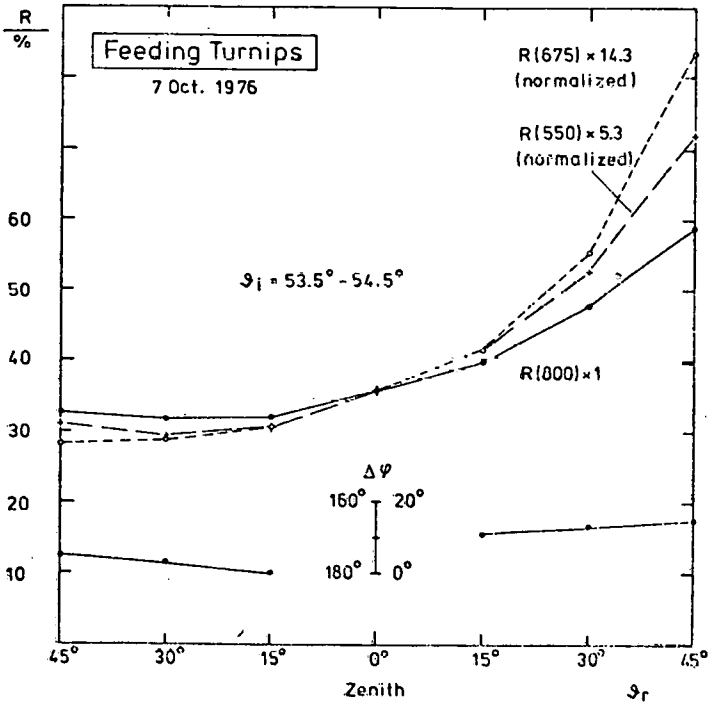

Fig. 13

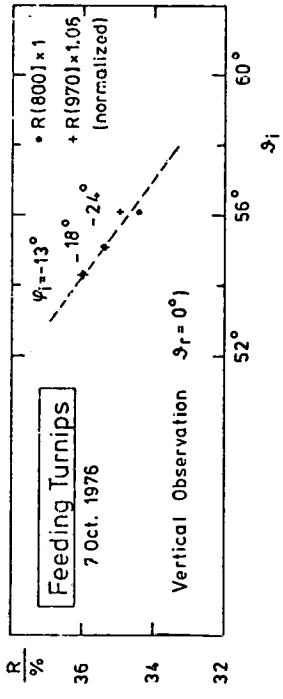

Fig. 16

MANGROVE INVENTORY OF THE PHILIPPINES

USING THE LANDSAT MULTISPECTRAL DATA

AND THE IMAGE 100 SYSTEM

Ricardo T. Biña, Robert Jara
Benjamin de Jesus, Jr., and Ernesto Lorenzo

Natural Resources Management Center
Visayas Avenue, Diliman, Quezon City
Republic of the Philippines

ABSTRACT

To determine the potentials of LANDSAT multispectral data in the inventory of Philippine mangrove forests, the Natural Resources Management Center conducted an investigation employing computerized processing techniques using the Image 100 interactive multispectral analysis system. The study applied two basic procedures, namely, the spectral signature acquisition method and the digital classification program. For ground truth, information came principally from ocular inspection of selected study sites. Preliminary results of the investigation yielded indications of the potentials of LANDSAT data in mapping and monitoring mangrove areas in general and in detecting the various growth and structural characteristics of mangroves.

INTRODUCTION

In the Philippines, the depletion of mangrove areas to satisfy the increasing demand for fishponds, lumber and other economic necessities has made immediate decisions imperative on resource managers for the judicious allocation of mangrove areas for purposes of preservation, conservation and utilization. To do this rationally, resource managers need a synoptic and updated information on the areal extent, distribution and ecological conditions of mangrove forests in the country. Evaluation of existing technologies for acquiring such information in the fastest, most cost-effective and economical way led the Department of Natural Resources (DNR) to consider the use of LANDSAT imageries. This consideration gave birth to the present mangrove inventory project being undertaken by the Natural Resources Management Center in cooperation with the DNR, with the former availing of its Image 100 multispectral analysis system for digital processing of LANDSAT data. In addition to the compilation of areal statistics and mapping of the mangrove areas, the inventory project is investigating the potential of LANDSAT multispectral data in assessing the various growth and structural conditions of mangrove communities. This paper reports on the initial activities completed, as well as on future plans for the project.

METHODS

For this study, thirty (30) LANDSAT scenes which covered the entire country were used. These satellite imageries were obtained from Landsat 1 and Landsat 2 overpasses during the period October 1972 to April 1976. Main sources of ground truth information, which supplemented the analysis of LANDSAT data, were direct field observations and topographic maps at scale of 1:50,000.

A. Mapping and areal measurement of mangrove forests

The following two basic procedures were employed in mapping the mangrove forests: (1) Signature acquisition in four MSS bands, and (2) digital classification of mangrove forests based on the obtained signatures.

Each LANDSAT scene was scanned to select suitable mangrove training areas on the basis of the known locations of extensive mangrove growth. Also considered in the choice of training sites were secondary information derived from topographic maps, land classification maps, air photos and related literatures. When all the training areas were adjudged, each was displayed on the CRT as a 3-band false color-composited imagery with the four MSS data stored in the refresh memory unit. An adjustable electronic cursor display identified for the computer the areas representing mangrove forests. The computer then scanned every pixel within the cursor and determined the range of gray level values of the four MSS bands. Based on these gray level values (or spectral signatures), the entire imagery was again scanned and every pixel falling within the computed spectral ranges was color-coded (alarmed). When the alarmed pixels include elements which do not belong to the mangrove category, modification of the spectral range was done by altering the upper and lower gray level limits in each band until every alarmed pixel belonged only to the specific mangrove category. Thus achieved, the modified mangrove spectral limits in the desired classification were retained.

The entire LANDSAT scene (185 km x 185 km) was projected on the CRT so that the spectral limits previously obtained from the training areas could be input to color-code all the mangrove areas in the whole LANDSAT scene imagery. The result was a false color-coded mangrove map superimposed on the original image data. The processed imagery was photographed for the production of thematic maps featuring binary theme overlays and alphanumeric theme prints.

For areal compilation, the entire LANDSAT scene was divided into 1 : 1 subscenes (one pixel per picture element) and each subscene containing known mangrove areas was loaded and displayed on the TV monitor. The spectral limits previously extracted from the supervised training were input to generate the alarmed mangrove pixels. Then the number of alarmed pixels were tabulated and the results displayed on the CRT. This procedure was repeated for the other subscenes as the areas involved in every LANDSAT scene were compiled.

B. Assessment of growth and structural conditions of mangrove communities

To assess the feasibility and potential of using LANDSAT data in determining the existing growth and structural conditions of mangrove forests, ground truth surveys were conducted in Bahile, Palawan (LANDSAT Scene ID No. 1154-01533), in Babatngon, Leyte (LANDSAT Scene ID No. 1186-01300), and in Pagbilao, Quezon (LANDSAT Scene ID No. 2455-01294). These sites were selected on the basis of the heterogeneity in land features, as well as forest characteristics, found in the test locations. In addition, different mangrove areas in Samar, Leyte, Bohol, Zamboanga City, and Palawan were surveyed for comparison, using helicopter/airplane/ground reconnaissance.

Imageries of the selected mangrove study sites were extracted from the LANDSAT CCT and displayed on the TV monitor. Based on ground data, features on the imageries corresponding to mangrove growth types, as well as other land cover categories, were identified. Then employing the signature acquisition programs, the four-band mean gray levels of each feature were determined and graphed to show the relationship among the four MSS bands together with the differences in the spectral signatures of the identified features.

RESULTS AND DISCUSSION

Figures 1,2 and 3 represent the different computer output maps of mangrove areas now being reproduced as parts of the outputs of this inventory project. Figure 1 is a TV display photograph of a 3-band false color composite of a 1 : 1 subscene of Babatngon, Leyte. The mangrove areas were defined by a false color different to those assigned to each MSS band. This kind of processed photographic output is very useful for "quick look" analysis of mangrove distribution in a given area, especially when the mangrove vegetation cannot be distinguished from other vegetation types in the raw MSS data. When applied to a whole LANDSAT scene, the false-color photograph also gives a ready and handy synoptic reference to the mangrove spatial distribution in an area of 185 km x 185 km. Such range of coverage should provide valuable information to planners and decision-makers and to researchers, as well. Direct photographs of the video display, however, suffer from the inherent distortions of the imagery in the video screen and so these are less likely to be useful in the preparation of mosaic maps. The most ideal system for this purpose, if the cost is not prohibitive, would be a digital film recorder through which a rectified imagery can be produced.

In Fig. 2, the same color-coded mangrove areas are presented in the form of a binary theme print superposed on a base map of 1:50,000 scale. The target theme is printed via the line printer and with the use of appropriate digital programs could be rectified and registered into a base map at any desired scale. The chief advantage of this thematic map is its facility to be superposed into any original resource map, thus allowing quick temporal comparison and change detection. As shown in Fig. 2, the stipled areas represent the former extent of mangrove areas when the same were compiled in 1949. The said areas have now been converted into fishponds, or left denuded. On the other hand, the shaded areas are the superposed binary theme prints obtained from the 1972 LANDSAT imagery, which now stands as the remaining mangrove growth as of the year the scene was taken. A compilation of this kind of map encompassing all mangrove areas in the country would be invaluable in establishing rates and trends of denudation in such localities.

The alphanumeric theme print shown in Fig. 3 provides a very convenient medium for assessing trends in land cover changes within and around the mangrove areas. Mapping of each land cover category was accomplished by using the same supervised technique for mapping the mangrove areas or by unsupervised digital clustering. The resulting thematic patterns were then rectified and registered to a base map as overlays. At present, attempts are being made to subcategorize the mangrove areas according to varying structural conditions. Should it prove feasible, the subcategories could be printed in alphanumeric form to be a source for a quick reference in assessing mangrove forest conditions.

Fig. 4 shows an example of a mangrove area digital measurement output as displayed on the CRT. Initial measurement is done by counting the number of false-colored pixels representing mangrove areas and then converting them into hectare unit through a specified conversion factor, depending on the scale of imageries used. A digital subprogram compiles all the measurements executed for each Landsat subscene and logs them to appropriate scene files.

Results of our ground surveys in the three study sites, as well as aerial reconnaissance in some other areas, show the futility of mapping species distribution out of the present LANDSAT resolution. Except for the genus Rhizophora and Avicennia, which tend to form the seaward limit of a mangrove area, the majority of the forest stands is a mixture of varying mangrove species of at least two kinds. This is seen even in an undisturbed primary mangrove forest like that in Bahile, Palawan, where Rhizophora apiculata and Bruguiera gymnorrhiza are so closely intermingled as to give the impression of a homogeneous stand when viewed from a distance.

In several instances, likewise, mangrove forest stands are difficult to recognize apart from other land cover types when visually examining LANDSAT imageries. This makes supervised classification quite difficult, too. The present dilemma could be attributed to the fact that as a result of economic

exploitation, most of the mangrove areas in the country are now in varying secondary and reproductive growth stages with the original mangrove species having been replaced, in several cases, by non-mangrove types. In Babatngon, Leyte, for example, the majority of the vegetation stands, though some portions of which still show remnants of the primary mangrove forest, are second-growth mangroves with varying ages, canopy cover and density. Interspersed with the stands are fishponds and logged-over areas overgrown by brush vegetation.

The variability of land cover features within the mangrove areas is reflected in the very wide range of LANDSAT reflectance values (in gray level) found in the three study sites (Fig. 5). While each curve represents the mean reflectance of land cover within and adjacent to the study sites, it could also be interpreted as a transitory stage in the continuous change in reflectance of a mangrove area as its original primary forest stand undergoes a series of transformations due to logging and conversion to some other land uses. Hence, by simply examining the reflectance ranges of a mangrove area in the LANDSAT imagery, an assessment of existing environmental conditions in said area can be made. An increase in the reflectance values for the near-infrared is indicative of canopy changes. A primary mangrove forest similar to the one in Bahile, Palawan would have a spectral signature very close to that of a tropical rainforest (Fig. 6). As the trees are cut down, corresponding spectral changes occur, especially in the near-infrared regions, so that if the mean reflectance values are taken, the resulting spectral signatures would be lower (Fig. 5).

The relationship between the near-infrared reflectance and mangrove canopy conditions is further indicated in Fig. 7, which shows the mean spectral signatures of various types of mangrove growth stands found in the study sites. As should be expected, the differences in reflectance values among the growth types become clearly apparent toward the near-infrared regions. Since species intermixing occur within these growth stands, the spectral signature variations in the near-infrared bands can be generally attributed to their differences in crown cover. The continuous decrease in canopy cover seen from the old growth stand down to the logged-over areas is reflected by the progressive decrease in reflectances for MSS 6 and MSS 7.

The study reveals that while LANDSAT near-infrared bands can be used to diagnose canopy conditions, classifying mangrove areas according to growth stand categories from LANDSAT data is still not practical. The following reasons are given:

1. A LANDSAT reflectance norm has yet to be defined for every growth type based on real-time ground truth and radiometrically corrected LANDSAT scenes. Aerial reconnaissance has shown that similar mangrove growth stands vary in their species mixes and thus affect the color of canopy cover to a large extent. Hence, there is always the possibility in digital mapping for similar growth types to be categorized separately due to reflectance variations within the same LANDSAT frame. It would therefore necessitate extensive sampling of different species mixes and correlating them to the LANDSAT reflectance values to establish the lower and upper reflectance bounds for each growth category.

2. Due to the economic exploitation of mangrove areas, which ranges from foliage gathering for animal feeds to outright logging, variations in canopy cover of similar growth types can be expected. If defoliation is interspersed so as to affect the spectral character of every pixel of a given growth stand, its spectral signature would necessarily differ from that of a similar but undisturbed stand. Such a spectral signature could simulate any other growth types, in which case, the resulting categories from digital classification would be confusing.

Further examination of the mangrove spectral signatures in Fig. 5 and Fig. 7 shows that while there is a wide variation in the gray levels for the near-infrared bands, the differences in reflectance for MSS 4 and MSS 5 are curiously not significant. Such range of gray levels in the visible bands can be taken as spectral characteristics for the mangroves in general, which makes digital recognition of mangrove areas also possible.

CONCLUSION

In general, most of the mangrove areas in the Philippines are recognizable from LANDSAT imageries, making it possible to conduct a rapid areal inventory and monitoring through digital processing. However, high variations in mangrove canopy cover and the heterogeneity of the species of most of the country's mangrove forests forestall and render virtually impossible the categorization of mangrove stands according to species at the present LANDSAT resolution. The infinite morphological and physiographic combinations that influence the LANDSAT reflectance likewise make it difficult to categorize the mangrove forests following the traditional classification i.e. old growth, young growth, reproduction-brush, etc. On the optimistic side, however, the study demonstrates that the sensitivity of MSS 6 and MSS 7 can be exploited to perform a diagnosis of the general canopy conditions of a mangrove stand.

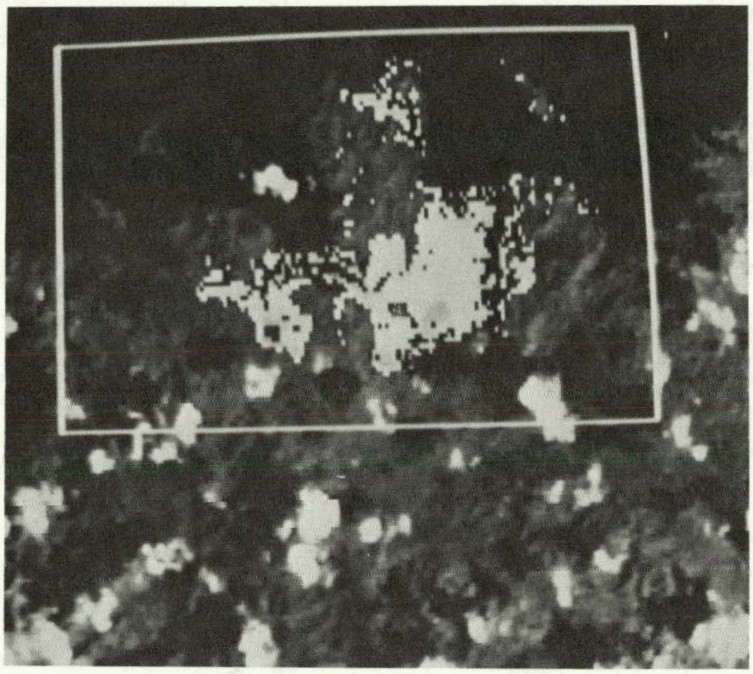

Figure 1. TV-display photograph showing mangrove areas in false-color (LANDSAT Scene No. 1186-01300, Babatngon, Leyte).

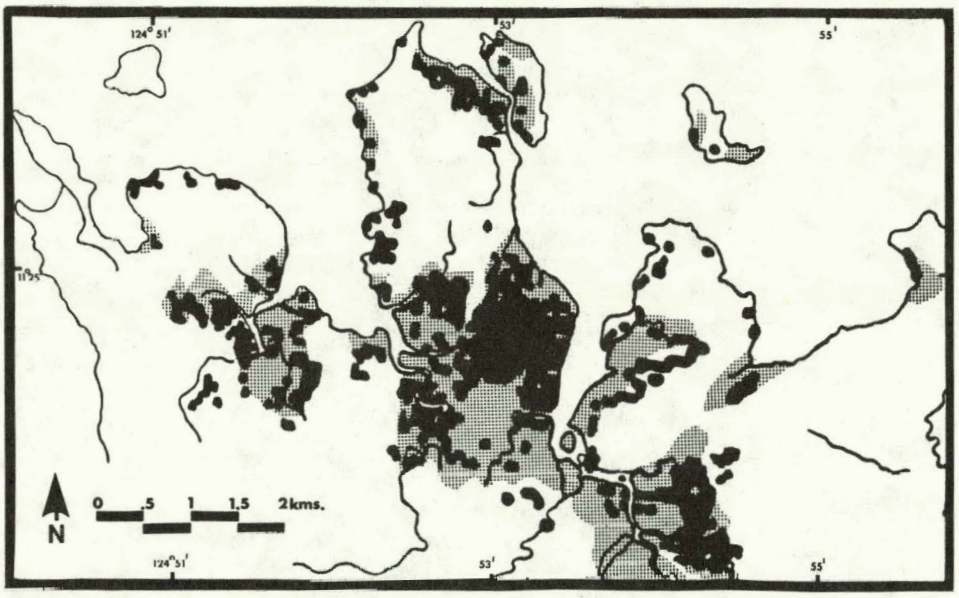

Figure 2. A binary theme print of mangroves in Babatngon, Leyte superposed on the 1:50,000 scale topographic map.

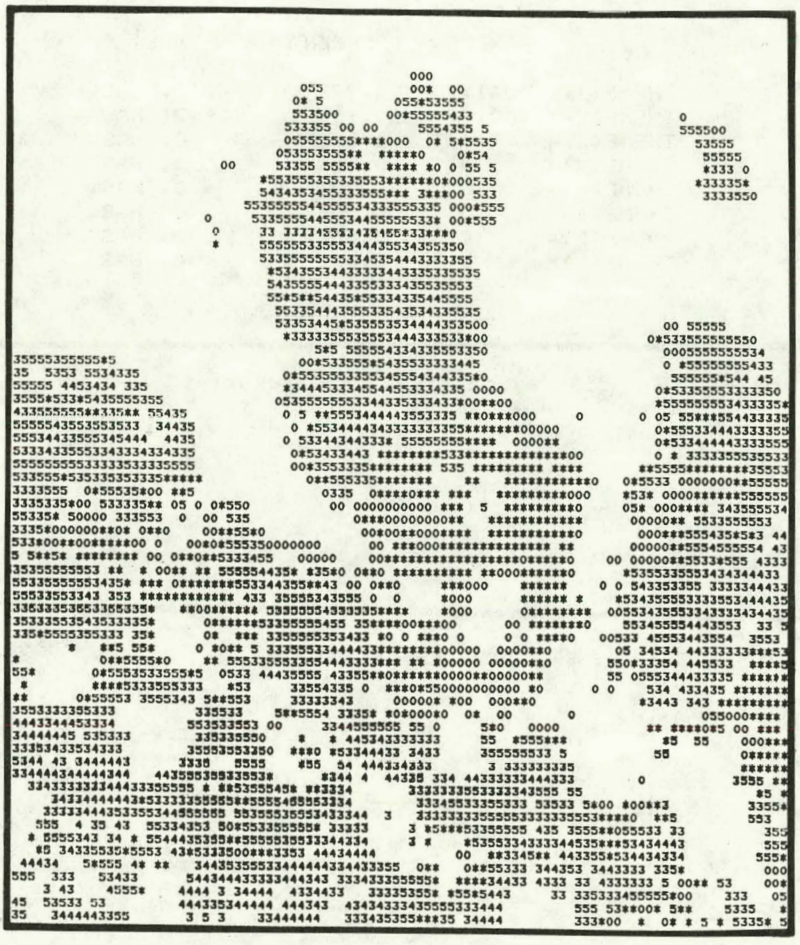

Figure 3. Computer-generated alpha-numeric theme print of Babatngon, Leyte showing the mangroves (*), logged-over areas (0), brush (3), open areas (4) and coconut (5).

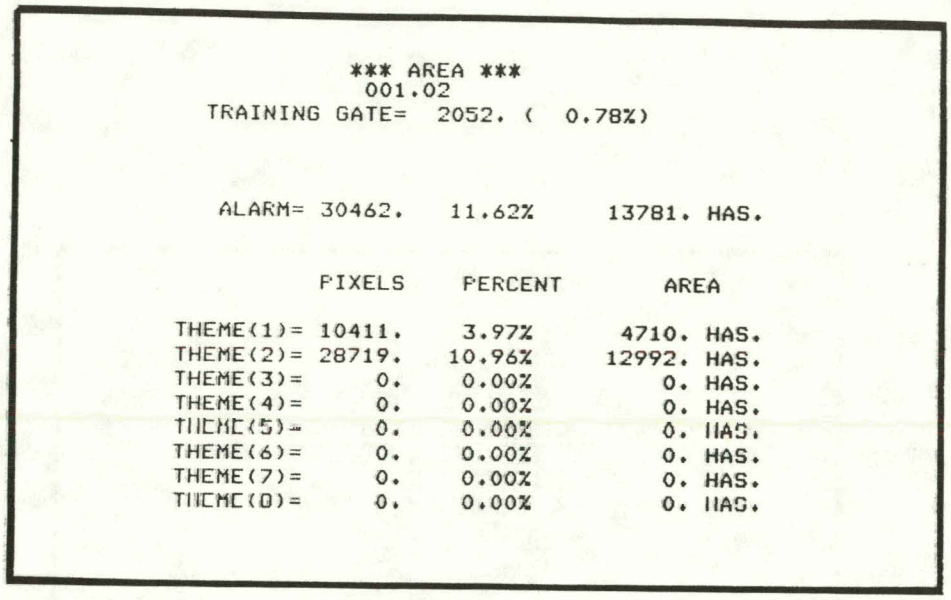

Figure 4. CRT display of areal measurement of identified mangrove areas.

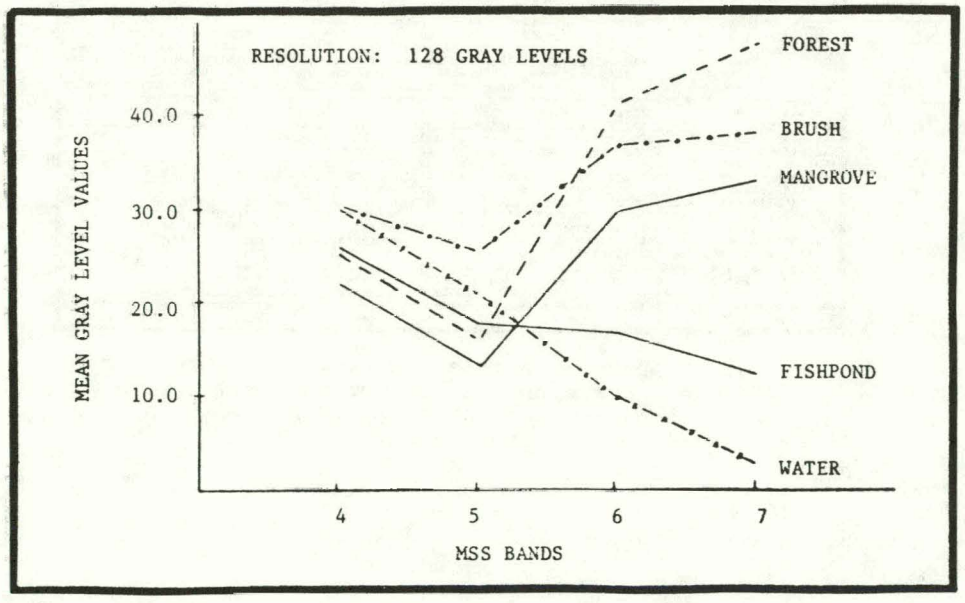

Figure 5. Mean spectral signatures of different land cover types within and around the mangrove area.

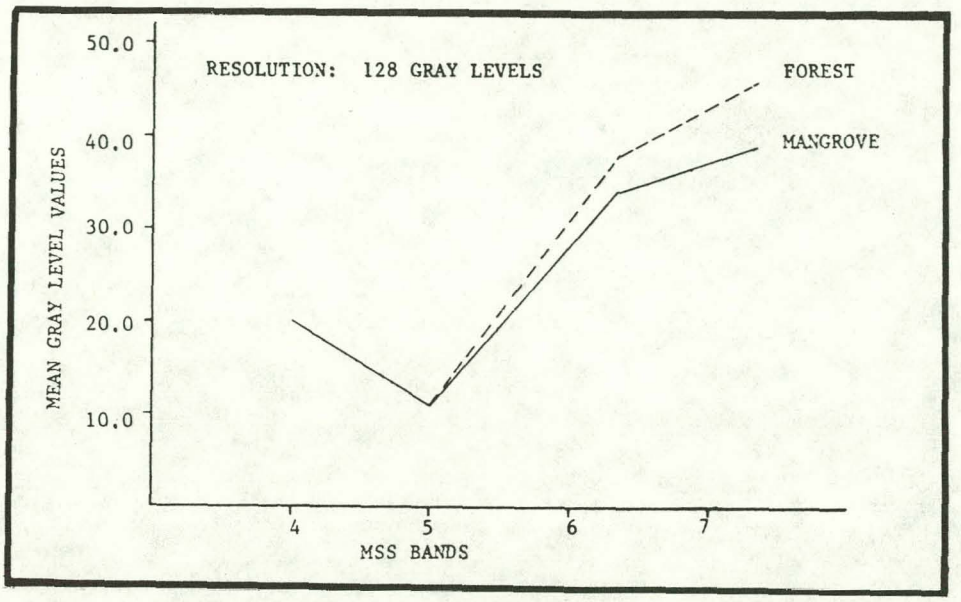

Figure 6. Mean spectral signatures of primary dipterocarp forests and mangroves in Bahile, Palawan.

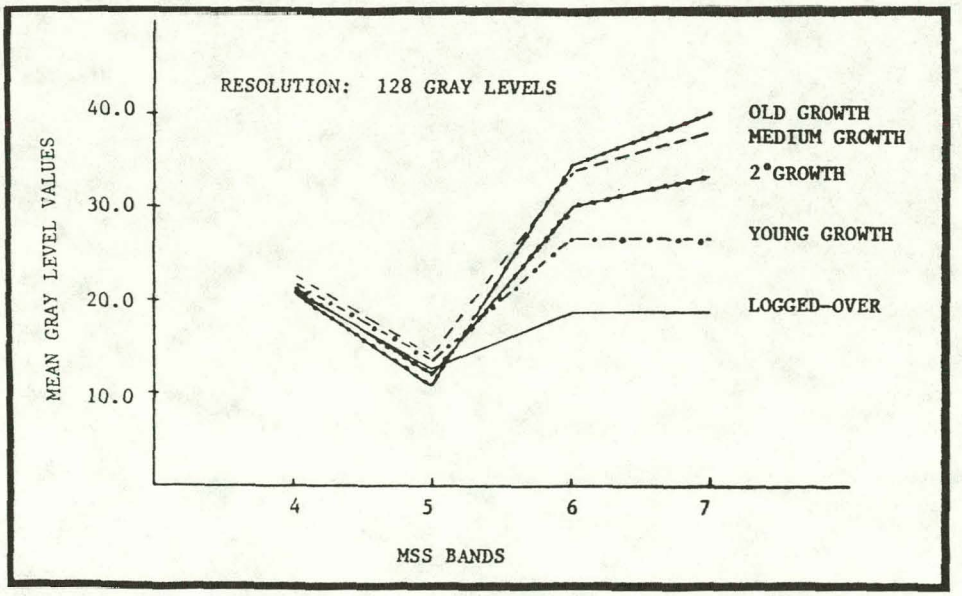

Figure 7. Mean spectral signatures of different mangrove growth conditions.

THIS PAGE

WAS INTENTIONALLY

LEFT BLANK

SESSION 15

FUTURE OPERATIONAL EARTH RESOURCES PROGRAMS

EDITORIAL NOTE:

This final session, chaired by Mr. E. M. Risley of the U.S. Department of the Interior, was designed to include both formal presentations by invited panelists (with backgrounds in various areas of program technology, management and jurisdiction) and open discussion among those panelists and symposium participants. Statements included here address scientific and technical characteristics, application areas, and legal, political and institutional concerns related to the future global application of technologies treated throughout the symposium.

In general, these speakers did not speak from prepared texts and statements included here, except as noted, were transcribed, from recordings made during this closing session in Manila. Views and comments included here are those of the individuals involved, and should not be construed as representing or reflecting official views, opinions, or positions of their agencies or organizations.

The following pages, in the order of presentation herein, include statements by:

Mr. E. M. Risley (Panel Chairman)	U.S. Department of the Interior
Mr. David Keller (Panelist)	Manager, Advanced Space Programs, General Electric Space Division
Dr. Clifford Spohn (Panelist)	Deputy Director, Satellite Services, U.S. National Oceanic & Atmospheric Adm.
Dr. W. M. Strome (Panelist)	Chief, Applications Division, Canada Centre for Remote Sensing
Dr. I. M. Pikus (Panelist)	Deputy Director, Office of Technology Policy & Space Affairs, U.S. Department of State
Mr. J. U. Hielkema (Panelist)	Technical Officer, U.N. Food and Agriculture Organization
Dr. D. S. Simonett	Chairman, Department of Geography, University of California, Santa Barbara, California
Mr. William Fischer	Chief Scientist, EROS Program, U.S. Geological Survey, Reston, Virginia
Dr. Robert Vincent	President, Geospectra Corporation, Ann Arbor, Michigan
Dr. Jerald J. Cook (Symposium Chairman)	Environmental Research Institute of Michigan, Ann Arbor, Michigan
Dr. John van Genderen	Fairey Surveys, Ltd., Berkshire, United Kingdom
(Dr. W. M. Strome)	
Brig. Sanchez Pena	Director, National Commission on Space Research, Buenos Aires, Argentina
Ing. F. M. Rudin	Director, National Geographic Institute, San Jose, Costa Rica
Dr. Celso R. Roque (Symposium Co-Chairman)	Executive Director, Natural Resources Management Center, Manila, Philippines

E. Risley:

Ladies and gentlemen, welcome to the final session of this inspiring symposium.

I think we all realize that over the past four days we have heard some extremely useful and educational discussions of the technology, and of its application...we've heard something about developing programs. I think we are all aware that we are dealing with powerful tools for the betterment of mankind. We know that these systems are here to stay and are going to become increasingly influential as we attempt to get a better handle on some of the pressing resource and environmental survey problems that face the world today. The current meeting opened with inspirational words by His Excellency President Marcos, and we hope to close in something of a round-table affair to consider some of the problems and the issues that are raised as we try to translate these technological developments into routine operational programs applied to a variety of pressing needs.

We'll try to present a representative sampling by five speakers, who come with considerable experience and professional competence in different areas. In addition, I have asked Mr. William Fischer and Dr. David Simonett to each provide a short critique following the prepared talks, and then I would like to open the meeting up to the floor, to the extent that time permits. Obviously, some of the issues to be discussed here today are cosmic in nature, and we will never resolve them; but at least we can flag them, and hopefully, we can identify some of the problems that lie ahead.

There are microphones on the floor and I would ask that speakers in the audience identify themselves and provide the group with a brief statement or with a question directed to one of our panel members, as you wish.

I would also like to point out that our speakers did not come with prepared statements; they speak for themselves as scientists; and their comments do not represent agency positions.

With that I would like to get on with the first of our five speakers, Mr. David Keller of the General Electric Company, Valley Forge. Mr. Keller had the very important responsibility of developing the highly successful Landsat-1, and is now engaged in the study of a variety of other satellites which are coming along. I think his remarks will set the framework for what we can expect in the near future; Mr. Keller.

D. Keller:

Thank you Ed. Good afternoon ladies and gentlemen. I arrived here on Monday and I am still in awe of being half way around the world and seeing so many friends and so many people working on the applications of Landsat data. I am here because of the technological acceleration of this century; because an airplane can bring me 12,000 miles in just a few hours.

Landsat is one of the illustrations of that technological advancement. Landsat has opened up a new understanding of our natural resources and how to manage them. Landsat-1, as most of you know, was launched in July of 1972 and operated for five and one-half years, before being turned off to make room for Landsat-3, which was launched just two months ago. Sandwiched in between was Landsat-2, which has now been operating for over 3 years; and which, in tandum with Landsat-3, has given us the capability of providing worldwide coverage every 9 days. Waiting in the wings is Landsat-D, which in the 1980's, will provide better data at a higher data rate; and, we hope, with much faster data dissemination.

The data detail from Landsat-D will also be much better. Landsat-2, as you know, provides an 80-meter instantaneous field of view. Landsat-3 (RBV), as

shown in some slides this week, improves on that by nearly 2:1; and Landsat-D will provide still further improvement, to a 30-meter IFOV with improved spectral performance. Whereas we now look at a resolution which is equivalent to a 4-hectare cell, with Landsat-D we will be able to study an image made up of 1-hectare cells.

The Landsat program has generated more scientific interest, in application over a wider range of disciplines, than any other space undertaking. These satellites have provided a half million images of the earth to more than 100 nations. The appeal and the usefulness of Landsat data has proven its value to user nations, regardless of the state of development of those nations. And from the talks given in the poster sessions this week, my impression that about 80 percent of the work reported at this symposium has been on the application of Landsat data. But I think the real value comes, as many of you have pointed out, from multiple data sources; when Landsat data are merged with what you already know, or when Landsat data trigger you to collect more data to enhance the application in which you are working.

I am the industry representative on the panel today, and from an industry viewpoint there are four considerations which I would like to touch upon briefly: (1) future spacecraft systems, (2) international participation, (3) data handling, and (4) industry's role in all of these.

The first of these considerations is the need for Landsat to become operational, and to lead to future spacecraft which will provide better data and better ways to observe the earth. In many ways the outstanding performance of the Landsat spacecraft has already made them operational; and what is a burning issue in the United States (i.e., should Landsat be an operational program) seems to be of trivial concern here, because most of you are presently using the data in an experimental-prototype operational sense.

The technology is here for further improvements in remote sensing from space. It keeps improving. We are not able to fully exploit the data from Landsat-1 and Landsat-2, and already Landsat-3 is here with its improved multispectral scanner, the thermal IR-channel, and the improved resolution of the RBV's. The Landsat family of spacecraft being planned by NASA is going to make an even further improvement. Arrays of solid state detectors are going to come; radar, at some time in the future; soil moisture measurements are coming on the Landsat family; Seasat will be launched in just another month or so, and although it's designed specifically for oceanic observations, some of the sensors, in particular the radar, will have applications over the land mass. There is a Magsat program; a Heat Capacity Mapping Mission; plans for Stereosat; shuttle is coming on line, and will have a large format camera; there will be increasing research related to soil moisture measurements; and to the development of microwave sensors for a variety of applications. We've just begun to exploit the technology of remote sensing from space. The international impact should be reflected in increased cooperation and participation among countries to exploit this capability which space will provide.

The second area is the growing international participation in remote sensing from space. Ground stations are already in place in Brazil, Canada, and Italy, and under varying stages of planning and development in Iran, Japan, the Philippines, Australia, Argentina, Sweden, and a cooperative project in Upper Volta. Japan, Germany, and France are all considering earth resources satellite systems. France, Japan, and the USSR already have Metsats, and India is about to develop one.

The accumulation of Metsats, Landsats, Seasats, Magsats, Stereosats, and the rest are a challenge to our use of data and to our applications work. We need to pull together those ground stations into a global network considerably enhancing the value of the overall system.

We are on a planet where only one-fourth of the surface is land, and by the end of this century we'll ask that land to support a population of about seven billion people. The more we know, and the sooner we know, the better we can manage what we have. The key is international cooperation, to serve

both our national needs, and our growing international needs.

Thinking is still in a very early stage, but there are encouraging signs that a global information system linking the space and ground systems of the world is a realistic possibility. This would facilitate the use of data from multiple sources, and would create still a further challenge in the design, development, and use of data bases to allow us to move data from one system to another, from one reference frame to another, from one spectral interval to another, and from one temporal interval to another. Much of the long range benefit of earth resources systems will come from our ability to intergrate these many data sources.

I have mentioned the importance of operational systems, and of international cooperation, and they are both critical. But a third consideration is even more critical; the need to improve our methods of handling data on the ground. We are collecting data at a remarkable pace, and the satellite systems I have just mentioned are going to further accelerate that pace.

In the Landsat case, current ground systems for tracking, receiving, and initial processing require about six weeks to deliver data to the user. As many of you know, it often takes a lot longer than that to acquire the data; and after acquisition, to get it processed, packaged, and ready for you. This is the situation with Landsat-2. Landsat-3 should offer some improvement in the speed with which the data are processed; and we expect that the Landsat-D ground system will provide processed data, ready for distribution, in 48 hours.

Data must continue to pass through four stages in its transformation into information: (1) data reception, (2) data processing, (3) data storage and dissemination and (4) data analysis and data interpretation leading up to the critical decision process. The revolution going on in the field of data processing technology is addressing the first three of these stages. We are processing more data faster and cheaper than we thought possible, even five or ten years ago; it's really within the scope of this meeting to work on the critical fourth stage; the interpretation, analysis, and the use of those data.

The fourth consideration I would like to touch upon is industry participation and future operational remote sensing systems. Most people in industry, in the United States at least, see the government as the key implementor in future systems; but still see a very major role for industry in such a program. Industry, we expect, will continue to supply the satellite sensors and the ground processing systems; industry is capable of operating data centers and photo labs; and industry can analyze the data in order to provide resource information to commercial and to government users. In addition, industry can help with the enormous training job that lies ahead. In cooperation with educational institutions and governments, industry can greatly aid the development of the skilled manpower force needed to maximize the return from remote sensing technology. Industry will develop smarter machines to analyze the data, but until we are able to mass produce the craftsmanship needed to handle the information that these machines extract...until that day we are still playing a game of catch-up.

The world does not face a shortage of manpower, only a critical shortage of trained manpower; and again, the organization of this kind of meeting, is addressing itself to that key issue.

So, industry's role is a multiple one, as a developer and supplier of systems and as an analyzer of data. Industry's role will continue to be a formidable one that can only be done in cooperation with the government within its' own country, and with political and industrial components of all other participating nations.

I mention these four concerns today, future spacecraft, international

cooperation, the need for improved and broader based ground systems and the industry commitment, because I feel that positive decisions in all four of these areas will greatly enhance the return the world receives from remote sensing.

About a dozen years ago, in Ann Arbor, I went to my first meeting of this remote sensing symposium as quite a neophyte; and I listened very carefully to this new world (to me). One paper stands out very much in my mind; a doctoral candidate from one of the universities, in Texas, I believe, reported on a Gemini photograph. He had done doctoral, or perhaps his post-doctoral, work, analyzing that photograph. In his analysis he identified nearly every one of the applications of remote sensing from space that we are working on today. He cited applications in agricultural resources, forest resources, water resources, pollution, sediment transport, aids to navigation, mapping, and all the rest. In those days this meeting was very much addressed to "Gee whiz, Wow. Look what you can see." Now we have progressed to the point where we are providing data on a very routine and systematic scale, around the earth, roughly every two weeks.

By the early 1980's, scarsely a decade into this program, we will be receiving seven times the data provided by the first experimental satellite, and with little or no increase in cost. As you people have shown here this week, the benefits are increasing, and we are doing great things to the cost-benefit ratios. Thank you.

E. Risley:

Thank you very much David. The host of systems alluded to by Mr. Keller raises the question of the formidable management problems to be faced. There is some precedent for earth observing systems in the form of meteorological satellites which have been operational for some time. We are fortunate to have with us today the Deputy Director of Satellite Services for the U.S. National Oceanographic and Atmospheric Administration, Dr. Clifford Spohn. Dr. Spohn received his PhD from MIT and has made a long career in meteorological systems. He is particularly familiar with the development of international weather programs; Dr. Spohn.

C. Spohn:

Thank you Ed. I am going to speak, for a few minutes, on where we in NOAA see ourselves going in operational environmental satellite activity. From our view point I can best express where we stand, if I borrow a phrase that my friends from Washington will all recognize: "The future is now."

For us in NOAA the future starts this summer, with the launch of the first Tiros-N satellite which will represent the third generation, insofar as the United States is concerned, of operational, polar, orbiting meteorological environmental satellites. In many respects, Tiros-N will simply be more (and better) of what we have already been providing with the present NOAA series. We will again have the scanning radiometer, which will provide the same visible infrared data that has been provided heretofore. In addition, we have added two more channels. One of these, at 3.9 microns, is in a part of the infrared spectrum which we expect to help us to do a better job of determining sea surface temperatures. The second is a channel in the near-IR, at just about 1 micron, which is expected to be particularly useful in distinguishing ice and liquid water, in studies on snowpack, ice cover, and similar uses of the data.

We will again have a sounding capability, but in addition to having what we trust is a much improved infrared sounder on this spacecraft, we will also have a stratospheric sounding unit and a microwave sounding unit. We believe that the combination of these will provide a more effective ability to measure vertical temperature variations in the atmosphere.

In addition we have added what, in many respects, is not truly a "remote sensing capability." Yet in another sense it is remote sensing, in that it permits the collection of data from remote areas where such collection would otherwise be difficult or impossible. I am referring to a data collection platform location system, the Argos system, which will permit this spacecraft to acquire data from a variety of ground-based and atmospheric-based platforms.

One of the striking things about Tiros-N is that it is truly an international satellite. The stratospheric sounding unit is being provided by Great Britain, and the Argos data collection platform location system is being provided by France. Thus we have an internationally-collected set of instruments, flown on a single space frame.

We will also have the capability, with this spacecraft, to increase the instrument complement as we progress through the series. We can already identify two instruments which will be added to the last three of these spacecraft. The first is the Earth Radiation Budget Sensor, which will be of particular interest to our friends in climatology; and the second is the Backscatter Ultraviolet Sensor, which will be of particular interest to those of us who are concerned with the distribution of ozone, and the effects on that distribution of aerosol usage on the surface of the earth and/or the flight of supersonic transport aircraft. It will provide, for the first time, for a continuing surveillance of the concentration and distribution of ozone.

In the geo-stationary area we are expecting, within the next two years, to launch what I will call a "generation-and-a-half" spacecraft. It will be the same spacecraft, with the same instrument complement, with one exception: the viewing instrument which we refer to as the VISSR (the Visible Infrared Spin-scan Radiometer) will now be altered and be called a VAS, (a VISSR Atmospheric Sounder). This instrument, having some additional channels and a capability for continuous scanning of a small portion of the earth's surface, is intended to provide us with the capability to obtain soundings from geostationary altitude.

I want to stress that the VAS, at this point, is an experiment. We will have the capability, if the experiment is not successful, to simply return to a normal VISSR-type operation, and thereby continue the activities that are currently provided through the geostationary spacecraft...i.e., the GOES spacecraft. However, if VAS is successful, we will then face the problem of making it into an operational system; one of those problems that we like to face.

Beyond these two, which represent changes in our systems that are authorized by the Congress, funded, and with spacecraft which are well on the way to construction, we can look to the further future. We are well aware that the Tiros-N series, and the GOES-series will both reach the end of the line by the mid-1980's. We are currently engaged, jointly with NASA, in a study to determine the type of spacecraft for both the polar mission and the geostationary mission; that is, the follow-on to the Tiros and GOES series for the latter half of the 1980's and through the decade of the 1990's.

At this point there is no final determination as to what the instrument complement, or the type of spacecraft, should be. The study has only begun. We expect that, in about two years, the current study will have reached a point where we can generate technical specifications, and approach our friends in industry (for whom Mr. Keller was speaking) to start them producing hardware that will represent the follow-on to the present series of spacecraft.

However, there are some guidelines that we can address with respect to what might be produced. First, one of the clear guidelines is to continue the services available from the space systems we are now operating; and, to the extent possible, deliver those services so that the ground systems which are now in operation can receive the data with little or no alteration. Advancing technology does force us, from time to time, to make changes which will impact

you, but let me assure you that we do our best to restrain those impacts to the extent we can. We are very cognizant of the investment in ground equipment, and in ground processing systems, that have been made, by all of you, in order to use our data.

We will also be looking very strongly at increasing our capability in the oceanic area. It's quite fair to say that, up to this point, our success has been largely atmospheric; and the success we have had in the oceanic area has been largely serendipitous. The instruments currently in use were designed for atmospheric purposes, and the fact that we have been able to find uses for them in the oceanic area has been fortuitous. With the System-85 studies we will be looking at the inclusion of instruments which are designed to provide oceanic parameters, and to extend, very markedly, our capabilities in the oceanic area.

With respect to a follow-on to Seasat, I can say very little at this time, except that there is consideration being given to the need for some type of continuation, if the Seasat effort is not to be abortive. The kinds of things which are being discussed (and none of these represent decisions; they have not even been submitted for consideration for funding) include a demonstration operational-project; that is, a quasi-operational system to operate for a given period, with the understanding that at the end of it's lifetime it can either be replaced by a fully operational system, or (if it was not a success) be terminated.

I would like to close with just one plea (and I think, in a sense, Mr. Keller also made the same plea); too often, unfortunately, the uses of data from space systems have been linked to particular satellites...there has been a Seasat project, or there has been a GOES project, looking at the use of the data from that instrument on that spacecraft. We need to broaden our view and look at all of these sources of data as complimentary, and work out ways to combine the data from various sources to solve a variety of problems which perhaps cannot be solved by the use of any single one by itself. Thank you.

E. Risley:

Thank you Cliff. Our third speaker is from Canada, Dr. Murray Strome, who holds the title of Chief of the Applications Division, Canada Centre for Remote Sensing, in Ottawa, Canada. He holds a PhD in electrical engineering and he has extensive experience in the area of Landsat data reception systems development; Dr. Strome.

EDITORIAL NOTE:

Dr. Strome's presentation, on behalf of Dr. L. W. Morley, Director General, Canada Centre for Remote Sensing, addressed current barriers to the effective utilization of remote sensing data, and to the realization of benefits potentially available from this powerful technology. At Dr. Strome's request, his remarks are represented here by the prepared text of Dr. Morley.

THIS PAGE

WAS INTENTIONALLY

LEFT BLANK

BARRIERS TO REALIZING REMOTE SENSING BENEFITS

L. W. Morley
Director General
Canada Centre for Remote Sensing
Ottawa, Canada

The advent of earth observation satellites: meteorological satellites, environmental monitoring satellites, resource satellites, data relay satellites, and in case I have left any out - remote sensing satellites, together with the new airborne remote sensing systems is ushering in a new era of ocean and land management. For the first time in man's history, he has (at least potentially) the means for continuously monitoring land, sea and air in a timely and synoptic fashion. True, a lot of this is still on paper; much more research needs to be done, but organizational, not technical problems, are now looming as the major barriers to the skilful management of our resources and control of our environment using both the old and the new techniques. We remote sensors in our naiveté have been guilty of assuming that somewhere out there in our society are the environmental control officers, the end-users, the resource managers and the decision makers who were trying honestly to do a good job but just did not have adequate information and as soon as they got it, their efficiency would increase enormously. After several years of trying to search out these people, we have come to the conclusion that they do not exist, at least not in the whole - only in part in any one person.

Our earth observation and management system resembles a fool who has enormous visual and sensory powers and a brain that can convert the data into information but who is then incapable of making logical decisions for action, based on this information. By this statement, I do not mean to impune our partial resource and environment managers. Our barriers are organizational. We are suffering from an overload of data and information of a potentially powerful nature which our organizational structures are not set up to cope with.

When we are dealing with data whose value does not decay rapidly with time (i.e. mapping) there is time for these data to be translated into information and to weave its way through our outmoded bureaucratic structure before it arrives, sometimes by luck, on the desk of a person who is in a position and has the means to do something about it (i.e. manage). On the other hand, we are not achieving benefits from data whose value does decay rapidly with time (monitoring), because by the time it is analyzed and begins threading its way to some happenstance manager, it's about as useful as last week's newspaper.

In analyzing the value of Landsat data, over the past six years for Canada, proven benefits from slow-decay data are substantial, but proven benefits from analysis of fast-decay data are almost non-existent. The exception that proves the rule is Landsat and NOAA data on sea-ice which will be discussed later. In the extensive potential cost/benefit analyses that were done for ERTS before launch, in both Canada and the U.S., the potential benefits from monitoring far exceeded those from mapping activities. Six years later, after the fact, the reverse proved to be true. In fact the benefits from monitoring in Canada were nearly zero. We must explain why.

Both for weather and sea ice, near real-time data gathering, analysis and dissemination operational systems exist. There are few, if any, real-time complete operational systems for hydrology and flood monitoring, forest monitoring and crop monitoring. The reason that they do not exist is that until satellite and airborne remote sensing, and satellite data relay systems came along, it was not possible to gather data synoptically and quickly enough to make it worthwhile setting up such centres. The fact that such systems do not exist for hydrology, forest and crop monitoring, means that real benefits cannot be realized in these fast data-decay areas.

Let us take the example of forestry. Forest inventory is slow-decay data. A forest inventory map is produced and it is useful to the manager for at least a few years. The remote sensing benefit is determined by calculating how much was saved by using remote sensing methods as opposed to conventional methods. Few seem to ask the question what is the benefit of a forest inventory map, whether produced by remote sensing or conventional methods. It is certainly useful to the timber company manager if he is looking for suitable trees to cut, but is not much use to the government forest manager who is trying to manage the forest for maximum sustainable yield. The information he needs is "change information". What is the change from last year, from last month or last week? His important decisions should be based on change detection. He has to monitor the forests to determine how much was cut from last year, how much new kill has been produced by the spruce budworm, how is the forest regeneration progressing; is the cutting so intensive that it is causing erosion; is the forest dry or wet and what is the fire danger, etc.? This is the kind of change information on which his decisions for action are based.

It was mentioned that the only monitoring activity in Canada that was achieving benefits from Landsat and NOAA imagery is the ice reconnaissance program. Perhaps it is this program that best demonstrates the thesis presented here. This program is properly organized in that Landsat and NOAA Quicklook data are faxed into ICE CENTRAL where the data are combined with aircraft reconnaissance data to make timely ice maps which are then faxed directly to the decision makers - in this case the ship captains. The point I wish to make here is that there is an organization in place capable of receiving quick-decay data, analysing it and getting the useful information out to the end-user.

In water resource management, adequate organizations do not exist to deal with real-time data in an operational way. It is not enough to know the quantity and quality of the water supply. We must know the change in order to regulate and to know the change, we must monitor.

Thus for much of resource and environmental management, change mapping or monitoring is what is required. Before airborne and satellite monitoring existed, it took so long to map, that it was never possible to map quickly enough to monitor.

The objective of land management is to manage in such a way as to maintain the productivity of an area. Here is where we observe the organizational barrier. In a given area, it is a mistake to have one agency responsible for forest inventory, another for forest fire control, another for hydrology, another for forest meteorology. It is better to divide the area into manageable regions and to investigate the monitoring of all environmental and resource data within the region. The actual management responsibility could be split up, but the cost of assembling all the relevant timely data and information should have a common information centre.

A paper on the importance of monitoring was published in "The New Scientist" on 2nd February 1978, entitled "Ecological Monitoring in East Africa" by Croze, et al. In this paper they cite many examples of how monitoring, as opposed to one-time mapping or infrequent mapping, is crucial to effective management. "Monitoring provides important feedback between environmental management and its effects ... Too often policy-makers were handed a geology or vegetation map or the number of livestock ..... by an ecologist who then believed his responsibility had ended."

I could conclude by suggesting that monitoring benefits which are far greater and more important than one-time or infrequent mapping benefits will never be achieved until the organization is set up for monitoring. Interdisciplinary Environmental Monitoring Centres need to be set up in regions of manageable size where all the satellite, airborne and ground data relating to that area are routinely analyzed in such a way as to reveal changes - daily, weekly, seasonal and yearly changes in the vegetation, the water, the rainfall and the temperature, etc., in the hydrosphere, the biosphere, the lithosphere and the atmosphere. All this is now possible for the first time in history and we must organize for it in order to achieve benefits.

E. Risley:

Our fourth speaker is Dr. Irwin Pikus, who has been formally educated in both science and law, holds a PhD in physics, and a JD degree in law. He has spent some 15 years working in the aerospace industry, and is currently with the U.S. Department of State, where he holds the title of Deputy Director of the Office of Technology Policy and Space Affairs. He has participated in the UN-Committee on Peaceful Uses of Outer Space. However, his views today are his own and not those of his agency. He will discuss some of the legal and political implications of space activities; Dr. Pikus.

I. Pikus:

Thank you Ed. Yes, my views today are my personal opinion, and should not be construed as the opinion of the U.S. government or any agency of that government.

We've heard, during the course of this meeting, some very excellent presentations on the scientific and technical aspects of remote sensing. Some of the members of our audience are economists and planners, and they have an interest in the applications of remote sensing to problems of development, commercial needs, and so on.

However, there is yet another community of interest that I would like to call to your attention, although briefly; and that is the community of lawyers and politicians who are interested in establishing a framework within which remote sensing activities might take place, without embarrassing, or causing distress, to any country.

Space is by nature supranational, and therefore it is appropriate that discussions of this legal and political framework take place in an international forum. In fact, to date, most of these discussions have taken place in the United Nations, in a main committee of the general assembly called the UN Committee on Peaceful Uses of Outer Space, sometimes called the Outer Space Committee for short. This committee has 47 members representative of virtually every geographical region; they represent virtually every level of economic development; and every country, except the People's Republic of China, who have launched satellites themselves, are members of this committee. The committee has two sub-committees; a scientific and technical sub-committee, and a legal sub-committee; and the three organs, the committee and its two sub-committees, meet once every year.

The job of the committee is to elaborate a legal and political framework for the conduct of space activities. To date they have produced four documents, or agreements, that have been signed by many nations. The first was the 1967-Treaty on Peaceful Uses of Outer Space, a treaty that provides guidelines to countries, principles according to which countries should conduct their activities in outer space. The hallmark of this treaty is that it is based on providing peaceful uses of outer space, giving benefit to all countries. It is interesting to note that in the United States the 1958-National Aeronautics and Space Act also provides that U.S. activities in outer space are for peaceful purposes, and for the benefit of all mankind. The '67-treaty also renounces sovereignty in outer space; that is, so to speak, there is an open skies policy. No country can assert sovereignty over any sector of space, or any portion of a celestial body.

There are a number of other provisions of this particular treaty. For example, one provision specifies that one may not orbit nuclear weapons, or the weapons of mass destruction. The treaty is a very comprehensive one in the sense that it deals with many many aspects of space activities, but it is also a general treaty.

The efforts of the committee have, since 1967, been devoted to elaborating various portions of these activities in space, and to formulating other additional agreements. For example, in 1968 there was opened, for signature, an agreement on rescue and return of astronauts and the return of space objects. In 1973 there was opened a convention on liability for damage caused by space objects. In 1976 there was opened a convention on the registration of objects launched into outer space. So you can see that this committee has been rather busy.

It's current deliberations are focused on several very interesting and important matters. For example, the question of direct broadcast of television by satellite has been occupying this committee for some time. As you can imagine it raises many questions of national interest. There are negotiations aimed at providing a treaty on the moon and other celestrial bodies. This is also a rather difficult matter.

There is a question as to whether the geostationary orbit, which obviously lies in outer space, is deserving of any special consideration or any special legal regime. And, of course, there is an effort (which has been going on for several years now) to elaborate a set of principles to guide the remote sensing of the earth and its natural environment.

Today I would like to very briefly note several of the more important issues pertaining to remote sensing that arise in this UN-context. I don't expect that we will be able to resolve them, they have not been resolved by the lawyers and politicians in their debates, and the reason I mention them is that I think it is important that there be discussion among the various communities of interest. The lawyers and politicians would do well to understand more of your discussions in scientific and technical areas, and I think it would be useful and perhaps interesting, to you to know something about the issues that the lawyers and politicians find curious and interesting.

The first issue is one that has not, as yet, been discussed to any great extent in the outer space committee. I guess we are not at the point where it really is a burning issue; but in the '67-treaty there is a provision made for the conduct of activities in space by non-governmental entities. In other words, private sector individuals, corporations, universities, or foundations can, in fact, conduct activities in space, provided that their governments authorize and continually supervise these activities. No set of criteria has yet been evolved which defines the basis under which such authorization should be granted, or on what basis such control should be exerted or supervision exercised. This matter has not yet been discussed to any great extent, but it no doubt will be, as time goes on.

A much more difficult, and thoroughly debated, issue is the question of the dissemination of data. We've seen, from the inception of the Landsat program, a very wide dissemination of data. Data has been available to anyone who wants it, first from the EROS Data Center, and more recently, from the various ground stations.

It's my feeling that this wide dissemination has provided the basis on which we have progressed so far in the technical and scientific studies that you have been supporting. I shutter to think of what might have happened if the data had not been available as broadly. It would have meant a very small community of scientists working on these problems, and I think that would certainly have hindered the development of remote sensing.

However, a number of countries look forward to the time when the resolution of available data will be very much improved, to the extent that it might in fact show things that could perhaps embarrass the country, or could serve to the disadvantage to a country, were it widely known.

I think everybody understands that this is a possibility. However, many countries believe that it is premature to try to regulate this sort of thing; that we really should wait until we see the scope of the problems, if there are to be any; and try to regulate on the basis of some specific knowledge of such problems. This is really a central issue in some of the debates in the UN, and I doubt that it will be easily resolved.

I think everyone has agreed that at least the "sensed state" should have access to the data. Certainly the "sensing state" is going to have such access. The real question is whether data should be disseminated to third states, with or without approval of the sensed state.

The resolution of Landsat imagery is said to be of the order of 80 meters. Of course this is the instantaneous field of view. There is some controversay within the UN, even within the scientific and technical subcommittee of the UN, as to what resolution really means. We are, after all, interested in the resolution of an image in a political and legal sense, something perhaps more difficult to define than in the case of a particular technological specification. I think this is an area where some good scientific examination would be very much appreciated by the community of lawyers and politicians.

We hear talk about the question of photographic resolution and its comparison with the size of pixels; and whether there should be a particular spatial resolution which is indicative of the level of sensitivity of individual nations. Should we vie for some regulation in the future, should that regulation be based on spatial resolution or are there other parameters which might be more important or more pertinent? Is spectral resolution important, and if there is to be regulation, how should that be factored into the criteria.

The third issue that I would like to briefly mention, is the question of the legal status of information developed through utilization of remotely sensed data. In the UN we have found it convenient to discuss data in two forms. One is called "raw data" and that includes raw data coming down from the satellite, preprocessed, and processed data. Another category is what we call "analyzed information", which is the result of one's effort to take the raw data from satellites and combine it with data from other sources, or models of one kind or another, or his own inate intelligence, and create some piece of information that has intrinsic value.

Some countries assert that the information developed about the natural resources of a country is as much under the soverign control of that country as are the natural resources themselves. This seems a rather anomalous point of view, but it's one that is subscribed to by many countries. On the other hand, there is the problem of one's work product. If one expends a certain amount of effort, and is creative, one generally can have some proprietary interest in the results ofone's labors. The central question is how does this proprietary interest square with the interest of countries, and information pertaining to their natural resources.

I don't want to belabor these points as we can discuss them in some detail, if you are interested, during the discussion period; but I think it is important for you to be aware of the fact that there is such discussion underway in the UN. I appreciate the opportunity to discuss these points with you. Thank you.

E. Risley:

Thank you Irv. Dr. Pikus has mentioned some of the formal relations between countries. Our next speaker will offer some reflections on the possible role of individuals...people who identify themselves as members of an international remote sensing community. Mr. Jelle Hielkema is a citizen of the Netherlands, currently on sabbatical leave from the UN-Food and Agriculture Organization. He holds a degree in soil science and has worked on the utilization of remote sensing techniques for desert locust survey and control; Mr. Hielkema.

J. Hielkema:

Thank you Ed. Ladies and gentlemen, I wish to state explicitly that my remarks here this afternoon are own own personal views as a private citizen... The content of my presentation should in no way be regarded as the official views of the Food and Agriculture Organization of the UN, by which I am employed.

EDITORIAL NOTE:

Mr. Hielkema's subsequent remarks are represented herein by prepared text, supplied via the session chairman, subsequent to the symposium in Manila.

One of the skills necessary in modern life is not to get frustrated. To develop and maintain this skill is difficult in our timeframe where we become increasingly dependent upon each other, on both personal and group levels, in national, regional, and even global contexts. Before continuing to work this out in relation to the International Remote Sensing community, I would like to state a few facts on which I think we can agree after all that has been presented to us during the last few days:

1. Satellite remote sensing is with us, we like it and it is here to stay.

2. Remote sensing is rapidly becoming a field of its own although it should not be seen entirely apart from the subject fields which it is meant to serve.

3. Satellite remote sensing is by definition of an international nature by way of its uniform, repetitive global coverage.

4. The biggest applications potential lies undoubtedly in the developing countries whereas the major applications development is concentrated in the industrial countries.

5. There is growing pressure for operational satellite remote sensing systems which guarantee timely data-availability in various formats on a global basis.

6. All of it is just beginning and the next decade will strengthen this new technology considerably and provide the user community with unprecedented capabilities to inventory and monitor the earth's natural resource base. We are working here in a field with only a little past and a lot of future.

In our language we have a saying which as follows: "de wrâld is ûzes mei elkoar". I assume that there is nobody in the audience who speaks this language but this saying can be translated as: "the world is ours together". The true meaning of this saying is that we, altogether, are responsible for each other's well being and that we should take care of this planet in a concerted, common approach. It is hard to think of a technological development whose initial use has spread so widely over a period of a half a decade and which may if properly used, have such an impact on man's ability to monitor and control his natural resource base on which we become more and more dependent.

However the six points mentioned earlier, contain several problem areas, which if we neglect to look into, will make especially the operational users community suffer from serious frustration in the years to come. Furthermore the most hard hit users will be those in the developing countries where the applications give the biggest return.

The U.S. Government deserves considerable credit for, firstly, developing an earth resources satellite system, including both the Landsat system and the polar orbiting and geosynchronous weather satellites, and secondly, for maintaining a completely open policy concerning the availability of data from these

systems on a worldwide basis. Furthermore NASA's extensive principal investigator program, the activities of the EROS Program, the United Nations seminars and training courses, the twelve sessions of this very successful symposium, the program of the U.S. AID and other international development agencies, the bilateral activities of universities and private companies have all contributed to the present state-of-the-art and the worldwide excitement about the use of this new technology.

However, after some six years of "show and tell", of worldwide experimentation and assessment of possible operational uses of earth resources satellite data, the time has come to rethink the serious issues facing us in the years to come, to determine where we stand, and to determine where we possibility want to go. Professor Adelman from the University of Maryland has rightly pointed out: "The historical record of technological developments is not a favourable one from the point of view of equity. The benefits of remote sensing, when current developments are extrapolated into the future, will serve only to make the rich even richer and the poor still poorer."

In light of this grim forecast, I consider that we all should, with whatever means are available to us, strive to insure that this technological development does not turn itself against man who invented it. We must make sure instead that it is truly used for the benefit of all mankind as expressed in the concepts developed by Pecora and Udall when defining the Landsat system.

In order to give some idea of the magnitude of the technology of the next few years, I should like to summarize for you information about on-going satellite system development. In the United States no less than five unmanned satellites, which will orbit and sense the earth for different purposes, will be launched this year. These are, in succession:

a. Landsat-C, successfully launched and put into orbit on the fifth of March, is largely comparable to Landsat-1 and -2. New features which should prove of considerable interest are the added thermal band on the multispectral scanner and the 40-meter spatial resolution, panchromatic, Return Beam Vidicon (RBV) Camera System which is essentially a new sensor because of the limited experience with a comparable RBV system on Landsat-1 and -2.

b. TIROS-n, scheduled for launch in late May but likely to be delayed, is the first of the next generation of polar orbiting weather satellites with considerable improvements over the current series of NOAA satellites. TIROS-N will be an all-digital system and will carry a one-kilometer resolution, multispectral sensing capability with a six-eight hour temporal interval.

In this connection I would like to remark that whereas the satellites of the Landsat system have clearly been oversold, for a variety of applications, both the polar orbiting and geostationary weather satellites have certainly been underrated. In my work I use data from both systems in a complementary way with considerable success.

c. Heat Capacity Mapping Mission (HCMM). This new experimental single sensor satellite will carry a one channel thermal sensor with a ground resolution of 500 meters. Its orbital configuration has been chosen in such a fashion that it will pass over the same area on earth at the peak of the diurnal heating and cooling cycle, enabling the mapping of thermal inertia properties of earth surface materials and monitoring of large area soil moisture changes in cloudfree areas.

d. Seasat-A. This will be an all weather day/night satellite primarily designed for observations of ocean dynamics. The satellite, scheduled for launch in the next month or two, will carry five sensors. One of the most interesting, both for oceanic and terrestrial applications, is the 25 meter L-band, synthetic aperture radar.

e. Nimbus-G, an experimental satellite designed for studying coastal environments with its 10-channel narrow band scanner, is to be launched in August, 1978.

Looking somewhat beyond this year but not further than 1981, two more significant developments need to be mentioned.

1. Space Shuttle/Spacelab. A new era will be entered in orbital remote sensing with the operations of the Space Shuttle launched into space as a rocket and returning to earth like an aircraft. The Shuttle will be a re-usable spacecraft capable of putting both manned and unmanned missions into orbit, performing repair-and refurbishing missions and likely to make satellite remote sensing considerably more cost effective and flexible.

2. Landsat-D. The first of the next generation of high resolution earth resources satellites will be launched in 1981. New improved sensors will be carried by Landsat-D in addition to the existing multispectral scanner. A new instrument, called the Thematic Mapper, will sense reflected radiation in seven carefully chosen spectral bands, with a ground resolution of 25 meters, increasing the data rate when compared to Landsat-1 and -2 by a factor of seven.

For researchers equipped with sophisticated image analysis facilities, Landsat-D will be the fulfillment of a dream. However, for the poorly-equipped operational user, although deeply convinced of the importance of using satellite data for his particular application, it may turn out to be a nightmare.

Here I come to the point of my first major concern; the global political-economic issue. It is not the principle of developing, launching and operating satellite systems that is at question but rather how to make all these billions of data bits effectively available to the global remote sensing community for the best use in discipline oriented applications. In addition to the activities of the United States, other industrialized countries like France, Germany and Japan have developments underway for launching their own earth resources satellite systems. This will further increase the total data rates. Remote sensing programmes may become a highly competitive rather than cooperative business at the expense of the data user community.

Obviously there can be serious compatibility problems which will put a severe constraint on the exchange of data and experience. The more serious problem for international relations is the fact that the existence of different national satellite systems with increasing spatial resolutions is likely to create areas of political sensitivity. I feel that it is the responsibility of the international remote sensing community gathered here, among others, to inform and convince national government authorities that this technology, when jointly developed and used for common purposes can tremendously help us. Equally, when manipulated and misused it can seriously hurt us and lead to international frustration and tension.

I feel further that after this considerable period of worldwide experimentation it is time to take steps to pull resources and expertise together and to develop meaningful applications at various levels of scale be they national, regional or global. I believe that we in the remote sensing community are quite convinced that we are faced with serious resource management problems on this planet and that remote sensing offers tremendous potential for coping with many of them. Therefore, it is only reasonable that we who understand the implications of remote sensing technology should initiate steps towards solving these problems. I am convinced that, given the present situation of the global economy, the benefits of satellite remote sensing will not finally be evaluated on the basis of scientific merit or interest but on the number of cost-effective applications for alleviating distress, especially among the less developed countries.

Technology transfer is a second problem area.

We will find ourselves very soon in the situation that we have enormous amounts of raw data gathered by various satellites sitting in centralized archives. We want to distribute, process, analyze and utilize this data and develop applications for its best use. As far as the developing countries are concerned, we envisage to do this by appropriate technology transfer. This symposium has clearly demonstrated that Landsat is an appropriate tool for a variety of applications but also that there is still a long way to go for another and much bigger variety of applications. The LACIE programme has shown the world that early forecasting of global wheat production is still a far cry; and that has been a costly message.

If we really want to undertake a serious attempt to help the developing countries absorb this technology for meaningful applications, we will have to pay more attention to the process and structure of the way by which this transfer will have to proceed. In the majority of the developing countries no framework, neither in terms of facilities nor in terms of personnel, was and still is available to immediately incorporate the new technology at the desired levels. At this time nearly every country in the world has some experience in the use of satellite remote sensing data however, the range or spread of levels of experience between countries in the same geographical region is striking if not to some extent alarming.

It is at this point that we really can start the transfer of technology in an appropriate way, now that philosophies of how to make best use of the available data types have had time to grow and can be seen in the right perspective of their potential. However to accomplish this second phase of transfer of technology, we have to take an in-depth look at the processes involved. What we have shown very much in the past was an eagerness to sell the technology and no doubt with the best of intentions. What we have lacked very much was the highly necessary followup and aftercare once a project or a training course has finished. In order to accommodate this much acknowledged problem better in the future, we will have to sit down together and rethink our development strategies in this field. There are considerable sources of experience on both sides which, if they can meet in a pragmatic and technical environment, can generate substantial positive development.

International cooperation is a third problem area.

Satellite remote sensing provides us with a unique and very powerful means to assess common problems at various selected scales like deforestation, desertification, waterlogging and salinity, flooding, insect infestations, etc. At the same time it forces us to very close international cooperation in projects which address these problems.

In the domain of earth resources satellite remote sensing considerable international dialogue will have to take place. There will have to be definition of common goals and objectives concerning the establishment and operation of both space and ground segments of future operational satellite systems. I feel this dialogue should start as soon as possible and, again, that those who constitute the global remote sensing users community should take an active part and perhaps a lead in this process. This can only successfully be achieved when the global remote sensing users community is willing and able to organize itself in a permanent body with international recognition. I view such a body as an international but in principal strictly technical forum where producers and users of this technology can meet in an unbiased way. If such a body should take shape in the years to come, groups of scientists and technicians would be enabled to work out meaningful cost-effective applications and implement them under the guidance of the national authorities involved.

Such an independent international forum could fulfill a number of important functions which I would like to summarize here.

1. Create a permanent working environment rather than a meeting place, for the international remote sensing community (the annual meetings of this symposium take care very well of the meeting requirement).

2. Examine and create ways and means which should lead to more effective and higher rate of technology transfer. With this I mean to say that considerable effort should be made to line up resources, expertise, and executing agencies.

3. Provide feedback from the users community to the technology producing agencies for definition of future space systems.

4. Create a place where technical disputes between groups or nations can be solved without going directly to a highly political environment. I often have the feeling that meetings end up in political disputes because of the sheer lack of technical arguments and understanding.

5. Coordinate global and regional activities in the field of remote sensing to avoid duplication and coordinate input to efforts to define a multilaterally-funded, operational earth resources satellite remote sensing system.

6. Organize an efficient system for storage and retrieval of worldwide research results in this field and manage a system for dissemination of this information.

7. Provide unbiased assistance to developing nations regardless of political background and assist in the establishment of national remote sensing bodies and technical facilities.

8. Provide a much-needed information channel to the general public. It is astonishing how seldom people can place you when you tell them that your work is in the field of remote sensing. In the end it is for the general public that we work and how can they appreciate our efforts without any reference framework.

I was extremely pleased with the proposal of President Marcos in his opening speech calling for an international forum to promote and coordinate international activities in this new field and I think this objective should be pursued without delay. It is quite clear that this cannot be accomplished overnight and it should not be done that way. What I would like to come out of these days, at the Twelfth Symposium, of learning, listening and talking is a consensus of opinion that there is enough interest to identify a small international group which will agree to sit down and study the various issues at stake now and in the years to come. This group could communicate over the next twelfth months and report to the next session of this symposium in Ann Arbor. From there, a next step could be taken for implementation of a carefully structured approach to the certainly not easy task of the institutionalizing of this new technological field.

E. Risley:

Thank you Mr. Hielkema. I have asked the Chairman of the Department of Geography at the University of California, Santa Barbara, Dr. David Simonett (chairman of this morning's Session 13) to react to some of the remarks he has heard during this session. At this point I would like to turn the microphone over to Dr. Simonett.

D. Simonett:

Thank you. In view of the fact that time is running along, I will be as brief as I can. Two speakers today have addressed the fact that benefits are increasing and that costs, relatively, are going down. Having been through the trauma of the principle scientist engaged in (what is notorious in the United States) a very conservative cost benefit evaluation, I can only echo that statement.

It is quite apparent that the best of us, at the best of time, are very inferior in making judgments of the future. When we are forced, through the cost-benefit-analysis, to rely upon the judgments of people who are new in the field, and in many instances have to protect professional investments in other ways of doing things, we automatically handicap the procedure. If I were to leave you with one warning...be very careful with cost benefit analysis.

Second, both Dr. Spohn and Mr. Hielkema made a point that I must say I completely echo...the benefits of meteorological satellites are essentially underrated. If I were to make one firm prognostication of the future it would be: a decade from now we will be measuring our success by the degree to which meteorological satellites bear the burden of analysis and costs, because they are intrinsically the low cost elements of the system.

I have one comment about the issue that Mr. Hielkema raised, using Irma Adelman's work at the University of Maryland...it is a serious business. We are engaging in high technology, and Irma has emphasized, from her studies of 25 developing nations over recent years, that during the last two decades there has been, in those 25 sample countries, a net transfer of wealth from the poorer 60 percent of the population to the upper 40 percent...if they were resource rich. In other words, in countries which have large mineral resources, there is a net possibility of transfer of wealth. It is a concern that I think we all have to think about.

There is another concern, of equal magnitude, that worries me very much; and that is that this flood of information is potentially going to open up, much more rapidly than would ordinarily be the case, a vast array of tappable natural resources. Rather than benefiting the developing world, this may actually act as a net "disbenefit," by producing so many available natural resources that international prices are reduced. This would act as a net transfer of wealth from the developing world to the developed world, comparable to what happens when coffee prices go down and a net transfer of wealth, from the developing world to the developed world takes place, which is greater in magnitude than all the U.S. AID programs over the last decade.

The final points I would like to make relate to the question of internationalization and disaster. A great deal of the technology transfer to date has been government to government. One of the things that is characteristic of the developing world is the small number of able scientists, although it is growing, and the fact that such persons are at a great preminum. Being in such demand they constantly get job opportunities and move up to better jobs; they manage; they no longer do themselves. Further, they manage different things than they were trained to do.. If I were to make one recommendation to international agencies it is: Remember the universities; they are in the business of training the next generation. If we continue to train only government people we will have a much slower "trickle-down" of the technology.

The final point is there are some areas of international development where perhaps the remote sensing technology lacks that concern I have just expressed about net transfer of wealth and net disbenefits. One example of this is in the area of international disaster assistance. Brazil, under United Nation's auspicies, will be running a UN-funded seminar on international disaster assistance, and the relationship of remote sensing to such assistance in October and November of this year. There are, from discussions I have had with a number of you, very real benefits in this area. Those of you who have ideas which you would like to call to the attention of a U.S.-National Academy of Science committee, currently looking at these issues, are urged to communicate to me your interest, knowledge, and concern in international disaster assistance, and the role to be played by remote sensing. Thank you.

E. Risley:

Thank you David for your thoughtful observations. I would now like to call on Mr. William Fischer, Chief Scientist of the EROS program of the USGS, and well known to many of you; Mr. Fischer.

W. Fisher:

I think it is perfectly evident that the technology is available to go anywhere we wish to go; Dr. Simonett and Dr. Spohn have made that very clear. I do want to comment on the very excellent policies that Dr. Spohn described, concerning the planning of new systems that won't impact too heavily on the ground systems that are currently owned and operated by other nations. I think this policy should be emulated in all of our planning.

I personally think Dr. Strome has an excellent point in asking why we are not using this technology in a monitoring sense. Perhaps we have to go back further, and begin to inject into our educational process, an understanding of dynamic phenomena, something normally not taught.

Another thing which should be noted is the need for continuity of data. We have to be assured the data are coming before we change our mechanism of monitoring. We can't fire all the people who are riding horseback over our national lands until we are sure that the satellite is going to be up there. I think this is a most important point.

There certainly needs to be more training. Traditionally, in the past this responsibility has shifted to the university, in time. The government has served only in an interim sense, and I suspect that this will continue to be the case. I would like to see the universities more and more involved, and I think this is true with everyone in government.

The major problem, of the future, as I see it, was touched upon by our friend from the State Department, that is, continued open availability of data. I think this is the most critical issue we are going to face in the next 10 to 15 years. It's political, in a sense, but it's highly desirable if we are to maintain significant remote sensing programs of an international nature, and if we are to head toward a goal of peace. Thank you.

E. Risley:

I'd like to ask if any of the panel members have supplemental comments they wish to make at this time; Dr. Strome.

W. Strome:

I would just like to echo one comment which others have alluded to, and some have mentioned. I would like to emphasize what, all too often, people in the remote sensing community seem to forget, that in most information systems remote sensing data represent only one piece of the puzzle. There are many elements to any kind of information system. If you want to do a management job, remote sensing data will be only one element. All too often we try to solve the whole problem with remote sensing alone. This, in turn, serves two purposes; one, it reduces the chances of success, and secondly, it tends to create greater aleniation of the user. Also, I would like to echo Mr. Fischer's last comment, although actually I feel in having attended some of the same meetings as Dr. Pikus, that in fact, the climate is improving. As more and more people become educated in the benefits and in the value of available remote sensing data, I see less and less resistence to the idea of a free dissemination of information. Thank you.

E. Risley:

If there are no more comments from the panel, I would like to thank the members who have given their time for their remarks here today and also to thank you for your patience. We are not closing the meeting at this point... instead we're opening it to the floor. If you have specific questions I would prefer that you come forward, at the end of this session, and talk with appropriate panel members. However, at this point, I invite anyone who may have a brief statement that they would like to make to come forward and identify themselves. Do we have anyone who would like to supplement, or react to, the remarks you have heard in this session? Dr. Vincent.

R. Vincent:

I would like to express my appreciation, first to the government of the Philippines and the Philippine people for their great hospitality; and second, to thank those of you who are speaking English as a language other than your native tongue. We who suffer from a monolingual plague very greatly appreciate that you are speaking our language...because we can't speak yours. It's not unappreciated that you should make such a sacrifice and try to speak so that we too can understand. Finally, to a certain extent, I disagree with a point expressed by Dr. Simonett. I think that geologists in particular recognize that we are only buying time until our energy resources and natural resources have been depleted to the point that we must devise alternative sources of energy, and hopefully, begin recycling our natural resources. I personally would like to see an acceleration in the discovery of natural resources, and if developing countries choose to hold their resources back for better prices in the future this is fine. However, I think that these decisions should be made on improved information rather than in ignorance of what new natural resources are available. I would say that geologists, in particular, need all the help they can get from this accelerated discovery of natural resources, and that satellites have certainly been a great aid in this regard.

E. Risley:

Thank you Dr. Vincent. Are there any other statements? Dr. Cook.

J. Cook:

Although not directly related to this afternoon's session, I would like to make a few brief announcements, and also to introduce certain other participants here today who wish to take this opportunity for brief remarks concerning different but related issues, which have arisen during the current meeting, or are related to future meetings in this series.

First, there are various rumors floating about, some valid, some not so valid, concerning a move, initiated here in Manila, toward organization of an international society for remote sensing. Among these rumors, perhaps the most valid is concerned with the meeting of an ad hoc group of participants, interested in the feasibility, as well as the possible nature and potential benefits, of such a society.

While I have been unable to attend all of the meetings of this ad hoc group, having been occupied with a variety of other matters during much of this week, and am therefore unaware of the intricacies of all that has transpired, I believe Dr. van Genderen, as one of the primary spokesmen for this group, is prepared to outline briefly the recent developments in this regard. It is my understanding that Dr. van Genderen would also like to speak briefly on behalf of a currently existing society, which has its' present headquarters in the United Kingdom, but which I am informed is quite international, both in make-up, and in its' constituency. Thus, without further ado, I would like to introduce Dr. John van Genderen, General Secretary of The Remote Sensing Society, as

well as a member of the Program Committee responsible for organizing this Twelfth Symposium; John.

J. van Genderen:

Thank you Jerry. Ladies and gentlemen, I am going to speak very briefly, and not just on behalf of the Remote Sensing Society, but also on behalf of the ad hoc group which has been discussing the whole question of the need for an international association for remote sensing, to cater to the needs of the remote sensing community, internationally. It was felt that this would be a good opportunity to initiate action along these linges, as we have, here in Manila, a very distinguished international gathering, and it is hoped that the enthusiasm generated by this meeting can similarly generate action to further the objectives of meeting our needs for an international society of remote sensing. The ad hoc group has discussed and explored various possibilities and alternatives, and concluded that one of the more practical is, in fact, to proceed within the framework of an existing remote sensing society such as that currently based within the U.K. This society already has a constitution; it already has a secretariate; library facilities; etc. This alternative would alter the existing society according to the needs of the remote sensing community, along various lines depending upon what its members require.

Among the methods that have been proposed to take advantage of this gathering, and to initiate action toward organizing an international society can already be seen outside this room. I notice that there are at least 50 or 60 names already on a sheet, which has only been circulated for a few hours, concerning the creation of an Asian remote sensing society. We would encourage you, if you are interested in supporting an international association, the exact form of which is perhaps at this moment not very clearly defined, to sign one of the sheets available at the registration desk. It's only by setting up national or regional associations that you, as a remote sensing community, can become better organized; and we can begin an interchange of ideas, of information, and of development in the various regions, and proceed toward establishment of a truly international society for remote sensing.

As you know there are already various journals devoted to this subject; there is already the International Symposium, of which we are attending the twelfth meeting at the moment; and it is hoped that, in some way, we may be able to integrate these various and diverse aspects into a logical and coherent framework to serve the needs of people interested in keeping up to date with trends in remote sensing.

Many of you have seen the brochure and the products of the existing Remote Sensing Society, such as its' newsletters and its' annual publications. To meet the needs of many of our overseas members, there would, of course, be a need to change this society; your requirements will be different than ours. However, I think one of the best ways to change this is to join the society. Membership gives you voting rights; it allows you to nominate your own regional representatives to the council; and it thereby allows you to change the society in which ever way you think is most suitable for its development and growth. So, without much further ado, I would encourage you all to sign the appropriate forms available at the registration desk before leaving Manila; and perhaps we will have an opportunity, at the next symposium in Ann Arbor, to evaluate the progress that has been made in the various regions. There are sheets available for Asia, Southeast-Asia, South America, North America, and various other regions. We will then have an opportunity, at our next assembly in Ann Arbor, to evaluate these developments and to determine what further action to take.

I would like to thank the organizers of this meeting for the opportunity to have introduced this topic to you. Finally, I think it's very unwise to make

too definite a recommendation at this stage, because much thinking remains to be done. However, I feel as a first step all of you should become more active in joining a society in order to foster our common goals of a better information exchange in the field of remote sensing. Thank you.

M. Strome:

In regard to the ad hoc group to which both Jerry and John have referred, perhaps it is worthwhile to let you know who the people are who have been spending considerable time at this conference, talking among themselves, and with a number of you, about various needs and alternatives for an international remote sensing society.

This ad hoc group was somewhat variable, and included different people from time to time; but some of those involved were myself, Jerry Cook, Ed Risley, John van Genderen, Jim Moore, Klaus Volger, Bill Fischer, Arch Park, Dr. Roque, and others I may have missed...I apologize. Perhaps I should rather apologize to those I've mentioned.

Nevertheless, I do want to explain why we have not made the suggestion that, right now, we form a new international society for remote sensing. I feel many people will wonder about that, since that is exactly what we started out to discuss. But I think some, perhaps many, of us had some reservations... perhaps I should note that none of us, except John van Genderen, is now a member of the Remote Sensing Society of which John has spoken...and I think many of us have reservations about giving a further boost, if you like, to this particular society over another, or successor, organization.

We did receive assurances from John that certain changes could be made in the existing society, to further enhance its' international character; and we, as a group, have made certain commitments toward fostering the development and realization of a truly international society.

I would like to have John explain some of the changes, or commitments to change, which he feels would make the existing society take on, what we feel would be, more of an international character. I think John would argue that it already has this international character, and while this may be true, to some of us it doesn't have that image. Perhaps John could take a minute to explain what they propose to do.

Finally, before I leave the podium, I would like to reiterate that a number of people in different areas have expressed an interest in organizing regional remote sensing societies. Since all of us in this ad hoc group feel (and I think the sentiment is shared by many of you here today) that local, regional or national societies should be encouraged, we urge you to help these regional organizers by signing one of the appropriate sheets in the lobby. Thank you.

J. van Genderen:

I shall try to respond very briefly to Dr. Strome's request by noting that the existing Remote Sensing Society will try to cater to the needs of the international community, firstly, by an invitation for every member from overseas to propose nominees for the council, and in this way to make the character of the society more truly international. The council also has the right to coopt members, and we shall certainly recommend that more international members be coopted onto the council. However, the main council is an elected body, and it is up to the international members to nominate and to vote for members from various regions.

Negotiation for an international journal is another point that has been raised; and this negotiation will take place immediately on completion of this

symposium. We will negotiate, first with Elsivier, who currently produce the journal "Remote Sensing of Environment", to see if there is some way that this can become an official journal for the international community, through the Remote Sensing Society, or through other regional remote sensing societies.

To show that the existing society is not just a 'UK-society', although it was founded in the United Kingdom, we will actively set about the formation of regional chapters (to use the American term for this...we would call them regional associations) which will be associated in some way, under the Remote Sensing Society, as the society already has the infrastructure and secretariat to provide the necessary support facilities.

Finally as to the question of actual society headquarters...at the moment it is in the UK. Some people have asked why isn't it somewhere else? I think this is a matter for discussion, and not for us to debate at this time; since, if it is moved somewhere else, we would have the same situation. Is it an American society if we move it to Ann Arbor? Is it a Japanese society if we move it to Tokyo? Here again, I think that is up to the members to decide. Thank you.

J. Cook:

Thank you John. I'm sure there is little doubt in any of our minds concerning the gratitude we would like to express to the Philippine government, and to the Philippine people, who have been our hosts here the past several days. However, most of us will not have the opportunity to do so personally. Here to speak for the Latin American participants attending this Twelfth Symposium is Brigadier Miguel Sanchez Peña, Presidente, Comisión Nacional de Investigaciones Espaciales, the National Commission on Space Research, Buenos Aires, Argentina; Brigadier Peña.

M.S. Peña:

Mr. Chairman, Dr. Cook, ladies and gentlemen; on behalf of the participants from Bolivia, Chile, Columbia, Costa Rica, Mexico, Peru, Suriname, and the Interamerican Development Bank, and on behalf of the government of Argentina, I would like to express our most profound appreciation to the Environmental Research Institute of Michigan, ERIM, and to the Natural Resources Management Center of the Philippines, for the very effective job they have done in planning and carrying out this Twelfth International Symposium on Remote Sensing of Environment. We would also like to thank the Government of the Philippines for their assistance and cooperation in having facilitated the organization of this symposium in Manila.

For all of us who have attended the numerous sessions here for the past few days, it has been an enlightening experience, both from an academic, and a practical point of view. We realize from the participant's presentations and comments, and the poster sessions, that the task ahead is quite challenging, especially when we consider the role of this technology in meeting the needs of the developing countries.

Above all we want to send a special message of gratitude to the people of the Philippines, for their constant kindness, and the warmth of their hospitality which has meant so much to all of us who have traveled half way around the world to participate in this international event. We shall not forget such human kindness, and we take this opportunity to reiterate our desire to reciprocate, in the nearest future, by having all of you attend a future Remote Sensing Symposium in Latin America. Our Latin American countries are open, and although it will be very difficult for us to be more kind or to surpass the hospitality we have had here in the Philippines, we welcome you.

Once more, thank you very much for your hospitality.

J. Cook:

Thank you Brigadier Peña. Following that most gracious message on behalf of our Latin American participants, and Brigadier Peña's invitation to all of you to attend a near-future Remote Sensing Symposium in Latin America, I am pleased to announce that the Executive Committee for this series has recently received, and unanimously accepted, an offer from the Government of Costa Rica, to hold the 1980-Symposium in San Jose, Costa Rica.

With us here today, to make this announcement official and, I'm sure, to once again invite you all to attend the 1980-Symposium in San Jose, is Ing. F. M. Rudin. Director, Instituto Geografico Nacional, Costa Rica; Ing. Rudin.

F. M. Rudin:

Thank you Mr. Chairman; distinguished members of the committee, ladies and gentlemen. Last year Costa Rica requested to be considered the host of the Fourteenth International Symposium on Remote Sensing of Environment, to be held in April 1980. Today the Executive Committee has made their announcement, selecting San Jose as the site for this event. The Costa Rican government would like to thank the committee for their decision, and at the same time, extend an invitation to the remote sensing community, all of you, to come to Costa Rica to meet in April 1980, where we will sincerely say to all of you "Bienvenida a Costa Rica". Thank you.

J. Cook:

Thank you Ing. Rudin. I should point out that, while final negotiations regarding the site for the 1980-Symposium are not yet complete, I have every reason to believe they will be finalized in the very near future. Thus, we will return to Ann Arbor, for the Thirteenth Symposium in April 1979, and then meet in San Jose in April 1980.

I would like to extend a personal welcome to each of you, both to Ann Arbor in 1979, and to San Jose in 1980; and assure you we will do all we can to provide as fine a meeting there as you have experienced here in Manila.

In regard to the latter point, this 1978-Manila Symposium, Dr. Roque and I began the organization of this event slightly less than one year ago today, with neither of us quite sure of where it would lead, or just what the outcome would be. I can only say, from my viewpoint, I could not have been more pleased; we could not have selected a better site than Manila, for our first non-U.S. symposium. This has been a truly monumental event that is rivaled, if at all, only by the first of these symposia, held in Ann Arbor, back in 1961; we all know where that meeting led.

On behalf of the Executive Committee, the Program Committee, and especially the participants here today, I would like to express our deepest gratitude to Dr. Roque and his staff. I think they deserve a rousing ovation.

C. Roque:

On behalf of the staff of the Natural Resources Management Center and the Government of the Philippines, I thank you, and extend our gratitude to all of you for giving us the opportunity to host this symposium. If there were any short comings, I apologize and beg your forgiveness; this is the first time my staff has undertaken a task like this. If we do it again we promise to do better. Thank you and "Mabuhay".

THIS PAGE

WAS INTENTIONALLY

LEFT BLANK

REPORT ON COMMERCIAL EXHIBITS

Sixteen corporations from five different countries participated in this year's Commercial Exhibits Section.

Because many of the close to 800 scientists and decision makers from over 50 countries had yet to see such a broad diversity of remote sensing technology centralized in one location, the Commercial Exhibits Section of this year's symposium was undoubtably one of the highlights of the meeting. The following is a report on the exhibitors' activities.

THE GENERAL ELECTRIC COMPANY, Earth Sciences Applications, 5030 Herzel Place, Beltsville, Maryland, U.S.A.

The General Electric exhibit was in three parts. The central section was dedicated to a 40" diameter mosaic of the Republic of the Philippines made up of color balanced Landsat imagery. Around the mosaic there were selected photographs and imagery of the Landsat system and remote sensing applications. The sections on each side of the central mosaic stressed the applications of remotely sensed data in the form of enhanced thematic imagery and display a typical Landsat ground station including descriptive schematic diagrams. Special printed handouts were available stressing the benefits of remote sensing and describing the basic design features of a ground station. The folder enclosing the handouts also had the Philippine mosaic on the cover.

DAEDALUS ENTERPRISES, INCORPORATED, P. O. Box 1869, Ann Arbor, Michigan, U.S.A.

The Daedalus display for the Twelfth International Symposium on Remote Sensing of Environment featured its digital multispectral scanning system. Display boards showed direct comparison with Landsat data and scanner data acquired by the Daedalus DS-1260 scanner flown in high altitude jet aircraft.

Also displayed was product information on Daedalus' new maritime patrol scanner, the model DS-1220/MP. This scanner is designed for dual channel operation in both the ultraviolet and infrared spectrums, and is currently used operationally for coastal surveillance by several countries.

NAC, INCORPORATED, 17 Kowa Building, No. 2-7, Nishiazabu, 1-chome, Minato-ku, Tokyo, JAPAN

NAC's exhibits contained demonstration items of NAC's remote sensing equipment: (1) Additive color viewer AC-90B, optical interpretation for Landsat film and airborne 9-1/2 inch multiband film; (2) Multi-color data system 4200E, three television camera systems for analysis of Landsat and airborne multiband film; (3) Mini multiband camera MD-470B, handheld multiband camera for ground truth; (4) Additive color mini viewer AC-70, small size additive color viewer for MD-470B camera film.

MACDONALD, DETTWILER AND ASSOCIATES, LIMITED, Nootka Building, 10280 Shellbridge Way, Richmond, British Columbia, CANADA

MacDonald, Dettwiler & Associates Ltd.'s (MDA) exhibit at the Twelfth International Symposium on Remote Sensing of Environment centered on the company's expertise in remote sensing and resource handling data systems. A photographic display illustrated the various MDA systems, including its Landsat line scan receiving and processing systems, meteorological data systems, and data acquisition and processing systems with a selection of satellite imagery produced by these systems.

BAUSCH AND LOMB, INCORPORATED, Optics Center, 1400 North Goodman, Rochester, New York, U.S.A.

Since the mid 1800's, Bausch & Lomb has been a leader in the development and manufacture of precision optical products. Among the important recent developments are the various models of the Zoom Transfer Scope™, graphical data transfer instruments, two of which were demonstrated at this symposium. These are simple, economical and efficient instruments for transferring photographic (or map) information onto a map or data base. Also shown was the latest in high quality optical stereoscopes complete with light table and scanning stage.

LOGETRONICS, INCORPORATED, 7001 Loisdale Road, Springfield, Virginia, U.S.A.

LogEtronics, Inc., manufacturers of specialized electronic aerial contact printers, were present at the Commercial Exhibits of the Twelfth International Symposium on Remote Sensing of Environment. On hand were examples of aerial prints exhibiting the image enhancement capabilities inherent in the equipment. Included were samples produced on the Mark IV Variable Dodging Contact Printer (black-and-white, normal color, and infra-red), the SP10/70C Dodging Continuous Strip Printer (black-and-white) and the Mark IVR5A Variable Dodging Contact/Projection Printer (70mm to 9 1/2 inch black-and-white projection prints).

AERO SERVICE, 8100 West Park Drive, Houston, Texas, U.S.A.

The booth of Aero Service Division, Western Geophysical Company of America, served as a means of displaying examples of Synthetic Aperture Radar (SAR) images produced by Aero Service in conjunction with Goodyear Aerospace Corporation, and employing the GEMS (Goodyear Electronic Mapping System) radar. Samples included the following: Original holographic data film; Original negatives; Enlargements at scales 1:100,000, 1:50,000 and 1:25,000; Controlled mosaics, scale 1:250,000; Extended dynamic range color image; Landsat-radar color composites.

In addition to the radar surveys, Aero Service performs airborne magnetometer, airborne scintillation spectrometer and other airborne geophysical surveys. Literature on these matters were on display.

GATES LEARJET CORPORATION, Box 11186, Tuscon, Arizona, U.S.A.

The Learjet exhibit featured some of the various configurations of their aircraft as well as photographic and scanner imagery taken at high and low altitudes.

Gates Learjet offers high performance aircraft ideally suited for remote sensing and aerial photography. These specially modified versions of the sleek Learjet are in use throughout the world. Smooth running jet engines provide a near vibration free platform for imagery of the highest quality. Capable of flying at all altitudes from sea level to 51,000 ft., the Learjet is the only aircraft capable of collecting imagery from the largest scale to the smallest.

CARL ZEISS, Jena, GERMAN DEMOCRATIC REPUBLIC

The Carl Zeiss exhibit featured their MKF-6 Multispectral Camera, MSP-4 Multispectral Projector and their interpretoskop.

The MKF-6 Multispectral Camera constitutes a major step forward from the experimental stage. The camera takes six photographs on black-and-white film through different narrow-band colour filters. The shutters are synchronized to an unparalleled degree to ensure perfect registration. The camera combines finest optical performance of the lenses with maximum mechanical stability that can stand the enormous thrust forces occurring when the carrier rocket is launched.

The MSP-4 Multispectral Projector, though specially designed for the visual

interpretation of multiband black-and-white exposures taken with the six-channel MKS-6 Multispectral Camera, can be employed for inspecting other multi-band, and even multi-temporal, imagery. The MSP-4 can mix four black-and-white photographs projected through different filters, and thus present a mixed colour picture with all the multi-spectral information at a glance. Varied false-colour presentations are possible that permit to derive distinctly differing hues from small spectral brightness differences in the objects explored, which would reveal little chromatic variation on conventional colour and false-colour photographs.

The Interpretoskop is a high performance optical photo-interpretation instument.

INTERPRETATION SYSTEMS, INCORPORATED, P. O. Box 1108, Lawrence, Kansas, U.S.A.

Interpretation Systems, Inc. presented their standard ISI System/30 which consisted of a density slicer and a pseudo 3-dimensional presentation.

PROSPACE, 129 rue d'Universite, Paris, FRANCE

Prospace is a non-profit office created in 1974 by CNES (the French Space Agency), and 42 other French firms and organizations active in the space field. Its aim is to help specialists throughout the world to become familiar with the field of expertise, facilities and products they can obtain from its members.

Visitors had the opportunity to obtain information and documentation on many aspects of French remote sensing equipment; i.e., Image taking; scanning radiometers, multispectral cameras, IR scanners; Data Processing: computers, High Density Data Recorders; Display: paper recorders, laser beam recorders, color graphic and video display consoles.

Prospace also presented the G.D.T.A. - Groupement pour le Developement de la Teledetection (French Aerospace Remote Sensing Development Organization), composed of CNES (French Space Agency), IGN (French National Geographic Institute), IFP (French Petroleum Institute) and BRGM (French Geological and Mining Research Bureau).

The G.D.T.A., which draws on the know-how, expertise and facilities of its members, has five main fields: study and promotion of sensor applications; remote sensing campaigns for users; promotion of the data available from Earth Observation Satellites (particularly Landsat and SPOT in the near future); study of data processing techniques and promotion of their use; collection and dissemination of documentation relevant to the remote sensing of the Earth's natural resources.

The ARGOS Location and Data Collection Satellites System was presented by the French Space Agency (Centre National d'Etudes Spatiales - CNES) and the French firm Electronique Marcel Dassault - E.M.D.

ARGOS will be an environmental (agriculture, hydrology, ecology, meteorology, geology, oceanology, seismology, etc.) data collection system operational between 1978 and 1985. The data will be transmitted from fixed or mobile platforms, such as land or ship installations, anchored or drifting buoys and balloons.

This program is the result of Franco-American cooperation between CNES, NASA and NOAA. Electronique Marcel Dassault produces all the ARGOS hardware for the satellites, and has also developed all types of compatible beacons.

EMR TELEMETRY, P. O. Box 3041, Sarasota, Florida, U.S.A.

EMR displayed their TIROS-N AVHRR Data Acquisition system and GMS HR FAX Image Acquisition system in pictorial block diagram form. Also on display was a mock-up of EMR's 850 series APT/WEFAX (LR-FAX) system complete with literature and sample photographs.

EMR representatives were available to discuss contents of these stations in detail including RF Antenna system, data processing and data display products.

OPTRONICS INTERNATIONAL SALES CORPORATION, 7 Stuart Road, Chelmsford, Massachusetts, U.S.A.

Optronics International Sales Corporation displayed imagery produced on their high-resolution, micro-positioning scanning/plotting systems. Imagery produced from Landsat data tapes and from scans of color infra-red aerial photographs comprise the primary display supported by color range/resolution test patterns. Additionally, Optronic's remote sensing experts provided information and literature on the application of digital image processing instrumentation relative to remote sensing research.

SOCIETE EUROPEENNE DE PROPULSION, Tour Nobel, Cedex No. 3, Paris, FRANCE

SEP exhibited a model of their VIZIR system, a high resolution laser beam recorder. Representatives were on hand to answer questions and distribute literature on SEP's many remote sensing and aerospace activities.

MOTOROLA AERIAL REMOTE SENSING, INCORPORATED, 4350 E. Camelback Road, Phoenix, Arizona, U.S.A.

MARS (Motorola Aerial Remote Sensing, Inc.) presented a display of remote sensing imagery and imagery products at its booth at the Twelfth International Symposium on Remote Sensing of Environment, held in Manila the 20th through the 26th of April.

MARS operates a highly sophisticated remote sensing aircraft containing 6 remote sensors utilized in various applications for natural resource identification mapping programs. The key sensor stressed by MARS is its unique SLAR (Side Looking Airborne Radar) with simultaneous dual look capability. This X-band radar system provides high resolution and high dynamic range imagery for processing into mosaics with interpretation by its experienced staff of scientists for geology, agriculture, forestry, mineralogy, hydrology and hydrocarbon applications.

Sample imagery of the SLAR system were featured in the MARS booth along with imagery from its magnetometer, infra-red line scanner, dual RC8 cameras and I^2S imaging systems. MARS provided literature, data and answered questions from interested guests during the symposium at the Philippine Plaza Hotel.

SPECIALIZED AIRCRAFT, P. O. Box 217, Camarillo, California, U.S.A.

Representatives from Specialized Aircraft were on hand to hand out literature on, and answer questions about, their Tri-Turbo-3, a modernization of the world famous Douglas DC-3/C-47 aircraft. This short take-off and landing aircraft is available for aerial missions, including the installation and flying of aerial remote sensors.

AUTHOR INDEX

Abotteen, R.A., 765
Adrien, P.M., 187
Ahern, F.J., 1267
Ahmad, M.S., 123
Aikoh, T., 1451
Akhavi, M.S., 503
Alford, W.L., 329
Ali, M.M., 887
Alpers, W., 1597
Andrawis, A.S., 1289, 1503
Aquino, E., 1401
Araya, M., 2131
Arnold, H.A., 175
Asanuma, I., 1707
Asaoka, O., 1827
Asmoro, P., 27
Attia, S.H., 857
Audirac, H., 1267
Austin, R.W., 1103
Ayyanger, R.S., 2323
Azim, A., 1391

Baker, R.H., 1287
Bare, J.E., 2205
Barney, T.W., 1653
Barringer, A.R., 257, 975
Basa, V., 1401
Beaubien, J., 1267
Bhattarai, K.D., 1503
Bijleveld, J.H., 2267
Bina, R.T., 1791, 2051, 2343
Birnie, R.W., 795
Blackey, E.A., 1027
Blatchford, D.R., 2027
Blyth, K., 2267
Bonn, F.J., 2101
Booncong, V., 1973
Bormann, R., 113
Boyne, H.S., 877, 957
Braconne, S., 2193
Brera, A.M., 1329
Breslau, L., 239, 1917
Brockmann, C.E., 131, 415
Bruce, R.C., 547
Bruce, W.D., 203
Bruneau, M., 1883
Bryant, N.A., 927
Bussey, H.E., 957
Buzby, C.E., 825

Campbell, R.W., 139
Cannon, T.K., 2081
Carpenter, K., 2051
Carrel, J.E., 1653
Carter, W.D., 387, 755, 1037
Cassinis, R., 145
Chahine, M.T., 1307
Chandrasekhar, S., 1769
Chang, A.T.C., 877
Chaudhury, M.U., 63, 887, 1391, 2277
Chen, S.C., 2091
Chen Yen-chuan, 535
Chen, Z., 2141
Cheosakul, P., 37
Chou Hsiu-chi, 535, 671
Choudhury, J.K., 1391
Christenson, J.W., 1083
Chu Shao-hou, 535
Cicone, R.C., 917
Clark, D.K., 621
Clemena, G.G., 867
Coberly, W.A., 775
Cochrane, G.R., 2109
Coiner, J.C., 547
Colwell, J.E., 845, 1149, 1391
Cook, J.J., 2373
Craib, K.B., 2081
Crespo, J., 2081
Crist, E.P., 917
Currey, D.T., 463

Danjoy, W.A., 947
Darmoyuwono, K., 1349
Daubner, L., 975
Davies, J.H., 257, 975
Davis, M.R., 1409
De Jesus, B., 1791, 2343
Dellwig, L.E., 2205
DeNoyer, J.M., 755
Dietrich, D.L., 1083, 1401
Dijardjana, 2071
Drake, B., 1115
Du Bois, F.P., 203
Dykstra, J.D., 795

Egli, E., 2285
El-Amin, H., 1563
El-Baz, F., 703
El Ghawaby, M.A., 857, 1563
El Kassas, I.A., 1563
Ellefsen, R.A., 2081
Ellerbruch, D.A., 877, 957
Ellis, P.J., 159
Ellyett, C.D., 1207
El Rakaiby, M.M., 1563
El Shazly, E.M., 857, 1563
El Shazly, M.M., 857, 1563
Emori, Y., 1707
Estes, J.E., 1319

Falconer, A., 1697
Fan Hsi-an, 535
Fernandez, J.C., 1513
Fischer, W., 2333
Fischer, W.A., 805, 2372
Fitzpatrick, E.A., 1849
Freezer, D.R., 2037
Fukimura, S., 1451
Fukuhara, M., 1707

Gaubert, A.M., 289
Geiser, U., 2285
Gelnett, R.H., 2205
Genda, H., 2019
Gilg, W., 1421
Gilmer, D.S., 845
Gleason, J.M., 917
Gnagy, J., 1091
Good, W., 1779
Gray, D., 1697
Green, A.A., 1697, 1755
Green, A.E.S., 991
Green, S.L., 743
Greenlee, D.D., 805
Guardia, R.E. Quiros, 139
Guerrero, D., 1287, 1489
Gurney, R.J., 2267
Gustafson, J.R., 271

Haack, B.N., 1391
Haba, Y., 1241
Hacker, R.B., 1895
Hady, M.A. Abdel, 857, 1563
Haefner, H., 2285
Hajic, E.J., 1025
Haketa, S., 1643
Hanuschak, G., 1013
Haraga, A.A., 857
Hardy, J.R., 1717
Hart, W.G., 1409
Haruyama, Y., 1947
Hayashi, S., 1707
Hernandez, P.F., 2091
Herrmann, H., 1279
Hick, P.T., 2027
Hielkema, J., 2366
Hofer, R., 1779
Honey, F.R., 2027, 2177
Horstmann, U., 1379
Hossain, A., 63, 213
Hossain, Q.T., 1391
Hovis, W.A., 621
Huang Hsuan, 653
Huang Run-heng, 671
Huddleston, H.F., 429
Hung, R.J., 2245
Huntington, J.F., 1755

Iikura, Y., 1309
Iisaka, J., 1451, 1707, 1827, 1957
Imanaka, M., 1957
Indrambarya, B., 37
Ingle, S.J., 1409
Irsyam, M., 1909
Ishii, Y., 1957
Ishiyama, T., 2019
Itakura, Y., 2121
Itten, K.T., 2285

Jackson, P.L., 1115
Jara, R., 1791, 2051, 2343

Jazayeri, B., 69
Jesch, R.L., 957
Jin Chi-i, 523
Joachim, R., 113
Johannsen, C.J., 1653
Jones, R.N., 957
Jones, W.L., 1597
Joo, Chong Yean, 35, 1741
Joseph, G., 1219
Joshi, P.M., 1503

Kalensky, Z.D., 1349
Kamat, D.S., 1219
Kan, E.P., 1809
Kaplan, L.D., 1307
Kauth, R., 999
Kautzleben, H., 113
Kawata, Y., 1241
Keller, D., 2354
Kammerer, A.J., 621
Kent, G.S., 1279
Khawasik, S.M., 857, 1563
Klankamsorn, B., 417, 1299
Kodaria, N., 505
Koepp, F., 1279
Koffler, N.F., 2091
Koutsandreas, J., 271
Koyama, T., 1451
Kraus, S.P., 1319
Krishnan, R., 1259
Kumar, R., 1729
Kusaka, T., 1241
Kuyper, W.H., 1009

Lachowski, H.M., 1083, 1401
Lambeck, P.F., 999
Larson, R.W., 297, 1115, 1127
Leido, J.J., 1
Lemus, L. Hidalgo, 1937
Le Toan, T., 1883
Leu Dar-ren, 523, 671
Levin, S., 11
Lim, J.B.R., 1489, 2051
Lin Hai, 523
Link, L.E., 907, 1073
Lo, C.P., 1339
Lodwick, G.D., 1461
Logan, T.L., 927
Long, K.S., 907
Lorenzo, E., 1791, 2343
Lowe, D.S., 277, 899
Lowry, R.T., 683
Lozano, F., 1871
Lu Nai-ping, 535
Lummaux, J.C., 2193
Luyendyk, B.P., 1025
Lyon, R.J.P., 835, 1985
Lyzenga, D.R., 887

MacDonald, J.S., 2163
MacLeod, N.H., 887, 1391, 2277
Madhavan Unni, N.V., 1471
Malila, W.A., 917
Malingreau, J.P., 1617, 2313
Mamiya, K., 81

Maracci, G., 1431
Marcos, F.E., 5
Marmelstein, A.D., 2315
Maruthachalam, M., 1769
Matsuoka, R., 1441
McDonnell, M.J., 1687
McFarland, W., 1653
McKeel, W.T., 867
McKim, H.L., 1027
Medina, M., 1871
Meeks, G.R., 719
Mehl, W., 1431
Mejia, C., 1871
Merkel, R.F., 719
Merry, C.J., 1927
Mertz, F.C., 1319
Messmore, J.A., 943
Meylan, D., 1779
Michino, T., 1349, 1643
Miller, J.M., 2255
Miller, L.D., 1167
Mishima, S., 1827
Misra, K.S., 1763
Missallati, A., 835
Miyakawa, G., 1643
Miyazaki, T., 1309
Miyazaki, Y., 1957
Montero, P.O., 1513
Moore, D.G., 443, 1155
Moore, G.K., 445
Moore, H.S., 507
Morain, S.A., 417, 587, 1199
Morgan, G.A., 599
Morgan, J.O., 1973
Morley, L.W., 2361
Morrissey, K., 1013
Morzier, C., 1779
Mosher, P.N., 1415
Mourlon, J.C., 235
Muhlfeld, R., 2199
Murai, S., 1441
Murayama, N., 505
Murthy, H.G.S., 179
Musy, A., 1779

Naderi, F., 69
Nakata, E., 1957
Nalepka, R.F., 1149
Nanayakkara, C., 1665
Nasu, M., 1481
Nataraian, S., 1259
Nor, S.M., 133
Nualchawee, K., 1167

Ochiai, H., 1451
Okayama, H., 2019
Okuda, T., 1441
Olson, C.E., 323
Omakupt, M., 2297
Ondrejka, R.J., 703
Orr, D.G., 805
Orth, R., 2163
Ortiz, A., 1583
Osterkamp, T.E., 2255

Park, A.B., 355
Parry, J.T., 1573
Parsons, A.J., 1849
Parthasarathy, A., 2011
Pascual, A., 1859
Pena, M.S., 125, 2376
Perez, J.A. Diez, 497, 1871
Pierce, T.H., 271
Pikus, I., 2363
Polcyn, F.C., 887, 1091, 1391
Potts, T.F., 1349
Pramanik, M.A.H., 63, 887, 2277
Praseno, D.P., 2071
Pratt, D.A., 1207
Prelat, A.E., 835, 1985
Puerner, J.H., 507
Punongbayan, R.S., 1287, 1489

Ragan, R.M., 481
Rajbhandari, M.D., 1503
Ramos, E.G., 1489
Raney, R.K., 683
Rao, K.R., 43
Rausch, G., 1421
Rawson, R.F., 1127
Rebel, D.L., 845
Reiniger, P., 2267
Renz, C.E., 1555
Reynolds, C.D., 1037
Rice, D.P., 1149
Richard, R.R., 719
Risley, E., 2354
Roberts, G.P., 1755
Rochon, G., 1267
Rodriquez, D. Bejarano, 1609
Rodriquez, H., 139
Rohde, W.G., 729
Roller, N.E.G., 845, 887, 1091, 1391
Roque, C.R., 17, 2377
Rosema, A., 2267
Rosenberg, A., 1307
Rowan, L.C., 387
Ruangsiri, P., 1545
Rudin, F.M., 139, 2377
Ruiz, P. Azuara, 1937
Ryan, J.F., 55
Ryerson, R.A., 1415

Sabhasri, S., 37
Sadowski, F.G., 917, 947
Saitoh, S., 1827
Sakata, T., 1229
Salman, A.B., 1563
Salomonson, V.V., 371, 481
Sanad, S., 857
Santoso, P., 2313
Sasso, R.R., 1319
Sayn-Wittgenstein, L., 1187
Sayson, V., 1489
Schanda, E., 297, 1779
Schlesinger, H.L., 743

Schmidt, D., 1379
Schoch, R., 2285
Scott, G.N., 825, 1053
Sekioka, M., 1679
Shahrokhi, F., 1329
Sharifi, M.A., 95
Sharp, W.L., 1837
Sheehan, C.A., 1037
Shelton, R.L., 567
Sherestha, P.P., 1503
Sherman, J.W., 639
Shimabukuro, Y.E., 2091
Shimoda, H., 1229
Shiue, J.C., 877
Short, N.M., 395
Shuchman, R.A., 1127
Siegal, B.S., 1743
Sigman, R., 1013
Silonga, W., 1859
Simonett, D.S., 427, 597, 1025, 2370
Sivertson, W.E., 1115
Slaney, V.R., 1995
Smith, A.M., 1015
Smith, J.T., 283
Smith, R.C., 1103
Smith, R.E., 2245
Smith, W.L., 395
Snider, F.G., 1743
Soejitno, T., 2217
Soejoeti, Z., 2071
Sorensen, B.M., 1431
Soto, M., 1871
Spinhirne, J.D., 991
Spohn, C., 2357
Sprigg, W.A., 513
Sriplung, N., 2045
Steffen, H., 2285
Steffensen, R., 1015
Strahler, A.H., 927
Strome, W.M., 355, 1415, 2372, 2375
Struve, H., 1073
Sturm, B., 1431
Suarez, M., 2227
Summers, R.A., 395
Susskind, J., 1307
Suwijanto, 1993

Tabata, T., 619
Takeda, K., 2019
Takemura, K., 2121
Tanaka, S., 2151
Tapley, I.J., 2177
Taranik, J.V., 1037
Tassone, G., 2267
Tateishi, R., 1441
Teodoro, C.F., 1513
Terashita, Y., 1241
Thillaigovindarajan, S., 1053, 1289
Thomas, G.S., 999
Thomas, I.L., 1367
Tilford, N.R., 1743
Tilmann, S.E., 567
Tom, C., 1167
Toyota, H., 1451
Trevett, J.W., 1799, 1919
Tseng, L.Y., 2141
Tsutsumi, S., 2121
Tubbs, J.D., 775
Tueller, P.T., 2177
Turner, R.E., 783

Ueno, S., 1241
Ulbricht, K.A., 1379
Umali, R., 1401

Vaidya, N.N., 1503
Van de Meene, E.A., 1985
van Genderen, J.L., 219, 2374, 2375
Vanselous, T.M., 621
Vass, P.A., 219
Velten, E.H., 1421
Vibulsresth, S., 37, 1545, 1973
Vincent, R.K., 825, 1053, 2373
Voelke, N., 2285
Vogel, T.C., 943
Vollmers, R.R., 2037

Wacharakitti, S., 587
Wagner, T.W., 277, 899
Warne, D.K., 1063
Waters, M.P., 1529
Weber, F.P., 1809
Werner, C.H., 1279
White, J.R., 239, 2307
Whitehouse, G., 1545
Wigton, W.H., 429, 1013
Wilson, W.H., 1103
Wiroatmodjo, P., 1671
Wong, F., 2163
Worcester, B.K., 1155
Work, E.A., 845
Worsfold, R.D., 1127
Wyssen, D., 1779

Yamamoto, Y., 1947
Yasuoka, Y., 1309
Yuhara, K., 1679

Zacher, W., 2051
Zimmerman, S., 1091